Property of
Flood Control District of MC Library
Please Return to
2801 W. Durango
Phoenix, AZ 85009

UNSTEADY FLOW MODELING USING DAMBRK AND DWOPER

WORKSHOP PROBLEM #1

#14

	1 (10)	2 (20)	3 (30)	4 (40)	5 (50)	6 (60)	7 (70)	8 (80)
1.	WORKSHOP	DAM						
	J. M. RUMANN	3335 W.	DURANGO	DIHDEWIXI, AZ				
2.	1	1	1	3	39.	0	0	0
SKIP 3.								
OPTIONAL 4.								
OMIT 5.								
6.	1610710.	851210	518160.	310075.	13499.	14125.	335.	0
	12342.	2330.	12320.	12305.	12290.	12275.	2260.	12245.
OPTIONAL 7.								
8.	5.	12323.	0.0	22445.	2190	1.25	22445.	1.0
9.	23417	23417.	12333.	0	9750 ~~6000~~	0	16009.	8199.
OPTIONAL 10.								
11.								
12.	2.0	57						
OMIT 13	800	800						
HYDROGRAPH 14	12.0	239	see table					
15	1.0	3.0	see table 3	7	9	11	13	15
16	~~12.0~~ 58	5	2	4	0	0	0	0
17	0	5						
	0							
see section 20 21	see table 22.50	2260	2300					
22	0	1024	2737					
25	0							

X-SECTIONS

	1	2	3	4	5	6	7	8
	0.0							
meaning								
28								
31	.5	.5	.5	.5				
32	0	0	0	0				
33	0	0	0	1/10.1/5				

WORK SHOP PROBLEM #2

1	2	3	4	5	6	7	8
10	20	30	40	50	60	70	80

ouiet Hydrograph

WORKSHOP #3

1	2	3	4	5	6	7	8
10	20	30	40	50	60	70	80

WORKSHOP -4

1	2	3	4	5	6	7	8
10	20	30	40	50	60	70	80

University of Texas, Austin

Property of
Flood Control District of MC Library
Please Return to
2801 W. Durango
Phoenix, AZ 85009

Unsteady Flow Modeling Using DAMBRK and DWOPER

April 21 - 25, 1986

Monday

8:15	Larry W. Mays, Introduction and Review of Hydrology and Hydraulics
10:15	Break
10:30	Larry W. Mays, Review of Open Channel Hydraulics
11:30	Larry W. Mays, Unsteady Flow Equations
12:30	Lunch
1:45	Larry W. Mays, Finite Difference Approximations
3:15	Larry W. Mays, Numerical Solution of Unsteady Flow Equations, Initial Conditions, Boundary Conditions, and Internal Boundary Conditions
5:00	Adjourn

Tuesday

8:15	Larry W. Mays, Numerical Solution of Unsteady Flow Equations
9:15	Danny L. Fread, Introduction to DAMBRK
10:15	Break
10:30	Danny L. Fread, Introduction to DAMBRK (continued)
12:30	Lunch
1:45	Danny L. Fread, Data Input, Output, and Application of DAMBRK to Teton (Slides)
3:15	Danny L. Fread and Larry W. Mays, Workshop, Application of DAMBRK
5:00	Adjourn

Friday

8:15	Larry W. Mays, Continuation of Workshop (DWOPER)
9:15	Larry W. Mays, Application of DWOPER
10:15	Break
10:30	Larry W. Mays, Storm Sewer (Network) Option in DWOPER, Application to Storm Sewers and a Flood Bypass Tunnel, and Microcomputer (IBM-PC) Demonstration of NETWORK
12:30	Adjourn

REVIEW OF HYDROLOGY

AND

HYDRAULICS

REVIEW OF HYDROLOGY AND HYDRAULICS

HYDROLOGIC CYCLE (HYDROLOGIC SYSTEMS)

ROUTING METHODS (CLASSIFICATION)

RAINFALL - RUNOFF ANALYSIS

DESIGN STORMS

HYDROLOGIC ROUTING

HEC-1 (DETERMINATION OF RESERVOIR INFLOW HYDROGRAPHS)

HYDROLOGIC CYCLE

NATIONAL 42-381 200 SHEETS 5 SQUARE

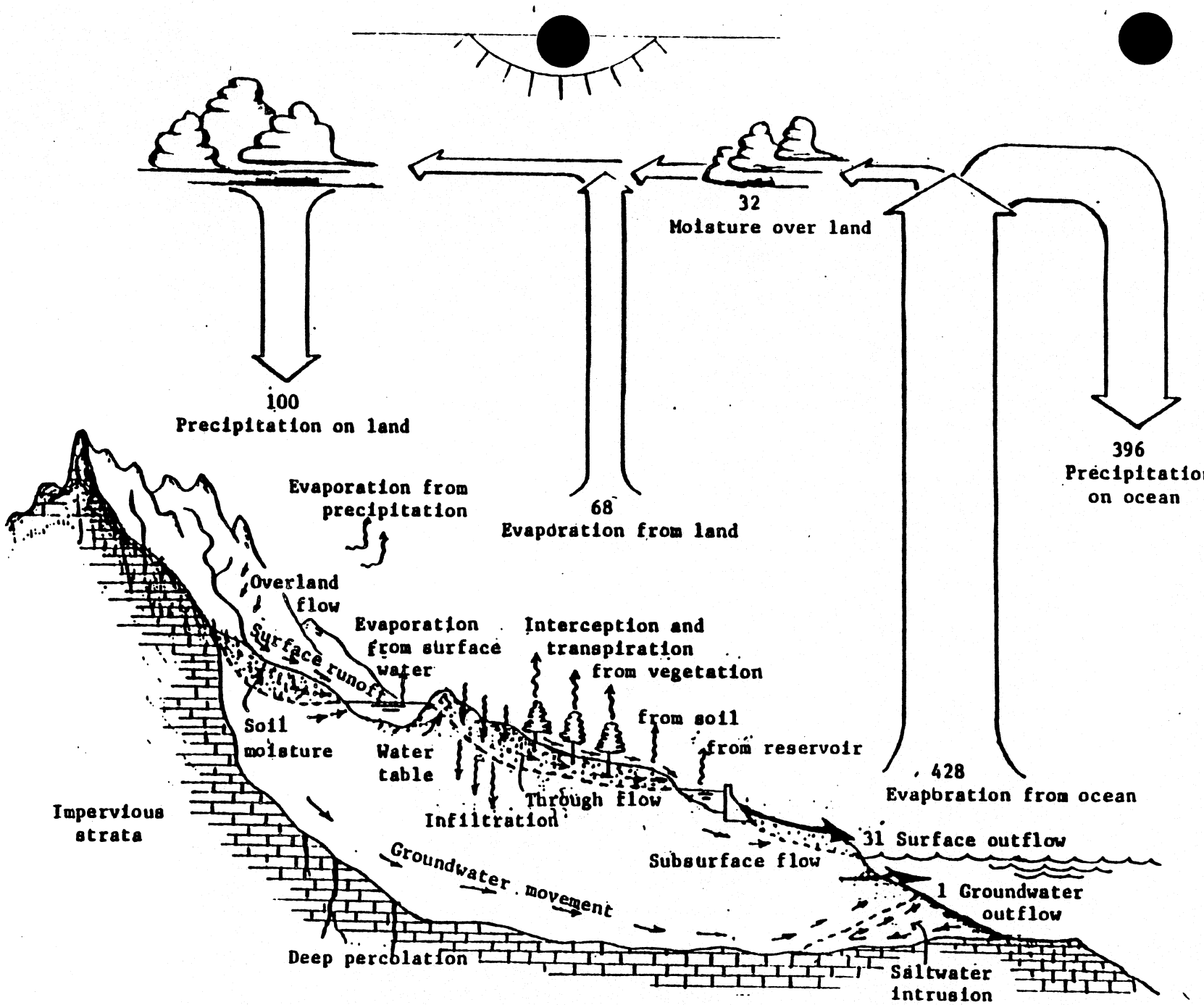

Fig. 1-1. Hydrologic cycle with global annual average water balance given in relative units

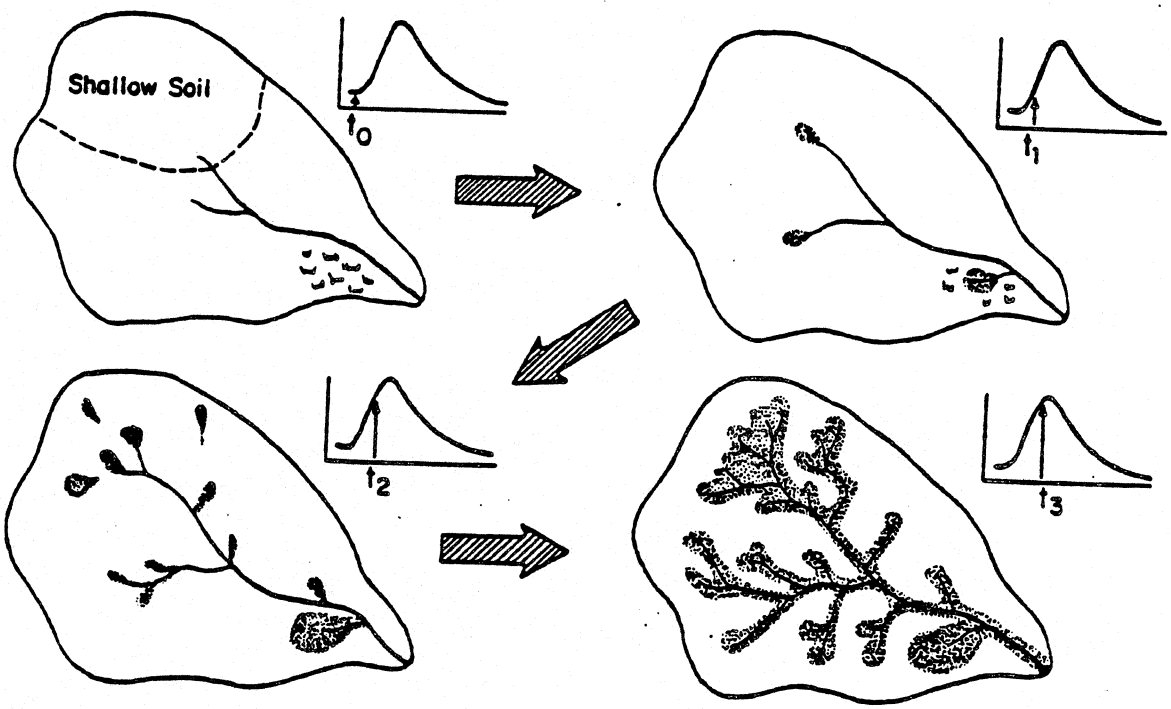

Fig. 6.3.3 The small arrows in the hydrographs show how streamflow increases as the variable source extends into swamps, shallow soils and ephemeral channels. The process reverses as streamflow declines. (after Hewlett,1982)

Source: Hewlett,J.D., Principles of Forest Hydrology,Univ. of Georgia Press, Athens, Ga., Fig.7-12, p.124, 1982

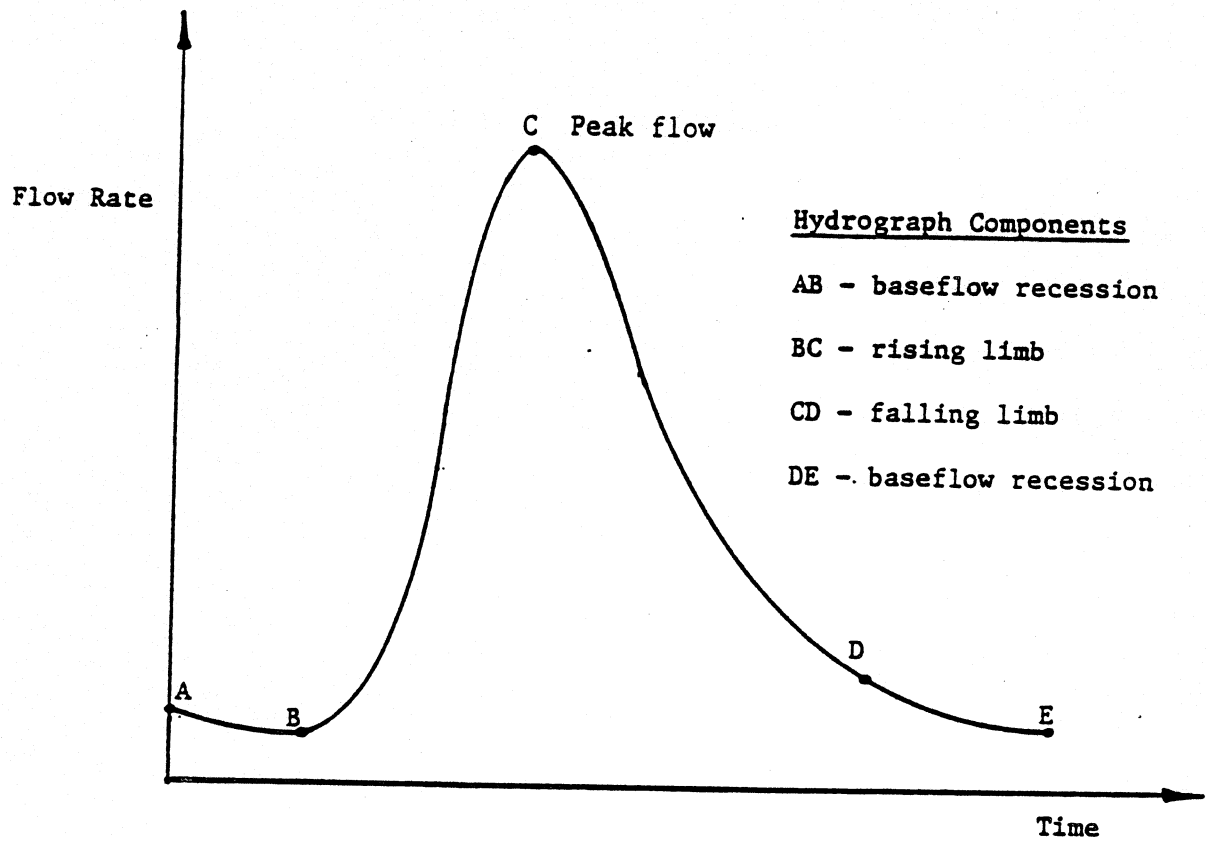

Figure 6.4.2 Components of the streamflow hydrograph during a storm.

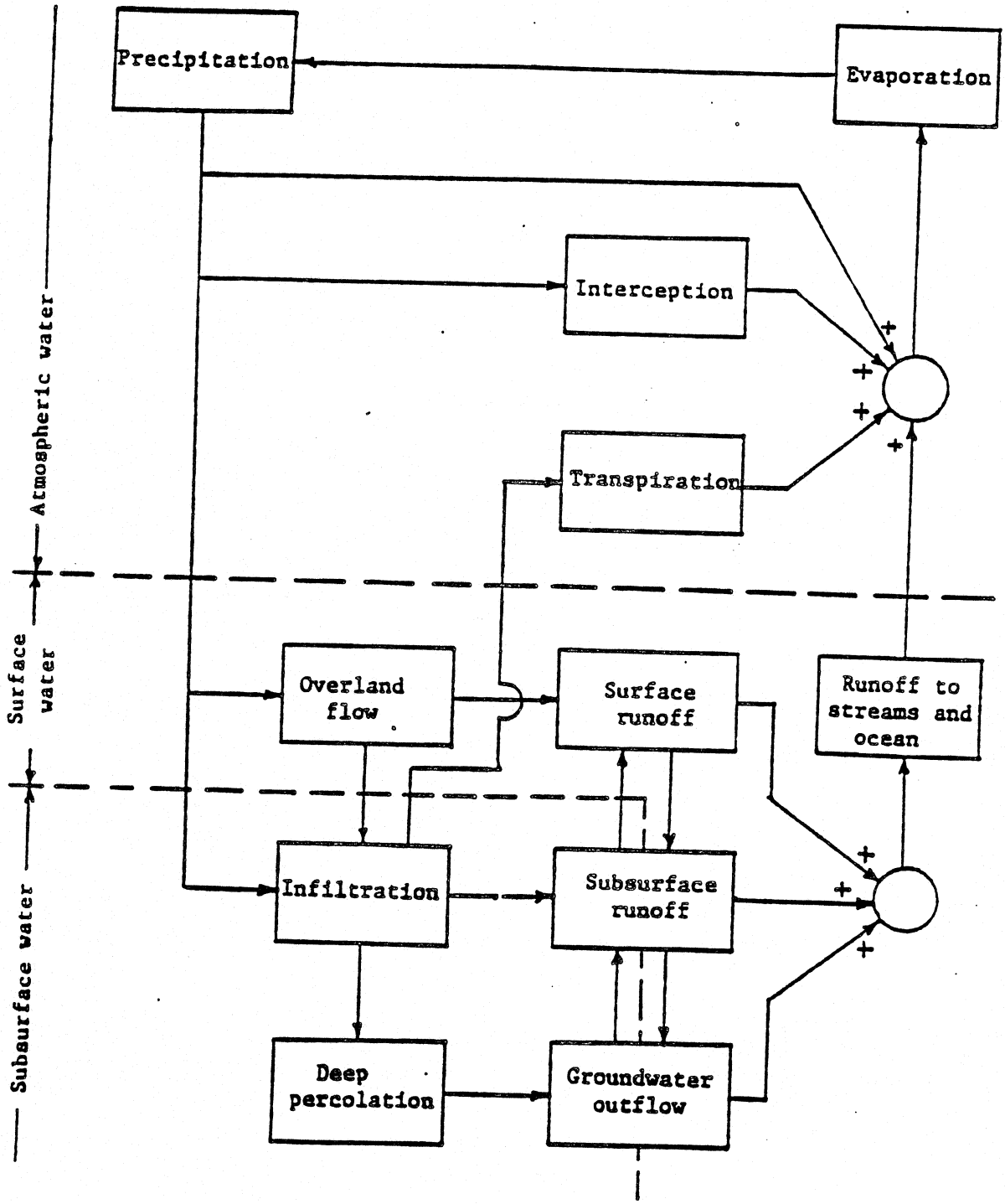

Fig. 2-1. Block-diagram representation of the global hydrologic system.

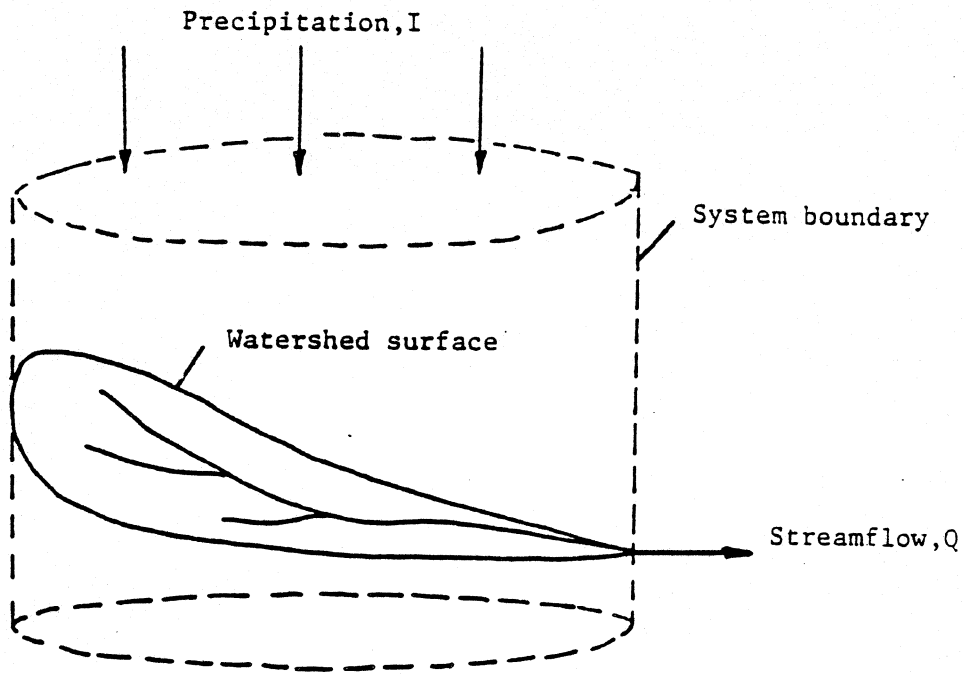

Fig. 2-3. The watershed as a hydrologic system.

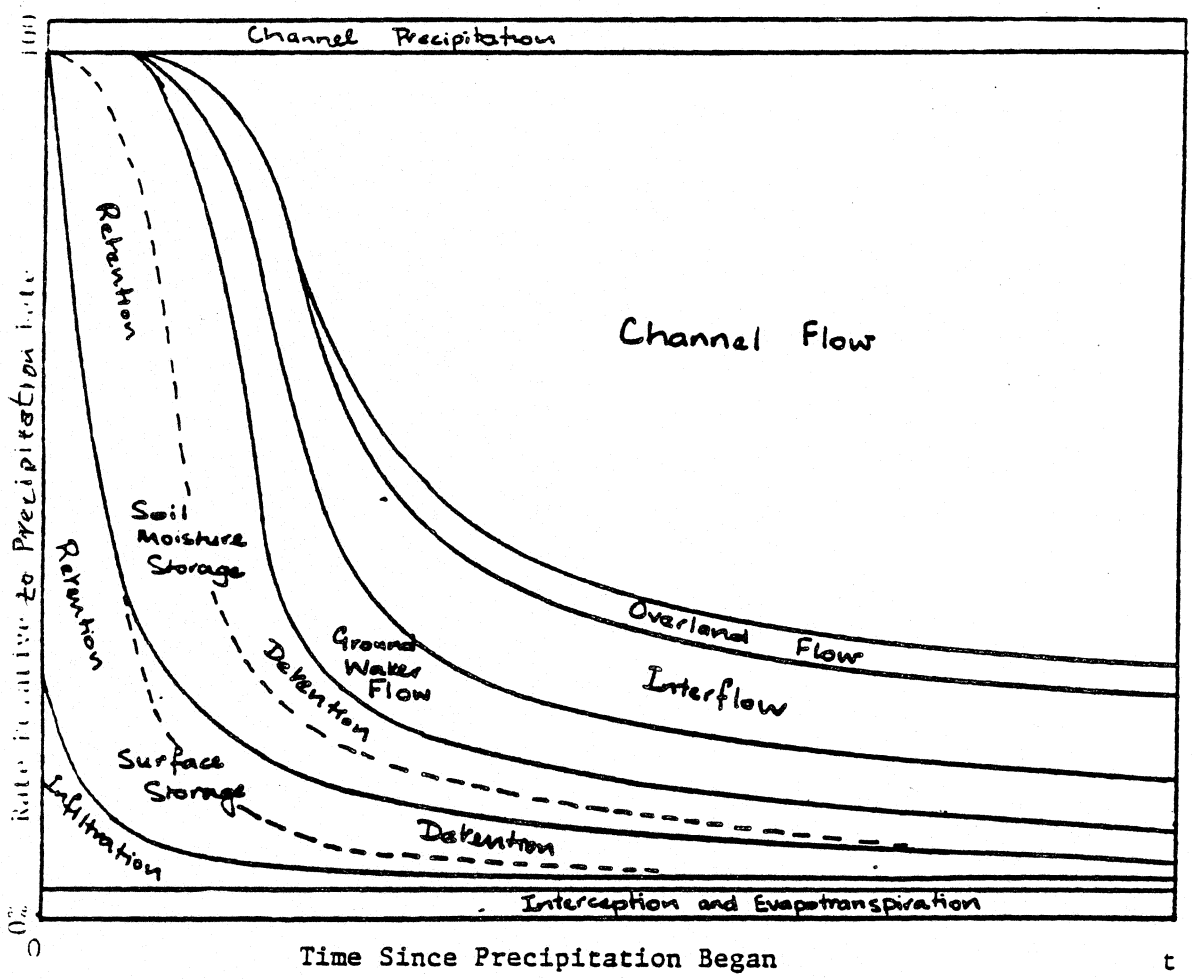

Figure 6.1.1 Schematic illustration of the disposal of precipitation on a watershed.

ROUTING METHODS

HYDROLOGIC VS HYDRAULIC

LUMPED VS DISTRIBUTED

NATIONAL 42-381 50 SHEETS 5 SQUARE 42-382 100 SHEETS 5 SQUARE 42-389 200 SHEETS 5 SQUARE

FLUID MECHANICS

CONSERVATION OF MASS

$$\oiint_A \rho V \cdot dA + \frac{\partial}{\partial t} \iiint_S \rho \, ds = 0$$

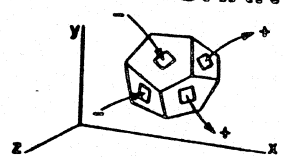

CONSERVATION OF MOMENTUM

$$\oiint_A V(\rho V \cdot dA) + \frac{\partial}{\partial t} \iiint_S V(\rho \, ds) = \oiint_A dF + \iiint_S dB$$

HYDRAULICS

constant $\rho \rightarrow$ conservation of volume

$$\frac{\partial (V y z)}{\partial x} dx + \frac{\partial (y z)}{\partial t} dx = 0$$

$$\frac{\partial (V y)}{\partial x} + \frac{\partial y}{\partial t} = 0$$

$$V \frac{\partial y}{\partial x} + y \frac{\partial V}{\partial x} + \frac{\partial y}{\partial t} = 0$$

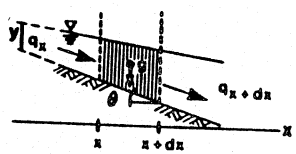

constant mass (ρ and volume) $\rightarrow$ conservation of acceleration

$$g \frac{\partial y}{\partial x} + V \frac{\partial V}{\partial x} + \frac{\partial V}{\partial t} = -\frac{\tau_0}{\rho y} + g\theta$$

DYNAMIC WAVE

$$\frac{\tau_0}{\rho y} = g\theta \rightarrow \tau_0 = \rho g y \theta$$

$$\tau_0 = c V^2 \rightarrow V = C \theta^{1/2} y^{1/2}, \quad q = V y = \alpha y^{3/2}$$

KINEMATIC WAVE

HYDROLOGY

flow rate $q = V y z$

$$\frac{q_x - q_{x+\Delta x}}{\Delta x} \Delta x + \frac{S_t - S_{t+\Delta t}}{\Delta t} = 0$$

$$(q_x - q_{x+\Delta x}) \Delta t = S_{t+\Delta t} - S_t$$

$$p \Delta t - q \Delta t = S_{t+\Delta t} - S_t$$

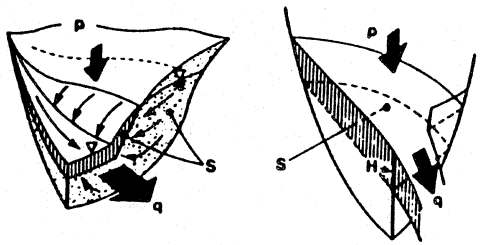

$$q = \alpha H^{\beta}, \quad S = \lambda H^{A} \rightarrow q = a S^{b}$$

FIG. 1. Progression of simplifications of equations of motion.

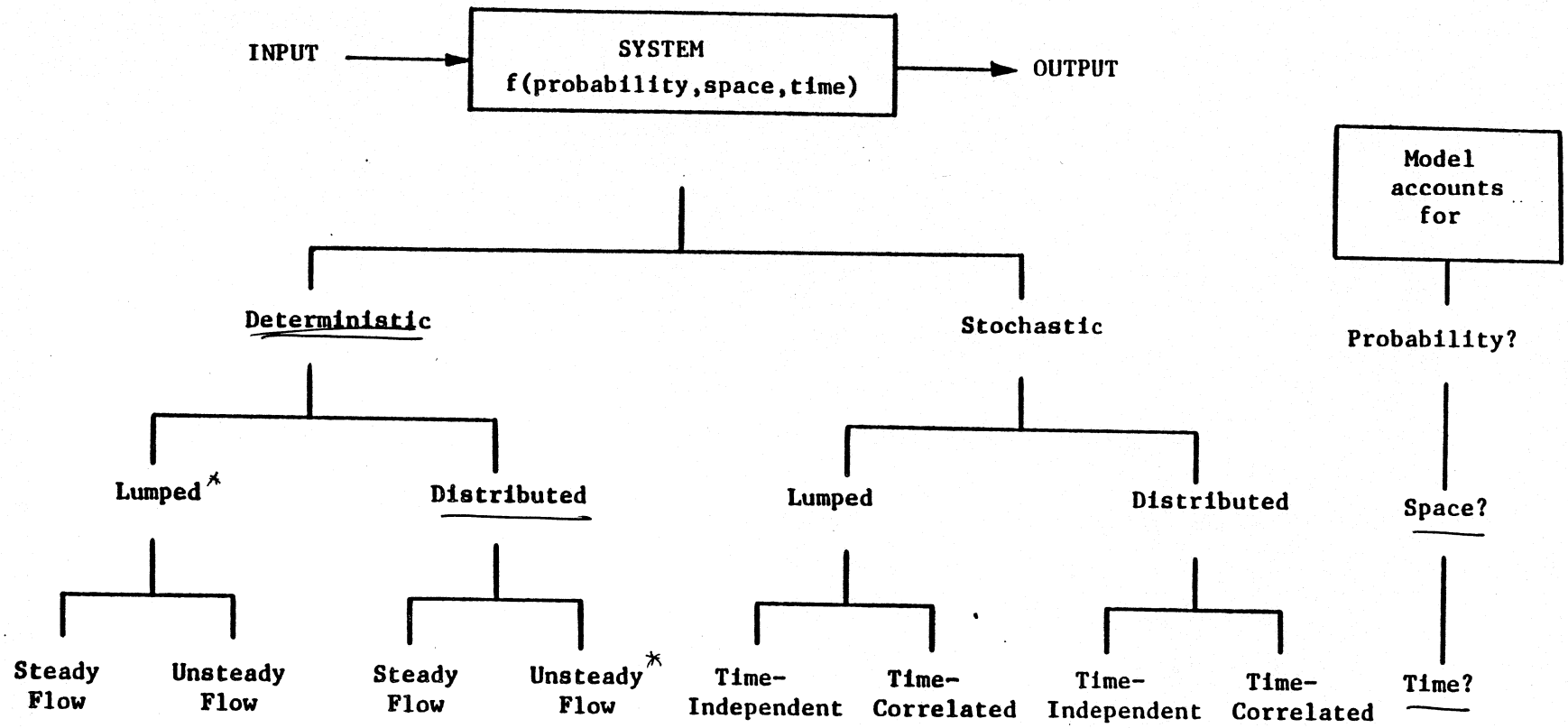

Fig. 2-5. Classification of Abstract Hydrologic Systems Models.

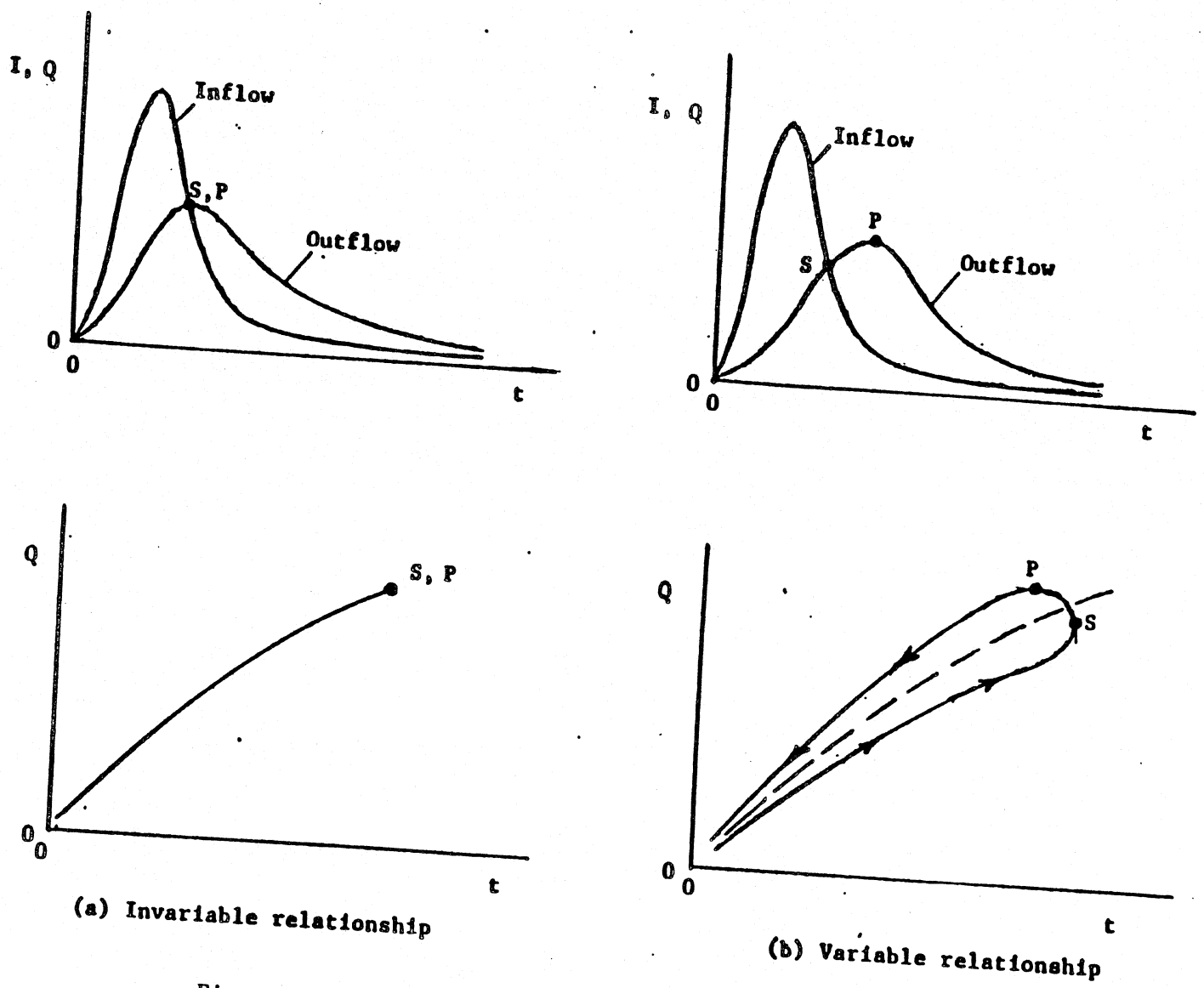

(a) Invariable relationship

(b) Variable relationship

Figure 9.2.1. Relationship Between Discharge and Storage

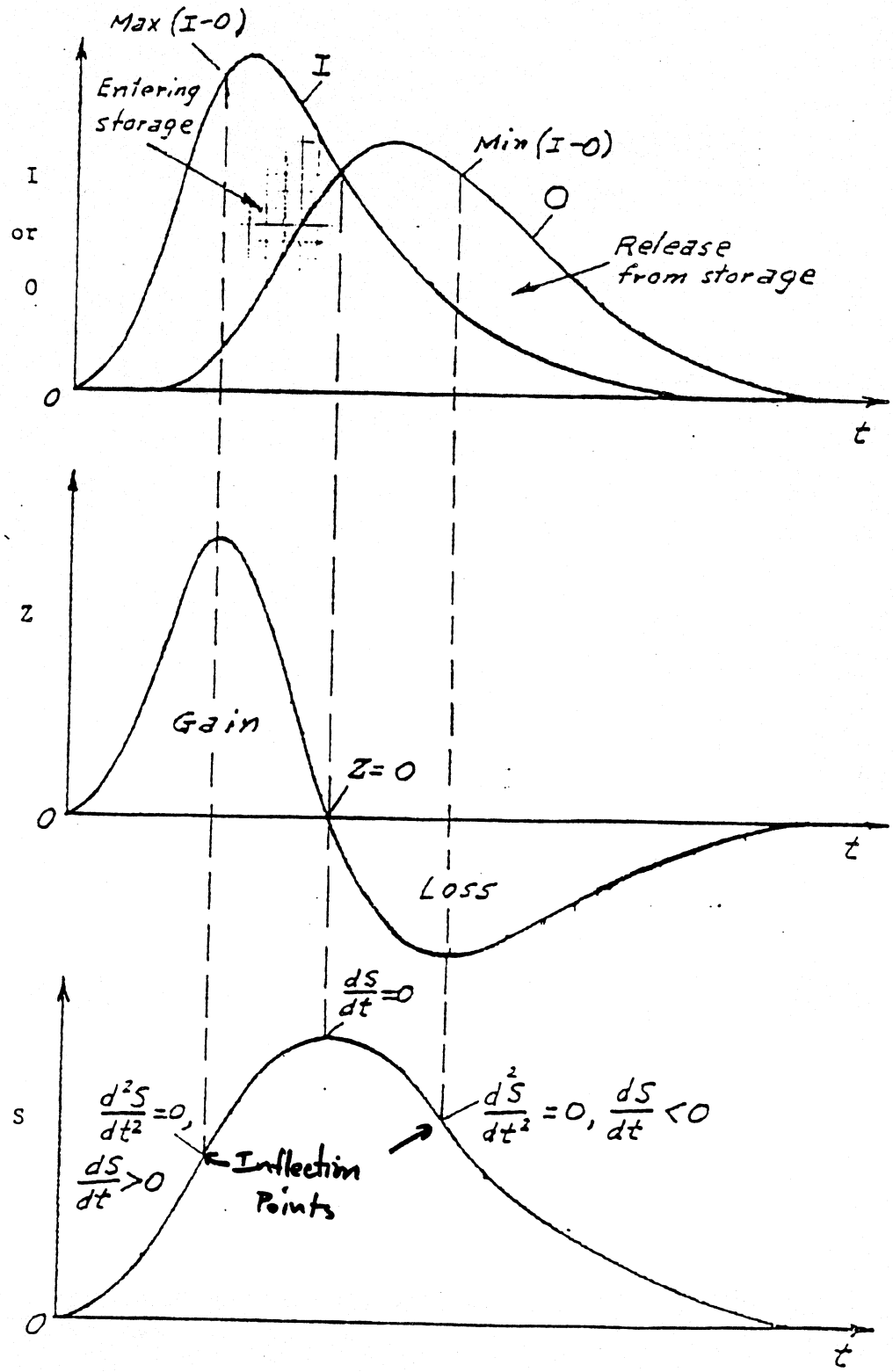

Fig. 2-2. Relations between input, output, throughput, and storage.

MUSKINGUM ROUTING

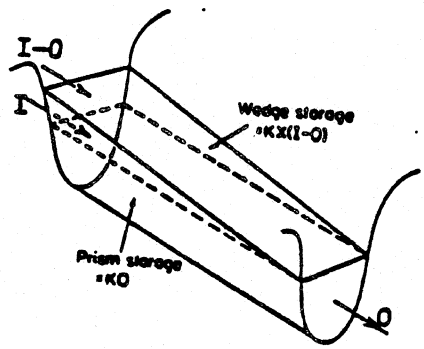

Figure 9.3.1.

Prism and Wedge Storages in a Channel Reach.

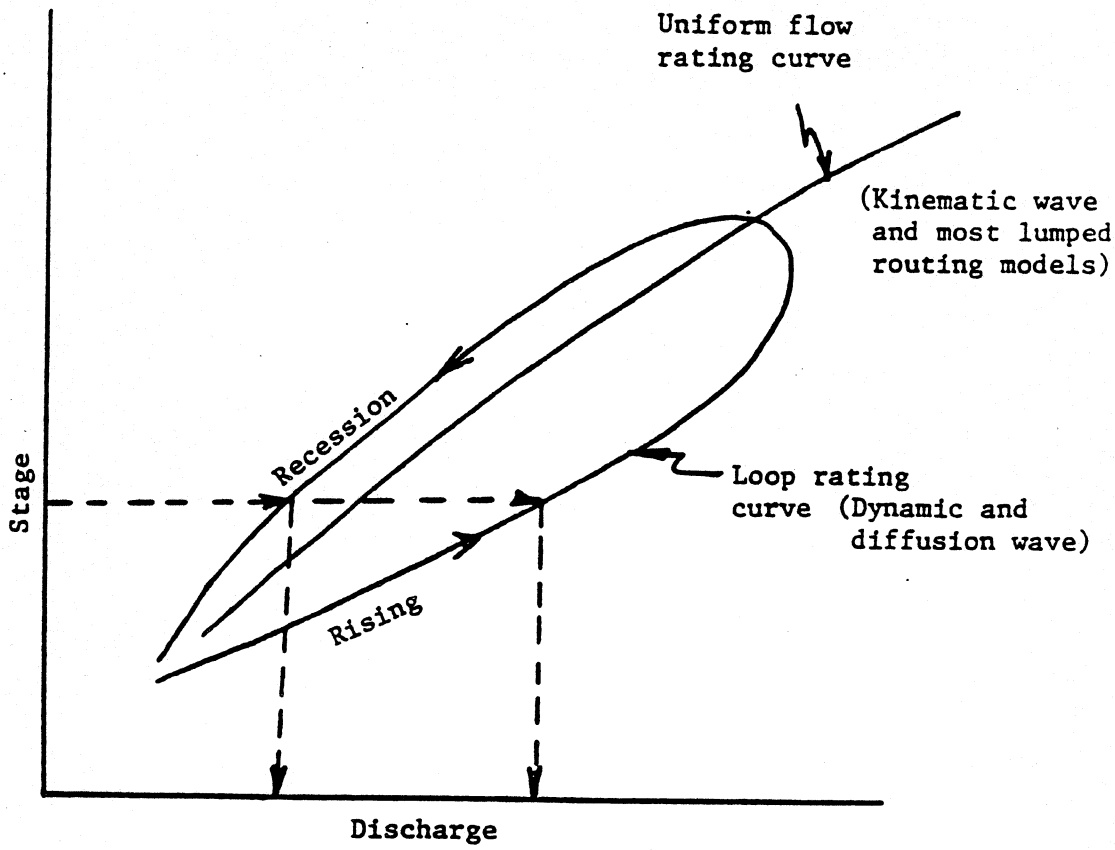

Figure 11.7 Loop Rating Curve

Table 11.1 Summary of Saint-Venant Equations*

Continuity Equation

Conservation form

$$\frac{\partial Q}{\partial x} + \frac{\partial A}{\partial t} = 0 \qquad (11.1.35)$$

Nonconservation form

$$\frac{\partial y}{\partial t} + \frac{A}{B}\frac{\partial V}{\partial x} + V\frac{\partial y}{\partial x} = 0 \qquad (11.1.36)$$

Momentum Equation

Conservation form

$\frac{1}{A}\frac{\partial Q}{\partial t}$	$+ \frac{1}{A}\frac{\partial}{\partial x}(Q^2/A)$	$+ g\frac{\partial y}{\partial x}$	$-g(S_o - S_f) = 0$ (11.1.37)	
local acceleration term	convective acceleration term	pressure term	slopes	
Nonconservation form				
$\frac{\partial V}{\partial t}$	$+ \frac{\partial V}{\partial x}$	$+ g\frac{\partial y}{\partial x}$	$-g(S_o - S_f) = 0$ (11.1.38)	
			Kinematic wave	
		Diffusion wave		
	Dynamic wave			

*Neglecting lateral inflow, $q = 0$, assuming $\beta = 1$ and $\tau_w = 0$.

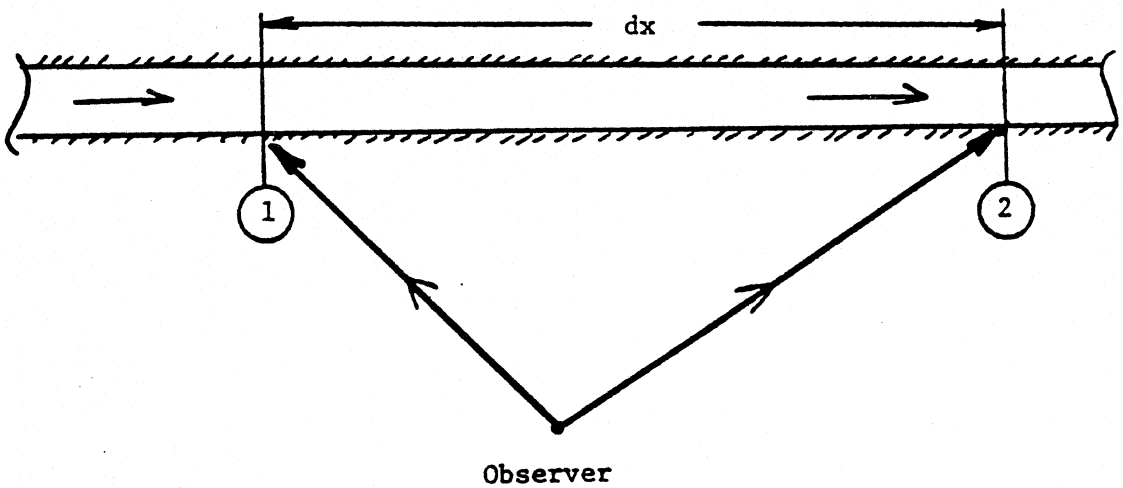

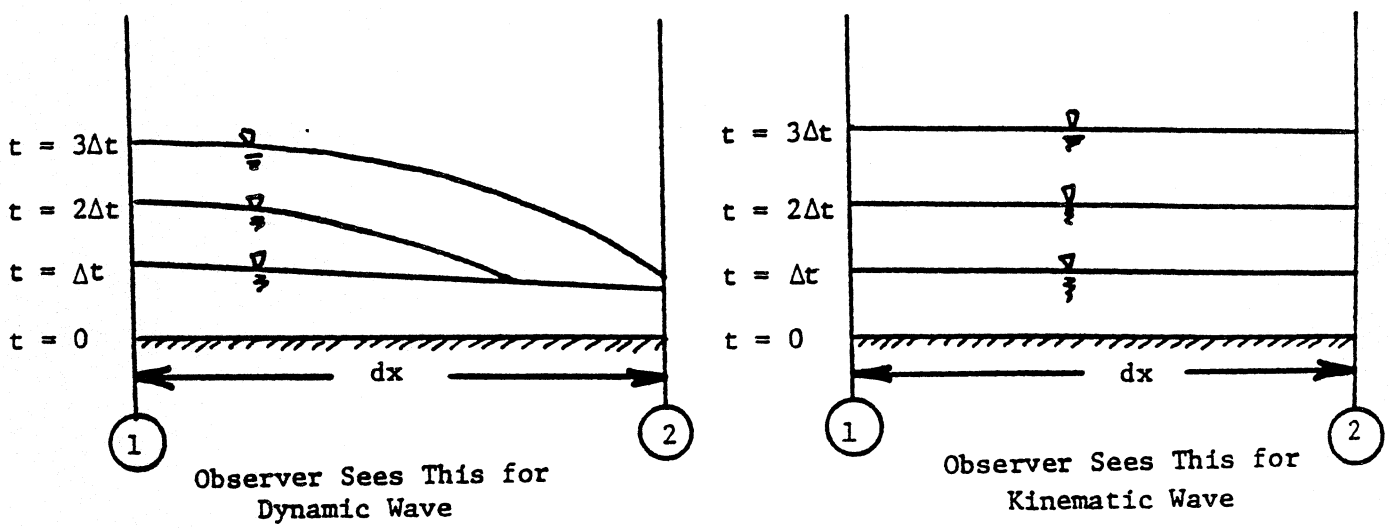

Figure 11.5 Kinematic vs. Dynamic Waves

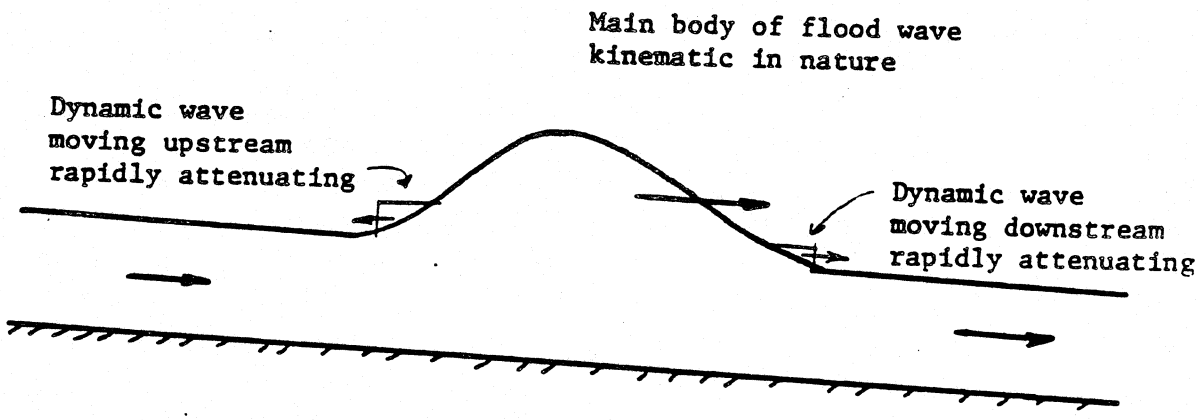

Figure 11.6 Movement of a Natural Flood Wave

Kinematic and Dynamic Wave

Continuity Equation

$$\frac{\partial Q}{\partial x} + \frac{\partial A}{\partial t} = q$$

Q - flow rate in channel (cfs)

A - cross-sectional area in channel (ft^2)

q - lateral inflow to the channel (cfs/ft)

x, t - distance along channel, time

Momentum Equation

$$\underbrace{S_f = S_o}_{\text{Kinematic}} + \overbrace{\frac{\partial y}{\partial x} + \frac{v}{g}\frac{\partial v}{\partial x} + \frac{1}{g}\frac{\partial v}{\partial t}}^{\text{Dynamic}}$$

S_f - friction slope (slope of energy grade line)

S_o - bed slope

y - flow depth

v - flow velocity

g - acceleration due to gravity

Advantages

Takes mechanics of flow directly into account

Can be applied to rainfall runoff and channel routing

Limitations

Requires numerical solution of (1) and (2)

Channel roughness sometimes arbitrary

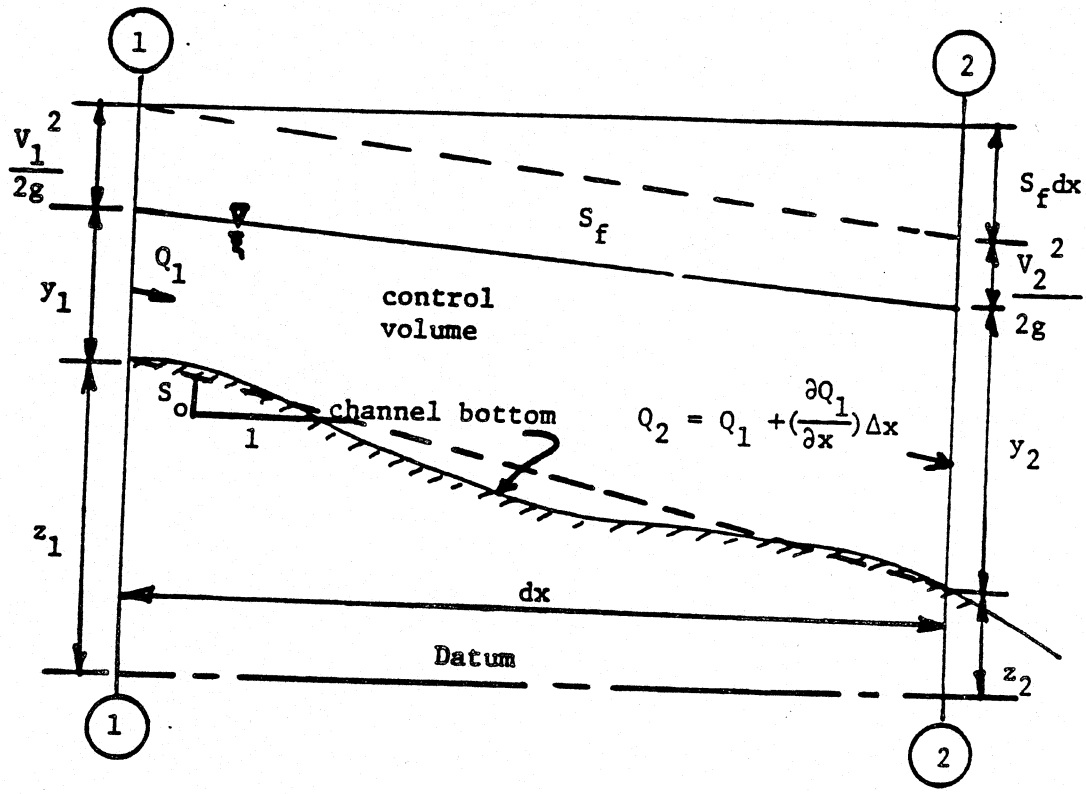

(a) PROFILE

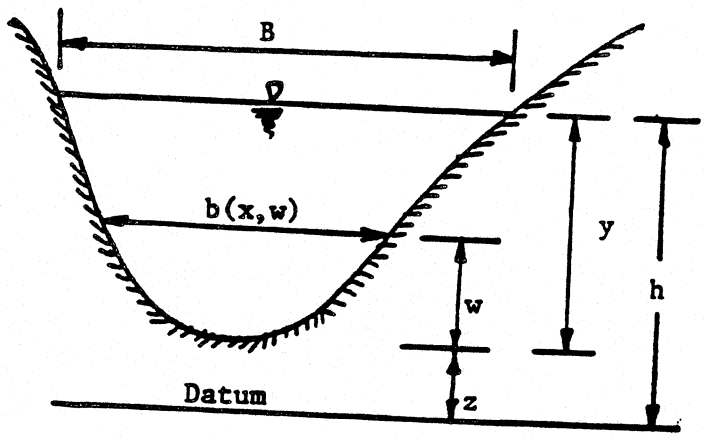

(b) CROSS-SECTION

Figure 11.1 Profile and Cross-Section of an Elemental Reach of Channel

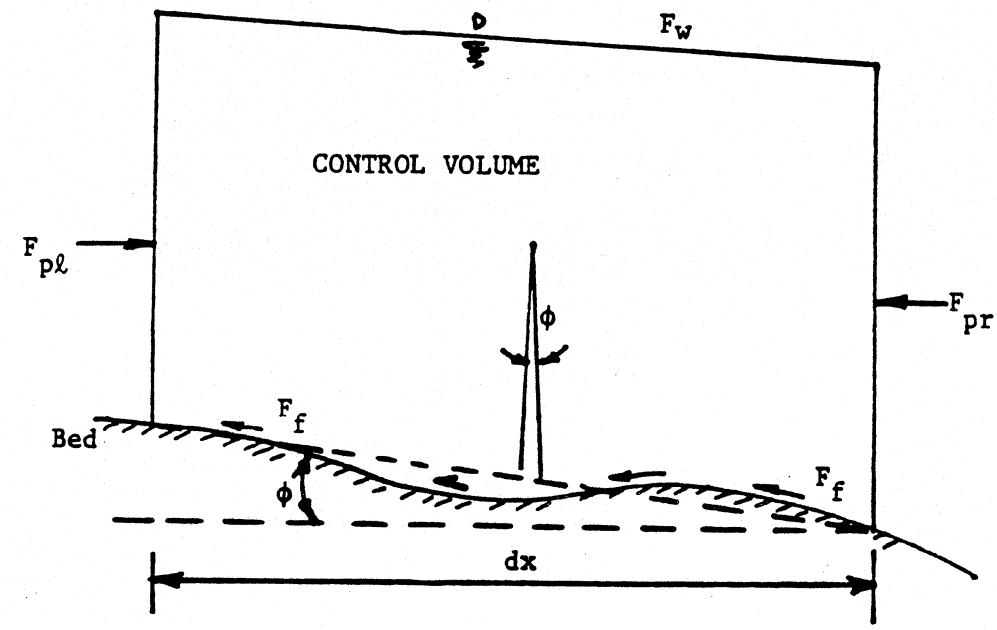

PROFILE

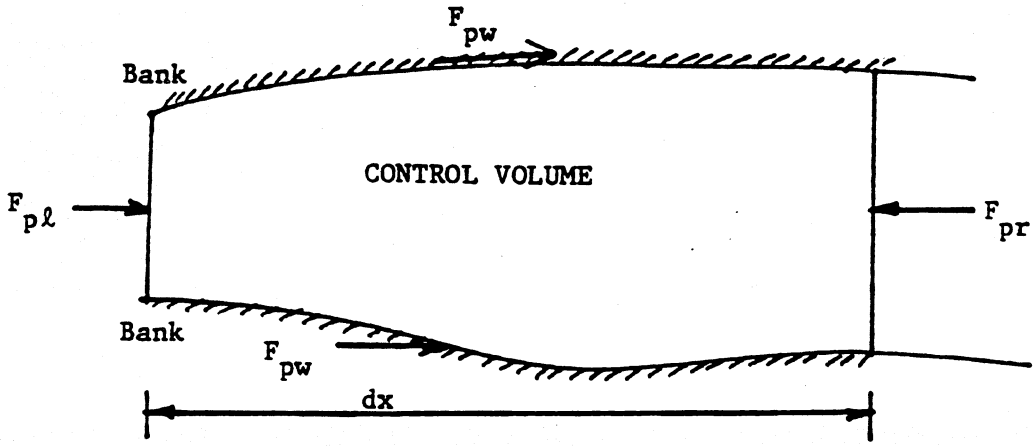

PLANVIEW

Figure 11.2 Forces Acting on Surface of Control Volume

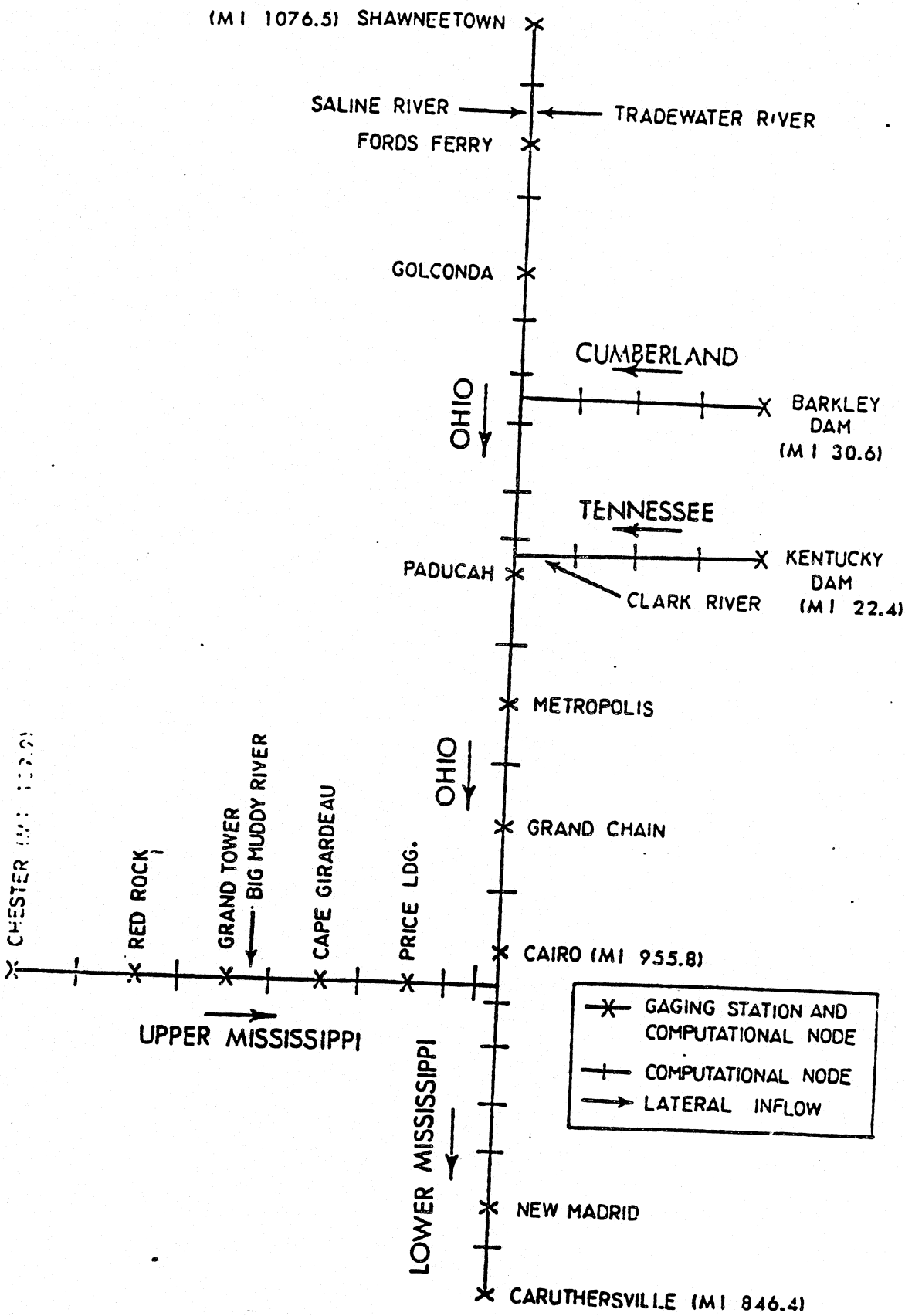

Figure 12.4 Schematic of Mississippi-Ohio-Cumberland-Tenessee (MOCT) River System (Fread, 1978)

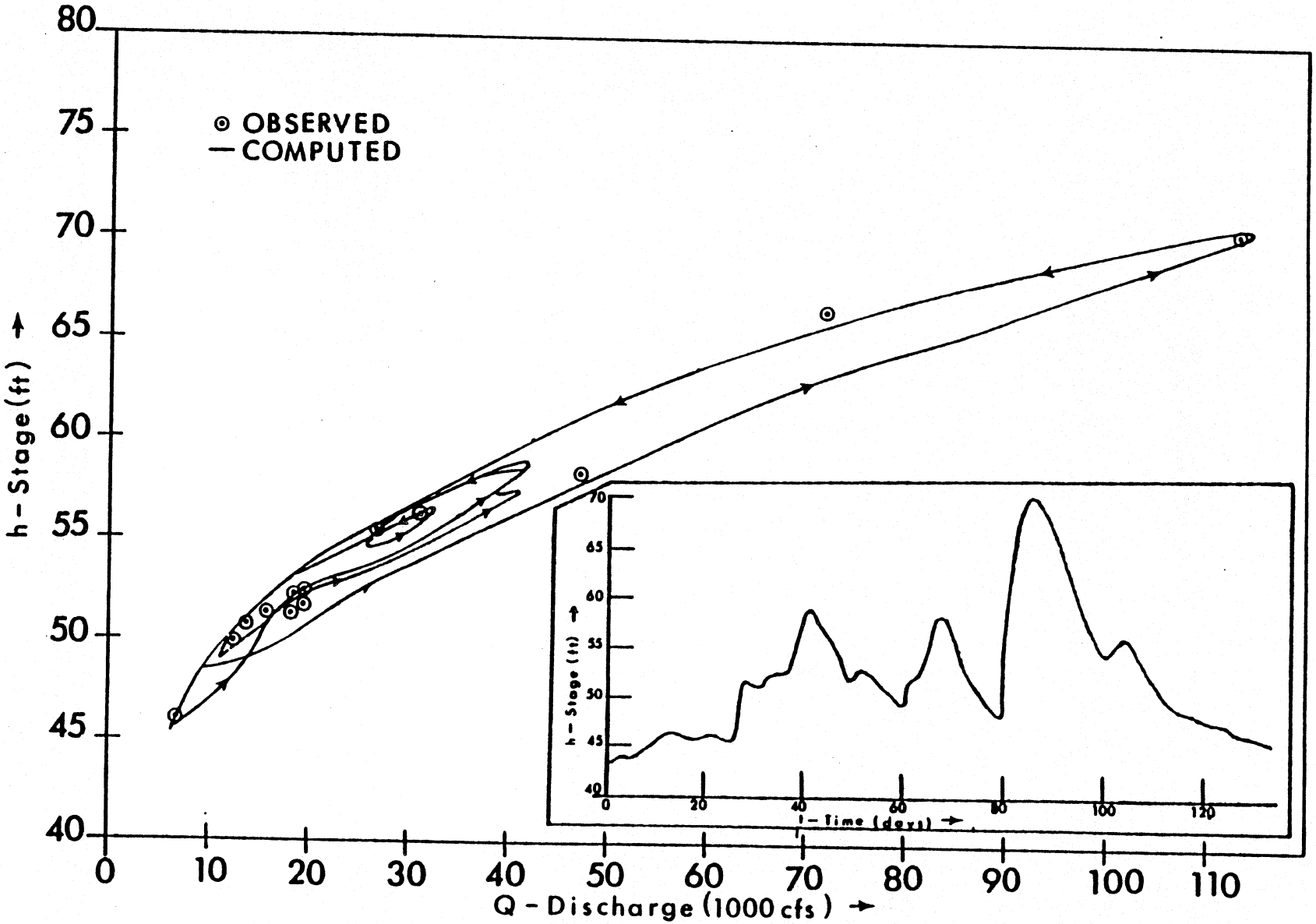

Figure 11.8 Stage-Discharge Relation for Red River, Alexandria, La. (2/5/64 - 6/17/64) (Fread, 1973d).

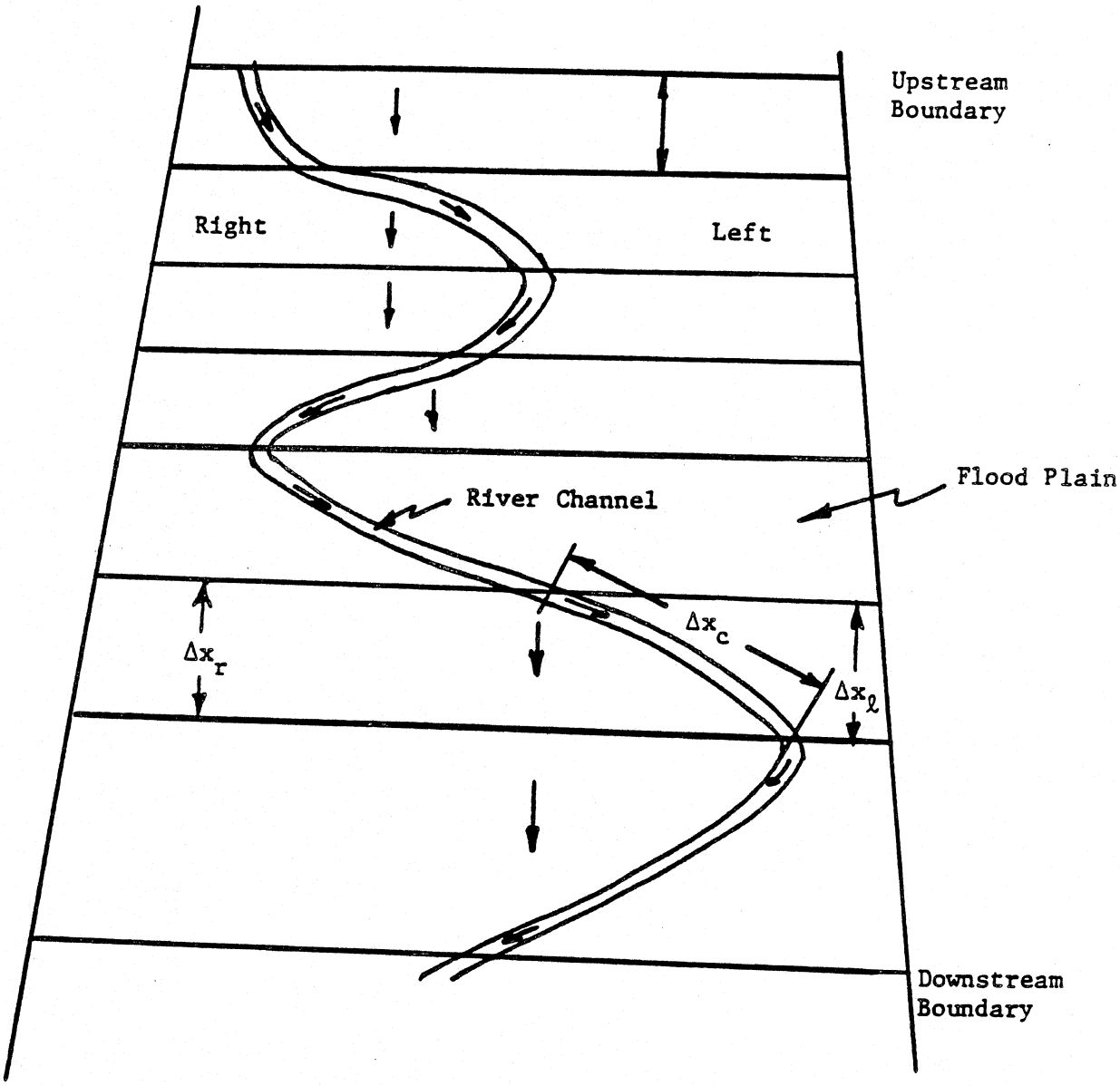

Figure 12.5 Meandering River in a Flood Plain

RAINFALL - RUNOFF ANALYSIS

NATIONAL 42-381 50 SHEETS 5 SQUARE 42-382 100 SHEETS 5 SQUARE 42-389 200 SHEETS 5 SQUARE

DESIGN FLOW

TWO BASIC PROBLEMS OF DESIGN

- WATER CONVEYANCE (PEAK FLOW)
- WATER STORAGE (FLOW HYDROGRAPH)

	NO FLOW DATA	WITH FLOW DATA
PEAK FLOW	① - RATIONAL METHOD - OTHER EMPIRICAL METHODS	② - FLOOD FREQUENCY ANALYSIS (LOG PEARSON TYPE III)
FLOW HYDROGRAPH	④ - SYNTHETIC UNIT HYDROGRAPH - KINEMATIC WAVE	③ - UNIT HYDROGRAPH

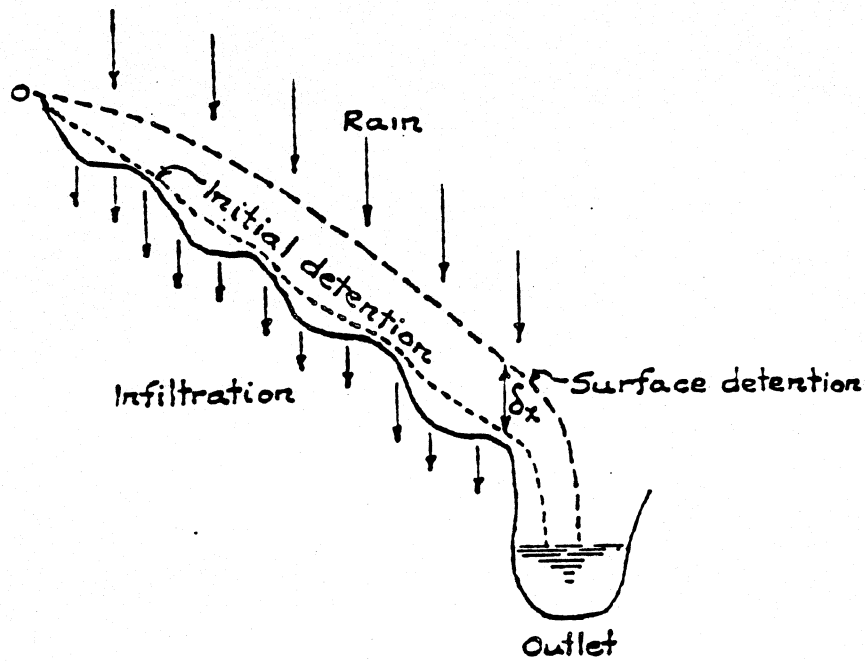

Figure 6.3.1 Overland flow on a slope produced by the excess of rainfall over infiltration (after Horton,1945)

Source: Horton, R.E., Erosional development of streams and their drainage basins; hydrophysical approach to quantitative morphology, Bull. Geol.Soc.Am.,Vol.56,p.314,Fig.13, 1945

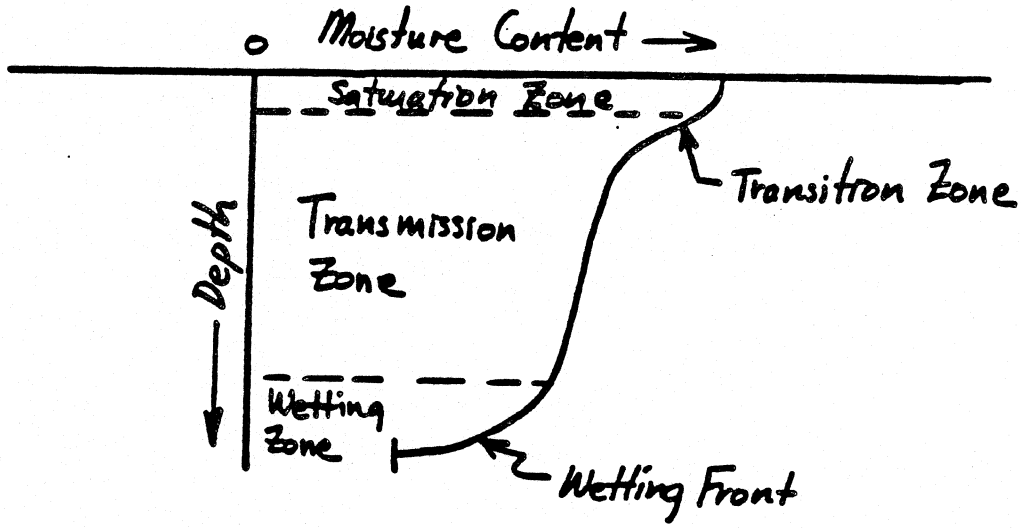

Figure 5.1.1 Soil Moisture Distribution

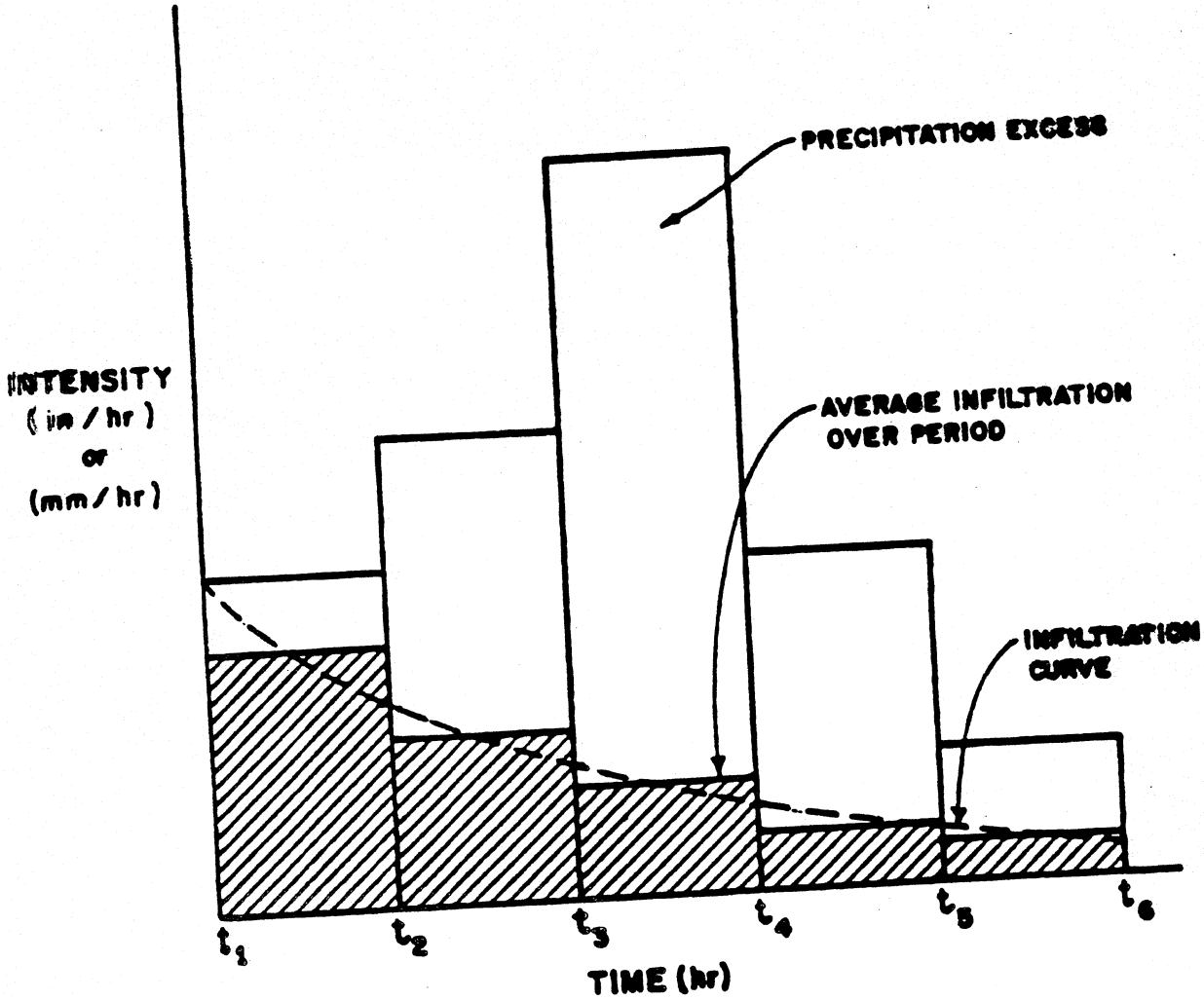

methods { horton
green-ampt
P index

Figure 3.2: Loss Rate; Rainfall Excess Hyetograph

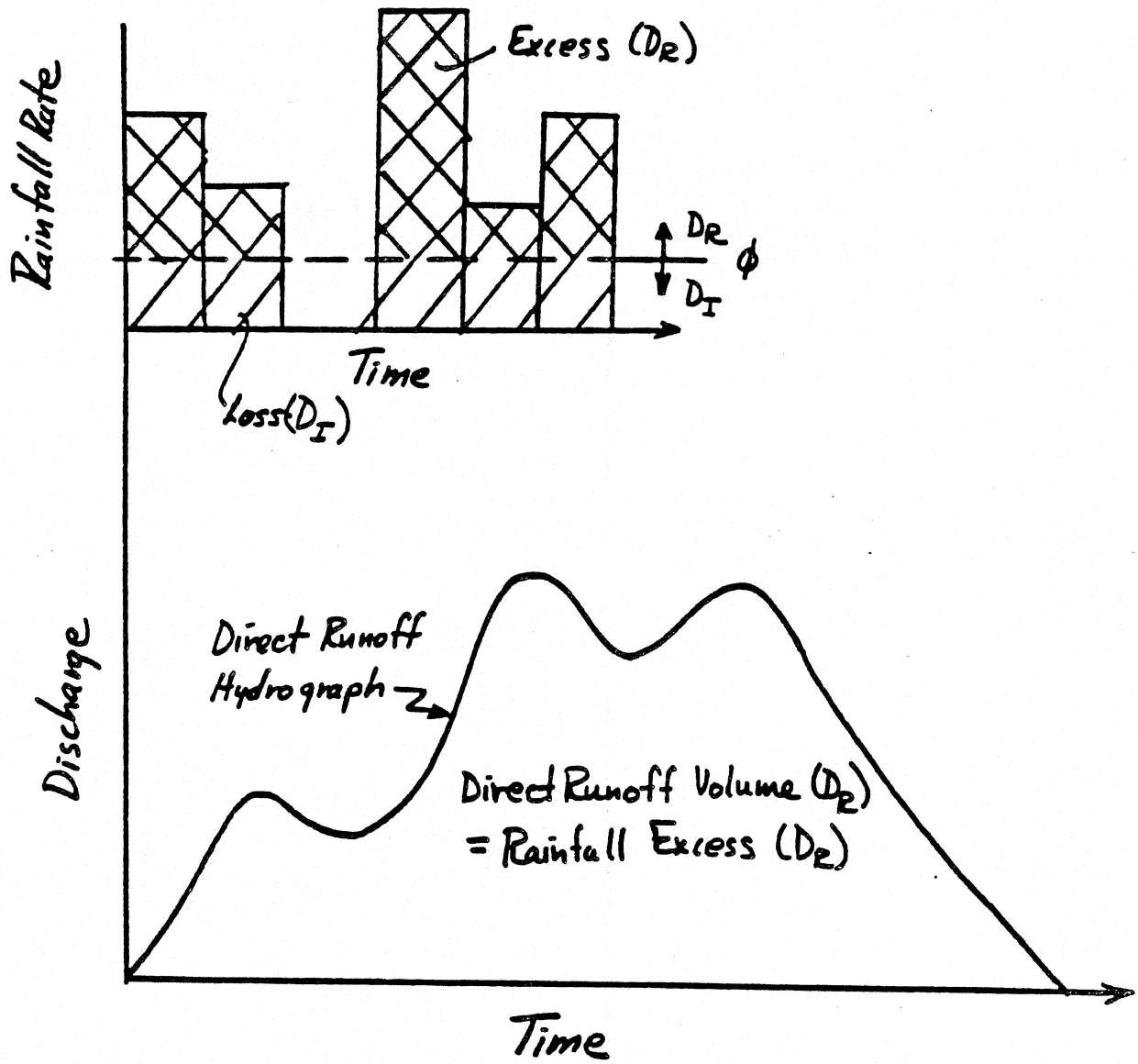

Figure 5.2.1 Loss Rate by the Φ index method.

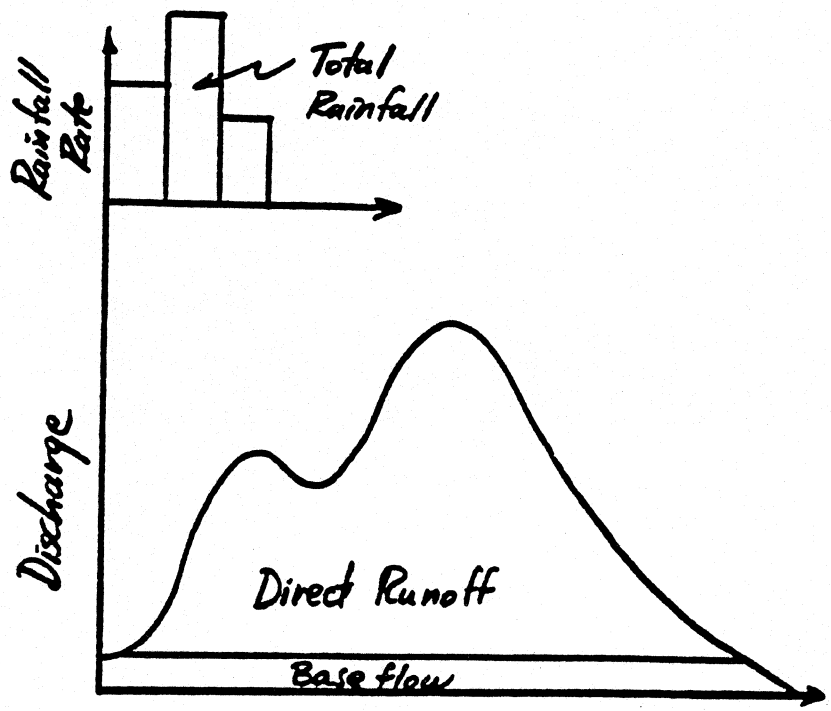

(a) Given Data for Watershed to Compute Infiltration Loss

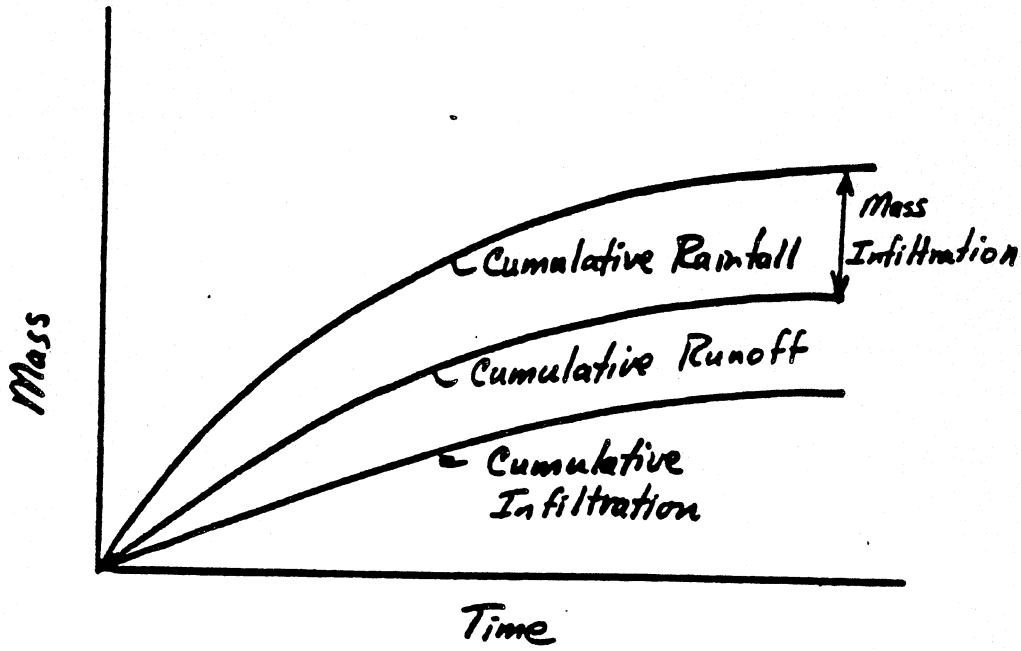

(b) Relationship of Cumulative Rainfall, Runoff and Infiltration

Figure 5.3.3 Computing Infiltration for a Watershed

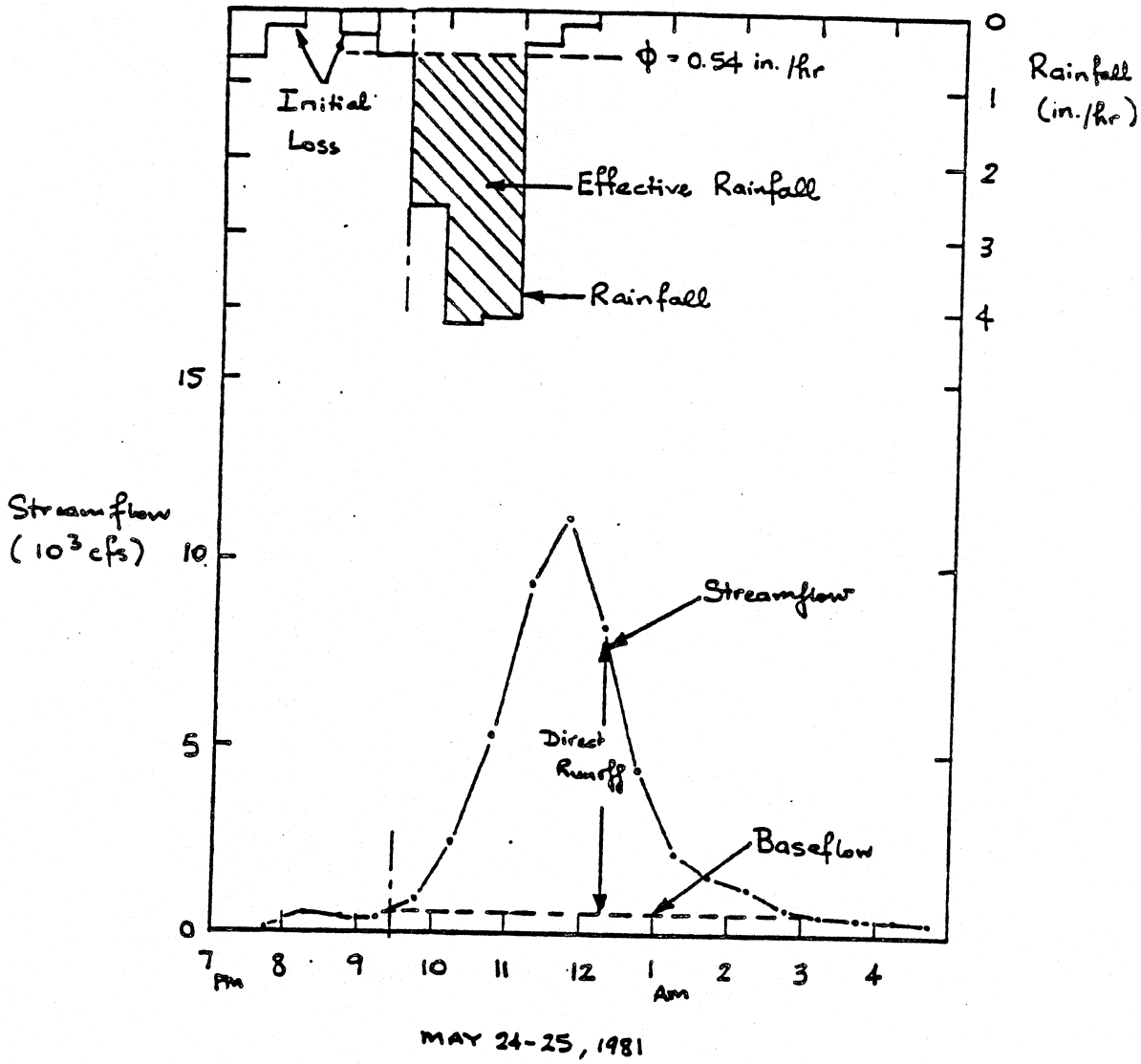

Fig. 6.5.2. Rainfall and streamflow for the storm of May 24-25, 1981 on Shoal Creek at Northwest Park, Austin, Texas.
Note: 1 cfs = 0.0283 m^3/s;
1 in/hr = 2.54 cm/hr.

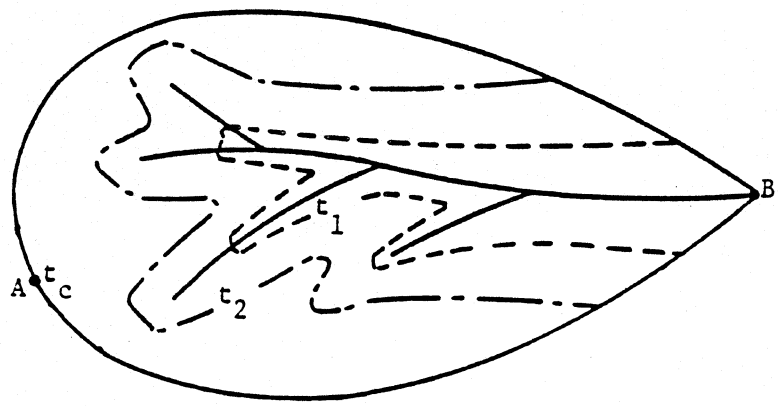

Fig. 6.8.1 Isochrones at t_1 and t_2 define the area contributing to flow at the outlet for rainfall of duration t_1 and t_2. Time of concentration, t_c, is the time of flow from the farthest point in the watershed (A) to the outlet (B).

Unit Hydrograph.

$$Q_n = \sum_{m=1}^{n} I_m U_{n-m+1}$$

Q_n direct runoff in time period n (cfs)

I_m effective rainfall in time period m (in)

U_{n-m+1} unit hydrograph in time period $n-m+1$ (cfs/in.)

Advantages

- Flow varies with time so complete hydrograph is produced
- Time varying abstractions and base flow can be accounted for.
- can synthesize unit hydrograph if flow data unavailable

Limitations

- no direct accounting for spatial variation or flow mechanics within the watershed.

Unit Hydrograph

Hydrograph of surface runoff which would be generated from a unit depth of rainfall excess uniformly distributed over the watershed and occurring within a specified duration of time.

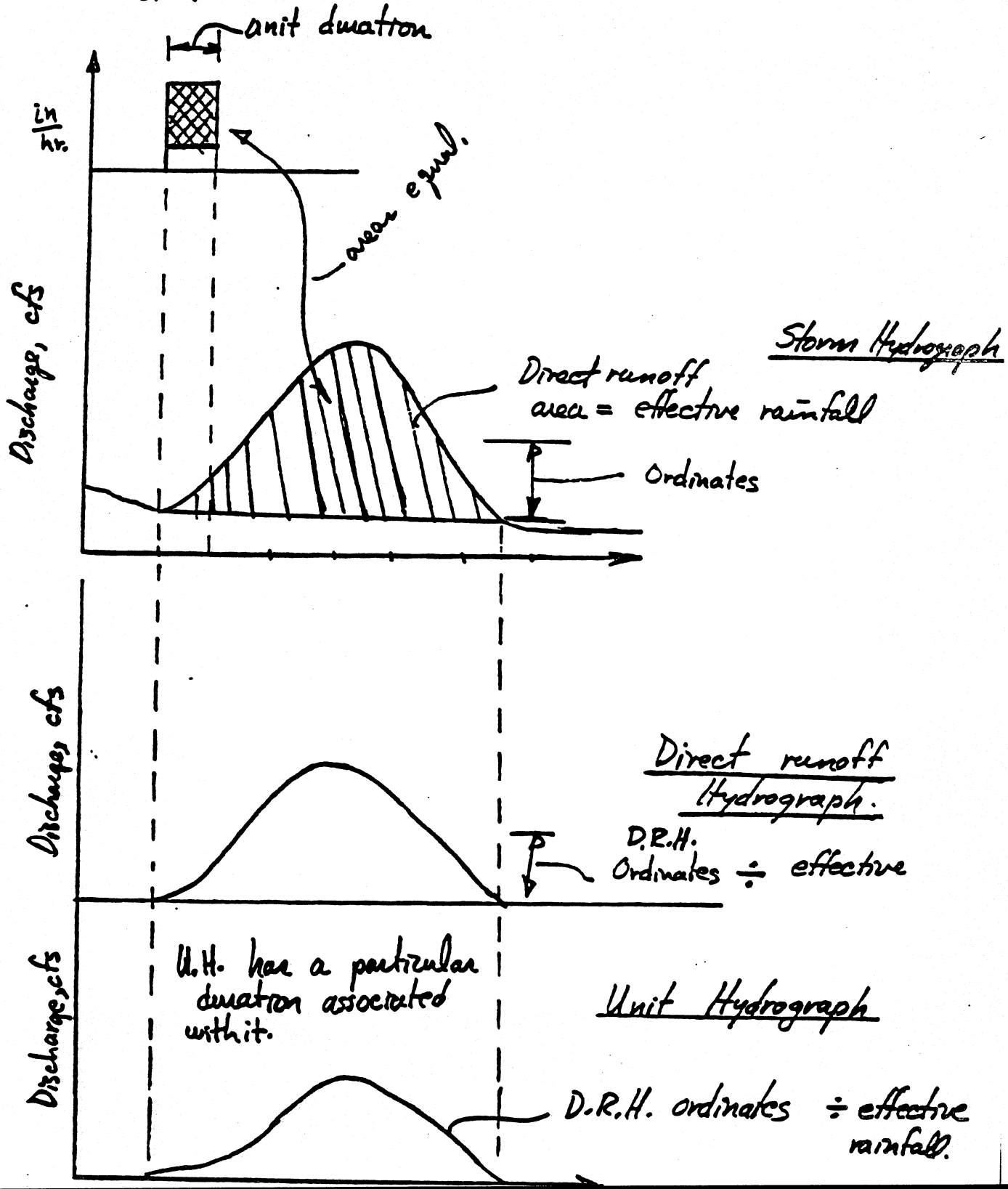

Unit Hydrographs for Multiple Period Storms.

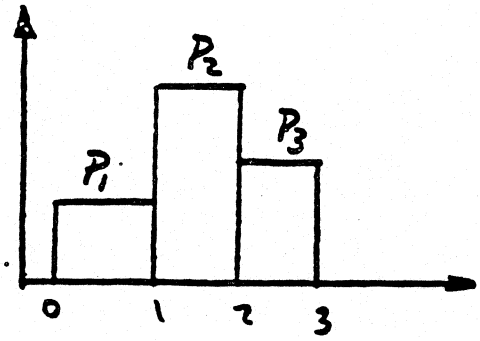

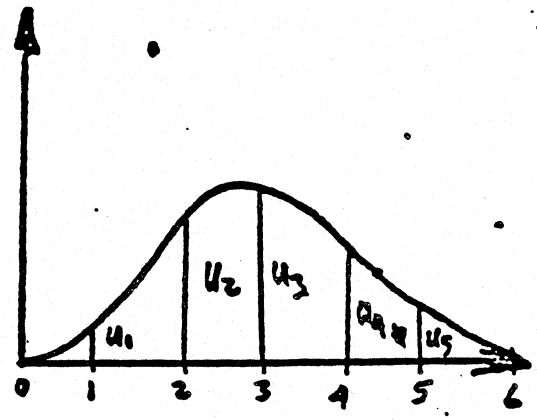

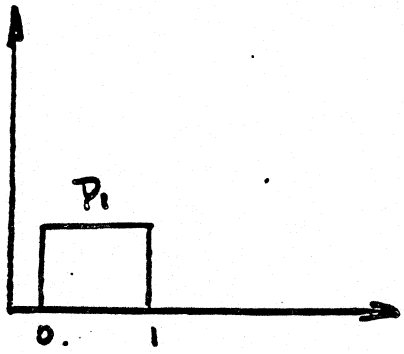

⇒

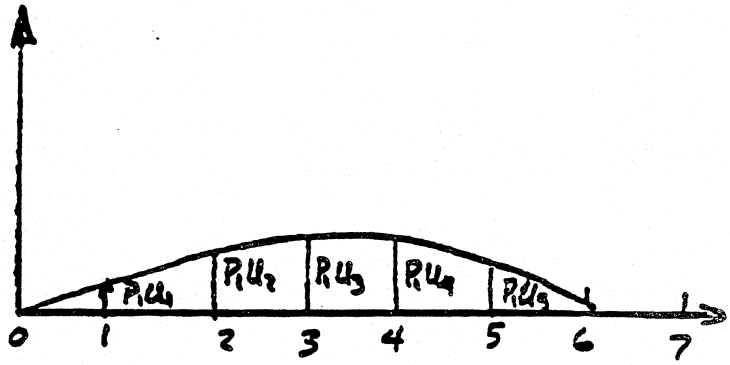

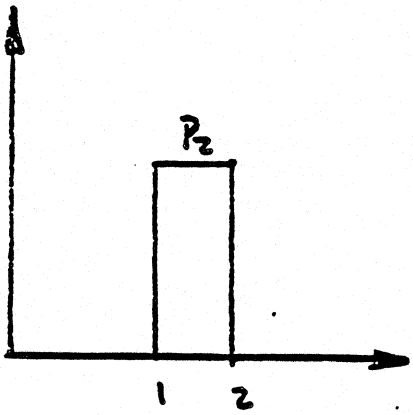

⇒

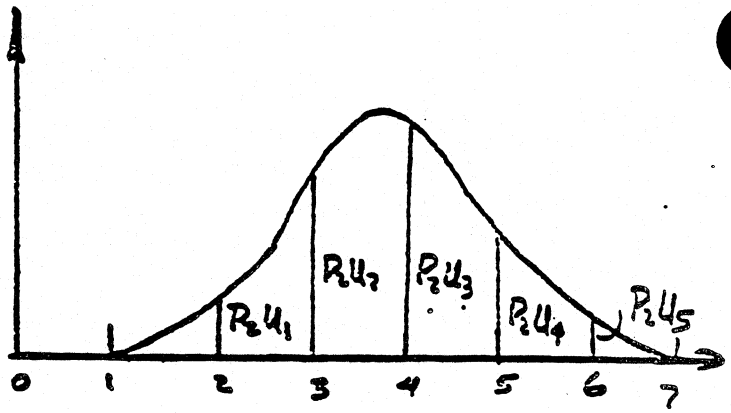

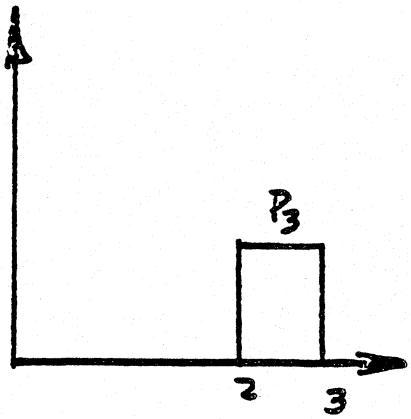

⇒

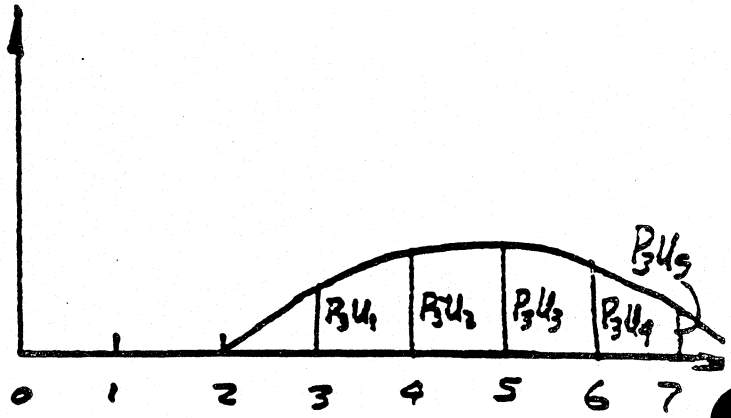

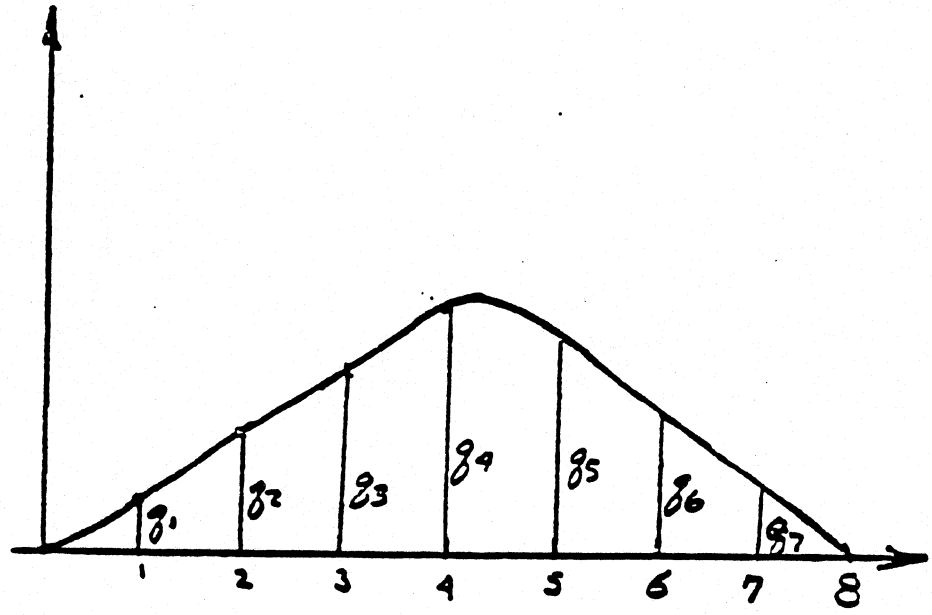

$$\left.\begin{aligned}
q_1 &= P_1 U_1 \\
q_2 &= P_2 U_1 + P_1 U_2 \\
q_3 &= P_3 U_1 + P_2 U_2 + P_1 U_3 \\
q_4 &= P_3 U_2 + P_2 U_3 + P_1 U_4 \\
q_5 &= P_3 U_3 + P_2 U_4 + P_1 U_5 \\
q_6 &= P_3 U_4 + P_2 U_5 \\
q_7 &= P_3 U_5
\end{aligned}\right\}$$

In matrix form.

$$P\,U = Q$$

Gaussian equations
matrix
overdetermined system of
equations

n = # storm hydrograph ordinates
j = # unit hydrograph ordinates
i = # of periods of rainfall excess

$$n = j + i - 1$$

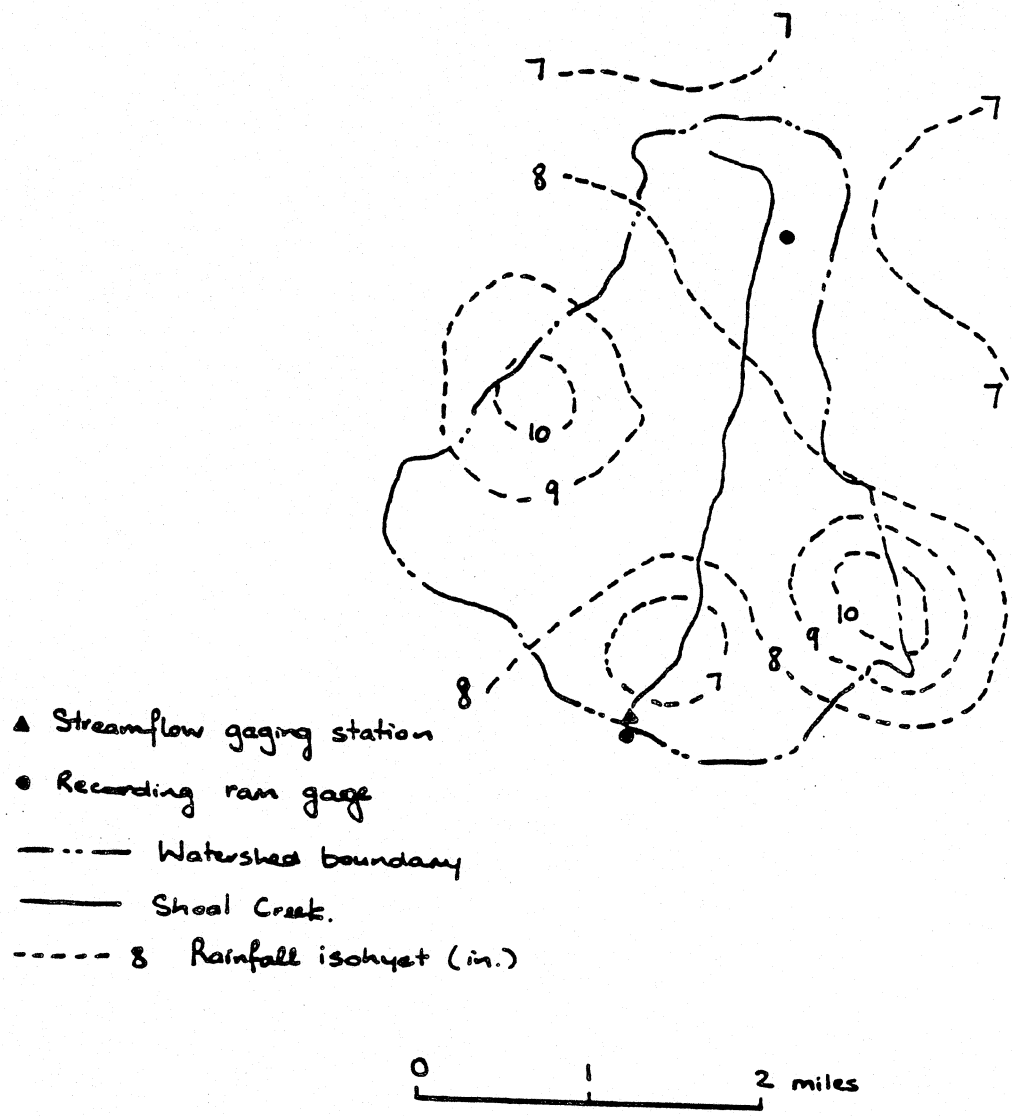

Fig. 8-5. Isohyetal map on the watershed of Shoal Creek for storm of 24-25 May 1981.

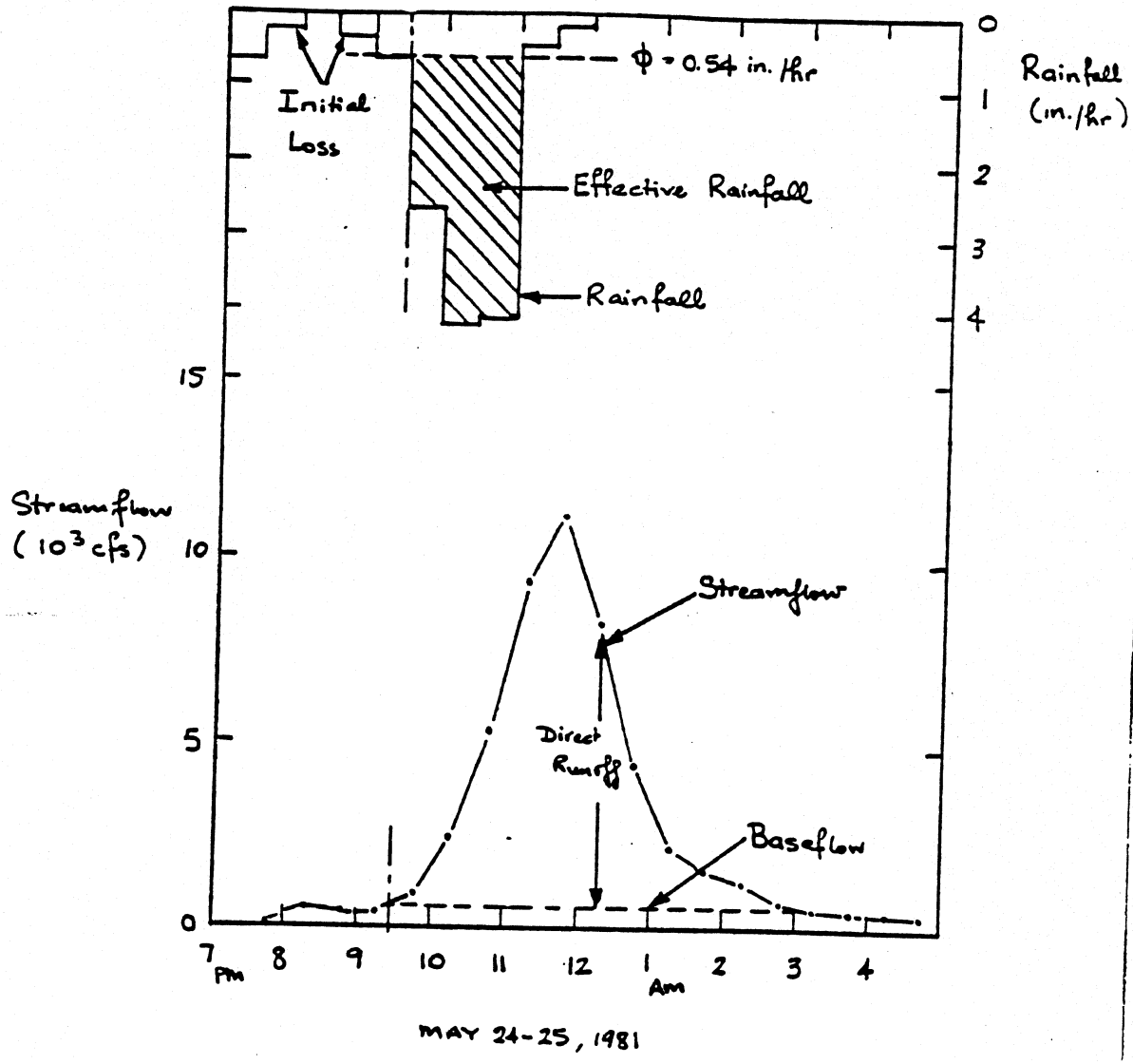

FIG. 8-6. Rainfall and streamflow for the storm of May 24-25, 1981 on Shoal Creek at Northwest Park, Austin, Texas

Note (1 cfs = 0.0283 m^3/s ; 1 in./hr = 2.54 cm/hr)

	Observed Data			Model Data			
	Time	Rainfall (in./½ hr)	Streamflow (cfs)	Time (½ hr)	ERH (in./½ hr)	DRH (cfs)	1½ hr Unit Hydrograph (cfs)
Col.	1	2	3	4	5	6	7
24 May	7:15 PM	0.33					
	7:45	0.11	0				
	8:15	0.00	103				
	8:45	0.15	467				
	9:15	0.26	346				
	9:45	1.33	283				
	10:15	2.20	828				
	10:45	2.08	2322	1	1.06	428	89
	11:15	0.20	5693	2	1.93	1922	400
	11:45	0.09	9523	3	1.81	5293	1103
25 May	12:15 AM		11013	4		9123	1901
	12:45		8223	5		10613	2211
	1:15		4316	6		7823	1630
	1:45		2242	7		3916	816
	2:15		1800	8		1842	384
	2:45		1250	9		1400	292
	3:15		740	10		850	177
	3:45		394	11		340	71
	4:15		354				
			303	Total	4.80	43,500	9074

Table 8-1. Rainfall and Streamflow Data for the Storm of May 24-25, 1981 in Shoal Creek at Northwest Park, Austin, Texas

Effective Rainfall (ERH) = Observed Rainfall - Losses (0.27 in./½ hr)
Direct Runoff (DRH) = Observed Streamflow - Baseflow (400 cfs)
1½ hr Unit Hydrograph = DRH ÷ 4.80.

																			Eqn.
428	=	$1.06u_1$																	(a)
1922	=	$1.93u_1$	+	$1.06u_2$															(b)
5293	=	$1.81u_1$	+	$1.93u_2$	+	$1.06u_3$													(c)
9123	=			$1.81u_2$	+	$1.93u_3$	+	$1.06u_4$											(d)
10613	=					$1.81u_3$	+	$1.93u_4$	+	$1.06u_5$									(e)
7823	=							$1.81u_4$	+	$1.93u_5$	+	$1.06u_6$							(f)
3916	=									$1.81u_5$	+	$1.93u_6$	+	$1.06u_7$					(g)
1842	=											$1.81u_6$	+	$1.93u_7$	+	$1.06u_8$			(h)
1400	=													$1.81u_7$	+	$1.93u_8$	+	$1.06u_9$	(i)
850	=															$1.81u_8$	+	$1.93u_9$	(j)
340	=																	$1.81u_9$	(k)

Table 8-2. Set of simultaneous equations for solution of ½-hour unit hydrograph for storm of 24-25 May, 1981, on Shoal Creek at Northwest Park, Austin, Texas

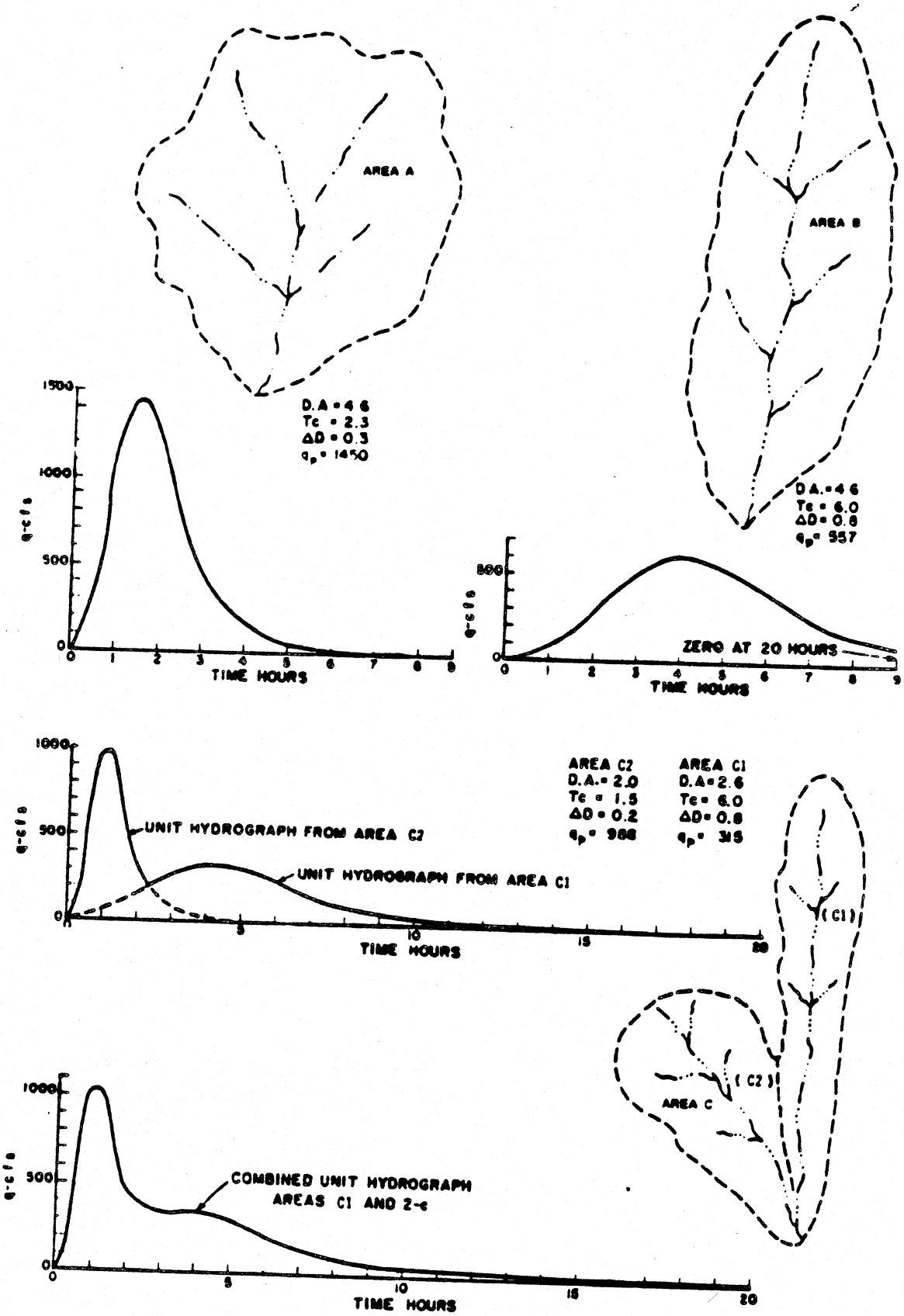

Figure 16.3 The effect of watershed shape on the peaks of unit hydrographs

intervals, the resulting hydrograph would simply be the sum of the two unit hydrographs, but with the second unit hydrograph beginning 1 time unit later.

While it is known that some assumptions of linearity involved in the unit hydrograph technique do not accurately apply, extensive experience indicates that the limitations of the technique are not a major handicap, considering the quality of rainfall and snowmelt data that are usually available, provided that the procedures involved are applied with appropriate knowledge and judgment.

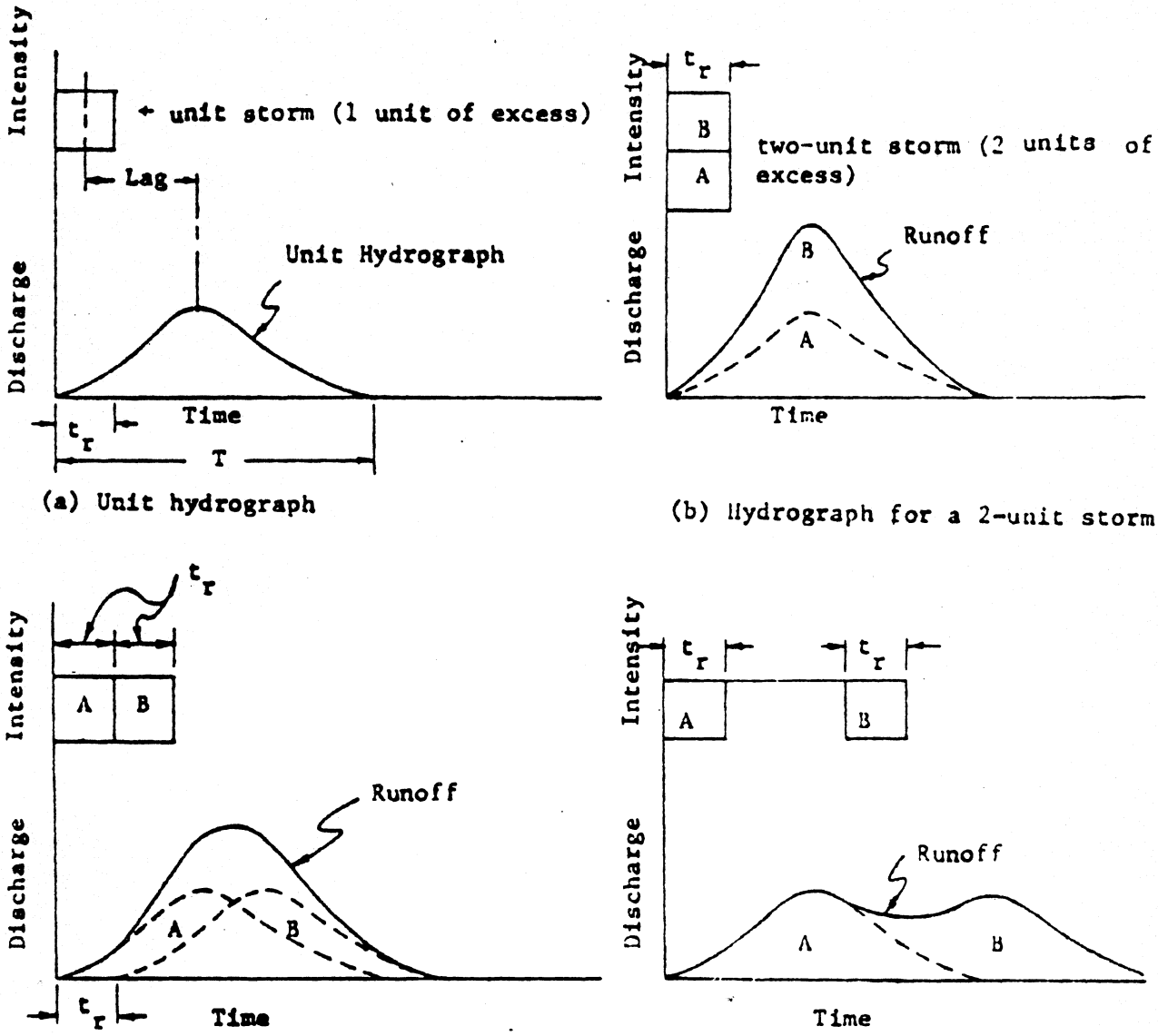

Fig. 5.02. Unit hydrograph relationships

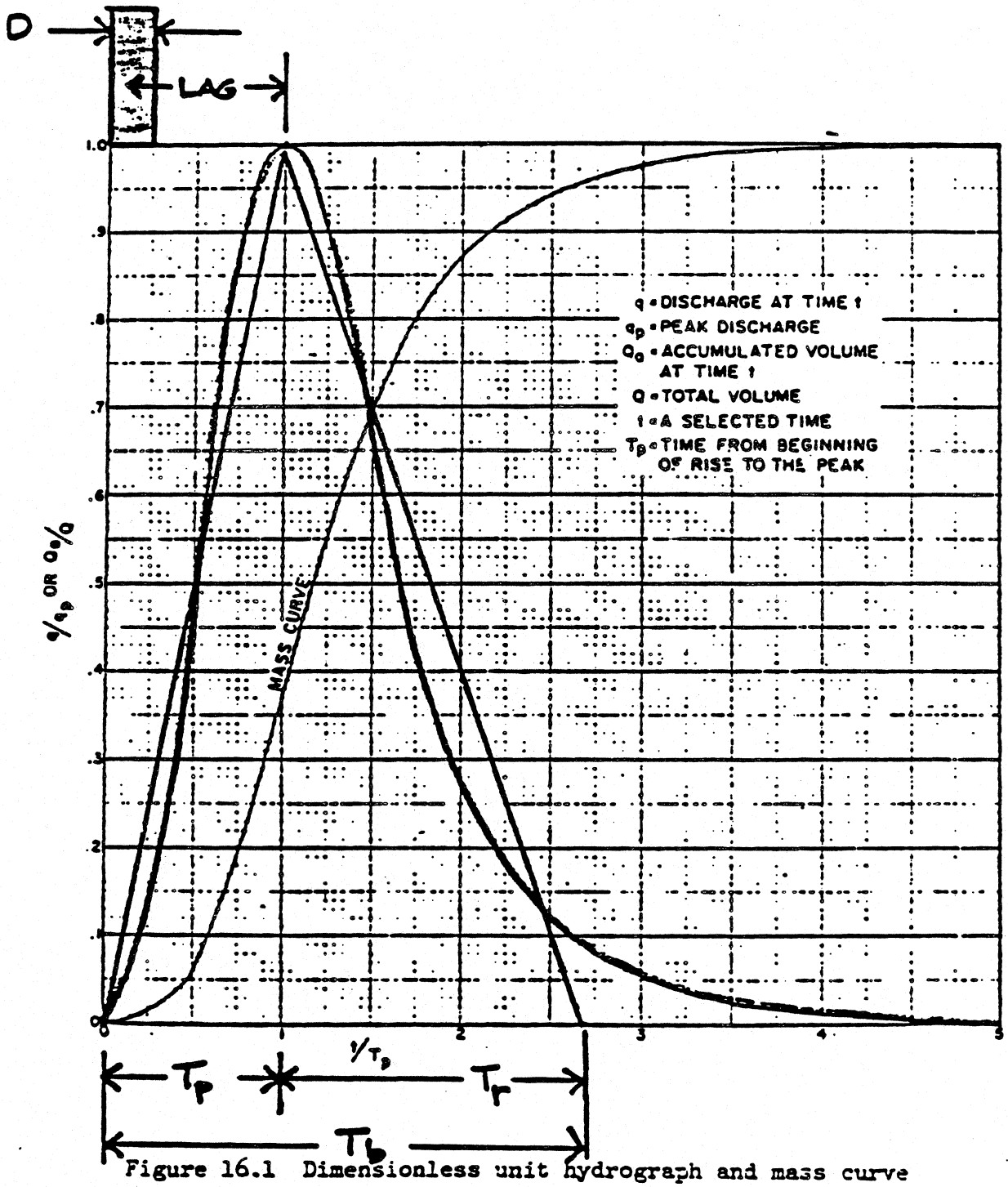

Figure 16.1 Dimensionless unit hydrograph and mass curve

SCS Synthetic Unit Hydrograph

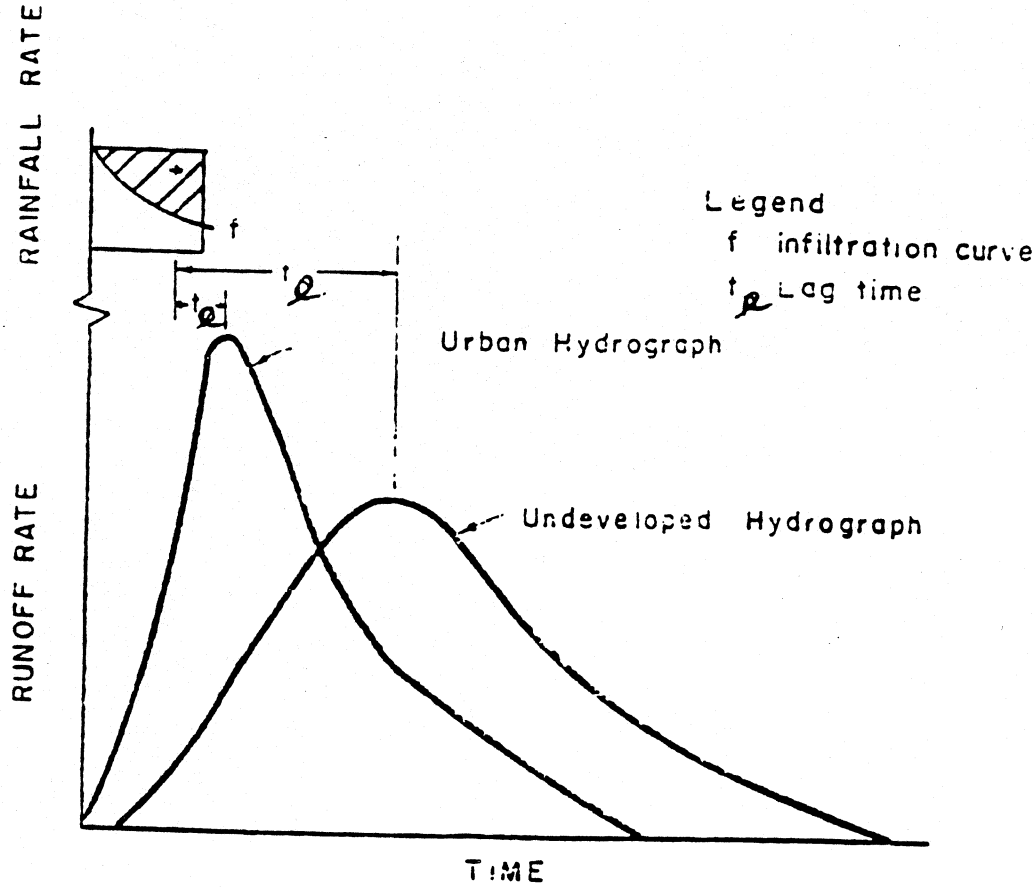

Figure 6.9.1. Effects of Urbanization on Flood Hydrograph

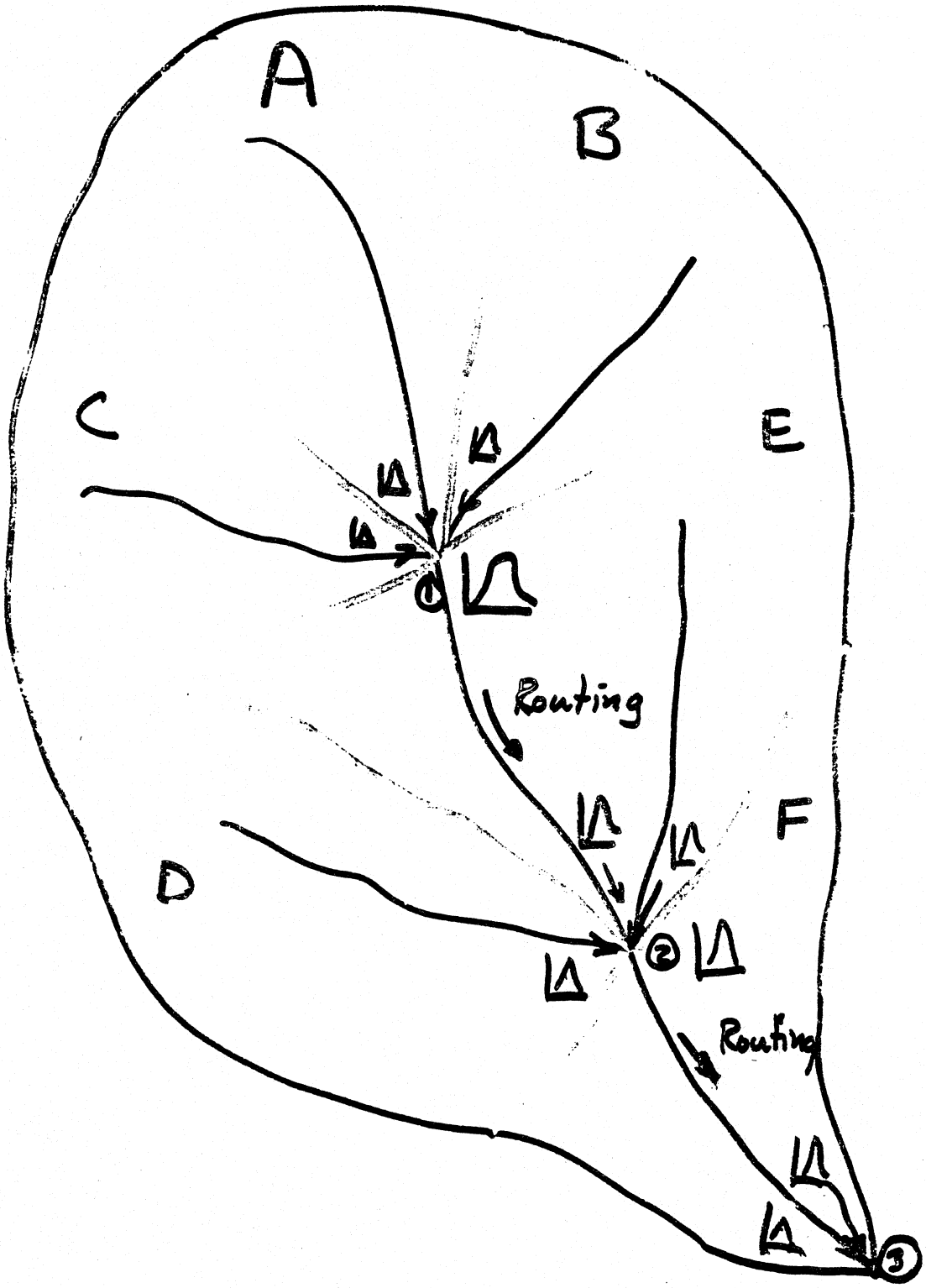

Watershed Outlet.

DESIGN STORMS

PROBABLE MAXIMUM FLOOD ESTIMATION

42-381 50 SHEETS 5 SQUARE
42-382 100 SHEETS 5 SQUARE
42-389 200 SHEETS 5 SQUARE
NATIONAL

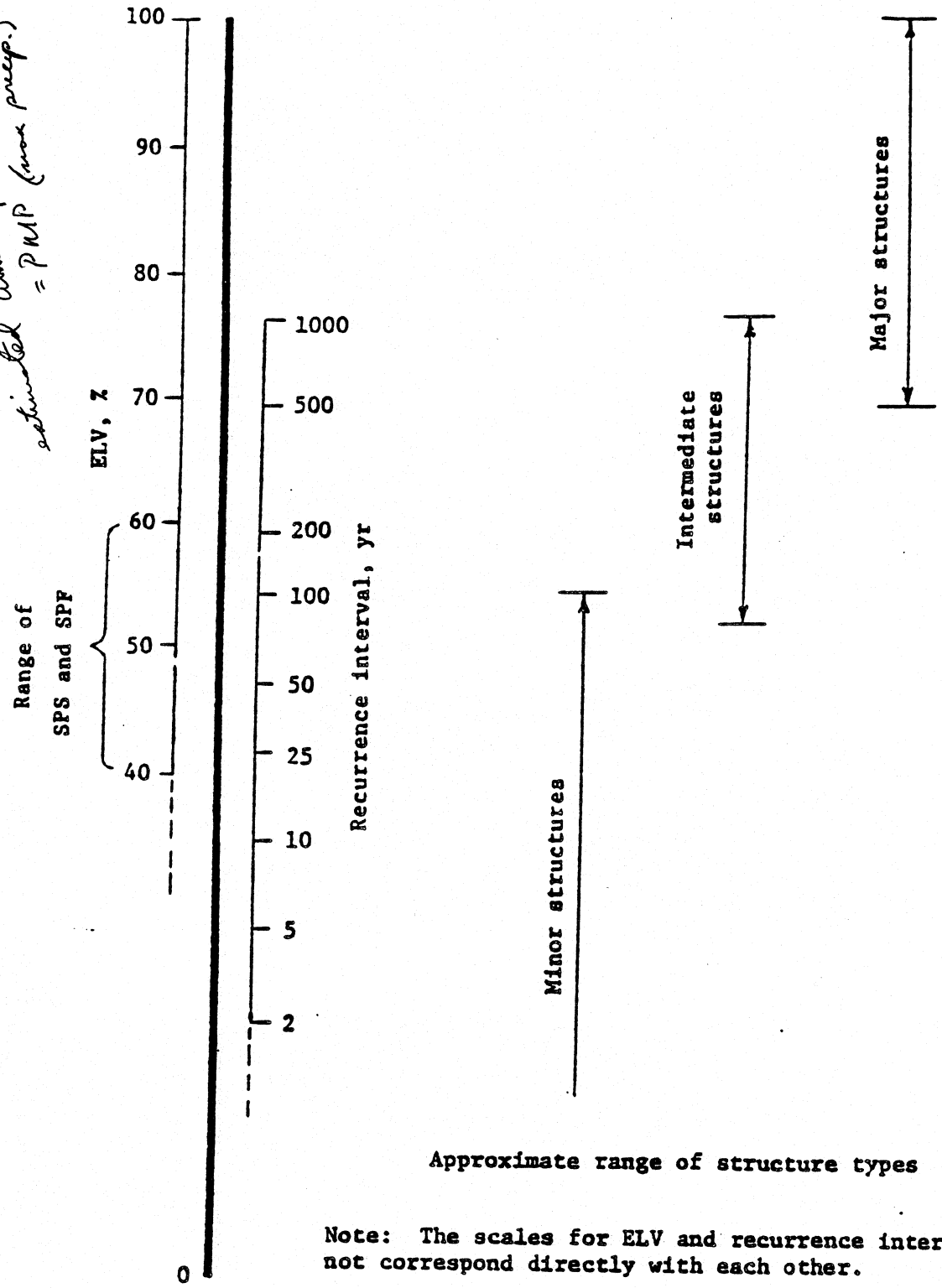

Approximate range of structure types

Note: The scales for ELV and recurrence interval do not correspond directly with each other.

Fig. 15-1. Scale of hydrologic design.

FLOOD FREQUENCY ANALYSIS

$$Q_T = \overline{Q} + K_T S$$

Q_T flood flow equalled or exceeded on average once in T yrs

$\overline{Q}$ mean of observed annual maximum flows

S standard deviation of observed annual max flows

K_T frequency factor

Advantages

Based on observed flows - no rainfall runoff calculation needed

Limitations

Strictly applicable only at site where flows are measured. Need at least ~~5-10~~ yrs data

Reference

U.S. Water Resources Council, "Guidelines for determining flood flow frequency", Bulletin 17B, US Govt Printing Office, Washington DC 1981

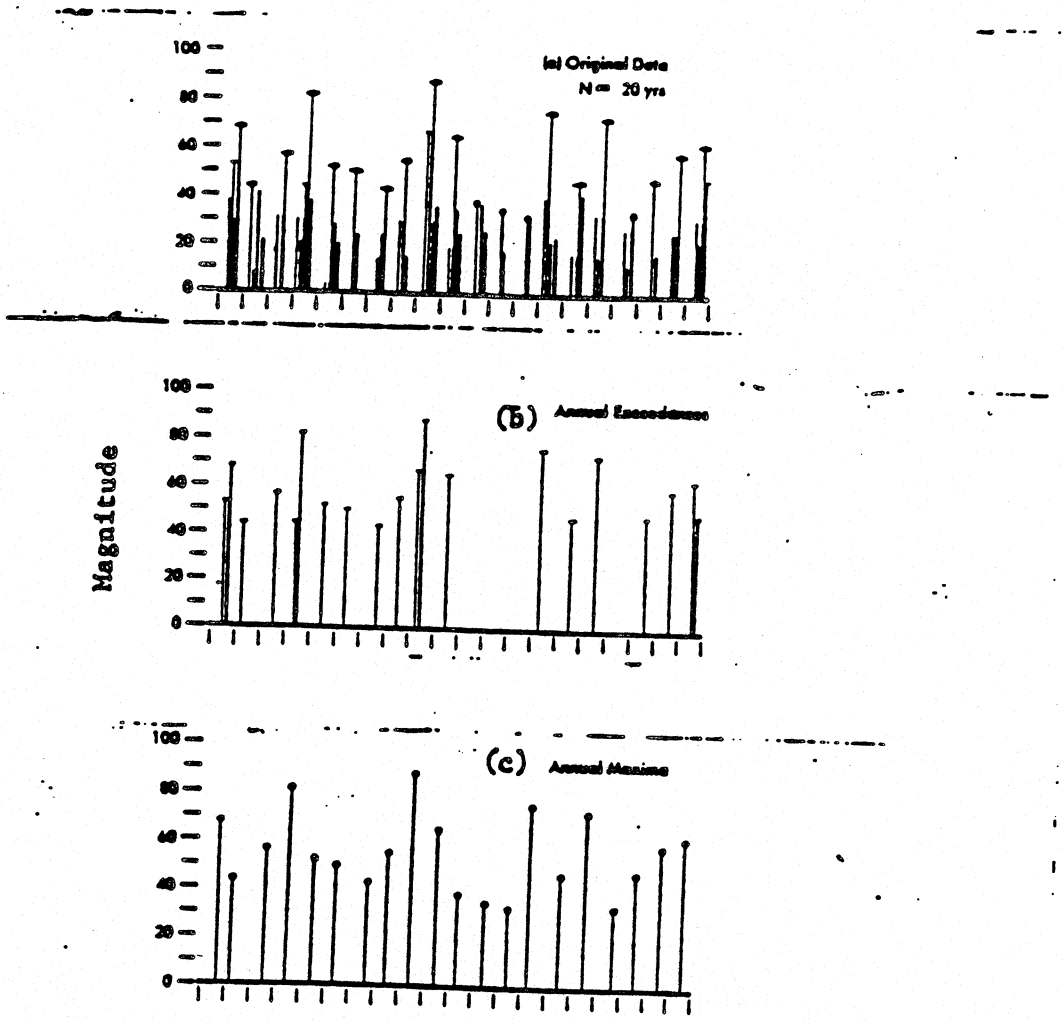

Figure 13.4.1. Hydrologic data arranged in the order of occurrence.

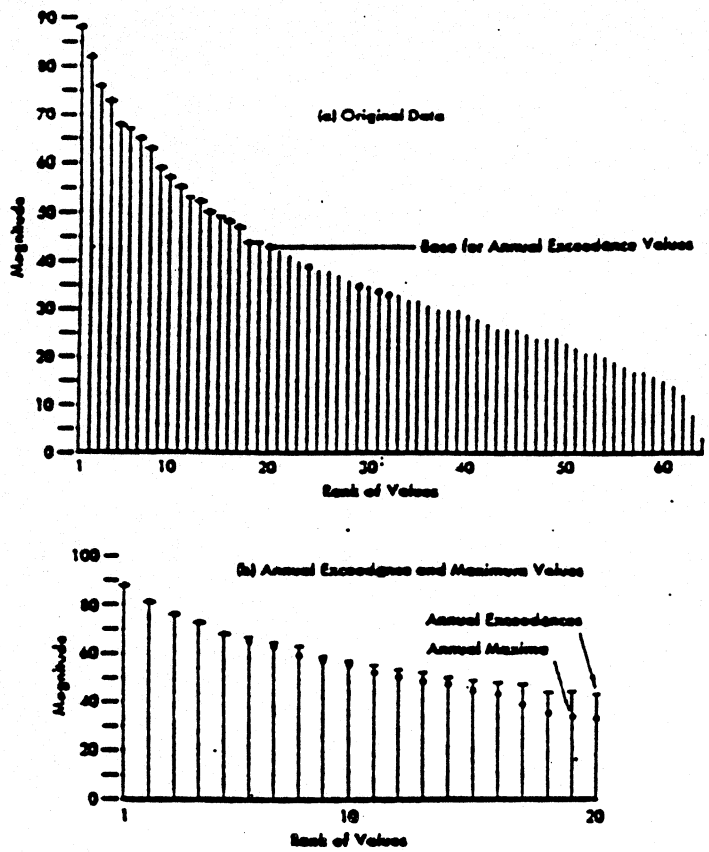

Figure 13.4.2. Hydrologic data arranged in the order of magnitude.

Table 13.6.1 Moment Formulas

Moment	Definition	Estimate
First	mean $= \mu = \int_{-\infty}^{\infty} x\, p(x)\,dx$	$\bar{x} = \frac{1}{n} \Sigma x_i$
Second	variance $= \sigma^2 = \int_{-\infty}^{\infty} (x-\mu)^2\, p(x)\,dx$	$s^2 = \frac{1}{n-1} \Sigma (x_i - \bar{x})^2$
	standard deviation $= \sigma$	$= s$
	coefficient of variation $= \frac{\sigma}{\mu}$	$= \frac{s}{\bar{x}}$
Third	skewness $= \alpha = \int_{-\infty}^{\infty} (x-\mu)^3\, p(x)\,dx$	$a = \frac{1}{(n-1)(n-2)} \Sigma (x_i - \bar{X})^3$
	coefficient of skewness $= g = \frac{\alpha}{\sigma^3}$	$= \frac{a}{s^3}$

Table 13.7.2

Distribution	Probability Density Function
Normal	$p(x) = \frac{1}{\sigma\sqrt{2\pi}} e^{-(x-\mu)^2/2\sigma^2}$
Gamma	$p(x) = \frac{1}{\beta^{\gamma}\Gamma(\gamma)} x^{\gamma-1} e^{-x/\beta}$
Pearson III	$p(x) = \frac{1}{\alpha\Gamma(\beta)} \left(\frac{x-\gamma}{\alpha}\right)^{\beta-1} \exp\left[-\frac{x-\gamma}{\alpha}\right]$
Extremal I (Gumbel)	$p(x) = \alpha \exp\{-\alpha(x-\beta) - \exp(x-\beta)\}$
Extremal III (Weibull)	$p(x) = \alpha x^{\alpha-1}\beta^{-\alpha} \exp\left[-\left(\frac{x}{\beta}\right)^{\alpha}\right]$
Beta	$p(x) = x^{\alpha-1}(1-x)^{\beta-1} \frac{\Gamma(\alpha+\beta)}{\Gamma(\alpha)\Gamma(\beta)}$
Log-Normal 2-Parameter	$p(x) = \frac{1}{x\sigma_y\sqrt{2\pi}} \exp\left\{-\frac{(\ln x - \mu_y)^2}{2\sigma_y^2}\right\}$
Log-Normal 3-Parameter	$p(x) = \frac{1}{(x-a)\sigma_y\sqrt{2\pi}} \exp\left\{-\frac{[\ln(x-a) - \mu_y]^2}{2\sigma_y^2}\right\}$
Log-Pearson III	$p(x) = \frac{1}{\alpha_y x\Gamma(\beta)} \left(\frac{\ln x - \gamma}{\alpha_y}\right)^{\beta-1} \exp\left[-\frac{(\ln x - \gamma)}{a_y}\right]$

54

U.S. DEPARTMENT OF COMMERCE
NATIONAL OCEANIC AND ATMOSPHERIC ADMINISTRATION

U.S. DEPARTMENT OF THE ARMY
CORPS OF ENGINEERS

HYDROMETEOROLOGICAL REPORT NO. 51

Probable Maximum Precipitation Estimates, United States East of the 105th Meridian

Prepared by
Louis C. Schreiner and John T. Riedel
Hydrometeorological Branch
Office of Hydrology
National Weather Service

WASHINGTON, D.C.
June 1978

Reprinted August 1980

For sale by the Superintendent of Documents, U.S. Government Printing Office
Washington, D.C. 20402

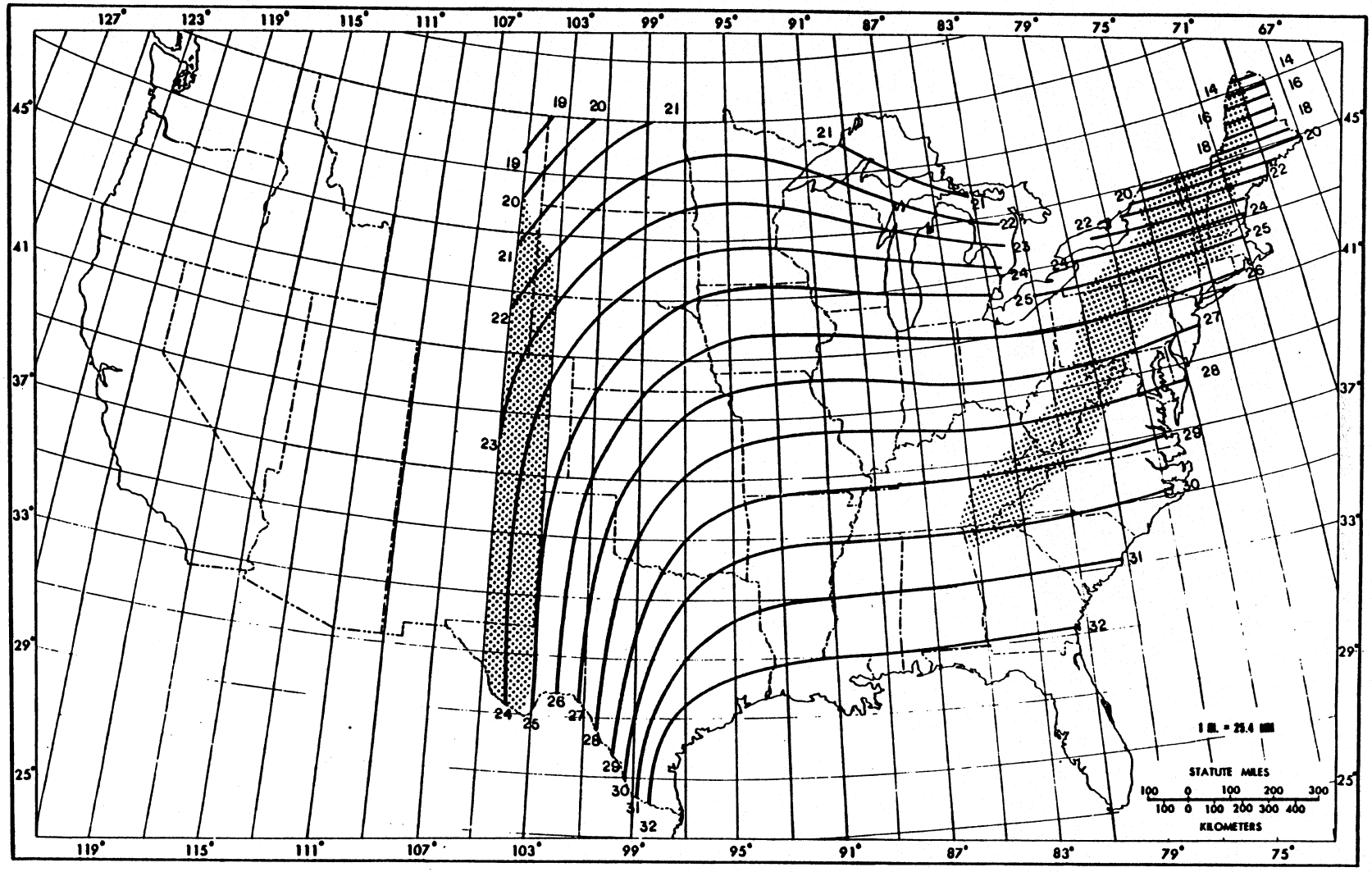

Figure 18.--All-season PMP (in.) for 6 hr 10 mi^2 (26 km^2).

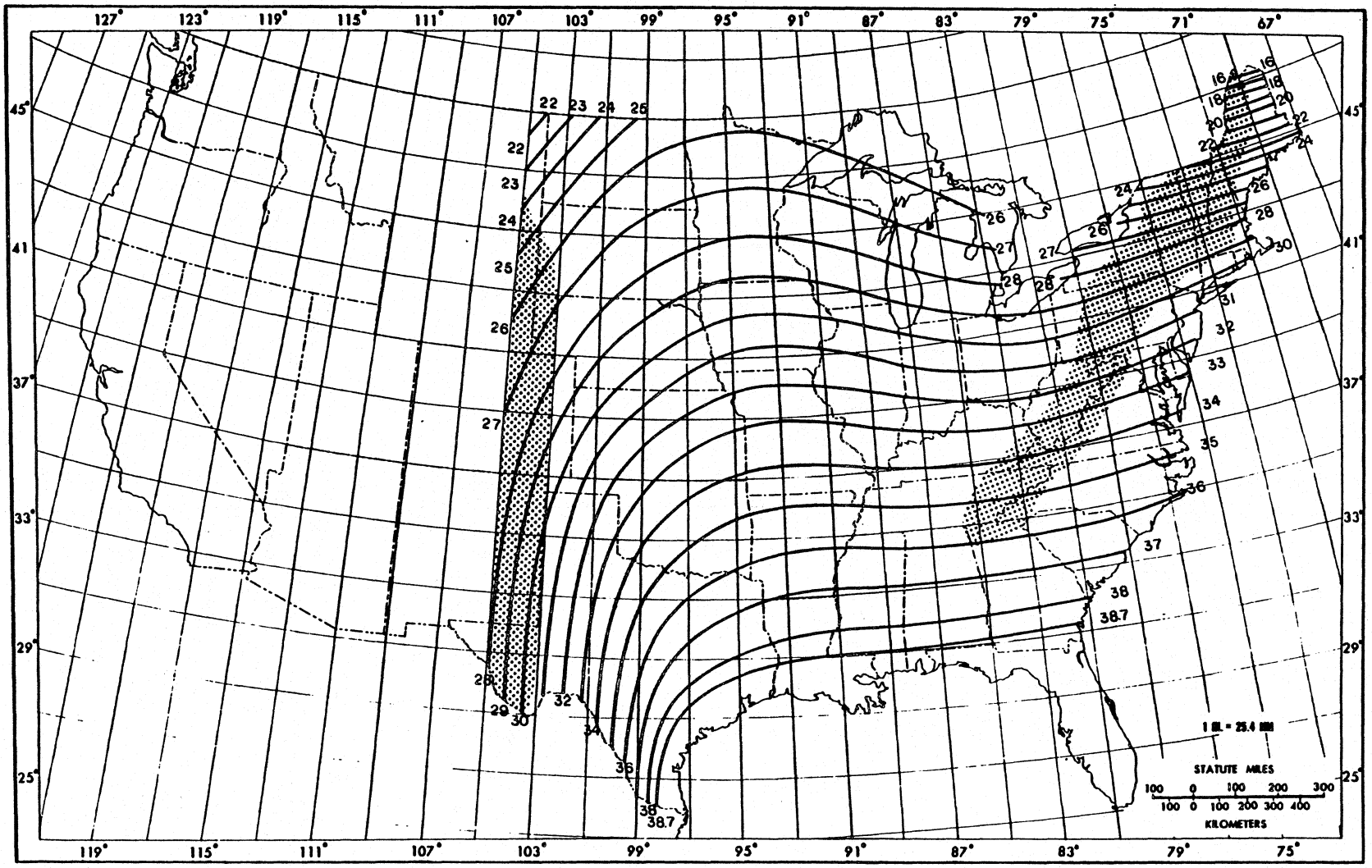

Figure 19.--All-season PMP (in.) for 12 hr 10 mi^2 (26 km^2).

516

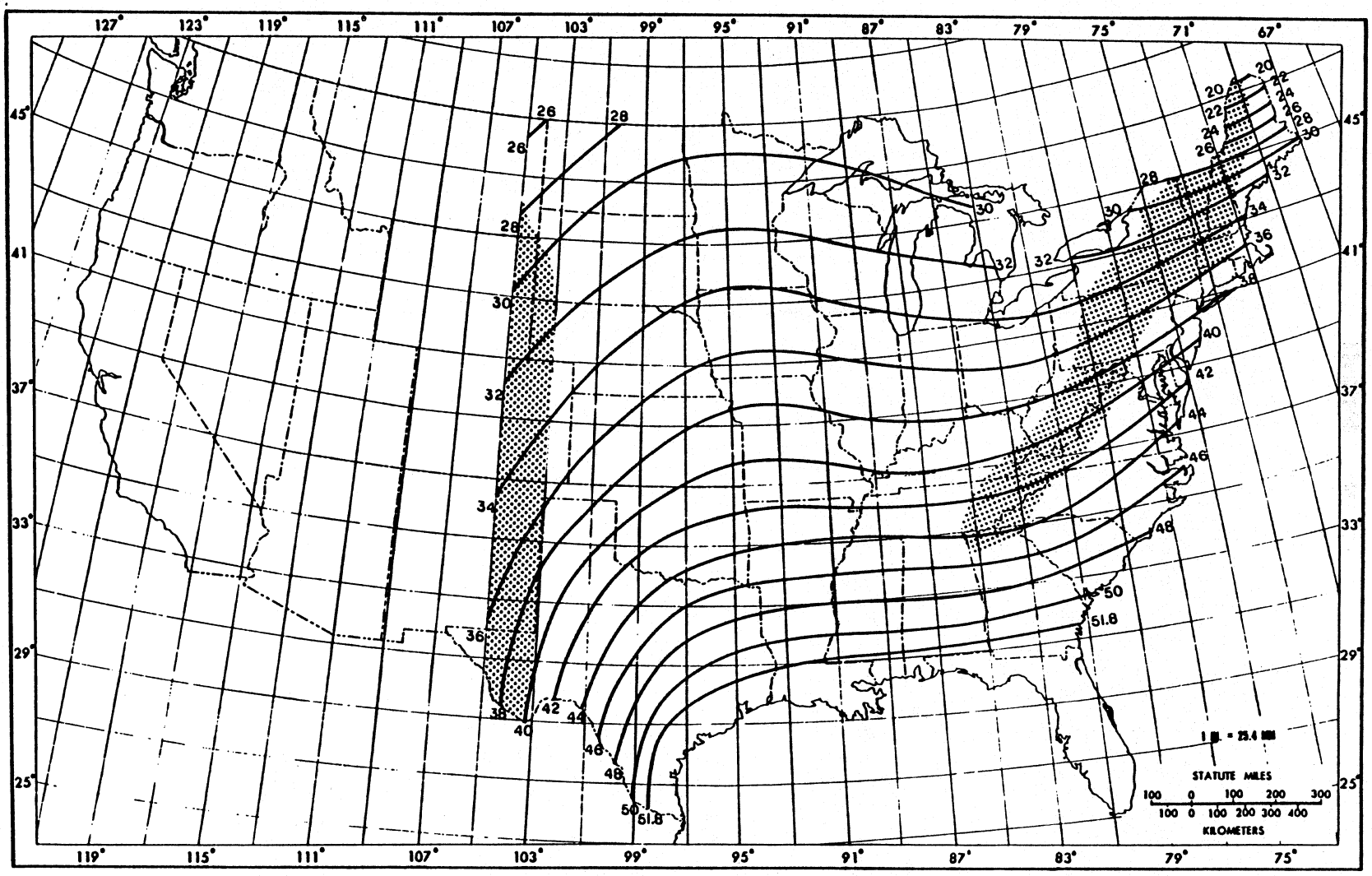

Figure 21.--All-season PMP (in.) for 48 hr 10 mi^2 (26 km^2).

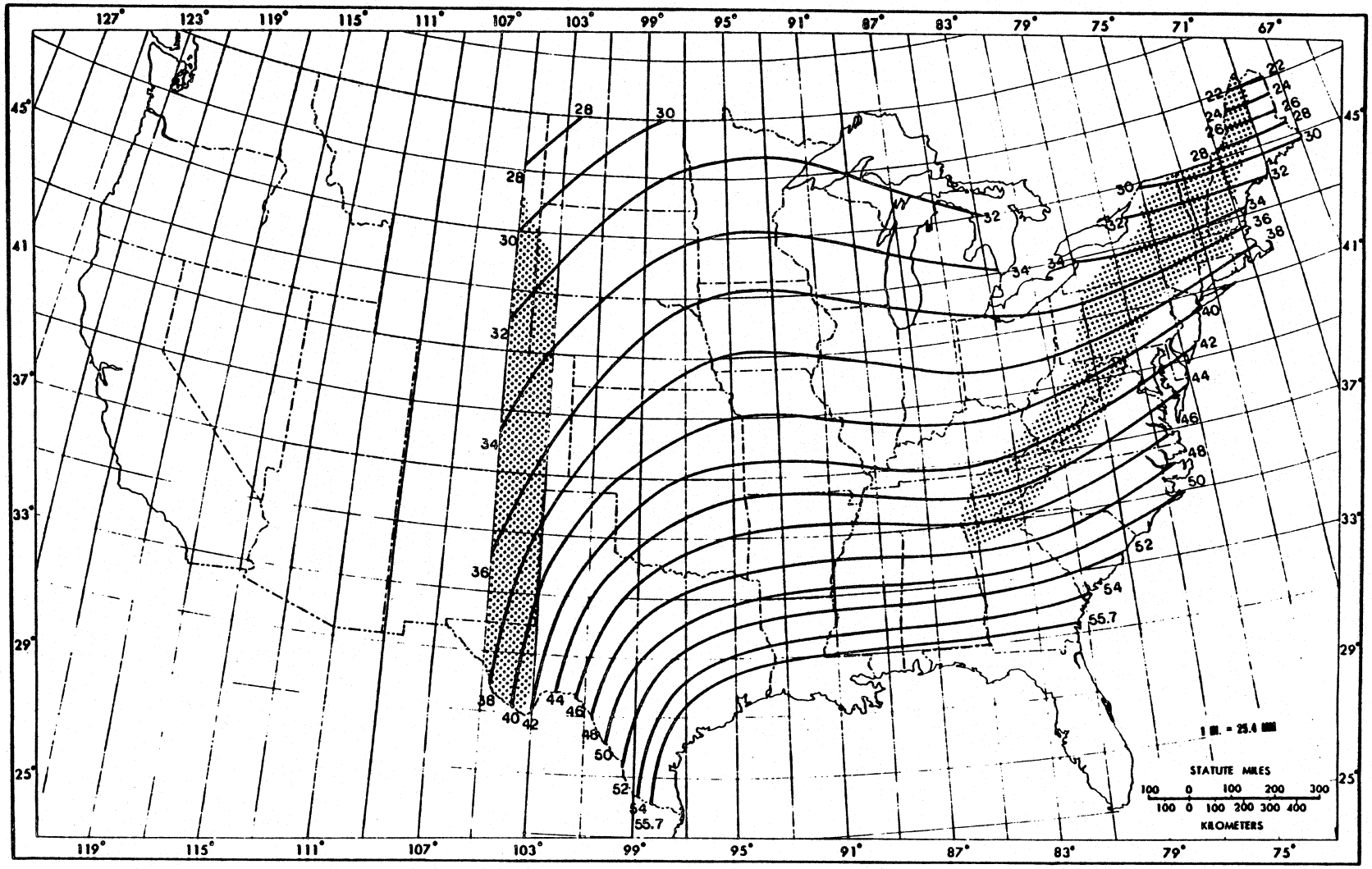

Figure 22.--All-season PMP (in.) for 72 hr 10 mi^2 (26 km^2).

U.S. DEPARTMENT OF COMMERCE
NATIONAL OCEANIC AND ATMOSPHERIC ADMINISTRATION

U.S. DEPARTMENT OF THE ARMY
CORPS OF ENGINEERS

59.

NOAA HYDROMETEOROLOGICAL REPORT NO. 52

Application of Probable Maximum Precipitation Estimates - United States East of the 105th Meridian

Prepared by
E.M. Hansen, L.C. Schreiner & J.F. Miller
Hydrometeorological Branch
Office of Hydrology
National Weather Service

WASHINGTON, D.C.
August 1982

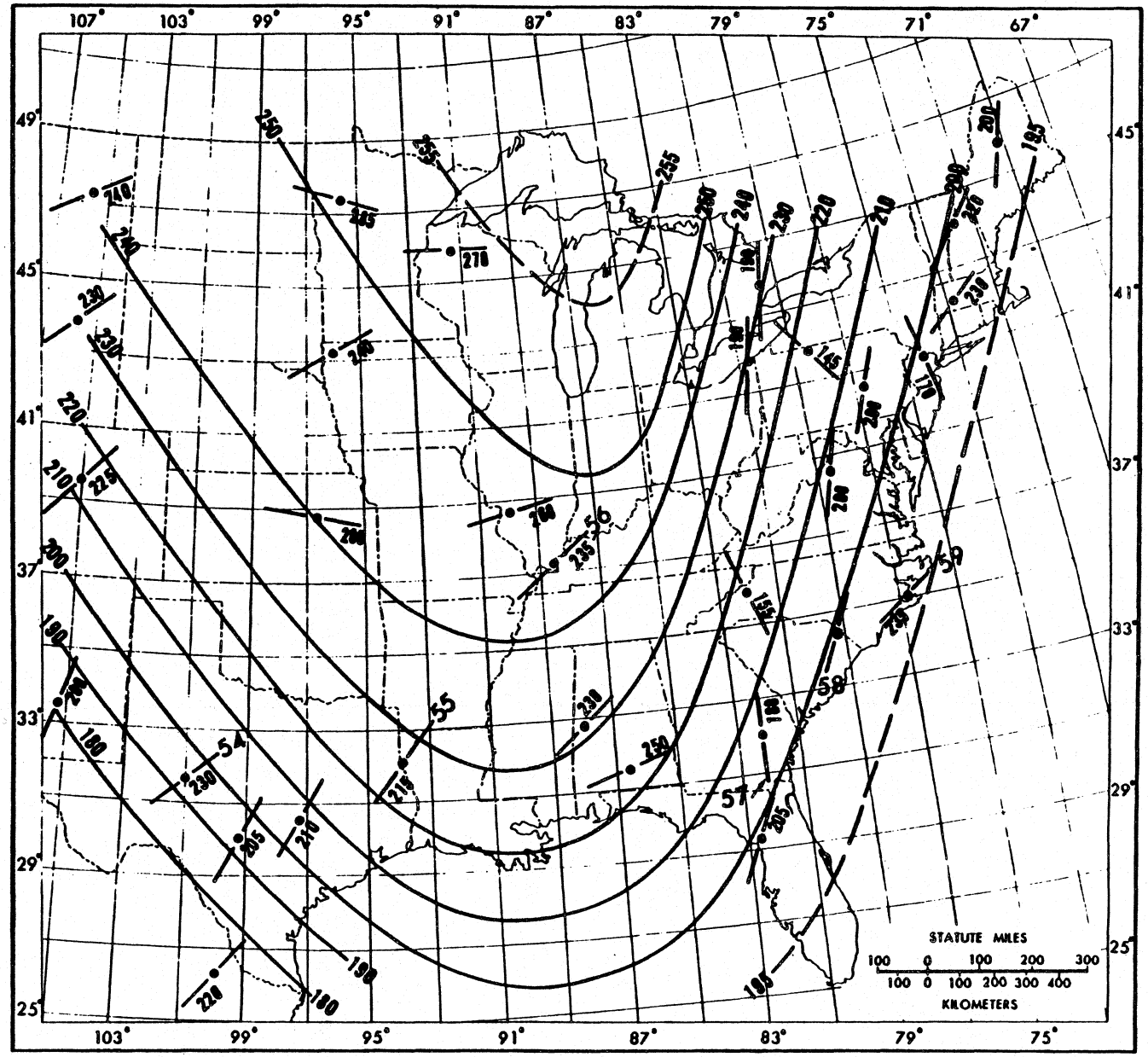

SUPPLEMENTAL STORMS

54. BROOME, TX
55. LOGANSPORT, LA
56. GOLCONDA, IL
57. GLENVILLE, GA
58. DARLINGTON, SC
59. BEAUFORT, NC

Figure 8.--Analysis of isohyetal orientations for selected major storms adopted as recommended orientation for PMP within ± 40°. Addition of 6 major storms not in figure 7 have been identified numerically above station locations and in the margin.

60.

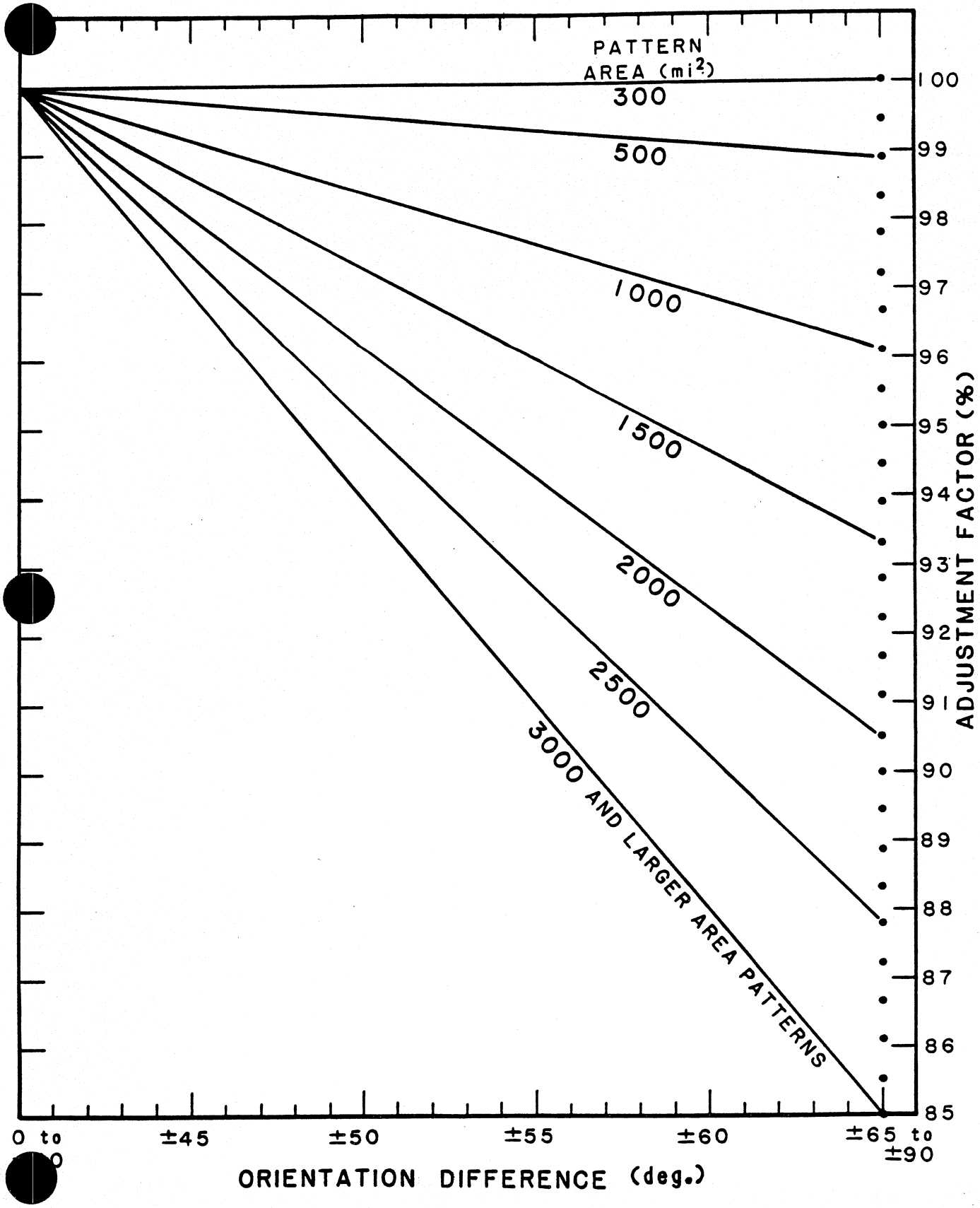

Figure 10.—Model for determining the adjustment factor to apply to isohyet values as a result of placing the pattern in figure 5 at an orientation differing from that given in figure 8 by more than 40°, for a specific location.

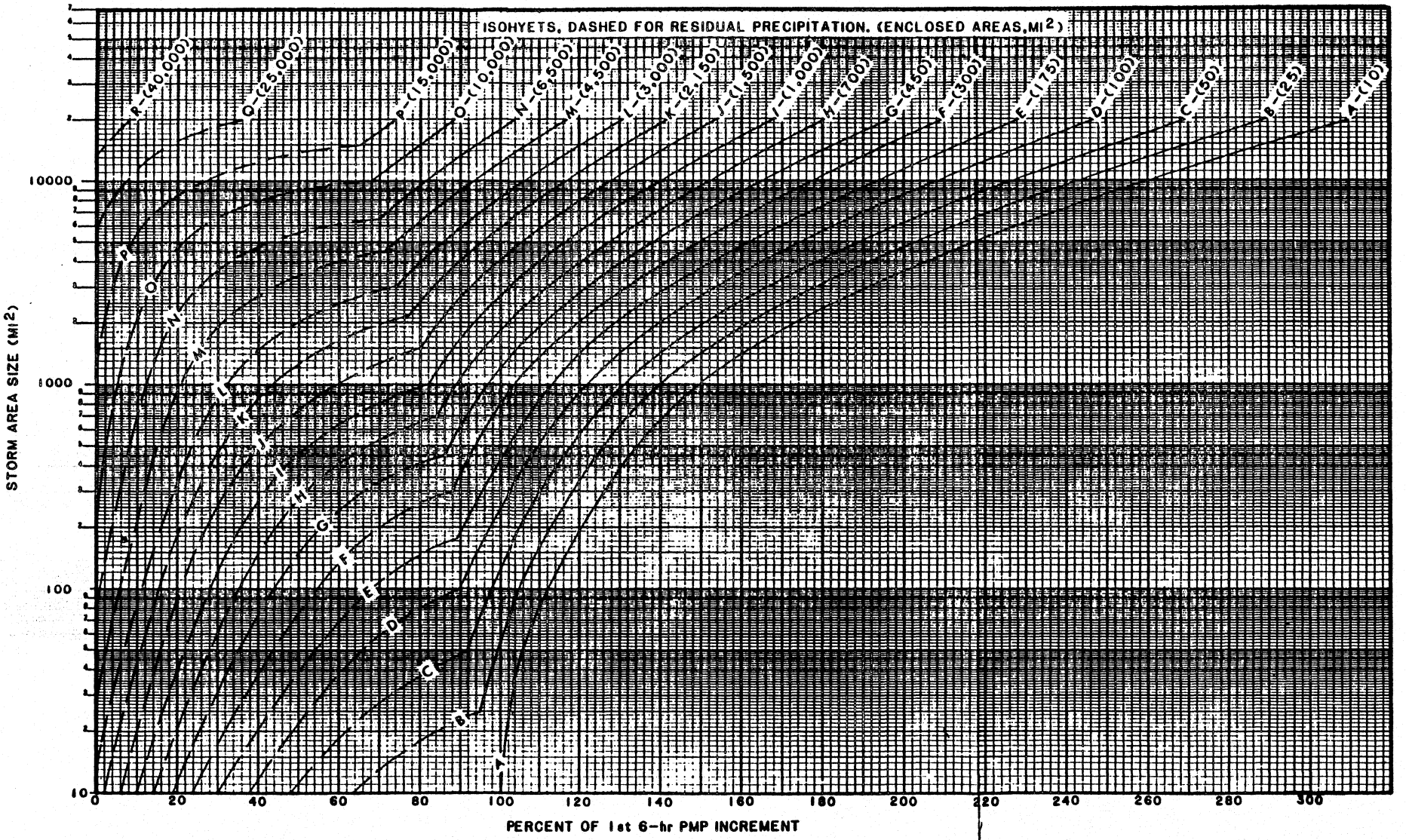

Figure 16.—Nomogram for the 1st 6-hr PMP increment and for standard isohyet area sizes between 10 and 40,000 mi²

29

Table 15.--1st 6-hr nomogram values at selected area sizes - Continued

Isohyet	Storm Area (mi^2) size											
	450	560	700	850	1000	1200	1500	1800	2150	2600	3000	3800
A	132	136	140	145	149	155	162	129	176	184	191	203
B	124	128	132	136	140	145	152	158	165	172	179	189
C	116	120	124	128	131	136	142	147	154	160	166	176
D	108	111	115	119	122	126	132	137	142	148	154	163
E	101	104	107	110	113	116	122	126	131	137	142	150
F	93	95	98	101	104	107	112	117	122	127	132	140
G	86*	89	92	94	97	100	105	108	113	118	122	130
H	63	72	84*	87	89	92	96	99	103	108	112	119
I	50	56	63	72	82*	85	88	91	95	99	102	108
J	38	43	48	54	60	68	80*	83	86	89	92	98
K	30	33	36	40	44	49	56	64	77*	80	83	89
L	23	25	27	30	32	35	41	46	52	62	74*	79
M	15	16	18	19	21	23	26	29	33	38	44	56
N	8	9	10	11	12	14	16	18	20	22	25	31
O	3	3	4	4	5	6	7	8	9	11	13	15
P	0	0	0	0	0	0	0	1	2	3	4	6
Q								0	0	0	0	0

*Indicates cusp.

Table 15.—1st 6-hr nomogram values at selected area sizes

Isohyet	Storm Area (mi^2) size											
	10	17	25	35	50	75	100	140	175	220	300	360
A	100*	101	102	104	106	109	112	116	119	122	126	129
B	64	78	95*	97	99	102	105	108	111	114	118	121
C	48	58	67	77	92*	95	98	101	103	106	110	113
D	38	46	52	59	66	77	90*	93	96	99	103	105
E	30	37	43	48	54	62	68	78	89*	92	96	98
F	24	30	34	39	44	50	55	61	66	73	88*	90
G	19	24	28	32	35	40	44	49	53	58	65	73
H	14	19	22	25	28	32	35	39	42	46	51	56
I	10	14	17	19	22	26	28	32	34	37	42	45
J	6	9	12	14	16	19	21	24	26	28	32	35
K	2	5	7	9	11	14	16	18	20	22	25	27
L	0	1	3	5	7	9	11	13	15	17	19	21
M		0	0	1	3	5	6	8	9	10	12	13
N				0	0	0	1	2	3	4	6	7
O							0	0	0	0	1	2
P											0	0

*Indicates cusp.

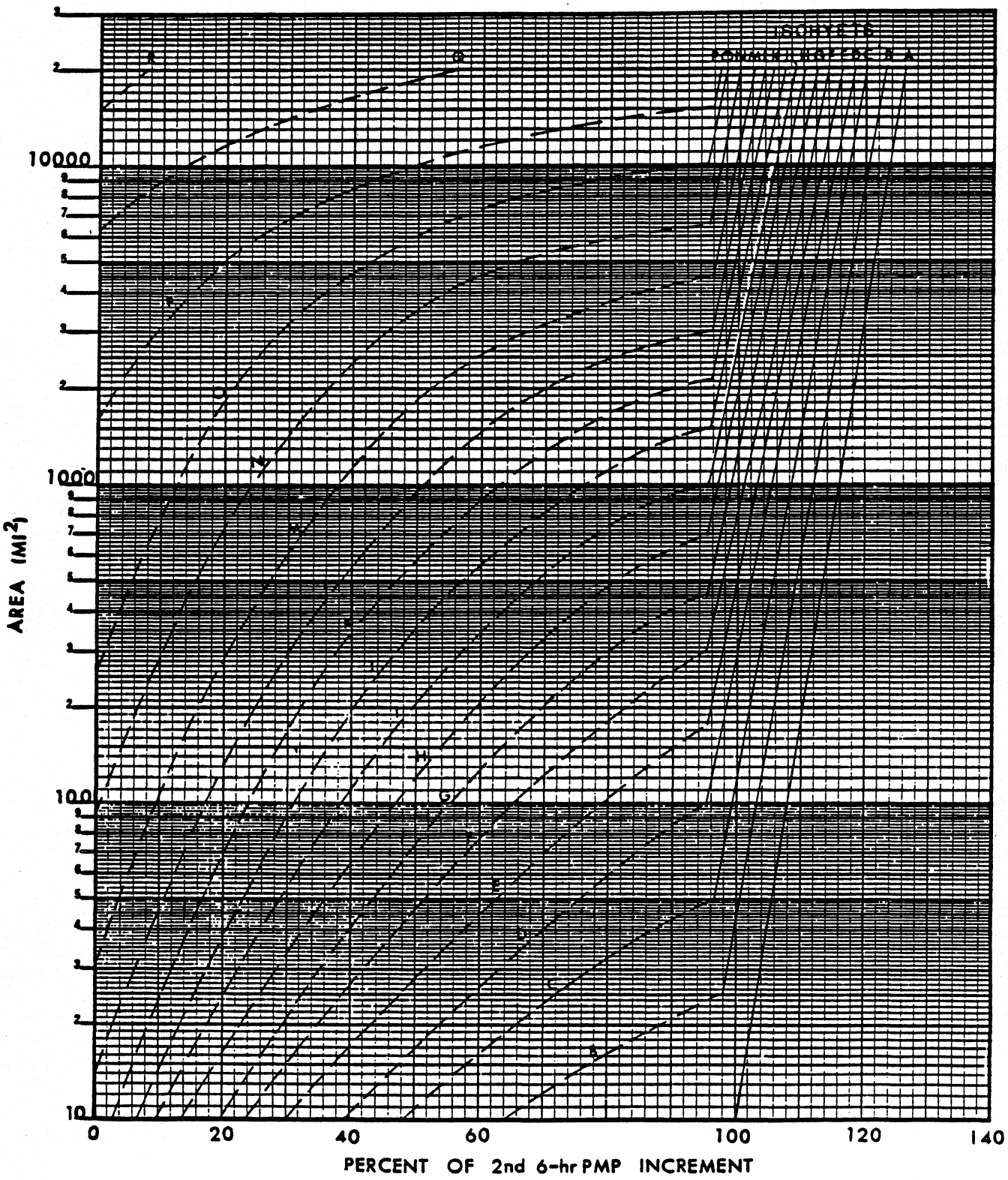

Figure 18.—Nomogram for the 2nd 6-hr PMP increment and for standard isohyet area sizes between 10 and 40,000 mi^2.

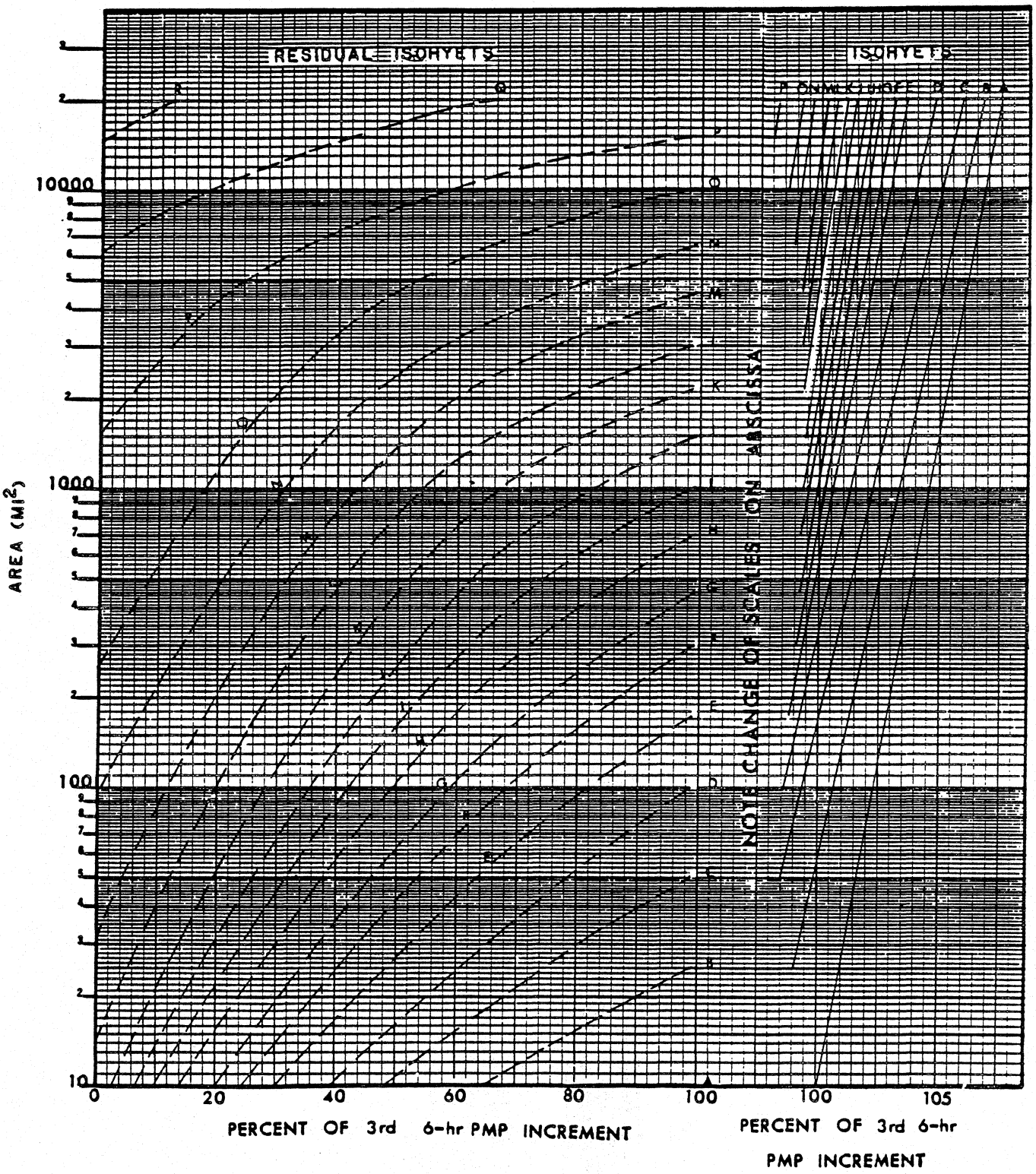

Figure 19.—Nomogram for the 3rd 6-hr PMP increment and for standard isohyet area sizes between 10 and 40,000 mi^2.

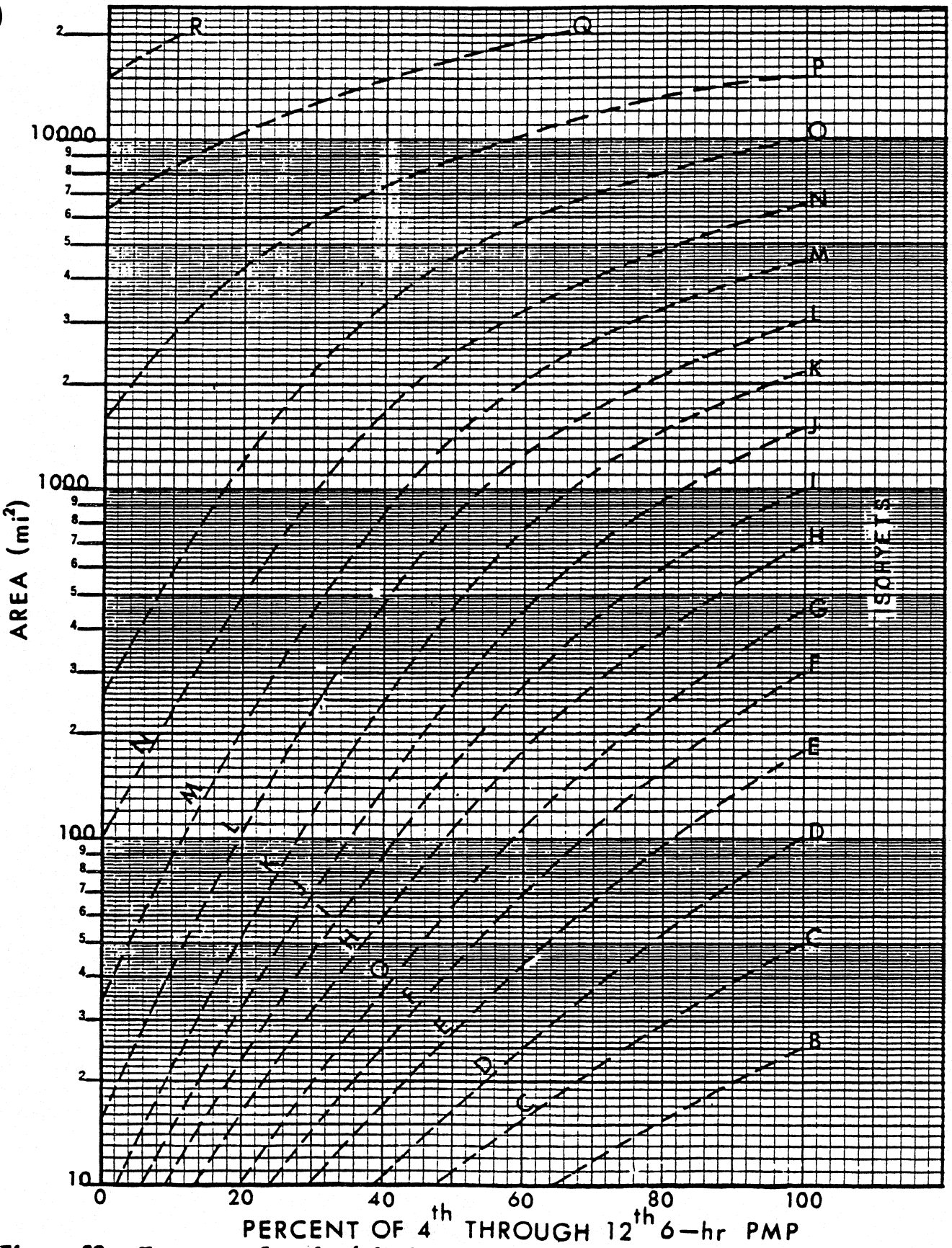

Figure 20.—Nomograms for the 4th through 12th 6-hr PMP increments and for standard isohyet area sizes between 10 and 40,000 mi^2.

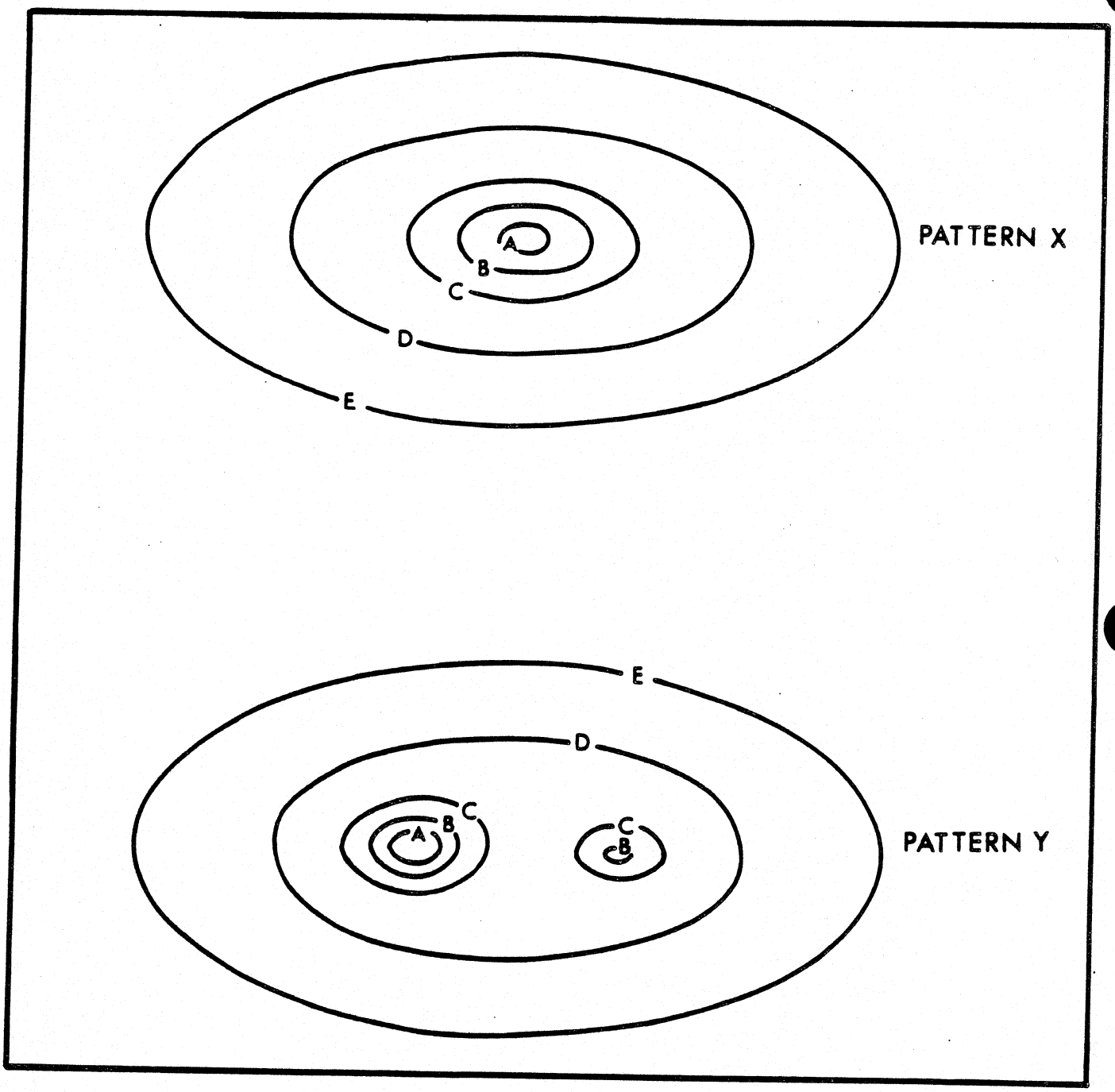

Figure 22.—Schematic showing an example of multiple centered isohyetal pattern (PMP portion only).

centers. In general, all else being equal, the more centers used, the lower the peak discharge. If multiple centers are to be considered, we therefore recommend a limit of two.

The process for deriving these centers within an elliptical pattern is based on the standard isohyets and their values for a single-centered pattern as

6-hr periods

1	2	3	4	5	6	7	8	9	10	11	12
11	10	8	5	1	2	3	4	6	7	9	12

F. Subdrainages

Should it be necessary to determine the areal distribution of PMP across subdrainages of a particular drainage, consider the following steps:

Step

1. With the pattern placed across the entire drainage as given in step B1, and incremental isohyet values as determined in step D3 and/or D5, planimeter the incremental areas contained between isohyets within each subdrainage.

2. Follow the computational procedure outlined in steps C5 to C8 to obtain the incremental subdrainage volumes for 6-hr periods 1 through 12.

3. The subdrainage volumes divided by the subdrainage areas yield the average depths across the subdrainage for each 6-hr increment.

   Note: If the subdrainage is crossed by the zero isohyet, the appropriate area for consideration is the subdrainage area inside the zero isohyet, not that of the total subdrainage.

4. If it is hydrologically critical to rearrange the temporal sequence of the incremental amounts determined in step F3 for a particular subdrainage, then it is necessary that the same arrangement be applied to all other subdrainages. This requirement is important and must be observed without exception. Demonstration of a subdrainage application is given in example 2a.

7.2 Example No. 1a

The first example demonstrates the computational procedure, and shows the affect on maximum volume determination that results from consideration of orientation of the isohyetal pattern.

The drainage used in this example is that of the Leon River in Texas above Belton Reservoir (approximately 3,660 mi^2) shown in figure 42, drawn to a scale of 1:1,000,000. Drainage center is about 31°45'N, 98°15'W.

The following steps correspond to those outlined in section 7.1 leading to determination of the area size of the isohyetal pattern that gives maximum volume, from which we then assign isohyet values.

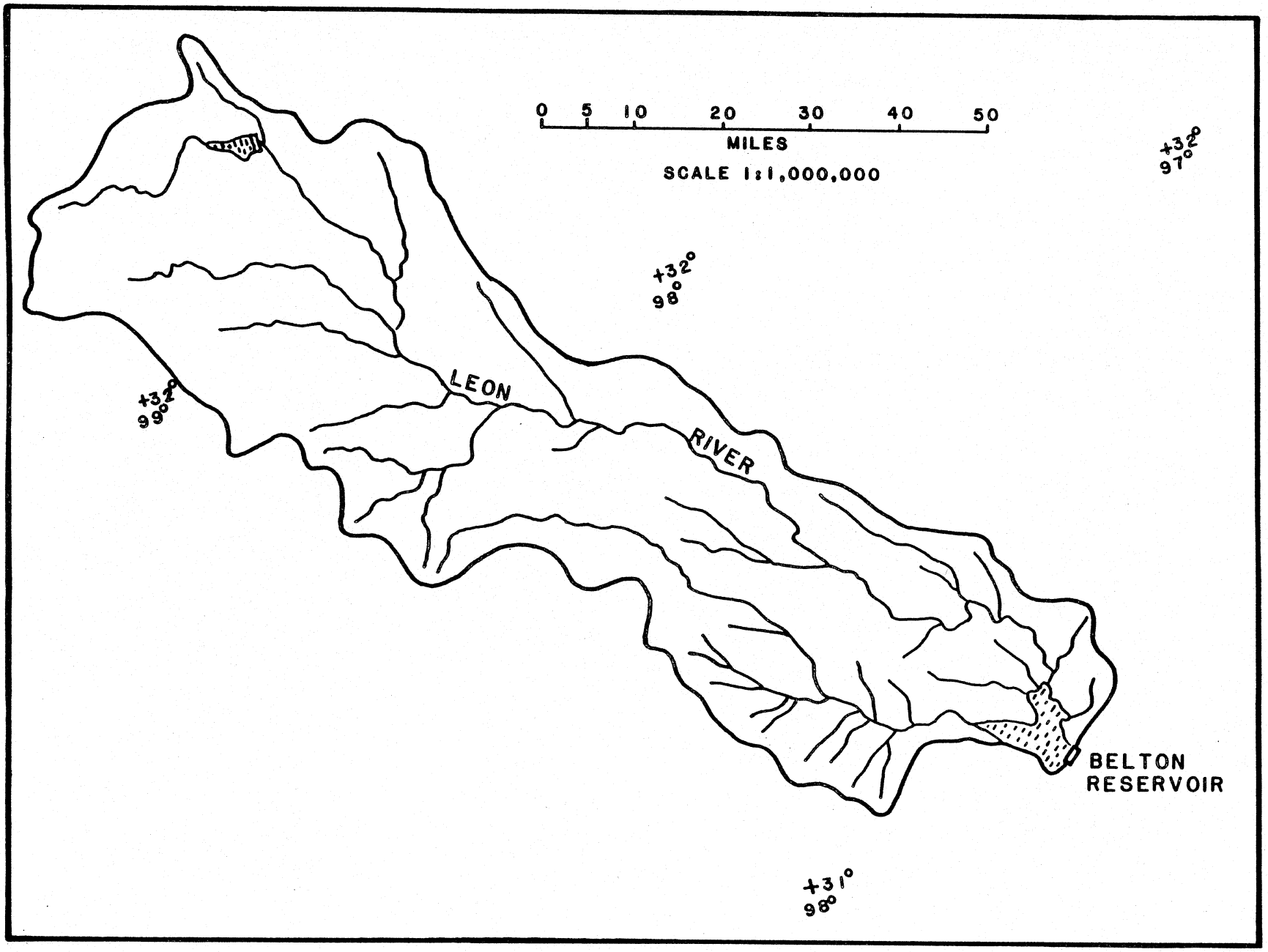

Figure 42.—Leon River, TX (3,660 mi^2) above Belton Reservoir showing drainage.

Step

A1. For the Leon River drainage above Belton Reservoir (31°45°N, 98°15'W) we obtain storm-area averaged PMP data from HMR No. 51, figures 18 through 47 as,

	Duration (hr)				
Area (mi^2)	6	12	24	48	72
10	29.8	36.2	41.8	46.7	49.8
200	22.3	27.4	33.0	37.5	41.4
1000	16.2	21.2	26.8	31.0	34.5
5000	9.3	13.1	18.1	22.6	25.9
10000	7.2	10.4	14.9	18.8	21.0
20000	5.2	8.2	11.7	15.4	18.4

A2. The depth-area-duration data in step A1 is plotted in figure 43, and smooth curves drawn. The decision on how to smooth these curves to the data points is left to the user, although it is cautioned they are to be parallel or converge slightly with increasing area size.

A3. From figure 43, we can read off values for the standard areas of isohyets both larger and smaller than the drainage area (3,660 mi^2).

	Duration (hr)				
Area (mi^2)	6	12	24	48	72
1000	16.1	20.7	26.1	30.5	34.1
1500	14.4	18.9	24.1	28.5	32.0
2150	12.9	17.2	22.3	26.7	30.2
3000	11.5	15.7	20.6	25.0	28.5
4500	9.8	13.9	18.6	22.8	26.4
6500	8.5	12.4	16.7	21.0	24.3
10000	7.1	10.6	14.8	18.8	22.0
15000	5.9	9.3	13.0	16.8	20.0

A4. The data in step A3 are plotted on linear paper and smooth depth-duration curves drawn as shown in figure 44. From these curves we interpolate 18-hr values:

Area (mi^2)	18-hr Duration
1000	23.7
1500	21.8
2150	20.0
3000	18.5
4500	16.5
6500	14.8
10000	13.0
15000	11.3

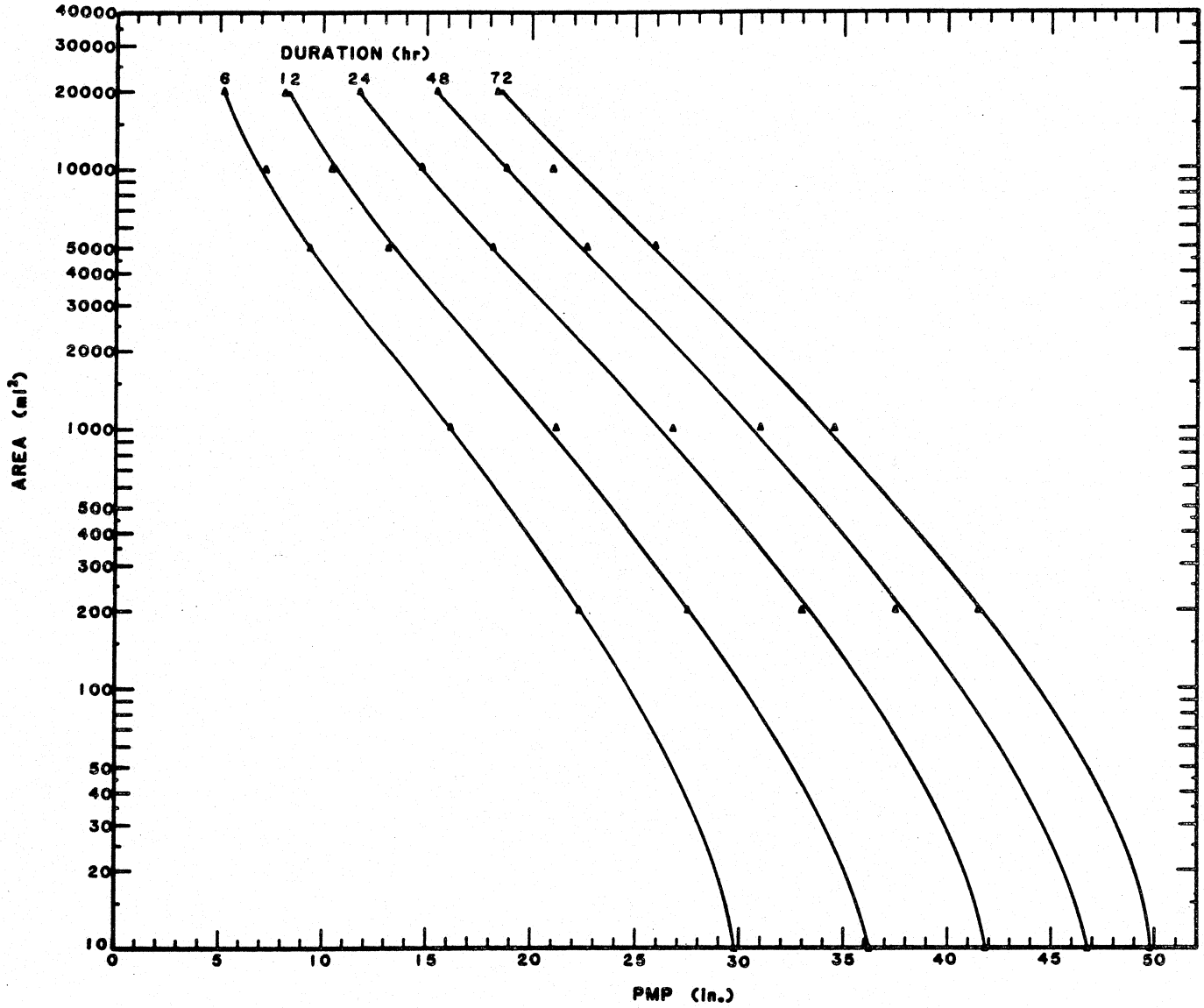

Figure 43.—Depth-area-duration curves for 31°45'N, 98°15'W applicable to the Leon River, TX drainage.

A5. Incremental differences for the 1st three 6-hr periods are obtained by successive subtraction of the values contained in steps A3 and A4.

	6-hr periods		
Area (mi^2)	1	2	3
1000	16.1	4.6	3.0
1500	14.4	4.5	2.9
2150	12.9	4.3	2.8
3000	11.5	4.2	2.8
4500	9.8	4.1	2.6
6500	8.5	3.9	2.4
10000	7.1	3.5	2.4
15000	5.9	3.4	2.0

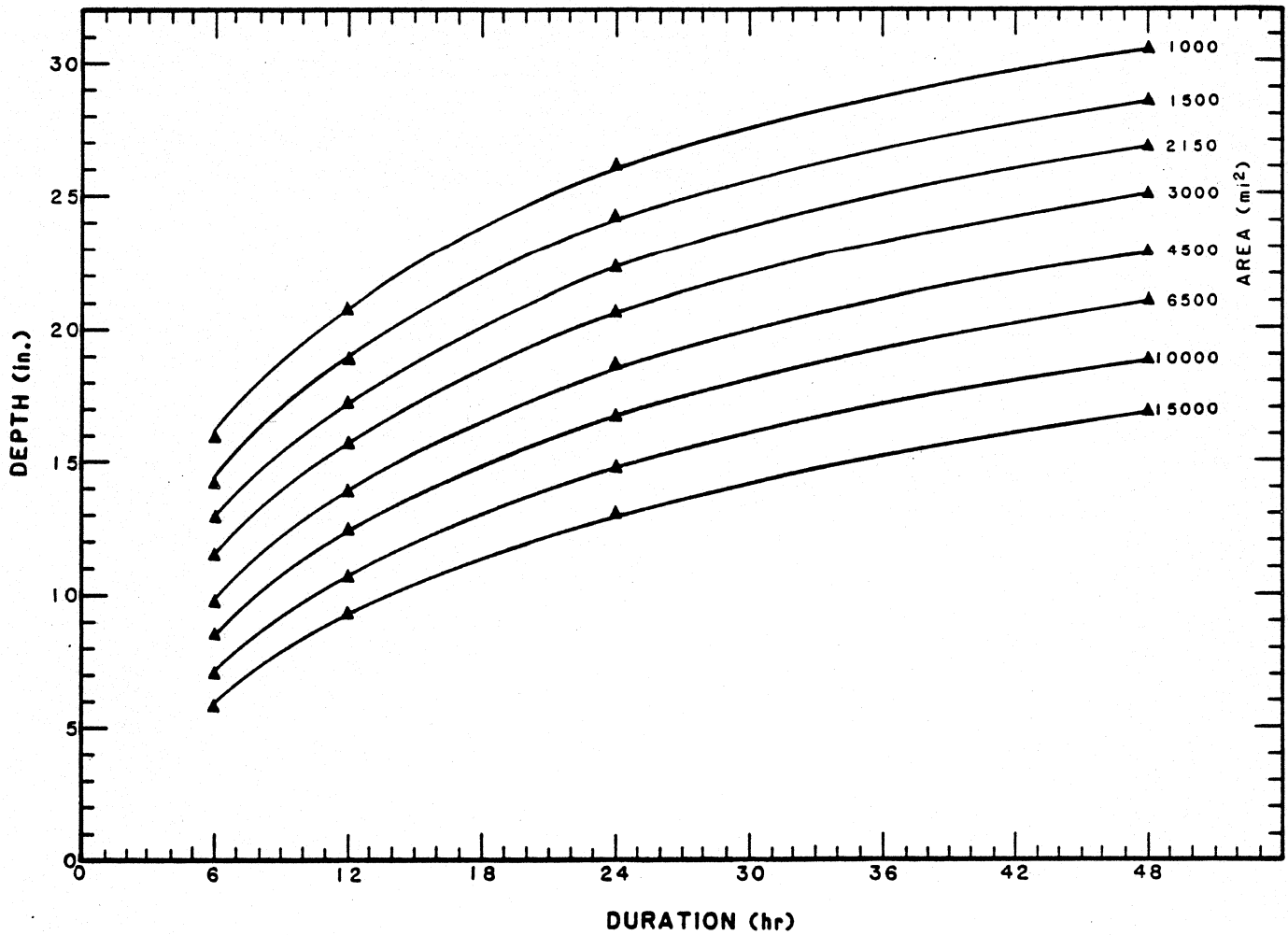

Figure 44.—Depth-duration curves for selected area sizes at 31°45'N, 98°15'W.

Plotting each set of 6-hr values against area and fitting the points by smooth lines as shown in figure 45 gives the following set of incremental data (read to hundredths).

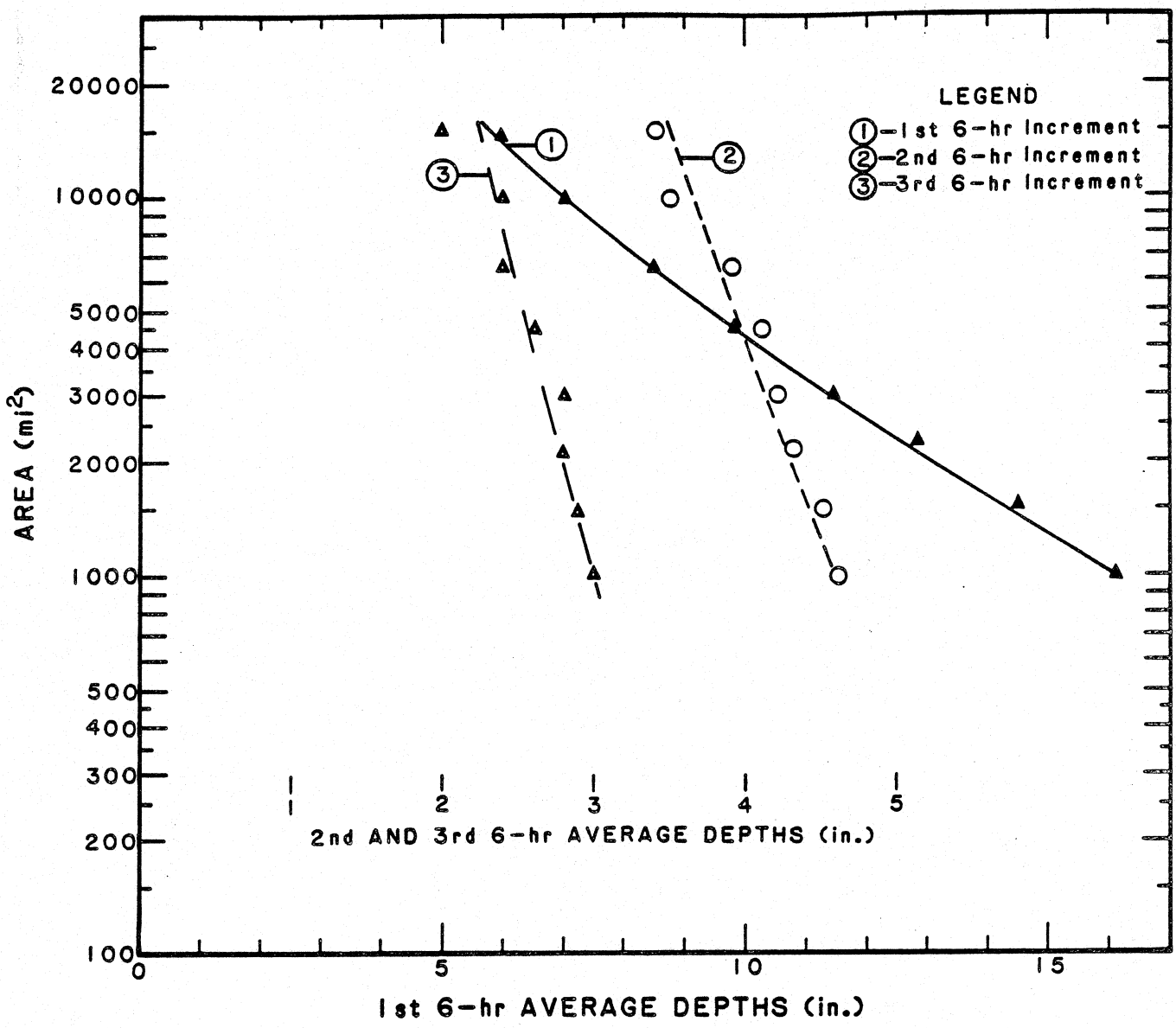

Figure 45.—Smoothing curves for 6-hr incremental values at selected area sizes for Leon River, TX drainage.

	6-hr periods		
Area (mi^2)	1	2	3
1000	16.10	4.60	3.01
1500	14.35	4.42	2.89
2150	12.82	4.27	2.79
3000	11.40	4.14	2.70
4500	9.80	3.96	2.58
6500	8.50	3.82	2.48
10000	7.05	3.66	2.36
15000	5.80	3.50	2.25

Note that within each column as a result of this smoothing, the values consistently decrease with increasing area size.

B1. The isohyetal pattern is then drainage-centered over the Leon River drainage drawn to 1:1,000,000 scale as shown in figure 46. Our judgment of best fit enclosed the "H" isohyet within the narrow outline of the drainage. The "N" isohyet encloses almost all the drainage.

B2. The orientation of the pattern, when fit as in figure 46 is roughly 134°/314°. The 134° misses by 1° our preferred range (135° to 315°) and we accordingly added 180° to get an orientation of 314°.

B3. For the location of the drainage center at 31°45'N and 98°15'W, figure 8 gives the PMP orientation of 208°. The angular difference is 314°-208°, or 106°. Since this difference, or its supplement, 74°, exceeds our range of ±40° for which no reduction to PMP is applied, we must adjust the storm-area averaged PMP for orientation of the pattern when aligned with the drainage.

B4. Figure 10 gives the following reductions for the various isohyet areas considered in step A3 and the orientation difference from PMP given in step B3.

Pattern area (mi^2)	Adjustment factor (%)
1000	96.1
1500	93.3
2150	89.7
3000	85.0
4500	85.0
6500	85.0
10000	85.0
15000	85.0

Multiply each of the final smoothed 6-hr incremental values in step A5 by the adjustment factors of step B4 to get the adjusted incremental values,

Pattern area (mi^2)	6-hr periods 1	2	3
1000	15.47	4.42	2.89
1500	13.39	4.12	2.70
2150	11.50	3.83	2.50
3000	9.69	3.52	2.30
4500	8.33	3.37	2.19
6500	7.22	3.25	2.11
10000	5.99	3.11	2.01
15000	4.93	2.98	1.91

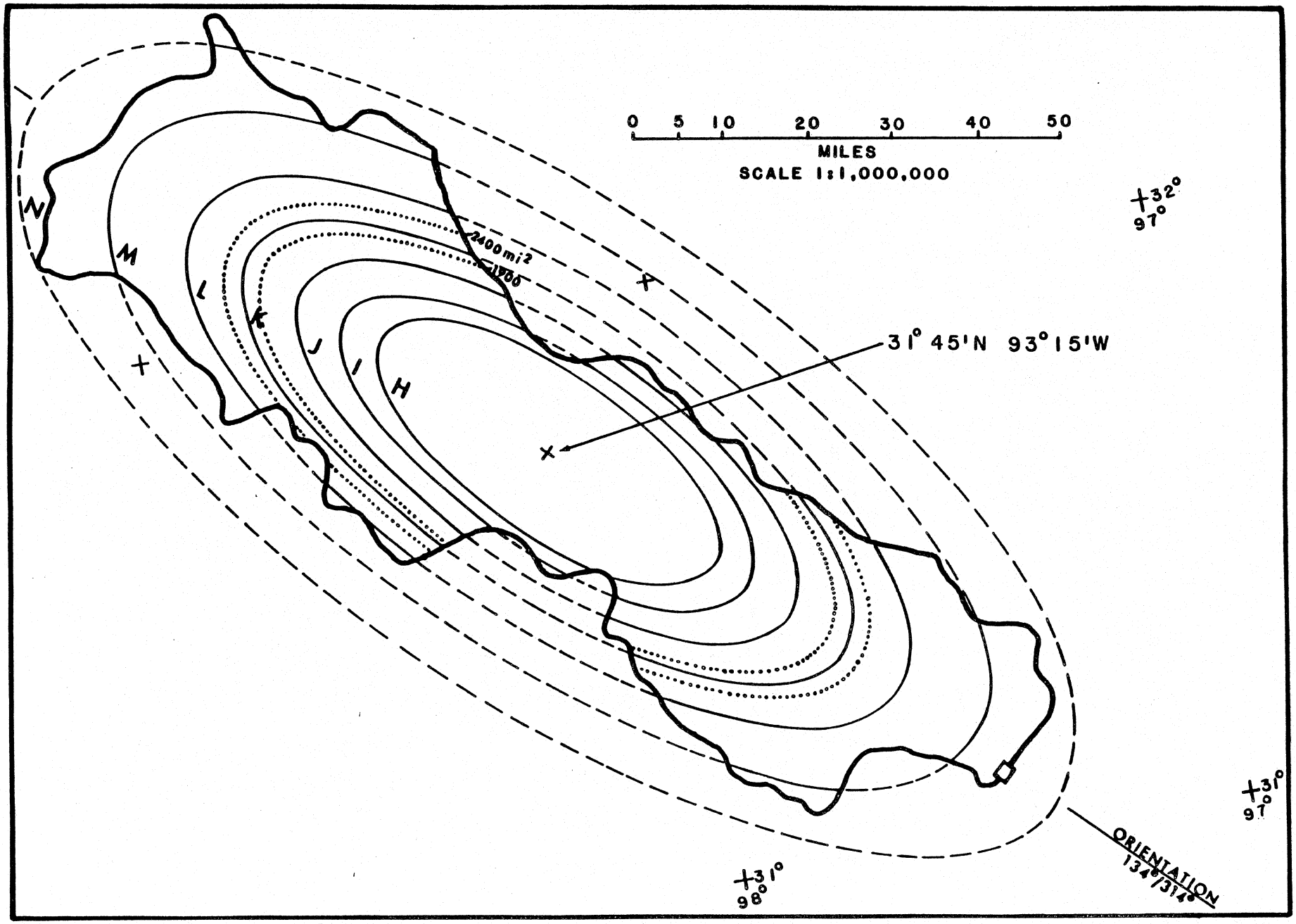

Figure 46.—Isohyetal pattern placed on the Leon River, TX drainage to give maximum precipitation volume.

C. Determine the maximum volume of precipitation for the PMP patterns corresponding to the 8 area sizes used in the previous steps. To do this, we recommend filling in the computation sheets as shown in table 22. Some preliminary considerations have been made regarding the fit of the isohyetal pattern over the drainage. First, the small (~10-mi^2) area of the drainage outside the N isohyet has been disregarded as insignificant to overall volume. Second, weight factors of 0.6 and 0.75 have been assigned (arbitrary judgment) to the average depth calculation for the L to M and M to N isohyetal areas, respectively (see step C6).

Following the procedure outlined in section C, we find the greatest volume for the 1st 6-hr increment occurs at 1,500 mi^2. We should then check the volumes obtained for the 2nd and 3rd 6-hr increments before accepting 1,500 mi^2 as our answer. For these additional increments it is not necessary to calculate volumes for all the areas considered in the 1st 6-hr increment, only those in the vicinity of the presumed area of maximum volume (1,500 mi^2). Thus, we have limited our calculations to areas between 1,000 and 3,000 mi^2 (table 22). Addition of the incremental volumes at corresponding area sizes shows, however, that the maximum volume has shifted from 1,500 mi^2 to 2,150 mi^2 for these accumulated volumes. (The sum of the 1st to 3rd volumes is shown by the solid line in fig. 47.)

It is of interest to narrow in on this maximum as to area size, and we chose to evaluate two supplementary PMP pattern areas at 1,900 and 2,400 mi^2. Isohyets for these area sizes have been added to figure 46 as dotted lines. The results from table 23 (dashed lines in figure 47) show a maximum volume occurs at an area size slightly less than that for the 2,150-mi^2 area pattern in the Leon River drainage.

Because of the shift of area size between the 1st and the sum of the 1st three increments, it has been recommended that the three greatest increments be determined in the computation procedure. This significantly increases the number of computations required.

Step

D1. Having concluded that the maximum volume occurs for a PMP pattern near 2,150 mi^2 when placed over the Leon River, we can now determine the values for each isohyet for all twelve 6-hr increments. Return to the smooth depth-duration curve for 2,150 mi^2 in step A4, and extend this curve to 72 hr before reading off the 6-hr values.

	Duration (hr)											
	6	12	18	24	30	36	42	48	54	60	66	72
Increm. PMP (in.)	12.9	17.2	20.0	22.3	23.8	25.0	26.0	26.8	27.7	28.5	29.2	29.9

Table 22.—Completed computation sheets for 1st, 2nd and 3rd 6-hr increments for Leon River, TX drainage

Increment: 1

Drainage: Leon River, TX Area: 3,660 mi^2 Date:

	I	II	III	IV	V	VI		I	II	III	IV	V	VI
Area size	Iso.	Nomo.	Amt. 15.47	Avg. depth	ΔA	ΔV	Area size	Iso.	Nomo.	Amt. 9.69	Avg. depth	ΔA	ΔV
	A	149	23.05	23.05	10	230.5		A	191	18.51	18.51	10	185.1
	B	140	21.66	22.36	15	335.4		B	179	17.93	17.93	15	258.9
1000/1	C	131	20.27	20.97	25	524.2	3000/1	C	166	16.09	16.72	25	418.0
	D	122	18.87	19.57	50	978.5		D	154	14.92	15.51	50	775.5
	E	113	17.48	18.18	75	1363.5		E	142	13.76	14.34	75	1075.5
	F	104	16.09	16.79	125	2098.8		F	132	12.79	13.28	125	1660.0
	G	97	15.01	15.55	150	2332.5		G	122	11.82	12.31	150	1846.5
	H	89	13.77	14.39	250	3597.5		H	112	10.85	11.34	250	2835.0
	I	82	12.69	13.23	271	3585.3		I	102	9.88	10.37	271	2810.3
	J	60	9.28	10.99	393	4319.1		J	92	8.91	9.39	393	3690.3
	K	44	6.81	7.69	488	3752.7		K	83	8.04	8.48	488	4138.2
	L	32	4.95	5.88	582	3422.2		L	74	7.17	7.61	582	4429.0
(.60 X)*	M	21	3.25	4.27	737	3146.9	(.60 X)	M	44	4.26	6.01	737	4428.4
(.75 X)	N	12	1.85	3.09	489	1511.0	(.75 X)	N	25	2.42	3.80	489	1858.2
					Sum = 31198.1							Sum = 30418.9	
Area size			Amt. 13.39				Area size			Amt. 8.33			
	A	162	21.69	21.69	10	216.9		A	212	17.66	17.66	10	176.6
	B	152	20.35	21.02	15	315.8		B	198	16.49	17.08	15	256.1
1500/1	C	142	19.01	19.68	25	492.0	4500/1	C	184	15.33	15.91	25	397.8
	D	132	17.67	18.34	50	917.0		D	170	14.16	14.75	50	737.5
	E	122	16.33	17.00	75	1275.0		E	157	13.08	13.62	75	1021.5
	F	112	14.99	15.66	125	1957.5		F	146	12.16	12.62	125	1577.5
	G	105	14.06	14.52	150	2178.0		G	135	11.25	11.71	150	1756.5
	H	96	12.85	13.46	250	3365.0		H	124	10.33	10.79	250	2697.5
	I	88	11.78	12.32	271	3338.7		I	113	9.41	9.87	271	2674.8
	J	80	10.71	11.24	393	4417.3		J	103	8.58	9.00	393	3537.0
	K	56	7.50	9.10	488	4440.8		K	93	7.75	8.16	488	3982.1
	L	41	5.49	6.50	582	3783.0		L	83	6.91	7.33	582	4266.1
(.60 X)	M	26	3.48	4.69	737	3456.5	(.60 X)	M	71	5.91	6.51	737	4797.9
(.75 X)	N	16	2.14	3.14	489	1535.5	(.75 X)	N	37	3.08	5.20	489	2542.8
					Sum = 31689.0							Sum = 30421.7	
Area size			Amt. 11.50				Area size			Amt. 7.22			
	A	176	20.24	20.24	10.	202.4		A	233	16.82	16.82	10	168.2
	B	165	18.98	19.61	15	294.2		B	218	15.74	16.28	15	244.2
2150/1	C	154	17.71	18.35	25	458.6	6500/1	C	203	14.66	15.20	25	380.0
	D	142	16.33	17.02	50	851.0		D	187	13.50	14.08	50	704.0
	E	131	15.07	15.70	75	1177.5		E	174	12.56	13.03	75	977.3
	F	122	14.03	14.55	125	1818.8		F	160	11.55	12.06	125	1507.5
	G	113	12.99	13.51	150	2026.5		G	148	10.69	11.12	150	1668.0
	H	103	11.58	12.42	250	3105.0		H	137	9.89	10.29	250	2572.5
	I	95	10.93	11.39	271	3086.7		I	125	9.03	9.46	271	2563.7
	J	86	9.89	10.41	393	4091.1		J	113	8.16	8.59	393	3375.9
	K	77	8.86	9.38	488	4577.4		K	103	7.44	7.80	488	3806.4
	L	52	5.98	7.42	582	4318.4		L	93	6.71	7.08	582	4120.6
(.60 X)	M	33	3.80	5.11	737	3766.1	(.60 X)	M	81	5.85	6.37	737	4694.7
(.75 X)	N	20	2.30	3.42	489	1672.4	(.75 X)	N	70	5.05	5.65	489	2762.8
					Sum = 31446.3							Sum = 29545.7	

* Weighting factor F (see text Section 7.1 Step C6)

Table 22.—Completed computation sheets for 1st, 2nd and 3rd 6-hr increments for Leon River, TX drainage - Continued

Increment: 1,2

Drainage: Leon River, TX Area: 3,660 mi^2 Date:

	I	II	III	IV	V	VI		I	II	III	IV	V	VI
Area size	Iso.	Nomo.	Amt. 5.99	Avg. depth	ΔA	ΔV	Area size	Iso.	Nomo.	Amt. 4.93	Avg. depth	ΔA	ΔV
	A	262	15.69	15.69	10	156.9		A	290	14.30	14.30	10	143.0
	B	243	14.56	15.12	15	226.8		B	271	13.36	13.83	15	207.4
10000/1	C	227	13.60	14.08	25	352.0	15000/1	C	253	12.47	12.92	25	323.0
	D	209	12.52	13.06	50	653.0		D	232	11.44	11.96	50	598.0
	E	194	11.62	12.07	75	905.2		E	214	10.55	11.00	75	825.0
	F	178	10.66	11.14	125	1392.5		F	196	9.66	10.10	125	1262.5
	G	166	9.94	10.30	150	1545.0		G	183	9.02	9.34	150	1411.0
	H	152	9.10	9.52	250	2380.0		H	168	8.28	8.65	250	2162.5
	I	140	8.39	8.74	271	2368.5		I	156	7.69	7.98	271	2162.6
	J	128	7.67	8.03	393	3155.8		J	143	7.05	7.37	393	2896.4
	K	117	7.01	7.34	488	3581.9		K	131	6.46	6.76	488	3298.9
	L	107	6.41	6.71	582	3905.2		L	120	5.92	6.19	582	3602.6
(.60 X)	M	93	5.57	6.07	737	4473.6	(.60 X)	M	106	5.22	5.64	737	4156.7
(.75 X)	N	82	4.91	5.40	489	2640.6	(.75 X)	N	94	4.63	5.07	489	2479.2
						Sum = 27737.0							Sum = 25518.8
Area size			Amt. 4.42				Area size			Amt. 4.12			
	A	116	5.13	5.13	10	51.3		A	117	4.82	4.82	10	48.2
	B	112	4.95	5.04	15	75.6		B	113	4.66	4.74	15	71.1
1000/2	C	108.5	4.80	4.88	25	121.9	1500/2	C	110	4.53	4.60	25	114.9
	D	105	4.64	4.72	50	236.0		D	107	4.41	4.47	50	223.5
	E	103	4.55	4.60	75	345.0		E	105	4.33	4.37	75	327.8
	F	101	4.46	4.51	125	563.8		F	103	4.24	4.29	125	535.6
	G	99	4.38	4.42	150	663.0		G	100.5	4.14	4.19	150	628.5
	H	97	4.29	4.34	250	1085.0		H	99	4.08	4.11	250	1027.5
	I	95	4.20	4.25	271	1151.8		I	97	4.00	4.04	271	1094.8
	J	76	3.36	3.78	393	1485.5		J	95.5	3.93	3.97	393	1560.2
	K	63	2.78	3.07	488	1498.2		K	75.5	3.11	3.52	488	1717.8
	L	51	2.25	2.52	582	1466.6		L	605	2.49	2.80	582	1629.6
(.60 X)	M	38	1.68	2.02	737	1488.7	(.60 X)	M	45	1.85	2.23	737	1643.5
(.75 X)	N	24	1.06	1.52	489	743.3	(.75 X)	N	31	1.28	1.71	489	836.2
						Sum = 10975.7							Sum = 11459.2
Area size			Amt. 3.83				Area size			Amt. 3.52			
	A	118.5	4.54	4.54	10	45.4		A	119.5	4.21	4.21	10	42.1
	B	114.5	4.39	4.47	15	67.0		B	116	4.08	4.15	15	62.2
2150/2	C	110.5	4.25	4.32	25	108.0	3000/2	C	112.5	3.96	4.02	25	100.5
	D	108.5	4.16	4.21	50	210.5		D	110	3.87	3.92	50	196.0
	E	106.5	4.08	4.12	75	309.0		E	108	3.80	3.84	75	288.0
	F	104.5	4.00	4.04	125	505.0		F	106	3.77	3.77	125	471.2
	G	102	3.91	3.96	150	594.0		G	104	3.66	3.70	150	555.0
	H	100	3.83	3.96	250	967.5		H	102	3.59	3.63	250	907.5
	I	99	3.79	3.81	271	1032.5		I	100.5	3.54	3.56	271	964.8
	J	97	3.72	3.76	393	1477.7		J	99	3.48	3.51	393	1379.4
	K	96	3.68	3.70	488	1805.6		K	97	3.41	3.45	488	1683.6
	L	73	2.80	3.24	582	1885.7		L	96	3.38	3.40	582	1978.8
(.60 X)	M	54	2.07	2.62	737	1930.9	(.60 X)	M	67	2.36	2.97	737	2188.9
(.75 X)	N	37.5	1.44	1.91	489	934.0	(.75 X)	N	45	1.58	2.17	489	1061.1
						Sum = 11872.8							Sum = 11879.1

Table 22.—Completed computation sheets for 1st, 2nd and 3rd 6-hr increments for Leon River, TX drainage - Continued

Increment: 3

Drainage: Leon River, TX Area: 3,660 mi^2 Date:

	I	II	III	IV	V	VI		I	II	III	IV	V	VI
Area size	Iso.	Nomo.	Amt. 2.89	Avg. depth	ΔA	ΔV	Area size	Iso.	Nomo.	Amt. 2.70	Avg. depth	ΔA	ΔV
	A	104.6	3.02	3.02	10	30.2		A	105	2.84	2.84	10	28.4
	B	103.3	2.98	3.00	15	45.0		B	103.8	2.80	2.82	15	42.3
1000/3	C	102.3	2.96	2.97	25	74.2	1500/3	C	102.7	2.77	2.785	25	69.6
	D	101.3	2.93	2.945	50	147.2		D	101.7	2.74	2.755	50	137.8
	E	100.6	2.91	2.92	75	219.0		E	101	2.73	2.735	75	205.1
	F	100.3	2.90	2.905	125	393.1		F	100.7	2.72	2.725	125	340.6
	G	99.9	2.89	2.895	150	434.2		G	100.3	2.71	2.715	150	407.2
	H	99.6	2.88	2.885	250	721.2		H	100	2.70	2.705	250	676.2
	I	99.3	2.87	2.875	271	779.1		I	99.7	2.69	2.695	271	730.3
	J	82.5	2.38	2.70	393	1061.1		J	99.4	2.68	2.685	393	1055.2
	K	67	1.94	2.16	488	1054.1		K	81	2.19	2.44	488	1190.7
	L	54	1.56	1.75	582	1018.5		L	65.5	1.77	1.98	582	1152.4
(.60 X)	M	43	1.24	1.43	737	1053.9	(.60 X)	M	51.5	1.39	1.62	737	1193.9
(.75 X)	N	31	.90	1.16	489	567.2	(.75 X)	N	38	1.03	1.30	489	635.7
					Sum =	7598.0						Sum =	7865.4
Area size			Amt. 2.50				Area size			Amt. 2.30			
	A	105.3	2.63	2.63	10	26.3		A	105.7	2.43	2.43	10	24.3
	B	104.2	2.60	2.615	15	39.2		B	104.6	2.41	2.42	15	36.3
2150/3	C	103.2	2.58	2.59	25	64.8	3000/3	C	103.5	2.38	2.40	25	60.0
	D	102	2.55	2.565	50	128.2		D	102.5	2.36	2.37	50	118.5
	E	101.3	2.53	2.54	75	190.5		E	101.7	2.34	2.35	75	176.3
	F	101	2.52	2.525	125	315.6		F	101.3	2.33	2.345	125	293.1
	G	100.6	2.52	2.52	150	378.0		G	100.9	2.32	2.335	150	350.2
	H	100.3	2.51	2.515	250	628.8		H	100.5	2.31	2.315	250	578.8
	I	100	2.50	2.505	271	678.8		I	100.2	2.30	2.305	271	624.6
	J	99.7	2.49	2.495	393	980.5		J	99.9	2.30	2.30	393	903.9
	K	99.5	2.49	2.49	488	1215.1		K	99.6	2.29	2.295	488	1120.0
	L	80.5	2.01	2.25	582	1309.5		L	99.3	2.28	2.285	582	1329.9
(.60 X)	M	61	1.52	1.81	737	1334.0	(.60 X)	M	76	1.75	2.07	737	1525.6
(.75 X)	N	46.5	1.16	1.43	489	699.3	(.75 X)	N	57	1.31	1.64	489	802.0
					Sum =	7988.6						Sum =	7943.5

Table 23.—Completed computation sheet for the 1st to 3rd 6-hr increments for supplemental isohyets on the Leon River, TX drainage

Increment: 1 to 3

Drainage: Leon River, TX Area: 3,660 mi^2 Date: _____

	I	II	III	IV	V	VI		I	II	III	IV	V	VI
Area size	Iso.	Nomo.	Amt. 12.12	Avg. depth	ΔA	ΔV	Area size	Iso.	Nomo.	Amt. 10.86	Avg. depth	ΔA	ΔV
	A	171	20.72	20.72	10	207.2		A	181	19.66	19.66	10	196.6
	B	160	19.39	20.06	15	300.9		B	169	18.35	19.00	15	285.0
1900/1	C	149	18.06	18.72	25	468.0	2400/1	C	158	17.16	17.76	25	444.0
	D	138	16.73	17.40	50	870.0		D	146	15.86	16.51	50	825.5
	E	128	14.51	16.12	75	1209.0		E	134	14.55	15.20	75	1140.0
	F	118	14.30	14.90	125	1862.5		F	125	13.58	14.06	125	1757.5
	G	110	13.33	13.82	150	2073.0		G	116	12.60	13.09	150	1963.5
	H	100	12.12	12.72	250	3180.0		H	106	11.51	12.06	250	3015.0
	I	93	11.27	11.70	271	3170.7		I	97	10.53	11.02	271	2986.4
	J	84	10.18	10.72	393	4213.0		J	88	9.56	10.04	393	3945.7
	-	78	9.45	9.82	345	3387.9		K	79	8.98	9.07	488	4426.2
	K	68	8.24	8.84	143	1264.1		-	76	8.25	8.42	211	1776.6
	L	48	5.82	7.03	582	4091.5		L	58	6.30	7.28	371	2700.9
(.60 X)	M	30	3.64	4.95	737	3548.2	(.60 X)	M	36	3.91	5.34	737	3935.6
(.75 X)	N	18	2.18	3.28	489	1603.9	(.75 X)	N	21	2.28	3.50	489	1711.5
					Sum =	31449.9						Sum =	31110.0
Area size			Amt. 3.93				Area size			Amt. 3.73			
	A	118	4.64	4.64	10	46.4		A	119	4.44	4.44	10	44.4
	B	116	4.56	4.60	15	69.0		B	115	4.29	4.36	15	65.4
1900/2	C	111	4.36	4.46	25	111.5	2400/2	C	112	4.18	4.24	25	106.0
	D	108	4.24	4.30	50	215.0		D	109	4.06	4.12	50	206.0
	E	106	4.16	4.20	75	315.0		E	107	3.99	4.025	75	301.9
	F	104	4.09	4.125	125	515.6		F	105	3.92	3.955	125	494.4
	G	102	4.01	4.05	150	607.5		G	103	3.84	3.88	150	582.0
	H	100	3.93	4.97	250	1242.5		H	101	3.77	3.805	250	951.2
	I	98	3.85	3.89	271	1054.2		I	99	3.69	3.73	271	1010.8
	J	96.5	3.79	3.82	393	1501.3		J	97.5	3.64	3.665	393	1440.3
	-	95.5	3.75	3.77	345	1300.6		K	96.5	3.60	3.62	488	1766.6
	K	86	3.38	3.57	143	510.5		-	96	3.58	3.59	211	757.5
	L	68	2.67	3.03	582	1763.5		L	78	2.91	3.25	371	1205.8
(.60 X)	M	50.5	1.98	2.39	737	1761.4	(.60 X)	M	57.5	2.14	2.60	737	1916.2
(.75 X)	N	37	1.48	1.86	489	909.5	(.75 X)	N	40	1.49	1.98	489	968.2
					Sum =	11923.5						Sum =	11816.7
Area size			Amt. 2.56				Area size			Amt. 2.43			
	A	105.2	2.69	2.69	10	26.9		A	105.4	2.56	2.56	10	25.6
	B	104.1	2.66	2.675	15	40.1		B	104.3	2.53	2.545	15	38.2
1900/3	C	103	2.64	2.65	25	66.2	2400/3	C	103.3	2.51	2.52	25	63.0
	D	102	2.61	2.625	50	131.2		D	102.3	2.48	2.495	50	124.8
	E	101.2	2.59	2.06	75	195.0		E	101.5	2.47	2.475	75	185.6
	F	100.8	2.58	2.585	125	323.1		F	101.0	2.45	2.46	125	307.5
	G	100.5	2.57	2.575	150	386.2		G	100.7	2.45	2.45	150	367.5
	H	100.2	2.56	2.565	250	641.2		H	100.3	2.44	2.445	250	611.2
	I	99.8	2.55	2.555	271	692.4		I	100.0	2.43	2.435	271	659.9
	J	99.6	2.55	2.55	393	1000.2		J	99.8	2.42	2.425	393	953.0
	-	99.4	2.54	2.545	345	878.0		K	99.4	2.42	2.42	488	1181.0
	K	92	2.36	2.45	143	350.4		-	99.3	2.41	2.415	211	509.6
	L	75	1.92	2.14	582	1245.5		L	86	2.09	2.25	371	834.8
(.60 X)	M	58	1.48	1.74	737	1285.3	(.60 X)	M	66	1.60	1.89	737	1392.9
(.75 X)	N	43	1.10	1.39	489	679.7	(.75 X)	N	49.5	1.20	1.50	489	733.5
					Sum =	7940.5						Sum =	7988.1

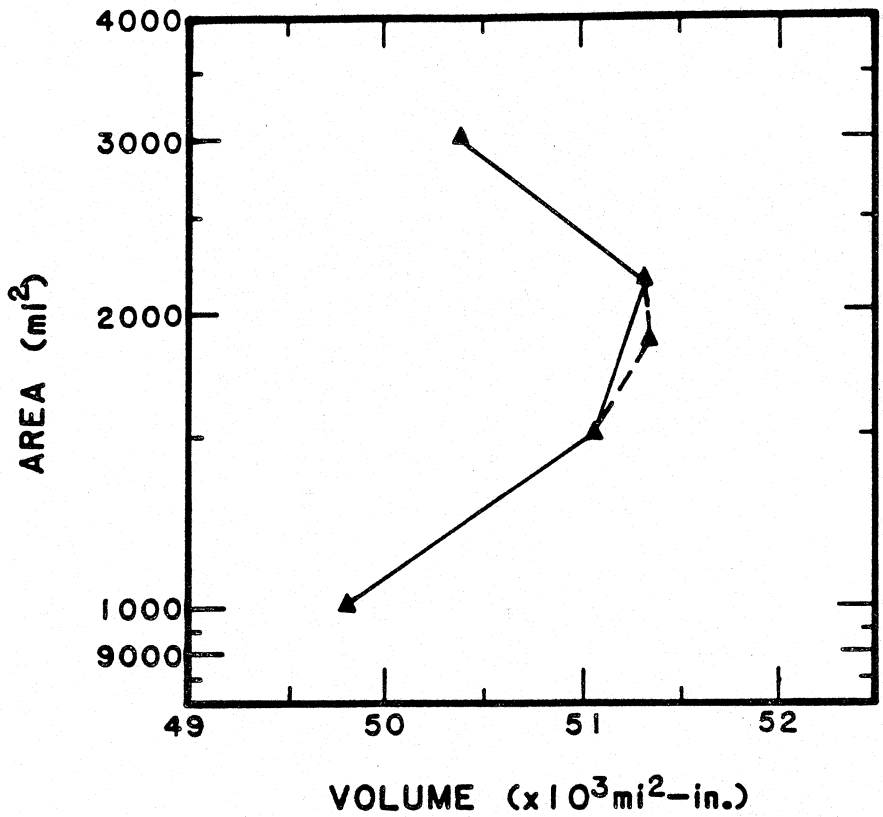

Figure 47.—Volume vs. area curve for 1st three 6-hr increments for Leon River, TX drainage.

D2. Successively subtract the 6-hr values in step D1.

6-hr periods

	1	2	3	4	5	6	7	8	9	10	11	12
Increm. PMP (in.)	12.9	4.3	2.8	2.3	1.5	1.2	1.0	0.8	0.9	0.8	0.7	0.7

We read slightly different values (read to hundreths) in smoothed data from figure 45 for the 1st three 6-hr increments, which we substitute here, for consistency.

Note that to assure a series of decreasing values it was necessary to reverse the values for the 8th and 9th increment. This does not cause any problem for our computations.

6-hr periods

	1	2	3	4	5	6	7	8	9	10	11	12
Increm. PMP (in.)	12.82	4.27	2.79	2.30	1.50	1.20	1.00	0.90	0.80	0.80	0.70	0.70

Multiply each of these 6-hr incremental PMP by 89.7% to reduce them for orientation.

	6-hr periods											
	1	2	3	4	5	6	7	8	9	10	11	12
Adj. PMP (in.)	11.50	3.83	2.50	2.06	1.34	1.08	0.90	0.81	0.72	0.72	0.63	0.63

D3. Isohyet values are then obtained by multiplying the 1st 6-hr value in step D2 by the percentages for 2,150 mi^2 from table 15 or the 1st 6-hr nomogram (fig. 16), the 2nd 6-hr value by the percentages in table 16 or figure 18, the 3rd 6-hr value by the percentages in table 17 or figure 19, and the fourth through 12th 6-hr values by the percentages in table 18 or figure 20 as shown in table 24. In section 3.5.3, we have explained that the fourth through 12th 6-hr increments are assumed uniform. Thus, a constant value is used through the extent of the area size of PMP, 2,150 mi^2 in this example.

Table 24.—Isohyet values (in.), Leon River, TX, for example 1a

Isohyet	6-hr periods 1	2	3	4	5	6	7	8	9	10	11	12
A	20.24	4.54	2.63	2.06	1.34	1.08	0.90	0.81	0.72	0.72	0.63	0.63
B	18.98	4.39	2.61	2.06	1.34	1.08	0.90	0.81	0.72	0.72	0.63	0.63
C	17.17	4.25	2.58	2.06	1.34	1.08	0.90	0.81	0.72	0.72	0.63	0.63
D	16.33	4.16	2.56	2.06	1.34	1.08	0.90	0.81	0.72	0.72	0.63	0.63
E	15.07	4.08	2.53	2.06	1.34	1.08	0.90	0.81	0.72	0.72	0.63	0.63
F	14.03	4.00	2.53	2.06	1.34	1.08	0.90	0.81	0.72	0.72	0.63	0.63
G	12.99	3.91	2.52	2.06	1.34	1.08	0.90	0.81	0.72	0.72	0.63	0.63
H	11.85	3.83	2.51	2.06	1.34	1.08	0.90	0.81	0.72	0.72	0.63	0.63
I	10.93	3.77	2.50	2.06	1.34	1.08	0.90	0.81	0.72	0.72	0.63	0.63
J	9.89	3.72	2.49	2.06	1.34	1.08	0.90	0.81	0.72	0.72	0.63	0.63
K	8.86	3.68	2.48	2.06	1.34	1.08	0.90	0.81	0.72	0.72	0.63	0.63
L	5.98	2.80	2.03	1.66	1.08	0.87	0.72	0.65	0.58	0.58	0.51	0.51
M	3.80	2.07	1.55	1.26	0.82	0.66	0.55	0.49	0.44	0.44	0.38	0.38
N	2.30	1.44	1.16	0.96	0.62	0.50	0.42	0.38	0.33	0.33	0.29	0.29

Note: The results shown in this matrix emphasize the fact that for the fourth through 12th 6-hr period the distribution of PMP is uniform across the PMP portion of the pattern (A through K) for each increment. However, isohyets L to N represent residual precipitation for the 2,150-mi^2 pattern and these isohyets are assigned decreasing values.

D4. The values in table 24 represent the incremental isohyetal values for the Leon River drainage with the 2,150-mi^2 PMP pattern placed as shown in figure 46. To obtain incremental average depths (PMP) for this drainage it is necessary to compute the incremental volumes as determined from the tabulated isohyetal values according to the procedures described for figure 41, and then divide each incremental volume by the drainage area. This results in the following incremental average depths. (See computations in table 25.)

Table 25.—Completed computation sheets showing typical format to get incremental drainage-average depths, Leon River, TX

Increment: 1 to 6

Drainage: Leon River, TX Area: 3,660 mi^2 Date: _____

	I	II	III	IV	V	VI		I	II	III	IV	V	VI
Area size	Iso.	Nomo.	Amt. 11.50	Avg. depth	ΔA	ΔV	Area size	Iso.	Nomo.	Amt. 2.06	Avg. depth	ΔA	ΔV
	A		20.24	20.24	10	202.4		A	100	2.06	2.06	10	20.6
	B		18.98	19.61	15	294.2		B	100	2.06	2.06	15	30.9
2150/1	C		17.71	18.35	25	458.8	2150/4	C	100	2.06	2.06	25	51.5
	D		16.33	17.02	50	851.0		D	100	2.06	2.06	50	103.0
	E		15.07	15.70	75	1177.5		E	100	2.06	2.06	75	154.5
	F		14.03	14.55	175	1818.8		F	100	2.06	2.06	125	257.5
	G		12.99	13.51	150	2026.5		G	100	2.06	2.06	150	309.0
	H		11.85	12.42	250	3105.0		H	100	2.06	2.06	250	515.0
	I		10.93	11.39	271	3086.7		I	100	2.06	2.06	271	558.3
	J		9.89	10.41	393	4091.1		J	100	2.06	2.06	393	809.6
	K		8.86	9.38	488	4577.4		K	100	2.06	2.06	488	1005.3
	L		5.98	7.42	582	4318.4		L	80.5	1.66	1.86	582	1082.5
(.60 X)	M		3.80	5.11	737	3766.1	(.60 X)	M	61	1.26	1.46	737	1076.0
(.75 X)	N		2.30	3.42	489	1672.4	(.75 X)	N	46.5	.96	1.11	489	542.8
				Total = 3660									
				Sum =		31446.3						Sum =	6516.5
				Avg. depth =		8.59					Avg. depth =		1.78
Area size			Amt. 3.83				Area size			Amt. 1.34			
	A				10	45.4		A	100	1.34	1.34	10	13.4
	B				15	67.0		B	100	1.34	1.34	15	20.1
2150/2	C				25	108.0	2150/5	C	100	1.34	1.34	25	33.5
	D				50	210.5		D	100	1.34	1.34	50	67.0
	E				75	309.0		E	100	1.34	1.34	75	100.5
	F				125	505.0		F	100	1.34	1.34	125	167.5
	G				150	594.0		G	100	1.34	1.34	150	201.0
	H				250	967.5		H	100	1.34	1.34	250	335.0
	I				271	1032.5		I	100	1.34	1.34	271	363.1
	J				393	1477.7		J	100	1.34	1.34	393	526.6
	K				488	1805.6		K	100	1.34	1.34	488	653.9
	L				582	1887.5		L	80.5	1.08	1.21	582	704.2
(.60 X)	M				737	1930.9	(.60 X)	M	61	0.82	0.95	737	700.2
(.75 X)	N				489	934.0	(.75 X)	N	46.5	0.62	0.72	489	352.1
				Sum =		11872.8						Sum =	4238.1
				Avg. depth =		3.24					Avg. depth =		1.16
Area size			Amt. 2.50				Area size			Amt. 1.08			
	A				10	26.3		A	100	1.08	1.08	10	10.8
	B				15	39.2		B	100	1.08	1.08	15	16.2
2150/3	C				25	64.8	2150/6	C	100	1.08	1.08	25	27.0
	D				50	128.2		D	100	1.08	1.08	50	54.0
	E				75	190.5		E	100	1.08	1.08	75	81.0
	F				125	315.6		F	100	1.08	1.08	125	135.0
	G				150	378.0		G	100	1.08	1.08	150	162.0
	H				250	628.8		H	100	1.08	1.08	250	270.0
	I				271	678.8		I	100	1.08	1.08	271	292.7
	J				393	980.5		J	100	1.08	1.08	393	424.4
	K				488	1215.1		K	100	1.08	1.08	488	527.0
	L				582	1309.5		L	80.5	0.87	0.98	582	570.4
(.60 X)	M				737	1334.0	(.60 X)	M	61	0.66	0.77	737	567.5
(.75 X)	N				489	699.3	(.75 X)	N	46.5	0.50	0.58	489	283.6
				Sum =		7988.6						Sum =	3421.6
				Avg. depth =		2.18					Avg. depth =		0.93

Table 25.—Completed computation sheets showing typical format to get incremental drainage-averaged depths, Leon River, TX. - Continued

Increment: 7 to 12

Drainage: Leon River, TX Area: 3,660 mi^2 Date:

	I	II	III	IV	V	VI
Area size	Iso.	Nomo.	Amt. 0.90	Avg. depth	ΔA	ΔV
	A	100	0.90	0.90	10	9
	B	100	0.90	0.90	15	13.5
2150/7	C	100	0.90	0.90	25	22.5
	D	100	0.90	0.90	50	45.0
	E	100	0.90	0.90	75	67.5
	F	100	0.90	0.90	125	112.5
	G	100	0.90	0.90	150	135.0
	H	100	0.90	0.90	250	225.0
	I	100	0.90	0.90	271	243.9
	J	100	0.90	0.90	393	353.7
	K	100	0.90	0.90	488	439.2
	L	80.5	0.72	0.81	582	471.4
(.60 X)	M	61	0.55	0.64	737	471.7
(.75 X)	N	46.5	0.42	0.49	489	239.6
					Sum =	2849.5
				Avg. depth =		0.78

	I	II	III	IV	V	VI
Area size	Iso.	Nomo.	Amt. 0.72	Avg. depth	ΔA	ΔV
	A	100	0.72	0.72	10	7.2
	B	100	0.72	0.72	15	10.8
2150/10	C	100	0.72	0.72	25	18.0
	D	100	0.72	0.72	50	36.0
	E	100	0.72	0.72	75	54.0
	F	100	0.72	0.72	125	90.0
	G	100	0.72	0.72	150	108.0
	H	100	0.72	0.72	250	180.0
	I	100	0.72	0.72	271	195.1
	J	100	0.72	0.72	393	282.9
	K	100	0.72	0.72	488	351.4
	L	80.5	0.58	0.65	582	378.3
(.60 X)	M	61	0.44	0.51	737	375.9
(.75 X)	N	46.5	0.33	0.39	489	190.7
					Sum =	2278.3
				Avg. depth =		0.62

	I	II	III	IV	V	VI
Area size	Iso.	Nomo.	Amt. 0.81	Avg. depth	ΔA	ΔV
	A	100	0.81	0.81	10	8.1
	B	100	0.81	0.81	15	12.2
2150/8	C	100	0.81	0.81	25	20.3
	D	100	0.81	0.81	50	40.5
	E	100	0.81	0.81	75	60.8
	F	100	0.81	0.81	125	101.3
	G	100	0.81	0.81	150	121.5
	H	100	0.81	0.81	250	202.5
	I	100	0.81	0.81	271	219.5
	J	100	0.81	0.81	393	318.3
	K	100	0.81	0.81	488	395.3
	L	80.5	0.65	0.73	582	424.9
(.60 X)	M	61	0.49	0.57	737	420.1
(.75 X)	N	46.5	0.38	0.44	489	215.2
					Sum =	2560.4
				Avg. depth =		0.70

	I	II	III	IV	V	VI
Area size	Iso.	Nomo.	Amt. 0.63	Avg. depth	ΔA	ΔV
	A	100	0.63	0.63	10	6.3
	B	100	0.63	0.63	15	9.5
2150/11	C	100	0.63	0.63	25	15.8
	D	100	0.63	0.63	50	31.5
	E	100	0.63	0.63	75	47.3
	F	100	0.63	0.63	125	78.8
	G	100	0.63	0.63	150	94.5
	H	100	0.63	0.63	250	157.5
	I	100	0.63	0.63	271	170.7
	J	100	0.63	0.63	393	247.6
	K	100	0.63	0.63	488	307.4
	L	80.5	0.51	0.57	582	331.7
(.60 X)	M	61	0.38	0.45	737	331.7
(.75 X)	N	46.5	0.29	0.34	489	166.3
					Sum =	1996.6
				Avg. depth =		0.54

	I	II	III	IV	V	VI
Area size	Iso.	Nomo.	Amt. 0.72	Avg. depth	ΔA	ΔV
	A	100	0.72	0.72	10	7.2
	B	100	0.72	0.72	15	10.8
2150/9	C	100	0.72	0.72	25	18.0
	D	100	0.72	0.72	50	36.0
	E	100	0.72	0.72	75	54.0
	F	100	0.72	0.72	125	90.0
	G	100	0.72	0.72	150	108.0
	H	100	0.72	0.72	250	180.0
	I	100	0.72	0.72	271	195.1
	J	100	0.72	0.72	393	282.9
	K	100	0.72	0.72	488	351.4
	L	80.5	0.58	0.65	582	378.3
(.60 X)	M	61	0.44	0.51	737	375.9
(.75 X)	N	46.5	0.33	0.39	489	190.7
					Sum =	2278.3
				Avg. depth =		0.62

	I	II	III	IV	V	VI
Area size	Iso.	Nomo.	Amt. 0.63	Avg. depth	ΔA	ΔV
	A	100	0.63	0.63	10	6.3
	B	100	0.63	0.63	15	9.5
2150/12	C	100	0.63	0.63	25	15.8
	D	100	0.63	0.63	50	31.5
	E	100	0.63	0.63	75	47.3
	F	100	0.63	0.63	125	78.8
	G	100	0.63	0.63	150	94.5
	H	100	0.63	0.63	250	157.5
	I	100	0.63	0.63	271	170.7
	J	100	0.63	0.63	393	247.6
	K	100	0.63	0.63	488	307.4
	L	80.5	0.51	0.57	582	331.7
(.60 X)	M	61	0.38	0.45	737	331.7
(.75 X)	N	46.5	0.29	0.34	489	166.3
					Sum =	1996.6
				Avg. depth =		0.54

	6-hr periods											
	1	2	3	4	5	6	7	8	9	10	11	12
Avg. PMP (in.)	8.59	3.24	2.18	1.78	1.16	0.93	0.78	0.70	0.62	0.62	0.54	0.54

These give a 72-hr total drainage-averaged PMP of 21.68 in., which can be compared to 27.4 in. for 3,660 mi^2 (from fig. 43), or a 21 percent reduction from HMR No. 51. The reduction is due to orientation and basin shape factors.

D5. a. At 31°45'N, 98°15'W, we read a 1/6-hr ratio of 0.306 from figure 39.

b. We adjust the scale for the nomogram in figure 40 such that the abscissa for the 20,000-mi^2 "A" isohyet reads 0.306.

c. With the scale set as in step D5b, we read ratios for the following isohyets.

Isohyet	1/6-hr ratio
A	.299
B	.298*
C	.297
D	.295*
E	.293
F	.2915*
G	.290
H	.2875*
I	.285
J	.282
K	.279

*interpolated isohyet on nomogram

d. Multiply the ratios in step D5c by the corresponding values from table 24 (1st 6-hr period only) to get the 1-hr isohyet values.

Isohyet	1-hr isohyet values
A	6.05
B	5.66
C	5.10
D	4.82
E	4.42
F	4.09
G	3.77
H	3.73
I	3.12
J	2.78
K	2.47

e. Plot the values in step D5d and those for the 4 greatest increments from table 24 and draw a smooth curve of best fit through these points with the origin as the starting point as shown in figure 48.

f. From figure 48, we can read isohyet values for any other duration less than 6 hr (see note in procedure step 7D5f).

g. The 4 greatest 6-hr incremental isohyet values for the M isohyet have also been plotted on figure 48 as an example of residual precipitation. It is apparent that this curve is flatter than those for the PMP portion of the pattern. Lesser errors are therefore likely in interpolating short duration isohyet values for residual precipitation than for those within the PMP area. (Note in procedure step 7D5f applies here and to 1-hr values for residual precipitation.)

7.3 Example 1b

As a comparison to the results of example 1a, we will now evaluate the maximum volume for the Leon River, Texas drainage when no adjustment for orientation is applied. In step B3, we obtained the orientation for PMP from figure 8 as 208° for 31°45'N, 98°15'W. Figure 10 indicates that within 40° of PMP orientation, no reduction need be applied to isohyets values. Subtracting 40° from 208°, we get an orientation of 168°. Thus, if we place the isohyetal pattern at an orientation of 168° on the Leon River drainage, as shown in figure 49, no adjustment is necessary. We must planimeter the areas between each of the incomplete isohyets, and then refer to step C in the procedure.

C. Complete the computational process of figure 41 for the area sizes considered in example 1a. We have omitted the 1,000- and 15,000-mi^2 areas based on the outcome of example 1a. Note that the nomogram percentages will be the same as those used in example 1a, but the amount heading column III is now unadjusted for orientation; i.e., smoothed values from figure 45.

Table 26 presents completed computations for this example. The preliminary maximum volume for the first 6-hr increment appears to occur between 6,500 and 10,000 mi^2. To check on this outcome, the 15,000-mi^2 area pattern volume was determined and was found to be significantly less than that at 10,000 mi^2. Computation of the 2nd and 3rd 6-hr increments for the standard isohyet areas between 4,500 and 15,000 mi^2 resulted in 18-hr volumes ranging between 45,000 and 49,000 mi^2-in.

Note that by not adjusting the isohyets for orientation, the PMP pattern area of maximum volume has greatly increased from 2,150 mi^2 in example 1a to 10,000 mi^2 in this example, but the total volume as decreased. This occurs because some of the larger isohyets become more effective as the isohyet values increase with increasing area, and combine with proportionately larger incremental areas. At the same time the volume contributed by the isohyets enclosing smaller areas has been markedly reduced.

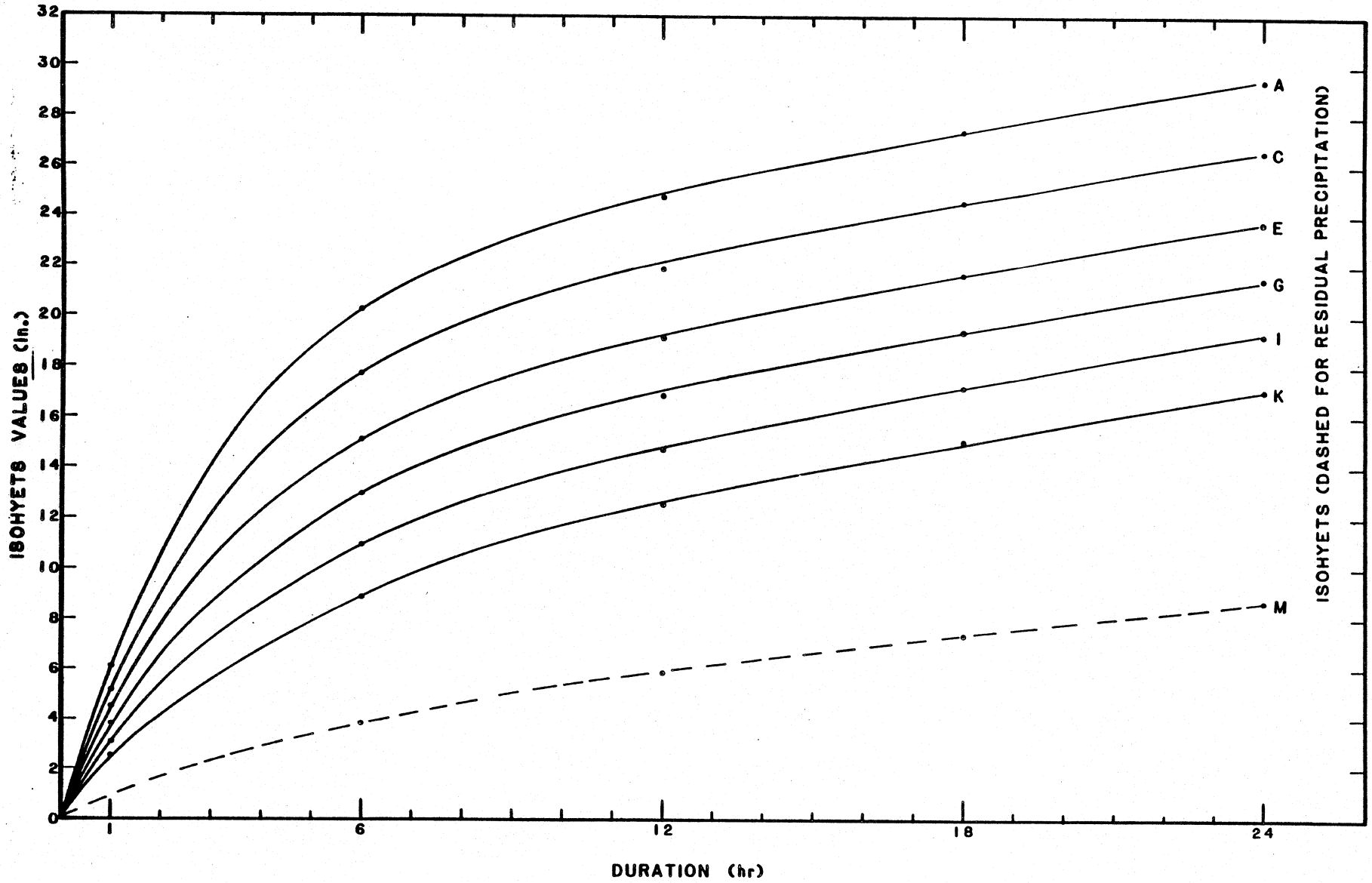

Figure 48.—Smoothed durational curves used to interpolate short-duration isohyet values for the Leon River, TX drainage.

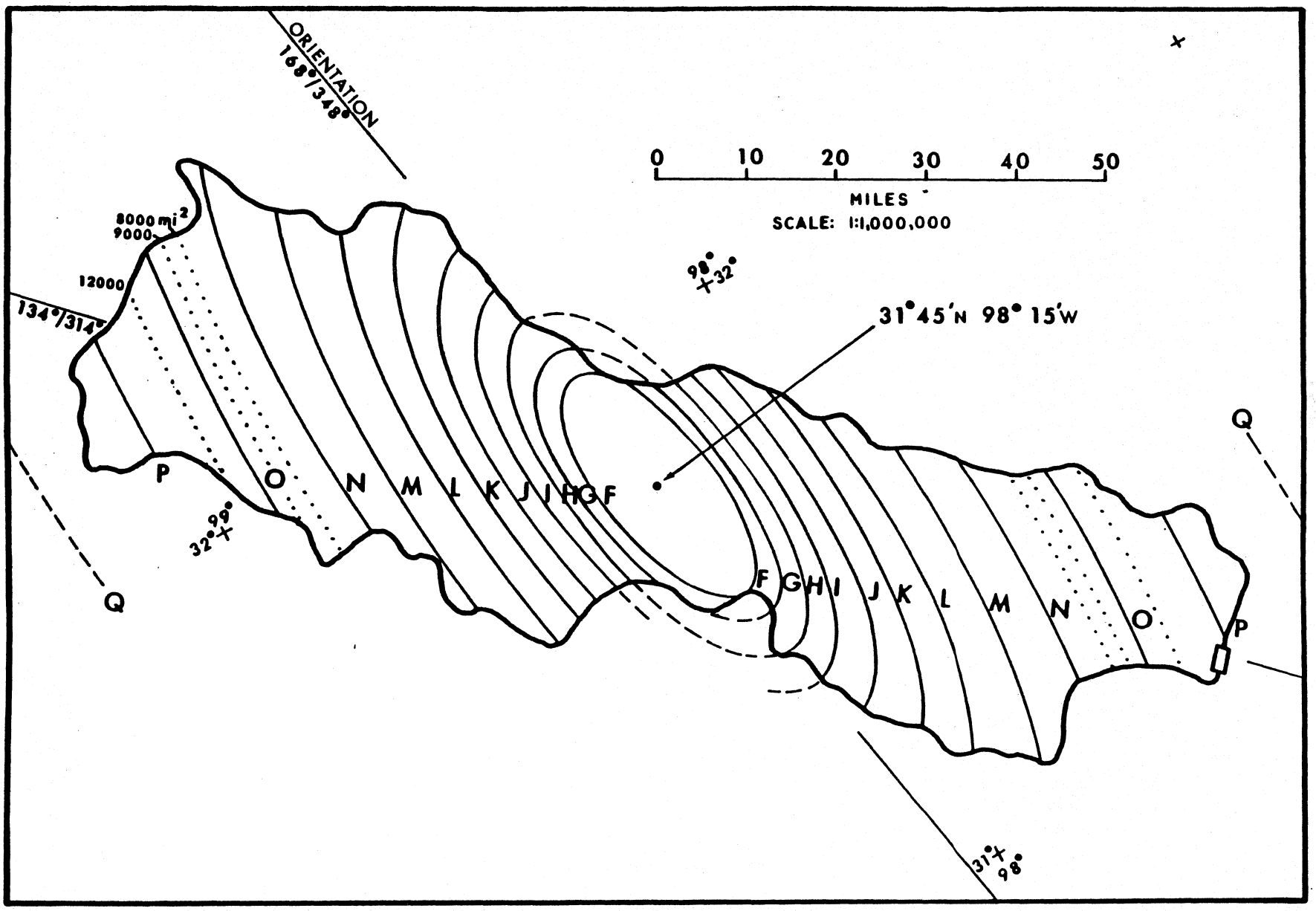

Figure 49.—Alternate placement of isohyetal pattern on Leon River, TX drainage such that no adjustment is applicable for orientation.

HYDROLOGIC ROUTING

NATIONAL 42-381 50 SHEETS 5 SQUARE 42-382 100 SHEETS 5 SQUARE 42-389 200 SHEETS 5 SQUARE

FLOOD ROUTING

I. Hydrologic (Lumped) Models

- Reservoir Routing
- Streamflow Routing

II Hydraulic (Distributed) Models

- Governing Equations (St. Venant)
- Hydrologic vs Hydraulic Routing
- Kinematic Wave
- Dynamic Wave (Implicit)
- DWOPER
- DAMBRK (Dam break analysis)
  - Users Manual
  - Application

Routing

Lumped - Hydrologic Routing

Reservoin (Level Pool)

Streamflow (Muskingum)

Distributed - Hydraulic Routing

Kinematic Wave

Muskingum - Cunge - constants vary

Dynamic Wave

NATIONAL 42-381 50 SHEETS 5 SQUARE 42-382 100 SHEETS 5 SQUARE 42-389 200 SHEETS 5 SQUARE

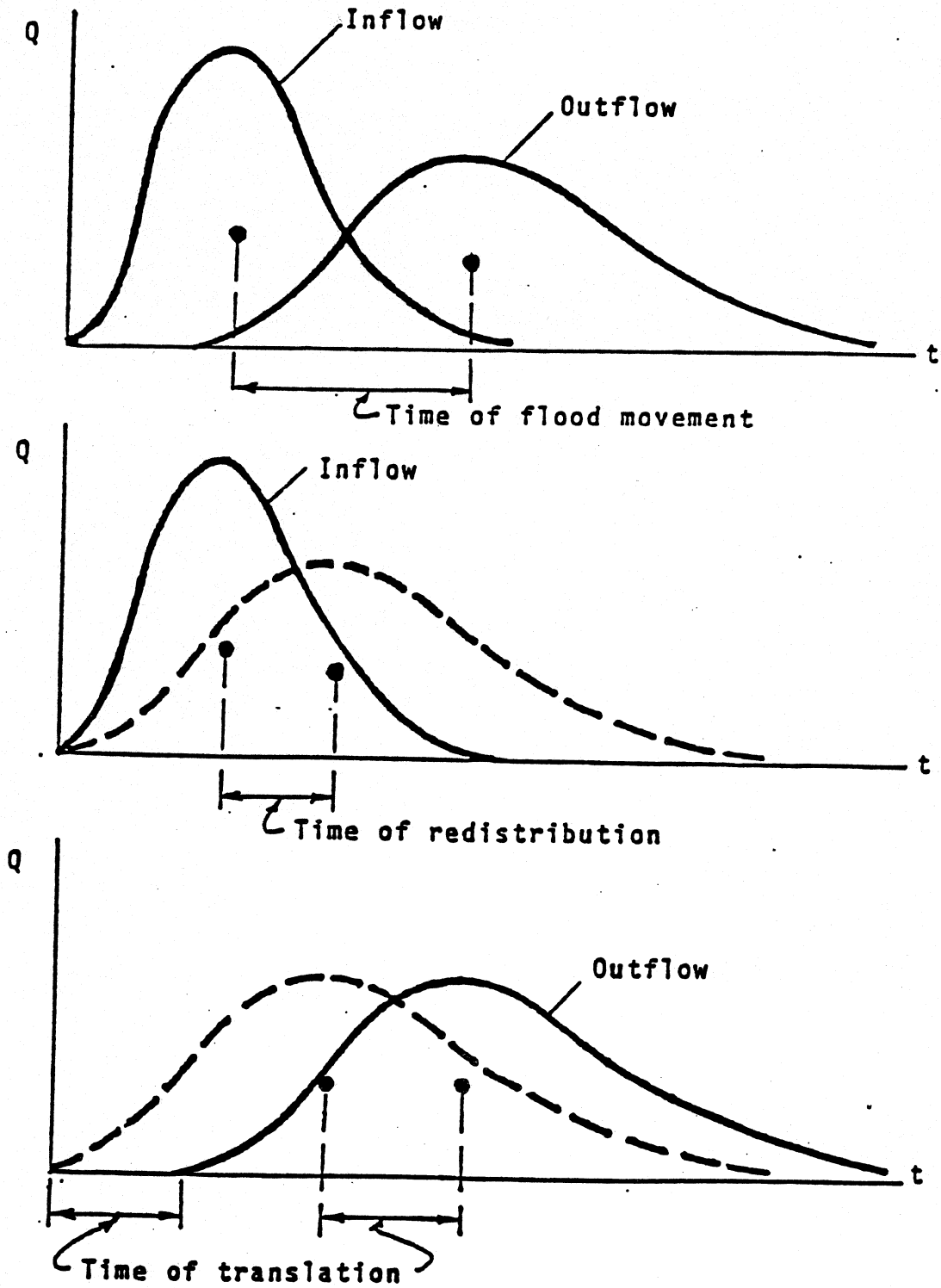

Figure 9.2.2. Theoretical Interpretation of the Time of Flood Movement

Storage Routing

$$\frac{dS}{dt} = I - Q$$ Continuity Equation

$$S = f(I, Q)$$ Storage Function

S - storage in pond or stream reach (ft^3)

I - inflow (cfs)

Q - outflow (cfs)

f - a function dependent on type of storage

Advantages

- Solution is exact when $S = f(Q)$ only (level pool)
- Readily worked out on calculator or small computor.

Limitations

- Solution is approximate for $S = f(I, Q)$ (rivers)
- Storage function may not account correctly for mechanics for flow.

Routing

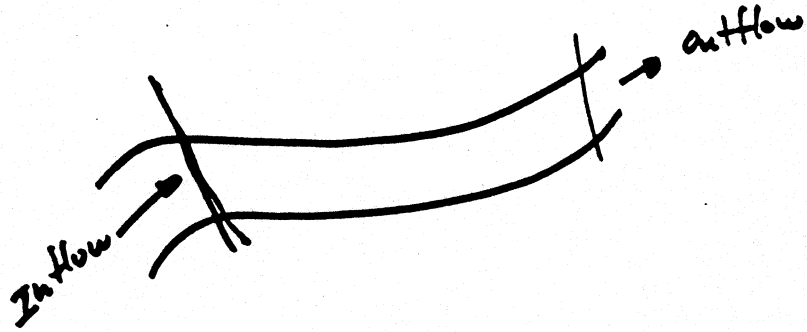

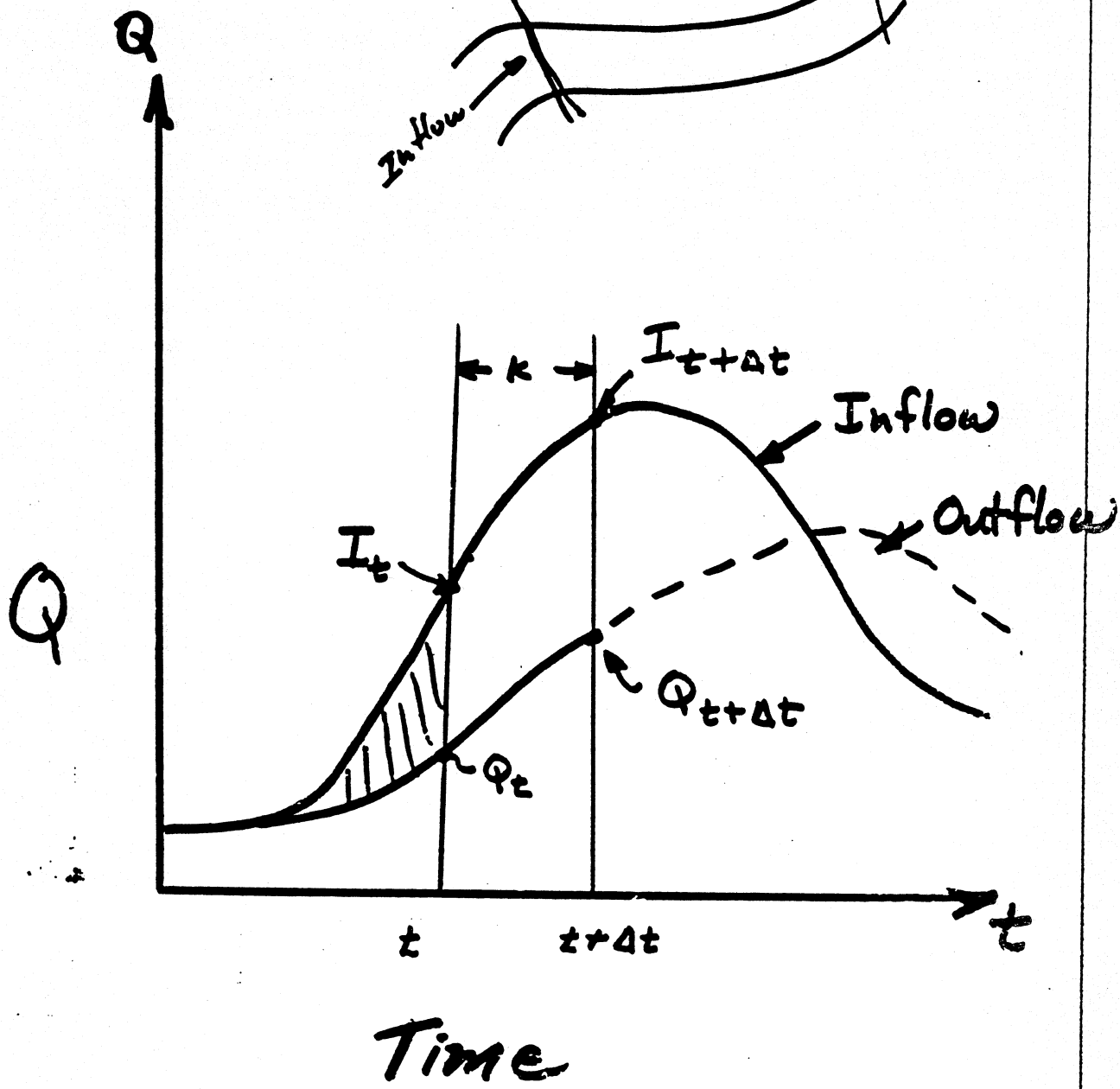

$$\bar{I} - \bar{Q} = \frac{dS}{dt}$$

$$\frac{I_t + I_{t+\Delta t}}{2} - \frac{Q_t + Q_{t+\Delta t}}{2} = \frac{S_{t+\Delta t} - S_t}{\Delta t}$$

Routing

Essentially a hydrograph is a record of the movement of a wave past a gaging station. As the wave moves downstream, its shape is changed by the addition of flow from tributaries, and velocities at various points along the wave differ. All hydrologic routing methods are founded upon the equation of continuity

$$\bar{I} - \bar{O} = \frac{ds}{dt}$$

where $\bar{I}$ = average rate of inflow for time dt
$\bar{O}$ = average rate of outflow for time dt
ds/dt = rate of change of storage

The above continuity equation can be rewritten as follows:

$$\frac{I_n + I_{n+1}}{2} - \frac{O_n + O_{n+1}}{2} = \frac{S_{n+1} - S_n}{\Delta t}$$

where n refers to time t and n+1 refers to time t + Δt. Also,

$$I_n + I_{n+1} + \left(\frac{2S_n}{\Delta t} - O_n\right) = \frac{2S_{n+1}}{\Delta t} + O_{n+1}$$

for which the only unknowns are S_{n+1} and O_{n+1} which are at times t + Δt.

Because there are two unknowns S_{n+1} and O_{n+1}, a second equation is needed which must relate the storage to the outflow.

Take, for example, a reservoir with a spillway. Knowing the head-discharge curve or elevation-discharge curve and the elevation-storage curve for the reservoir, we can obtain a useful relationship.

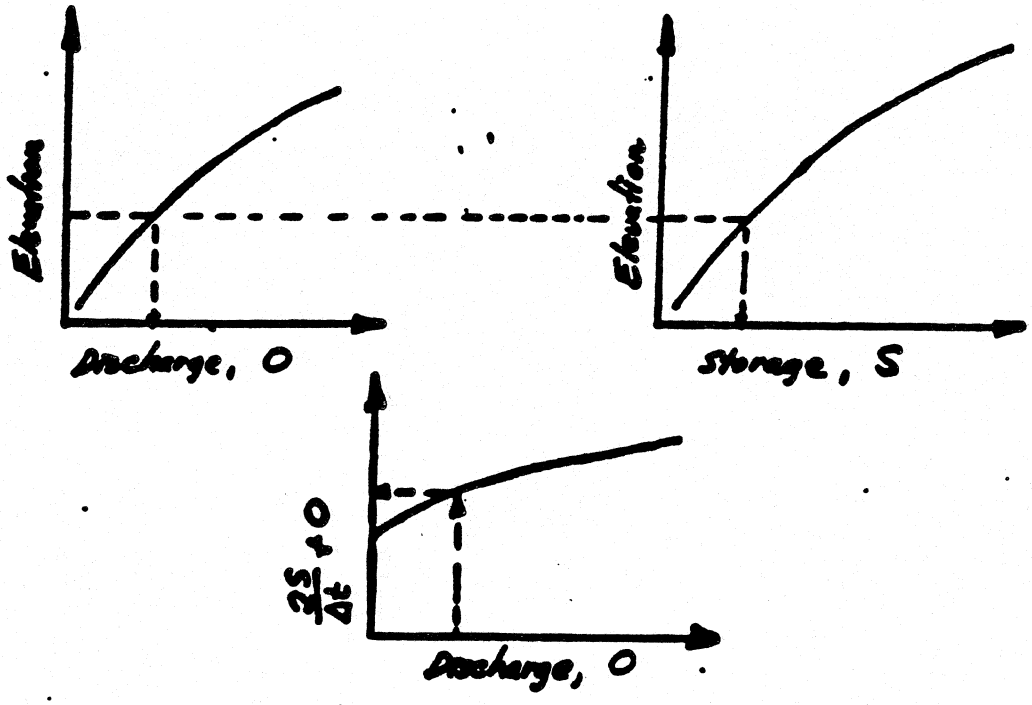

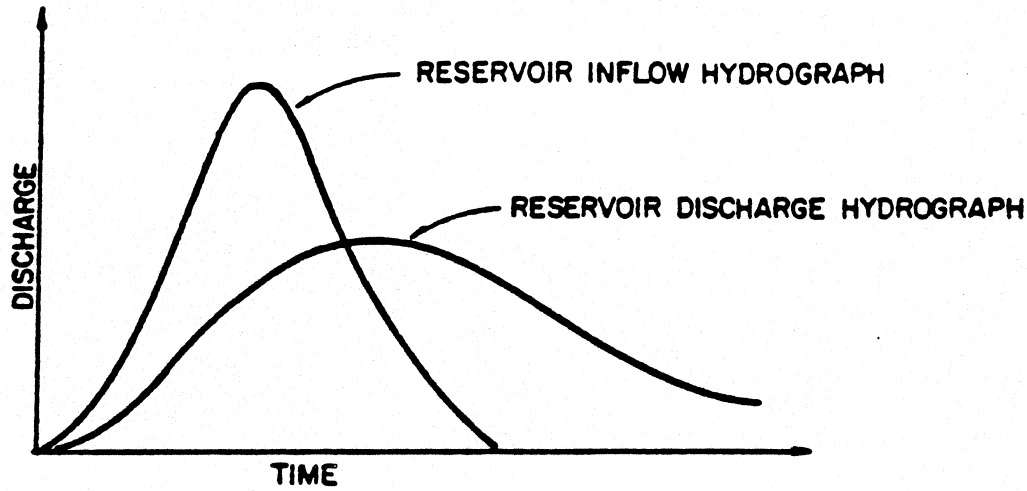

FIGURE 9.2.3a RESERVOIR INFLOW AND OUTFLOW

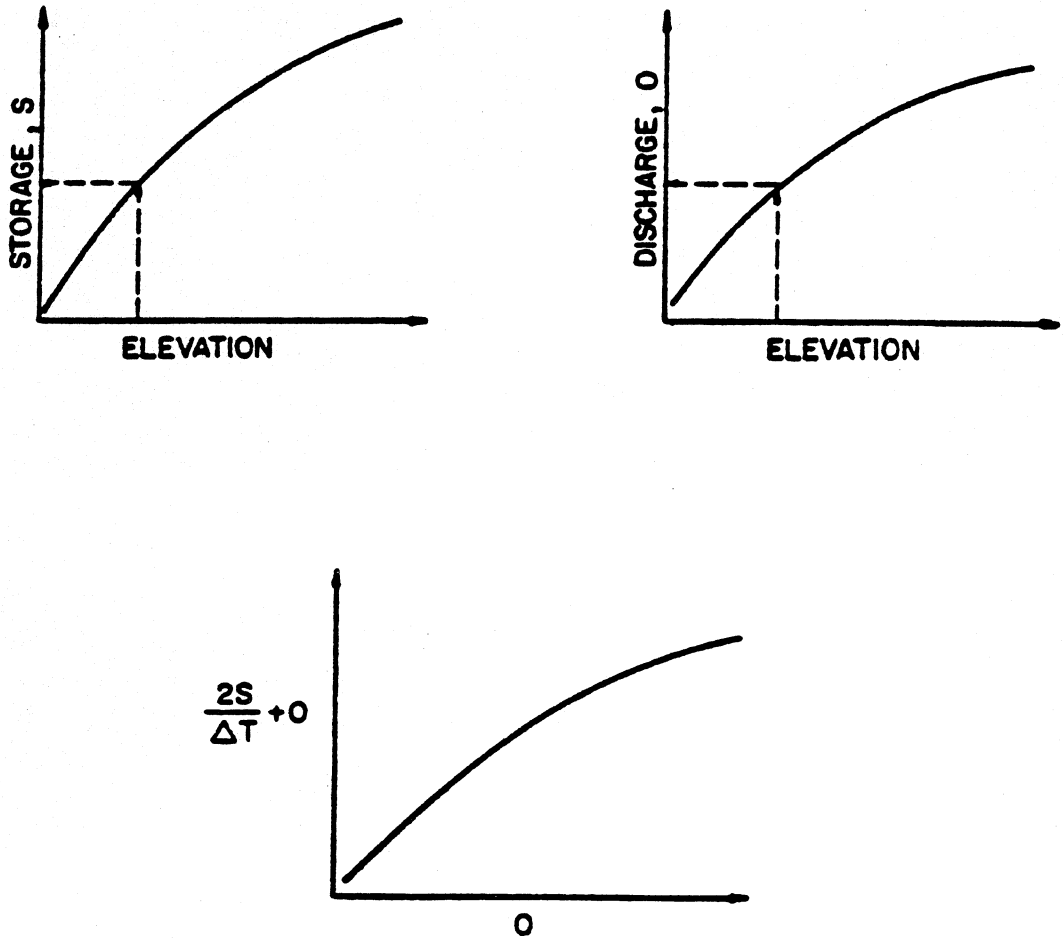

FIGURE 9.2.3b DEVELOPMENT OF RESERVOIR ROUTING CURVE

Table 9.2.1 Spillway Discharge Equations*

Spillway Type	Equation	Notation
Uncontrolled overflow ogee crest	$Q = CLH^{3/2}$	Q = discharge, cfs C = variable coefficient of discharge L = effective length of crest H = total head on the crest including velocity of approach head.
Gate controlled ogee crest	$Q = \frac{2}{3}\sqrt{2g}\ CL\left(H_1^{3/2}-H_2^{3/2}\right)$	H_1 = total head to bottom of the orifice H_2 = total head to top of the orifice C = coefficient which differs with gate and crest arrangement
Morning Glory spillway	$Q = C_0(2\pi R_s)H^{3/2}$	C_o = coefficient related to H and R_s R_s = radius to the outside periphery of the overflow crest H = total head
Culvert (submerged inlet control)	$Q = CdWD\sqrt{2gH}$	W = entrance width D = height of opening

* Refer to Design of Small Dams, Bureau of Reclamation, U.S. Department of the Interior, 1973.

Problem 1

For a reservoir with the outflow-elevation curve (Fig. A) and the storage-elevation curve (Fig. B), route the storm inflow hydrograph for the upstream end of the reservoir through the reservoir. Use 10 minute time intervals. The reservoir is full to the bottom of the spillway at elevation 1160. What is the maximum height of water in the reservoir? At what elevation should the top of the dam be placed to obtain 5 ft. of free board? What is the reduction in peak discharge and the delay in time to peak?

Developing the $\frac{2S}{t} + O$ vs. O curve for a routing period of 10 min (600 sec)

(1)	(2)	(3)	(4)	(5)
Elevation (ft)	Storage ($10^6 \times ft^3$)	$\frac{2S}{\Delta t}$ (cfs)	O (cfs)	$\frac{2S}{\Delta t} + O$ (cfs)
1150	22.5	75,000	0	75,000
1155	32	106,666	0	106,000
1160	42	140,000	0	140,000
1162	48	160,000	140	160,140
1164	54	180,000	400	180,400
1166	62	206,667	760	207,427
1168	71	236,666	1180	237,846
1170	80	266,666	1640	268,306
1172	87	290,000	2060*	292,060

Col(2) = Storage vs. Elev. Curve (Fig B)

Col(3) = $\frac{2S}{t} = \frac{2S}{600}$ (cfs)

Col(4) = Outflow vs. Elev. Curve (Fig A)

Col(5) = Col(3) + Col(4)

* = Estimated value from chart.

Routing the Storm Hydrograph through the Reservoir.

(1)	(2)	(3)	(4)	(5)	(6)
Time (min)	Inflow (cfs)	$I_n + I_{n+1}$	$\frac{2S_n}{t} - O_n$ (cfs)	$\frac{2S_{n+1}}{t} + O_{n+1}$ (cfs)	O_{n+1} (cfs)
0	0		140,000	140,000	0
		100			
10	100		140,090	140,100	5
		750			
20	650		140,820	140,840	10
		2200			
30	1550		142,980	143,020	20
		3550			
40	2000		146,470	146,530	30
		4475			
50	2475		150,825	150,945	60
		4475			
60	2000		155,100	155,300	100
		3750			
70	1750		158,610	158,850	120
		1650			
80	900		159,960	160,260	150
		1425			
90	525		161,075	161,385	155
		925			
100	400		161,680	162,000	160
		600			
110	200		161,950.	162,280	165
		250			
120	50		161,880	162,200	160
		75			
130	25		161,641	161,955	157
		25			
140	0			161,666	150

Initially at Elev. 1160' → $\frac{2S}{t} + O = 140{,}000$ cfs & $O = 0$ cfs

Col (2) = From Fig C → Storm Inflow Hydrograph.

Col (3) = $I_n + I_{n+1}$

Col (4) = $\left(\frac{2S_n}{t} - O_n\right) = \left(\frac{2S_n}{t} + O_n\right) - 2O_n$

Col (5) = $(I_n + I_{n+1}) + \left(\frac{2S_n}{t} - O_n\right) = \left(\frac{2S_{n+1}}{t} + O_{n+1}\right)$

Col (6) = From graph of $\frac{2S}{t} + O$ vs. O

SS# _____

Problem 4

For a reservoir located in Klump, Texas, eight miles from Bleiblerville, Texas, having an uncontrolled ogee spillway, a morning glory spillway, and a siphon spillway (elevation -discharge curves shown in Figure 4B) route the storm inflow hydrograph (Figure 4.A) through the reservoir. The elevation-storage curve for the reservoir is shown in Figure 4.C. Use a routing interval of 60 min. The reservoir level is initially at elevation 990.

Determine $\frac{2S}{\Delta t} + O$ vs O Curve.

Elevation	Discharge (ft^3/sec)	Storage (10^6) (ft^3)	$\frac{2S}{\Delta t} + O$ $\times 10^3$	O
990	0	10	5.55	0
993	360	20	11.47	360
995	550	24.5	14.16	550
998	1700	28.7	17.64	1700
1000	2260	32.5	20.32	2260
1004	2780	37.5	20.83	2780
1007	3970	41.0	26.47	3970
1010	4410	44.	28.85	4410
1015	4940	50.	32.72	4940
1020	5390	58.	37.61	5390

Routing Computations

Inflow	$I_n + I_{n+1}$	$\frac{2S}{\Delta t} - O$	$\frac{2S}{\Delta t} + O$	O
1000	3000	5550		0
2000	7000	8250	8550	150
5000	10000	13250	15250	1000
5000	10000	16650	23250	3300
5000	6000	18650	26650	4000
1000	2000	17450	24650	3600
1000	2000	15250	19450	2100
1000	2000	14050	17250	1600
1000	2000	13650	16050	1200
1000	2000	13450	15650	1100
1000	2000	13350	15450	1050
1000	2000	13350	15350	1000
			15350	1000

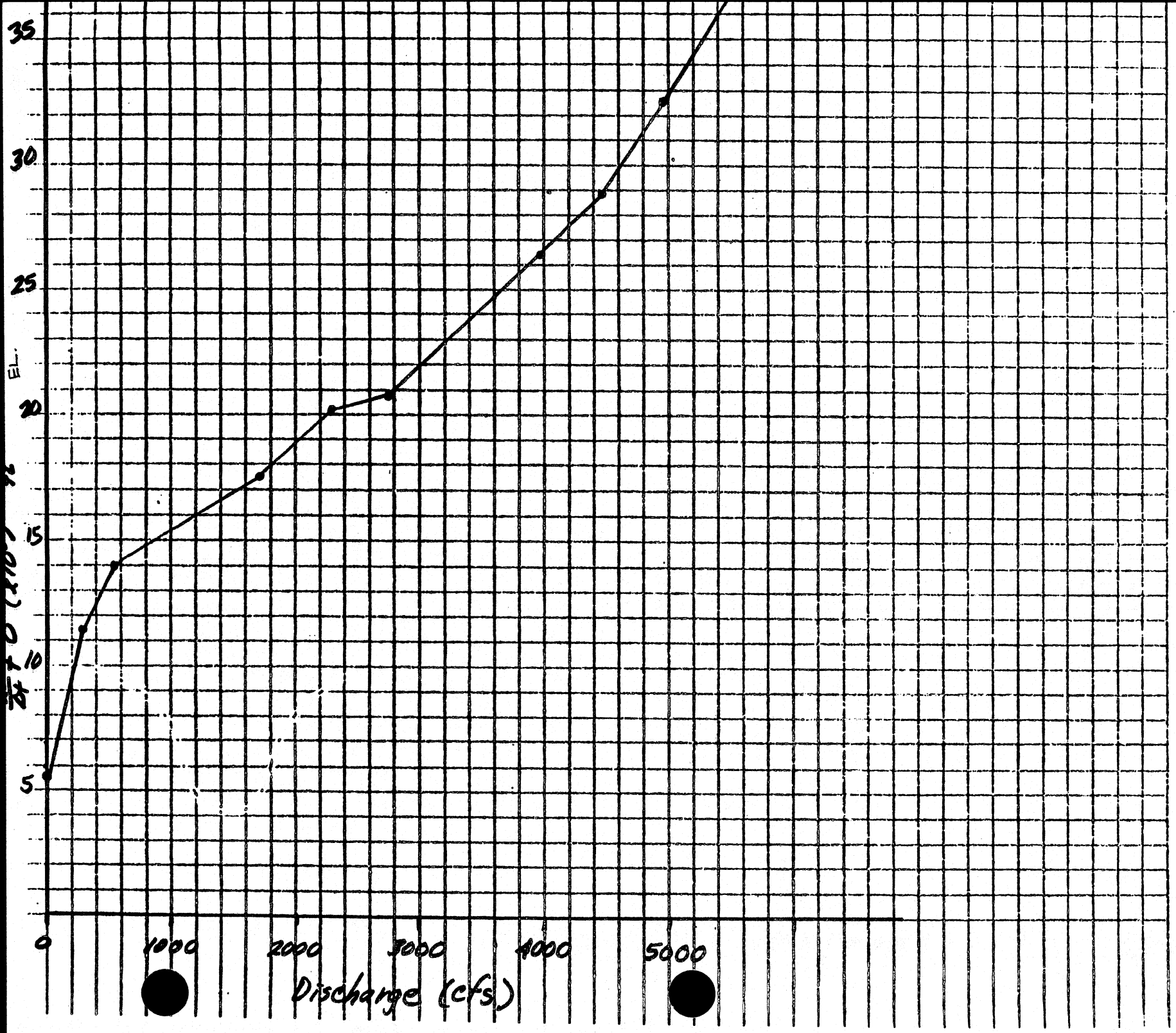
35
30
25
20
15
10
5
EL.
0
1000
2000
3000
4000
5000
Discharge (cfs)

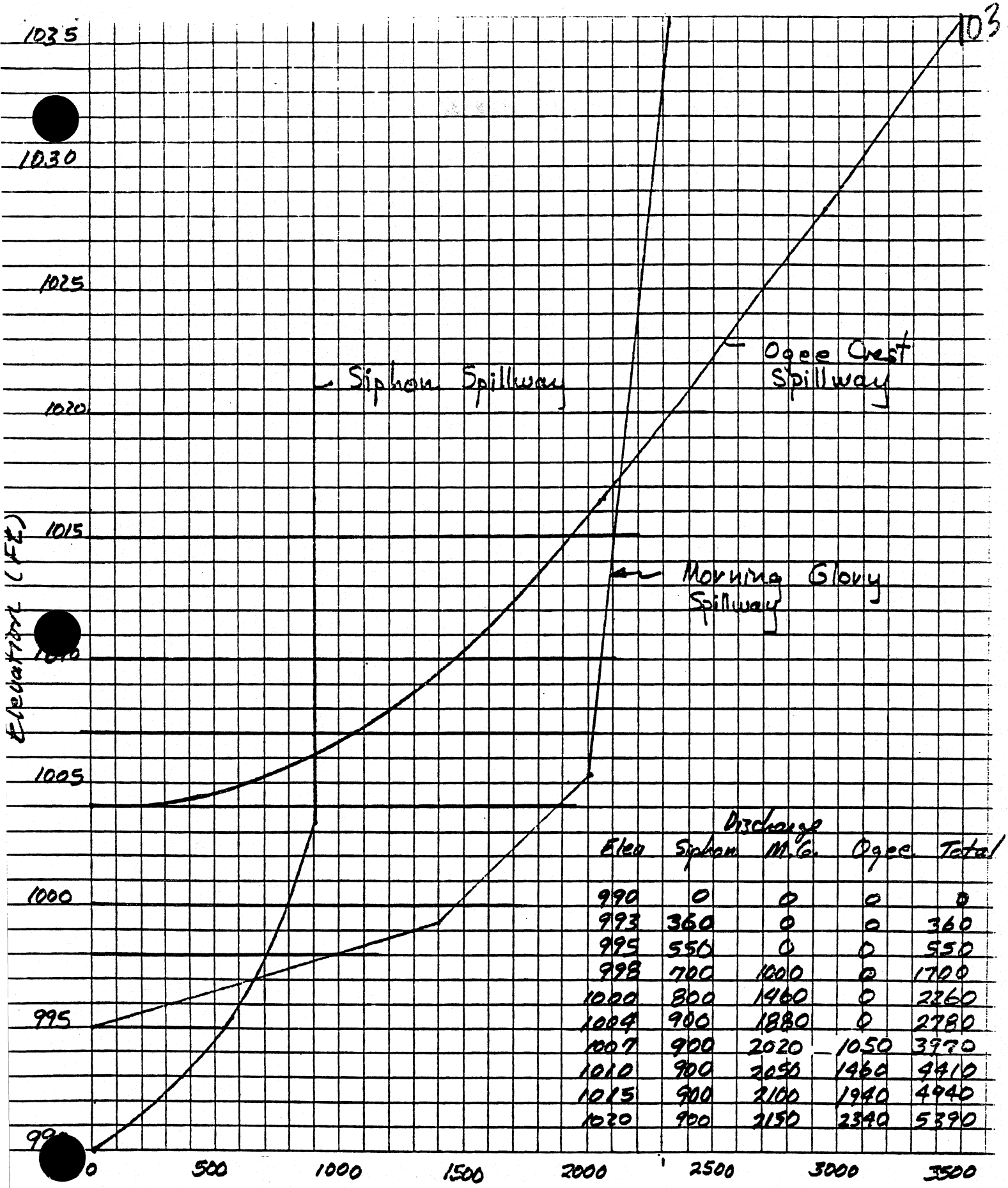

Elev	Discharge Siphon	M.G.	Ogee	Total
990	0	0	0	0
993	360	0	0	360
995	550	0	0	550
998	700	1000	0	1700
1000	800	1460	0	2260
1004	900	1880	0	2780
1007	900	2020	1050	3970
1010	900	2050	1460	4410
1015	900	2100	1940	4940
1020	900	2150	2340	5390

Discharge (cfs)

Figure 4.B

FLOOD ROUTING TECHNIQUES FOR STREAMS

References:
a. EM 1110-2-1408, "Routing of Floods Through River Channels," US Army Corps of Engineers, March 1960.
b. "Storage and Flood Routing," US Geological Survey, Water Supply Paper 1543-B, 1960.
c. Chow, Ven Te, Open Channel Hydraulics, Chapter 20, pp 604-613.
d. Henderson, F. M., Open Channel Flow, MacMillan, Chapter 9, 1966.

1. Purpose of Flood Routing

a. Hydrograph reuted from point A to point B

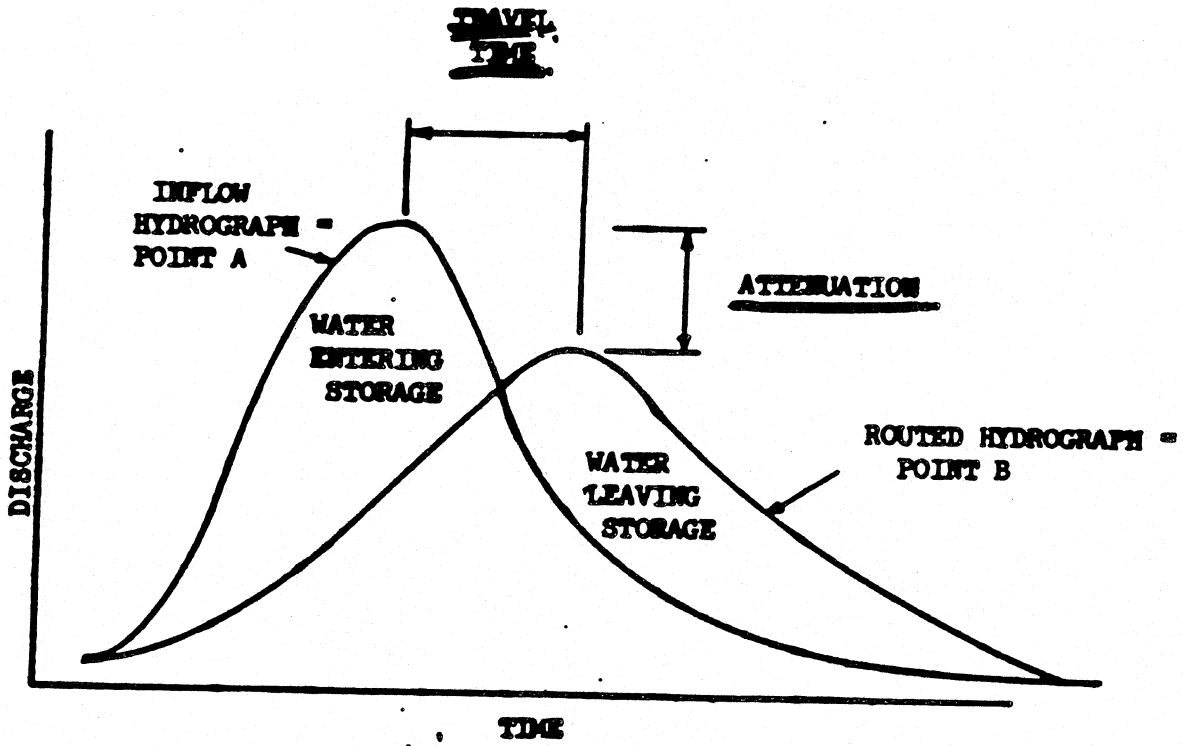

FLOOD ROUTING IN RIVERS

After the runoff hydrograph from a watershed area has been determined, it is routed to the next downstream point and the runoff hydrograph for the intervening area is added to the routed hydrograph to determine the total hydrograph to be expected at the downstream point. Figure 1 is a graphical representation of the above statement.

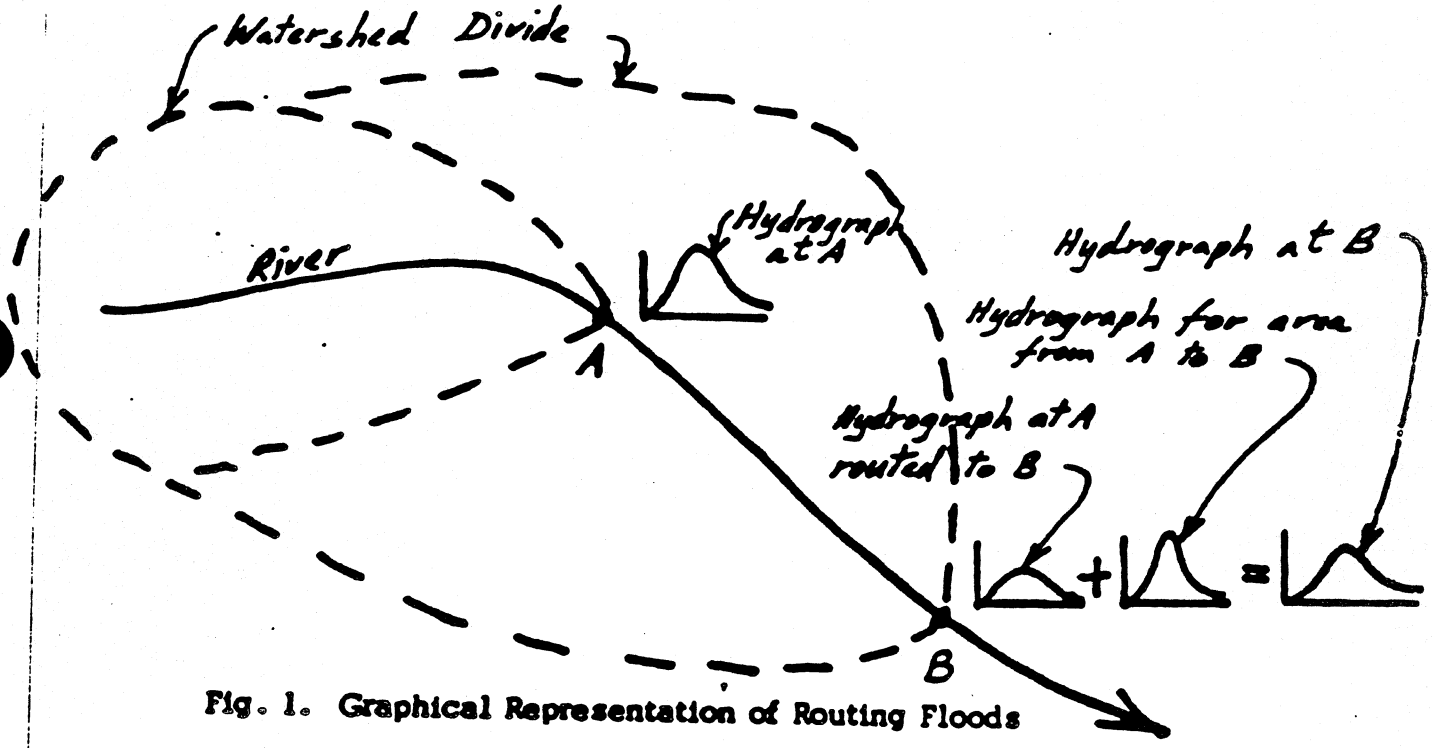

Fig. 1. Graphical Representation of Routing Floods

Flood routing is accomplished by several methods, and the most general and frequently used is that developed by Muskingum.

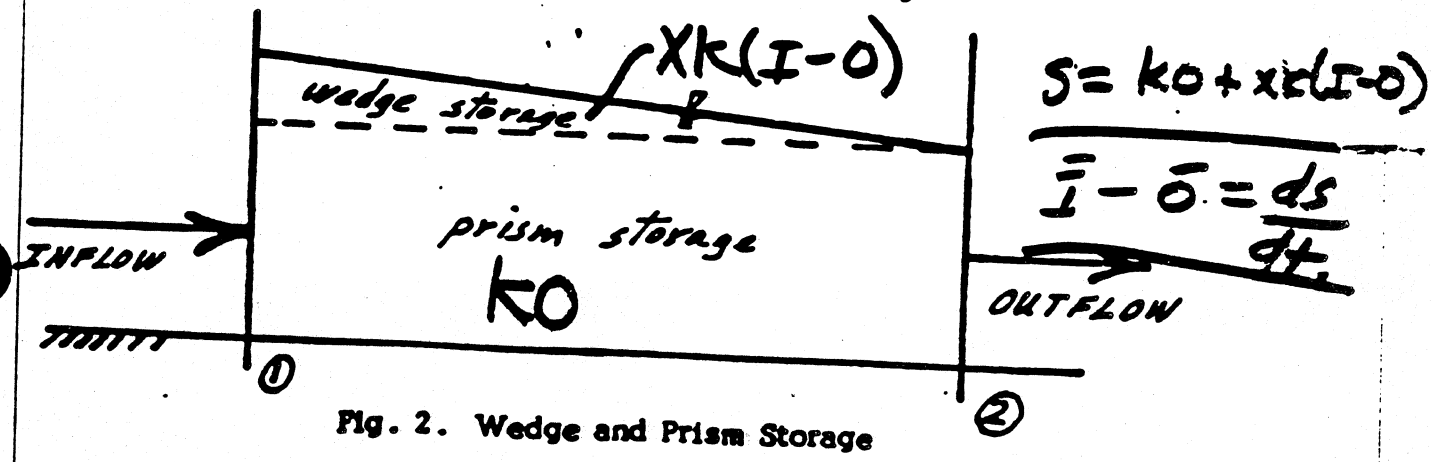

Fig. 2. Wedge and Prism Storage

Volume $\neq$ f(outflow) because

Inflow = $f(d_1)$ and Outflow = $f(d_2)$

Therefore,

Volume = f(Inflow, Outflow)

Prism storage = f(Outflow) = f(O)

Wedge storage = f(Inflow, Outflow) = f(I,O)

Assuming a linear system,

Prism storage = KO and

Wedge storage = XK(I−O)

Then K is a constant factor and X is a weighting factor for K.

$$\text{Volume} = S = KO + XK(I-O)$$

$$S = K[O+X(I-O)]$$

$$S = K[XI+(1-X)O] \qquad (1)$$

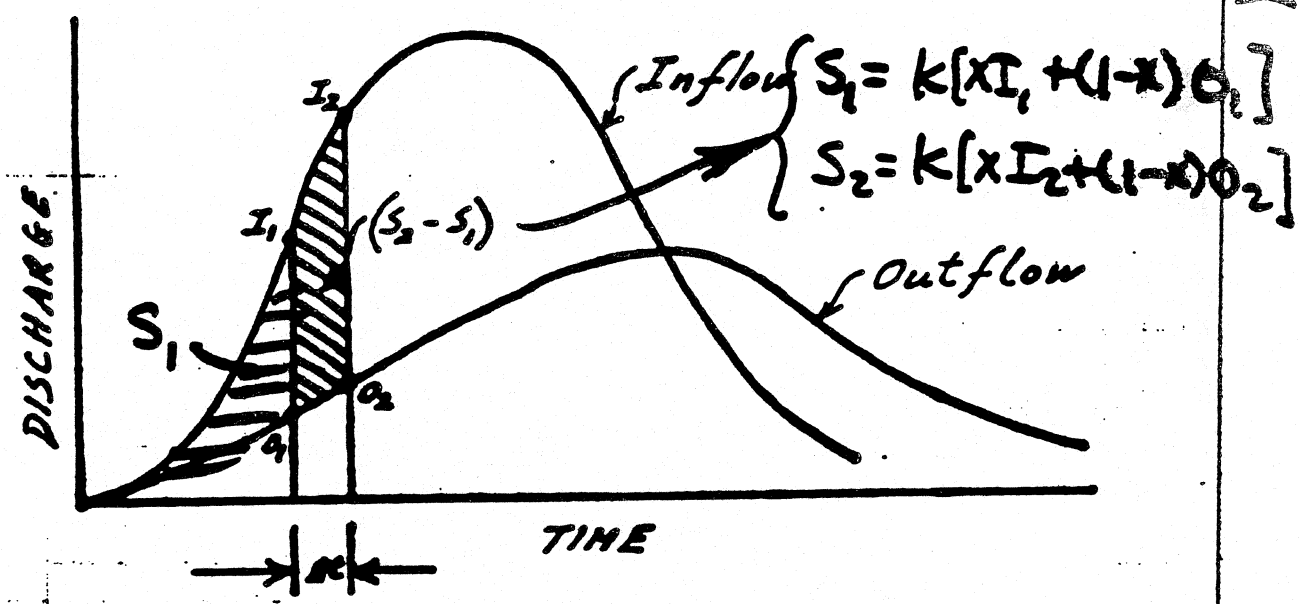

Fig. 3. Change in Storage for Flood Routing

From the Continuity Equation

$$I - O = \frac{\Delta s}{\Delta t} \qquad (2)$$

In Figure 3, from t_1 to t_2

From Eqn. 1 $S_2 - S_1 = K[X(I_2 - I_1) + (1-X)(O_2 - O_1)]$

<u>Continuity</u> $$\frac{S_{n+1} - S_n}{\Delta t} = \frac{I_n + I_{n+1}}{2} - \frac{O_n + O_{n+1}}{2}$$

$$S_{n+1} - S_n = \left(\frac{I_n + I_{n+1}}{2}\right)\Delta t - \left(\frac{O_n + O_{n+1}}{2}\right)\Delta t$$

<u>Muskingum Storage</u>

$$S = k\left[xI + (1-x)O\right]$$

$$S_n = k\left[xI_n + (1-x)O_n\right]$$

$$S_{n+1} = k\left[xI_{n+1} + (1-x)O_{n+1}\right]$$

$$S_{n+1} - S_n = k\left[x(I_{n+1} - I_n) + (1-x)(O_{n+1} - O_n)\right]$$

<u>Equating</u>

$$\left(\frac{I_n + I_{n+1}}{2}\right)\Delta t - \left(\frac{O_n + O_{n+1}}{2}\right)\Delta t =$$

$$k\left[x(I_{n+1} - I_n) + (1-x)(O_{n+1} - O_n)\right]$$

$$O_{n+1} = C_0 \cdot I_{n+1} + C_1 \cdot I_n + C_2 O_n$$

$$C_0 = \frac{-kx + 0.5\Delta t}{k - kx + 0.5\Delta t}$$

$$C_2 = \frac{k - kx - 0.5\Delta t}{k - kx + 0.5\Delta t}$$

$$C_1 = \frac{kx + 0.5\Delta t}{k - kx + 0.5\Delta t}$$

From Eqn. 2 $S_2 - S_1 = \left(\frac{I_1 + I_2}{2}\right) \Delta t - \left(\frac{O_1 + O_2}{2}\right) \Delta t$

Equate the two equations and solve for O_2

$$O_2 = C_0 I_2 + C_1 I_1 + C_2 O_1 \tag{3}$$

where

$$C_0 = \frac{-KX - 0.5\Delta t}{K-KX + 0.5\,\Delta t} \tag{4}$$

$$C_1 = \frac{KX + 0.5\,\Delta t}{K-KX + 0.5\,\Delta t} \tag{5}$$

$$C_2 = \frac{K-KX - 0.5\,\Delta t}{K-KX + 0.5\,\Delta t} \tag{6}$$

It can be shown that K is equal to the lag time or the time between the centroids of the inflow and outflow hydrographs.

Using data from an actual flood measured at the inflow and outflow points of the reach, the value of K is measured, and using trial values of X, plots of XI + (1-X)O versus S are drawn.

The best value of X is that which causes the data to plot most nearly as a single valued curve. The Muskingum Method assumes this curve is a straight line with slope $\frac{dS}{dq}$ equivalent to K. The units of K depend on the units of flow and storage; if flow is in cfs and storage in sfd, K is in days. The determination of the Muskingum storage coefficients is shown in Figure 4.

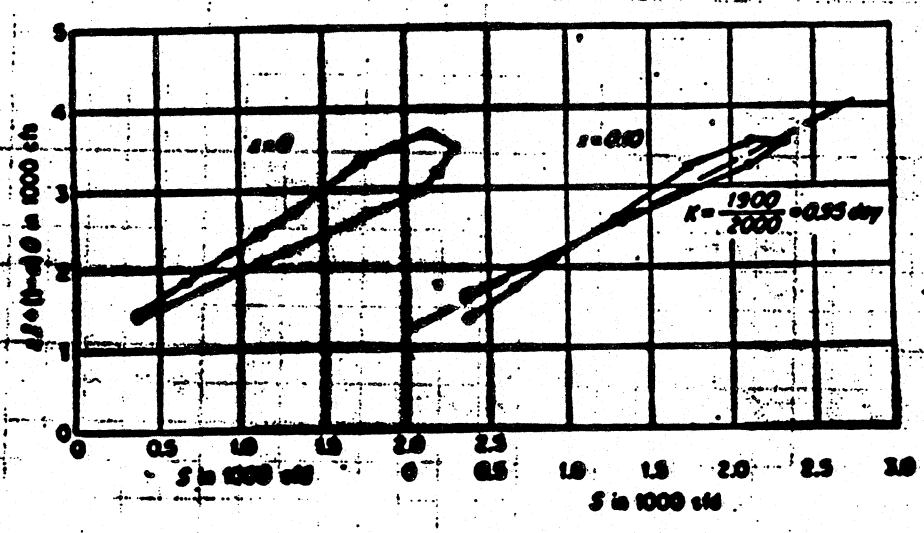

Fig. 4. Determination of the Muskingum Storage Constants (Ref. 3)

Determining k & x from known inflow & known outflow hydrograph

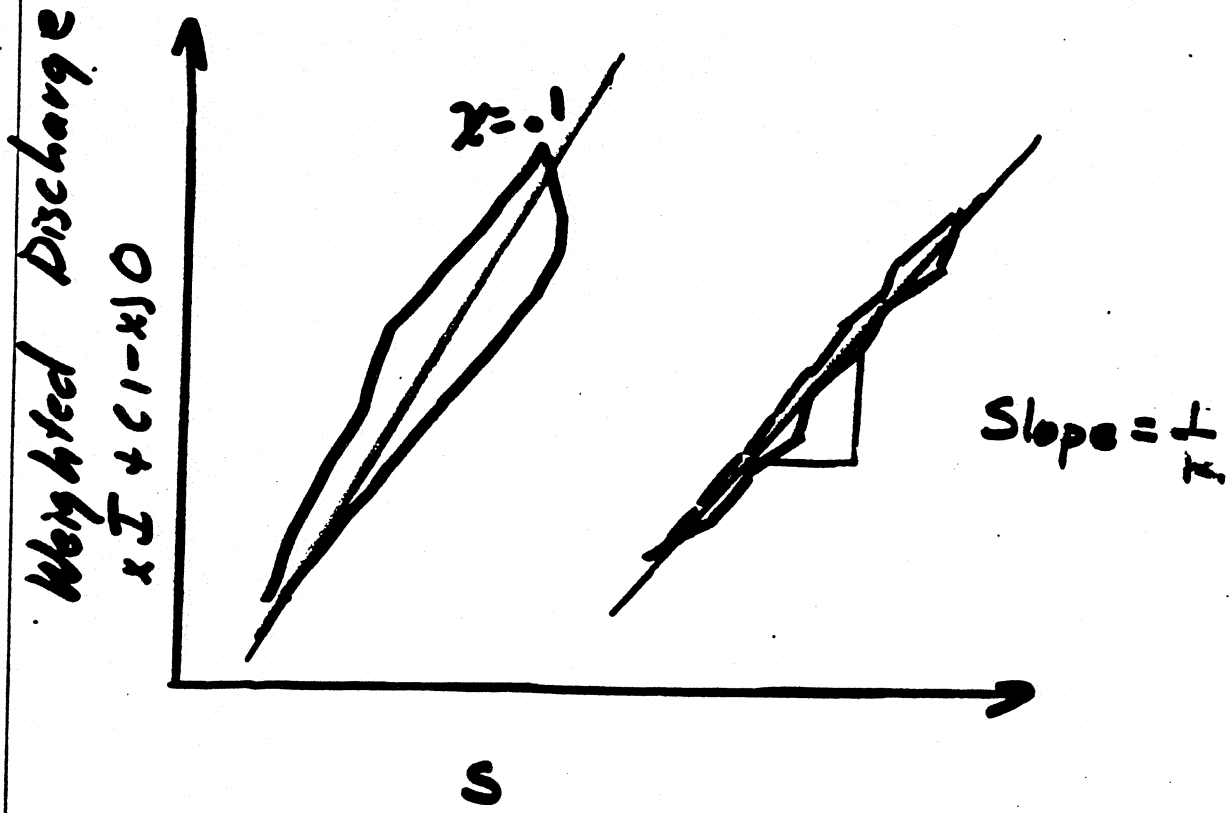

$$S = k\,[\text{weighted discharge}]$$

$$\downarrow$$

$$S = k\,[xI + (1-x)O]$$

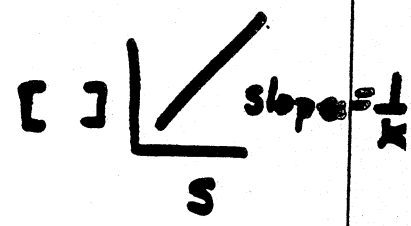

Without Inflow & outflow hydrographs

$k \approx$ travel time

$x \approx 0.2$

REVIEW OF HEC-1

111.

Computer Program 723-X6-L2010

HEC-1

Flood Hydrograph Package

Users Manual

September 1981

US Army Corps of Engineers
Water Resources Support Center

The Hydrologic Engineering Center
609 Second Street
Davis, California 95616

(916) 440-2105
(FTS) 448-2105

```
*****************************************
*                                       *
*   FLOOD HYDROGRAPH PACKAGE  (HEC-1)   *
*          FEBRUARY 1981                *
*        REVISED 27 JUL 83              *
*                                       *
*  RUN DATE  9 AUG 83    TIME  10:48:31 *
*                                       *
*****************************************
```

```
*************************************
*                                   *
*    U.S. ARMY CORPS OF ENGINEERS   *
*  THE HYDROLOGIC ENGINEERING CENTER *
*          609 SECOND STREET        *
*       DAVIS, CALIFORNIA 95616     *
*  (916) 440-3285 OR (FTS) 448-3285 *
*                                   *
*************************************
```

```
X     X  XXXXXXX   XXXXX          X
X     X  X        X     X        XX
X     X  X        X              X
XXXXXXX  XXXX     X       XXXXX  X
X     X  X        X              X
X     X  X        X     X        X
X     X  XXXXXXX   XXXXX         XXX
```

THIS PROGRAM REPLACES ALL PREVIOUS VERSIONS OF HEC-1 KNOWN AS HEC1 (JAN 73), HEC1GS, HEC1DB, AND HEC1KW.

THE DEFINITIONS OF VARIABLES -RTIMP- AND -RTIOR- HAVE CHANGED FROM THOSE USED WITH THE 1973-STYLE INPUT STRUCTURE. THE DEFINITION OF -AMSKK- ON RM-CARD WAS CHANGED WITH REVISIONS DATED 28 SEP 81. SEE SEPTEMBER 1981 INPUT DESCRIPTION FOR NEW DEFINITIONS.

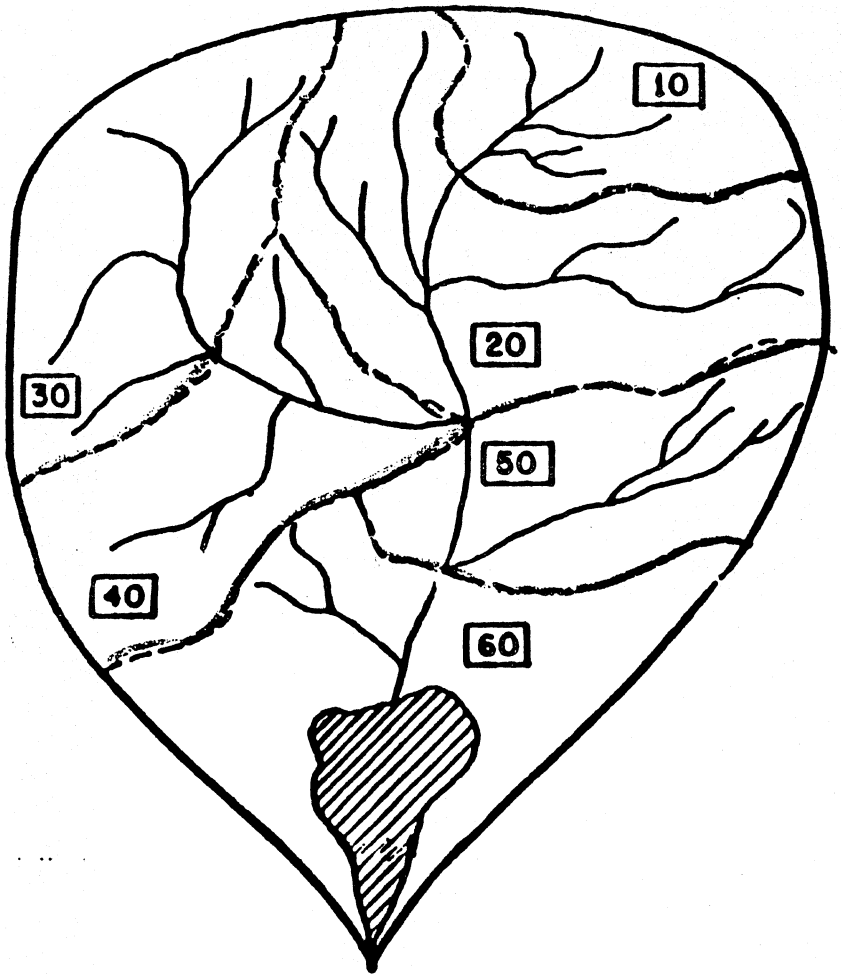

Figure 2.1: Example River Basin

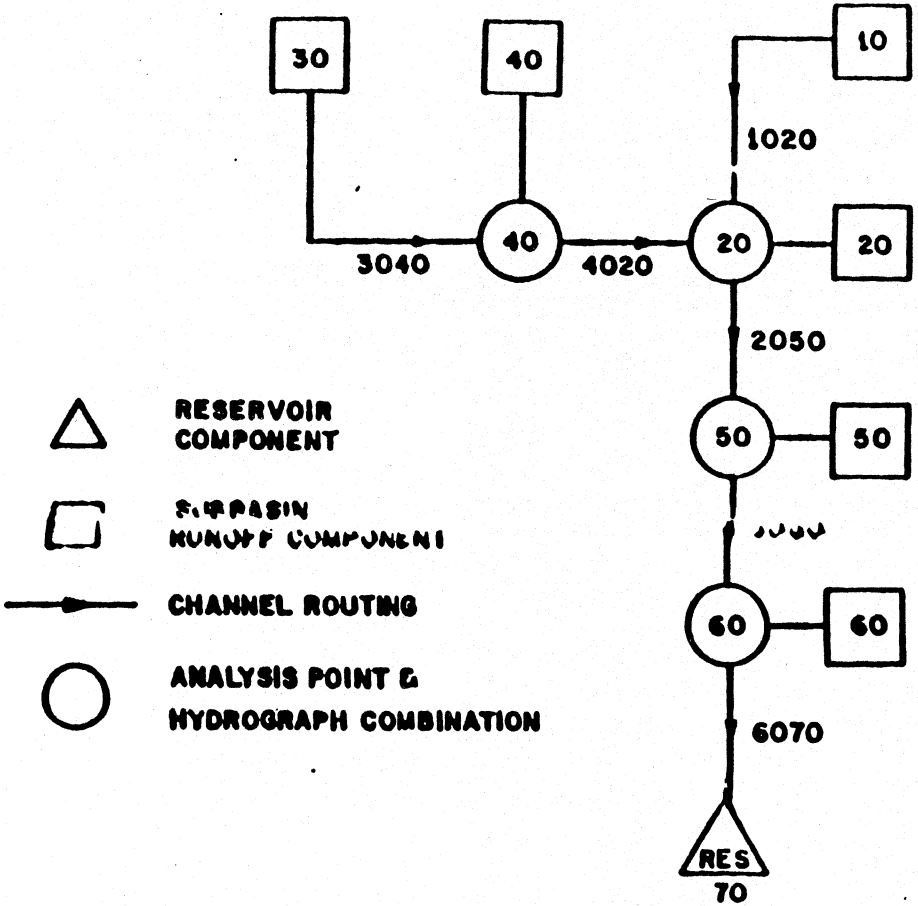

Figure 2.2: River Basin Schematic

HEC, 1981

113.

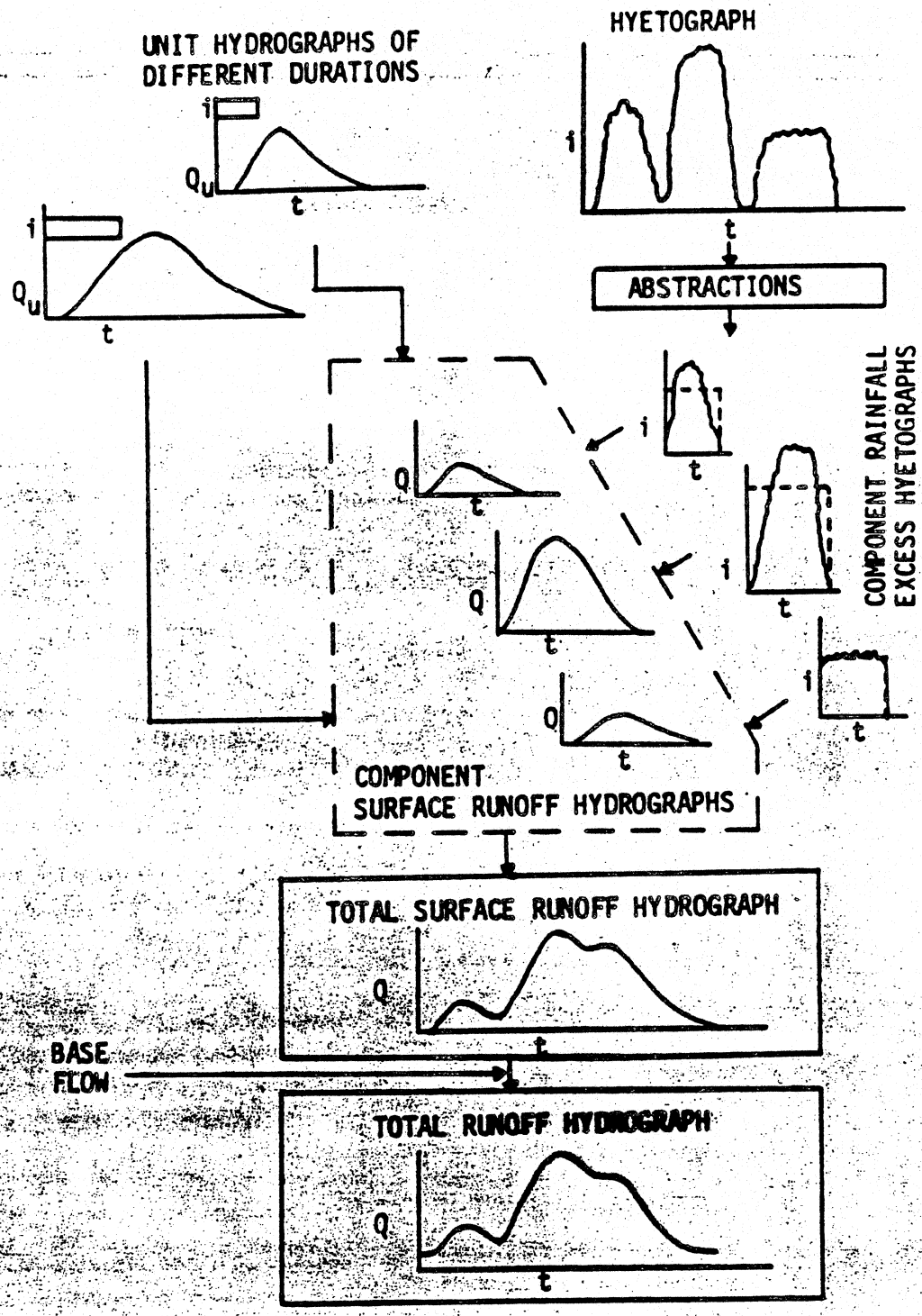

Fig. 31. Schematic diagram of unit hydrograph method

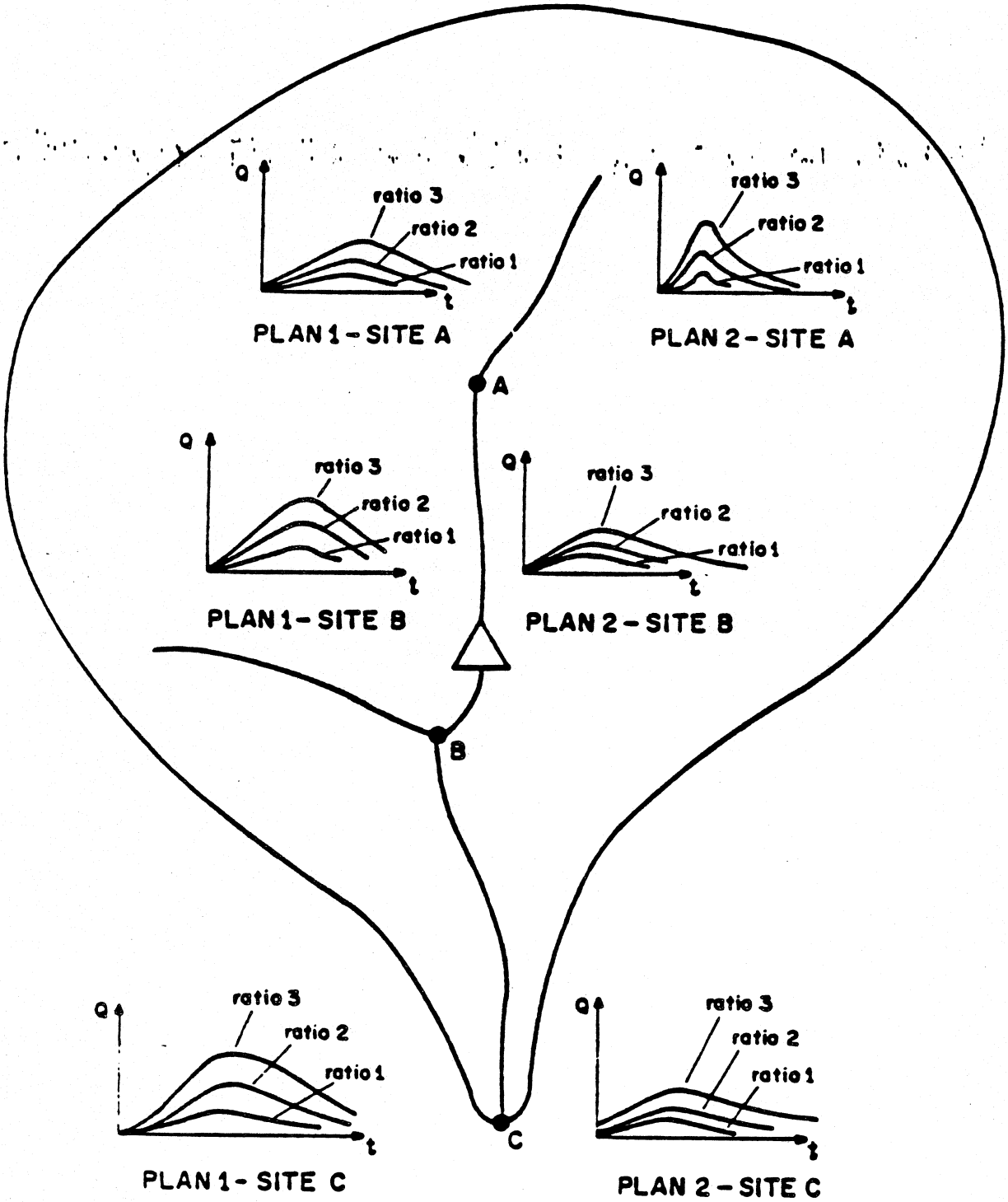

Figure 5.1. Multiflood and Multiplan Hydrographs

HEC, 1981

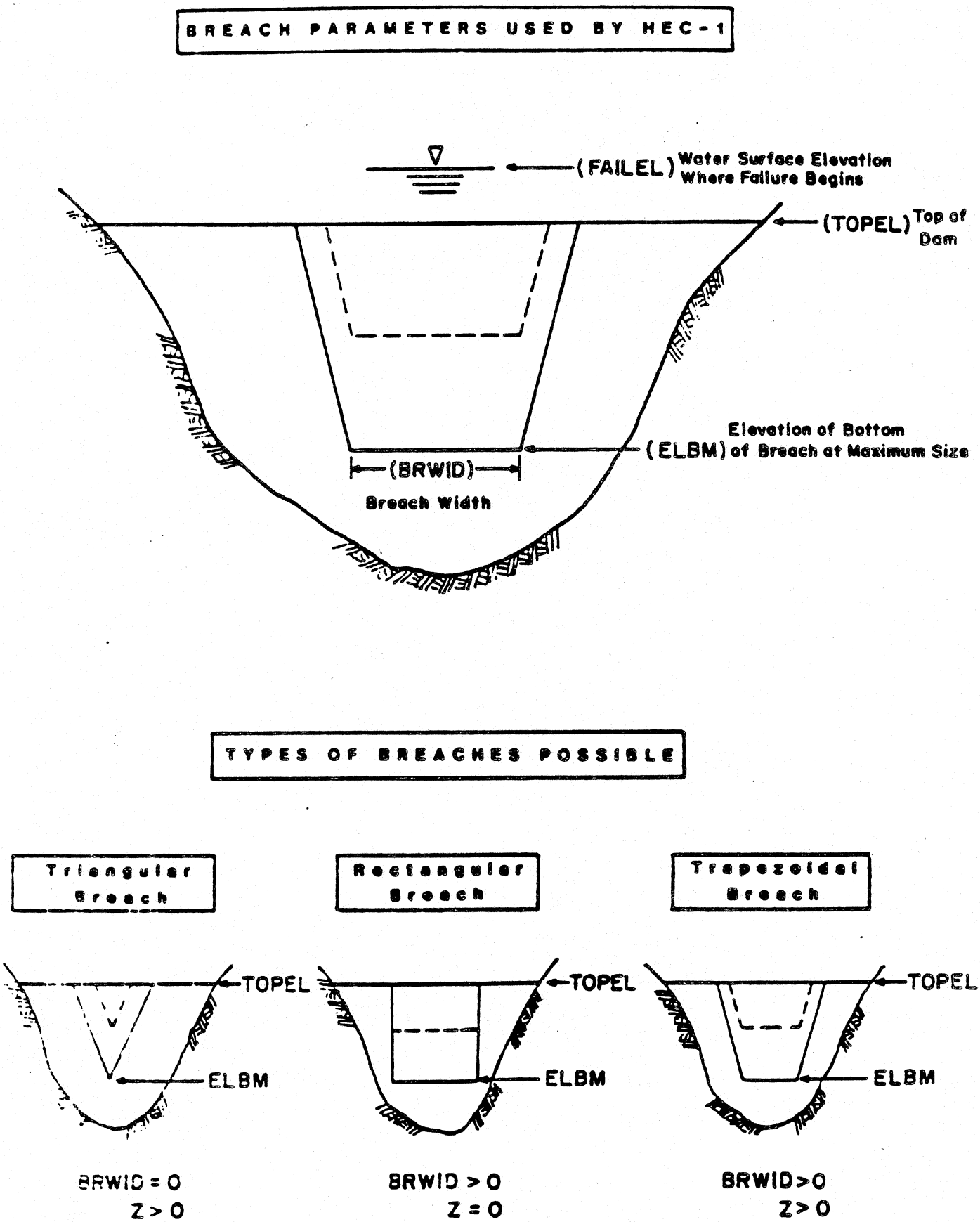

HEC, 1981

Figure 6.3. HEC-1 Dam Breach Parameters

Q_{OD} = CØOD * DAMW h_1^{EXPD}

where

h_1 = current WSE - TØPEL

CØOD = discharge coefficient

EXPD = exponent of head

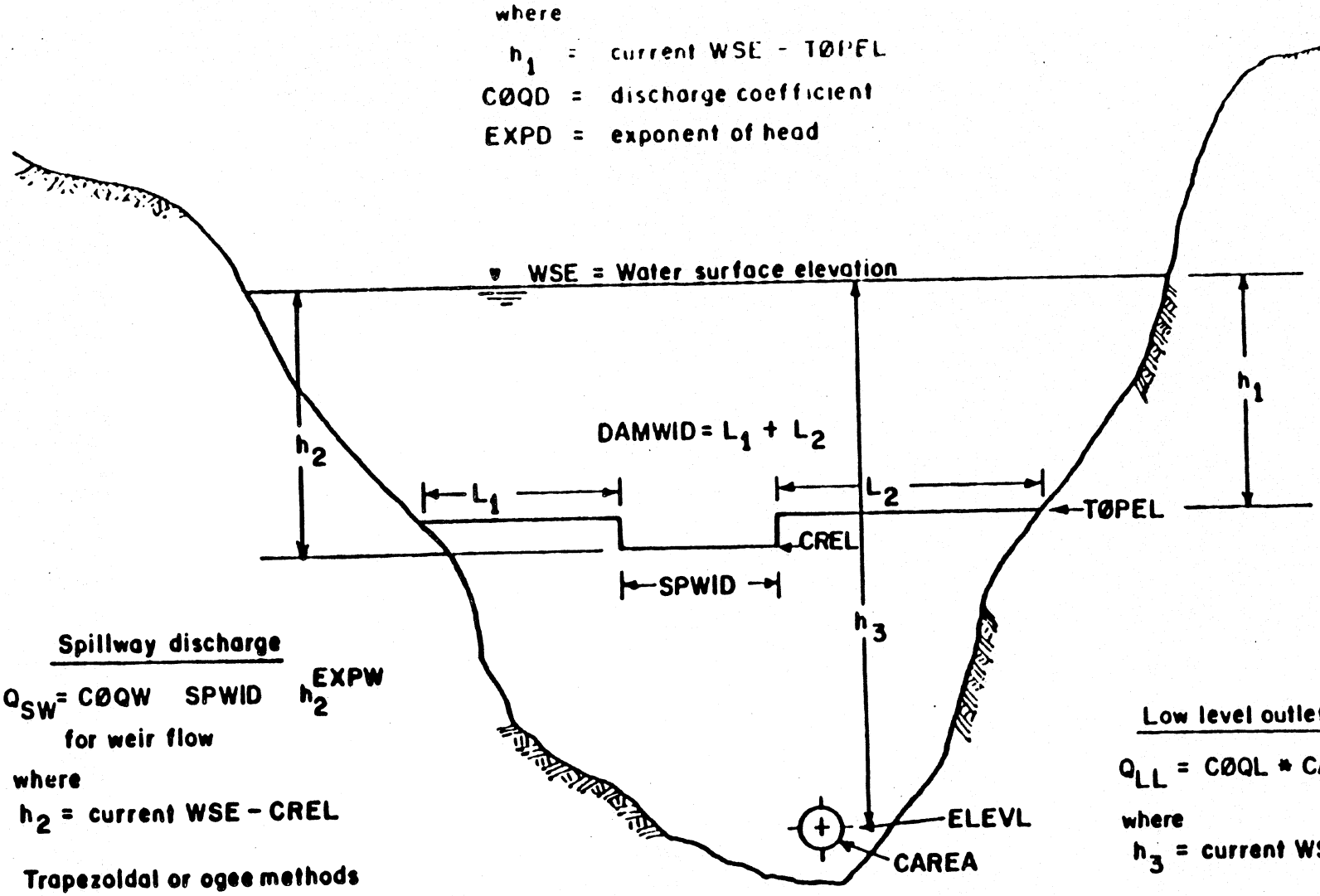

Spillway discharge

Q_{SW} = CØQW SPWID h_2^{EXPW}

for weir flow

where

h_2 = current WSE - CREL

Trapezoidal or ogee methods may also be used

Low level outlet discharge

Q_{LL} = CØQL * CAREA * $\sqrt{2g}$ h_3^{EXPL}

where

h_3 = current WSE - ELEVL

Figure 6.1. Spillway Adequacy and Dam Overtopping Variables in HEC-1

HEC, 1981

117

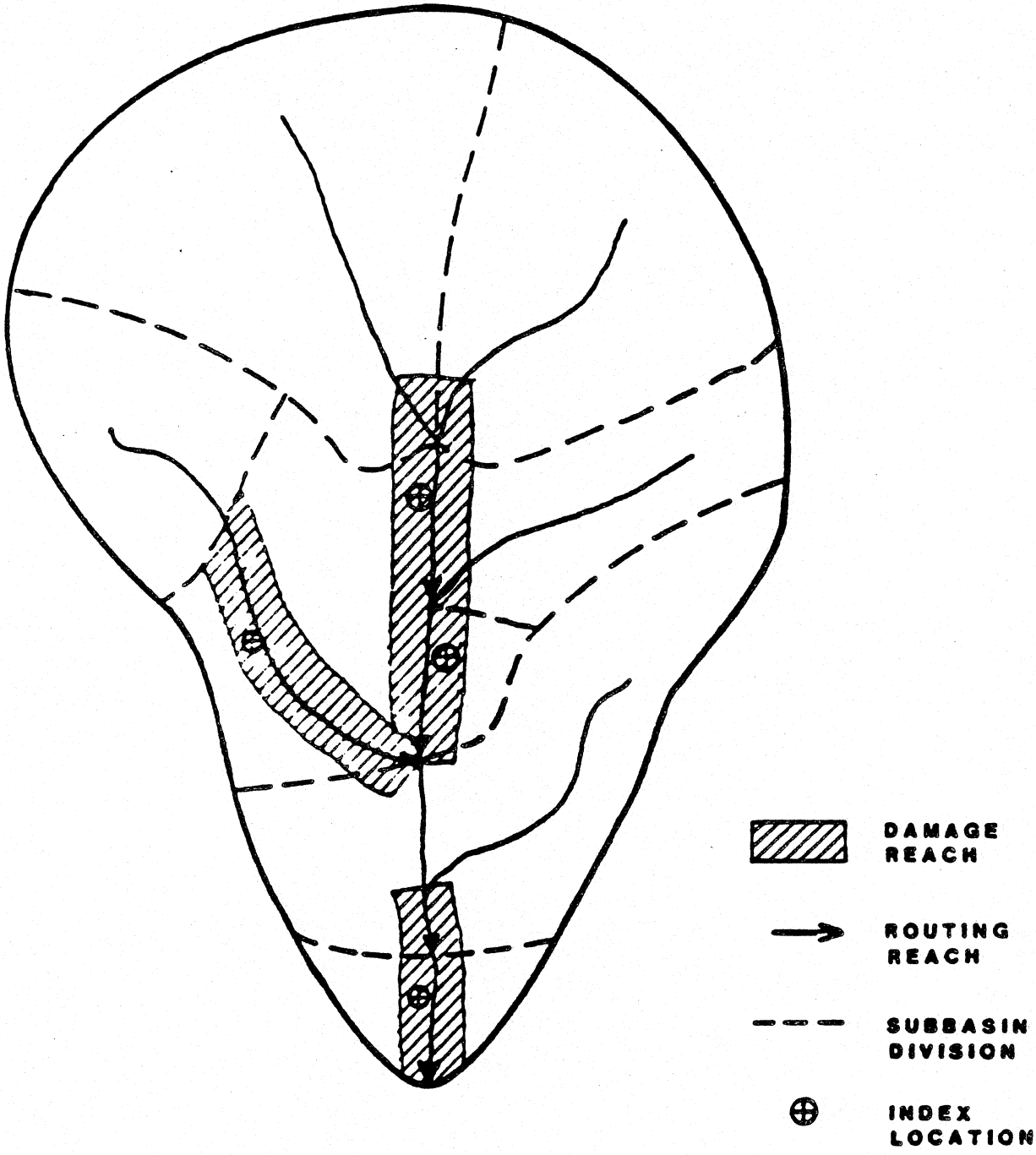

Figure 8.1. Flood Damage Reduction Model HEC, 1981

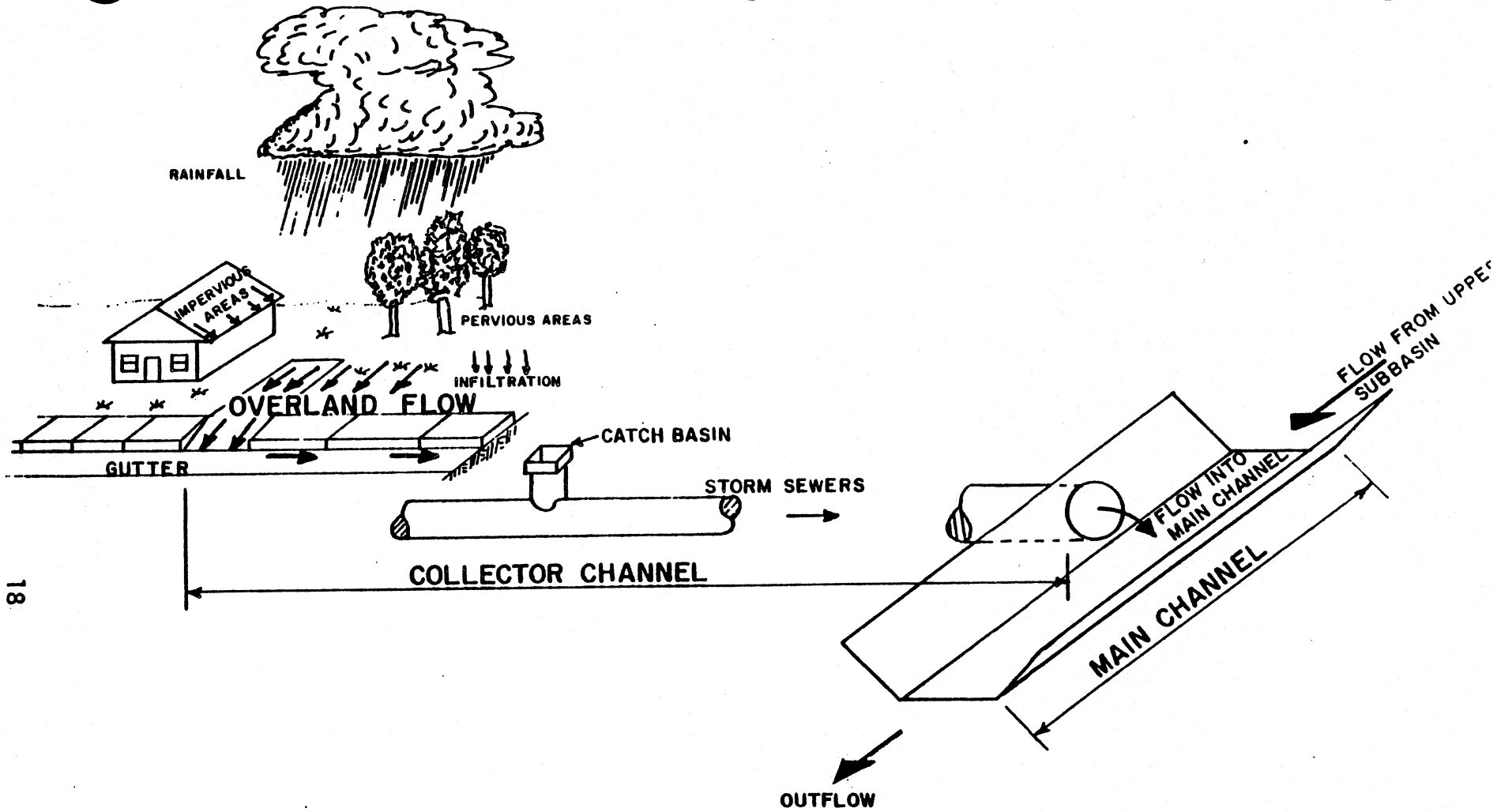

Figure 1.5 Typical Urban Drainage Pattern (HEC)

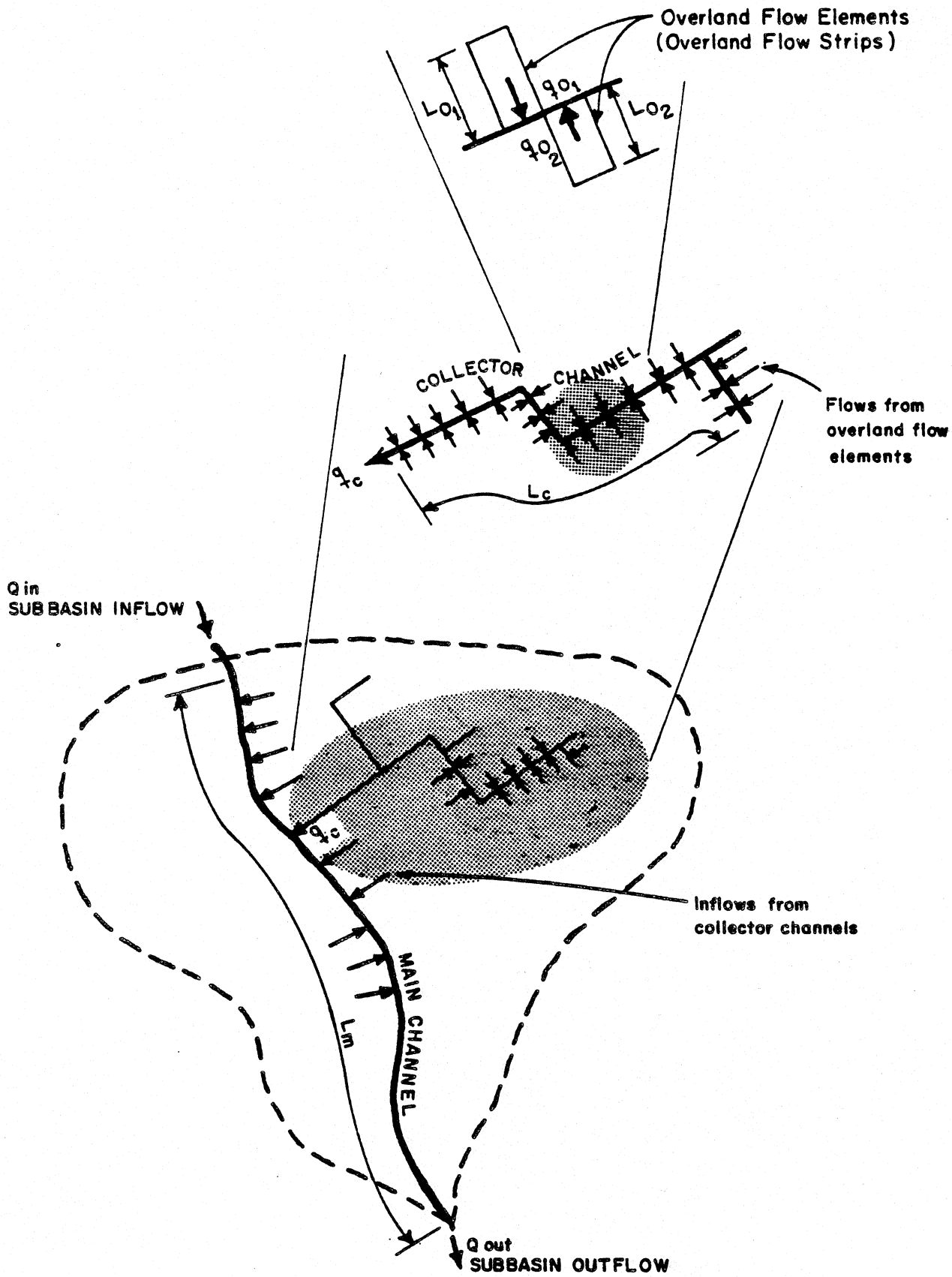

Figure 1.4. Relationships Between Flow Elements HEC, 1981

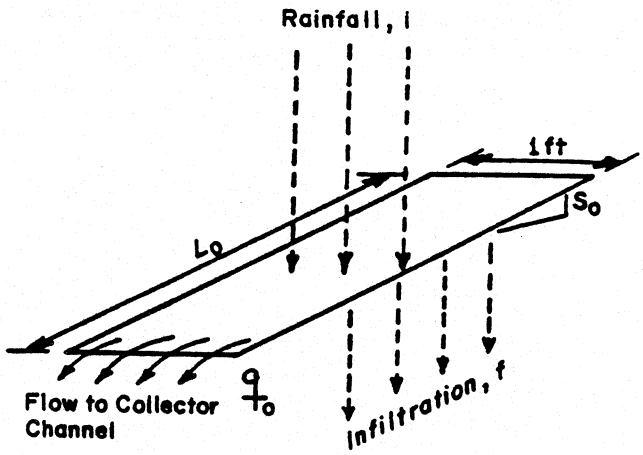

Overland Flow Element

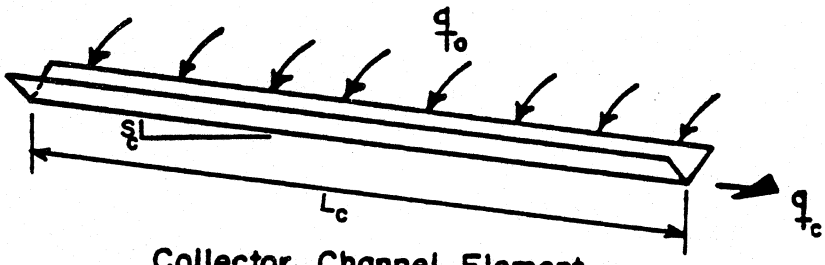

Collector Channel Element

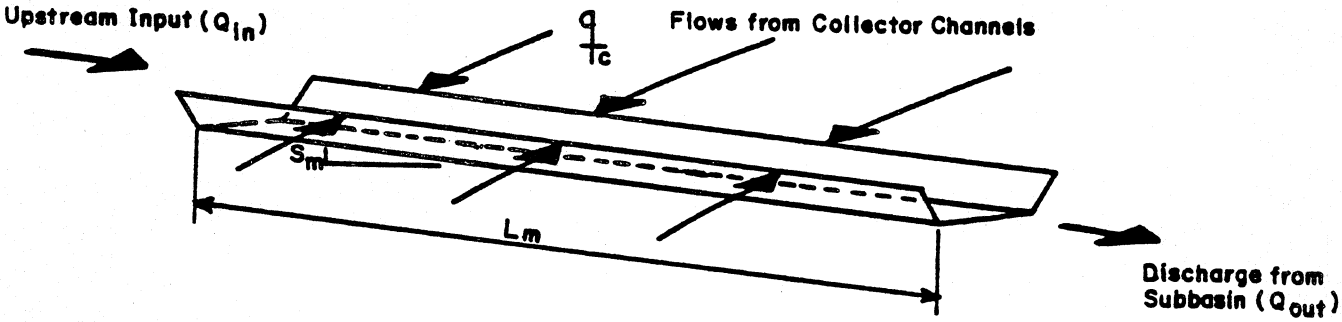

Main Channel Element

Figure 1.3 Elements Used in Kinematic Wave Calculations (HEC)

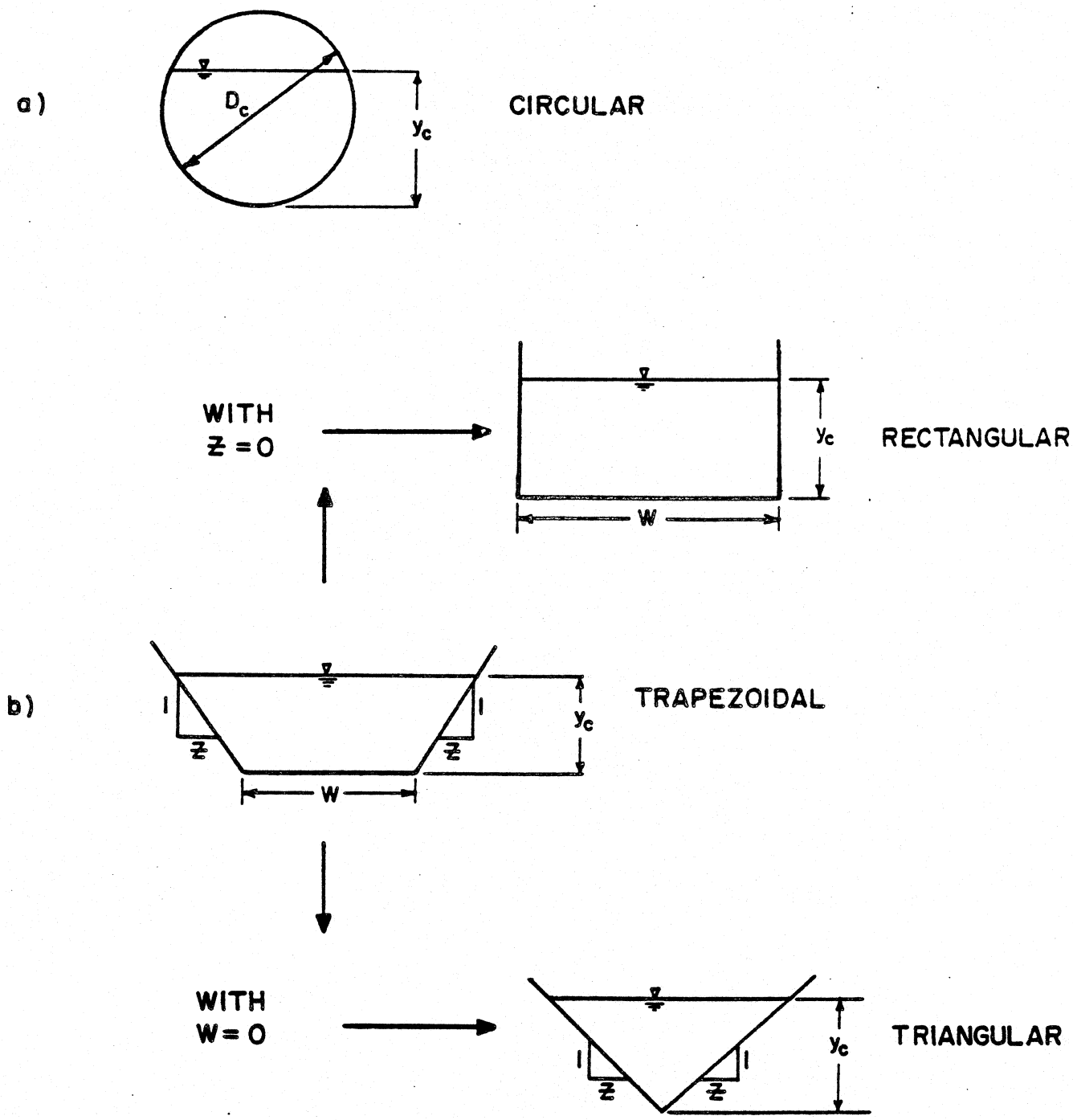

Figure 1.7 Two Basic Channel Shapes and their Variations Used by the HEC-1 Flood Hydrograph Package for Kinematic Wave Stream Routing (HEC)

US Army Corps
of Engineers

The Hydrologic
Engineering Center

Probable Maximum Flood Estimation - Eastern United States

by

Paul B. Ely

John C. Peters

Technical Paper No. 100
September 1984

Papers in this series have resulted from technical activities of the Hydrologic Engineering Center. Versions of some of these have been published in technical journals or in conference proceedings. The purpose of this series is to make the information available for use in the Center's training program and for distribution within the Corps of Engineers.

The findings in this report are not to be construed as an official Department of the Army position unless so designated by other authorized documents.

The contents of this report are not to be used for advertising, publication, or promotional purposes. Citation of trade names does not constitute an official endorsement or approval of the use of such commercial products.

PROBABLE MAXIMUM FLOOD ESTIMATION – EASTERN UNITED STATES[1]

Paul B. Ely and John C. Peters[2]

ABSTRACT: In 1982, the National Weather Service (NWS) published criteria for developing the spatial and temporal precipitation distribution characteristics of Probable Maximum Storms. The criteria, which are intended for use in the United States east of the 105th meridian, involve four variables: (1) location of the storm center, (2) storm-area size, (3) storm orientation, and (4) temporal arrangement of precipitation amounts. A computer program has been developed which applies the NWS criteria to produce hyetographs of spatially-averaged precipitation for a basin, or for each subbasin if the basin is subdivided. The basis and operational characteristics of the program are described, and an application is illustrated in which the program is used in conjunction with a precipitation-runoff simulation program (HEC-1) to compute a Probable Maximum Flood.
(KEY TERMS: Probable Maximum Flood; design storm.)

INTRODUCTION

In 1978, the United States National Weather Service (NWS) published estimates for Probable Maximum Precipitation (PMP) for the eastern part of the country, east of the 105th meridian (NWS, 1978). The estimates apply to areas of 10 to 10,000 sq. mi. and durations of 6 to 72 hours. The National Weather Service has also published applications criteria (NWS, 1982) that can be used with the PMP estimates to develop spatial and temporal characteristics of a Probable Maximum Storm (PMS). A PMS thus developed can be used with a precipitation-runoff simulation model to calculate a Probable Maximum Flood (PMF) hydrograph. The PMF is used in the hydraulic design of project components for which virtually complete security from flood-induced failure is desired; for example, the spillway of a major dam or protection works for a nuclear power plant.

The NWS criteria for defining a PMS require that the magnitude of four variables be established: (1) location of the storm center, (2) storm-area size, (3) storm orientation, and (4) temporal arrangement of precipitation amounts. Additional variables that influence the magnitude of a PMF include antecedent moisture conditions and the initial state of a reservoir or reservoir system. The four PMS variables are generally chosen to produce the maximum peak discharge or runoff volume at the point of interest. It is therefore necessary to calculate runoff as a part of the trial and error process of establishing the magnitude of the PMS variables.

A computer program has been developed (HEC, 1983b) for applying the NWS procedure for defining a PMS. The program, called HMR52, has an optional capability to pass calculated hyetographs to a data storage system for subsequent retrieval by computer program HEC-1 (HEC, 1981), with which runoff is calculated. This paper describes the basis for the new program and describes its application in conjunction with HEC-1.

COMPUTER PROGRAM HMR52

The NWS criteria define the PMS in terms of a set of elliptical isohyets for a series of 'standard' area sizes – 10, 25, 50, 100, etc., up to 60,000 sq. mi. The basis for, and method of, assigning precipitation depths to the isohyets are provided in Hydrometeorological Report No. 52 (NWS, 1982). For runoff determination, a watershed is generally divided into subbasins, and a hyetograph (i.e., time distribution) of average precipitation for each subbasin is required. The output from HMR52 consists essentially of a set of subbasin hyetographs.

The sequence of computations in HMR52 is first to calculate a PMS for the total watershed and then to determine the corresponding subbasin hyetographs. Input items for HMR52 include the following:

1. X-Y coordinates for the total watershed and for each subbasin. These could be obtained with a digitizer.
2. Depth-area-duration PMP data from Hydrometeorological Report No. 51 (NWS, 1978).
3. Preferred storm orientation from Hydrometeorological Report No. 52 (NWS, 1982).
4. X-Y coordinates of the storm center.
5. Storm-area size.
6. Storm orientation.
7. Temporal arrangement of six-hour depths.
8. Time interval for hyetographs.

Although PMS variables are generally based on the production of peak discharge or maximum runoff volume, maximization of the average depth of precipitation over the watershed is, in many cases, a virtually equivalent criterion. The HMR52 program contains an option by which storm area size

[1] Paper No. 84017 of the *Water Resources Bulletin.*
[2] Hydraulic Engineers, Hydrologic Engineering Center, 609 Second Street, Davis, California 95616.

and/or orientation can be optimized with maximization of average depth as an objective function. Although the program does not have capability to optimize the location of the storm center, the program will locate the storm center at the basin centroid if location of the storm center is not specified. The programmed optimization procedure is as follows:

1. The major axis of the storm is oriented such that the moment of inertia (second moment) of the basin area about this axis is a minimum. The depth of basin-average precipitation is determined for an array of storms corresponding to the standard storm-area sizes. The storm-area size which produces the maximum average depth is selected as the critical storm-area size (i.e., see Table 1a).

2. Using the critical storm-area size, the depth of basin-average precipitation is determined for an array of storms for which storm orientation varies in 10-degree increments over the range of possible orientations. The orientation producing the maximum average depth is determined and two additional storms, with orientations of $\pm 5^{\circ}$ from this orientation, are developed. The orientation that produces the maximum average depth is selected as the critical orientation (i.e., see Table 1b).

Six-hour incremental precipitation amounts for each storm identified in the optimization process are arranged in order of decreasing magnitude, as illustrated in Tables 1a and 1b. The time interval for incremental precipitation used for definition of the optimized (or user-specified) storm is selected by the user in the range of five minutes to six hours. Precipitation is assumed to occur with uniform intensity during each six-hour period outside of the 24-hour period of maximum precipitation.

The user can specify the arrangement of six-hour increments throughout the storm or just the position of the maximum six-hour increment, which may occur in any position after the first 24 hours of the storm. If the position of the largest six-hour increment is not specified, it is placed in the seventh position (hours 37-42) by default. Figure 1 illustrates a program-generated hyetograph for which Δt is one hour. Criteria and guidelines for determining the temporal arrangement of precipitation are given in Hydrometeorological Report No. 52 (NWS, 1982).

RUNOFF SIMULATION

The HMR52 program has capability to write subbasin hyetographs to a disk file, or to a special Data Storage System (HEC, 1982), for subsequent runoff simulation with computer program HEC-1 (HEC, 1981). An advantage of using the Data Storage System is that a graphics program called DSPLAY (HEC, 1983a) can be used to plot the precipitation hyetographs as well as hydrographs calculated with HEC-1.

The HEC-1 program can be used to simulate the runoff generation, routing and combining operations required for complex multi-subbasin watersheds. Generally the unit hydrograph approach to runoff simulation is employed, although capability to calculate runoff with kinematic wave methodology is also available (HEC, 1979).

In addition to the subbasin hyetographs, input items for HEC-1 would include:

1. Subbasin areas.
2. Unit hydrograph, loss rate, and base flow parameters for each subbasin.
3. Streamflow routing parameters for each routing reach.
4. Storage-outflow criteria and an initial storage for reservoirs, if reservoir routing is to be performed.

ILLUSTRATION

The joint use of HMR52 and HEC-1 for PMF estimation is illustrated in the following hypothetical example. Figure 2 shows the 288 sq. mi. watershed above Jones Reservoir. HMR52 is used to develop PMS hyetographs for the four subbasins shown in Figure 2, and HEC-1 is used to calculate a PMF inflow hydrograph to the reservoir and to route the PMF through the reservoir.

For this illustration, no values are specified for storm center, storm-area size, orientation, and temporal arrangement. The program therefore places the storm center at the basin centroid and obtains storm-area size and orientation by maximizing the depth of precipitation. A default two-hour temporal distribution is used.

Table 1a is HMR52 output that summarizes storm depths for various storm-area sizes and for a storm orientation that minimizes the moment of inertia of the basin area about the major axis of the elliptical storm pattern. As may be seen from the table, a storm-area size of 300 sq. mi. produces the largest depth.

Table 1b summarizes depths obtained by varying storm orientation in 10° increments and a storm-area size of 300 sq. mi. The last two storms in the table have orientations which are 5° to either side of the best previous orientation. By coincidence, the best previous orientation is 285°, so the last two storms (280° and 290° orientations) are repeats of storms calculated previously.

With PMS variables thus defined, hyetographs are calculated for the four subbasins. Table 2 shows precipitation amounts for Subbasin 1. The four hyetographs, runoff and routing parameters, etc., are used as input to HEC-1, which calculates discharge hydrographs for locations of interest. Table 3 shows HEC-1 summary output resulting from the storm generated by HMR52. Peak discharge and maximum average discharges for durations of 6, 24, and 72 hours are tabulated for each location.

The objective in calculating a PMF is to obtain the largest flood that can reasonably occur. Because of hydrologic characteristics of a watershed, the largest flood may not result from the storm that produces the greatest average depth of precipitation. Results from several trials that were made in calculating the PMF for Jones Reservoir are shown in Table 4. These trials represent a sensitivity analysis with respect to position of the peak six-hour interval, storm area, storm

TABLE 1a. Selection of Storm-Area Size – Varying Storm Area Size and Fixed Orientation.

Storm Area (sq. miles)	Orientation (degrees)	Basin-Averaged Incremental Depths for Six-Hour Periods (inches)												Sum of Depths for Three Peak Six-Hour Periods (inches)
10	285	9.62	1.35	0.71	0.48	0.37	0.30	0.25	0.21	0.19	0.17	0.15	0.14	11.69
25	285	12.06	1.96	1.05	0.71	0.54	0.44	0.37	0.32	0.28	0.25	0.22	0.20	15.07
50	285	13.82	2.40	1.28	0.88	0.67	0.54	0.45	0.39	0.34	0.30	0.27	0.25	17.50
100	285	14.81	2.76	1.48	1.01	0.77	0.62	0.52	0.45	0.39	0.35	0.32	0.29	19.05
175	285	15.23	2.99	1.59	1.09	0.83	0.67	0.56	0.48	0.42	0.39	0.34	0.31	19.82
300	285	15.38	3.21	1.67	1.13	0.86	0.69	0.58	0.50	0.44	0.39	0.35	0.32	20.25
450	285	15.07	3.32	1.68	1.13	0.85	0.69	0.57	0.49	0.43	0.39	0.35	0.32	20.07
700	285	14.40	3.40	1.66	1.11	0.83	0.67	0.56	0.48	0.42	0.37	0.34	0.31	19.46
1,000	285	13.76	3.42	1.63	1.08	0.81	0.67	0.54	0.47	0.41	0.36	0.33	0.30	18.82
1,500	285	13.04	3.33	1.58	1.04	0.78	0.63	0.52	0.45	0.39	0.35	0.32	0.29	17.95
2,150	285	12.23	3.22	1.51	0.99	0.75	0.60	0.50	0.43	0.38	0.33	0.30	0.27	16.95
3,000	285	11.31	3.05	1.42	0.93	0.70	0.56	0.47	0.40	0.35	0.32	0.28	0.26	15.78
4,500	285	10.84	3.05	1.41	0.92	0.70	0.56	0.47	0.40	0.35	0.31	0.28	0.26	15.30
6,500	285	10.45	3.00	1.37	0.89	0.67	0.54	0.45	0.39	0.34	0.30	0.27	0.25	14.82
10,000	285	9.76	2.97	1.31	0.85	0.63	0.51	0.42	0.36	0.32	0.28	0.26	0.23	14.05
15,000	285	9.04	2.86	1.30	0.85	0.64	0.52	0.43	0.37	0.33	0.29	0.26	0.24	13.21
20,000	285	8.34	2.78	1.30	0.85	0.64	0.52	0.44	0.38	0.33	0.29	0.26	0.24	12.41

TABLE 1b. Selection of Storm Orientation – Fixed Storm Area Size and Varying Orientation.

m Area miles)	Orientation (degrees)	Basin-Averaged Incremental Depths for Six-Hour Periods (inches)												Sum of Depths for Three Peak Six-Hour Periods (inches)
300	140	14.85	3.14	1.64	1.11	0.84	0.68	0.57	0.49	0.43	0.38	0.34	0.32	19.62
300	150	14.60	3.10	1.62	1.10	0.83	0.67	0.56	0.48	0.42	0.38	0.34	0.31	19.31
300	160	14.37	3.07	1.60	1.09	0.83	0.66	0.56	0.48	0.42	0.37	0.34	0.31	19.04
300	170	14.18	3.04	1.59	1.08	0.82	0.66	0.55	0.48	0.42	0.37	0.33	0.30	18.81
300	180	14.03	3.02	1.58	1.07	0.81	0.66	0.55	0.47	0.41	0.37	0.33	0.30	18.63
300	190	13.96	3.01	1.58	1.07	0.81	0.65	0.55	0.47	0.41	0.37	0.33	0.30	18.54
300	200	13.96	3.01	1.57	1.07	0.81	0.65	0.55	0.47	0.41	0.37	0.33	0.30	18.54
300	210	14.04	3.02	1.58	1.07	0.81	0.65	0.55	0.47	0.41	0.37	0.33	0.30	18.64
300	220	14.19	3.03	1.59	1.08	0.82	0.66	0.55	0.47	0.42	0.37	0.33	0.30	18.81
300	230	14.40	3.07	1.60	1.09	0.82	0.66	0.56	0.48	0.42	0.37	0.34	0.31	19.06
300	240	14.63	3.10	1.62	1.10	0.83	0.67	0.56	0.48	0.42	0.38	0.34	0.31	19.34
300	250	14.88	3.14	1.63	1.11	0.84	0.68	0.57	0.49	0.43	0.38	0.34	0.31	19.65
300	260	15.11	3.17	1.65	1.12	0.85	0.68	0.57	0.49	0.43	0.38	0.35	0.32	19.93
300	270	15.28	3.19	1.66	1.13	0.85	0.69	0.58	0.50	0.43	0.39	0.35	0.32	20.13
300	280	15.37	3.20	1.66	1.13	0.86	0.69	0.58	0.50	0.44	0.39	0.35	0.32	20.24
300	290	15.37	3.21	1.67	1.13	0.86	0.69	0.58	0.50	0.44	0.39	0.35	0.32	20.25
300	300	15.28	3.19	1.66	1.13	0.86	0.69	0.58	0.50	0.44	0.39	0.35	0.32	20.14
300	310	15.10	3.17	1.65	1.12	0.85	0.68	0.57	0.49	0.43	0.39	0.35	0.32	19.92
300	280	15.37	3.20	1.66	1.13	0.86	0.69	0.58	0.50	0.44	0.39	0.35	0.32	20.24
300	290	15.37	3.21	1.67	1.13	0.86	0.69	0.58	0.50	0.44	0.39	0.35	0.32	20.24

orientation and storm-center location. A sensitivity analysis of this kind should be performed when using the HMR52/HEC-1 PMF estimation procedure. Characteristics of the trials as follows:

Trial 1 – Storm center, area size, orientation, and temporal distribution were selected by the program. Figure 3 shows the storm pattern used for Trials 1 and 2.

Trial 2 – Same as Trial 1, except a temporal distribution is used in which the peak six-hour interval is shifted to the 10th position (hours 54-60). This change increased the peak flow slightly and was used for subsequent trials.

Trial 3 – Same as Trial 2, except the isohyetal pattern was manually centered on the watershed.

Trial 4 – Same as Trial 3, except that a storm-area size of 175 sq. mi. was specified.

Trial 5 – A storm center was determined considering only Subbasins 1, 2, and 3. The centering was chosen because these subbasins produce most of the runoff.

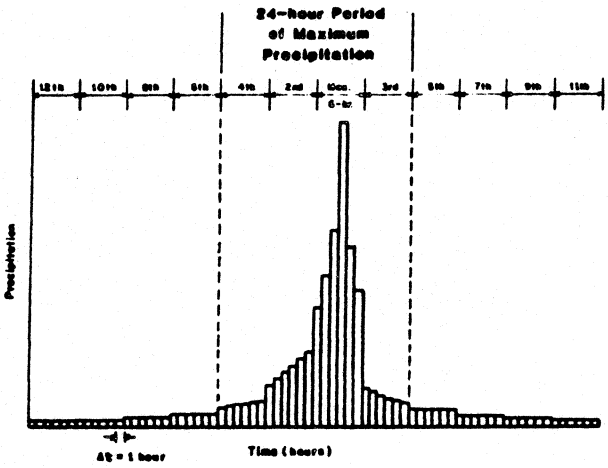

Figure 1. Example One-Hour Distribution of PMS Rainfall.

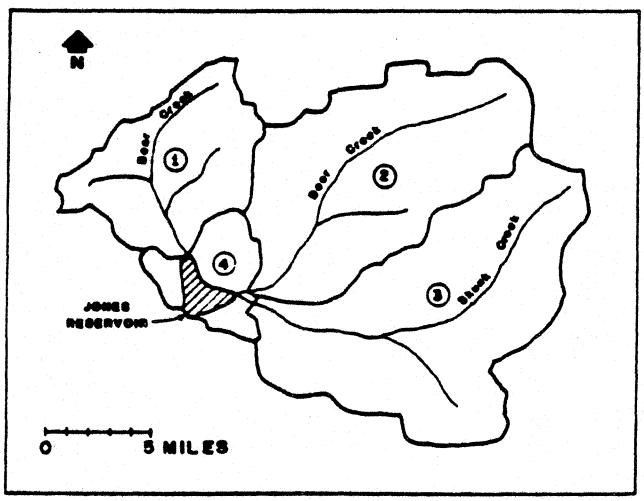

Figure 2. Jones Reservoir Watershed.

As may be noted from Table 4, there is very little difference in results for the five trials. Trial 2 produced the maximum peak inflow and outflow. However the results from Trial 1, using program defaults, could readily be adopted for the PMF, because the difference in peak inflow and outflow differed by only 0.4 percent and 0.7 percent, respectively, from the maximum values.

Although this illustration is hypothetical, studies performed to date indicate that, in most cases, default values in HMR52 will suffice to develop the PMS. However, in the case of a highly unusual basin shape or of a basin with marked spatially heterogeneous runoff characteristics, a number of trials may be warranted.

TABLE 2. Precipitation for Subbasin 1.

		Precipitation (inches)		
	Time	Six-Hour Increment	Two-Hour Increment	Cumulative
Day 1	0000		– –	– –
	0200		0.11	0.11
	0400		0.11	0.22
	0600	0.33	0.11	0.33
	0800		0.13	0.46
	1000		0.13	0.59
	1200	0.40	0.13	0.72
	1400		0.17	0.89
	1600		0.17	1.06
	1800	0.51	0.17	1.23
	2000		0.23	1.46
	2200		0.23	1.70
	2400	0.70	0.23	1.93
Day 2	0200		0.34	2.28
	0400		0.38	2.66
	0600	1.15	0.43	3.09
	0800		0.82	3.91
	1000		1.05	4.95
	1200	3.24	1.37	6.32
	1400		3.94	10.27
	1600		8.99	19.26
	1800	15.51	2.57	21.83
	2000		0.67	22.50
	2200		0.55	23.05
	2400	1.69	0.48	23.53
Day 3	0200		0.29	23.82
	0400		0.29	24.11
	0600	0.87	0.29	24.40
	0800		0.20	24.60
	1000		0.20	24.79
	1200	0.59	0.20	24.99
	1400		0.15	25.14
	1600		0.15	25.29
	1800	0.45	0.15	25.44
	2000		0.12	25.55
	2200		0.12	25.67
	2400	0.36	0.12	25.79

SUMMARY

The National Weather Service has published criteria and procedures for PMS development in the United States east of the 105th meridian. A PMS can be input to a precipitation-runoff simulation program such as HEC1 to develop PMF estimates. A computer program, HMR52, has been developed to facilitate PMS development. The program contains capability to optimize storm-area size and orientation with maximization of average depth as an objective function. In many cases this capability will produce values for storm parameters that are appropriate for PMF development.

TABLE 3. HEC-1 Summary Output for Trial 1
(Runoff Summary – flow in cubic feet per second, time in hours, area in square miles).

Operation	Station	Peak Flow	Time of Peak	Average Flow for Maximum Period			Basin Area
				6-Hour	24-Hour	72-Hour	
Hydrograph at	1	29,528	48.00	28,056	20,818	11,805	51.80
Hydrograph at	4	26,798	42.00	21,758	12,922	8,339	20.30
Two Combined at	1+4	43,374	44.00	42,278	33,231	20,144	72.10
Hydrograph at	2	48,055	50.00	46,176	36,320	20,357	98.60
Hydrograph at	3	44,777	52.00	43,877	36,318	20,591	116.90
Two Combined at	2+3	90,924	52.00	88,749	72,386	40,948	215.50
Two Combined at	Inflow	127,493	50.00	124,553	103,675	61,092	287.60
Routed to	Jones	94,664	60.00	91,656	74,403	42,765	287.60

TABLE 4. Summary of PMF Calculations.

Trial	Position of Peak 6-Hr. Interval	Storm Area (sq. mi.)	Orientation (degrees)	Storm Center (x miles)	Storm Center (y miles)	Total Rainfall (inches)	Peak Inflow (cfs)	Peak Outflow (cfs)
1	7	300	285	32.2	83.8	25.50	127,500	94,650
2	10	300	285	32.2	83.8	25.50	127,800	95,300
3	10	300	285	31.0	83.6	25.44	127,650	95,250
4	10	175	290	31.0	83.6	24.86	125.200	91,650
5	10	300	296	32.7	84.0	25.41	127,200	93,900

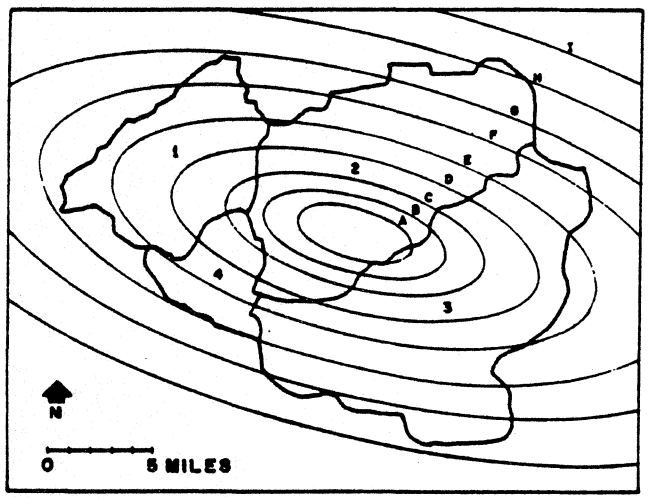

Figure 3. Storm Pattern for Trials 1 and 2.

LITERATURE CITED

Hydrologic Engineering Center, 1979. Introduction and Application of Kinematic Wave Routing Techniques Using HEC-1. Training Document 10. U.S. Army Corps of Engineers, Davis, California.

Hydrologic Engineering Center, 1981. HEC-1 Flood Hydrograph Package – Users Manual. U.S. Army Corps of Engineers, Davis, California.

Hydrologic Engineering Center, 1982. The Hydrologic Engineering Center Data Storage System (HEC-DSS) – An Overview. U.S. Army Corps of Engineers, Davis, California.

Hydrologic Engineering Center, 1983a. HEC-DSS Display Module Users Manual. U.S. Army Corps of Engineers, Davis, California.

Hydrologic Engineering Center, 1983b. HMR52 Probable Maximum Storm (Eastern United States) Users Manual – Draft. U.S. Army Corps of Engineers, Davis, California.

National Weather Service, 1978. Probable Maximum Prescription Estimates, United States East of the 105th Meridian. Hydrometeorological Report No. 51, National Oceanic and Atmospheric Administration, Washington, D.C.

National Weather Service, 1982. Application of Probable Maximum Precipitation Estimates – United States East of the 105th Meridian. Hydrometeorological Report No. 52, National Oceanic and Atmospheric Administration, Washington, D.C.

Unclassified

SECURITY CLASSIFICATION OF THIS PAGE *(When Data Entered)*

REPORT DOCUMENTATION PAGE

READ INSTRUCTIONS BEFORE COMPLETING FORM

1. REPORT NUMBER
Technical Paper No. 100

2. GOVT ACCESSION NO.

3. RECIPIENT'S CATALOG NUMBER

4. TITLE *(and Subtitle)*
Probable Maximum Flood Estimation - Eastern United States

5. TYPE OF REPORT & PERIOD COVERED

6. PERFORMING ORG. REPORT NUMBER

7. AUTHOR*(s)*
Paul B. Ely and John C. Peters

8. CONTRACT OR GRANT NUMBER*(s)*

9. PERFORMING ORGANIZATION NAME AND ADDRESS
U.S. Army Corps of Engineers
The Hydrologic Engineering Center
609 Second Street, Davis, CA 95616

10. PROGRAM ELEMENT, PROJECT, TASK AREA & WORK UNIT NUMBERS

11. CONTROLLING OFFICE NAME AND ADDRESS

12. REPORT DATE
June 1984

13. NUMBER OF PAGES
5

14. MONITORING AGENCY NAME & ADDRESS*(if different from Controlling Office)*

15. SECURITY CLASS. *(of this report)*
Unclassified

15a. DECLASSIFICATION/DOWNGRADING SCHEDULE

16. DISTRIBUTION STATEMENT *(of this Report)*
Distribution of this publication is unlimited.

17. DISTRIBUTION STATEMENT *(of the abstract entered in Block 20, if different from Report)*

18. SUPPLEMENTARY NOTES
This is Paper No. 84017, published in Vol. 20, No. 3 of the Water Resources Bulletin in June 1984. (American Water Resources Assocation)

19. KEY WORDS *(Continue on reverse side if necessary and identify by block number)*
Probable Maximum Flood; design storm.

20. ABSTRACT *(Continue on reverse side if necessary and identify by block number)*
In 1982, the National Weather Service (NWS) published criteria for developing the spatial and temporal precipitation distribution characteristics of Probable Maximum Storms. The criteria, which are intended for use in the United States east of the 105th meridian, involve four variables: (1) location of the storm center, (2) storm-area size, (3) storm orientation, and (4) temporal arrangement of precipitation amounts. A computer program has been developed which applies the NWS criteria to produce hyetographs of spatially-averaged precipitation for a basin, or for each subbasin (CONTINUED)

DD FORM 1 JAN 73 1473 EDITION OF 1 NOV 65 IS OBSOLETE

Unclassified

SECURITY CLASSIFICATION OF THIS PAGE *(When Data Entered)*

if the basin is subdivided. The basis and operational characteristics of the program are described, and an application is illustrated in which the program is used in conjunction with a precipitation-runoff simulation program (HEC-1) to compute a Probable Maximum Flood.

TECHNICAL PAPERS (TP)

Technical papers are written by the staff of the HEC, sometimes in collaboration with persons from other organizations, for presentation at various conferences, meetings, seminars and other professional gatherings.

This listing includes publications starting in 1978.

HEC NUMBER	TITLE	HEC PRICE	NTIS NUMBER
		$2.00 Each	
TP-52	Potential Use of Digital Computer Ground Water Models, D. L. Gundlach, Apr 78, 38 pp.		ADA-106 251
TP-53	Development of Generalized Free Surface Flow Models Using Finite Element Techniques, D. M. Gee and R. C. MacArthur, Jul 78, 21 pp.		ADA-106 252
TP-54	Adjustment of Peak Discharge Rates for Urbanization, D. L. Gundlach, Sep 78, 7 pp.		ADA-106 253
TP-55	The Development and Servicing of Spatial Data Management Techniques in the Corps of Engineers, R. P. Webb and D. W. Davis, Jul 78, 26 pp.		ADA-106 254
TP-56	Experiences of the Hydrologic Engineering Center in Maintaining Widely Used Hydrologic and Water Resource Computer Models, B. S. Eichert, Nov 78, 16 pp.		ADA-106 255
TP-57	Flood Damage Assessments Using Spatial Data Management Techniques, D. W. Davis and R. P. Webb, May 78, 27 pp.		ADA-106 256
TP-58	A Model for Evaluating Runoff-Quality in Metropolitan Master Planning, L. A. Roesner, H. M. Nichandros, R. P. Shubinski, A. D. Feldman, J. W. Abbott, and A. O. Friedland, Apr 72, 81 pp.		ADA-106 257

TECHNICAL PAPERS (TP)(Continued)

HEC NUMBER	TITLE	HEC PRICE	NTIS NUMBER
		$2.00 Each	
TP-59	Testing of Several Runoff Models on an Urban Watershed, J. Abbott, Oct 78, 53 pp.		ADA-106 258
TP-60	Operational Simulation of a Reservoir System with Pumped Storage, G. F. McMahon, V. R. Bonner and B. S. Eichert, Feb 79, 32 pp.		ADA-106 259
TP-61	Technical Factors in Small Hydropower Planning, D. W. Davis, Feb 79, 35 pp.		ADA-109 757
TP-62	Flood Hydrograph and Peak Flow Frequency Analysis, A. D. Feldman, Mar 79 21 pp.		ADA-109 758
TP-63	HEC Contribution to Reservoir System Operation, B. S. Eichert and V. R. Bonner, Aug 79, 28 pp.		ADA-109 759
TP-64	Determining Peak-Discharge Frequencies in an Urbanizing Watershed: A Case Study, S. F. Daly and J. C. Peters, Jul 79, 15 pp.		ADA-109 760
TP-65	Feasibility Analysis in Small Hydropower Planning, D. W. Davis and B. W. Smith, Aug 79, 20 pp.		ADA-109 761
TP-66	Reservoir Storage Determination by Computer Simulation of Flood Control and Conservation Systems, B. S. Eichert, Oct 79, 10 pp.		ADA-109 762
TP-67	Hydrologic Land Use Classification Using LANDSAT, R. J. Cermak, A. D. Feldman and R. P. Webb, Oct 79, 26 pp.		ADA-109 763
TP-68	Interactive Nonstructural Flood-Control Plannng, D. T. Ford, Jun 80, 12 pp.		ADA-109 764

TECHNICAL PAPERS (TP)(Continued)

HEC NUMBER	TITLE	HEC PRICE	NTIS NUMBER
		$2.00 Each	
TP-69	Critical Water Surface by Minimum Specific Energy Using the Parabolic Method, B. S. Eichert, 1969, 15 pp.		ADA-951 599
TP-70	Corps of Engineers Experience with Automatic Calibration of a Precipitation-Runoff Model, D. T. Ford, E. C. Morris, and A. D. Feldman, May 80, 12 pp.		ADA-109 765
TP-71	Determination of Land Use from Satellite Imagery for Input to Hydrologic Models, R. P. Webb, R. Cermak, and A. D. Feldman, Apr 80, 18 pp.		ADA-109 766
TP-72	Application of the Finite Element Method to Vertically Stratified Hydrodynamic Flow and Water Quality, R. C. MacArthur and W. R. Norton, May 80, 12 pp.		ADA-109 767
TP-73	Flood Mitigation Planning Using HEC-SAM, D. W. Davis, Jun 80, 17 pp.		ADA-109 756
TP-74	Hydrographs by Single Linear Reservoir Model, J. T. Pederson, J. C. Peters, and O. J. Helweg, May 80, 17 pp.		ADA-109 768
TP-75	HEC Activities in Reservoir Analysis, V. R. Bonner, Jun 80, 10 pp.		ADA-109 769
TP-76	Institutional Support of Water Resource Models, J. C. Peters, May 80, 23 pp.		ADA-109 770
TP-77	Investigation of Soil Conservation Service Urban Hydrology Techniques, D. G. Altman, W. H. Espey, Jr. and A. D. Feldman, May 80, 14 pp.		ADA-109 771
TP-78	Potential for Increasing the Output of Existing Hydroelectric Plants, D. W. Davis and J. J. Buckley, Jun 81, 20 pp.		ADA-109 772

TECHNICAL PAPERS (TP)(Continued)

HEC NUMBER	TITLE	HEC PRICE	NTIS NUMBER
		$2.00 Each	
TP-79	Potential Energy and Capacity Gains from Flood Control Storage Reallocation at Existing U. S. Hydropower Reservoirs, B. S. Eichert and V. R. Bonner, Jun 81, 18 pp.		ADA-109 787
TP-80	Use of Non-Sequential Techniques in the Analysis of Power Potential at Storage Projects, G. M. Franc, Jun 81, 18 pp.		ADA-109 788
TP-81	Data Management Systems for Water Resources Planning, D. W. Davis, Aug 81, 12 pp.		ADA-114 650
TP-82	The New HEC-1 Flood Hydrograph Package, A. D. Feldman, P. B. Ely and D. M. Goldman, May 81, 28 pp.		ADA-114 360
TP-83	River and Reservoir Systems Water Quality Modeling Capability, R. G. Willey, Apr 82, 15 pp.		ADA-114 192
TP-84	Generalized Real-Time Flood Control System Model, B. S. Eichert and A. F. Pabst, Apr 82, 18 pp.		ADA-114 359
TP-85	Operation Policy Analysis: Sam Rayburn Reservoir, D. T. Ford, R. Garland and C. Sullivan, Oct 81, 16 pp.		ADA-123 526
TP-86	Training the Practitioner: The Hydrologic Engineering Center Program, W. K. Johnson, Oct 81, 20 pp.		ADA-123 568
TP-87	Documentation Needs for Water Resources Models, W. K. Johnson, Aug 82, 16 pp.		ADA-123 558
TP-88	Reservoir System Regulation for Water Quality Control, R.G. Willey, Mar 83, 18 pp.		ADA-130 829
TP-89	A Software System to Aid in Making Real-Time Water Control Decisions, A. F. Pabst and J. C. Peters, Sep 83, 17 pp.		ADA-138 616

TECHNICAL PAPERS (TP)(Continued)

HEC NUMBER	TITLE	HEC PRICE	NTIS NUMBER
		$2.00 Each	
TP-90	Calibration, Verification and Application of a Two-Dimensional Flow Model, D. M. Gee, Sep 83, 6 pp.		ADA-135 668
TP-91	HEC Software Development and Support, B. S. Eichert, Nov 83, 12 pp.		ADA-139 009
TP-92	Hydrologic Engineering Center Planning Models D. T. Ford and D. W. Davis, Dec 83, 17 pp.		ADA-139 010
TP-93	Flood Routing Through A Flat, Complex Floodplain Using A One-Dimensional Unsteady Flow Computer Program, J. C. Peters, Dec 83, 8 pp.		ADA-139 011
TP-94	Dredged-Material Disposal Management Model, D. T. Ford, Jan 84, 18 pp.		ADA-139 008
TP-95	Inflitration and Soil Moisture Redistribution in HEC-1, A. D. Feldman, Jan 84,		ADA-141 626
TP-96	The Hydrologic Engineering Center Experience in Nonstructural Planning, W. K. Johnson and D. W. Davis, Feb 84, 7 pp.		ADA-141 860
TP-97	Prediction of the Effects of a Flood Control Project on a Meandering Stream, D. M. Gee, Mar 84, 12 pp.		ADA-141 951
TP-98	Evolution in Computer Programs Causes Evolution in Training Needs: The Hydrologic Engineering Center Experience, V. R. Bonner, Jul 84, 20 pp.		
TP-99	Reservoir System Analysis for Water Quality, J. H. Duke, D. J. Smith and R. G. Willey, Aug 84, 27 pp.		

TECHNICAL PAPERS (TP)(Continued)

HEC NUMBER	TITLE	HEC PRICE	NTIS NUMBER
		$2.00 Each	
TP-100	Probable Maximum Flood Estimation - Eastern United States, P. B. Ely and J. C. Peters, Jun 84, 5 pp.		
TP-101	Use of Computer Program HEC-5 For Water Supply Analysis, R. J. Hayes and Bill S. Eichert, Aug 84, 7 pp.		

WATER RESOURCES BULLETIN
VOL. 22, NO. 1 AMERICAN WATER RESOURCES ASSOCIATION FEBRUARY 1986

DISCUSSION[1]

"Probable Maximum Flood Estimation – Eastern United States," by Paul B. Ely and John C. Peters[2]

James H. Eychaner[3]

Ely and Peters (1984) presented a detailed computer-based method to estimate the probable maximum flood (PMF) at sites in the United States east of the 105th meridian. In contrast with the effort involved in that computation, I was able to estimate a peak discharge in less than 60 seconds that was within 17 percent of the value for their example site.

An excellent first approximation to the probable maximum flood is available in a set of graphs showing enveloping curves for maximum observed floods (Crippen and Bue, 1977). The floods are the largest known through September 1974 for 883 sites in the conterminous United States with drainage less than 10,000 mi^2. The data are listed in a table, displayed in graphs of peak discharge by drainage area for 17 regions, and summarized by enveloping curves. By knowing only the location of a basin and its drainage area, the user can inspect the graphs for an immediate estimate of peak discharge.

The graphical method is based on runoff data, which is what we are ultimately interested in, rather than relying on extensive manipulations of rainfall data. It is also applicable to 48 states instead of only those east of the Rocky Mountains. The method has some limitations, of course. It applies only to basins without significant regulation of extreme floods, and it does not produce an estimate of the complete hydrograph.

Ely and Peters (1984) reported a probable maximum unregulated discharge of 127,800 ft^3/s for their hypothetical example basin of 228 mi^2 but did not give its location. Crippen and Bue (1977) divided the area east of the 105th meridian into 12 regions. The enveloping-curve discharge for eight of those regions ranges from 110,000 to 150,000 ft^3/s (86 to 117 percent of 127,800). I would be very confident in the 127,800 ft^3/s value if it were for a basin in eastern Kansas where the enveloping curve gives 130,000 ft^3/s. However, if the basin were near the gulf coast of Texas where the enveloping curve gives 500,000 ft^3/s, I would carefully evaluate the reasons for the discrepancy before accepting either figure.

Although the rainfall-based method for estimating the probable maximum flood provides great detail and flexibility, the results should be checked against simple graphs of extreme runoff events. For preliminary analyses, the graphs alone may be sufficient. Crippen (1982) has presented equations that describe the enveloping curves. These equations could easily be written into Ely and Peters' computer package so that results from runoff data could be checked concurrently with the detailed computations using rainfall data.

Finally, although the data base used by Crippen and Bue (1977) is now more than 10 years old, the enveloping curves for several regions have been checked against more recent data and found to remain valid. The U.S. Geological Survey has work in progress to update the graphs for additional regions. The positions of the enveloping curves seem fairly stable because an adequate sample size and record length have been reached. The stability of the curves may also indicate that geophysical limits are being approached (Wolman and Costa, 1984).

LITERATURE CITED

Ely, P. B. and J. C. Peters, 1984. Probable Maximum Flood Estimation – Eastern United States. Water Resources Bulletin 20(3):391-395.

Crippen, J. R., 1982. Envelope Curves for Extreme Flood Events. American Society of Civil Engineers, Journal of Hydraulic Engineering 108(HY10):1208-1212.

Crippen, J. R. and C. D. Bue, 1977. Maximum Floodflows in the Conterminous United States. U.S. Geological Survey Water-Supply Paper 1887, 52 pp.

Wolman, M. G. and J. E. Costa, 1984. Envelope Curves for Extreme Flood Events (discussion). American Society of Civil Engineers, Journal of Hydraulic Engineering 110(HY1):77-78.

[1]Discussion No. 85303D of the *Water Resources Bulletin.*
[2]Paper No. 84017 of the *Water Resources Bulletin* 20(3):391-395.
[3]Hydrologist, U.S. Geological Survey, 300 West Congress St., Tucson, Arizona 85701.

VOL. 22, NO. 1 WATER RESOURCES BULLETIN
AMERICAN WATER RESOURCES ASSOCIATION FEBRUARY 1986

Reply to

DISCUSSION
by James H. Eychaner[1]
"Probable Maximum Flood Estimation – Eastern United States"[2]

Paul B. Ely and John C. Peters[3]

The authors concur with Mr. Eychaner's comments regarding the utility of envelope curves for checking the peak discharge associated with a probable maximum flood (PMF) estimate. However, for spillway design purposes, the volume associated with the reservoir-inflow hydrograph is of utmost importance. As is indicated by Mr. Eychaner, the envelope curves developed by Crippen (1982) provide a check only of peak discharge.

The example used by the authors for the hypothetical Jones Reservoir is based on hydrometeorological criteria for a watershed located in Region 4, for which the envelope curve would indicate a peak discharge of 143,000 cfs. This is about 12 percent greater than the PMF estimate obtained in the authors' example.

LITERATURE CITED

Crippen, J. R., 1982. Envelope Curves for Extreme Flood Events. American Society of Civil Engineers, Journal of Hydraulic Engineering 108(HY10):1208-1212.

[1] Discussion No. 85303D of the *Water Resources Bulletin* 22(1):137.
[2] Paper No. 84017 of the *Water Resources Bulletin* 20(3):391-395.
[3] Respectively, Hydraulic Engineer and Software Consultant, Arcata, California; and Hydraulic Engineer, The Hydrologic Engineering Center, 609 Second St., Davis, California 95616.

REVIEW

OF

OPEN CHANNEL HYDRAULICS

NATIONAL 42-381 50 SHEETS 5 SQUARE 42-382 100 SHEETS 5 SQUARE 42-389 200 SHEETS 5 SQUARE

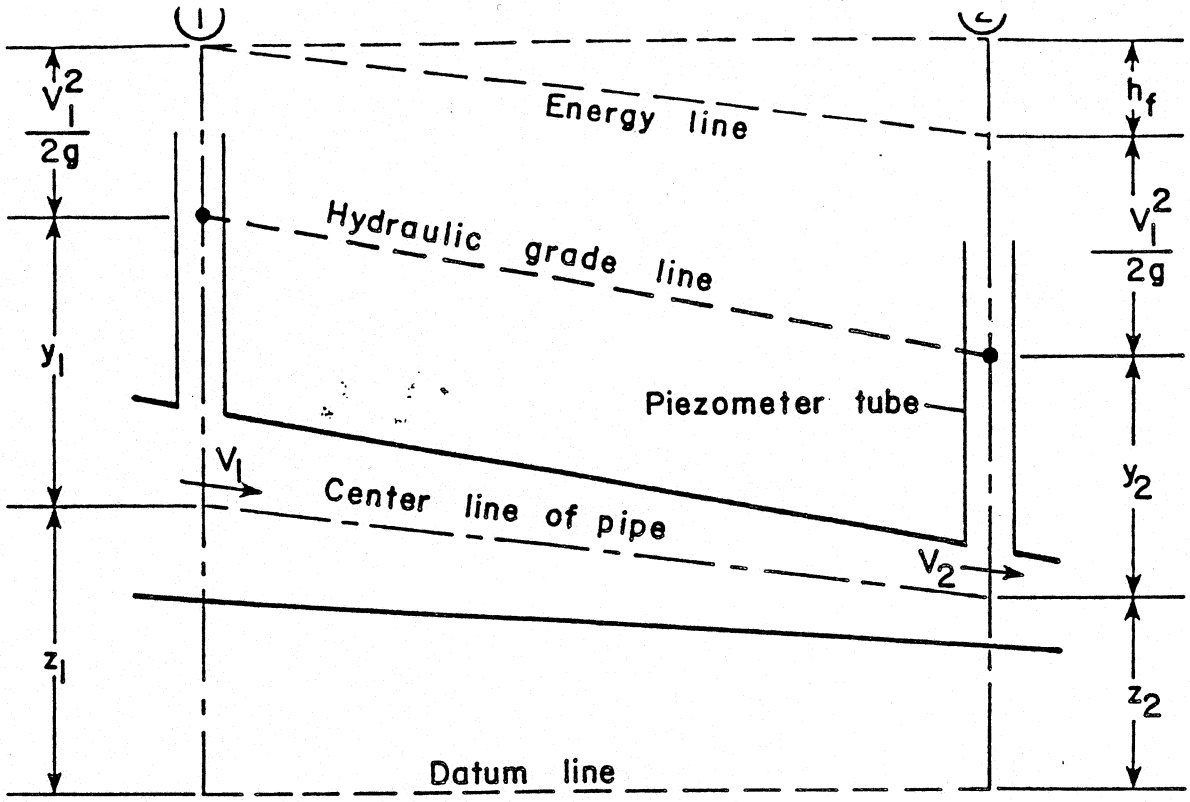

Pipe flow

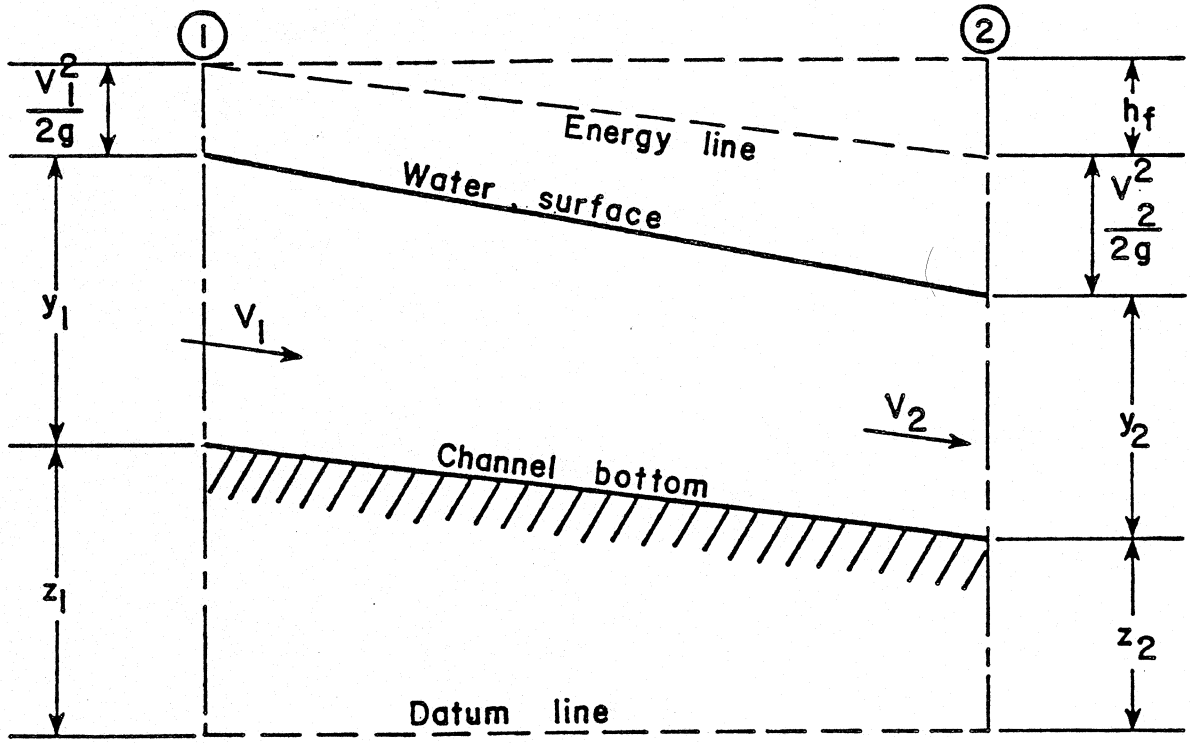

Open - channel flow

OPEN CHANNEL HYDRAULICS

III. Equations for Analysis

A. Continuity $Q = A_1 V_1 = A_2 V_2$; Q known.

Closed conduits - A known, V can be calculated.

Open channel - A and V unknown.

A and V both functions of water depth y.

y unknown.

B. Energy Bernoulli Equation

Closed Conduit

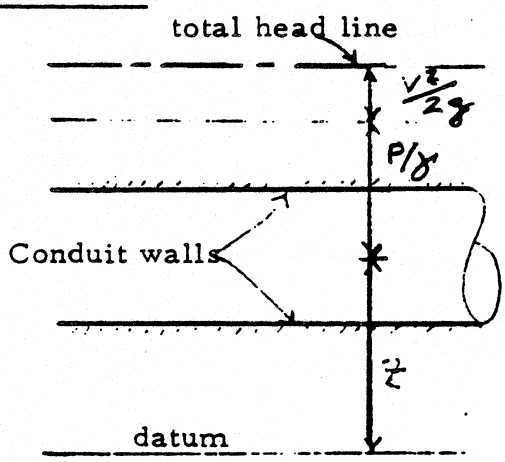

$$H = Z + \frac{P}{\gamma} + \frac{V^2}{2g}$$

Open Channel

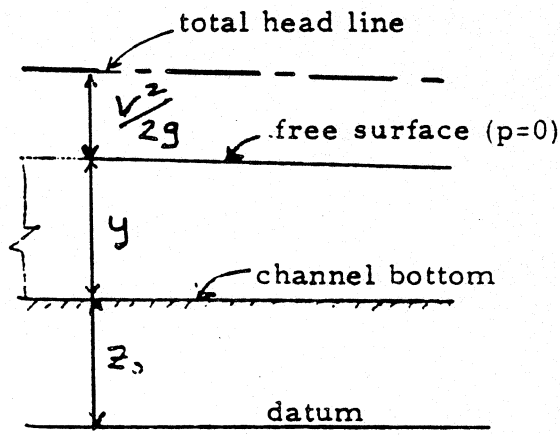

$$H = Z_o + y + \frac{\alpha V^2}{2g}$$ [for hydrostatic pressure distribution]

H and Z_o are known, so we are interested in $y + \frac{\alpha V^2}{2g}$

$$H = Z_o + E_o$$

where $E_o = y + \frac{\alpha V_o^2}{2g}$ = specific energy

$E_o = f(y)$ for $Q = \text{const.}$

$$\alpha = \text{Energy Coefficient} = \frac{\Sigma V^3 \Delta A}{\overline{V}^3 A}$$

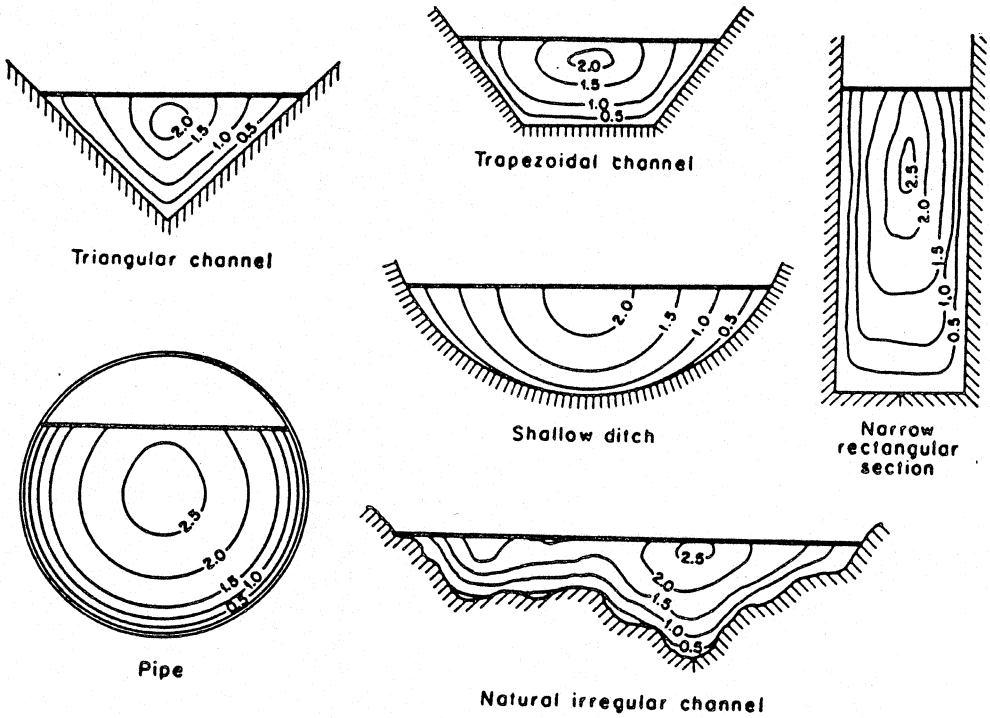

FIG. 2-4. Typical curves of equal velocity in various channel sections.

☆ - Chow

Channels	Value of α			Value of β		
	Min	Av	Max	Min	Av	Max
Regular channels, flumes, spillways	1.10	1.15	1.20	1.03	1.05	1.07
Natural streams and torrents	1.15	1.30	1.50	1.05	1.10	1.17
Rivers under ice cover	1.20	1.50	2.00	1.07	1.17	1.33
River valleys, overflooded	1.50	1.75	2.00	1.17	1.25	1.33

energy

momentum

correction coefficients

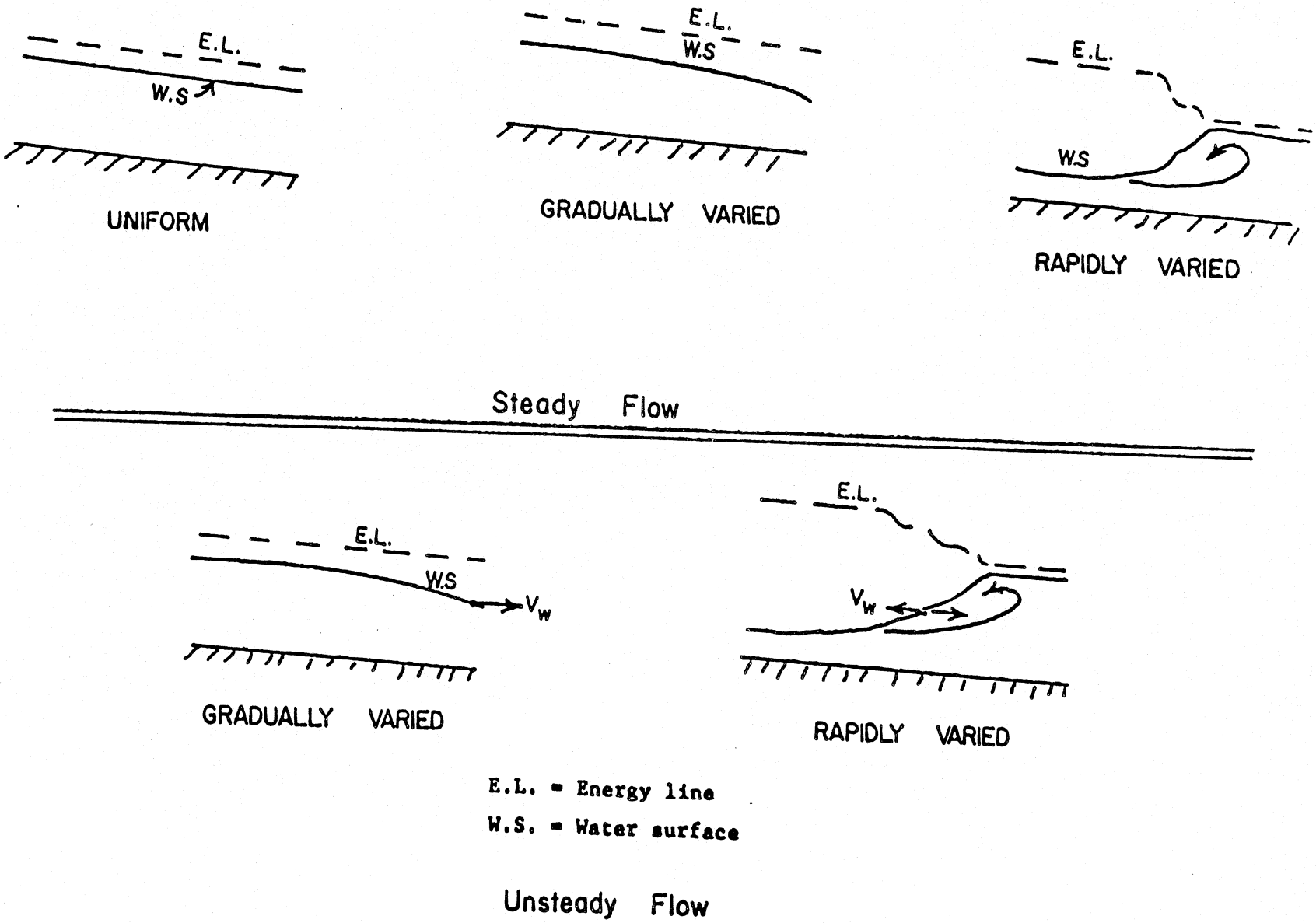

Figure 1.2 Possible Types of Open Channel Flow
(From Thomas, July 1975)

Classification of Flow

1. Steady or unsteady
2. Uniform or nonuniform (varied) { Gradually varied (G. V. F.) / Rapidly varied (R. V. F.)

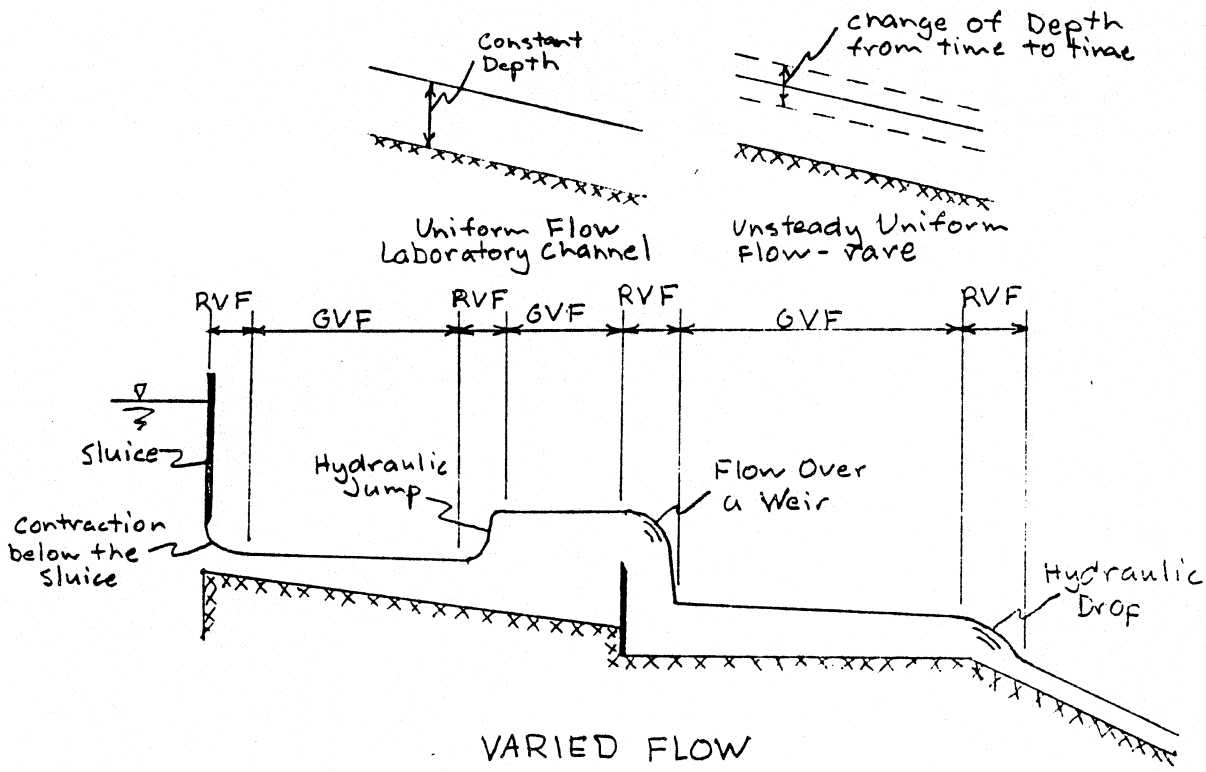

VARIED FLOW

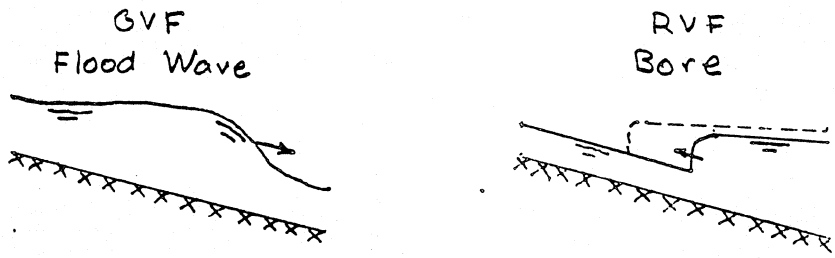

UNSTEADY FLOW

State of Flow

1. Effect of viscosity: laminar or turbulent (measured by viscosity relative to inertia by Reynold's number).

$$R = \frac{VL}{\gamma}$$

L = char. length, ft.
γ = ft^2/sec kinematic viscosity

Nonuniform Flow (Varied Flow)

As a rule, uniform flow is found only in artificial channels of constant shape and slope, and is rarely found in natural streams because of changes in depth, width, and slope along the channel.

In an open stream on a falling grade, the effect of gravity is to tend to produce a flow with a continually increasing velocity along the path. The gravity force is opposed by the frictional resistance. The frictional force increases with velocity, while gravity is constant; so eventually the two will be in balance, and uniform flow may occur. When the two forces are not in balance, the flow is nonuniform.

Two types of nonuniform flow:

Gradually varied flow - changing conditions extend over a long distance (either subcritical or supercritical flow)

Rapidly varied flow - changing conditions take place very rapidly and the transition is thus confined to a short distance

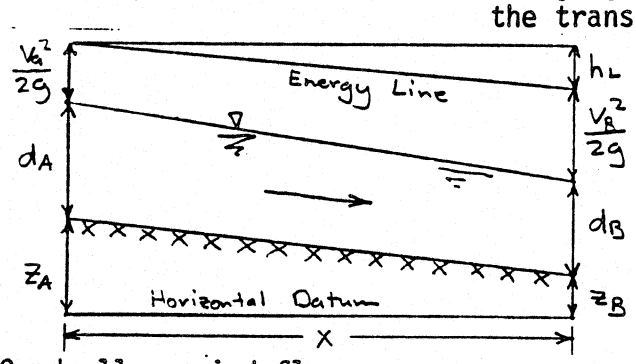

Definition sketch for nonuniform flow in an open channel

Gradually varied flow.

The principal forces involved in flow in an open channel are inertia, gravity, hydrostatic force due to change in depth and friction.

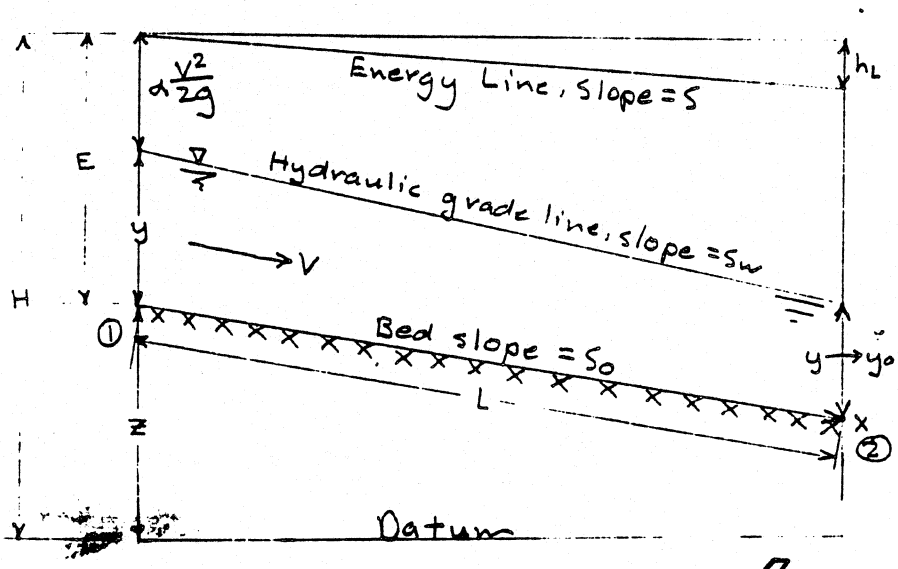

Energy relations for non-uniform flow and Franzini.

2. Effect of gravity: ratio of intertial forces to gravity forces by Froude number

$$F = \frac{V}{\sqrt{gh}} \qquad h = \text{depth, ft.}$$

$F < 1$, subcritical	$V < \sqrt{gh}$
$F = 1$, critical	$V = \sqrt{gh}$
$F > 1$, supercritical	$V > \sqrt{gh}$

<u>Uniform Flow</u>

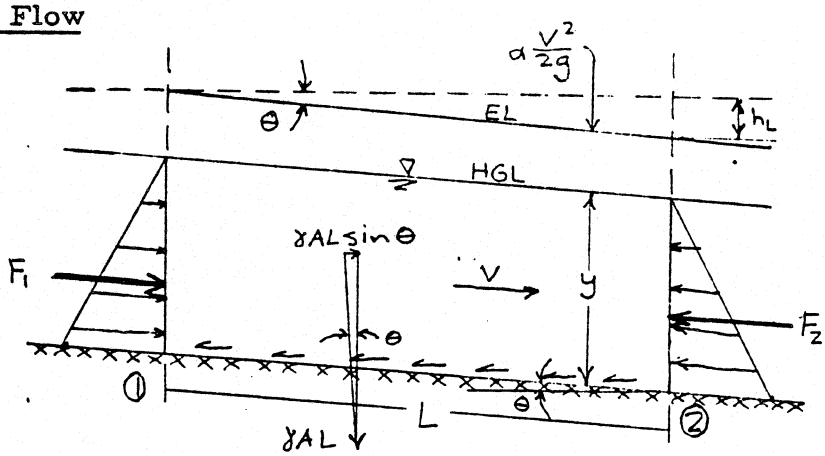

RESISTANCE TO UNIFORM FLOW

Uniform flow, so depths at upstream and downstream ends of section are same:

hydrostatic press. forces

$$F_1 + \underbrace{\gamma AL \sin\theta}_{\text{gravity comp.}} = F_2 + \underbrace{\tau_o PL}_{\text{force to resist boundary shear}}$$

$F_1 = F_2$ (because same depth)

$$\gamma AL \sin\theta = \tau_o PL$$

$\sin\theta$ = slope of H. G. L. = $h_L/L = S$

$$\gamma A \cancel{L} S = \tau_o P \cancel{L}$$

$$\tau_o = \gamma A/P \; S = \gamma RS$$

$$\text{Shear stress} = f \rho \frac{V^2}{8} = \tau_o$$

$$f \rho \frac{V^2}{8} = \gamma RS$$

$$V^2 = 8 \frac{\gamma}{\rho f} RS = \frac{8g}{f} RS \qquad g = \frac{\gamma}{\rho}$$

$$V = \sqrt{\frac{8gRS}{f}}$$

Chezy Equation (average velocity of flow):

$$V = C\sqrt{RS} \qquad \text{where } C = \sqrt{8g/f} \Rightarrow L^{1/2}T^{-1}$$

Through experimental work by Manning:

$$C = \frac{1.49}{n} R^{1/6} \qquad \text{(in English units)}$$

$$C = \frac{R^{1/6}}{n} \qquad \text{(metric)}$$

Manning's Equation:

$$\left.\begin{aligned} V &= \frac{1.49}{n} R^{2/3} S^{1/2} \quad \text{English units} \\ V &= \frac{1}{n} R^{2/3} S^{1/2} \quad \text{Metric} \end{aligned}\right\} \quad 1.49 = (3.28)^{1/3}$$

$$Q = AV = \frac{1.49}{n} AR^{2/3}S^{1/2} \qquad \text{English}$$

$$\text{or} \qquad = \frac{1}{n} AR^{2/3} S^{1/2} \qquad \text{Metric}$$

n = Manning's roughness factor

Valid when channel slope $\prec$ 0.1.

Illustrative example 10.1: Find the depth for uniform flow in this channel when the flow rate is 225 cfs if $S_o = 0.0006$ and n is assumed to be 0.016. Compute the corresponding value of ϵ.

$$A = (10 + 2y)y$$

and $$R = \frac{A}{P} = \frac{(10 + 2y)y}{10 + 2 \times \sqrt{5}\, y}$$

Thus $$Q = 225 = \frac{1.49}{0.016}(10 + 2y)y\left[\frac{(10 + 2y)y}{10 + 2 \times \sqrt{5}\, y}\right]^{2/3}(0.0006)^{1/2}$$

By trial, $y_o = 3.4$ ft, uniform flow depth,

$$A = [10 + 2(3.4)]3.4 = 57.0 \text{ ft}^2$$

$$P = 10 + 2 \times \sqrt{5}\,(3.4) = 25.2 \text{ ft}$$

$$R = \frac{A}{P} = \frac{57.0}{25.2} = 2.26 \text{ ft}$$

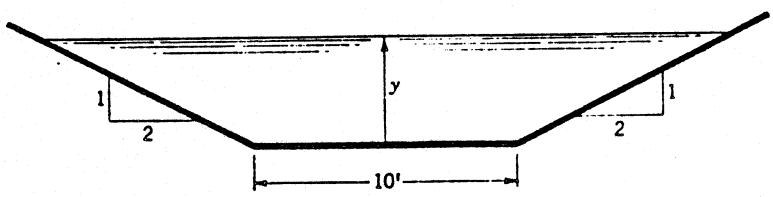

Table 2-1. Geometric Elements of Channel Sections

Section	Area A	Wetted perimeter P	Hydraulic radius R	Top width T	Hydraulic depth D	Section factor Z
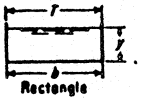 Rectangle	by	$b + 2y$	$\frac{by}{b + 2y}$	b	y	$by^{1.5}$
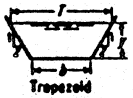 Trapezoid	$(b + zy)y$	$b + 2y\sqrt{1 + z^2}$	$\frac{(b + zy)y}{b + 2y\sqrt{1 + z^2}}$	$b + 2zy$	$\frac{(b + zy)y}{b + 2zy}$	$\frac{[(b + zy)y]^{1.5}}{\sqrt{b + 2zy}}$
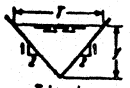 Triangle	zy^2	$2y\sqrt{1 + z^2}$	$\frac{zy}{2\sqrt{1 + z^2}}$	$2zy$	$\frac{1}{2}y$	$\frac{\sqrt{2}}{2}zy^{2.5}$
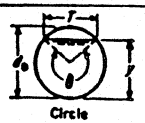 Circle	$\frac{1}{8}(\theta - \sin\theta)d_0^2$	$\frac{1}{2}\theta d_0$	$\frac{1}{4}\left(1 - \frac{\sin\theta}{\theta}\right)d_0$	$(\sin\frac{1}{2}\theta)d_0$ or $2\sqrt{y(d_0 - y)}$	$\frac{1}{8}\left(\frac{\theta - \sin\theta}{\sin\frac{1}{2}\theta}\right)d_0$	$\frac{\sqrt{2}}{32}\frac{(\theta - \sin\theta)^{1.5}}{(\sin\frac{1}{2}\theta)^{0.5}}d_0^{2.5}$
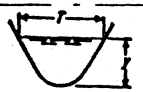 Parabola	$\frac{2}{3}Ty$	$T + \frac{8}{3}\frac{y^2}{T}$ *	$\frac{2T^2y}{3T^2 + 8y^2}$ *	$\frac{3}{2}\frac{A}{y}$	$\frac{2}{3}y$	$\frac{2}{3}\sqrt{6}\,Ty^{1.5}$
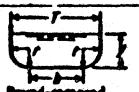 Round-cornered rectangle ($y > r$)	$\left(\frac{\pi}{2} - 2\right)r^2 + (b + 2r)y$	$(\pi - 2)r + b + 2y$	$\frac{(\pi/2 - 2)r^2 + (b + 2r)y}{(\pi - 2)r + b + 2y}$	$b + 2r$	$\frac{(\pi/2 - 2)r^2}{b + 2r} + y$	$\frac{[(\pi/2 - 2)r^2 + (b + 2r)y]^{1.5}}{\sqrt{b + 2r}}$
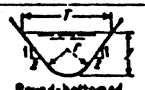 Round-bottomed triangle	$\frac{T^2}{4z} - \frac{r^2}{z}(1 - z\cot^{-1}z)$	$\frac{T}{z}\sqrt{1 + z^2} - \frac{2r}{z}(1 - z\cot^{-1}z)$	$\frac{A}{P}$	$2[z(y - r) + r\sqrt{1 + z^2}]$	$\frac{A}{T}$	$A\sqrt{\frac{A}{T}}$

* Satisfactory approximation for the interval $0 < z \leq 1$, where $z = 4y/T$. When $z > 1$, use the exact expression $P = (T/2)[\sqrt{1 + z^2} + 1/z \ln(z + \sqrt{1 + z^2})]$.

Solution of Manning's Equation by Newton-Raphson Method

There is no general analytical solution to Manning's equation for determining the flow depth given the flow rate. The Newton-Raphson method may be applied iteratively to give a numerical solution. Suppose that at iteration i (i = 1, 2, ...) the depth y_i is selected and from this the flow rate Q_i is computed from

$$Q_i = \frac{1.49}{n} S_o^{1/2} A_i R_i^{2/3} \tag{6.7.4}$$

and compared with the actual flow Q. where A_i and R_i are the area and hydraulic radius corresponding to y_i. The object is to select y so that the error

$$f(y_i) = Q_i - Q \tag{6.7.5}$$

is acceptably small. The gradient of f with respect to y is

$$\left(\frac{\partial f}{\partial y}\right)_i = \frac{\partial Q_i}{\partial y} \tag{6.7.6}$$

because Q is a constant. Hence, assuming Manning's n is constant,

$$\left(\frac{\partial f}{\partial y}\right)_i = \frac{\partial}{\partial y}\left(\frac{1.49}{n} S_o^{1/2} A_i R_i^{2/3}\right)$$

$$= \frac{1.49}{n} S_o^{1/2} \left(\frac{2AR^{-1/3}}{3} \frac{\partial R}{\partial y} + R^{2/3} \frac{\partial A}{\partial y}\right)_i$$

$$= \underbrace{\left[\frac{1.49}{n} S_o^{1/2} A_i R_i^{2/3}\right]}_{Q_i}\left(\frac{2}{3R} \frac{\partial R}{\partial y} + \frac{1}{A} \frac{\partial A}{\partial y}\right)_i$$

$$\left(\frac{\partial f}{\partial y}\right)_i = Q_i \left(\frac{2}{3R}\frac{\partial R}{\partial y} + \frac{1}{A}\frac{\partial A}{\partial y}\right)_i \tag{6.7.7}$$

where the subscript i outside the brackets indicates that the contents are evaluated for $y = y_i$. If the error function f is plotted versus y (Fig. 6.7.3), the gradient $\left(\frac{\partial f}{\partial y}\right)_i$ is given by

$$\left(\frac{\partial f}{\partial y}\right)_i = \frac{0 - f(y_i)}{y_{i+1} - y_i} \tag{6.7.8}$$

where y_{i+1} is the depth extrapolated along the tangent at $y = y_i$ which will make the error zero.

Solving,

$$y_{i+1} = y_i - \frac{f(y_i)}{(\partial f/\partial y)_i} \tag{6.7.9}$$

which is the fundamental equation of the Newton-Raphson method. So, iterations i = 1, 2, ..., are continued until there is no significant change in y and the error in the computed flow is acceptably small.

Substituting from Eqs (6.7.5) and (6.7.7)

$$y_{i+1} = y_i - \frac{1 - Q/Q_i}{\left(\frac{2}{3R}\frac{\partial R}{\partial y} + \frac{1}{A}\frac{\partial A}{\partial y}\right)_i} \tag{6.7.10}$$

for a rectangular channel A = By, R = By/(B + 2y); so, after some manipulation

$$y_{i+1} = y_i - \frac{1 - Q/Q_i}{\left[\frac{5B + 6y_i}{3y_i(B + 2y_i)}\right]}$$

13

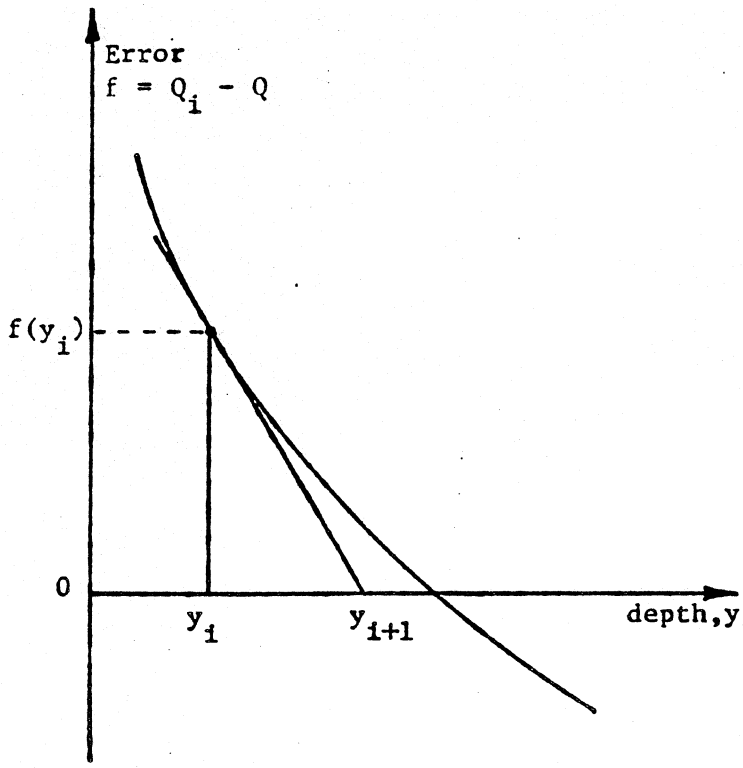

Figure 6.7.3 The Newton-Raphson method extrapolates the tangent of the error function at the current depth y_i to obtain the depth for the next iteration y_{i+1}

The values for $\frac{2}{3R}\frac{\partial R}{\partial y} + \frac{1}{A}\frac{\partial A}{\partial y}$ for other cross-sections are given in Table 6.7.1.

Example 6.7.3.

Calculate the flow depth in a 2 ft wide rectangular channel having $n = 0.015$, $S_o = 0.025$, $Q = 9.26$ cfs.

Solution.

$$Q_i = \frac{1.49}{n} S_o^{1/2} \frac{(By_i)^{5/3}}{(B + 2y_i)^{2/3}}$$

$$= \frac{1.49}{0.015} (0.025)^{1/2} \frac{(2y_i)^{5/3}}{(2 + 2y_i)^{2/3}}$$

$$Q_i = \frac{31.41\ y_i^{5/3}}{(1 + y_i)^{2/3}}$$

and $$\frac{5B + 6y_i}{3y_i\ (B + 2y_i)} = \frac{10 + 6y_i}{3y_i\ (2 + 2y_i)}$$

$$= \frac{1.667 + y_i}{y_i(1 + y_i)}$$

$$\therefore\ y_{i+1} = y_i - \frac{(1 - 9.26/Q_i)\ y_i(1 + y_i)}{1.667 + y_i}$$

From an arbitrarily chosen starting depth of $y = 1.00$ ft, the solution to three significant figures is achieved after 3 iterations.

Section	Area A	Wetted Perimeter P	Hydraulic Radius R	Top Width T	$\frac{2}{3R}\frac{\partial R}{\partial y} + \frac{1}{A}\frac{\partial A}{\partial y}$
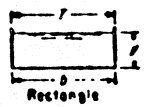 Rectangle	By	$B + 2y$	$\frac{By}{B + 2y}$	B	$\frac{5B + 6y}{3y(B + 2y)}$
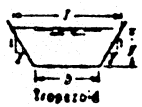 Trapezoid	$(B + zy)y$	$B + 2y\sqrt{1 + z^2}$	$\frac{(B + zy)y}{B + 2y\sqrt{1 + z^2}}$	$B + 2zy$	$\frac{(B + 2zy)(5B + 6y\sqrt{1 + z^2})}{3y\,(B + zy)(B + 2y\sqrt{1 + z^2})}$ $+4zy^2\sqrt{1+z^2}$
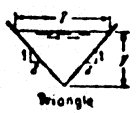 Triangle	zy^2	$2y\sqrt{1 + z^2}$	$\frac{zy}{2\sqrt{1 + z^2}}$	$2zy$	$\frac{8}{3y}$
Circle	$1/8(\theta - \sin\theta)d_o^2$	$1/2\,\theta\,d_o$	$1/4\left(1 - \frac{\sin\theta}{\theta}\right)d_o$	$(\sin 1/2\,\theta)d_o$ or $2\sqrt{y(d_o - y)}$	$\frac{1}{y}\left[\frac{3\theta - \theta\cos\theta - 2\sin\theta}{3(\theta - \sin\theta)}\right]$

Table 6.7.1 Geometrical Functions for Channel Elements [after Chow (1959) with additions]

Source: Chow, V.T., Open-Channel Hydraulics, McGraw-Hill, New York, 1959, Table 2.1, p. 21.

Iteration, i	1	2	3	4
y_i (ft)	1.00	0.601	0.577	0.577
Q_i (cfs)	19.787	9.82	9.26	9.26

Example 6.7.4.

Compute the velocity and depth of flow at 200 ft increments along a 1000 ft long rectangular channel having width 2 ft, roughness n = 0.015, slope S_o = 0.025, fed by a lateral flow of 0.00926 cfs/ft.

Solution.

The method of Example 6.7.3 is applied repetitively to compute y for Q = 0.00926 L. The velocity v = Q/By = Q/2y.

Distance Along Channel, L (ft)	0	200	400	600	800	1000
Flow Rate, Q (cfs)	0	1.85	3.70	5.56	7.41	9.26
Depth, y (ft)	0	0.20	0.31	0.41	0.49	0.58
Velocity, v (ft/sec)	0	4.63	5.97	6.86	7.56	8.02

The previous examples in this section have assumed steady flow on the watershed. In reality, under a constant intensity rainfall, the steady flow at equilibrium is approached asymptotically at a time of equilibrium t_e in the manner illustrated by Fig. 6.7.4. Thus the flow is varying both in space and time on the watershed surface and in the stream channel. Detailed solution for the depth and velocity of this flow is taken up in Chapter 10.

Specific Energy

Many problems of open-channel flow are solved by a special application of the energy principle using the channel bottom as the datum plane. The concept and use of specific energy, the distance between channel bottom and energy line, are useful in the explanation and analysis of new and old problems of open-channel flow.

Considering the following figure:

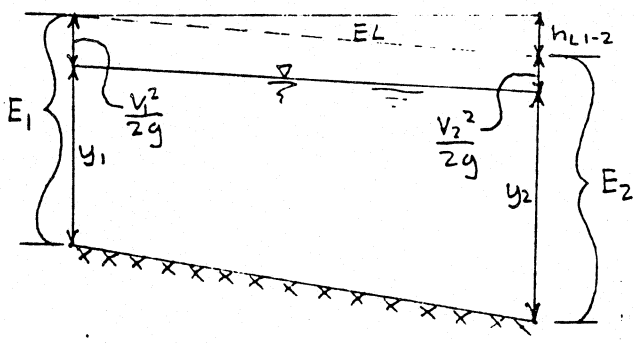

It is not possible to predict the character of the change of specific energy between sections 1 and 2. Although the energy line must fall in the direction of flow, the specific energy may increase or decrease, depending upon other factors.

$$\text{Specific energy} \quad E = y + \frac{V^2}{2g}$$

$$= y + \frac{1}{2g}\left(\frac{Q}{A}\right)^2$$

Now consider a flow in a wide channel of rectangular cross-section. The assumption of a wide channel allows us to use q = flow rate/unit width of channel and y = depth.

So $V = \frac{q}{y}$

Then $E = y + \frac{1}{2g}\left(\frac{q}{y}\right)^2$

or $q = \sqrt{2g(y^2E - y^3)}$ Relation of flowrate, depth and specific energy

Plotting this relationship gives a specific energy diagram and the q-curve below.

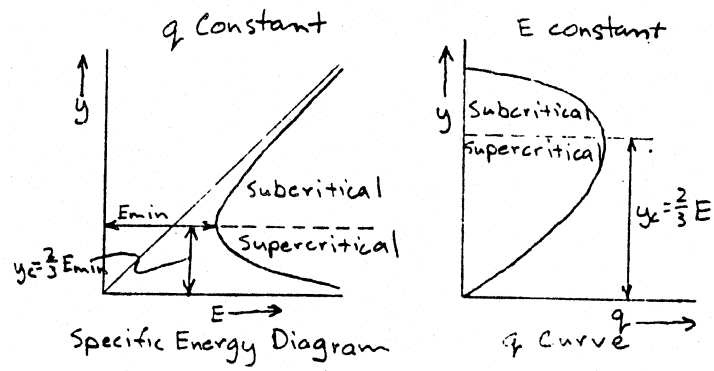

Specific Energy and q-Curve

Merely different plots of the same equation. Minimum E and maximum q are equivalent. The depth associated with these points is the <u>critical depth</u>, y_c or d_c.

Point out supercritical and subcritical areas.

An increase in depth $\begin{cases} \text{increase in energy in subcritical} \\ \text{decrease in specific energy in supercritical flow} \end{cases}$

For a given specific energy two depths (alternate depth) and thus two flow situations (one subcritical and one supercritical).

Therefore, from this analysis we can see the importance in calculating the critical depth to identify the type of flow.

$$\frac{dE}{dy} = 0 \quad \Rightarrow \quad \frac{d}{dy}\left[y + \frac{1}{2g}\left(\frac{q}{y}\right)^2\right] = 0$$

$$q = \sqrt{g\, y_c^3} \quad \text{or} \quad y_c = \sqrt[3]{\frac{q^2}{g}}$$

$$\frac{dq}{dy} = 0 \quad \Rightarrow \quad \frac{d}{dy}\left[\sqrt{2g\,(y^2E - y^3)}\right] = 0$$

$$y_c = \frac{2E_{min}}{3} \quad \text{or} \quad E_{min} = \frac{3y_c}{2}$$

Using $q = \sqrt{2g\,(y^2E - y^3)}$ and substitute in $E_{min} = \frac{3y_c}{2}$ gives $q = \sqrt{gy_c^3}$.
Therefore, critical depth is dependent upon flowrate only.

Critical velocity - velocity at critical depth

$$q = V_c y_c \quad \text{and} \quad q = \sqrt{gy_c^3}$$

$$V_c y_c = \sqrt{gy_c^3} \Rightarrow V_c = \sqrt{gy_c}$$

19

$\sqrt{gy}$ = celerity or velocity of propagation of a small wave on the surface of a liquid of depth y .

Subcritical flow	$v < \sqrt{gy}$	so small waves will progress upstream
Supercritical flow	$v > \sqrt{gy}$	small waves will not progress upstream
Mild slope	$y_n > y_c$	subcritical flow
where	y_n = normal depth, depth at which uniform flow will occur in an open channel (from Manning's equation).	
Steep slope	$y_n < y_c$	supercritical

Problem 5

For a rectangular channel of 20 ft. width, construct a family of specific energy curves and a family of specific force curves for Q = 0,50, 100, and 300 cfs. Draw the locus of the critical depth point on these curves. For each flow rate, what is the minimum energy found from these curves?

Solution:

a)

$$y_c = \sqrt[3]{\frac{q^2}{g}} \leftarrow q = \frac{Q}{b}$$

$$E = y + \frac{V^2}{2g} \leftarrow V = \frac{Q}{A}$$

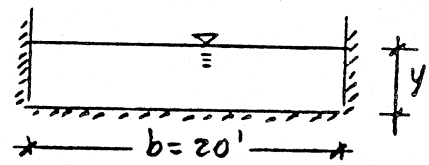

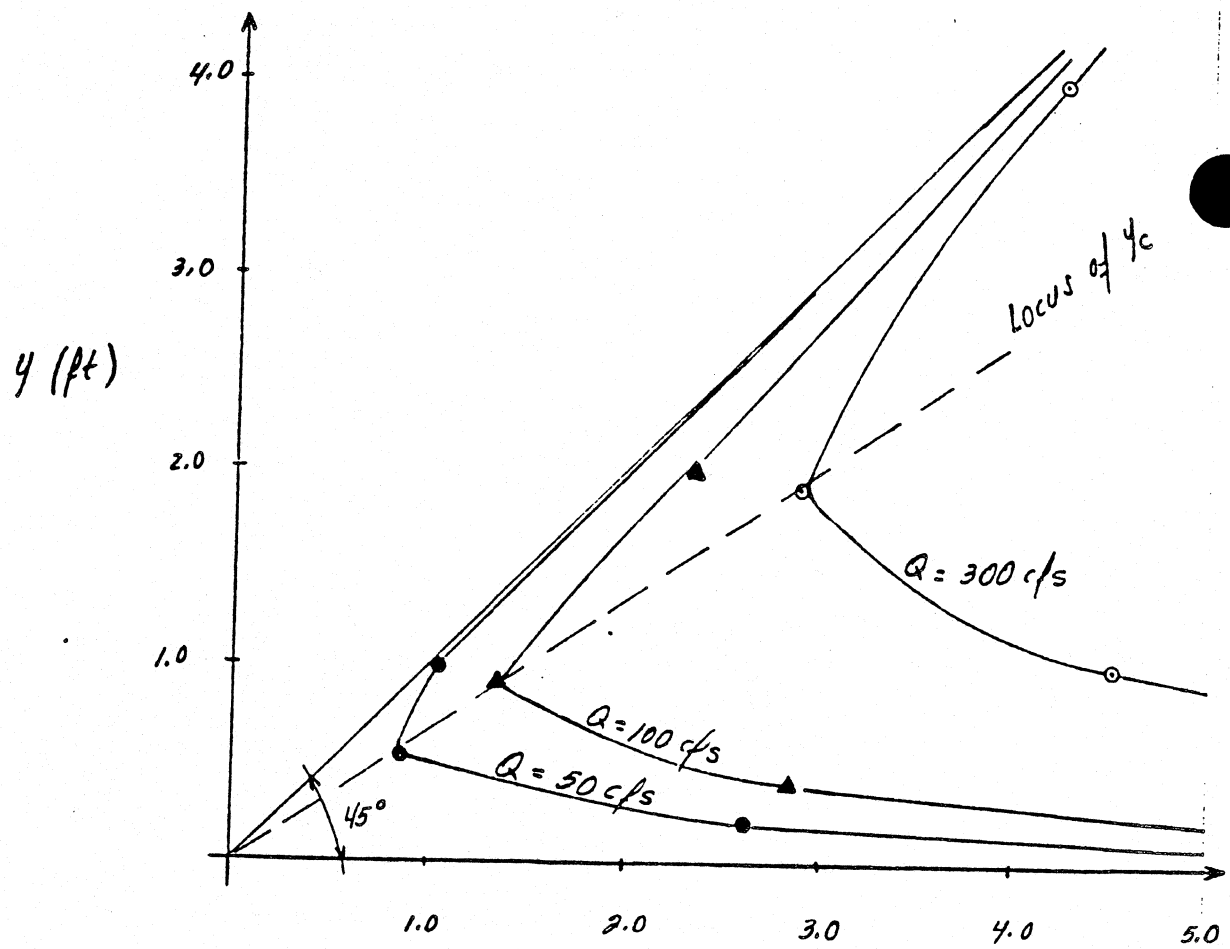

(E = y, for Q = 0)

b) $q = \frac{Q}{b} \rightarrow y_c = \sqrt[3]{\frac{q^2}{g}}$

$$F = \frac{q^2 b}{g\, y} + \frac{b y^2}{2}$$

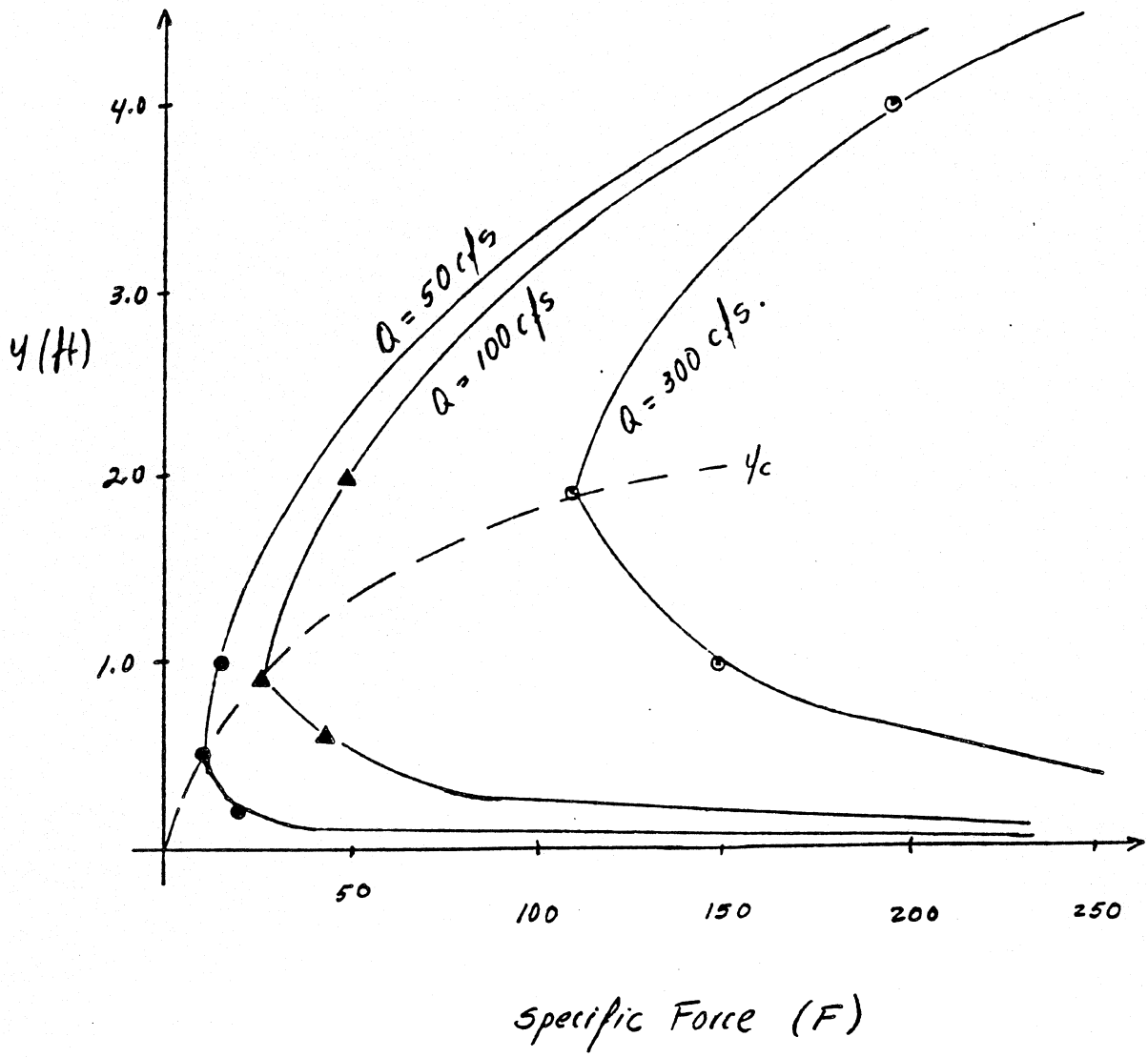

IV. Specific Energy and Critical Flow

A. Equations

$$E_o = y + \frac{\alpha Q^2}{2gA^2} = y + \frac{\alpha V^2}{2g}$$

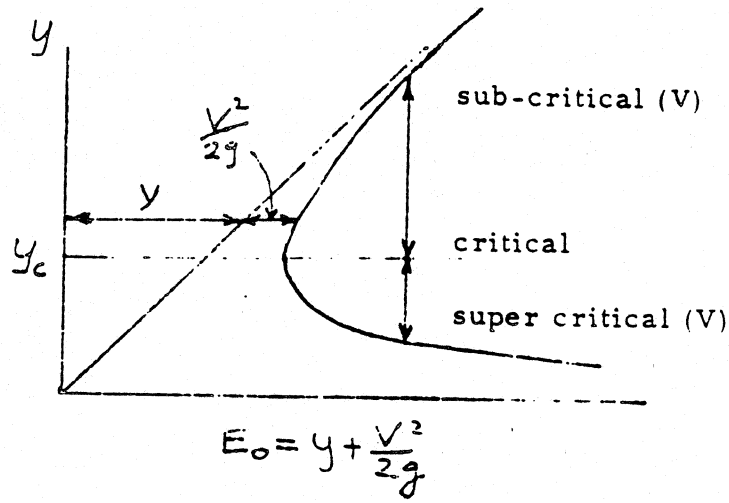

Min E_o is "critical" flow

For min E_o

$$\frac{dE_o}{dy} = 1 - \frac{2\alpha Q^2}{2gA^3}\frac{dA}{dy} = 0$$

$$\frac{\alpha Q^2 T}{gA^3} = 1$$

or $\frac{\alpha V^2}{2g} = \frac{A}{2T} = \frac{1}{2}$ y avg.

B. Significance of Critical Flow

1. Min E_o for Q=const.
2. Max Q for E_o =const.
3. Flow velocity $V = V_c$=Velocity of surface wave = $\sqrt{gy}$

   Froude No. $F_r = 1.0$
4. For a decrease in E_o, depth moves toward y_c; an increase in E_o, depth moves away from y_c.
5. When $V=V_c$ standing waves occurs, i.e. depth is not constant.
6. $V < V_c$, flow is <u>sub critical</u> and <u>depth is controlled from downstream,</u> $F_r < 1.0$.

7. $V > V_c$, flow is <u>super critical</u> and <u>depth is controlled from upstream</u>, $F_r > 1.0$.

8. When flow passes downward through critical conditions a <u>control</u> exists, i.e. the water surface elevation is fixed for given Q and cross section.

V. Non-Uniform Flow

A. Purpose

Control points known, i.e. water depth at specific stations along channel.

Need method to calculate water surface profile, i.e. depth y vs. station x.

B. Non-Uniform Flow Equations - Prismatic Channel

Consider total Head H and calculate rate of change with distance x.

$$H = Z_o + y + \frac{V^2}{2g}$$

$$\frac{dH}{dX} = \frac{dZ_o}{dx} + \frac{dy}{dx} - 2\,\frac{Q^2}{2gA^3}\,\frac{dA}{dy}\,\frac{dy}{dx}$$

$$-S_f = -S_o + \frac{dy}{dx} - \frac{Q^2 T}{g A^3}\,\frac{dy}{dx}$$

gradually varied flow equation

$$\frac{dy}{dx} = \frac{S_o - S_f}{1 - \frac{Q^2 T}{gA^3}} = \frac{1}{f(y)}$$ for a given Q and cross section

Integrate $\frac{dy}{dx} = \frac{1}{f(y)}$ to find profile y vs x.

$$dx = \int f(y)\,dy = \left(\frac{1 - \frac{Q^2 T}{gA^3}}{S_o - S_f} \right) dy$$

Consider sign of numerator of f(y) for flow depth y above, equal to, or less than critical depth y_c, and sign of denominator for depths above, equal to, or less than normal depth y_n (depth for uniform flow).

		Sign		
numerator	$\left(1 - \frac{Q^2 T}{gA^3}\right)$	$y > y_c$	$y = y_c$	$y < y_c$
		+	0	-
denominator	$(S_o - S_f)$	$y > y_n$	$y = y_n$	$y < y_n$
		+	0	-

C. Profile Types

For mild slope-

Channel slope $S_o <$ critical slope S_c

and normal depth $y_n >$ critical depth y_c

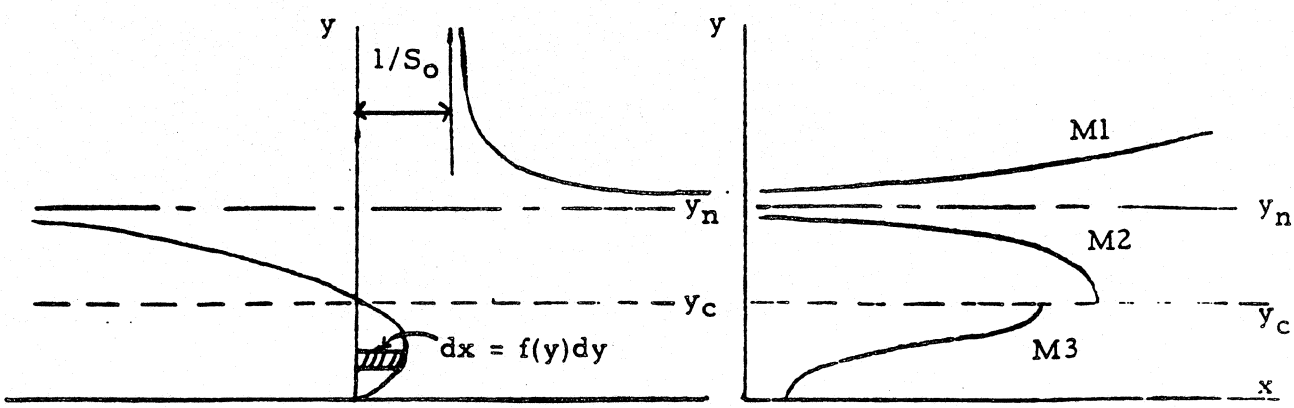

For steep slope-

Channel slope S_o > critical slope S_c

and normal depth y_n < critical depth y_c

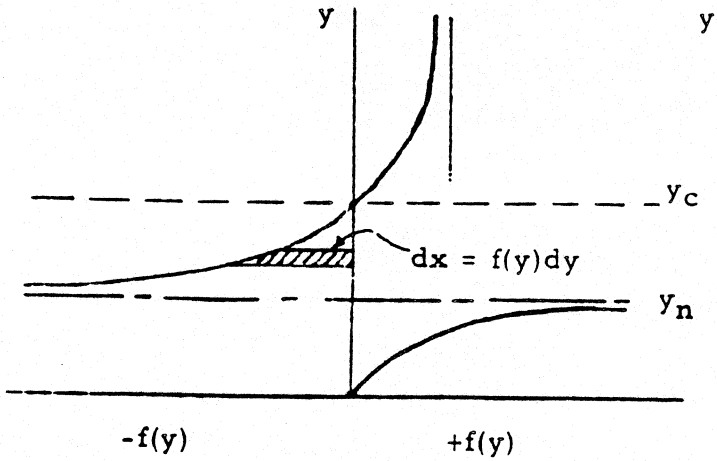

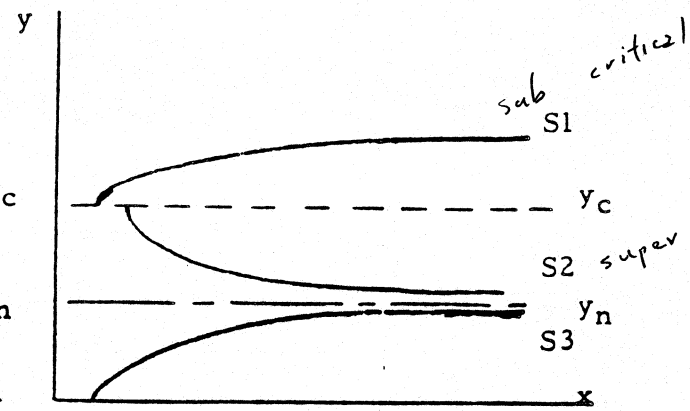

For critical slope

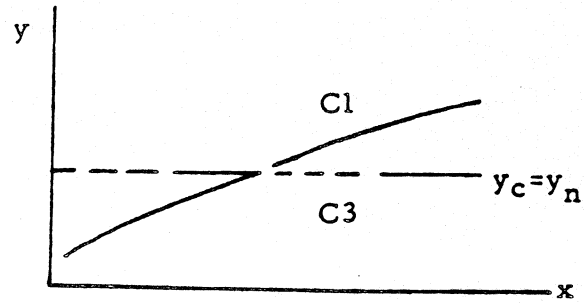

For horizontal slope

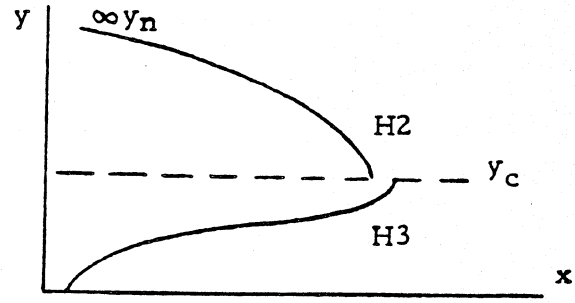

For adverse slope

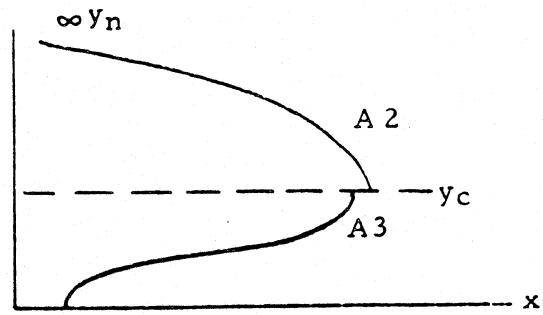

These are all the possible gradually varied flow profiles. Their general shape is shown, but in a particular case the coordinates of the profile depend on numerical values of

$$f(y) = \frac{1 - \frac{Q^2 T}{g A^3}}{S_o - S_f}$$

On the following page is a summary of these profiles with some examples shown at the right. The figure is reproduced by permission from Daugherty & Franzini, Fluid Mechanics with Engineering Applications, McGraw-Hill Book Company.

D. Flow Analysis

It is useful to analyze possible flow situations.

Procedure - Determine critical depth y_c and normal depth y_n for each channel or reach.

- Identify control points.
- Sketch water surface profile upstream and downstream from each control point.

Slope	Designation	Relation of Y, Y_n, Y_c.	dy/dx	Sketch.
Mild	M-1	$Y > Y_n > Y_c$	$\frac{+}{+} = +$	
	M-2	$Y_n > Y > Y_c$	$\frac{-}{+} = -$	
	M-3	$Y_n > Y_c > Y$	$\frac{-}{-} = +$	

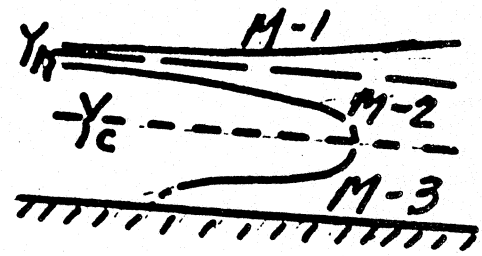

Critical	C_1	$Y > Y_c = Y_n$	$\frac{+}{+} = +$	
	C_2	$Y = Y_n = Y_c$ Uniform flow at critical		
	C_3	$Y_n = Y_c > Y$	$\frac{-}{-} = +$	

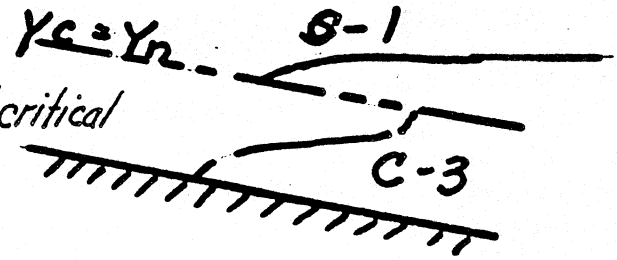

Steep.	S1	$Y > Y_c > Y_n$	$\frac{+}{+} = +$	
	S-2	$Y_c > Y > Y_n$	$\frac{+}{-} = -$	
	S-3	$Y < Y_n < Y_c$	$\frac{-}{-} = +$	

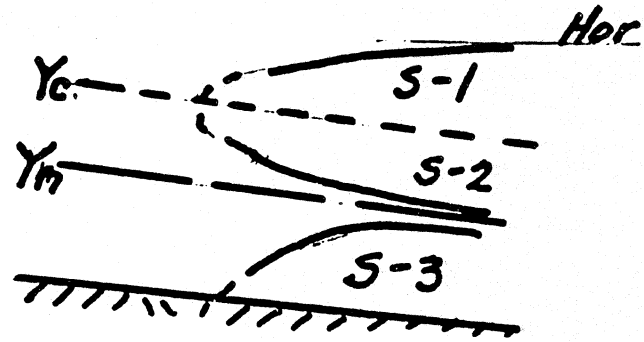

HORIZONTAL

H-2	$\frac{-}{+} = -$
H-3	$\frac{-}{-} = +$

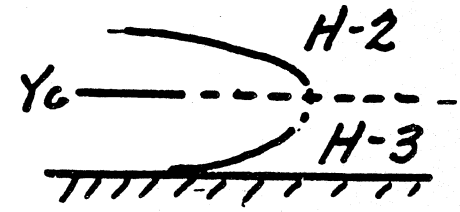

ADVERSE $\frac{-}{+} = -$

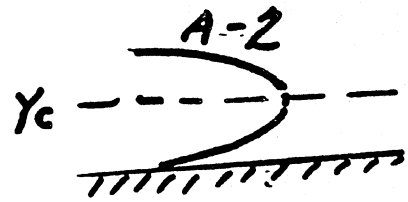

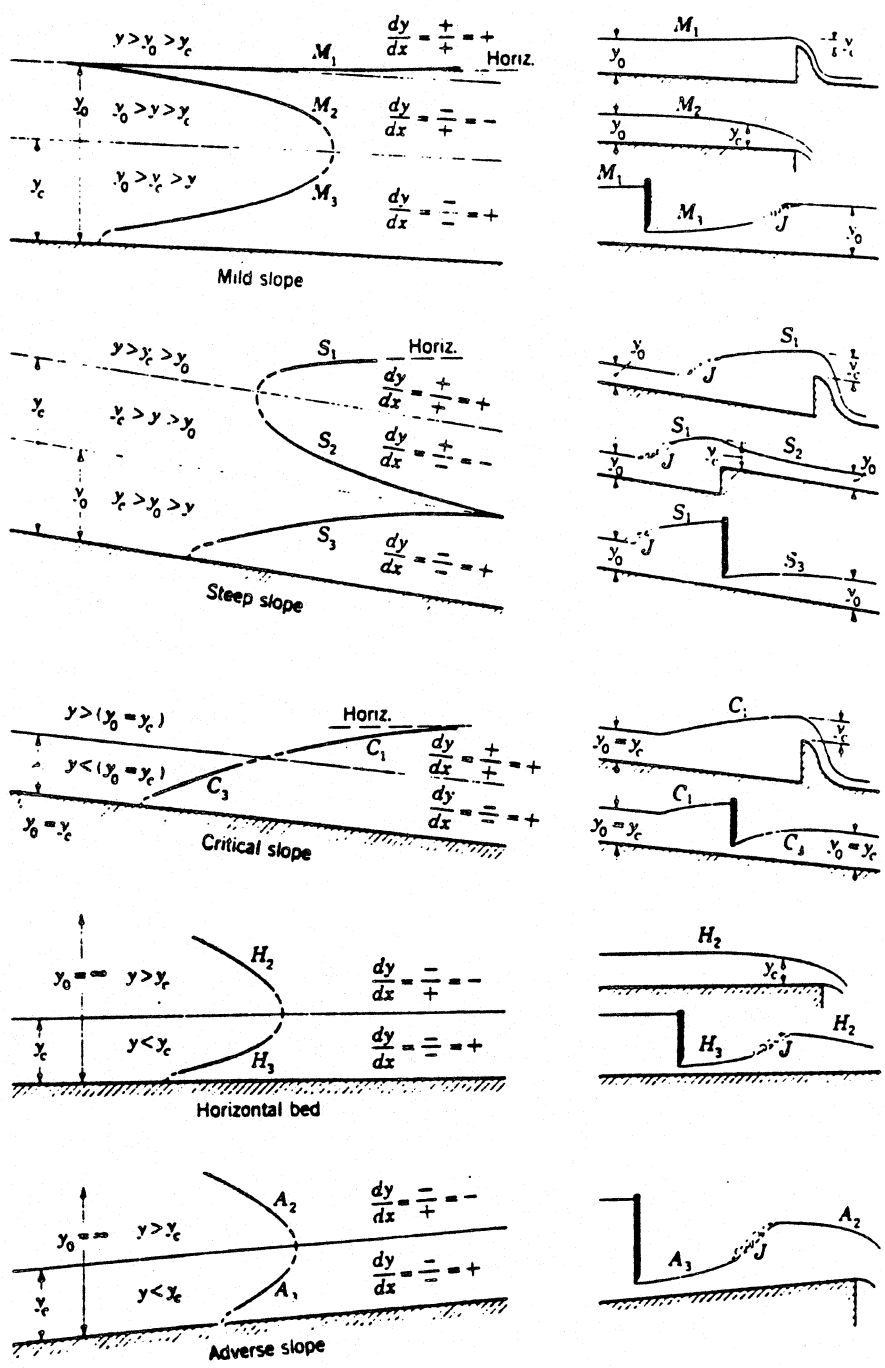

Various types of nonuniform flow.

TABLE 9-1. TYPES OF FLOW PROFILES IN PRISMATIC CHANNELS

Channel slope	Designation			Relation of y to y_n and y_c			General type of curve	Type of flow
	Zone 1	Zone 2	Zone 3	Zone 1	Zone 2	Zone 3		
Horizontal $S_0 = 0$	None			$y > y_n > y_c$			None	None
		$H2$			$y_n > y > y_c$		Drawdown	Subcritical
			$H3$		$y_n > y_c > y$		Backwater	Supercritical
Mild $0 < S_0 < S_c$	$M1$			$y > y_n > y_c$			Backwater	Subcritical
		$M2$			$y_n > y > y_c$		Drawdown	Subcritical
			$M3$		$y_n > y_c > y$		Backwater	Supercritical
Critical $S_0 = S_c > 0$	$C1$			$y > y_c = y_n$			Backwater	Subcritical
		$C2$			$y_c = y = y_n$		Parallel to channel bottom	Uniform-critical
			$C3$		$y_c = y_n > y$		Backwater	Supercritical
Steep $S_0 > S_c > 0$	$S1$			$y > y_c > y_n$			Backwater	Subcritical
		$S2$			$y_c > y > y_n$		Drawdown	Supercritical
			$S3$		$y_c > y_n > y$		Backwater	Supercritical
Adverse $S_0 < 0$	None			$y > (y_n)^* > y_c$			None	None
		$A2$			$(y_n)^* > y > y_c$		Drawdown	Subcritical
			$A3$		$(y_n)^* > y_c > y$		Backwater	Supercritical

* y_n in parentheses is assumed a positive value.

COMPUTATION METHODS

I. Direct Step Method - For Prismatic Channels

SOLVING FOR "L"

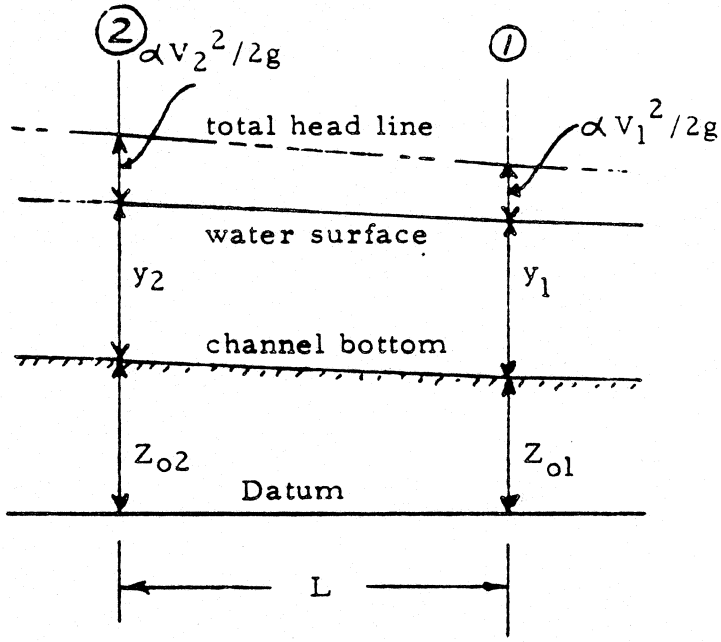

DIRECT STEP IS VERTICAL SOLUTION

STANDARD STEP IS HORIZONTAL SOLUTION

$$Z_{o2} + y_2 + \alpha \frac{V_2^2}{2g} = Z_{o1} + y_1 + \alpha_1 \frac{V_1^2}{2g} + H_L$$

$$Z_{o2} + E_{o2} = Z_{o1} + E_{o1} + H_L$$

$$H_L = \left(\frac{S_{f1} + S_{f2}}{2} \right) L$$

S_f = slope of total head line

Evaluate S_f from Manning Equation.

$$Q = \frac{1.49}{n} AR^{2/3} S_o^{1/2} = K S_o^{1/2} \quad \text{(uniform flow)}$$

$$\text{conveyance } K = \frac{1.49}{n} AR^{2/3}$$

Assume for non-uniform flow that slope of total lead line S_f is the same as slope S_o for uniform flow at same depth and Q in channel, i.e.

$$S_f = \frac{Q^2}{K^2}$$

Then solving Bernoulli's Equation

$$L = \frac{E_{o2} - E_{o1}}{\frac{1}{2}\left(\frac{Q^2}{K_1^2} + \frac{Q^2}{K_2^2}\right) - S_o}$$

To calculate water surface profile

1) Calculate upstream if flow is sub/critical, calculate downstream if flow is super/critical.
2) Start at point in channel where depth is known and call this y_1.
3) Calculate y_n and y_c for channel and determine type of profile and its general shape.
4) Choose y_2 slightly larger (or smaller depending on type of profile) and calculate

$$L = \frac{y_2 - y_1 + \alpha_2 \frac{V_2^2}{2g} - \alpha_1 \frac{V_1^2}{2g}}{\frac{Q^2}{2}\left(\frac{1}{K_1^2} + \frac{1}{K_2^2}\right) - S_o}$$

which gives location of assumed depth y_2.

5) Repeat starting with point 2 and continue until profile is delineated.

ILLUSTRATIVE EXAMPLE 10-1 A discharge of 160 cfs occurs in a rectangular open channel 6 ft wide with $S_0 = 0.002$ and $n = 0.012$. If the channel ends in a free outfall, calculate the depth at the brink, d_n, and d_c. Determine the shape of the water-surface profile for a distance of 100 ft upstream from the brink.

$$Q = \frac{1.49}{n} AR^{2/3}S^{1/2} = \frac{1.49}{0.012} \times 6d_n \times \left(\frac{6d_n}{6 + 2d_n}\right)^{2/3} \times 0.002^{1/2} = 160 \text{ cfs}$$

By trial $d_n = 3.5$ ft. Critical depth occurs when

$$\frac{Q^2}{g} = \frac{A^3}{B} \quad \text{or} \quad \frac{160^2}{32.2} = \frac{(6d_c)^3}{6}$$

from which $d_c = 2.81$ ft. Since $d_n > d_c$, the flow is subcritical and the water-surface profile is M_2 (Fig. 10-5). The depth at the outfall is approximately $0.7d_c = 2.0$ ft. Critical depth occurs at about $4d_c = 11$ ft upstream from the brink. Computations for the water-surface profile are shown in Table 10-2.

TABLE 10-2 Computation of Water-surface Profile for Illustrative Example 10-1

d, ft	A, sq ft	$B + 2d$, ft	R, ft	V, ft/sec	$\frac{V^2}{2g}$, ft	$d + \frac{V^2}{2g}$, ft	$\Delta\left(d + \frac{V^2}{2g}\right)$, ft	V_{avg}, ft/sec	R_{avg}, ft	S_f	$S - S_0$	x, ft	Σx,* ft
2.81	16.86	11.62	1.451	9.49	1.398	4.208							
							0.005	9.34	1.463	0.00341	0.00141	4	4
2.90	17.40	11.80	1.475	9.20	1.313	4.213							
							0.014	9.04	1.488	0.00312	0.00112	12	16
3.00	18.00	12.00	1.500	8.89	1.227	4.227							
							0.022	8.74	1.512	0.00284	0.00084	26	42
3.10	18.60	12.20	1.525	8.60	1.149	4.249							
							0.029	8.47	1.536	0.00262	0.00062	47	89
3.20	19.20	12.40	1.548	8.33	1.078	4.278							

*Summation x is measured from the point of critical depth 11 ft upstream from the brink.

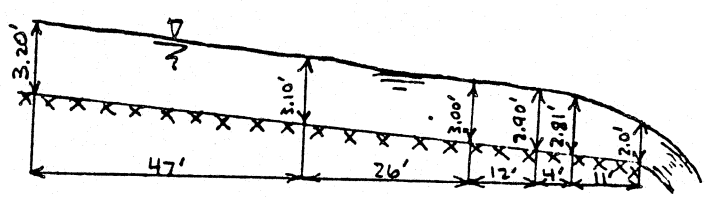

For supercritical flow at outfall, the depth at the brink will be only slightly less than the normal depth which is necessarily below the critical depth.

Problem 4

a. Now for n = 0.025, S_o = 0.0016, and a discharge of 400 cfs, compute the normal depth and velocity. Also identify the type of flow (supercritical, critical, or subcritical).

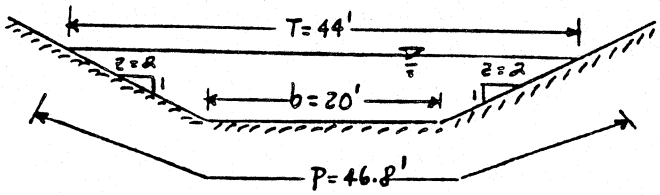

b. Now for a dam placed across the channel described in part a, compute the backwater profile created by the dam which backs up the water to a depth of 5 ft. immediately behind the dam. This profile should extend from the dam site to an upstream section where the depth of flow is 1% greater than the normal depth. Present this profile in a tabular form and plot it on graph paper.

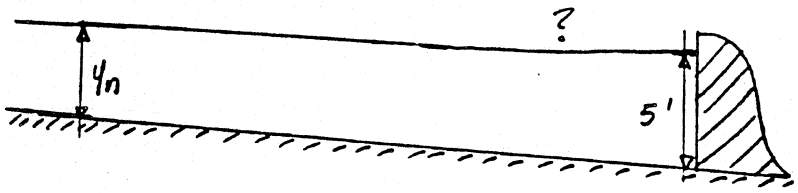

Solution.

a) $P = b + 2y\sqrt{1+z^2}$

$= 20 + 2 \cdot 6\sqrt{1+4}$

$= 46.8'$

$A = (b + zy)y$

$= 0.5(20 + 4 \times 6) \times 6$

$= 192.0 \text{ ft}^2$

$R = (b + zy)y \,/\, b + 2y\sqrt{1+z^2} = 192/46.8 = 4.10'$

→ Find d_n: (normal depth)

$$R = \frac{d_n(10+d_n)}{10 + d_n\sqrt{5}} \quad \text{and} \quad A = d_n(20 + 2d_n)$$

and $V = \frac{Q}{A} = \frac{400}{d_n(20+2d_n)}$

Substituting the given quantities and the above expressions in the Manning formula and simplifying,

$$V = \frac{1.49}{n} R^{2/3} S^{1/2}$$

$$\frac{200}{d_n(10+d_n)} = \frac{1.49}{0.025}\left[\frac{d_n(10+d_n)}{10 + d_n\sqrt{5}}\right]^{2/3} 0.0016^{1/2}$$

$$7{,}680 + 1{,}720\, d_n = \left[d_n(10+d_n)\right]^{2.5}$$

Solving by trial-and-error, $d_n = 3.36$ ft.

this is the normal depth

$V = 4.45$ fps.

→ Find y_c : (critical depth)

The hydraulic depth and water area of the trapezoidal section are expressed in terms of the depth y as:

$$D = \frac{y(10+y)}{10+2y} \quad \text{and} \quad A = y(20+2y)$$

Velocity is $\quad V = \frac{Q}{A} = \frac{400}{y(20+2y)}$

At y_c, the specific energy is minimum, thus

$$\frac{V^2}{2g} = \frac{D}{2} \quad \text{or use} \quad \frac{Q^2}{g} = \frac{A^3}{T}$$

substituting and simplifying,

$$2{,}484(5+y) = [y(10+y)]^3$$

Solving by trial-and-error → $y_c = 2.15$ ft

This the critical depth.

Since normal depth $(d_n) = 3.36' >$ critical depth $(y_c) = 2.15$

Flow is subcritical.

b) Results obtained by the Direct Step Method:

$\alpha = 1.10$ energy coefficient. $\left(\alpha \frac{V^2}{2g}\right)$

(CDC 6600 Computer results)

37

Y (ft.)	A (ft²)	R (ft.)	V (ft/sec)	E (ft.)	ΔE (ft.)	S_f	$\bar{S}_f$	Δx (ft.)	x (ft.)
5.000	150.000	3.541	2.667	5.121	0.000000	.000371	0.000000	0.00	0.00
4.900	146.020	3.484	2.739	5.028	.093288	.000400	.000385	76.81	76.81
4.800	142.080	3.426	2.815	4.935	.092793	.000432	.000416	78.37	155.18
4.700	138.180	3.369	2.895	4.843	.092250	.000467	.000450	80.19	235.37
4.600	134.320	3.311	2.978	4.751	.091655	.000506	.000487	82.32	317.69
4.500	130.500	3.252	3.065	4.660	.091002	.000549	.000527	84.85	402.54
4.400	126.720	3.194	3.157	4.570	.090283	.000596	.000573	87.88	490.42
4.300	122.980	3.135	3.253	4.481	.089491	.000649	.000623	91.58	582.01
4.200	119.280	3.076	3.353	4.392	.088616	.000708	.000679	96.17	678.17
4.100	115.620	3.016	3.460	4.304	.087647	.000773	.000741	101.99	780.16
4.000	112.000	2.956	3.571	4.218	.086571	.000846	.000810	109.57	889.73
3.900	108.420	2.896	3.689	4.132	.085375	.000928	.000887	119.82	1009.55
3.800	104.880	2.835	3.814	4.048	.084041	.001021	.000975	134.37	1143.91
3.700	101.380	2.774	3.946	3.966	.082549	.001124	.001073	156.51	1300.42
3.600	97.920	2.712	4.085	3.885	.080877	.001242	.001183	194.04	1494.47
3.500	94.500	2.651	4.233	3.806	.078996	.001375	.001309	271.02	1765.49
3.400	91.120	2.588	4.390	3.729	.076875	.001527	.001451	515.66	2281.15

38

Computer Results using $\alpha = 1.0$ $\left(\frac{V^2}{2g}\right)$

Y (ft)	A (ft²)	R (ft)	V (ft/sec)	E (ft)	ΔE (ft)	Sf	S̄f	ΔX (ft)	X (ft.)
5.000	150.000	3.541	2.667	5.110	0.000000	.000371	0.000000	0.00	0.00
4.900	146.020	3.484	2.739	5.017	.093899	.000400	.000385	77.31	77.31
4.800	142.080	3.426	2.815	4.923	.093448	.000432	.000416	78.93	156.24
4.700	138.180	3.369	2.895	4.830	.092955	.000467	.000450	80.80	237.04
4.600	134.320	3.311	2.978	4.738	.092414	.000506	.000487	83.00	320.04
4.500	130.500	3.252	3.065	4.646	.091820	.000549	.000527	85.61	405.65
4.400	126.720	3.194	3.157	4.555	.091167	.000596	.000573	88.74	494.40
4.300	122.980	3.135	3.253	4.464	.090446	.000649	.000623	92.56	586.96
4.200	119.280	3.076	3.353	4.375	.089651	.000708	.000679	97.29	684.25
4.100	115.620	3.016	3.460	4.286	.088770	.000773	.000741	103.29	787.54
4.000	112.000	2.956	3.571	4.198	.087792	.000846	.000810	111.11	898.65
3.900	108.420	2.896	3.689	4.111	.086704	.000928	.000887	121.68	1020.34
3.800	104.880	2.835	3.814	4.026	.085491	.001021	.000975	136.69	1157.03
3.700	101.380	2.774	3.946	3.942	.084135	.001124	.001073	159.51	1316.54
3.600	97.920	2.712	4.085	3.859	.082615	.001242	.001183	198.22	1514.76
3.500	94.500	2.651	4.233	3.778	.080906	.001375	.001309	277.57	1792.33
3.400	91.120	2.588	4.390	3.699	.078977	.001527	.001451	529.76	2322.09

Flow Profile For $\alpha = 1.0$

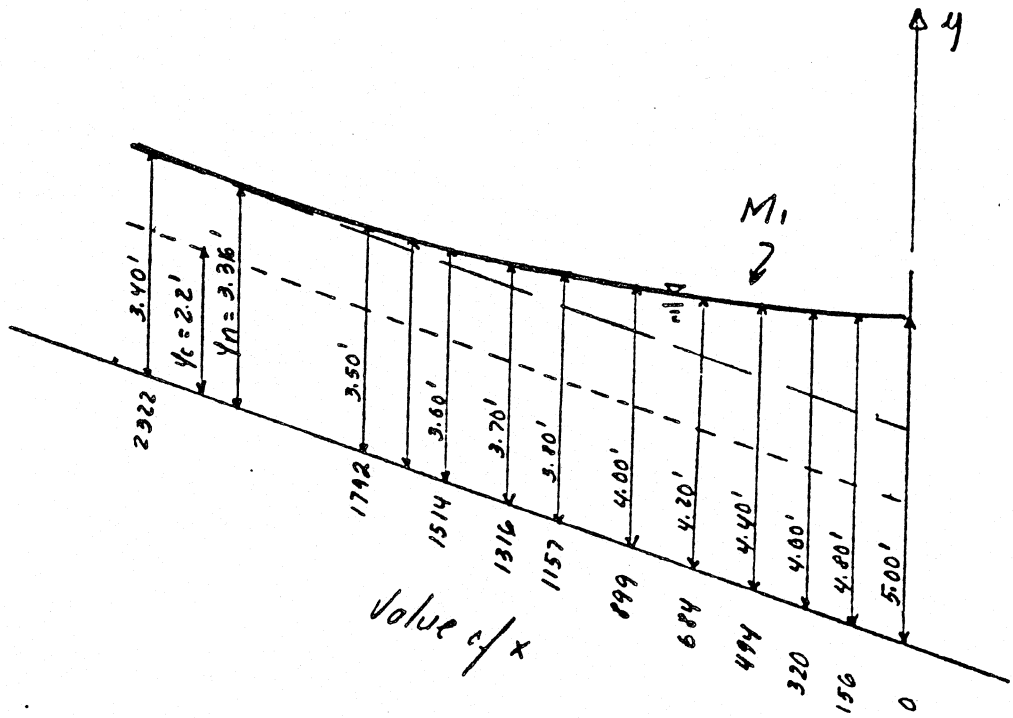

II. Standard Step Method - For Natural Channels

The standard step method is much like the direct step method except in the standard step method the length of channel reach is chosen in advance and the depth y_2 is determined by trial. This method is necessary in most natural channels because natural channels vary in slope and cross section. The natural channel must be approximated by dividing it into reaches such that the channel properties for the reach may be considered as an average of the properties at each end of the reach.

For this computation the equation may be more conveniently written as follows:

$$Z_{o2} + y_2 + \alpha_2 \frac{V_2^2}{2g} = H_2$$

$$H_2' = Z_{o1} + y_1 + \frac{\alpha_1 V_1^2}{2g} + \frac{Q^2}{2}\left(\frac{1}{K_1^2} + \frac{1}{K_2^2}\right) L$$

where the symbols and subscripts are the same as used for the direct step method.

The computation procedure may be described as follows:

1) Start at a point in the channel where the depth is known and call this y_1.

2) Determine the type of profile and its general shape.

3) Choose y_2 slightly larger (or smaller depending on the type of profile) and calculate H_2 and H_2'.

4) If H_2 is not equal to H_2' assume a new value of y_2 and repeat until H_2 and H_2' agree within an acceptable tolerance.

5) The value of y_2 from step 4 becomes the starting point for the next reach and the process is repeated for each successive channel reach.

In HEC-2 a modified procedure is used. Instead of checking the agreement between the elevations of the total head line H_2 and H_2' the check is made on the water-surface elevation. This procedure may be described in general as follows:

1) Start at a point in the channel where the depth is known and call the corresponding water surface elevation WSELK.

2) Choose a water surface elevation slightly larger or smaller than WSELK (depending on the type of profile in the channel), and call it WSELA.

4) Calculate the water surface elevation at other end of the reach, CWSEL, as follows:

$$CWSEL = WSELK + \frac{1}{2}\left(\frac{Q^2}{K_1^2} + \frac{Q^2}{K_2^2}\right) L + \frac{\alpha_1 V_1^2}{2g} - \frac{\alpha V_2^2}{2g}$$

5) If the calculated water surface elevation CWSEL does not agree with the assumed water surface elevation WSELA within the specified tollerance, assume a new WSELA and repeat the process until CWSEL and WSELA agree within the tollerance.

In these calculations α is expressed in terms of the Conveyance and area as follows:

$$\alpha = \frac{\Sigma V^3 \Delta A}{\bar{V}^3 A} = \frac{\Sigma \frac{K^3}{\Delta A^3} S^{\frac{1}{2}} \Delta A}{\frac{K^{-3}}{A^3} S^{\frac{1}{2}} A} = \frac{\Sigma \frac{K^3}{\Delta A^2}}{\frac{\bar{K}^3}{A^2}}$$

Also a term is added to account for head loss due to expansion or contraction of the cross section in the reach. The head loss is expressed as

$$ho = C_e \left| \Delta\left(\alpha \frac{V^2}{2g}\right) \right| \text{ for an expansion}$$

and $ho = C_c \left| \Delta\left(\alpha \frac{V^2}{2g}\right) \right|$ for a contraction.

A number of different computer programs for calculating water surface profiles have been developed by different agencies. HEC-2 is one of the most general and capable of handling many complex situations. A recent review of the programs for calculating water surface profiles is given by Troy L. Lovell in his paper, "Computer Applications to Backwater Problems," a copy of which is included with these notes.

HENDERSON

EXAMPLE 5-4 Longitudinal Profile in a Natural River by the Standard Step Method

$$Q = 90{,}000 \text{ cusecs}, \quad n = 0.033$$

$$\frac{2g \times 0.033^2}{1.49^2} = 0.0316 \qquad S_f = 0.0316 \frac{v^2/2g}{R^{4/3}}$$

1	2	3	4	5	6	7	8	9	10	11	12	13	14
River mile	*River stage, ft*	*Area, A sq ft*	$\frac{v^2}{2g}$ *ft*	*Total head, H ft*	*P ft*	*R ft*	$R^{4/3}$	*Friction slope, S_f*	*Average S_f over reach*	*Length of reach ft*	h_f *ft*	h_e *ft*	*Total head, H ft*
36.55	65.21	11,950	0.88	66.09	623	19.2	51.4	0.00054	–	–	–	–	66.09
~~36.70~~	~~65.5~~	~~10,700~~	~~1.10~~	~~66.60~~	~~514~~	~~20.8~~	~~57.2~~	~~0.00061~~	~~0.00057~~	~~792~~	~~0.45~~	~~0.00~~	~~66.54~~
36.70	65.44	10,670	1.10	66.54	514	20.8	57.2	0.00061	0.00057	792	0.45	0.00	66.54
~~36.95~~	~~66.4~~	~~7,700~~	~~2.12~~	~~68.52~~	~~500~~	~~15.4~~	~~38.3~~	~~0.00175~~	~~0.00118~~	~~1320~~	~~1.56~~	~~0.00~~	~~68.10~~
36.95	65.96	7,450	2.26	68.22	497	15.0	37.0	0.00193	0.00127	1320	1.68	0.00	68.22
Bridge, Rounded Piers, Opening: Span Ratio = 0.94													
36.97	66.4	7,700	2.12	68.52	500	15.4	38.3	0.00175	–	–	–	–	68.52
~~37.10~~	~~68.0~~	~~8,900~~	~~1.58~~	~~69.58~~	~~551~~	~~16.2~~	~~41.0~~	~~0.00122~~	~~0.00149~~	~~686~~	~~1.02~~	~~0.00~~	~~69.54~~
37.10	67.94	8,850	1.61	69.55	550	16.1	40.7	0.00125	0.00150	686	1.03	0.00	69.55
~~37.30~~	~~69.0~~	~~11,050~~	~~1.03~~	~~70.03~~	~~637~~	~~17.4~~	~~45.1~~	~~0.00072~~	~~0.000985~~	~~1056~~	~~1.04~~	~~0.13~~	~~70.72~~
37.30	69.75	11,500	0.95	70.70	645	17.8	46.5	0.00065	0.00095	1056	1.00	0.13	70.68

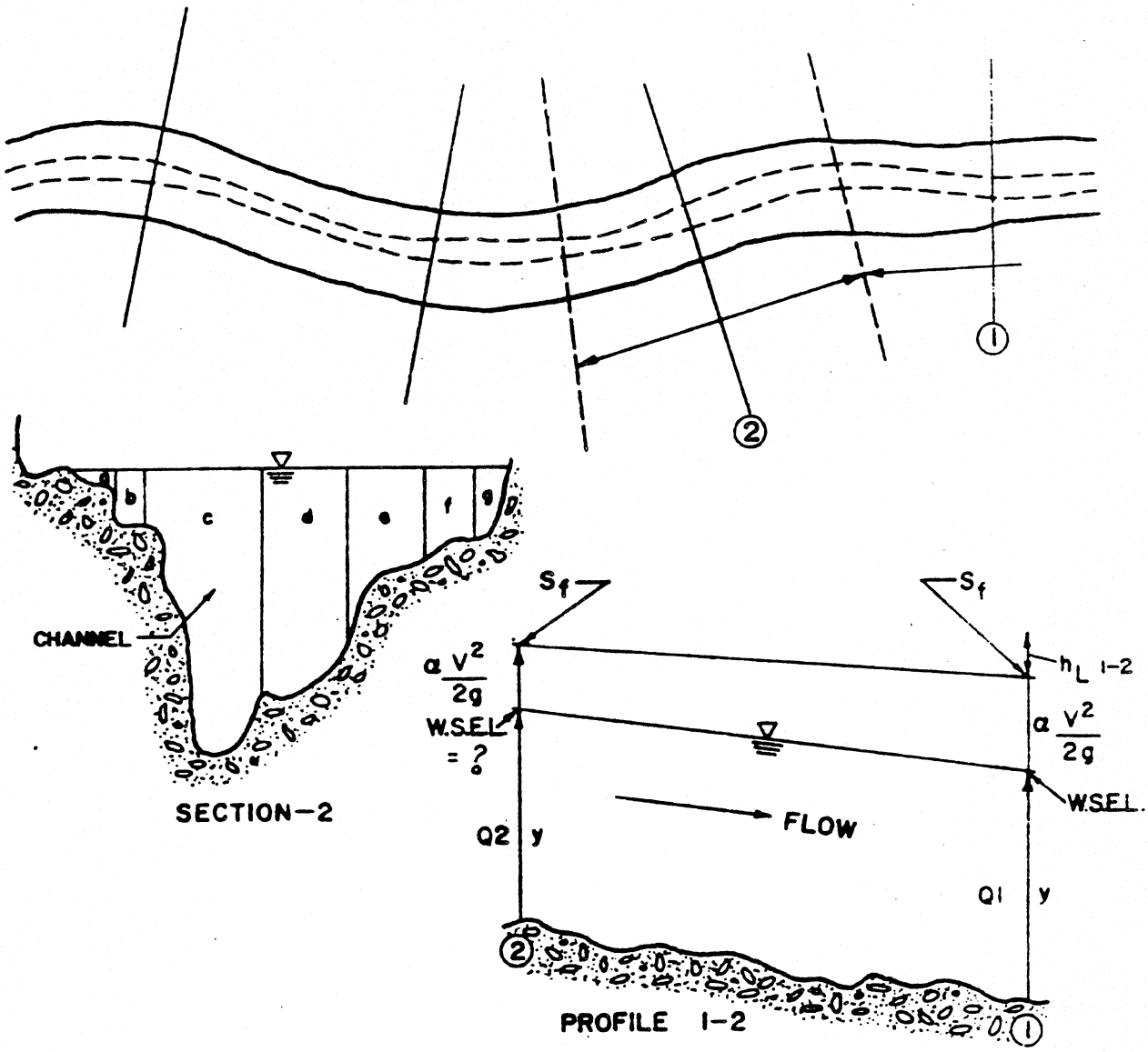

Computation Procedure

Conditions are known @ 1

- Assume WSEL (2)
- *** Compute conveyance— $K(2) = \Sigma K_a + K_b + \ldots + K_g$
  where: $K = \frac{1.49}{n} AR^{2/3}$
- *** Compute representative rate of friction loss
  $$K_{av} = \frac{K(1) + K(2)}{2} \cdot S_{av} = \frac{Q2}{K_{av}^{\ 2}}$$
- Compute WSEL(2)
  $$WSEL(2) = WSEL(1) + \alpha \frac{V_1^2}{2g} + S_{av} \cdot L_w + C \cdot \frac{|\Delta\alpha V^2|}{2g} - \alpha \frac{V_2^2}{2g}$$

Compare and repeat until criterion met.

Fig. . Schematic of Computation Procedure

PROFILES

1 Critical Depth

2 Computed assuming Subcritical Flow

3 Computed assuming Supercritical Flow

NOTE:

If critical depth is computed, no water surface below critical depth will be accepted for subcritical flow and no water surface elevation above will be accepted for supercritical flow (critical will be assumed)

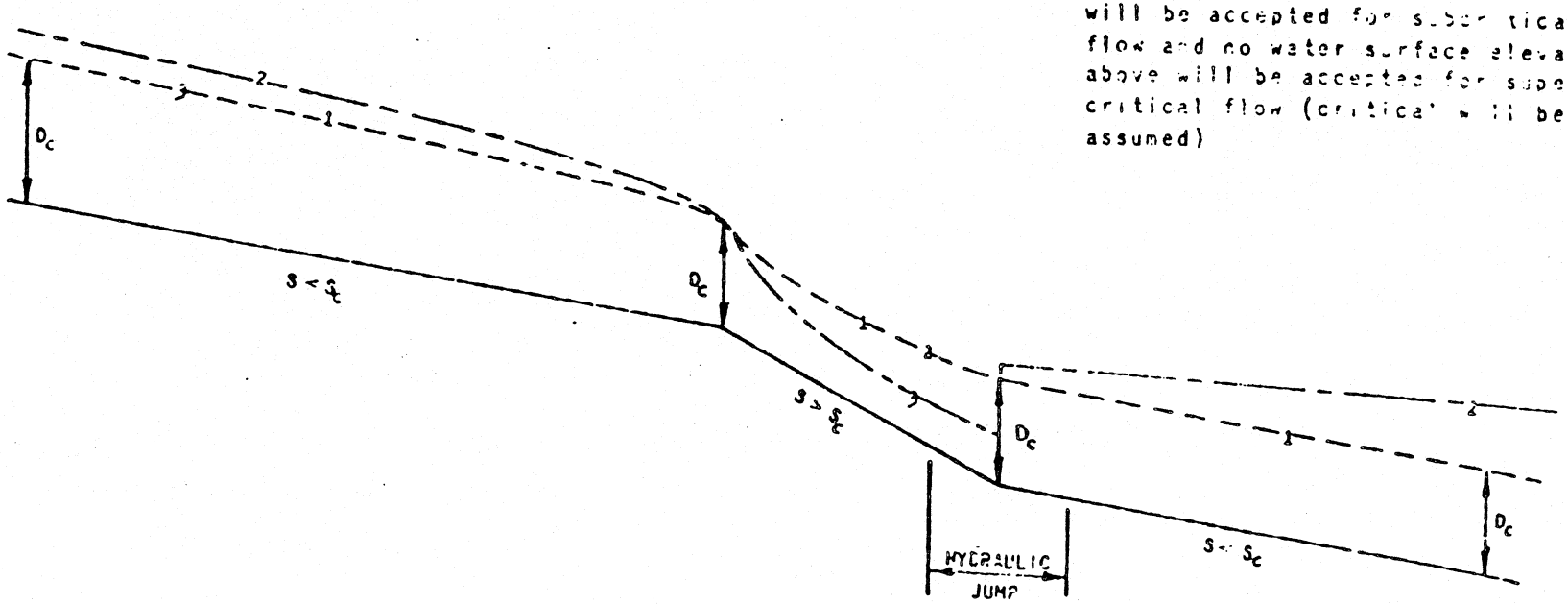

ILLUSTRATION OF PROFILE DETERMINATION FOR SUBCRITICAL AND SUPERCRITICAL FL IN ADJACENT [illegible] REAM

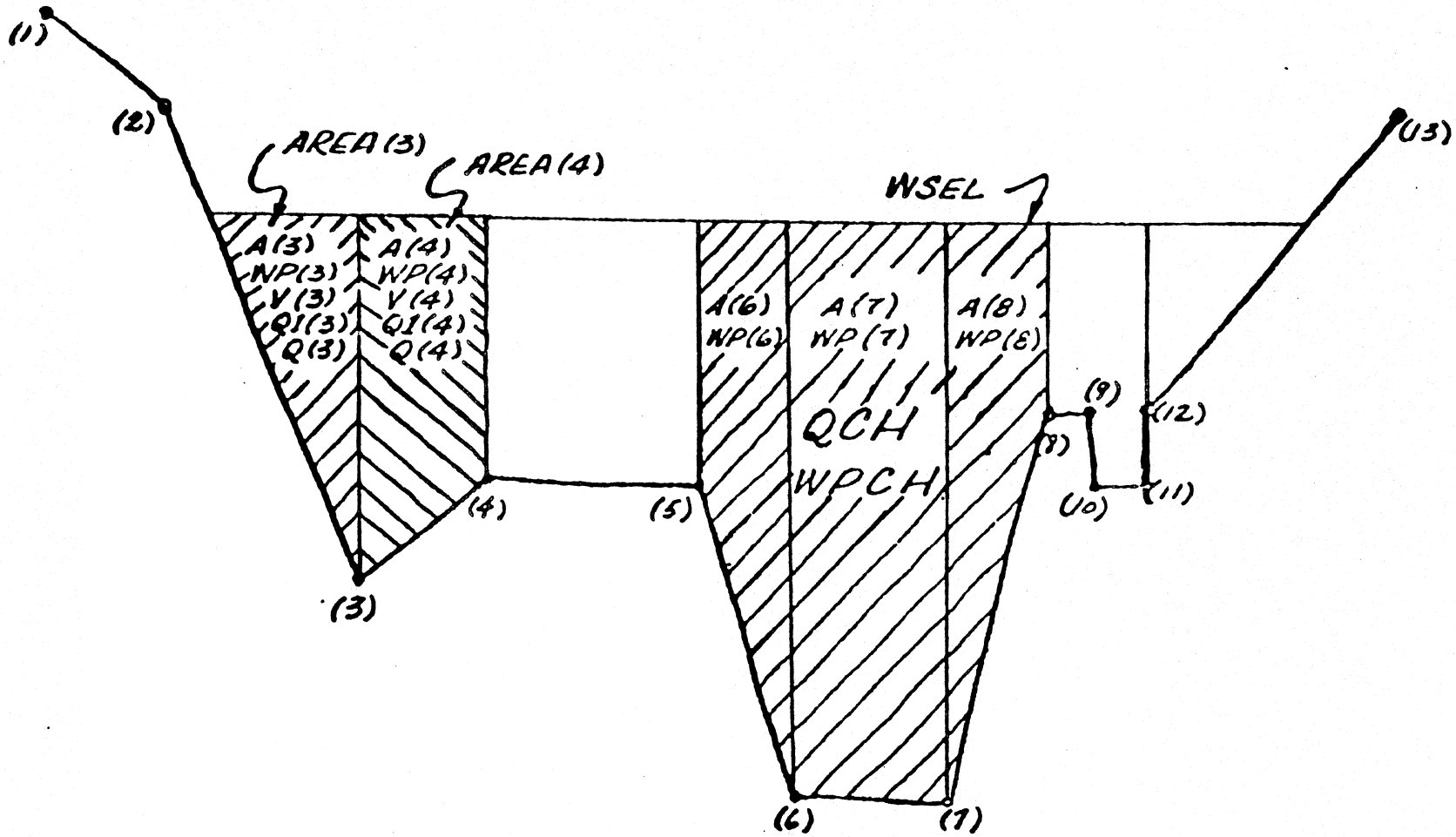

TYPICAL CROSS SECTION

EXHIBIT 1

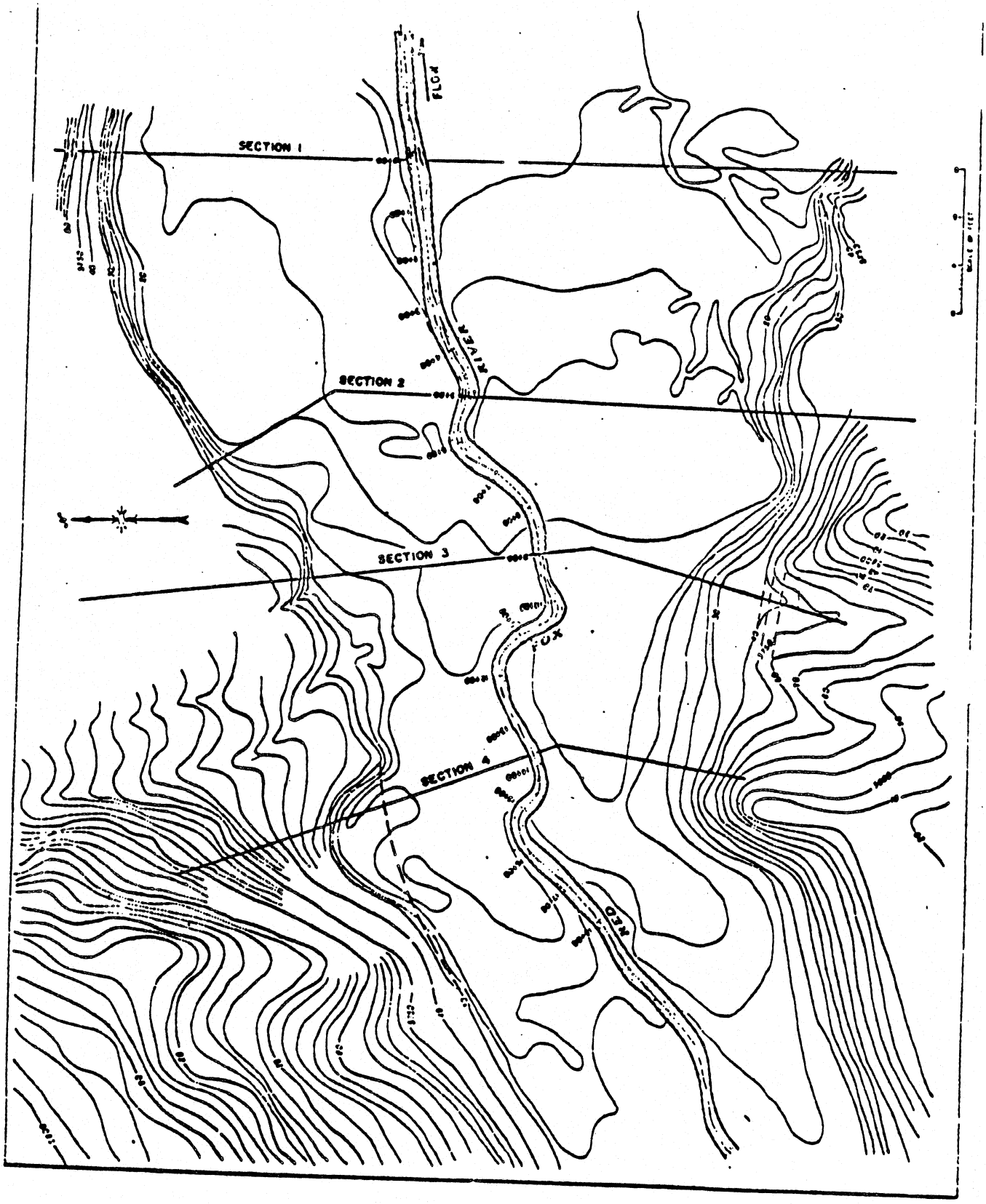
SECTION 1
SECTION 2
SECTION 3
SECTION 4
FLOW
RIVER
FOX
RED

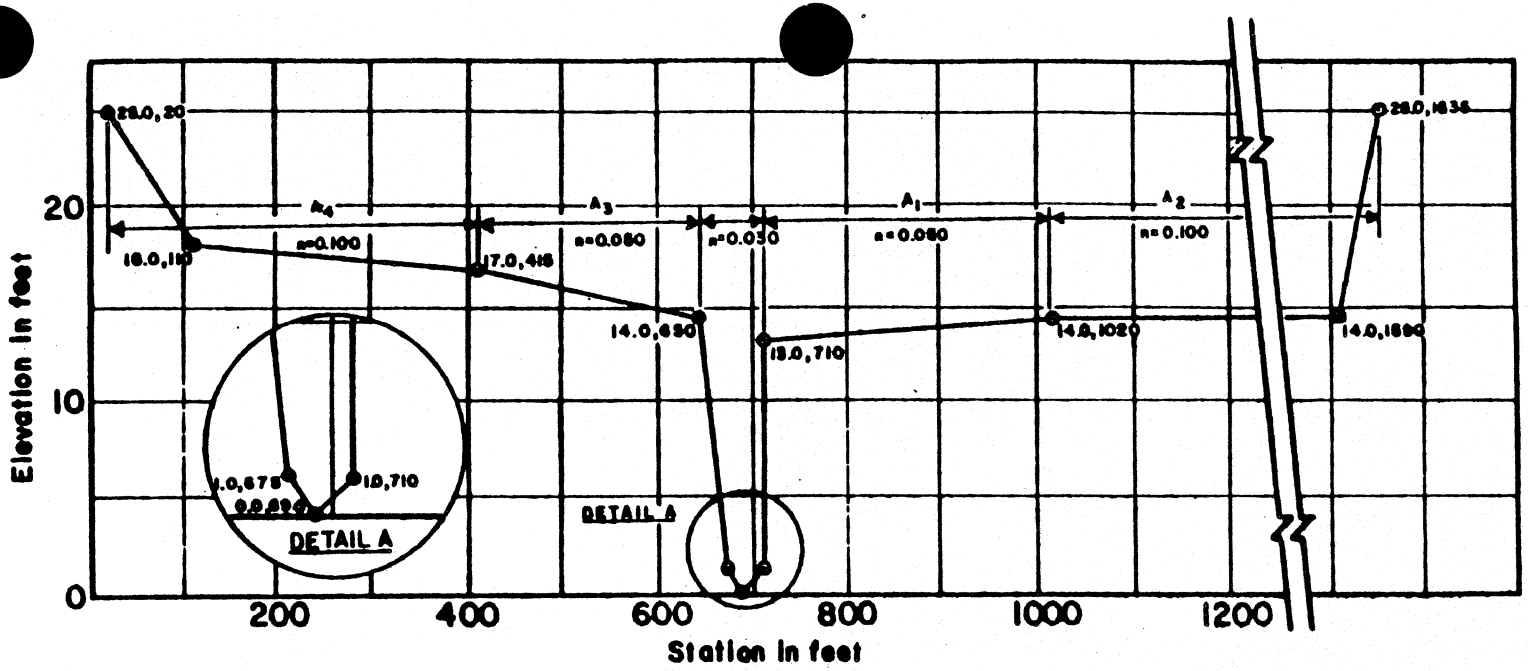

Cross section No. 1

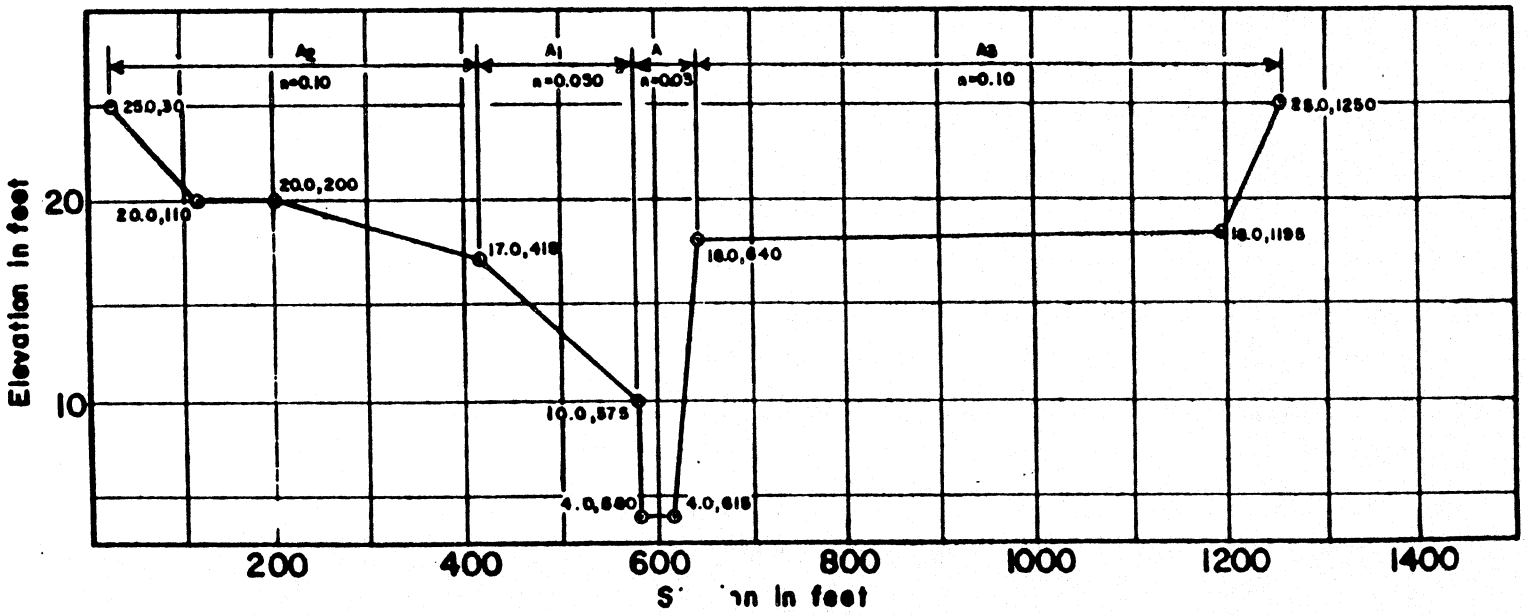

Cr[illegible] ction No. 2

48

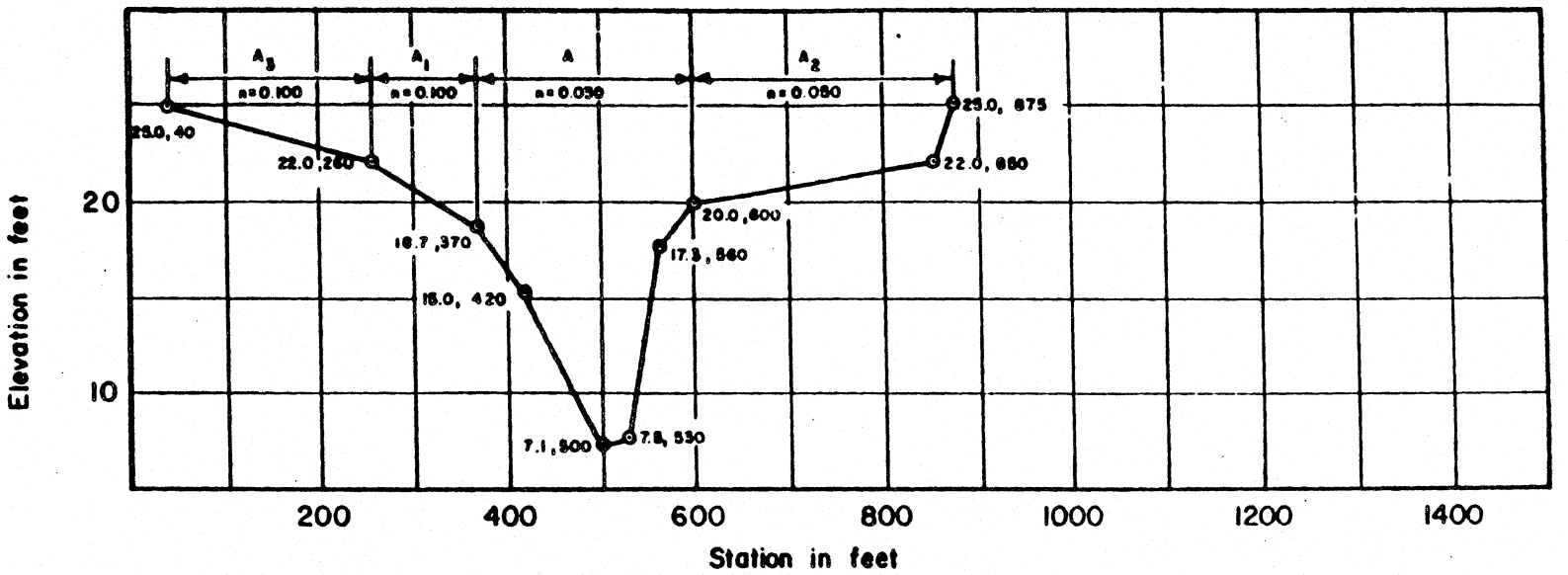

Cross section No. 3

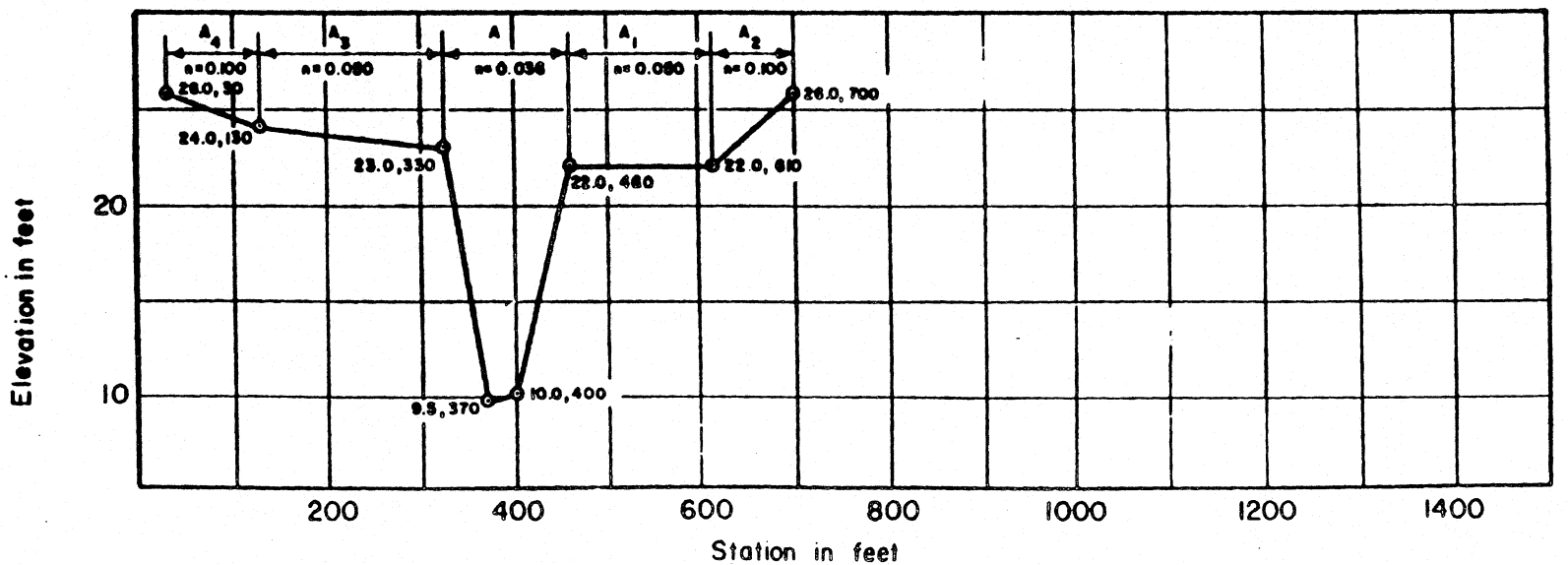

Cross section No. 4

RED FOX RIVER, COLORADO

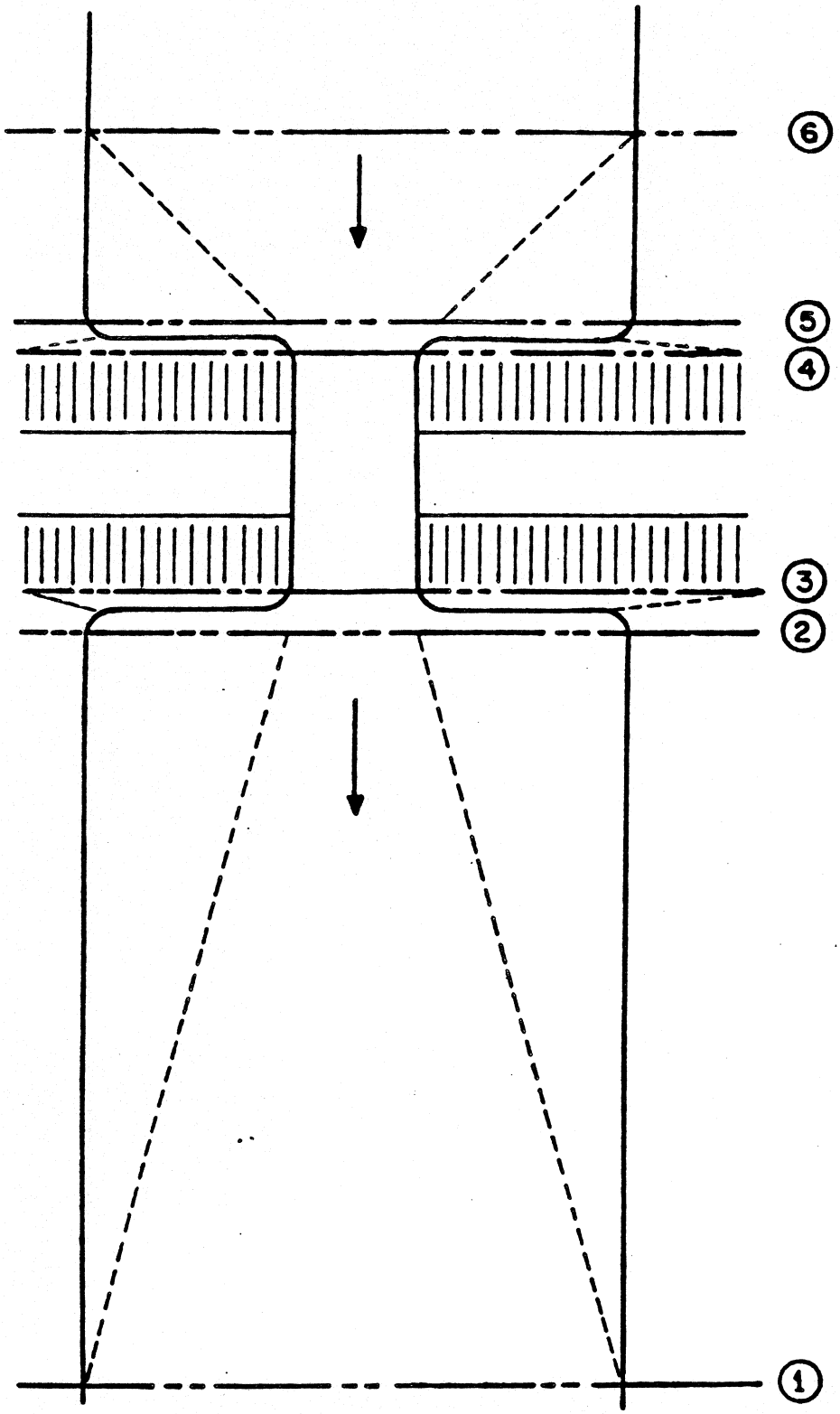

NORMAL BRIDGE CROSS SECTION LOCATIONS

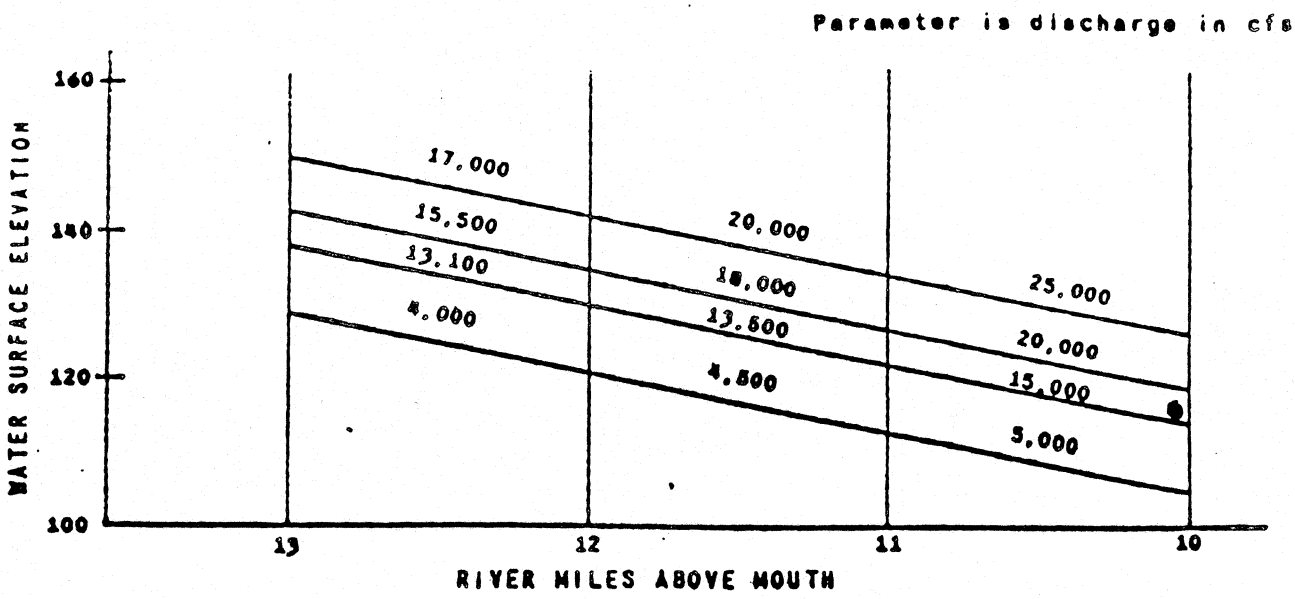

PROFILE

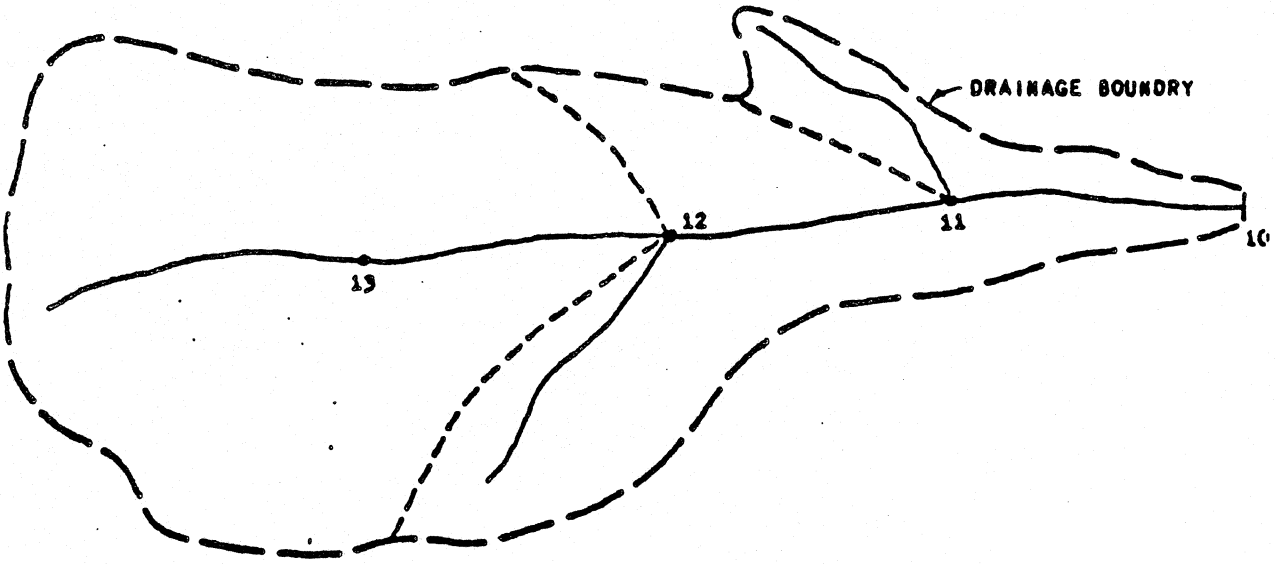

PLAN

NEED FOR CHANGING
DISCHARGE FOR
BACKWATER COMPUTATIO

STARTING WATER SURFACE PROFILES - TRIBUTARIES

PROBLEM: The starting water surface elevation for backwater computations at the first cross section on a main stream tributary is often a difficult figure to obtain. Figures 1 and 2 illustrate the problem.

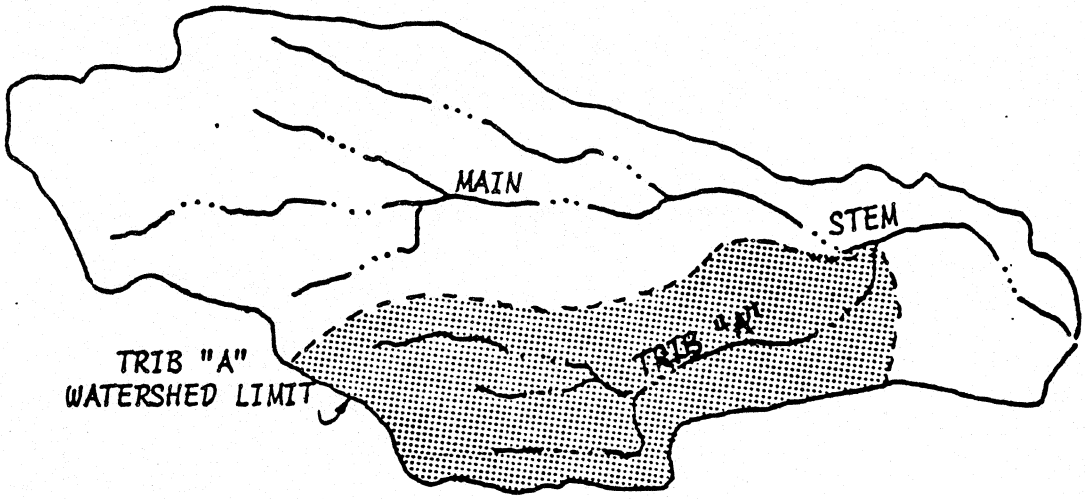

FIGURE 1- MAIN STEM WATERSHED

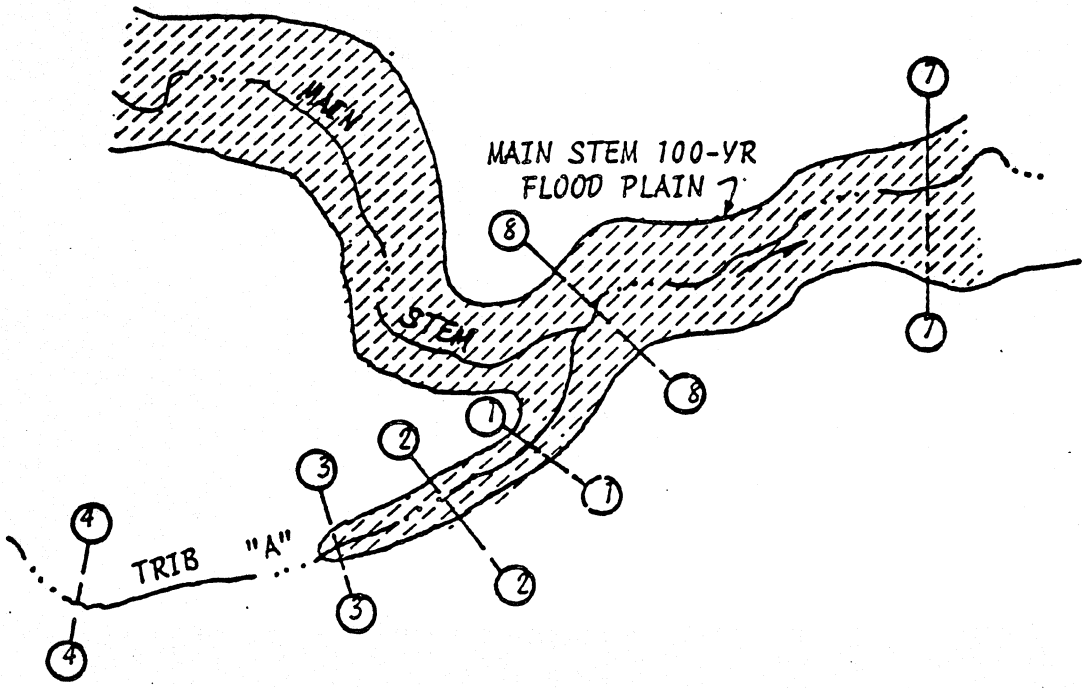

FIGURE 2- CROSS-SECTION LAYOUT

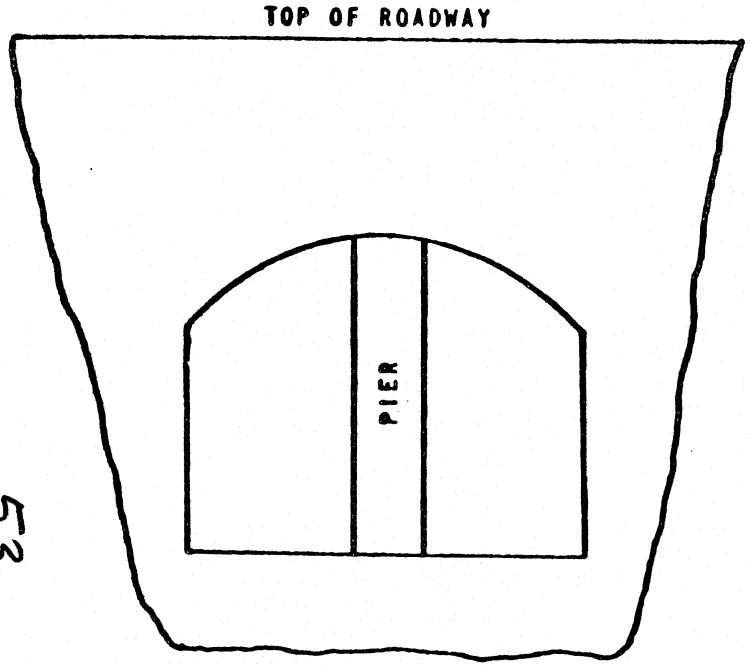

SECTION AA

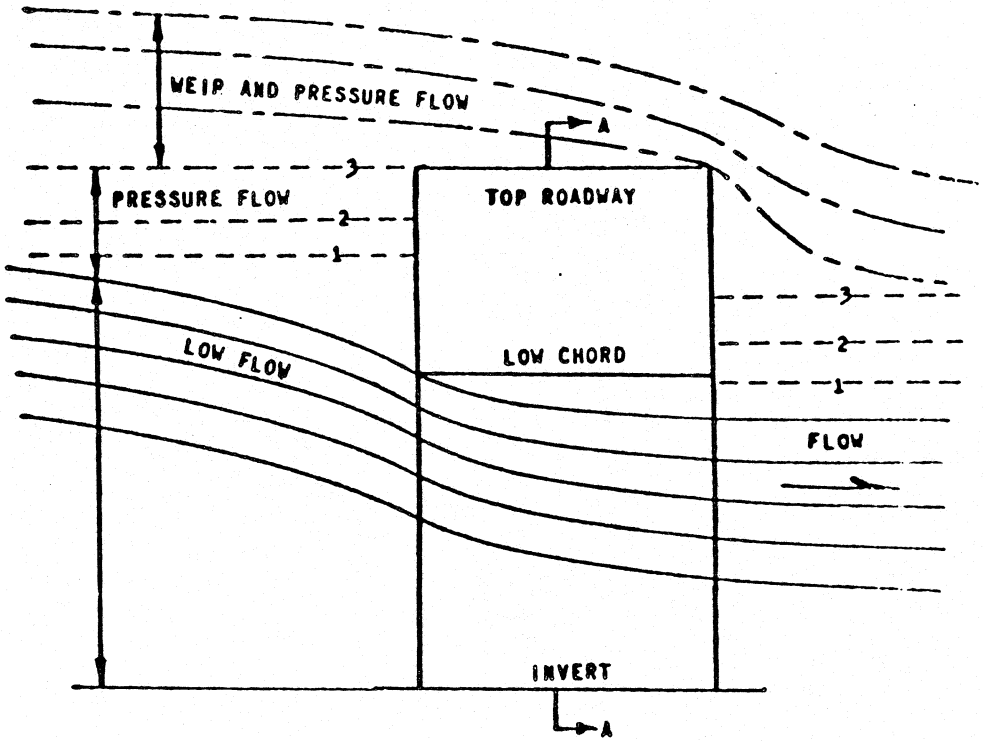

PROFILE

CLASSIFICATION OF FLOW
TYPICAL BRIDGE

SPLIT FLOW ANALYSIS
EXAMPLE PROBLEM

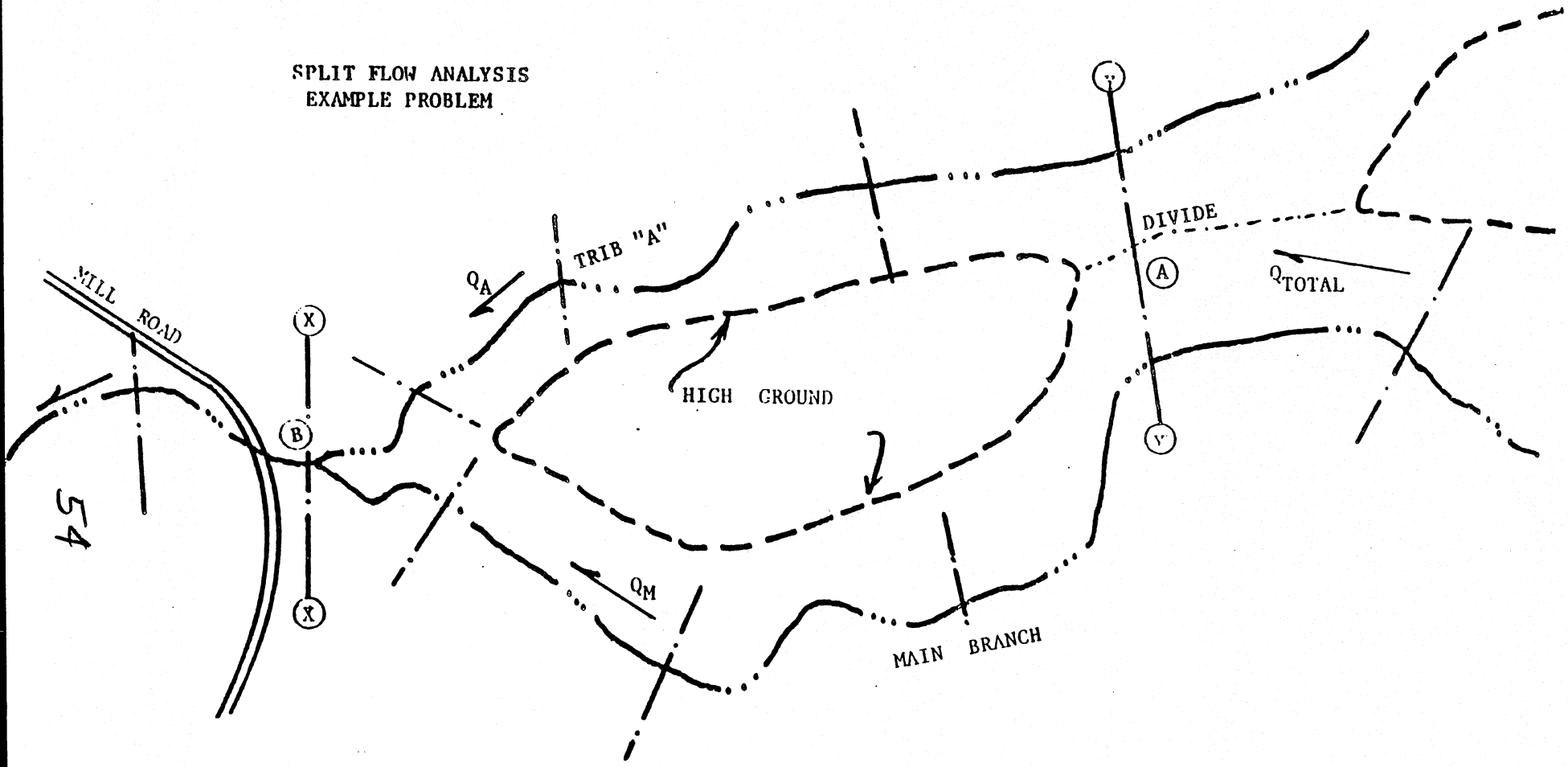

FIGURE 1
SF-2

Best Hydraulic Section

The conveyance of a channel section increases with increase in the hydraulic radius or with decrease in the wetted perimeter. This is evident from Manning's equation for uniform flow:

$$Q = \frac{1.49}{n} A R^{2/3} S^{1/2}$$

for A, S, and n constant. Therefore, from a hydraulic viewpoint, the channel section having the smallest wetted perimeter for a given area has the maximum conveyance. This section has the best hydraulic section (highest hydraulic efficiency).

The geometric elements of some best sections are listed in the table below:

TABLE 7-2. BEST HYDRAULIC SECTIONS

Cross section	Area A	Wetted perimeter P	Hydraulic radius R	Top width T	Hydraulic depth D
Trapezoid, half of a hexagon	$\sqrt{3}\,y^2$	$2\sqrt{3}\,y$	$\frac{1}{2}y$	$\frac{4}{3}\sqrt{3}\,y$	$\frac{3}{4}y$
Rectangle, half of a square	$2y^2$	$4y$	$\frac{1}{2}y$	$2y$	y
Triangle, half of a square	y^2	$2\sqrt{2}\,y$	$\frac{1}{4}\sqrt{2}\,y$	$2y$	$\frac{1}{2}y$
Semicircle	$\frac{\pi}{2}y^2$	πy	$\frac{1}{2}y$	$2y$	$\frac{\pi}{4}y$
Parabola, $T = 2\sqrt{2}\,y$	$\frac{4}{3}\sqrt{2}\,y^2$	$\frac{8}{3}\sqrt{2}\,y$	$\frac{1}{2}y$	$2\sqrt{2}\,y$	$\frac{2}{3}y$

In general, a channel section should be designed for the best hydraulic efficiency but should be modified for practicability. The most efficient section may not always be practical because of difficulties in construction. The principle of the best hydraulic section applies only to the design of non-erodible channels.

Wide Rectangular Channels

$$A = By$$

$$P = B + 2y$$

$$R = \frac{By}{B + 2y} = \frac{y}{1 + 2y/B}$$

As $B \rightarrow \infty$, $R \rightarrow y$. So, for wide rectangular channel, a common assumption is $R = y$.

CHANNEL RESISTANCE

I. Resistance Factors

Although many different resistance factors have been proposed for open channel flow, the one most widely used and the most useful one at the present time is the Manning "n." It occurs in the Manning equation for uniform flow

$$Q = \frac{1.49}{n} A R^{2/3} S^{1/2}$$

and as stated previously is also used to evaluate the slope of the total head line S_f for non-uniform flow when the channel section properties A and R are calculated for the existing flow depth in non-uniform flow.

Several different methods of estimating n are available.

A. Descriptive Tables

One of the most complete using descriptive comments on channel materials and characteristics is given by Chow. These tables are reproduced on pages III-7 to III-10 and are self-explanatory.

B. Cowan Procedure

The Cowan procedure offers an alternative method for estimating n and may be useful for resolving uncertainties in selecting n from tables. The range of values for each component of n in the equation

$$n = (n_0 + n_1 + n_2 + n_3 + n_4)\ m_5$$

are given in the tables on page III-11 reproduced from Chow.

C. USGS Water Supply Paper 1849, Roughness Characteristics of Natural Channels.

This book summarizes the results of many measurements of n in natural streams. In addition to word descriptions and cross sections of the channels, color photographs are included which are very helpful in giving a more complete description of the channel conditions. As a further aid in recording the appearance of channels with measured n values, some USGS offices have sets of color stereo slides of the measured streams.

D. Strickler Equation

The Strickler Equation is useful for estimating n for a channel in alluvial material when the resistance is due to the grain roughness and not due to ripple or dune formations on the bed. Information on the size distribution of the sediment bed must be obtained. The equation can be developed from Nikuradse's results and may be either of the following two forms:

$$n = 0.034\, d^{1/6} \quad \text{(d = mean sediment size in feet)}$$

$$n = 0.31\, d^{1/6} \quad \text{(d = 75\% finer size in feet)}$$

E. Grassed Channels

Based on work by the Soil Conservation Service and reported in Chow, the resistance of grassed channels is related to the

product of the channel velocity V and the channel hydraulic radius R. This product is representative of a Reynolds Number. For a given channel the retardence level is determined by the grass characteristics. The tables on the following pages give a description of the grass characteristics for each retardance level and for each retardence level curves relating n to the product VR.

II. Composite Sections

For some channels the resistance coefficient (Mannings n) varies across the cross section. One of the most common causes of this variation is the presence of brush or trees on the flood plain causing a high resistance there as compared with the main channel. Variations in bed and bank material may also cause the resistance to vary across the main stream channel.

Method of Analysis
Division of Channel Cross-section

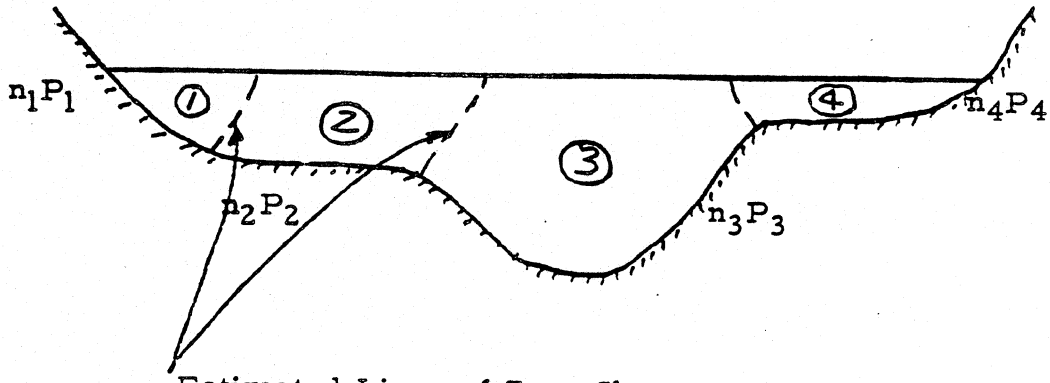

Estimated Lines of Zero Shear
(Perpendicular to isovelocity lines)

EXAMPLE CROSS SECTIONS SHOWING SUBSECTIONS FOR CHANGES IN 'n' VALUES

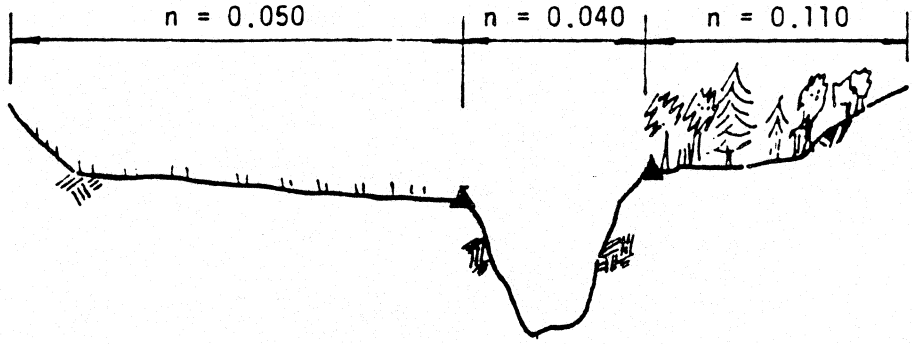

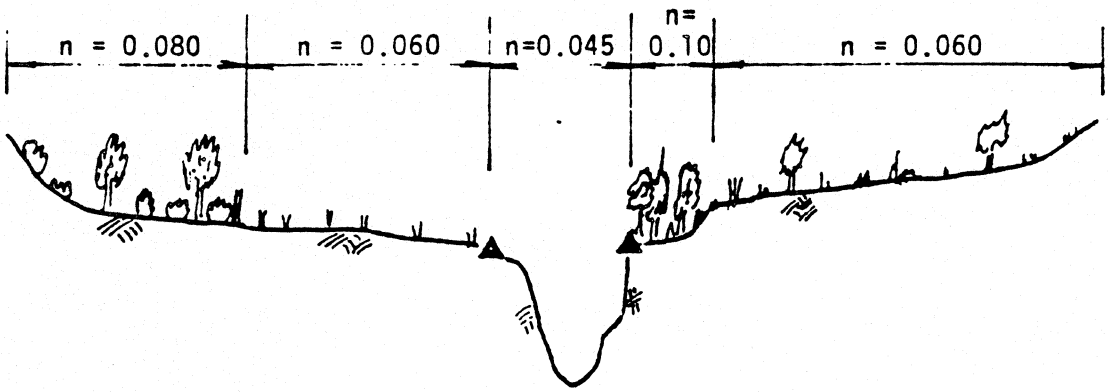

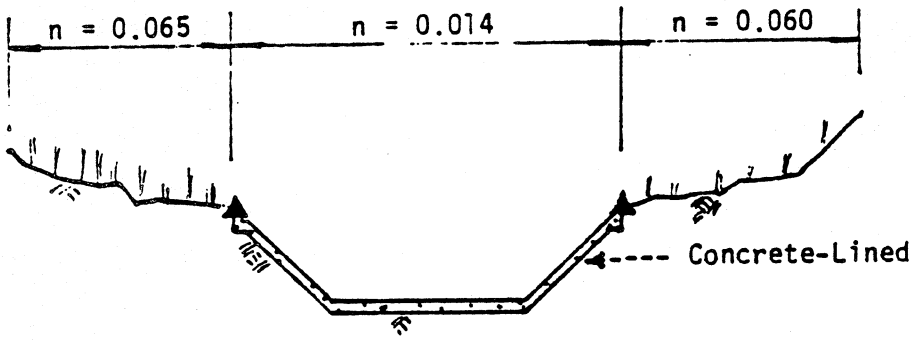

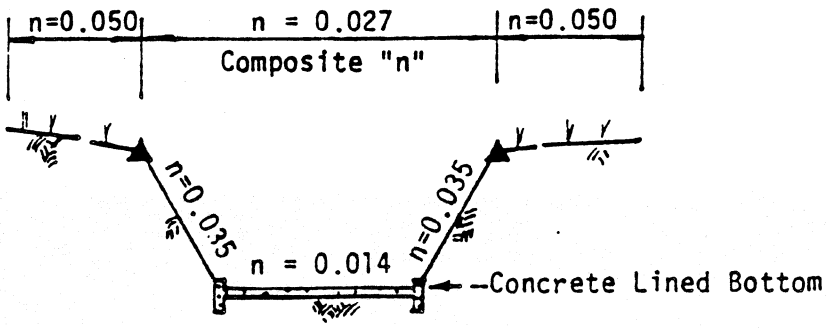

▲ Denotes Left (STACHL) and Right (STACHR) Channel Limits

$$Q \text{ total} = Q_1 + Q_2 + Q_3 + Q_4$$

For each subdivision n = Manning n

P = Perimeter

A = Area of subdivision

$$Q_1 = \frac{1.49}{n_1} A_1 R_1^{2/3} S^{1/2} = K_1 S^{1/2}$$

where $K_1 = \frac{1.49}{n_1} A_1 R_1^{2/3}$ and similar relations

apply to each subdivision.

$$\text{Then } Q_{total} = \sum_1^N K_i \; S_f^{1/2}$$

$$\text{or } S_f^{1/2} = \frac{Q_{total}}{\sum_1^N K_i}$$

Any individual Q_i may be found from

$$Q_i = K_i \; \frac{Q_{total}}{\sum_1^N K_i}$$

An n value for the composite section may be calculated as follows:

$$Q_{total} = K_o S_f^{1/2} = \sum K_i S_f^{1/2}$$

$$\frac{1.49}{n_o} A_o R_o^{2/3} S_f^{1/2} = 1.49 \, S_f^{1/2} \sum \frac{A_i R_i^{2/3}}{n_i}$$

$$\frac{P_o R_o^{5/3}}{n_o} = \sum \frac{P_i R_i^{5/3}}{n_i}$$

or

$$n_o = \frac{P_o R_o^{5/3}}{\sum_1^N \frac{P_i R_i^{5/3}}{n_i}}$$

Where the subscript o refers to the total cross section and the subscript i refers to any one subdivision.

For convenience the subdivisions may be formed by vertical lines through selected points in the bottom of the channel cross section. This is satisfactory for most natural channels which are much wider in relation to depth than they appear to be in common cross section plots in which the vertical scale is exaggerated. These vertical lines serve to subdivide the area, but they should not be included as wetted perimeter in calculating the hydraulic radius of the subdivision.

The analysis presented above is based on the idea that the discharge for a composite channel is the sum of the discharges through the elements and that the Manning equation applies to each element. Other assumptions have been made to calculate composite n values, including (1) that the total force resisting flow is the sum of the resisting forces developed in each element, and (2) that the mean velocity in each element is the same and equal to the mean velocity for the entire cross section. Of these assumptions the last one seems the most unrealistic and the one described in detail, which is the one used in HEC-2, the most realistic.

VALUES OF THE ROUGHNESS COEFFICIENT n

(Boldface figures are values generally recommended in design)

Type of channel and description	Minimum	Normal	Maximum
A. CLOSED CONDUITS FLOWING PARTLY FULL			
A-1. Metal			
a. Brass, smooth	0.009	**0.010**	0.013
b. Steel			
1. Lockbar and welded	0.010	0.012	0.014
2. Riveted and spiral	0.013	0.016	0.017
c. Cast iron			
1. Coated	0.010	0.013	0.014
2. Uncoated	0.011	0.014	0.016
d. Wrought iron			
1. Black	0.012	0.014	0.015
2. Galvanized	0.013	0.016	0.017
e. Corrugated metal			
1. Subdrain	0.017	0.019	0.021
2. Storm drain	0.021	**0.024**	0.030
A-2. Nonmetal			
a. Lucite	0.008	0.009	0.010
b. Glass	0.009	**0.010**	0.013
c. Cement			
1. Neat, surface	0.010	0.011	0.013
2. Mortar	0.011	0.013	0.015
d. Concrete			
1. Culvert, straight and free of debris	0.010	0.011	0.013
2. Culvert with bends, connections, and some debris	0.011	**0.013**	0.014
3. Finished	0.011	0.012	0.014
4. Sewer with manholes, inlet, etc., straight	0.013	0.015	0.017
5. Unfinished, steel form	0.012	0.013	0.014
6. Unfinished, smooth wood form	0.012	**0.014**	0.016
7. Unfinished, rough wood form	0.015	0.017	0.020
e. Wood			
1. Stave	0.010	0.012	0.014
2. Laminated, treated	0.015	0.017	0.020
f. Clay			
1. Common drainage tile	0.011	**0.013**	0.017
2. Vitrified sewer	0.011	0.014	0.017
3. Vitrified sewer with manholes, inlet, etc.	0.013	0.015	0.017
4. Vitrified subdrain with open joint	0.014	**0.016**	**0.018**
g. Brickwork			
1. Glazed	0.011	0.013	0.015
2. Lined with cement mortar	0.012	0.015	0.017
h. Sanitary sewers coated with sewage slimes, with bends and connections	0.012	0.013	0.016
i. Paved invert, sewer, smooth bottom	0.016	0.019	0.020
j. Rubble masonry, cemented	0.018	0.025	0.030

VALUES OF THE ROUGHNESS COEFFICIENT *n* (*continued*)

Type of channel and description	Minimum	Normal	Maximum
B. LINED OR BUILT-UP CHANNELS			
B-1. Metal			
a. Smooth steel surface			
1. Unpainted	0.011	0.012	0.014
2. Painted	0.012	0.013	0.017
b. Corrugated	0.021	0.025	0.030
B-2. Nonmetal			
a. Cement			
1. Neat, surface	0.010	0.011	0.013
2. Mortar	0.011	0.013	0.015
b. Wood			
1. Planed, untreated	0.010	0.012	0.014
2. Planed, creosoted	0.011	0.012	0.015
3. Unplaned	0.011	0.013	0.015
4. Plank with battens	0.012	0.015	0.018
5. Lined with roofing paper	0.010	0.014	0.017
c. Concrete			
1. Trowel finish	0.011	0.013	0.015
2. Float finish	0.013	0.015	0.016
3. Finished, with gravel on bottom	0.015	0.017	0.020
4. Unfinished	0.014	0.017	0.020
5. Gunite, good section	0.016	0.019	0.023
6. Gunite, wavy section	0.018	0.022	0.025
7. On good excavated rock	0.017	0.020	
8. On irregular excavated rock	0.022	0.027	
d. Concrete bottom float finished with sides of			
1. Dressed stone in mortar	0.015	0.017	0.020
2. Random stone in mortar	0.017	0.020	0.024
3. Cement rubble masonry, plastered	0.016	0.020	0.024
4. Cement rubble masonry	0.020	0.025	0.030
5. Dry rubble or riprap	0.020	0.030	0.035
e. Gravel bottom with sides of			
1. Formed concrete	0.017	0.020	0.025
2. Random stone in mortar	0.020	0.023	0.026
3. Dry rubble or riprap	0.023	0.033	0.036
f. Brick			
1. Glazed	0.011	0.013	0.015
2. In cement mortar	0.012	0.015	0.018
g. Masonry			
1. Cemented rubble	0.017	0.025	0.030
2. Dry rubble	0.023	0.032	0.035
h. Dressed ashlar	0.013	0.015	0.017
i. Asphalt			
1. Smooth	0.013	0.013	
2. Rough	0.016	0.016	
j. Vegetal lining	0.030	.....	0.500

VALUES OF THE ROUGHNESS COEFFICIENT *n* (*continued*)

Type of channel and description	Minimum	Normal	Maximum
C. EXCAVATED OR DREDGED			
a. Earth, straight and uniform			
1. Clean, recently completed	0.016	0.018	0.020
2. Clean, after weathering	0.018	0.022	0.025
3. Gravel, uniform section, clean	0.022	0.025	0.030
4. With short grass, few weeds	0.022	0.027	0.033
b. Earth, winding and sluggish			
1. No vegetation	0.023	0.025	0.030
2. Grass, some weeds	0.025	0.030	0.033
3. Dense weeds or aquatic plants in deep channels	0.030	0.035	0.040
4. Earth bottom and rubble sides	0.028	0.030	0.035
5. Stony bottom and weedy banks	0.025	0.035	0.040
6. Cobble bottom and clean sides	0.030	0.040	0.050
c. Dragline-excavated or dredged			
1. No vegetation	0.025	0.028	0.033
2. Light brush on banks	0.035	0.050	0.060
d. Rock cuts			
1. Smooth and uniform	0.025	0.035	0.040
2. Jagged and irregular	0.035	0.040	0.050
e. Channels not maintained, weeds and brush uncut			
1. Dense weeds, high as flow depth	0.050	0.080	0.120
2. Clean bottom, brush on sides	0.040	0.050	0.080
3. Same, highest stage of flow	0.045	0.070	0.110
4. Dense brush, high stage	0.080	0.100	0.140
D. NATURAL STREAMS			
D-1. Minor streams (top width at flood stage <100 ft)			
a. Streams on plain			
1. Clean, straight, full stage, no rifts or deep pools	0.025	0.030	0.033
2. Same as above, but more stones and weeds	0.030	0.035	0.040
3. Clean, winding, some pools and shoals	0.033	0.040	0.045
4. Same as above, but some weeds and stones	0.035	0.045	0.050
5. Same as above, lower stages, more ineffective slopes and sections	0.040	0.048	0.055
6. Same as 4, but more stones	0.045	0.050	0.060
7. Sluggish reaches, weedy, deep pools	0.050	0.070	0.080
8. Very weedy reaches, deep pools, or floodways with heavy stand of timber and underbrush	0.075	0.100	0.150

VALUES OF THE ROUGHNESS COEFFICIENT *n* (*continued*)

Type of channel and description	Minimum	Normal	Maximum
b. Mountain streams, no vegetation in channel, banks usually steep, trees and brush along banks submerged at high stages			
1. Bottom: gravels, cobbles, and few boulders	0.030	0.040	0.050
2. Bottom: cobbles with large boulders	0.040	0.050	0.070
D-2. Flood plains			
a. Pasture, no brush			
1. Short grass	0.025	0.030	0.035
2. High grass	0.030	0.035	0.050
b. Cultivated areas			
1. No crop	0.020	0.030	0.040
2. Mature row crops	0.025	0.035	0.045
3. Mature field crops	0.030	0.040	0.050
c. Brush			
1. Scattered brush, heavy weeds	0.035	0.050	0.070
2. Light brush and trees, in winter	0.035	0.050	0.060
3. Light brush and trees, in summer	0.040	0.060	0.080
4. Medium to dense brush, in winter	0.045	0.070	0.110
5. Medium to dense brush, in summer	0.070	0.100	0.160
d. Trees			
1. Dense willows, summer, straight	0.110	0.150	0.200
2. Cleared land with tree stumps, no sprouts	0.030	0.040	0.050
3. Same as above, but with heavy growth of sprouts	0.050	0.060	0.080
4. Heavy stand of timber, a few down trees, little undergrowth, flood stage below branches	0.080	0.100	0.120
5. Same as above, but with flood stage reaching branches	0.100	0.120	0.160
D-3. Major streams (top width at flood stage >100 ft). The *n* value is less than that for minor streams of similar description, because banks offer less effective resistance.			
a. Regular section with no boulders or brush	0.025	....	0.060
b. Irregular and rough section	0.035	..	0.100

VALUES FOR THE COMPUTATION OF THE ROUGHNESS COEFFICIENT

Channel conditions		Values		
Material involved	Earth	n_0	0.020	
	Rock cut		0.025	
	Fine gravel		0.024	
	Coarse gravel		0.028	
Degree of irregularity	Smooth	n_1	0.000	
	Minor		0.005	
	Moderate		0.010	
	Severe		0.020	
Variations of channel cross section	Gradual	n_2	0.000	
	Alternating occasionally		0.005	
	Alternating frequently		0.010–0.015	
Relative effect of obstructions	Negligible	n_3	0.000	
	Minor		0.010–0.015	
	Appreciable		0.020–0.030	
	Severe		0.040–0.060	
Vegetation	Low	n_4	0.005–0.010	
	Medium		0.010–0.025	
	High		0.025–0.050	
	Very high		0.050–0.100	
Degree of meandering	Minor	m_5	1.000	1.0 -1.2
	Appreciable		1.150	1.2-1.5
	Severe		1.300	1.5→

CLASSIFICATION OF DEGREE OF RETARDANCE FOR VARIOUS KINDS OF GRASS*

Retardance	Cover	Condition
A Very high	Weeping love grass	Excellent stand, tall (av 30 in.)
	Yellow bluestem ischaemum	Excellent stand, tall (av 36 in.)
B High	Kudzu	Very dense growth, uncut
	Bermuda grass	Good stand, tall (av 12 in.)
	Native grass mixture (little bluestem, blue grama, and other long and short Midwest grasses)	Good stand, unmowed
	Weeping love grass	Good stand, tall (av 24 in.)
	Lespedeza sericea	Good stand, not woody, tall (av. 19 in.)
	Alfalfa	Good stand, uncut (av 11 in.)
	Weeping love grass	Good stand, mowed (av 13 in.)
	Kudzu	Dense growth, uncut
	Blue grama	Good stand, uncut (av 13 in.)
C Moderate	Crab grass	Fair stand, uncut (10 to 48 in.)
	Bermuda grass	Good stand, mowed (av 6 in.)
	Common lespedeza	Good stand, uncut (av 11 in.)
	Grass-legume mixture—summer (orchard grass, redtop, Italian rye grass, and common lespedeza)	Good stand, uncut (6 to 8 in.)
	Centipede grass	Very dense cover (av 6 in.)
	Kentucky bluegrass	Good stand, headed (6 to 12 in.)
D Low	Bermuda grass	Good stand, cut to 2.5 in. height
	Common lespedeza	Excellent stand, uncut (av 4.5 in.)
	Buffalo grass	Good stand, uncut (3 to 6 in.)
	Grass-legume mixture—fall, spring (orchard grass, redtop, Italian rye grass, and common lespedeza)	Good stand, uncut (4 to 5 in.)
	Lespedeza sericea	After cutting to 2 in. height, very good stand before cutting
E Very low	Bermuda grass	Good stand, cut to 1.5 in. height
	Bermuda grass	Burned stubble

* U.S. Soil Conservation Service

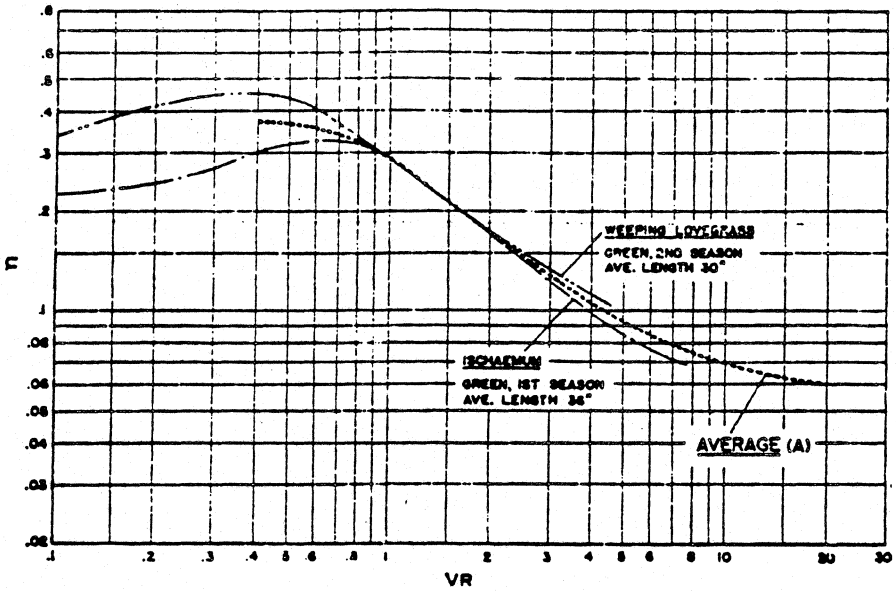

(*a*) Curves for A or very high vegetal retardance.

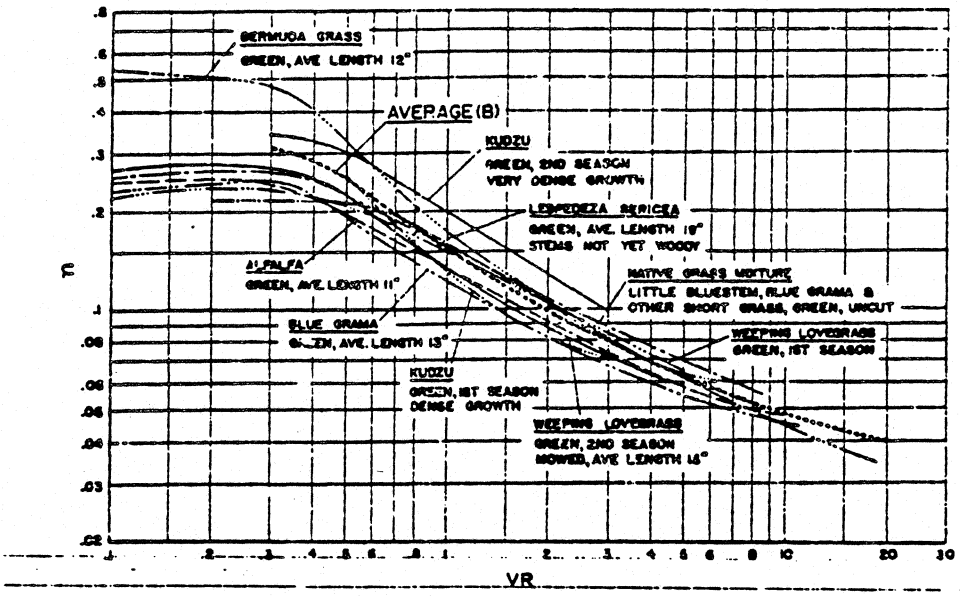

(*b*) Curves for B or high vegetal retardance.

Experimental *n-VR* curves. (*U.S. Soil Conservation Service.*)

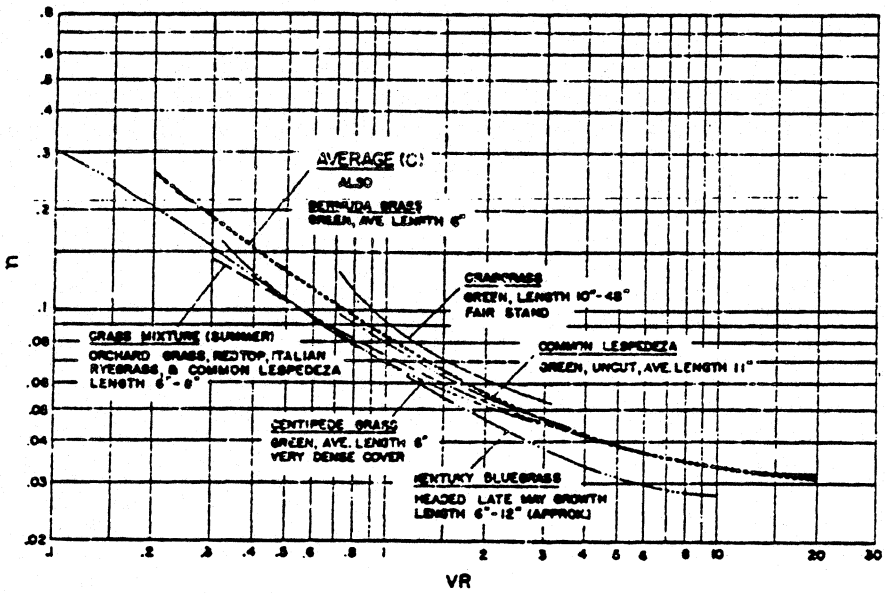

(*c*) Curves for C or moderate vegetal retardance.

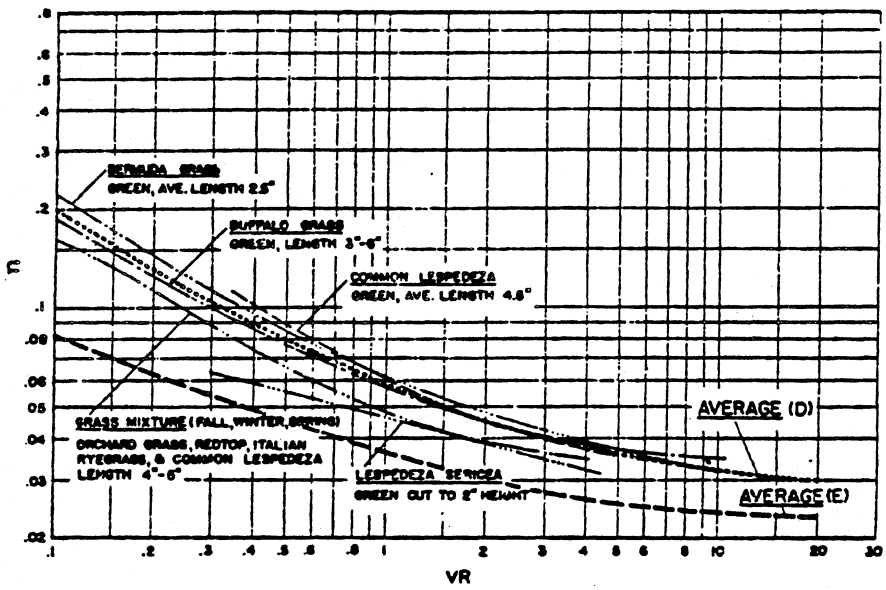

(*d*) Curves for D or low vegetal retardance, and an average curve for E or very low vegetal retardance.

GUIDE IN SELECTION OF VEGETAL RETARDANCE*

Stand	Average length of grass, in.	Degree of retardance
Good	>30	A Very high
	11–24	B High
	6–10	C Moderate
	2–6	D Low
	<2	E Very low
Fair	>30	B High
	11–24	C Moderate
	6–10	D Low
	2–6	D Low
	<2	E Very low

* U.S. Soil Conservation Service

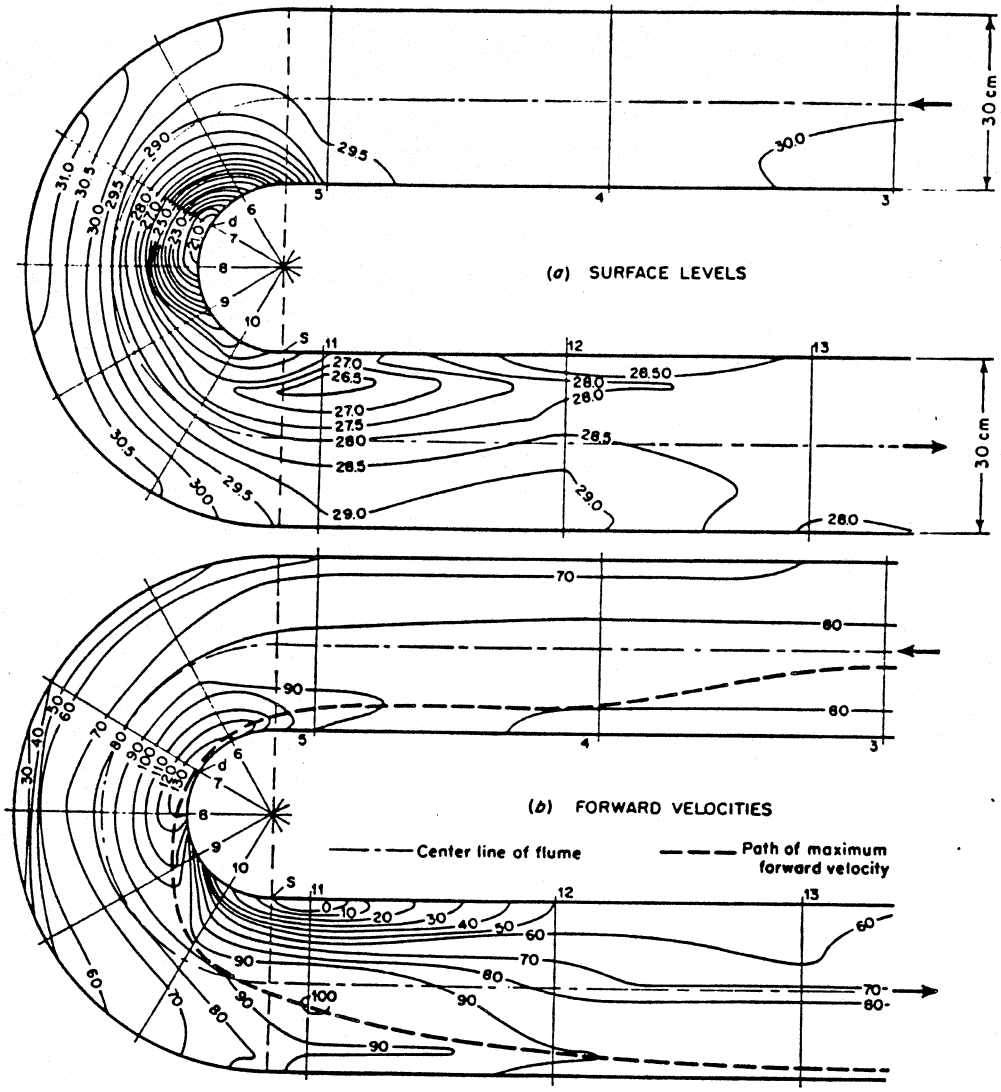

FIG. 16-3. Contour lines of equal surface levels and forward velocities in flow around a 180° bend. (*After A. Shukry* [2].) Surface levels measured in cm (= 0.3937 in.) and velocities in cm/sec (= 0.03281 fps). r_c/b = 1.00; y_A/b = 1.00; and, with V_A = 77.8 cm/sec (= 2.55 fps), R_A = 73,500, where subscript A refers to conditions at the inlet-approach section of the bend.

Rapidly Varied Flow

One important example of rapidly varied flow is a hydraulic jump. A hydraulic jump occurs when the supercritical flow has its velocity reduced to subcritical. A rapid or sudden discontinuity occurs in the surface with violent turbulence occuring. In other words, there is a change in flow from supercritical to subcritical in which there is a loss of energy across the jump. The loss of energy is a very important concept in design.

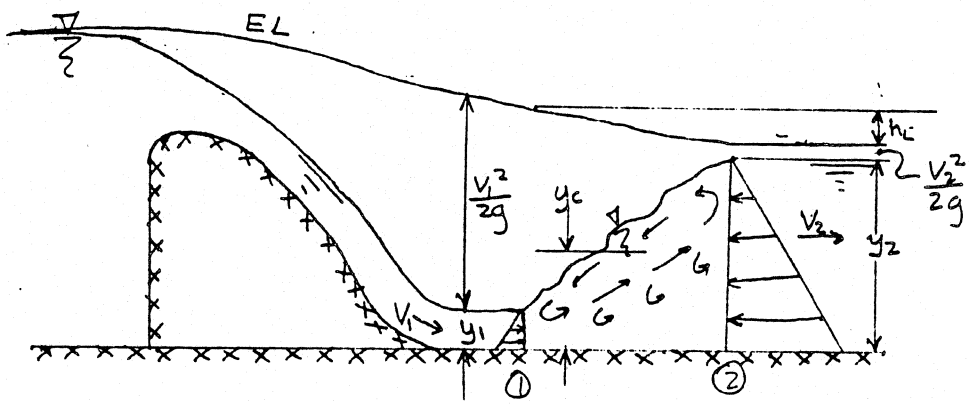

Consider a rectangular channel and apply the impulse-momentum principle, neglecting friction.

$$\Sigma F_x = \underbrace{F_1 - F_2}_{\text{hydrostatic forces}} = (V_2 - V_1)\frac{\gamma q}{g} \qquad \left(\frac{\gamma}{g} = \rho\right)$$

$$\frac{\gamma y_1^2}{2} - \frac{\gamma y_2^2}{2} = (V_2 - V_1)\frac{\gamma}{g} q$$

$$V_2 = q/y_2 \quad \text{and} \quad V_1 = q/y_1$$

$$\frac{\gamma}{2} y_1^2 - \frac{\gamma y_2^2}{2} = (q/y_2 - q/y_1)\frac{\gamma}{g} q$$

$$\frac{\gamma}{2} y_1^2 - \frac{\gamma}{2} y_2^2 = q^2 \frac{\gamma}{g} (1/y_2 - 1/y_1)$$

$$\frac{q^2}{gy_1} + \frac{y_1^2}{2} = \frac{q^2}{gy_2} + \frac{y_2^2}{2}$$

Can solve for $$y_2/y_1 = 1/2\left[-1 + \sqrt{1 + \frac{8q^2}{gy_1^3}}\right]$$

$$= 1/2\left[-1 + \sqrt{1 + \frac{8V_1^2}{gy_1}}\right]$$

or $$y_2 = -\frac{y_1}{2} + \sqrt{\frac{y_1^2}{4} \quad \frac{2V_1^2 y_1}{g}}$$

which gives the sequent depth of a jump.

$$f_m = \text{"force" quantity} = \frac{q^2}{y_1 g} + \frac{y_1^2}{2} = \frac{q^2}{y_2 g} + \frac{y_2^2}{2}$$

for q = 2 cfs/ft

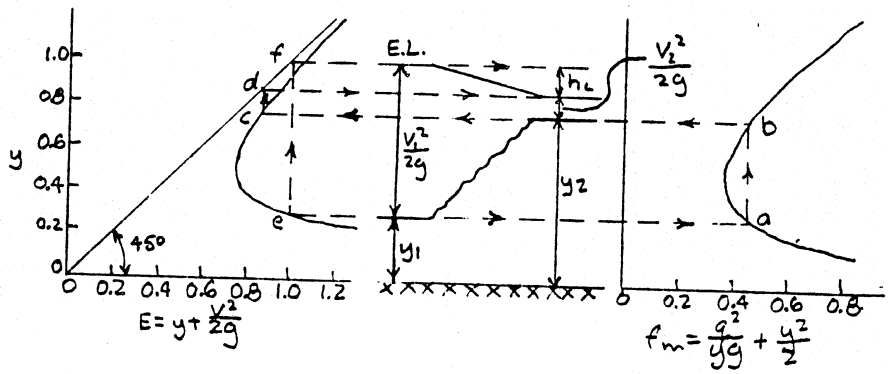

Energy and Momentum Relations in Hydraulic Jump

Loss of energy in the jump does not effect the force quantity (same before and after the jump). A vertica line intersecting the f_m curve serves to locate two <u>conjugate</u> depths y_1 and y_2. These depths represent possible combinations of depths that occur before and after the jump.

For the depth y_1 then we can draw a vertical line ab to get y_2. This depth, y_2, can then be transposed to the specific energy diagram to determine the value cd of $V_2^2/2g$.

$V_1^2/2g$ is the vertical distance ef, and the headloss hj caused by the jump is the drop in energy from 1 to 2, or

$$hj = (y_1 + \frac{V_1^2}{2g}) - (y_2 + \frac{V_2^2}{2g})$$

SECTION 1.0

THEORETICAL DEVELOPMENT OF DYNAMIC (DISTRIBUTED) FLOOD ROUTING MODELS

Table 1.1. Summary of Saint-Venant Equations*

Continuity Equation

Conservation form

$$\frac{\partial Q}{\partial x} + \frac{\partial A}{\partial t} = 0 \qquad (1.35)$$

Nonconservation form

$$\frac{\partial y}{\partial t} + \frac{A}{B}\frac{\partial V}{\partial x} + V\frac{\partial y}{\partial x} = 0 \qquad (1.36)$$

Momentum Equation

Conservation form

$$\frac{1}{A}\frac{\partial Q}{\partial t} + \frac{1}{A}\frac{\partial}{\partial x}(Q^2/A) + g\frac{\partial y}{\partial x} \quad -g(S_o - S_f) = 0 \qquad (1.37)$$

local acceleration term | convective acceleration term | pressure term

Nonconservation form (unit width element)

$$\frac{\partial V}{\partial t} + V\frac{\partial V}{\partial x} + g\frac{\partial y}{\partial x} \quad -g(S_o - S_f) = 0 \qquad (1.38)$$

Kinematic wave

Diffusion wave

Dynamic wave

*Neglecting lateral inflow, $q = 0$, assuming $\beta = 1$ and $\tau_w = 0$.

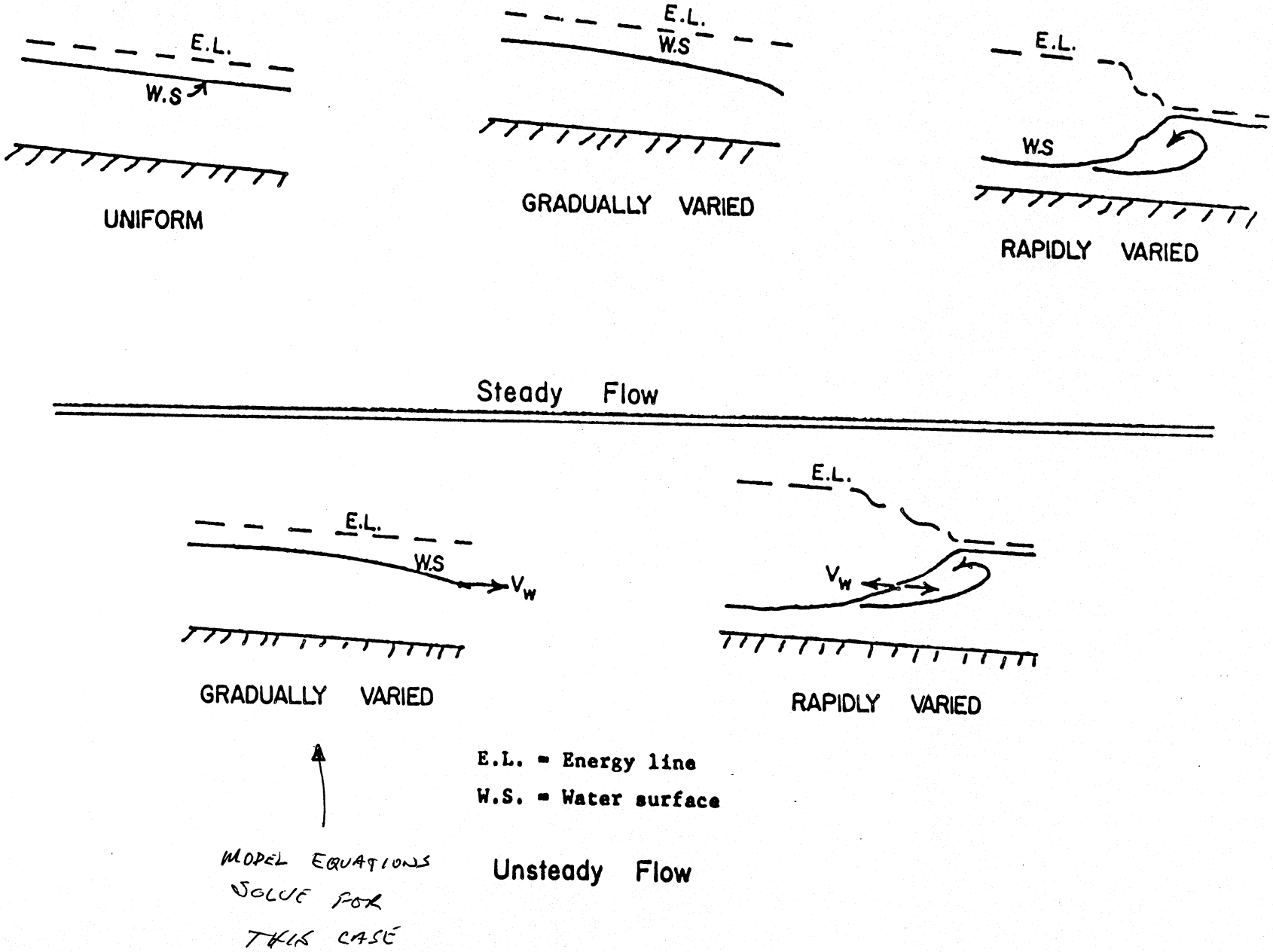

Figure 1.2 Possible Types of Open Channel Flow
(From Thomas, July 1975)

ASSUMPTIONS OF SAINT-VENANT EQUATIONS

1.) Flow is one-dimensional in the sense that flow characteristics (depth, velocity, etc.) are considered to vary only in the longitudinal (x-direction) of the channel.

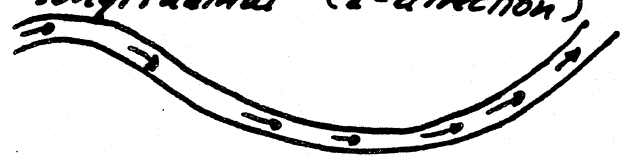

2.) Water surface is horizontal across any section perpendicular to the longitudinal axis.

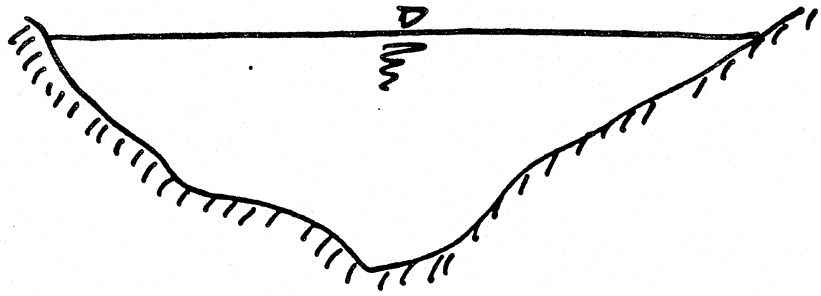

3.) Flow is gradually varied with hydrostatic pressure prevailing at all points in the flow.

4.) Longitudinal axis of the channel can be approximated by a straight-line.

5.) Bottom slope of the channel is small.

$\tan\phi \approx \sin\phi$ $\qquad \phi = 10^\circ \rightarrow 1.5\%$ variation

6.) Bed of the channel is fixed, i.e. no scouring or deposition is assumed to occur.

7.) Resistance coefficient for steady uniform tubulent flow is considered applicable. and an empirical resistance equation such as the Manning equation describes the resistance effect.

$$Q = \frac{1.49}{n} A R^{2/3} S_f^{1/2}$$

8.) Flow is incompressible and homogeneous in density.

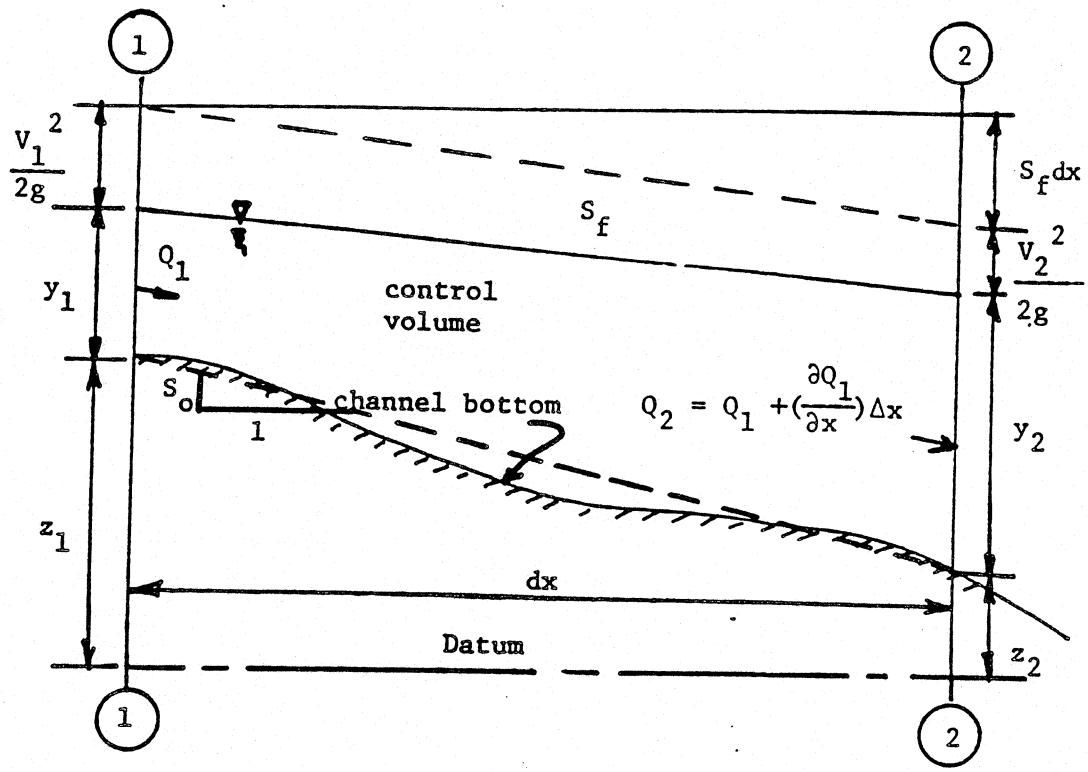

(a) PROFILE

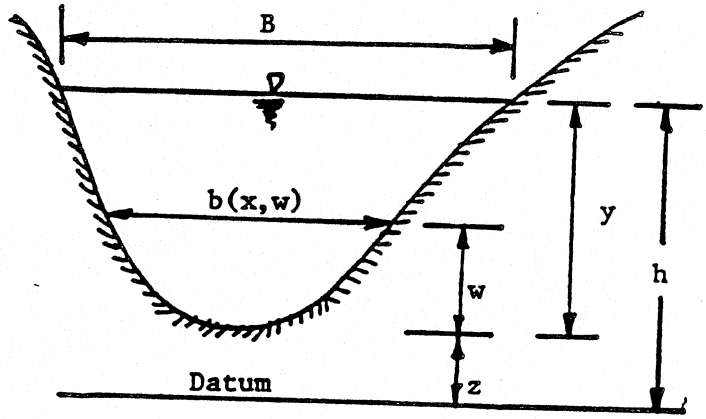

(b) CROSS-SECTION

Figure 1.1. Profile and Cross-Section of an Elemental Reach of Channel

Law of Conservation of Mass

$$I_{mass} - O_{mass} = \frac{dS_{mass}}{dt}$$

I_{mass} = mass inflow to Δx or dx reach during time dt

$$I_{mass} = \rho Q + \rho \cdot q \cdot dx.$$

lateral inflow per dx distance.

ASSUMPTION #1 ?

O_{mass} = mass outflow from Δx reach during time dt

$$O_{mass} = \rho Q + \left(\frac{\partial Q}{\partial x}\right) dx$$

$\frac{dS}{dt}_{mass}$ = time rate of change of mass

$\rho \cdot A \cdot dx$ = amount of mass in dx reach

$$\frac{dS_{mass}}{dt} = \frac{\partial(\rho A\, dx)}{\partial t}$$

$$(\rho Q + \rho q\, dx) - \left(\rho Q + \rho\left(\frac{\partial Q}{\partial x}\right) dx\right) = \frac{\partial(\rho A\, dx)}{\partial t}$$

Simplifying

$$\rho q \cancel{dx} - \rho\left(\frac{\partial Q}{\partial x}\right)\cancel{dx} = \frac{\partial(\rho A)}{\partial t}\cancel{dx}$$

$$\cancel{\rho} q - \cancel{\rho}\frac{\partial Q}{\partial x} = \frac{\partial(\rho A)}{\partial t} = \cancel{\rho}\frac{\partial A}{\partial t}$$

$$q - \frac{\partial Q}{\partial x} = \frac{\partial A}{\partial t} \quad \text{or} \quad \boxed{\frac{\partial Q}{\partial x} + \frac{\partial A}{\partial t} - q.}$$

CONSERVATION OF Momentum

CONSERVATION OF MOMENTUM
(NEWTON'S SECOND LAW)

SUM OF FORCES ACTING ON CONTROL VOLUME + NET RATE OF MOMENTUM INFLOW = TIME RATE OF MOMENTUM ACCUMULATION IN CONTROL VOLUME

FORCES:

1. GRAVITY FORCE DUE TO WEIGHT OF FLUID
2. FORCE DUE TO FRICTIONAL RESISTANCE
3. UNBALANCED PRESSURE FORCE
4. FORCE DUE TO SHEAR STRESS FROM WIND

CONSERVATION OF MOMENTUM

$$\sum F + (I_{mom} - O_{mom}) = \frac{dS_{mom}}{dt}$$

$$\sum F = \underset{\text{(Gravity)}}{F_g} + \underset{\text{(Friction)}}{F_f} + \underset{\text{(Wind)}}{F_w} + \underset{\text{(Pressure)}}{F_p}$$

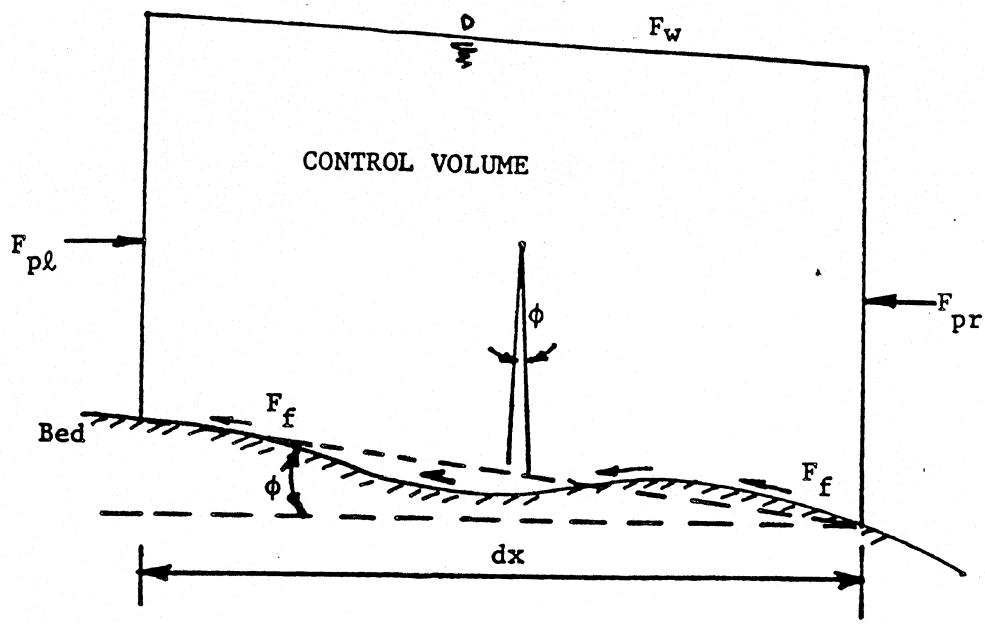

PROFILE

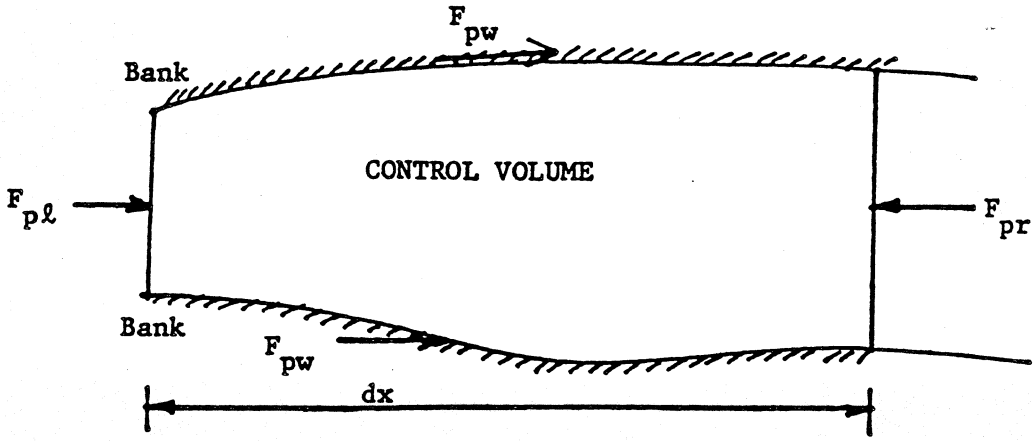

PLANVIEW

Figure 1.2 Forces Acting on Surface of Control Volume

Gravity Force

$$F_g = \rho g A \, dx \sin\phi$$

$$\tan\phi \approx \sin\phi$$

$$\tan\phi = -\frac{dz}{dx} = S_o \quad \text{channel bottom slope}$$

$$F_g = \rho g A S_o * dx$$

Frictional Force

Manifested by shear stress, τ along the bottom & sides of the control volume

$$F_f = -\tau P \, dx$$

Express shear stress in terms of friction slope S_f

$$\tau = \rho g \frac{A}{P} S_f = \overset{\gamma}{\rho} g R S_f$$

$$F_f = -\tau P dx = -\left(\rho g \frac{A}{P} S_f\right) P \cdot dx$$

$$\therefore F_f = -\rho g A S_f \cdot dx.$$

Wind Shear Force.

$$F_w = -\tau_w \cdot B \cdot dx$$

B: width of free surface

τ_w: wind shear stress $(\pm)$

Unbalanced Pressure Force

– further discussion on this is given on 1-1 through

$$F_p = -eg A \frac{\partial y}{\partial x} dx$$

$$\Sigma F = F_g + F_f + F_w + F_p$$
$$= eg A S_o dx - eg A S_f dx - \tau_w B dx - eg A \frac{\partial y}{\partial x} dx.$$

Momentum

Rate of flow of momentum in the x-direction is the product of the mass rate of flow eQ and the velocity component in the x-direction

left side along channel

$$I_{mom} = e\beta VQ + e\beta v_x q\, dx.$$

momentum correction factor to account for nonuniformity of the velocity in the vertical and horizontal direction $\beta = 1.0$ to 1.3

$\beta = 1.0 \Rightarrow$ uniform velocity

$$O_{mom} = e\left[\beta VQ + \frac{\partial(\beta VQ)}{\partial x} dx\right]$$

left side

change

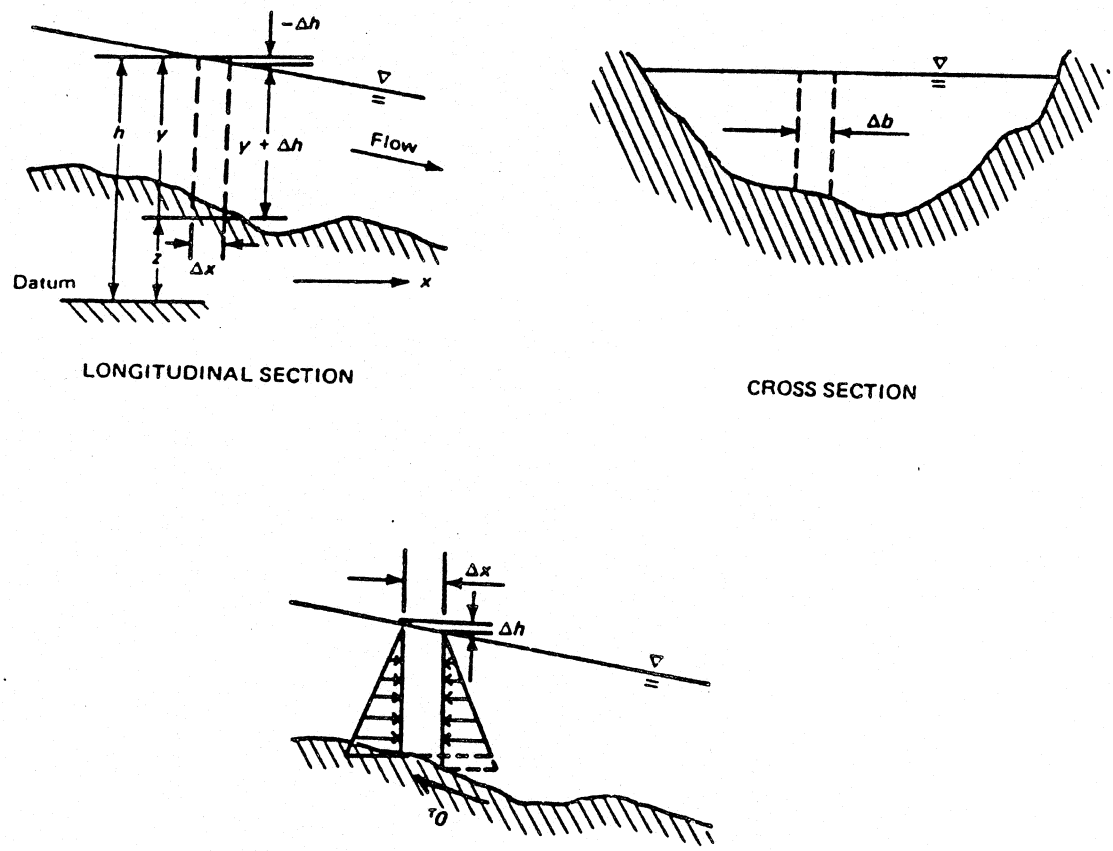

FIGURE 3.—Definition sketches for the equation of motion.

Net rate of flow of momentum entering the channel (control volume)

$$N_{mom} = I_{mom} - O_{mom}$$

$$= \left[e(\beta V Q + \beta v_x g \cdot dx) - e\left(\beta V Q + \frac{\partial(\beta V Q)}{\partial x} dx\right)\right]$$

$$= e\left[\beta g v_x - \frac{\partial(\beta V Q)}{\partial x}\right] dx$$

Time rate of accumulation of momentum in the control volume is

$$S_{mom} = e \frac{\partial Q}{\partial t} dx$$

Applying Law of Conservation of Momentum

$$\sum F + N_{mom} = S_{mom}$$

$$\overbrace{\rho g A S_o dx - \rho g A S_f dx - \tau_w B\, dx - \rho g A \frac{dy}{dx} dx}^{\sum F}$$

$$+ \underbrace{e\left[\beta g v_x - \frac{\partial(\beta V Q)}{\partial x}\right] dx}_{N_{mom}} = \underbrace{e \frac{\partial Q}{\partial t} dx}_{S_{mom}}$$

Divide by $e\,dx$

$$\frac{\partial Q}{\partial t} + \frac{\partial(\beta V Q)}{\partial x} + \underbrace{\left(gA\frac{\partial y}{\partial x} - gAS_o + gAS_f\right)}_{\parallel} - \beta g v_x + \frac{\tau_w}{e}B = 0$$

$$gA\left(\frac{\partial y}{\partial x} - S_o + S_f\right)$$

$$\frac{\partial Q}{\partial t} + \frac{\partial(\beta V Q)}{\partial x} + gA\left(\frac{\partial y}{\partial x} - S_o + S_f\right) - \beta g v_x + \frac{\tau_w}{e}B = 0$$

$h = y + z$

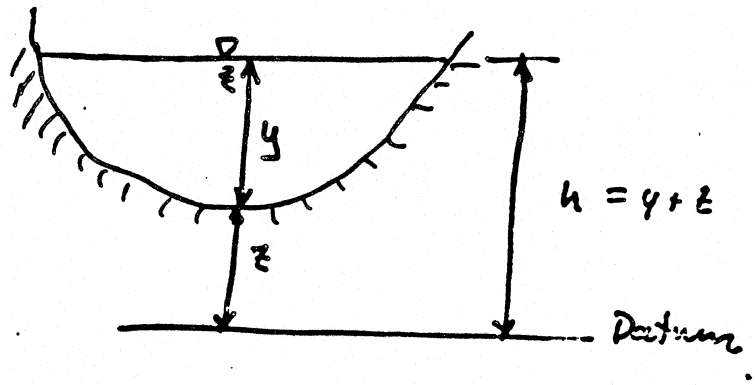

$$\frac{\partial h}{\partial x} = \frac{\partial y}{\partial x} + \frac{\partial z}{\partial x} \qquad \text{where} \quad S_o = -\frac{\partial z}{\partial x} \text{ or } \frac{\partial z}{\partial x} = -S_o$$

$$\frac{\partial h}{\partial x} = \frac{\partial y}{\partial x} - S_o$$

CONSERVATION FORM OF ~~SOL~~ MOMENTUM EQUATION

$$\frac{\partial Q}{\partial t} + \frac{\partial(\beta V Q)}{\partial x} + gA\left(\frac{\partial h}{\partial x} + S_f\right) - \beta g v_x + \frac{\tau_w}{e}B = 0$$

Table 1.1. Summary of Saint-Venant Equations*

Continuity Equation

Conservation form

$$\frac{\partial Q}{\partial x} + \frac{\partial A}{\partial t} = 0 \qquad (1.35)$$

Nonconservation form

$$\frac{\partial y}{\partial t} + \frac{A}{B}\frac{\partial V}{\partial x} + V\frac{\partial y}{\partial x} = 0 \qquad (1.36)$$

Momentum Equation

Conservation form

$$\frac{1}{A}\frac{\partial Q}{\partial t} + \frac{1}{A}\frac{\partial}{\partial x}(Q^2/A) + g\frac{\partial y}{\partial x} - g(S_o - S_f) = 0 \qquad (1.37)$$

local acceleration term | convective acceleration term | pressure term

Nonconservation form (unit width element)

$$\frac{\partial V}{\partial t} + V\frac{\partial V}{\partial x} + g\frac{\partial y}{\partial x} - g(S_o - S_f) = 0 \qquad (1.38)$$

Kinematic wave

Diffusion wave

Dynamic wave

*Neglecting lateral inflow, $q = 0$, assuming $\beta = 1$ and $\tau_w = 0$.

Kinematic Wave Model

Kinematic refers to the study of motion exclusive of the influence of mass and force whereas in dynamics these forces are included.

$$\frac{\partial Q}{\partial x} + \frac{\partial A}{\partial t} = q \qquad \text{Continuity}$$

$$S_o - S_f = 0 \qquad \text{Momentum}$$

Inertial & pressure terms are neglected in the momentum equation therefore kinematic wave will propagate only in the downstream direction.

Dynamic wave will propagate in both the upstream and downstream directions.

From Manning's Eq. $Q = \frac{k_{SI}}{n} A R^{2/3} S_f^{1/2}$

$$S_o \simeq S_f = \frac{n^2 Q^2}{[illegible] R^{4/3} A^2}$$

1.0 THEORETICAL DEVELOPMENT OF DYNAMIC (DISTRIBUTED) FLOOD ROUTING MODELS

The nature of flood waves propagating through a river or a network of rivers is a complex problem to describe. The impetus to develop complex models such as dynamic wave models to describe flood wave propagation more accurately has resulted from man's desire to build and live along rivers. The accuracy of predicting flow rates and the resulting water surface elevations is needed to provide better forecasts of floods. The importance of being able to accurately route floods is also reflected in the large number of routing methods that have been developed. Another major impetus to develop dynamic wave routing models has been from the need for more accurate and consequently more advanced hydrologic simulation models, and in particular the development of urban watershed simulation models and urban drainage design models. As a consequence, there have been several distributed routing models based upon the dynamic wave model developed to more accurately simulate the hydrologic-hydraulic response of urban watersheds. The passage of a flood wave along a river channel or an urban drainage system is an <u>unsteady</u>, <u>nonuniform</u> flow, unsteady because it varies in time, nonuniform because flow properties such as water surface elevation, velocities, and discharge are not constant along the channel.

The one-dimensional distributed routing methods are classified into <u>kinematic wave routing</u>, <u>diffusion wave routing</u>, and <u>dynamic wave routing</u> methods. Kinematic waves govern the flow when the inertial and pressure forces are not important, i.e., the gravitational force of the flow is balanced by the resistance forces.

The kinematic wave approximation is useful for applications where the channel slopes are steep and backwater effects are negligible. When the pressure forces become important but the inertial forces remain unimportant, a diffusion wave model which describes the resistance forces in terms of the pressure force is applicable. Essentially both the kinematic wave model and the diffusion wave model are helpful in describing downstream wave propagation when the channel slope is greater than about 0.5 ft/mi and there are no waves propagating upstream due to downstream disturbances such as tides, downstream tributary inflows, or downstream reservoir operations. When both the inertial and pressure forces are important, such as in mild sloped rivers, and backwater effects from downstream disturbances are not negligible, then both the inertial force terms and pressure force terms in the momentum equation are important to describe the resistance forces. Under these circumstances the dynamic wave routing method is required, which involves numerical solution of the full Saint-Venant equations. Dynamic routing was first used by Stoker (1953) and Isaacson, et al. (1954) in their pioneering investigation of flood routing for the Ohio River. This chapter describes the theoretical development of dynamic wave routing models using <u>implicit finite difference approximations</u> to solve the Saint-Venant equations.

20

Distributed flow routing models can be used to describe the transformation of storm rainfall to runoff over a watershed to produce a flow hydrograph at the watershed outlet, and then to take this hydrograph as the input at the upstream end of a river or pipe system and route it to the downstream end. The true flow process in either of these applications varies in all three space dimensions; for example, the velocity in a river varies along the river, across it, and also from the water surface to the river bed. For many practical purposes the spatial variation in velocity across the channel and with respect to the depth can be ignored so that the flow process can be approximated as varying in only one space dimension - along the flow channel, or in the direction of flow. The Saint-Venant equations, dirst developed by Barre De Saint-Venant (1871), describe the one-dimensional, unsteady open channel flow that is applicable in this case.

1.1 Derivation of Saint-Venant Equations

The following assumptions are necessary for derivation of the Saint-Venant equations:

1. The flow is one-dimensional so that depth and velocity vary only in the longitudinal direction of the channel. This implies that the velocity is constant and the water surface elevation is constant across any section perpendicular to the longitudinal axis.
2. Flow is assumed to vary gradually along the channel so that hydrostatic pressure prevails and vertical accelerations are neglected (Chow, 1959).
3. The longitudinal axis of the channel is approximated as a straight line.
4. The bottom slope of the channel is small and the channel bed is fixed, neglecting the effects of scour and deposition.

5. Resistance coefficients for steady uniform turbulent flow are applicable so that equations such as Manning's can be used to describe resistance effects.

6. The fluid is incompressible and of constant density throughout the flow.

Conservation of Mass

The conservation of mass (continuity equation) expresses that the mass inflow to a control volume (I_{mass}) minus the mass outflow from the control volume (O_{mass}) is equal to the time rate of change of stored mass (S_{mass}) within the control volume, i.e.,

$$I_{mass} - O_{mass} = \frac{dS_{mass}}{dt} \tag{1.1}$$

Considering the control volume of a channel of length dx shown in Figure 1.1, the mass inflow, the mass outflow, and the time rate of change of mass are, respectively,

$$I_{mass} = \rho\,(Q+qdx) \tag{1.2}$$

$$O_{mass} = \rho\,(Q + \frac{\partial Q}{\partial x}\,dx) \tag{1.3}$$

$$\frac{dS_{mass}}{dt} = \frac{\partial\,(\rho A dx)}{\partial t} \tag{1.4}$$

where ρ is the density of water, Q is the discharge, q is the lateral inflow per unit channel length per unit time, x is the longitudinal distance along the channel, and A is the cross-sectional area of flow.

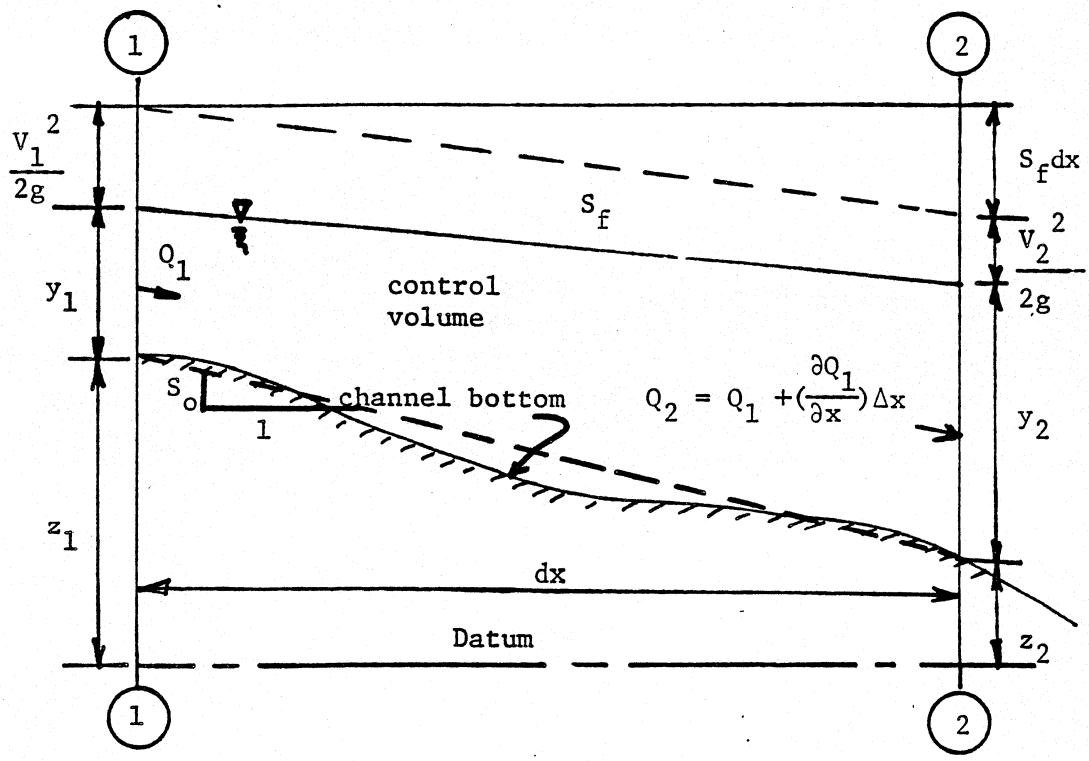

(a) PROFILE

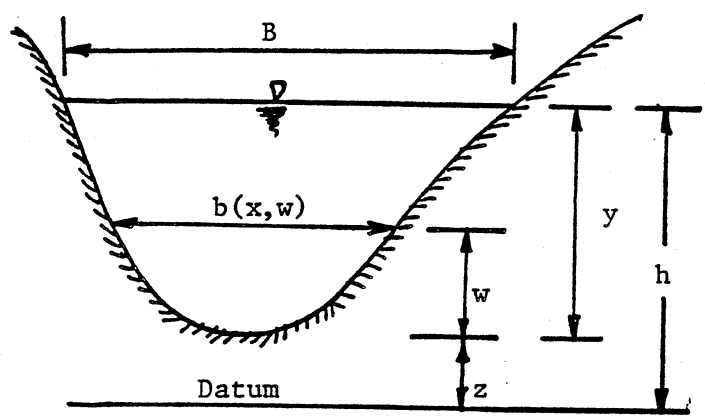

(b) CROSS-SECTION

Figure 1.1. Profile and Cross-Section of an Elemental Reach of Channel

Substituting equations (1.2 - 1.4) into (1.1) gives

$$\rho(Q+qdx) - \rho(Q+\frac{\partial Q}{\partial x}dx) = \frac{\partial(\rho A dx)}{\partial t} \tag{1.5}$$

and simplifying gives the <u>conservation form</u> of the continuity equation,

$$\frac{\partial Q}{\partial x} + \frac{\partial A}{\partial t} - q = 0 \tag{1.6}$$

which is for a prismatic or nonprismatic channel. A <u>prismatic channel</u> is one in which the flow cross-section is unvarying and the channel bottom slope is constant.

For some finite difference solution techniques, such as the method of characteristics, the <u>non-conservation form</u> of the continuity equation is desirable. The non-conservation form of the continuity equation can be derived considering that for a prismatic channel A is a function of y and for a non-prismatic channel A is a function of both x and y. For a prismatic channel then

$$\frac{\partial A}{\partial t} \simeq B\frac{\partial y}{\partial t} \quad (\text{assuming } \frac{\partial B}{\partial t} \approx 0) \tag{1.7}$$

where B is the top width of flow (see Fig. 1.1a).

The $\partial Q/\partial x$ can be expressed using the continuity equation, $Q = AV$, where V is the average flow velocity so that

$$\frac{\partial Q}{\partial x} = A\frac{\partial V}{\partial x} + V\frac{\partial A}{\partial x} \tag{1.8}$$

and

$$\frac{\partial A}{\partial x} = B \frac{\partial y}{\partial x} \tag{1.9}$$

which assumes dA = Bdy. Substituting equations (1.7 - 1.9) into (1.6) and rearranging gives

$$V\frac{\partial y}{\partial x} + \frac{A}{B}\frac{\partial v}{\partial x} + \frac{\partial y}{\partial t} - q/B = 0 \tag{1.10}$$

The nonconservation form for a nonprismatic channel can be derived in a similar manner, except the term $\partial A/\partial x$ is expressed as

$$\frac{\partial A}{\partial x} = \left.\frac{\partial A}{\partial x}\right|_y + B\frac{\partial y}{\partial x} \tag{1.11}$$

where the subscript y denotes that y is constant when taking the derivative. Substituting equations (1.7), (1.8), and (1.11) into (1.6) and rearranging gives the nonconservation form

$$V\frac{\partial y}{\partial x} + \frac{A}{B}\frac{\partial v}{\partial x} + \frac{\partial y}{\partial t} + \frac{V}{B}\left[\frac{\partial A}{\partial x}\right]_y - \frac{q}{B} = 0 \tag{1.12}$$

Conservation of Momentum

The conservation of momentum states that the sum of forces (ΣF) acting on a control volume (Fig. 1.1) plus the net rate of momentum entering the control volume ($I_{mom} - O_{mom}$) are equal to the time rate of accumulation of momentum within the control volume (S_{mom}/dt). This is stated as Newton's second law

$$\Sigma F + (I_{mom} - O_{mom}) = \frac{dS_{mom}}{dt} \tag{1.13}$$

The sum of the forces acting on the control volume are

$$\Sigma F = F_g + F_f + F_w + F_p \tag{1.14}$$

where F_g is the gravity force along the channel due to the weight of the water in the control volume, F_f is the friction force along the bottom and sides of the control volume, F_w is the wind shear force, and F_p is the unbalanced pressure force (see Fig. 1.2). The gravity force is expressed as

$$F_g = \rho g A \, S_o \, dx \tag{1.15}$$

where S_o is the channel bottom slope, $\partial z/\partial x$. Frictional forces are derived as

$$F_f = -\rho g \, A \, S_f \, dx \tag{1.16}$$

where the friction slope, S_f, is based upon using resistance equations such as Manning's. The wind shear force is caused by frictional resistance of wind against the free surface of the water expressed as

$$F_w = -\tau_w \, B \, dx \tag{1.17}$$

where τ_w is the wind shear stress and the negative sign indicates that the wind is in opposite direction to the flow.

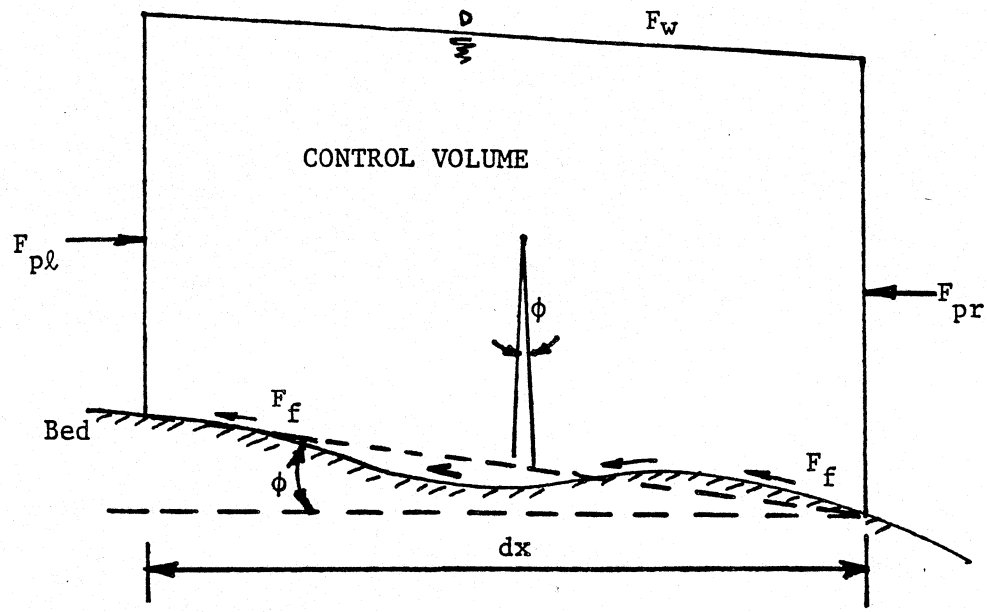

PROFILE

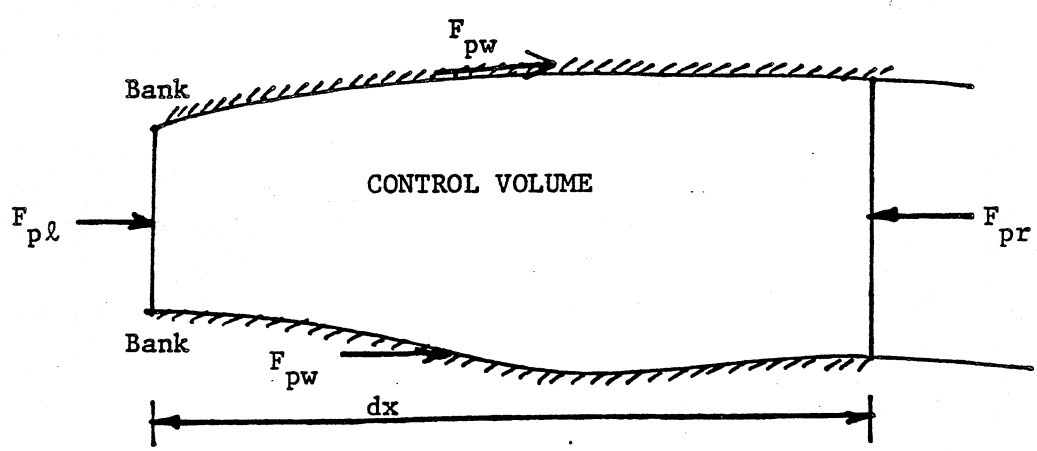

PLANVIEW

Figure 1.2 Forces Acting on Surface of Control Volume

Referring to Figure 1.2, the unbalanced pressure force is a resultant of the hydrostatic forces on the left side of the control volume, $F_{P\ell}$, the hydrostatic force on the right side of the control volume, F_{Pr}, and the pressure force exerted by the banks on the control volume, F_{Pb},

$$F_p = F_{P\ell} - F_{Pr} + F_{Pb} \tag{1.18}$$

The hydrostatic force on the left side of the control volume (referring to Fig. (1.2a) is

$$F_{P\ell} = \int_0^y \rho g(y-w) \frac{\partial b}{\partial x} dw \tag{1.19}$$

where w and b are defined in Fig. 1.1b. The hydrostatic force on the right side of the control volume is

$$F_{Pr} = \left[F_{P\ell} + \frac{\partial F_{P\ell}}{\partial x} dx \right] \tag{1.20}$$

where $\partial F_{P\ell}/\partial x$ is determined using the Leibnitz rule for differentiation of an integral (Abramowitz and Stegun, 1972),

$$\frac{\partial F_{P\ell}}{\partial x} = \int_0^y \rho g \frac{\partial y}{\partial x} bdw + \int_0^y \rho g(y-w) \frac{\partial b}{\partial x} dw \tag{1.21a}$$

$$= \rho g A \frac{\partial y}{\partial x} + \int_0^y \rho g(y-w) \frac{\partial b}{\partial x} dw \tag{1.21b}$$

because $A = \int_0^y bdw$. The force due to the banks is

$$F_{Pb} = \left[\int_0^y \rho g(y-w) \frac{\partial b}{\partial x} \, dw \right] dx \tag{1.22}$$

Substituting Equation (1.20) into Equation (1.18) gives

$$F_P = F_{P\ell} - F_{P\ell} + \frac{\partial F_{P\ell}}{\partial x} dx + F_{Pb} \tag{1.23a}$$

$$= - \frac{\partial F_{P\ell}}{\partial x} dx + F_{Pb} \tag{1.23b}$$

Now substituting Equations (1.21b) and (1.22) into (1.23b) and simplifying gives

$$F_P = - \rho g A \frac{\partial y}{\partial x} dx \tag{1.24}$$

The sum of forces can be expressed by substituting Equations (1.15-(1.17), and (1.24) into Equation (1.14)

$$\Sigma F = \rho g \, AS_o dx - \rho g \, AS_f dx - \tau_w \, Bdx - \rho g \, A \frac{\partial y}{\partial x} dx \tag{1.25}$$

The inflowing momentum to the control volume can be expressed as

$$I_{mom} = \rho(\beta VQ + \beta v_x q dx) \tag{1.26a}$$

where $\rho \beta VQ$ is the momentum entering the left side of the channel and $\rho \beta \, v_x q dx$ is the momentum entering from the lateral inflow which has a velocity v_x, in

the x-direction and β is the momentum correction factor. β is known as the momentum coefficient or Boussinesq coefficient to account for the nonuniform distribution of velocities in open channel flow in computing the momentum. $\beta = \frac{\int v^2 dA}{V^2 A}$ where v is the velocity of a small section of area dA. β can range from 1.01 for straight prismatic channels to 1.33 for river valleys with flood-plains. See Chow (1959) or Henderson (1966) for further details. The momentum leaving the control volume is

$$O_{mom} = \rho\left[\beta VQ + \frac{\partial(\beta VQ)}{\partial x}\right] dx \qquad (1.26b)$$

The net flow of momentum can then be expressed as

$$I_{mom} - O_{mom} = \rho\left[\beta VQ + \beta v_x q dx - \beta VQ - \frac{\partial(BVQ)}{\partial x} dx\right] \qquad (1.27a)$$

$$= \left[\rho\, \beta v_x q - \frac{\partial(\beta VQ)}{\partial x}\right] dx \qquad (1.27b)$$

The time rate of accumulation of momentum in the control volume is

$$\frac{dS_{mom}}{dt} = \rho \frac{\partial Q}{\partial t} dx \qquad (1.28)$$

The momentum Equation 1.13) can now be written by substituting Equations (1.25), (1.27), and (1.28) into Equation (1.13),

$$\rho g\, AS_o dx - \rho g\, AS_f dx - \tau_w B dx - \rho g\, A \frac{\partial y}{\partial x}\, dx +$$

$$\rho \left[\beta v_x - \frac{\partial(\beta VQ)}{\partial x} \right] dx = \rho \frac{\partial Q}{\partial t}\, dx \tag{1.29}$$

Dividing through by $\rho\, dx$ gives the conservation form of the momentum equation

$$\frac{\partial Q}{\partial t} + \frac{\partial(\beta VQ)}{\partial x} + g\, A \left(\frac{\partial y}{\partial x} - S_o + S_f\right) - \beta q v_x + \frac{\tau_w}{\rho} B = 0 \tag{1.30}$$

The depth y in Equation (1.30) can be replaced by the water surface elevation h using (see Fig. (1.1b)

$$h = y + z \tag{1.31}$$

where z is the elevation of the channel bottom above the datum. The derivative of Equation (1.31) with respect to the longitudinal distance along the channel is

$$\frac{\partial h}{\partial x} = \frac{\partial y}{\partial x} + \frac{\partial z}{\partial x} \tag{1.32}$$

where $\partial z/\partial x = -S_o$ so

$$\frac{\partial h}{\partial x} = \frac{\partial y}{\partial x} - S_o \tag{1.33}$$

The conservation of momentum can now be expressed in terms of h as

$$\frac{\partial Q}{\partial t} + \frac{\partial (\beta Q^2/A)}{\partial x} + gA\left(\frac{\partial h}{\partial x} + S_f\right) - \beta q v_x + \frac{\tau_w}{\rho} B = 0 \qquad (1.34)$$

The nonconservation form of the momentum equation (Eq. (1.38 in Table (1.1) can be derived in a similar manner as the nonconservation form of the conservation equation.

1.2 Classification of Distributed Routing Models

The Saint-Venant equations can have various approximate forms, each defining a one-dimensional distributed routing model. Equations (1.6) and (1.34), each written in the conservation form then the nonconservation form, neglecting lateral inflow, wind effect and eddy losses are used to define the different approximate one-dimensional distributed routing models as shown in Table 1.1.

The momentum equation consists of terms for the physical processes that define the resistance effects of flow by the energy grade line or friction slope. These terms in the conservation form that affect the energy slope are: a) the local acceleration term that describes the change in energy due to the change in velocities over time; b) the convective acceleration term that describes the change in energy due to change in velocity along the river; c) the pressure term that describes the change in energy due to change in the water surface elevation along the river; and d) the channel bottom slope. The local and convective acceleration terms essentially describe the effect of inertial forces on the flow. Other physical processes that can affect the energy are: eddy losses due to abrupt changes in river cross sections; wind effect, and lateral inflow which is the flow entering and leaving the river channel.

Through the incorporation of the local acceleration, the convective acceleration, and the pressure terms, these flow phenomena relating to effects such

Table 1.1. Summary of Saint-Venant Equations*

Continuity Equation

Conservation form

$$\frac{\partial Q}{\partial x} + \frac{\partial A}{\partial t} = 0 \qquad (1.35)$$

Nonconservation form

$$\frac{\partial y}{\partial t} + \frac{A}{B}\frac{\partial V}{\partial x} + V\frac{\partial y}{\partial x} = 0 \qquad (1.36)$$

Momentum Equation

Conservation form

$$\frac{1}{A}\frac{\partial Q}{\partial t} + \frac{1}{A}\frac{\partial}{\partial x}(Q^2/A) + g\frac{\partial y}{\partial x} \quad -g(S_o - S_f) = 0 \qquad (1.37)$$

local acceleration term | convective acceleration term | pressure term

Nonconservation form (unit width element)

$$\frac{\partial V}{\partial t} + V\frac{\partial V}{\partial x} + g\frac{\partial y}{\partial x} \quad -g(S_o - S_f) = 0 \qquad (1.38)$$

Kinematic wave

Diffusion wave

Dynamic wave

*Neglecting lateral inflow, $q = 0$, assuming $\beta = 1$ and $\tau_w = 0$.

as backwater effects can be incorporated in the distributed routing methods. Lumped routing methods do a poor job of simulating the flow conditions when backwater effects are significant and the river slopes are mild because these methods have no mechanisms to describe the energy or momentum effects. Other advantages of the distributed methods over the lumped methods will become evident as the reader studies this chapter.

The simplest distributed (hydraulic) routing model is the kinematic wave approximation which neglects the local acceleration, convective acceleration and pressure terms in the momentum equation. The diffusion wave approximation neglects the local and convective acceleration terms but incorporates the pressure term. The dynamic wave model considers all the acceleration and pressure terms in the momentum equation.

To illustrate the various types of flow the momentum equation (1.38) can be rearranged to define

$$-\frac{1}{g}\frac{\partial V}{\partial t} - \frac{V}{g}\frac{\partial V}{\partial x} - \frac{\partial y}{\partial x} + S_o = S_f \qquad (1.39)$$

steady uniform flow

steady nonuniform flow

unsteady nonuniform flow.

1.3 Movement of Flood Waves

To illustrate the movement of flood waves a monoclinal (dipping in one direction) flood wave is considered. A monoclinal flood wave which is a step increase in discharge moving downstream is shown in Figure 1.3. The monoclinal flood wave is influenced by bed slope and channel friction and can

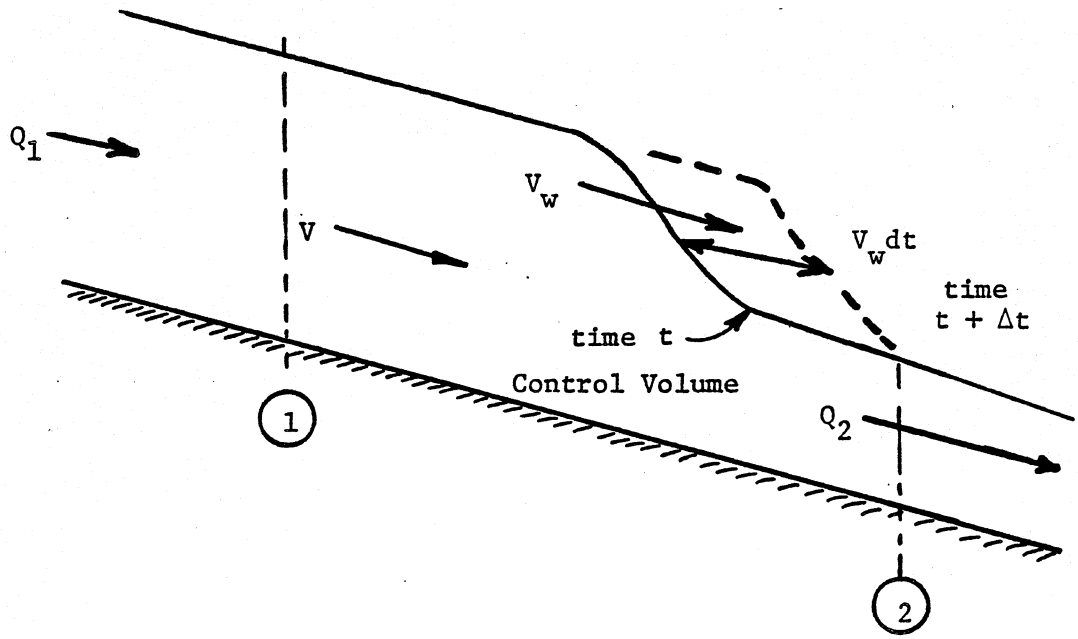

Figure 1.3. Monoclinal Wave

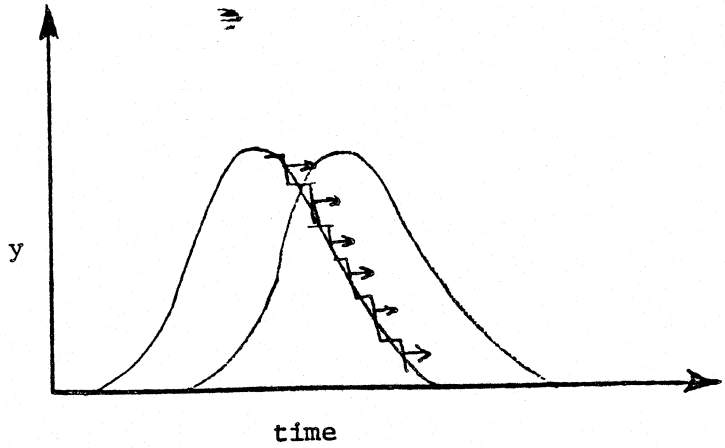

(a) Kinematic Wave as an Accumulation of Monoclinal Waves

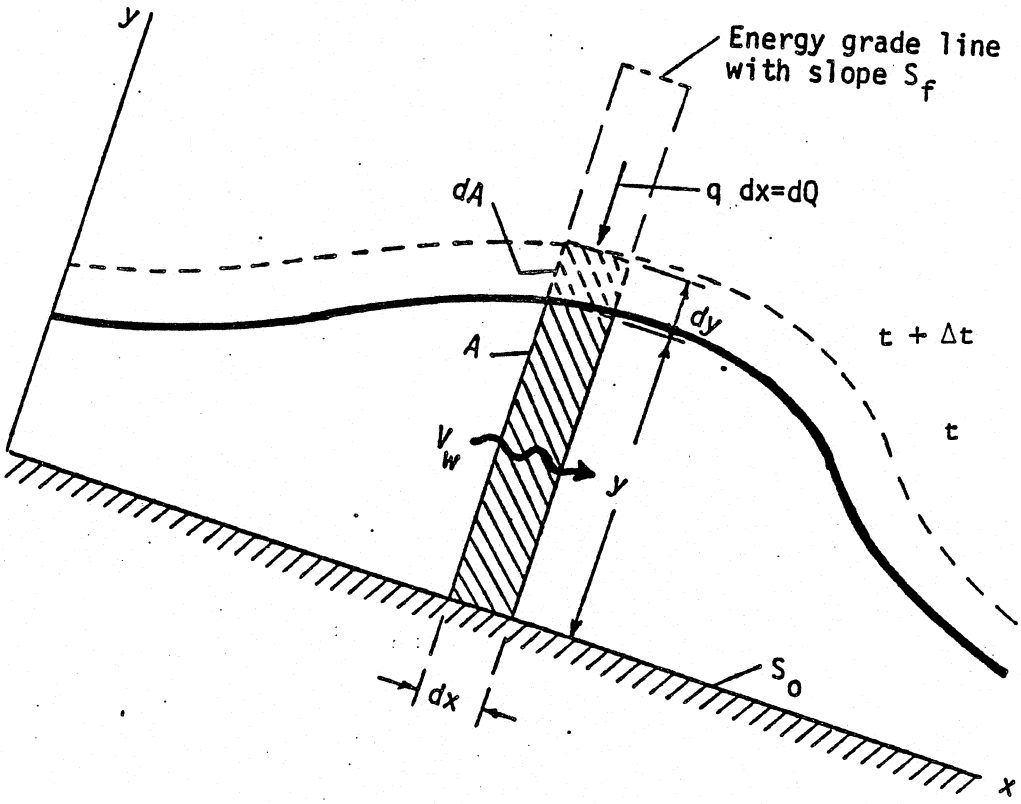

(b)

Figure .1.4. The Sketch for a Kinematic Wave

extend over a considerable length of a channel or river. The mean velocity of the water body is V and the speed of the flood wave is V_w. The monoclinal wave velocity can be rationalized by considering the control volume in Figure 1.3 and writing a simplified continuity equation as

$$\frac{(A_1 - A_2) \cdot V_w \cdot dt}{dt} = Q_1 - Q_2 \qquad (1.40)$$

which can be solved for V_w as

$$V_w = \frac{Q_1 - Q_2}{A_1 - A_2} \qquad (1.41)$$

As the wave becomes small $Q_1 \rightarrow Q_2$ and $A_1 \rightarrow A_2$ then the wave velocity is

$$V_w = \frac{dQ}{dA} = \frac{d(AV)}{dA} = V + A\frac{dV}{dA} \qquad (1.42)$$

The wave velocity can also be expressed as

$$V_w = \frac{1}{B} \cdot \frac{dQ}{dy} \qquad (1.43)$$

where $dA = B \cdot dy$.

This above argument assumes no subsidence or flattening out of the flood wave and also assumes that a unique relation between Q and A exists, i.e. a <u>uniform flow condition</u> ($S_o = S_f$). Hence total derivatives are used instead of partial derivatives as earlier.

The kinematic wave is a direct result of a unique relation between Q and A or Q and y, and can be thought of as a series of superimposed monoclinal waves as illustrated in Figure 1.4. Kinematic waves govern the flow when the inertial

and pressure forces are not important. Dynamic waves govern the flow when inertial and pressure forces are important such as in the movement of long waves in shallow water, e.g. a large flood wave in a wide river. In the kinematic wave the force component of the weight due to gravity is balanced by the resistive forces due to friction ($S_o = S_f$). Kinematic waves do not accelerate appreciably and the flow remains uniform along the channel within the differential length dx.

Figure 1.5 illustrates the difference in the kinematic and dynamic wave movements from the viewpoint of a stationary observer on the river bank. For the kinematic wave the energy-grade line parallels the channel bottom slope within the differential length, dx (Figure 1.4). Within the differential length, dx, the flow is steady uniform as implied by the momentum equation (1.39), and the change in discharge can be expressed as $dA \frac{dx}{dt}$. From Eq. (1.43) then the change in depth in the differential length dx can be expressed as

$$\frac{dy}{dt} = \frac{1}{B}\frac{dQ}{dx} \qquad (1.44)$$

Both the kinematic and dynamic wave movements are present in natural flood waves. In many cases the channel slope dominates in the momentum equation (1.39), therefore, most of the flood would move as a kinematic wave. Lighthill and Whitham (1955) proved that the speed of the main part of a natural flood wave approximates that of a kinematic wave. If the other terms, ($\frac{\partial V}{\partial t}$, $V\frac{\partial V}{\partial x}$, and $\frac{1}{g}\frac{\partial y}{\partial x}$), are not negligible then a dynamic wave front exists as shown in Figure 1.6.

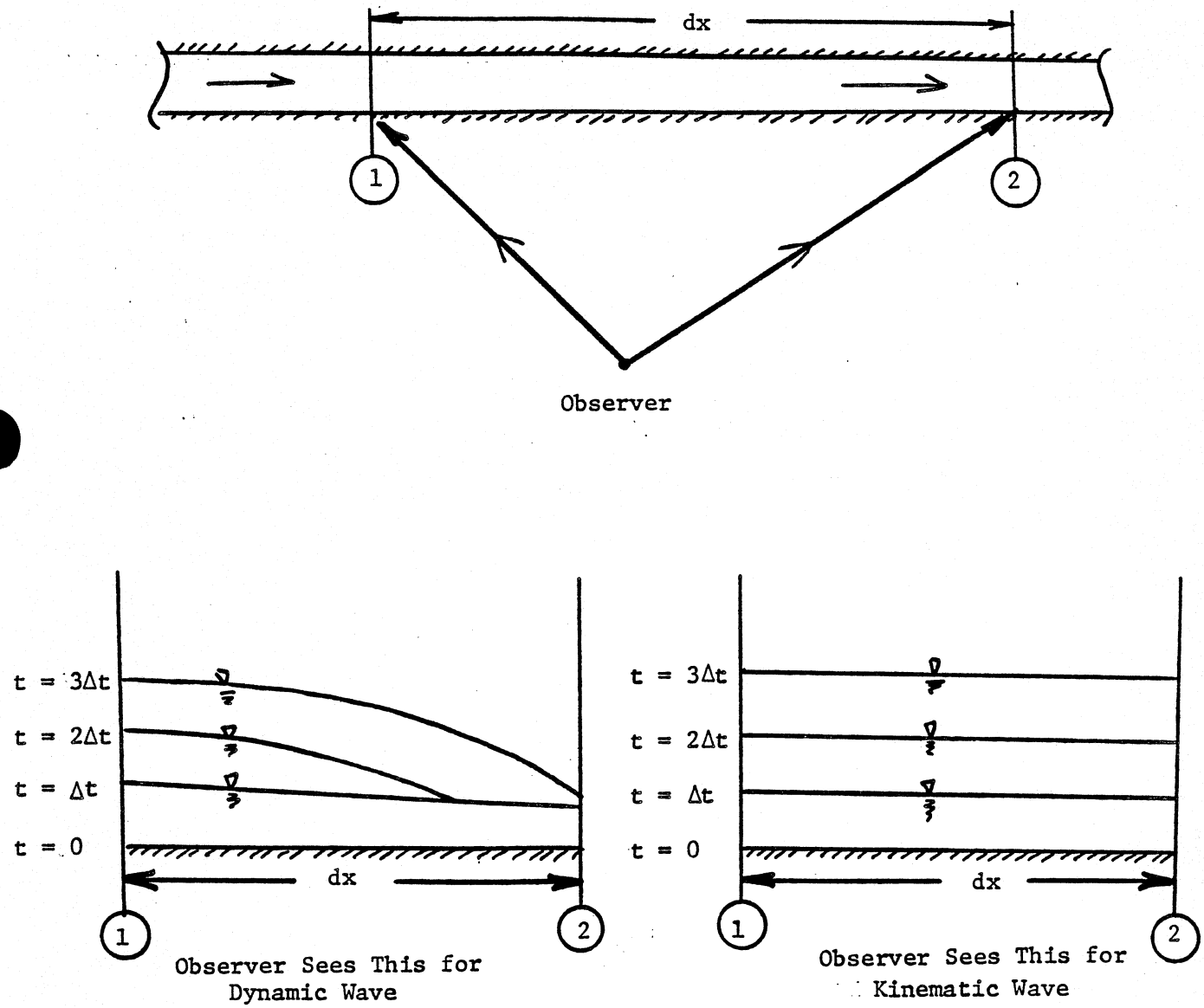

Figure 1.5. Kinematic vs. Dynamic Waves

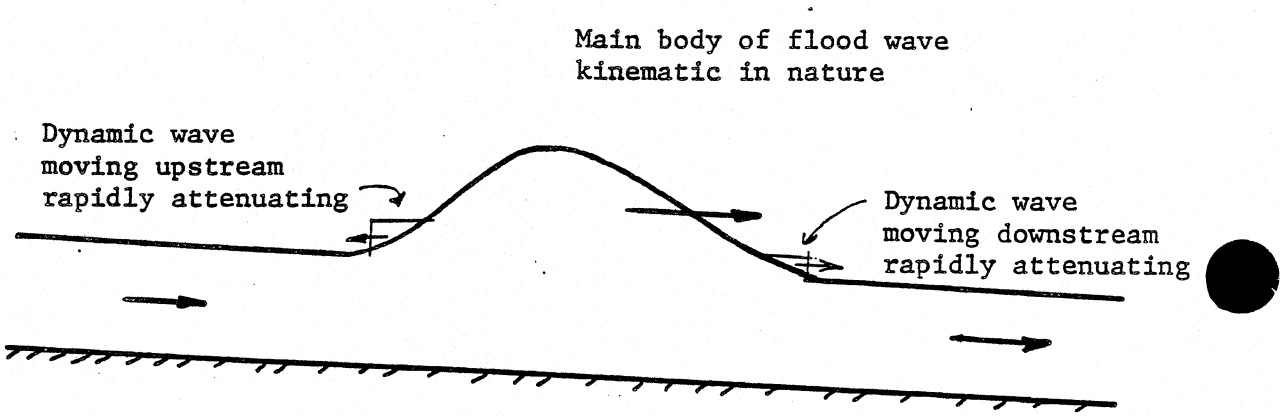

Figure 1.6. Movement of a Natural Flood Wave

If a wave is exactly kinematic ($S_f = S_o$), the kinematic wave speed varies with dQ/dy or dQ/dA. As a result the kinematic wave should theoretically advance downstream with the front of the wave getting steeper. However, the wave does not get longer or attenuate so it does not subside and the flood peak stays at the same maximum depth. As the front of the wave becomes steeper the other slope terms ($\frac{\partial V}{\partial t}$, $\frac{V\partial V}{\partial x}$, $\frac{1}{g}\frac{\partial y}{\partial x}$), become more important and introduce dispersion and attenuation. The wave velocity of a subsiding flood wave departs from the kinematic wave velocity because (1) the discharge is not just a function of depth alone and (2) at the wave crest the Q and y do not remain constant.

Lighthill and Whitham (1955) illustrated that the profile of a wave front can be determined combining the Chezy equation

$$Q = CA\sqrt{RS_f} \tag{1.45}$$

and the momentum equation (11.1.39)

$$Q = CA\sqrt{R(S_o - \frac{\partial y}{\partial x} - \frac{V}{g}\frac{\partial V}{\partial x} - \frac{1}{g}\frac{\partial v}{\partial t})} \tag{1.46}$$

in which C is the Chezy coefficient and R is the hydraulic radius. The velocity can also be determined from equation (1.46).

1.4 Dynamic Stage-Discharge Relation

Figure 1.7 shows a loop rating curve defining the stage-discharge relationship. The uniform flow rating curve is typical of hydrologic routing methods in which S = f(Q) or S = f(I, Q) and the loop rating curve is typical of distributed (hydraulic) routing methods. Referring to Eqs. (1.45 or 1.46) it is evident that the influences of the slope terms in addition to S_o can be

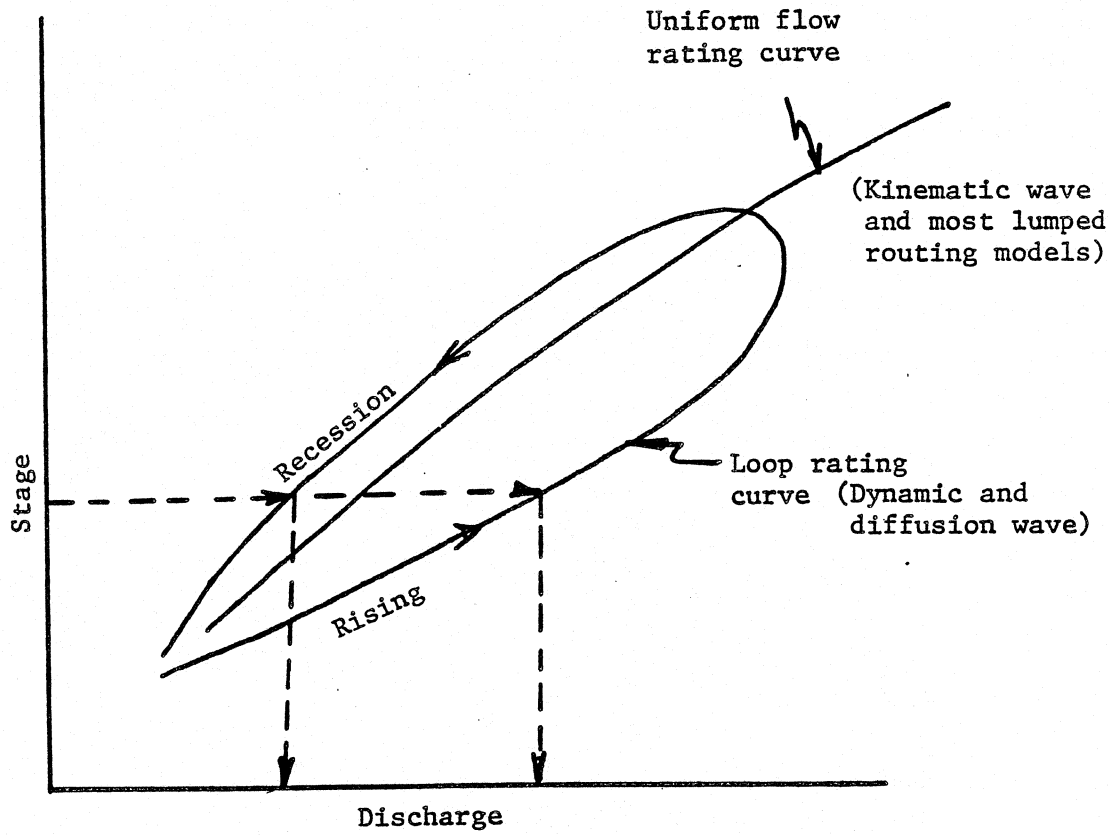

Figure 1.7. Loop Rating Curve

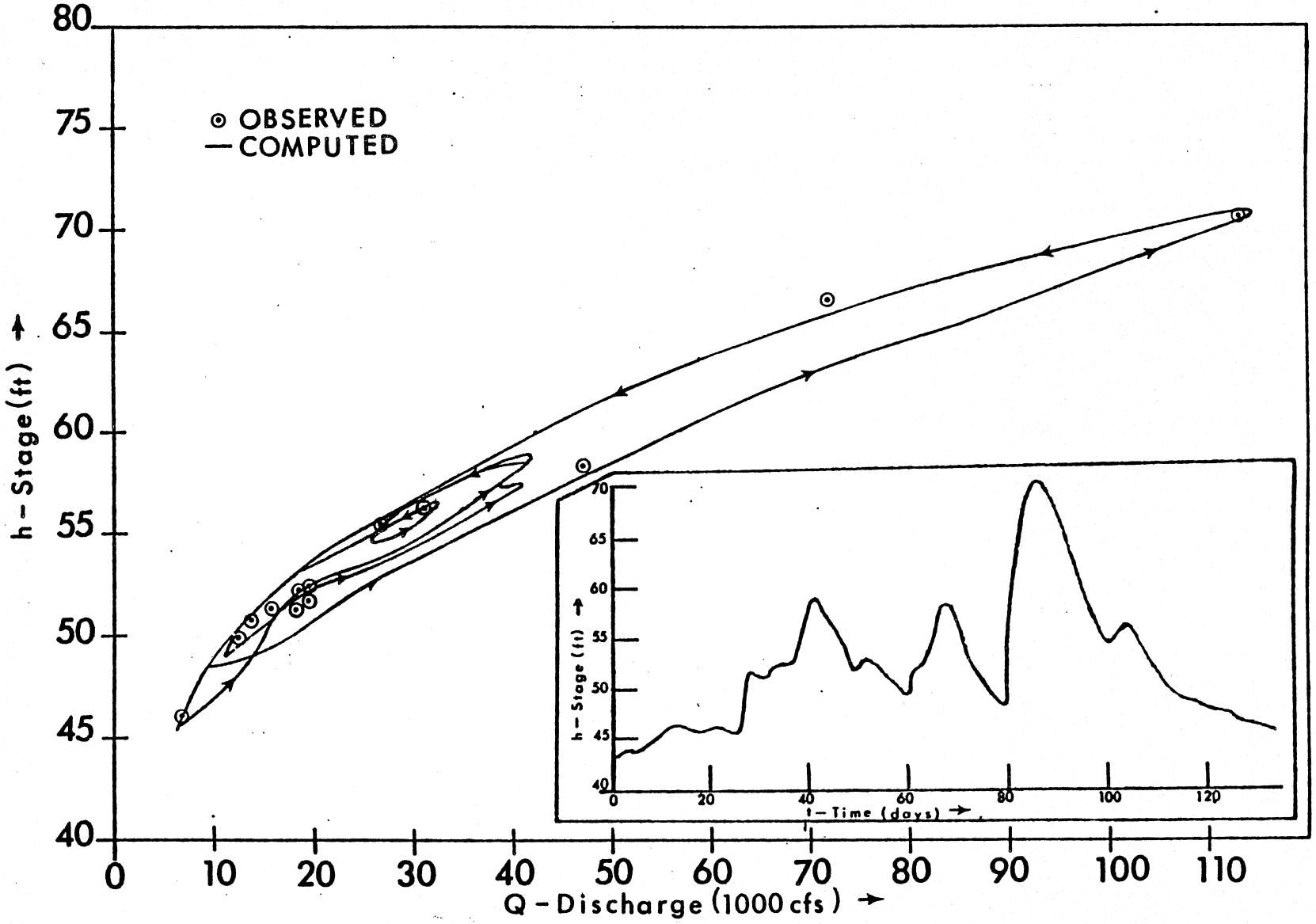

Figure 1.8. Stage-Discharge Relation for Red River, Alexandria, La. (2/5/64 - 6/17/64) (Fread, 1973d).

important, in which case the depth or stage is not just a function of discharge, but also is a function of the variable energy slope. For a given stage the discharge is usually lower on the rising limb of a flood hydrograph than on the recession limb.

Fread (1973d, 1975a) developed an equation for the dynamic relation between stage and discharge when the energy slope is variable due to changing discharge. This model can be used to determine discharge when the rate of change of stage is known (for stream gaging) or to determine stage when the rate of change of discharge is known (for stream forecasting). An application of this stage-discharge model is shown in Figure 1.8 to the Red River.

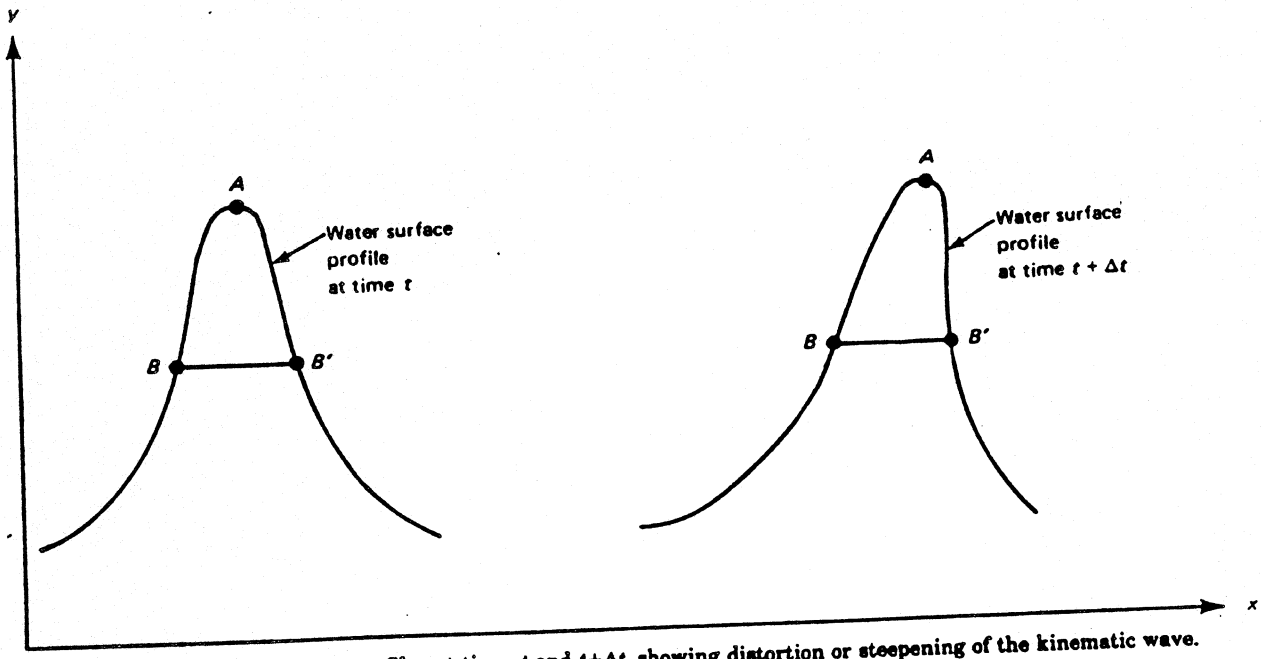

FIGURE 4.—Water-surface profiles at time, t and $t+\Delta t$, showing distortion or steepening of the kinematic wave.

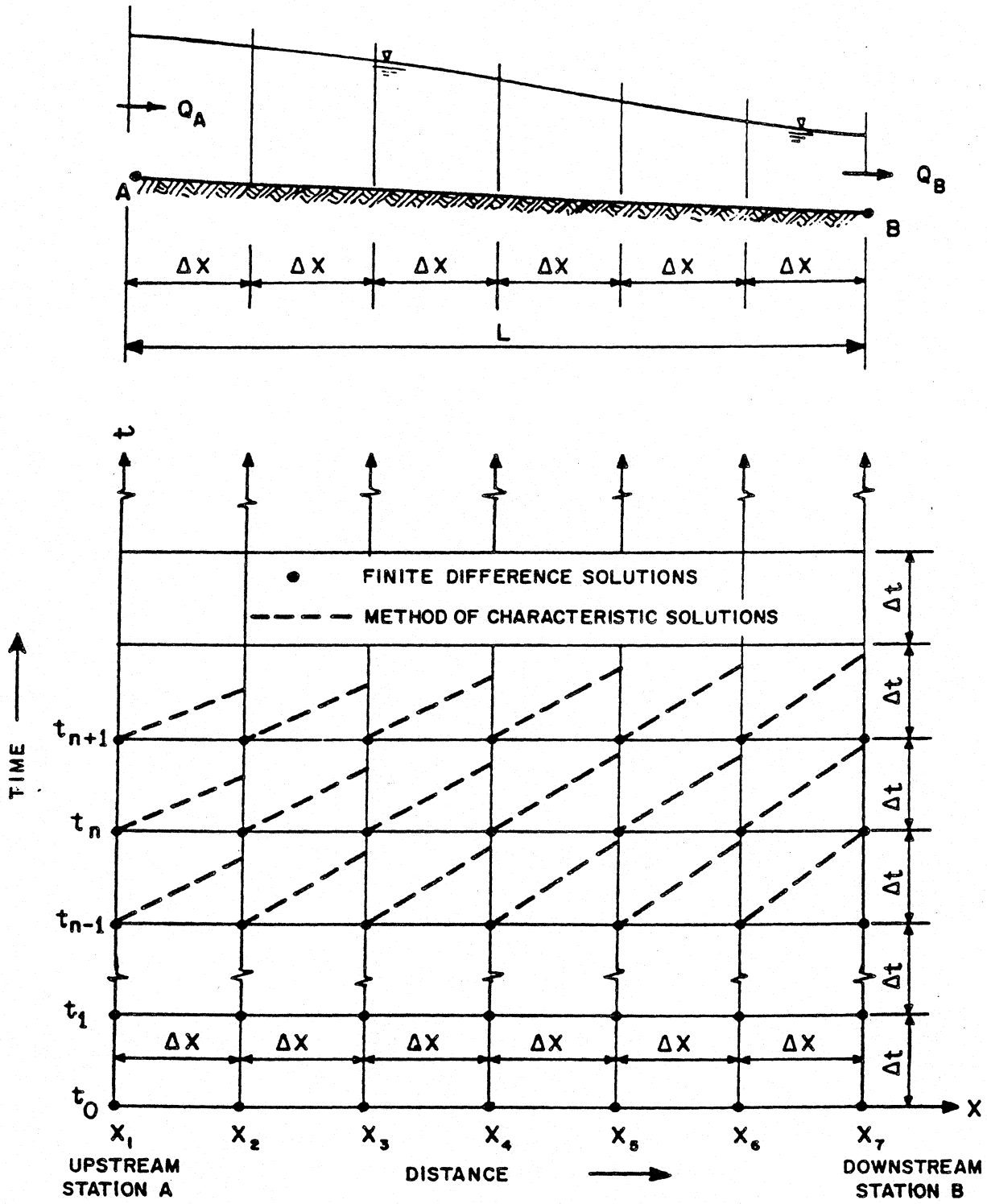

Figure 1.8 Characteristic Curves on a Fixed $\Delta X - \Delta t$ Grid

46

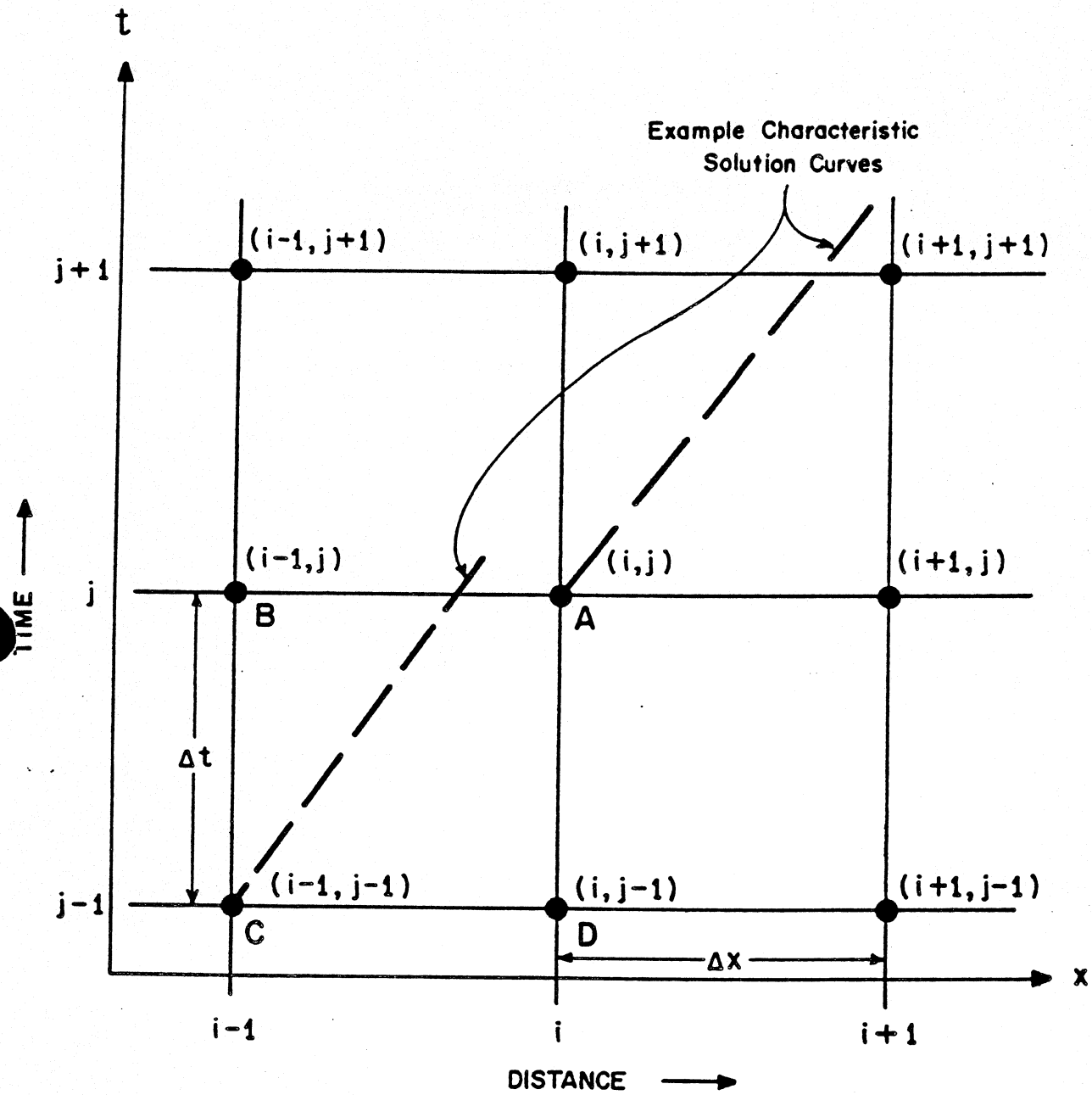

Figure 1.9 Space-Time Grid Used for Finite Difference Method

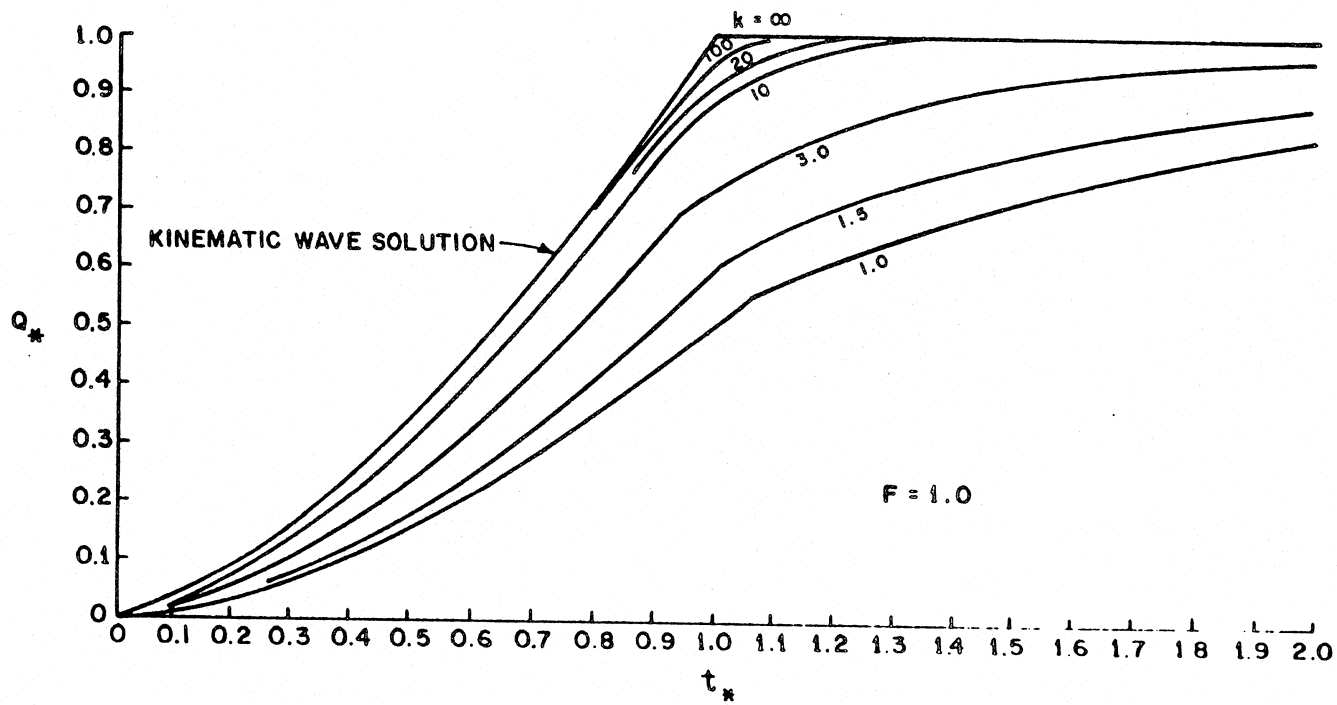

Figure 1.6 The Rising Hydrograph – Variation with k, for F = 1

(from Liggett and Woolhiser, 1967)

SECTION 2.0

SOLUTION OF SAINT-VENANT EQUATIONS

FINITE DIFFERENCES

FINITE DIFFERENCE APPROXIMATION

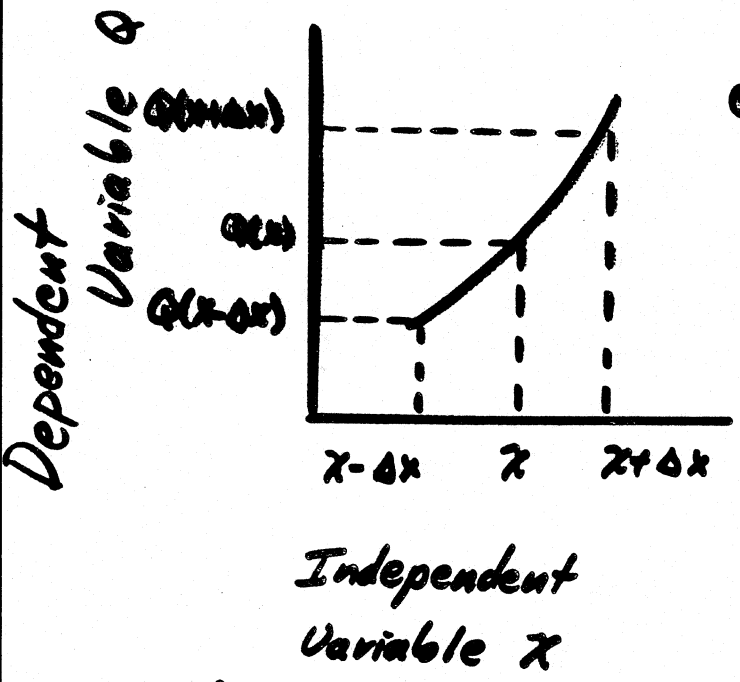

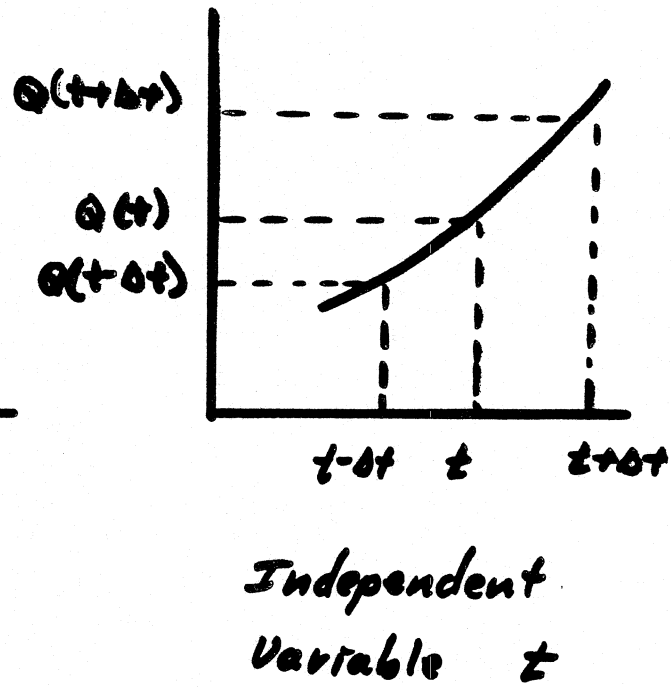

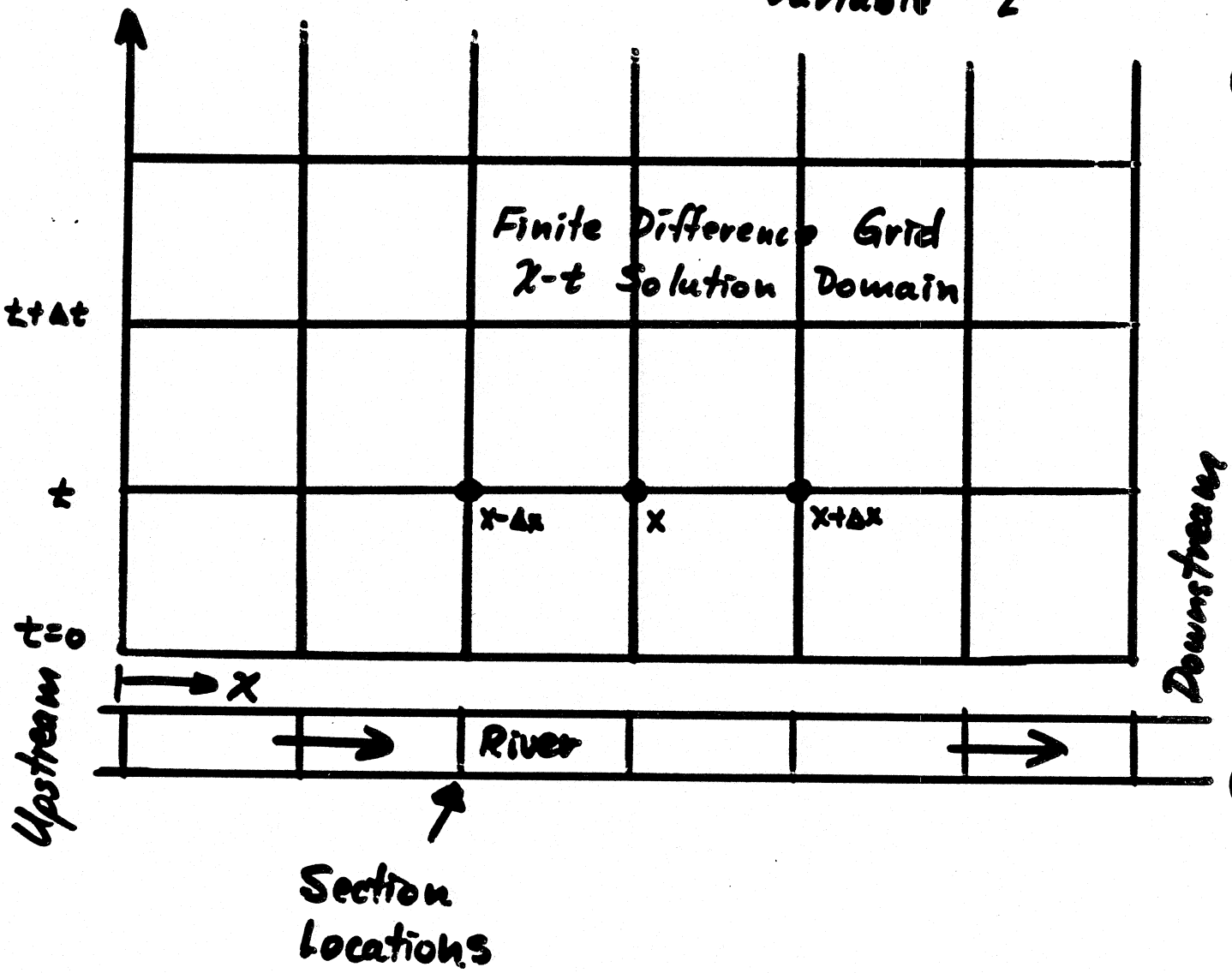

Independent Variables x & t ←

Dependendent Variables Q, H ←

Q, Y

V, Y

V, H

V, A

$\vdots$

Consider the dependent variable u
& the independent variable x

$u(x)$

To find $u(x+\Delta x)$ and $u(x-\Delta x)$ use a
<u>Taylor's series expansion</u>

At $x+\Delta x$

$$u(x+\Delta x) = u(x) + \Delta x \cdot u'(x) + \frac{1}{2}\Delta x^2 u''(x) + \frac{1}{6}\Delta x^3 u'''(x) + \cdots$$

At $x-\Delta x$

$$u(x-\Delta x) = u(x) - \Delta x\, u'(x) + \frac{1}{2}\Delta x^2 u''(x) - \frac{1}{6}\Delta x^3 u'''(x) + \cdots$$

$u'(x) \Rightarrow$ 1st derivative

$u''(x) \Rightarrow$ 2nd derivative

$\vdots$ $\vdots$

Central Differences

$$u(x+\Delta x) - u(x-\Delta x) = 2\Delta x\, u'(x) + \cancel{O(\Delta x^3)} \to 0$$

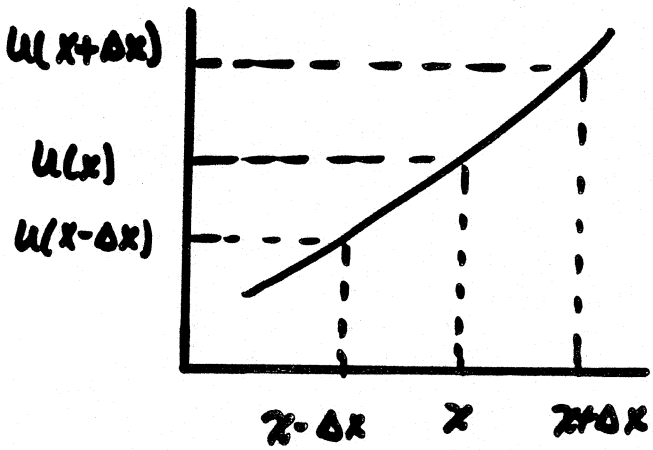

$$u'(x) \approx \frac{u(x+\Delta x) - u(x-\Delta x)}{2\Delta x} \qquad \frac{\partial Q}{\partial x} = \frac{Q_{x+\Delta x} - Q_{x}}{2\Delta x}$$

Forward Differences

$$u(x+\Delta x) - u(x) = \Delta x\, u'(x) + \cancel{O(\Delta x^2)} \to 0$$

$$u'(x) \approx \frac{u(x+\Delta x) - u(x)}{\Delta x} \qquad \frac{\partial Q}{\partial x} = \frac{Q_{x+\Delta x} - Q_{x}}{\Delta x}$$

Backward Differences

$$u(x) - u(x-\Delta x) = \Delta x\, u'(x) + \cancel{O(\Delta x^2)} \to 0$$

$$u'(x) = \frac{u(x) - u(x-\Delta x)}{\Delta x} \qquad \frac{\partial Q}{\partial x} = \frac{Q_{x} - Q_{x-\Delta x}}{\Delta x}$$

Explicit Scheme

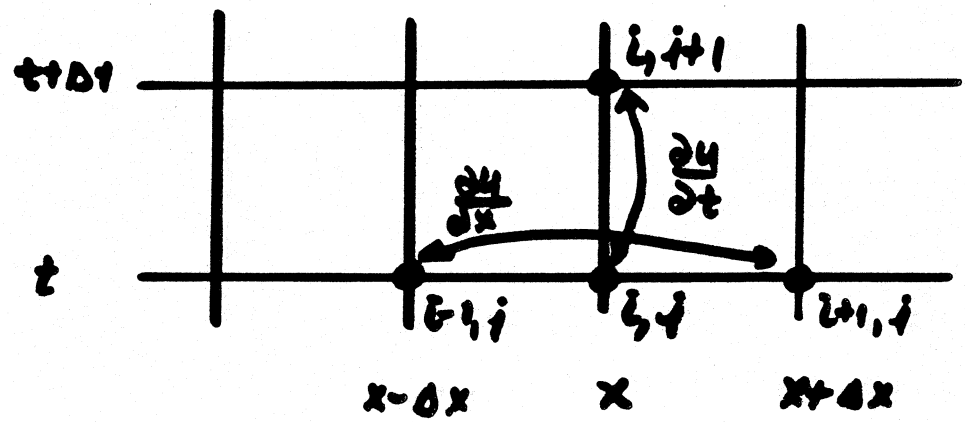

$$\frac{\partial u}{\partial t} = \frac{u_i^{j+1} - u_i}{\Delta t} \qquad \text{Forward}$$

$$\frac{\partial u}{\partial x} = \frac{u_{i+1}^{j} - u_{i-1}^{j}}{2\Delta x} \qquad \underline{\text{Central}}$$

Explicit Diffusion Scheme

$$\frac{\partial u}{\partial t} = \frac{u_i^{j+1} - \frac{1}{2}\left(u_{i+1}^{j} + u_{i-1}^{j}\right)}{\Delta t}$$

$$\frac{\partial u}{\partial x} = \frac{u_{i+1}^{j} - u_{i-1}^{j}}{2\Delta x}$$

based on writing derivatives of on known time line

implicit scheme " are written on known and unknown time line

Dynamic Wave Model - Explicit Diffusion Scheme

ST. VENANT EQ

CONTINUITY

$$\frac{\partial Q}{\partial x} + \frac{\partial A}{\partial t} - q = 0$$

MOMENTUM

$$\frac{\partial Q}{\partial t} + \frac{\partial (Q^2/A)}{\partial x} + gA\left(\frac{\partial h}{\partial x} + S_f\right) - q v_x = 0$$

Let $\frac{\partial A}{\partial t} = B\frac{\partial y}{\partial t}$

$y = h - z$

$\frac{\partial h}{\partial x} = \frac{\partial y}{\partial x} - S_o$

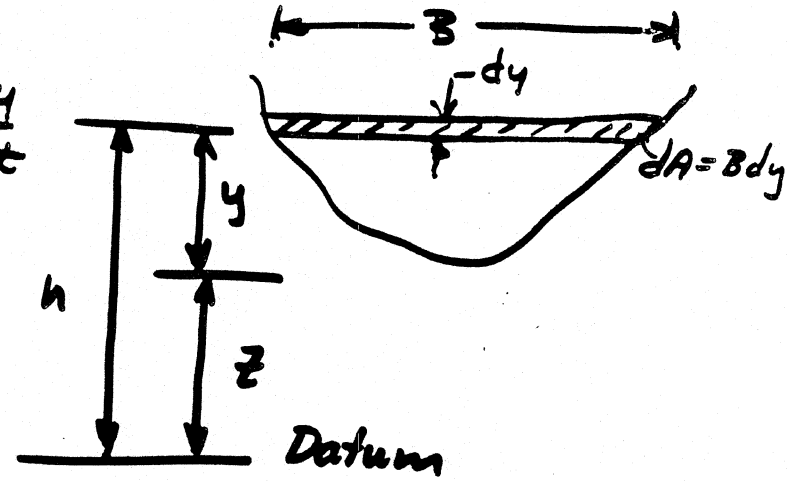

Making these substitutions the above equations are expressed as:

$$\frac{\partial y}{\partial t} + \frac{1}{B}\frac{\partial Q}{\partial x} - q/B = 0$$

lateral inflow term

Time derivative

$$\frac{\partial Q}{\partial t} + \frac{\partial (Q^2/A)}{\partial x} + gA\left(\frac{\partial y}{\partial x} - S_o + S_f\right) - q v_x = 0$$

Dependent variables are Q & y

$$\frac{\partial y}{\partial t} = \frac{y_i^{j+1} - \frac{1}{2}\left(y_{i+1}^{j} + y_{i-1}^{j}\right)}{\Delta t}$$

$$\frac{\partial Q}{\partial t} = \frac{Q_i^{j+1} - \frac{1}{2}\left(Q_{i+1}^{j} + Q_{i-1}^{j}\right)}{\Delta t}$$

$$\frac{\partial y}{\partial x} = \frac{y_{i+1}^{j} - y_{i-1}^{j}}{2\Delta x}$$

spatial derivative

$$\frac{\partial Q}{\partial x} = \frac{Q_{i+1}^{j} - Q_{i-1}^{j}}{2\Delta x}$$

$$\frac{\partial (Q^2/A)}{\partial x} = \frac{(Q^2/A)_{i+1}^{j} - (Q^2/A)_{i-1}^{j}}{2\Delta x}$$

Average values are used for non-derivative terms.

Cont'd

$$\left\{ \frac{y_i^{j+1} - \frac{1}{2}(y_{i+1}^{j} + y_{i-1}^{j})}{\Delta t} + \frac{1}{\frac{1}{2}(B_{i+1}^{j} + B_{i-1}^{j})}\left[\left(\frac{Q_{i+1}^{j} - Q_{i-1}^{j}}{2\Delta x}\right) - \frac{1}{2}\left(q_{i+1/2}^{j} + q_{i-1/2}^{j}\right)\right] = 0 \right.$$

Only unknown is y_i^{j+1}

$$y_i^{j+1} = \frac{1}{2}(y_{i+1}^{j} + y_{i-1}^{j}) - \frac{\Delta t}{\frac{1}{2}(B_{i+1}^{j} + B_{i-1}^{j})}\left[\frac{Q_{i+1}^{j} - Q_{i-1}^{j}}{2\Delta x} - \frac{1}{2}\left(q_{i+1/2}^{j} + q_{i-1/2}^{j}\right)\right]$$

Momentum

$$\frac{Q_i^{j+1} - \frac{1}{2}\left(Q_{i+1}^{j} + Q_{i-1}^{j}\right)}{\Delta t} + \frac{\left(\frac{Q^2}{A}\right)_{i+1}^{j} - \left(\frac{Q^2}{A}\right)_{i-1}^{j}}{2\Delta x}$$

$$+ \frac{1}{2} g \left(A_{i+1}^{j} + A_{i-1}^{j}\right)\left[\frac{y_{i+1}^{j} - y_{i-1}^{j}}{2\Delta x} - S_o + \frac{1}{2}\left(S_{f\,i+1}^{j} + S_{f\,i-1}^{j}\right)\right]$$

$$- \frac{1}{2}\left[\left(g v_x\right)_{i+1/2}^{j} + \left(g v_x\right)_{i-1/2}^{j}\right] = 0$$

Unknown is discharge Q_i^{j+1}

$$Q_i^{j+1} = \frac{1}{2}\left(Q_{i+1}^{j} + Q_{i-1}^{j}\right) - \frac{\Delta t}{2\Delta x}\left[\left(\frac{Q^2}{A}\right)_{i+1}^{j} - \left(\frac{Q^2}{A}\right)_{i-1}^{j}\right]$$

$$- \frac{g\Delta t}{2}\left(A_{i+1}^{j} + A_{i-1}^{j}\right)\left[\frac{y_{i+1}^{j} - y_{i-1}^{j}}{2\Delta x} - S_o\right.$$

$$\left. + \frac{1}{2}\left(S_{f\,i+1}^{j} + S_{f\,i-1}^{j}\right)\right] + \frac{\Delta t}{2}\left[\left(g v_x\right)_{i+1/2}^{j}\right.$$

$$\left. + \left(g v_x\right)_{i-1/2}^{j}\right] = 0$$

Numerical Stability

CURRENT CONDITIONS

$$\Delta t \le \frac{\Delta x_i}{\left(\frac{Q}{A}\right)_i + \sqrt{g\left(\frac{A}{B}\right)_i}} \qquad \text{(min. for all } i\text{)}$$

MANNING CONDITIONS

$$\Delta t \le \frac{2.208\, A_i R_i^{4/3}}{g\, n_i^2\, |Q_i|} \qquad \text{(min. for all } i\text{)}$$

Note: As hydraulic depth $\left(\frac{A}{B}\right)$ increases Computational time step is substantially reduced

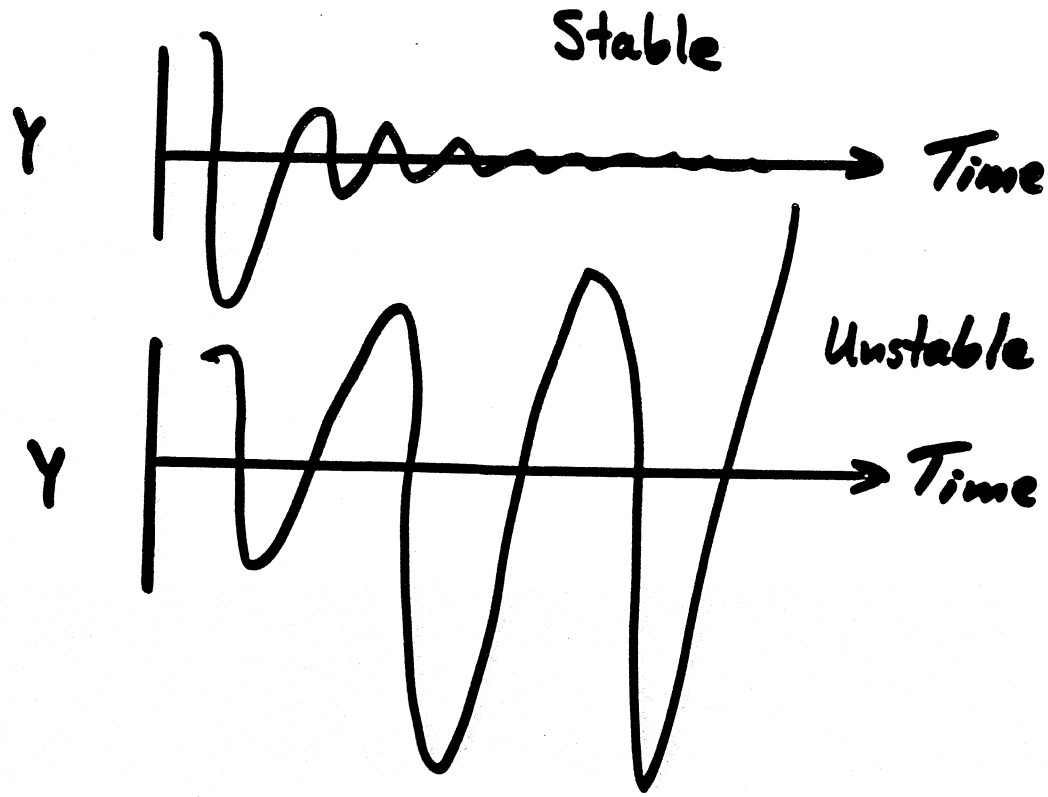

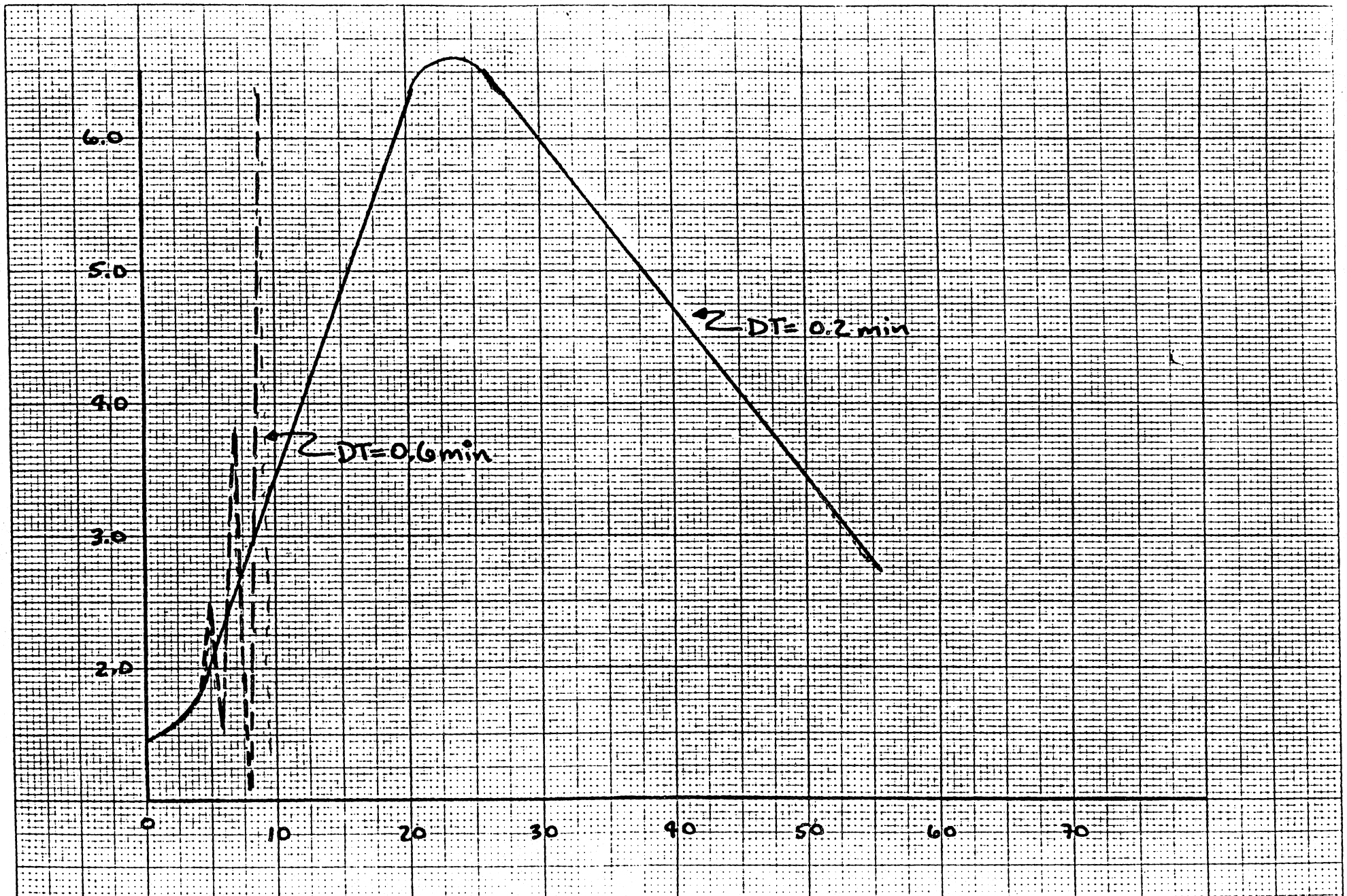

Figure 3. Discharge Hydrograph for Channel Section 8

Consider a Linear <u>Kinematic Wave</u> Model

$$\frac{\partial Q}{\partial x} + \frac{\partial A}{\partial t} = q \qquad \text{CONTINUITY}$$

$$S_o - S_f = 0 \quad \Rightarrow \quad \text{MOMENTUM}$$

Kinematic refers to study of motion exclusive of the influence of mass and force whereas in dynamics these forces are included.

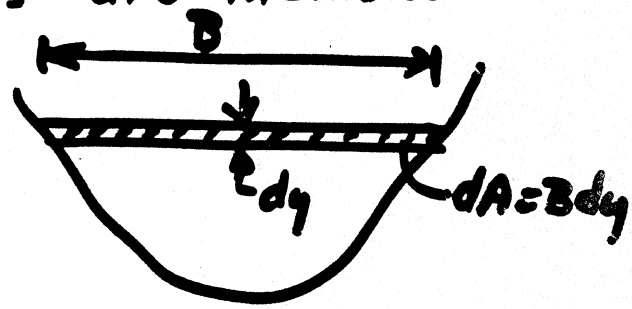

$$\frac{\partial A}{\partial t} = B\frac{\partial y}{\partial t}$$

$$\frac{\partial Q}{\partial x} = \frac{\partial Q}{\partial y}\cdot\frac{\partial y}{\partial x}$$

$$\frac{\partial Q}{\partial y}\cdot\frac{\partial y}{\partial x} + B\frac{\partial y}{\partial t} = 0$$

$$\frac{1}{B}\frac{\partial Q}{\partial y}\cdot\frac{\partial y}{\partial x} + \frac{\partial y}{\partial t} = 0 \quad \text{where} \quad \frac{dy}{dt} = \frac{dx}{dt}\frac{\partial y}{\partial x} + \frac{\partial y}{\partial t} = 0$$

Observer moving at velocity $\frac{dx}{dt}$ with the flow would see discharge flow Q to be constant.

$$\frac{dx}{dt} = V_w = \frac{1}{B}\frac{dQ}{dy} = \frac{dQ}{dA} \qquad \text{wave celerity}$$

Linear Scheme

$$\frac{\partial Q}{\partial x} + \frac{\partial A}{\partial t} = q$$

$$S_o = S_f \quad \Rightarrow \quad A = \alpha Q^{\beta}$$

$$\frac{\partial A}{\partial t} = \frac{\partial A}{\partial Q}\frac{\partial Q}{\partial t}$$

$$\frac{\partial A}{\partial Q} = \alpha \beta Q^{\beta-1}$$

By Manning's Eq.

$$Q = \frac{1.49}{n}\frac{A^{5/3}}{P^{2/3}} S_f^{1/2}$$

$$A = \underbrace{\left[\frac{n P^{2/3}}{1.49 S_f}\right]^{3/5}}_{\alpha} Q^{3/5}$$

$$\beta = 3/5$$

$$\frac{\partial Q}{\partial x} + \alpha \beta Q^{\beta-1}\frac{\partial Q}{\partial t} = q$$

Dependent Variable is Q

Finite difference approximations

$$\frac{\partial Q}{\partial x} = \frac{Q_{i+1}^{j+1} - Q_i^{j+1}}{\Delta x}$$

$$\frac{\partial Q}{\partial t} = \left(\frac{Q_{i+1}^{j+1} - Q_{i+1}^{j}}{\Delta t}\right)$$

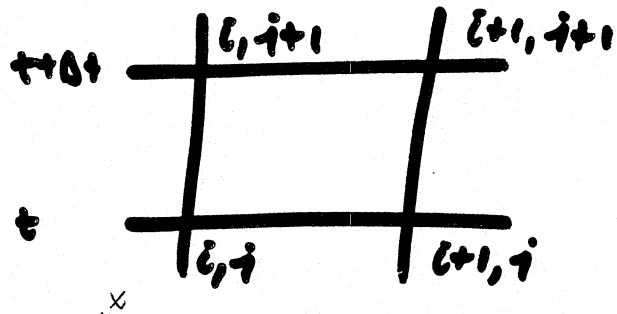

omit

$$\frac{Q_{i+1}^{j+1} - Q_i^{j+1}}{\Delta x} + \alpha\beta\left(\frac{Q_{i+1}^{j} + Q_i^{j}}{2}\right)^{\beta-1}\left(\frac{Q_{i+1}^{j+1} - Q_{i+1}^{j}}{\Delta t}\right) = \frac{1}{2}\left(q_{i+1}^{j+1} + q_{i+1}^{j}\right)$$

$$Q_{i+1}^{j+1} = \left[\frac{\Delta t}{\Delta x} Q_i^{j+1} + \alpha\beta Q_{i+1}^{j}\left(\frac{Q_{i+1}^{j} + Q_i^{j+1}}{2}\right)^{\beta-1} + \Delta t/2\left(q_{i+1}^{j+1} + q_{i+1}^{j}\right)\right]\left[\frac{\Delta t}{\Delta x} + \alpha\beta\left(\frac{Q_{i+1}^{j} + Q_i^{j+1}}{2}\right)^{\beta-1}\right]^{-1}$$

Weighted 4-Point Implicit Scheme

$$\frac{\partial Q}{\partial x} + \frac{\partial A}{\partial t} = 0 \qquad \text{Full Dynamic Wave}$$

$$\frac{1}{A}\frac{\partial Q}{\partial t} + \frac{1}{A}\frac{\partial}{\partial x}(Q^2/A) + gA\left(\frac{\partial h}{\partial x} + S_f\right) - \beta g v_x + W_f B = 0$$

Need finite difference expressions for the various terms.

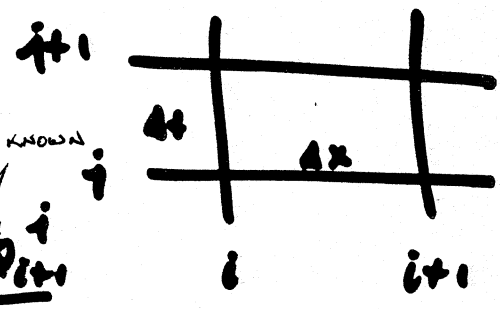

Time Derivative

UNKNOWN KNOWN

$$\frac{\partial Q}{\partial t} = \frac{\dfrac{Q_i^{j+1} + Q_{i+1}^{j+1}}{2} - \dfrac{Q_i^{j} + Q_{i+1}^{j}}{2}}{\Delta t}$$

if $\theta = 0$ derivative is explicit
$= 1$ " " fully implicit

Spatial Derivative

$$\frac{\partial Q}{\partial x} = \theta\left(\frac{Q_{i+1}^{j+1} - Q_i^{j+1}}{\Delta x}\right) + (1-\theta)\left(\frac{Q_{i+1}^{j} - Q_i^{j}}{\Delta x}\right)$$

WEIGHTING FACTOR
BETWEEN 0-1
USUALLY 0.55

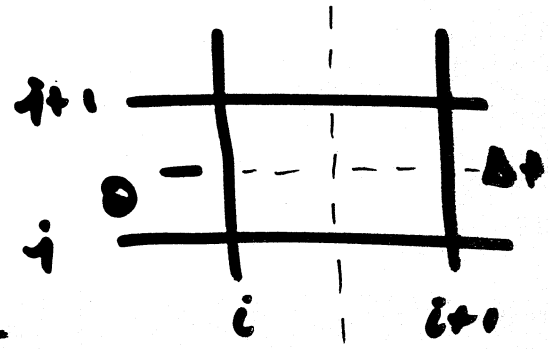

Other terms

$$q = \theta q_i^{j+1} + (1-\theta) q_i^{j}$$

LATERAL INFLOW

$$f(\bar{x}^{k+1}) = f(\bar{x}^{k}) + J(\bar{x}^{k})(\bar{x}^{k+1} - \bar{x}^{k})$$

Jacobian matrix
1st partials at $\bar{x}^k$

$$J(\bar{x}^k)\underbrace{(\bar{x}^{k+1} - x^k)}_{\Delta\bar{x}^k} = -f(x^k)$$

Solve for $\Delta\bar{x}^k$ above repeatedly until $\Delta\bar{x}^k <$ error.

$$h_i^{k+1} - h_i^k = dh_i \Rightarrow h_i^{k+1} = h_i^k + dh_i$$

$$Q_i^{k+1} - Q_i^{k+1} = dQ_i \Rightarrow Q_i^{k+1} = Q_i^k + dQ_i$$

2.0 Solution of Saint-Venant Equations - Finite Difference

The Saint-Venant equations for distributed (hydraulic) routing are not amenable to general analytical solutions except in a few special simple cases. The Saint-Venant equations are partial differential equations which must be solved using numerical methods. Most numerical methods for the solution of differential equations basically replace the derivatives in the equations by finite differences in order to transform the differential equations into finite-difference algebraic equations. The solution of the finite-difference algebraic equations can be performed quite simply on computers. Methods of finite differences may be classified as direct methods and characteristic methods. In the direct methods, the representation of finite differences is based directly on the original equations. In the characteristic methods, the Saint-Venant equations are first transformed to the characteristic form and the latter is used in finite-difference representation.

A finite-difference method may employ either an explicit scheme or an implicit scheme in solution. The explicit method is the simplest but can be unstable, which is to say that small computation (time and space) steps are required for convergence of the numerical procedures. The method is convenient since results are given at fixed locations and times, and it can treat slightly varying channel geometry from section to section. It is least efficient and hence not suitable for routing flood flows over a long time.

The implicit method is mathematically the most complicated, but with the use of computers this is not a serious problem once the method is programmed. The method is stable for large computation steps with no loss of accuracy and hence works much faster than the other two methods. Also, it can handle significantly varying channel geometry.

The characteristic method is the most accurate although it involves no more sophisticated mathematical analysis than the explicit method. It can handle gradually varying channel geometry but is not suitable for natural channels if the times and locations at which results are given are not fixed ahead of time. This method can use larger time steps than the explicit method and still is accurate and stable. In this method and the implicit method, large computation steps cause errors increasing with the size of step. However, the use of smaller time steps than necessary results in little improvement in the accuracy of the results.

2.1 Finite Difference Approximations

Finite difference approximations can be derived considering a function u(x) as shown in Fig. 10.2.1. A Taylor series expansion of u(x) at x + Δx is

$$u(x+\Delta x) = u(x) + \Delta x\, u'(x) + 1/2\, \Delta x^2\, u''(x) + 1/6 \Delta x^3 u'''(x) + \ldots \tag{2.1}$$

and the Taylor series expansion at x - Δ x is

$$u(x-\Delta x) = u(x) - \Delta x u'(x) + 1/2 \Delta x^2 u''(x) - 1/6\, \Delta x^3\, u'''(x) + \ldots \tag{2.2}$$

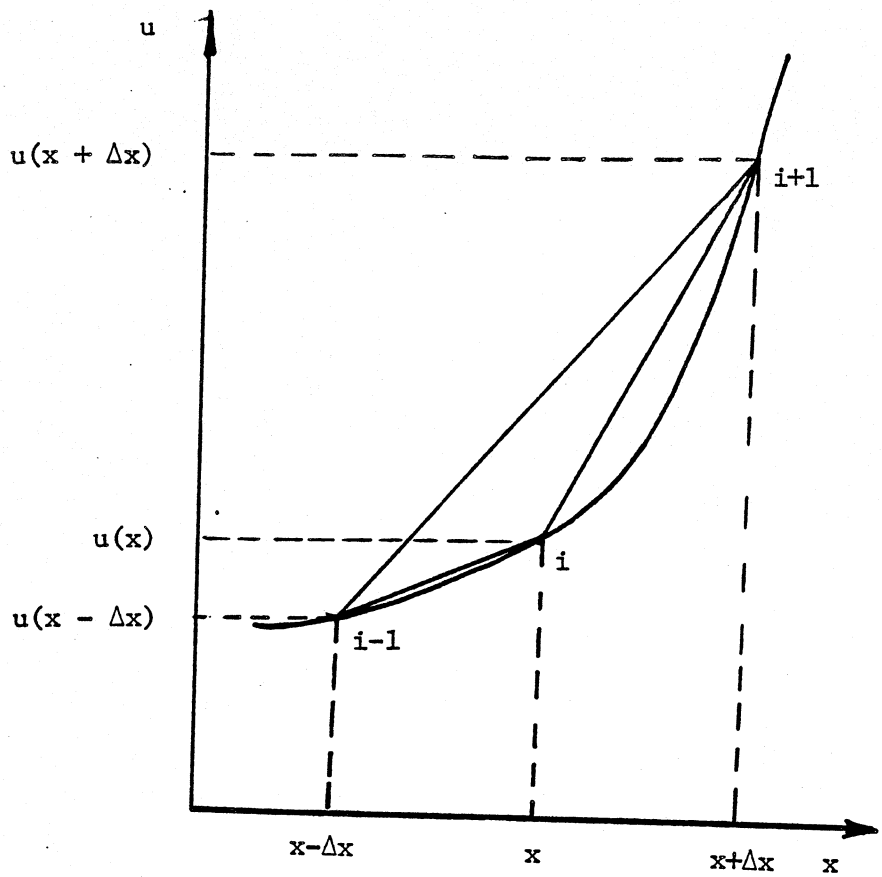

Figure 2.1. Function u(x) for finite difference approximations

where $u'(x)$, $u''(x)$, and $u'''(x)$ are the first, second, and third derivative of $u(x)$.

A <u>central difference approximation</u> is defined by subtracting the expansion equations (2.1) and (2.2)

$$u(x + \Delta x) - u(x - \Delta x) = 2\,\Delta x\, u'(x) + O(\Delta x^3) \tag{2.3}$$

where $O(\Delta x^3)$ represents the third and higher order terms. Then solving for $u'(x)$ assuming $O(\Delta x^3) \approx 0$ results in

$$u'(x) \approx \frac{u(x+\Delta x) - u(x-\Delta x)}{2\,\Delta x} \tag{2.4}$$

which has an error of approximation of order Δx^2. This approximation error due to dropping the higher order terms is also referred to as a <u>truncation error</u>.

A <u>forward difference</u> is defined by subtracting $u(x)$ from the expansion, Eq. (2.1) as

$$u(x+\Delta x) - u(x) = \Delta x\, u'(x) + O(\Delta x^2) \tag{2.5}$$

Solving for $u'(x)$ and assuming the second and higher order terms are negligible, $O(\Delta x^2) \approx 0$, gives

$$u'(x) \approx \frac{u(x+\Delta x) - u(x)}{\Delta x} \tag{2.6}$$

which has an error of approximation of order Δx.

The <u>backward-difference</u> approximation is defined by subtracting the expansion, Eq. 2.2 from $u(x)$,

$$u(x) - u(x-\Delta x) = \Delta x\, u'(x) + O(\Delta x^2) \tag{2.7}$$

so that solving for u'(x)

$$u'(x) \approx \frac{u(x) - u(x-\Delta x)}{\Delta x} \tag{2.8}$$

An x-t plane (Fig. 2.2) consisting of a rectangular net of discrete points is used to represent the continuous solution domain defined by the independent variable (x and t) in the Saint-Venant equations. The lines parallel to the x-axis are spaced by the time increment Δt. The discrete points in the solution domain are defined by the subscript i for the x position and the superscript j for the time line.

2.2 Explicit Methods

Explicit methods advance the solution of the Saint-Venant equations point by point along a time line until the equations have been solved at all the points along the time line, then the solution procedure goes to the next time line. The unknowns at a given location on a time line are found by extrapolating from the known hydraulic quantities in adjacent locations on the previous time line. The extrapolation follows the Saint-Venant equations and associated initial and boundary conditions. Application of explicit methods to solve the Saint Venant equation include Stoker (1953), Isaacson, et al. (1954, 1956, 1958), Amein and Fang (1969), Martin and DeFazio (1969), Ragan (1965), Liggett and Woolhiser (1967), Garrison, et al. (1969), Strelkoff (1970), and Johnson (1974).

Explicit Scheme

The finite difference representation is shown by the mesh of points on the time-distance plane shown in Fig. 2.2. Assuming that at time t, all the hydraulic quantities u for u^j_{i-1}, u^j_{i+1} are known, the problem is to determine

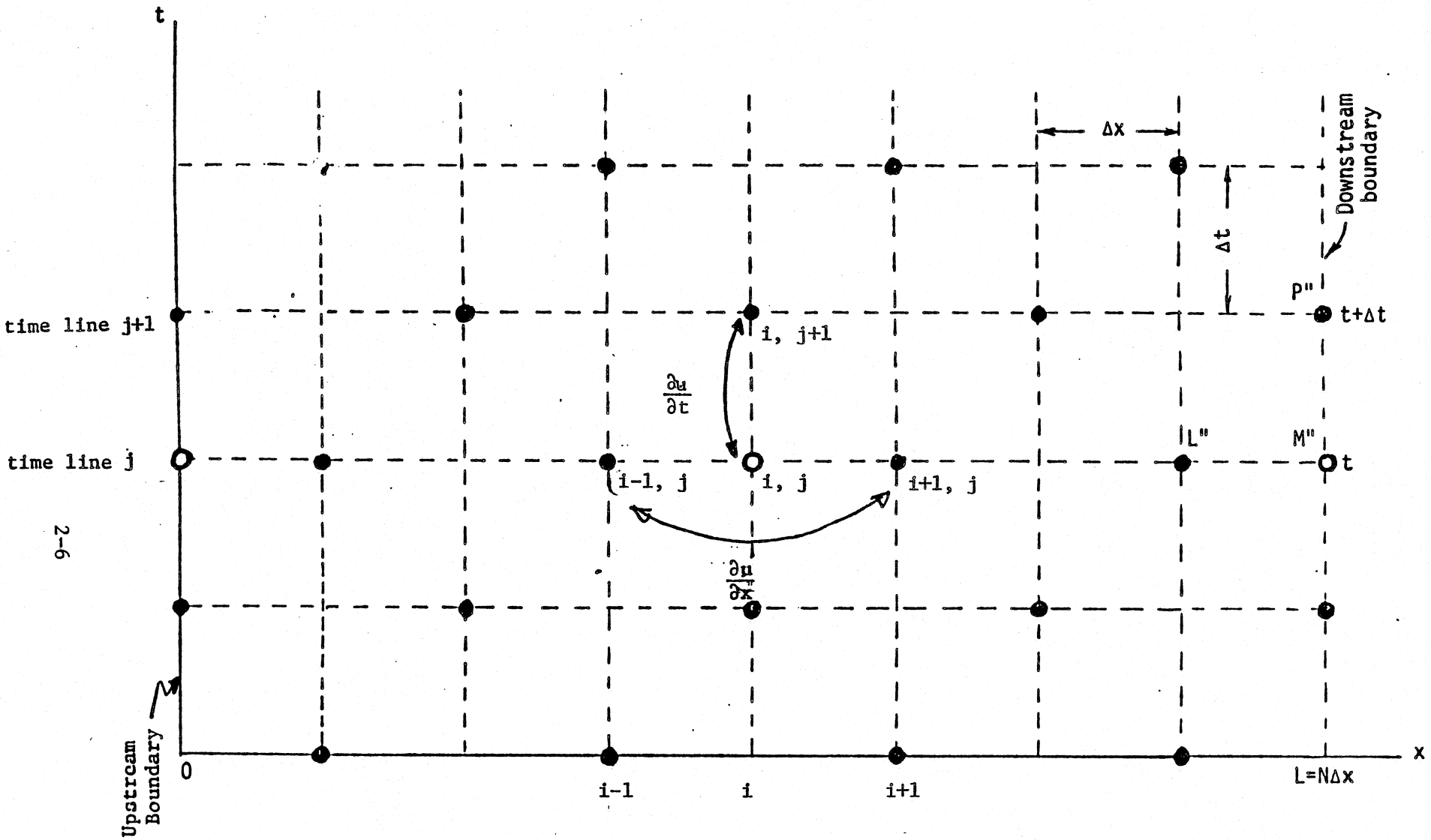

Figure 2.2. Finite-difference scheme on x-t plane for the explicit method

the unknown quantity at point (i, j+1) at time $t + \Delta t$, i.e. u_i^{j+1}. Assume then that all hydraulic quantities have been computed through time t, i.e., all quantities are known on time line j in Fig. 10.2.2. It is required to determine the quantities at time $t + \Delta t$ or on time line j+1. The partial derivatives at point (i, j+1) can be approximated in terms of the quantities at adjacent points (i-1, j), (i, j), and (i+1, j) using

$$\frac{\partial u_i^{j+1}}{\partial t} = \frac{u_i^{j+1} - u_i^j}{\Delta t} \tag{2.9}$$

$$\frac{\partial u_i^j}{\partial x} = \frac{u_{i+1}^j - u_{i-1}^j}{2\Delta x} \tag{2.10}$$

A forward difference scheme is used for the time derivative (2.9) and a central difference scheme is used for the spatial derivative (2.10).

The discretization of the finite difference grid of time and space in the integration of the finite-difference equations introduces numerical errors in the computations. A finite difference scheme is stable if such errors are not amplified during successive computations. Their numerical stability of the computations depends on the relative grid size. The necessary but insufficient condition for stability is given by the Courant condition (Courant and Friedrichs, 1948)

$$\Delta t \leq \frac{\Delta x_i}{V + \sqrt{gD_i}} \tag{2.11}$$

where $\sqrt{gD}$ is the wave velocity, D is the hydraulic depth. The Courant condition requires that the time step be less than the time for a water particle to travel the distance Δx_i. If the Δt is chosen such that the Courant condition is not satisfied, then the time interval is too large such that in effect there would be an accumulation or piling up of water.

The Courant condition implies that the time step Δt must be chosen such that point (i, j+1) lies within the area bounded by the characteristics from points (i-1, j) and (i+1, j). For computational purposes Δx is usually specified and kept fixed throughout the computations whereas Δt is determined at each time step. Essentially Δt_i is computed at each grid point i on time line j and the smallest Δt_i is used. Because the explicit method is unstable unless Δt is small, it is sometimes advisable to determine the minimum Δt_i at a time line j then reduce the min Δt_i by some percentage. The Courant condition does not guarantee stability, and therefore, is only a guideline.

2.3 Initial and Boundary Conditions

Initial conditions define values of the dependent variables for values of the independent x at the initial time line for t = 0 on the x-t plane. The initial condition then defines the state of the flow within the channel or river prior to passage of a flood wave. The initial values of independent variables (x and t) and the dependent variables (e.g. V and y or Q and h) are required for grid points IC_1, IC_2, . . . , IC_N in Fig. 2.3 The initial condition could be defined assuming uniform flow throughout the river or channel or could be determined by backwater computations for a known water surface elevation or discharge.

Boundary conditions are used to introduce the unsteady disturbance, such as a flood wave or tidal flows, into the channel or river system. Boundary conditions define the known relationships that exist between the independent variables x and t and the unknown dependent variables at the upstream and downstream ends of the channel or river. The boundary conditions are independent of the Saint-Venant equations. Also, the boundary conditions must be valid throughout the time of a flood passage. The upstream boundary conditions refer to the grid points UBC_1, UBC_2, . . . , UBC_4 in Fig. 2.3 and the downstream boundary condition refers to the grid points DBC_1, DBC_2, ...

The upstream boundary condition (i = 1) can be specified as either a known stage hydrograph,

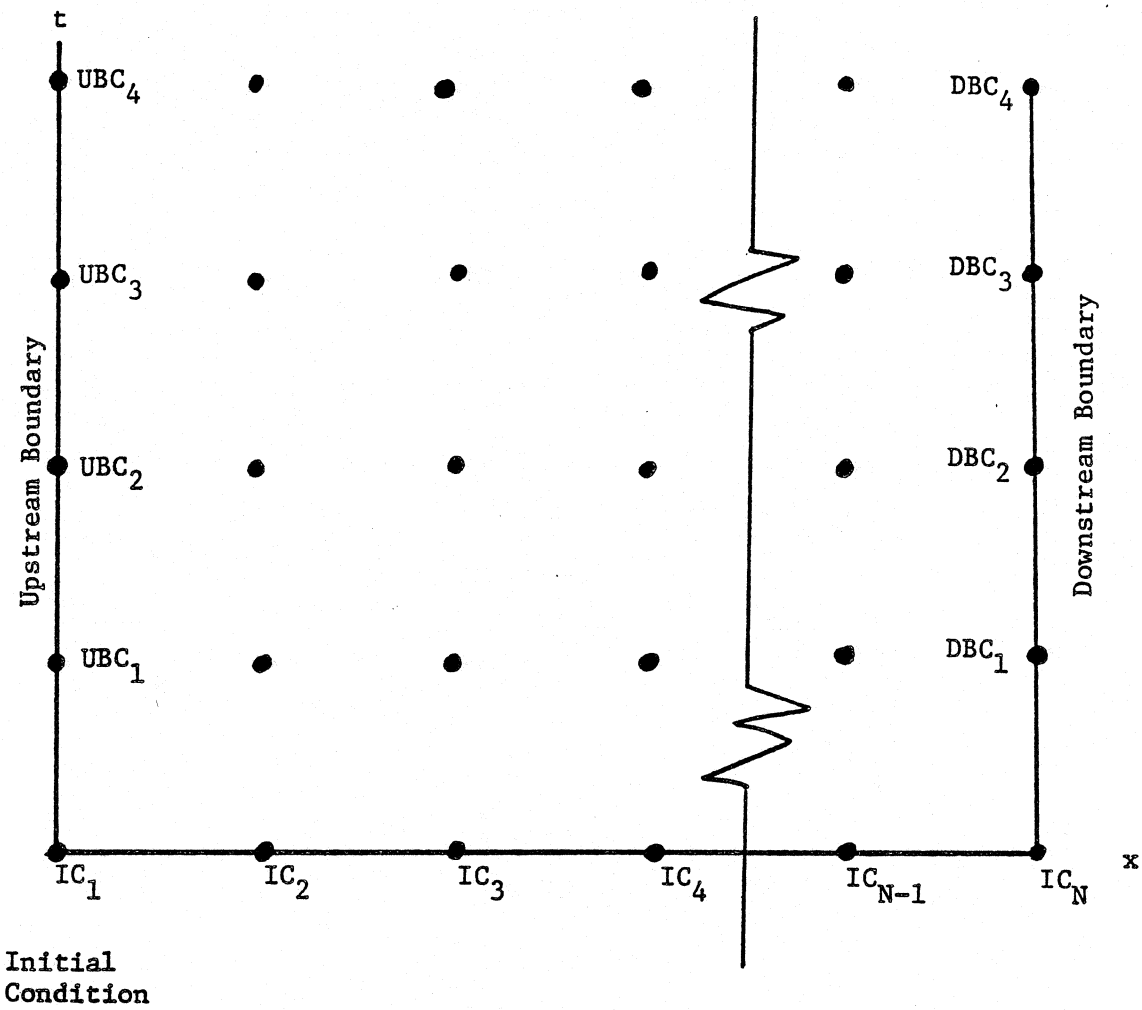

Figure 2.3 Initial and Boundary Conditions

$$h_1^{j+1} = h(t^{j+1}) \tag{2.12}$$

as a known discharge hydrograph,

$$Q_1^{j+1} = Q(t^{j+1}) \tag{2.13}$$

where h (t^{j+1}) is the known water surface elevation and Q (t^{j+1}) is the known discharge at the upstream boundary at time t^{j+1}.

It should be emphasized once again that the kinematic wave model cannot describe downstream disturbances that propagate upstream, therefore downstream boundary conditions are not considered in kinematic wave schemes. However, downstream boundary conditions will be briefly described for later use with the dynamic wave models. The downstream boundary condition (i=N) can be in the form of a known stage hydrograph, a known discharge hydrograph, or a known relationship between stage and discharge such as a rating curve. The stage-discharge relation can be expressed as

$$Q_N^{j+1} = f(h_N^{j+1}) \tag{2.14}$$

For forecasting and simulation, the upstream boundary is either a stage or discharge hydrograph while the downstream boundary is usually a stage-discharge curve.

The stage-discharge relation could be a unique function, i.e., a single value rating curve expressed in tabular form using linear interpolation for intermediate values. A loop rating curve (Fig. 1.7) could also be used which expresses the relation between stage and discharge also as a function of the friction slope S_f (Fread, 1973c, 1975a). The loop rating curve could be expressed as

$$Q_N^{j+1} = 1.486 \left(\frac{AR^{2/3}}{n}\right)_N^{j+1} \left(\frac{h_{N-1}^{j+1} - h_N^{j+1}}{\Delta x_{N-1}}\right)^{1/2} \tag{2.15}$$

SECTION 3.0

DYNAMIC WAVE MODEL USING IMPLICIT METHOD

3.0 DYNAMIC WAVE MODEL USING IMPLICIT METHOD

Implicit Method

Implicit finite difference methods usually advance the solution of the Saint-Venant equation from one time line to the next simultaneously for all points along the time line. A system of algebraic equations is generated from the Saint-Venant equation applied simultaneously to all the N net points along the x-axis. The implicit methods were developed because of the limitation on the time step size required for numerical stability of the explicit methods. Applications of implicit methods to solve the Saint-Venant equations include

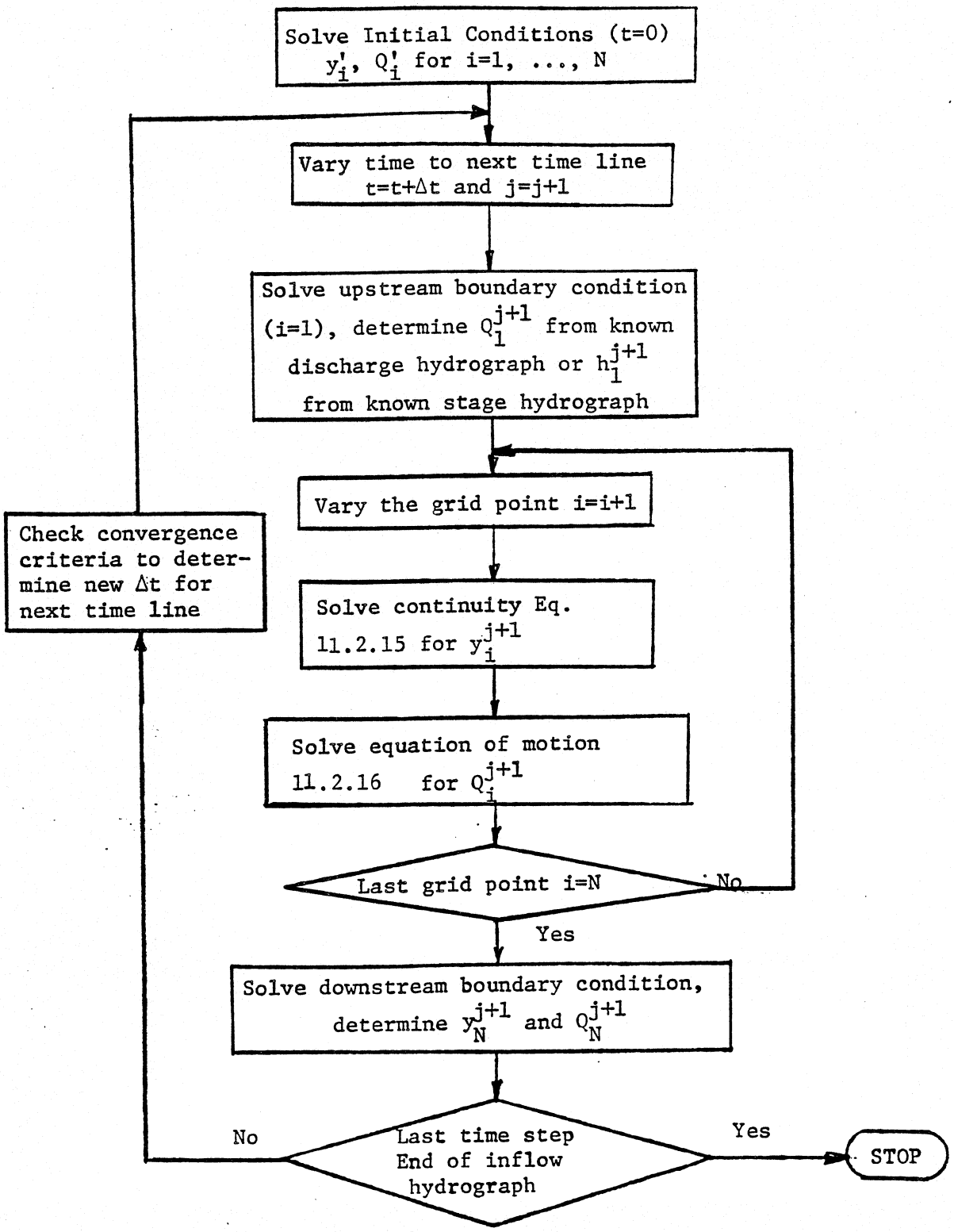

Figure 3.1 Flowchart for Solving Saint Venant Equations Using Explicit Method

Preissmann (1961); Preissman and Cunge (1961); Vasiliev, et al. (1965); Isaacson (1966); Abbott and Ionescu (1967); Amein (1968); Baltzer and Lai (1968); Dronkers (1969); Amein and Fang (1970); Gunavatnam and Perkins (1970); Kamphuis (1970); Contractor and Wiggert (1972); Quinn and Wylie (1972); Fread (1973b, c); Chen (1973); Chaudhury and Contractor (1973); SOGREAH (1973); Fread (1974a, b); Price (1974); Greco and Panattoni (1975); Amein (1975); Amein and Chu (1975); Chen and Simons (1975); Fread (1975 b); Wood, et al. (1975); Fread (1976a, b); Kanda and Kitada (1977); Ponce, et al. (1978b); Price (1980); Hoff-Claussen, et al. (1981); and Sojoberg (1981).

The four point weighted implicit finite difference scheme considers the spatial derivates and non-derivative terms positioned between adjacent time lines at a point M using the weights θ and (1-θ), as shown in Fig. B.2. The time derivatives are approximated by

$$\frac{\partial u}{\partial t} \approx \frac{u_i^{j+1} + u_{i+1}^{j+1} - u_i^j - u_{i+1}^j}{2\,\Delta t} \tag{3.1}$$

and the spatial derivatives and non-derivative terms are positioned between adjacent time lines according to the weights θ and (1-θ) by the following approximations:

$$\frac{\partial u}{\partial x} \approx \frac{\theta(u_{i+1}^{j+1} - u_i^{j+1})}{\Delta x} + (1-\theta)\,\frac{(u_{i+1}^j - u_i^j)}{\Delta x} \tag{3.2}$$

$$\overline{u} = \frac{\theta(u_i^{j+1} + u_{i+1}^{j+1})}{2} + (1-\theta)\,\frac{(u_i^j + u_{i+1}^j)}{2} \tag{3.3}$$

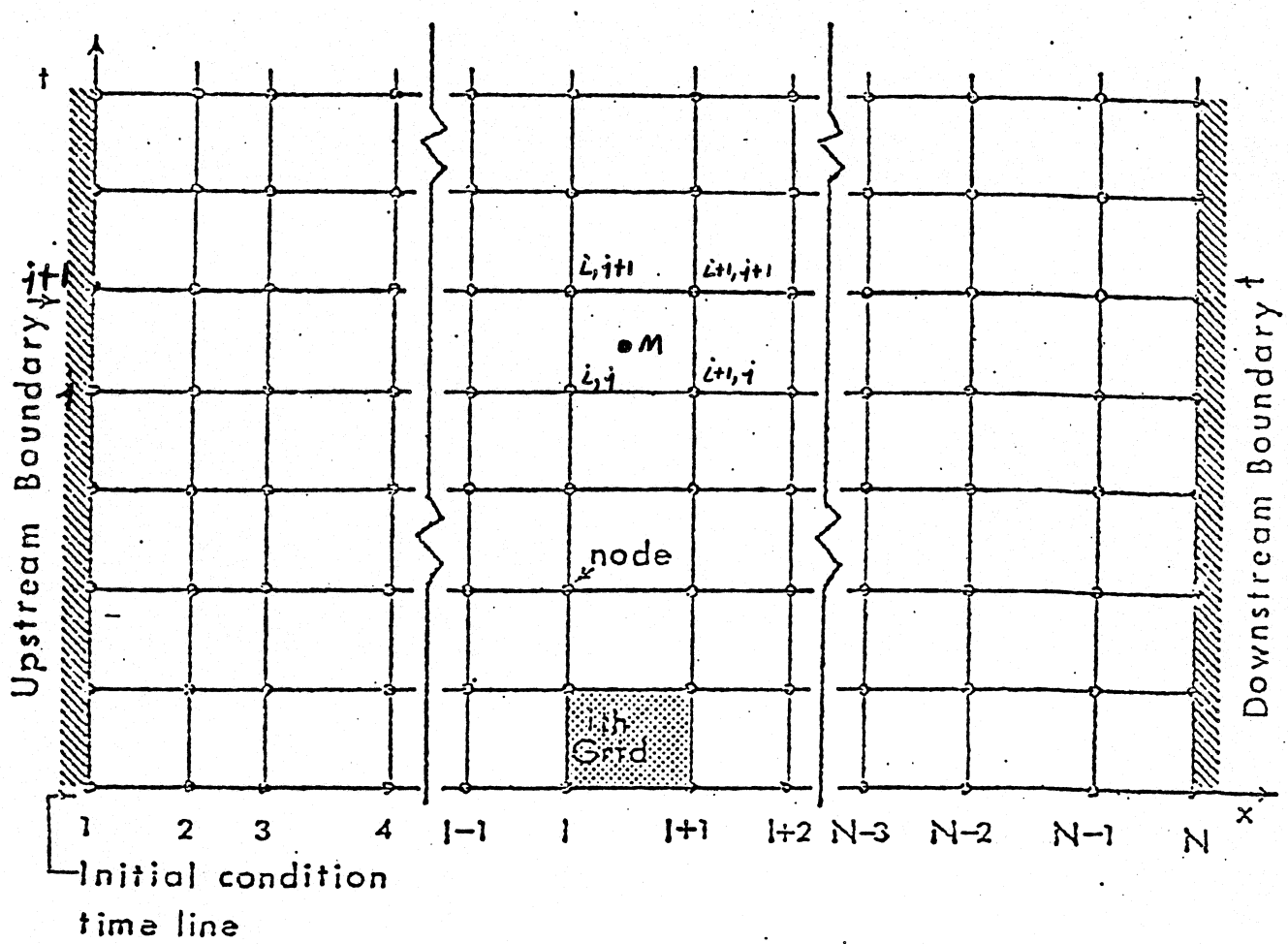

Figure 3.2 x-t Solution Plane (Fread, 1974a)

Weighted 4-Pt. Implicit Scheme

Time Derivative :

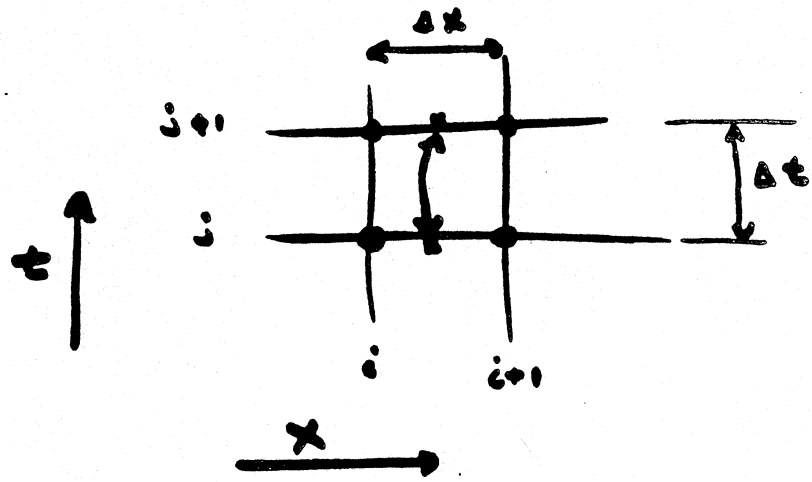

$$\frac{\partial Q}{\partial t} \simeq \frac{\dfrac{Q_i^{j+1} + Q_{i+1}^{j+1}}{2} - \dfrac{Q_i^{j} + Q_{i+1}^{j}}{2}}{\Delta t}$$

Spatial Derivative :

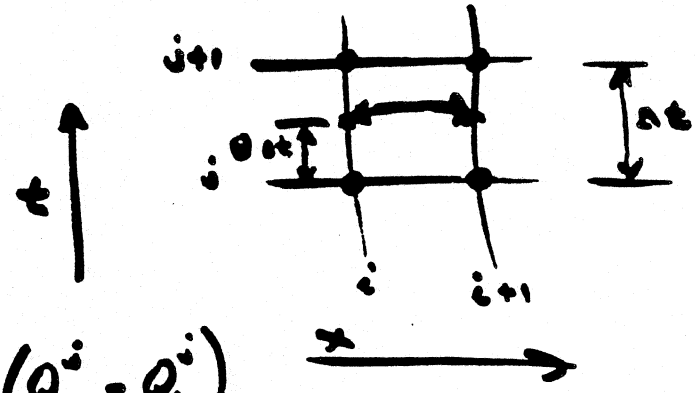

$$\frac{\partial Q}{\partial x} \simeq \theta\frac{\left(Q_{i+1}^{j+1} - Q_i^{j+1}\right)}{\Delta x} + (1-\theta)\frac{\left(Q_{i+1}^{j} - Q_i^{j}\right)}{\Delta x}$$

Other terms: $q = \theta\, q_i^{j+1} + (1-\theta)\, q_i^{j}$

A major difference between the explicit and implicit methods is that implicit methods are conditionally stable for all time steps whereas the explicit methods are numerically stable only for two time steps less than a critical value determined by the Courant condition or the friction criteria, described in the previous section. Another major difference is that the implicit method is considerably computationally more complex (Fread, 1976). Fread (1974a) has shown that the weighted four-point scheme is unconditionally linearly stable for any time step if $0.5 \leq \theta \leq 1.0$. This scheme has a second-order accuracy when $\theta = 0.5$ and a first order accuracy when $\theta = 1.0$.

3.1 Finite Difference Equation for Implicit Method

The conservation form of the Saint-Venant equation is used because this form provides the versatility required to simulate a wide range of flows from gradual long-duration flood waves in rivers to abrupt waves similar to those caused by dam breaks (Fread, 1976). Conservation forms of the Saint-Venant equations are expressed as

dead storage over bank area

$$\frac{\partial Q}{\partial x} + \frac{\partial (A + A_o)}{\partial t} - q = 0 \tag{3.4}$$

eddy losses lateral inflow wind

$$\frac{\partial Q}{\partial t} + \frac{\partial (\beta Q^2/A)}{\partial x} + gA\left(\frac{\partial h}{\partial x} + S_f + S_e\right) - \beta q v_x + W_f B = 0 \tag{3.5}$$

where the terms are defined as: x = longitudinal distance along the channel or river; t = time; A = cross sectional area of flow; A_o = off channel dead storage; q = lateral inflow or outflow per unit length along the channel; h = water surface elevation; v_x = velocity of lateral flow in the direction of the channel flows; S_f = friction slope; S_e = eddy loss slope; B = top width of the channel at the water surface; W_f = wind resistance effect; β = momentum correction factor; and g = acceleration due to gravity.

The weighted four-point finite difference approximations previously given by Eqs. (3.1) and (3.2) are used to derive the dynamic routing model. These approximations are

$$\frac{\partial Q}{\partial x} = \theta\left(\frac{Q_{i+1}^{j+1} - Q_i^{j+1}}{\Delta x_i}\right) + (1-\theta)\left(\frac{Q_{i+1}^{j} - Q_i^{j}}{\Delta x_i}\right) \tag{3.6}$$

$$\frac{\partial h}{\partial x} = \theta\left(\frac{h_{i+1}^{j+1} - h_i^{j+1}}{\Delta x_i}\right) + (1-\theta)\left(\frac{h_{i+1}^{j} - h_i^{j}}{\Delta x_i}\right) \tag{3.7}$$

$$\frac{\partial (A+A_o)}{\partial t} = \frac{(A+A_o)_i^{j+1} + (A+A_o)_{i+1}^{j+1} - (A+A_o)_i^{j} - (A+A_o)_{i+1}^{j}}{2\Delta t_j} \tag{3.8}$$

$$\frac{\partial Q}{\partial t} = \frac{Q_i^{j+1} + Q_{i+1}^{j+1} - Q_i^{j} - Q_{i+1}^{j}}{2\Delta t_j} \tag{3.9}$$

The spatial derivatives, $\frac{\partial Q}{\partial x}$ and $\frac{\partial h}{\partial x}$, are positioned between adjacent time lines according to the weighting factors θ and $(1-\theta)$. The non-derivative

terms, such as q, A, etc. are also positioned between adjacent time lines using the weighting factors, such as

$$q = \theta\left(\frac{q_{i+1}^{j+1} + q_i^{j+1}}{2}\right) + (1-\theta)\left(\frac{q_i^j + q_{i+1}^j}{2}\right) \tag{3.10}$$

$$A = \theta\left(\frac{A_{i+1}^{j+1} + A_i^{j+1}}{2}\right) + (1-\theta)\left(\frac{A_i^j + A_{i+1}^j}{2}\right) \tag{3.11}$$

The difference equation for the conservation form of the continuity equation (3.4) is determined by substituting the finite difference approximations, Eqs. (2.6), (3.8), and (3.10) into Eq. (3.4), i.e.,

$$\theta\left[\frac{(Q_{i+1}^{j+1} - Q_i^{j+1})}{\Delta x_i} - q_i^{j+1}\right] + (1-\theta)\left[\frac{(Q_{i+1}^j - Q_i^j)}{\Delta x_i} - q_i^j\right] + \frac{(A+A_o)_i^{j+1} + (A+A_o)_{i+1}^{j+1} - (A+A_o)_i^j - (A+A_o)_{i+1}^j}{2\Delta t_j} = 0 \tag{3.12}$$

In a similar manner, the difference equation for the conservation form of the momentum equation is

$$\frac{(Q_i^{j+1} + Q_{i+1}^{j+1} - Q_i^j - Q_{i+1}^j)}{2\Delta t_j} + \theta\left\{\frac{(\beta Q^2/A)_{i+1}^{j+1} - (\beta Q^2/A)_i^{j+1}}{\Delta x_i} + g\bar{A}_i^{j+1}\left[\frac{(h_{i+1}^{j+1} - h_i^{j+1})}{\Delta x_i} + \bar{S}_{f_i}^{j+1} + \bar{S}_{e_i}^{j+1}\right] - (\overline{\beta q v_x})_i^{j+1} + (\bar{W}_f\bar{B})_i^{j+1}\right\}$$
$$+ (1-\theta)\left\{\frac{(\beta Q^2/A)_{i+1}^j - (\beta Q^2/A)_i^j}{\Delta x_i} + g\bar{A}_i^j\left[\frac{(h_{i+1}^j - h_i^j)}{\Delta x_i} + \bar{S}_{f_i}^j + \bar{S}_{e_i}^j\right] - (\overline{\beta q v_x})_i^j + (\bar{W}_f\bar{B})_i^j\right\} = 0 \tag{3.13}$$

The four-point finite difference equation for the continuity equation can be further modified by multiplying Eq. (3.12) by Δx_i to obtain

$$\theta \left[Q_{i+1}^{j+1} - Q_i^{j+1} - \bar{q}_i^{j+1} \Delta x_i \right] + \left[(1-\theta) \; Q_{i+1}^{j} - Q_i^{j} - \bar{q}_i^{j} \; \Delta x_i \right]$$

$$+ \left(\frac{\Delta x_i}{2\Delta t_j}\right) \left[(A+A_o)_i^{j+1} + (A+A_o)_{i+1}^{j+1} - (A+A_o)_i^{j} - (A+A_o)_{i+1}^{j} \right] = 0 \qquad (3.14)$$

Similarly the equation of motion can be modified by multiplying Eq. (3.13) by Δx_i to obtain

$$\left(\frac{\Delta x_i}{2\Delta t_j}\right) \left(Q_i^{j+1} + Q_{i+1}^{j+1} - Q_i^{j} - Q_{i+1}^{j}\right) + \theta \left[(\beta Q^2/A)_{i+1}^{j+1} - (\beta Q^2/A)_i^{j+1} \right]$$

$$+ g\bar{A}_i^{j+1} \left[h_{i+1}^{j+1} - h_i^{j+1} + \bar{S}_{f_i}^{j+1} \Delta x_i + \bar{S}_{e_i}^{j+1} \Delta x_i \right]$$

$$- \overline{(\beta q v_x)}_i^{j+1} \Delta x_i + (\bar{W}_f \bar{B})_i^{j+1} \Delta x_i + (1-\theta) \left[(\beta Q^2/A)_{i+1}^{j} \right]$$

$$- (\beta Q^2/A)_i^{j} + g\bar{A}_i^{j} \left[h_{i+1}^{j} - h_i^{j} + \bar{S}_{f_i}^{j} \Delta x_i + \bar{S}_{e_i}^{j} \Delta x_i \right]$$

$$- \overline{(\beta q v_x)}_i^{j} \Delta x_i + (\bar{W}_f \bar{B})_i^{j} \Delta x_i = 0 \qquad (3.15)$$

where the average values (with $^{-}$) over a reach are defined as

$$\bar{\beta}_i = \frac{\beta_i + \beta_{i+1}}{2} \tag{3.16}$$

$$\bar{A}_i = \frac{A_i + A_{i+1}}{2} \tag{3.17}$$

$$\bar{B}_i = \frac{B_i + B_{i+1}}{2} \tag{3.18}$$

$$\bar{S}_{f_i} = \frac{\bar{n}_i^2 \, |\bar{Q}_i| \, \bar{Q}_i}{2.208 \, \bar{A}_i^2 \, \bar{R}_i^{4/3}} \tag{3.19}$$

$$\bar{Q}_i = \frac{Q_i + Q_{i+1}}{2} \tag{3.20}$$

$$\bar{R}_i = \bar{A}_i / \bar{B}_i \tag{3.21}$$

$$\bar{S}_{e_i} = \frac{K_{e_i}}{2g\Delta x_i} \left[\left(\frac{Q}{A}\right)^2_{i+1} - \left(\frac{Q}{A}\right)^2_i \right] \tag{3.22}$$

$$\bar{W}_{f_i} = C_{w_i} \, (\cos \omega)^2 \, |\bar{V}_{r_i}| \, \bar{V}_{r_i} \tag{3.23}$$

$$\bar{V}_{r_i} = \pm \bar{V}_{w_i} + \bar{Q}_i / \bar{A}_i \tag{3.24}$$

The terms having superscript j are known from either (1) initial conditions or (2) a solution of the Saint-Venant equation for a previous time line. The terms g, Δx_i $\bar{\beta}_i$, K_{e_i}, C_{w_i}, and V_{w_i} are known and must be specified independent of the solution. The unknown terms are Q_i^{j+1}, Q_{i+1}^{j+1} h_i^{j+1}, h_{i+1}^{j+1}, A_i^{j+1}, A_{i+1}^{j+1}, B_i^{j+1}, B_{i+1}^{j+1}, and h_i^{j+1}. However, all the terms can be expressed as functions of the unknowns, Q_i^{j+1}, Q_{i+1}^{j+1}, h_i^{j+1}, h_{i+1}^{j+1}, so that there are actually only four unknowns. The unknowns are raised to powers other than unity so that Eqs. (3.14) and (3.15) are nonlinear.

The continuity equation (3.14) and the momentum equation (3.15) are considered at each of the (N-1) rectangular grids shown in Fig. 3.1 between the upstream boundary at i=1 and the downstream boundary at i = N. There are four unknowns in Eqs. (3.14) and (3.15), so that a system of (2N-2) nonlinear equations with 2N unknown is obtained. An upstream boundary condition and a downstream boundary condition provide two additional equations so that the system of nonlinear equations is determinate.

The upstream boundary condition (i=1) can be specified as either a known stage hydrograph or a known discharge hydrograph, or a known relationship between stage and discharge such as a rating curve.

2.3).

3.2 Solution Method for System of Finite Difference Equations

The following discussion for the solution of a system of finite difference equations follows that of Fread (1976). The system of nonlinear finite difference equations can be expressed in functional form in terms of the unknown and Q at time level j+1 expressed as

$$
\begin{aligned}
&B_1(h_1, Q_1) = 0 && \text{upstream boundary condition} \\
&C_1(h_1, Q_1, h_2, Q_2) = 0 && \text{continuity for grid 1} \\
&M_1(h_1, Q_1, h_2, Q_2) = 0 && \text{momentum for grid 1} \\
&\quad\vdots \\
&C_i\ (h_i, Q_i, h_{i+1}, Q_{i+1}) = 0 && \text{continuity for grid i} \qquad 3.25) \\
&M_i(h_i, Q_i, h_{i+1}, Q_{i+1}) = 0 && \text{momentum for grid i} \\
&\quad\vdots \\
&C_{N-1}(h_{N-1}, Q_{N-1}, h_N, Q_N) = 0 && \text{continuity eq. for grid N-1} \\
&M_{N-1}(h_{N-1}, Q_{N-1}, h_N, Q_N) = 0 && \text{momentum for grid N-1} \\
&B_N(h_N, Q_N) = 0 && \text{downstream boundary condition}
\end{aligned}
$$

This system of 2N nonlinear equations with 2N unknowns is solved for each time step by applying the Newton-Raphson method. The computational procedure for each time t+1 starts by assigning trial values to the 2N unknowns at time t+1. These trial values of Q and h can be the known values at time t, from either the intial condition if t = 1 or from the values of Q and h for the previous time step t. Using the trial values in the system of Eqs. 3.25) results in 2N residuals. For the k - th iteration these residuals can be expressed as

7 GRIDS X 2 EQUATIONS = 14 EQUATIONS + 2 BOUNDARY = 16 EQS

(7+1) NODES X 2 $\frac{\text{UNKNOWN}}{\text{NODE}}$ = 16 UNKNOWNS ← DETERMINATE

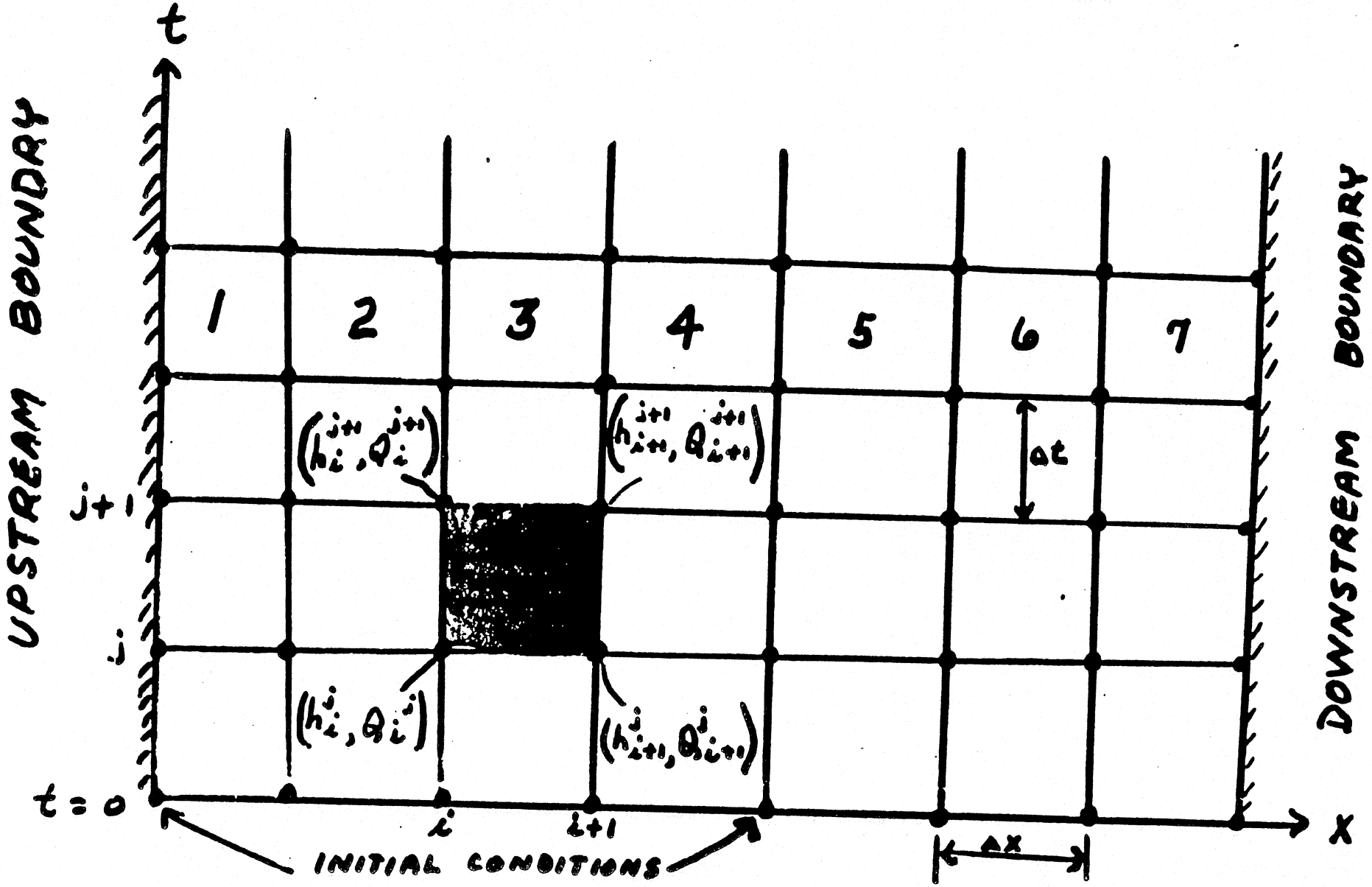

X-t SOLUTION DOMAIN

$$B_1\ (h_1^k,\ Q_1^k) = RB_1^k$$ residual for upstream boundary

$$C_1(h_1^k,\ Q_1^k,\ h_2^k,\ Q_2^k) = RC_1^k$$ residual for continuity at grid 1

$$M_1\ (h_1^k,\ Q_1^k,\ h_2^k,\ Q_2^k) = RM_1^k$$ residual for momentum at grid 1

$$\vdots$$

$$C_i\ (h_i^k,\ Q_i^k,\ h_{i+1}^k,\ Q_{i+1}^k) = RC_i^k$$ residual for momentum at grid i

(3.26)

$$M_i(h_i^k,\ Q_i^k,\ h_{i+1}^k,\ Q_{i+1}^k) = RM_i^k$$ residual for momentum at grid i

$$\vdots$$

$$C_{N-1}\ (h_{N-1}^k,\ Q_{N-1}^k,\ h_N^k,\ Q_N^k) = RC_{N-1}^k$$ residual for continuity at grid N-1

$$M_{N-1}\ (h_{N-1}^k,\ Q_{N-1}^k,\ h_N^k,\ Q_N^k) = RM_{N-1}^k$$ residual for momentum at grid N-1

$$B_N\ (h_N^k,\ Q_N^k) = RB_N^k$$ residual for downstream boundary

where the residuals for the k-th iteration are RB_1^k, RC_1^k, RM_1^k . . ., RC_{N-1}^k, RM_{N-1}^k and RB_N^K. The basic idea of solving the system of equations is to find values of the unknown Q and h so that the residuals are forced to zero or very close to zero.

The system of equations are solved by the Newton-Rhapson method for solving a system of nonlinear algebraic equations simultaneously by a functional iterative technique. Now consider the system of equations (3.26)

denoted in vector form as

$$f(\bar{x}) = 0 \tag{3.27}$$

where $\bar{x} = (Q_1, h_1, Q_2, h_2, \ldots Q_N, h_N)$ and for iteration k, $\bar{x}^k = (Q_1^k, h_1^k, Q_2^k, h_2^k, \ldots, Q_N^k, H_N^k)$. The nonlinear system can be linearized to

$$f(\bar{x}^{k+1}) \simeq f(\bar{x}^k) + J(\bar{x}^k) \; (\bar{x}^{k+1} - \bar{x}^k) \tag{3.28}$$

where $J(\bar{x}^k)$ is the Jacobian which is a coefficient matrix made up of the first partial derivatives evaluated at $\bar{x}^k$. The right-hand side of Eq. 3.28) is the linear vector function of $\bar{x}^k$. Basically, an iterative procedure is used to force $f(\bar{x})$ to zero which is then the solution of Eq. (3.25). This can be accomplished by setting $f(\bar{x}^{k+1}) = 0$ rearranging (3.28) to

partial terms

(dQ's, dh's)

residuals

$$J(\bar{x}^k) \; (\underbrace{\bar{x}^{k+1} - x^k}_{\Delta\bar{x}^k}) = - f(\bar{x}^k) \tag{3.29}$$

and solving for $(\bar{x}^{k+1} - x^k) = \Delta\bar{x}^k$ which is the correction vector. Then the improved estimate of the solution vector $\bar{x}^{k+1}$ can be determined from knowing $\Delta\bar{x}^k$. The process is repeated until $(\bar{x}^{k+1} - \bar{x}^k)$ is less than some specified tolerance, at which time the iteration process has converged.

The system of linear equations represented by (3.29) consists of $J(\bar{x}^k)$ which is the partial derivative of the system of Eqs. (3.2) and $-f(\bar{x}^k)$ are the residuals defined in (3.26). The system of equations (3.29) for solving (3.14) are the following.

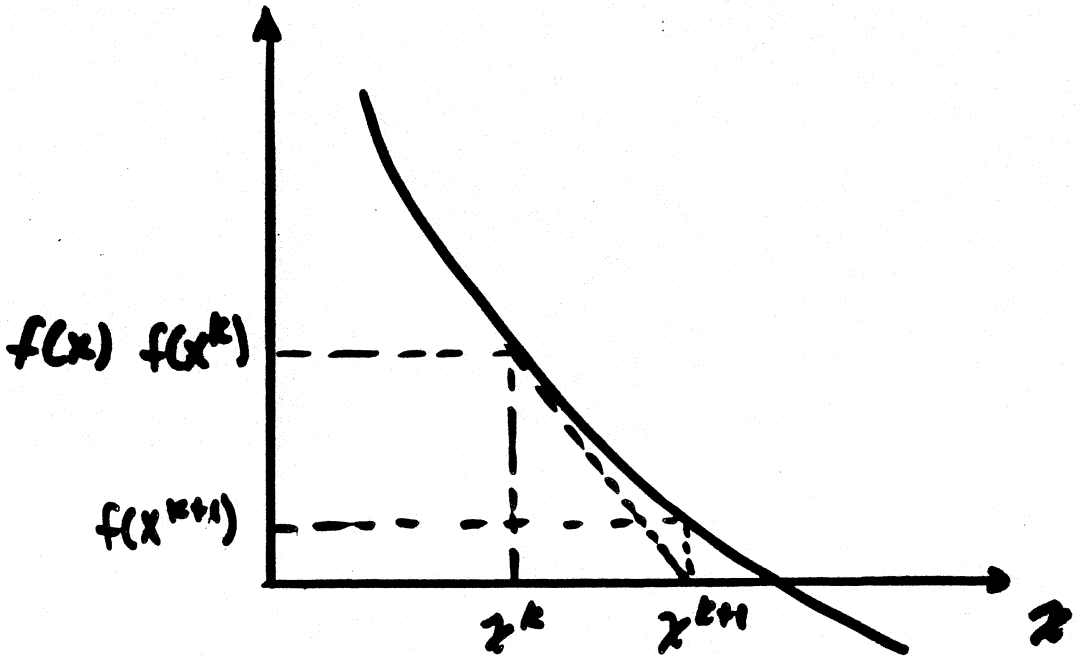

$$\frac{df}{dx} = f'(x) = \frac{f(x^{k+1}) - f(x^k)}{x^{k+1} - x^k}$$

TAYLOR EXPANSION — $f(x^{k+1}) = f(x^k) + f'(x)\left(x^{k+1} - x^k\right)$

Attempting to force $f(x^{k+1}) \to 0$

$$0 \approx f(x^k) + f'(x)\left(x^{k+1} - x^k\right)$$

Now consider a system of nonlinear equations $f(\bar{x}) = 0$

where $\bar{x} = (Q_1, h_1, Q_2, h_2, \ldots, Q_N, h_N)$

For iteration k

$$\bar{x}^k = (Q_1^k, h_1^k, Q_2^k, h_2^k, \ldots, Q_N^k, h_N^k)$$

$$
\begin{aligned}
&\frac{\partial B_1}{\partial h_1} dh_1 + \frac{\partial B_1}{\partial Q_1} dQ_1 = -RB_1^k \\
&\frac{\partial C_1}{\partial h_1} dh_1 + \frac{\partial C_1}{\partial Q_1} dQ_1 + \frac{\partial C_1}{\partial h_2} dh_2 + \frac{\partial C_1}{\partial Q_2} dQ_2 = -RC_1^k \\
&\frac{\partial M_1}{\partial h_1} dh_1 + \frac{\partial M_1}{\partial Q_1} dQ_1 + \frac{\partial M_1}{\partial h_2} dh_2 + \frac{\partial M_1}{\partial Q_2} dQ_2 = -RM_1^k \\
&\qquad\qquad\vdots \\
&\frac{\partial C_i}{\partial h_i} dh_i + \frac{\partial C_i}{\partial Q_i} dQ_i + \frac{\partial C_i}{\partial h_{i+1}} dh_{i+1} + \frac{\partial C_i}{\partial Q_{i+1}} dQ_{i+1} = -RC_i^k \\
&\frac{\partial M_i}{\partial h_i} dh_i + \frac{\partial M_i}{\partial Q_i} dQ_i + \frac{\partial M_i}{\partial h_{i+1}} dh_{i+1} + \frac{\partial M_i}{\partial Q_{i+1}} dQ_{i+1} = -RM_i^k \\
&\qquad\qquad\vdots \\
&\frac{\partial C_{N-1}}{\partial h_{N-1}} dh_{N-1} + \frac{\partial C_{N-1}}{\partial Q_{N-1}} dQ_{N-1} + \frac{\partial C_{N-1}}{\partial h_N} dh_N + \frac{\partial C_{N-1}}{\partial Q_N} dQ_N = -RC_{N-1}^k \\
&\frac{\partial M_{N-1}}{\partial h_{N-1}} dh_{N-1} + \frac{\partial M_{N-1}}{\partial Q_{N-1}} dQ_{N-1} + \frac{\partial M_{N-1}}{\partial h_N} dh_N + \frac{\partial M_{N-1}}{\partial Q_N} dQ_N = -RM_{N-1}^k \\
&\frac{\partial B_N}{\partial h_N} dh_N + \frac{\partial B_N}{\partial Q_N} dQ_N = -RB_N^k
\end{aligned}
\tag{3.30}
$$

Fread (1976) provides detailed descriptions of the partial derivatives.

Gaussian elimination or matrix inversion can be used to solve the set of equations (Conte, 1965). The coefficient matrix, the Jacobian, consisting of the partial derivatives is a sparse matrix with a band width of, at most, four elements along the main diagonal of the matrix. Fread (1971c) developed a very efficient solution technique to solve such a system of equations taking advantage of the banded (quad-diagonal) structure of the coefficient matrix.

Solving Eq. (3.30) provides values of dh_i and dQ_i. The values of the unknowns at the (k+1) - th iteration are determined using

$$h_i^{k+1} = h_i^k + dh_i \tag{3.31}$$

$$Q_i^{k+1} = Q_i^k + dQ_i \tag{3.32}$$

The flow chart in Fig. 3.2 outlines the procedure to solve the system of difference equations for one time step using the Newton-Rhapson method.

UNKNOWN VARIABLE = dependent variables = Q - dis.
= h - ws

NONLINEAR EQS ARE EXPRESSED LINEARLY

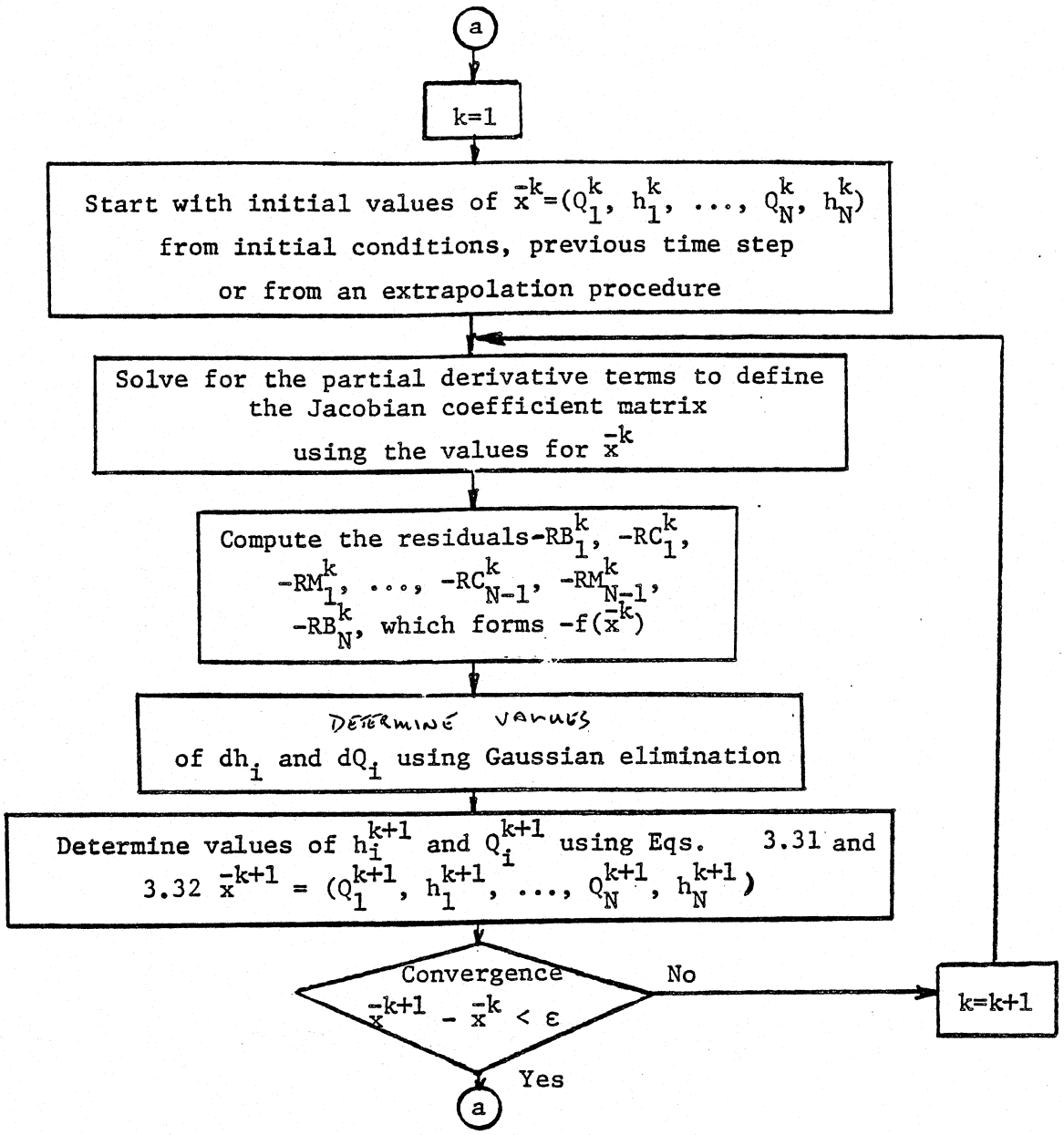

Ready to start next time step.

Figure 3.2 Procedure to Solve System of Difference Equations at One Time Step Using Newton-Rhapson Method.

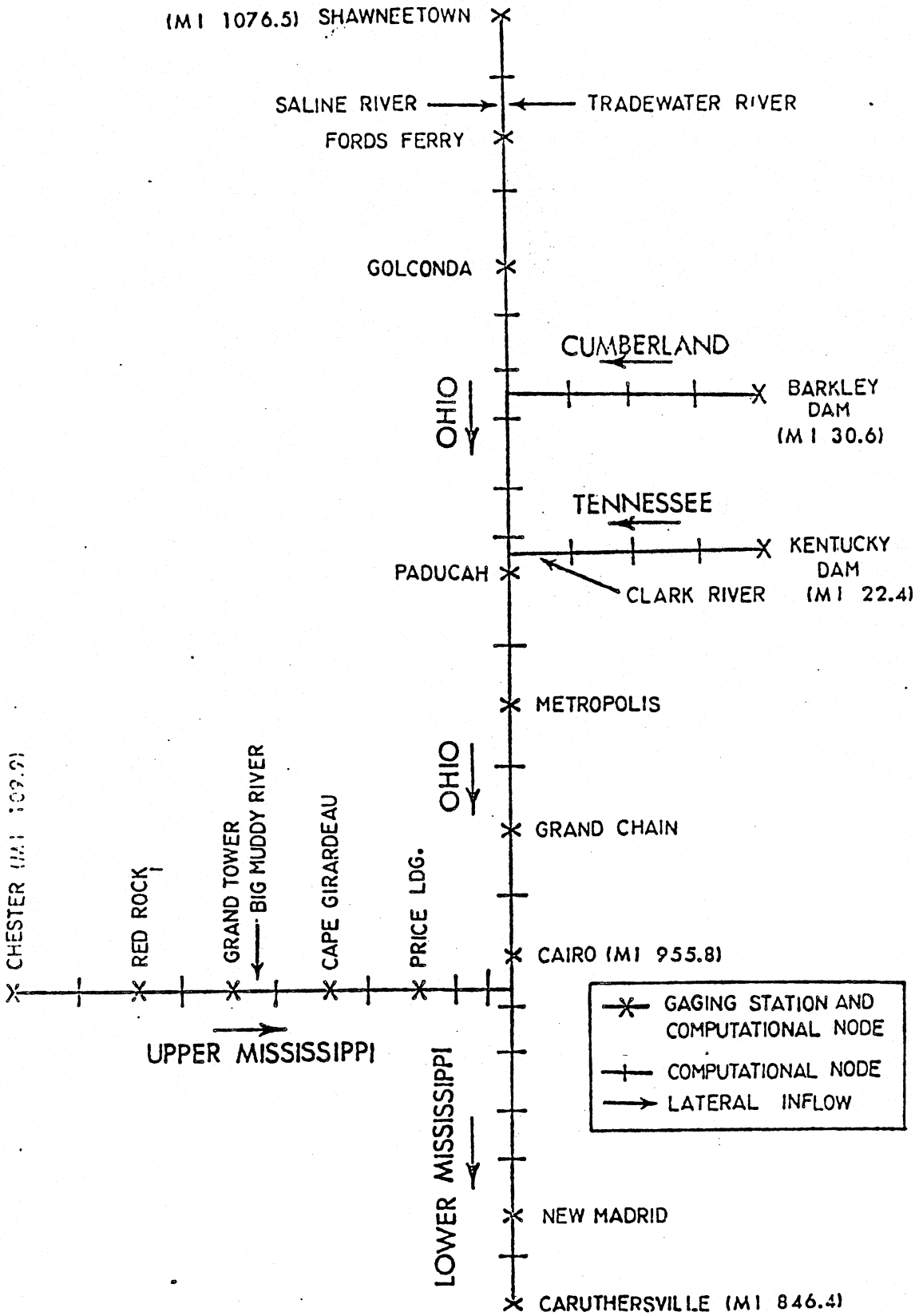

Figure 3.3 Schematic of Mississippi-Ohio-Cumberland-Tenessee (MOCT) River System (Fread, 1978)

D.L. Fread

Solution of System of Difference Equations

Upon applying the difference Equations (4.22) and (4.23) to each of the (N-1) grids shown in Fig. 4.4 and including an upstream boundary equation and a downstream boundary equation, the following system of non-linear equations (expressed in functional form) is obtained:

$$\left.\begin{array}{l}
B_1(h_1, Q_1) = 0 \\
C_1\ (h_1, Q_1, h_2, Q_2) = 0 \\
M_1\ (h_1, Q_1, h_2, Q_2) = 0 \\
\cdots\cdots\cdots\cdots\cdots\cdots \\
C_i\ (h_i, Q_i, h_{i+1}, Q_{i+1}) = 0 \\
M_i\ (h_i, Q_i, h_{i+1}, Q_{i+1}) = 0 \\
\cdots\cdots\cdots\cdots\cdots\cdots \\
C_{N-1}(h_{N-1}, Q_{N-1}, h_N, Q_N) = 0 \\
M_{N-1}(h_{N-1}, Q_{N-1}, h_N, Q_N) = 0 \\
B_N\ (h_N, Q_N) = 0
\end{array}\right\} \qquad (4.42)$$

where the B function represents the boundary conditions and the C and M functions represent respectively the Continuity Equation (4.22) and the Momentum Equation (4.23) applied to each grid. Thus, if there are N-1 grids and two boundaries, a total of 2N equations are included in Equations (4.42). The terms within the parenthesis are the unknown variables h and Q at time level j+1.

A generalized functional iterative method known as the Newton-Raphson method [Isaacson, 1966] first used by Amein and Fang [1970], can be used to obtain an efficient solution to the non-linear system. The development of the Newton-Raphson method for a general system of non-linear equations is described in Appendix B and is quite similar to the more commonly known Newton-Raphson method of solving a single non-linear equation as described in Appendix A.

The system of 2N non-linear equations with 2N unknowns is solved by applying the Newton-Raphson method. Computations are begun by assigning trial values to the 2N unknowns. Substitution of the trial values into the system of non-linear equations yields a set of 2N residuals. A residual is the value of the right-hand side of the equation after the trial value is substituted in Equations (4.42). Solutions to

Equations (4.42) are obtained when the trial values converge to the actual values. This is accomplished by adjusting the trial values until each residual vanishes or is reduced to a tolerable quantity. Convergence is also obtained when successive trial values of the discharge and stage unknowns differ by less than a quantity known as the convergence criterion, ε. Actually, the discharges $(Q_i^{j+1}, Q_{i+1}^{j+i})$ have one specified convergence criterion ε_Q and the water surface elevations $(h_i^{j+1}, h_{i+1}^{j+1})$ have another convergence criterion ε_h. The Newton-Raphson method provides the means for correcting the trial values in a series of iteration steps until the residuals are reduced to tolerable values.

If only one iteration step is performed at each Δt time step, i.e., the first approximation is corrected only once, the non-linear formulation of the finite difference approximation of the Saint-Vanant equations degenerates to the equivalent of a linear finite difference formulation such as used by Chen and Simons [1975]. The use of only one iteration (correction) is advantageous when the flow change is small over the selected routing interval (Δt), where the time step is selected by considerations of fixed data input or output intervals such as used in forecasting. When the time step can be selected independent of these considerations, the computational advantage of a linear solution procedure is negated by increasing the time step used in the non-linear solution beyond that needed in the linear solution to produce a desired accuracy.

In order to illustrate the Newton-Raphson method, let it be assumed that the computations have been carried through the k-th iteration cycle so that values of the unknowns have been approximated through the k-th cycle. It is desired to approximate the values of the 2N unknowns through the (k+1)-th cycle. Let the residuals be represented by RB_1^k, RC_1^k, RM_1^k ... RC_i^k, RM_i^k ... RC_{N-1}^k, RM_{N-1}^k, RB_N^k in which RB, RC, and RM are associated with the functions B, C, and M, respectively. The values of the residuals at the k-th iteration cycle are:

$$\left.\begin{array}{l}
B_1\ (h_1^k,\ Q_1^k) = RB_1^k \\
C_1\ (h_1^k,\ Q_1^k,\ h_2^k,\ Q_2^k) = RC_1^k \\
M_1\ (h_1^k,\ Q_1^k,\ h_2^k,\ Q_2^k) = RM_1^k \\
\cdots\cdots\cdots\cdots\cdots\cdots \\
\cdots\cdots\cdots\cdots\cdots\cdots \\
C_i\ (h_i^k,\ Q_i^k,\ h_{i+1}^k,\ Q_{i+1}^k) = RC_i^k \\
M_i\ (h_i^k,\ Q_i^k,\ h_{i+1}^k,\ Q_{i+1}^k) = RM_i^k
\end{array}\right\} \quad (4.43)$$

$$
\left.
\begin{aligned}
&\cdots\cdots\cdots\cdots\cdots\cdots\cdots\cdots\cdots\cdots \\
&C_{N-1}\,(h^k_{N-1},\ Q^k_{N-1},\ h^k_N,\ Q^k_N) = RC^k_{N-1} \\
&M_{N-1}\,(h^k_{N-1},\ Q^k_{N-1},\ h^k_N,\ Q^k_N) = RM^k_{N-1} \\
&B_N\,(h^k_N,\ Q^k_N) = RB^k_N
\end{aligned}
\right\} \quad (4.43\text{--con.})
$$

The residuals and the partial derivatives of the system of Equations (4.42) are related according to the Newton-Raphson algorithm, developed in Appendix B, by the following:

$$
\left.
\begin{aligned}
&\frac{\partial B_1}{\partial h_1}\,dh_1 + \frac{\partial B_1}{\partial Q_1}\,dQ_1 = -RB^k_1 \\
&\frac{\partial C_1}{\partial h_1}\,dh_1 + \frac{\partial C_1}{\partial Q_1}\,dQ_1 + \frac{\partial C_1}{\partial h_2}\,dh_2 + \frac{\partial C_1}{\partial Q_2}\,dQ_2 = -RC^k_1 \\
&\frac{\partial M_1}{\partial h_1}\,dh_1 + \frac{\partial M_1}{\partial Q_1}\,dQ_1 + \frac{\partial M_1}{\partial h_2}\,dh_2 + \frac{\partial M_1}{\partial Q_2}\,dQ_2 = -RM^k_1 \\
&\cdots\cdots\cdots\cdots\cdots\cdots\cdots\cdots\cdots\cdots\cdots\cdots \\
&\frac{\partial C_i}{\partial h_i}\,dh_i + \frac{\partial C_i}{\partial Q_i}\,dQ_i + \frac{\partial C_i}{\partial h_{i+1}}\,dh_{i+1} + \frac{\partial C_i}{\partial Q_{i+1}}\,dQ_{i+1} = -RC^k_i \\
&\frac{\partial M_i}{\partial h_i}\,dh_i + \frac{\partial M_i}{\partial Q_i}\,dQ_i + \frac{\partial M_i}{\partial h_{i+1}}\,dh_{i+1} + \frac{\partial M_i}{\partial Q_{i+1}}\,dQ_{i+1} = -RM^k_i \\
&\cdots\cdots\cdots\cdots\cdots\cdots\cdots\cdots\cdots\cdots\cdots\cdots\cdots\cdots \\
&\frac{\partial C_{N-1}}{\partial h_{N-1}}\,dh_{N-1} + \frac{\partial C_{N-1}}{\partial Q_{N-1}}\,dQ_{N-1} + \frac{\partial C_{N-1}}{\partial h_N}\,dh_N + \frac{\partial C_{N-1}}{\partial Q_N}\,dQ_N = -RC^k_{N-1} \\
&\frac{\partial M_{N-1}}{\partial h_{N-1}}\,dh_{N-1} + \frac{\partial M_{N-1}}{\partial Q_{N-1}}\,dQ_{N-1} + \frac{\partial M_{N-1}}{\partial h_N}\,dh_N + \frac{\partial M_{N-1}}{\partial Q_N}\,dQ_N = -RM^k_{N-1} \\
&\frac{\partial B_N}{\partial h_N}\,dh_N + \frac{\partial B_N}{\partial Q_N}\,dQ_N = -RB^k_N
\end{aligned}
\right\} \quad (4.44)
$$

Equations (4.44) are a system of 2N linear equations with 2N unknowns $[(dh_i,\ dQ_i)\ i=1,N]$. Any standard method for solving a linear system of equations such as Gaussian elimination or matrix inversion can be

$M \times M$ where $M = N$ linear algebraic equations. (Quad-diagonal system)

VACOBIAN MATRIX

$$
\begin{bmatrix}
\frac{\partial B_1}{\partial h_1} & \frac{\partial B_1}{\partial Q_1} & & & & & & & & & & \\
\frac{\partial C_1}{\partial h_1} & \frac{\partial C_1}{\partial Q_1} & \frac{\partial C_1}{\partial h_2} & \frac{\partial C_1}{\partial Q_2} & & & & & & & & \\
\frac{\partial M_1}{\partial h_1} & \frac{\partial M_1}{\partial Q_1} & \frac{\partial M_1}{\partial h_2} & \frac{\partial M_1}{\partial Q_2} & & & & & & & & \\
 & & \frac{\partial C_2}{\partial h_2} & \frac{\partial C_2}{\partial Q_2} & \frac{\partial C_2}{\partial h_3} & \frac{\partial C_2}{\partial Q_3} & & & & & & \\
 & & \frac{\partial M_2}{\partial h_2} & \frac{\partial M_2}{\partial Q_2} & \frac{\partial M_2}{\partial h_3} & \frac{\partial M_2}{\partial Q_3} & & & & & & \\
 & & & & & & \ddots & & & & & \\
 & & & & & & & \frac{\partial C_{N-1}}{\partial h_{N-1}} & \frac{\partial C_{N-1}}{\partial Q_{N-1}} & \frac{\partial C_{N-1}}{\partial h_N} & \frac{\partial C_{N-1}}{\partial Q_N} & \\
 & & & & & & & \frac{\partial M_{N-1}}{\partial h_{N-1}} & \frac{\partial M_{N-1}}{\partial Q_{N-1}} & \frac{\partial M_{N-1}}{\partial h_N} & \frac{\partial M_{N-1}}{\partial Q_N} & \\
 & & & & & & & & & \frac{\partial B_N}{\partial h_N} & \frac{\partial B_N}{\partial Q_N} &
\end{bmatrix}
\times
\begin{bmatrix}
dh_1 \\ dQ_1 \\ dh_2 \\ dQ_2 \\ dh_3 \\ dQ_3 \\ \vdots \\ dh_{N-1} \\ dQ_{N-1} \\ dh_N \\ dQ_N
\end{bmatrix}
=
\begin{bmatrix}
-RB_1^k \\ -RC_1^k \\ -RM_1^k \\ -RC_2^k \\ -RM_2^k \\ 0 \\ \vdots \\ -RC_{N-1}^k \\ RM_{N-1}^k \\ -RB_N^k
\end{bmatrix}
$$

UNKNOWNS

RESIDUALS

MATRIX FORM

$$[A]\,X = R$$

$[A]$ - $n \times n$ SQUARE MATRIX (BANDED)

X - COLUMN VECTOR

R - COLUMN VECTOR

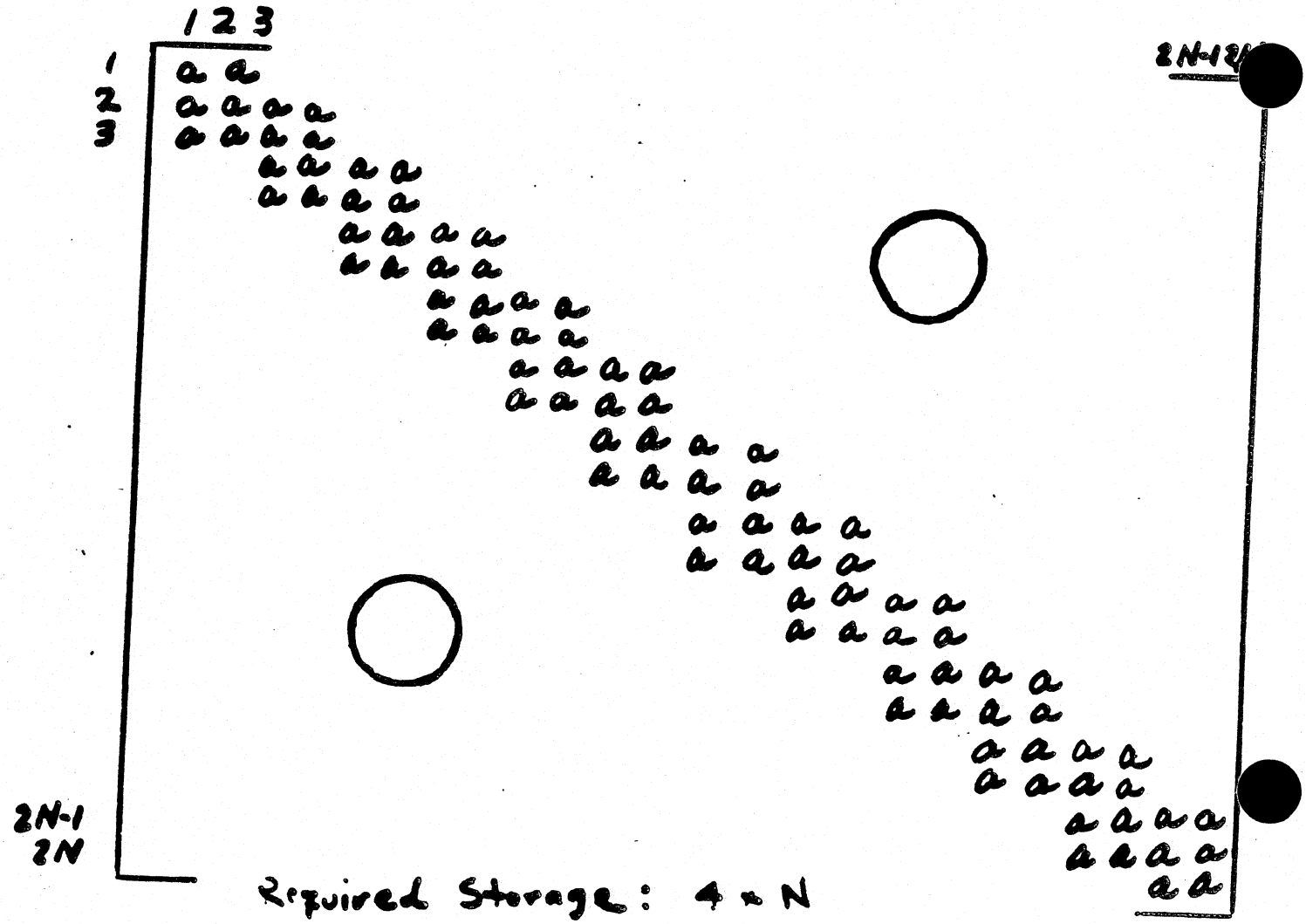

Required Storage: $4 \times N$

Required Computation: $38\,N$

used for its solution. However, since the coefficient matrix denoted as the Jacobian in Appendix B consisting of the partial derivative terms of Equations (4.44) is a sparse-matrix with a band width of at most four components along the main diagonal of the matrix, as illustrated in Appendix C, a very efficient solution technique developed by Fread [1971c] and described in Appendix C is used to minimize the required computer computation time and storage.

The solution of Equations (4.44) will provide values of dh_i and dQ_i. Then, the values of the unknowns at the (k+1)-th iteration cycle are obtained from the following relationships:

$$h_i^{k+1} = h_i^k + dh_i \tag{4.45}$$

$$Q_i^{k+1} = Q_i^k + dQ_i \tag{4.46}$$

The procedure is applied as many times as desired until the difference between values of any unknown in two consecutive iteration cycles is less than the appropriate convergence criterion, ε_h or ε_Q.

The terms in Equations (4.44) consist of three categories. The first is the unknowns $[(dh_i, dQ_i), i=1,N]$. The second is the residuals, which are noted to have a negative sign associated with them. The residuals as indicated in Equations (4.43) are determined by substituting the values of h_i^k and Q_i^k in Equations (4.42) and computing the resultant numerical value. It is evident that the residual associated with the boundary conditions given by Equations (4.33), (4.34), (4.36), or (4.37) is zero, while the residual of Equations (4.38)-(4.41) may be non-zero. The last category of terms is the partial derivatives. These are evaluated for the C_i and M_i functions according to the following expressions:

$$\frac{\partial C_i}{\partial h_i} = \frac{\Delta x_i}{2\Delta t_j} (B + B_o)_i^{j+1} \tag{4.47}$$

$$\frac{\partial C_i}{\partial Q_i} = -\Theta \tag{4.48}$$

$$\frac{\partial C_i}{\partial h_{i+1}} = \frac{\Delta x_i}{2\Delta t_j} (B + B_o)_{i+1}^{j+1} \tag{4.49}$$

$$\frac{\partial C_i}{\partial Q_{i+1}} = \Theta \tag{4.50}$$

where B_o is the top width of the off-channel dead storage cross-sectional area:

$$\frac{\partial M_i}{\partial h_i} = \Theta\left[\left(\frac{\beta Q^2 B}{A^2}\right)_i^{j+1} + g\overline{A}_i^{j+1}\left(-1 + \frac{\partial \overline{S}_f}{\partial h_i}\Delta x_i + \frac{\partial \overline{S}_e}{\partial h_i}\Delta x_i\right)\right.$$

$$\left. + \frac{gB_i^{j+1}}{2}\left(h_{i+1}^{j+1} - h_i^{j+1} + \overline{S}_{f_i}^{j+1}\Delta x_i + \overline{S}_{e_i}^{j+1}\Delta x_i\right) + \left(\frac{\overline{W}_f B}{2}\right)_i^{j+1}\Delta x_i\right] \quad (4.51)$$

$$\frac{\partial M}{\partial Q_i} = \left(\frac{\Delta x_i}{2\Delta t_j}\right) + \Theta\left[-2\left(\frac{\beta Q}{A}\right)_i^{j+1} + g\overline{A}_i^{j+1}\left(\frac{\partial \overline{S}_f}{\partial Q_i}\Delta x_i + \frac{\partial \overline{S}_e}{\partial Q_i}\Delta x_i\right)\right] \quad (4.52)$$

$$\frac{\partial M}{\partial h_{i+1}} = \Theta\left[-\left(\frac{\beta Q^2 B}{A^2}\right)_{i+1}^{j+1} + g\overline{A}_i^{j+1}\left(1 + \frac{\partial \overline{S}_f}{\partial h_{i+1}}\Delta x_i + \frac{\partial \overline{S}_e}{\partial h_{i+1}}\Delta x_i\right)\right.$$

$$\left. + \frac{gB_{i+1}^{j+1}}{2}\left(h_{i+1}^{j+1} - h_i^{j+1} + \overline{S}_{f_i}^{j+1}\Delta x_i + \overline{S}_{e_i}^{j+1}\Delta x_i\right) + \left(\frac{\overline{W}_f B}{2}\right)_i^{j+1}\Delta x_i\right] \quad (4.53)$$

$$\frac{\partial M}{\partial Q_{i+1}} = \left(\frac{\Delta x_i}{2\Delta t_j}\right) + \Theta\left[2\left(\frac{\beta Q}{A}\right)_{i+1}^{j+1} + g\overline{A}_i^{j+1}\left(\frac{\partial \overline{S}_f}{\partial Q_{i+1}}\Delta x_i + \frac{\partial \overline{S}_e}{\partial Q_i}\Delta x_i\right)\right] \quad (4.54)$$

in which:

$$\frac{\partial \overline{S}_f}{\partial h_i} = 2\overline{S}_{f_i}\left(\frac{d\overline{n}/dh_i}{\overline{n}_i} - \frac{5B_i}{6\overline{A}} + \frac{dB_i/dh_i}{3\overline{B}}\right) \quad (4.55)$$

$$\frac{\partial \overline{S}_f}{\partial h_{i+1}} = 2\overline{S}_{f_i}\left(\frac{d\overline{n}/dh_{i+1}}{\overline{n}_i} - \frac{5B_{i+1}}{6\overline{A}} + \frac{dB_{i+1}/dh_{i+1}}{3\overline{B}}\right) \quad (4.56)$$

$$\frac{\partial \overline{S}_f}{\partial Q_i} = 2\overline{S}_{f_i}\left(\frac{d\overline{n}/dQ_i}{\overline{n}_i} + \frac{1}{2\overline{Q}}\right) \quad (4.57)$$

$$\frac{\partial S_f}{\partial Q_{i+1}} = 2\overline{S}_{f_i}\left(\frac{d\overline{n}/dQ_{i+1}}{\overline{n}_i} + \frac{1}{2\overline{Q}}\right) \quad (4.58)$$

$$\frac{\partial \overline{S}_e}{\partial h_i} = \frac{2\ \overline{S}_{e_i}\ B_i\ V_i^2}{A_i\ (V_{i+1}^2 - V_i^2)} \tag{4.59}$$

$$\frac{\partial \overline{S}_e}{\partial h_{i+1}} = \frac{-2\ \overline{S}_{e_i}\ B_{i+1}\ V_{i+1}^2}{A_{i+1}\ (V_{i+1}^2 - V_i^2)} \tag{4.60}$$

$$\frac{\partial \overline{S}_e}{\partial Q_i} = \frac{-2\ \overline{S}_{e_i}\ V_i}{(V_{i+1}^2 - V_i^2)\ A_i} \tag{4.61}$$

$$\frac{\partial \overline{S}_e}{\partial Q_{i+1}} = \frac{2\ \overline{S}_{e_i}\ V_{i+1}}{(V_{i+1}^2 - V_i^2)\ A_{i+1}} \tag{4.62}$$

where:

$$dB_i/dh_i = \Delta B_i/\Delta h_i \tag{4.63}$$

$$V_i = Q_i/A_i \tag{4.64}$$

$$V_{i+1} = Q_{i+1}/A_{i+1} \tag{4.65}$$

$$d\overline{n}/dh_i = \frac{\Delta \overline{n}}{\Delta \hat{h}} \frac{d\hat{h}}{dh_i} \tag{4.66}$$

$$d\overline{n}/dQ_i = \frac{\Delta \overline{n}}{\Delta \hat{Q}} \frac{d\hat{Q}}{dQ_i} \tag{4.67}$$

$$\hat{h} = \frac{h_m + h_{m+1}}{2} \tag{4.68}$$

$$\hat{Q} = \frac{Q_m + Q_{m+1}}{2} \tag{4.69}$$

and

$$\left.\begin{aligned} d\hat{h}/dh_i &= 0 && \text{if } i \neq m \\ d\hat{h}/dh_i &= 1/2 && \text{if } i = m \end{aligned}\right\} \tag{4.70}$$

$$\left.\begin{aligned} d\hat{Q}/dQ_i &= 0 && \text{if } i \neq m \\ d\hat{Q}/dQ_i &= 1/2 && \text{if } i = m \end{aligned}\right\} \tag{4.71}$$

Whereas the i and i+1 subscripts in Equations (4.47)-(4.71) donote each node location along the routing reach, the m and m+1 subscripts donote the upstream and downstream node locations between which the Manning $\overline{n}$ relationship with stage or discharge is considered constant with respect to distance along the routing reach.

The partial derivatives for the B_1 and B_N functions are evaluated as follows:

$$\frac{\partial B_1}{\partial h_1} = 1 \tag{4.72}$$

$$\frac{\partial B_1}{\partial Q_1} = 0 \tag{4.73}$$

when the upstream boundary is a stage hydrograph, Equation (4.33), or:

$$\frac{\partial B_1}{\partial h_1} = 0 \tag{4.74}$$

$$\frac{\partial B_1}{\partial Q_1} = 1 \tag{4.75}$$

when the upstream boundary is a discharge hydrograph, Equation (4.34), and:

$$\frac{\partial B_N}{\partial h_N} = 1 \tag{4.76}$$

$$\frac{\partial B_N}{\partial Q_N} = 0 \tag{4.77}$$

when the downstream boundary is a stage hydrograph, Equation (4.36), or:

$$\frac{\partial B_N}{\partial h_N} = 0 \tag{4.78}$$

$$\frac{\partial B_N}{\partial Q_N} = 1 \tag{4.79}$$

when the downstream boundary is a discharge hydrograph, Equation (4.37), or:

$$\frac{\partial B_N}{\partial h_N} = -\frac{(Q_{k+1} - Q_k)}{(h_{k+1} - h_k)} \tag{4.80}$$

$$\frac{\partial B_N}{\partial Q_N} = 1 \tag{4.81}$$

when the downstream boundary is a stage-discharge single value rating curve, Equation (4.39), or:

$$\frac{\partial B_N}{\partial h_N} = \left[-1.486\left(\frac{AR^{2/3}}{n}\right)_N^{j+1}\left(\frac{h_{N-1}^{j+1} - h_N^{j+1}}{\Delta x_{N-1}}\right)^{1/2}\right]\left[\frac{-dn/dh_N}{n_N} + \frac{5}{3}\left(\frac{B}{A}\right)_N^{j+1}\right.$$

$$\left. - \frac{2}{3}\left(\frac{dB/dh}{B}\right)_N^{j+1} - \frac{1}{2(h_{N-1}^{j+1} - h_N^{j+1})}\right] \tag{4.82}$$

$$\frac{\partial B_N}{\partial Q_N} = 1 \tag{4.83}$$

when the downstream boundary is a stage-discharge loop rating curve, Equation (4.40), or:

$$\frac{\partial B_N}{\partial h_N} = -ab(h_N^{j+1} - h_w)^{b-1} \tag{4.84}$$

$$\frac{\partial B_N}{\partial Q_N} = 1 \tag{4.85}$$

when the downstream boundary is a weir type stage-discharge relation, Equation (4.41).

Relaxation Algorithm for System of Rivers

The implicit formulation of the Saint-Venant equations is well suited for simulating unsteady flows in a system of rivers such as the one shown in Fig. 4.7, since the response of the system as a whole is determined for each time step. Also, because the implicit technique is stable for large time steps, it can provide an efficient means of obtaining the transient response of river systems subjected to floods of several days' or even weeks' duration.

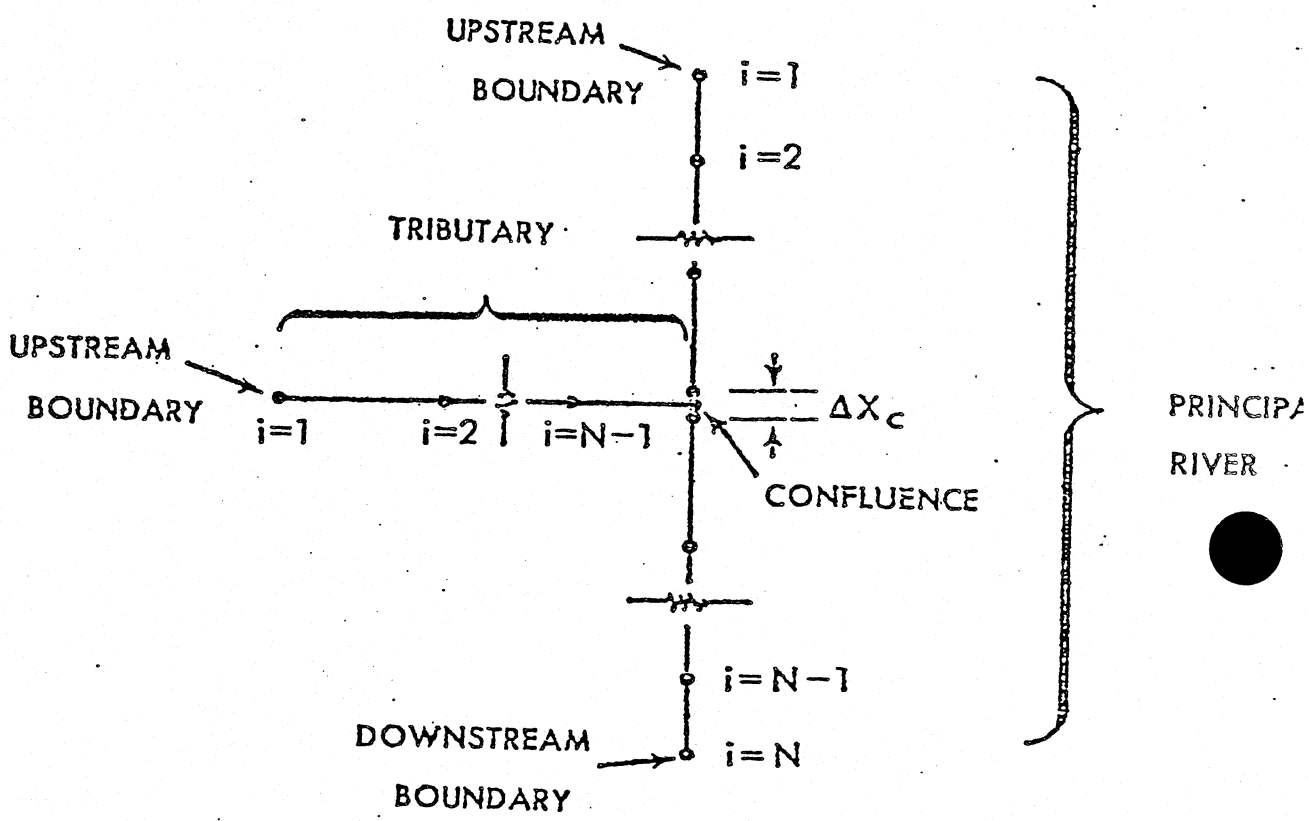

Fig. 4.7.--Application of implicit solution technique to system of rivers.

The following criteria should be considered in developing a technique for applying the implicit method of dynamic routing to a river system: (1) the continuous storage and dynamic interactions at the confluence of the tributary and the principal (main stem) river must be properly simulated; (2) an efficient matrix solution algorithm such as presented in Appendix C must be used; and (3) the technique must be adaptable to a river with several tributaries. An algorithm satisfying the above criteria can be devised by applying the implicit technique to one river at a time and the separate transient responses so obtained are coupled by conserving mass and momentum of flow in each river at the confluence. A complete conservation is accomplished by treating the tributary flow at the confluence as lateral flow q when the transient response of the principal river is obtained. (Losses at the confluence other than friction are not considered.) Since the tributary flow depends in part on the water surface elevation at the confluence, and vice versa, an iterative or relaxation procedure is necessary. The application of the implicit technique of dynamic flood routing to the river system shown in Fig. 4.7 is summarized by the following algorithm [Fread, 1973c].

1. Specify the initial conditions and the upstream boundary condition for the principal river and the tributary; specify the downstream boundary condition for the principal river.

2. Estimate the tributary flow Q_{te} occurring at the confluence for the time $t+\Delta t$.

3. Solve the implicit difference Equations (4.22) and (4.23) for the principal river by using a lateral inflow $Q_{te}/\Delta x_c$ along the finite reach Δx_c (the width of the tributary); the solution obtained for the water surface elevation at the midpoint of Δx_c is denoted as h_c.

4. Solve the implicit difference Equations (4.22) and (4.23) for the tributary by using h_c as the downstream boundary condition; the solution obtained for the tributary flow at the downstream boundary is denoted as Q_{ts}.

5. If $|Q_{te}-Q_{ts}| < \varepsilon_c$, a predetermined error tolerance, increment the time and return to step 2; otherwise:

$$Q_{te} = \alpha_c Q_{ts} + (1 - \alpha_c) Q_{te} \tag{4.86}$$

where α_c is a weighting factor ($0.5 \leq \alpha_c \leq 1.0$) and return to step 3.

The rate of convergence of the algorithm can be increased by using parabolic extrapolation to obtain Q_{te} in step 2. The convergence can be accelerated further by a proper selection of the weighting factor α_c. Usually, one to two iterations is required for convergence when a reasonable value of the error tolerance ε_c is used.

The above algorithm is very easily extended to a river having several tributaries by simply repeating steps 2-5 for each tributary.

Updating of Initial Conditions When Forecasting

A procedure for updating the initial conditions when in a day-to-day forecast mode was developed. The updating procedure consists of using the most recent observed stages along the river system to correct the initial conditions (stages and discharges at all computational points in the river system). With the initial conditions corrected so as to most nearly agree with the current state of the river system, any errors produced by the model in computing the forecast stages and discharges will be due to the influence of the model parameters, e.g., Manning's n, during the time interval associated with the forecast. Thus, errors produced by the model during time periods prior to the current time associated with the updated initial conditions will not be carried over into the current forecast period. Of course, if the upstream boundary hydrograph which is forecast by another model is in error, this will be propagated during the solution of the Saint-Venant equations and accordingly produce an error in all forecast stages and discharges.

The updating procedure relies entirely on observed stages at gaging stations within the river system. Since there are more computational points than gaging stations, linear interpolation is used to approximate the updated stages at computational points between two gaging stations. Near junctions of major tributaries, particular procedures are used to provide the best approximation of stage at the computational points. These procedures are tailored to suit the location of gaging stations relative to particular junctions.

Discharges are also updated using the observed stages and the previously computed stages and discharges associated with the time of the initial conditions according to a simplified momentum balance given by the following:

$$S_{f_o} + \frac{\partial h_o}{\partial x} = S_{f_c} + \frac{\partial h_c}{\partial x} \tag{4.87}$$

in which S_f is the friction slope and $\partial h/\partial x$ is the water surface slope. The subscripts o and c designate observed and computed values, respectively.

Upon substituting Equation (4.27) for S_f in Equation (4.87) and approximating the water surface slope with a central finite difference expression, i.e.,

$$\frac{\partial h}{\partial x} \simeq \frac{(h_{i+1} - h_{i-1})}{(\Delta x_{i-1} + \Delta x_i)} \tag{4.88}$$

the following expression for the observed discharge is obtained:

$$Q_{o_i} = \frac{A_{o_i}}{\left(\dfrac{n_{o_i} B_{o_i}^{2/3}}{1.486\, A_{o_i}^{2/3}}\right)} \left[\left(\frac{Q_{c_i} n_{c_i} B_{c_i}^{2/3}}{1.486\, A_{c_i}^{5/3}}\right)^2 + \frac{\left(h_{c_{i+1}} - h_{c_{i-1}} + h_{o_{i-1}} - h_{o_{i+1}}\right)}{(\Delta x_{i-1} + \Delta x_i)}\right]^{1/2} \quad (4.89)$$

in which the subscript i denotes the particular node location along the river.

Equation (4.89) provides estimated values of the observed discharges such that the momentum of the observed flow defined by the observed stages and discharges is equal to the momentum of the computed flow as defined by the computed stages and discharges. Equation (4.89) is applied to each computational point after the observed stages have been assigned to each point either directly or by linear interpolation.

APPENDIX A

SOLUTION OF NON-LINEAR EQUATION BY NEWTON-RAPHSON ITERATION

A non-linear equation may be solved by a functional iterative technique such as Newton-Raphson Iteration. Consider the following equation expressed in functional form:

$$f(x) = 0 \tag{A.1}$$

Non-linearity arises when the equation contains the variable x raised to any power other than unity. The solution of Equation (A.1) is obtained in an iterative manner, proceeding from a first solution estimate x^k towards succeeding improved estimates x^{k+1}, which tend to converge toward the solution denoted as X in Fig. A.1. The orderly procedure by which the improved solution estimate x^{k+1} is obtained so that it converges to an acceptable solution is known as Newton-Raphson Iteration [Conte, 1967; Fread, 1971b] and is described as follows.

A non-linear equation such as Equation (A.1) may be linearized by using only the first two terms of its Taylor series expansion at x^k, i.e.,

$$f(x) = f(x^k) + f'(x^k)\ (x - x^k) \tag{A.2}$$

where the prime (') denotes a derivative evaluated at x^k, i.e., $f'(x) = df(x)/dx$. The right side of Equation (A.2) is the linear function of x^k that best approximates the non-linear function f(x) which is evaluated at x^k. An iterative procedure, which will cause $f(x^k)$ to approach zero as the quantity $(x-x^k)$ approaches zero, can be obtained from Equation (A.2) by setting f(x) equal to zero and replacing x with x^{k+1}, which will be an improved solution estimate for x if the iterative procedure is convergent. Hence, Equation (A.2) takes the form:

$$x^{k+1} = x^k - f(x^k)/f'(x^k) \tag{A.3}$$

where the k superscript denotes the number of iteration.

Equation (A.3), the general iteration algorithm of Newton, is repeated until the difference $(x^{k+1} - x^k)$ is less than ε_1, or until $f(x^k)$ is less than ε_2. When either occurs, the iteration process has converged; i.e., x^{k+1} has approached X to within the prescribed error tolerance ε_1 or ε_2. The case of convergence according to the ε_2 criterion is illustrated in Fig. A.1.

The convergence of the iteration process depends on a good first solution estimate $x^{k=1}$. If the estimate is sufficiently close to X, convergence is attained; and it is at a quadratic rate, i.e., second order, since the iterative procedure involves the first derivative.

The non-linear equations which are solved by the Newton-Raphson iterative algorithm in this report are time dependent finite-difference equations. A first estimate of the solution is obtained by using the solution associated with the time $t-\Delta t$. Using this as the initial estimate, the iteration process will converge. The convergence process can be hastened when the first solution estimate $x^{k=1}$ is made closer to the acceptable solution. A simple linear extrapolation is used to provide better first solution estimates. Thus:

$$x_j^{k=1} = x_{j-1} + \alpha(x_{j-1} - x_{j-2}) \tag{A.4}$$

where the j subscript denotes the solution at time t and j-1 denotes the solution at time $t-\Delta t$, etc. The weighting factor α varies from zero to unity. A value of 0.5 is usually a safe value which will insure convergence within a few iterations.

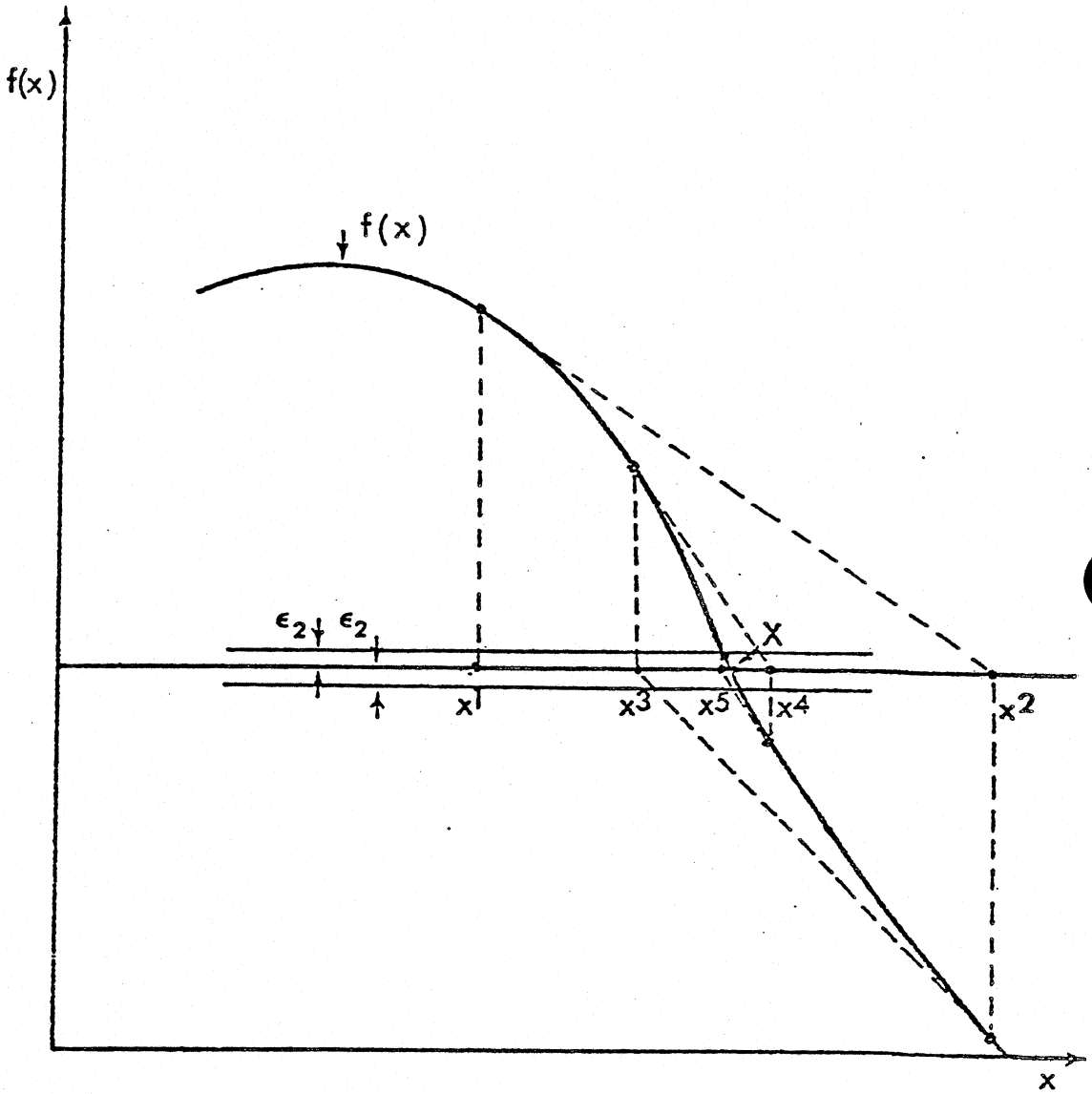

Fig. A.1.—Graphical illustration of convergence process of Newton-Raphson iteration.

APPENDIX B

SOLUTION OF NON-LINEAR SYSTEM OF EQUATIONS BY NEWTON-RAPHSON ITERATION

A system of non-linear algebraic equations may be solved simultaneously by a functional iterative technique known as Newton-Raphson Iteration [Isaacson and Keller, 1966]. Consider the following M-dimensional system of non-linear algebraic equations:

$$\begin{aligned} f_1 \; (x_1^j, x_2^j \; . \; . \; . \; . \; . \; . \; . \; x_M^j) &= 0 \\ \vdots \\ f_M \; (x_1^j, x_2^j \; . \; . \; . \; . \; . \; . \; . \; x_M^j) &= 0 \end{aligned} \tag{B.1}$$

or in vector notation:

$$f \; (\vec{X}^j) = 0 \tag{B.2}$$

The superscript j denotes a particular system of equations. When the algebraic non-linear equations emanate from finite difference approximations of time dependent partial differential equations, j denotes the particular time level at which solutions to the differential equations are sought.

The solution vector $\vec{X}^j$ of Equation (B.1) is obtained in an iterative manner, proceeding from a first solution estimate $\vec{X}^k$ towards succeeding improved estimates $\vec{X}^{k+1}$, which tend to converge toward the solution vector $\vec{X}^j$. The orderly procedure by which the improved solution estimate $\vec{X}^{k+1}$ is obtained such that it converges toward $\vec{X}^j$ is known as Newton-Raphson Iteration and may be described as follows.

The non-linear system $f(\vec{X})$ may be linearized by using the first two terms of its Taylor Series expansion at $\vec{X}^k$, i.e.,

$$f(\vec{X}^j) \simeq f(\vec{X}^k) + \sum_{i=1}^{M} f_i'(\vec{X}^k) \; (\vec{X}_i^j - \vec{X}_i^k) \tag{B.3}$$

where:

$$f_i'(\vec{X}^k) = \frac{\partial f(\vec{X}^k)}{\partial X_i} \tag{B.4}$$

Equation (B.3) may be expressed in a concise form as:

$$f(\vec{X}^j) \simeq f(\vec{X}^k) + \underset{\sim}{J}'(\vec{X}^k) \; \Delta\vec{X} \tag{B.5}$$

where $\underset{\sim}{J}' \; (\vec{X}^k)$ is the Jacobian, a coefficient matrix made up of the partial derivatives evaluated at $\vec{X}^k$, and $\Delta\vec{X}$ is a correction term

defined as:

$$\Delta\vec{X} = \vec{X}_i^j - \vec{X}_i^k \tag{B.6}$$

The right-hand side of Equation (B.5) is the linear vector function of $\vec{X}^k$ that best approximates the non-linear function $f(\vec{X})$, evaluated at $\vec{X}^k$. An iterative procedure is desired which will cause the vector function $f(\vec{X}^k)$ to approach zero as $\Delta\vec{X}$, the correction vector, approaches zero. Therefore, the right-hand side of Equation (B.5) is used to construct the general iteration algorithm, i.e.,

$$\underset{\sim}{J}'(\vec{X}^k)\ \Delta\vec{X} = -f(\vec{X}^k) \tag{B.7}$$

In Equation (B.7), $\Delta\vec{X}$ is now defined as the difference between an improved solution vector $\vec{X}^{k+1}$ and the old solution vector $\vec{X}^k$.

The right-hand side of Equation (B.7) is the negative of the residual or error vector produced by using the solution estimate vector $\vec{X}^k$ in Equation (B.2). The Jacobian is known since it is evaluated as $\vec{X}^k$.

The linear system of equations represented in vector form by Equation (B.7) may be solved for the unknown linear correction vector $\Delta\vec{X}$ by a suitable matrix solution technique. A variation of Gaussian elimination was chosen as the most efficient matrix solution technique; it is described in Appendix C.

The correction vector is used to obtain an improved solution vector estimate $\vec{X}^{k+1}$ of the solution vector $\vec{X}^j$. The process is repeated until $\Delta\vec{X}$ is less than ε which is a suitable tolerance vector. When this occurs, the iteration process has converged, i.e., $\vec{X}^{k+1}$ has approached $\vec{X}^j$ within the prescribed tolerance ε. The convergence of the iteration process depends on a good first solution vector estimate $\vec{X}^{k=1}$. If the estimate is sufficiently close to $\vec{X}^j$, convergence is attained at a quadratic rate since the iterative procedure is second order (involves the first derivative).

When applying the Newton-Raphson Iteration to non-linear finite difference approximations to the Saint-Venant equations, the first estimate solution vector $\vec{X}^{k=1}$ can be chosen sufficiently close to $\vec{X}^j$ to allow convergence. A reasonably accurate initial condition provides the first $\vec{X}^{k=1}$, and linear or parabolic extrapolated first estimates may be used thereafter. Linear extrapolations are obtained from the following expression:

$$\vec{X}^{k=1} = \vec{X}^{j-1} + \frac{\alpha\ \Delta t^j}{\Delta t^{j-1}}\left(\vec{X}^{j-1} - \vec{X}^{j-2}\right) \tag{B.8}$$

where Δt^j and Δt^{j-1} are the values of the time steps between the time levels corresponding to the solution vectors, $\vec{X}^j$ and $\vec{X}^{j-1}$, respectively.

The weighting factor α varies from zero to unity. If the time steps are constant, the following parabolic extrapolation algorithm yields parabolic extrapolations for the first estimate solution vectors:

$$\vec{X}^{k=1} = \vec{X}^{j-3} + 3\,(\vec{X}^{j-1} - \vec{X}^{j-2}) \qquad \text{(B.9)}$$

If the time steps are not constant, linear extrapolation is used for all extrapolated first estimate vectors.

APPENDIX C

COMPACT GAUSSIAN ELIMINATION ALGORITHM FOR QUAD-DIAGONAL SYSTEMS

Consider the following system of linear algebraic equations in vector notation:

$$\underset{\sim}{J'}\vec{X} = \vec{R} \tag{C.1}$$

where $\underset{\sim}{J'}$ is a coefficient matrix of M x M dimensions with known components $J'_{i,j}$; $\vec{X}$ is a column vector with M unknown X_i components, and $\vec{R}$ is a column vector with M specified R_i components.

The components of $\underset{\sim}{J'}$ may be arranged in numerous patterns; however, the structure shown below is characteristic of the Jacobian described in Appendix B and generated by four-point finite difference approximations of the Saint-Venant equations.

$$\underset{\sim}{J'} = \begin{bmatrix} J'_{1,1} & J'_{1,2} & & & & & & \\ J'_{2,1} & J'_{2,2} & J'_{2,3} & J'_{2,4} & & & & \\ J'_{3,1} & J'_{3,2} & J'_{3,3} & J'_{3,4} & & & & \\ & J'_{4,3} & J'_{4,4} & J'_{4,5} & J'_{4,6} & & & \\ & J'_{5,3} & J'_{5,4} & J'_{5,5} & J'_{5,6} & & & \\ & & \cdots & \cdots & \cdots & \cdots & & \\ & & \cdots & \cdots & \cdots & \cdots & & \\ & & \cdots & \cdots & \cdots & \cdots & & \\ & & J'_{M-2,M-3} & J'_{M-2,M-2} & J'_{M-2,M-1} & J'_{M-2,M} & & \\ & & J'_{M-1,M-3} & J'_{M-1,M-2} & J'_{M-1,M-1} & J'_{M-1,M} & & \\ & & & & J'_{M,M-1} & J'_{M,M} & & \end{bmatrix} \tag{C.2}$$

The components of $\underset{\sim}{J'}$ are banded about the main diagonal with, at most, four components contained in any one row. A matrix structured in this way lends itself to the development of an efficient solution algorithm. The compact solution algorithm developed by Fread [1971c] and presented herein is based on a modified Gaussian elimination method, which is a well-known direct solution technique for a system of linear equations.

The compact algorithm differs from the general Gaussian elimination method in that it requires substantially less computations and computer core storage. The number of computations required by Gaussian elimination

is of the order $(M^2 + M^3)/2$, while the compact algorithm requires 19 (M-1) computations. The core storage required by the Gaussian method is M x M words while that required by the compact algorithm is M x 4 words. The number of computations is reduced by eliminating all computations involving the many zero components in $\underset{\sim}{J}'$. The core storage is reduced by transforming $\underset{\sim}{J}'$ into a compact form $\underset{\sim}{J}$ shown below.

$$\underset{\sim}{J} = \begin{bmatrix} J_{1,1} & J_{1,2} & & \\ J_{2,1} & J_{2,2} & J_{2,3} & J_{2,4} \\ J_{3,1} & J_{3,2} & J_{3,3} & J_{3,4} \\ J_{4,1} & J_{4,2} & J_{4,3} & J_{4,4} \\ \cdots & \cdots & \cdots & \cdots \\ \cdots & \cdots & \cdots & \cdots \\ \cdots & \cdots & \cdots & \cdots \\ J_{M-2,1} & J_{M-2,2} & J_{M-2,3} & J_{M-2,4} \\ J_{M-1,1} & J_{M-1,2} & J_{M-1,3} & J_{M-1,4} \\ & & J_{M,3} & J_{M,4} \end{bmatrix} \tag{C.3}$$

The arrangement of the components in $\underset{\sim}{J}$ resulted from the J' components being shifted horizontally such that the relative positions of the components in any one row were not altered. The transformation is accomplished by a simple change of the jth index of the $J'_{i,j}$ components. Thus, after transforming $\underset{\sim}{J}'$ into $\underset{\sim}{J}$, Equation (C.1) becomes:

$$\underset{\sim}{J}\vec{X} = \vec{R} \tag{C.4}$$

Equation (C.4) can be solved for the solution vector $\vec{X}$ by a compact Gaussian elimination algorithm for quad-diagonal systems. The solution algorithm consists of two parts. The first transforms the augmented matrix $\underset{\sim}{J/R}$ into an upper triangular matrix by an elimination process. The second part computes the X solution vector by a back-substitution process. The solution algorithm consisting of 23 steps follows:

1. Set k = 0 and i = 2

2. $F = -J_{i,1}/J_{i-1,k+1}$ (C.5)

3. $J_{i,2} = F \cdot J_{i-1,k+2} + J_{i,2}$ (C.6)

4. $R_i = F \cdot R_{i-1} + R_i$ (C.7)

5. $F = -J_{i+1,1}/J_{i-1,k+1}$ (C.8)

6. $J_{i+1,2} = F \cdot J_{i-1,k+2} + J_{i+1,2}$ (C.9)

7. $R_{i+1} = F \cdot R_{i-1} + R_{i+1}$ (C.10)

8. $F = -J_{i+1,2}/J_{i,2}$ (C.11)

9. $J_{i+1,3} = F \cdot J_{i,3} + J_{i+1,3}$ (C.12)

10. $J_{i+1,4} = F \cdot J_{i,4} + J_{i+1,4}$ (C.13)

11. $R_{i+1} = F \cdot R_i + R_{i+1}$ (C.14)

12. Set $k = 2$

13. If $i < (M-2)$ increment i by 2 and return to step 2; otherwise, proceed to step 14.

14. Set $k = 2$ and $i = M-1$

15. $F = -J_{M,3}/J_{i,3}$ (C.15)

16. $J_{M,4} = F \cdot J_{i,4} + J_{M,4}$ (C.16)

17. $R_M = F \cdot R_i + R_M$ (C.17)

18. $X_M = R_M/J_{M,4}$ (C.18)

19. $X_i = (R_i - J_{i,k+2} \cdot X_{i+1})/J_{i,k+1}$ (C.19)

20. If $i = 1$, <u>stop</u>; otherwise, decrease i by 1 and proceed to step 21.

21. $X_i = (R_i - J_{i,4} \cdot X_{i+2} - J_{i,3} \cdot X_{i+1})/J_{i,2}$ (C.20)

22. Decrease i by 1

23. If $i > 1$, return to step 19; otherwise, set $k = 0$ and return to step 19.

Steps 1-18 reduce the augmented matrix $\underset{\sim}{J/R}$ to an upper triangular form. Steps 19-23 perform the back-substitution by which the solution vector $\underset{\sim}{X}$ is obtained.

5. Develop the finite difference equations (full dynamic wave model) for the trapezoidal channel described below. Write out the equations for the particular grid shown below.

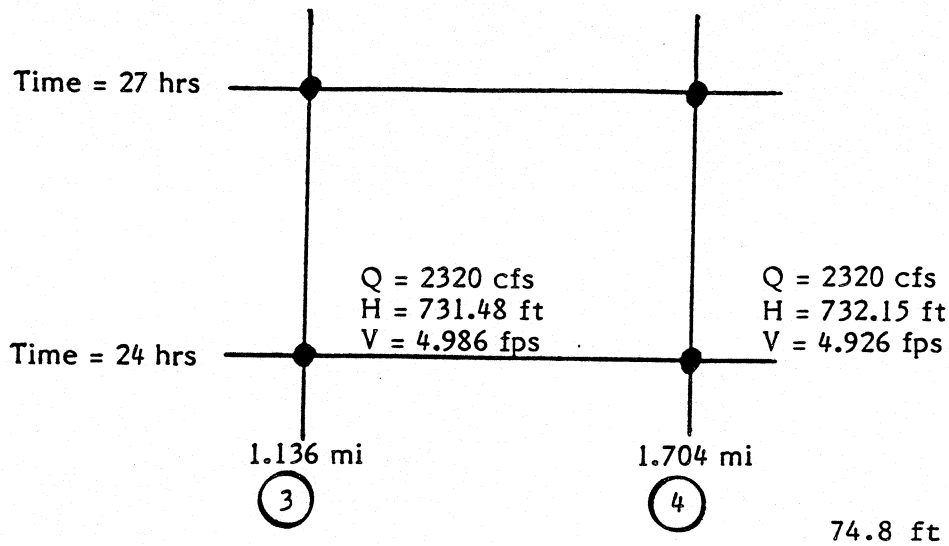

Manning's N = 0.018
No overbank flow
Assume $\beta = 1.0$
No Lateral inflow
No wind effect
$\theta = 0.55$

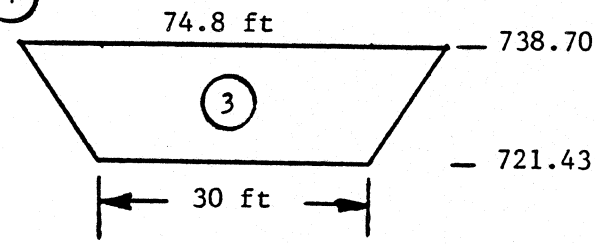

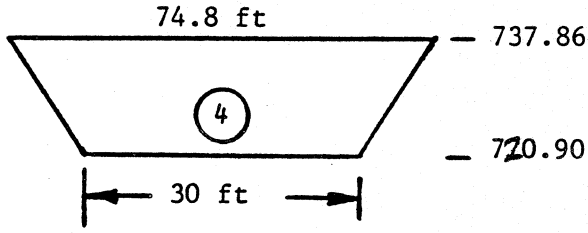

INITIAL AND BOUNDARY CONDITIONS

- INITIAL CONDITIONS
- UPSTREAM AND DOWNSTREAM BOUNDARY CONDITIONS
- INTERNAL BOUNDARY CONDITIONS

7 GRIDS X 2 EQUATIONS = 14 EQUATIONS + 2 BOUNDARY = 16 EQS

(7+1) NODES X 2 $\frac{\text{UNKNOWN}}{\text{NODE}}$ = 16 UNKNOWNS ← DETERMINATE

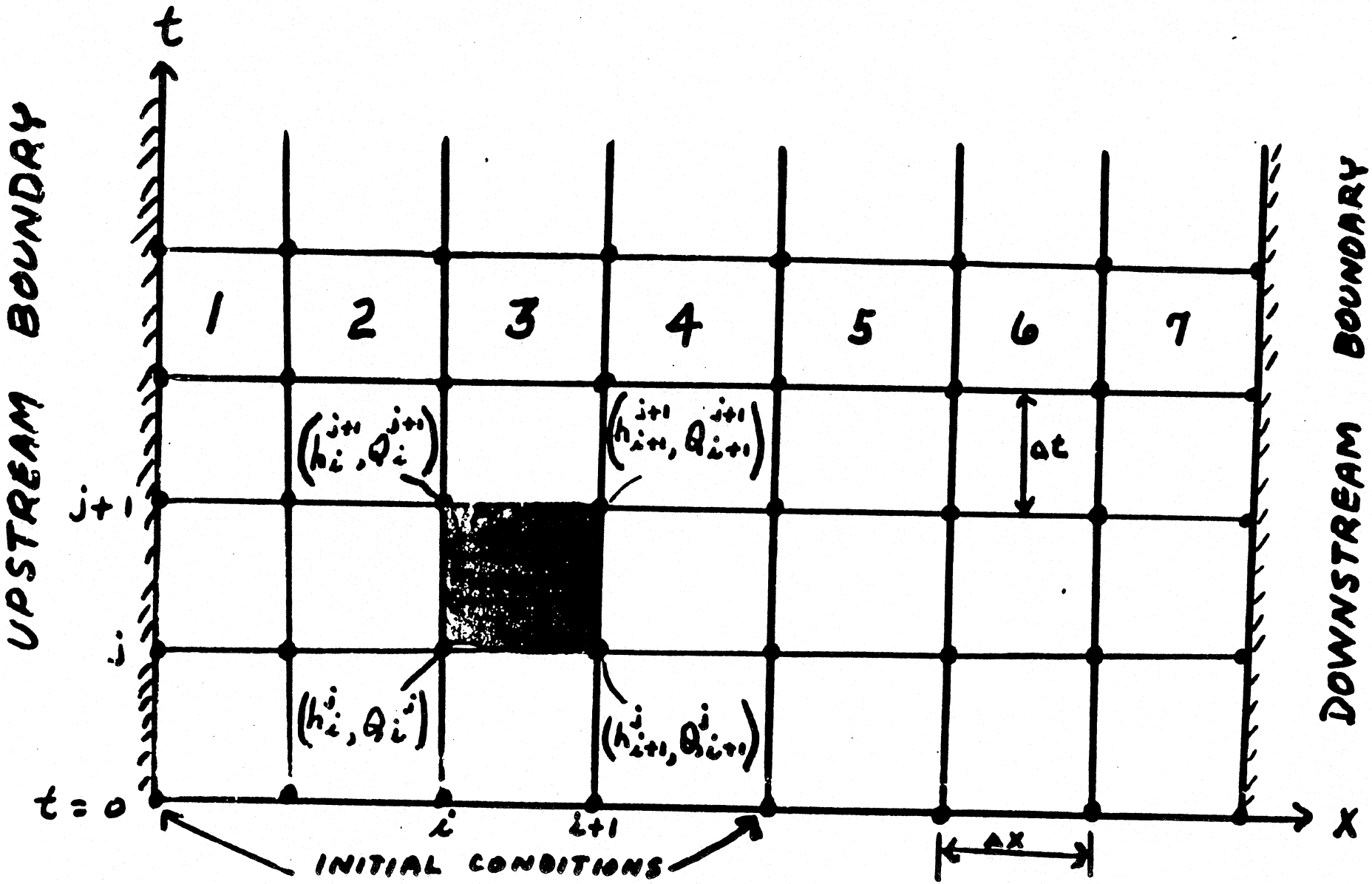

X-t SOLUTION DOMAIN

continuity equation for each grid

$$\theta\left(Q_{i+1}^{j+1} - Q_i^{j+1} - \bar{q}_i^{j+1}\,\Delta x_i\right) + (1-\theta)\left(Q_{i+1}^{j} - Q_i^{j} - \bar{q}_i^{j}\,\Delta x_i\right)$$

$$+ 0.5\,\Delta x_i/\Delta t^j\left[(A + A_o)_i^{j+1} + (A + A_o)_{i+1}^{j+1} - (A + A_o)_i^{j}\right.$$

$$\left. - (A + A_o)_{i+1}^{j}\right] = 0$$

momentum eq. for each grid

$$0.5\,\Delta x_i/\Delta t^j\left(Q_{i+1}^{j+1} + Q_i^{j+1} - Q_i^{j} - Q_{i+1}^{j}\right) + \theta\left[(Q^2/A)_{i+1}^{j+1}\right.$$

$$- (Q^2/A)_i^{j+1} + g\,\bar{A}_i^{j+1}\left(h_{i+1}^{j+1} - h_i^{j+1} + \Delta x_i\,\bar{S}_{f_i}^{j+1} + \Delta x_i\,\bar{S}_{e_i}^{j+1}\right)$$

$$\left. + \Delta x_i\left(L + \bar{W}_f\bar{B}\right)_i^{j+1}\right] + (1-\theta)\left[(Q^2/A)_{i+1}^{j} - (Q^2/A)_i^{j} + g\bar{A}_i^{j}\right.$$

$$\left.\left(h_{i+1}^{j} - h_i^{j} + \Delta x_i\,\bar{S}_{f_i}^{j} + \Delta x_i\,\bar{S}_{e_i}^{j}\right) + \Delta x_i\left(L + \bar{W}_f\bar{B}\right)_i^{j}\right] = 0$$

where: $\bar{A}_i = 0.5\,(A_i + A_{i+1})$

$$\bar{B}_i = 0.5\,(B_i + B_{i+1})$$

$$\bar{S}_{f_i} = \frac{\bar{n}_i^{\,2}\,|\bar{Q}_i|\,\bar{Q}_i}{2.21\,\bar{A}_i^{\,2}\,R_i^{\,4/3}} = |\bar{Q}_i|\,\bar{Q}_i/\bar{K}_{c_i}^2$$

$$\bar{Q}_i = 0.5\,(Q_i + Q_{i+1})$$

$$R_i = \bar{A}_i/\bar{B}_i$$

$$\bar{K}_{c_i} = 0.5\,(K_{c_i} + K_{c_{i+1}})$$

$$\bar{S}_{e_i} = K_{e_i}\left[(Q/A)_{i+1}^2 - (Q/A)_i^2\right]/(2g\Delta x_i)$$

$$\bar{W}_{f_i} = C_{w_i}\,|\bar{V}_{r_i}|\,\bar{V}_{r_i}$$

$$\bar{V}_{r_i} = \bar{Q}_i/\bar{A}_i - \bar{V}_{w_i}\cos\omega$$

INITIAL CONDITIONS

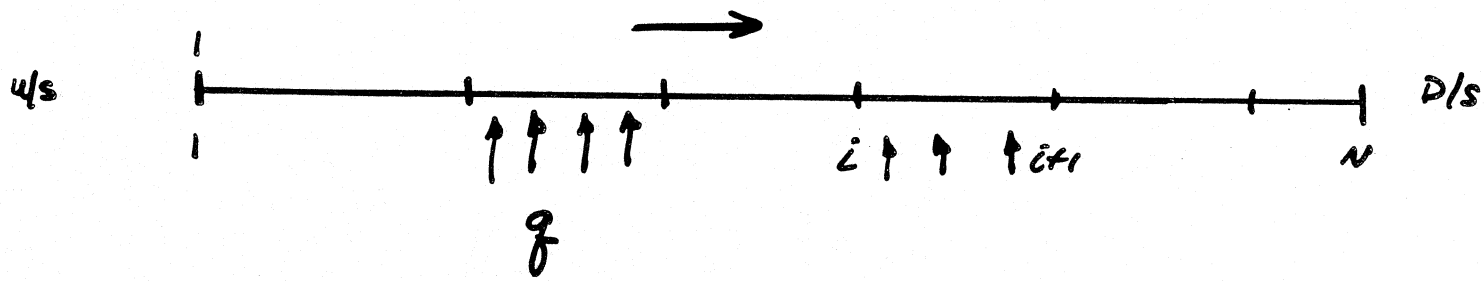

STEADY FLOW CONDITION

Consider momentum equation:

$$\cancel{\frac{\partial Q}{\partial t}}^{\,0} + \frac{\partial (Q^2/A)}{\partial x} + gA\left(\frac{\partial h}{\partial x} + S_f\right) - \cancel{q u_x}^{\,0} = 0$$

$$\frac{\partial (Q^2/A)}{\partial x} + gA\left(\frac{\partial h}{\partial x} + S_f\right) = 0$$

$$\frac{(Q^2/A)_{i+1} - (Q^2/A)_i}{\Delta x_i} + g\left(\frac{A_i + A_{i+1}}{2}\right)\left[\frac{h_{i+1} - h_i}{\Delta x_i} + \frac{n^2 (Q_i + Q_{i+1})^2 (B_i + B_{i+1})^{4/3}}{2.2\,(A_i + A_{i+1})^{10/3}}\right]$$

$$\left(\frac{Q^2}{A}\right)_{i+1} - \left(Q^2/A\right)_i + g\bar{A}_i\left(h_{i+1} - h_i + \Delta x_i\,\bar{S}_{f_i}\right) = 0$$

Starting with given surface water elevation $\underline{h_N}$ use Newton-Rhapson method to solve

Newton-Rhapson Method for Initial Conditions

Scalar form because only one unknown.

$$x^{k+1} = x^k - f(x^k)/f'(x^k) \qquad k \Rightarrow \text{iteration}$$

where $x = h_i$

$$f(x^k) = \left(\frac{Q^2}{A}\right)_{i+1} - \left(\frac{Q^2}{A}\right)_i + g\bar{A}_i\left(h_{i+1} - h_i + \Delta x_i \bar{S}_f\right)$$

$$f'(x^k) = \frac{df(x^k)}{dh_i} = \left(\frac{Q^2 B}{A^2}\right)_i + 0.5g\, B_i\left(h_{i+1} - h_i + \bar{S}_f \Delta x_i\right) + g\bar{A}_i\left[-1 + \Delta x_i \frac{d\bar{S}_f}{dh_i}\right]$$

where

$$\frac{d\bar{S}_f}{dh} = 2\bar{S}_f\left[\frac{d\bar{n}}{dh}/n - \frac{5B}{6\bar{A}} + \frac{dB/dh}{3\bar{B}}\right]$$

$$= \frac{-\bar{S}_f \; dK_c/dh}{\bar{K}_c}$$

$\bar{K}_c \leftarrow$ CONVEYANCE

$$\bar{S}_f = \frac{\bar{n}_i^2 |\bar{Q}_i| \bar{Q}_i}{2.21\, \bar{A}_i^2 R_i^{4/3}} = |\bar{Q}_i| \bar{Q}_i / \bar{K}_{c_i}^2$$

$$\bar{Q}_i = \tfrac{1}{2}(Q_i + Q_{i+1})$$

$$\bar{K}_{c_i} = \tfrac{1}{2}(K_{c_i} + K_{c_{i+1}})$$

X-t Solution Domain

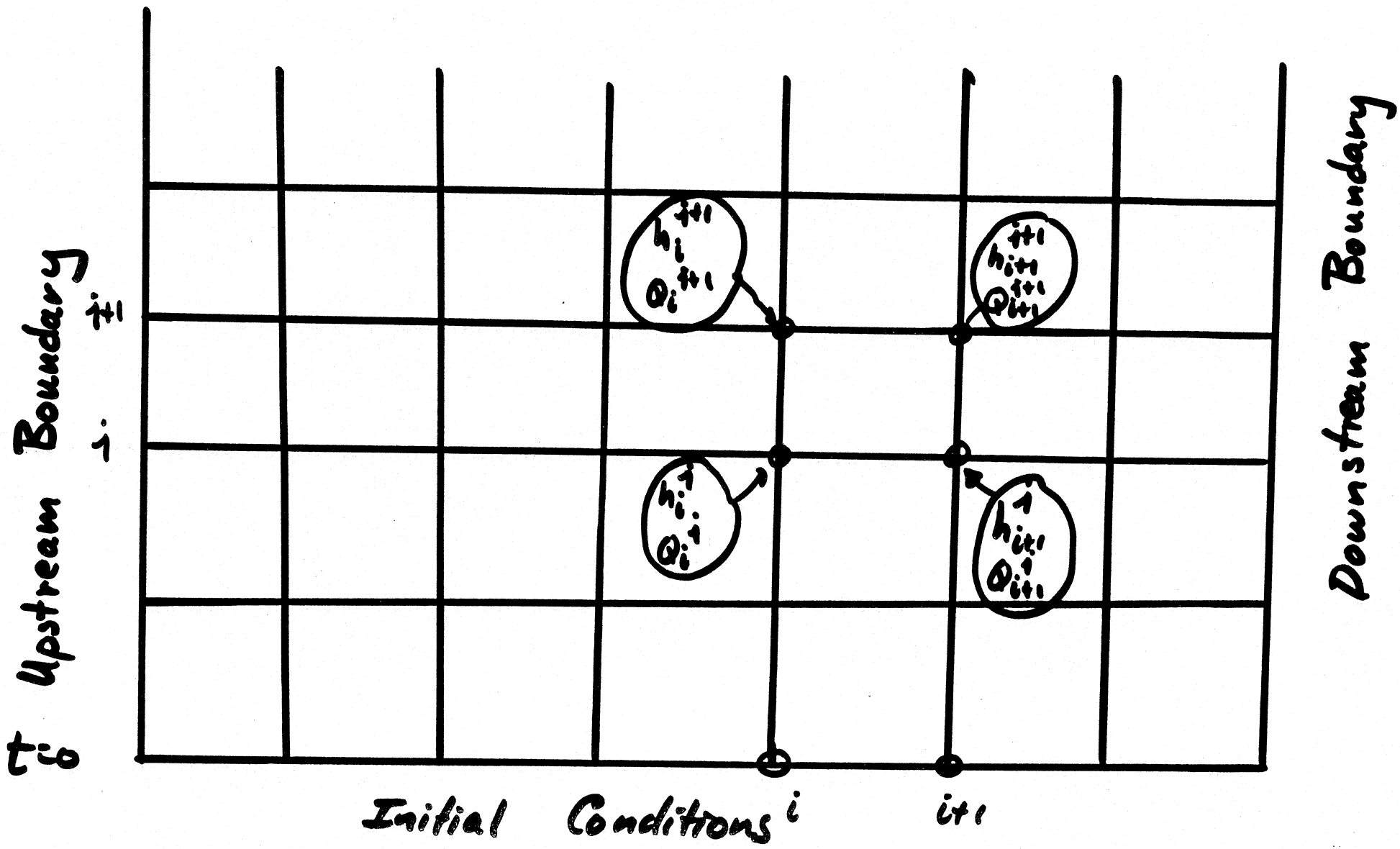

Upstream Boundary Conditions $(i=1)$

Discharge Hydrograph $\quad Q_1^{j+1} = Q(t)$

Stage Hydrograph $\quad h_1^{j+1} = h(t)$

Downstream Boundary Conditions $(i=N)$

1. Discharge Hydrograph $\quad Q_N^{j+1} = Q'(t)$
2. Stage Hydrograph $\quad h_N^{j+1} = h'(t)$
3. Critical Flow $\quad Q_N^{j+1} = QC$

$$QC = \left(\sqrt{g/B}\, A^{3/2}\right)_N^{j+1}$$

4. Rating Curve (piece-wise linear)

$$Q_N^{j+1} = Q'$$

$$Q' = Q_k + (Q_{k+1} - Q_k)(h_N^{j+1} - h_k)/(h_{k+1} - h_k)$$

5. Looped Rating Curve $\quad Q_N^{j+1} = QN$

$$QN = 1.49\left(\frac{A^{5/3}}{nB^{2/3}}\right)_N^{j+1}\left(\frac{h_{N-1}^{j} - h_N}{\Delta x_{N-1}}\right)^{1/2} = k_c\left(\frac{h_{N-1}^{j} - h_N^{j}}{\Delta x_{N-1}}\right)^{1/2}$$

3. Critical Flow $\quad Q_N^{j+1} = QC$

$$QC = \left(\sqrt{g/B}\, A^{3/2}\right)_N^{j+1}$$

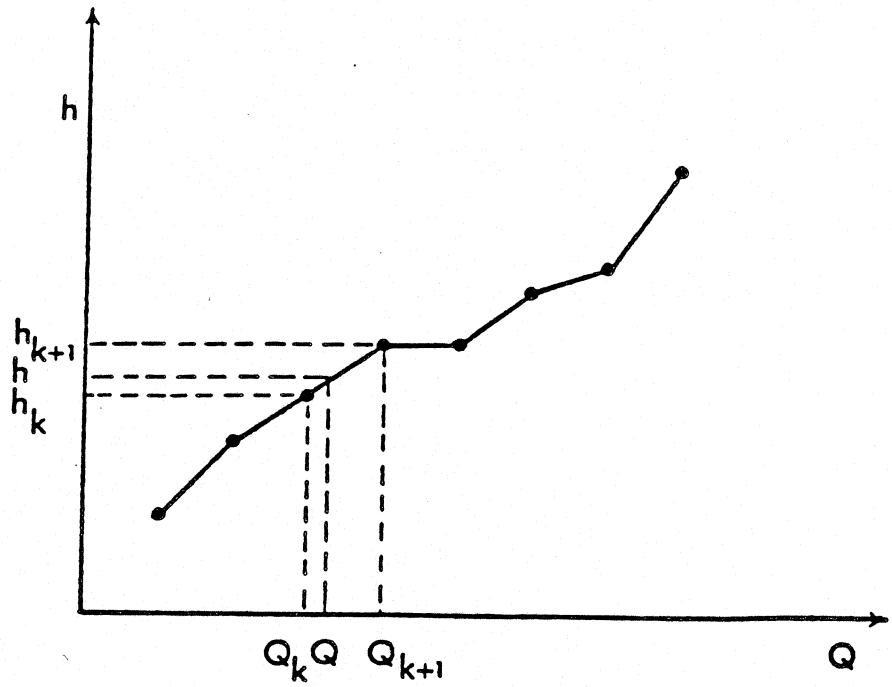

Fig. 4.5.--Single-value rating curve.

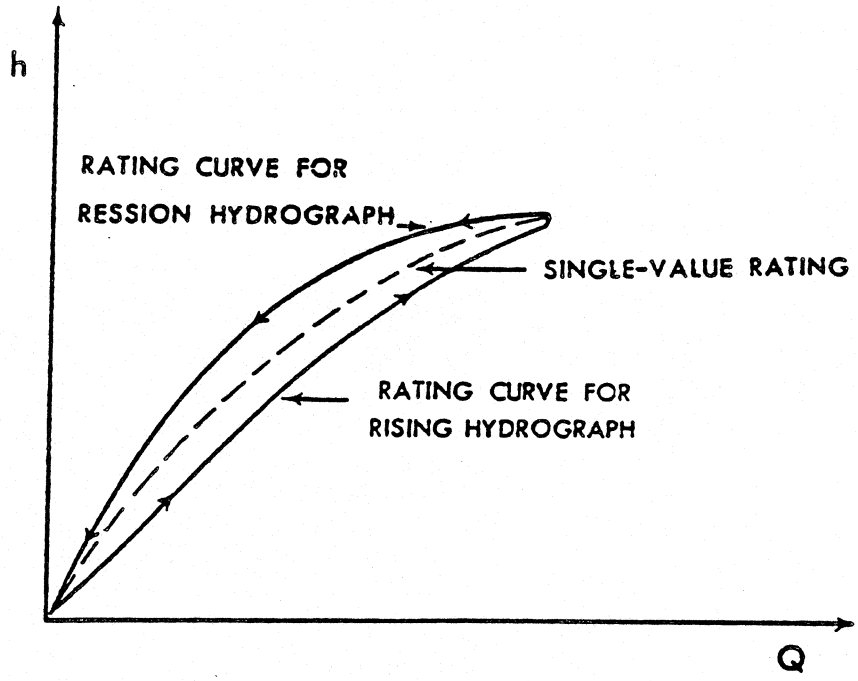

Fig. 4.6.--Loop rating curve.

Cross-sections required at upstream and downstream ends of internal boundary condition.

"Internal" Boundary Condition

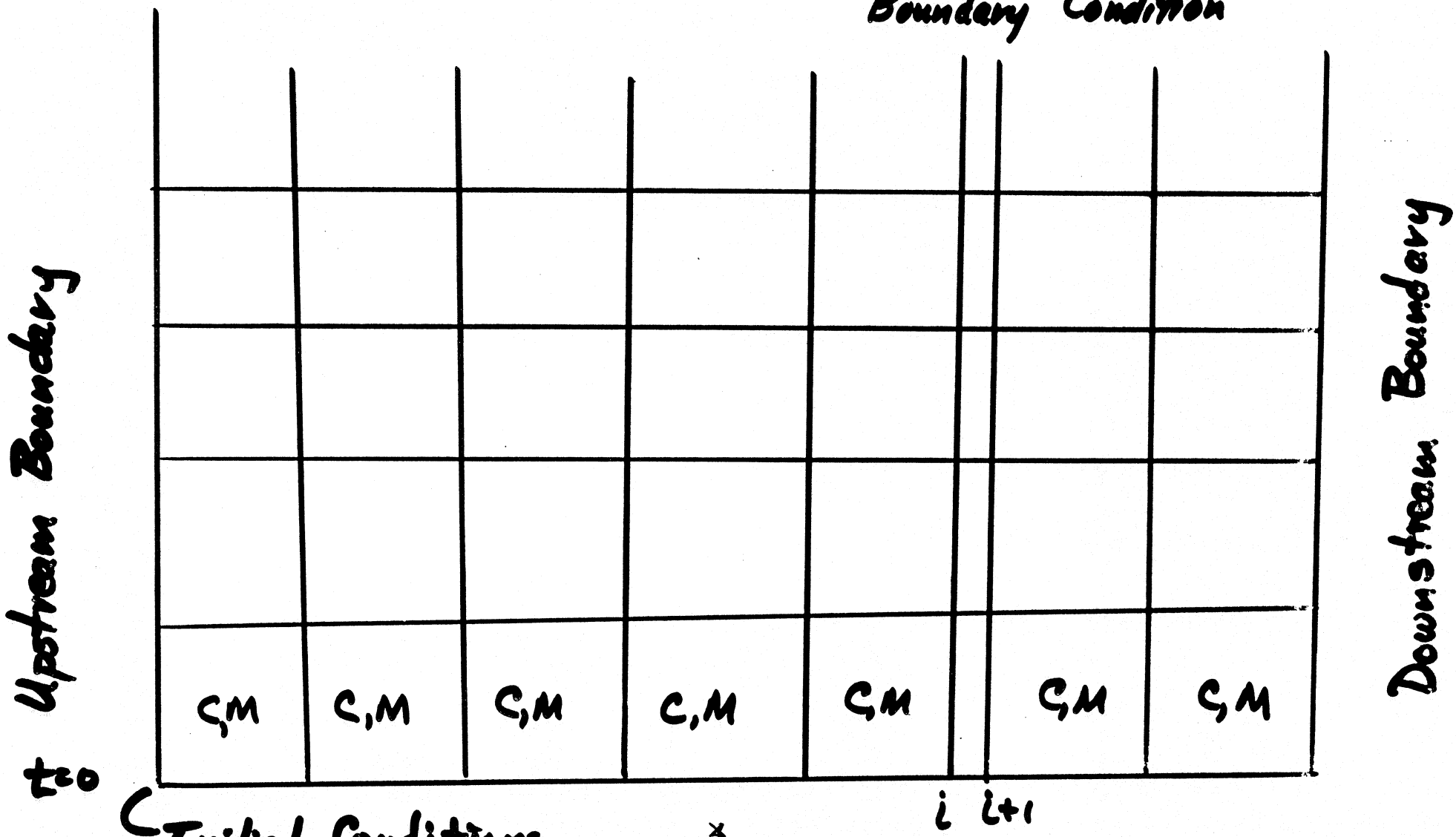

Initial Conditions

C => Continuity

M => Momentum

* 2 equations required for internal boundary condition.

Internal Boundary Conditions

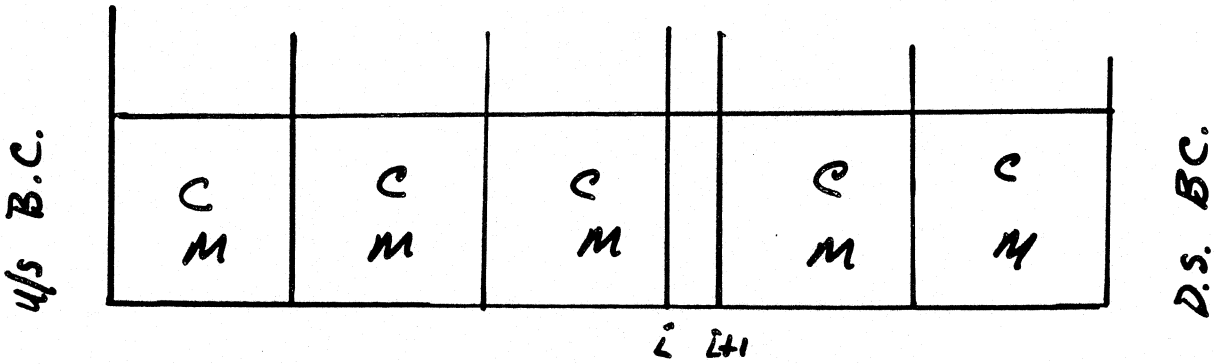

U/S B.C.

C $\frac{\partial Q}{\partial x} + \frac{\partial A}{\partial t} - q = 0$

M $\frac{\partial Q}{\partial t} + \frac{\partial (Q^2/A)}{\partial x} + g\left(\frac{\partial h}{\partial x} + S_f\right) - q v_x = 0$

⋮

D/S BC

Internal Boundary Equations

$Q_i - Q_{i+1} = 0$

$Q_i = f(h_i, h_{i+1}, \ldots)$

ST. VENANT EQ. CAN'T BE USED ON INTERNAL BOUNDARY CONDITIONS

$$\theta\,(Q_{i+1}^{j+1} - Q_i^{j+1} - \bar{q}_i^{j+1}\,\Delta x_i) + (1-\theta)\,(Q_{i+1}^{j} - Q_i^{j} - \bar{q}_i^{j}\,\Delta x_i)$$

$$+ 0.5\,\Delta x_i/\Delta t^j[(A + A_o)_i^{j+1} + (A + A_o)_{i+1}^{j+1} - (A + A_o)_i^{j}$$

$$- (A + A_o)_{i+1}^{j}] = 0$$

$$0.5\,\Delta x_i/\Delta t^j(Q_{i+1}^{j+1} + Q_i^{j+1} - Q_i^{j} - Q_{i+1}^{j}) + \theta[(Q^2/A)_{i+1}^{j+1}$$

$$- (Q^2/A)_i^{j+1} + g\,\bar{A}_i^{j+1}\,(h_{i+1}^{j+1} - h_i^{j+1} + \Delta x_i\,\bar{S}_{f_i}^{j+1} + \Delta x_i\,\bar{S}_{e_i}^{j+1})$$

$$+ \Delta x_i(L + \bar{W}_f\bar{B})_i^{j+1}] + (1-\theta)\,[(Q^2/A)_{i+1}^{j} - (Q^2/A)_i^{j} + g\bar{A}_i^{j}$$

$$(h_{i+1}^{j} - h_i^{j} + \Delta x_i\,\bar{S}_{f_i}^{j} + \Delta x_i\,\bar{S}_{e_i}^{j}) + \Delta x_i(L + \bar{W}_f\bar{B})_i^{j}] = 0$$

where: $\bar{A}_i = 0.5\,(A_i + A_{i+1})$

$$\bar{B}_i = 0.5\,(B_i + B_{i+1})$$

$$\bar{S}_{f_i} = \frac{\bar{n}_i^{\,2}|\bar{Q}_i|\bar{Q}_i}{2.21\,\bar{A}_i^{\,2}\,R_i^{\,4/3}} = |\bar{Q}_i|\bar{Q}_i/\bar{K}_{c_i}^2$$

$$\bar{Q}_i = 0.5\,(Q_i + Q_{i+1})$$

$$R_i = \bar{A}_i/\bar{B}_i$$

$$\bar{K}_{c_i} = 0.5\,(K_{c_i} + K_{c_{i+1}})$$

$$\bar{S}_{e_i} = K_{e_i}[(Q/A)_{i+1}^2 - (Q/A)_i^2]/(2g\Delta x_i)$$

$$\bar{W}_{f_i} = C_{w_i}|\bar{V}_{r_i}|\bar{V}_{r_i}$$

$$\bar{V}_{r_i} = \bar{Q}_i/\bar{A}_i - \bar{V}_{w_i}\cos\omega$$

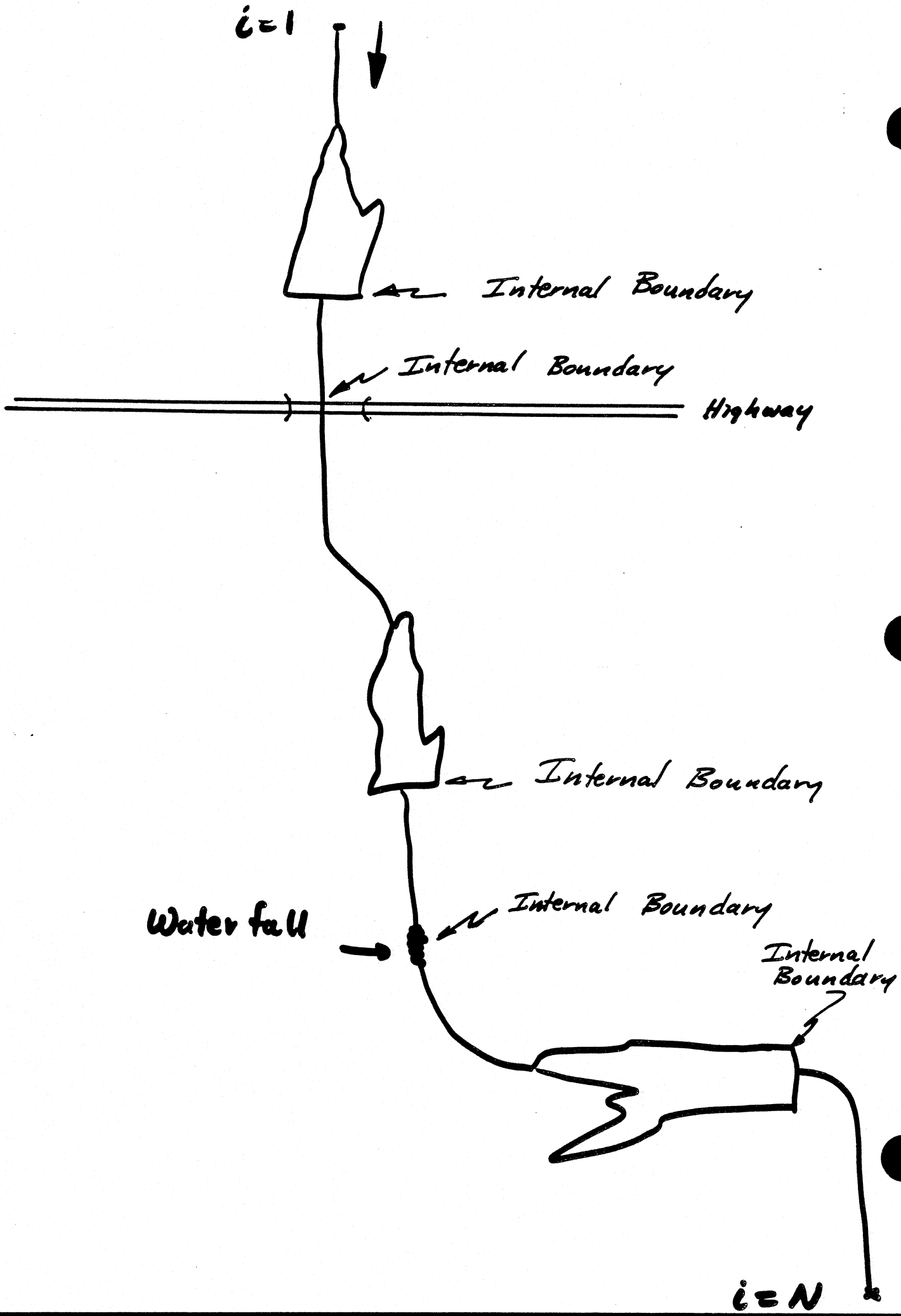
i=1
Internal Boundary
Internal Boundary
Highway
Internal Boundary
Internal Boundary
Water fall
Internal Boundary
i=N

Internal Boundary Conditions

Locations along a waterway where the Saint-Venant equations are not applicable. Flow is rapidly varied rather than gradually varied.

Critical flow

$$Q_i^{i+1} - \sqrt{g}\,\left(A^{3/2}/B^{1/2}\right)_i^{i+1} = 0$$

Dam

(Spillway flow (uncontrolled overflow, fixed gate, or time-dependent gate))

(Crest over flow)

(Constant or head-independent flow)

(Breach flow due to time-dependent failure of a dam)

$$Q_{dam} = Q_s + Q_{co} + Q_c + Q_B$$

Bridge - Embankment

Total flow $Q_{be} = Q_{bo} + Q_{em} + Q_{br}$

Q_{bo}: flow bridge openning

Q_{em}: flow over embankment

Q_{br}: flow through time-dependent breach.

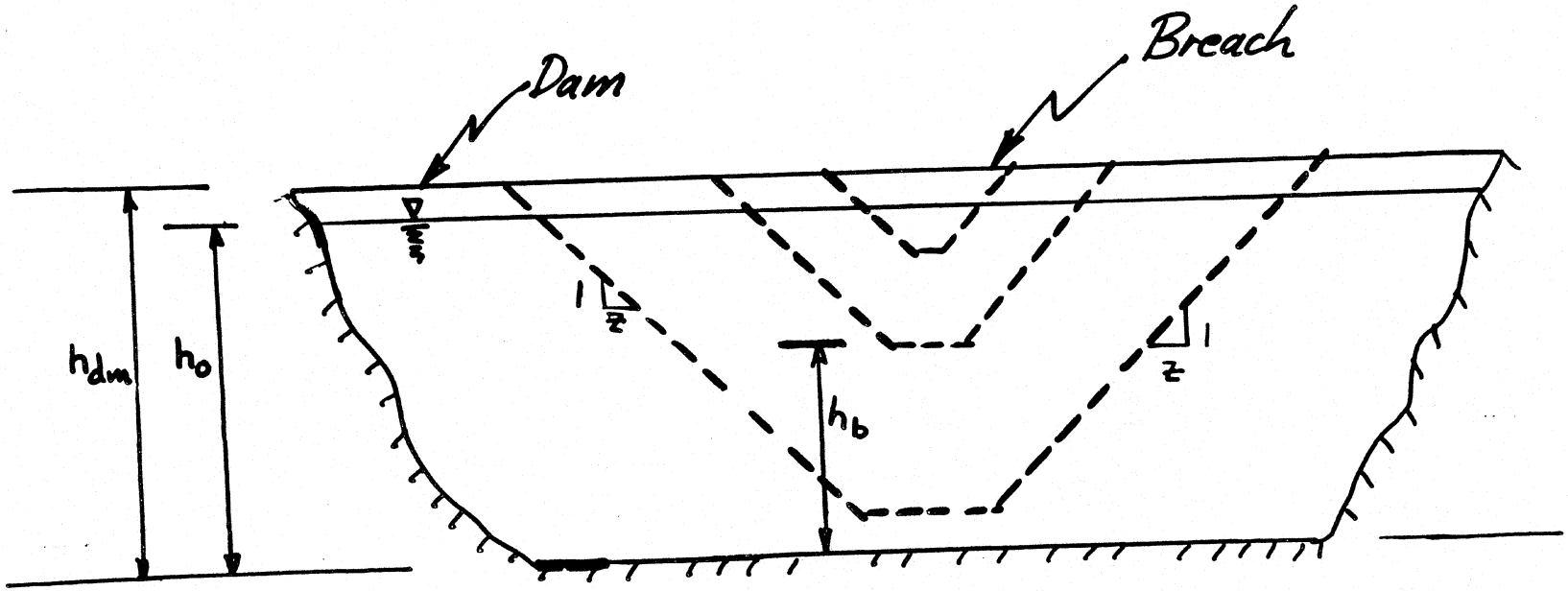

Front View of Dam Showing Breach Formation

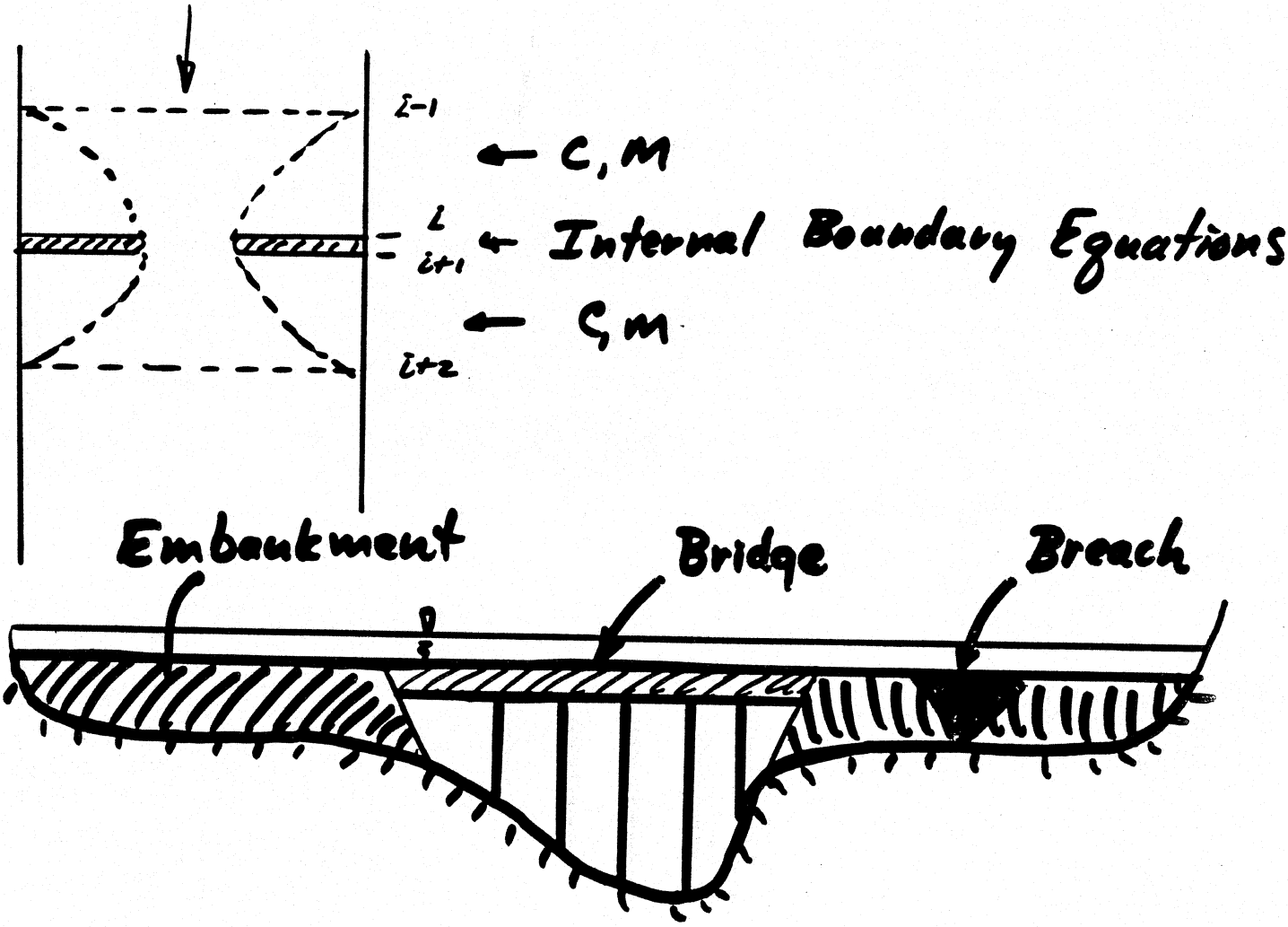

Internal Boundary Equations

(1) $Q_i = Q_{i+1}$

(2) $Q_i = Q_s + Q_b$

$$Q_s = C_b \sqrt{2g}\, A_{i+1} (h_i - h_{i+1})^{1/2} + C_d k_s (h - h_e)^{3/2}$$

$$Q_b = k_s \left[3.1 \hat{B} \frac{t_b}{\hat{q}} (h - h_b)^{3/2} + 2.45 z (h - h_b)^{5/2} \right]$$

Lock & Dam

$$h_i^{i+1} - h_t = 0$$

target pool

Rating Curve (Single-valued rating curve)

$$Q_i^{i+1} = Q'$$

$$Q' = Q_k + (Q_{k+1} - Q_k)(h_i^{i+1} - h_k)/(h_{k+1} - h_k)$$

where $Q_i^{i+1} = f(h_i^{i+1})$

Time Dependent Gate Operations

TIME DEPENDENT GATE OPERATIONS
(e.g. IRRIGATION CANALS)

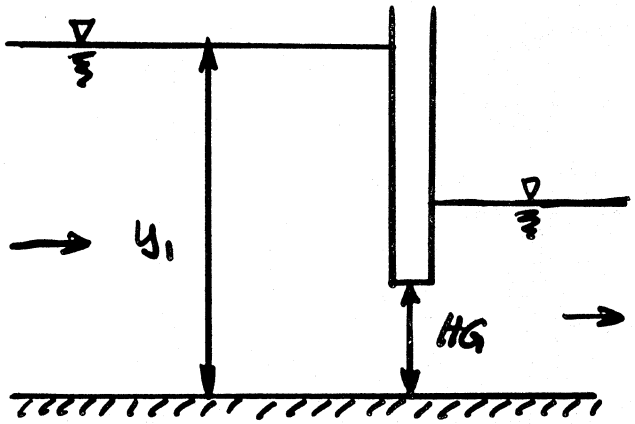

CONTINOUS BOTTOM SLOPE

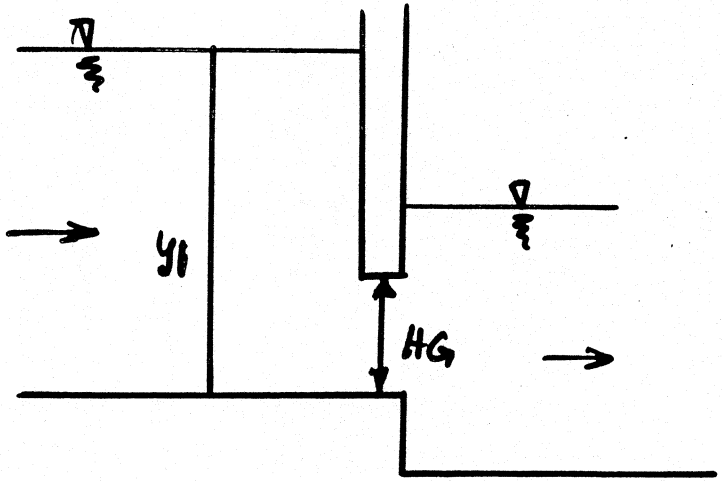

DISCONTINOUS BOTTOM SLOPE

MEANDERING CHANNELS IN A FLOOD PLAIN

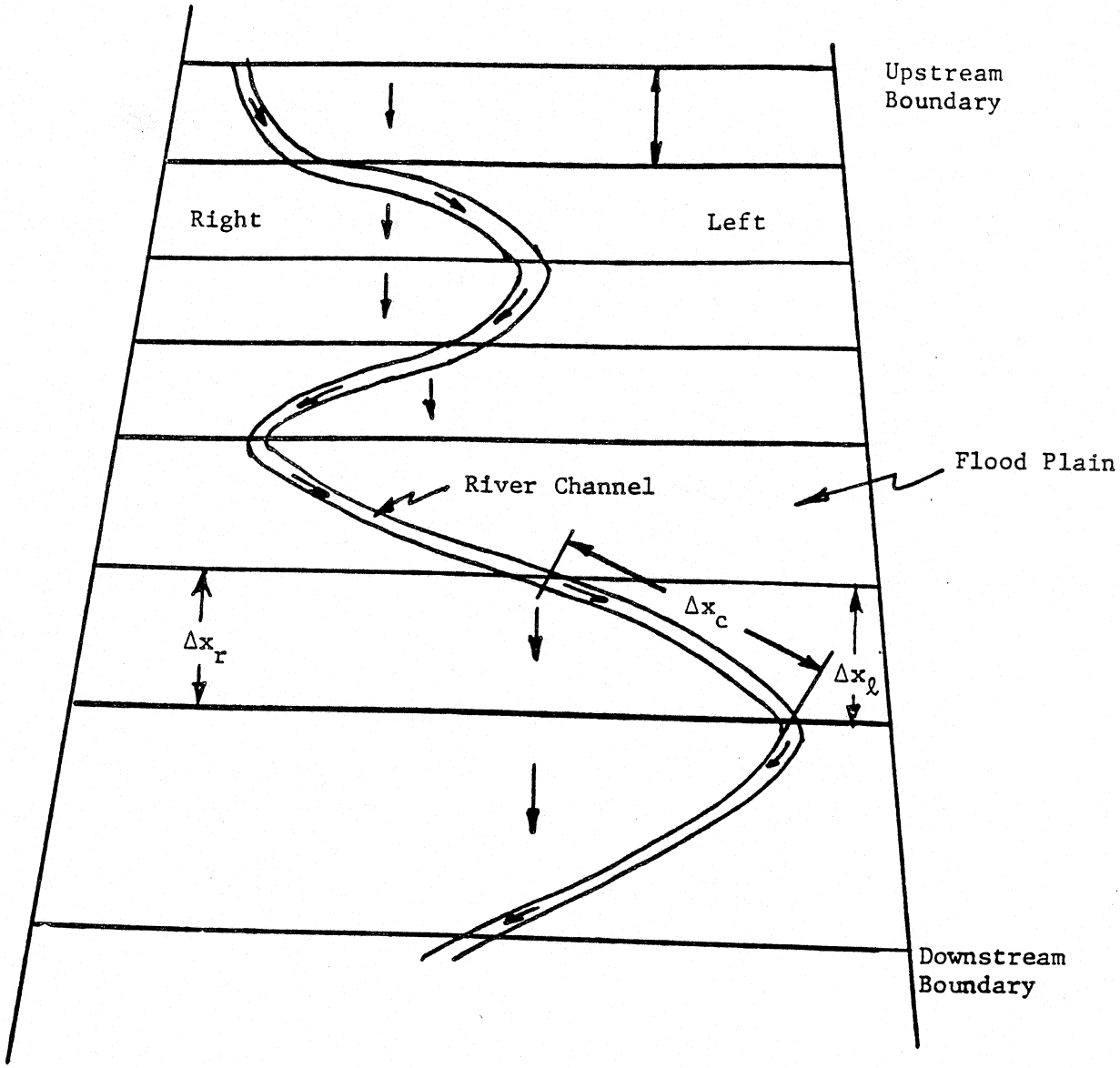

Figure 4.6 Meandering River in a Flood Plain

$$\theta\left(Q_{i+1}^{j+1} - Q_i^{j+1} - \bar{q}_i^{j+1}\,\Delta x_i\right) + (1-\theta)\left(Q_{i+1}^{j} - Q_i^{j} - \bar{q}_i^{j}\,\Delta x_i\right)$$

$$+ 0.5\,\Delta x_i/\Delta t^j\left[(A + A_o)_i^{j+1} + (A + A_o)_{i+1}^{j+1} - (A + A_o)_i^{j}\right.$$

$$\left. - (A + A_o)_{i+1}^{j}\right] = 0$$

$$0.5\,\Delta x_i/\Delta t^j\left(Q_{i+1}^{j+1} + Q_i^{j+1} - Q_i^{j} - Q_{i+1}^{j}\right) + \theta\left[(Q^2/A)_{i+1}^{j+1}\right.$$

$$- (Q^2/A)_i^{j+1} + g\,\bar{A}_i^{j+1}\left(h_{i+1}^{j+1} - h_i^{j+1} + \Delta x_i\,\bar{S}_{f_i}^{j+1} + \Delta x_i\,\bar{S}_{e_i}^{j+1}\right)$$

$$\left. + \Delta x_i\left(L + \bar{W}_f\bar{B}\right)_i^{j+1}\right] + (1-\theta)\left[(Q^2/A)_{i+1}^{j} - (Q^2/A)_i^{j} + g\bar{A}_i^{j}\right.$$

$$\left.\left(h_{i+1}^{j} - h_i^{j} + \Delta x_i\,\bar{S}_{f_i}^{j} + \Delta x_i\,\bar{S}_{e_i}^{j}\right) + \Delta x_i\left(L + \bar{W}_f\bar{B}\right)_i^{j}\right] = 0$$

where: $\bar{A}_i = 0.5\,(A_i + A_{i+1})$

$$\bar{B}_i = 0.5\,(B_i + B_{i+1})$$

$$\bar{S}_{f_i} = \frac{\bar{n}_i^{\,2}\,|\bar{Q}_i|\,\bar{Q}_i}{2.21\,\bar{A}_i^{\,2}\,R_i^{\,4/3}} = |\bar{Q}_i|\,\bar{Q}_i/\bar{K}_{c_i}^2$$

$$\bar{Q}_i = 0.5\,(Q_i + Q_{i+1})$$

$$R_i = \bar{A}_i/\bar{B}_i$$

$$\bar{K}_{c_i} = 0.5\,(K_{c_i} + K_{c_{i+1}})$$

$$\bar{S}_{e_i} = K_{e_i}\left[(Q/A)_{i+1}^2 - (Q/A)_i^2\right]/(2g\Delta x_i)$$

$$\bar{W}_{f_i} = C_{w_i}\,|\bar{V}_{r_i}|\,\bar{V}_{r_i}$$

$$\bar{V}_{r_i} = \bar{Q}_i/\bar{A}_i - \bar{V}_{w_i}\cos\omega$$

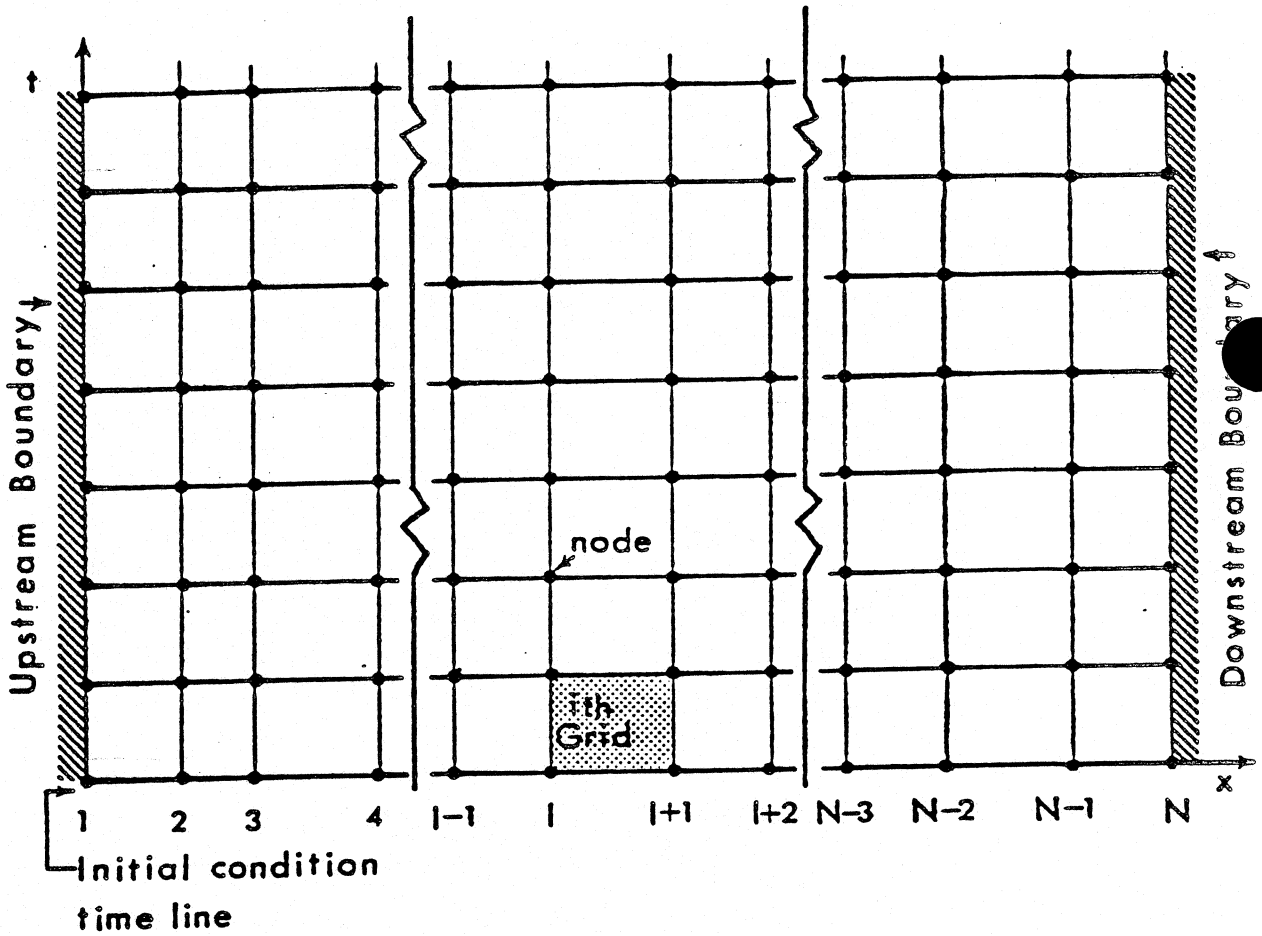

Fig. 4.4.--x-t solution plane showing time lines, nodes, grids, upstream and downstream boundaries, and initial condition time line.

Meandering Rivers with Flood Plains

$$A = A_c + A_L + A_R + A_S$$

Channel — left floodplain — right floodplain — Dead Storage

$$\frac{\partial (k_c Q)}{\partial x_c} + \frac{\partial (k_\ell Q)}{\partial x_\ell} + \frac{\partial (k_r Q)}{\partial x_r} + \frac{\partial (A_c + A_\ell + A_r + A_s)}{\partial t} = 0$$

$$\frac{\partial Q}{\partial t} + \frac{\partial (k_c^2 Q^2 / A_c)}{\partial x_c} + \frac{\partial (k_\ell^2 Q^2 / A_\ell)}{\partial x_\ell} + \frac{\partial (k_r^2 Q^2 / A_r)}{\partial x_r}$$

$$+ g A_c \left(\frac{\partial h}{\partial x_c} + S_{fc} + S_e \right) + g A_\ell \left(\frac{\partial h}{\partial x_\ell} + S_{f\ell} \right)$$

$$+ g A_r \left(\frac{\partial h}{\partial x_r} + S_{fr} \right) = 0$$

$$k_c = \frac{1}{1 + \frac{Q_\ell}{Q_c} + \frac{Q_r}{Q_c}} \qquad k_r = \frac{Q_r / Q_c}{1 + \frac{Q_\ell}{Q_c} + \frac{Q_r}{Q_c}}$$

$$k_\ell = \frac{Q_\ell / Q_c}{1 + \frac{Q_\ell}{Q_c} + \frac{Q_r}{Q_c}}$$

$$\frac{Q_l}{Q_c} = \frac{n_c}{n_l} \frac{A_l}{A_c} \left(\frac{R_l}{R_c}\right)^{2/3} \left(\frac{\Delta x_c}{\Delta x_l}\right)^{1/2}$$

$$\frac{Q_r}{Q_c} = \frac{n_c}{n_r} \frac{A_r}{A_c} \left(\frac{R_r}{R_c}\right)^{2/3} \left(\frac{\Delta x_c}{\Delta x_r}\right)^{1/2}$$

$$S_{f\,l} = \frac{n_l \,|k_l Q|\, k_l Q}{2.21\, A_l^{\,2}\, R_l^{\,4/3}}$$

Hydrological Forecasting
Edited by M. G. Anderson and T. P. Burt
© 1985 John Wiley and Sons Ltd.

CHAPTER 14

Channel routing

D. L. Fread
Hydrologic Research Laboratory,
National Weather Service, NOAA

14.1. INTRODUCTION

Channel routing is a mathematical method (model) to predict the changing magnitude, speed, and shape of a flood wave as it propagates through waterways such as canals, rivers, reservoirs, or estuaries. The flood wave can emanate from precipitation runoff (rainfall or snowmelt), reservoir releases (spillway flows or dam-failures), and tides (astronomical and/or wind-generated).

Channel routing has long been of vital concern to man as he has sought to predict the characteristic features of a flood wave in his efforts to improve the transport of water through man-made or natural waterways and to determine necessary actions to protect life and property from the effects of flooding. Commencing with investigations as early as the seventeenth century, mathematical techniques to predict wave propagation have continually been developed. With the contribution of Saint-Venant in 1871, the basic theory for one-dimensional analysis of flood wave propagation was formulated; however, due to the mathematical complexity of Saint-Venant's theoretical equations, simplifications were necessary to obtain feasible solutions for the salient characteristics of the wave. Thereafter, a profusion of simplified flood routing methods appeared in the literature. It is only within the last 25 years, with the advent of high-speed electronic computers, that the complete Saint-Venant equations could be solved with varying degrees of feasibility.

14.1.1 Scope

In this chapter an overview of the various types of one-dimensional channel routing models is presented first. Then a detailed description is given of a particular routing model (FLDWAV) which is representative of the current state of the art. This model has wide applicability and feasible computational

requirements, and it is popular with many hydrologists and engineers. It also serves as a framework in which many flood routing complexities can be described and solution techniques presented. Selected applications of the model are presented. Finally, some suggestions are offered concerning future requirements and directions in channel routing development.

All mathematical notation used herein is defined when first presented.

14.2 SYNOPSIS OF CHANNEL ROUTING MODELS

Commencing with investigations by such eminent scientists as Newton (1687), Laplace (1776), Poisson (1816), Boussinesq (1871), and culminating in the one-dimensional equations of unsteady flow derived by Saint-Venant (1871), the theoretical foundation for channel routing was essentially achieved. The original Saint-Venant equations consist of the conservation of mass equation:

$$\frac{\partial(AV)}{\partial x}+\frac{\partial A}{\partial t}=0 \tag{14.1}$$

and the conservation of momentum equation:

$$\frac{\partial V}{\partial t}+V\frac{\partial V}{\partial x}+g\left(\frac{\partial h}{\partial x}+S_f\right)=0 \tag{14.2}$$

in which t is time, x is distance along the longitudinal axis of the waterway, A is cross-sectional area, V is velocity, g is the gravity acceleration constant, h is the water surface elevation above a datum, and S_f is the friction slope which may be evaluated using a steady flow empirical formula such as the Chezy or Manning equation. These are quasi-linear hyperbolic partial differential equations with two dependent parameters (V and h) and two independent parameters (x and t). A is a known function of h, and S_f is a known function of V and h. No analytical solutions can be obtained. Derivations of the Saint-Venant equations can be found in the following references: Stoker (1957), Chow (1959), Henderson (1966), Strelkoff (1969), and Liggett (1975).

Due to the complexities of the Saint-Venant equations, their solution was not feasible, and various simplified approximations of flood wave propagation continued to be developed. An excellent summary of such is presented by Miller and Yevjevich (1975). The simplified methods may be categorized as: (1) purely emprical; (2) linearization of the Saint-Venant equations; (3) hydrological, i.e., based on the conservation of mass and an approximate relation between flow and storage; and (4) hydraulic, i.e., based on the conservation of mass and a simplified form of the conservation of momentum equation. In recent years a fifth category of flood routing models, based on the complete Saint-Venant equations, have become economically feasible as a result of advances in computing equipment and improved numerical solution techniques. Following is a brief review of several models in each of the five categories.

14.3 EMPIRICAL MODELS

Some routing models are purely empirical, based on intitution and observations of past flood waves. Empirical models are limited to applications with sufficient observations of inflows and outflows of a reach of waterway to calibrate the essential empirical relationships or routing coefficients. They give their best results when applied to slowly fluctuating rivers with negligible lateral inflows and backwater effects. They require minimal computational resources; however, considerable effort can be required to derive the empirical parameters.

14.3.1 Lag models

Lag is defined as the difference in time between inflow and outflow within a routing reach. The successive average-lag method developed by Tatum (1940), assumes that there is a point downstream where the flow (I_2) at time (t_2) is equal to an average flow, i.e. ($I_1 + I_2/2$. Tatum (1940) found that the number of successive averages occurring within a reach was approximately the time of travel of the wave divided by the reach length. Outflow (O) at the end of the reach is computed by:

$$O_{n+1}=C_1I_1+C_2I_2+\ldots C_{n+1}I_{n+1} \tag{14.3}$$

where n is the number of subreaches (successive averages) within the routing reach. The routing coefficients used in the method can be obtained via Tatum's approach or by trial and error using observed inflow and outflow hydrographs. The routing coefficients in equation (14.3) may also be obtained via a least-squares correlation of inflow and outflow hydrographs as described by Linsley *et al.* (1949). A similar lag model known as the progressive average-lag method was reported by Harris (1970).

14.3.2 Gauge relations

Empirical relationships which relate the flow at a downstream point to that at an upstream station known as gauge relations are described by Linsley *et al.* (1949). Gauge relations can be based on flow, water elevations, or a combination of each. The effect of lateral inflows is automatically contained in the empirical relation.

14.4 LINEARIZED MODELS

The complexity of the Saint-Venant equations has caused many scientists and engineers to simplify them in order to obtain solutions. The simplifications have been to either totally ignore the least important nonlinear terms and/or to linearize the remaining nonlinear terms in the equations. Given a sufficiently simplified form of the equations, they can be integrated analytically to obtain solutions of velocity and water surface elevation for any pair of (x,t) values at a relatively small expenditure of computational effort. Usually the most common simplifying assumptions are: (1) ignore the second term in equation (14.2); (2) constant cross-sectional area, usually rectangular; (3) constant channel bottom slope, often assumed to be zero; (4) the friction slope term is linearized with respect to velocity and depth; (5) no lateral inflow; and (6) the routed flood wave has a simple shape that is amenable to an analytical expression. These simplifications usually invoke severe limitations on the conditions for which the solution is valid. The applicability of a particular linearized model is limited by the assumptions in its derivation. The complete linearized model, Harley (1967), is the least restricted, although it is not appropriate when backwater effects exist due to the presence of tides, significant lateral inflows, dams, bridges, or cross-sectional irregularities.

14.4.1 Classical wave models

Neglecting lateral inflow, frictional resistance and nonlinear terms $V\partial A/\partial x$ and $V\,\partial V/\partial x$ in equations (14.1) and (14.2) respectively, the following classical linear wave equations may be obtained:

$$\frac{\partial^2 V}{\partial t^2} = gD\frac{\partial^2 V}{\partial x^2} \quad \text{and} \quad \frac{\partial^2 h}{\partial t^2} = gD\frac{\partial^2 h}{\partial x^2} \tag{14.4}$$

where D is the average depth. The analytical solutions of equations (14.4) have the following form (Abbott, 1966):

$$V = C_1'(x - \sqrt{gD}t) + C_2'(x + \sqrt{gD}t) \tag{14.5}$$

where C_1' and C_2' are functions determined by initial flow conditions and the boundary conditions.

Also, by assuming a rectangular cross-section, zero bottom slope, linearized resistance, and neglecting the $V\partial V/\partial x$ term, the following equation may be obtained after combining the resulting simplified forms of equations (14.1) and (14.2) and eliminating h;

$$gD\frac{\partial^2 V}{\partial x^2} = \frac{\partial^2 V}{\partial t^2} + gC_0'\frac{\partial V}{\partial t} \tag{14.6}$$

in which C_0' is a constant depending on the linearized resistance term. Equation (14.6) is in the form of the telegraph-equation which has been extensively studied (Dronkers, 1964).

14.4.2 Simple impulse response models

Linear systems theory has been used to develop routing techniques (Dooge, 1973). In this approach the routing model is assumed to be composed of linear reservoirs connected by linear channels. According to linear systems theory, any linear system is completely and uniquely characterized by its unit impulse response. By knowing the unit impulse response all possible system outputs may be determined for all possible inputs. The input–output relationship is defined by the convolution integral:

$$O(t) = \int_0^t I(t)H(t-\tau')d\tau' \tag{14.7}$$

in which $O(t)$ is the routed flow, $I(t)$ is the inflow, and $H(t-\tau')$ is the unit impulse response. The unit impulse response for a distributed linear reservoir was given by Maddaus (1969) as:

$$H_N(x,t) = \frac{1}{N}\sum_{m=1}^{N}\frac{e^{-(t-m\tau')/K}}{K\Gamma(m)}\left(\frac{t-m\tau'}{K}\right)^{m-1} \quad \ldots\ t > mt' \tag{14.8}$$

where N is the number of linear elements, $\Gamma(\ )$ is the gamma function, K is the characteristic linear reservoir time constant, and τ is a time constant. The parameters, k and τ, are obtained by a fitting procedure described by Maddaus. A similar unit-response approach for routing through a single linear reservoir was reported by Sauer (1973). This approach is analogous to the unit hydrograph used by hydrologists to compute rainfall runoff. Also, it is related to the lag methods.

14.4.3 Complete linearized models

Linearized models of the complete Saint-Venant equations were developed by Lighthill and Whitham (1955) and Harley (1967). If equations (14.1) and (14.2) are rewritten for a unit-width channel and in terms of unit discharge (q') and depth (y), and then combined and linearized about a reference flow velocity $(V_0 = q_0'/y_0)$, the following linearized equation is obtained:

$$(gy_0^3 - V_0^2)\frac{\partial^2 q'}{\partial x^2} - 2V_0\frac{\partial^2 q'}{\partial x\partial t} - \frac{\partial^2 q'}{\partial t^2} = 3gS_0\frac{\partial q'}{\partial qx} + 2g\frac{S_0}{V_0}\frac{\partial q'}{\partial t} \tag{14.9}$$

in which S_0 is the channel bottom slope. Harley *et al.* (1970) obtained the following unit response function for equation (14.9):

$$H(x,t) = e^{-Px}\,\delta(t - x/C_1) + h'(x/C_1 - x/C_2)e^{sx-rt}\,I[2h'm']/m' \tag{14.10}$$

where:

$$C_1 = V_0 + \sqrt{gy_0} \tag{14.11}$$

$$C_2 = V_0 - \sqrt{gy_0} \tag{14.12}$$

$$F = V_0/\sqrt{gy_0} \tag{14.13}$$

$$P = S_0(2-F)/[2y_0(F^2+F)] \tag{14.14}$$

$$r = S_0V_0(2+F^2)/(2y_0F^2) \tag{14.15}$$

$$s = S_0/(2y_0) \tag{14.16}$$

$$h' = S_0V_0[(4-F^2)(1-F^2)]^{1/2}/(4y_0F^2) \tag{14.17}$$

$$m' = [(t-x/C_1)(t-x/C_2)]^{1/2} \tag{14.18}$$

and $I[\ \ ]$ is a first-order Bessel function of the first kind and δ is the delta function. This model is similar to the diffusion analogy model developed by Hayami (Chow, 1959); however, it does not over-attenuate the flood wave as much as the simpler diffusion analogy model. The accuracy of the model is very dependent on the reference flow.

14.4.4 Multiple linearized models

Keefer and McQuivey (1974) presented an improved method for linearized models in which they introduced a multiple linearization technique for both the complete linearized model of Harley and the diffusion analogy model of Hayami (Chow, 1959); they concluded the latter was more practical.

14.5 HYDROLOGICAL MODELS

Significant river improvement projects in the early 1900s provided the impetus for development of an array of simplified flood routing methods. These have been termed hydrological models. They are based on the conservation of mass equation (14.1) written in the following form:

$$I - O = \Delta S/\Delta t \tag{14.19}$$

in which ΔS is the change in storage within the reach during a Δt time increment; the storage (S) is assumed to be related to inflow (I) and/or outflow (O), i.e.,

$$S = K[XI + (1-X)O] \tag{14.20}$$

in which K is a storage constant with dimensions of time (seconds), and X is a weighting coefficient, $0 \leqslant X \leqslant 1$. All hydrological models are limited to applications where the depth–discharge relation is single-valued. Thus backwater effects from tides, significant tributary inflow, dams or bridges are not considered by these models, nor are they well-suited for very mild sloping waterways where looped depth–discharge ratings may exist. Most hydrological models are also limited to applications where observed inflow–outflow hydrographs exist. When using the observed hydrographs to calibrate the routing coefficients, variations in flood wave shapes within the observed data set are not considered, and only the average wave shape is reflected in the fitted routing coefficients. Generally, the hydrological models have two parameters which can be calibrated to effectively reproduce the flood wave speed and its attenuated peak.

14.5.1 Storage routing models

Storage routing models attributed to Puls (1928) and Goodrich (1931) were developed by assuming X in equation (14.20) to be zero, i.e. storage is dependent only on outflow. Expressing equation (14.19) in centred finite difference form, the following reservoir routing model is obtained:

$$\frac{I_1+I_2}{2} - \frac{O_1+O_2}{2} = \frac{S_2-S_1}{\Delta t} \tag{14.21}$$

which can be rearranged as:

$$\frac{2S_2}{\Delta t} + O_2 = I_1 + I_2 + \frac{2S_1}{\Delta t} - O_1 \tag{14.22}$$

which can be solved step-by-step for the left-hand side since O_1 and S_1 are known at time $t=0$. An $S_2 = f(0)$ relationship obtained from observed inflow–outflow hydrographs allows the outflow (O_2) to be determined.

14.5.2 Muskingum model

If equation (14.20) with non-zero values for K and X is used for the storage relationship and this is substituted in equation (14.21), the following is obtained for computing O:

$$O_2 = C_1I_2 + C_2I_1 + C_3O_1 + C_4 \tag{14.23}$$

where:

$$C_0 = K - KX + \Delta t/2 \tag{14.24}$$

$$C_1 = -(KX - \Delta t/2)/C_0 \tag{14.25}$$

$$C_2 = (KX + \Delta t/2)/C_0 \tag{14.26}$$

$$C_3 = (K - KX - \Delta t/2)/C_0 \tag{14.27}$$

$$C_4 = 0.5(q_1 + q_2)\ \Delta x\ \Delta t/C_0 \tag{14.28}$$

Equation (14.23), which has been expanded to include the effects of lateral inflow (q) along the Δx routing reach, is the widely used Muskingum routing model first developed by McCarthy (1938). The parameters K and X are determined from observed inflow–outflow hydrographs using any of the following techniques (Singh and McCann, 1980): (1) least-squares or its equivalent, the graphical method; (2) method of moments; (3) method of cumulants; and (4) direct optimization method. Among the many descriptions and variations of the Muskingum model are: Linsley *et al.* (1949); Nash (1959); Diskin (1967), Strupczewski and Kundzewicz (1980); and Dooge *et al.* (1982).

14.5.3 Muskingum–Cunge model

A significant improvement of the Muskingum model was developed by Cunge (1969). Cunge derived equation (14.23) using the assumption of a single-valued depth–discharge relation, the classical kinematic wave equation (see equation (14.43)), and applying a four-point implicit finite difference approximation technique. Equation (14.23) remains the same, but the following expressions for K and X are determined:

$$K = \Delta x/c \tag{14.29}$$

$$X = 0.5[1 - q_0'/(cS_0\ \Delta x)] \tag{14.30}$$

where

$$c = \mathrm{d}Q/\mathrm{d}A \tag{14.31}$$

in which c is the kinematic wave speed corresponding to a unit-width reference discharge q_0', Δx is the reach length and S_0 is the channel bottom slope. Equation (14.31) may be expressed in an alternative form, i.e.:

$$c = 1.27\beta S_0^{0.3}/(q_0'^{\,0.4} n^{0.6}) \tag{14.32}$$

where:

$$\beta = 5/3 - 2/3\ \frac{A_0}{B_0^2}\ \mathrm{d}B/\mathrm{d}y \tag{14.33}$$

in which A_0 is the cross-sectional area corresponding to the total reference discharge (Q_0), B_0 is the channel width corresponding to Q_0, y is the depth of flow, and the Manning equation is used to relate friction, depth and velocity. Depending on the cross-section shape, β may have values in the range, $1 < \beta \leqslant 5/3$. Selection of the appropriate time step (Δt) is given by;

$$\Delta t = T_r/M \tag{14.34}$$

where T_r is the time of rise of the inflow hydrograph and M is an integer whose value ranges from 5 to 20, depending on the extent of variation in the inflow hydrograph. The selection of Δx affects the accuracy of the solution. It is related to Δt and is limited by the following inequality (Ponce, 1981):

$$\Delta x \leqslant 0.5[c\Delta t + q_0'/(cS_0)] \tag{14.35}$$

While the Muskingum–Cunge model does not require observed inflow–outflow hydrographs to establish the routing coefficients as required in the Muskingum model, best results are obtained if the wave speed (c) is determined from actual flow data. Also, the model is restricted to applications where backwater is not significant and channel rating curves do not have significant loops.

The Muskingum–Cunge model (Miller and Cunge, 1975; Weinmann and Laurenson, 1979) has created much interest in recent years as a highly versatile simplified routing model. Koussis (1978) and Ponce and Yevjevich (1978) have extended the model by using variable parameters c and B for temporally varying Q. Another model similar to the Cunge modification of the Muskingum model has been proposed by Koussis (1980).

14.5.4 Kalinin–Miljukov model

Another variation of the Muskingum model is the Kalinin–Miljukov model (Miller and Cunge, 1975), developed in 1958 in the USSR. This model has the following form:

$$O_2 = O_1 + (I_1 - O_1)K_1 + (I_2 - I_1)K_2 \tag{14.36}$$

where:

$$K_1 = 1 - \mathrm{e}^{-c\Delta t/\Delta x} \tag{14.37}$$

$$K_2 = 1 - K_1\Delta x/(c\Delta t) \tag{14.38}$$

$$\Delta x = O/S_0(\Delta y/\Delta O) \tag{14.39}$$

in which $\Delta y/\Delta O$ is the slope of the depth–outflow rating curve. Equation (14.36) is identical to the Muskingum model if in the latter, $K = \Delta x/c$ and $X = 0$.

Another variation of the Muskingum model is the SSARR routing model (Rockwood, 1958) which Miller and Cunge (1975) show is similar to the Muskingum model with X assumed to be zero.

14.5.5 Lag and route model

Another hydrological storage routing model is the Lag and K model (Linsley *et al.*, 1949). First, the inflow is lagged and then the outflow (O_2) at time (t_2) is determined by substituting the relation $S_1 - S_1 = K(O_2 - O_1)$ in equation (14.21) and solving for O_2, i.e.:

$$O_2 = [I_1 + I_2 - O_1(1 - 2K/\Delta t)]/(1 + 2K/\Delta t) \tag{14.40}$$

The extent of lag and the K parameter may be constants, or they can be functions of the inflow and outflow, respectively. Another lag and route model has been proposed by Quick and Pipes (1975).

14.6 SIMPLIFIED HYDRAULIC MODELS

The advent of computers made possible the development of another category of routing models based on equation (14.1) and various simplifications of equation (14.2). These models are classified as kinematic, diffusion, or quasi-steady depending on the terms retained in equation (14.2). The range of applicability of the kinematic and diffusion models has recently been treated by Ponce *et al.* (1978) who utilized a linear stability analysis of the finite difference form of the Saint-Venant equations. They compared wave attenuation factors and celerities and concluded that bottom slope and wave shape determine the range of their suitable applicability. In general, the steeper slopes associated with overland flow or steep streams with slow-rising floods are amenable to the use of kinematic models. The diffusion models have a wider range of applicability and can accommodate milder bottom slopes. However, there still remain many practical combinations of mild sloping channels and flood wave shapes that are not suitable for either diffusion or kinematic approximations and should be treated with the complete Saint-Venant equations.

14.6.1 Kinematic model

Interest in the kinematic model was initiated by Lighthill and Whitham (1955). There have been many forms of the kinematic model proposed; however, the basic assumption used in their derivation is that equation (14.2) can be simplified and expressed in the following form:

$$S_f - S_0 = 0 \tag{14.41}$$

in which $\partial h/\partial x = \partial y/\partial x - S_0$. Equation (14.41) implies that the momentum of the unsteady flow is assumed to be the same as that of steady uniform flow as described by the Chezy or Manning equation or a similar expression in which discharge is a single-valued function of depth, i.e. $\partial A/\partial Q = \mathrm{d}A/\mathrm{d}y = 1/c$ in which Q is discharge (flow) and c is the kinematic wave speed from equation (14.31) or (14.32). Also, since

$$\frac{\partial A}{\partial t} = \frac{\partial A}{\partial Q}\frac{\partial Q}{\partial t} \tag{14.42}$$

and $Q = AV$, equation (14.1) can be written as the classical kinematic equation, i.e.

$$\frac{\partial Q}{\partial t} + c\frac{\partial Q}{\partial x} = 0 \tag{14.43}$$

which can be solved by explicit or implicit finite difference methods, the latter being more efficient in most river applications. The kinematic wave model is limited to applications where single-valued depth–discharge ratings exist, and where backwater effects are insignificant, since in kinematic models flow disturbances can only propagate in the downstream direction. Also, the kinematic model modifies the flood wave through attenuation and dispersion via the errors inherent in the finite difference solution technique. The phenomenon of numerical damping merely mimics the actual physical damping of a flood wave since there is no mechanism in the basic kinematic equation to cause such damping. The kinematic wave models are very popular in applications to overland flow routing of precipitation runoff, e.g., Wooding (1965) and Woolhiser and Liggett (1967). Kinematic wave models have been used in channel routing by Harley *et al.* (1970) in the MIT catchment model and in the Hydrocomp model (Linsley, 1971).

14.6.2 Diffusion model

Another type of simplified hydraulic model is the diffusion model or zero-inertia model. The latter designation is derived from the basic assumption of this model that the inertia terms (first two) in equation (14.2) are insignificant. Thus, equation (14.2) takes the following form:

$$S_f + \partial h/\partial x = 0 \tag{14.44}$$

Equation (14.44) may be expressed in terms of channel conveyance K_c which is a single-valued function of elevation (h), i.e.,

$$Q = -K_c(h_x/|h_x|)(|h_x|)^{1/2} \tag{14.45}$$

where $h_x = \partial h/\partial x$. Equation (14.45) allows for upstream directed flows. Brakensiek (1965) solved equations (14.1) and (14.45) with a four-point centred implicit finite difference solution technique for reasons of computational efficiency. Harder and Armacost (1966) used an explicit finite difference solution technique for the diffusion routing model used by the Army Corps of Engineers (Harrison and Bueltel, 1973) on the Missouri River. This model is restricted to small time steps due to the numerical stability constraint given by:

$$\Delta t \leqslant BS_0^{1/2}\,\Delta x^2/(K_c + S_0\,\Delta x\,\Delta K_c/\Delta h) \tag{14.46}$$

in which B is the wetted top width of the channel. The nonlinear diffusion wave model is a significant improvement over the kinematic model because of the inclusion in equation (14.44) of the water surface slope term ($\partial h/\partial x$) of equation (14.1). This term allows the diffusion model to describe the attenuation (diffusion effect) of the flood wave. It also allows the specification of a boundary condition at the downstream extremity of the routing reach to account for backwater effects. It does not use the intertial (first two

terms) of equation (14.2) and, therefore, is limited to slow to moderately rising flood waves in channels of rather uniform geometry. Since inclusion of the inertial terms in an implicit (finite difference) solution of equation (14.44) in conjunction with equation (14.1) results in only a small increase in computational effort, the resulting dynamic model is generally preferred over the diffusion model due to the wider range of applicability of the dynamic wave model.

14.6.3 Quasi-steady model

A third type of simplified hydraulic model is the quasi-steady hydraulic model in which equation (14.1) is used along with equation (14.2) with all its terms except $\partial V/\partial t$. This simplification saves very little in computational effort and introduces more error than the simpler diffusion model. The quasi-steady model has been infrequently used, and its further use is not recommended.

14.7 COMPLETE HYDRAULIC MODELS

After the advent of high-speed computers, Stoker (1953) and Isaacson *et al.* (1954) first attempted to use the complete Saint-Venant equations for flood routing on the Ohio River. Since then, much effort has been expended in the development of the complete (dynamic wave) models. They are categorized according to the method of solution, i.e. direct or characteristic methods. In the direct methods finite difference approximations for the partial derivatives are substituted directly into equations (14.1) and (14.2), and solutions are obtained for incremental times (Δt) and distances (Δx) along the waterway. In the method of characteristics, the partial differential equations (14.1) and (14.2) are first transformed into an equivalent set of four ordinary differential equations which are then approximated with finite differences to obtain solutions. Dynamic models can be classified further as either explicit or implicit, depending on the type of finite difference scheme used in the solution. Explicit schemes transform the differential equations into a set of easily solved algebraic equations. However, implicit schemes transform the differential equations into a set of algebraic equations which must be solved simultaneously; the set of simultaneous equations may be either linear or nonlinear, the latter requiring an iterative solution procedure.

14.7.1 Characteristic models

Several methods of characteristic models were developed in the 1960s. Most were explicit, e.g. Liggett and Woolhiser (1967), Streeter and Wylie (1967), and Ellis (1970). Implicit characteristic models were reported by Amein (1966) and Wylie (1970). Characteristic models can have a curvilinear grid or a rectangular grid in the x–t solution domain (Abbott, 1966). The former is not practical for application in natural waterways of irregular geometry. The latter, known as the Hartree method, requires interpolation formulae meshed within the finite difference solution procedure. These restrictions have tended to discourage the application of characteristic models for flood routing. The characteristic models for prismatic channels are based on the following four total differential equations:

$$\mathrm{d}x/\mathrm{d}t - V - \sqrt{gA/B} = 0 \tag{14.47}$$

$$\mathrm{d}V/\mathrm{d}t + \sqrt{gB/A}\ \mathrm{d}y/\mathrm{d}t + g(S_f - S_0) + q(V - v_x)/A - \sqrt{gB/A}q/B = 0 \tag{14.48}$$

$$\mathrm{d}x/\mathrm{d}t - V + \sqrt{gA/B} = 0 \tag{14.49}$$

$$\mathrm{d}V/\mathrm{d}t - \sqrt{gB/A}\ \mathrm{d}y/\mathrm{d}t + g(S_f - S_0) + q(V - v_x)/A + \sqrt{gB/A}q/B = 0 \tag{14.50}$$

Equations (14.47)–(14.50) are equivalent to the Saint-Venant partial differential equations (14.1) and (14.2) except that lateral inflow (q) has been included. The term v_x is the velocity of the lateral inflow in the x-direction along the axis of the waterway, A is cross-sectional area, B is cross-sectional top width, and y is depth.

14.7.2 Explicit models

Explicit finite difference models advance the solution of the Saint-Venant equations point by point along one time line in the x–t solution domain until all the unknowns associated with that time line have been evaluated. Then, the solution is advanced to the next time line. In an explicit scheme the spatial derivatives and non-derivative terms are evaluated on the time line where the values of all variables are known. Only the time derivatives contain unknowns. Thus, in an explicit model, two linear algebraic equations are generated from the two Saint-Venant equations at each net point (node). Since the two equations can be solved directly for the unknowns, the equations are described as 'explicit'.

The development of explicit models began with the pioneering work of Stoker (1953). Among those who have reported on explicit models are Liggett and Woolhiser (1967), Martin and DeFazio (1969), and Strelkoff (1970). Dronkers (1969), Balloffet (1969) and Kamphuis (1970) applied explicit models to analyze tidal movement in estuaries. Garrison *et al.* (1969) and Johnson (1974) applied the explicit models for flood routing in rivers and reservoirs. Many variations of the explicit method have been developed, each based on a type of explicit finite difference scheme, e.g. the Stoker scheme, the diffusion scheme, and the leapfrog scheme. Descriptions and analyses of several explicit finite difference schemes have been given by Liggett and Cunge (1975).

In explicit models, equations (14.1) and (14.2) are usually expressed in the following form to enable an explicit solution of their finite difference approximations:

$$A\frac{\partial V}{\partial x}+V\frac{\partial A}{\partial x}+B_T\frac{\partial y}{\partial t}-q=0 \tag{14.51}$$

$$\frac{\partial V}{\partial t}+V\frac{\partial V}{\partial x}+g\left(\frac{\partial y}{\partial x}-S_0+S_f\right)+\frac{(V-v_x)q}{A}=0 \tag{14.52}$$

in which B_T is the wetted top width of the total cross-sectional area (active and inactive or off-channel storage areas). Also, the effect of lateral inflow (q) is included in equations (14.51) and (14.52).

Explicit models, although relatively simple compared to implicit models, have a restriction in the size of the computational time step (Δt) in order to achieve numerical stability. In the Stoker scheme the maximum permissible time step (Δt) is given by the following inequality (Garrison *et al.*, 1969):

$$\Delta t \leqslant \Delta x/[V+\sqrt{gA/B}+gn^2\,|V|\,\Delta x/(c_1R^{4/3})] \tag{14.53}$$

in which n is the Manning roughness coefficient, $c_1=1.0$ in metric units and $c_1=2.21$ in English units, and R is the hydraulic radius. The first two terms in the denominator are associated with the well-known Courant condition for stability of explicit schemes in frictionless flow. The third term accounts for the effects of friction. This inequality, or some slight modification thereof, is representative of all explicit models. An inspection of equation (14.53) indicates that the computational time step is substantially reduced as the hydraulic depth (A/B) increases. Thus, in large rivers it is not uncommon for time steps on the order of a few minutes or even seconds to be required for numerical stability even though the flood wave may be very gradual, having a duration in the order of weeks. Such small time steps cause the explicit method to be very inefficient in the use of computer time. Another disadvantage of explicit schemes is the requirement of equal Δx distance steps.

14.7.3 Implicit models

Implicit finite difference schemes advance the solution of the Saint-Venant equations from one time line to the next simultaneously for all points along the time line (the x-axis of the waterway) in the x–t solution domain of Figure 14.1. Thus, in an implicit model, a system of $2N$ algebraic equations is generated when finite difference approximations of the Saint-Venant equations are applied simultaneously to the N cross-sections along the x-axis. The system of algebraic equations so generated may be either linear or nonlinear, depending on the way non-derivative terms are approximated.

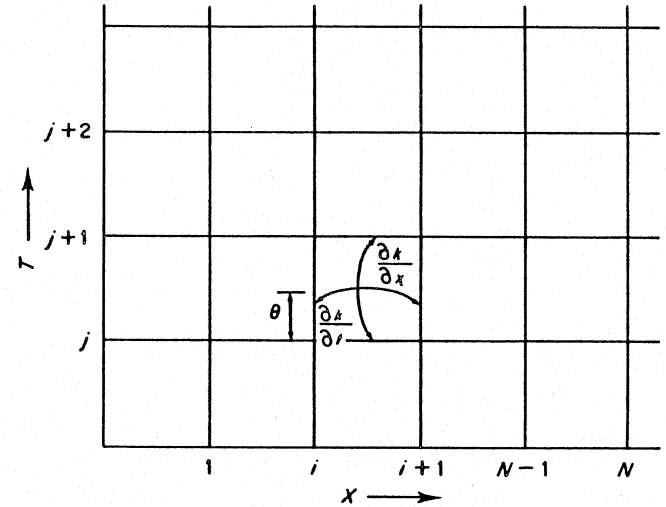

Figure 14.1 Discrete x–t solution domain

Implicit models were developed because of the limitations on the size of the time step required for numerical stability of explicit models. The use of implicit models was suggested by Isaacson *et al.* (1956) and first appeared in the literature in the early 1960s with the work of Preissmann (1961) and Vasiliev *et al.* (1965). Later, Abbott and Ionescu (1967), Baltzer and Lai (1968), Dronkers (1969), Amein and Fang (1970), Kamphuis (1970), Contractor and Wiggert (1972), Quinn and Wylie (1972), Fread (1973), Chaudhry and Contractor (1973), Greco and Panattoni (1975), Amein and Chu (1975), Chen and Simons (1975), Bennett (1975), and Fread (1976), were among those reporting their research with implicit methods.

Analysis of the numerical stability and accuracy of various implicit schemes has been reported by Cunge (1966), Abbott and Ionescu (1967), Dronkers (1969), Gunaratnam and Perkins (1970), Fread (1974), Liggett and Cunge (1975), and Ponce and Simons (1977). Within the simplifications required in making the numerical stability analyses, the various implicit methods were found to be unconditionally linearly stable, i.e. the simplified linearized versions of the Saint-Venant equations were numerically stable independent of the size of the time or distance steps. However, Chaudhry and Contractor (1973), Fread (1974) and Cunge (1975a) found that instability could occur for the implicit schemes if the time steps were too large and the x-derivative terms were not sufficiently weighted towards the future time line when modelling rapidly varying transients. Also, time steps are restricted in size for reasons of accuracy; Δt is found to depend upon the shape of the wave, the Courant condition, the Δx step size, and the type of implicit scheme used. Nonlinearities

due to irregular cross-sections having widths that vary rapidly in the x-direction along the waterway or in the vertical direction can also cause numerical instabilities.

Implicit models are computationally more complex than explicit models. Depending on the type of implicit scheme (linear or nonlinear), the number of computations during a time step are several times greater than that of an explicit scheme. This extra computational requirement is very much greater if the method of solving the system of simultaneous equations is not efficient by taking advantage of the banded-structure of the coefficient matrix of the system of equations. Efficient solution techniques include the following: (1) a compact penta-diagonal elimination method described by Fread (1971) which makes use of the banded structure of the coefficient matrix of the system of equations, or (2) the double-sweep method developed in Europe (Liggett and Cunge, 1975). If the implicit scheme is linear, only one solution of the system of equations is required at each time step. However, if the implicit scheme is nonlinear, an iterative solution is necessary, and this requires one or more solutions of the system of equations at each time step. The use of the Newton–Raphson iterative method for nonlinear systems of equations (Amein and Fang, 1970) provides a very efficient solution if selected convergence criteria are practical. If the Newton–Raphson method is applied only once, the nonlinear implicit model is essentially equivalent to the linearized implicit models with respect to computational effort and performance.

Nonlinear implicit methods can be based on the conservation form of the Saint-Venant equations including lateral flow q (inflow is positive, outflow is negative) and off-channel (inactive flow) storage area A_0, with dependent variables discharge (Q) and water elevation (h), i.e.,

$$\frac{\partial Q}{\partial x} + \frac{\partial (A + A_0)}{\partial t} - q = 0 \tag{14.54}$$

$$\frac{\partial Q}{\partial t} + \frac{\partial (Q^2/A)}{\partial x} + gA\left(\frac{\partial h}{\partial x} + S_f\right) + L = 0 \tag{14.55}$$

where $L = -qv_x$ for lateral inflow, $L = -qQ/A$ for bulk lateral outflow, and $L = -qQ/(2A)$ for seepage lateral outflow. An important advantage of equations (14.54) and (14.55) when they are expressed in finite difference form is their ability to accurately describe steep-fronted waves in waterways of non-prismatic geometry.

Linear implicit methods often utilize an expanded form of equations (14.54) and (14.55) such as that used by Chen and Simons (1975), i.e.

$$\frac{\partial Q}{\partial x} + B_T \frac{\partial y}{\partial t} - q = 0 \tag{14.56}$$

$$\frac{\partial Q}{\partial t} + 2\frac{Q}{A}\frac{\partial Q}{\partial x} - \frac{Q^2}{A^2}\left[B\frac{\partial y}{\partial x} + \left(\frac{\partial \tilde{A}}{\partial x}\right)\right] + gA\left(\frac{\partial y}{\partial x} - S_0 + S_f\right) + L = 0 \tag{14.57}$$

in which B_T is the total top width (active and inactive), $(\partial \tilde{A}/\partial x)$ is the variation of A with respect to x with the depth (y) held constant, and S_f is expanded in a Taylor series in order to linearize this highly nonlinear term, i.e.,

$$S_f^{t+\Delta t} = S_f^t + (\partial S_f/\partial Q)^t (Q^{t+\Delta t} - Q^t) + (\partial S_f/\partial y)^t (y^{t+\Delta t} - y^t) \tag{14.58}$$

in which the superscripts (t and $t + \Delta t$) indicate at which time line the term is evaluated. In linear methods the accuracy of the solution is quite dependent on the size of Δt if the flow is rapidly changing with time due to the assumption of linearity of flow throughout a time step.

Implicit schemes have generally been four-point, i.e., the conservation of mass and momentum equations have been applied to the flow existing between two adjacent cross-sections. The weighted four-point scheme allows a convenient flexibility in the placement of x-derivative and non-derivative terms between two adjacent time lines in the x–t solution domain. The weighting factor must be equal to or greater than 1/2 to provide unconditional linear stability with respect to time step size, and the accuracy of the scheme generally decreases as the weighting factor approaches unity, i.e., when the terms are expressed entirely at the forward time line. A few six-point schemes have been proposed, e.g. Abbott and Ionescu (1967) and Vasiliev *et al.* (1965), but they have the disadvantage of requiring regular Δx intervals whereas the four-point schemes allow variable Δx spacing. Also, the six-point schemes treat the boundary conditions in a more complicated manner than the four-point schemes.

14.7.4 Finite element models

The method of finite elements (Gray *et al.*, 1977) can also be applied to the complete Saint-Venant equations, e.g. Cooley and Moin (1976). Although this method of solution is popular in two-dimensional unsteady flow models, it does not appear to offer any advantages over the four-point nonlinear implicit models for the Saint-Venant one-dimensional equations of unsteady flow. Also, the mathematical basis for finite element solution schemes is not as easily understood as the finite difference approach. It seems that the personal preference of the model developer is the determining factor in selection of finite element or finite difference solution methods for the Saint-Venant equations.

14.7.5 Two-dimensional models

The unsteady flow equations when formulated in the x-direction as in equations (14.1) and (14.2), and also in the horizontal direction perpendicular to

the x-axis, become two-dimensional equations which form the basis for an array of models summarized by Hinwood and Wallis (1975a,b) and Abbott (1976), Abbott and Cunge (1975), Grupert (1976), and the simplified models described by Cunge (1975b) and Vicens *et al.* (1975). These models are beyond the intended scope and have been omitted from consideration herein. They are considerably more expensive to calibrate and execute on high-speed computers than the one-dimensional models. They are often used as an alternative modelling approach whenever a large amount of flow information is desired in complex unsteady flows associated with oceans and bays and water quality prediction therein and in estuarial networks.

14.8 MODEL SELECTION

Channel routing has been an important type of engineering analysis, and this importance, along with its inherent complexity, have resulted in the proliferation of routing models. The literature abounds with a wide spectrum of usable and reasonably accurate mathematical models for channel routing when each is used within the bounds of its limitations.

The selection of a channel routing model for a particular application is influenced by the relative importance one places on the following factors: (1) model accuracy; (2) the accuracy required in the application; (3) the type and availability of required data; (4) the available computational facilities; (5) the computational costs; (6) the extent of flood wave information desired; (7) one's familiarity with a given model; (8) the extent of documentation, range of applicability, and availability of a 'canned' or packaged routing model; (9) the complexity of the mathematical formulation if the routing model is to be totally developed from 'scratch' (coded for computer); and (10) one's capability and time available to develop a particular type of routing model. Taking all factors into consideration, and recognizing that each application may change the relative importance of each factor, it is apparent that there is no universally superior routing model.

In the absence of significant backwater effects, the hydrological storage routing models offer the advantage of simplicity. They hydrological models have two parameters which can be calibrated to effectively reproduce the simple characterisics of a flood wave such as its celerity and crest attenuation. The accuracy considerations restrict the hydrological and kinematic models to applications where the depth–discharge relation is essentially single-valued. Following the analysis of Ponce and Simons (1977), and Ponce *et al.* (1978) approximate criteria for their acceptable range of application can be formulated. For kinematic-type models including the Muskingum model, the following criterion will restrict routing errors to less than about 5 per cent:

$$T_r S_0^{1.6}/(q_0'^{\,0.2} n^{1.2}) \geqslant 0.014 \qquad (14.59)$$

A similar criterion for diffusion-type models including the Muskingum–Cunge model is:

$$T_r S_0^{1.15}/(q_0' n)^{0.3} \geqslant 0.0003 \qquad (14.60)$$

in which T_r is time of rise (hours) of the inflow hydrograph, S_0 is the channel slope, q_0' is a unit-width reference discharge, and n is the Manning coefficient.

Inspection of equations (14.59) and (14.60) reveals the importance of the parameters, T_r and S_0. Also it is apparent that the diffusion models are applicable for a wider range of bottom slopes and hydrographs than the kinematic models. In instances of a gently sloping channel and rapidly rising flood wave, when the combination of S_0 and T_r becomes small enough that equation (14.60) cannot be satisfied, the complete hydraulic (dynamic wave) models are required. The simple Muskingum–Cunge model can be used effectively in many applications where equation (14.60) is satisfied and backwater effects are not significant. However, as the trend continues for increasing computational speed and storage capabilities of computers at decreasing costs, accessibility to inexpensive computational resources should increase the feasibility of using the dynamic wave models for a wider range of applications.

Among the models reviewed, the hydraulic models based on the complete Saint-Venant equations have the capability to correctly simulate the widest spectrum of wave types and waterway characteristics. Since the dynamic wave models contain only one calibration parameter (the roughness coefficient), they are very amenable to the calibration process. Also, since the roughness coefficient can be estimated with some degree of accuracy from inspection of waterways or, better still, from minimal depth–discharge data, any of the hydraulic flood routing models or the Muskingum–Cunge model can be used when there is a scarcity of pertinent inflow–outflow observations such as in the case of ungauged rivers or proposed man-made changes to waterways. The hydraulic (dynamic wave) models are preferred over all other models when: (1) the backwater effect is important due to tides, significant tributary inflows, dams, and/or bridges; and (2) the upstream propagation of waves can occur from large tides and storm surges or very large tributary inflows. The implicit dynamic wave model is the most efficient and versatile, although the most complex, of the complete hydraulic models. A detailed description of such a model follows.

14.9 STRUCTURE OF THE DYNAMIC WAVE MODEL (FLDWAV)

The FLDWAV model is a synthesis of two widely used models, DWOPER (Fread, 1978) and DAMBRK (Fread, 1980). In addition, FLDWAV has significant modelling capabilities not available in either of the other models. FLDWAV is a generalized dynamic wave model for one-dimensional unsteady flows in a single or branched waterway. It is based on an implicit four-point,

nonlinear) finite difference solution of the Saint-Venant equation. The following special features are included in FLDWAV: variable Δt and Δx computational intervals; irregular cross-sectional geometry; off-channel storage; roughness coefficients which vary with discharge or water surface elevation, and distance along the waterway; capability to generate linearly interpolated cross-sections and roughness coefficients between input cross-sections; automatic computation of initial steady flow and water elevations at all cross-sections along the waterway; external boundaries of discharge or water surface elevation time series (hydrographs), a single-valued or looped depth–discharge relation (tabular or computed); time-dependent lateral inflows (outflows); internal boundaries which enable the treatment of time-dependent dam failures, spillway flows, gate controls, bridge flows, bridge-embankment overtopping flow; short-circuiting of floodplain flow in a valley with a meandering river; levee failure and/or overtopping; a special computational technique to provide numerical stability when treating flows which change from supercritical to subcritical or, conversely, with time and distance along the waterway; and an automatic calibration technique for determining the variable roughness coefficient by using observed hydrographs along the waterway.

FLDWAV is coded in FORTRAN IV and the computer program is of modular design with each subroutine requiring less than 64,000 bytes of storage. Overall program storage requirement is approximately 256,000 bytes. Program array sizes are variable with the size of each array set internally via the input parameters used to describe the particular unsteady flow application for which the model is being used. Input data to the program is free or fixed-format. Program output is user-selective and consists of tabular and/or graphical displays.

14.10 BASIC ALGORITHM

FLDWAV is based on an implicit finite difference solution of the conservation form of the Saint-Venant equations of unsteady flow. In their conservation form, the equations consist of the conservation of mass equation, i.e.,

$$\frac{\partial Q}{\partial x} + \frac{\partial (A + A_0)}{\partial t} - q = 0 \tag{14.61}$$

and the conservation of momentum equation, i.e.,

$$\frac{\partial Q}{\partial t} + \frac{\partial (Q^2/A)}{\partial x} + gA\left(\frac{\partial h}{\partial x} + S_f + S_e\right) + L + W_f B = 0 \tag{14.62}$$

where:

$$S_f = \frac{n^2 |Q| Q}{2.21 A^2 R^{4/3}} = \frac{|Q| Q}{K_c^2} \tag{14.63}$$

$$S_e = \frac{K_e \partial (Q/A)^2}{2g\, \partial x} \tag{14.64}$$

$$W_f = C_w |V_r| V_r \tag{14.65}$$

in which x is distance along the longitudinal axis of the waterway, t is time, Q is discharge, A is active cross-sectional area, A_0 is inactive (off-channel storage) cross-sectional area, q is lateral inflow (positive) or outflow (negative), g is the gravity acceleration constant, h is water surface elevation, B is wetted top width of cross-section, L is the momentum effect of lateral inflow, S_f is friction slope computed from Manning's equation, n is the Manning n, R is the hydraulic radius approximated by (A/B), K_c is the channel conveyance factor, S_e is the local loss slope, K_e is an expansion (negative) or contraction (positive) coefficient, W_f is the wind term, C_w is non-dimensional wind coefficient, V_r is the velocity of the wind (V_w) relative to the velocity of the channel flow where the acute angle between the wind direction and channel flow direction is ω and V_w is $(-)$ if aiding the flow.

In an implicit finite difference solution of equations (14.61) and (14.62), the continuous x–t solution domain in which solutions of h and Q are sought is represented by a rectangular net of discrete points as shown in Figure 14.1. The net points (nodes) may be at equal or unequal intervals of Δt and Δx along the t and x axes, respectively. Each node is identified by a subscript (i) which designates the x position and a superscript (j) for the time line. A four-point weighted, implicit difference approximation is used to transform the nonlinear partial differential equations of Saint-Venant into nonlinear algebraic equations. The four-point weighted difference approximations are:

$$\frac{\partial K}{\partial t} = (K_i^{j+1} + K_{i+1}^{j+1} - K_i^j - K_{i+1}^j)/(2\,\Delta t^j) \tag{14.66}$$

$$\frac{\partial K}{\partial x} = \theta/\Delta x_i (K_{i+1}^{j+1} - K_i^{j+1}) + (1-\theta)/\Delta x_i (K_{i+1}^j - K_i^j) \tag{14.67}$$

$$K = 0.5\theta(K_i^{j+1} + K_{i+1}^{j+1}) + 0.5(1-\theta)(K_i^j + K_{i+1}^j) \tag{14.68}$$

where K is a dummy parameter representing any variable in the above differential equations, θ is a weighting factor varying from 0.5 to 1, i is a subscript denoting the sequence number of the cross-section or Δx reach, and j is a superscript denoting the sequence number of the time line in the x–t solution domain. A θ value of 0.5 is known as the 'box' scheme while $\theta = 1$ is the 'fully implicit' scheme. To insure unconditional linear numerical stability and provide good accuracy, θ values nearer to 0.5 are recommended (Fread, 1974). Accuracy decreases as θ departs from 0.5 and approaches 1.0. This effect becomes more pronounced as the time step size increases. FLDWAV allows θ to be an

input parameter. A value of 0.55 to 0.60 is often used to minimize loss of accuracy while avoiding weak or pseudo-instability which sometimes results when θ of 0.5 is used.

Substitution of the finite difference approximations defined by equations (14.66)–(14.68) into equations (14.61) and (14.62) for the derivatives and non-derivative terms and multiplying through by Δx_i yields the following difference equations:

$$\theta(Q_{i+1}^{j+1} - Q_i^{j+1} - \bar{q}_i^{j+1}\,\Delta x_i) + (1-\theta)(Q_{i+1}^{j} - Q_i^{j} - \bar{q}_i^{j}\,\Delta x_i) + 0.5\,\Delta x_i/\Delta t^j[(A+A_0)_i^{j+1} + (A+A_0)_{i+1}^{j+1} - (A+A_0)_i^j - (A+A_0)_{i+1}^j] = 0 \tag{14.69}$$

$$0.5\,\Delta x_i/\Delta t^j(Q_{i+1}^{j+1} + Q_i^{j+1} - Q_i^j - Q_{i+1}^j) + \theta[(Q^2/A)_{i+1}^{j+1} - (Q^2/A)_i^{j+1} + g\bar{A}_i^{j+1}(h_{i+1}^{j+1} - h_i^{j+1} + \Delta x_i\bar{S}_{f_i}^{j+1} + \Delta x_i\bar{S}_{e_i}^{j+1}) + \Delta x_i(L + \bar{W}_f\bar{B})_i^{j+1}] + (1-\theta)[(Q^2/A)_{i+1}^j - (Q^2/A)_i^j + g\bar{A}_i^j(h_{i+1}^j - h_i^j + \Delta x_i\bar{S}_{f_i}^j + \Delta x_i\bar{S}_{e_i}^j) + \Delta x_i(L + \bar{W}_f\bar{B})_i^j] = 0 \tag{14.70}$$

where:

$$\bar{A}_i = 0.5(A_i + A_{i+1}) \tag{14.71}$$

$$\bar{B}_i = 0.5(B_i + B_{i+1}) \tag{14.72}$$

$$\bar{S}_{f_i} = \frac{\bar{n}_i^2\,|\bar{Q}_i|\,\bar{Q}_i}{2.21\bar{A}_i^2 R_i^{4/3}} = |\bar{Q}_i|\,\bar{Q}_i/\bar{K}_{c_i}^2 \tag{14.73}$$

$$\bar{Q}_i = 0.5(Q_i + Q_{i+1}) \tag{14.74}$$

$$R_i = \bar{A}_i/\bar{B}_i \tag{14.75}$$

$$\bar{K}_{c_i} = 0.5(K_{c_i} + K_{c_{i+1}}) \tag{14.76}$$

$$\bar{S}_{e_i} = K_{e_i}[(Q/A)_{i+1}^2 - (Q/A)_i^2]/(2g\,\Delta x_i) \tag{14.77}$$

$$\bar{W}_{f_i} = C_{w_i}\,|\bar{V}_{r_i}|\,\bar{V}_{r_i} \tag{14.78}$$

$$\bar{V}_{r_i} = \bar{Q}_i/\bar{A}_i - \bar{V}_{w_i}\cos\omega \tag{14.79}$$

$$\bar{L}_i = -(\bar{q}v_{x_i}) \quad \text{(lateral inflow)} \tag{14.80}$$

$$L_i = -(\bar{q}\bar{Q}/\bar{A})_i \quad \text{(bulk lateral outflow)} \tag{14.81}$$

$$L_i = -(0.5\bar{q}\bar{Q}/\bar{A})_i \quad \text{(seepage lateral outflow)} \tag{14.82}$$

The bar (–) above the variables represents the average of the variable over the reach length (Δx_i) between cross-sections i and $i+1$. The subscript (i) associated with $\bar{q}$, $\bar{v}_x$, $\bar{A}$, $\bar{B}$, $\bar{S}_f$, $\bar{Q}$, $\bar{S}_e$, $\bar{W}_f$, $\bar{V}_r$, and $\bar{V}_w$ represents the number of the reach (Δx_i) rather than the cross-section (node) number. Node numbers commence with 1 and terminate with N, while reach numbers commence with 1 and terminate with $(N-1)$.

Equations (14.69) and (14.70) are nonlinear with respect to the unknowns h and Q at the points i and $i+1$ on the $j+1$ time line. All terms associated with the jth time line are known from either the initial conditions or previous computations. The initial conditions are values of h and Q at each computational point (node) along the x-axis for the first time line ($j=1$).

Equations (14.69) and (14.70) are two nonlinear algebraic equations which cannot be solved in a direct (explicit) manner since there are four unknowns h and Q, at points i and $(i+1)$ on the $(j+1)$ time line and only two equations. However, if similar equations are formed for each of the $(N-1)$ Δx reaches between the upstream and downstream boundaries, a total of $(2N-2)$ equations with $2N$ unknowns results. (N denotes the total number of computational points or cross-sections.) Then prescribed boundary conditions, one at the upstream extremity of the waterway and one at the downstream extremity, provide the additional two equations required for the system to be determinate. The resulting system of $2N$ nonlinear equations with $2N$ unknowns is solved by the Newton–Raphson method which was first applied by Amein and Fang (1970) to an implicit nonlinear formulation of the Saint-Venant equations.

14.10.1 Newton–Raphson method

The Newton–Raphson method is a functional iterative technique to solve a system of nonlinear equations. The technique is derived from a Taylor series expansion of the nonlinear function in which all terms of second and higher order are neglected. The resulting algorithm is:

$$J'(X^k)\,\Delta X = -f(X^k) \tag{14.83}$$

in which X^k is a vector quantity, J' is the Jacobian (a coefficient matrix made up of the partial derivatives evaluated with X^k values), $f(X^k)$ is the nonlinear equation evaluated with X^k values, and ΔX is a vector containing the $2N$ unknowns. Equation (14.83) represents a system of equations in which the unknown vector ΔX is linear. Solution of equation (14.83) for the unknown ΔX is by an appropriate matrix inversion technique such as Gauss elimination. The ΔX vector actually represents the difference between an initial estimate of the true solution and an improved estimate, i.e.

$$\Delta X = X^{k+1} - X^k \tag{14.84}$$

in which k is the number of iteration, X^k is the initial estimate (guess) and X^{k+1} is the improved estimate. Convergence of the iterative solution is attained in usually one or two iterations when the ΔX vector containing the

unknown discharges (Q_i^{j+1}, Q_{i+1}^{j+1}) and water elevations (h_i^{j+1}, h_{i+1}^{j+1}) becomes less than convergence criteria which are specified for each application of FLDWAV. Typical values are 0.01 feet for convergence of water elevation (ϵ_h) while the convergence for the discharge is specified in ft^3/s according to the following relation;

$$\epsilon_Q = \epsilon_h \hat{B} \hat{V} \tag{14.85}$$

in which $\hat{B}$ and $\hat{V}$ are the representative channel width and velocity, respectively.

The convergence process depends on a good first estimate for the vector X^k. A reasonably accurate initial condition of the discharges and water elevations at $t=0$ provides the first X^k. Thereafter, X^k first estimate values can be obtained using extrapolated values from solutions at previous time steps according to the following algorithm:

$$X^k = X^{j-1} + (X^{j-1} - X^{j-2})\alpha' \ \Delta t^j/\Delta t^{j-1} \tag{14.86}$$

where Δt^j and Δt^{j-1} are values of time steps between the time lines corresponding to the solution vectors, X^j and X^{j-1}, respectively. The weighting actor α' can be specified over the range of zero to unity.

The Jacobian matrix, $J'(X^k)$, is composed of elements ($a_{l,k}$) located along the main-diagonal with two elements in rows 1 and $2N$ which represent the upstream and downstream external boundaries, respectively; and all other rows have four elements which represent the partial derivatives of equations (14.69) and (14.70) with respect to the four unknowns (Q_i^{j+1}, h_i^{j+1}, Q_{i+1}^{j+1}, h_{i+1}^{j+1}). Each adjacent pair of rows represent the application of equations (14.69) and (14.70) to each Δx_i reach along the waterway proceeding from the upstream to the downstream boundary.

Letting $\hat{C}$ represent equation (14.69) and $\hat{M}$ represent equation (14.70), their derivatives can be expressed as follows:

$$a_{l,k} = \partial\hat{C}/\partial Q_i^{j+1} = -\theta \tag{14.87}$$

$$a_{l,k+1} = \partial\hat{C}/\partial h_i^{j+1} = (B+B_0)_i^{j+1} 0.5 \ \Delta x_i/\Delta t^j \tag{14.88}$$

$$a_{l,k+2} = \partial\hat{C}/\partial Q_{i+1}^{j+1} = \theta \tag{14.89}$$

$$a_{l,k+3} = \partial\hat{C}/\partial h_{i+1}^{j+1} = (B+B_0)_{i+1}^{j+1} 0.5 \ \Delta x_i/\Delta t^j \tag{14.90}$$

$$\begin{aligned} a_{l+1,k} &= \partial\hat{M}/\partial Q_i^{j+1} = 0.5 \ \Delta x_i/\Delta t^j + \theta\{-2(Q/A)_i^{j+1} \\ &\quad + g\bar{A}_i^{j+1} \ \Delta x_i[(\partial\bar{S}_f/\partial Q)_i^{j+1} + (\partial\bar{S}_e/\partial Q)_i^{j+1}] + \Delta x_i(\partial L/\partial Q)_i^{j+1}\} \end{aligned} \tag{14.91}$$

$$\begin{aligned} a_{l+1,k+1} &= \partial\hat{M}/\partial h_i^{j+1} = \theta\{(BQ^2/A^2)_i^{j+1} + 0.5gB_i^{j+1}(h_{i+1}^{j+1} - h_i^{j+1} \\ &\quad + \Delta x_i\bar{S}_{f_i}^{j+1} + \Delta x_i\bar{S}_{e_i}^{j+1}) + g\bar{A}_i^{j+1}[-1 + \Delta x_i(\partial\bar{S}_f/\partial h)_i^{j+1} \\ &\quad + \Delta x_i(\partial\bar{S}_e/\partial h)_i^{j+1}] + \Delta x_i[(\partial L/\partial h)_i^{j+1} + 0.5(\overline{W}_f \ dB/dh)_i^{j+1}]\} \end{aligned} \tag{14.92}$$

$$\begin{aligned} a_{l+1,k+2} &= \partial\hat{M}/\partial Q_{i+1}^{j+1} = 0.5 \ \Delta x_i/\Delta t^j + \theta\{2(Q/A)_i^{j+1} \\ &\quad + g\bar{A}_i^{j+1} \ \Delta x_i[(\partial\bar{S}_f/\partial Q)_{i+1}^{j+1} + (\partial\bar{S}_e/\partial Q)_{i+}^{j+}] + \Delta x_i(\partial L/\partial Q)_{i+1}^{j+1}\} \end{aligned} \tag{14.93}$$

$$\begin{aligned} a_{l+1,k+3} &= \partial\hat{M}/\partial h_{i+1}^{j+1} = \theta\{(-BQ^2/A^2)_{i+1}^{j+1} + 0.5gB_{i+1}^{j+1}(h_{i+1}^{j+1} - h_i^{j+1} \\ &\quad + \Delta x_i\bar{S}_{f_i}^{j+1} + \Delta x_i\bar{S}_{e_i}^{j+1}) + g\bar{A}_i^{j+1}[1 + \Delta x_i(\partial\bar{S}_f/\partial h)_{i+1}^{j+1} \\ &\quad + \Delta x_i(\partial\bar{S}_e/\partial h)_{i+1}^{j+1}] \ \Delta x_i[(\partial L/\partial h)_{i+1}^{j+1} + 0.5(\overline{W}_f \ dB/dh)_{i+1}^{j+1}]\} \end{aligned} \tag{14.94}$$

where:

$$\partial\bar{S}_f/\partial Q = \bar{S}_f/(1/\bar{Q} + 1/\bar{n} \ \Delta\bar{n}/\Delta\tilde{Q}) \tag{14.95}$$

$$\partial\bar{S}_f/\partial h = 2\bar{S}_f\left[\frac{d\bar{n}/dh}{\bar{n}} - \frac{5B}{6\bar{A}} + \frac{dB/dh}{3\bar{B}}\right] = \frac{-\bar{S}_f \ dK_c/dh}{\bar{K}_c} \tag{14.96}$$

$$dB/dh = \Delta B/\Delta h \tag{14.97}$$

$$d\bar{n}/dh = 0.5 \ \Delta\bar{n}/\Delta\bar{h} \tag{14.98}$$

$$dK_c/dh = \Delta K_c/\Delta h \tag{14.99}$$

$$(\partial\bar{S}_e/\partial Q)_i^{j+1} = [-K_eQ/(g \ \Delta x A^2)]_i^{j+1} \tag{14.100}$$

$$(\partial\bar{S}_e/\partial Q)_{i+1}^{j+1} = [K_eQ/(g \ \Delta x A^2)]_{i+1}^{j+1} \tag{14.101}$$

$$(\partial\bar{S}_e/\partial h)_i^{j+1} = [K_eQ^2B/(g \ \Delta x A^3)]_i^{j+1} \tag{14.102}$$

$$(\partial\bar{S}_e/\partial h)_{i+1}^{j+1} = [-K_eQ^2B/(g \ \Delta x A^3)]_{i+1}^{j+1} \tag{14.103}$$

$$\partial L/\partial Q = 0 \tag{14.104}$$

(lateral inflow)

$$\partial L/\partial h = 0 \tag{14.105}$$

$$\partial L/\partial Q = -0.5\bar{q}/\bar{A} \tag{14.106}$$

(bulk lateral outflow)

$$\partial L/\partial h = 0.5\bar{q}\bar{Q}B/\bar{A}^2 \tag{14.107}$$

$$\partial L/\partial Q = -0.25\bar{q}/\bar{A} \tag{14.108}$$

(seepage outflow)

$$\partial L/\partial h = 0.25\bar{q}\bar{Q}B/\bar{A}^2 \tag{14.109}$$

In equations (14.87)–(14.94), the subscripts (l and k) denote the row and column of the element ($a_{l,k}$) within the Jacobian matrix. The subscript (l) has a value of 2 for the first Δx reach and increments by 2 for each successive Δx reach proceeding from the upstream boundary to downstream boundary. The subscript (k) has a value of 1 for the first Δx reach and increments by 2 for each successive Δx reach.

Thus, the Newton–Raphson method generates a system of $2N \times 2N$ linear equations. The Jacobian or coefficient matrix of the system is composed of the partial derivative expressions evaluated at the first estimate, X^k. The right-hand side of equation (14.83) is the residual, a vector whose values are obtained by evaluating equations (14.69) and (14.70) using the X^k estimate values for the unknown discharges and water surface elevations. Solution of the linear system described by equation (14.83) provides corrections to the first trial (estimated) values of the unknowns.

14.10.2 Matrix solution

An efficient matrix solution technique is critical to the feasibility of an implicit model. Equation (14.83) is solved by a special modification of the Gauss elimination method for solving a system of linear equations. Using matrix notation, equation (14.83) takes the following form:

$$[A]X = R \tag{14.110}$$

in which $[A]$ = the coefficient matrix with elements $a_{l,k}$ and X, R are column vectors having components x_l and r_l respectively. The coefficient matrix is banded with most of the elements being zero except for four elements in each row along the main diagonal of the matrix. An efficient solution technique was developed by Fread (1971) in which (1) the computations do not involve any of the many zero elements, thus reducing the required number of operations (addition, subtraction, division, multiplication) from $(16/3N^3 + 8N^2 + 14/3N)$ to $(38N - 19)$; and (2) stores only the non-zero elements, thus reducing the storage required for the $[A]$ matrix from $2N \times 2N$ to $2N \times 4$, where N is the total number of cross-sections along the waterway. The compaction of the original matrix into $2N \times 4$ size causes the subscript k in equations (14.87)–(14.94) not to increment for each successive Δx reach, i.e. $k = 1,2,3,4$, for all l rows.

Equation (14.109) may be efficiently solved by the following compact, penta-diagonal, modified Gauss elimination algorithm. The computations to eliminate the elements below the main diagonal proceed according to $l = 2,4,6 \ldots 2N-2$ and are:

$$a_{l,2} = a_{l,1}/a_{l-1,k'+1}a_{l-1,k'+2} + a_{l,2} \tag{14.111}$$

$$r_l = -a_{l,1}/a_{l-1,k'+1}r_{l-1} + r_l \tag{14.112}$$

$$a_{l+1,2} = -a_{l+1,1}/a_{l-1,k'+1}a_{l-1,k'+2} + a_{l+1,2} \tag{14.113}$$

$$r_{l+1} = -a_{l+1,1}/a_{l-1,k'+1}r_{l-1} + r_{l+1} \tag{14.114}$$

$$a_{l+1,3} = -a_{l+1,2}/a_{l,2}a_{l,3} + a_{l+1,3} \tag{14.115}$$

$$a_{l+1,4} = -a_{l+1,2}/a_{l,2}a_{l,4} + a_{l+1,4} \tag{14.116}$$

$$r_{l+1} = -a_{l+1,2}/a_{l,2}r_l + r_{l+1} \tag{14.117}$$

in which $k' = 0$ when $l = 2$ and $k' = 2$ when $l > 2$. The x_l components of the solution vector X are obtained through a back-substitution procedure commencing at $l = 2N$ and proceeding sequentially to $l = 1$. Thus,

$$x_{2N} = (-a_{2N,3}/a_{2N-1,3}r_{2N-1} + r_{2N})/(-a_{2N,3}/a_{2N-1,3}a_{2N-1,4} + a_{2N,4}) \tag{14.118}$$

$$x_l = (r_l - a_{l,k'+2}x_{l+1})/a_{l,k'+1} \quad \ldots\ l = 2N-1, 2N-3, \ldots 3,1 \tag{14.119}$$

$$x_l = (r_l - a_{l,4}x_{l+2} - a_{l,3}x_{l+1})/a_{l,2}.\ l = 2N-2, 2N-4, \ldots 4,2 \tag{14.120}$$

in which $k' = 2$ when $l > 1$ and $k' = 0$ when $l = 1$.

14.10.3 Enhancement of computational algorithm

FLDWAV contains an automatic procedure which increases the robust nature of the four-point, nonlinear implicit finite difference algorithm. This enhancement is quite useful when treating rapidly rising hydrographs in channels where the cross-sections have large variations in the vertical and/or along the x-axis. This situation may cause computational problems which are manifested by non-convergence in the Newton–Raphson iteration or by erroneously low computed depths at the leading edge of steep-fronted waves. When either of these manifestations are sensed, an automatic procedure consisting of two parts is implemented.

The first reduces the current time step (Δt) by a factor of 1/2 and repeats the computations. If the same problem persists, Δt is again halved and the computations repeated. This continues until a successful solution is obtained or the time step has been reduced to 1/16 of the original size. If a successful solution is obtained, the computational process proceeds to the next time level using the original Δt. If the solution using $\Delta t/16$ is unsuccessful, the θ weighting factor is increased by 0.1 and a time step of $\Delta t/2$ [illegible]ed. Upon

achieving a successful solution, θ and the time step are restored to their original values. Unsuccessful solutions are treated by increasing θ and repeating the computation until $\theta = 1.0$ whereupon the automatic procedure terminates and the solution with $\theta = 1.0$ and $\Delta t/2$ is used to advance the solution forward in time now using the original θ and the Δt values. Often, computational problems can be overcome via one or two reductions in the time step.

14.11 EXTERNAL BOUNDARIES AND INITIAL CONDITIONS

External boundaries which consist of the upstream and down extremities of the waterway must be specified in order to obtain solutions to the Saint-Venant equations. In fact, in most unsteady flow applications, the unsteady disturbance is introduced to the waterway at one or both of the external boundaries.

14.11.1 Upstream boundary

Either a specified discharge or water elevation time series (hydrographs) can be used as the upstream boundary in FLDWAV. If a discharge hydrograph $Q(t)$ is used, the boundary equation is:

$$\hat{B}_1 = Q_1^{j+1} - Q(t) = 0 \tag{14.121}$$

in which case the partial derivatives for the Jacobian are:

$$a_{1,k} = \partial\hat{B}_1/\partial Q_1 = 1 \tag{14.122}$$

$$a_{1,k+1} = \partial\hat{B}_1/\partial h_1 = 0 \tag{14.123}$$

If a water elevation time series $h(t)$ is used, the boundary equation is:

$$\hat{B}_1 = h_1^{j+1} - h(t) = 0 \tag{14.124}$$

in which case the partial derivatives are:

$$a_{1,k} = \partial\hat{B}_1/\partial Q_1 = \epsilon \tag{14.125}$$

$$a_{1,k+1} = \partial\hat{B}_1/\partial h_1 = 1 \tag{14.126}$$

where ϵ is an arbitrarily small value, e.g. 0.0001. This prevents a zero value for the element $a_{1,1}$ which allows the matrix solution technique previously described to proceed without an interchange of rows needed to eliminate the zero main-diagonal element.

The hydrographs used as upstream boundary conditions should not be affected by the flow conditions downstream of the upstream boundary.

14.11.2 Downstream boundary

Specified discharge or water elevation time series may be used as the downstream boundary condition. For a discharge hydrograph $Q'(t)$, the boundary equation is:

$$\hat{B}_N = Q_N^{j+1} - Q'(t) = 0 \tag{14.127}$$

and the partial derivatives for the Jacobian are:

$$a_{2N,k+2} = \partial\hat{B}_N/\partial Q_N = 1 \tag{14.128}$$

$$a_{2N,k+3} = \partial\hat{B}_N/\partial h_N = 0 \tag{14.129}$$

In a water elevation time series $h'(t)$ such as an observed or predicted tide, the boundary equation is;

$$\hat{B}_N = h_N^{j+1} - h'(t) = 0 \tag{14.130}$$

and

$$a_{2N,k+2} = \partial\hat{B}_N/\partial Q_N = 0 \tag{14.131}$$

$$a_{2N,k+3} = \partial\hat{B}_N/\partial h_N = 1 \tag{14.132}$$

Another frequently used downstream boundary is a relation between discharge and depth or water elevation such as a single-valued rating curve expressed in tabular (piece-wise linear) form consisting of points (Q_k, h_k). Any discharge Q' can be obtained from the table for any associated water elevation (h_N^{j+1}) at the downstream boundary by the following linear interpolation formula:

$$Q' = Q_k + (Q_{k+1} - Q_k)(h_N^{j+1} - h_k)/(h_{k+1} - h_k) \tag{14.133}$$

In this case the downstream boundary equation is:

$$\hat{B}_N = Q_N^{j+1} - Q' = 0 \tag{14.134}$$

and

$$a_{2N,k+2} = \partial\hat{B}_N/\partial Q_N = 1 \tag{14.135}$$

$$a_{2N,k+3} = \partial\hat{B}_N/\partial h_N = -(Q_{k+1} - Q_k)/(h_{k+1} - h_k) \tag{14.136}$$

The downstream boundary can be a loop-rating curve based on the Manning equation for normal flow. The loop is produced by using the water surface slope rather than the channel bottom slope. In this case the downstream boundary equation is:

$$\hat{B}_N = Q_N^{j+1} - QN = 0 \tag{14.137}$$

where:

$$QN = 1.49\left(\frac{A^{5/3}}{nB^{2/3}}\right)_N^{j+1}\left(\frac{h_{N-1}^j - h_N^j}{\Delta x_{N-1}}\right)^{1/2} = K_{c_N}\left(\frac{h_{N-1}^j - h_N^j}{\Delta x_{N-1}}\right)^{1/2} \tag{14.138}$$

and $$a_{2N,k+2} = \partial\hat{B}_N/\partial Q_N = 1 + QN/n_N^{j+1}(\Delta n/\Delta Q)_N^{j+1} \tag{14.139}$$

$$a_{2N,k+3} = \partial\hat{B}_N/\partial h_N = \frac{QN}{3}\left(3\,\frac{\Delta n/\Delta h}{n} + 2\,\frac{\Delta B/\Delta h}{B} - \frac{5B}{A}\right)_N^{j+1} = \frac{-QN}{K_{cN}}\,\frac{\Delta K_c}{\Delta h} \tag{14.140}$$

The downstream boundary can be a critical flow section; the downstream boundary equation is:

$$\hat{B}_N = Q_N^{j+1} - QC = 0 \tag{14.141}$$

where $$QC = (\sqrt{g/B}A^{3/2})_N^{j+1} \tag{14.142}$$

and $$a_{2N,k+2} = \partial\hat{B}_N/\partial Q_N = 1 \tag{14.143}$$

$$a_{2N,k+3} = \partial\hat{B}_N/\partial h_N = \frac{QC}{2}\left(\frac{\Delta B/\Delta h}{B} - 3\,\frac{B}{A}\right)_N^{j+1} \tag{14.144}$$

The flow at the downstream boundary should not be affected by flow conditions further downstream. Of course, there are always some minor influences on the flow due to the presence of cross-sectional irregularities downstream of the chosen boundary location; however, these usually can be neglected unless the irregularity is very pronounced such as to cause significant backwater or drawdown effects. Reservoirs or major tributaries located below the downstream boundary which cause backwater effects at the chosen boundary location should be avoided. When this situation is unavoidable, the reach of channel for which the Saint-Venant equations are being used should be extended on downstream to a location below where the tributary enters or to the dam in the case of the reservoir. Sometimes the routing reach may be shortened and the downstream boundary shifted upstream to a point where backwater effects are negligible.

14.11.3 Initial conditions

Initial conditions of water surface elevation (h) and discharge (Q) must be specified at time $t = 0$ to obtain solutions of the Saint-Venant equations. Initial conditions may be specified for FLDWAV by any of the following: (1) from observations at gauging stations with interpolated values for intermediate cross-sections; these must be sufficiently accurate to result in convergence of the Newton–Raphson solution of the Saint-Venant finite difference equations (the errors dampen-out after several time steps); (2) computed values from a previous unsteady flow solution (this is frequently used in day-to-day flood forecasting); and (3) computed values from a steady flow backwater solution.

In the case of steady flow, the discharge at all cross-sections can be determined by:

$$Q_{i+1} = Q_i + \bar{q}_i\,\Delta x_i \qquad \ldots\ i = 1,2,3,\ \ldots\ N-1 \tag{14.145}$$

in which Q_1 is the assumed steady flow at the upstream boundary at time $t = 0$, and $\bar{q}_i$ is the known average lateral inflow (outflow) along each Δx reach at $t = 0$. The water surface elevations (h_i) are computed according to the following steady flow simplification of the momentum equation (14.62):

$$(Q^2/A)_{i+1} - (Q^2/A)_i + g\bar{A}_i(h_{i+1} - h_i + \Delta x_i\bar{S}_{f_i}) = 0 \tag{14.146}$$

in which $\bar{A}_i$ and $\bar{S}_{f_i}$ are defined by equations (14.71) and (14.73), respectively. The computations proceed in the upstream direction ($i = N-1, \ldots 3,2,1$) for subcritical flow (they proceed in the downstream direction for supercritical flow). The starting water surface elevation (h_N) can be specified or obtained from the appropriate downstream boundary condition for a discharge of Q_N. Equation (14.146) can be solved by the Newton–Raphson method as applied to a single nonlinear equation. In this case, if equations (14.83) and (14.84) are combined, the following recursive relationship can be written in scalar form;

$$x^{k+1} = x^k - f(x^k)/f'(x^k) \tag{14.147}$$

in which x represents the unknown (h_i), k is the number of iterations, $f(x^k)$ is equation (14.146) evaluated with the trial solution x^k, and $f'(x^k)$ is the derivative of equation (14.146) with respect to the unknown (h_i) and evaluated at x^k. The derivative expression follows:

$$f'(x^k) = \mathrm{d}f(x^k)/\mathrm{d}h_i = (Q^2B/A^2)_i + 0.5gB_i(h_{i+1} - h_i + \bar{S}_{f_i}\,\Delta x_i) + g\bar{A}_i[-1 + \Delta x_i(\mathrm{d}\bar{S}_{f_i}/\mathrm{d}h_i)] \tag{14.148}$$

in which $\mathrm{d}\bar{S}_f/\mathrm{d}h_1$ is defined by equation (14.96).

14.12 INTERNAL BOUNDARIES

There may be locations such as a dam, bridge, or waterfall (short rapids) along a waterway where the Saint-Venant equations are not applicable. At these locations the flow is rapidly varied rather than gradually varied as necessary for the applicability of the Saint-Venant equations. Empirical water elevation –discharge relations such as weir-flow can be utilized for simulating rapidly varying flow. In FLDWAV, unsteady flows are routed along the waterway including points of rapidly varying flow by utilizing internal boundaries. At internal boundaries, cross-sections are specified for the upstream and downstream extremities of the section of waterway where rapidly varying flow occurs. The Δx reach length between the two cross-sections can be any appropriate value from zero to the actual measured distance. Since, as with any other Δx reach, two equations (the Saint-Venant equations) are required,

the internal boundary Δx reach requires two equations. The second of the required equations represents the conservation of mass with negligible time-dependent storage, i.e.,

$$\hat{B}_{I2} = Q_i^{j+1} - Q_{i+1}^{j+1} = 0 \tag{14.149}$$

and the derivatives for the Jacobian are:

$$a_{l+1,k} = \partial\hat{B}_{I2}/\partial Q_i = 1 \tag{14.150}$$

$$a_{l+1,k+1} = \partial\hat{B}_{I2}/\partial h_i = 0 \tag{14.151}$$

$$a_{l+1,k+2} = \partial\hat{B}_{I2}/\partial Q_{i+1} = -1 \tag{14.152}$$

$$a_{l+1,k+3} = \partial\hat{B}_{I2}/\partial h_{i+1} = 0 \tag{14.153}$$

The first of the two required equations is an empirical rapidly varied flow relation. Several examples of rapidly varied flow internal boundary equations follow.

14.12.1 Critical flow

If the internal boundary is used to represent critical flow, the following equation is used in conjunction with equation (14.149):

$$\hat{B}_{I1} = Q_i^{j+1} - \sqrt{g}(A^{3/2}/B^{1/2})_i^{j+1} = 0 \tag{14.154}$$

and the derivatives are:

$$a_{l,k} = \partial\hat{B}_{I1}/\partial Q_i = 1 \tag{14.155}$$

$$a_{l,k+1} = \partial\hat{B}_{I1}/\partial h_i = 0.5\sqrt{g}[\Delta B/\Delta h(A/B)^{3/2} - 3(AB)^{1/2}]_i^{j+1} \tag{14.156}$$

14.2.2 Dam

At a dam, the internal boundary can represent any combination of flow such as spillway flow (uncontrolled overflow, fixed gate, time-dependent gate), crest overflow, constant (head-independent) flow, or breach flow due to a time-dependent failure of the dam. The general equation for flow at a dam is:

$$\hat{B}_{I1} = Q_i^{j+1} - Q_d = 0 \tag{14.157}$$

where:

$$Q_d = Q_{br} + Q_s \tag{14.158}$$

in which Q_{br} is the time-dependent breach flow which may be zero and Q_s is the sum of all other types of flow. The breach flow can be expressed as broad-crested weir flow corrected for submergence effects, i.e.

$$Q_{br} = K_s Q_{br}' \tag{14.159}$$

where:

$$Q_{br}' = 3.1b(h_i^{j+1} - h_{br})^{3/2} + 2.45z(h_i^{j+1} - h_{br})^{5/2} \tag{14.160}$$

$$K_s = 1. - 27.8(h_r - 0.67)^3 \quad \ldots h_r > 0.67 \tag{14.161}$$

$$K_s = 1. \quad \ldots h_r \leqslant 0.67 \tag{14.162}$$

$$h_r = (h_{i+1}^{j+1} - h_{br})/(h_i^{j+1} - h_{br}) \tag{14.163}$$

$$b = \hat{b} \quad \ldots t_{br} > \tau_{br} \tag{14.164}$$

$$b = \hat{b}t_{br}/\tau_{br} \quad \ldots t_{br} \leqslant \tau_{br} \tag{14.165}$$

$$h_{br} = h_{bm} \quad \ldots t_{br} > \tau_{br} \tag{14.166}$$

$$h_{br} = h_d - (h_d - h_{bm})t_{br}/\tau_{br} \quad \ldots t_{br} \leqslant \tau_{br} \tag{14.167}$$

in which K_s is a submergence correction factor due to the effects of the water surface elevation (h_{i+1}) downstream of the dam, b is the instantaneous width of the breach bottom, $\hat{b}$ is the final maximum width of the breach bottom, t_{br} is the time since beginning of breach formation, τ_{br} is the interval of time necessary for the breach to completely form, h_b is the elevation of the breach bottom, h_{bm} is the final elevation of the breach bottom (usually assumed to be the bottom of the dam), h_d is the elevation of the crest of the dam, and z is the side slope of the breach (1 : vertical to z : horizontal). The values of $\hat{b}$, τ_{br}, h_{br}, h_d, h_{bm}, and z must be known or assumed from previous breached dams. The breach starts forming when h_i^{j+1} equals or exceeds h_f, a specified elevation representing the amount of overtopping required for failure to commence. The sum of all other flows (Q_s) is:

$$Q_s = K_{ss}Q_{ss} + Q_g + K_{cs}Q_{cs} + Q_t \tag{14.168}$$

$$Q_{ss} = c_s L_s (h_i^{j+1} - h_s)^{3/2} \tag{14.169}$$

$$Q_g = \sqrt{2g}c_g A_g (h_i^{j+1} - h_g)^{1/2} \tag{14.170}$$

$$Q_{cs} = c_d L_d (h_i^{j+1} - h_d)^{3/2} \tag{14.171}$$

$$K_{ss} = 1. - 27.8(h_{rs} - 0.67)^3 \quad \ldots h_{rs} > 0.67 \tag{14.172}$$

$$h_{rs} = (h_{i+1}^{j+1} - h_s)/(h_i^{j+1} - h_s) \tag{14.173}$$

$$K_{cs} = 1. - 27.8(h_{rc} - 0.67)^3 \quad \ldots h_{rc} > 0.67 \tag{14.174}$$

$$h_{rc} = (h_{i+1}^{j+1} - h_d)/(h_i^{j+1} - h_d) \tag{14.175}$$

in which K_{ss} and K_{cs} are submergence correction factors for the spillway and dam crest, respectively; c_s, c_g, and c_d are discharge coefficients for the spillway, gate(s) and dam crest, respectively; L_s is the length of the spillway; A_g is the area of the gate opening; L_d is the length of the dam crest after subtracting L_s; h_s is the elevation of the spillway crest; h_g is the elevation of the centre of the gate(s); and Q_t is a constant, head-independent outflow. Also, time-dependent gate parameters (c_g and A_g) may be specified via tabular, piecewise linear, values and associated times (t). For further information on the expected range of the parameters in equations (14.157)–(14.175), see Fread (1980).

The partial derivatives of equation (14.157) are:

$$a_{I,k} = \partial \hat{B}_{I1}/\partial Q_i = 1 \tag{14.176}$$

$$a_{I,k+1} = \partial \hat{B}_{I1}/\partial h_i = -K_s \partial Q'_{br}/\partial h_i - Q'_{br}\partial K_s/\partial h_i - \partial Q_s/\partial h_i \tag{14.177}$$

where:

$$\partial Q'_{br}/\partial h_i = 4.65b(h_i^{j+1} - h_{br})^{1/2} + 6.13z(h_i^{j+1} - h_{br})^{3/2} \tag{14.178}$$

$$\partial K_s/\partial h_i = 83.4(h_r - 0.67)^2 h_r/(h_i^{j+1} - h_{br}) \tag{14.179}$$

$$\begin{aligned}\partial Q_s/\partial h_i = {} & 1.5K_{ss}c_sL_s(h_i^{j+1} - h_s)^{1/2} + 83.4Q_{ss}(h_{rs} - 0.67)^2 \\ & h_{rs}/(h_i^{j+1} - h_s) \\ & + 0.5\sqrt{2g}c_gA_g/(h_i^{j+1} - h_g)^{1/2} + 1.5K_{cs}c_dL_d(h_i^{j+1} - h_d)^{1/2} \\ & + 83.4Q_{cs}(h_{rc} - 0.67)^2 h_{rc}/(h_i^{j+1} - h_d)\end{aligned} \tag{14.180}$$

and

$$a_{I,k+2} = \partial \hat{B}_{I1}/\partial Q_{i+1} = 0 \tag{14.181}$$

$$a_{I,k+3} = \partial \hat{B}_{I1}/\partial h_{i+1} = -Q'_{br}\partial K_s/\partial h_{i+1} - \partial Q_s/\partial h_{i+1} \tag{14.182}$$

where:

$$\partial K_s/\partial h_{i+1} = -83.4(h_r - 0.67)^2/(h_i^{j+1} - h_{br}) \tag{14.183}$$

$$\begin{aligned}\partial Q_s/\partial h_{i+1} = {} & -83.4Q_{ss}(h_{rs} - 0.67)^2/(h_i^{j+1} - h_s) \\ & - 83.4Q_{cs}(h_{rc} - 0.67)^2/(h_i^{j+1} - h_d)\end{aligned} \tag{14.184}$$

14.12.3 Bridge-embankment

Another internal boundary condition can be the flow occurring at a bridge and perhaps over its embankment which impedes flow in the floodplain. The total flow (Q_{be}) which may be a combination of flow through the bridge opening (Q_{bo}), flow over the embankment (Q_{em}), and flow through a time-dependent breach in the embankment (Q_{br}). The internal boundary equation for flow at a bridge embankment is:

$$\hat{B}_{i1} = Q_i^{j+1} - Q_{be} \tag{14.185}$$

where:

$$Q_{be} = Q_{bo} + Q_{em} + Q_{br} \tag{14.186}$$

$$Q_{bo} = \sqrt{2g}c_bA_{i+1}^{j+1}(h_i^{j+1} - h_{i+1}^{j+1})^{1/2} \tag{14.187}$$

$$Q_{em} = K_{em}L_{em}c_{em}(h_i^{j+1} - h_{em})^{3/2} \tag{14.188}$$

$$K_{em} = 1. - 27.8(h_{re} - 0.67)^3 \quad \ldots\ h_{re} > 0.67 \tag{14.189}$$

$$h_{re} = (h_{i+1}^{j+1} - h_e)/(h_i^{j+1} - h_{em}) \tag{14.190}$$

in which c_b is the bridge flow coefficient which accounts for piers, angle of flow approach, etc. (see Chow, 1959); c_{em}, Lem, K_{em} are the discharge coefficient, length of embankment, and submergence correction factor, respectively, for the embankment overflows (Fread, 1980); and the flow through a breach of the the embankment (Q_{br}) is defined as in equations (14.159)–(14.167) except h_d is replaced with h_e, the top of the embankment.

The partial derivatives of equation (14.185) are:

$$a_{I,k} = \partial \hat{B}_{I1}/\partial Q_i = 1 \tag{14.191}$$

$$\begin{aligned}a_{I,k+1} = {} & \partial \hat{B}_{I1}/\partial h_i = -0.5Q_{bo}/(h_i^{j+1} - h_{i+1}^{j+1}) - 1.5Q_{em}/(h_i^{j+1} - h_{em}) \\ & + 83.4Q_{em}/K_{em}(h_{re} - 0.67)^2 h_{re}/(h_i^{j+1} - h_{em}) - \partial Q_{br}/\partial h_i\end{aligned} \tag{14.192}$$

$$a_{I,k+2} = \partial \hat{B}_{I1}/\partial Q_{i+1} = 0 \tag{14.193}$$

$$\begin{aligned}a_{I,k+3} = {} & \partial \hat{B}_{I1}/\partial h_{i+1} = Q_{bo}[0.5/(h_i^{j+1} - h_{i+1}^{j+1}) - B_i^{j+1}/A_i^{j+1}] \\ & + 83.4Q_{em}/K_{em}(h_{re} - 0.67)^2/(h_i^{j+1} - h_{em}) - \partial Q_{br}/\partial h_{i+1}\end{aligned} \tag{14.194}$$

in which $\partial Q_{br}/\partial h_i$ is similar to the expression $K_s\,\partial Q'_{br}/\partial h_i + Q'_{br}\partial K_s/\partial h_i$ in equation (14.177) and ∂h_{i+1} is similar to the expression ($Q'_{br}\partial K_s/\partial h_{i+1}$) in equation (14.182) except h_d is replaced by h_e.

14.12.4 Lock and dam

A waterway may include small dams with manually operated gates to pass the flow so as to maintain a desired depth for safe navigation upstream of the dam. A lock is provided for navigation of boats, barges, etc. past the dam. Although the actual gate operations may not be known in the application of FLDWAV, the assumed maintenance of a constant water elevation provides the internal boundary equation, i.e.

$$\hat{B}_{I1} = h_i^{j+1} - h_t = 0 \tag{14.195}$$

in which h_t is the target pool elevation which the dam operator attempts to maintain via operation of the gates. The target pool elevation may be a constant value or it may be an assumed function of time. When the computed elevation (h_{i+1}) exceeds a specified elevation, the flow is assumed then to be governed by the Saint-Venant equations.

The partial derivatives of equation (14.195) are all zero except one, i.e.

$$a_{I,k+1} = \partial B_{I1}/\partial h_i = 1 \tag{14.196}$$

14.12.5 Rating curve

A rating curve as described previously in section 14.11 can be used as an internal boundary in which the downstream flow is assumed to have negligible effect on the flow passing the internal boundary section. The internal boundary equation is:

$$\hat{B}_{I1} = Q_i^{j+1} - Q' = 0 \tag{14.197}$$

in which Q' is defined by equation (14.133). The partial derivatives are:

$$a_{I,k} = \partial \hat{B}_{I1}/\partial Q_i = 1 \tag{14.198}$$

$$a_{I,k+1} = \partial \hat{B}_{I1}/\partial h_i = -(Q_{k+1} - Q_k)/(h_{k+1} - h_k) \tag{14.199}$$

$$a_{I,k+2} = \partial \hat{B}_{I1}/\partial Q_{i+1} = 0 \tag{14.200}$$

$$a_{I,k+3} = \partial \hat{B}_{I1}/\partial h_{i+1} = 0 \tag{14.201}$$

14.13 CROSS-SECTIONS

14.13.1 Active flow sections

That portion of the channel cross-section in which flow occurs is termed active. In FLDWAV the active flow cross-sections may be of regular or irregular geometrical shape. Each cross-section is specified as tabular values of channel width and elevation, which together constitute a piecewise linear relationship. Experience has shown that in almost all instances the cross-section may be sufficiently described with approximately eight or less sets of widths and associated elevations. A low-flow cross-sectional area which can be zero is used to describe the cross-section below the minimum specified elevation, below which the water elevation must not recede. The total cross-sectional area below each of the widths is initially computed within the model. During the solution of the unsteady flow equations any areas or widths associated with a particular water surface elevation are linearly interpolated from the piecewise linear relationships of width and elevation which were specified or the area–elevation sets initially generated within the model.

Cross-sections at gauging station locations are generally used as computational points in the x–t plane. Cross-sections are also specified at points along the river where significant cross-sectional changes occur or at points where major tributaries enter. Typically, cross-sections are spaced farther apart for large natural channels than for small channels, since the degree of variation in the cross-sectional characteristics is less for the larger channels. Spacing can range from a few hundred feet to a few miles. In addition to the consideration of cross-sectional variation in the selecton of Δx reaches, the solution accuracy also affects the choice of Δx. For best accuracy, the maximum reach length (Δx_m) is related to Δt as follows:

$$\Delta x_m \leqslant c\Delta t \tag{14.202}$$

in which c is the wave speed of the essential characteristic of the unsteady flow such as the mid-point of the hydrograph. The wave speed may be initially estimated from equation (14.32) or from observed flows, and the time step (Δt) is selected according to equation (14.34). Since c may vary with distance along the channel, Δx_m may not be constant along the channel.

In some applications the total number of cross-sections due to geometrical variation can be reduced by using a distance-weighted average section. The width ($\bar{B}$) of the average section can be computed from the widths of the other sections which are to be averaged by:

$$\bar{B} = 0.5[(B_i + B_{i+1})\,\Delta d_i + (B_{i+1} + B_{i+2})\,\Delta d_{i+1} + \ldots (B_{I'-1} + B_{I'})\,\Delta d_{I'-1}]/\sum_1^{I'} \Delta d_i \tag{14.203}$$

in which $\bar{B}$ is the distance-weighted width for a particular depth of flow, B_i is width of the ith section along a reach having a total of (I') sections to be averaged, and Δd_i is the distance between the individual sections. The total reach length ($\sum \Delta d_i$) of equation (14.203) must be less than Δx_m of equation (14.202).

14.13.2 Off-channel storage

A cross-section may contain portions where the flow velocity in the x-direction is negligible relative to the velocity in the active portion. The inactive portion of the cross-section is known as dead or off-channel storage. Off-channel storage areas can be used to effectively account for embayments, ravines, or tributaries which connect to the flow channel but do not pass flow and serve only to store the flow. Another effective use of off-channel storage is to model a heavily wooded floodplain which stores a portion of the flood waters passing through the channel. In each of these cases the use of zero velocity for the portion of the flood waters contained in the dead storage area results in a more

realistic simulation of the actual flow than using an average velocity derived from the main flow channel and the dead storage area. The dead storage cross-sectional properties are described in the same manner as the active cross-sectional areas.

14.13.3 Linearly interpolated cross-sections

Within FLDWAV, there is an option to generate additional cross-sections between any two adjacent specified cross-sections. The properties of the additional sections are linearly interpolated. This facilitates adherence to equation (14.202) for appropriate Δx reach lengths. Both active and off-channel storage widths are generated via the interpolation procedure.

14.14 CHANNEL FRICTION

The Manning n is used to describe the resistance of flow due to channel roughness caused by bed forms, bank vegetation, obstructions, bend effects, and eddy losses. The Manning n is defined for each Δx reach as a specified function of water elevation or discharge according to a tabular (piecewise linear) relation between n and the independent variable (h or Q). Linear interpolation is used in FLDWAV to obtain n for values of h or Q intermediate to the tabular values.

Alternatively, the friction effects can be represented by channel conveyance (K_c) which may be specified in FLDWAV as a tabular function of water elevation. Conveyance is related to the Manning n and cross-sectional properties, i.e.

$$K_c = 1.49AR^{2/3}/n \tag{14.204}$$

The use of K_c rather than n has an advantage in applications where the cross-section consists of an in-bank portion and a rather wide, flat floodplain. The hydraulic radius (R) can be somewhat discontinuous when the water surface expands onto the floodplain. This discontinuity can be treated by specifying conveyance as a function of elevation which is smoothed in the vicinity of the discontinuity. This provides more realistic flows and helps to avoid numerical problems during the computations.

The channel routing computations are often sensitive to the Manning n or K_c. In the absence of necessary data (observed stages and discharges), n can be estimated; however, best results are obtained when the Manning n is adjusted to reproduce historical observations of water elevation and discharge. The adjustment process or calibration may be either trial-and-error or an automatic iterative procedure. The automatic calibration algorithm is desc later.

14.15 LATERAL INFLOWS

FLDWAV incorporates small tributary inflows or overland flow via the lateral inflow term (q) in equations (14.61) and (14.62). These are considered independent of flows occurring in the river to which they are added. They are specified as a time series of flows with constant or variable time intervals. They can be specified for any Δx reach along the river as the sum of all lateral inflows within the Δx reach. Outflows may be simulated by assigning a negative sign to the specified flows. Linear interpolation is used for flows at times other than the specified intervals.

14.16 MODIFIED SAINT-VENANT EQUATIONS FOR FLOODPLAIN FLOWS

Unsteady flow in a natural river which meanders through a wide floodplain is complicated by large differences in geometric and hydraulic characteristics between the river channel and the floodplain, as well as the extreme differences in the hydraulic roughness coefficient. The flow is further complicated by the meandering of the main channel within the floodplain; this causes a portion of the total flow to 'short-circuit' and proceed downstream along the more direct course afforded by the floodplain rather than along the more circuitous route of the meandering channel. This tendency for short-circuiting of the flow is enhanced by the greater longitudinal slope associated with the floodplain than that of the main channel; however, the short-circuiting effect is diminished by the greater hydraulic roughness of the floodplain. Further complexities are created by portions of the floodplain which act as dead storage areas, wherein the flow velocity is negligible.

FLDWAV contains a modified form of the Saint-Venant equations for an alternative method for routing floods in meandering rivers with floodplains. A modification of the one-dimensional Saint-Venant equations avoids the obvious use of the more complex and computationally time-consuming two-dimensional equations. The one-dimensional equations are modified such that the flow in the meandering channel and floodplain are identified separately. Thus, the differences in both hydraulic properties and flow-path distance are taken into account in a physically meaningful way, but one that is one-dimensional in concept. This development differs from conventional one-dimensional treatment of unsteady flows in rivers with floodplains, wherein the flow is either averaged across the total cross-sectional area (channel and floodplain) or the floodplain is treated as off-channel storage and the reach lengths of the channel and floodplain are assumed to be identical.

The Saint-Venant equations are modified (Fread, 1976) as follows:

$$\frac{\partial(K_{cn}Q)}{\partial x_{cn}} + \frac{\partial(K_{lf}Q)}{\partial x_{lf}} + \frac{\partial(K_{rf}Q)}{\partial x_{rf}} + \frac{\partial(A_{cn} + A_{lf} + A_{rf} + A_0)}{\partial t} - q = \tag{14.205}$$

$$\frac{\partial Q}{\partial t}+\frac{\partial(K_{cn}^2Q^2/A_{cn})}{\partial x_{cn}}+\frac{\partial(K_{lf}^2Q^2/A_{lf})}{\partial x_{lf}}+\frac{\partial(K_{rf}^2Q^2/A_{rf})}{\partial x_{rf}}+gA_{cn}\left(\frac{\partial h}{\partial x_{cn}}+S_{fcn}+S_e\right)$$

$$+gA_{lf}\left(\frac{\partial h}{\partial x_{lf}}+S_{flf}\right)+gA_{rf}\left(\frac{\partial h}{\partial x_{rf}}+S_{frf}\right)=0 \qquad (14.206)$$

The parameters (K_{cn}, K_{lf}, K_{rf}) proportion the total flow (Q) into the channel, left floodplain, and right floodplain, respectively. These are defined as follows:

$$K_{cn}=1/(1+k_l+k_r) \qquad (14.207)$$

$$K_{lf}=k_l/(1+k_l+k_r) \qquad (14.208)$$

$$K_{rf}=k_r/(1+k_l+k_r) \qquad (14.209)$$

and

$$k_l=\frac{Q_{lf}}{Q_{cn}}=\frac{n_{cn}A_{lf}}{n_{lf}A_{cn}}\left(\frac{R_{lf}}{R_{cn}}\right)^{2/3}\left(\frac{\Delta x_{cn}}{\Delta x_{lf}}\right)^{1/2} \qquad (14.210)$$

$$k_r=\frac{Q_{rf}}{Q_{cn}}=\frac{n_{cn}A_{rf}}{n_{rf}A_{cn}}\left(\frac{R_{rf}}{R_{cn}}\right)^{2/3}\left(\frac{\Delta x_{cn}}{\Delta x_{rf}}\right)^{1/2} \qquad (14.211)$$

Equations (14.210) and (14.211) represent the ratio of flow in the channel section to flow in the left and right floodplain sections; the flows are expressed in terms of the Manning equation with the energy slope approximated by the water surface slope ($\Delta h/\Delta x$). The friction slope terms in equation (14.206) are similar to equation (14.73).

Equations (14.205) and (14.206) are approximated with the weighted, four-point finite difference expressions of equations (14.66)–(14.68). The resulting finite difference equations, similar to equations (14.69) and (14.70), are solved by the Newton–Raphson iterative method for nonlinear equations using the special penta-diagonal matrix technique described by equations (14.111)–(14.120). The coefficients K_{lf} or K_{rf} are considered to be zero until the water elevation is sufficient to produce wetted top widths, B_{lf} or B_{rf}, greater than 1 ft. Thus, any terms associated with the left or right floodplain in equations (14.205) and (14.206) are set to zero, as are the derivatives associated with the terms. This avoids numerical difficulties such as division by zero, etc. during the computer solution.

14.17 SUPERCRITICAL OR MIXED FLOW

In the preceding presentation it was assumed the flow is always subcritical at each cross-section along the routing reach. When the flow becomes supercritical it requires special treatment of the external boundaries. Supercritical flow may occur all along a channel reach, or it may occur at intermittent locations along the routing reach. The former is easier to treat, while the latter ('mixed flow') is more difficult. The flow may be mixed in both time and location along the channel. The locations of each type of flow (supercritical or subcritical) must be determined at each time step, and various types of boundary conditions must be used with each partial reach of supercritical or subcritical flow.

Supercritical flow occurs when the Froude number (F_i) is greater than that for critical flow, i.e.

$$F_i=Q_i/(\sqrt{g/B_i}A_i^{3/2})>F_c \qquad (14.212)$$

in which F_c is the Froude number for critical flow. A value of 1.0 is used for F_c, although this may be slightly changed to account for numerical effects. Subcritical flow occurs when $F_i<F_c$, and critical flow occurs when $F_i=F_c$. *A priori* estimation of the occurrence of supercritical flow is conveniently determined through use of the channel bottom slope, i.e. supercritical flow occurs if $S_0>S_c$, where S_c (the critical slope) may be expressed as follows:

$$S_c=gn^2/[2.21(A/B)^{1/3}] \qquad (14.213)$$

14.17.1 Supercritical flow

If the entire routing reach is supercritical flow, the downstream boundary condition is no longer required since flow disturbances cannot propagate upstream; hence, the downstream boundary is superfluous. However, in order to have a determinate system of implicit difference equations, there must be $2N$ equations to match the $2N$ unknowns. The additional equation needed to make a determinate system is an additional upstream boundary equation in the form of a depth-discharge relation, i.e.,

$$\hat{B}_2=Q_1^{j+1}-QS=0 \qquad (14.214)$$

where:

$$QS=\left(\frac{1.486A^{5/3}}{nB^{2/3}}\right)_1^{j+1}\left(\frac{h_1^j-h_2^j}{\Delta x_1}\right)^{1/2}=K_{c1}\left(\frac{h_1^j-h_2^j}{\Delta x_1}\right)^{1/2} \qquad (14.215)$$

The partial derivatives of equation (14.214) for the Jacobian are:

$$a_{2,1}=\partial\hat{B}_2/\partial Q_1=1 \qquad (14.216)$$

$$a_{2,2}=\partial\hat{B}_2/\partial h_1=\frac{QS}{3}\left(\frac{3\,\mathrm{d}n/\mathrm{d}h}{n}-\frac{5B}{A}+\frac{2\,\mathrm{d}B/\mathrm{d}h}{B}\right)_1^{j+1}=-\frac{QS}{K_{c1}}\frac{\Delta K_{c1}}{\Delta h_l} \qquad (14.217)$$

and the subscript (l) of equations (14.87)–(14.94) starts with a value of 3 and progresses to a value of $2N-2$ in steps of 2. The matrix solution given by equations (14.111)–(14.120) must be slightly modified since there are two upstream boundary equations and none at the downstream boundary. When determining the initial conditions, equation (14.145) can be used although the unknown is h_{i+1} and the first term for equation (14.146) becomes $(-Q^2B/A^2)_{i+1}$, B_i becomes B_{i+1}, and the -1 in the brackets becomes $+1$.

The computations proceed from upstream to downstream ($i = 1, 2, \ldots 2N-1$); and h_i is determined by solving the Manning equation, (14.215) for h_i^{j+1} and the term $(h_1^j - h_2^j)/\Delta x_1$ is replaced with the channel bottom slope between the first and second cross sections.

14.17.2 Mixed flow

When the flow changes with either time or distance along the routing reach from supercritical to subcritical or conversely, the flow is described as 'mixed'. During each time step, subreaches are delineated where supercritical or subcritical flow exists by computing the Froude number at each cross-section and grouping consecutive Δx_i reaches into either subcritical or supercritical subreaches. Then, the Saint-Venant equations are applied and solutions obtained for each subreach, commencing with the most upstream subreach and progressing downstream until each subreach has been solved. Appropriate external boundary equations are used for each subreach.

Where the flow changes from subcritical to supercritical the downstream boundary for the subcritical subreach is the critical flow equation (14.140). The two upstream boundary equations for the supercritical subreach are:

$$\hat{B}_{I1} = Q_1^{j+1} - Q' = 0 \tag{14.218}$$

$$\hat{B}_{I2} = h_1^{j+1} - h_c = 0 \tag{14.219}$$

$$a_{1,1} = \partial \hat{B}_{I1}/\partial Q_1 = 1 \tag{14.220}$$

$$a_{1,2} = \partial \hat{B}_{I1}/\partial h_1 = 0 \tag{14.221}$$

$$a_{2,1} = \partial \hat{B}_{I2}/\partial Q_1 = 0 \tag{14.222}$$

$$a_{2,2} = \partial B_{I2}/\partial h_1 = 1 \tag{14.223}$$

in which Q' is the computed flow at the downstream boundary of subcritical subreach, Q_1^{j+1} is the flow at the same cross-section which is now the first section of the supercritical subreach, h_c is the critical water surface elevation computed at the downstream boundary of the subcritical subreach, and h_1^{j+1} is the water elevation of the first section of the supercritical subreach. The supercritical subreach does not require a downstream boundary equation.

Where the flow changes from supercritical to subcritical, the upstream boundary equation for the subcritical subreach is:

$$\hat{B}_{I1} = Q_1^{j+1} - Q'' = 0 \tag{14.224}$$

in which Q'' is the computed flow at the last cross-section of the supercritical reach and Q_1^{j+1} is the flow at the first cross-section of the subcritical subreach. The [illegible]stream boundary for the subcritical subreach would be equatio[illegible]

(14.140) if another supercritical subreach exists below the subcritical subreach or the appropriate condition described by equations (14.126)–(14.140) if the subcritical subreach is the last subreach in the routing reach. The depth of flow at the first section of the subcritical subreach is determined by the downstream boundary condition and the Saint-Venant equations applied to the subcritical subreach. A hydraulic jump occurs between the last section of the supercritical subreach and the first section of subcritical subreach, although an equation for such is not directly used. To account for the possible movement of the hydraulic jump, the following procedure is utilized before advancing to the next time step: (1) the water elevation at the first section of the subcritical subreach is extrapolated to several upstream cross-sections near the downstream end of the supercritical subreach; (2) the sequent depths (water elevations) of the same sections in the supercritical reach are computed; and (3) the sequent elevations are compared with the extrapolated elevations, and the first section of the subcritical subreach is determined as that section nearest the intersection of two elevations.

14.18 THE CHANNEL NETWORKS

The implicit formulation of the Saint-Venant equations is well-suited from the standpoint of accuracy for simulating unsteady flows in a network of channels since the response of the system as a whole is determined within a certain convergence criterion for each time step. However, a network of channels presents complications in achieving computational efficiency when using the implicit formulation. Equations representing the conservation of mass and momentum at the confluence of two channels produce a Jacobian matrix in the Newton–Raphson method with elements which are not contained within the narrow band along the main diagonal of the matrix. The column location of the elements within the Jacobian depends on the sequence numbers of the adjacent cross-sections at the confluence. The generation of such 'off-diagonal' elements produces a 'sparse' matrix containing relatively few non-zero elements. Unless special matrix solution techniques are used for the sparse matrix, the computation time required to solve the matrix by conventional matrix solution techniques is so great as to make the implicit method unfeasible. The same situation also occurs for the linearized implicit methods which must also solve a system of linear equations similar to the Jacobian. One of two algorithms can be selected in FLDWAV for an efficient computational treatment of channel networks.

The first, called the 'relaxation' algorithm, is restricted to a dendritic (tree-type) network of channels in which the main channel has any number of tributary channels joining with it. Sometimes, dendritic systems with second-order tributaries (tributaries of tributaries) can be accommodated in the relaxation technique by reordering the dendritic system, i.e. s[illegible]g another

branch of the system as the main channel. In the relaxation algorithm no sparse matrix is generated; the Jacobian is always banded as it is for a single channel reach.

The second, called the 'network' algorithm, can be used on almost any natural system of channels (dendritic systems having any order of tributaries; bifurcating channels such as those associated with islands, deltas, flow bypasses between parallel channels; and tributaries joining bifurcated channels). The network algorithm produces a sparse matrix which is solved by a special matrix technique which is described later. The relaxation algorithm is slightly more efficient than the network algorithm, but the former does not have the versatility of the latter.

14.18.1 Relaxation algorithm

During a time step the relaxation algorithm solves the Saint-Venant equations first for the main channel and then separately for each tributary of the first-order dendritic network. The tributary flow at each confluence with the main channel is treated as lateral flow (q) which is first estimated when solving Saint-Venant equations for the main channel. Each tributary flow depends on its upstream boundary condition, lateral inflows along its reach, and the water surface elevation at the confluence (downstream boundary for the tributary) which is obtained during the simulation of the main channel. Due to the interdependence of the flows in the main channel and its tributaries, the following iterative or relaxation algorithm (Fread, 1973) is used:

$$q^* = \alpha q + (1-\alpha)q^{**} \tag{14.225}$$

in which α is a weighting factor ($0 < \alpha \leqslant 1$), q is the computed tributary flow at each confluence, q^{**} is the previous estimate of q, and q^* is the new estimate of q. Convergence is attained when q is sufficiently close to q^{**}, i.e. $|q - q^{**}| < \epsilon_Q$. Usually, one or two iterations is sufficient; however, the weighting factor has an important influence on the algorithm's efficiency. Optimal values of α can reduce the iterations by as much as half. *A priori* selection of α is difficult since it varies with each dendritic system. Good first approximations for α are in the range $0.6 \leqslant \alpha \leqslant 0.8$.

The acute angle (ω_t) that the tributary makes with the main channel is a specified parameter. This enables the inclusion of the momentum effect of the tributary inflow via the term ($-qv_x$) of equation (14.80) as used in the momentum equation, equation (14.62). The velocity of the tributary inflow is given by:

$$V_x = (Q/A)_N \cos \omega_t \tag{14.226}$$

in which N denotes the last cross-section of the tributary.

14.18.2 Network algorithm

The network algorithm is used when the channel network consists of any or all of the following: (1) second- and higher-order tributaries; (2) bifurcations around islands with either zero, one, or two bypasses through the island; (3) dendritic branches joining any portion of the bifurcated branches; and (4) a dendritic network associated with river delta formations. The algorithm is based on the treatment of the channel junctions (confluences, bifurcations) as internal boundary conditions using the following three equations:

$$\hat{B}_{I1} = Q_i^{j+1} + Q_{i'}^{j+1} - Q_{i'+1}^{j+1} - \Delta s/\Delta t^j = 0 \tag{14.227}$$

$$\hat{B}_{I2} = 2g(h_i^{j+1} - h_{i'+1}^{j+1}) + (Q^2/A^2)_i^{j+1} - \Upsilon(Q^2/A^2)_{i'+1}^{j+1} = 0 \tag{14.228}$$

$$\hat{B}_{I3} = 2g(h_{i'}^{j+1} - h_{i'+1}^{j+1}) + (Q^2/A^2)_{i'}^{j+1} - \Upsilon(Q^2/A^2)_{i'+1}^{j+1} = 0 \tag{14.229}$$

where:

$$\frac{\Delta s}{\Delta t} = \Delta x_i/(6\ \Delta t^j)\tilde{B}(h_i^{j+1} + h_{i'}^{j+1} + h_{i+1}^{j+1} - h_i^j - h_{i'}^j - h_{i'+1}^j) \tag{14.230}$$

$$i' = i + m + 1 \tag{14.231}$$

$$\tilde{B} = B_i^j + B_{i'+1}^j + B_{i'}^j \cos \omega_t \tag{14.232}$$

$$\Upsilon = 1 + C_m + C_f \tag{14.233}$$

$$C_m = (0.1 + 0.83Q_{i'}^j/Q_{i'+1}^j)(\omega_t/90)^\mu \tag{14.234}$$

$$C_f = 2g\ \Delta x_i \bar{n}^2/[2.21(\bar{D}^{4/3})^j] \tag{14.235}$$

in which $\bar{D}$ is the average depth in the junction, $\bar{n}$ is the Manning n for the junction, ω_t is the acute angle between the upstream reach and the branch, μ is an exponent taken as unity, and m is the total number of Δx reaches located upstream (downstream) along the branching channel. The parameters C_m and C_f are related to the head loss due to mixing (Lin and Soong, 1979) and friction effects, respectively. They can be specified as zero values in FLDWAV.

The partial derivatives of equation (14.227) for the Jacobian are:

$$a_{l,l-1} = \partial\hat{B}_{I1}/\partial Q_i = 1 \tag{14.236}$$

$$a_{l,l} = \partial\hat{B}_{I1}/\partial h_i = -\tilde{B}\ \Delta x_i/(6\ \Delta t^j) \tag{14.237}$$

$$a_{l,l+k'} = \partial\hat{B}_{I1}/\partial Q_{i'} = 1 \tag{14.238}$$

$$a_{l,l+k'+1} = \partial\hat{B}h_{i'} = -\tilde{B}\ \Delta x_i/(6\ \Delta t^j) \tag{14.239}$$

$$a_{l,l+k'+2} = \partial\hat{B}_{I1}/Q_{i'+1} = -1 \tag{14.240}$$

$$a_{l,l+k'+3} = \partial\hat{B}_{I1}/\partial h_{i'+1} = -\tilde{B}\ \Delta x_i/(6\ \Delta t^j) \tag{14.241}$$

The derivatives of equation (14.228) are:

$$a_{l',l'-k'} = \partial\hat{B}_{I2}/\partial Q_i = 2(Q/A^2)_i^{j+1} \tag{14.242}$$

$$a_{l',l'-k'+1} = \partial\hat{B}_{I2}/\partial h_i = 2g - 2(Q^2B/A^3)_i^{j+1} \tag{14.243}$$

$$a_{l',l'-1} = \partial\hat{B}_{I2}/Q_{i'+1} = 2\Upsilon(Q/A^2)_{i'+1}^{j+1} \tag{14.244}$$

$$a_{l',l'} = \partial\tilde{B}_{I2}/\partial h_{i'+1} = -2g - 2\Upsilon(Q^2B/A^3)_{i'+1}^{j+1} \tag{14.245}$$

The partial derivatives of equation (14.229) are;

$$a_{l'+1,l'-1} = \partial\hat{B}_{I3}/\partial Q_{i'} = 2(Q/A^2)_{i'}^{j+1} \tag{14.246}$$

$$a_{l'+1,l'} = \partial\hat{B}_{I3}/\partial h_{i'} = 2g - 2(Q^2B/A^3)_{i'}^{j+1} \tag{14.247}$$

$$a_{l'+1,\,l'+1} = \partial\hat{B}_{I3}/\partial Q_{i'+1} = -2\Upsilon(Q/A^2)_{i'+1}^{j+1} \tag{14.248}$$

$$a_{l'+1,l'+2} = \partial\hat{B}_{I3}/\partial h_{i'+1} = -2g + 2\Upsilon(Q^2B/A^3)_{i'+1}^{j+1} \tag{14.249}$$

The subscript (l) is determined by the sequence number of the most upstream cross-section. The subscripts (l', k', k'') are automatically determined so as to minimize the number of off-diagonal elements in the Jacobian and to minimize the creation of new off-diagonal elements during the elimination phase of the matrix solution. Also, the way in which the cross-sections are assigned sequential numbers within the channel network is most important in effecting the desired minimization. The numbering scheme is as follows: numbers run consecutively in the downstream direction until a dendritic-type junction is reached; then the most upstream section of the dendritic branch is given the next consecutive number and the numbes increase in the downstream direction along this branch until another junction is reached; then the most upstream section of that dendritic branch is numbered and the numbers increase in the downstream direction along that branch until a new junction is reached; this is repeated until all sections have been numbered, including the first cross-section of the branch of the very first dendritic-type junction; then the numbers continue to increase along the downstream branch of this junction. Bifurcations are numbered in a similar manner.

Computational efficiency is achieved by use of a specially developed matrix solution technique of the Gauss elimination type which operates on only non-zero elements in the matrix through use of a specified code number for each cross-section in the network of channels. The specified code number is as follows: (1) regular cross-section, (2) upstream boundary, (3) downstream boundary, (4) dendritic-type junction, (5) dendritic-type junction emanating from a bifurcated channel branch, (6) upstream junction of a bifurcation around an island, (7) downstream junction of a bifurcation around an island, (8) bifurcation-type junction emanating from another bifurcated channel and joining with a third bifurcated channel, and (9) bifurcation-type junction emanating from a bifurcated channel and joining into the other branch of the bifurcated channel.

Three subroutines in the FLDWAV program accomplish the special treatment of channel networks. The first determines the appropriate row and column numbers of the derivative elements in the Jacobian, the second evaluates the derivatives, and the third solves the matrix. The Jacobian is a $2N \times 2N$ matrix. The number of operations (addition, subtraction, multiplication, division) required to solve the matrix is approximately $(102 + 46J)N$, where J is he total number of junctions. This is compared with $(95N - 48)$ operations for the relaxation algorithm, $(38N - 19)$ for a single channel using equations (14.111)–(14.119), and $16/3N^3 + 8N^2 + 14/3N)$ for a standard Gauss elimination method for solving a $2N \times 2N$ matrix. Generally, the simulation of a channel network requires about two to three times as much computational effort as a single channel when each have N cross-sections.

14.19 LEVEE EFFECTS

Flows which overtop a levee located along either side or both sides of a channel may be simulated in FLDWAV, since any number of Δx reaches may bypass flow via a broadcrested weir-flow equation to another channel which represents the floodplain (beyond the levee). If the system of channels including floodplain channels is treated by the relaxation technique, the floodplain channel may either directly connect back into the waterway at some downstream location, or it may be disconnected as in the case of the floodplain within a ringed levee where the flow is ponded with no exit. If the channel system is treated by the network technique, the floodplain must hydraulically connect with the waterway. The hydraulic connection may be either a natural confluence or a flap-gated gravity drainage pipe. The flow in the floodplain can affect the overtopping levee flows via a submergence correcton factor K_{le} similar to that used at internal boundaries of dams. The flow may also pass from the waterway to the floodplain through a time-dependent crevasse (breach) in the levee using a breach-flow equation similar to that used at internal boundaries of dams.

The overtopping and/or breach flow is routed through the floodplain which is considered to be a tributary of the waterway along which the levee is located. The tributary (floodplain) channel must have a fictitious low-flow channel in which a small steady flow occurs at all times before the lateral inflow from the overtopped (breached) levee enters. The low flow which is specified via the upstream boundary condition for the tributary is necessary so that the Saint-Venant equations applied to the tributary can be continuously solved during the simulation; however, at the hydraulic connection with the channel, the fictitious low flow is not added to the channel flow, nor is it included in the flow that ponds within a ringed levee.

Depending on the relative elevations in the channel and floodplain (tributary), the overtopping levee flow can reverse its direction and flow from the floodplain back into the channel. Each Δx_i reach for the channel has a corresponding Δx_m reach along the floodplain channel. Each Δx_i reach has a submergence correcton factor (K_{le}), a broadcrested weir flow coefficient (C_{le}), and a mean elevation (h_{le}) of the top of the levee. The effect of the levee flow is achieved by considering it to be lateral inflow of outflow (q) in equations (14.61) and (14.62). When routing the flow in the channel, if the flow overtops the levee and enters the floodplain it is considered to be bulk lateral outflow. When routing the flow in the floodplain the levee overtopping flow is considered to be lateral inflow. In either case the overtopping flow is computed as follows:

$$q_{le_i} = S_g C_{le_i} K_{le_i} (\hat{h} - h_{le_i})^{3/2} \quad \ldots \hat{h} > h_{le_i} \tag{14.250}$$

where

$$S_g = (\hat{h} - \tilde{h})/|\hat{h} - \tilde{h}| \tag{14.251}$$

$$\hat{h} = \bar{h}_i \quad \ldots \bar{h}_i > h_{t_m} \tag{14.252}$$

$$\hat{h} = \bar{h}_{t_m} \quad \ldots \bar{h}_i < h_{t_m} \tag{14.253}$$

$$\tilde{h} = \bar{h}_{t_m} \quad \ldots \bar{h} > h_{t_m} \tag{14.254}$$

$$\tilde{h} = \bar{h}_i \quad \ldots \bar{h}_i < h_{t_m} \tag{14.255}$$

$$\bar{h}_i = 0.5(h_i^{j+1} + h_{i+1}^{j+1}) \tag{14.256}$$

$$\bar{h}_{t_m} = 0.5(h_{t_m}^{j+1} + h_{t_{m+1}}^{j+1}) \tag{14.257}$$

$$K_{le_i} = 1 \quad \ldots \gamma \leqslant 0.67 \tag{14.258}$$

$$K_{le_i} = 1. - 27.8(\gamma - 0.67)^3 \quad \ldots \gamma > 0.67 \tag{14.259}$$

$$\gamma = (\tilde{h} - h_{le_i})(\hat{h} - h_{le_i}) \tag{14.260}$$

in which S_g determines the appropriate sign (− for outflow, + for inflow), $\bar{h}_i$ is the average water elevation along the Δx_i reach, h_{t_m} is the average water elevation along the same Δx reach of the floodplain. Of course, the lateral flow may be zero when the water elevation in either channel does not overtop the levee or when the elevations are exactly the same, i.e.

$$q_{le_i} = 0 \quad \ldots \hat{h} < h_{le_i},\ \tilde{h} < h_{le_i} \tag{14.261}$$

$$q_{le_i} = 0 \quad \ldots \hat{h} = \tilde{h} \tag{14.262}$$

Additional terms must be included in certain elements of the Jacobian in the Newton–Raphson solution to account for the effect of the levee lateral inflow (outflow). In equation (14.88) the following additional term is required:

$$-\theta\, \Delta x_i\, \partial q/\partial h_i = -\theta\, \Delta x_i q_{le_i} \left[\frac{1.5\, \partial \hat{h}/\partial h_i}{(\hat{h} - h_{le_i})} - \frac{83.4(\gamma - 0.67)^2\, \partial \gamma/\partial h_i}{K_{le_i}} \right] \tag{14.263}$$

where:

$$\partial \hat{h}/\partial h_i = 0.5 \quad \ldots \bar{h}_i > \bar{h}_{t_m} \tag{14.264}$$

$$\partial \hat{h}/\partial h_i = 0 \quad \ldots \bar{h}_i \leqslant \bar{h}_{t_m} \tag{14.265}$$

$$\partial \gamma/\partial h_i = -0.5\gamma/(\hat{h} - h_{le_i}) \quad \ldots \bar{h}_i > \bar{h}_{t_m},\ \gamma > 0.67 \tag{14.266}$$

$$\partial \gamma/\partial h_i = 0.5/(\hat{h} - h_{le_i}) \quad \ldots \bar{h}_i < \bar{h}_{t_m},\ \gamma > 0.67 \tag{14.267}$$

In equation (14.90) the additional term is $\partial q/\partial h_{i+1}$ which is given by the same expression as in equation (14.263) except h_i is replaced with h_{i+1}. When applying the Saint-Venant equations to the Δx_m reach of floodplain, equation (14.263) is used to introduce the additional terms in equations (14.88) and (14.90). However, in this case the expression in equations (14.243)–(14.267) must be slightly modified, i.e. $\hat{h}$, $\tilde{h}$ and h_i are replaced with $\bar{h}_t$, $\bar{h}_i$ h_{i_m}, respectively.

The overtopping levee flow is assumed to enter perpendicular to the direction of flow in the floodplain. Thus, the lateral flow does not affect the conservation of momentum equation (14.62) except when it is considered to be bulk lateral outflow. In this case, equations (14.106) and (14.107) are appropriate.

14.20 MODEL CALIBRATION (AUTOMATIC)

Calibration is the process by which values of model parameters are adjusted until results of simulations correspond to measured (observed) flow conditions. A critical task in the calibration of dynamic wave models such as FLDWAV is the determination of the Manning n which often varies with discharge or stage, and with distance along the waterway. Calibration may be a manual trial-and-error process; however, FLDWAV has an option to automatically determine the optimum Manning n which will minimize the difference between computed and observed hydrographs via a highly efficient optimization technique (Fread and Smith, 1978). The technique can be applied to a single reach of waterway or any dendritic system which can be simulated with the relaxation method. The Manning n or conveyance factor (K_c) may be constant or have a piecewise linear variation with either discharge or water elevation for each reach of the waterway bounded by gauging stations from which observed water elevation hydrographs are available.

In the automatic calibration technique optimum Manning n values are sequentially determined for each reach bounded by gauging stations, commencing with the most upstream reach and progressing reach-by-reach in the downstream direction. Dendritic river systems are decomposed into a series of

single reaches connected by appropriate external boundary conditions. Tributaries are calibrated before the main-stem waterway and their flows are added to the main stem as lateral inflows. An observed discharge hydrograph is specified at the upstream boundary of each waterway, while an observed water elevation hydrograph at the downstream gauging station of each reach is used as the downstream boundary condition. The computed water elevation hydrograph at the upstream boundary is tested against the observed hydrograph at that point. Statistics of bias (Φ_j) and root-mean-square (r.m.s.) error are computed for $j = 1,2,3, \ldots J$ ranges of discharge or water elevation so that the Manning n or K_c can be calibrated as a function of discharge or stage. For each range of discharge, an improved estimate of the optimum Manning n (n_j^{k+1}) is obtained via a modified Newton–Raphson iterative method, i.e.

$$n_j^{k+1} = n_j^k - \frac{\Phi_j^k(n_j^k - n_j^{k-1})}{(\Phi_j^k - \Phi_j^{k-1})} \qquad \ldots k > 2;\ j = 1, 2, \ldots J \quad (14.268)$$

in which the k superscript denotes the number of iterations and Φ_j is the bias for the jth range. Equation (14.268) can be applied only for the second and successive iterations; therefore, the first iteration is made using the following estimator:

$$n_j^{k+1} = n_j^k(1.0 - 0.01\Phi_j^k/|\Phi_j^k|) \qquad \ldots k = 1;\ j = 1, 2, \ldots J \quad (14.269)$$

in which a small percentage change in the Manning n is made in the correct direction as determined by the term $(-\Phi_j^k/|\Phi_j^k|)$. The convergence properties of equation (14.268) are quadratic with convergence usually obtained within three to five iterations. Improved Manning n values obtained via equation (14.268) are used and the cycle repeated until a minimum r.m.s. error for the reach is found. Then, the discharges computed at the downstream boundary using the otimum Manning n are stored internally and specified as the upstream boundary condition for the next downstream reach.

Computational requirements for the calibration technique are less than twice that required for an application of FLDWAV to the same waterway without the calibration option utilized.

14.21 SELECTED APPLICATIONS OF FLDWAV

Four applications of FLDWAV are presented. They include: (1) a long, very mild sloping large river with a slow rising flood wave; (2) a dendritic river system consisting of four mild sloping large rivers with moderately rising flood waves and mutual backwater effects among the channels of the network; (3) a large, very mild sloping dendritic river system affected by a large tide at its mouth; and (4) a moderately sloping river subjected to a rapidly rising dam-break wave. These applications represent a wide spectrum of wave and channel characteristics for which the dynamic wave model is particularly well-suited and potentially the most accurate of the routing models.

14.21.1 Lower Mississippi

FLDWAV was applied to a 291.7 mile reach of the Lower Mississippi River from Red River Landing to Venice shown schematically in Figure 14.2. Six intermediate gauging stations at Baton Rouge, Donaldsonville, Reserve, Carrollton, Chalmette, and Point a la Hache were used to evaluate the simulations. This reach of the Lower Mississippi is contained within levees for most of its length, although some overbank flow occurs along portions of the upper 70 miles. Throughout the reach the alluvial river meanders between deep bends and relatively shallow crossings; the sinuosity coefficient is 1.6. The low flow depth varies from a minimum of 30 ft at some crossings to a maximum depth of almost 200 ft in some bends. The average channel width is approximately $\frac{1}{2}$ mile. The average channel bottom slope is a very mild, 0.0000064. The Manning n varies from about 0.012 to 0.030. The discharge varies from low flows of about 100,000 cfs to flood discharges of over 1,200,000 cfs. A total of 25 cross-sections located at unequal intervals ranging from 5 to 20 miles were used to describe the 291.7 mile reach.

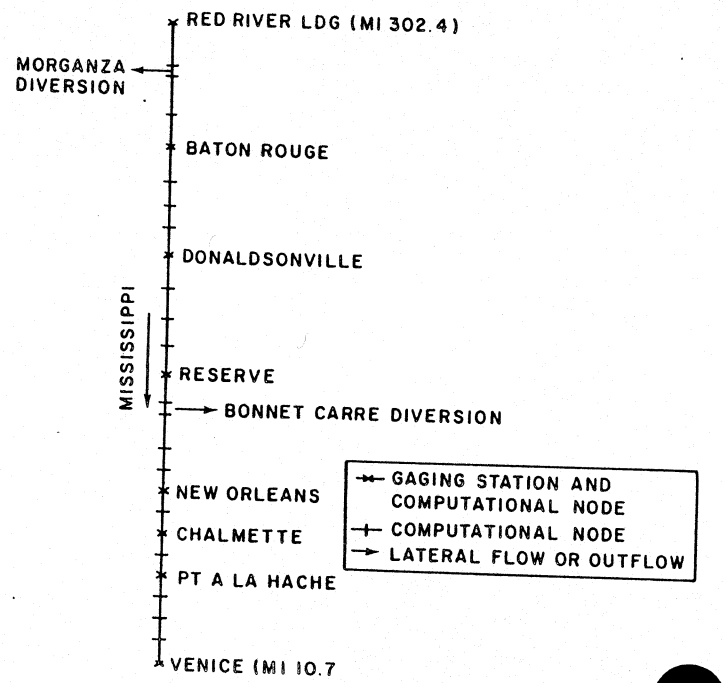

Figure 14.2 Schematic of Lower Mississippi River

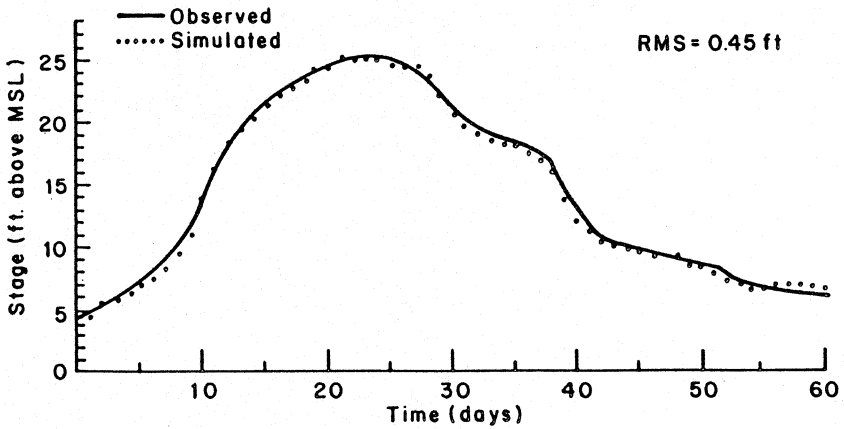

Figure 14.3 Observed vs. simulated stages at Donaldsonville for 1966 flood

The reach was first automatically calibrated by FLDWAV for the 1969 spring flood. Time steps of 24 hours were used. Then, using the calibrated set of Manning *n* vs. discharge for each reach bounded by gauging stations, the 1969 flood was simulated using water elevation (stage) hydrographs for upstream and downstream boundaries at Red River Landing and Venice, respectively. The simulated stage hydrographs at the six intermediate gauging stations were compared with the observed hydrographs. The r.m.s. error was used as a statistical measure of the accuracy of the calibration. The r.m.s. error varied from 0.17 to 0.36 ft with an average value of 0.25 ft.

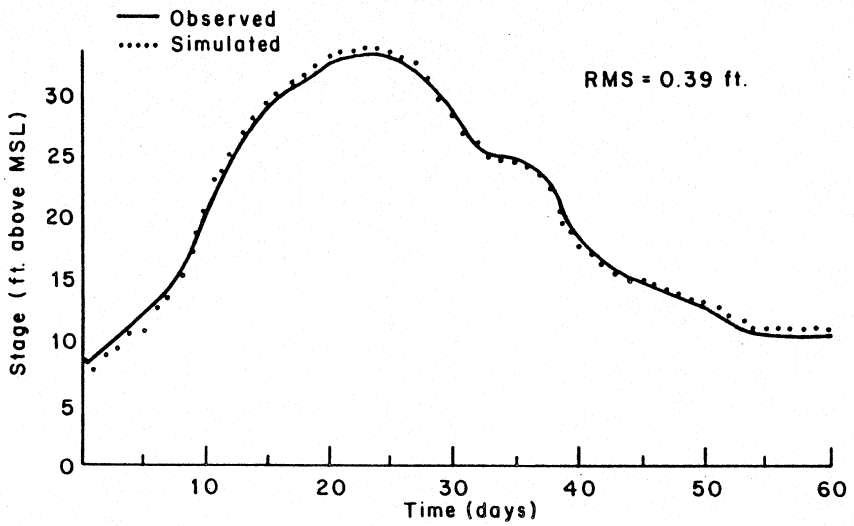

Figure 14.4 Observed vs. simulated stages at Baton Rouge for 1966 flood

Table 14.1 Summary of flood simulations in Lower Mississippi River (Red River Landing to Venice) for the years 1959–1971

Year	Average r.m.s. error (ft.)	Peak discharge (1000 cfs)
1959	0.62	750
1960	0.31	850
1961	0.47	1220
1962	0.61	1155
1963	0.38	905
1964	0.51	1140
1965	0.44	1040
1966	0.38	1090
1967	0.38	700
1968	0.36	980
1969*	0.25	1065
1970	0.91	1080
1971	0.46	940

*Calibrated

Several historical floods from the period 1959–71 were then simulated using the calibrated Manning *n* values obtained from the 1969 flood. An example of simulted vs. observed stages is shown in Figures 14.3 and 14.4 for the 1966 flood. Average r.m.s. errors for all six stations for each of the simulated floods are shown in Table 14.1. The average r.m.s. error for all the floods was 0.47 ft. This compares with 0.25 ft for the calibrated flood of 1969, indicating that for this reach of the Mississippi there is not a significant change in the channel roughness from one flood event to another. A calibration run required 7 s on an IBM 360/195 computer system while a normal simulation run required 6 s.

14.21.2 Mississippi–Ohio–Cumberland–Tennessee System

A dendritic channel system consisting of 393 miles of the Mississippi–Ohio–Cumberland–Tennessee (MOCT) River System was also simulated using FLDWAV. A schematic of the river system is shown in Figure 14.5. Eleven intermediate gauging stations located at Fords Ferry, Golconda, Paducah, Metropolis, Grand Chain, Cairo, New Madrid, Red Rock, Grand Tower, Cape Girardeau, and Price Landing were used to evaluate the simulation.

In applying FLDWAV to this system the main channel was considered to be the Ohio–Lower Mississippi segment with the Cumberland, Tennessee, and Upper Mississippi considered as first-order tributaries. The channel bottom slope is mild, varying from about 0.000047 to 0.000095. Each branch of the river system is influenced by backwater from downstream branches. Total discharge through the system varies from low flows of approximately

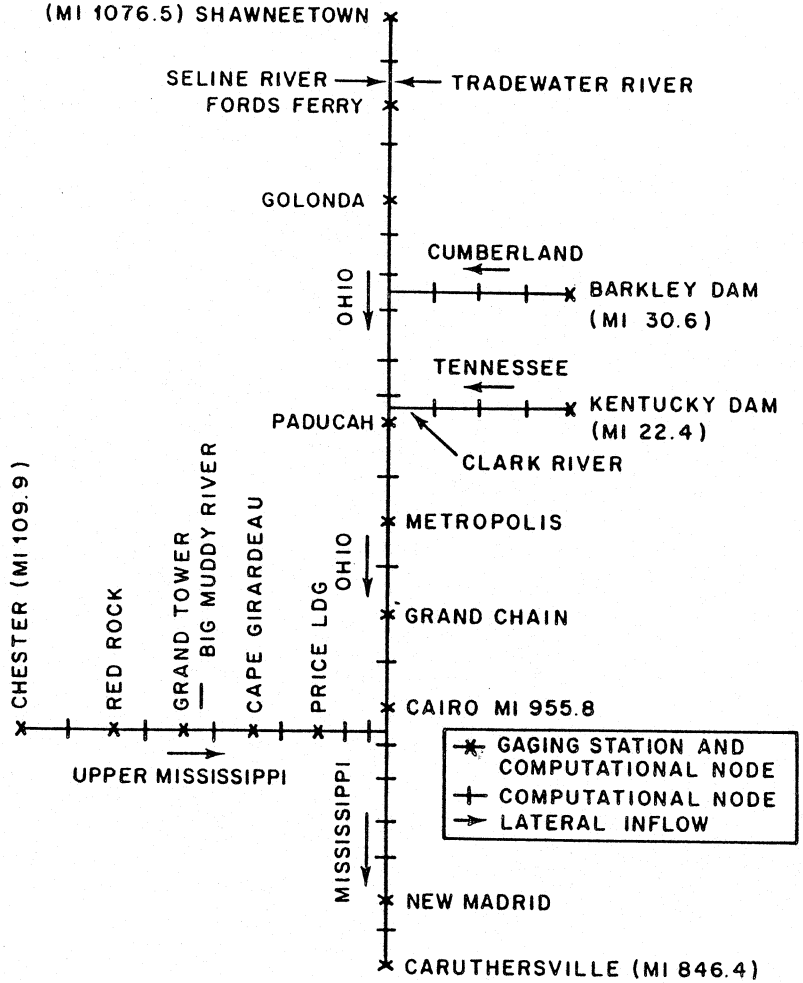

Figure 14.5 Schematic of Mississippi–Ohio–Cumberland–Tennessee (MOCT) River System

120,000 cfs to flood flows of 1,700,000 cfs. A total of 45 cross-sections located at unequal intervals ranging from 0.5 to 20 miles were used to describe the MOCT river system.

The MOCT system was calibrated to determine the n–Q relationship for each of 15 reaches bounded by gauging stations. Time steps of 24 h were used. About 25 s of IBM 360/195 CPU time were required by FLDWAV to perform the calibration; a simulation run required only about 15 s. The flood of 1970 was used in the automatic calibration process. The average r.m.s. error for all 15 rea[illegible]vas 0.60 ft. Typical comparisons of observed and simulated stages

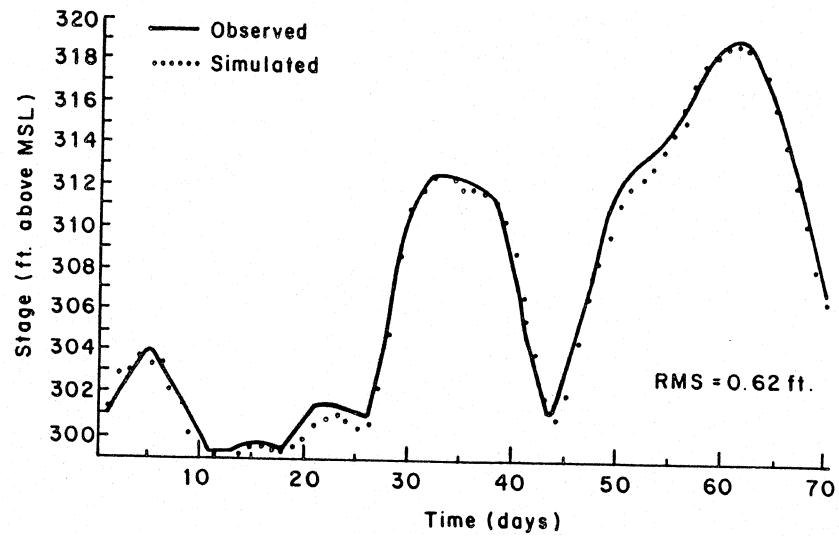

Figure 14.6 Observed vs. simulated stages at Cairo for 1970 flood

for the Cairo and Cape Girardeau gauging stations are shown in Figures 14.6 and 14.7 respectively.

Using the calibrated n–Q relations, the 1969 flood was simulated. Stage hydrographs at Shawneetown and Chester and discharge hydrogaphs at

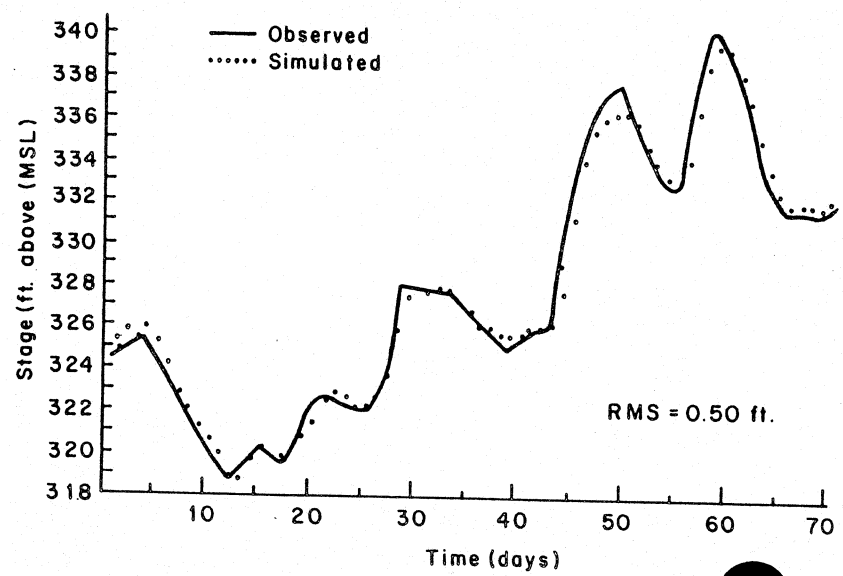

Figure 14.7 Observed vs. simulated stages at Cape Girardeau for [illegible] flood

Barkely Dam and Kentucky Dam were used as upstream boundary conditions, and a rating curve was used as the downstream boundary condition at Caruthersville. The average r.m.s. error for the 11 intermediate gauging stations was 0.56 ft.

14.21.3 Columbia–Willamette System

FLDWAV was applied to the 130-mile reach of the lower Columbia River below Bonneville Dam, including the 25-mile tributary reach of the lower Willamette River. A schematic of the river system is shown in Figure 14.8.

This reach of the Columbia has a very flat slope (0.000011) and the flows are affected by the tide from the Pacific Ocean. The tidal effect extends as far upstream as the tailwater of Bonneville Dam during periods of low flow. Reversals in discharge during low flow are possible as far upstream as Vancouver. A total of 25 cross-sections located at unequal distance intervals ranging from 0.6 to 12 miles were used to describe the river system. One-hour time steps were used in the simulations which required about 11 s on an IBM 360/5 computer system.

The system was first calibrated for a 4-day period in August 1973. Seven

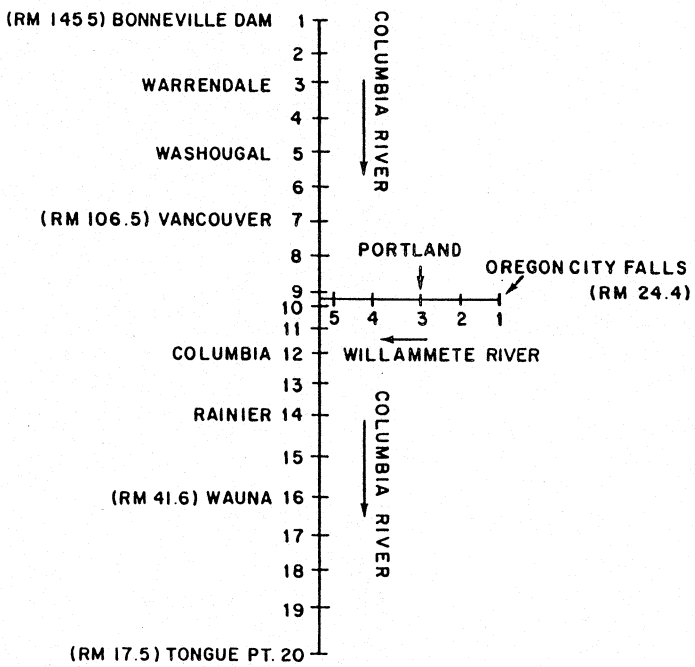

Figure 14.8 Schematic of lower Columbia–Willamette River System

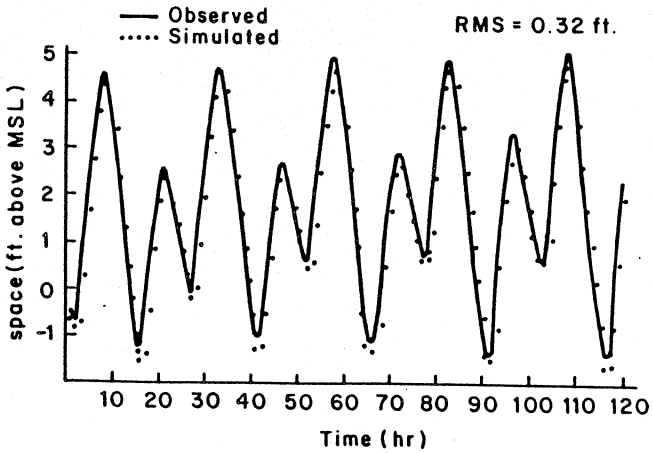

Figure 14.9 Observed vs. simulated stages at Wauna

intermediate gauging stations at Warrendale, Washougal, Vancouver, Portland, Columbia City, Rainier, and Wauna were used along with the gauging stations at the extremities of the system, i.e., Bonneville, Oregon Falls, and Tongue Point. Another 5-day period in August 1973 was then simulated using the calibrated n–Q relations. Upstream and downstream boundaries were observed discharges and stages, respectively. The average r.m.s. error for all stations in the simulation run was 0.21 ft. Some examples of simulated and observed stage hydrographs for Portland and Wauna are shown in Figures 14.9 and 14.10, respectively.

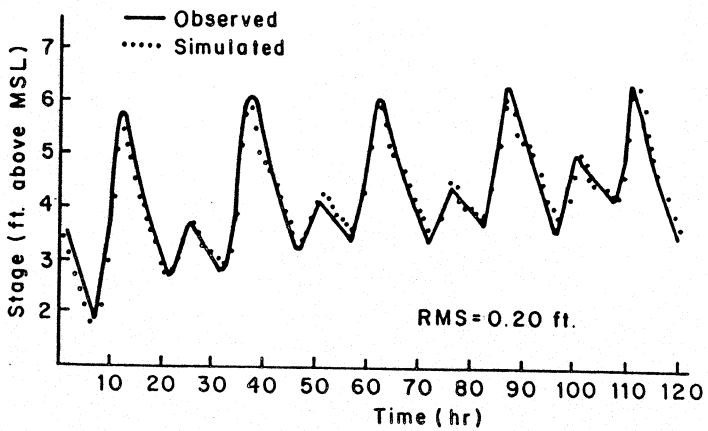

Figure 14.10 Observed vs. simulated stages at Portland

14.21.4 Teton Dam-break flood

The Teton Dam, a 300-ft high earthen dam with a 3000-ft long crest, failed on 5 June 1976, killing 11 people, making 25,000 people homeless, and inflicting about $400 million in damages to the downstream Teton–Snake River Valley. Data from the US Geological Survey provided observations on the approximate development of the breach, description of the reservoir storage, downstream cross-sections and estimate values of the Manning's n approximately every 5 miles, indirect peak discharge measurement at three sites, flood peak travel times, and flood peak elevations. The inundated area is shown in Figure 14.11.

The following breach parameters were used in DAMBRK to reconstitute the downstream flooding due to the failure of Teton Dam: $\tau_{br} = 1.25$ h, $\bar{b} = 150$ ft, $z = 0$, $h_{bm} = 0.0$, $h_f = h_d = 261.5$ ft, $Q = 16{,}000$ cfs. The initial depth of the reservoir was 261.5 ft. Cross-sections at 12 locations shown in Figure 14.11 along the 60-mile reach of the Teton–Snake River Valley below the dam were used. The average bottom slope of the 60-mile reach is 0.00135. Five top widths were used to describe each cross-section. The downstream valley consists of a narrow canyon (approximately 1000 ft wide) for the first 5 miles and thereafter a wide valley which was inundated to a width of about 9 miles. The estimated Manning n values vary from 0.028 to 0.047. Additional cross-sections were interpolated such that computational reach lengths varied from 0.5 to 1.5 miles. The downstream boundary was assumed to be channel flow control as represented by a loop rating curve giving by equation (14.136).

The computed outflow hydrograph is shown in Figure 14.11. It has a peak value of 1,652,300 cfs, a time to peak of 1.25 h, and a total duration of about 6 h. The peak is about 20 times greater than the flood of record. The temporal variation of the computed outflow volume compared within 5 per cent of observed values. The computed peak discharge values along the 60-mile downstream valley are shown in Figure 14.12 along with three observed (indirect measurement) values at miles 8.5, 43.0, and 59.5. The average difference between the computed and observed values is 4.8 per cent. Most apparent is the extreme attenuation of the peak discharge as the flood wave propagates through the valley. Losses due to infiltration and detention storage behind irrigation levees were assumed to vary from zero to a maximum of -0.30 cfs/ft and were acounted for by the lateral outflow (q) in equation (14.61).

The a priori selection of the breach parameters (τ_{br} and $\bar{b}$) causes the greatest uncertainty in simulating dam-break flood waves. However, sensitivity studies (Fread, 1980) show that large differences in the discharges near the Teton Dam rapidly diminish in the downstream direction. After 15 miles the variation diminished to (+15 to −8 per cent) for variations in $\bar{b}$ of a factor of 2 and in τ_{br} [illegible] factor from 0.3 to 2. The tendency for extreme peak attenuation

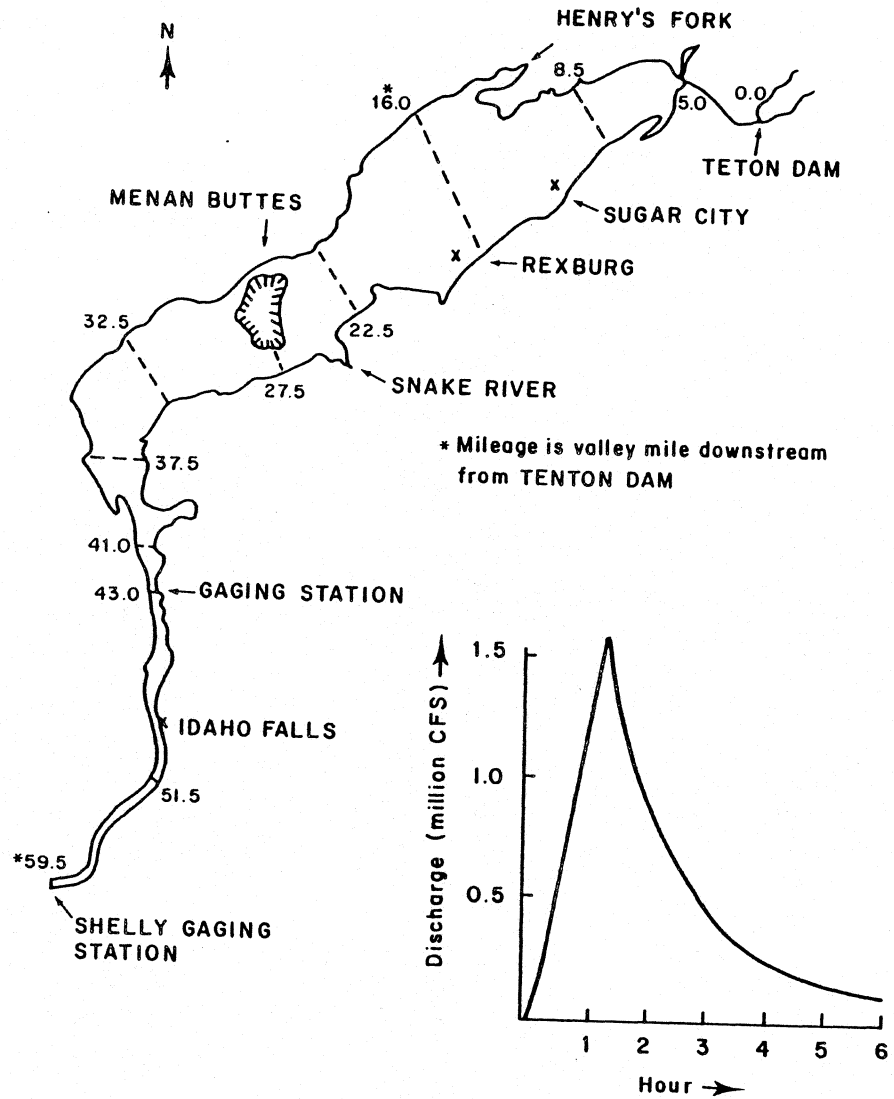

Figure 14.11 Outflow hydrograph and flood area downstream of Teton Dam

and rapid damping of differences in the peak discharge is accentuated in the case of Teton Dam due to the presence of the very wide valley. Had the narrow canyon extended all along the 60-mile reach to the Shelly gauge, the peak discharge would not have attenuated as much and the differences in peak discharges due to variations in $\bar{b}$ and τ_{br} would be more persiste[illegible] this in-tance the peak discharge (cfs) would have attenuated to about 3[illegible] rather

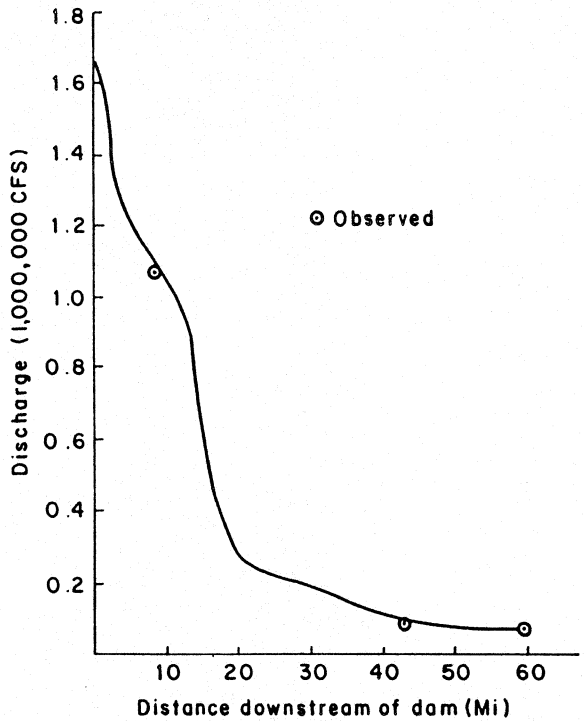

Figure 14.12 Profile of peak discharge from Teton Dam failure

than 67,000 and the differences in peak discharges at mile 59.5 would have been about 27 per cent, as opposed to less than 5 per cent for the actual wide valley.

Computed peak elevations compared favourably with observed values. The average absolute error was 1.5 ft, while the average arithmetic error was only −0.2 ft. The computed travel time of the flood wave was compared with observed values at the locations of the discharge measurements; they differed by less than 10 per cent.

A typical simulation of the Teton flood involved 78 Δx reaches, 55 h of prototype time, and an initial time step (Δt) of 0.06 h which was automatically increased gradually to 0.5 h as the wave propagated downstream and natural dispersion increased the time of rise. Such a simulation run required only 19 s on an IBM 360/195 computer system.

14.22 A VIEW TOWARDS FUTURE DIRECTIONS IN CHANNEL ROUTING

The hydrological models (especially the Muskingum–Cunge model) will continue to be much used, particularly as components of precipitation-runoff

catchment models for routing overland flow and channel flow associated with the network of headwater streams which feed larger, more mild sloping collecting streams. Therefore it is important that the strengths and limitations of the simplified models be set forth and their relationship to other routing models, especially the complete models, be understood through analyses similar to those by Cunge (1969), Miller and Cunge (1975), Ponce *et al.* (1978), and Koussis (1978, 1980). The analysis should quantify a model's characteristics in terminology familiar to hydraulic engineers.

It appears that the trend for increasing computational speed and storage capabilities of both large and small computers will be sustained throughout the 1980s. Also, the accessibility to such computational resources will become more commonplace and economically feasible to both large and small agencies, universities, and engineering consulting firms. For these reasons, and their great range of applicability, flood routing models based on the complete Saint-Venant equations will continue to receive much attention from model developers and increasing use in the engineering community. Since the implicit dynamic models are the most promising of the complete hydraulic models for many flood routing applications due to their superior computational efficiency, many future improvements will likely be associated with this type of model. Some future improvements may include the following: (1) Develop an improved one-dimensional modelling of meandering rivers with short-circuiting floodplain flow and large differences between channel and floodplain properties such as hydraulic roughness and wave celerity; some effort in this area has been made by Radojkovic (1976), Fread (1976), Tingsanchali and Ackermann (1976), and Weiss and Midgley (1978). (2) Analysis of effects of nonlinear terms in the Saint-Venant equations on the stability and accuracy of implicit solution algorithms. (3) Develop manual and/or automatic smoothing techniques to overcome nonlinear instabilities due to rapid variations of cross-sectional properties with elevation and distance along the waterway.

A significant area of general improvement consists of expanding flood routing models to account for significant effects of bridges, breached or overtopped levees, ice covers, ice jams, flow exchanges with groundwater aquifers due to bed and bank seepage and floodplain infiltration, and bed elevation and bed roughness changes caused by sediment transport. There exists a large body of knowledge in each of these areas; however, the incorporation of this into flood routing models has not received enough attention. Some work in this area has been done, e.g. Chen and Simons (1975) and Ponce *et al.* (1979) concerning bed elevation changes due to sediment transport; Pinder and Sauer (1971), Freeze (1972), Hall and Moench (1972), Cooley and Westphal (1974), and Pogge and Chiang (1977) concerning the flow exchange between the waterway and ajacent aquifer; Uzner and Kennedy (1976) concerning ice jams; and Balloffet (1969), Cunge (1975b), Fread (1978, 1980) concerning effects of levees, bridge/embankments, and other man-made structures.

Calibration of flood routing models is most essential for good results. The calibration process for diffusion and dynamic hydraulic models when applied to a complex system of waterways is often time-consuming and requires considerable experience. There is a need for the development of objective calibration methodologies which may be trial–error and/or automatic, e.g., Yeh and Becker (1973), and Fread and Smith (1978).

Flood routing models should be developed having a modular design. This will permit convenient selection of various combinations of external and internal boundary conditions permitting the same mdoel to be used for a wide range of applications.

There is also a need for the development of updating techniques to improve real-time simulation of unsteady flows such as in flood forecasting. Approaches include the use of filter theory, e.g., the Kalman filter technique (Chiu and Isu, 1978).

Automated data processing techniques are needed to allow the inexpensive and rapid development of the cross-section and roughness parameters of the hydraulic-type models. The sources of data should include remote sensing as well as conventional on-site surveys and measurements (Lai *et al.*, 1980).

REFERENCES

Abbott, M. B. (1966) *An Introduction to the Method of Characteristics*. New York: American Elsevier.

Abbott, M. B. (1976) 'Discussion of review of models of tidal waters by J. B. Hinwood and I. G. Wallis', *J. Hydraulic Div.*, ASCE, **102** (HY8), 1145–1148.

Abbott, M. B., and Cunge, J. A. (1975) 'Two-dimensional modeling of tidal deltas and estuaries'. In Mahmood, K., and Yevjevich, V. (eds), *Unsteady Flow in Open Channels*, Fort Collins, Colorado: Water Resources Publications, Chapter 18, pp. 763–812.

Abbott, M. B., and Ionescu, F. (1967) 'On the numerical computation of nearly horizontal flows'. *J. Hydraulic Res.*, **5**(2), 97–117.

Amein, M. (1966) 'Streamflow routing on computer by characteristics'. *Water Resources Res.* **2**(1), 123–130.

Amein, M., and Chu, H. L. (1975) 'Implicit numerical modeling of unsteady flows'. *J. Hydraulic Div.*, ASCE, **101** (HY6), 93–108.

Amein, M., and Fang, C. S. (1970) 'Implicit flood routing in natural channels'. *J. Hydraulic Div.*, ASCE, **96** (HY12), 2481–2500.

Balloffet, A. (1969) 'One-dimensional analysis of floods and tides in open channels'. *J. Hydraulic Div.*, ASCE, **95** (HY4), 1429–1451.

Baltzer, R. A. and Lai, C. (1968) 'Computer simulation of unsteady flow in waterways'. *J. Hydraulic Div., ASCE,* **94** (HY4), *1083–1117.*

Bennett, J. P. (1975) 'General model to simulate flow in branched estuaries'. In *Symp. on Modeling Techniques*, Vol. I, 2nd Annual Symp. of Waterways, Harbors, and Coastal Engng. Div., ASCE, pp. 643–662.

Boussinesq, J. (1871) 'Theory of the liquid intumescence, called a solitary wave or a wave [illegible]nslation, propagated in a channel of rectangular cross section'. *Comptes Rend[illegible]d. Sci., Paris*, **72**, 755–759.

Brakensiek, D. L. (1965). 'An implicit flood routing method'. Paper presented at Hydraulic Div. Specialty Conf., ASCE, Tucson, Arizona.

Chaudhry, Y. M., and Contractor, D. N. (1973) 'Application of implicit method to surges in channels'. *Water Resources Res.*, **9**(6), 1605–1612.

Chen, Y. H., and Simons, D. B. (1975) 'Mathematical modeling of alluvial channels'. In *Symp. on Modeling Techniques*, Vol. I, 2nd Annual Symp. of Waterways, Harbors, and Coastal Engng. Div., ASCE, pp. 466–483.

Chiu, C.-L., and Isu, E. O. (1978) 'Kalman filter in open channel flow estimation'. *J. Hydraulic Div.*, ASCE, **104** (HY8), 1137–1152.

Chow, V. T. (1959) *Open-Channel Hydraulics*, New York: McGraw-Hill Book Co., pp. 601–604.

Contractor, D. N., and Wiggert, J. M. (1972) *Numerical Studies of Unsteady Flow in the James River*. Bul. 51, VPI-WRRC 51, Water Resources Research Center, Virginia Poly Institute and State Univ., Blacksburg, Virginia.

Cooley, R. L., and Westphal, J. A. (1974) *An Evaluation of the Theory of Groundwater and River-water Interchange, Winnemucca Reach of the Humbolt River, Nevada*. Tech. Report Series H-W No. 19, Center for Water Resources Research, Desert Research Institute, Reno, Nevada.

Cooley, R. L., and Moin, S. A. (1976) 'Finite element solution of Saint-Venant equations'. *J. Hydraulic Div.*, ASCE, **102** (HY6), 759–775.

Cunge, J. A. (1966) *Etude d'un Schema de Differences Finies Applique a l'integration Numerique d'un Certain Type d'equation Hyperbolique d'ecoulement* [Study of a Finite Difference Scheme, Applied to Numerical Integration of the Certain Type of Hyperbolic Flow Equation]. Thesis, Grenoble University, France.

Cunge, J. A. (1969) 'On the subject of a flood propagation computation method (Muskingum method)'. *J. Hydraulic Res.*, **7**(2), 205–230.

Cunge, J. A. (1975a) 'Rapidly varying flow in power and pumping canals'. In Mahmood, K., and Yevjevich, V. (eds), *Unsteady Flow in Open Channels*, Vol. II. Fort Collins, Colorado: Water Resources Publications, Chapter 14, pp. 539–586.

Cunge, J. A. (1975b) 'Two-dimensional modeling of flood plains'. In Mahmood, K., and Yevjevich, V. (eds), *Unsteady Flow in Open Channels*, Vol. II. Fort Collins, Colorado: Water Resources Publications, Chapter 17, pp. 705–762.

Diskin, M. H. (1967) 'On the solution of the Muskingum method of flood routing equation', *J. Hydrol.*, **5**, 286–289.

Dooge, J. C. I. (1973) *Linear Theory of Hydraulic Systems*, Tech. Bul. No. 1468, USDA Agricultural Research Service, Beltsville, Maryland.

Dooge, J. C. I., Strupczewski, W. G., and Napiorkowski, J. J. (1982) 'Hydrodynamic derivation of storage parameters of the Muskingum model'. *J. Hydrol.*, **54**, 371–387.

Dronkers, J. J. (1964) *Tidal Computations in Rivers and Coastal Waters*. New York: Interscience Publishers, Inc.

Dronkers, J. J. (1969) 'Tidal computations for rivers, coastal areas, and seas'. *J. Hydraulic Div.*, ASCE, **95** (HY1), 29–77.

Ellis, J. (1970) 'Unsteady flow in channel of variable cross section', *J. Hydraulic Div.*, ASCE, **96** (HY10), 1927–1945.

Fread, D. L. (1971) 'Discussion of implicit flood routing in natural channels by M. Amein and C. S. Fang'. *J. Hydraulic Div.*, ASCE, **97** (HY7), 1156–1159.

Fread, D. L. (1973) 'Technique for implicit dynamic routing in rivers with tributaries'. *Water Resources Res.*, **9**(4), 918–926.

Fread, D. L. (1974) *Numerical Properties of Implicit Four-point Fini[illegible]ifference Equations of Unsteady Flow*. NOAA Tech. Memo NWS HYDRO-18[illegible] Department of Commerce, National Weather Service, Silver Spring, Maryla[illegible]

Fread, D. L. (1976) 'Flood routing in meandering rivers with flood plains'. In *Symp. on Inland Waterways for Navigation, Flood Control and Water Diversion*, Vol. I, ASCE, pp. 16–35.

Fread, D. L. (1978) 'NWS operational dynamic wave model'. In *Verification of Mathematical and Physical Models*, Proc. of 26th Annual Hydr. Div. Specialty Conf., ASCE, College Park, Maryland, pp. 455–464.

Fread, D. L. (1980) 'Capabilities of NWS model to forecast flash floods caused by dam failures'. In *Proc. of 2nd Conf. on Flash Floods*, Atlanta, Georgia, American Met. Soc., pp. 171–178.

Fread, D. L. and Smith, G. F. (1978) 'Calibration technique for 1-D unsteady flow models'. *J. Hydraulic Div.*, ASCE, **104** (HY7), 1027–1044.

Freeze, R. A. (1972). 'Role of subsurface flow in generating surface runoff, 1. Base flow contributions to channel flow'. *Water Resources Res.*, **8**(3), 609–623.

Garrison, J. M., Granju, J. P. and Price, J. T. (1969) 'Unsteady flow simulation in rivers and reservoirs'. *J. Hydraulic Div.*, ASCE, **95** (HY5), 1559–1576.

Goodrich, R. D. (1931) 'Rapid calculation of reservoir discharge'. *Civil Eng.*, **1**, 417–418.

Gray, W. G., Pinder, G. F. and Brebbia, C. A. (1977) *Finite Elements in Water Resources*. London: Pentech Press.

Greco, F., and Panattoni, L. (1975) 'An implicit method to solve Saint-Venant equations'. *J. Hydraulic.*, **24**, 171–185.

Grupert, J. P. (1976) 'Numerical computation of two-dimensional flows'. *J. Waterways, Harbors, Coastal Engng. Div.*, ASCE, **102**(WW1), 1–12.

Gunaratnam, D. J. and Perkins, F. E. (1970) *Numerical Solution of Unsteady Flows in Open Channels*. Hydrodynamic Lab. Report 127, Dept. of Civil Engng., Massachusetts Institute of Technology, Cambridge, Massachusetts.

Hall, F. R., and Moench, A. F. (1972) 'Application of the convolution equation to stream-aquifer relationships'. *Water Resources Res.*, **8**(2), 487–493.

Harder, J. A., and Armacost, L. V. (1966) *Wave Propagation in Rivers*. Hydraulic Engng. Lab., Report No. 1, Series 8, University of California, Berkeley, California.

Harley, B. M. (1967) *Linear Routing in Uniform Channels*. Thesis, University College, Cork, Ireland.

Harley, B. M., Perkins, F. E., and Eagleson, P. S. (1970) *A Modular Distributed Model of Catchment Dynamics*. Hydrodynamics Lab. Report 133, Department of Civil Engineering, Massachusetts Institute of Technology, Cambridge, Massachusetts.

Harris, G. S. (1970) 'Real time routing of flood hydrographs in storm sewers'. *J. Hydraulic Div.*, ASCE, **96** (HY6), 1247–1260.

Harrison, A. S., and Bueltel, C. J. (1973) *Computer Simulation of Missouri River Floods, Part I*, U.S. Army Corps of Engineers, Missouri River Div., Omaha, Nebraska.

Henderson, F. M. (1966) *Open Channel Flow*. New York: Macmillan Co., pp. 285–287.

Hinwood, J. B., and Wallis, I. G. (1975a) 'Classification of models of tidal waters'. *J. Hydraulic Div.*, ASCE, **101** (HY10), 1315–1331.

Hinwood, J. B., and Wallis, I. G. (1975b) 'Review of models of tidal waters'. *J. Hydraulic Div.*, ASCE, **101** (HY11), 1405–1421.

Isaacson, E., Stoker, J. J., and Troesch, A. (1954) *Numerical Solution of Flood Prediction and River Regulation Problems, Report II*. New York University Institute of Mathematical Science, IMM-205, New York.

Isaacson, E., Stoker, J. J., and Troesch, A. (1956) *Numerical Solution of Flood Prediction and River Regulation Problems, Report III*. New York University Institute of Mathematical Science, IMM-NYU-235, New York.

Johnson, B. H. (1974) *Unsteady Flow Computations on the Ohio–Cumberland–Tennessee–Mississippi River System*. Tech. Report H-74-8, Hydraulics Lab., Waterways Experiment Station, US Army Corps of Engineers, Vicksburg, Mississippi.

Kamphuis, J. W. (1970) 'Mathematical tidal study of St. Lawrence River'. *J. Hydraulic Div.*, ASCE, **96** (HY3), 643–664.

Keefer, T. N., and McQuivey, R. S. (1974) 'Multiple linearization flow routing model'. *J. Hydrolic Div.*, ASCE, **100** (HY7), 1031–1046.

Koussis, A. D. (1978) 'Theoretical estimations of flood routing parameters'. *J. Hydraulic Div.*, ASCE, **104** (HY1), 109–115.

Koussis, A. D. (1980) 'Comparison of Muskingum method difference schemes'. *J. Hydraulic Div.*, ASCE, **106** (HY5), 925–929.

Lai, C., Schaffranek, R. W., and Baltzer, R. A. (1980) 'An operational system for implementing simulation models: a case study'. In *Proc. of Verification of Mathematical and Physical Models*, 26th Annual Hydrol. Div. Specialty Conf., ASCE, College Park, Maryland, pp. 415–454.

Laplace, P. S. (1776) *Recherches sur Quelques Points due Systeme du Monde* [Researches on Some Points of World System]. Memoirs, Vol. 9, Acad. Sci., Paris.

Liggett, J. A., and Woolhiser, D. A. (1967) 'Difference solutions of the shallow-water equation'. *J. Engng. Mech. Div.*, ASCE, **95** (EM2), 39–71.

Liggett, J. A. (1975) 'Basic equations of unsteady flow'. In Mahmood, K., and Yevjevick, V. (eds), *Unsteady Flow in Open Channels*, Vol. I. Fort Collins, Colorado: Water Resource Publications, Chapter 2, pp. 29–62.

Liggett, J. A., and Cunge, J. A. (1975) 'Numerical methods of solution of the unsteady flow equations'. In Mahmood, K., and Yevjevich, V. (eds), *Unsteady Flow in Open Channels*, Vol. I. Fort Collins, Colorado: Water Resources Publications, Chapter 4, pp. 89–182.

Lighthill, M. J., and Whitham, G. B. (1955) 'On kinematic floods, I: Flood movements in long rivers'. In *Proc. Royal Society Lond.*, **A229**, 281–316.

Lin, J. O., and Soong, H. K. (1979) 'Junction losses in open channel flows'. *Water Resources Res.*, **15**(2), 414–418.

Linsley, R. K. (1971) *A Critical Review of Currently Available Hydrologic Models for Analysis of Urban Stormwater Runoff*. Report, Hydrocomp International Inc., Palo Alto, California.

Linsley, R. K., Kohler, M. A., and Paulhus, J. L. H. (1949) *Applied Hydrology*. New York: McGraw Hill Book Co., pp. 502–530.

Maddaus, W. O. (1969) *A Distributed Linear Representation of Surface Runoff*. Hydrodynamics Lab. Report 115, Massachusetts Institute of Technology, Cambridge, Massachusetts.

Martin, C. S. and DeFazio, F. G. (1969) 'Open channel surge simulation by digital computer'. *J. Hydraulic Div.*, ASCE, **95** (HY6), 2049–2070.

McCarthy, G. T. (1938) 'The unit hydrograph and flood routing'. Paper presented at Conf. of the North Atlantic Div. of US Corps of Engineers, New London, Connecticut.

Miller, W. A., and Cunge, J. A. (1975) 'Simplified equations of unsteady flow'. In Mahmood, K., and Yevjevich, V. (eds) *Unsteady Flow in Open Channels*, Vol. I. Fort Collins, Colorado: Water Resources Publications, Chapter 5, pp. 183–257.

Miller, W. A., and Yevjevich, V. (1975) *Unsteady Flow in Open Channels*. Bibliography, Vol. III. Fort Collins, Colorado: Water Resources Publications.

Nash, J. E. (1959) 'A note on the Muskingum method of flood routing'. *J. Geophys. Res.*, **64**, 1053–1056.

Newton, Sir, I. (1687) 'Propositions'. Book 2 in *Principia*, pp. 44–46, Royal Society, London.

Pinder, G. F., and Sauer, S. P. (1971) 'Numerical simulation of flood wave modification due to bank storage effects'. *Water Resources Res.*, **7**(1), 63–70.

Pogge, E. C., and Chiang, W.-L. (1977) *Further Development of a Stream–Aquifer System Model*. Kansas Water Resources Research Institute, University of Kansas, Lawrence, Kansas.

Poisson, S. D. (1816) *Memoir on the Theory of Waves*. Memoirs, Vol. 1. Acad. Sci., Paris, pp. 71–186.

Ponce, V. M. (1981). *Development of an Algorithm for the Linearized Diffusion Method of Flood Routing*. SDSU Civil Engineering Series No. 81144, San Diego State University, San Diego, California.

Ponce, V. M., and Simons, D. B. (1977) 'Shallow wave propagation in open channel flow'. *J. Hydraulic Div.*, ASCE, **103** (HY12), 1461–1476.

Ponce, V. M., and Yevjevich, V. (1978) 'Muskingum–Cunge method with variable parameters'. *J. Hydraulic Div.*, ASCE, **104** (HY12), 1663–1667.

Ponce, V. M., Indlekofer, H., and Simons, D. B. (1979) 'The convergence of implicit bed transient models'. *J. Hydraulic Div.*, ASCE, **105** (HY4), 351–363.

Ponce, V. M., Li, R. M., and Simons, D. B. (1978) 'Applicability of kinematic and diffusion models'. *J. Hydraulic Div.*, ASCE, **104** (HY3), 353–360.

Preissmann, A. (1961) 'Propagation of translatory waves in channels and rivers'. In *Proc., First Congress of French Assoc. for Computation*, Grenoble, France, pp. 433–442.

Puls, L. G. (1928) *Construction of Flood Routing Curves*. House Document 185, US 70th Congress, 1st session, Washington, DC, pp. 46–52.

Quick, M. C., and Pipes, A. (1975) 'Nonlinear channel routing by computer'. *J. Hydr. Div.*, ASCE, **101** (HY6), 651–664.

Quinn, F. H., and Wylie, E. B. (1972) 'Transient analysis of the Detroit River by the implicit method'. *Water Resources Res.*, **8**(6), 1461–1469.

Radojkovic, M. (1976) 'Mathematical modelling of rivers with flood plains'. In *Symp. on Inland Waterways for Navigation, Flood Control and Water Diversions*, Vol. I, ASCE, pp. 56–64.

Rockwood, D. M. (1958) 'Columbia Basin stream flow routing computer'. *Transactions*, ASCE, **126**(4), 32–56.

Saint-Venant, B. De (1871) 'Theory of unsteady water flow, with application to river floods and to propagation of tides in river channels'. *Computes Rendus Acad. Sci., Paris*, **73**, 148–154, 237–240. (Translated into English by US Corps of Engineers, No. 49-g, Waterways Experiment Station, Vicksburg, Mississippi, 1949.)

Sauer, V. B. (1973) 'Unit-response method of open-channel flood routing'. *J. Hydraulic Div.*, ASCE, **99** (HY1), 179–193.

Singh, V. P., and McCann, R. C. (1980) 'Some notes on Muskingum method of flood routing'. *J. Hydrol.*, **48**(3), 343–361.

Stoker, J. J. (1953). *Numerical Solution of Flood Prediction and River Regulation Problems; Derivation of Basic Theory and Formulation of Numerical Methods of Attack*. Report I, New York Univeristy Institute of Mathematical Science, Report No. IMM-NYU-200, New York.

Stoker, J. J. (1957). *Water Waves*. New York: Interscience, pp. 452–455.

Streeter, V. L., and Wylie, E. B. (1967) *Hydraulic Transients*. New York: McGraw Hill Book Co., pp. 239–259.

Strelkoff, T. (1969) 'The one-dimensional equations of open-channel flow'. *J. Hydraulic Div.*, ASCE, **95** (HY3), 861–874.

Strelkoff, T. (1970) 'Numerical solution of Saint-Venant equations'. *J. Hydraulic Div.*, ASCE, **96** (HY1), 223–252.

Strupczewski, W., and Kundzewicz, Z. (1980) 'Translatory characteristics of the Muskingum method of flood routing—a comment'. *J. Hydrol.*, **98**, 363–368.

Tatum, F. E. (1940) *A Simplified Method of Routing Flood Flows Through Natural Valley Storage*. Unpublished memo, US Engineers Office, Rock Island, Illinois.

Tingsanchali, T., and Ackermann, N. L. (1976) 'Effects of overbank flow in flood computations'. *J. Hydraulic Div.*, ASCE, **102** (HY7), 1013–1025.

Uzner, M. S., and Kennedy, J. F. (1976) 'Theoretical model of river ice jams'. *J. Hydraulic Div.*, ASCE, **102** (HY9), 1365–1383.

Vasiliev, O. F., Gladyshev, M. T., Pritvits, N. A., and Sudobicher, V. G. (1975) 'Methods for the calculation of shock waves in open channels'. In *Proc., 11th Congress IAHR*, Leningrad, USSR, paper 3.44.

Vicens, G. J., Harley, B. M., and Schaake, J. C. (1975) 'Flow 2D: a two-dimensional flow model for flood plains and estuaries'. In *Symp. Modeling Techniques*, Vol. II. 2nd Annual Symp. of Waterways, Harbors, and Coastal Engng. Div., ASCE, pp. 1487–1504.

Weinmann, P. E., and Laurenson, E. M. (1979) 'Approximate flood routing methods: a review'. *J. Hydraulic Div.*, ASCE, **105** (HY13), Proc., Paper 15057.

Weiss, H. W., and Midgley, D. C. (1978) 'Suite of mathematical flood plain models'. *J. Hydraulic Div.*, ASCE, **104** (HY3), 361–376.

Wooding, R. A. (1965) 'A hydraulic model for the catchment-stream problem, I, kinematic wave theory'. *J. Hydrol.*, **3**.

Woolhiser, D. A., and Liggett, J. A. (1967) 'Unsteady one-dimensional flow over a plane—the rising hydrograph'. *Water Resources Res.*, **3**(3), 753–771.

Wylie, E. B. (1970) 'Unsteady free-surface flow computations' *J. Hydraulic Div.*, ASCE, **96** (HY11), 2241–2251.

Yeh, W. W.-G. and Becker, L. (1973). 'Linear programming and channel flow identification'. *J. Hydraulic Div.*, ASCE, **99** (HY11), 2013–2021.

APPLICABILITY CRITERIA FOR KINEMATIC AND DIFFUSION ROUTING MODELS[1]

INTRODUCTION

Many simplified flood routing models may be categorized as either kinematic-type or diffusion-type models. The Muskingum Model (McCarthy, 1938), Reservoir Routing Model (Goodrich, 1931), SSARR Model (Rockwood, 1958), Kinematic Model (Lighthill and Whitham, 1955), and the SWMM Model (Huber et al., 1975) are kinematic-type models. The Muskingum-Cunge Model (Cunge, 1969) is a diffusion-type model. These models are limited to applications where the inertial effects are insignificant and, in the case of the kinematic-type models, the water surface slope is constant with time and is closely approximated by the channel bottom slope.

This paper develops criteria to quantify the acceptable range of application for kinematic and diffusion models. The criteria are developed by estimating the magnitude of the terms in the conservation of momentum equation which are neglected by the kinematic and diffusion models. The omitted terms are normalized with the channel bottom slope; this ratio is expressed with hydraulic variables (channel bottom slope, peak discharge, Manning n, time of rise of inflow hydrograph, cross-section parameters) whose values are readily available prior to routing. The criteria are applicable for a wide range of practical channel shapes and typical inflow hydrograph shapes.

Ponce et al. (1978) also presented criteria for selecting appropriate applications for kinematic and diffusion models. Their results, which were obtained for a sinusoidal shaped wave in a wide channel by using a linear analysis technique, are compared with those developed herein. Realistic hydrograph shape, cross-section shape, nonlinearity and non-prismatic channel characteristics are considered in the approach presented in this paper.

Kinematic and diffusion models are also limited to applications where insignificant backwater effects exist and where wave propagation is in the downstream flow direction only. No attempt is made herein to quantify these restrictions.

All notation is defined in Appendix A--Notation.

THEORETICAL DEVELOPMENT

The conservation of momentum of one-dimensional unsteady flow is described by the following:

$$\partial V/\partial t + V\,\partial V/\partial x + g(\partial y/\partial x - S_o + S) = 0 \qquad (1)$$

[1]D. L. Fread, Senior Research Hydrologist, Hydrologic Research Laboratory, National Weather Service, Silver Spring, Maryland 20910.

Solving Eq. (1) for the friction slope (S) and then dividing through by the channel bottom slope (S_o), one obtains:

$$\frac{S}{S_o} = \overset{(1)}{1} - \overset{(2)}{\frac{\partial y/\partial x}{S_o}} - \overset{(3)}{\frac{V\,\partial V/\partial x}{g\,S_o}} - \frac{\partial V/\partial t}{g\,S_o} \tag{2}$$

The conservation of mass of one-dimensional unsteady flow is described by the following:

$$A\,\partial V/\partial x + V\,\partial A/\partial x + B\,\partial y/\partial t = 0 \tag{3}$$

Also, the term ($\partial A/\partial x$) may be approximated as:

$$\partial A/\partial x \simeq B\,\partial y/\partial x + y\,\partial B/\partial x \tag{4}$$

and the hydraulic depth (D) is by definition,

$$D = A/B \tag{5}$$

Now, solving Eq. (3) for $\partial V/\partial x$, the following is obtained:

$$\partial V/\partial x = -V/A\,\partial A/\partial x - B/A\,\partial y/\partial t \tag{6}$$

Upon substituting Eqs. (4) and (5) into Eq. (6) and then multiplying through by V, the following expression for the term ($V\,\partial v/\partial x$) is obtained:

$$V\,\partial V/\partial x = -V^2/D\,\partial y/\partial x - V^2/B\,\partial B/\partial x - V/D\,\partial y/\partial t \tag{7}$$

Using the kinematic approximation for $\partial y/\partial x$ (Henderson, 1966), i.e.,

$$\partial y/\partial x = -1/c\,\partial y/\partial t \tag{8}$$

where c is the kinematic wave speed which can be evaluated using the following:

$$c = KV \tag{9}$$

in which K is a cross-sectional shape factor, $7/6 \leq K \leq 5/3$. Hence, by substituting Eq. (9) into Eq. (8), the expression for $\partial y/\partial x$ becomes:

$$\partial y/\partial x = -\partial y/\partial t/(KV) \tag{10}$$

Returning now to Eq. (2), the following is obtained by substituting Eqs. (7) and (10) into Eq. (2):

$$\frac{S}{S_o} = \overset{(1)}{1} + \overset{(2)}{\frac{\partial y/\partial t}{K\,V\,S_o}} + \overset{(3)}{\frac{1}{g\,S_o}\left[\frac{V^2}{B}\,\partial B/\partial x + (1-1/K)\,\frac{V}{D}\,\partial y/\partial t - \partial V/\partial t\right]} \tag{11}$$

Let the time derivatives be represented by the following expressions:

$$\partial y/\partial t = M\, y_p/T \tag{12}$$

$$\partial V/\partial t = M\, V_p/T \tag{13}$$

in which y_p is the peak depth, V_p is the peak velocity, and M is a multiplier which adjusts the straight line approximation for the rising limb of the hydrograph to that maximum slope associated with the rising limb of a hydrograph having a gamma distribution. An expression for M is developed by differentiating the gamma function, evaluating this expression at $t = 2T/3$ and then forming a ratio of the evaluated expression to the straight line approximation. (See Appendix B for the derivation of M). The resulting expression for M is:

$$M = \alpha/2\ (2/3)^{\alpha}\ e^{\alpha/3} \tag{14}$$

where: $$\alpha = 1/(T_g/T_r - 1) \tag{15}$$

in which T_g is the time (hr.) from beginning of rise to the center of gravity of the hydrograph, and T_r is the time (hr.) from the beginning of rise to the peak of the hydrograph. The minimum value for M is one when the rising limb is a straight line; and its maximum value of about 2.5 occurs when T_g/T_r is 1.09 and $t = 2T_r/3$. Thus, $1 < M < 2.5$ represents the range for the multiplier parameter (M).

It is more convenient if the time of rise (T_r) is expressed in hrs.; therefore, Eqs. (12-13) become:

$$\partial y/\partial t = M\, y_p/(3600\ T_r) \tag{16}$$

$$\partial V/\partial t = M\, V_p/(3600\ T_r) \tag{17}$$

in which T_r is the time of rise (hr.) of the hydrograph.

The velocity (V) in the preceding equations is assumed to be the velocity occurring when $t = 2T_r/3$, i.e.,

$$V = 2\ V_p/3 \tag{18}$$

since the velocity at the beginning of rise is assumed negligible compared to V_p. Upon substituting Eqs. (16-18) into Eq. (11) and simplifying, the following is obtained:

$$\frac{S}{S_o} = \overset{(1)}{1} + \overset{(2)}{\frac{0.000417\ M\ y_p}{T_r\ S_o\ K\ V_p}} + \overset{(3)}{\frac{0.00000863\ M\ V_p}{T_r\ S_o}}\left[\beta + (1-1/K)\ \frac{2\ y_p}{3D} - 1\right] \tag{19}$$

where: $$\beta = \frac{1600\ T_r\ V_p}{M\ B}\ \Delta\bar{B}/\Delta x \tag{20}$$

REPRESENTATION OF HYDRAULIC PARAMETERS

In order to evaluate the terms in Eq. (19) before routing an inflow hydrograph, it is necessary to express the parameters (y_p, V_p, K, D, B) in terms of parameters which are known a priori. To accomplish this, as well as account for the effect of cross-sectional shape, the channel geometry is approximated as:

$$B = k\ y^m \tag{21}$$

$$A = \frac{k\ y^{m+1}}{m+1} \tag{22}$$

$$D = A/B = y/(m+1) \tag{23}$$

in which k and m are fitted parameters for the observed variation of B with y. Scaling is accomplished via k, and m accounts for the shape. Rectangular (wide channel), parabolic, and triangular shaped channels have m values of 0, 0.5, and 1.0, respectively. A value of m > 1 represents an expanding V-shape section in which the width (B) increases at a nonlinear rate with depth (y). This shape is appropriate for many natural cross sections composed of a relatively narrow in-bank channel and a rather wide over-bank (floodplain) section.

Using the Manning equation, the unit-width peak discharge (q_p) is given by:

$$q_p = 1.49/n\ S_o^{1/2}\ D_p^{5/3} \tag{24}$$

Then, substituting Eq. (23) into Eq. (24) and solving for y_p, the following is obtained:

$$y_p = (q_p/a)^{0.6} \tag{25}$$

where: $$a = 1.49\ S_o^{1/2}/[n\ (m+1)^{5/3}] \tag{26}$$

Also, the unit-width discharge (q_p) can be expressed as Q_p/B or

$$q_p = a\ \left(\frac{Q_p}{k\ a}\right)^{5/(3m+5)} \tag{27}$$

in which Q_p is the peak discharge of the inflow hydrograph.

Using the Manning equation, the peak velocity (V_p) can be expressed as:

$$V_p = 1.49/n\ S_o^{1/2}\ D_p^{2/3} \tag{28}$$

Substituting peak values for V and D (using Eq. (23) for the latter) results in the following:

$$V_p = 1.49/n\ S_o^{1/2}\ [y_p/(m+1)]^{2/3} \tag{29}$$

Now, substituting Eq. (25) into Eq. (29) yields an expression for V_p:

$$V_p = (m+1)\ a^{0.6}\ q_p^{0.4} \tag{30}$$

The ratio (V_p/y_p) can be obtained from Eq. (25) and (30). Thus,

$$V_p/y_p = (m+1)\ a^{1.2}/q_p^{0.2} \tag{31}$$

The cross-sectional factor (K) in Eq. (9) is given by the following:

$$K = 5/3 - 2/3\ dB/dy\ A/B^2 \tag{32}$$

Upon substituting Eqs. (21-22) into Eq. (32) and simplifying, the following is obtained:

$$K = (3m+5)/[3(m+1)] \tag{33}$$

The ratio $[2\ y_p/(3D)]$ in Eq. (19) may be obtained as follows:

$$2\ y_p/(3D) = \frac{2\ y_p}{3(2\ y_p/3)/(m+1)} = m+1 \tag{34}$$

Then, the term in brackets of Eq. (19) can be evaluated using Eqs. (33), and (34). Thus,

$$\beta + (1-1/K)\ 2\ y_p/(3D) - 1 = \beta - (m+3)/(3m+5) \tag{35}$$

The ratio (V_p/B) is obtained using Eqs. (21) and (30). Thus,

$$V_p/B = 1.5^m(m+1)a^{0.6(m+1)}/(k\ q_p^{0.6m-0.4}) \tag{36}$$

Then, using Eq. (36), the nonprismatic term (β), Eq. (20), can be expressed as follows:

$$\beta = \frac{1600\ T_r\ 1.5^m(m+1)\ a^{0.6(m+1)}}{M\ k\ q_p^{0.6m\ -\ 0.4}}\ \Delta\bar{B}/\Delta x \tag{37}$$

in which $\Delta\bar{B}/\Delta x$ is the average variation of the width (B) along the routing reach (Δx); this is the nonprismatic characteristic of the routing reach.

DIFFUSION ROUTING MODELS

Diffusion-type routing models are based on the following approximation for S:

$$S = S_o - \partial y/\partial x \tag{38}$$

Therefore, only the inertial effect represented by the third (3) term in Eqs. (2), (11), and (19) is omitted. The error due to the omission of this term is denoted as E_r, expressed as a decimal fraction. The following inequality expresses the relationship that must exist if the omitted term should not cause a relative error in the conservation of momentum equation greater than E_r:

$$E_r > \frac{0.00000863\ M\ V_p}{T_r\ S_o} [\beta + (1-1/K)2\ y_p/(3D) - 1] \tag{39}$$

Using Eqs. (30) and (35), Eq. (39) can be expressed as follows:

$$E_r > \frac{0.000011\ M\ q_p^{0.4}}{T_r\ S_o^{0.7}\ n^{0.6}} |\beta - (m+3)/(3m+5)| \tag{40}$$

Replacing E_r with E/100, in which E is in percent, Eq. (40) can be rearranged as follows:

$$\frac{T_r\ S_o^{0.7}\ n^{0.6}}{M\ \Phi'\ q_p^{0.4}} > 0.0011/E \tag{41}$$

where: $\Phi' = |\beta - (m+3)/(3m+5)|$ (42)

In Eq. (42), E is a quantitative index related to the maximum error (percent) that is tolerated when the inequality is satisifed. When the channel is prismatic ($\Delta\bar{B}/\Delta x = 0$) with rectangular cross-section (m=0) and assuming M = 2.5, Eq. (41) becomes:

$$\frac{T_r\ S_o^{0.7}\ n^{0.6}}{q_p^{0.4}} > 0.0017/E \tag{43}$$

KINEMATIC ROUTING MODELS

Kinematic-type routing models are based on the assumption of a single-valued depth-discharge relation, i.e.,

$$\partial A/\partial Q = dA/dQ = 1/c \tag{44}$$

Eq. (44) implies that the friction slope (S) is constant and equal to the bottom slope, i.e.,

$$S = S_o \tag{45}$$

or $$S/S_o = 1 \tag{46}$$

Therefore, kinematic models omit the second (2) and third (3) terms of Eqs. (2), (11), and (19). The error due to the omission of these terms is denoted as E_r expressed as a decimal fraction. The following inequality expresses the relationship that must exist if the omitted terms should not cause a relative error of conservation of momentum greater than E_r:

$$E_r > \frac{0.000417\ M\ y_p}{T_r\ S_o\ K\ V_p} + \frac{0.00000863\ M\ V_p}{T_r\ S_o} [\beta + (1-1/K)\ 2\ y_p/(3D) - 1] \tag{47}$$

Substituting Eqs. (30), (31), (33), (35), and (42) into Eq. (47), the following is obtained:

$$E_r > \frac{0.000777\ M\ q_p^{0.2}\ n^{1.2}\ (m+1)^2}{T_r\ S_o^{1.6}\ (3m+5)} + \frac{0.000011\ M\ q_p^{0.4}\ \Phi'}{T_r\ S_o^{0.7}\ n^{0.6}} \tag{48}$$

Replacing E_r with E/100, in which E is in percent, Eq. (48) can be rearranged in the following form:

$$E > \frac{0.0777\ M\ q_p^{0.2}\ n^{1.2}\ \Phi\ (1+I)}{T_r\ S_o^{1.6}} \tag{49}$$

where: $\Phi = (m+1)^2/(3m+5)$ (50)

$$I = 0.014\ S_o^{0.9}\ q_p^{0.2}\ \Phi'/(\Phi\ n^{1.8}) \tag{51}$$

The parameter (I) acounts for the term (3) in Eq. (47). It represents less than about 17% of term (2) for flows with Froude numbers (F) less than 0.5 and only represents 4% of term (2) when the Froude number is 0.25. The parameter (I) can also be expressed in terms of the Froude number (F), i.e., $I = 0.22\ F^2\ \Phi'/\Phi$.

Rearranging Eq. (49), the following criterion is obtained for kinematic models:

$$\frac{T_r\ S_o^{1.6}}{M\ (1+I)\ \Phi\ q_p^{0.2}\ n^{1.2}} > 0.078/E \tag{52}$$

If the inequality in Eq. (52) is satisfied, the maximum error that will be incurred using a kinematic model is E (percent). If the channel is prismatic, rectangular, M is assumed to be 2.5, and the Froude number is about 0.5 such that I may be approximated as 0.15, Eq. (52) reduces to the following:

$$\frac{T_r\ S_o^{1.6}}{q_p^{0.2}\ n^{1.2}} > 0.045/E \tag{53}$$

COMPARISON WITH CRITERIA OF PONCE AND SIMONS

Ponce and Simons (1977) developed an analytical solution to a linearized version of the unsteady flow equations, Eqs. (1) and (3), for a sinusoidal shaped wave propagating in a wide channel. Ponce et al. (1978) used this information to define the limits of applicability of the kinematic and diffusion type models.

<u>Kinematic Criterion</u>. In the case of kinematic models, they presented the following criterion for routing errors at the 5% level:

$$\frac{T_D\ S_o\ V_o}{D_o} > 171 \tag{54}$$

in which T_D is the duration (sec.) of the inflow hydrograph. Using Eqs. (23), and (30) and the approximation that $T_D = (2)(3600)T_r$, Eq. (54) may be rewritten in the following equivalent form:

$$\frac{T_r \; S_o^{1.6}}{q_p^{0.2} \; n^{1.2}} > 0.014 \tag{55}$$

For a wide channel (m = 0), with M taken to be about 1.7 for a sinusoidal shaped hydrograph, I = 0.15, and E = 5, Eq. (52) becomes:

$$\frac{T_r \; S_o^{1.6}}{q_p^{0.2} \; n^{1.2}} > 0.006 \tag{56}$$

The left-hand-side of Eq. (56) is identical with that of Eq. (55), although the right-hand-side of Eq. (55) is about two times that of Eq. (56).

Diffusion Criterion. In the case of diffusion models, Ponce et al. (1978) presented the following criterion:

$$T_D \; S_o \sqrt{g/D_o} > 30 \tag{57}$$

Substituting Eqs. (23) and (31) into Eq. (57) allows it to be rewritten in the following equivalent form:

$$\frac{T_r \; S_o^{1.15}}{(q_p \; n)^{0.3}} > 0.0003 \tag{58}$$

Eq. (58) can be rewritten in the following form:

$$\frac{T_r \; S_o^{0.7} \; n^{0.6}}{q_p^{0.4}} > 0.0003 \; f \tag{59}$$

where f varies from about 0.5 to 1.5 depending on a typical range of values for $S_o^{-0.5}$ and n.

Eq. (41), with E = 5, M = 1.7, I = 0.15, and m = 0, becomes:

$$\frac{T_r \; S_o^{0.7} \; n^{0.6}}{q_p^{0.4}} > 0.00024 \tag{60}$$

Eqs. (59) and (60) are identical, although the right-hand-side of Eq. (59) can be from one-half to about two times that of Eq. (60). Thus, it is considered that this approach is in general agreement with that of Ponce et al. (1978) while being able to account for channel shape, more realistic shaped hydrographs than the sinusoidal approximation, and non-prismatic channel geometry.

SENSITIVITY OF CRITERIA

The kinematic criterion, Eq. (52), and diffusion criterion, Eq. (41), may be expressed in the following common form:

$$\frac{\gamma}{T_r S_o} < E \tag{61}$$

where: $\gamma = \gamma_k = 0.08\ M\ (1+I)\ \Phi\ q_p^{0.2}\ n^{1.2}/S_o^{0.6}$ (kinematic) (62)

$$\gamma = \gamma_d = 0.001\ M\ \Phi'\ q_p^{0.4}\ S_o^{0.3}/n^{0.6} \quad \text{(diffusion)} \tag{63}$$

Eq. (60) is shown in Fig. 1 in which E is plotted against $(T_r S_o)$ for various values of γ.

If M is set at 2.5 (a conservative value for natural hydrographs), the practical range of values for q_p, n, S_o, and m result in the following ranges for γ_k and γ_d:

$$0.01 < \gamma_k < 10 \tag{64}$$

$$0.001 < \gamma_d < 0.1 \tag{65}$$

The diffusion and kinematic regions are denoted in Fig. 1 where it may be noted that the error (E) is smaller for a much larger range of the value $(T_r\ S_o)$ for the range of possible values of γ_d. Therefore, the diffusion models have a wider range of acceptable application than the kinematic models. Also, E is strongly dependent on $(T_r\ S_o)$, while γ is weakly dependent on S_o and q_p; γ is strongly dependent upon m, M, and n.

Sensitivity characteristics of the criteria are apparent from Figs. 2 and 3 which show the kinematic and diffusion criteria, respectively, as a function of the dominant factors (S_o and T_r). Also, the variation of S_o and T_r for a fixed E value of 5 percent is shown in the inset of each figure. Notice how much greater the allowable T_r must be for the kinematic criterion compared with the allowable T_r for the diffusion criterion, particularly at the mild slopes. The kinematic criteria is strongly a function of the channel slope.

SUMMARY AND CONCLUSIONS

Index criteria for the applicability of kinematic and diffusion type routing models are developed from an analysis of the magnitude of the normalized errors in the momentum equation due to omission of certain terms. The criteria are easily evaluated from the parameters (T_r, S_o, n, q_p, m) which are available prior to the routing computations.

The criteria are:

$$\frac{T_r\ S_o^{1.6}}{M\ (1+I)\ \Phi\ q_p^{0.2}\ n^{1.2}} > 0.078/E \quad \text{(kinematic models)} \tag{66}$$

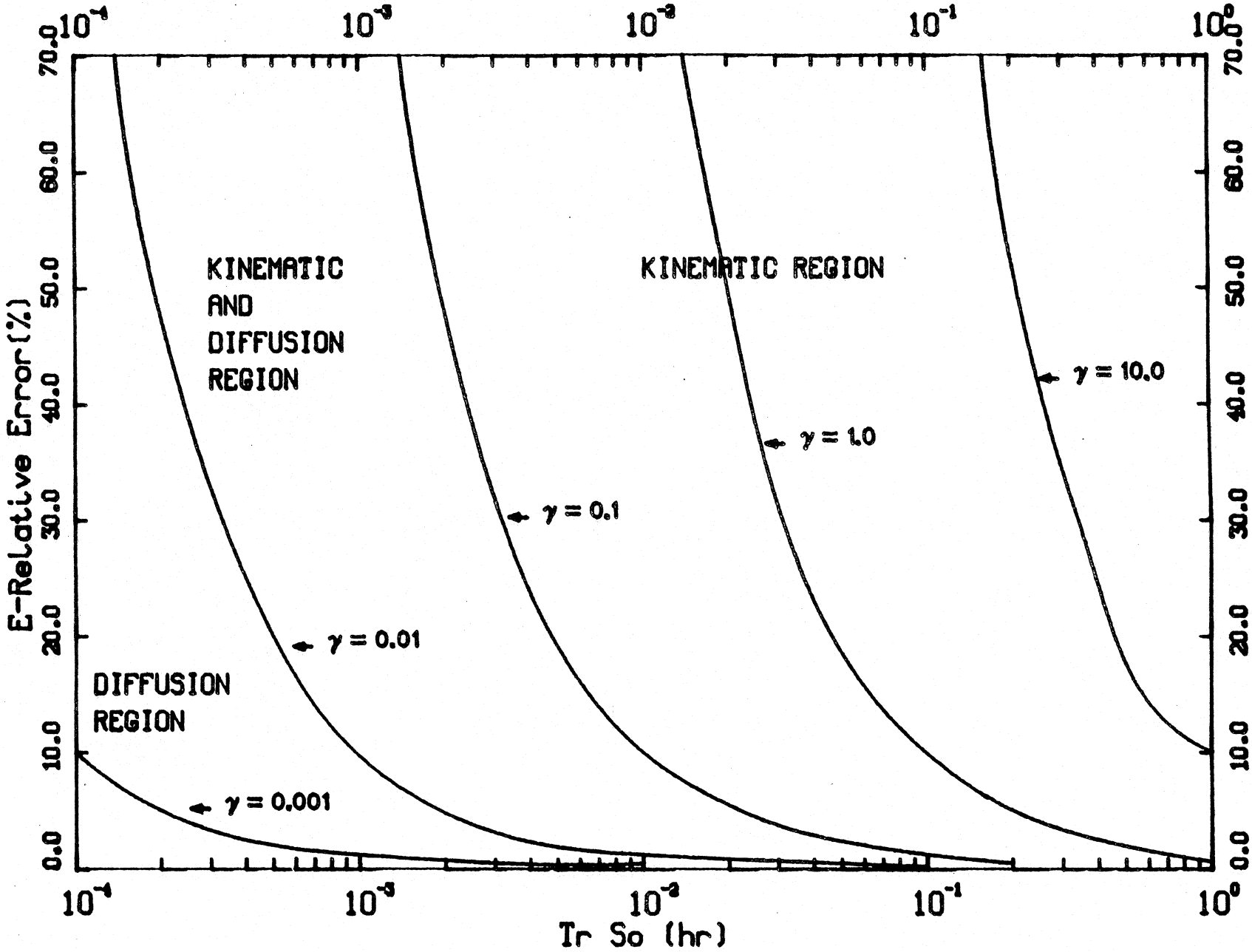

Figure 1. Kinematic and diffusion criteria showing E as a function of T_r and S_o and γ.

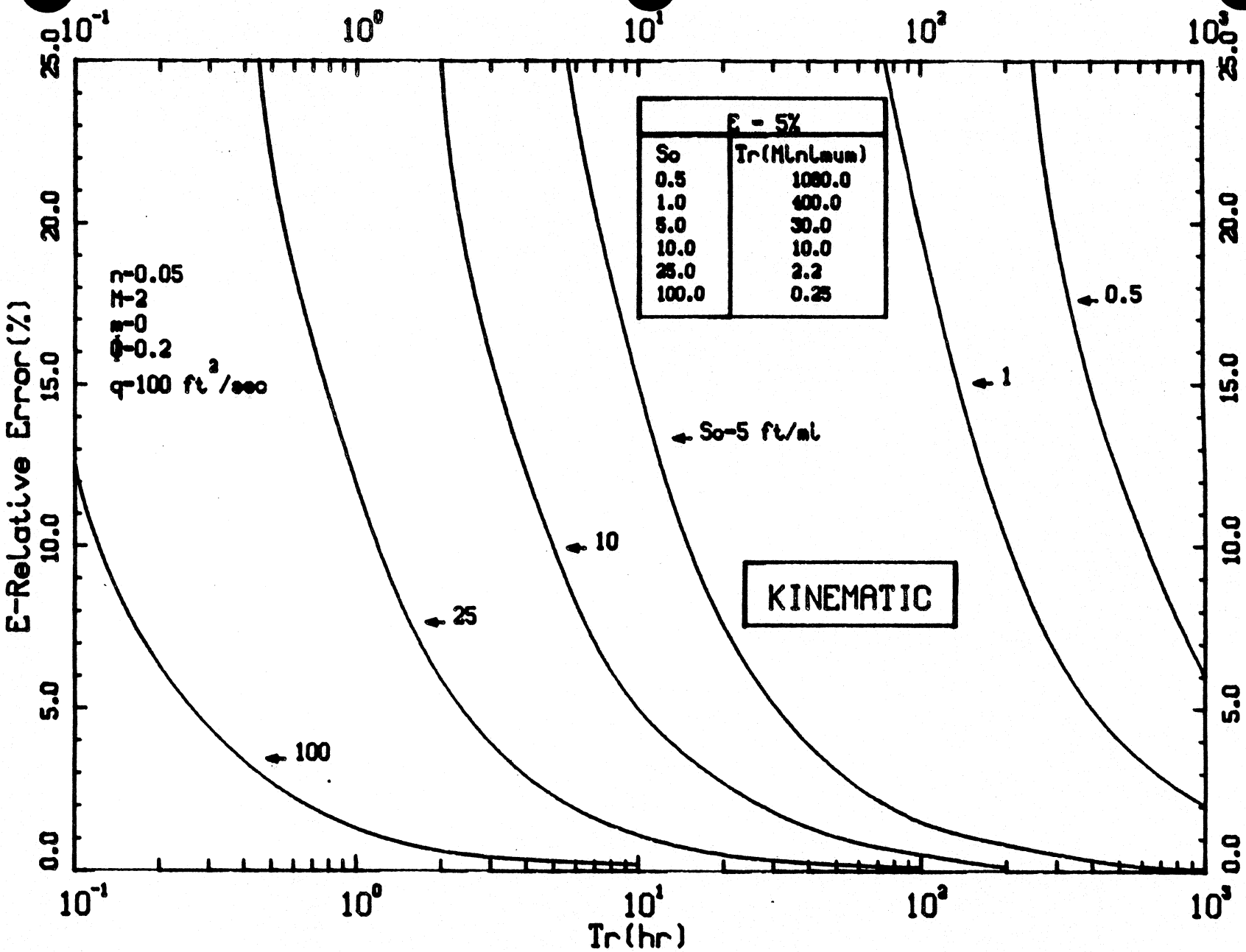

Figure 2. Kinematic criterion showing E as a function of T_r and S_o.

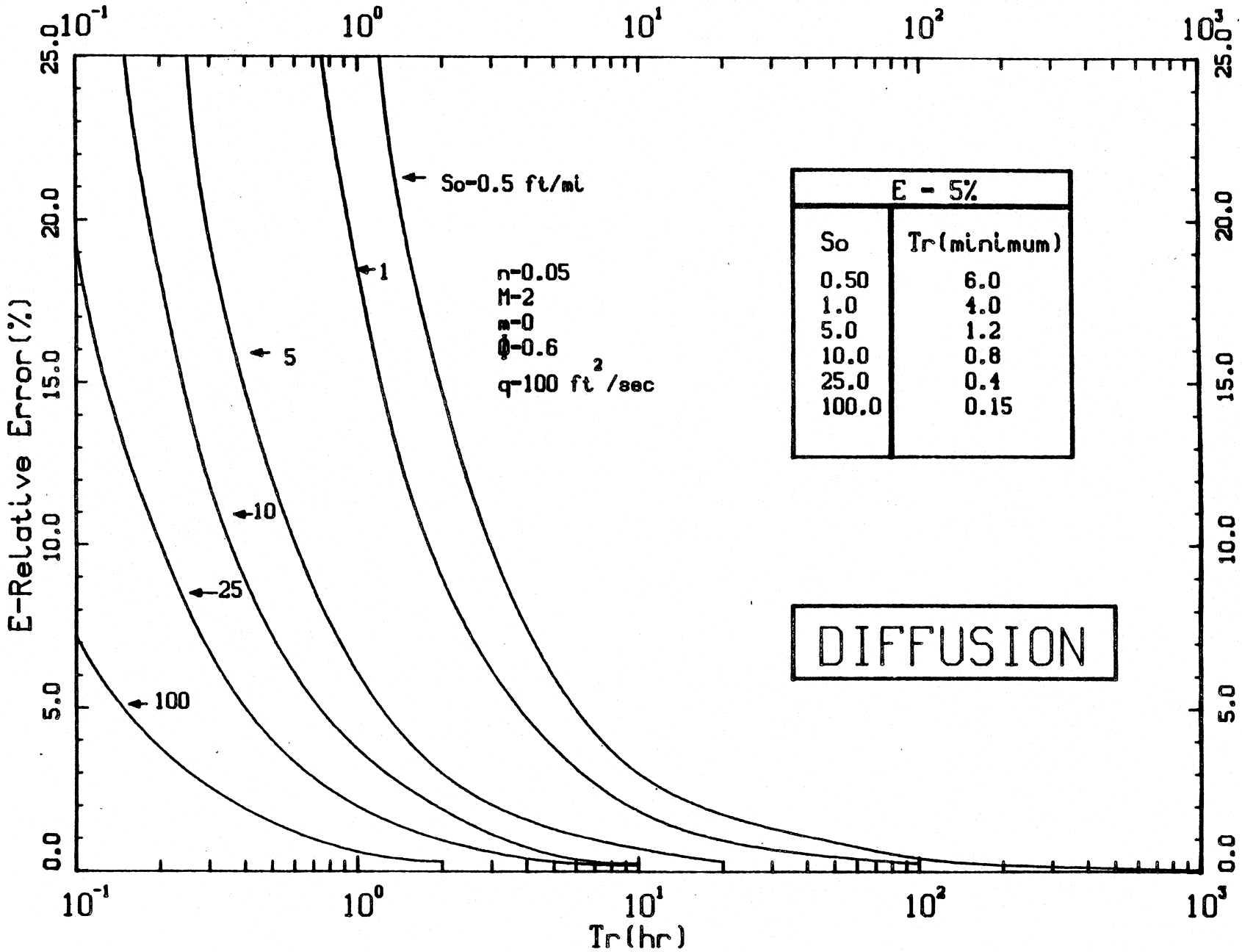

Figure 3. Diffusion criterion [illegible]wing E as a function of T_r and S_o.

$$\frac{T_r\, S_o^{0.7}\, n^{0.6}}{M\, \Phi'\, q_p^{0.4}} > 0.001/E \qquad \text{(diffusion models)} \qquad (67)$$

where: $$q_p = a\, [Q_p/(k\, a)]^{5/(3m+5)} \qquad (68)$$

$$a = 1.49\, S_o^{1/2}/[n(m+1)^{5/3}] \qquad (69)$$

$$M = \alpha/2\, (2/3)^{\alpha}\, e^{\alpha/3} \qquad 1 < M < 2.5 \qquad (70)$$

$$\alpha = 1/(T_g/T_r - 1) \qquad 1.025 < T_g/T_r < 1.45 \qquad (71)$$

$$I = 0.014\, S_o^{0.9}\, q_p^{0.2}\, \Phi'/(\Phi\, n^{1.8}) \qquad (72)$$

$$\Phi = (m+1)^2/(3m+5) \qquad (73)$$

$$\Phi' = |\beta - (m+3)/(3m+5)| \qquad (74)$$

$$\beta = \frac{1.5^m\, 1600\, (m+1)\, T_r\, a^{0.6(m+1)}}{k\, M\, q_p^{0.6m-0.4}}\, \Delta\bar{B}/\Delta x \qquad (75)$$

in which $\Delta\bar{B}/\Delta x$ is a measure of the average nonprismatic characteristic of the channel reach. The applicability criteria include the effects of channel shape, non-prismatic geometry, realistic hydrograph shape, channel slope, roughness, and peak discharge.

Sensitivity studies show that the diffusion criteria permits a much larger range of channel characteristics and inflow hydrographs (characterized by the time of rise) to be treated with diffusion-type models than with kinematic models for the same level of error index (E).

REFERENCES

Cunge, J.A. (1969). 'On the subject of a flood propagation computation method (Muskingum method)', J. Hydr. Research, Vol. 7, No. 2, pp. 205-230.

Goodrich, R.D. (1931). 'Rapid calculation of reservoir discharge,' Civil Engineering, Vol. 1, pp. 417-418.

Henderson, F.M. (1966). Open Channel Flow, Macmillan Co., New York, pp. 285-287.

Huber, W.C., Heany, J.P., Meding, M.A., Peltz, W.A., Sheikh, H., and Smith, G.F. (1975). Storm Water Management Model User's Manual, Nat. Environ. Res. Ctr., U.S. Environ. Prot. Agency, Cincinnati, Ohio, Document EPA-670/2-75-017.

Lighthill, M.J. and Whitham, G.B. (1955). 'On kinematic floods I, Flood movements in long rivers', in Proc., Royal Society, A229, London, pp. 281-316.

McCarthy, G.T. (1938). The Unit Hydrograph and Flood Routing, Paper presented at Conf. of the North Atlantic Div. of U.S. Corps of Engineers, New London, Connecticut.

Ponce, V.M. and Simons, D.B. (1977). 'Shallow wave propagation in open channel flow', J. Hydr. Div., Vol. 103, No. HY12, pp. 1461-1476.

Ponce, V.M., Li, R.M., and Simons, D.B. (1978). 'Applicability of kinematic and diffusion models', J. Hydr. Div., ASCE, Vol. 104, No. HY3, pp. 353-360.

Rockwood, D.M. (1958). 'Columbia Basin stream flow routing computer', Transactions, ASCE, Vol. 126, Part 4, pp. 32-56.

APPENDIX A

Notation

A	cross-sectional area, L^2
a	hydraulic parameter defined by Eqs. (26), (68)
B	wetted top width, L
c	kinematic wave speed, L/T
D	hydraulic depth, L
D_o	hydraulic depth in Eq. (54), L
D_p	hydraulic depth associated with peak flow, L
d	total derivative
E	relative (normalized) error in momentum equation, percent
E_r	Relative (normalized) error in momentum equation, dimensionless ratio
e	exponential function
F	Froude number, dimensionless
g	acceleration due to gravity
I	effect on error due to omission of inertial terms, defined by Eqs. (5), (71)
K	cross-section factor for kinematic wave speed, defined by Eqs. (32), (33)
k	fitted scale parameter for cross section, dimensionless
m	fitted shape parameter for cross section, dimensionless
M	multiplier parameter to correct straight-line approximation of temporal derivatives, defined by Eqs. (14), (70)
n	Manning roughness coefficient
p	subscript denoting that it is associated with the peak flow
Q_p	peak discharge, L^3/T
q_p	peak unit-width discharge, L^2/T, defined by Eqs. (27), (68)
S	friction slope, dimensionless
S_o	channel bottom slope, dimensionless
T	time to peak of inflow hydrograph, T (sec.)
T_D	time of duration of inflow hydrograph, T (sec.)
T_g	time to center of gravity of inflow hydrograph, T (hr.)
T_r	time to peak of inflow hydrograph, T (hr.)
t	time, T (sec.)
V	velocity, L/T
V_p	velocity associated with peak flow, L/T, defined by Eqs. (28), (29), (30)
x	distance along the channel axis, L
y	flow depth, L
y_p	flow depth associated with peak flow, L, defined by Eq. (25)
α	hydrograph parameter of gamma function
β	hydraulic parameter for nonprismatic channel effects, defined by Eqs. (37), (75)
Δ	incremental
γ	hydraulic parameter used in Eq. (60) and defined by Eqs. (62) and (63)
γ_d	hydraulic parameter for diffusion criterion, defined by Eq. (63)
γ_k	hydraulic parameter for kinematic criterion, defined by Eq. (62)
Φ	parameter associated with cross-section shape, defined by Eqs. (50) (73)
Φ'	parameter associated with cross-section shape and β, defined by Eqs. (42), (74)
∂	partial derivative

APPENDIX B

Derivation of Parameter (M)

The assumption that $\partial y/\partial t = y_p/T$ is suitable when the rising limb of the inflow hydrograph is a straight line. This occurs for most dam-break hydrographs and reservoir releases associated with hydropower. However, runoff-generated hydrographs do not tend to have a straight-line rising limb but rather have more of an $\int$-shape. The three-parameter gamma function can be used to describe a hydrograph having such a rising limb. Thus,

$$Q(t) = Q_p \ (t/T_r)^{\alpha} \ e^{\alpha(1-t/T_r)} \qquad \text{(B-1)}$$

where: $\alpha = 1/(T_g/T_r - 1)$

in which T_g is the time to center of gravity of the hydrograph, T_r is the time to the peak of the hydrograph, t is time, and Q_p is the peak discharge.

If Eq. (B-1) is differentiated with respect to time, the following is obtained:

$$\frac{dQ}{dt}(t) = \frac{\alpha}{T_r} Q_p \left(\frac{t}{T_r}\right)^{\alpha} \left(\frac{1-t/T_r}{t/T_r}\right) e^{\alpha(1-t/T_r)} \qquad \text{(B-2)}$$

Now, Eq. (B-2) may be evaluated at any given time (t) to determine the instantaneous slope (dQ/dt). Selecting the time ($t = 2T_r/3$) and substituting this into Eq. (B-2) gives:

$$\frac{dQ}{dt}(t) = 2T_r/3) = \frac{\alpha}{T_r} Q_p \ (2/3)^{\alpha} \ (1/2) \ e^{\alpha/3} \qquad \text{(B-3)}$$

Evaluating the slope at $t = 2T_r/3$ is appropriate for hydrographs with $1.025 < T_g/T_r < 1.45$.

Let M be defined as follows:

$$M = \frac{dQ/dt}{Q_p/T_r} \qquad \text{(B-4)}$$

Thus, M is the ratio of the instantaneous slope of the hydrograph to the straight line approximation (Q_p/T_r). Therefore, dQ/dt may be obtained by multiplying (Q_p/T_r) by M.

Substitution of Eq. (B-3) into Eq. (B-4) produces the following general expression for M:

$$M = \alpha/2 \ (2/3)^{\alpha} \ e^{\alpha/3} \qquad \text{(B-5)}$$

where M applies for points located at time ($t = 2T_r/3$) on the rising limb of the inflow hydrograph which is approximated by a gamma function.

RIVERS '76

FLOOD ROUTING IN MEANDERING RIVERS WITH FLOOD PLAINS

by

D. L. Fread[1]

ABSTRACT

Unsteady flow in a natural river which meanders through a wide flood plain is complicated by large differences in hydraulic resistance and cross-sectional geometry of the river channel and the flood plain. The unsteady flow is further complicated by the tendency for a portion of the flow to "short-circuit" along the more direct route afforded by the flood plain rather than following the longer route along the meandering channel. Thus, the wave attenuation and the time of travel of the portion of the flow in the channel differs from that in the flood plain due to differences in the hydraulic properties and flow-path distances of the channel and flood plain.

A mathematical model for routing floods in meandering rivers with flood plains is presented. The technique is based on a modified form of the complete one-dimensional equations of unsteady flow and thus avoids the obvious use of the more complex and computationally time consuming two-dimensional equations. The one-dimensional equations are modified such that the flow in the meandering channel and flood plain are identified separately. Thus, the differences in both hydraulic properties and flow-path distance are taken into account in a physically meaningful way, but one that is one-dimensional in concept. This development differs from conventional one-dimensional treatment of unsteady flows in rivers with flood plains wherein the flow is either averaged across the total cross-sectional area (channel and flood plain) or the flood plain is treated as off-channel storage, and the reach lengths of the channel and flood plain are assumed to be identical.

The modified equations contain the same two unknowns (discharge and water surface elevation) as the conventional equations; hence, the same numerical solution techniques applicable to the conventional one-dimensional unsteady flow equations may be used. In this paper, a weighted four-point implicit finite difference technique is used for reasons of its versatility and computing efficiency.

The mathematical model is compared with two conventional flood-plain routing models and found to produce appropriately smaller wave attenuation and travel time, especially when channel meander is a factor. The mathematical model is used to simulate a number of hydrographs for varying flood plain to channel ratios of flow-path distance, roughness, and width in order to determine both qualitatively and quantitatively the modifying effects of flood plains on floods propagating through meandering rivers. Wave attenuation and travel time are found to increase as flood-plain roughness and width increase and as the extent of channel meander decreases.

[1]Research Hydrologist, Hydrologic Research Laboratory, National Weather Service, Silver Spring, Md. 20910.

INTRODUCTION

Unsteady flow in a natural river which meanders through a wide flood plain is complicated by large differences in geometric and hydraulic characteristics between the river channel and the flood plain, as well as the extreme differences in the hydraulic roughness coefficient. The flow is further complicated by the meandering of the main channel within the flood plain, which causes a portion of the total flow to "short-circuit" and proceed downstream along the more direct course afforded by the flood plain rather than along the more circuitous route of the meandering channel. This tendency for short-circuiting of the flow is enhanced by the greater longitudinal slope associated with the flood plain than that of the main channel; however, the short-circuiting effect is diminished by the greater hydraulic roughness of the flood plain. Further complexities are created by portions of the flood plain which act as dead storage areas, wherein the flow velocity is negligible. Another flow complexity occurs due to the interaction of the flows in the main channel and the flood plain; the direction of the lateral exchange of flow between the two watercourses depends on whether the flood wave is rising or receding, which, in turn, affects the magnitude of the associated energy loss.

In the literature [Liggett and Cunge, 1975; Miller and Cunge, 1975], it is evident that the one-dimensional mathematical models proposed for simulating unsteady flows in natural rivers have, for the most part, ignored the above flow complexities. Most either treat the flood plain or some portion of it as off-channel dead storage, or the main river channel and the flood plain are lumped together to form a composite channel in which the significantly different particle velocities and wave speeds of the flows in the main channel and in the flood plain are averaged together. Each of these techniques provides only a rough approximation of the actual flow, while the problem of short-circuiting is usually ignored; although, Perkins [1970] approached the problem by linearly adjusting the channel flow-path length as the flood plain is inundated.

The purpose of this paper is to present a one-dimensional mathematical model for simulating unsteady flows in a meandering river within a wide flood plain. Although the proposed model is also an approximation of the complex flow in such a natural watercourse, it does directly consider the influence of the unequal flow velocities and different degrees of roughness in the main river channel and the flood plain, the influence of different lengths and slopes of the flow paths of the channel and the flood plain, and the influence of dead storage areas. The energy loss due to the interaction of channel and flood-plain flows, as well as the problems of simulating helicoidal flow at river bends, traveling eddies, etc., which are associated with natural river channels are not considered in the proposed model.

MATHEMATICAL MODEL

Governing Equations

The basic concept of the model is to treat the flows in the river channel and the flood plain separately and from a one-dimensional point of view [Fread, 1975]. Thus, the model is based on a modified form of the one-dimensional equations of unsteady flow and thereby avoids the obvious use of the more complex and computationally time-consuming two-dimensional equations. This approach is warranted since the purpose of the model is to route floods and thus determine the celerity and transformation of the flood wave as it proceeds downstream through the river channel and the flood plain. These characteristics of the flood wave are influenced predominantly by the one-dimensional motion of the flood wave along the longitudinal axes of the river and the flood plain.

In order to treat the flows in the channel and flood plain separately, it is important that the geometric, roughness, and flow-path characteristics of both the river channel and flood plain be preserved in the governing one-dimensional equations. Using a subscript "c" to denote variables pertaining to the river channel, the complete one-dimensional equations of unsteady flow in a prismatic or non-prismatic river channel of arbitrary cross-sectional shape [Liggett, 1975; Stoker, 1957] are:

$$\frac{\partial A_c}{\partial t} + \frac{\partial Q_c}{\partial x_c} = 0 \tag{1}$$

$$\frac{\partial Q_c}{\partial t} + \frac{\partial (Q_c^{\,2}/A_c)}{\partial x_c} + gA_c\left(\frac{\partial h_c}{\partial x_c} + S_c\right) = 0 \tag{2}$$

Likewise, using a subscript "f" to denote variables pertaining to the flood plain, the one-dimensional equations of unsteady flow can be written for the flood-plain flow as follows:

$$\frac{\partial A_f}{\partial t} + \frac{\partial A_s}{\partial t} + \frac{\partial Q_f}{\partial x_f} - q = 0 \tag{3}$$

$$\frac{\partial Q_f}{\partial t} + \frac{\partial (Q_f^{\,2}/A_f)}{\partial x_f} + gA_f\left(\frac{\partial h_f}{\partial x_f} + S_f\right) - qv_{1x} = 0 \tag{4}$$

The variables in Eqs. 1-4 are defined as follows: Q = the discharge, L^3/T; A = the cross-sectional area, L^2; A_s = the off-channel dead storage area, L^2; h = the water surface elevation, L; S = the friction slope, L/L; q = the lateral inflow, L^2/T; v_{1x} = the velocity of the lateral inflow in the direction of x-axis of the flood plain, L/T; x = distance along the longitudinal axes of the channel or flood plain, L; t = time, T; and g = the acceleration due to gravity, L/T^2.

Upon adding the flows in the channel and the flood plain, the equations of unsteady flow for the combined flow become:

$$\frac{\partial (A_c + A_f + A_s)}{\partial t} + \frac{\partial Q_c}{\partial x_c} + \frac{\partial Q_f}{\partial x_f} - q = 0 \tag{5}$$

$$\frac{\partial (Q_c + Q_f)}{\partial t} + \frac{\partial (Q_c^{\,2}/A_c)}{\partial x_c} + \frac{\partial (Q_f^{\,2}/A_f)}{\partial x_f} + gA_c\left(\frac{\partial h_c}{\partial x_c} + S_c\right)$$

$$+ gA_f\left(\frac{\partial h_f}{\partial x_f} + S_f\right) - qv_{1x} = 0 \tag{6}$$

Eqs. 5-6 contain only four unknowns, Q_c, Q_f, h_c, and h_f because A can be expressed as a function of h, S can be expressed as a function of Q and h, and q, v_{1x}, g, x, t are known quantities. Since there are only two equations, it is desirable to reduce the number of unknowns to two.

Following a one-dimensional approach, the water surface is assumed to be horizontal across the river channel and the flood plain; therefore:

$$h_c = h_f = h \tag{7}$$

Thus, h_c and h_f can be replaced by h in Eqs. 5-6, thereby eliminating one of the four unknowns.

It is further assumed that the friction slope in the channel and in the flood plain can be expressed by Manning's equation, in which the slope S is approximated as:

$$S \approx \Delta h/\Delta x \tag{8}$$

This approximation neglects the contribution of inertia effects in evaluating the friction loss, yet is reasonable in the case of slowly varying transients such as flood waves moving through meandering rivers.

An approximate ratio of the flow in the flood plain to that in the river channel can be found using Manning's equation with S approximated by Eq. 8. Thus

$$\frac{Q_f}{Q_c} = \frac{\dfrac{1.486}{n_f} A_f R_f^{\,2/3} \left(\dfrac{\Delta h}{\Delta x_f}\right)^{1/2}}{\dfrac{1.486}{n_c} A_c R_c^{\,2/3} \left(\dfrac{\Delta h}{\Delta x_c}\right)^{1/2}} \tag{9}$$

in which n = the Manning's roughness coefficient, $T/L^{1/3}$; R = the hydraulic radius, L, which is approximated herein by A/B, where B is the top width of the water surface within the cross section, L; $\Delta h/\Delta x$ = the change in water surface elevation per incremental distance along the channel or flood plain axis, L/L.

The above flow ratio is defined as:

$$\psi = \frac{Q_f}{Q_c} = \frac{n_c A_f}{n_f A_c}\left(\frac{R_f}{R_c}\right)^{2/3}\left(\frac{\Delta x_c}{\Delta x_f}\right)^{1/2} \tag{10}$$

The total flow in the channel and flood plain is the sum of two separate flows, i.e.,

$$Q = Q_c + Q_f \tag{11}$$

From Eq. 10, it is seen that

$$Q_f = \psi Q_c \tag{12}$$

Then, substituting Eq. 12 in Eq. 11, the following is obtained:

$$Q_c = \phi Q \tag{13}$$

where

$$\phi = \frac{1}{1+\psi} \tag{14}$$

Likewise, using Eqs. 11-12, the following can be obtained also:

$$Q_f = TQ \tag{15}$$

where

$$T = \frac{\psi}{1+\psi} \tag{16}$$

Since ϕ and T are both functions of ψ, which, in Eq. 10, is seen to be a function of only one unknown variable (h), Eqs. 13 and 15 can be used to express Q_c and Q_f in terms of Q and h. Thus, upon substituting Eqs. 7, 11, 13, and 15 in Eqs. 5-6, only two unknowns, Q (total discharge) and h (water surface elevation), remain, i.e.,

$$\frac{\partial A}{\partial t} + \frac{\partial(\phi Q)}{\partial x_c} + \frac{\partial(TQ)}{\partial x_f} - q = 0 \tag{17}$$

$$\frac{\partial Q}{\partial t} + \frac{\partial(\phi^2 Q^2/A_c)}{\partial x_c} + \frac{\partial(T^2 Q^2/A_f)}{\partial x_f} + gA_c\left(\frac{\partial h}{\partial x_c} + S_c\right)$$

$$+ gA_f\left(\frac{\partial h}{\partial x_f} + S_f\right) - qv_{1x} = 0 \tag{18}$$

in which

$$A = A_c + A_f + A_s \tag{19}$$

Eqs. 17-18 are the governing differential equations of one-dimensional flow in a natural meandering river with a flood plain. Eq. 17 conserves the mass of the flow and Eq. 18 conserves the momentum.

Eq. 18 neglects momentum considerations for the lateral exchange of flow between the channel and the flood plain. The exchange is assumed to be completely described by the equation of continuity (Eq. 17).

Eqs. 17-18 constitute a system of partial differential equations of the hyperbolic type. They contain two independent variables, x and t, and two dependent variables, h and Q; the remaining terms are either functions of x, t, h, and/or Q, or they are constants. These equations are not amenable to analytical solutions except in cases where the channel geometry and boundary conditions are uncomplicated and the non-linear properties of the equations are either neglected or made linear. The equations may be solved numerically by performing two basic steps. First, the partial differential equations are represented by a corresponding set of finite difference algebraic equations; and second, the system of algebraic equations is solved in conformance with prescribed initial and boundary conditions.

Numerical Solution

Eqs. 17-18 are modified forms of the conventional one-dimensional equations of unsteady flow (Eqs. 1-2). They contain the same two unknowns (water surface elevation and discharge) as the conventional equations; hence, the same numerical solution techniques applicable to the conventional equations may be used. Accordingly, Eqs. 17-18 can be solved by either explicit or implicit finite difference techniques [Liggett and Cunge, 1975]. Explicit methods, although simpler in application, are not suitable for the simulation of long-term unsteady flow phenomena, such as flood waves in rivers, because they are restricted by mathematical stability considerations to very small computational time steps (on the order of a few minutes). Such small time steps cause the explicit methods to be very inefficient in the use of computer time. Implicit finite difference techniques, however, have no restrictions on the size of the time step due to mathematical stability; however, convergence considerations may require its size to be limited to something less than a few hundred times that of the explicit method, depending on the hydraulic properties of the unsteady flow and the size of the distance step.

Of the various implicit schemes that have been developed, the "weighted four-point" scheme first used by Preissman [1961] and recently by Quinn and Wylie [1973], Chaudry and Contractor [1973] and Fread [1974b] appears most advantageous since it can readily be used with unequal distance steps and its stability-convergence properties can be controlled easily. In the weighted four-point implicit finite difference scheme, the continuous x-t region in which solutions of h and Q are sought is represented by a rectangular net of discrete points. The net points are determined by the intersection of lines drawn parallel to the x and t axes. Those

parallel to the x axis represent time lines; they have a spacing of Δt, which need not be constant. Those parallel to the t axis represent discrete locations or nodes along the river (x axis); they have a spacing of Δx, which also need not be constant. Each point in the rectangular network can be identified by a subscript (i) which designates the x position and a superscript (j) which designates the time line.

The time derivatives are approximated by a forward difference quotient centered between the ith and i+1 points along the x axis, i.e.,

$$\frac{\partial K}{\partial t} \approx \frac{K_i^{j+1} + K_{i+1}^{j+1} - K_i^j - K_{i+1}^j}{2\,\Delta t} \tag{20}$$

where K represents any variable.

The spatial derivatives are approximated by a forward difference quotient positioned between two adjacent time lines according to weighting factors of θ and $1-\theta$, i.e.,

$$\frac{\partial K}{\partial x} \approx \theta\left(\frac{K_{i+1}^{j+1} - K_i^{j+1}}{\Delta x}\right) + (1-\theta)\left(\frac{K_{i+1}^j - K_i^j}{\Delta x}\right) \tag{21}$$

Variables other than derivatives are approximated at the time level where the spatial derivatives are evaluated by using the same weighting factors, i.e.,

$$K \approx \theta\left(\frac{K_i^{j+1} + K_{i+1}^{j+1}}{2}\right) + (1-\theta)\left(\frac{K_i^j + K_{i+1}^j}{2}\right) \tag{22}$$

A θ weighting factor of 1.0 yields the fully implicit or backward difference scheme used by Baltzer and Lai [1968], Dronkers [1969]. A weighting factor of 0.5 yields the box scheme used by Amein and Fang [1970], Contractor and Wiggert [1971]. The influence of the θ weighting factor on the accuracy of the computations was examined by Fread [1974a], who concluded that the accuracy decreases as θ departs from 0.5 and approaches 1.0. This effect becomes more pronounced as the magnitude of the computational time step increases. In this paper, a weighting factor of 0.55 is used so as to minimize the loss of accuracy associated with greater values while avoiding the possibility of a weak or pseudo instability noticed by Baltzer and Lai [1968], Quinn and Wylie [1972], Chaudhry and Contractor [1973], and Fread [1975] when a θ of 0.5 is used.

When the finite difference operators defined by Eqs. 20-22 are used to replace the derivatives and other variables in Eqs. 17-18, the following weighted four-point implicit difference equations are obtained:

$$\frac{A_i^{j+1} + A_{i+1}^{j+1} - A_i^j - A_{i+1}^j}{2\,\Delta t_j} + \theta\left(\frac{(\Phi Q)_{i+1}^{j+1} - (\Phi Q)_i^{j+1}}{\Delta x_{c_i}} - q_{i+1/2}^{j+1}\right)$$

$$+ (1-\theta)\left(\frac{(TQ)_{i+1}^j - (TQ)_i^j}{\Delta x_{f_i}} - q_{i+1/2}^j\right) = 0 \tag{23}$$

$$\frac{Q_i^{j+1} + Q_{i+1}^{j+1} - Q_i^j - Q_{i+1}^j}{2\,\Delta t_j} + \theta\left[\frac{(\Phi^2Q^2/A_c)_{i+1}^{j+1} - (\Phi^2Q^2/A_c)_i^{j+1}}{\Delta x_{c_i}}\right.$$

$$+ \frac{(T^2Q^2/A_f)_{i+1}^{j+1} - (T^2Q^2/A_f)_i^{j+1}}{\Delta x_{c_i}} + g\bar{A}_c^{j+1}\left(\frac{h_{i+1}^{j+1} - h_i^{j+1}}{\Delta x_{c_i}} + \bar{S}_c^{j+1}\right)$$

$$\left. + g\bar{A}_f^{j+1}\left(\frac{h_{i+1}^{j+1} - h_i^{j+1}}{\Delta x_{f_i}} + \bar{S}_f^{j+1}\right) - (qv_{1x})_{i+1/2}^{j+1}\right]$$

$$+ (1-\theta)\left[\frac{(\Phi^2Q^2/A_c)_{i+1}^j - (\Phi^2Q^2/A_c)_i^j}{\Delta x_{c_i}} + \frac{(T^2Q^2/A_f)_{i+1}^j - (T^2Q^2/A_f)_i^j}{\Delta x_{f_i}}\right.$$

$$\left. + g\bar{A}_c^j\left(\frac{h_{i+1}^j - h_i^j}{\Delta x_{c_i}} + \bar{S}_c^j\right) + g\bar{A}_f^j\left(\frac{h_{i+1}^j - h_i^j}{\Delta x_{f_i}} + \bar{S}_f^j\right) - (qv_{1x})_{i+1/2}^j\right] = 0 \tag{24}$$

where

$$\bar{S}_f = \frac{n\,\bar{Q}|\bar{Q}|}{2.21\,\bar{A}^2\bar{R}^{4/3}} \tag{25}$$

in which,

$$\bar{Q} = 0.5\,(Q_i + Q_{i+1}) \tag{26}$$

$$\bar{A} = 0.5\,(A_i + A_{i+1}) \tag{27}$$

$$\bar{R} = 0.5\,(R_i + R_{i+1}) \tag{28}$$

Eqs. 23-24 constitute a system of algebraic equations that are non-linear with respect to the unknowns, i.e., the values of the dependent variables h and Q at the net points i and i+1 at the time line designated as j+1.

The terms associated with the jth time line are known from either the initial conditions or previous computations. The initial conditions refer to values of h and Q at each node along the x axis for the first time line (j=1). They are obtained from a previous unsteady flow solution, or they can be estimated since small errors in the initial conditions dampen out within a few time steps.

Eqs. 23-24 cannot be solved in an explicit or direct manner for the unknowns since there are four unknowns and only two equations. However, if Eqs. 23-24 are applied to each of the (N-1) rectangular grids between the upstream and downstream boundaries, a total of (2N-2) equations with 2N unknowns can be formulated. (N denotes the total number of nodes.) Then, prescribed boundary conditions, one at the upstream boundary and one at the downstream boundary, provide the necessary two additional equations required for the system to be determinate. The resulting system of 2N non-linear equations with 2N unknowns is solved by a functional iterative procedure, the Newton-Raphson method [Amein and Fang, 1970].

Computations for the iterative solution of the non-linear system are begun by assigning trial values to the 2N unknowns. Substitution of the trial values into the system of non-linear equations yields a set of 2N residuals. The Newton-Raphson method provides a means for correcting the trial values until the residuals are reduced to a suitable tolerance level. This is usually accomplished in one or two iterations through use of linear or parabolic extrapolation for the first trial values. If the Newton-Raphson corrections are applied only once, i.e., there is no iteration, the non-linear system of difference equations degenerates to the equivalent of a quasi-linear difference formulation which may require smaller time steps than the non-linear formulation for the same degree of numerical accuracy.

A system of 2N x 2N linear equations relates the corrections to the residuals and to a Jacobian coefficient matrix composed of partial derivatives of each equation with respect to each unknown variable in that equation. The coefficient matrix of the linear system has a banded structure which allows the system to be solved by a compact quad-diagonal Gaussian elimination algorithm [Fread, 1971], which is very efficient with respect to computing time and storage. The required storage is 2N x 4 and the required computational steps are approximately 38N.

The boundary conditions consist of a description of either water surface elevation (h) or discharge (Q) as a function of time at the upstream and downstream extremities of the study reach. The downstream boundary may also be a specified relationship between h and Q such as an empirical rating curve or normal stage-discharge relationship corrected for unsteady effects. For example, the upstream boundary could be given by the following:

$$Q_1^{j+1} - Q(t) = 0 \tag{29}$$

where Q(t) is the specified temporal variation of Q at the upstream boundary; and the downstream boundary could be given by the following stage-discharge relationship:

$$Q_N^{j+1} - 1.49\left(\frac{AR^{2/3}S^{1/2}}{n}\right)_N^{j+1} = 0 \tag{30}$$

where S is approximated by Eq. 8.

COMPARISON WITH CONVENTIONAL MODELS

The model developed herein is referred to as the "channel-flood plain" model to distinguish it from two other conventional models of rivers having flood plains with which it will be compared. The other models are denoted as the "off-channel storage" model and the "composite channel" model.

The off-channel storage model treats the flood plain as off-channel dead storage. In this model the effect of the flood plain on unsteady flows is assumed to be completely described by the continuity equation (Eq. 1) in which the term A_c is replaced by A, which is defined as:

$$A = A_c + A_f \tag{31}$$

In this model, the velocity of the flow in the flood plain is assumed negligible and its momentum effects are not considered in Eq. 2.

The composite section model treats the channel and flood plain as one continuous cross-sectional area. In this model the term A_c in each of Eqs. 1-2 is replaced by A, as defined by Eq. 31. An equivalent Manning roughness coefficient (n_e), which is a weighted average of n_c and n_f, is used. It is based on the assumption that the total force resisting the flow is equal to the sum of the forces resisting the flow in the channel and in the flood plain. It is given by:

$$n_e = [(P_c n_c^2 + P_f n_f^2)/(P_c + P_f)]^{1/2} \tag{32}$$

where P is the wetted perimeter of the cross-sectional area.

The same weighted four-point implicit finite difference method is used for the numerical solution procedure in the off-channel storage and composite channel models as was previously described for the channel-flood plain model.

An idealized meandering river with a significant flood plain (Fig. 1) and uniform cross section (Fig. 2) is used in the comparison of the simulation characteristics of the three models. The discharge-hydrograph is specified for the upstream end of a 100-mile reach of meandering river with a bottom slope of 1 foot/mile. The three models are used to compute the discharge hydrograph at the downstream boundary. In order to minimize numerical errors, 1-hour time steps and 1-mile distance steps are used. The extent of meander or sinousity is specified by the flow-path length ratio:

$$L_r = L_c/L_f \tag{33}$$

where L_c is the length of the meandering channel and L_f is the length of the flood plain between the upstream and downstream boundaries. For the comparison

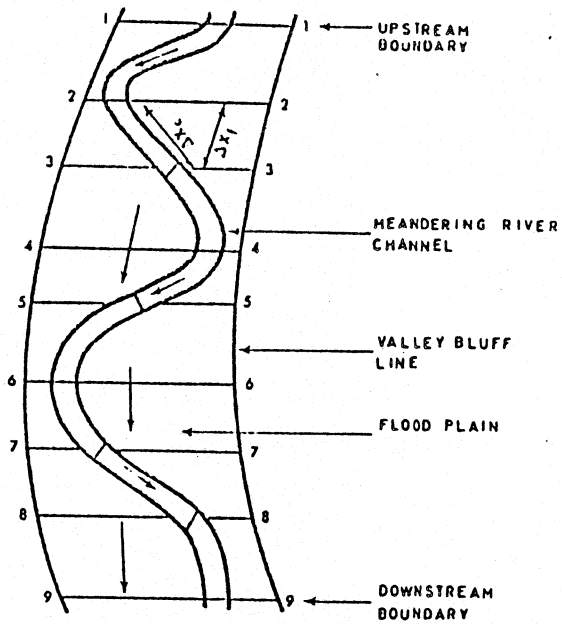

FIG. 1 DEFINITION PLAN OF IDEALIZED MEANDERING RIVER WITH FLOOD PLAIN

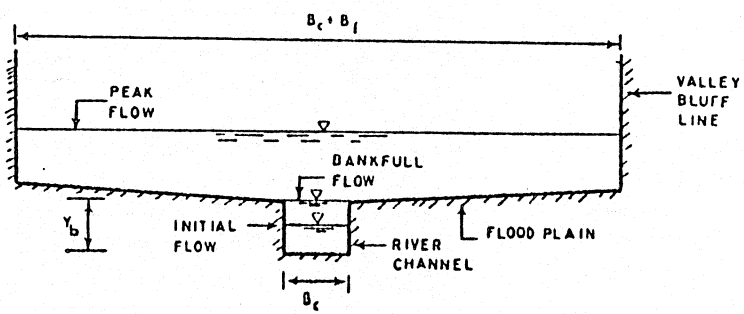

FIG. 2 CROSS-SECTION 5-5 OF IDEALIZED RIVER

simulations, the pertinent characteristics of the channel and flood plain are: L_r = 1.0, 1.5, 2.0; n_c = 0.03; n_f = 0.06; B_c = 500 feet; B_f = 2,000 feet; Y_b = 10 feet; the flood plain slopes upward from the river to the valley bluff line at a rate of 1 foot per 1,000 feet; and there is no lateral inflow.

Typical computed hydrographs of the channel-flood plain model and the off-channel storage model are shown in Fig. 3. The composite model is not shown since computational problems are encountered when simulating the sudden change in top width (B) as the flow spills onto the wide flat flood plain.

For a critical assessment of the differences between the models, attention is focused on the attenuation (α_p) and travel time (τ_p) of the hydrograph peaks (Q_p). These are normalized to the attenuation (α_b) and travel time (τ_b) associated with the flow condition (Q_b) when the river channel is bankfull. Normalization about the bankfull condition focuses on the differences in the computed attenuation and travel time of each model due to the presence of the flood plain. Simulations are also obtained from the composite channel model with the flow simulation starting with the flood plain inundated sufficiently to eliminate the problem of large changes in the top width per change in flow depth as the flow spills onto the flood plain. These results can be compared with the other models since only the hydrograph peaks are of interest.

The attenuation characteristics of the three flood-plain models are shown in Fig. 4. The off-channel storage model attenuates the hydrograph much more than the other two models. The composite channel model is similar to the channel-flood plain model, particularly at the larger flows and when there is no channel meander (L_r=1.0). As the sinuosity of the river channel increases, the composite channel model deviates farther from the channel-flood plain model, the former attenuating the hydrograph more than the latter.

The travel time characteristics of the three models are shown in Fig. 5. Again, the off-channel storage model deviates significantly from the other two models as manifested by its considerably greater travel times. The composite channel model deviates more and more from the channel-flood plain model as the sinuosity (L_r) and the peak flow (Q_p) increase.

The channel-flood plain model produces results which approach those of the off-channel storage model as the flood-plain roughness and width increase and as the sinuosity decreases. Although the composite section model has the inherent problem of simulating the condition when the flow spills onto a wide flat flood plain, its simulation characteristics approach those of the channel-flood plain model as the difference in channel and flood-plain roughness decreases, as the sinuosity decreases, and as the flood-plain width decreases.

FLOOD WAVE MODIFICATIONS DUE TO FLOOD PLAINS

The channel-flood plain model was used to obtain a qualitative and quantitative description of the modifying effects that flood plains have on flood waves propagating through meandering river channels. Hydrographs having a wide range of peak values were routed through the idealized meandering river and flood plain (Figs. 1-2) described previously. The modifying effects of

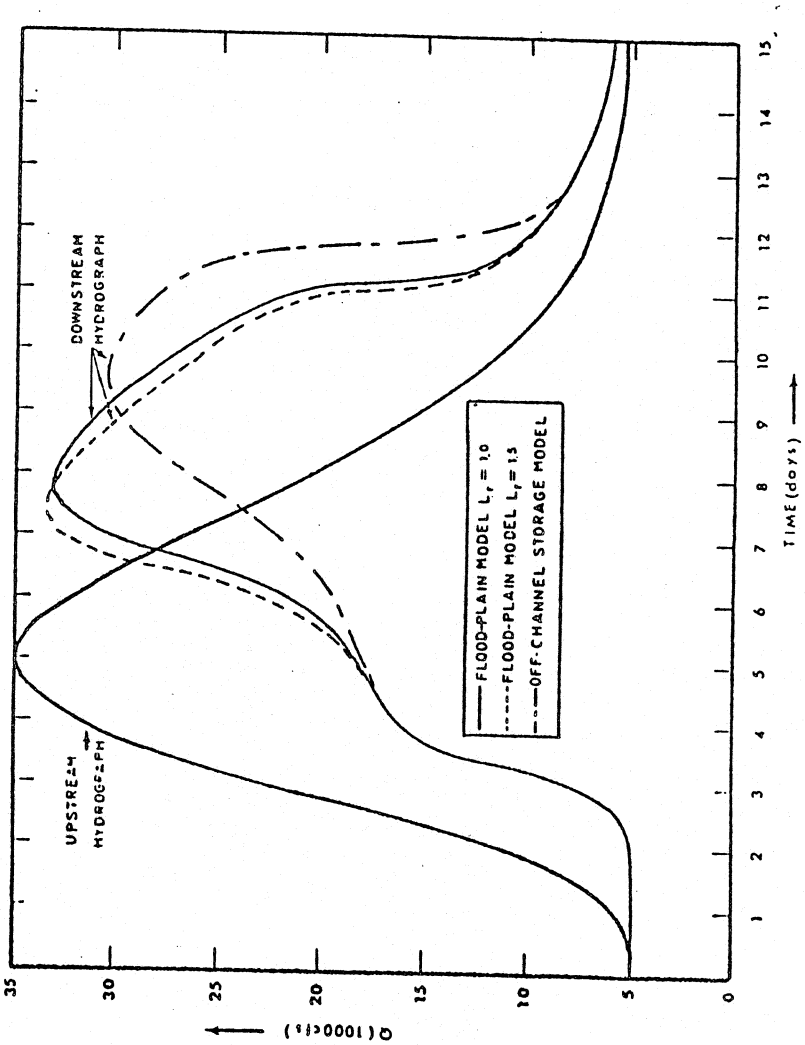

FIG. 3 TYPICAL HYDROGRAPHS OF CHANNEL-FLOOD PLAIN AND OFF-CHANNEL STORAGE MODELS

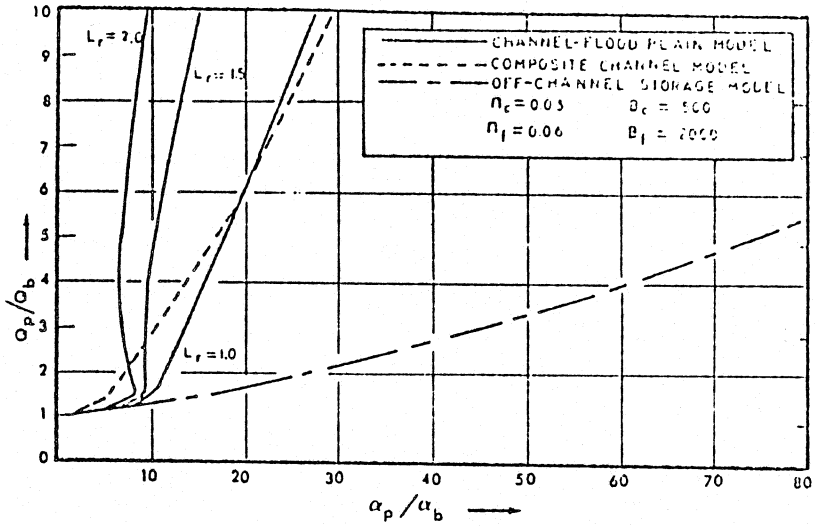

FIG. 4 ATTENUATION CHARACTERISTICS OF THREE FLOOD-PLAIN MODELS

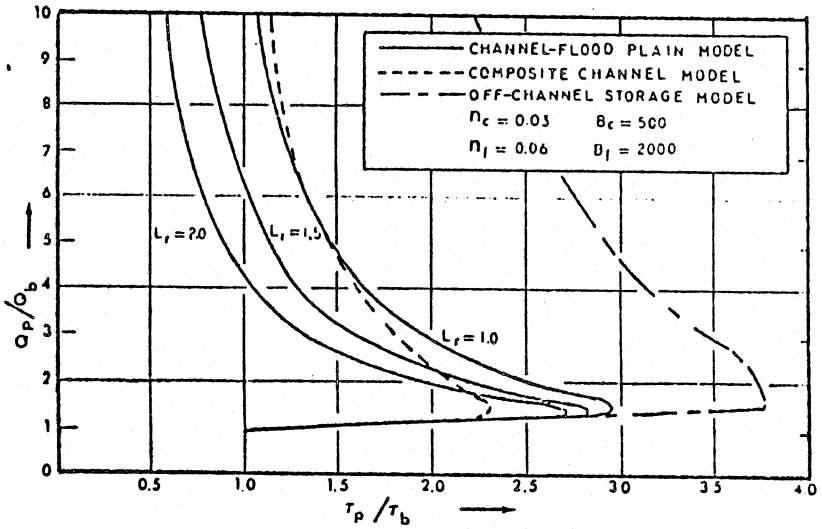

FIG. 5 TRAVEL TIME CHARACTERISTICS OF THREE FLOOD-PLAIN MODELS

the flood plain on the attenuation and travel time of the hydrograph peaks were sought for varying channel and flood plain characteristics such as flow-path distance, hydraulic roughness, and width. The flood plain effects are expressed in terms of a normalized attenuation (α_p/α_b) and travel time (τ_p/τ_b) for varying discharges normalized to the bankfull flow, i.e., (Q_p/Q_b).

The extent of channel sinuosity (L_r) is an important factor in affecting the attenuation. This is evident in Fig. 6, where the attenuation decreases significantly as the sinuosity increases. The travel time (Fig. 7) also decreases as the channel meander increases. The decrease in attenuation and travel time results when a portion of the flow short-circuits along the shorter path afforded by the flood plain rather than following the longer circuitous channel. For a given sinuosity, attenuation tends to increase and travel time decrease as the flow increases; however, the trends are reversed when the flood plain flows and depths are small.

The relative roughness of the flood plain to the channel, i.e.,

$$n_r = n_f/n_c \tag{34}$$

has an important effect on the attenuation and travel time characteristics. Attenuation (Fig. 8) and travel time (Fig. 9) increase significantly as the relative roughness of the flood plain to channel increases.

Similarly, the relative width of the flood plain to the channel, i.e.,

$$B_r = B_f/B_c \tag{35}$$

affects the attenuation and travel time characteristics. Attenuation (Fig. 10) and travel time (Fig. 11) increase as the width ratio (B_r) increases.

In Figs. 8-11, the attenuation increases and travel time decreases as the flow increases, except at low flood plain flows where the trends are reversed.

SUMMARY

A mathematical model has been developed to route floods in natural meandering rivers with wide flood plains. The governing equations are modifications of the conventional one-dimensional equations of unsteady flow. The modified equations preserve the identity of the essential one-dimensional flow properties of the flow in the river channel and in the flood plain; also, the flow-path lengths and slopes of each watercourse are preserved, which allows the problem of flow short-circuiting to be realistically modeled. The modified equations contain the same two unknowns as the conventional equations; this allows the convenient application of conventional numerical solution techniques. An efficient and versatile weighted four-point implicit scheme has been applied to the governing equations.

The channel-flood plain model developed herein has been compared with two conventional methods of treating the flood plain. The channel-flood plain model provided results which differed from the other models, especially where channel sinuosity and associated flow short-circuiting are factors. The

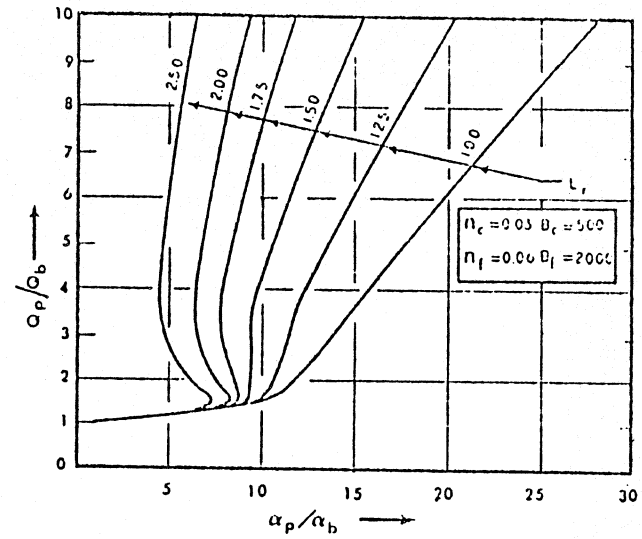

FIG. 6 EFFECT OF CHANNEL SINUOSITY (L_r) ON FLOOD ATTENUATION

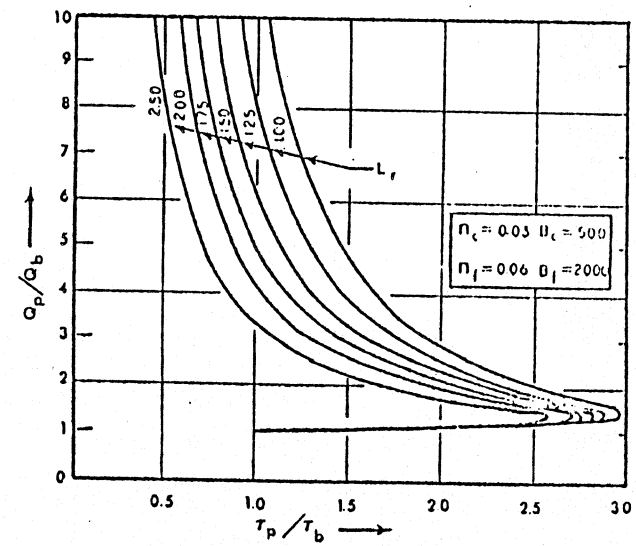

FIG. 7 EFFECT OF CHANNEL SINUOSITY (L_r) ON FLOOD TRAVEL TIME

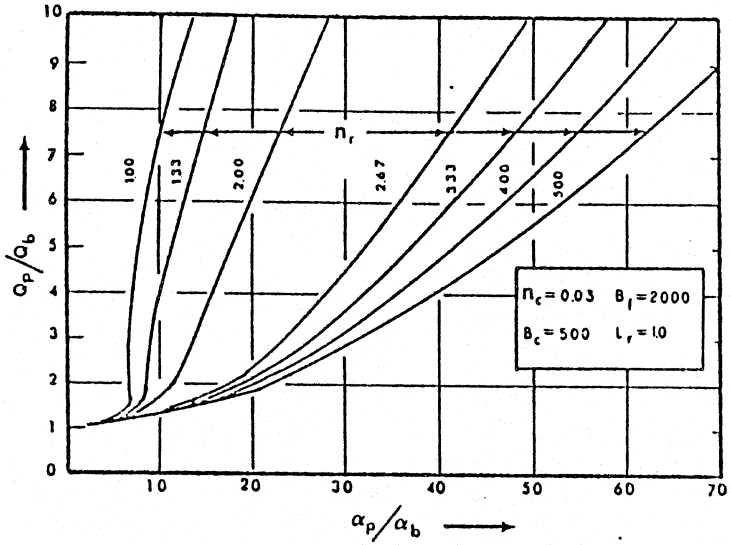

FIG. 8 EFFECT OF ROUGHNESS RATIO (n_r) ON FLOOD ATTENUATION

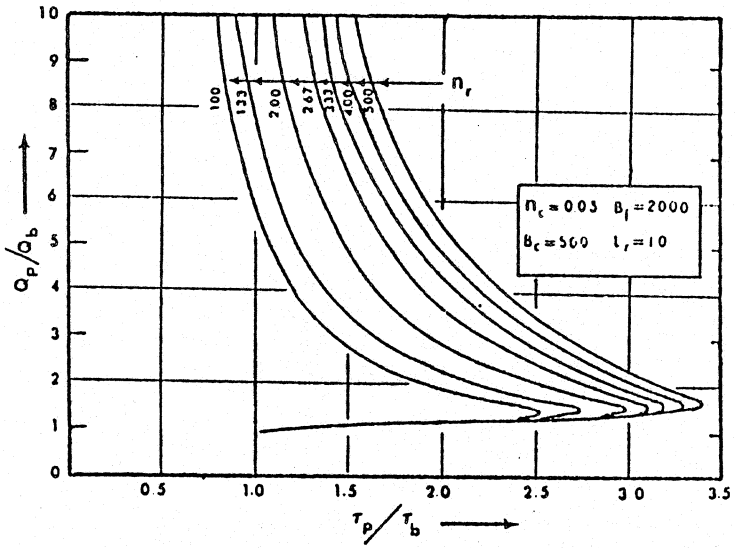

FIG. 9 EFFECT OF ROUGHNESS RATIO (n_r) ON FLOOD TRAVEL TIME

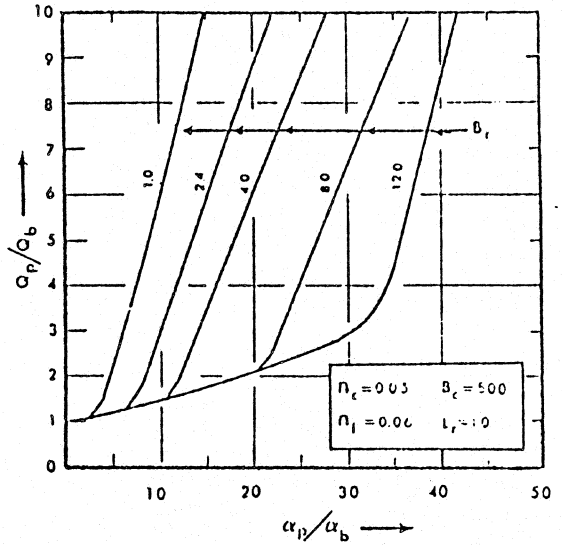

FIG. 10 EFFECT OF WIDTH RATIO (B_r) ON FLOOD ATTENUATION

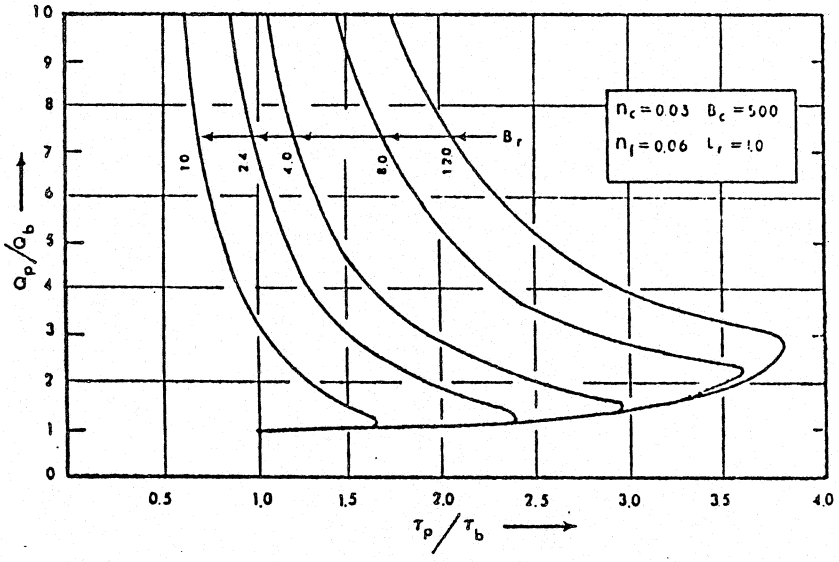

FIG. 11 EFFECT OF WIDTH RATIO (B_r) ON FLOOD TRAVEL TIME

compu[illegible]nal problem associated with a composite channel model when the flow spills onto a wide flat flood plain is not encountered in the channel-flood plain model.

The channel-flood plain model has been used to simulate flows in an idealized meandering river with a flood plain. Flood peak attenuation and travel time were found to increase as flood-plain roughness and width increase and as channel sinuosity decreases. Attenuation increases and travel time decreases as the flood-plain flow increases except at low flood-plain flows when the trends are reversed.

REFERENCES

Amein, M., and C. S. Fang, Implicit flood routing in natural channels, J. Hydraul. Div. Amer. Soc. Civil Engr., 96 (HY12), 2481-2500, 1970.

Baltzer, R. A. and C. Lai, Computer simulation of unsteady flows in water-ways, J. Hydraul. Div. Amer. Soc. Civil Engr., 94 (HY4), 1083-1117, 1968.

Chaudhry, Y. M., and D. N. Contractor, Application of implicit method to surges in channels, Water Resour. Res., 9 (6), 1605-1612, 1973.

Contractor, D. N. and J. M. Wiggert, Numerical studies of unsteady flow in the James River, Bulletin 51, VPI-WRRC-Bull 51, Water Resour. Res. Ctr., Virginia Poly Inst. and State Univ., Blacksburg, Va., May 1972.

Dronkers, J. J., Tidal computations for rivers, coastal areas, and seas, J. Hydraul. Div. Amer. Soc. Civil Engr., 95 (HY1), 29-77, 1969.

Fread, D. L., Discussion of implicit flood routing in natural channels, M. Amein and C. S. Fang, J. Hydraul. Div. Amer. Soc. Civil Engr., 97 (HY7), 1156-1159, 1971.

Fread, D. L., Numerical properties of implicit four-point finite difference equations of unsteady flow, NOAA Tech. Memo NWS HYDRO-18, U.S. Dept. of Commerce, NOAA, National Weather Service, 1974a.

Fread, D. L., Implicit dynamic routing of floods and surges in the Lower Mississippi, presented at AGU Natl. Mtg., Wash., D.C., April 1974b.

Fread, D. L., Discussion of comparison of four numerical methods for flood routing, R. K. Price, J. Hydraul. Div. Amer. Soc. Civil Engr., 101 (HY3), 565-567, 1975.

Liggett, J. A., Basic equations of unsteady flow, Unsteady Flow in Open Channels, edited by K. Mahmood and V. Yevjevich, Vol. I, Chapter 3, 29-62, Water Resour. Pub., Ft. Collins, Colorado, 1975.

Liggett, J. A. and J. A. Cunge, Numerical methods of solution of the unsteady flow equations, Unsteady Flow in Open Channels, edited by K. Mahmood and V. Yevjevich, Vol. I, Chapter 4, 89-182, Water Resour. Pub., Ft. Collins, Colorado, 1975.

Miller, W. A. and J. A. Cunge, Examples of one-dimensional flow [illegible]ling, Unsteady Flow in Open Channels, edited by K. Mahmood and V. Yevjevich, Vol. I, Chapter 11, 407-484, Water Resour. Pub., Ft. Collins, Colorado, 1975.

Perkins, F. E., Flood plain modeling, Water Resour. Bull., 6 (3), 375-383, 1970.

Preissmann, A., Propagation des intumescences dans les canaux et rivières, 1st Congrès de l'Assoc. Francaise de Calcul, Grenoble, 433-442, 1961.

Quinn, F. H. and E. B. Wylie, Transient analysis of the Detroit River by the implicit method, Water Resour. Res., 8 (6), 1461-1469, 1972.

Stoker, J. J., Water Waves, Interscience Pub., Inc., New York, 1957.

MODELLING DAM-BREAK FLOODS
OR OTHER TRANSIENT FLOWS

using

NWS Models: DAMBRK
SMPDBK
BREACH
DWOPER

MODELING DAM BREAK FLOODS

using:

1. NWS "DAMBRK" Flood Forecasting Model
   HYDROGRAPHS AT ANY POINT ON ANY RIVER SYSTEM W/WOUT DAMS
2. NWS "SMPDBK" Simplified Dam Break Model
   PEAK VALUES ONLY - WITH DAMS
3. NWS "BREACH" Erosion Model for Earthen Dams
   GENERATES HYDROGRAPH AT EARTH DAM BREACH ONLY

LOOK INTO STUDY ON GLEN CANYON DAM FAILURE

~~300~~ 35 million cfs hydrograph peak

100 ft. of flow for 75 hrs over Hoover Dam

(1) DAM FAILURE:

WORLD WIDE STATISTICS

Piping, Seepage, Slides, Earthquake	40 →	50 %
Overtopping	30 →	35 %
Misc.	15 →	30 %

(2) OVERTOPPING:

Only overtopping can be predicted by a few of the current Dam-Breach Flood Models.

Overtopping prediction subject to errors in the Rainfall-Runoff Hydrologic Model used to predict the inflow to the reservoir.

Extent of overtopping to cause dam-failure is not well understood. It is highly dependent on the type of dam (concrete or earthfill).

Earthfill —— Duration and Magnitude of overtopping flow

Concrete —— Magnitude of overtopping flow

MAXIMUM POSSIBLE WAVE

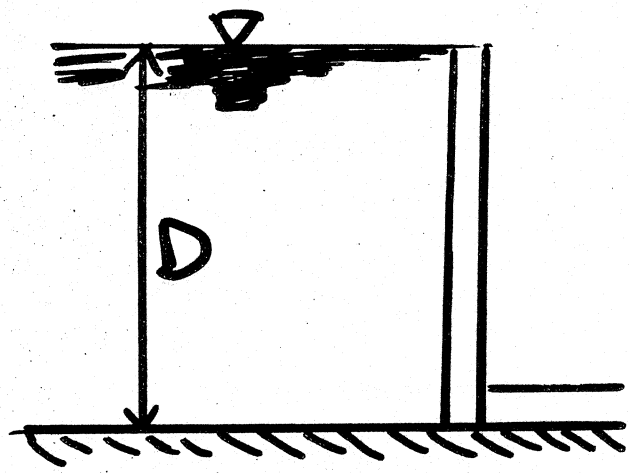

BEFORE FAILURE

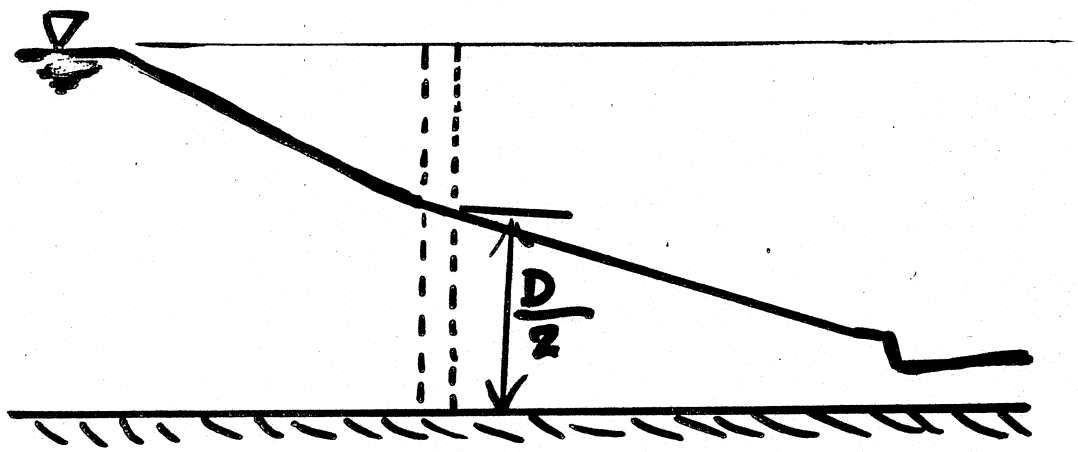

JUST AFTER COMPLETE AND SUDDEN FAILURE

FLOOD WAVE ATTENUATION

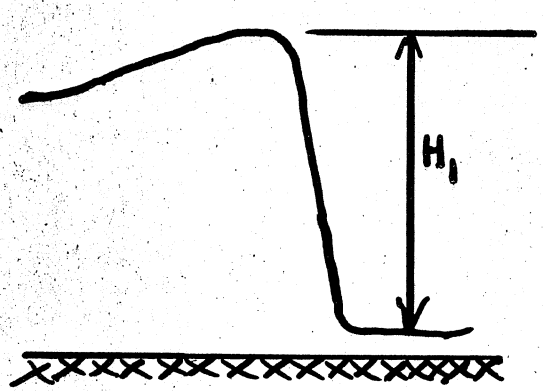

NEAR DAM

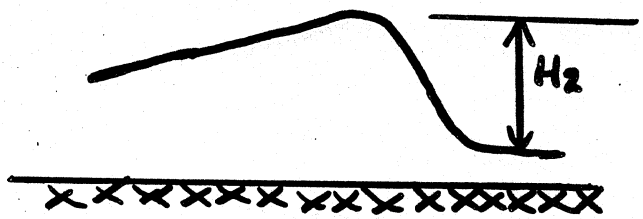

FEW MILES FROM DAM

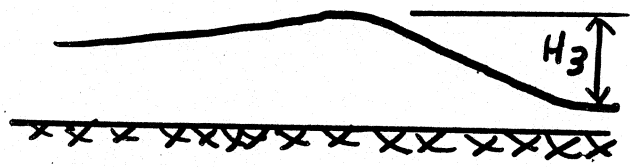

SEVERAL MILES FROM DAM

TETON : $H_1 \simeq 57$ ft AT DAM

$H_2 \simeq 14$ ft AT 9 MILES

$H_3 \simeq 9$ ft AT 60 MILES

TRAVEL TIME OF FLOOD WAVE PEAK

TETON : 1 TO 4 MI/hr

	MI.	HR.
REXBURG -	16	5
IDAHO FALLS -	50	34

slope = 7'/mile

BUFFALO CREEK : 4 TO 7 MI/hr

	MI.	HR.
STOWE -	7	1
MAN -	16	3

slope 80'/mile

TOCCOA : 4 MI/hr

	MI.	HR.
COLLEGE -	0.7	.2

OUTFLOW FROM DAM

EFFECTED BY:
1. SIZE AND SHAPE OF BREACH AS A FUNCTION OF TIME
2. HT. OF DAM
3. STORAGE VOLUME OF RESERVOIR
4. INFLOW TO RESERVOIR
5. DOWNSTREAM CHANNEL CONDITIONS (CHANNEL SIZE, ROUGHNESS) WHICH MAY CAUSE SUBMERGED WEIR FLOW THRU BREACH

DAM-BREAK WAVE TRANSFORMATION

EFFECTED BY:
1. INITIAL SHAPE
2. STORAGE VOLUME OF DOWNSTREAM VALLEY
3. ACCELERATION COMPONENTS OF WAVE
4. RESISTANCE TO FLOW THRU DOWNSTREAM VALLEY

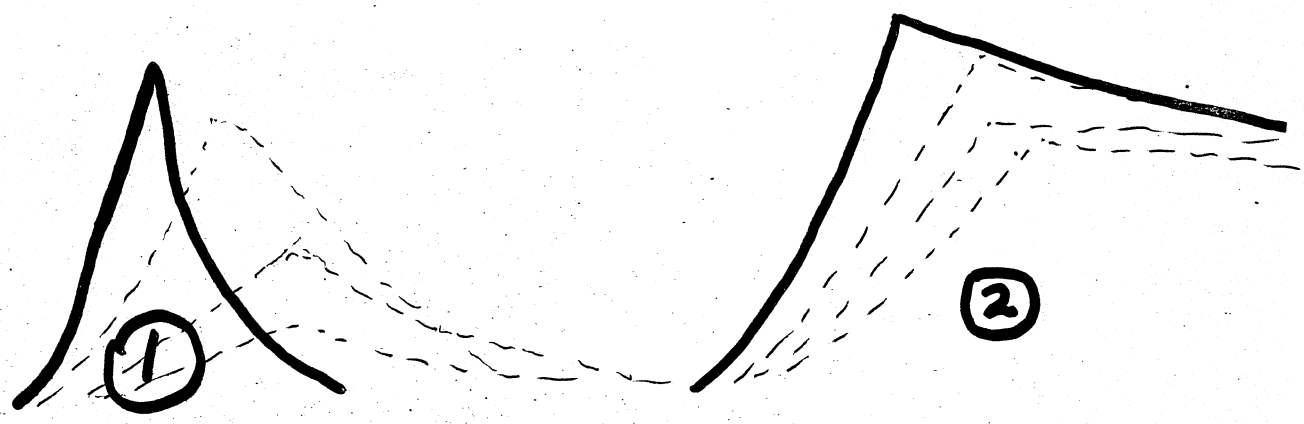

1 ---- SMALL STORAGE VOLUME IN RESERVOIR

2 ..... LARGE STORAGE VOLUME IN RESERVOIR

DAM-BREACH FLOOD ROUTING MODELS

SOME IMPROVEMENTS DURING LAST DECADE :

1) Breach Dynamics

   a) Time of formation

   b) Size

   c) Shape

2) 1-Dimensional Eqs. of Unsteady Flow

3) Effects of Downstream Dams and/or Bridge-Embankments on Flood Propagation

Not with standing the above improvements, errors of 2 feet or more can be expected in the flood peak profile.

This is evidenced by comparison of various Dam-Breach Flood Models with the observed flooding produced by the Teton, Toccoa, Laurel Run, and Buffalo Creek dam-failure floods.

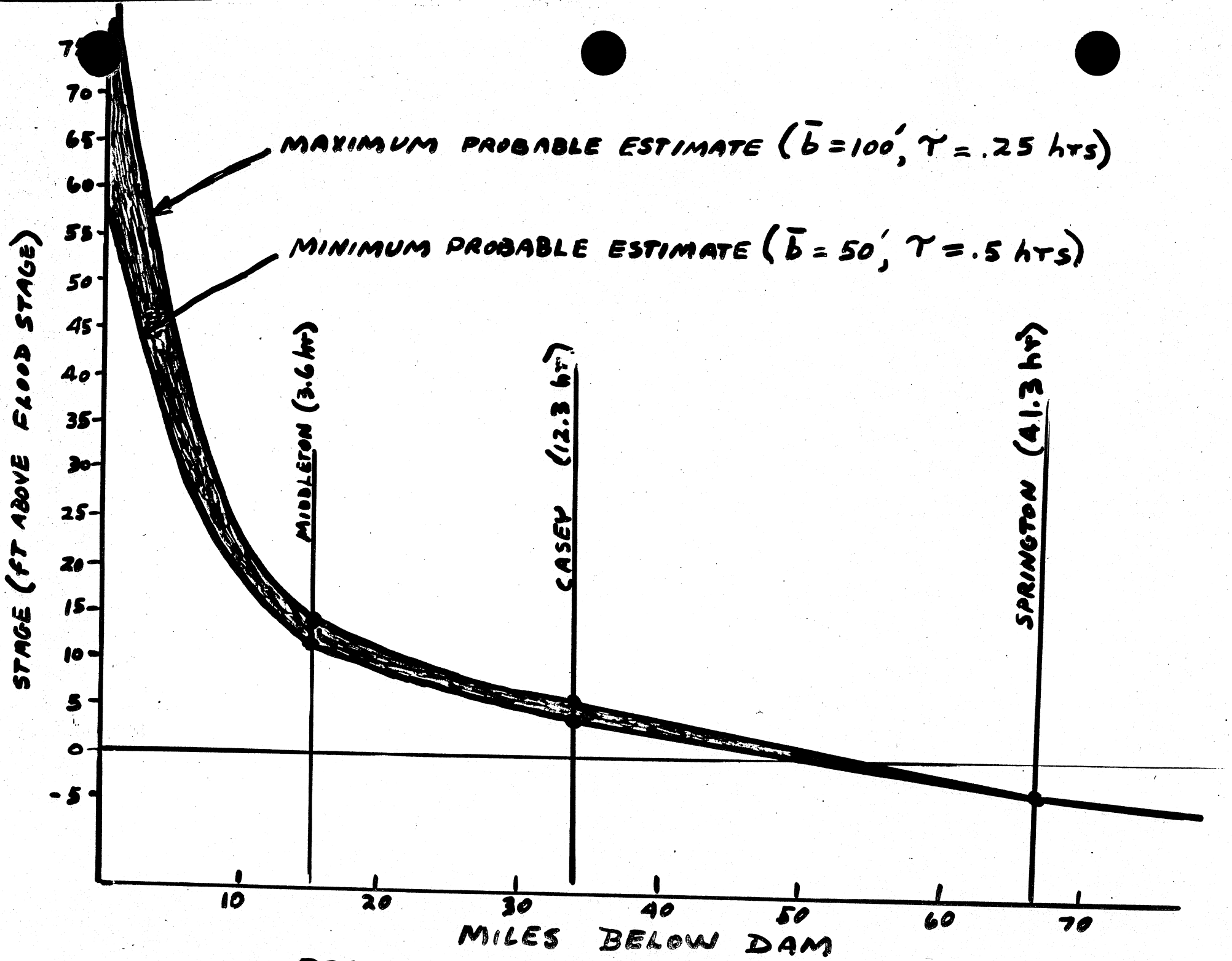

PRE-FORECAST FLASH FLOOD ENVELOPE

A Synopsis of NWS Models for Predicting the Flooding Due to Dam Failures

✓ **BREACH** : Earthen dams — size & timing of breach

✓ **DAMBRK** : concrete or Earthen dams
develop outflow hydrograph
determine extent & timing of flooding at various locations downstream of dam

✓ **SMPDBK** : Same thing as DAMBRK but in a much more simple manner usually more approximate results

D.L. FREAD (301-427-7640)
National Weather Service
Rm 530, Gramax Bldg.
8060 13th St.
Silver Spring, MD. 20910

Main-Frame
Mini

Mag Tape: DAMBRK, SMPDBK, BREACH, DWOPER, CROSS-SECT } Fortran #60 (45)
9 Trk, unlabled, 1600 BPI,

Micro

IBM Floppy PC: SMPDBK — Fortran / Basic

NO CHARGE

John Haestad (203-753-9800)

37 Brookside Rd.

Waterbury Conn. 06708

Micro	IBM PC	DAMOKK DWOPER	approx. $600 (US) each

DAMBRK

Dam Break Flood Forecasting Model

DAM-BREAK FLOOD FORECASTING MODEL

SOME GENERAL REQUIREMENTS :

1. WIDE APPLICABILITY

2. REASONABLY SMALL COMPUTATIONAL REQUIREMENTS

3. DATA INPUT WHICH VARIES FROM A MINIMUM LEVEL TO A MAXIMUM LEVEL 2-90 X-SECTIONS

4. DATA INPUT MUST BE OBTAINABLE WITH AVAILABLE SOURCES

5. COMPUTATIONAL SCHEME MUST BE ROBUST (STABLE)

DAM-BREAK MODEL COMPONENTS

THE THREE COMPONENTS CAN BE RUN TOGETHER OR SEPERATELY.

1. BREACH DESCRIPITION (SHAPE vs. TIME)

2. RESERVOIR ROUTING TO PRODUCE OUTFLOW HYDROGRAPH

   a. STORAGE ROUTING

   b. DYNAMIC ROUTING

3. DOWNSTREAM FLOOD ROUTING

FEATURES OF NWS DAM-BREAK FLOOD FORECASTING MODEL

OUTFLOW FROM RESERVOIR :

reservoir inflow at least 2 pts. needed to define this

reservoir storage characteristics : volume - surface areas

spillway (uncontrolled and gated) and turbine flows
head independent

can't break dam onto dry river.

crest overflow

breach outflow (broad crested weir flow with submergence correction)
... can be simulated to model spillway failures

Features cont'd

BREACH CHARACTERICSTICS :

time dependent geometry

triangular , rectangular or trapezoidal shape —— controlled by z factor

assumed to be linear

erosion formed breach with time dependent width starting at top of dam

piping formed breach with time dependent width starting at any prescribed elevation

no piping can occur when the head is at the same elevation

collapse failure , constant width , approaching instantaneous

RESERVOIR ROUTING :

storage type , assumes level pool condition

Downstream dams are always dynamic

dynamic type ,considers negative wave and/or inflow flood wave effects

DOWNSTREAM ROUTING (DYNAMIC):

Features cont'd

one–dimensional unsteady flow equations

conservation form of equations

weighted 4–pt implicit non–linear finite difference solution

variable time step 1/20 TH TIME TO FAILURE PEAK AND THEREFORE VARIES DOWNSTREAM

variable reach lengths between cross–sections

option to create cross–sections via linear interpolation

off channel storage effects

subcritical or supercritical flows

lateral inflows from tributaries

lateral outflow (loss function)

Manning roughness coefficient function of distance and stage

expansion– contraction losses

downstream boundary–generated loop rating or flow control structure caused by change in energy grade

initial conditions automatically computed via gradually varied steady flow eq.

internal computational checks to provide robust computational procedure

Features cont'd.

ADDITIONAL CAPABILITIES OF MODEL

- multiple dam capabilities
- supercritical reach/subcritical reach sequence capability
- bridge embankment effects
- model easily used for only downstream routing
- tributary dam failure can be analyzed by two applications of model
- feasible computational requirements (Teton analysis required less than 20 sec. cpu time) 55 HRS 60 video
- minimal data acceptance for generating approximate results

BREACH PARAMETERS

width

time of failure

JOHNSON & ILLES, 1976
WATER POWER AND DAM CONSTRUCTION
DEC 1976 PP. 43-45

300 DAM FAILURES WORLD WIDE

1946-1955 : 2000 DAMS CONSTRUCTED AND 12 MAJOR FAILURES

1956-1965 : 2500 DAMS CONSTRUCTED AND 24 MAJOR FAILURES

CAUSE OF FAILURE	% OF TOTAL
OVERTOPPING	35
PIPING, SEEPAGE, SLIDES	25
MISC.	40
	100

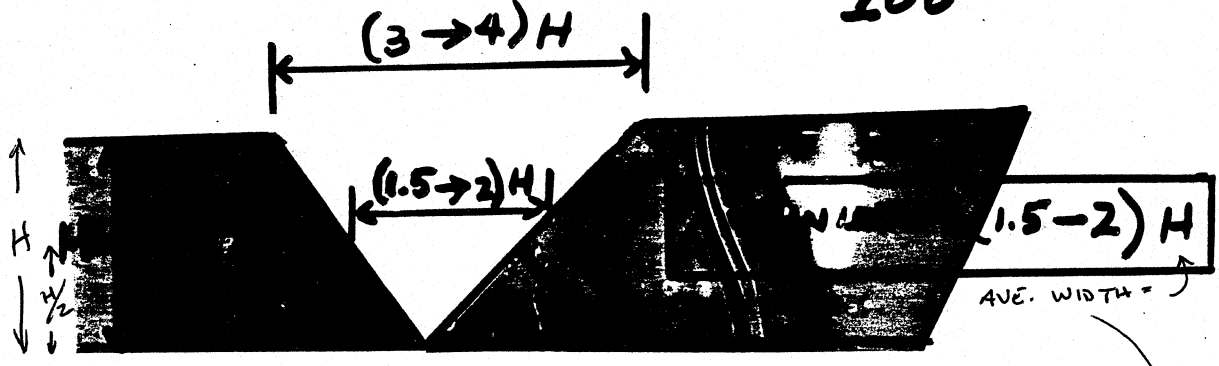

INITIAL V-SHAPED BREACH

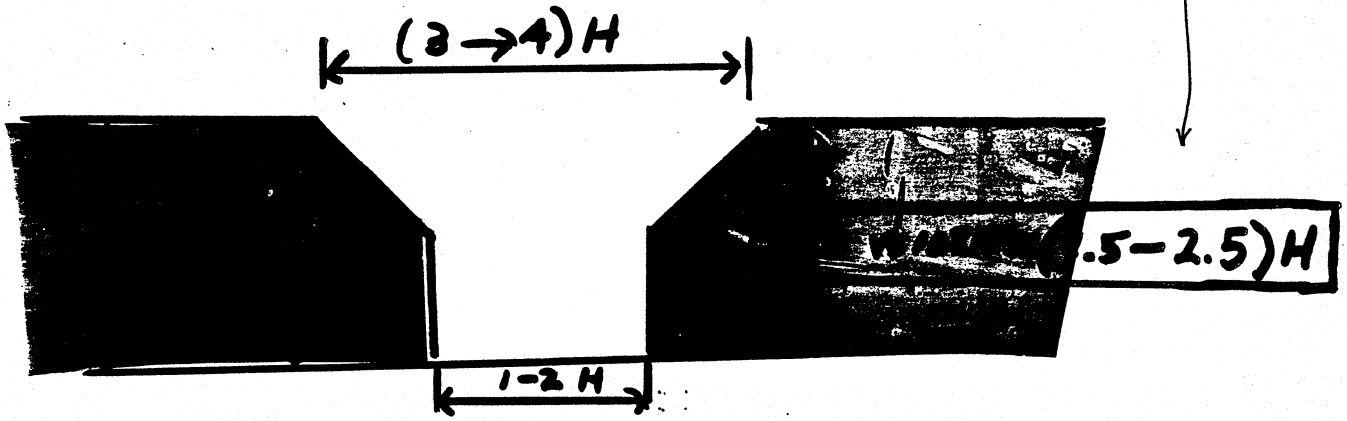

FINAL SHAPED BREACH IF OUTFLOW DURATION IS SUFFICIENT

HEC-1 - DAM BREACH OPTION IS SOMEWHAT DIFFERENT THAN NWS MODEL IN THAT POINT BREACH VERSUS FULL BROAD CRESTED DOESN'T EXIST IT IS ALWAYS BROAD. ALSO THE DROWN OUT BY TAILWATER WON'T OCCUR.

Table 1. Physical and Breach Parameters for 20 Historical Dam Failures

		Length ft	Height ft	Storage 1000 ac-ft	H_{se} ft	h_f ft	TF hr	t_e hr	BTW ft	BBW ft	DBD ft	Q_{max} 1000 cfs	R inches	A sq mi
1.	Bradfield Dam	1254	95	2.4	84			0.75				40		
2.	Canyon Lake Dam	500	20	0.8			0.10						10	
3.	Condty Dam	860	36	0.252			"short"	"short"	220	60				
4.	Higian Dam	3253	35	3.67								14		
5.	Elk City Dam	1850	30	0.6	27.5	1-1.5			150	*	30		5.75/2	23.5
6.	Brindale Dam	700	36		29		"short"		130	*	15			450
7.	Frias Dam	204				3.0	0.25		204	*	49			
8.	Grand Rapids Dam	**	25	0.18		"small"	"short"	"short"	40	20	25			
9.	Hatchtown Dam	780	63	13	58	-10	"short"	1.0	640	400	63			
10.	Horse Creek Dam	2300	40	2.5					↑	↑	↑			
11.	Kaddam Dam		41	174		1.5			450	*				
12.	Lake Barcroft Dam		69[2]	2.53		1.3	"long"	"long"	75	*	36		9.0	
13.	Lower Otay Dam	565	130	40		1-2	0.25	2.5	565	*	130		9.14	
14.	Machhu II Dam	13700	197	81.9		2.0	2.0		1768	*	197		21/21	
15.	Oakford Park Dam	350	20			2-3	1.0		75	*	10-20		5.1	
16.	Schaffer Dam	1100	90	3.19			"short"	0.5	↑	↑	↑	153		
17.	Sherburne Dam	300	34	0.064	29				150	*		34		
18.	South Fork Dam	930	72	15.4	65	0.4	0.75	3.5	400	*			10/36	
19.	Swift Dam	740		30			"short"		↑	↑	↑			
20.	Winston Dam	435	24	0.538	20	1.0	5.0	5.0	70	60	24		6.0	7.5

H_{se} = spillway elevation above the foundation
h_f = maximum water depth over the dam during failure by overtopping
TF = failure time from inception to completion of breach
t_e = time taken to empty reservoir after the beginning of failure
BTW = breach top width
BBW = breach bottom width
DBD = depth of breach from top of dam
Q_{max} = maximum outflow rate after dam breach
R = depth of rainfall/duration in hours (if known)

A = area of drainage basin above dam
"short" = time of few minutes, less than 0.5 hour
"long" = time of few hours, longer than 1.0 hour
"small" = depth of few inches, less than 0.5 foot
* = breach width not specified for top or bottom
↑ = most of the dam failed
** = circular reservoir with radius = 230 feet
1 = piping failure
2 = 36 feet where embankment failed

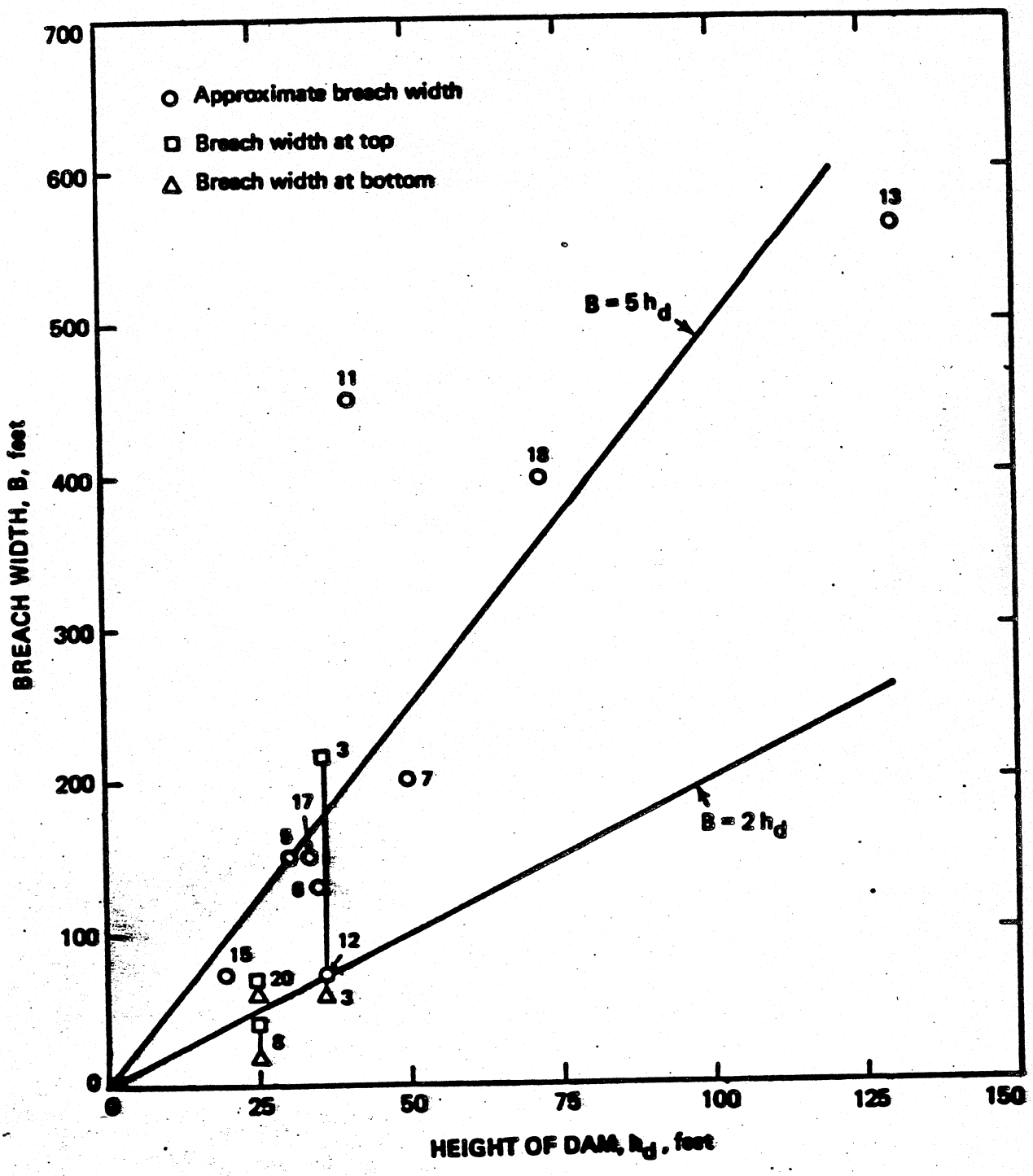

Figure 2. Breach width versus height of dam

BREACH CHARACTERISTICS

FOR BALL-PARK FIGURES TO USE IN MODELING

TYPE OF DAM	AVG. BREACH WIDTH ($\bar{b}$)	TIME OF FAILURE (T) hrs
EARTH (WELL CONSTRUCTED)	$2H_d < \bar{b} < 5H_d$	$0.1 \leq T \leq 0.5$
EARTH	$2H_d < \bar{b} < 5H_d$	$0.1 \leq T \leq 0.5$
SLAG PILE	$\bar{b} \geq 0.8\ W$	$T \leq .2$
CONCRETE (GRAVITY)	$\bar{b} \leq 0.5\ W$	$T \leq .2$
CONCRETE (ARCH)	$\bar{b} \geq 0.8\ W$	$T \leq .1$

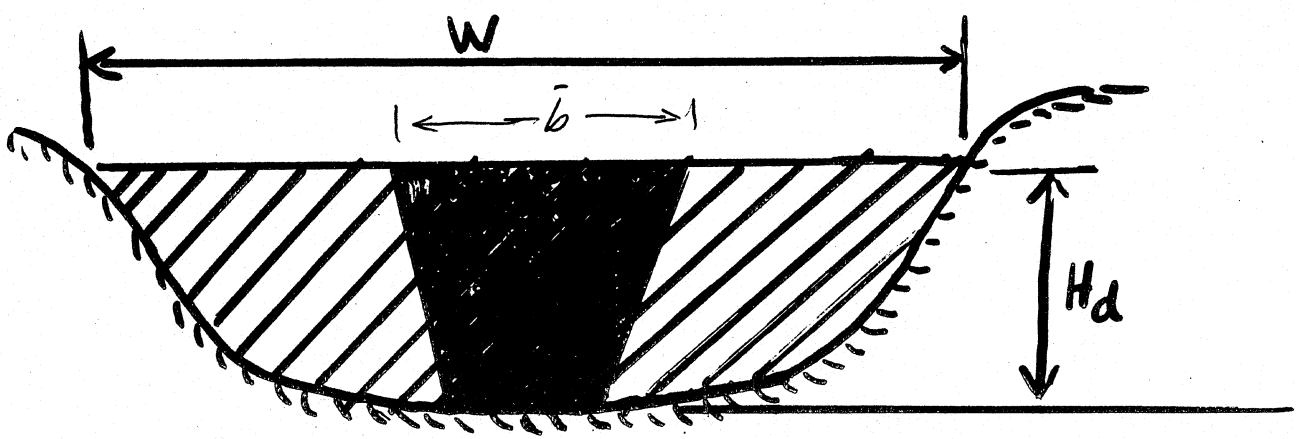

TRIANGULAR BREACH :

$Z > 0$

$BB = 0$

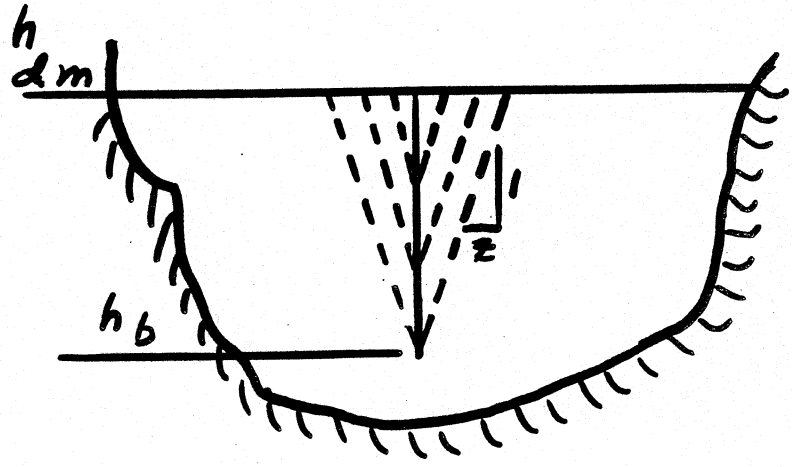

RECTANGULAR BREACH :

$Z = 0$

$BB > 0$

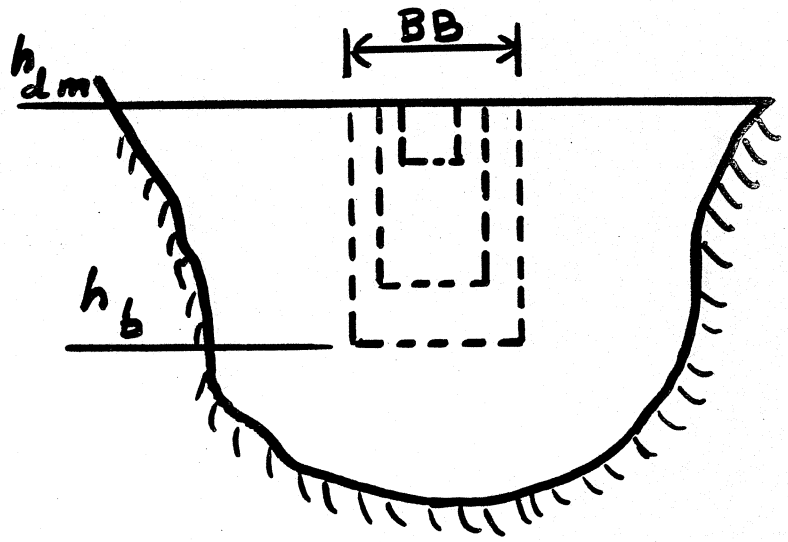

TRAPEZOIDAL BREACH:

$Z > 0$

$BB > 0$

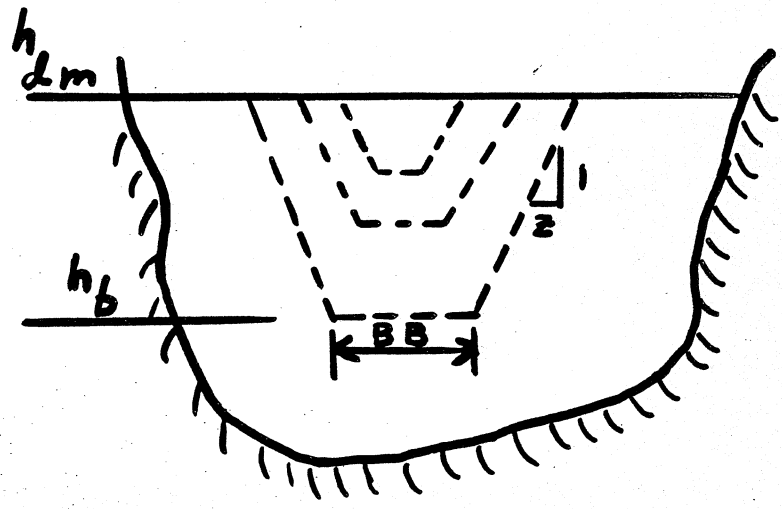

"Estimation of Breach Size"

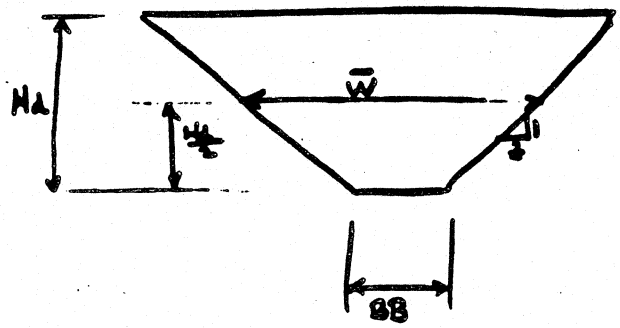

$$H_{k1} = \frac{0.04\ c\ \cos\phi}{1-\cos(90-\phi)}$$

$$H_{k2} = \frac{0.04\ c\ \cos\phi\ \sin(45+\phi/2)}{1-\cos(45-\phi/2)}$$

$$H_{k3} = \frac{0.04\ c\ \cos\phi\ \sin(22.5+3\phi/4)}{1-\cos(22.5-\phi/4)}$$

$BB = 5/3\ Hd$ . . . . . $0.8\ Hd \le H_{k1}$

$BB = 5/3\ H_{k1}$ . . . . . $0.8\ Hd > H_{k1}$

$\theta = 90$ . . . . . $0.8\ Hd \le H_{k1}$

$\theta = 45 + \phi/2$ . . . . . $0.8\ Hd > H_{k1}$

$\theta = 22.5 + 3\phi/4$ . . . . . $0.8\ Hd > H_{k2}$

$\theta = 11.3 + 7\phi/8$ . . . . . $0.8\ Hd > H_{k3}$

$$Z = \frac{1}{\tan\theta}$$

$$\bar{W} = BB + Z\ Hd$$

AVERAGE BREACH WIDTH

Earthen Dams:

$0.1 \le \overset{(h_w)}{TFH} \le 0.5$

$Hd \le \bar{W} \le 5\ Hd$

Concrete:

$0.05 \le \overset{(h_w)}{TFH} \le 0.1$

$\bar{W}$ = crest length (Arch)

$\bar{W}$ = 1 or more construction lifts (Gravity)

Material	D50 (mm)	(± 5%) ϕ (deg)	c (lb/ft²)
Gravel	> 5	38	< 50
Silty Gravel	> 5	34	50 – 300
Clayey Gravel	> 5	31	100 – 400
Sand	0.1 – 5	37	200 – 900
Silty Sand	0.1 – 5	34	700 – 1200
Clayey Sand	0.1 – 5	30	1000 – 2000
Silt	< 0.1	23 – 33	800 – 1600
Clay	< 0.1	15 – 25	1500 – 2000

"Estimation of Breach Size (Teton example)"

$C \approx 300$ lb/ft²

$\phi \approx 37$

$H_d = 262$

$$H_{K1} = \frac{0.04\ 300 \cos(37)}{1 - \cos(45-37)} = 24$$

$$H_{K2} = \frac{0.04\ 300\ \cos(37)\ \sin(45 + 37/2)}{1 - \cos(45 - 37/2)} = 82$$

$$H_{K3} = \frac{0.04\ 300\ \cos(37)\ \sin[22.5 + 0.75(37)]}{1 - \cos(22.5 - 37/4)} = 277$$

$$0.8\ H_d = 0.8(262) = 210$$

Since, $210 > 24$ $\quad BB = 5/3(24) = \underline{\underline{40}}$

Since, $210 > 82$ $\quad \theta = 22.5 + 0.75(37) = 50.3$

$$z = \frac{1}{\tan(50.3)} = \underline{\underline{0.83}}$$

$$\overline{W} = 40 + 0.83(262) = 257$$

$$W = 40 + 2(0.83)(262) = 475 \quad (\overset{\text{Actual}}{500})$$

effects of sedimentation are not handled very well but can be addressed with some assumptions

RESERVOIR

HYDRAULICS

NOTE:

BREACH STARTS FORMING WHEN $h \geq HF$

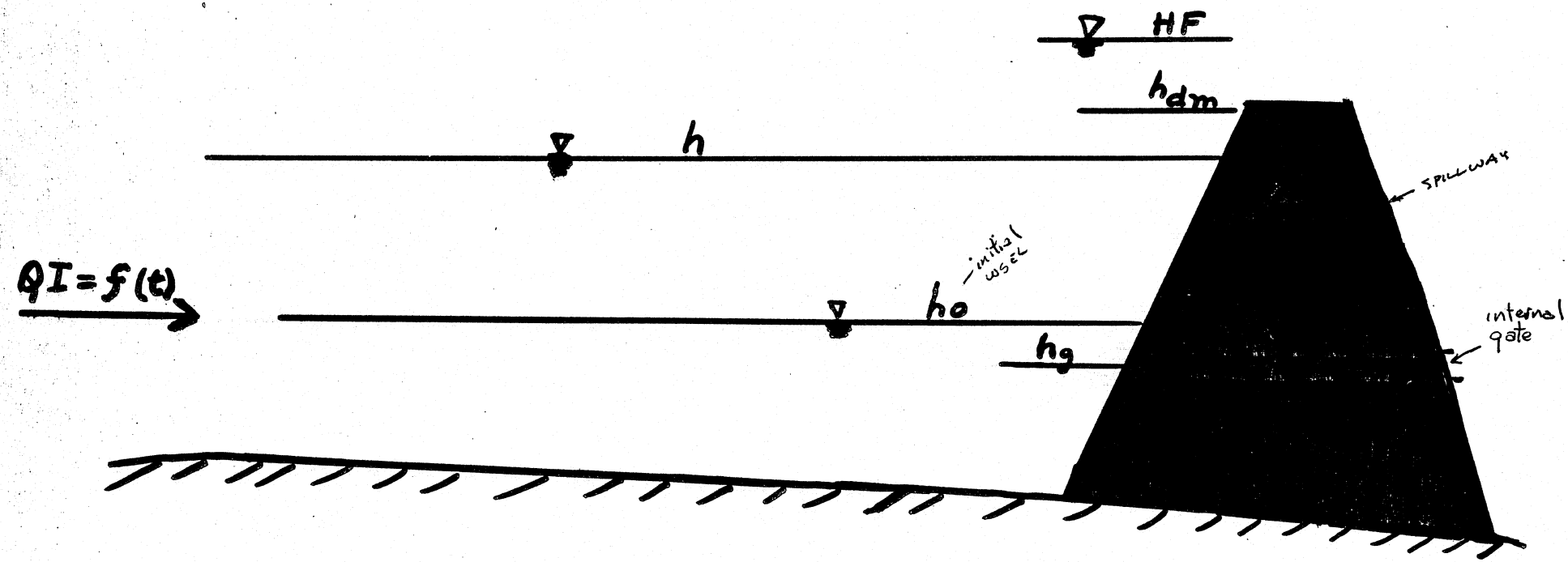

PROFILE VIEW

DAM BREACH OUTFLOW

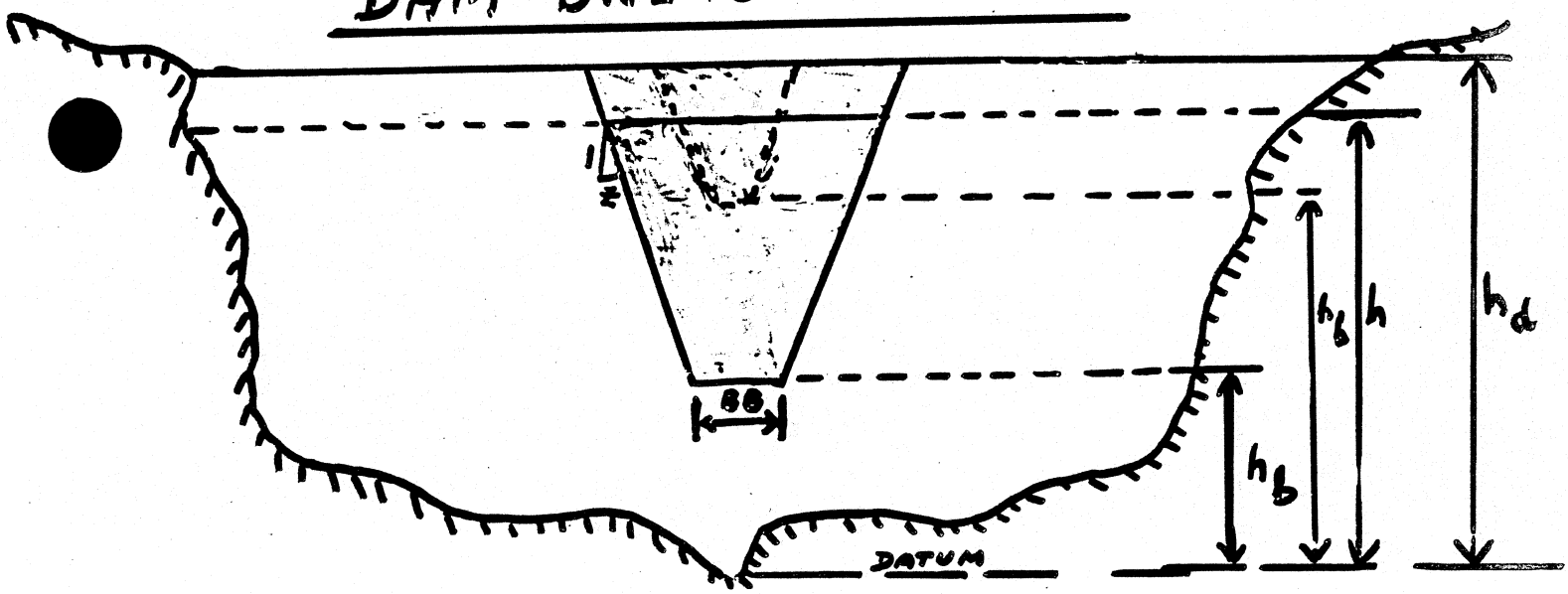

$$Q = Q_b + Q_s \quad \text{.....(38)}$$

Q_b → BREACH FLOW; Q_s → SPILLWAY + OTHER OUTFLOW

$$Q_b = K_s C_v \left[3.1\ BB\ \frac{t_b}{T} (h-h_b)^{1.5} + 2.45\ z (h-h_b)^{2.5} \right] \quad \text{.....(26)}$$

K_s: SUBMERGENCE CORRECTION FACTOR; C_v: velocity approach correction; T: time of failure

$$Q_s = K_{ss}\, C_s (h-h_s)^{1.5} + C_g (h-h_g)^{0.5} + C_d (h-h_d)^{1.5} + Q_t \quad \text{.....(27)}$$

SPILLWAY FLOW — GATE FLOW — CREST FLOW — TURBINE FLOW

WHERE:

$$\begin{cases} K_s = 1.0 \quad \text{.....} \quad r \le 0.67 \\ K_s = 1.0 - 27.8 (r - 0.67)^3 \quad \text{.....} \quad r > 0.67 \\ r = \dfrac{h - h_t}{h - h_b} \end{cases}$$

$$\begin{cases} K_{ss} = 1.0 \quad \text{.....} \quad rs \le 0.67 \\ K_{ss} = 1.0 - 27.8 (rs - 0.67)^3 \quad \text{.....} \quad rs > 0.67 \\ rs = \dfrac{h - h_t}{h - h_s} \end{cases}$$

$$C_v = 1.0 + .023 \frac{V^2}{h - h_b} \quad \text{.....(28)}$$

OUTFLOW HYDROGRAPH

I). RESERVOIR (LEVEL POOL) ROUTING

$$I - Q = \frac{\Delta S}{\Delta t} \quad \text{----------} (29)$$

$$\Delta S = \left(\frac{A_s + A_s'}{2}\right)(h - h')$$

$$(A_s + A_s')\frac{(h - h')}{\Delta t} + Q + Q' - I - I' = 0 \quad \text{----------} (30)$$

A_s = SURFACE AREA

A_s' = SURFACE AREA AT $t - \Delta t$

h = WATER SURFACE ELEVATION

h' = WATER SURFACE ELEVATION AT $t - \Delta t$

Δt = TIME STEP

Q = TOTAL INSTANTANEOUS OUTFLOW

Q' = OUTFLOW AT $t - \Delta t$

I = INFLOW

I' = INFLOW AT $t - \Delta t$

II). DYNAMIC WAVE ROUTING

DOWNSTREAM BOUNDARY —— $Q = Q_b + Q_s$ ----- (38)

$$A_s(h) + A_s' \frac{h-h'}{\Delta t} + Q(h) + Q' - I - I' = 0 \qquad (1)$$

where: $Q(h) = c_1 (h-h_b)^{3/2} + c_2 (h-h_b)^{5/2} + c_3 (h-h_s)^{3/2} + c_4 (h-h_g)^{1/2} + c_5 (h-h_d)^{3/2} + Q_T$

Solve Eq (1) by Newton-Raphson Iteration for h

Then use h to compute $Q(h)$

Then advance to next time and repeat

FLOOD ROUTING

Saint-Venant Eq.s of Unsteady Flow :

NEGATIVE FLOWS CAN OCCUR WHEN THE INFLOW HYDROGRAPH IS LARGE ENOUGH THAT IT WILL PROPAGATE UPSTREAM AT THE CONFLUENCE OF TWO STREAMS.

Conservation of mass :

$$\frac{\partial Q}{\partial x} + \frac{\partial (A + A_o)}{\partial t} - q = 0$$

Conservation of momentum :

other lateral inflow effects

$$\frac{\partial Q}{\partial t} + \frac{\partial Q^2/A}{\partial x} + gA\left(\frac{\partial h}{\partial x} + S_f + S_e\right) - L = 0$$

$$S_f = \frac{n^2 Q|Q|}{2.2 A^2 R^{4/3}}$$

$$R = A/B$$

$$S_e = \frac{K}{2g}\frac{\partial (Q/A)^2}{\partial x}$$

$$L = qV_x$$

Q = flow, cfs
A = cross-sect Area, ft^2
B = top width, ft
x = distance along river, ft
t = time, sec
q = lateral inflow (+) or outflow (-)
h = water surface elev., ft
g = 32.2 ft/sec^2

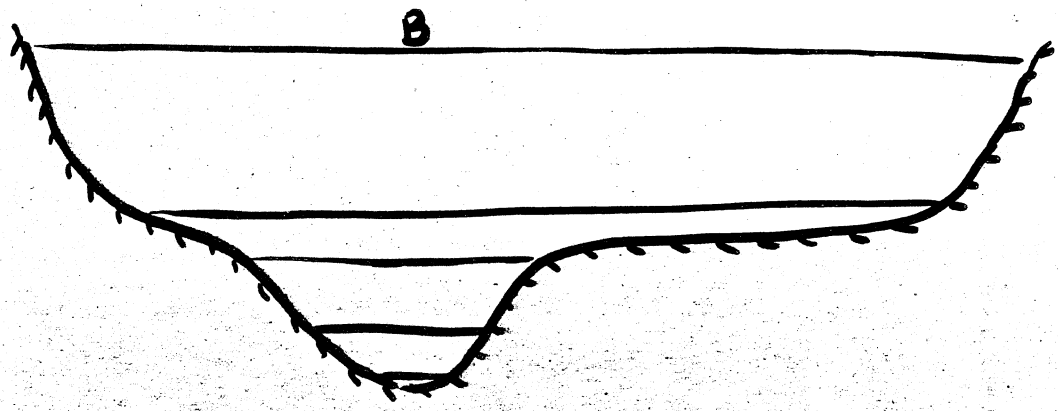

$$\frac{\partial Q}{\partial t} + \frac{\partial (Q^2/A)}{\partial x} + gA\left(\frac{\partial h}{\partial x} + S_f\right) = 0$$

$$\frac{\partial Q}{\partial t} + \frac{\partial (Q^2/A)}{\partial x} + gA\left(\frac{\partial y}{\partial x} - S_0 + S_f\right) = 0$$

friction gravity pressure inertia

$$S_f = S_0 - \frac{\partial y}{\partial x} - \frac{1}{gA}\left[\frac{\partial (Q^2/A)}{\partial x} + \frac{\partial Q}{\partial t}\right]$$

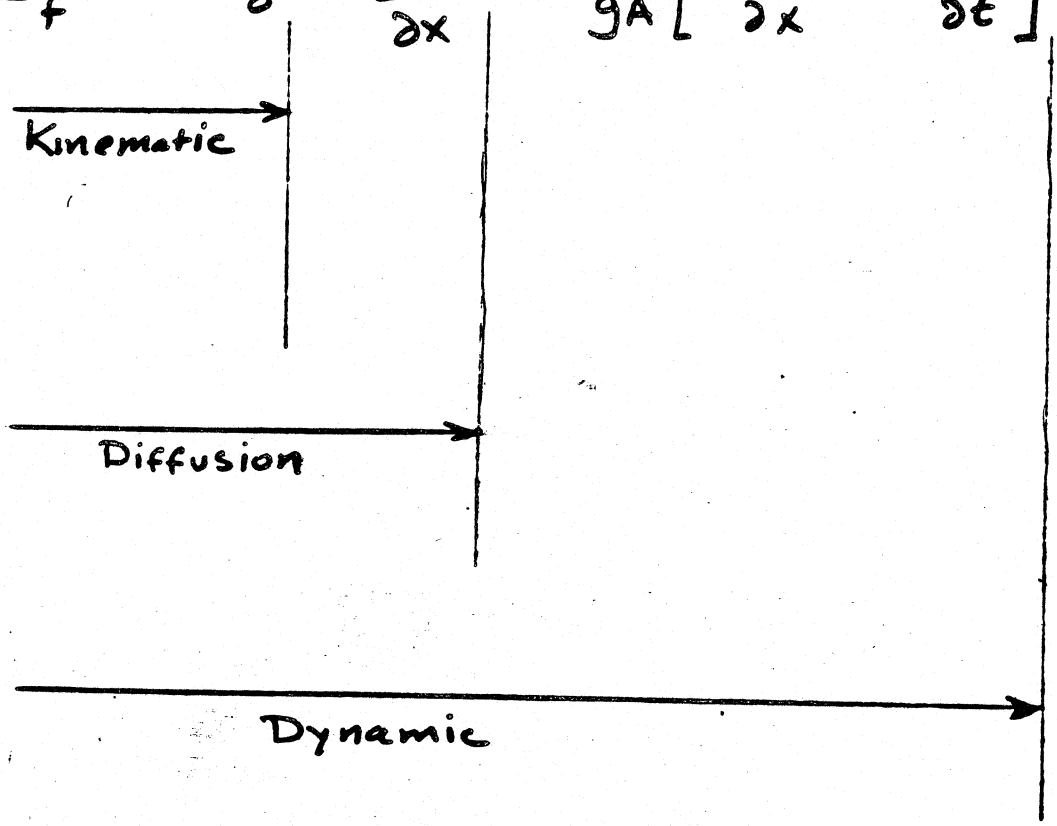

2. Routing Model Selection

Kinematic:

$$\frac{T_p S_o^{1.6}}{\phi n^{1.2} q_p^{0.2}} > \frac{0.2}{E}$$

Diffusion:

$$\frac{T_p S_o^{0.7} n^{0.6}}{\phi' q_p^{0.4}} > \frac{0.003}{E}$$

$$q_p = a\left(\frac{\theta_p}{\kappa a}\right)^{\frac{5}{3m+5}} \qquad a = \frac{1.49 S_o^{1/2}}{n(m+1)^{5/3}}$$

$$\phi = \frac{(m+1)^2}{3m+5}$$

$$\phi' = \frac{m+3}{3m+5}$$

* m = x-sect shape parameter

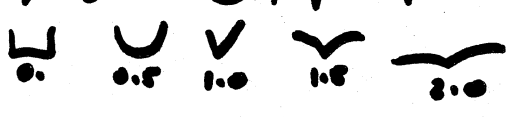

T_p = time of rise of hydrograph, hr

S_o = bottom slope ft/ft

n = Manning n

q_p = unit width peak discharge, $\frac{ft^3/sec}{ft}$

E = allowable routing error, percent

Weighted 4-Pt. Implicit Scheme

Time Derivative :

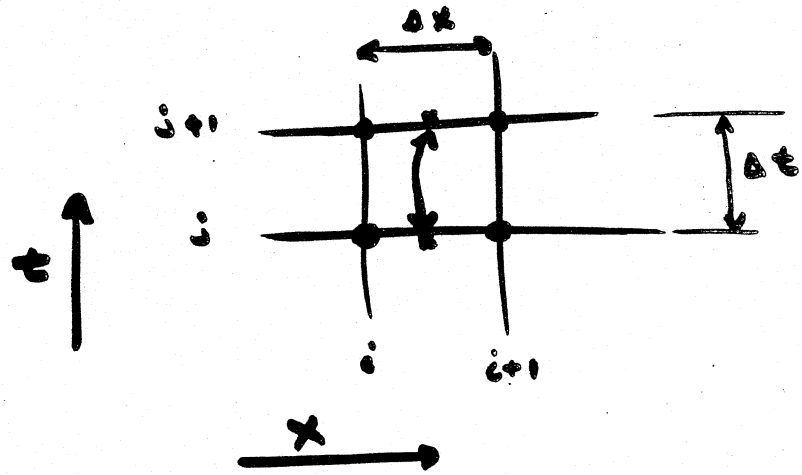

$$\frac{\partial Q}{\partial t} \simeq \frac{\dfrac{Q_i^{j+1} + Q_{i+1}^{j+1}}{2} - \dfrac{Q_i^{j} + Q_{i+1}^{j}}{2}}{\Delta t}$$

Spatial Derivative :

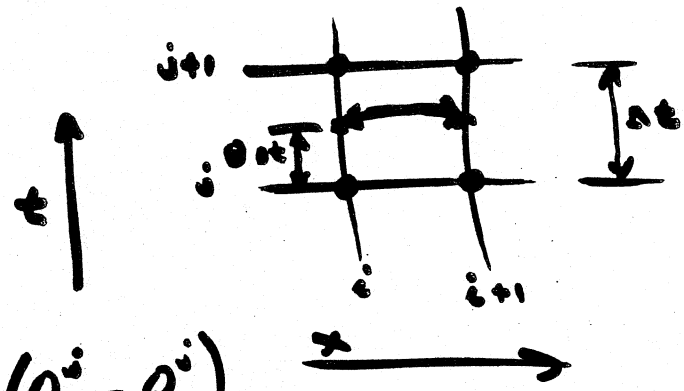

$$\frac{\partial Q}{\partial x} \simeq \theta\left(\frac{Q_{i+1}^{j+1} - Q_i^{j+1}}{\Delta x}\right) + (1-\theta)\left(\frac{Q_{i+1}^{j} - Q_i^{j}}{\Delta x}\right)$$

Other terms : $\quad q = \theta\, q_i^{j+1} + (1-\theta)\, q_i^{j}$

Unsteady Flow Difference Equations :

$$\theta\left(Q_{i+1}^{j+1} - Q_i^{j+1} - q_i^{j+1}\Delta x_i\right) + (1-\theta)\left(Q_{i+1}^{j} - Q_i^{j} - q_i^{j}\Delta x_i\right)$$

$$+ \frac{\Delta x_i}{2\,\Delta t_j}\left(A_i^{j+1} + A_{i+1}^{j+1} - A_i^{j} - A_{i+1}^{j}\right) = 0$$

$$\frac{\Delta x_i}{2\,\Delta t_j}\left(Q_i^{j+1} + Q_{i+1}^{j+1} - Q_i^{j} - Q_{i+1}^{j}\right) + \theta\Big[\left(Q^2/A\right)_{i+1}^{j+1} - \left(Q^2/A\right)_i^{j+1}$$

$$+ g\bar{A}_i^{j+1}\left(h_{i+1}^{j+1} - h_i^{j+1} + \bar{S}_{f_i}^{j+1}\Delta x_i\right)\Big] + \theta\Big[\left(Q^2/A\right)_{i+1}^{j} - \left(Q^2/A\right)_i^{j}$$

$$+ g\bar{A}_i^{j}\left(h_{i+1}^{j} - h_i^{j} + \bar{S}_{f_i}^{j}\Delta x_i\right)\Big] = 0$$

where:

$$\bar{A}_i = \frac{A_i + A_{i+1}}{2}$$

$$\bar{S}_{f_i} = \frac{n_i^2\,|\bar{Q}|\,\bar{Q}}{2.2\,\bar{A}^2\,\bar{R}^{4/3}}$$

$$\bar{Q}_i = \frac{Q_i + Q_{i+1}}{2}$$

$$\bar{R} = \frac{\bar{A}}{\bar{P}}$$

$$\bar{P} = \frac{P_i + P_{i+1}}{2}$$

Boundary Conditions

upstream: Flow $Q_1^{j+1} = Q(t)$

Water Elev. $h_1^{j+1} = h(t)$ (not in DAMBRK)

downstream: 1.) Flow $Q_N^{j+1} = Q'(t)$

2.) Water Elev $h_N^{j+1} = h'(t)$

3.) Critical Flow $Q_N^{j+1} = \sqrt{g}\left(\frac{A^{3/2}}{B^{1/2}}\right)_N^{j+1}$

4.) Rating Curve $Q_N^{j+1} = Q'$

$$Q' = Q_K + (Q_{K+1} - Q_K)\frac{(h_N^{j+1} - h_K)}{h_{K+1} - h_K}$$

5.) Synthetic Loop Rating $Q_N^{j+1} = \frac{1.49}{n}\left(AR^{2/3}\right)_N^{j+1} S^{1/2}$

$$S = \frac{h_{N-1}^j - h_N^j}{\Delta x_{N-1}}$$

5a.) trouble using this on very flat slopes

5b.) inverse slopes aren't accepted either as a boundary condition

LOCATION OF DOWNSTREAM BOUNDARY

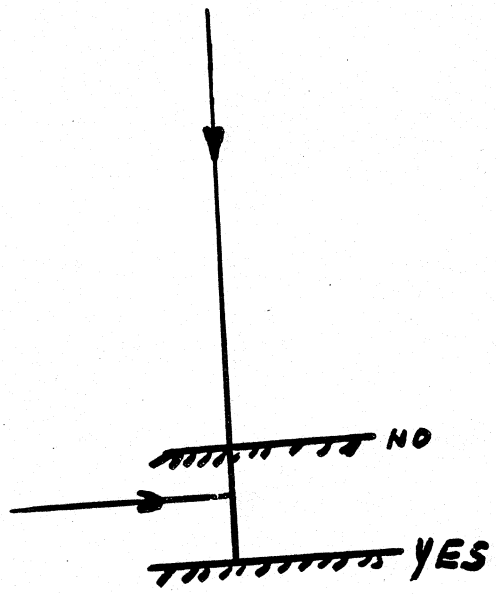

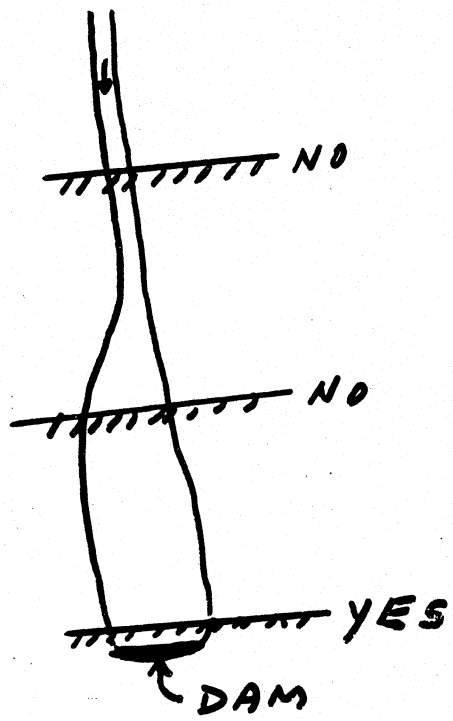

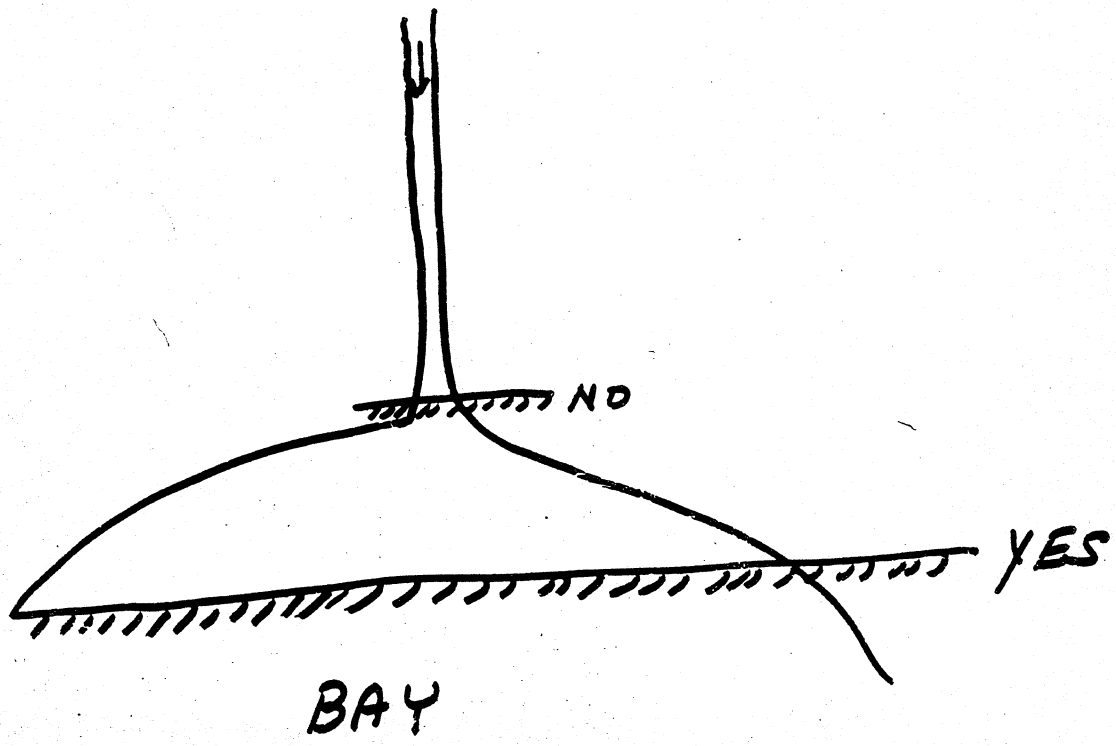

INITIAL CONDITIONS

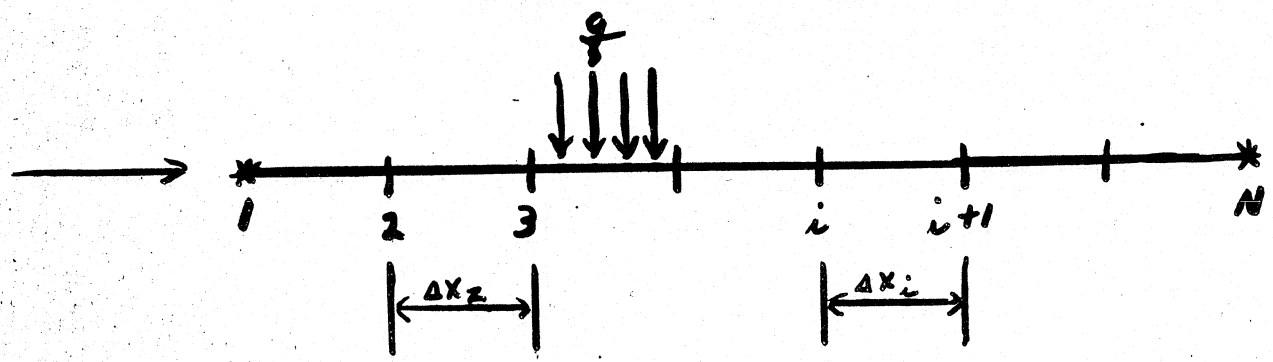

* GAGING STATION

STEADY FLOW CONDITION :

$$Q_{i+1} = Q_i + q_i \Delta X_i \qquad i = 1, 2, 3, \ldots\ldots N-1$$

GIVEN : h_N

$$\cancel{\frac{\partial Q}{\partial t}}^{\,0} + \frac{\partial Q^2/A}{\partial X} + gA\left(\frac{\partial h}{\partial X} + S_f\right) - \cancel{q V_X}^{\,0} = 0$$

$$\frac{(Q^2/A)_{i+1} - (Q^2/A)_i}{\Delta X_i} + g\left(\frac{A_i + A_{i+1}}{2}\right)\left[\frac{h_{i+1} - h_i}{\Delta X_i} + \frac{n^2 (Q_i + Q_{i+1})^2 (B_i + B_{i+1})^{4/3}}{2.2 (A_i + A_{i+1})^{10/3}}\right] = 0$$

SPECIFIED FLOW CONDITIONS :

GIVEN : Q_i $\qquad i = 1, 2, \ldots\ldots N$

GIVEN : h_K $\qquad$ WHERE K = LOCATION OF GAGING STATIONS

h_i $\qquad i \neq K$ DETERMINE h_i BY LINEAR INTERPOLATION BETWEEN h_K

7 GRIDS X 2 EQUATIONS = 14 EQUATIONS + 2 BOUNDARY = 16 EQS

(7+1) NODES X 2 $\frac{\text{UNKNOWN}}{\text{NODE}}$ = 16 UNKNOWNS ← DETERMINATE

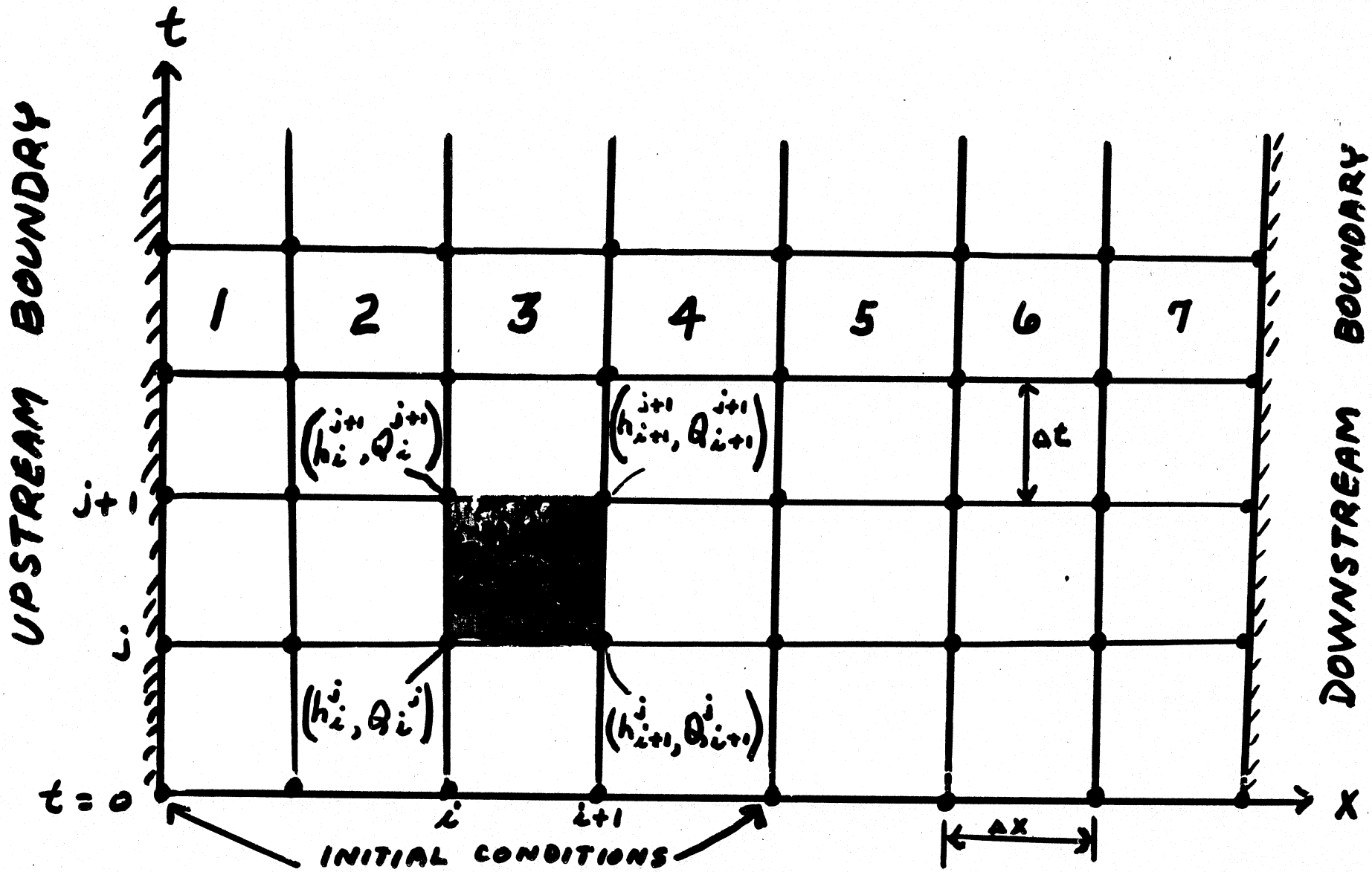

X–t SOLUTION DOMAIN

NEWTON RAPHSEN ITERATION FOR NONLINEAR EQUATIONS

$$f(x) = 0$$

$$x^{K+1} = x^{K} - \frac{f(x^K)}{f'(x^K)}$$

<u>OR</u>

$$f'(x^K)(x^{K+1} - x^K) = -f(x^K)$$

$$\frac{\partial C_1}{\partial h_1^{j+1}}\overbrace{\left(h_1^{j+1} - h_1^{j+1}\right)}^{\Delta h_1} + \frac{\partial C_1}{\partial Q_1^{j+1}}\overbrace{\left(Q_1^{j+1} - Q_1^{j+1}\right)}^{\Delta Q_1} + \frac{\partial C_1}{\partial h_2^{j+1}}\overbrace{\left(h_2^{j+1} - h_2^{j+1}\right)}^{\Delta h_2} + \frac{\partial C_1}{\partial Q_2^{j+1}}\overbrace{\left(Q_2^{j+1} - Q_2^{j+1}\right)}^{\Delta Q_2} = C_1\left(h_1^{j+1}, Q_1^{j+1}, h_2^{j+1}, Q_2^{j+1}\right)$$

$$\frac{\partial M_1}{\partial h_1^{j+1}}\left(h_1^{j+1} - h_1^{j+1}\right) + \frac{\partial M_1}{\partial Q_1^{j+1}}\left(Q_1^{j+1} - Q_1^{j+1}\right) + \frac{\partial M_1}{\partial h_2^{j+1}}\left(h_1^{j+1} - h_1^{j+1}\right) + \frac{\partial M_1}{\partial Q_2^{j+1}}\left(Q_1^{j+1} - Q_1^{j+1}\right) = M_1\left(h_1^{j+1}, Q_1^{j+1}, h_2^{j+1}, Q_2^{j+1}\right)$$

$$\frac{\partial C_2}{\partial h_2} \quad \text{———}$$

$$\frac{\partial M_2}{\partial h_2} \quad \text{———}$$

$$\frac{\partial B_d}{\partial h_3} \quad \text{———}$$

200 X-SECTION LIMIT

TO CHANGE THIS, CHANGE ARRAY STATEMENT FROM 200 TO WHATEVER

MATRIX FORM

DOUBLE OTHER ARRAY STATEMENTS

CHANGE ~~KMX~~ STATEMENT

$$[A]\,X = R$$

700 TIME STEPS CURRENT LIMIT. KTSP.

$[A]$ - $n \times n$ SQUARE MATRIX (BANDED)

X - COLUMN VECTOR

R - COLUMN VECTOR

CHANGE PLOT OF 6 HYDROGRAPHS LIMIT CAN ALSO BE MADE.

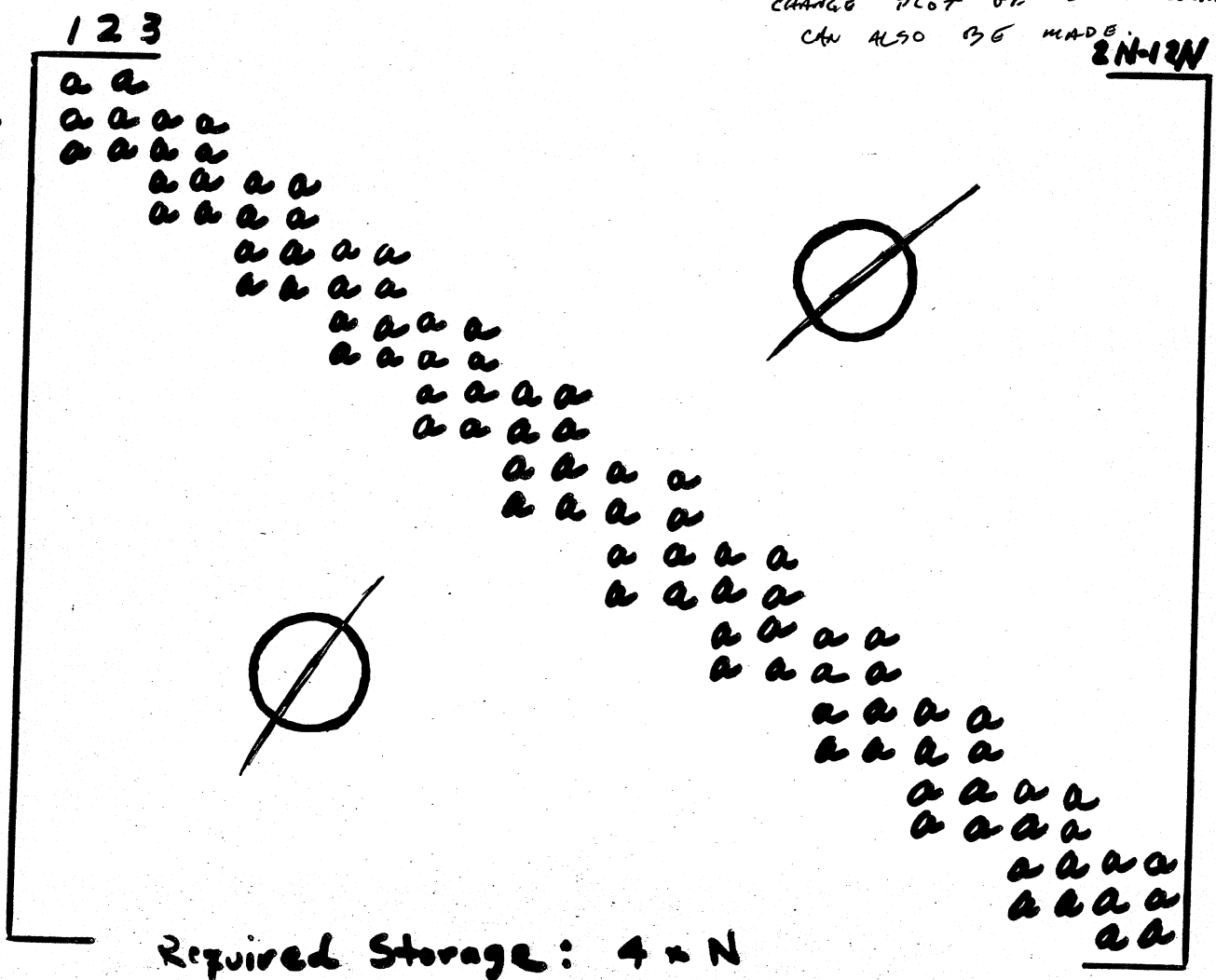

Required Storage: 4 × N

Required Computation: 38 N

(2) INTERNAL BOUNDARIES

- DAMS (SPILLWAY AND/OR BREACH FLOWS)
- BRIDGES - EMBANKMENTS
- CRITICAL FLOW (FALLS, SHORT STEEP RAPIDS)
- RATING CURVE

JUNCTIONS
Gates

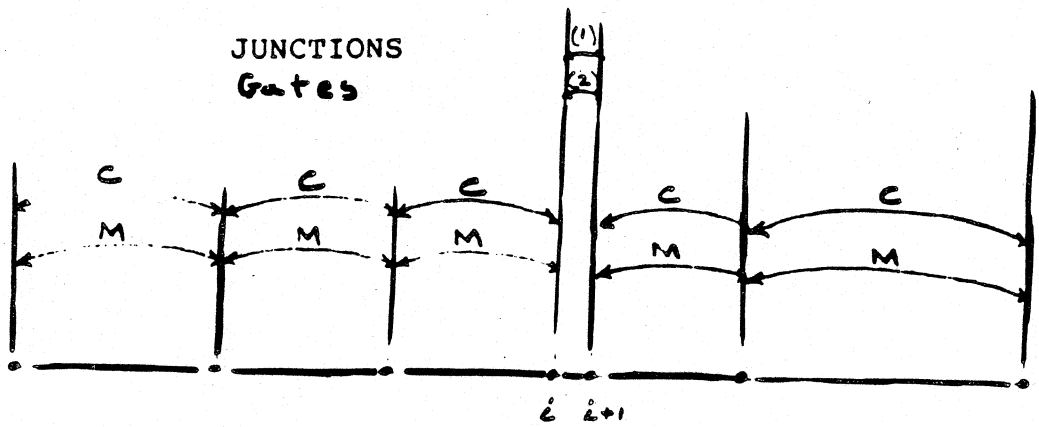

C ..... $\partial Q/\partial x + \partial A/\partial t - q = 0$

M ..... $\partial Q/\partial t + \partial(Q^2/A)/\partial x + gA\left(\frac{\partial h}{\partial x} + S_f\right) - qv_x = 0$

} ST. VENANT EQUATIONS

B ..... EXTERNAL BOUNDARY EQUATION

(1) .... $Q_i - Q_{i+1} = 0$

(2) ... $Q_i = f\left(h_i, h_{i+1} \ldots\ldots\ldots\right)$

} INTERNAL BOUNDARY EQUATIONS

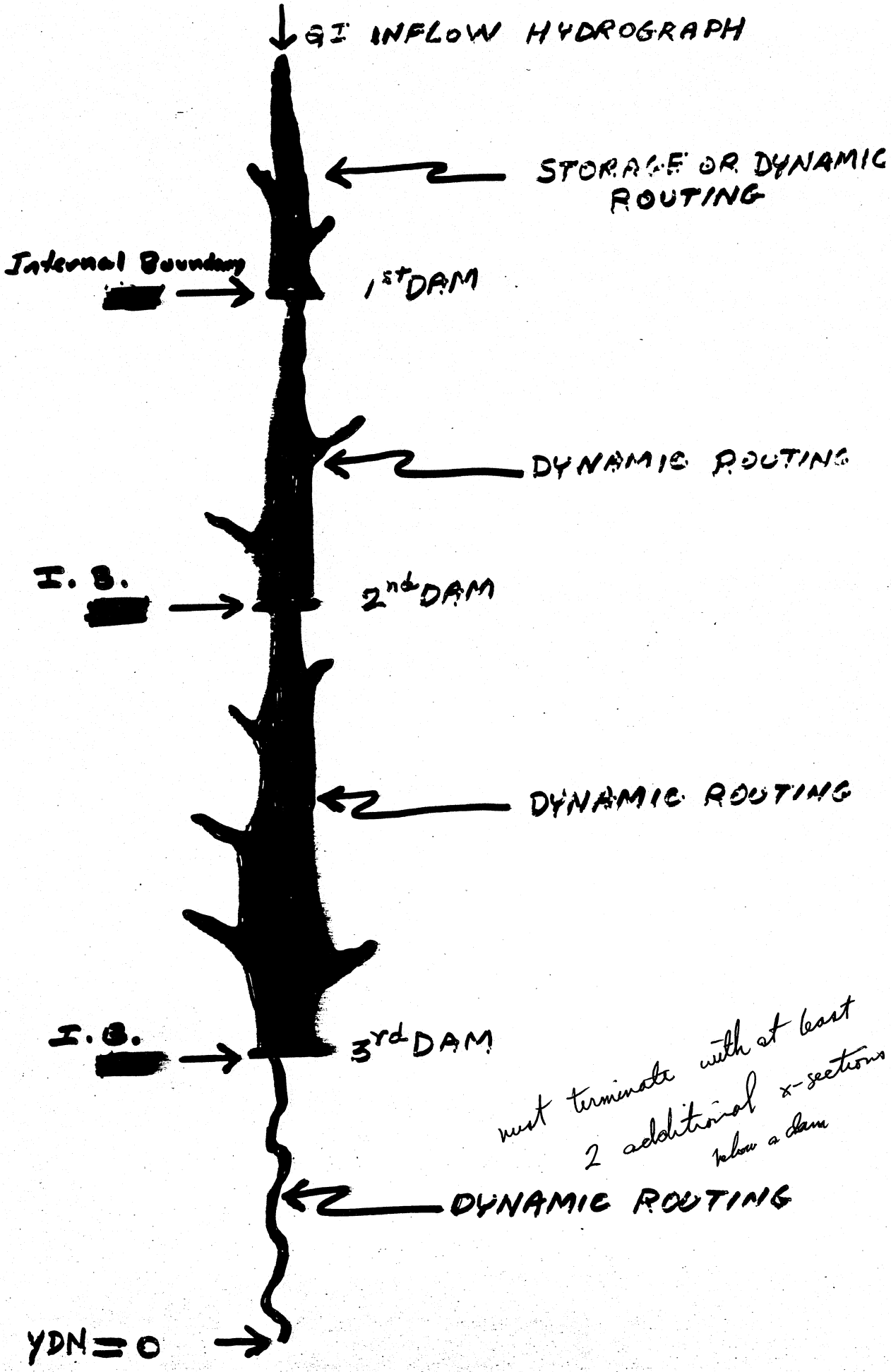

SCHEMATIC OF MULTIPLE DAM FAILURE OPTION

DAM (SPILLWAY and/or Breach Flow)

FRONT

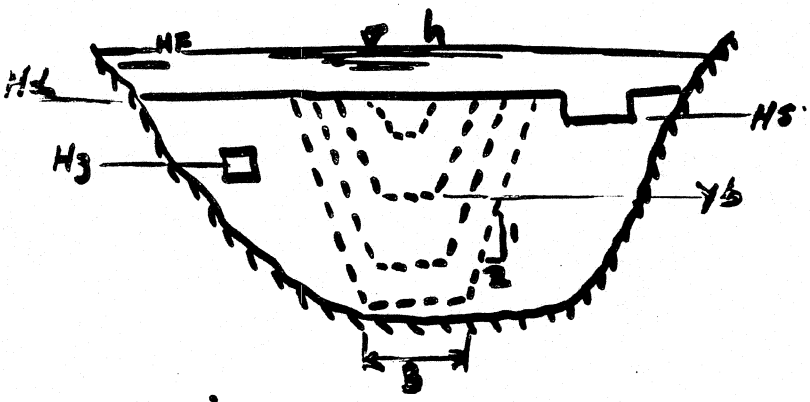

SIDE

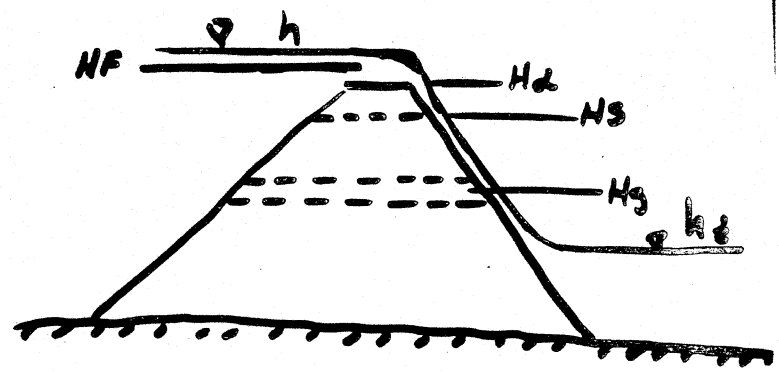

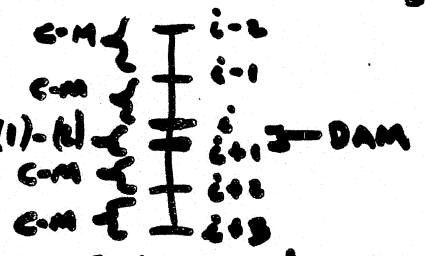

C = Continuity Eq.
M = Momentum Eq.

Schematic

(1) $Q_i = Q_{i+1}$

(2) $Q_i = Q_s + Q_b$ or $Q_s = f(h)$ .... rating curve

$$Q_s = Q_t + c_s k_{ss}(h-H_s)^{3/2} + c_g(h-H_g)^{1/2} + c_o k_{so}(h-H_d)^{3/2}$$

$$Q_b = k_{sd}\left[3.1\, B\, \frac{t_b}{T}(h-Y_b)^{3/2} + 2.48\, Z\,(h-Y_b)^{5/2}\right]$$

(B: rectangular; Z: V-TYPE)

$k_{ss} = 1. - 27.8(r_s - 0.67)^3 \qquad r_s > 0.67$

$r_s = (h_t - H_s)/(h - H_s)$

$k_{so} = 1. - 27.8(r_o - 0.67)^3 \qquad r_o > 0.67$

$r_o = (h_t - H_d)/(h - H_d)$

$k_{sd} = 1. - 27.8(r_d - 0.67)^3 \qquad r_d > 0.67$

$r_d = (h_t - Y_b)/(h - Y_b)$

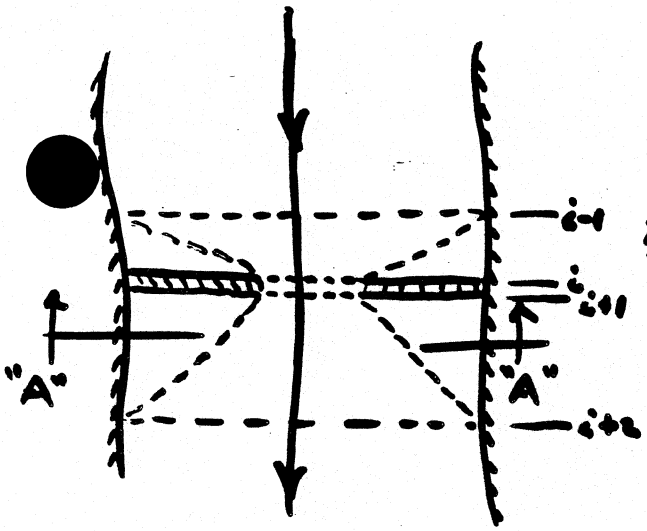

PLAN

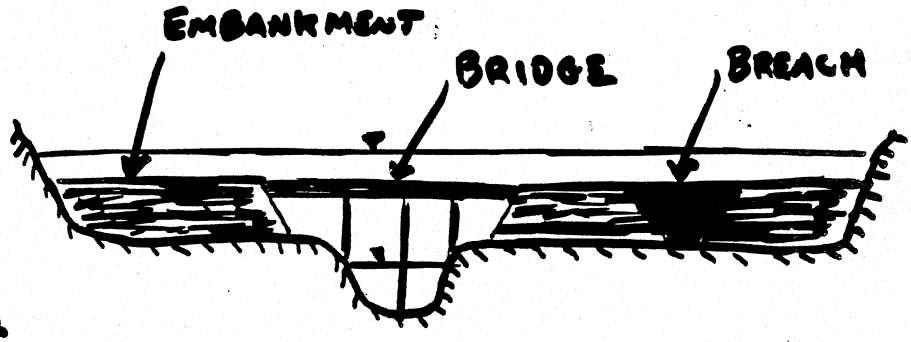

SEC "A"-"A"

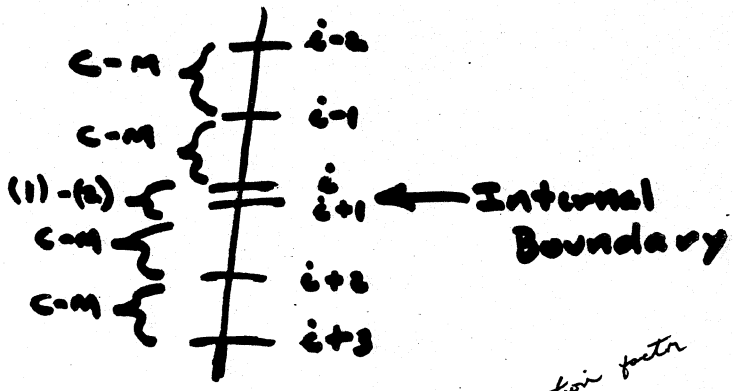

(1) $Q_i = Q_{i+1}$

(2) $Q_i = Q_s + Q_b$

$$Q_s = \underbrace{C_b \sqrt{2g}\, A_{i+1}\left(h_i - h_{i+1}\right)^{1/2}}_{\text{BRIDGE FLOW}} + \underbrace{C_d\, K_s \left(h - h_e\right)^{3/2}}_{\text{EMBANKMENT OVER FLOW}}$$

← .7 to .8 bridge factor from Chow

← submergence correction factor

$$Q_b = \underbrace{K_s\left[3.1\, \hat{B}\, \frac{t_b}{T}\left(h - h_b\right)^{3/2} + 2.45\, z\left(h - h_b\right)^{5/2}\right]}_{\text{BREACH FLOW}}$$

from D.O.T. tests

(6) LINEARLY INTERPOLATED CROSS SECTIONS

* NEEDS SAME NUMBER OF POINTS BETWEEN X-SECTIONS TO INTERPOLATE.

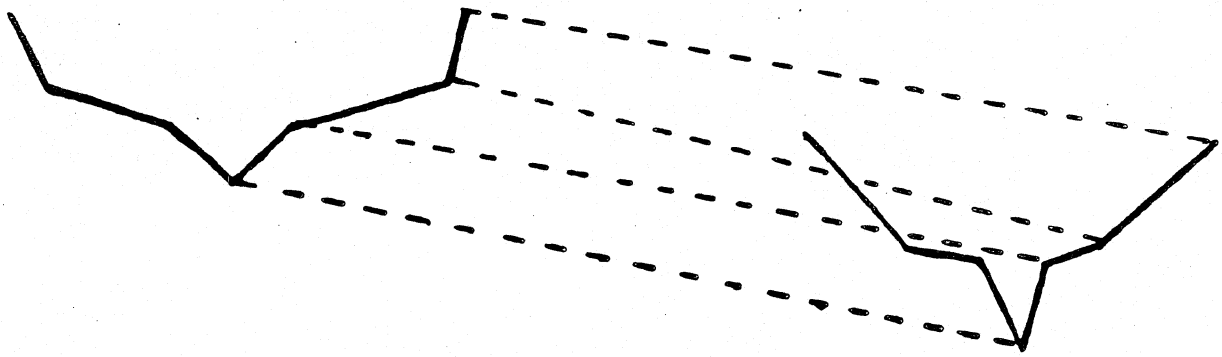

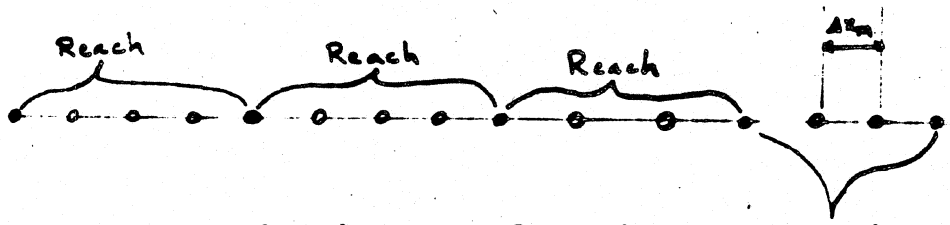

Δxm_i ..... $1 < i <$ No. of Reaches Reach

- Input Cross Section

○ Interpolated Cross Section

8 TOPWIDTHS LIMIT?

VERY RESTRICTIVE

[redacted]

[redacted]

DAMBRK Application

"Teton Flood"

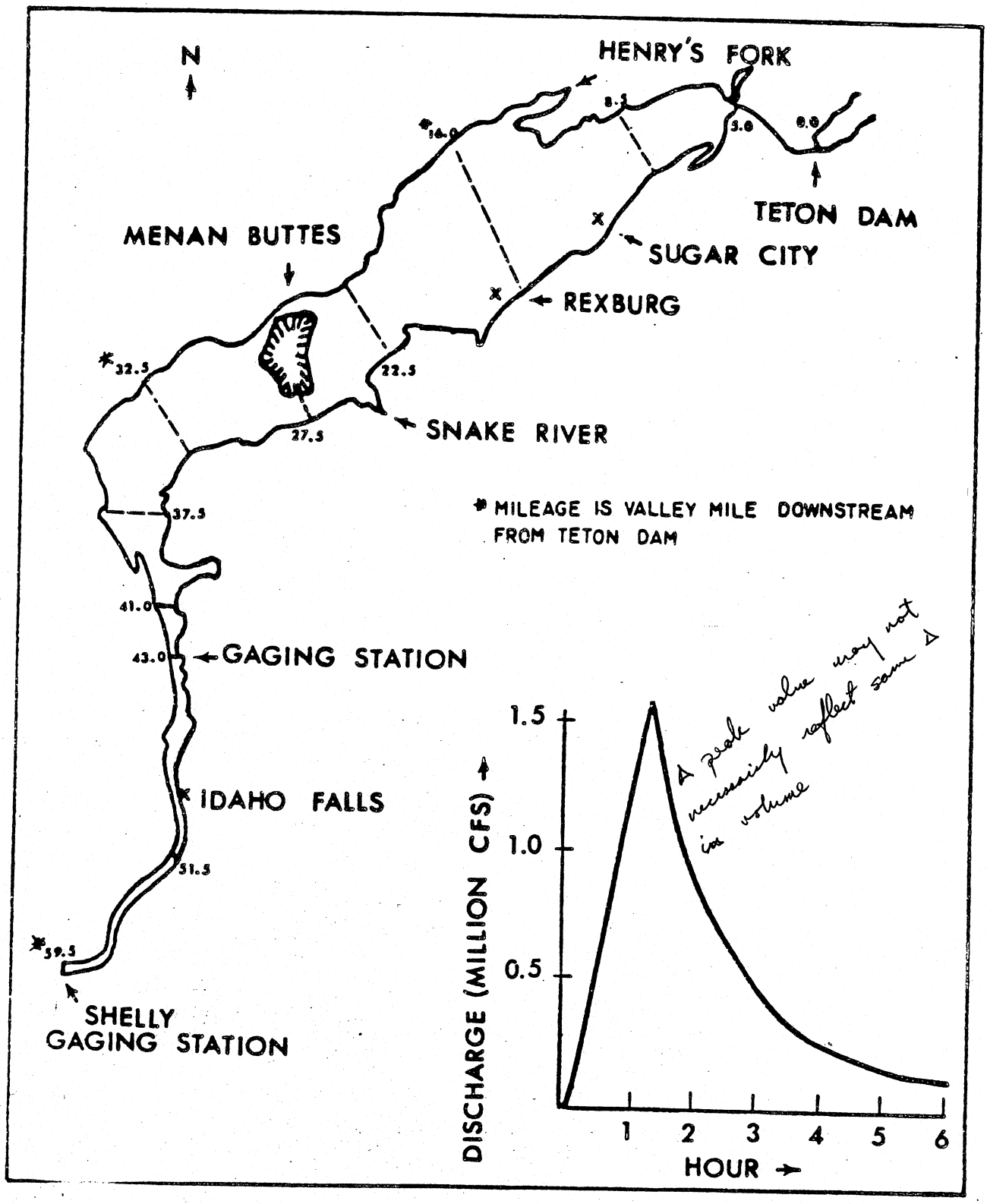

Fig. 2 — OUTFLOW HYDROGRAPH AND FLOODED AREA DOWNSTREAM OF TETON DAM

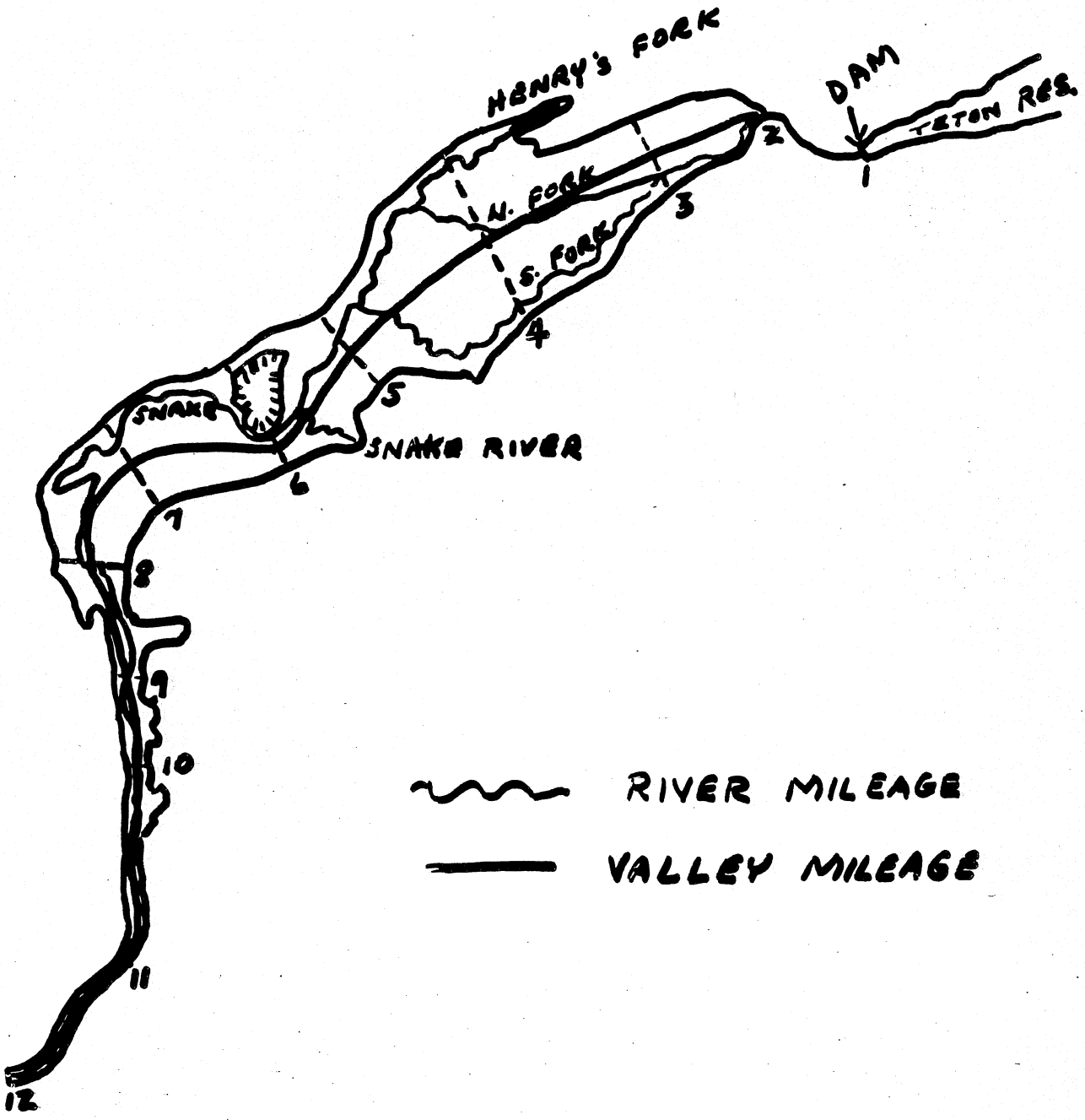

FLOODED AREA DOWNSTREAM OF TETON DAM

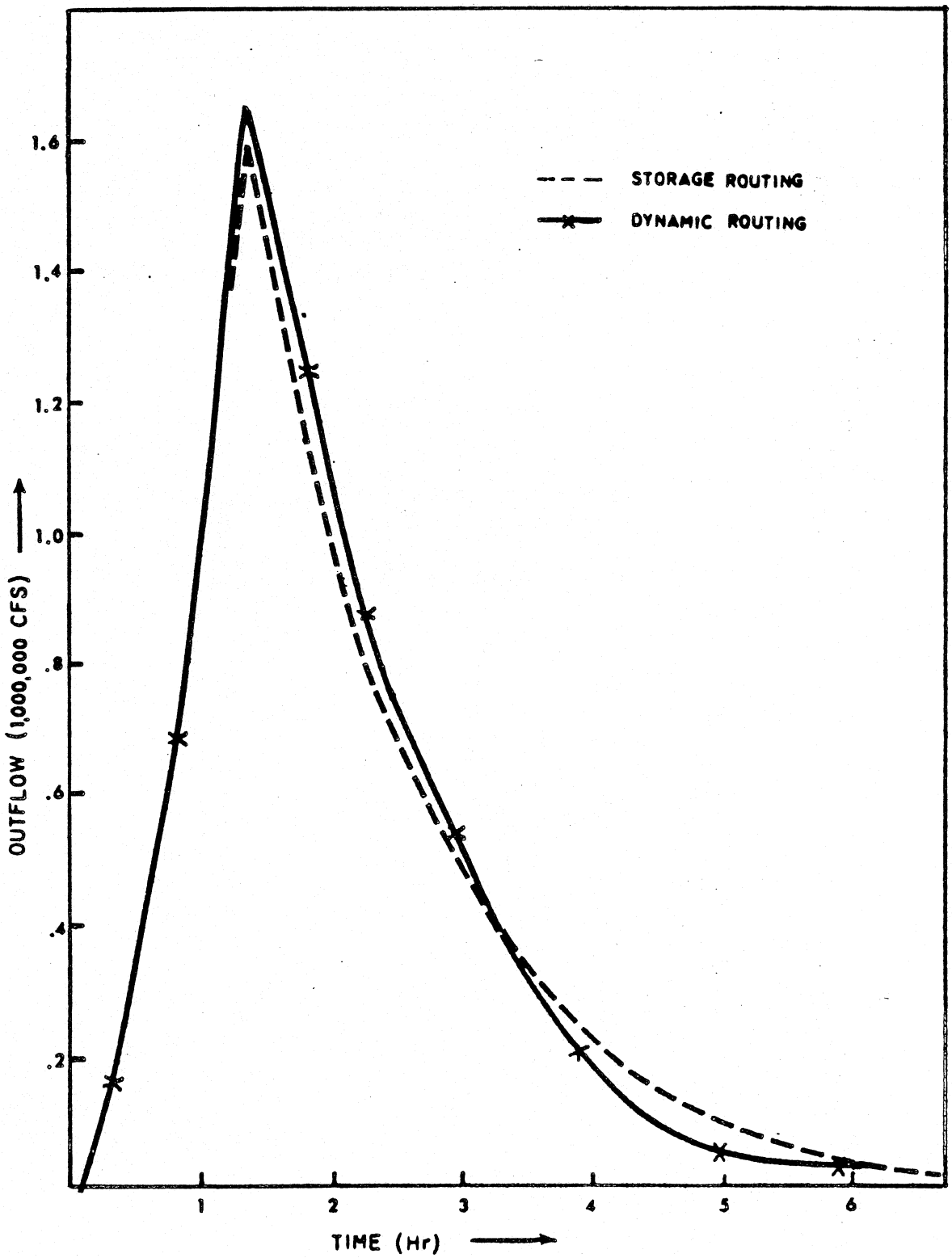

Fig. 4 — OUTFLOW HYDROGRAPH FROM TETON DAM FAILURE

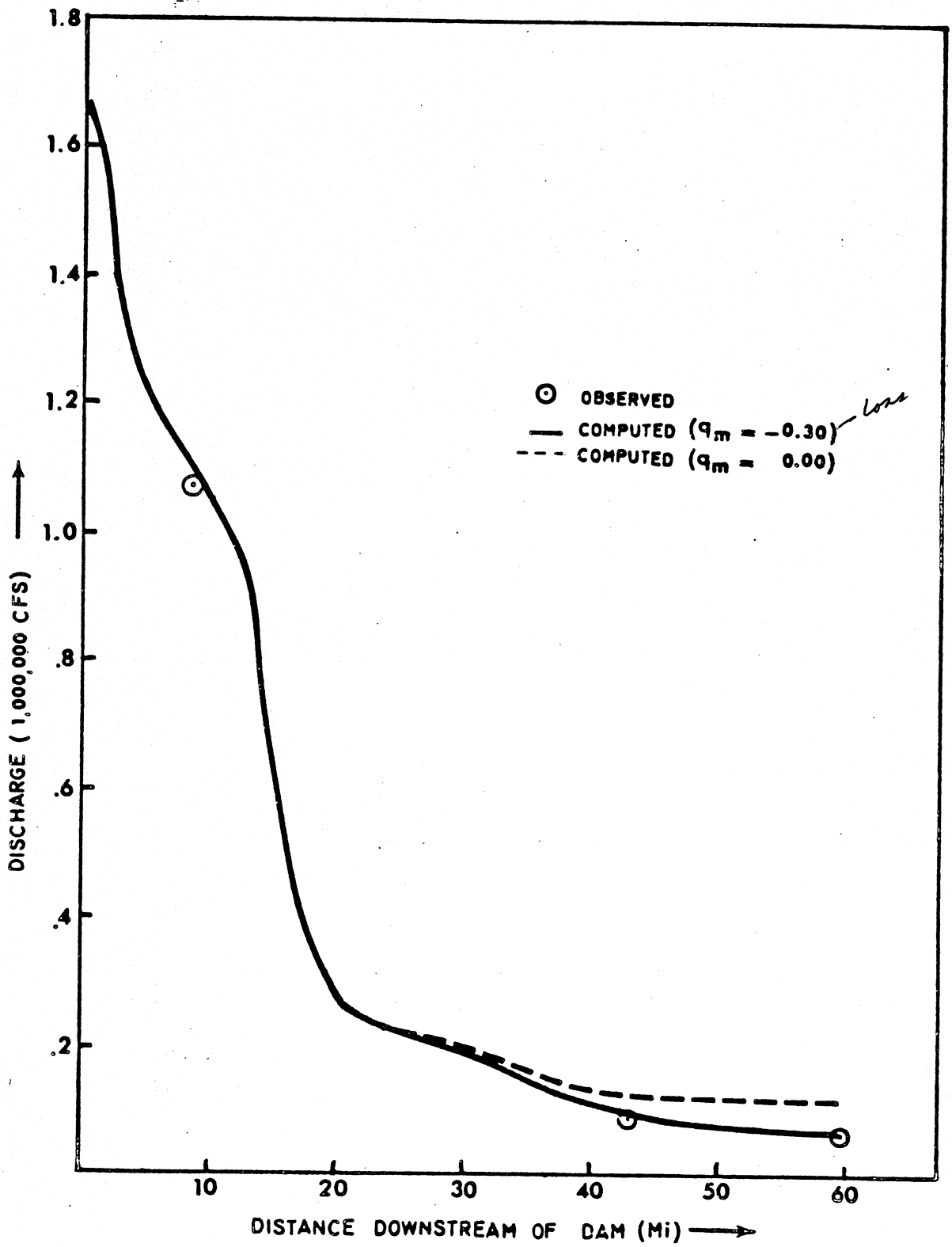

Fig. 5 – PROFILE OF PEAK DISCHARGE FROM TETON DAM FAILURE

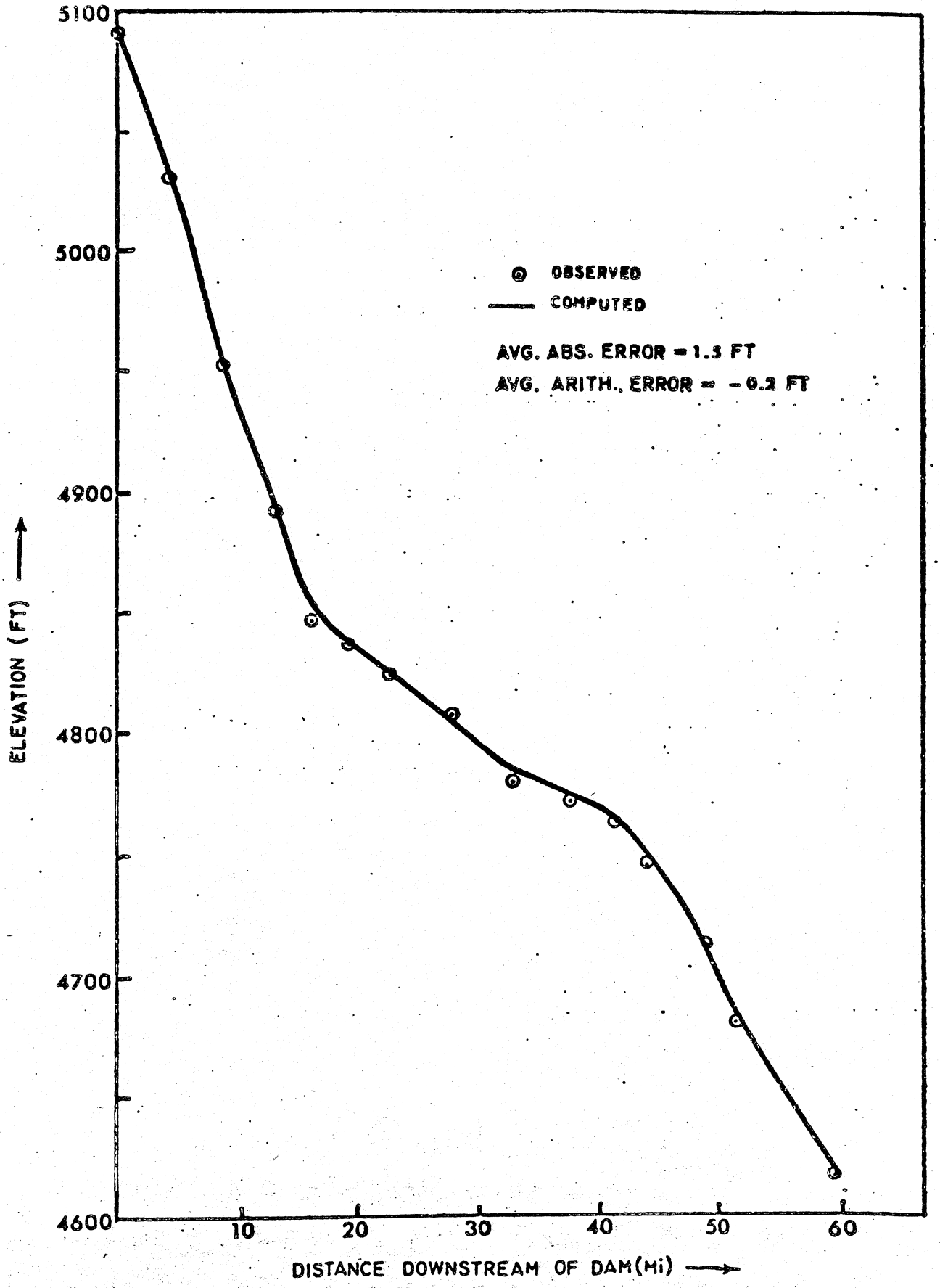
5100
5000
4900
4800
4700
4600
ELEVATION (FT)
10
20
30
40
50
60
DISTANCE DOWNSTREAM OF DAM(Mi)
OBSERVED
COMPUTED
AVG. ABS. ERROR = 1.5 FT
AVG. ARITH. ERROR = -0.2 FT

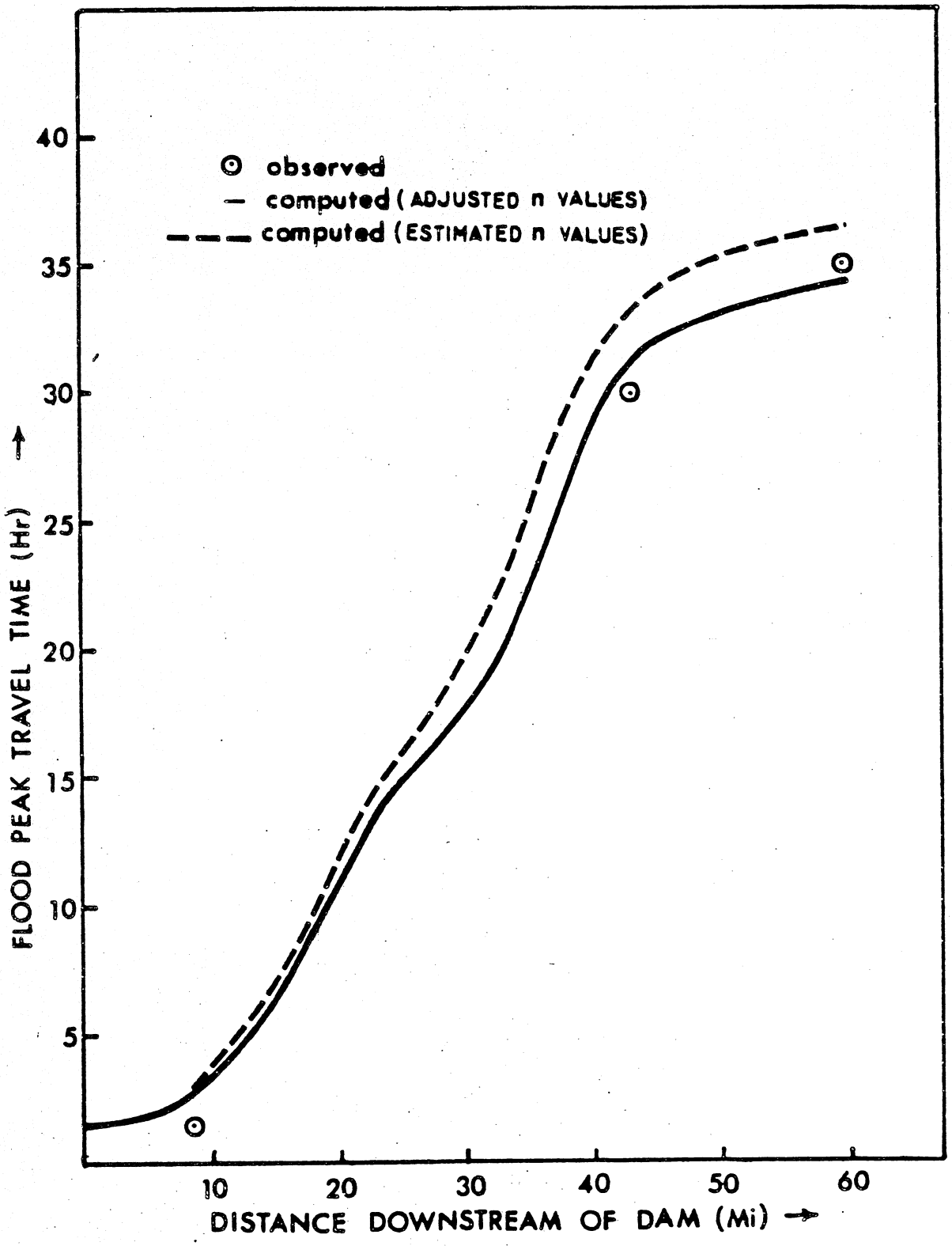

Fig. 8 — TRAVEL TIME OF FLOOD PEAK FROM TETON DAM FAILURE

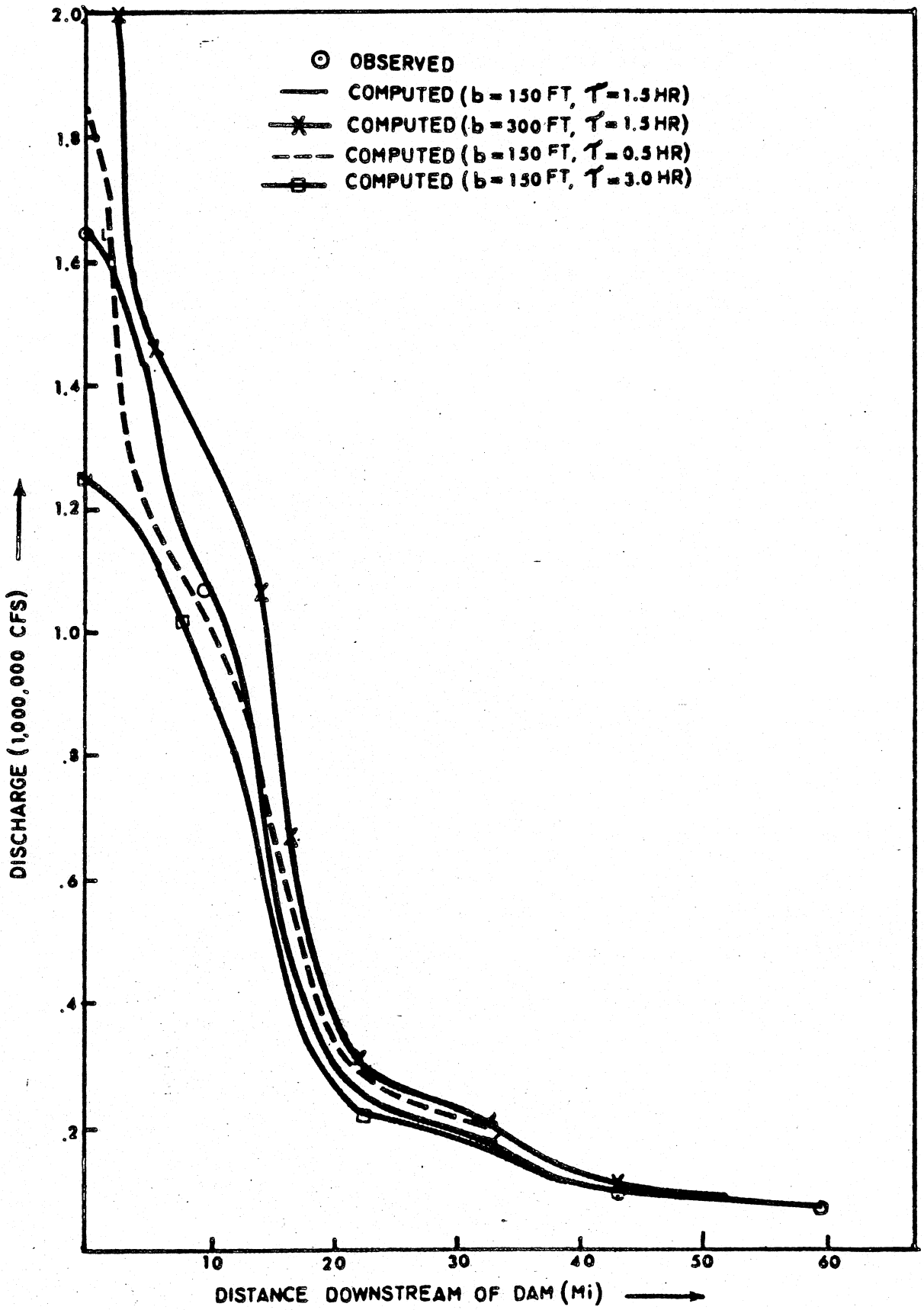

Fig. 6 — PROFILE OF PEAK DISCHARGE FROM TETON DAM FAILURE SHOWING SENSITIVITY OF VARIOUS INPUT PARAMETERS

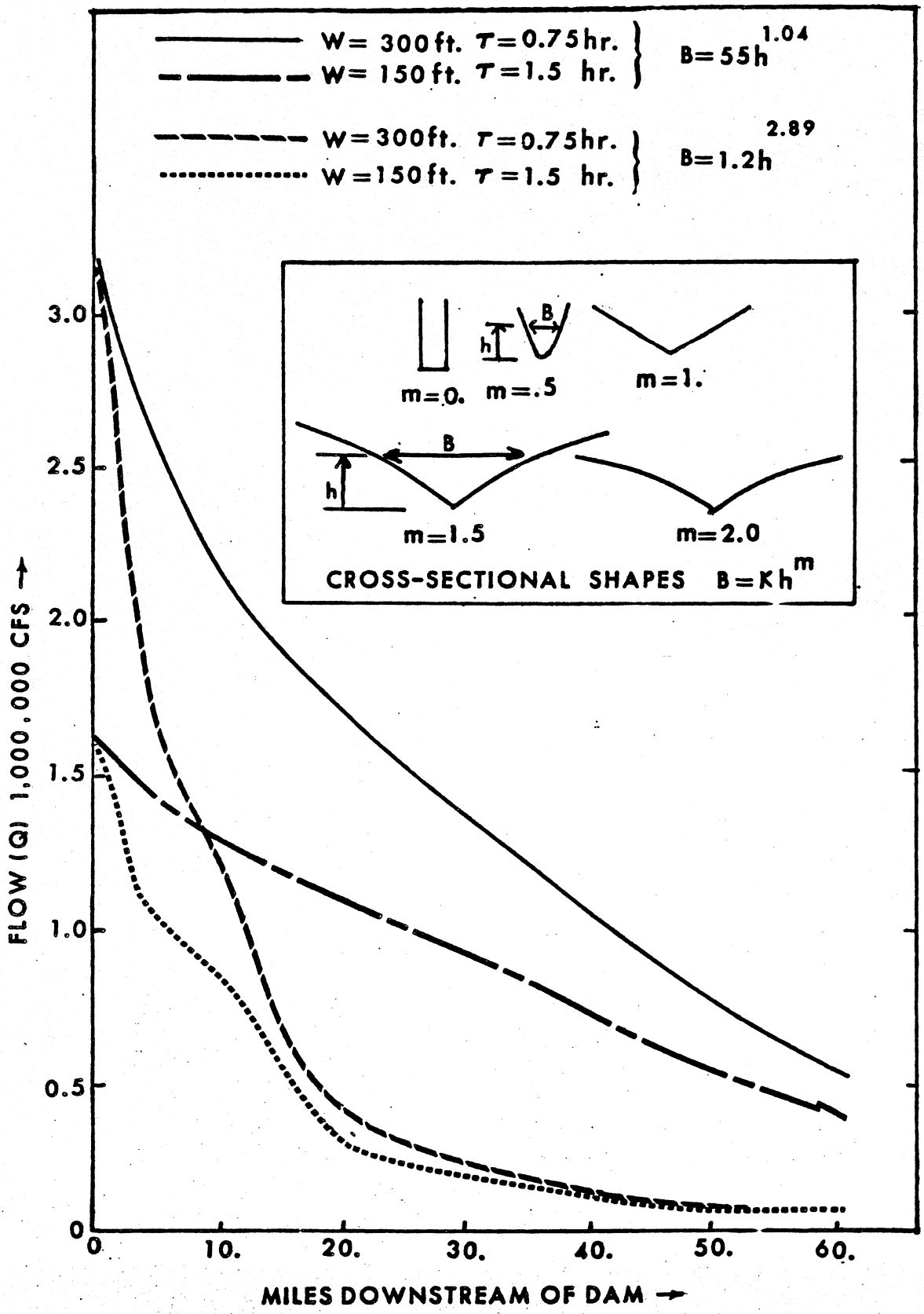

FIG. 1 - VARIATION OF PEAK FLOW DOWNSTREAM OF DAM

DATA INPUT

Description

OPTION 1

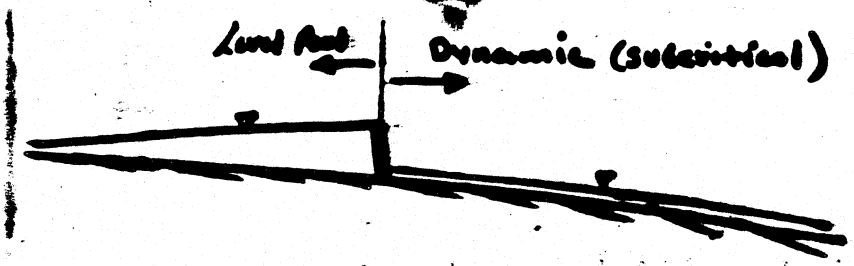

KUZ = 0

KKN = 1

MULDAM = 0

KSUPC = 0

Input data cards : 1-4 (1-4), 6-58 (6-58) ARE NECESSARY

OPTION 2

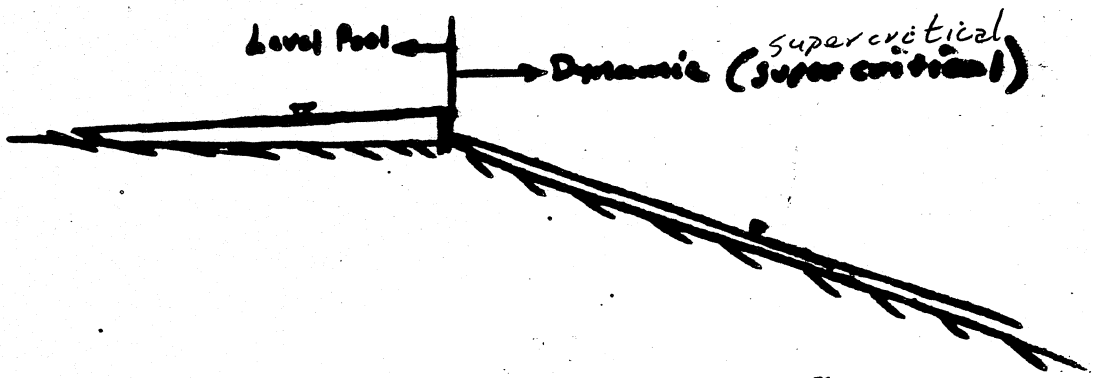

KUZ = 0

KKN = 1

MULDAM = 0

KSUPC = 1

Input data cards : 1-4, 6-58

OPTION 3

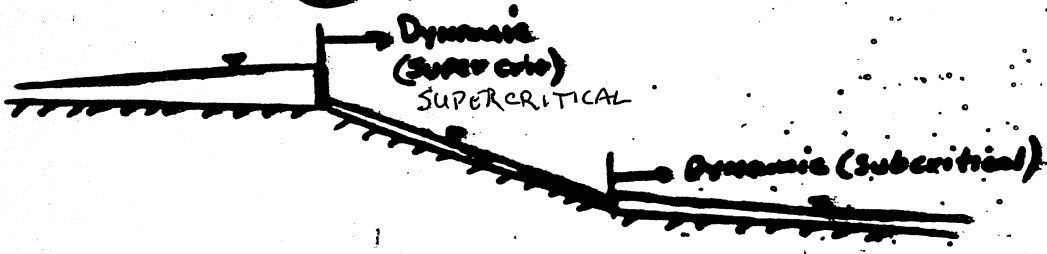

KUZ = 0

KKN = 2

0 = MULDAM

1 or 0 = KSUPC

Input data cards : 1-4, 6-39, 15-45, 15-45, ...

SEE CURRENT DOCUMENTATION

OPTION (7) SIMILAR TO HEC-2

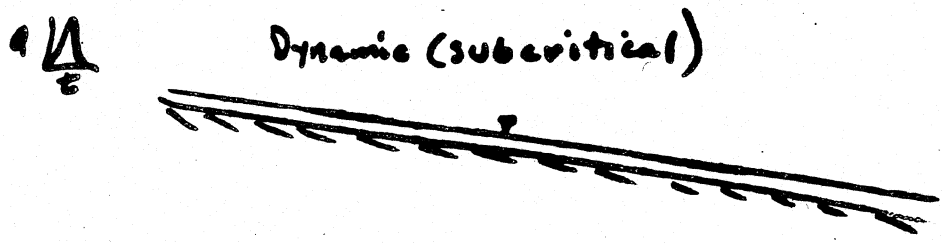

KUI = 0
KKN = 9
MULDAM = 0
KSUPC = 0

Input data Cards : 1-4, 12-39

OPTION (8)

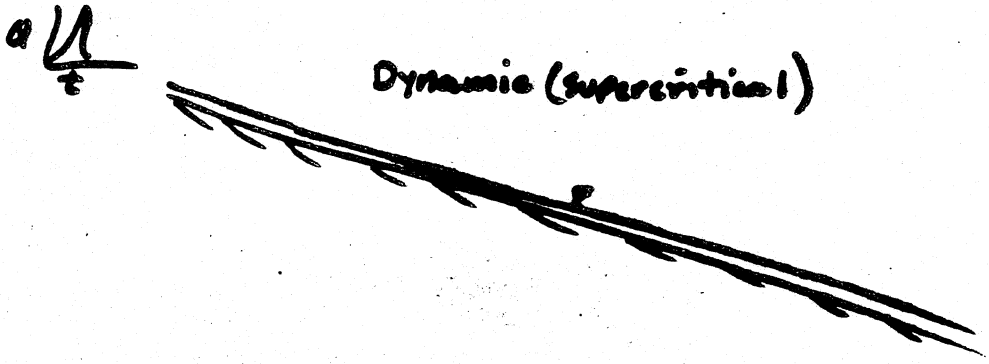

KUI = 0
KKN = 9
MULDAM = 0
KSUPC = 1

Input data cards: 1-4, 12-39

OPTION (11)

NO SUPERCRITICAL APPLICATIONS

Dynamic (sub)

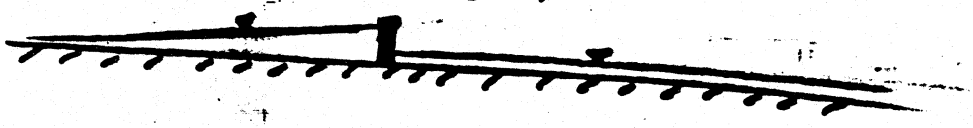

KUI = 1
KUZ = 1
KKN = 1
MULDAM = 1
MULGAM = 1
KSUPC = 0

Input data cards: 1-5, 8-11, 12-48

OPTION (12)

Dynamic (sub)

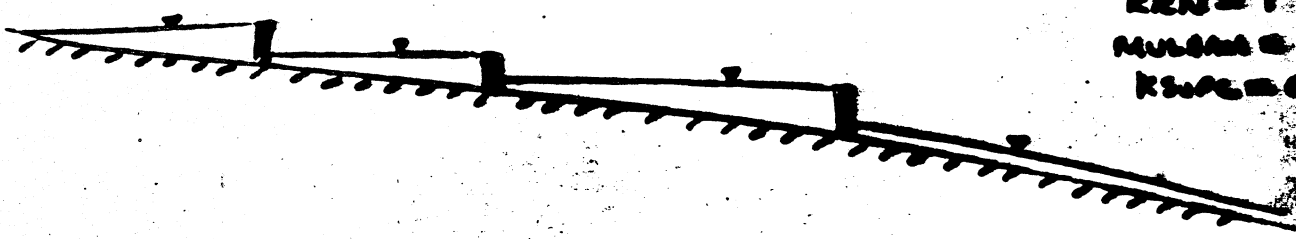

KUZ = 1
KKN = 1
MULGAM = 3
KSUPC = 0

Input data cards: 1-5, 8-11, 8-11, ... 8-11, 12-48

① TETON DAM TETON-SNAKE RIVER HYDRO LAB

GRAMAX RM 530E SILVER SPRING, MD. 20910

② 1 0 0 3 — OUTPUT CONTROL 2

⑥ 1936. 1157. 576. 217. 0. SURFACE AREA

⑦ 5288.5 5228.5 5098.5 5038.5 5027.0 ELEVATION OF RESERVIOR

⑧ 17. 5288.5 0. 5027. 150. 1.25 5027.

5288.5 5288.5 0. 0. 0. 0. 0. 13000. DAM SPILLWAY ? OTHER INFO.

0. 55. — TIME

13000. 13000. — FLOW

0. 55. TIMES

12 — x-sec. 5 Top width 6 hydrograph 4 0 0 0

1 2 3 7 10 12 — hydrograph plots at x-sec's.

0. 5047. —

5027. 5037. 5051. 5107. 5112.

0. 590. 820. 1130. 1200. TOP WIDTHS

0. DEAD STORAGE

NO BLANK LINES

TETON SIMULATION (CONT'D)

X-Section Data

5.0 4985.

4965.	4980.	5015.	5020.	5025.
0.	850.	1100.	1200.	1300.
0.	0.	3500.	4300.	5300.

8.5 4946.

4920.	4930.	4942.	4953.	4958.
0.	800.	4000.	11000.	15000.
0.	0.	0.	7000.	10000.

16.0 4830.

4817.	4827.	4845.	4847.	4852.
0.	884.	4000.	11000.	22000.
0.	0.	30000.	27000.	25000.

22.5 4820.

4805.	4812.	4814.	4825.	4830.
0.	1000.	1200.	11000.	16000.
0.	0.	0.	6000.	8000.

27.5 4800.

4788.	4792.	4802.	4808.	4810.
0.	286.	7000.	10000.	11000.
0.	0.	0.	3500.	5000.

32.5 4777.

4762.	4774.	4777.	4780.	4785.
0.	352.	5000.	10000.	18000.
0.	0.	9000.	16000.	24000.

TETON SIMULATION (CONT'D)

37.5 4767.

4752.	4763.	4768.	4773.	4778.
0.	450.	3500.	6000.	9000.
0.	0.	4000.	8500.	12000.

41.0 4756.

4736.	4756.	4761.	4763.	4768.
0.	540.	2000.	4000.	6000.
0.	0.	3700.	3700.	5500.

43.0 4749.

4729.	4737.	4749.	4757.	4759.
0.	250.	587.	1750.	2000.
0.	0.	0.	1500.	2000.

51.5 4674.

4654.	4659.	4668.	4678.	4683.
0.	70.	352.	400.	420.
0.				

59.5 4612.

4601.	4604.	4606.	4615.	4620.
0.	245.	450.	500.	520.
0.				

TETON SIMULATION (CONT'D)

Mannings "n"

.08	.08	.08	.08	.08
.05	.05	.05	.05	.05
.031	.031	.031	.031	.031
.034	.034	.034	.034	.034
.038	.038	.038	.038	.038
.037	.037	.037	.037	.037
.034	.034	.034	.034	.034
.034	.034	.034	.034	.034
.034	.034	.034	.034	.034
.036	.036	.036	.036	.036
.036	.036	.036	.036	.036

.5 .5 .5 .75 1.0 1.0 1.0 1.0 — LINEAR INTERPRETATIONS

1.0 1.1 1.4

CONTRACTION EXPANSION

0. -.90 0. 0. 0.1 -.50 0. 0.

0. 0. 0.

65000. -.30 0. 0. 0. 0.

DOWNSTREAM BOUNDARY CONDITION

sudden increases in mannings "n" can cause problems

APPENDIX A

INPUT DATA STRUCTURE FOR DAM-BREAK (DAMBRK): 07/18/84

Input card group no.

(1) MDAM, MRVR, MNAME - 20 A 4 Format

MDAM	Name of dam (col. 1-20).
MRVR	Name of reservoir (col. 21-40).
MNAME	Agency name (col. 41-60).

MESAGE - 20 A 4 Format

MESAGE	Agency address--street, room (col. 1-40). Agency Address--city, state, zip code (col. 41-72).

(2) KKN, KUI, MULDAM, KDMP, ITEH, NPRT, KFLP, KSL - 8 I 10 Format

KKN	Parameter which is associated with KSUPC on card (16). If KSUPC=0, KKN=1; if KSUPC=1, KKN should be given a value of 1 if the downstream channel valley below the dam is entirely supercritical flow or KKN should be given a value of 2 if the downstream reach is divided into two reaches (an upstream reach having supercritical flow and a downstream reach having subcritical flow). If KKN=9, a hydrograph is read in and then routed through the downstream valley.
KUI	Parameter used to select type of reservoir routing for determining outflow hydrograph; if KUI=0, storage routing is used; if KUI=1, dynamic routing is used.
MULDAM	Parameter used to select option for routing through multiple reservoirs sequentially located downstream of first dam. If one or more dams are located downstream of first dam, MULDAM=1, if no dams are downstream of first dam, then MULDAM=0. Any number of downstream sequentially located dams may be simulated by letting KKN=1 + no. of downstream dams.
KDMP	Parameter for printing; users outside of the National Weather Service set KDMP=3. KDMP=0, print only title page; KDMP=1, title page, abstract, variable descriptions; KDMP=2, same as KDMP=1 plus input data; KDMP=3, title page plus input data; KDMP=4, same as KDMP=2, then stop; if KDMP=5, IOPUT on card (4) allowing selective printout of computations is read-in and KDMP is reset to 3.

ITEH	Parameter denoting number of hydrograph ordinates of inflow hydrograph to reservoir; maximum value of 50 is allowed; if ITEH=0, the inflow hydrograph is generated via a mathematical function.
NPRT	Parameter to control print output for JNK=9, NPRT is the total number of cross-sections at which hydraulic information is printed-out during dynamic routing; if NPRT=0, the program uses a variable NPRT computed by the program and prints-out hydraulic information at NPRT intervals of cross-sections along the routing reach.
KFLP	Parameter denoting the use of the special flood-plain routing feature; if KFLP=0, the special flood-plain feature is <u>not</u> used; if KFLP=1, the special flood-plain routing is used.
KSL	Parameter denoting simulation of landslide; if KSL=0, <u>no</u> landslide; if KSL=1, a landslide occurring along one bank of the reservoir is simulated; if KSL=2, the landslide occurs along both banks of reservoir.

(3) NPT(K) - 8 I 10 Format

NPT(K)	Sequential number of cross-section at which hydraulic information is printed-out; this card is omitted if NPRT=0; K index goes from 1 to NPRT where NPRT $\leq$ 30.

(4) IOPUT(K) - 10 I 1, 2 I 2 Format

IOPUT(K) Optional print parameter that may override the JNK parameter, (card 16). K index goes from 1 to 12. If IOPUT(K)=0, allow the output to be printed; if IOPUT(K)=1, suppress the output. The following output can be controlled:

Col	
1	Slope profile plot
2	Summary tables of input x.s. and reaches
3	Initial conditions table - flow and "L" tables (reversed)
4	Initial conditions table - backwater elevation table (forward)
5	Dynamic routing - at upstream and downstream boundaries
6	Dynamic routing - at each multiple dam site (similar to depletion table)
7	Summary plots - peak elevation, discharge, time to peak, and time to flood elevation
8	Arrays for selected hydrograph plots
9	List of input cross-sectional information
10	Reservoir depletion table

Col	
11-12	This value reperesents the time at which printing of output will commence. All output will be suppressed until this time is reach.
13-14	The interval at which the output will be printed.

Note: This information can only be controlled if the JNK parameter allowed it to be printed originally.

(5) IDAM(K) - 8 I 10 Format

IDAM(K) Number of cross-section coincident with the upstream face of each dam; K index goes from 1 to MULDAM. This parameter is only read-in when the simultaneous computation of the complete system is desired (see note on page A-21 for further information on the use of this computational option).

(6) SA(K) - 8 F 10.0 Format

SA(K) Surface area (acres) or volume (acre-ft) of reservoir at elevation HSA(K). If KUI=1 and KKN≠1 or KKN=9, omit card (6). Maximum of 8 values allowed.

(7) HSA(K) - 8 F 10.0 Format

HSA(K) Elevation (ft) at which reservoir surface area SA(K) is defined; elevation is referenced to a datum plane corresponding to mean sea level (m.s.l.). If KUI=1 and KKN≠1 or KKN=9, omit card (7). Elevations start at highest and proceed to lowest. Maximum of 8 values allowed. Lowest elevation must be YBMIN as defined on card (8).

(8) RLM, YO, Z, YBMIN, BB, TFH, DATUM, VOL - 8 F 10.0 Format

RLM	Length (mi) of reservoir.
YO	Elevation (ft) of water surface in reservoir when computation commences; elevation is referenced to m.s.l. datum.
Z	Side slope (1:vertical to z:horizontal) of breach.
YBMIN	Lowest elevation (ft) that bottom of breach reaches; elevation is referenced to m.s.l. datum.

BB	Width (ft) of base of breach.
TFH	Time (hr) from beginning of breach formation until it reached its maximum size.
DATUM	Elevation (m.s.l.) of bottom of dam.
VOL	Parameter indicating if SA(K) is surface area (acres) or volume (acre-ft); if VOL=0.0, SA(K) is acres; if VOL=1.0, SA(K) is acre-ft.

(9) HF, HD, HSP, HGT, CS, CG, CDO, QT - 8 F 10.0 Format

HF	Elevation (ft) of water when failure of dam commences; elevation is referenced to m.s.l. datum; if HF is less than HD, the breach is formed by "piping."
HD	Elevation (ft) of top of dam; elevation is referenced to m.s.l. datum.
HSP	Elevation (ft) of uncontrolled spillway crest; elevation is referenced to m.s.l. datum.
HGT	Elevation (ft) of center of gate openings; elevation is referenced to m.s.l. datum.
CS	Discharge coefficient for uncontrolled spillway; it is equal to the coefficient of discharge (2.6-3.2) times the length (ft) of the spillway.
CG	Discharge coefficient for gate flow; it is equal to the coefficient of discharge (0.60-0.80) times the area of gates.
CDO	Discharge coefficient for uncontrolled weir flow over the top of the dam; it is equal to the coefficient of discharge (2.6-3.2) times the length of the dam crest (ft) less the length of the uncontrolled spillway and gates.
QT	Discharge (cfs) through turbines; this flow is assumed constant from start of computations until the dam is completely breached; thereafter, QT is assumed to be zero. QT may also be considered leaking or constant spillway flow.

<u>Note:</u> Omit cards (8) and (9) if KKN=9.

(10) QSPILL(K,L) - 8 F 10.0 Format

QSPILL(K,L)	Flow (cfs) of spillway or gate rating curve; K goes from 1 to maximum of 8; L goes from 1 to MULDAM (card (2)) which may be a maximum of 10; if MULDAM=0, L goes from 1 to 1.

(11) HEAD(K,L) - 8 F 10.0 Format

HEAD(K,L)	Head (ft) above spillway crest or gate center; head is associated with spillway flow or gate flow in rating curve; K goes from 1 to maximum of 8; L goes from 1 to MULDAM.

Note: Repeat cards 10-11 as L index goes from 1 to MULDAM. If MULDAM=0, L index goes from 1 to 1.

Note: Cards (10) and (11) are read-in only if either HSP is non-zero and CS is zero, or HGT is non-zero and CG is zero. This option allows a rating curve to be used for either the uncontrolled spillway or submerged gate rather than an equation for each using a constant discharge coefficient as in Eq. (17).

(12) DHF, TEH - 2 F 10.0 Format

DHF	Interval (hr) between QI(K) input hydrograph ordinates; enter 0.0 if intervals are not equal.
TEH	Time (hrs) from beginning of routing until routing is terminated.

(13) QO, RHO, GAMA, TPG - 4 F 10.0 Format

QO	Initial steady discharge (cfs).
RHO	Ratio of peak flow to initial flow of inflow hydrograph.
GAMA	Ratio of time from initial steady flow to center of gravity of inflow hydrograph to time to peak of inflow hydrograph.
TPG	Time from initial flow to peak flow of inflow (hr).

Note: Omit card 13 if ITEH (card 2) is nonzero.
If card 13 is included, then omit cards (14) and (15).

(14) QI(K) - 8 F 10.0 Format

QI(K)	Inflow (cfs) at upstream end of reservoir for each interval of time during the failure and until time TEH is reached; K goes from 1 to ITEH which can assume a maximum value of 50; if ITEH=0, omit this card.

(15) TI(K) - 8 F 10.0 Format

TI(K) Time associated with QI(K) inflows; if DHF (card 12) is non-zero, or if ITEH (card 2) is equal to zero, omit this card, K goes from 1 to ITEH.

(16) NS, NCS, NTT, JNK, KSA, KSUPC, LQ, KCG - 8 I 10 Format

NS Number of cross-sections used to describe the channel and valley downstream of dam; first cross-section should be immediately downstream of dam; last cross-section should be at farthest point downstream of dam where flood information is desired; other cross-sections can be located as desired by user; maximum of 90 and minimum of 2 cross-sections can be used to describe the downstream channel valley.

NCS Maximum numer of top widths used to describe a cross-section.

NTT Total number of cross-sections at which discharge hydrographs will be plotted; maximum number is limited to 6. The location of the cross-sections at which plots are provided is specified by the parameter NT(K), which is on card (17). If NTT=0, no plots are provided. If NTT=a negative value between 1 and 6, the profile plots are suppressed.

JNK Parameter to specify the type of output other than plots which will be provided; if JNK=0, a minimum of output is provided—this includes all input data and hydrograph plots; if NTT=0, no hydrographs or other output printed; if JNK=1, reservoir depletion table printed, profile of downstream crests and times, and designated hydrographs; if JNK=4, additional information is printed at each time step for debugging; if JNK=9, information is printed for debugging.

KSA Parameter to enable downstream channel-valley cross-sections to be specified by a surface area vs. elevation table similar to the SA(K) and HSA(K) values described above; if KSA=1, downstream channel-valley cross-sections will be described by input data consisting of a single table of surface area vs. elevations as indicated for cards (24) and (25); if KSA=0, this option is not used.

Also, a parameter to indicate type of cross section smoothing. If KSA<0, then smoothing of cross sections will be automatically performed. Type of smoothing is specified on card (18).

KSUPC — Parameter to indicate if flow is supercritical. If KSUPC=0, flow through entire downstream channel-valley reach is subcritical and no special treatment is required; if KSUPC=1, the flow is known to be supercritical in either an upstream portion of the downstream channel-valley or throughout the entire downstream reach. When flow is supercritical, special computational procedures are used within the program. If only the upstream portion of the reach has supercritical flow, two sets of downstream channel-valley inputs commencing with card no. (16) are read in.

LQ — Parameter denoting the total number of lateral inflow hydrographs along the downstream channel-valley; a maximum of 10 hydrographs, each with 50 ordinates, are allowed.

KCG — Number of ordinates in spillway gate control curve of gate coefficient (CGCG) vs. time (TCG) described on cards (43) and (46). If KCG is negative, it is the total number of floodplain compartments. Maximum of 16 allowed.

Note: For debugging, JNK=4 or 9 is preferred.

(17) NT(K) - 6 I 10 Format

NT(K) — Number of cross-section (1 through NS) at which hydrograph plots are desired; K goes from 1 to NTT: if NTT=0, card no. (17) is omitted.

(18) SMF, NTSM, NSMR - F10.2, 2 I 10

SMF — Smoothing factor, $0.5 \leq SMF \leq 0.9$.

NTSM — Parameter indicating type of smoothing. If NTSM=1, smoothing of widths along x-axis; if NTSM=2, smoothing of widths in vertical where maximum width/ft change is |KSA|*50; if NTSM=3, smoothing of elevations along x-axis; NTSM=4, type 1 and type 2 smoothing; if NTSM=5, type 1, 2, and 3 smoothing.

NSMR — Number of separate smoothing reaches within the total routing reach.

(19) NUSM(K), NDSM(K) - 2 I 10

NUSM(K) — Upstream cross section number of Kth smoothing reach.

NDSM(K) — Downstream cross section number of Kth smoothing reach.

Note: Card (19) is read-in for each Kth smoothing reach as K goes from 1 to NSMR.

Note: Omit cards 18 and 19 if KSA $\geq$ 0 (card 16)

(20) XS(I), FSTG(I), XSL(I), XSR(I) - 4 F 10.0 Format

XS(I)	Location (mi) of cross-sections used to describe downstream channel-valley; mileage must increase in the downstream direction from dam. If KFLP=1 (card (2)), XS(I) is mileage measured along center of channel.
FSTG(I)	Elevation (m.s.l.) at which flooding commences; may be left blank.
XSL(I)	If KFLP=0, leave blank; if KFLP=1, XSL(I) is the mileage (location) of the Ith cross-section along the left (looking upstream) flood-plain.
XSR(I)	If KFLP=0, leave blank; if KFLP=1, XSR(I) is the mileage (location) of the Ith cross-section along the right flood-plain.

(21) HS(K,I) - 8 F 10.0 Format

HS(K,I)	Elevation (ft), referenced to m.s.l. datum, corresponding to each top width (BS(K,I)) on card (22) used to describe cross-section; K goes from 1 to NCS; NCS values of HS(K,I) are punched on a single card. NCS is limited to a maximum of 8. Start with lowest HS and proceed to highest value of HS.

(22) BS(K,I) - 8 F 10.0 Format

BS(K,I)	Top width (ft) of active flow portion of channel-valley cross-section corresponding to each elevation HS(K,I); K goes from 1 to NCS; NCS values of BS(K,I) are punched on a single card; NCS is limited to maximum of 8. This card is omitted if KSA=1.

(23) BSL(K,I) - 8 F 10.0 Format

BSL(K,I)	Top width (ft) of active flow portion of left flood-plain corresponding to each elevation HS(K,I); K goes from 1 to NCS; NCS values of BSL(K,I) are punched on a single card; NCS is limited to a maximum of 8. This card is omitted if KFLP=0 (card (2)).

(24) BSR(K,I) - 8 F 10.0 Format

BSR(K,I) Top width (ft) of active flow portion of right flood-plain corresponding to each elevation HS(K,I). This card is omitted if KFLP=0.

(25) BSS(K,I) - 8 F 10.0 Format

BSS(K,I) Top width (ft) of off-channel storage portion of channel-valley cross-section corresponding to each elevation HS(K,I); K goes from 1 to NCS; NCS values of BSS(K,I) are punched on a single card; NCS is limited to maximum of 8; this card is omitted if KSA=1 (card (16)).

(26) DSA(K,I) - 8 F 10.0 Format

DSA(K,I) Surface area (acres) of active flow portion of down-stream channel-valley cross-section corresponding to each elevation HS(K,I); K goes from 1 to NCS; NCS values of DSA(K,I) are punched on a single card; NCS is limited to maximum of 8; this card is omitted if KSA $\leq$ 0.

(27) SSA(K,I) - 8 F 10.0 Format

SSA(K,I) Surface area (acres) of off-channel storage portion of channel valley cross-section corresponding to each elevation HS(K,I); K goes from 1 to NCS; NCS values of SSA(K,I) are punched on a single card; NCS is limited to maximum of 8; this card is omitted if KSA=0.

<u>Note:</u> Cards (20)-(25) are repeated for each cross-section as in the index I goes from 1 to NS.
When KSA=1, the cards are read-in as follows: (20), (21), (26), (27), (20), (21); this option is limited to the case of NS=2.

(28) CM(K,I) - 8 F 10.0 Format

CM(K,I) Manning n for channel corresponding to each elevation HS(K,I); K goes from 1 to NCS: NCS values of CM(K,I) are punched on a single card; NCS is limited to maximum of 8; the Manning n represents the roughness enountered by the flow through the reach bounded by cross-sections at locations I and I+1.

(29) CML(K,I) - 8 F 10.0 Format

CML(K,I) Manning n for left flood-plain corresponding to each elevation HS(K,I); K goes from 1 to NCS; NCS values of CM(K,I) are punched on a single card; NCS is limited to a maximum of 8. This card is omitted if KFLP=0 (card 2).

(30) CMR(K,I) - 8 F 10.0 Format

CMR(K,I) Manning n for right flood-plain corresponding to each elevation HS(K,I). This card is omitted if KFLP=0.

Note: Cards (28, 29, 30) are repeated for (NS-1) reaches.

(31) DXM(I) - 8 F 10.0 Format

DXM(I) Minimum Δx distance (mi) between cross-sections used in the computations. If DXM(I) is less than the distance between two adjacent cross-sections among the NS cross-sections read in, then intermediate cross-sections are created within the program via an interpolation procedure. (NS-1) values of DXM(I) are punched on one or more cards (8 values to a card); maximum no. of DXM(I) values is limited to 89; values assigned to DXM(I) should not result in more than 200 cross-sections produced by the interpolation procedure. (DXM values should be determined by the relationship C times Δt, where C is the approximate speed of the flood wave.)

(32) FKC(I) - 8 F 10.0 Format

FKC(I) Contraction-expansion coefficient; contraction values vary from 0.1 to 0.3, expansion values vary from -0.5 to -1.0; if contraction-expansion effects are negligible, enter 0.0 for FKC(I); (NS-1) values of FKC(I) are punched on one or more cards (8 values to a card); maximum no. of FKC(I) values is limited to 89.

(33) QMAXD, QLL, DTHM, YDN, SOM, F1I, EPSY, TFI - 8 F 10.0 Format

QMAXD	Estimated maximum discharge (cfs) at downstream extremity of channel-valley reach; can be read in as 0.0 for initial run; subsequent runs can have a value of QMAXD as determined by the routing computations during the initial run. Only required when QLL is non-zero.
QLL	Maximum lateral outflow (cfs/ft) producing the volume losses experienced by the passage of the dam-break flood wave through the downstream valley; QLL has a negative sign and is computed by Eq. (63) in paper.
DTHM	Initial Δt time step size (hr); if 0.0 is read in, the value of DTHM is computed by the program; if DTHM<0.0, DTHM represents the divisor MDT for determining the time step (DTH=TFH/MDT) and DTHM is reset to zero. See note on page A-23.
YDN	Initial elevation of water surface at downstream end of routing reach; if channel control exists at this location, enter 0.0; YDN is non-zero if a dam or other control structure exists at the downstream end of the routing reach; if YDN=0.25, a single value rating curve of water surface elevation (m.s.l.) vs. discharge exists at downstream end; if YDN=0.5, critical flow such as waterfall exists at downstream end; if YDN=0.75, a specified water surface elevation (m.s.l.) such as a tide exists at the downstream end; if YDN=1.0, channel control exists at downstream end, but this signals the program that initial water surface elevations will be read-in at the NS cross-sections via card (48).
SOM	Slope of downstream channel (ft/mi) for first mile below dam.
F1I	Theta (θ) weighting factor in finite difference solution; if left blank, a value of 0.60 is used in program; if 0.5 is used, θ is set internally to 0.60 and the model is capable of allowing negative flows to occur; if 0.51 is used, θ is set internally to 0.60 and the model routing is done by the diffusion method instead of dynamic routing.
EPSY	Convergence criterion for stage (ft) in Newton-Raphson iterative solution of finite difference unsteady flow equations; varies from .01 to .1 ft; if left blank, program use 0.01 ft. Also, can be used to specify the exponent m used in Eq. 65 in the paper; if EPSY<0.50, m=4; if EPSY>0.5, m=EPSY and EPSY is automatically set to 0.01.
TFI	Time (hr) when time step changes from DTHM to TFH/MDT. See time step note on page A-23.

(34) NPLD - I 10

NPLD — Number of last floodplain compartment on same side of river where first floodplain compartment (FPC) is located; if no flow is transferred from one FPC to an adjacent FPC, let NPLD=0. Omit this card if KCG=0.

(35) NPXI(K), NQLP(K), PWELV(K), PCWR(K), PEO(K), QMINP(K) - 2 I 10, 4 F 10.0

NPXI(K) — Number of cross section immediately upstream of Δx reach where inflow to K^{th} FPC occurs.

NQLP(K) — Parameter indicating if pump discharge within the Kth FPC will be specified by a discharge hydrograph; 0 if no, 1 if yes.

PWELV(K) — Average elevation (ft. msl) of crest of weir (levee) along Δx reach where inflow to K^{th} FPC occurs.

PCWR(K) — Coefficient of discharge for weir flow along Δx reach where inflow to K^{th} FPC occurs; ranges in value from 2.6 to 3.2.

PEO(K) — Initial elevation (ft. msl) of water surface in K^{th} FPC at time = 0.

QMINP(K) — Minimum discharge (cfs) of total number of pumps in K^{th} FPC at all times.

(36) PSA(I,K) - 8 F 10.0

PSA(I,K) — Total volume (acre-ft) of Kth FPC below each elevation (PEL(I,K)); I index goes from 1 to 8.

(37) PEL(I,K) - 8 F 10.0

PEL(I,K) — Elevation (ft. msl) associated with each volume (PSA(I,K); elevations start at the lowest and proceed to the highest; I index goes from 1 to 8; last specified elevation should be greater than any expected water elevation within the FPC.

(38) QPU(I,K) - 8 F 10.0

QPU(I,K) — Inflow (cfs) to K^{th} FPC other than that transmitted over the weir (levee) from the main river; I index goes from 1 to ITEH (card no. 2).

(39) QLP(I,K) - 8 F 10.0

QLP(I,K) Specified total pump discharge (cfs) for K^{th} FPC; I index goes from 1 to ITEH (card no. 2); omit this card if NQLP(K)=0.

(40) COFF(I,K) - 8 F 10.0

COFF(I,K) Coefficient of discharge for flow over levee separating the Kth and $K^{th}+1$ FPC; coefficient is product of the broad-crested weir coefficient (2.6 to 3.2) and the length (ft) of the weir crest; the coefficient varies with elevation (HCFF(I,K)); I index goes from 1 to 8; omit this card if NPLD=0.

(41) HCFF(I,K) - 8 F 10.0

HCFF(I,K) Elevation (ft. msl) associated with the discharge coefficients (COFF(I,K)); elevations start at the lowest point along the levee crest and proceed upward; I index goes from 1 to 8; omit this card if NPLD=0.

Note Omit card no. 34 to 45 if KCG$\geq$0; otherwise repeat card no. 33 to 41 as K index goes from 1 to ABS(KCG).

(42) NPM - I 10

NPM Total number of pumps in all the FPC.

Note> Omit card no. 43 to 45 if NPM=0.

(43) IPMPL(L), NXPO(L), PEMN(L), PEMX(L) - 2 I 10, 2 F 10.0

IPMPL(L) Number of the Kth FPC in which the Lth pump is located.

NXPO(L) Number of the cross section immediately upstream of Δx reach where the Lth pump discharges into main river.

PEMN(L) Elevation (ft. msl) of water in K^{th} FPC when L^{th} pump starts pumping.

PEMX(L) Elevation (ft. msl) of water in K^{th} FPC when Lth pump stops pumping.

(44) DHP(I,L) - 8 F 10.0

DHP(I,L) Head (ft) associated with L^{th} pump rating curve; I index goes from 1 to 8; head starts at smallest and proceeds to greatest; negative head may be specified. Omit this card if NQLP(K)=0.

(45) OP(I,L) - 8 F 10.0

OP(I,L) Pump discharge (cfs) associated with L^{th} pump rating curve; I index goes from 1 to 8; each value is associated with its corresponding DHP(I,L) value. Omit this card if NQLP(K)=0.

Note Repeat card no. 43 to 45 as L index goes from 1 to NPM.

(46) LQX(K) - 8 I 10 Format

LQX(K) Number of cross-section immediately upstream of lateral inflow/outflow; K goes from 1 to LQ (card (16)). If LQX(K) is specified as a negative number, this indicates that the reach may have outflow via broad-crested weir flow.

(47) QL(L,K) - 8 F 10.0 Format

QL(L,K) Lateral inflow (cfs) for k^{th} lateral inflow point; L index goes from 1 to ITEH (card (2)); ordinates of lateral inflow hydrograph have same times as those of reservoir inflow hydrograph (QI(L)) on card (14)); K index goes from 1 to LQ.
If LQX(K) is negative, two values only are specified on card (47) according to a 2 F 10.2 format. The first (WELV(K)) is the crest elevation (msl) at which overflow occurs (this represents the average crest elevation along the reach). The second (CWR(K)) is the discharge coefficient ranging in value from 2.6 to 3.2 with 3.0 a most common value.

Note: Omit cards (46) and (47) if LQ=0 (on card no. 16).

(48) YD(I) - 8 F 10.0 Format

YD(I) Initial water surface elevations (m.s.l.) along routing reach; this is used only if YDN=1.0; if YDN≠1.0, omit this card and program computes the initial water surface elevations.

(49) RH(K) - 8 F 10.0 Format

RH(K) Elevation (m.s.l.) points on single value rating curve for downstream boundary, read in only if YDN (card no. 33) = 0.25; K index goes from 1 to maximum of 8.

(50) RQ(K) - 8 F 10.0 Format

RQ(K) Discharge (cfs) associated with elevation points on single value rating curve for downstream boundary, read in only if YDN=0.25.

(51) STN(K) - 8 F 10.0 Format

STN(K) Specified water surface elevation (m.s.l.) at downstream boundary such as a tide; K goes from 1 to ITEH, read in only if YDN=0.75.

(52) TTN(K) - 8 F 10.0 Format

TTN(K) Time (hrs) associated with STN(K); K goes from 1 to ITEH, read in only if YDN=0.75.

(53) NSLI - I 10 Format

NSLI Total no. of cross-sections (read-in) where landslide occurs; maximum no. allowed is 6; also maximum total cross-sections (including interpolated ones created by DXM values on card (31)) is limited to 31; omit if KSL=0 (card (2)).

(54) NXSLI(K), TSL, HSL(K), HSM(K), HSU(K), THKSL(K), ALPHA, POR - I 10, 7 F 10.2 Format

NXSLI(K)	Sequential number of cross-section where landslide occurs; K index goes from 1 to NSLI.
TSL	Time of duration for landslide (usually in the range of 15 seconds to a few minutes); unit must be in hrs.
HSL(K)	Elevation (ft above m.s.l.) of lowest portion of landslide mass; K goes from 1 to NSLI.
HSM(K)	Elevation (ft above m.s.l.) of middle portion of landslide mass--at this elevation, the landslide mass has the greatest thickness into the bank; K goes from 1 to NSLI.
HSU(K)	Elevation (ft above m.s.l.) of highest portion of landslide mass, K goes from 1 to NSLI.
THKSL(K)	Greatest thickness (depth into the bank) in ft of the landslide mass at elevation HSM(K); K goes from 1 to NSLI.
ALPHA	Angle of repose that deposited material from the landslide assumes in the bottom of the reservoir, in degrees.
POR	Porosity of landslide material, decimal fraction.

Note: Omit cards (53) and (54) if KSL=0.

Note: Card (54) is repeated for each K as it goes from 1 to NSLI.

(55) ICG(K) - 8 I 10 Format

ICG(K)	Parameter indicating if a dam has time-dependent gate flow; if yes, ICG(K)=1; if no, ICG(K)=0; K goes from 1 to M, where M=MULDAM if MULDAM$\geq$1 and M=1 if MULDAM=0.

(56) CGCG(L,K) - 8 F 10.0 Format

CGCG(L,K)	Spillway gate coefficient equal to area of gates (opened at time TCG(L,K)) x coefficient of discharge; L goes from 1 to KCG (see card 16); and K goes from 1 to the total number of dams having time-dependent gate control.

(57) GBL(L,K) - 8 F 10.0 Format

GBL(L,K)	Distance (ft) from bottom of gate to gate sill (HGT-card(9)); This distance is time dependent and is associated with the time array TCG(L,K); L and K index are same as described on card (56).

(58) TCG(L,K) - 8 F 10.0 Format

TCG(L,K)	Time (hrs) associated with CGCG(L,K); L goes from 1 to KCG; and K goes from 1 to the total number of dams having time-dependent gate control.

Note: Omit cards (55), (56, (57), and (58) if KCG=0 (on card no. 16).

(59) Z, YBMIN, BB, TFH - 4 F 10.0 Format

Z	Side slope (1:vertical to z:horizontal) of breach of downstream dam.
YBMIN	Lowest elevation (ft) that bottom of breach reaches; elevation is referenced to m.s.l. datum.
BB	Width (ft) of base of breach of downstream dam.
TFH	Time (hr) from beginning of breach formation of downstream dam until it reaches its maximum size.

(60) HF, HD, HSP, HGT, CS, CG, CDO, QT - 8 F 10.0 Format

HF	Elevation (ft) of water when failure of downstream dam commences; elevation is referenced to m.s.l. datum.
HD	Elevation (ft) of top of downstream dam; elevation is referenced to m.s.l. datum.
HSP	Elevation (ft) of uncontrolled spillway crest; elevation is referenced to m.s.l. datum.
HGT	Elevation (ft) of center of gate openings; elevation is referenced to m.s.l. datum.
CS	Discharge coefficient for uncontrolled spillway; it is equal to the coefficient of discharge (2.6-3.2) times the length (ft) of the spillway.
CG	Discharge coefficient for gate flow; it is equal to the coefficient of discharge (0.10-0.80) times the area of gates.
CDO	Discharge coefficient for uncontrolled weir flow over the top of the downstream dam; it is equal to the coefficient of discharge (2.6-3.2) times the length of the downstream dam crest (ft) less the length of the uncontrolled spillway and gates.

QT	Discharges (cfs) through turbines; this flow is assumed constant from start of computations until the downstream dam is completely breached; thereafter QT is assumed to be zero.

(61) QSPILL(K,1) - 8 F 10.0 Format

QSPILL(K,1)	Flow (cfs) of spillway or gate rating curve; k goes from 1 to maximum of 8.

(62) HEAD(K,1) - 8 F 10.0 Format

HEAD(K,1)	Head (ft) above spillway crest or gate center; head is associated with spillway flow or gate flow in rating curve.

Note: Cards (61) and (62) are read-in only if either HSP is non-zero and CS is zero or HGT is non-zero and CG is zero. This option allows a rating curve to be used for either the uncontrolled spillway or submerged gate rather than an equation for each using a constant discharge coefficient as in Eq. (17).

(63) UPSH, SOM, CMN - 3 F 10.0 Format

UPSH	Dummy variable, leave blank.
SOM	Slope of downstream channel (ft/mi) for first few miles below dam.
CMN	Average Manning's n for downstream channel for first few miles below dam.

Note: Cards (59-63) are omitted if KUI=0 and MULDAM=0 or if KKN=9.

Note: If KUI=1 and dynamic routing is used for the reservoir routing procedure, cards (6) and (7) are omitted and cards (8)-(58) and (51) apply to the reservoir characteristics. Then, cards (16)-(58) are read in again; this time they apply to the downstream channel and valley.

Note: If KKN=9, only a downstream routing is used to route a read-in hydrograph (cards (12)-(15)). Also, cards (16)-(25) and (28)-(58) are required.

<u>Note</u>: The program has the capability of simulating a total of 12 different cases. These are outlined as follows:

Option 1: Reservoir storage routing to compute outflow hydrograph from reservoir with subcritical dynamic routing of outflow hydrograph through entire length of downstream valley—KUI=0, KKN=1, KSUPC=0, MULDAM=0.
Input data cards—1-4, 6-58.

Option 2: Reservoir storage routing to compute outflow hydrograph from reservoir with supercritical dynamic routing of outflow hydrograph through entire length of downstream valley—KUI=0, KKN=1, KSUPC=1, MULDAM=0.
Input data cards—1-4, 6-58.

Option 3: Reservoir storage routing to compute outflow hydrograph from reservoir with supercritical dynamic routing of outflow hydrograph through upstream portion of downstream valley and subcritical dynamic routing through downstream portion of downstream valley—KUI=0, KKN=2, KSUPC=1, MULDAM=0.
Input data cards—1-4, 6-52, 16-58.

Option 4: Same as Option 1 except reservoir dynamic routing to compute outflow hydrograph from reservoir—KUI=1, KKN=2, KSUPC=0, MULDAM=0.
Input data cards—1-4, 8-58, 63, 16-52.

Option 5: Same as Option 2 except reservoir dynamic routing to compute outflow hydrograph from reservoir—KUI=1, KKN=2, KSUPC=1, MULDAM=0.
Input data cards—1-4, 8-58, 63, 16-52

Option 6: Same as Option 3 except reservoir dynamic routing to compute outflow hydrograph from reservoir—KUI=1, KKN=3, KSUPC=1, MULDAM=0.
Input data cards—1-4, 8-58, 63, 16-52, 16-52.

Option 7: Subcritical dynamic routing of input hydrograph through a channel-valley—KUI=0, KKN=9, KSUPC=0, MULDAM=0.
Input data cards—1-4, 12-52. (See note on page A-20.)

Option 8:	Supercritical dynamic routing of input hydrograph through a channel-valley--KUI=0, KKN=9, KSUPC=1, MULDAM=0. Input data cards--1-4, 12-52. (See note on page A-20.)
Option 9: "Sequential Method"	Reservoir storage routing to compute outflow hydrograph from reservoir with subcritical dynamic routing of outflow hydrograph through downstream channel-reservoir having a dam which may fail--KUI=0, KKN=2, KSUPC=0, MULDAM=1. Input data cards--1-4, 6-63, 16-63, ... 16-52.
Option 10: "Sequential Method"	Reservoir dynamic routing to compute outflow hydrograph from reservoir with subcritical dynamic routing of outflow hydrograph through downstream channel-reservoir having a dam which may fail--KUI=1, KKN=3, KSUPC=0, MULDAM=1. Input data cards--1-4, 8-58, 63, 16-63, ... 16-52.
Option 11: "Simultaneous Method"	Simultaneous computation method for single dam or bridge (structure) using dynamic routing in the reach upstream of the structure and downstream of the structure with special internal boundary conditions for flow thru the structure--KUI=1, KKN=1, MULDAM=1, KSUPC=0. Input data cards--1-5, 8-11, 12-58. See note on page A-21 for input variables for bridge and embankment.
Option 12: "Simultaneous Method"	Simultaneous computation method for multiple dams and/or bridges (structures) using dynamic routing for all reaches with special internal boundary conditions for flow thru each structure--KUI=1, KKN=1, MULDAM=no. of dams and/or bridges, KSUPC=0. Input data cards--1-5, 8-11, 8-11, 8-11, ... 12-58. See note on page A-21 for input variables and embankments.

"SIMULTANEOUS METHOD" OF COMPUTATION OF COMPLETE SYSTEM:

This option treats the upstream reservoir, any intermediate reservoir, and the downstream channel as one system. Cross sections are numbered consecutively from the very upstream end of the most upstream reservoir to the downstream extremity of the downstream channel. Cross sections are specified for the upstream and downstream sides of each dam. This option is most useful for problems in which the tailwater below a dam is affected by backwater from downstream dams or other constrictions. It is necessary when using this option to specify KKN=1, KUI=1, MULDAM $\geq$ 1 to read-in card (5). Also, cards (6) and (7) are omitted, and cards (8) and (9) are repeated for each dam in

the system. Cards (59), (60), (61), (62), and (63) are not applicable for this option. MULDAM is defined as the number of dams in the system.

BRIDGE COMPUTATION

The simultaneous method can be used for either multiple dams or bridges. Cards (8) and (9) are used to describe the flow thru and across the bridge and embankment. The bridge embankment may be allowed to breach. If breaching is not considered possible, HF on card (9) is set to a very large value so that the water surface will not reach it. On card (8), RLM must be left blank as well as YO; other variables on card (8) are associated with the breach of the embankment and are defined essentially the same as shown on page A-4. The variables other than HF on card (9) are defined as follows: HD—height (ft m.s.l.) of crest of uppermost portion of road embankment; HSPD—length (ft) of crest of uppermost portion of road embankment measured across valley and perpendicular to flow; HGTD—height (ft m.s.l.) of crest of lower portion (emergency overflow) of road embankment (if non-existent, leave blank); CSD—length (ft) of crest of lower portion of road embankment measured across valley and perpendicular to flow; CGD—width of top of road embankment as measured parallel to flow; CDOD—coefficient of discharge of flow thru bridge opening (see: Chow, "Open-Channel Hydraulics" pp. 476-490); QT—time step to be used when the upper road embankment is overtopped. QT is only needed when the first structure in the routing reach is a bridge and when the inflow hydrograph is a slowly rising hydrograph. It should be left blank at all other times. If it is left blank when needed, the default value is 0.5 hr. Instead of reading in the length of the upper road embankment, a table of length of embankment (ft) vs. water surface elevation (ft msl) may be read in on cards (9) and (10) respectively. HSPD is then read in as zero.

ROUTING SPECIFIED INFLOW HYDROGRAPH (Options 7 and 8)

Options (7) and (8) are for routing a specified inflow hydrograph through the downstream valley, i.e., there is no upstream reservoir and associated outflow hydrograph as computed by DAMBRK. These options do not enable the treatment of bridges or dams located along the downstream valley.

LEVEL POOL ROUTING USING OPTIONS 11 AND 12

The storage routing (level pool) technique based on Eq. (18) may also be used simultaneously with the dynamic routing technique for simulating the unsteady flow through the downstream channel-valley. Eq. (18) is combined with Eq. (65) to form the upstream boundary condition and the dam is treated as an internal boundary via Eqs. (51-52). The advantages of this combination of the two routing techniques within a simultaneous computation method are: (1) simple routing technique for reservoir, (2) dynamic routing for downstream dam-break hydrograph, and (3) more accurate computation of tail-water elevation than via Eq. (11).

Level pool routing may be used with options 11 and 12 by: (1) including cards (6) and (7) after card (5); (2) IDAM(1) will always be 1, i.e., the first cross-section represents the upstream face of the first dam (level pool routing can only be used for the first or upstream reservoir).

FLOODPLAIN COMPARTMENTS (FPC)

Each FPC may have only one Δx-reach in which flow from the river enters the FPC or, if the differential head favors the FPC, the flow goes from the FPC to the river. This Δx-reach is designated by NXPI(K), where the K index goes from 1 to the total number of FPC's (KCG).

Each FPC may have only one Δx-reach in which the FPC pump(s) return water to the river. The Δx-reach is designated by NXPO(L), where the L index goes from 1 to the total number of pumps (NPM).

A particular Δx-reach cannot be used for more than one FPC; thus, NXPI(1)≠NXPI(2).

A particular Δx-reach cannot be used for both types of flow exchange (weir flow or pump flow); thus, NXPI(K)≠NXPO(L).

An FPC may pass flow to an adjacent FPC via broad-crested weir flow with submergence correction. Also, the most downstream FPC may pass flow on downstream via overtopping weir flow. FPC's are numbered from upstream to downstream, commencing on one side of the river and then the other side of the river.

TIME STEP SELECTION

The time step size used to route the hydrograph through the downstream channel-valley can be user controlled with the DTHM and TFI parameters on card (33). If a constant time step is desired, the user reads in DTHM (time step size) and leaves TFI blank.

If DTHM and TFI are both read in as zero, the model will generate an initial time step size based on the inflow hydrograph - TP/MDT where TP is the time from start of rise to peak of the hydrograph and MDT is the assumed to be 20 unless specified differently by reading in a negative DTHM value. This time step is used until time TFI (the time just prior to dam failure) is exceeded. If KUI=0 (card 2), this value is computed as the time to peak of the outflow hydrograph minus the time to failure. If KUI=1, TFI is set equal to TEH (card 12). If the time exceeds TFI or if the dam fails, the time step is cut back to TFH/MDT. If DTHM and TFI are read in as nonzero values, the DTHM is used until time TFI is exceeded and then the time step is cut back to TFH/MDT.

If TFI is read in as a nonzero value and DTHM is read in as zero, the model will compute DTHM=TP/MDT and use that time step until TFI is exceeded and then cut back to TFH/MDT.

UPDATE FEATURE:

If the parameters (BB, Z, TFH, HD, YO, HF) are the only ones that may have a different value than contained on all input data cards (1)-(63), the following UPDATE procedure can be used:

Place the following two cards immediately before card (1):

UPDATE (with U starting in column 1)
BB, Z, TFH, HD, YO, HF — 6F10.0

where BB, Z, etc., are defined as described previously on cards (8)-(9). If any of these values do not change, leave the appropriate space blank. The update feature is only applicable for Options 1-6.

DAMBRK OUTPUT

1. Output Structure.

Table 1 lists the output items that are available from DAMBRK. The primary input variable that controls level of output is JNK, which appears on card 10. Table 1 indicates output items that are obtained for various values of JNK.

Definitions of variables for the Reservoir Depletion Table are provided in the program output.

Definitions of variables for Initial Conditions are provided in Table 2.

Definitions of variables for the trace (JNK = 4) of the dynamic routing computations are shown in Table 3.

Table 4 illustrates tables of cross section properties available with JNK = 2.

Table 5 illustrates output available with a detailed trace of the dynamic routing computations (JNK = 3, 5 or 9). Variables NPRT (card 2) and NPT (card 2') can be used to specify cross sections, including interpolated cross sections, for which information is desired.

Hydrograph plots are requested with variable NTT on card 10. Up to six plots may be requested. Sequence numbers of cross sections (e.g., 5 for fifth cross section) for which plots are desired are input on card 11.

Variable KDMP on card 2 should be set to 3. Other values for KDMP are only applicable when operating DAMBRK on the National Weather Service computer system.

2. Example.

The handout following this lecture outline illustrates output for the problem for which input was prepared in the lecture on input requirements.

```
*******************************
*******************************
***                         ***
***  SUMMARY OF INPUT DATA  ***
***                         ***
*******************************
*******************************
```

INPUT CONTROL PARAMETERS FOR TETON

PARAMETER	VARIABLE	VALUE
NUMBER OF DYNAMIC ROUTING REACHES	KKN	1
TYPE OF RESERVOIR ROUTING	KUI	0
MULTIPLE DAM INDICATOR	MULDAM	0
PRINTING INSTRUCTIONS FOR INPUT SUMMARY	KDMP	3
NO. OF RESERVOIR INFLOW HYDROGRAPH POINTS	ITEH	2

TETON RESERVOIR

TABLE OF ELEVATION VS SURFACE AREA

ELEVATION (FT) HSA(K)	SURFACE AREA (ACRES) SA(K)
5324.00	2100.0
5250.00	1500.0
5150.00	800.0
5070.00	300.0
5025.00	0.0
0.00	0.0
0.00	0.0
0.00	0.0

TETON RESERVOIR AND BREACH PARAMETERS

PARAMETER	UNITS	VARIABLE	VALUE
LENGTH OF RESERVOIR	MI	RLN	10.00
ELEVATION OF WATER SURFACE	FT	YO	5301.50
SIDE SLOPE OF BREACH		Z	0.00
ELEVATION OF BOTTOM OF BREACH	FT	YBMIN	5040.00
WIDTH OF BASE OF BREACH	FT	BB	150.00
TIME TO MAXIMUM BREACH SIZE	HR	TFH	1.25
ELEVATION (MSL) OF BOTTOM OF DAM	FT	DATUM	5025.00
ELEVATION OF WATER WHEN BREACHED	FT	HF	5301.50
ELEVATION OF TOP OF DAM	FT	HD	5332.00
ELEVATION OF UNCONTROLLED SPILLWAY CREST	FT	HSP	5305.00
ELEVATION OF CENTER OF GATE OPENINGS	FT	HGT	5040.00
DISCHARGE COEF. FOR UNCONTROLLED SPILLWAY		CS	300.00
DISCHARGE COEF. FOR GATE FLOW		CG	0.00
DISCHARGE COEF. FOR UNCONTROLLED WEIR FLOW		CDO	9000.00
DISCHARGE THRU TURBINES	CFS	QT	940.00

QSPILL(K)	HEAD(K)
0.	0.0
500.	40.0
849.	105.0
850.	284.3
0.	0.0
0.	0.0
0.	0.0
0.	0.0

DHF(INTERVAL BETWEEN INPUT HYDROGRAPH ORDINATES) = 6.00 HRS.

TEH(TIME AT WHICH COMPUTATIONS TERMINATE) = 6.00 HRS.

INFLOW HYDROGRAPH TO TETON

****

3580. 3580.

TIME OF INFLOW HYDROGRAPH ORDINATES

0.00 6.00

CROSS-SECTIONAL PARAMETERS FOR TETON
BELOW TETON

PARAMETER	VARIABLE	VALUE
NUMBER OF CROSS-SECTIONS	NS	3
MAXIMUM NUMBER OF TOP WIDTHS	NCS	4
NUMBER OF CROSS-SECTIONAL HYDROGRAPHS TO PLOT	NTT	3
TYPE OF OUTPUT OTHER THAN HYDROGRAPH PLOTS	JNK	4
CROSS-SECTIONAL SMOOTHING PARAMETER	KSA	0
DOWNSTREAM SUPERCRITICAL OR NOT	KSUPC	0
NO. OF LATERAL INFLOW HYDROGRAPHS	LB	0

NUMBER OF CROSS-SECTION WHERE HYDROGRAPH DESIRED
(MAX NUMBER OF HYDROGRAPHS = 6)
****

1 2 3

CROSS-SECTIONAL VARIABLES FOR TETON
BELOW TETON

PARAMETER	UNITS	VARIABLE
LOCATION OF CROSS-SECTION	MI	XS(I)
ELEVATION (MSL) OF FLOODING AT CROSS-SECTION	FT	FSTG(I)
ELEV CORRESPONDING TO EACH TOP WIDTH	FT	HS(K,I)
TOP WIDTH CORRESPONDING TO EACH ELEV (ACTIVE FLOW PORTION)	FT	BS(K,I)
TOP WIDTH CORRESPONDING TO EACH ELEV (OFF-CHANNEL PORTION)	FT	BSS(K,I)
SURFACE AREA CORRESPONDING TO EACH ELEV (ACTIVE FLOW PORTION)	ACRES	DSA(K,I)
SURFACE AREA CORRESPONDING TO EACH ELEV (OFF-CHANNEL PORTION)	ACRES	SSA(K,I)
NUMBER OF CROSS-SECTION		I
NUMBER OF ELEVATION LEVEL		K

CROSS-SECTION NUMBER 1
****

XS(I) = 0.0 FSTG(I) = 0.00

HS ...	5025.0	5050.0	5150.0	5225.0
BS ...	0.0	400.0	510.0	630.0
BSS ...	0.0	0.0	0.0	0.0

CROSS-SECTION NUMBER 2
****

XS(I) = 2.2 FSTG(I) = 0.00

HS ...	5005.0	5028.0	5078.0	5158.0
BS ...	0.0	607.0	930.0	1122.0
BSS ...	0.0	0.0	0.0	0.0

CROSS-SECTION NUMBER 3
****

XS(I) = 5.0 FSTG(I) = 0.00

HS ...	4982.0	5010.0	5060.0	5140.0
BS ...	0.0	1450.0	3869.0	4021.0
BSS ...	0.0	0.0	0.0	0.0

MANNING N ROUGHNESS COEFFICIENTS FOR THE GIVEN REACHES
(CM(K,I),K=1,NCS) WHERE I = REACH NUMBER
****

REACH 1 ...	.040	.040	.040	.040
REACH 2 ...	.040	.040	.040	.040

TABLE 4

CROSS SECTION PROPERTIES (JNK = 2)

I	FKC(I)	DX
1	0.00	.44
2	0.00	.44
3	0.00	.44
4	0.00	.44
5	0.00	.44
6	0.00	.56
7	0.00	.56
8	0.00	.56
9	0.00	.56
10	0.00	.56

I	X(I)	(HS(K,I),K=1,NCS)			
1	0.00	5025.0	5050.0	5150.0	5225.0
2	.44	5021.0	5045.6	5135.6	5211.6
3	.88	5017.0	5041.2	5121.2	5198.2
4	1.32	5013.0	5036.8	5106.8	5184.8
5	1.76	5009.0	5032.4	5092.4	5171.4
6	2.20	5005.0	5028.0	5078.0	5158.0
7	2.76	5000.4	5024.4	5074.4	5154.4
8	3.32	4995.8	5020.8	5070.8	5150.8
9	3.88	4991.2	5017.2	5067.2	5147.2
10	4.44	4986.6	5013.6	5063.6	5143.6
11	5.00	4982.0	5010.0	5060.0	5140.0

I	X(I)	(CM(K,I),K=1,NCS)			
1	0.00	.0400	.0400	.0400	.0400
2	.44	.0400	.0400	.0400	.0400
3	.88	.0400	.0400	.0400	.0400
4	1.32	.0400	.0400	.0400	.0400
5	1.76	.0400	.0400	.0400	.0400
6	2.20	.0400	.0400	.0400	.0400
7	2.76	.0400	.0400	.0400	.0400
8	3.32	.0400	.0400	.0400	.0400
9	3.88	.0400	.0400	.0400	.0400
10	4.44	.0400	.0400	.0400	.0400
11	5.00	.0400	.0400	.0400	.0400

I	X(I)	(BS(K,I),K=1,NCS)			
1	0.00	0.0	400.0	510.0	630.0
2	.44	0.0	441.4	594.0	728.4
3	.88	0.0	482.8	678.0	826.8
4	1.32	0.0	524.2	762.0	925.2
5	1.76	0.0	565.6	846.0	1023.6
6	2.20	0.0	607.0	930.0	1122.0
7	2.76	0.0	775.6	1517.8	1701.8
8	3.32	0.0	944.2	2105.6	2281.6
9	3.88	0.0	1112.8	2693.4	2861.4
10	4.44	0.0	1281.4	3281.2	3441.2
11	5.00	0.0	1450.0	3869.0	4021.0

I	X(I)	(AS(K,I),K=1,NCS)			
1	0.00	0.0	5000.0	50500.0	93250.0
2	.44	0.0	5429.2	52022.2	102273.4
3	.88	0.0	5841.9	52273.9	110208.7
4	1.32	0.0	6238.0	51255.0	117055.8
5	1.76	0.0	6617.5	48965.5	122814.7
6	2.20	0.0	6980.5	45405.5	127485.5
7	2.76	0.0	9307.2	66642.2	195426.2
8	3.32	0.0	11802.5	88047.5	263535.5
9	3.88	0.0	14466.4	109621.4	331813.4
10	4.44	0.0	17298.9	131363.9	400259.9
11	5.00	0.0	20300.0	153275.0	468875.0

I	X(I)	(BSS(K,I),K=1,NCS)			
1	0.00	0.0	0.0	0.0	0.0
2	.44	0.0	0.0	0.0	0.0
3	.88	0.0	0.0	0.0	0.0
4	1.32	0.0	0.0	0.0	0.0
5	1.76	0.0	0.0	0.0	0.0
6	2.20	0.0	0.0	0.0	0.0
7	2.76	0.0	0.0	0.0	0.0
8	3.32	0.0	0.0	0.0	0.0
9	3.88	0.0	0.0	0.0	0.0
10	4.44	0.0	0.0	0.0	0.0
11	5.00	0.0	0.0	0.0	0.0

CROSS-SECTIONAL VARIABLES FOR TETON
BELOW TETON

PARAMETER	UNITS	VARIABLE
MINIMUM COMPUTATIONAL DISTANCE USED BETWEEN CROSS-SECTIONS	MI	DXM(I)
CONTRACTION - EXPANSION COEFFICIENTS BETWEEN CROSS-SECTIONS		FKC(I)

REACH NUMBER	DXM(I)	FKC(I)
1	.417	0.000
2	.500	0.000

DOWNSTREAM FLOW PARAMETERS FOR TETON
BELOW TETON

PARAMETER	UNITS	VARIABLE	VALUE
MAX DISCHARGE AT DOWNSTREAM EXTREMITY	CFS	QMAXD	0.0
MAX LATERAL OUTFLOW PRODUCING LOSSES	CFS/FT	QLL	0.000
INITIAL SIZE OF TIME STEP	HR	DTHM	0.000
INITIAL WATER SURFACE ELEVATION DOWNSTREAM	FT	YDN	.50
SLOPE OF CHANNEL DOWNSTREAM OF DAM	FT/MI	SOM	17.00
THETA WEIGHTING FACTOR		THETA	0.00

NUMBER OF INTERMEDIATE STATIONS (N) = 11 (MAXIMUM ALLOWABLE = 200

TOTAL VOLUME IN RESERVOIR BEHIND
TETON = 253752.4 ACRE-FEET

DEFINITION OF VARIABLES IN RESERVOIR DEPLETION TABLE

PARAMETER	UNITS	VARIABLE
TIME STEP FROM START OF ANALYSIS		I
ITERATIONS NECESSARY TO SOLVE FLOW EQUATIONS		K
ELAPSED TIME FROM START OF ANALYSIS	HRS	TTP(I)
OUTFLOW FROM BREACH	CFS	Q(I)
ELEVATION OF WATER SURFACE AT DAM	FT	H2
ELEVATION OF BOTTOM OF BREACH	FT	YB
EST DEPTH OF FLOW IMMEDIATELY DOWNSTREAM	FT	D
SUBMERGENCE COEFFICIENT		SUB
VELOCITY CORRECTION		VCOR
TOTAL VOLUME DISCHARGED FROM TIME OF BREACH	AC-FT	OUTVOL
BREACH WIDTH FT BB		
RECTANGULAR BREACH DISCHARGE COEFFICIENT		COFR
INFLOW TO RESERVOIR	CFS	QI(I)

RESERVOIR DEPLETION TABLE

I	K	TTP(I)	Q(I)	H2	YB	D	SUB	VCOR	OUTVOL	BB	COFR	QI(I)
***	**	******	********	*******	*******	*******	****	****	*********	****	****	*****
1	0	0.00	1789	5301.50	5301.50	5031.84	1.00	1.00	0.0	0.0	3.10	3580.
2	2	.03	1901	5301.50	5296.27	5032.14	1.00	1.00	3.8	3.0	3.10	3580.
3	3	.05	2419	5301.50	5291.04	5033.23	1.00	1.00	8.3	6.0	3.10	3580.
4	3	.08	3524	5301.50	5285.81	5034.76	1.00	1.00	14.4	9.0	3.10	3580.
5	3	.10	5350	5301.50	5280.58	5036.51	1.00	1.00	23.6	12.0	3.10	3580.
6	3	.13	8007	5301.50	5275.35	5038.35	1.00	1.00	37.4	15.0	3.10	3580.
7	1	.15	11597	5301.50	5270.12	5040.24	1.00	1.00	57.6	18.0	3.10	3580.
8	3	.18	16202	5301.49	5264.89	5042.15	1.00	1.00	86.4	21.0	3.10	3580.
9	3	.20	21903	5301.47	5259.66	5044.07	1.00	1.00	125.7	24.0	3.10	3580.
10	3	.23	28773	5301.45	5254.43	5045.99	1.00	1.00	178.1	27.0	3.10	3580.
11	3	.25	36879	5301.42	5249.20	5047.90	1.00	1.00	245.9	30.0	3.10	3580.
12	3	.28	46282	5301.37	5243.97	5049.81	1.00	1.00	331.8	33.0	3.10	3580.
13	3	.30	57041	5301.32	5238.74	5051.42	1.00	1.00	438.6	36.0	3.10	3580.
14	3	.33	69207	5301.26	5233.51	5053.04	1.00	1.00	569.0	39.0	3.10	3580.
15	3	.35	82830	5301.18	5228.28	5054.73	1.00	1.00	726.0	42.0	3.10	3580.
16	3	.38	97955	5301.09	5223.05	5056.47	1.00	1.00	912.8	45.0	3.10	3580.
17	3	.40	114623	5300.98	5217.82	5058.25	1.00	1.00	1132.4	48.0	3.10	3580.
18	3	.43	132872	5300.85	5212.59	5060.09	1.00	1.00	1388.1	51.0	3.10	3580.
19	3	.45	152736	5300.70	5207.36	5061.97	1.00	1.00	1683.1	54.0	3.10	3580.
20	3	.48	174245	5300.52	5202.13	5063.89	1.00	1.00	2020.9	57.0	3.10	3580.
21	3	.50	197427	5300.33	5196.90	5065.85	1.00	1.00	2404.9	60.0	3.10	3580.
22	3	.53	222303	5300.10	5191.67	5067.85	1.00	1.00	2838.5	63.0	3.10	3580.
23	3	.55	248895	5299.85	5186.44	5069.88	1.00	1.00	3325.3	66.0	3.10	3580.
24	3	.58	277218	5299.57	5181.21	5071.95	1.00	1.00	3868.8	69.0	3.10	3580.
25	3	.60	307284	5299.25	5175.98	5074.04	1.00	1.00	4472.6	72.0	3.10	3580.
26	3	.63	339103	5298.91	5170.75	5076.17	1.00	1.00	5140.4	75.0	3.10	3580.
27	3	.65	372680	5298.52	5165.52	5078.32	1.00	1.00	5875.7	78.0	3.10	3580.
28	3	.68	408015	5298.10	5160.29	5080.50	1.00	1.00	6682.2	81.0	3.10	3580.
29	3	.70	445108	5297.64	5155.06	5082.70	1.00	1.00	7563.5	84.0	3.10	3580.
30	3	.73	483951	5297.13	5149.83	5084.93	1.00	1.00	8523.3	87.0	3.10	3580.
31	3	.75	524534	5296.58	5144.60	5087.17	1.00	1.00	9565.1	90.0	3.10	3580.
32	3	.77	566845	5295.98	5139.37	5089.43	1.00	1.00	10692.6	93.0	3.10	3580.
33	3	.80	610864	5295.34	5134.14	5091.70	1.00	1.00	11909.2	96.0	3.10	3580.
34	3	.82	656570	5294.64	5128.91	5093.99	1.00	1.00	13218.5	99.0	3.10	3580.
35	3	.85	703938	5293.89	5123.68	5096.28	1.00	1.00	14624.0	102.0	3.10	3580.
36	3	.87	752936	5293.08	5118.45	5098.59	1.00	1.00	16129.1	105.0	3.10	3580.
37	3	.90	803532	5292.21	5113.22	5100.90	1.00	1.00	17737.0	108.0	3.10	3580.
38	3	.92	855685	5291.28	5107.99	5103.22	1.00	1.00	19451.1	111.0	3.10	3580.
39	3	.95	909354	5290.29	5102.76	5105.54	1.00	1.00	21274.4	114.0	3.10	3580.
40	3	.97	964492	5289.23	5097.53	5107.87	1.00	1.00	23210.2	117.0	3.10	3580.
41	3	1.00	1021045	5288.11	5092.30	5110.19	1.00	1.00	25261.4	120.0	3.10	3580.
42	3	1.03	1078958	5286.91	5087.07	5112.51	1.00	1.00	27430.8	123.0	3.10	3580.
43	3	1.05	1138170	5285.64	5081.84	5114.83	1.00	1.00	29721.3	126.0	3.10	3580.
44	3	1.08	1198615	5284.29	5076.61	5117.13	1.00	1.00	32135.3	129.0	3.10	3580.
45	3	1.10	1260222	5282.86	5071.38	5119.43	1.00	1.00	34675.4	132.0	3.10	3580.

103	3	2.56	756040	5178.17	5040.00	5096.50	1.00	1.00	178459.3	150.0	3.10	3580.
104	3	2.59	739157	5176.10	5040.00	5095.72	1.00	1.00	180515.2	150.0	3.10	3580.
105	3	2.63	720890	5173.85	5040.00	5094.87	1.00	1.00	182723.5	150.0	3.10	3580.
106	3	2.67	701159	5171.39	5040.00	5093.93	1.00	1.00	185089.4	150.0	3.10	3580.
107	3	2.71	679891	5168.72	5040.00	5092.91	1.00	1.00	187616.9	150.0	3.10	3580.
108	3	2.76	657016	5165.81	5040.00	5091.80	1.00	1.00	190308.3	150.0	3.10	3580.
109	3	2.81	632477	5162.65	5040.00	5090.59	1.00	1.00	193163.8	150.0	3.10	3580.
110	3	2.87	606226	5159.23	5040.00	5089.28	1.00	1.00	196181.2	150.0	3.10	3580.
111	3	2.94	578235	5155.52	5040.00	5087.85	1.00	1.00	199354.9	150.0	3.10	3580.
112	3	3.01	548498	5151.52	5040.00	5086.30	1.00	1.00	202675.9	150.0	3.10	3580.
113	3	3.09	517077	5147.22	5040.00	5084.62	1.00	1.00	206130.7	150.0	3.10	3580.
114	3	3.17	484095	5142.60	5040.00	5082.81	1.00	1.00	209701.3	150.0	3.10	3580.
115	3	3.27	449705	5137.68	5040.00	5080.87	1.00	1.00	213364.6	150.0	3.10	3580.
116	3	3.37	414102	5132.45	5040.00	5078.79	1.00	1.00	217092.2	150.0	3.10	3580.
117	3	3.49	377526	5126.91	5040.00	5076.58	1.00	1.00	220850.0	150.0	3.10	3580.
118	3	3.61	340286	5121.09	5040.00	5074.23	1.00	1.00	224598.1	150.0	3.10	3580.
119	3	3.75	302765	5115.01	5040.00	5071.76	1.00	1.00	228291.6	150.0	3.10	3580.
120	3	3.91	265416	5108.70	5040.00	5069.17	1.00	1.00	231881.4	150.0	3.10	3580.
121	3	4.08	228765	5102.21	5040.00	5066.47	1.00	1.00	235316.0	150.0	3.10	3580.
122	3	4.26	193399	5095.61	5040.00	5063.70	1.00	1.00	238543.4	150.0	3.10	3580.
123	3	4.46	159946	5088.98	5040.00	5060.87	1.00	1.00	241514.8	150.0	3.10	3580.
124	3	4.69	129042	5082.43	5040.00	5058.04	1.00	1.00	244188.0	150.0	3.10	3580.
125	3	4.93	101260	5076.09	5040.00	5055.24	1.00	1.00	246531.4	150.0	3.10	3580.
126	3	5.20	77113	5070.09	5040.00	5052.55	1.00	1.00	248527.9	150.0	3.10	3580.
127	3	5.50	56873	5064.55	5040.00	5050.01	1.00	1.00	250177.6	150.0	3.10	3580.
128	3	5.83	40602	5059.60	5040.00	5047.04	1.00	1.00	251497.8	150.0	3.10	3580.
129	3	6.19	28191	5055.36	5040.00	5044.22	1.00	1.00	252522.6	150.0	3.10	3580.

PARAMETER	UNITS	VARIABLE	VALUE
INITIAL FLOW	CFS	Q(1)	1790.
MAX FLOW	CFS	QM	1649635.
FINAL FLOW	CFS	Q(NU)	28191.
TIME TO MAX FLOW	HRS	TP	1.25
NUMBER OF TIME STEPS		NNU	129
TOTAL VOLUME DISCHARGED FROM RESERVOIR	AC-FT	DISVOL	252523.

46	3	1.13	1322915	5281.35	5066.15	5121.72	1.00	1.00	37343.9	135.0	3.10	3580.
47	3	1.15	1386612	5279.75	5060.92	5124.00	1.00	1.00	40143.0	138.0	3.10	3580.
48	3	1.18	1451228	5278.06	5055.69	5126.25	1.00	1.00	43074.7	141.0	3.10	3580.
49	3	1.20	1516670	5276.28	5050.46	5128.50	1.00	1.00	46140.7	144.0	3.10	3580.
50	3	1.23	1582840	5274.41	5045.23	5130.72	1.00	1.00	49342.7	147.0	3.10	3580.

RESERVOIR DEPLETION TABLE

I	K	TTP(I)	Q(I)	H2	YB	D	SUB	VCOR	OUTVOL	BB	COFR	QI(I)
***	**	******	********	*******	*******	*******	****	****	*********	****	****	*****
51	3	1.25	1649635	5272.44	5040.00	5132.91	1.00	1.00	52682.0	150.0	3.10	3580.
52	3	1.28	1627280	5270.42	5040.00	5129.26	1.00	1.00	56067.3	150.0	3.10	3580.
53	3	1.30	1606037	5268.41	5040.00	5128.58	1.00	1.00	59407.5	150.0	3.10	3580.
54	3	1.33	1584956	5266.41	5040.00	5127.88	1.00	1.00	62704.0	150.0	3.10	3580.
55	3	1.35	1564039	5264.41	5040.00	5127.18	1.00	1.00	65957.0	150.0	3.10	3580.
56	3	1.38	1543284	5262.42	5040.00	5126.48	1.00	1.00	69167.1	150.0	3.10	3580.
57	3	1.40	1522691	5260.43	5040.00	5125.78	1.00	1.00	72334.4	150.0	3.10	3580.
58	3	1.43	1502260	5258.46	5040.00	5125.09	1.00	1.00	75459.4	150.0	3.10	3580.
59	3	1.45	1481989	5256.49	5040.00	5124.39	1.00	1.00	78542.3	150.0	3.10	3580.
60	3	1.48	1461878	5254.52	5040.00	5123.70	1.00	1.00	81583.5	150.0	3.10	3580.
61	3	1.50	1441926	5252.56	5040.00	5123.00	1.00	1.00	84583.3	150.0	3.10	3580.
62	3	1.53	1422133	5250.61	5040.00	5122.31	1.00	1.00	87542.0	150.0	3.10	3580.
63	3	1.55	1402509	5248.67	5040.00	5121.62	1.00	1.00	90460.0	150.0	3.10	3580.
64	3	1.58	1383065	5246.74	5040.00	5120.94	1.00	1.00	93337.7	150.0	3.10	3580.
65	3	1.60	1363806	5244.81	5040.00	5120.25	1.00	1.00	96175.4	150.0	3.10	3580.
66	3	1.63	1344731	5242.90	5040.00	5119.57	1.00	1.00	98973.4	150.0	3.10	3580.
67	3	1.65	1325839	5240.99	5040.00	5118.89	1.00	1.00	101732.3	150.0	3.10	3580.
68	3	1.68	1307130	5239.09	5040.00	5118.22	1.00	1.00	104452.3	150.0	3.10	3580.
69	3	1.70	1288601	5237.21	5040.00	5117.54	1.00	1.00	107133.8	150.0	3.10	3580.
70	3	1.73	1270253	5235.33	5040.00	5116.87	1.00	1.00	109777.3	150.0	3.10	3580.
71	3	1.75	1252084	5233.46	5040.00	5116.20	1.00	1.00	112383.0	150.0	3.10	3580.
72	3	1.78	1234094	5231.60	5040.00	5115.53	1.00	1.00	114951.4	150.0	3.10	3580.
73	3	1.80	1216281	5229.75	5040.00	5114.87	1.00	1.00	117482.8	150.0	3.10	3580.
74	3	1.83	1198645	5227.91	5040.00	5114.20	1.00	1.00	119977.5	150.0	3.10	3580.
75	3	1.85	1181185	5226.08	5040.00	5113.54	1.00	1.00	122436.0	150.0	3.10	3580.
76	3	1.88	1163999	5224.26	5040.00	5112.89	1.00	1.00	124858.6	150.0	3.10	3580.
77	3	1.90	1146788	5222.45	5040.00	5112.23	1.00	1.00	127245.7	150.0	3.10	3580.
78	3	1.93	1129850	5220.65	5040.00	5111.58	1.00	1.00	129597.6	150.0	3.10	3580.
79	3	1.95	1113083	5218.85	5040.00	5110.93	1.00	1.00	131914.7	150.0	3.10	3580.
80	3	1.98	1096489	5217.07	5040.00	5110.28	1.00	1.00	134197.3	150.0	3.10	3580.
81	3	2.00	1080064	5215.30	5040.00	5109.64	1.00	1.00	136445.8	150.0	3.10	3580.
82	3	2.03	1063809	5213.53	5040.00	5108.99	1.00	1.00	138660.5	150.0	3.10	3580.
83	3	2.05	1047723	5211.78	5040.00	5108.35	1.00	1.00	140841.9	150.0	3.10	3580.
84	3	2.08	1031804	5210.03	5040.00	5107.7[illegible]	[illegible]00	1.00	142990.2	150.0	3.10	3580.
85	3	2.10	1016052	5208.29	5040.00	5107.0[illegible]	[illegible]00	1.00	145105.7	150.0	3.10	3580.
[illegible]	3	[illegible]	[illegible]	5204.57	5040.00	5104.45	1.00	1.00	147188.9	150.0	3.10	3580.

TABLE 2

DEFINITIONS OF VARIABLES FOR THE INITIAL CONDITIONS TABLE

I	=	Sequence number of cross section (from upstream to downstream)
K	=	Number of iterations required to solve steady flow equations
X(I)	=	Miles downstream from dam
YD(I)	=	Initial water surface elevation (feet) to be used in simulation
QDI(I)	=	Initial discharge (cfs)
FRD	=	Froude number
SOM	=	Slope of channel bottom (feet/mile) at downstream boundary for subcritical flow or at upstream boundary for supercritical flow.
YNORM(I)	=	Calculated water surface elevation for normal flow conditions

INITIAL CONDITIONS

I	K	X(I)	YD(I)	QDI(I)	FRB	SON
11	3	5.00	4985.12	1789.87	1.00	8.21
11	0	5.00	4986.12	1789.87		
10	3	4.44	4992.19	1789.87	.26	
9	3	3.88	4996.37	1789.87	.34	
8	3	3.32	5001.51	1789.87	.30	
7	3	2.76	5006.29	1789.87	.33	
6	3	2.20	5011.39	1789.87	.33	
5	2	1.76	5015.49	1789.87	.34	
4	3	1.32	5019.75	1789.87	.34	
3	3	.88	5023.99	1789.87	.35	
2	3	.44	5028.27	1789.87	.35	
1	3	0.00	5032.57	1789.87	.35	

I	X(I)	YD(I)	YNORM(I)
1	0.00	5032.57	5032.57
2	.44	5028.27	5028.27
3	.88	5023.99	5023.99
4	1.32	5019.75	5019.75
5	1.76	5015.49	5015.49
6	2.20	5011.39	5011.39
7	2.76	5006.29	5006.29
8	3.32	5001.51	5001.51
9	3.88	4996.37	4996.37
10	4.44	4992.19	4992.19
11	5.00	4986.12	4986.12

TIME PARAMETERS OF OUTFLOW HYDROGRAPH IMMEDIATELY DOWNSTREAM OF DAM

PARAMETER	UNITS	VARIABLE	VALUE
TIME TO FAILURE	HR	TFH	1.250
TIME TO START OF RISING LIMB OF HYDROGRAPH	HR	TFO	0.000
TIME TO PEAK	HR	TP	1.250
TIME STEP SIZE	HR	DTHI	.063

TABLE 3

DEFINITIONS OF VARIABLES FOR DYNAMIC ROUTING OUTPUT (JNK = 4)

TT	=	Time (hours)
DTH	=	Time step (hours)
ITERR	=	Number of iterations required to solve unsteady flow equations
QU(1)	=	Discharge (cfs) at upstream boundary
YU(1)	=	Water surface elevation (feet) at upstream boundary
QU(N)	=	Discharge (cfs) at downstream boundary
YU(N)	=	Water surface elevation (feet) at downstream boundary
FRDM	=	Maximum Froude number in entire routing reach
IFR	=	Sequence number of cross section at which FRDM occurs

```
TT =   0.000        DTH =   .063        ITERR =  0
QU(1) =   1789.87   YU(1) =   5032.57   QU(N) =   1789.87   YU(N) =   4986.12  FRDN= .50   IFR= 11

TT =   0.000        DTH =   .063        ITERR =  2
QU(1) =   1789.87   YU(1) =   5032.56   QU(N) =   2081.50   YU(N) =   4985.32  FRDN=1.00   IFR= 11

TT =   0.000        DTH =   .063        ITERR =  2
QU(1) =   1789.87   YU(1) =   5032.60   QU(N) =   1815.36   YU(N) =   4985.14  FRDN=1.00   IFR= 11

TT =   .063         DTH =   .063        ITERR =  2
QU(1) =   2971.96   YU(1) =   5033.61   QU(N) =   1798.58   YU(N) =   4985.13  FRDN=1.00   IFR= 11

TT =   .125         DTH =   .063        ITERR =  3
QU(1) =   8007.94   YU(1) =   5036.91   QU(N) =   1780.65   YU(N) =   4985.12  FRDN=1.00   IFR= 11

TT =   .188         DTH =   .063        ITERR =  3
QU(1) =   19053.26  YU(1) =   5041.24   QU(N) =   1779.94   YU(N) =   4985.12  FRDN=1.00   IFR= 11

TT =   .250         DTH =   .063        ITERR =  3
QU(1) =   36879.58  YU(1) =   5045.88   QU(N) =   1779.22   YU(N) =   4985.12  FRDN=1.00   IFR= 11

TT =   .313         DTH =   .063        ITERR =  3
QU(1) =   63124.44  YU(1) =   5050.53   QU(N) =   1781.02   YU(N) =   4985.12  FRDN=1.00   IFR= 11

TT =   .375         DTH =   .063        ITERR =  3
QU(1) =   97955.67  YU(1) =   5054.97   QU(N) =   1779.06   YU(N) =   4985.12  FRDN=1.00   IFR= 11

TT =   .438         DTH =   .063        ITERR =  4
QU(1) =   142804.90 YU(1) =   5059.48   QU(N) =   1799.30   YU(N) =   4985.13  FRDN=1.00   IFR= 11

TT =   .500         DTH =   .063        ITERR =  4
QU(1) =   197427.22 YU(1) =   5064.07   QU(N) =   1777.45   YU(N) =   4985.11  FRDN=1.00   IFR= 11

TT =   .563         DTH =   .063        ITERR =  5
QU(1) =   263056.87 YU(1) =   5068.80   QU(N) =   1511.03   YU(N) =   4984.92  FRDN=1.00   IFR= 11
```

TABLE 5

DYNAMIC ROUTING OUTPUT (JHK = 3, 5 or 9)

TT = 5.797 DTH = .063 ITERR = 1
QU(1) = 42259.04 YU(1) = 5049.49 QU(N) = 74642.63 YU(N) = 4995.89 FRDN=1.00 IFR= 11

X(I)	Y	V	A	B	BT	Q	CMN	FKC	WAVHT	DH	FRD	DISVOL
0.00	5049.49	8.81	4796.	392.	392.	42.259	.0400	0.00	16.93	12.2	.4	
.44	5045.00	8.63	5167.	431.	431.	44.593	.0400	0.00	16.71	12.0	.4	
.88	5040.55	8.47	5535.	470.	470.	46.868	.0400	0.00	16.61	11.8	.4	
1.32	5036.16	8.32	5905.	510.	510.	49.154	.0400	0.00	16.33	11.6	.4	
1.76	5031.77	8.22	6266.	550.	550.	51.518	.0400	0.00	16.39	11.4	.4	
2.20	5027.29	8.23	6556.	588.	588.	53.961	.0400	0.00	15.72	11.1	.4	
2.76	5021.88	7.69	7458.	694.	694.	57.386	.0400	0.00	15.85	10.7	.4	
3.32	5016.81	7.36	8339.	794.	794.	61.362	.0400	0.00	14.98	10.5	.4	
3.88	5012.04	7.09	9295.	892.	892.	65.867	.0400	0.00	16.17	10.4	.4	
4.44	5007.88	6.59	10743.	1010.	1010.	70.763	.0400	0.00	15.11	10.6	.4	
5.00	4995.89	14.94	4995.	719.	719.	74.643	.0400	0.00	10.97	6.9	1.0	

X(I) = Miles downstream from dam

V = Mean velocity (feet/second)

A = Effective-flow area (square feet)

B = Top width of effective flow (feet)

BT = Total top width (feet)

Q = Discharge (1000 cfs)

CMN = Composite Manning's n

FKC = Expansion or contraction coefficient

WAVHT = Depth of water above or below initial water surface elevation (feet)

DH = Hydraulic depth, A/B (feet)

FRD = Froude number

PROFILE OF CRESTS AND TIMES FOR TETON
BELOW TETON

RVR MILE FROM DAM	MAX ELEV (FT)	MAX FLOW (CFS)	TIME MAX ELEV(HR)	MAX VEL (FT/SEC)	MAX VEL (MI/HR)	FLOOD ELEV (FT)	TIME FLOOD ELEV (HR)
0.00	5115.37	1608692	1.23	48.31	32.94	0.00	0.00
.44	5109.66	1618659	1.30	43.53	29.68	0.00	0.00
.88	5103.11	1623350	1.30	40.17	27.39	0.00	0.00
1.32	5096.46	1620645	1.36	37.23	25.39	0.00	0.00
1.76	5092.04	1607247	1.36	33.07	22.55	0.00	0.00
2.20	5071.19	1597143	1.30	40.72	27.77	0.00	0.00
2.76	5067.73	1599715	1.36	28.14	19.19	0.00	0.00
3.32	5060.63	1592067	1.42	23.50	16.02	0.00	0.00
3.88	5053.89	1564901	1.42	20.77	14.16	0.00	0.00
4.44	5047.31	1551490	1.42	18.64	12.71	0.00	0.00
5.00	5028.65	1538917	1.42	27.60	18.82	0.00	0.00

1

13

K	TIP(K)	YC(K,I),I=1,NTT)		
1	0.000	5032.57	5011.39	4986.12
2	0.000	5032.56	5011.51	4985.32
3	0.000	5032.60	5011.36	4985.14
4	.063	5033.61	5011.42	4985.13
5	.125	5036.91	5011.40	4985.12
6	.188	5041.24	5011.41	4985.12
7	.250	5045.88	5011.42	4985.12
8	.313	5050.53	5011.30	4985.12
9	.375	5054.97	5012.28	4985.12
10	.438	5059.48	5017.46	4985.13
11	.500	5064.07	5024.10	4985.11
12	.563	5068.80	5030.97	4984.92
13	.594	5071.23	5034.18	4985.63
14	.656	5076.01	5039.38	4985.71
15	.672	5077.21	5040.63	4984.17
16	.703	5077.81	5041.25	4983.40
17	.734	5078.11	5041.56	4983.02
18	.797	5086.15	5046.59	4986.03
19	.859	5091.21	5051.96	4976.36
20	.922	5095.88	5054.69	5003.64

K	TTP(K)	QC(K,I),I=		
*****	********	**********		
1	0.000	1.79	1.79	1.79
2	0.000	1.79	1.74	2.08
3	0.000	1.79	1.85	1.82
4	.063	2.97	1.76	1.80
5	.125	8.01	1.80	1.78
6	.188	19.05	1.78	1.78
7	.250	36.88	1.80	1.78
8	.313	63.12	1.66	1.78
9	.375	97.96	2.98	1.78
10	.438	142.80	15.35	1.80
11	.500	197.43	51.45	1.78
12	.563	263.06	117.10	1.51
13	.594	299.77	157.03	2.61
14	.656	381.51	240.85	2.75
15	.672	403.60	262.63	.72
16	.703	414.64	273.52	-.29
17	.734	420.16	278.97	-.80
18	.797	605.36	392.45	3.38
19	.859	722.31	549.40	81.18
20	.922	849.17	708.69	226.24
21	.984	985.70	845.83	404.81
22	1.047	1130.77	994.55	593.77
23	1.109	1283.73	1153.36	775.15
24	1.172	1443.15	1314.77	953.64
25	1.234	1607.89	1483.64	1136.76
26	1.297	1608.69	1597.14	1316.40
27	1.359	1556.26	1593.13	1464.92
28	1.422	1504.81	1535.92	1538.92
29	1.484	1454.40	1490.44	1536.02
30	1.547	1404.96	1442.79	1503.27
31	1.609	1356.65	1393.11	1468.01
32	1.672	1309.47	1346.43	1427.20
33	1.734	1263.44	1299.51	1382.50
34	1.797	1218.51	1254.32	1338.46
35	1.859	1174.70	1210.08	1294.42
36	1.922	1131.97	1166.97	1250.82
37	1.984	1090.33	1125.05	1208.33
38	2.047	1049.73	1084.12	1166.66
39	2.109	1010.21	1044.32	1126.01
40	2.172	971.70	1005.53	1086.38
41	2.234	934.22	967.79	1047.72
42	2.297	897.74	931.05	1010.07
43	2.359	862.27	895.31	973.40
44	2.422	827.75	860.55	937.69
45	2.484	794.22	826.75	902.94
46	2.547	761.66	793.91	869.13

DISCHARGE HYDROGRAPH FOR TETON ... STATION NUMBER 1
BELOW TETON AT MILE 0.00

GAGE ZERO = 5025.00 MAX ELEVATION REACHED BY FLOOD WAVE = 5115.37
FLOOD STAGE NOT AVAILABLE
MAX STAGE = 90.37 AT TIME = 1.23 HOURS
MAX FLOW = 1608693 AT TIME = 1.30 HOURS

HR	STAGE	FLOW
0.0	7.6	1790
.2	17.2	22619
.4	31.8	115895
.6	46.7	307943
.8	61.4	611210
1.0	76.4	1021967
1.2	88.5	1517283
1.4	88.2	1522819
1.6	85.2	1363900
1.8	82.1	1216318
2.0	78.7	1080181
2.2	75.3	954834
2.4	71.8	839833
2.6	68.2	734746
2.8	64.7	639139
3.0	61.1	552657
3.2	57.6	474841
3.4	54.2	405855
3.6	50.9	344701
3.8	47.7	291523
4.0	44.6	245123
4.2	41.7	204882
4.4	38.9	170397
4.6	36.4	141113
4.8	33.9	116342
5.0	31.7	95348
5.2	29.6	77803
5.4	27.8	63836
5.6	26.1	52033
5.8	24.5	42126

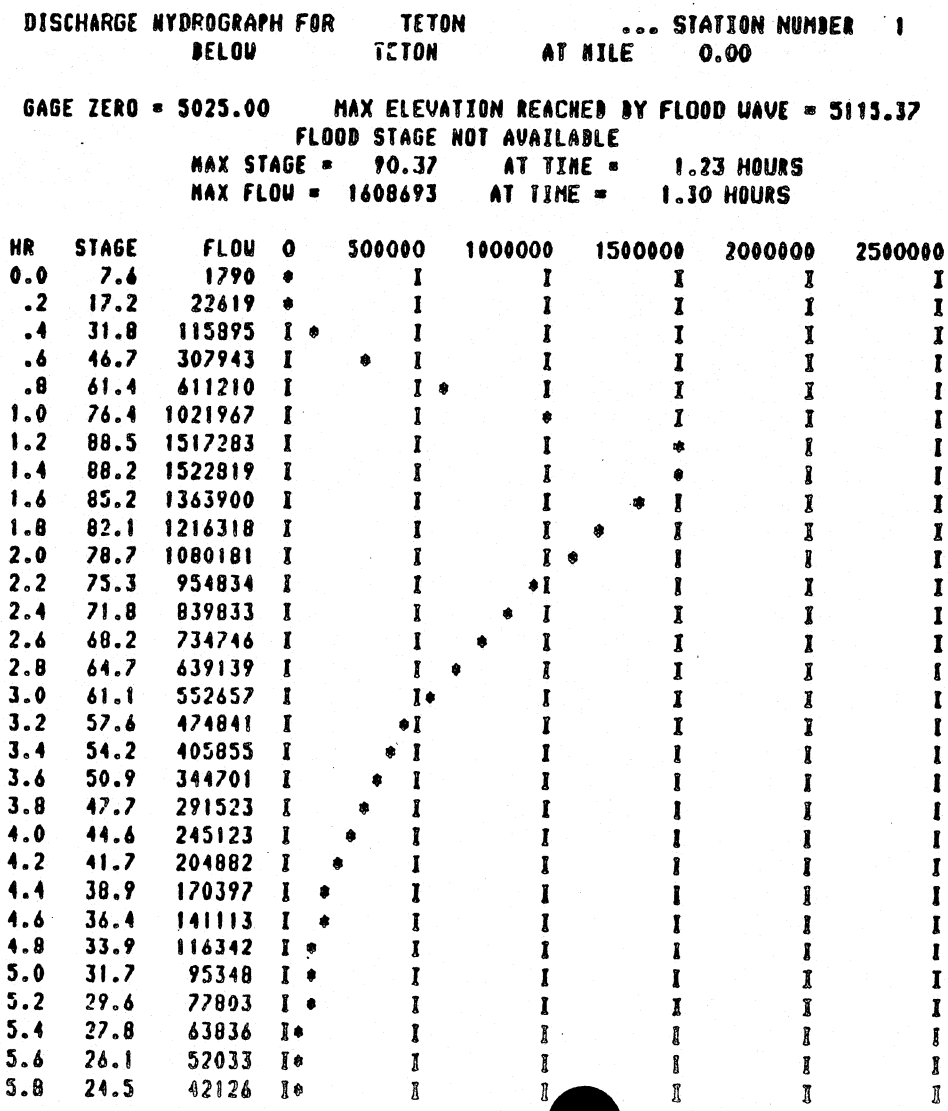

DISCHARGE HYDROGRAPH FOR TETON ... STATION NUMBER 6
BELOW TETON AT MILE 2.20

GAGE ZERO = 5005.00 MAX ELEVATION REACHED BY FLOOD WAVE = 5071.19
FLOOD STAGE NOT AVAILABLE
MAX STAGE = 66.19 AT TIME = 1.30 HOURS
MAX FLOW = 1597144 AT TIME = 1.30 HOURS

HR	STAGE	FLOW	0	500000	1000000	1500000	2000000	2500000
0.0	6.4	1790	*	I	I	I	I	I
.2	6.4	1787	*	I	I	I	I	I
.4	9.4	7927	*	I	I	I	I	I
.6	29.7	165413	I *	I	I	I	I	I
.8	41.9	400293	I *	I	I	I	I	I
1.0	55.9	883009	I	I *	I	I	I	I
1.2	64.3	1390759	I	I	I *	I	I	I
1.4	65.2	1555942	I	I	I	I*	I	I
1.6	64.2	1400566	I	I	I *	I	I	I
1.8	62.9	1252111	I	I	I *	I	I	I
2.0	61.1	1114815	I	I	I *	I	I	I
2.2	59.1	988549	I	I	*	I	I	I
2.4	56.9	872714	I	I *	I	I	I	I
2.6	54.7	766791	I	I *	I	I	I	I
2.8	52.4	670343	I	I *	I	I	I	I
3.0	50.0	582967	I	I *	I	I	I	I
3.2	47.6	504138	I	*	I	I	I	I
3.4	45.2	433850	I	*I	I	I	I	I
3.6	42.8	371534	I *	I	I	I	I	I
3.8	40.5	316790	I *	I	I	I	I	I
4.0	38.3	268926	I *	I	I	I	I	I
4.2	36.1	227306	I *	I	I	I	I	I
4.4	34.0	191303	I *	I	I	I	I	I
4.6	32.0	160344	I *	I	I	I	I	I
4.8	30.1	133929	I *	I	I	I	I	I
5.0	28.3	111678	I *	I	I	I	I	I
5.2	26.6	92964	I *	I	I	I	I	I
5.4	25.1	77098	I *	I	I	I	I	I
5.6	23.7	64051	I*	I	I	I	I	I
5.8	22.3	53827	I*	I	I	I	I	I

DISCHARGE HYDROGRAPH FOR TETON ... STATION NUMBER 11
BELOW TETON AT MILE 5.00

GAGE ZERO = 4982.00 MAX ELEVATION REACHED BY FLOOD WAVE = 5028.65
FLOOD STAGE NOT AVAILABLE
MAX STAGE = 46.65 AT TIME = 1.42 HOURS
MAX FLOW = 1538917 AT TIME = 1.42 HOURS

HR	STAGE	FLOW
0.0	4.1	1790
.2	3.1	1780
.4	3.1	1787
.6	3.6	2622
.8	4.5	7267
1.0	28.4	452052
1.2	39.7	1036044
1.4	46.3	1513018
1.6	45.8	1473303
1.8	44.1	1336261
2.0	42.2	1197913
2.2	40.3	1068992
2.4	38.4	950190
2.6	36.6	841183
2.8	34.8	741565
3.0	33.0	650958
3.2	31.3	568781
3.4	29.6	494714
3.6	27.9	428604
3.8	26.4	370046
4.0	24.8	318428
4.2	23.3	273052
4.4	21.9	233404
4.6	20.6	198924
4.8	19.3	169105
5.0	18.0	143544
5.2	16.9	121868
5.4	15.8	103425
5.6	14.8	87721
5.8	13.9	74455

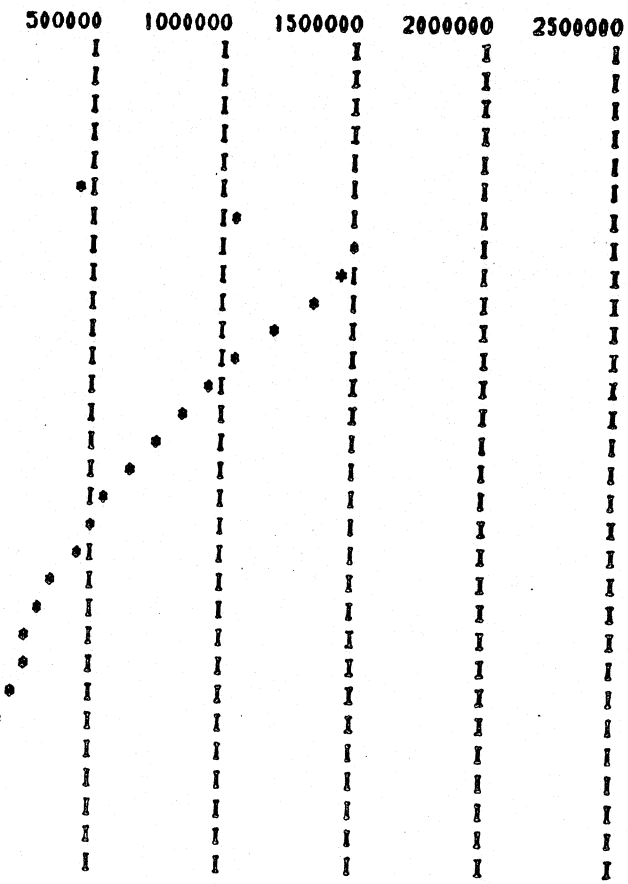

TP = 1.42 TFOO = .17 = 1538917.43 TFH = 1.23

TABLE 1 OU OPTIONS

OUTPUT ITEM	JNK					
	1	2	3	4	5	9
Input Data	X	X	X	X	X	X
Cross Section Properties for all Cross Sections (Linear and Interpolated)		X				
Reservoir Depletion Table (Results of Storage Routing)	X	X	X	X	X	X
Initial Conditions		X		X	X	X
Dynamic Routing Trace Information at Upstream and Downstream Cross Sections				X	X	X
Dynamic Routing Trace Information at Selected Cross Sections			X		X	X
Crest Profile Table (Peak Discharges And Elevations, Travel Times)	X			X	X	X
Dicharge And Elevation Hydrographs (Tabulated for up to Six Cross Sections)				X		X
Printer Plots of Hydrographs for up to Six Cross Sections	X	X	X	X	X	X
Flow Loss Data		X				

DAMBRK: THE NWS DAM-BREAK FLOOD FORECASTING MODEL

D. L. Fread

Office of Hydrology, National Weather Service (NWS)
Silver Spring, Maryland 20910

July 18, 1984

1. INTRODUCTION

Catastrophic flash flooding occurs when a dam is breached and the impounded water escapes through the breach into the downstream valley. Usually the response time available for warning is much shorter than for precipitation-runoff floods. Dam failures are often caused by overtopping of the dam due to inadequate spillway capacity during large inflows to the reservoir from heavy precipitation runoff. Dam failures may also be caused by seepage or piping through the dam or along internal conduits, slope embankment slides, earthquake damage and liquefaction of earthen dams from earthquakes, and landslide-generated waves within the reservoir. Middlebrooks (1952) describes earthen dam failures occurring within the U.S. prior to 1951. Johnson and Illes (1976) summarize 300 dam failures throughout the world.

The potential for catastrophic flooding due to dam failures has recently been brought to the Nation's attention by several dam failures such as the Buffalo Creek coal-waste dam, the Toccoa Dam, the Teton Dam, and the Laurel Run Dam. A report by the U.S. Army (1975) gives an inventory of the Nation's approximately 50,000[a] dams with heights greater than 25 ft. or storage volumes in excess of 50 acre-ft. The report also classifies some 20,000 of these as being "so located that failure of the dam could result in loss of human life and appreciable property damage..."

The National Weather Service (NWS) has the responsibility to advise the public of downstream flooding when there is a failure of a dam. Although this type of flood has many similarities to floods produced by precipitation runoff, the dam-break flood has some very important differences which make it difficult to analyze with the common techniques which have worked so well for the precipitation-runoff floods. To aid NWS flash flood hydrologists who are called upon to forecast the

[a]Superseded by April 1981 Corps of Engineers National Non-Federal Dam Inventory (66,804) and an additional 3,000 Federal dams.

downstream flooding (flood inundation information and warning times) resulting from dam-failures, a numerical model (DAMBRK) has been recently developed. Herein is presented an outline of the model's theoretical basis, its predictive capabilities, and ways of utilizing the model for forecasting of dam-break floods. The DAMBRK model may also be used for a multitude of purposes by planners, designers, and analysts who are concerned with possible future or historical flood inundation mapping due to dam-break floods and/or reservoir spillway floods, or any specified flood hydrograph.

2. MODEL DEVELOPMENT

The DAMBRK model attempts to represent the current state-of-the-art in understanding of dam failures and the utilization of hydrodynamic theory to predict the dam-break wave formation and downstream progression. The model has wide applicability; it can function with various levels of input data ranging from rough estimates to complete data specification; the required data is readily accessible; and it is economically feasible to use, i.e., it requires a minimal computation effort on large computing facilities.

The model consists of three functional parts, namely: (1) description of the dam failure mode, i.e., the temporal and geometrical description of the breach; (2) computation of the time history (hydrograph) of the outflow through the breach as affected by the breach description, reservoir inflow, reservoir storage characteristics, spillway outflows, and downstream tailwater elevations; and (3) routing of the outflow hydrograph through the downstream valley in order to determine the changes in the hydrograph due to valley storage, frictional resistance, downstream bridges or dams, and to determine the resulting water surface elevations (stages) and flood-wave travel times.

DAMBRK is an expanded version of a practical operational model first presented in 1977 by the author (Fread, 1977). That model was based on previous work by the author on modeling breached dams (Fread and Harbaugh, 1973) and routing of flood waves (Fread, 1974, 1976). There have been a number of other operational dam-break models that have appeared recently in the literature, e.g., Price, et al. (1977), Gundlach and Thomas (1977), Thomas (1977), Keefer and Simons (1977), Chen and Druffel (1977) Balloffet, et al. (1974), Balloffet (1977), Brown and Rogers (1977), Rajar (1978), Brevard and Theurer (1979). DAMBRK differs from each of these models in the treatment of the breach formation, the outflow hydrograph generation, and the downstream flood routing.

2.1 Breach Description

The breach is the opening formed in the dam as it fails. The actual failure mechanics are not well understood for either earthen or concrete dams. In previous attempts to predict downstream flooding due to dam failures, it was usually assumed that the dam failed completely and instantaneously. Investigators of dam-break flood waves such as

Ritter (1892), Schocklitsch (1917), Re (1946), Dressler (1954), Stoker (1957), Su and Barnes (1969), and Sakkas and Strelkoff (1973) assumed the breach encompasses the entire dam and that it occurs instantaneously. Others, such as Schocklitsch (1917) and Army Corps of Engineers (1960), have recognized the need to assume partial rather than complete breaches; however, they assumed the breach occurred instantaneously. The assumptions of instantaneous and complete breaches were used for reasons of convenience when applying certain mathematical techniques for analyzing dam-break flood waves. These assumptions are somewhat appropriate for concrete arch-type dams, but they are not appropriate for earthen dams and concrete gravity-type dams.

Earthen dams which exceedingly outnumber all other types of dams do not tend to completely fail, nor do they fail instantaneously. The fully formed breach in earthen dams tends to have an average width ($\bar{b}$) in the range ($h_d < \bar{b} < 3h_d$) where h_d is the height of the dam. The middle portion of this range for $\bar{b}$ is supported by the summary report of Johnson and Illes (1976). Breach widths for earthen dams are therefore usually much less than the total length of the dam as measured across the valley. Also, the breach requires a finite interval of time for its formation through erosion of the dam materials by the escaping water. Total time of failure may be in the range of a few minutes to a few hours, depending on the height of the dam, the type of materials used in construction, the extent of compaction of the materials, and the extent (magnitude and duration) of the overtopping flow of the escaping water. Piping failures occur when initial breach formation takes place at some point below the top of the dam due to erosion of an internal channel through the dam by escaping water. As the erosion proceeds, a larger and larger opening is formed; this is eventually hastened by caving-in of the top portion of the dam.

Concrete gravity dams also tend to have a partial breach as one or more monolith sections formed during the construction of the dam are forced apart by the escaping water. The time for breach formation is in the range of a few minutes.

Poorly constructed earthen dams and coal-waste slag piles which impound water tend to fail within a few minutes, and have average breach widths in the upper range or even greater than those for the earthen dams mentioned above.

Cristofano (1965) attempted to model the partial, time-dependent breach formation in earthen dams; however, this procedure requires critical assumptions and specification of unknown critical parameter values. Also, Harris and Wagner (1967) used a sediment transport relation to determine the time for breach formation, but this procedure requires specification of breach size and shape in addition to two critical parameters for the sediment transport relation.

For reasons of simplicity, generality, wide applicability, and the uncertainty in the actual failure mechanism, the NWS DAMBRK model allows the forecaster to input the failure time interval (τ) and the terminal

size and shape of the breach (Fread and Harbaugh, 1973). The shape (see Fig. 1) is specified by a parameter (z) identifying the side slope of the breach, i.e., 1 vertical: z horizontal slope. The range of z values is: $0 < z < 2$. Rectangular triangular, or trapezoidal shapes may be specified in this way. For example, Z=0 and b>0 produces a trapezoidal shape. The final breach size is controlled by the z parameter and another parameter (b) which is the terminal width of the bottom of the breach. As shown in Fig. 1, the model assumes the breach bottom width starts at a point and enlarges at a linear rate over the failure time interval (τ) until the terminal width is attained and the breach bottom has eroded to the elevation h_{bm} which is usually, but not necessarily, the bottom of the reservoir or outlet channel bottom. If τ is less than 10 minutes, the width of the breach bottom starts at a value of b rather than at a point. This represents more of a collapse failure than an erosion failure.

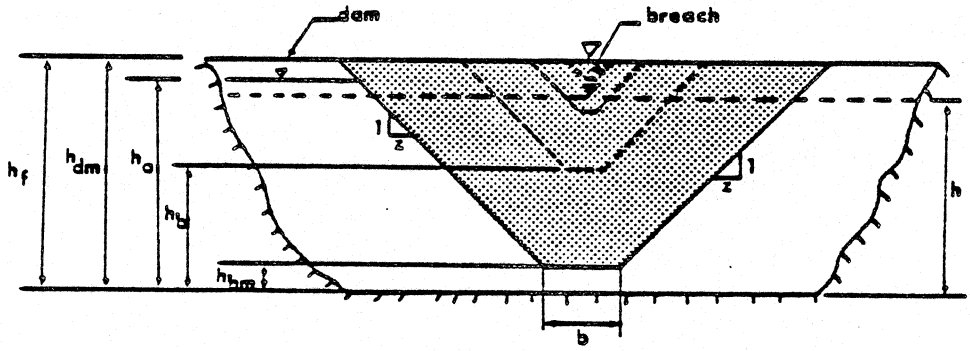

Fig.1- FRONT VIEW OF DAM SHOWING FORMATION OF BREACH

During the simulation of a dam failure, the actual breach formation commences when the reservoir water surface elevation (h) exceeds a specified value, h_f. This feature permits the simulation of an over-topping of a dam in which the breach does not form until a sufficient amount of water is flowing over the crest of the dam. A piping failure may be simulated when h_f is specified less than the height of the dam, h_d.

Selection of breach parameters before a breach forms, or in the absence of observations, introduces a varying degree of uncertainty in the model results; however, errors in the breach description and thence in the resulting time rate of volume outflow are rapidly damped-out as the flood wave advances downstream. For conservative forecasts which err on the side of larger flood waves, values for b and z should produce an average breach width ($\bar{b}$) in the uppermost range for a certain type of dam. Failure time (τ) should be selected in the lower range to produce a maximum outflow. Of course, observational estimates of $\bar{b}$ and τ should be used when available to update forecasts when response time is sufficient as in the case of forecast points several miles downstream of

the structure. Flood wave travel rates are often in the range of 2-10 miles per hour. Accordingly, response times for some downstream forecast points may therefore be sufficient for updated forecasts to be issued.

2.2 Reservoir Outflow Hydrograph

The total reservoir outflow consists of broad-crested weir flow through the breach and flow through any spillway outlets, i.e.,

$$Q = Q_b + Q_s \tag{1}$$

The breach outflow (Q_b) is computed as:

$$Q_b = c_1(h-h_b)^{1.5} + c_2)h-h_b)^{2.5} \tag{2}$$

where:

$$c_1 = 3.1\ b_i\ c_v\ k_s \tag{3}$$

$$c_2 = 2.45\ z\ c_v\ k_s \tag{4}$$

$$h_b = h_d - (h_d - h_{bm})\ \frac{t_b}{\tau} \qquad \text{if} \qquad t_b < \tau \tag{5}$$

$$h_b = h_{bm} \qquad \text{if} \qquad t_b > \tau \tag{6}$$

$$b_i = b\ t_b/\tau \qquad \text{if} \qquad t_b < \tau \tag{7}$$

$$c_v = 1.0 + 0.023\ Q^2/[B_d^2\ (h-h_{bm})^2\ (h-h_b)] \tag{8}$$

$$k_s = 1.0 \qquad \text{if} \qquad \frac{h_t - h_b}{h - h_b} < 0.67 \tag{9}$$

otherwise:

$$k_s = 1.0 - 27.8\ \left[\frac{h_t - h_b}{h - h_b} - 0.67\right]^3 \tag{10}$$

in which h_b is the elevation of the breach bottom, h is the reservoir water surface elevation, b_i is the instantaneous breach bottom width, t_b is time interval since breach started forming, c_v is correction for velocity of approach (Brater, 1959), Q is the total outflow from the reservoir, B_d is width of the reservoir at the dam, k_s is the submergence correction for tailwater effects on weir outflow (Benard, 1954),

and h_t is the tailwater elevation (water surface elevation immediately downstream of dam).

The tailwater elevation (h_t) is computed from Manning's equation, i.e.,

$$Q = \frac{1.49}{n} S^{1/2} \frac{A^{5/3}}{B^{2/3}} \tag{11}$$

in which n is the Manning roughness coefficient, A is the cross-sectional area of flow, B is the top width of the wetted cross-sectional area, and S is the energy slope. Each term in Eq. (11) applies to a representative channel reach immediately downstream of the dam. The S parameter can be specified by the user; it does not change with time; if it is not specified, the model uses the channel bottom slope of the first third of the downstream valley reach. Since A and B are functions of h_t and Q is the total discharge given by Eq. (1), Eq. (11) provides a sufficiently accurate value for h_t if there are no backwater effects immediately below the dam due to downstream constrictions, dams, bridges, or significant tributary inflows. When these affect the tailwater, Eq. (11) is not used and another procedure, referred to herein as the "simultaneous method," which is described in a following section on multiple dams and bridges is used.

If the breach is formed by piping, Eq. (2)-(9) are replaced by the following orifice flow equation:

$$Q_b = 4.8\ A_p(h-\bar{h})^{1/2} \tag{12}$$

where:

$$A_p = [2b_i+4z(h_f-h_b)]\ (h_f-h_b) \tag{13}$$

$$\bar{h} = h_t \qquad \text{if} \qquad h_t < 2h_f - h_b \tag{14}$$

$$\bar{h} = h_t \qquad \text{if} \qquad h_t > 2h_f - h_b \tag{15}$$

and h_d is replaced by h_f in Eq. (5) to compute h_b.

However, if $\bar{h} = h_f$ and

$$h - h_b < 2.2(h_f-h_b) \tag{16}$$

the flow ceases to be orifice flow and the broad-crested weir flow, Eq. (2), is used.

The spillway outflow (Q_s) is computed as:

$$Q_s = c_s L_s (h-h_s)^{1.5} + c_g A_g (h-h_g)^{0.5} + c_d L_d (h-h_d)^{1.5} + Q_t \qquad (17)$$

in which c_s is the uncontrolled spillway discharge coefficient, h_s is the uncontrolled spillway crest elevation, c_g is the gated spillway discharge coefficient, h_g is the center-line elevation of the gated spillway, c_d is the discharge coefficient for flow over the crest of the dam L_s is the spillway length, A_g is the gate flow area, L_d is the length of the dam crest less L_s, and Q_t is a constant outflow term which is head independent. The uncontrolled spillway flow or the gated spillway flow can also be represented as a table of head-discharge values. The gate flow may also be specified as a function of time.

The total outflow is a function of the water surface elevation (h). Depletion of the reservoir storage volume by the outflow causes a decrease in h which then causes a decrease in Q. However, any inflow to the reservoir tends to increase h and Q. In order to determine the total outflow (Q) as function of time, the simultaneous effects of reservoir storage characteristics and reservoir inflow require the use of a reservoir routing technique. DAMBRK utilizes a hydrologic storage routing technique based on the law of conservation of mass, i.e.,

$$I - Q = dS/dt \qquad (18)$$

in which I is the reservoir inflow, Q is the total reservoir outflow, and dS/dt is the time rate of change of reservoir storage volume. Eq. (18) may be expressed in finite difference form as:

$$(I+I')/2 - (Q+Q')/2 = \Delta S/\Delta t \qquad (19)$$

in which the prime (') superscript denotes values at the time $t-\Delta t$ and the Δ approximates the differential. The term ΔS may be expressed as:

$$\Delta S = (A_s+A_s') (h-h')/2 \qquad (20)$$

in which A_s is the reservoir surface area coincident with the elevation (h).

Combining Eqs. (1), (2), (17), (19) and (20) result in the following expression:

$$(A_s+A_s') (h-h')/\Delta t + c_1(h-h_b)^{1.5} + c_2(h-h_b)^{2.5} + c_s(h-h_b)^{1.5}$$

$$+ c_g(h-h_g)^{0.5} + c_d(h-h_d)^{1.5} + Q_t + Q' - I - I' = 0 \qquad (21)$$

Since A_s is a function of h and all other terms except h are known, Eq. (21) can be solved for the unknown h using Newton-Raphson iteration.

Having obtained h, usually within two or three iterations, Eq. (2) and (17) can be used to obtain the total outflow (Q) at time (t). In this way the outflow hydrograph Q(t) can be developed for each time (t) as t goes from zero to some terminating value (t_e) sufficiently large for the reservoir to be drained. In Eq. (21) the time step (Δt) is chosen sufficiently small to incur minimal numerical integration error. This value is preset in the model to $\tau/50$.

The hydrologic storage routing technique, Eq. (18), implies that the water surface elevation within the reservoir is level. This assumption is quite adequate for gradually occurring breaches with no substantial reservoir inflow hydrographs. However, when 1) the breach is specified to form almost instantaneously so as to produce a negative wage within the reservoir, and/or 2) the reservoir inflow hydrograph is significant enough to produce a positive wave progressing through the reservoir, a routing technique which simulates the negative and/or positive wave(s) occurring within the reservoir could be used for greater accuracy in computing the reservoir outflow through the breach and/or spillways. Such a technique is referred to as dynamic routing. Since this technique is used for routing the dam-break flood wave through the downstream valley, the application of it in lieu of reservoir storage routing will be presented after the downstream routing technique is presented.

2.3 Downstream Routing

After computing the hydrograph of the reservoir outflow, the extent of and time of occurrence of flooding in the downstream valley is determined by routing the outflow hydrograph through the valley. The hydrograph is modified (attenuated, lagged, and distorted) as it is routed through the valley due to the effects of valley storage, frictional resistance to flow, flood wave acceleration components, and downstream obstructions and/or flow control structures. Modifications to the dam-break flood wave are manifested as attenuation of the flood peak elevation, spreading-out or dispersion of the flood wave volume, and changes in the celerity (translation speed) or travel time of the flood wave. If the downstream valley contains significant storage volume such as a wide flood plain, the flood wave can be extensively attenuated and its time of travel greatly increased. Even when the downstream valley approaches that of a uniform rectangular-shaped section, there is appreciable attenuation of the flood peak and reduction in the wave celerity as the wave progresses through the valley.

A distinguishing feature of dam-break waves is the great magnitude of the peak discharge when compared to runoff-generated flood waves having occurred in the past in the same valley. The dam-break flood is usually many times greater than the runoff flood of record. The above-record discharges make it necessary to extrapolate certain coefficients used in various flood routing techniques and make it impossible to fully calibrate the routing technique.

Another distinguishing characteristic of dam-break floods is the very short duration time, and particularly the extremely short time from beginning of rise until the occurrence of the peak. The time to peak is in almost all instances synonymous with the breach formation time (τ) and therefore is in the range of a few minutes to a few hours. This feature, coupled with the great magnitude of the peak discharge, causes the dam-break flood wave to have acceleration components of a far greater significance than those associated with a runoff-generated flood wave.

There are two basic types of flood routing methods, the hydrologic and the hydraulic methods. The hydrologic methods are more of an approximate analysis of the progression of a flood wave through a river reach than are the hydraulic methods. The hydrologic methods are used for reasons of convenience and economy. They are most appropriate as far as accuracy is concerned when the flood wave is not rapidly varying, i.e., the flood wave acceleration effects are negligible compared to the effects of gravity and channel friction. Also, they are best used when the flood waves are very similar in shape and magnitude to previous flood waves for which stage and discharge observations are available for calibrating the hydrologic routing parameters (coefficients).

For routing dam-break flood waves, a particular hydraulic method known as the dynamic wave method is chosen. This choice is based on its ability to provide more accuracy in simulating the dam-break flood wave than that provided by the hydrologic methods, as well as other hydraulic methods such as the kinematic wave and diffusion wave methods. Of the many available hydrologic and hydraulic routing techniques, only the dynamic wave method accounts for the acceleration effects associated with the dam-break waves and the influence of downstream unsteady backwater effects produced by channel constrictions, dams, bridge-road embankments, and tributary inflows. Also, the dynamic wave method can be used economically, i.e., the computational costs can be made insignificant if advantages of certain numerical solution techniques are utilized.

The dynamic wave method based on the complete equations of unsteady flow is used to route the dam-break flood hydrograph through the downstream valley. This method is derived from the original equations developed by Barre De Saint-Venant (1871). The only coefficient that must be extrapolated beyond the range of past experience is the coefficient of flow resistance. It so happens that this is usually not a sensitive parameter in effecting the modifications of the flood wave due to its progression through the downstream valley. The applicability of Saint-Venant equations to simulate abrupt waves such as the dam-break wave has been demonstrated by Terzidis and Strelkoff (1970) and by Martin and Zovne (1971) who used a "through computation" method which ignores the presence of shock waves. DAMBRK uses the "through computation" method as opposed to isolating a single shock wave should it occur, and then applying the shock equations to it and using the Saint-Venant equations for all other portions of the flow.

The Saint-Venant unsteady flow equations consist of a conservation of mass equation, i.e.,

$$\frac{\partial Q}{\partial x} + \frac{\partial (A+A_o)}{\partial t} - q = 0 \tag{22}$$

and a conservation of momentum equation, i.e.,

$$\frac{\partial Q}{\partial x} + \frac{\partial (Q^2/A)}{\partial x} + gA(\frac{\partial h}{\partial x} + S_f + S_e) = 0 \tag{23}$$

where A is the active cross-sectional area of flow, A_o is the inactive (off-channel storage) cross-sectional area, x is the longitudinal distance along the channel (valley), t is the time, q is the lateral inflow or outflow per linear distance along the channel (inflow is positive and outflow is negative in sign), g is the acceleration due to gravity, S_f is the friction slope, and S_e is the expansion-contraction slope. The friction slope is evaluated from Manning's equation for uniform, steady flow, i.e.,

$$S_f = \frac{n^2 |Q| Q}{2.21\ A^2\ R^{4/3}} \tag{24}$$

in which n is the Manning coefficient of frictional resistance and R is the hydraulic radius defined as A/B where B is the top width of the active cross-sectional area. The term (S_e) is defined as follows:

$$S_e = \frac{k\ \Delta(Q/A)^2}{2g\ \Delta x} \tag{25}$$

in which k (Morris and Wiggert, 1972) is the expansion-contraction coefficient varying from 0.0 to ±1.0 (+ if contraction, - if expansion), and $\Delta(Q/A)^2$ is the difference in the term $(Q/A)^2$ at two adjacent cross-sections separated by a distance Δx. L is the momentum effect of lateral flow assumed herein to enter or exit perpendicular to the direction of the main flow. This term has the following form: 1) lateral inflow, L = 0; 2) seepage lateral outflow, L = -0.5qQ/A; and 3) bulk lateral outflow, L = -qQ/A.

Eqs. (22)-(23) were modified by the author (Fread, 1975, 1976) and Smith (1978) to better account for the differences in flood wave properties for flow occurring simultaneously in the river channel and the overbank flood plain of the downstream valley. As modified, Eqs. (22)-(23) become:

$$\frac{\partial (K_c Q)}{\partial x_c} + \frac{\partial (K_\ell Q)}{\partial x_\ell} + \frac{\partial (K_r Q)}{\partial x_r} + \frac{\partial A}{\partial t} - q = 0 \tag{26}$$

$$\frac{\partial Q}{\partial t} + \frac{\partial(K_c^2 Q^2/A_c)}{\partial x_c} + \frac{\partial(K_\ell^2 Q^2/A_\ell)}{\partial x_\ell} + \frac{\partial(K_r^2 Q^2/A_r)}{\partial x_r} + gA_c \left[\frac{\partial h}{\partial x_c} + S_{fc} + S_e\right] + gA_\ell \left[\frac{\partial h}{\partial x_\ell} + S_{f\ell}\right] + gA_r \left[\frac{\partial h}{\partial x_r} + S_{fr}\right] = 0 \tag{27}$$

in which the subscripts (c), (ℓ), and (r) represent the channel, left flood-plain, and right flood-plain sections, respectively. The parameters (K_c, K_ℓ, K_r) proportion the total flow (Q) into channel flow, left flood-plain flow, and right flood-plain flow, respectively. These are defined as follows:

$$K_c = \frac{1}{1+k_\ell+k_r} \tag{28}$$

$$K_\ell = \frac{k_\ell}{1+k_\ell+k_r} \tag{29}$$

$$K_r = \frac{k_r}{1+k_\ell+k_r} \tag{30}$$

in which

$$k_\ell = \frac{Q_\ell}{Q_c} = \frac{n_c}{n_\ell}\frac{A_\ell}{A_c}\left[\frac{R_\ell}{R_c}\right]^{2/3}\left[\frac{\Delta x_c}{\Delta x_\ell}\right]^{1/2} \tag{31}$$

$$k_r = \frac{Q_r}{Q_c} = \frac{n_c}{n_r}\frac{A_r}{A_c}\left[\frac{R_r}{R_c}\right]^{1/2}\left[\frac{\Delta x_c}{\Delta x_r}\right]^{1/2} \tag{32}$$

Eqs. (31)-(32) represent the ratio of flow in the channel section to flow in the left and right flood-plain (overbank) sections, where the flows are expressed in terms of the Manning equation in which the energy slope is approximated by the water surface slope ($\Delta h/\Delta x$).

The friction slope terms in Eq. (27) are given by the following:

$$S_{fc} = \frac{n_c^2 |K_c Q| K_c Q}{2.21\, A_c^2 R_c^{4/3}} \tag{33}$$

$$S_{f\ell} = \frac{n_\ell^2 |K_\ell Q| K_\ell Q}{2.21\, A_\ell^2 R_\ell^{4/3}} \tag{34}$$

$$S_{fr} = \frac{n_r^2 |K_r Q| K_r Q}{2.21\, A_r^2 R_r^{4/3}} \tag{35}$$

In Eq. (26), the term A is the total cross-sectional area, i.e.,

$$A = A_c + A_\ell + A_r + A_o \tag{36}$$

where A_o is the off-channel storage (inactive) area.

Eqs. (22)-(23) and (26)-(27) constitute a system of partial differential equations of the hyperbolic type. They contain two independent variables, x and t, and two dependent variables, h and Q; the remaining terms are either functions of x, t, h, and/or Q, or they are constants. These equations are not amenable to analytical solutions except in cases where the channel geometry and boundary conditions are uncomplicated and the non-linear properties of the equations are either neglected or made linear. The equations may be solved numerically by performing two basic steps. First, the partial differential equations are represented by a corresponding set of finite difference algebraic equations; and second, the system of algebraic equations is solved in conformance with prescribed initial and boundary conditions.

Eqs. (22)-(23) and (26)-(27) can be solved by either explicit or implicit finite difference techniques (Liggett and Cunge, 1975). Explicit methods, although simpler in application, are restricted by mathematical stability considerations to very small computational time steps (on the order of a few minutes or even seconds). Such small time steps cause the explicit methods to be very inefficient in the use of computer time. Implicit finite difference techniques (Preissmann, 1961; Amein and Fang, 1970; Strelkoff, 1970), however, have no restrictions on the size of the time step due to mathematical stability; however, convergence considerations may require its size to be limited (Fread, 1974a).

Of the various implicit schemes that have been developed, the "weighted four-point" scheme first used by Preissmann(1961), and more recently by Chaudhry and Contractor (1973) and Fread (1974b, 1978) appears most advantageous since it can readily be used with unequal distance steps and its stability-convergence properties can be easily controlled. In the weighted four-point implicit finite difference scheme, the continuous x-t region in which solutions of h and Q are sought, is represented by a rectangular net of discrete points. The net points are determined by the intersection of lines drawn parallel to the x and t axes. Those parallel to the x axis represent time lines; they have a spacing of Δt, which also need not be constant. Each point in the rectangular network can be identified by a subscript (i) which designates the x position and a superscript (j) which designates the time line.

The time derivatives are approximated by a forward difference quotient centered between the ith and i+1 points along the x axis, i.e.,

$$\frac{\partial K}{\partial t} = \frac{K_i^{j+1} + K_{i+1}^{j+1} - K_i^j - K_{i+1}^j}{2\ \Delta t_j} \tag{37}$$

where K represents any variable.

The spatial derivatives are approximated by a forward difference quotient positioned between two adjacent time lines according to weighting factors of Θ and $1-\Theta$, i.e.,

$$\frac{\partial K}{\partial x} = \Theta \left[\frac{K_{i+1}^{j+1} - K_i^{j+1}}{\Delta x_i}\right] + (1-\Theta) \left[\frac{K_{i+1}^{j} - K_i^{j}}{\Delta x_i}\right] \tag{38}$$

Variables other than derivatives are approximated at the time level where the spatial derivatives are evaluated by using the same weighting factors, i.e.,

$$K = \Theta \left[\frac{K_i^{j+1} + K_{i+1}^{j+1}}{2}\right] + (1-\Theta) \left[\frac{K_i^{j} + K_{i+1}^{j}}{2}\right] \tag{39}$$

A Θ weighting factor of 1.0 yields the fully implicit or backward difference scheme used by Baltzer and Lai (1968). A weighting factor of 0.5 yields the box scheme used by Amein and Fang (1970). The influence of the Θ weighting factor on the accuracy of the computations was examined by Fread (1974a), who concluded that the accuracy decreases as Θ departs from 0.5 and approaches 1.0. This effect becomes more pronounced as the magnitude of the computational time step increases. Usually, a weighting factor of 0.60 is used so as to minimize the loss of accuracy associated with greater values while avoiding the possibility of a weak or pseudo instability noticed by Baltzer and Lai (1968), and Chaudhry and Contractor (1973); however, Θ may be specified other than 0.60 in the data input to the DAMBRK model.

When the finite difference operators defined by Eqs. (37)-(39) are used to replace the derivatives and other variables in Eqs. (22)-(23), the following weighted four-point implicit difference equations are obtained:

$$\Theta \left[\frac{Q_{i+1}^{j+1} - Q_i^{j+1}}{\Delta x_i}\right] - \Theta\, q_i^{j+1} + (1-\Theta) \left[\frac{Q_{i+1}^{j} - Q_i^{j}}{\Delta x_i}\right] - (1-\Theta)\, q_i^{j}$$

$$+ \left[\frac{(A+A_o)_i^{j+1} + (A+A_o)_{i+1}^{j+1} - (A+A_o)_i^{j} - (A+A_o)_{i+1}^{j}}{2\Delta t_j}\right] = 0 \tag{40}$$

$$\left(\frac{Q_i^{j+1} + Q_{i+1}^{j+1} - Q_i^{j} - Q_{i+1}^{j}}{2\Delta t_j}\right) + \Theta \left[\frac{(Q^2/A)_{i+1}^{j+1} - (Q^2/A)_i^{j+1}}{\Delta x_i} + g\,\bar{A}^{j+1}\right.$$

$$\left.\left(\frac{h_{i+1}^{j+1} - h_i^{j+1}}{\Delta x_i} + \bar{S}_f^{j+1} + S_{ce}^{j+1}\right)\right] + (1-\Theta) \left[\frac{(Q^2/A)_{i+1}^{j} - (Q^2/A)_i^{j}}{\Delta x_i}\right.$$

$$\left. + g\,\bar{A}^{j} \left(\frac{h_{i+1}^{j} - h_i^{j}}{\Delta x_i} + \bar{S}_f^{j} + S_{ce}^{j}\right)\right] = 0 \tag{41}$$

where:

$$\bar{A} = (A_i + A_{i+1})/2 \tag{42}$$

$$\bar{S}_f = n^2 \bar{Q}|\bar{Q}|/(2.2 \bar{A}^2 \bar{R}^{4/3}) \tag{43}$$

$$\bar{Q} = (Q_i + Q_{i+1})/2 \tag{44}$$

$$\bar{R} = \bar{A}/\bar{B} \tag{45}$$

$$\bar{B} = (B_i + B_{i+1})/2 \tag{46}$$

The terms associated with the jth time line are known from either the initial conditions or previous computations. The initial conditions refer to values of h and Q at each node along the x axis for the first time line (j=1).

Eqs. (40)-(41) cannot be solved in an explicit or direct manner for the unknowns since there are four unknowns and only two equations. However, if Eqs. (40)-(41) are applied to each of the (N-1) rectangular grids between the upstream and downstream boundaries, a total of (2N-2) equations with 2N unknowns can be formulated. (N denotes the total number of nodes). Then, prescribed boundary conditions, one at the upstream boundary and one at the downstream boundary, provide the necessary two additional equations required for the system to be determinate. The resulting system of 2N non-linear equations with 2N unknowns is solved by a functional iterative procedure, the Newton-Raphson method (Amein and Fang, 1970).

Computations for the iterative solution of the non-linear system are begun by assigning trial values to the 2N unknowns. Substitution of the trial values into the system of non-linear equations yields a set of 2N residuals. The Newton-Raphson method provides a means for correcting the trial values until the residuals are reduced to a suitable tolerance level. This is usually accomplished in one or two iterations through use of linear extrapolation for the first trial values. If the Newton-Raphson corrections are applied only once, i.e., there is no iteration, the non-linear system of difference equations degenerates to the equivalent of a quasi-linear formulation which may require smaller time steps than the non-linear formulation for the same degree of numerical accuracy.

A system of 2N x 2N linear equations relates the corrections to the residuals and to a Jacobian coefficient matrix composed of partial derivatives of each equation with respect to each unknown variable in that equation. The coefficient matrix of the linear system has a banded

structure which allows the system to be solved by a compact quad-diagonal Gaussian elimination algorithm (Fread, 1971), which is very efficient with respect to computing time and storage. The required storage is 2N x 4 and the required number of computational steps is approximately 38N.

The DAMBRK model has the option to use either Eqs. (22)-(23) or Eqs. (26)-(27). The former is a somewhat simpler treatment in which a total or composite cross-section is used, whereas the latter set utilizes a more detailed representation of the flow cross-section. Eqs. (26)-(27) are recommended when the channel is sufficiently large to carry a significant portion of the total flow and the channel has a rather meandrous path through the downstream valley.

2.4 Initial and Boundary Conditions

In order to solve the unsteady flow equations the state of the flow (h and Q) must be known at all cross-sections at the beginning (t=0) of the simulation. This is known as the initial condition of the flow. The DAMBRK model assumes the flow to be steady, non-uniform flow where the flow at each cross-section is initially computed to be:

$$Q_i = Q_{i-1} + q_{i-1}\,\Delta x_{i-1} \qquad i=2,3,\ldots N \tag{47}$$

where Q_1 is the known steady discharge at the dam, i.e., the upstream boundary of the downstream valley, and q_i is any lateral inflow from tributaries existing between the cross-sections spaced at intervals of Δx along the valley. The steady discharge from the dam at t=0 must be non-zero, i.e., a dry downstream channel is not amenable to simulation by DAMBRK. This is not an important restriction, especially when maximum flows and peak stages are of paramount interest in the dam-break flood. The tributary lateral inflow must be specified by the forecaster throughout the simulation period. If these flows are relatively small, they may be safely ignored.

The water surface elevations associated with the steady flow must also be computed at t=0. This is accomplished by solving the following equation:

$$\frac{(Q^2/A)_{i+1} - (Q^2/A)_i}{\Delta x_i} + g\left[\frac{A_i+A_{i+1}}{2}\right]\left[\frac{h_{i+1}-h_i}{\Delta x_i}\right.$$

$$\left. + \frac{n^2(Q_i+Q_{i+1})^2\,(B_i+B_{i+1})^{4/3}}{2.2\,(A_i+A_{i+1})^{10/3}}\right] = 0 \tag{48}$$

This equation may be easily solved using the Newton-Raphson method by starting at a specified elevation at the downstream extremity of the

valley and solving for the adjacent upstream elevation step by step until the upstream boundary is reached. The downstream specified elevation may be obtained from a solution of the Manning equation if the flow is governed only by the channel conditions; however, if a flow control structure produces a back-up of the flow at this location, the forecaster must directly specify the water surface elevation existing at the downstream boundary at $t=0$.

In addition to initial conditions, boundary conditions at the upstream and downstream sections of the valley must be specified for all times ($t=0$ to $t=t_e$ where t_e is the future time at which the simulation ceases).

At the upstream boundary the reservoir outflow hydrograph $Q(t)$ provides the necessary boundary condition.

At the downstream boundary an appropriate stage-discharge relation is used. If the flow at the downstream extremity is channel-controlled, the following relation is used:

$$Q_N = \frac{1.49}{n} A_N^{5/3}/B_N^{2/3} \left[\frac{h_{N-1}-h_N}{\Delta x_{N-1}}\right]^{1/2} \tag{49}$$

Eq. (49) reproduces the hysteresis effect in stage-discharge relations often observed as a loop-rating curve. The loop (hysteresis) is produced by the temporal variations in the water surface slope. If the flow at the downstream boundary is controlled by a flow control structure such as a dam, the following relation is used:

$$Q_N = Q_b + Q_s \tag{50}$$

where the breach flow (Q_b) is defined by Eq. (2) and the spillway flow (Q_s) is defined by Eq. (17) in which the various terms apply to the dam at the downstream boundary. Since the resulting expressions for Q_b and Q_s are in terms of the water surface elevation, h_N, Eq. (50) is a stage-discharge relation.

The downstream boundary condition may also be specified as a single-value rating curve in which the stage-discharge values are input as tabular values. Linear interpolation is used for determining intermediate values. The downstream boundary may also be a known water surface elevation as a function of time, e.g., a tidal condition.

2.5 Multiple Dams and Bridges

The DAMBRK model can simulate the progression of a dam-break wave through a downstream valley containing a reservoir created by another downstream dam, which itself may fail due to being sufficiently overtopped by the wave produced by the failure of the upstream dam. In fact, an unlimited number of reservoirs located sequentially along the

valley can be simulated. In DAMBRK there is a choice of two methods for simulating dam-break flows in a valley having multiple dams.

In the first method, which is known as the "sequential method," the downstream boundary condition for the dynamic routing component is given by Eq. (50) rather than Eq. (49). The properties of the downstream dam, spillways, breach description, and elevation of flow which precipitates the failure of the dam, are used in Eq. (50). In this way, backwater effects of the downstream dam are included in the routing of the outflow hydrograph from the upstream dam. The most upstream reservoir may be simulated using either storage or dynamic routing.

When the tailwater below a dam is affected by flow conditions downstream of the tailwater section (e.g., backwater produced by a downstream dam, flow constriction, bridge, and/or tributary inflow), the flow occurring at the dam is computed by the second method known as the "simultaneous method" which uses an internal boundary condition at the dam. In this method the dam is treated as a short Δx reach in which the flow through the reach is governed by the following two equations rather than either Eqs. (22)-(23) or Eqs. (26)-(27):

$$Q_i = Q_{i+1} \tag{51}$$

$$Q_i = Q_b + Q_s \tag{52}$$

in which Q_b and Q_s are breach flow and spillway flow as described in Eqs. (2) and (17). In this way the flows, Q_i and Q_{i+1}, and the elevations, h_i and h_{i+1}, are in balance with the other flows and elevations occurring simultaneously throughout the entire flow system; the system may consist of additional dams which are treated as additional internal boundary conditions via Eqs. (51)-(52). Either storage or dynamic routing may be used in the most upstream reservoir. This method can also be used for a flow system having a single dam, only.

Highway/railway bridges and their associated earthen embankments which are located at points downstream of a dam may also be treated as internal boundary conditions. Eqs. (51)-(52) are used at each bridge; the term Q_s in Eq. (52) is computed by the following expression:

$$Q_s = 8.02\ C\ A_{i+1}(h_i - h_{i+1})^{1/2} + cc_u\ L_u\ k_u(h_i - h_{cu})^{3/2} + cc_\ell\ L_\ell\ k_\ell(h_i - h_{c\ell})^{3/2} \tag{53}$$

in which

$$k_u = 1.0 \qquad \text{if} \qquad h_{ru} < 0.76 \tag{54}$$

$$k_u = 1.0 - c_u(h_{ru} - 0.76)^3 \quad \text{if} \quad h_{ru} > 0.76 \tag{55}$$

$$c_u = 133(h_{ru}-0.78) + 10 \quad \text{if} \quad 0.76 \leq h_{ru} \leq 0.96 \tag{56}$$

$$c_u = 400(h_{ru}-0.96) + 34 \quad \text{if} \quad h_{ru} > 0.96 \tag{57}$$

$$h_{ru} = (h_{i+1}-h_{cu})/(h_i-h_{cu}) \tag{58}$$

$$cc_u = 3.02(h_i-h_{cu})^{0.015} \quad \text{if} \quad 0 < h_u \leq 0.15 \tag{59}$$

$$cc_u = 3.06 + 0.27(h_u-0.15) \quad \text{if} \quad h_u > 0.15 \tag{60}$$

$$h_u = (h_i-h_{cu})/w_u \tag{61}$$

in which C is a coefficient of bridge flow (see Chow, 1959), A_{i+1} is the cross-section flow area of the bridge opening at section i+1 (downstream end of bridge), h_{cu} is the elevation of the upper embankment crest, h_i is the water surface elevation at section i (upstream end of bridge), h_{i+1} is the water surface elevation at section i+1, L_u is the length of the upper embankment crest perpendicular to flow direction), k_u is the submergence correction factor for flow over the upper embankment crest, and w_u is the width (parallel to flow direction) of the crest of the upper embankment. In Eq. (53), the terms with an (ℓ) subscript refer to a lower embankment crest and these terms are defined by Eqs. (54)-(61) in which the (u) subscripts are replaced with (ℓ) subscripts. Eqs. (54)-(61) were developed from basic information on flow over road embankments as reported by the U.S. Dept. of Transportation (1978).

2.6 Supercritical Flow

The DAMBRK model can simulate the flow through the downstream valley when the flow is supercritical. This type of flow occurs when the slope of the downstream valley exceeds about 50 ft/mi. Slopes less than this usually result in the flow being subcritical to which all preceding comments pertaining to the downstream routing apply. When the flow is supercritical, any flow disturbances cannot travel back upstream; therefore, the downstream boundary becomes superfluous. Thus, for supercritical flow, a downstream boundary condition is not required; however, another equation in addition to the reservoir outflow hydrograph is needed for the upstream boundary condition. To satisfy this requirement, an equation similar to Eq. (49) is used at the upstream boundary, i.e.,

$$Q_1 = \frac{1.486}{n} A_1^{5/3}/B_1^{5/3} \left[\frac{h_1-h_2}{\Delta x_1}\right]^{1/2} \tag{62}$$

A modified compact quad-diagonal Gaussian elimination algorithm similar to the one previously described is required for solving the unsteady flow equations when supercritical flow exists. The modification results when the form of the Jacobian coefficient matrix is slightly changed due to the need for two upstream boundary conditions and none at the downstream boundary.

The DAMBRK model is constructed to accommodate supercritical flow for either the entire channel reach or for only an upstream portion of the entire reach. The supercritical flow regime is assumed to be applicable throughout the duration of the flow. Multiple reservoirs on supercritical valley slopes must be treated using a storage routing technique such as Eq. (18) rather than the dynamic routing technique.

2.7 Routing Losses

Often in the case of dam-break floods, where the extremely high flows inundate considerable portions of channel overbank or valley flood plain, a measurable loss of flow volume occurs. This is due to infiltration into the relatively dry overbank material, detention storage losses, and sometimes short-circuiting of flows from the main valley into other drainage basins via canals or overtopping natural ridges separating the drainage basins. Such losses of flow may be taken into account via the term q in Eq. (22) or Eq. (26). An expression describing the loss is given by the following:

$$q_m = -0.00458\ V_L\ P/(L\ \bar{T}) \tag{63}$$

in which V_L is the outflow volume (acre-ft) from the reservoir; P is the volume loss ratio; L is the length (mi) of downstream channel through which the loss occurs; and T is the average duration (hr) of the flood wave throughout the reach length L; and q_m is the maximum lateral outflow (cfs/ft) occurring along the reach L throughout the duration of flow. The mean lateral outflow is proportioned in time and distance along the reach L such that $q_i^j=0$ when $Q_i^j=Q_i^1$ and $q_i^j=q_m$ when $Q_i^j=Q_{max_i}$. Thus:

$$q_i^j = \frac{(Q_i^j - Q_i^1)}{(Q_{max_i} - Q_i^1)}\ q_m \tag{64}$$

$$Q_{max_i} = Q_{max_N} + (Q_{max} - Q_{max_N})\ \left(\frac{X_N - X_i}{L}\right)^m \tag{65}$$

where Q_i^1 is the initial flow, Q_{max_i} is the estimated maximum flow at each flood node, Q_{max_N} is the maximum routed discharge at the downstream section (X_n), Q_{max} is the maximum discharge at the dam and m is a fitted

exponent. The parameter P may vary from only a few percent to more than 30, depending on the conditions of the downstream valley.

2.8 Tributary Inflows/Outflows

Unsteady flows associated with tributaries downstream of the dam can be added to the unsteady flow resulting from the dam failure. This is accomplished via the term q in Eq. (22) or Eq. (26). The tributary flow is distributed along a single Δx reach. Backwater effects of the dam-break flow on the tributary flow are ignored, and the tributary flow is assumed to enter perpendicular to the dam-break flow. Outflows are assigned negative values. Outflows which occur as broad-crested weir flow over a levee or natural crest may be simulated. The crest elevation, discharge coefficient, and location along the river-valley must be specified. The head is computed as the average water surface elevation, along the length of the crest, less the crest elevation.

2.9 Floodplain Compartments

The DAMBRK model can simulate the exchange of flow between the river and floodplain compartments. The floodplain compartments are formed by a levee which runs parallel to the river on either or both sides of the river, and other levees or road embankments which run perpendicular to the river. Flow transfer between a floodplain compartment and the river is assumed to occur along one Δx reach and is controlled by broad-crested weir flow with submergence correction. Flow can be either away from the river or into the river, depending on the relative water surface elevations of the river and the floodplain compartment. The river elevations are computed via Eqs. (40-41), and the floodplain water surface elevations are computed by a simple storage routing relation, i.e.,

$$V_\ell^{t} = V_\ell^{t-\Delta t} + \left(I^{t} - O^{t}\right) \Delta t/43560 \tag{66}$$

in which V_ℓ is the volume (acre-ft) in the floodplain compartment at time t or $t-\Delta t$ referenced to the water elevation, I is the inflow from the river or adjacent floodplain compartments, and O is the outflow from the floodplain compartment to the river and/or to adjacent floodplain compartments. Flow transfer between adjacent floodplain compartments is also controlled by broad-crested weir flow with submergence correction. The broad-crested weir flow is according to the following:

$$I = c\, s_b \left(h_r - h_{fp}\right)^{3/2} \tag{67}$$

$$O = c\, s_b \left(h_{fp} - h_r\right)^{3/2} \tag{68}$$

in which c is a specified discharge coefficient, h_r is the river elevation, h_{fp} is the water surface elevation of the floodplain, and s_b is the submergence correction factor, i.e.

$$s_b = 1.0 \qquad h_r < 0.67 \tag{69}$$

$$s_b = 1.0 - 27.8\,(H_r - 0.67)^3 \qquad h_r > 0.67 \tag{70}$$

$$H_r = (h_r - h_w)/(h_{fp} - h_w) \tag{71}$$

and h_w is the specified elevation of the crest of the levee. The floodplain elevation (h_{fp}) is obtained iteratively via a table look-up algorithm from the specified table of volume-elevation values. The outflow from a floodplain compartment may also include that from one or more pumps associated with each floodplain compartment. Each pump has a specified discharge-head relation given in tabular form along with start-up and shut-off operation instructions depending on specified water surface elevations. The pumps discharge to the river.

2.10 Reservoir Dynamic Routing

As mentioned earlier, an option is provided in the DAMBRK model to use dynamic routing rather than storage routing to compute the reservoir outflow hydrograph. The dynamic routing is identical to the above description with the exception of boundary conditions. The upstream boundary condition is a discharge hydrograph given by the following:

$$Q_1^{j+1} - I(t) = 0 \tag{72}$$

where I(t) is the known reservoir inflow hydrograph. The downstream boundary condition is a stage-discharge relation given by Eq. (50). The initial water surface elevations are computed by solving Eq. (48), the steady gradually varied backwater equation, using h_o which is the elevation of the water surface at the dam site when the computation commences. The reservoir dynamic routing procedure must contend with the lowering of the water surface elevation at the upstream boundary as the reservoir volume is depleted by the outflow through the breach. If this depth becomes small and approaches a value less than the normal depth, the computations become unstable. To avoid this computational problem, the upstream depth is constantly monitored; if it becomes less than the initial normal depth (d_n), the location of the upstream boundary condition is shifted downstream one node at a time until the depth at the node is greater than d_n.

2.11 Landslide-Generated Waves

Reservoirs are sometimes subject to landslides which rush into the reservoir, displacing a portion of the reservoir contents and, thereby,

creating a very steep water wave which travels up and down the length of the reservoir (Davidson and McCartney, 1975). This wave may have sufficient amplitude to overtop the dam and precipitate a failure of the dam, or the wave by itself may be large enough to cause catastrophic flooding downstream of the dam without resulting in the failure of the dam as perhaps in the case of a concrete dam such as the Viaont Dam flood of 1963.

The capability to generate waves produced by landslides is provided within DAMBRK. The volume of the landslide mass, its porosity, and time interval over which the landslide occurs, are input to the model. In the model, the landslide mass is deposited within the reservoir in layers during small computational time steps, and simultaneously the original dimensions of the reservoir are reduced accordingly. The time rate of reduction in the reservoir cross-sectional area (Koutitas, 1977) creates the wave during the solution of the unsteady flow, Eqs. (22)-(23), which are applied to the cross-sections describing the reservoir characteristics. The upstream boundary condition is given by Eq. (72), and the downstream boundary condition is given by Eq. (50). The initial conditions are obtained as described by Eqs. (47)-(48) for steady non-uniform flow.

Wave runup is not considered in the model. For near vertical faces of concrete dams the runup may be neglected; however, for earthen dams the angle of the earth fill on the reservoir side will result in a surge which will advance up the face of the dam to a height approximately equal to 2.5 times the height of the landslide-generated wave (Morris and Wiggert, 1972).

2.12 Selection of Δt and Δx

Rapidly rising hydrographs, such as the dam-break outflow hydrograph, can cause computational problems (instability and non-convergence) when applied to numerical approximations of the unsteady flow equations. This is the case even when an implicit, non-linear finite difference solution technique is used. However, many computational problems can be overcome by proper selection of time step (Δt) size. During the limited testing of the model presented herein, two types of computational problems arose. First, if the time step were too large relative to the rate of increase of discharge during that time step, errors occurred in the computed water surface elevation in the vicinity of the wave front. These water surface elevations would tend to dip toward the channel bottom and quickly cause negative areas to be computed which would then cause the computations to "blow up." Second, too large a time step would also cause the Newton-Raphson iteration to not converge. The first computational problem is similar to that experienced by Cunge (1975). Both of the computational problems were successfully treated by reducing the time step size by a factor of 0.5 whenever negative areas were computed, or when a reasonable number of iterations were exceeded. With the reduced time step, the computations were repeated. If the same problems persisted, the time step was again halved and the computations repeated. Usually, one or two reductions

would be sufficient. The computational process was then advanced to the next time level by the original unreduced time step. Computations were initially begun with Δt time steps (hr) computed via the following relation:

$$\Delta t = \tau/M \tag{73}$$

in which τ is the time (hr) from the beginning of rise to the peak of the outflow hydrograph and M is the divisor for determining the time step. A reasonable value for M is 20 for subcritical flow and 40 for supercritical flow.

Distance steps (Δx) are selected in the following range:

$$\Delta x \leq c\ \Delta t \tag{74}$$

where c is the wave speed in mi/hr and Δx is in miles. The dam-break hydrograph tends to be a very peaked-type of hydrograph and, as such, tends to dampen and flatten out as it advances downstream. Accordingly, the time step may be increased as the wave progresses downstream; therefore, smaller values of Δx are selected immediately downstream of the dam, with a gradual increase in size at greater distances downstream of the dam. Also, the smaller values of Δx are associated with the smaller values of τ. This methodology of selecting Δx and Δt values follows the guidelines set forth in an analysis made by Fread (1974a) of the numerical properties of the four-point implicit solution of the unsteady flow equations.

Distance steps may need to be reduced in size where severe expansions or contractions in the cross sections occur.

Since the flood wave dampens out as it moves downstream, the Δt time step may be increased as the computations advance in time. The following scheme is used:

$$\Delta t = T_p/M \qquad t \leq t_b + 2\tau \tag{75}$$

where T_p is the time between the start of rise of the hydrograph and the peak of the hydrograph at selected locations along the downstream valley. Six evenly spaced locations along the downstream valley commencing at the dam site are monitored to determine T_p. The peak must have occurred at one of the locations before T_p can be evaluated. Since T_p increases at locations farther and farther downstream of the dam, the T_p which exists for the most downstream location is used in Eq. (75). An option exists to maintain throughout the computations and time step size specified in the data input. The units of Δt, t_b, and T_p are hours.

3. DATA REQUIREMENTS

The DAMBRK model was developed so as to require data that was accessible to the forecaster. The input data requirements are flexible

insofar as much of the data may be ignored (left blank on the input data cards or omitted altogether) when a detailed analysis of a dam-break flood inundation event is not feasible due to lack of data or insufficient data preparation time. Nonetheless, the resulting approximate analysis is more accurate and convenient to obtain than that which could be computed by other techniques. The input data can be categorized into two groups.

The first data group pertains to the dam (the breach, spillways, and reservoir storage volume). The breach data consists of the following parameters: τ (failure time of breach, in hours); b (final bottom width of breach); z (side slope of breach); h_{bm} (final elevation of breach bottom); h_o (initial elevation of water in reservoir); h_f (elevation of water when breach begins to form); and h_d (elevation of top of dam). The spillway data consists of the following: h_s (elevation of uncontrolled spillway crest); c_s (coefficient of discharge of uncontrolled spillway); h_g (elevation of center of submerged gated spillway); c_g (coefficient of discharge of gated spillway); c_d (coefficient of discharge of crest of dam); and Q_t (constant, head independent discharge from dam). The storage parameters consist of the following: a table of surface area (A_s) in acres or volume in acre-ft. and the corresponding elevations within the reservoir. The forecaster must estimate the values of τ b, z, h_{bm}, and h_f. The remaining values are obtained from the physical description of the dam, spillways, and reservoir. In some cases h_s, c_s, h_g, c_g, and c_d may be ignored and Q_t used in their place.

The second group pertains to the routing of the outflow hydrograph through the downstream valley. This consists of a description of the cross-sections, hydraulic resistance coefficients, and expansion coefficients. The cross-sections are specified by location mileage, and tables of top width (active and inactive) and corresponding elevations. The active top widths may be total widths as for a composite section, or they may be left flood-plain, right flood-plain, and channel widths. The top widths can be obtained from USGS topography maps, 7 1/2' series, scale 1:24000. The channel widths are usually not as significant for an accurate analysis as the overbank widths (the latter are available from the topo maps). The number of cross-sections used to describe the downstream valley depends on the variability of the valley widths. A minimum of two must be used. Additional cross-sections are created by the model via linear interpolation between adjacent cross-sections specified by the forecaster. This feature enables only a minimum of cross-sectional data to be input by the forecaster according to such criteria as data availability, variation, preparation time, etc. The number of interpolated cross-sections created by the model is controlled by the parameter DXM which is input for each reach between specified cross-sections. The hydraulic resistance coefficients consist of a table of Manning's n vs. elevation for each reach between specified cross-sections. The expansion-contraction coefficients (k) are specified as non-zero values at sections where significant expansion or contractions occur. The k parameters may be left blank in most analyses.

4. MODEL TESTING

The DAMBRK model has been tested on five historical dam-break floods to determine its ability to reconstitute observed downstream peak stages, discharges, and travel times. Those floods that have been used in the testing are: 1976 Teton Dam, 1972 Buffalo Creek Coal-WAste Dam, 1889 Johnstown Dam, 1977 Toccoa (Kelly Barnes) Dam, and the 1977 Laurel Run Dam floods. However, only the Teton and Buffalo Creek floods will be presented herein.

4.1 Teton Dam Flood

The Teton Dam, a 300 ft. high earthen dam with a 3,000 ft. long crest and 250,000 acre-ft of stored water, failed on June 5, 1976, killing 11 people, making 25,000 homeless, and inflicting about $400 million in damages to the downstream Teton-Snake River Valley. Data from a Geological Survey Report by Ray, et al. (1977) provided observations on the approximate development of the breach, description of the reservoir storage, downstream cross-sections and estimates of Manning's n approximately every 5 miles, indirect peak discharge measurements at 3 sites, flood-peak travel times, and flood-peak elevations. The inundated area is shown in Fig. 2.

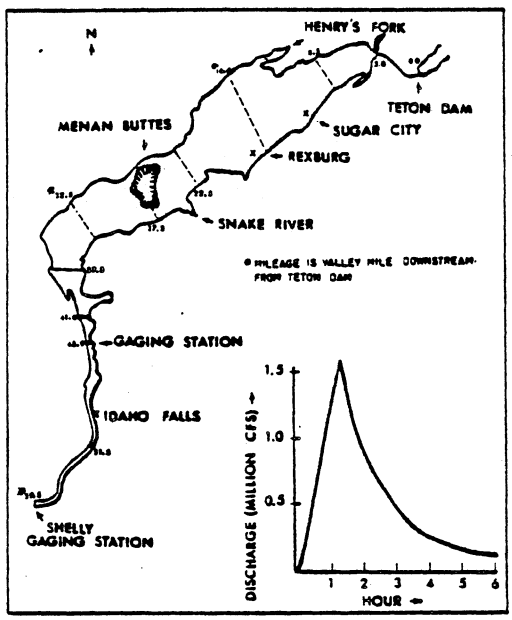

Fig. 2 — OUTFLOW HYDROGRAPH AND FLOODED AREA DOWNSTREAM OF TETON DAM

The following breach parameters were used in DAMBRK to reconstitute the downstream flooding due to the failure of Teton Dam: $\tau = 1.25$ hrs., $b = 150$ ft., $z = 0$, $h_{bm} = 0.0$, $h_f = h_d = h_o = 261.5$ ft. Cross-sectional properties at 12 locations shown in Fig. 2 along the 60-mile reach of the Teton-Snake River Valley below the dam were used. Five top widths were used to describe each cross-section. The downstream valley

consisted of a narrow canyon (approx. 1,000 ft. wide) for the first 5 miles and thereafter a wide valley which was inundated to a width of about 9 miles. Manning's n values ranging from 0.028 to 0.047 were provided from field estimates by the Geological Survey. DXM values between cross-sections were assigned values that gradually increased from 0.5 miles near the dam, to a value of 1.5 miles near the downstream boundary at the Shelly gaging station (valley mile 59.5 downstream from the dam). The reservoir surface area-elevation values were obtained from Geological Survey topo maps. The downstream boundary was assumed to be channel flow control as represented by a loop rating curve given by Eq. (49).

The computed outflow hydrograph is shown in Fig. 2. It has a peak value of 1,652,300 cfs (cubic feet per second), a time to peak of 1.25 hrs., and a total duration of about 6 hours. This peak discharge is about 20 times greater than the flood of record at Idaho Falls. The temporal variation of the computed outflow volume compared within 5 percent of observed values as shown in Fig. 3. In Fig. 4 a comparison

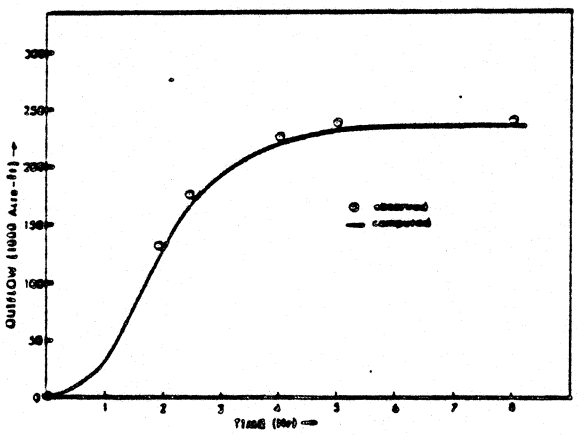

Fig. 3 – OUTFLOW VOLUME FROM TETON DAM

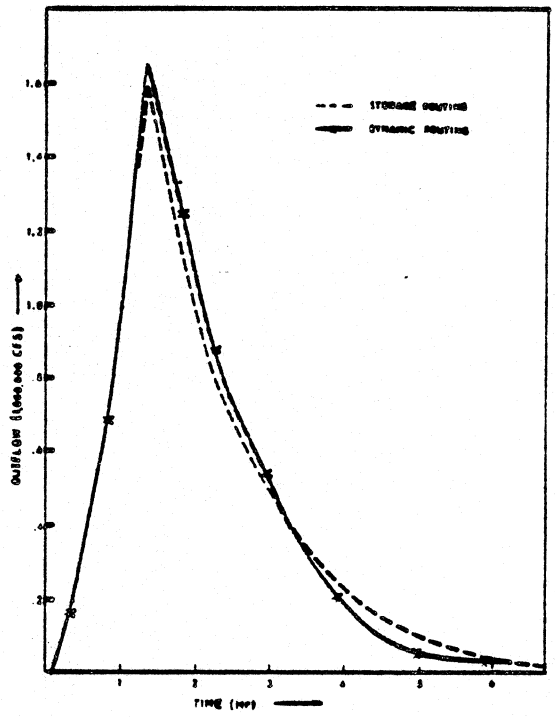

Fig. 4 – OUTFLOW HYDROGRAPH FROM TETON DAM FAILURE

is presented of Teton reservoir outflow hydrographs computed via reservoir storage routing and reservoir dynamic routing. Since the breach of the Teton Dam formed gradually over approximately a one-hour interval, a steep negative wave did not develop. Also, the inflow to the reservoir was not very significant. For these two reasons, the reservoir surface remained essentially level during the reservoir drawdown and the dynamic routing yielded almost the same outflow hydrograph as the level pool, storage routing technique.

The computed peak discharge values along the 60-mile downstream valley are shown in Fig. 5 along with three observed (indirect measurement) values at miles 8.5, 43.0, and 59.5. The average difference between the computed and observed values is 4.8 percent. Most apparent is the extreme attenuation of the peak discharge as the flood wave progresses through the valley. Two computed curves are shown in Fig. 5; one in which no losses were assumed, i.e., $q_m = 0$; and a second in which the losses were assumed to vary from zero to a maximum of $q_m = -0.30$ cfs/ft and were accounted for the model through the q term in Eq. (22). Losses were due to infiltration and detention storage behind irrigation levees amounting to about 25 percent of the reservoir outflow volume. Eq. (63) was used to compute q_m.

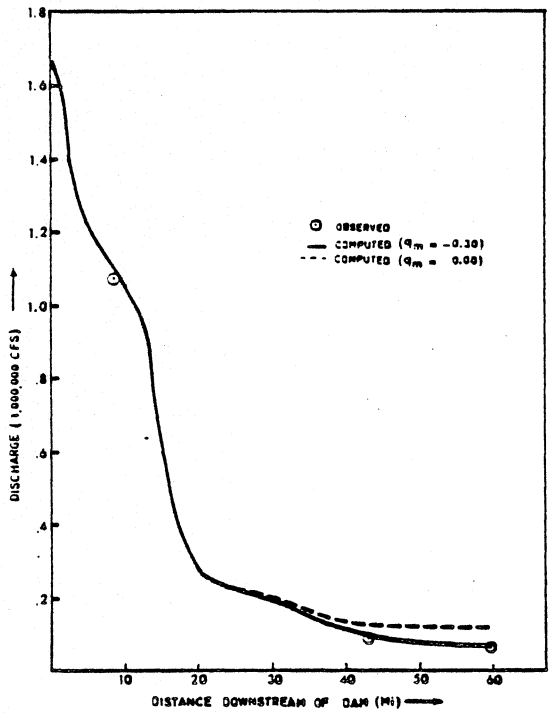

Fig. 5 – PROFILE OF PEAK DISCHARGE FROM TETON DAM FAILURE

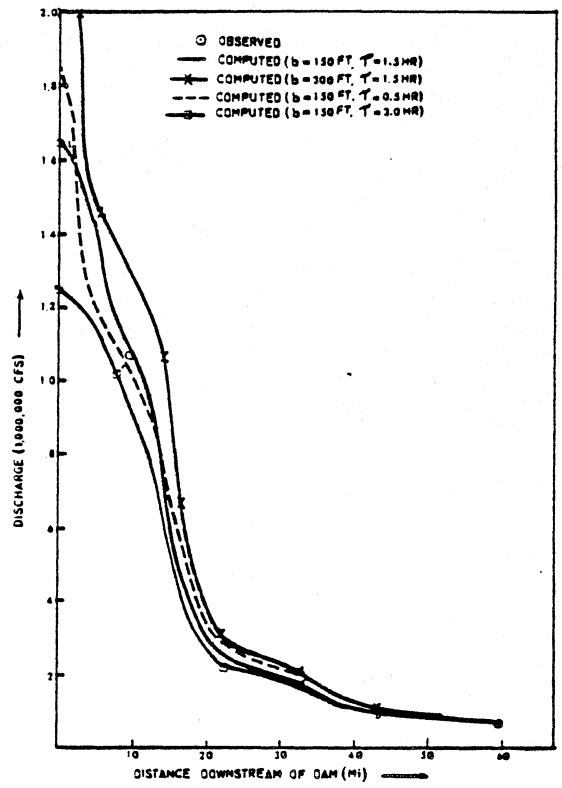

Fig. 6 – PROFILE OF PEAK DISCHARGE FROM TETON DAM FAILURE SHOWING SENSITIVITY OF VARIOUS INPUT PARAMETERS

The a priori selection of the breach parameters (τ and b) causes the greatest uncertainty in forecasting dam-break flood waves. The sensitivity of downstream peak discharges to reasonable variations in τ and b are shown in Fig. 6. Although there are large differences in the discharges (+45 to -25 percent) near the dam, these rapidly diminish in the downstream direction. After 10 miles the variation is +20 to -14 percent, and after 15 miles the variation has further diminished (+15 to -8 percent). The tendency for extreme peak attenuation and rapid damping of differences in the peak discharge is accentuated in the case of Teton Dam due to the presence of the very wide valley. Had the

narrow canyon extended all along the 60-mile reach to Shelly, the peak discharge would not have attenuated as much and the differences in peak discharges due to variations in τ and $\bar{b}$ would be more persistent. In this instance, the peak discharge would have attenuated to about 350,000 rather than 67,000 as shown in Fig. 6, and the differences in peak discharges at mile 59.5 would have been about 27 percent as opposed to less than 5 percent as shown in Fig. 6.

Computed peak elevations compared favorably with observed values, as shown in Fig. 7. The average absolute error was 1.5 ft., while the average arithmetic error was only -0.2 ft.

The computed flood-peak travel times and three observed values are shown in Fig. 8. The differences between the computed and observed are about 10 percent for the case of using the estimated Manning's n values and about 1 percent if the n values are slightly increased by 7 percent.

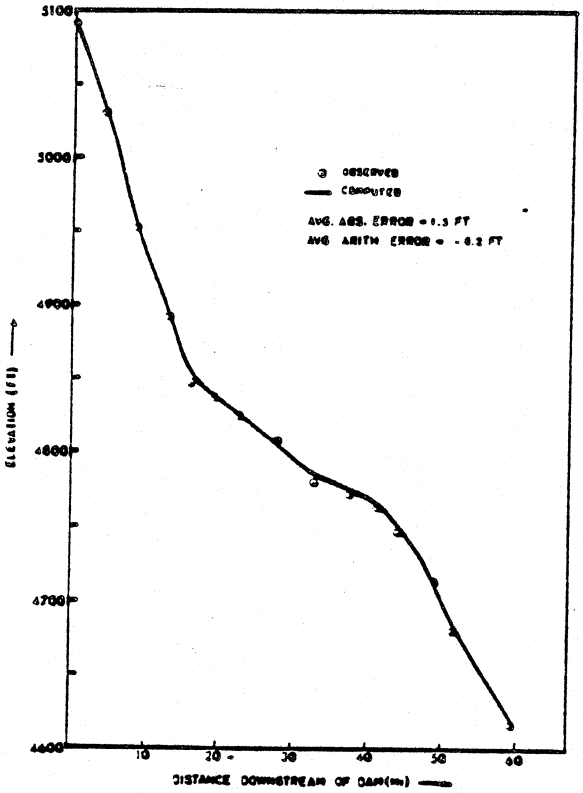

Fig. 7 — PROFILE OF PEAK FLOOD ELEVATION FROM TETON DAM FAILURE

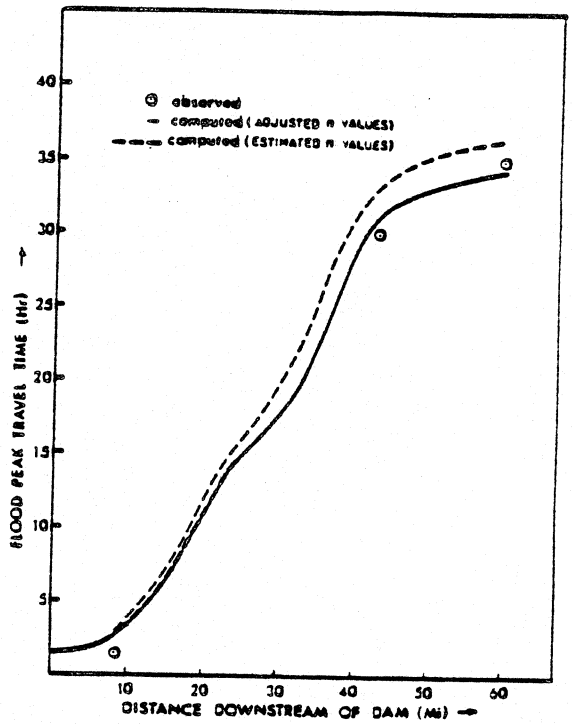

Fig. 8 — TRAVEL TIME OF FLOOD PEAK FROM TETON DAM FAILURE

As mentioned previously, the Manning's n must be estimated, especially for the flows above the flood of record. The sensitivity of the computed states and discharges of the Teton flood due to a substantial change (20 percent) in the Manning's n was found to be as follows: 1) 0.5 ft in computed peak water surface elevations or about 2 percent of the maximum flow depths, 2) 16 percent deviation in the computed peak discharges, 3) 0.8 percent change in the total attenuation of peak

discharge incurred in the reach from Teton Dam to Shelly, and 4) 15 percent change in the flood-peak travel time at Shelly. These results indicate that Manning's n has little effect on peak elevations or depths; however, the travel time is affected by nearly the same percent that the n values are changed.

A typical simulation of the Teton flood as described above involved 78 Δx reaches, 55 hrs. of prototype time, and an initial time step (Δt) of 0.06 hrs. Such a simulation run required only 19 seconds of CPU time on an IBM 360/195 computer system; the associated cost was less than $5 per run.

4.2 Buffalo Creek Flood

The DAMBRK model was also applied to the failure of the Buffalo Creek coal-waste dam which collapsed on the Middle Fork, a tributary of Buffalo Creek (See Fig. 9) in southwestern West Virginia near Saunders. The dam failed very rapidly on February 26, 1972, and released about

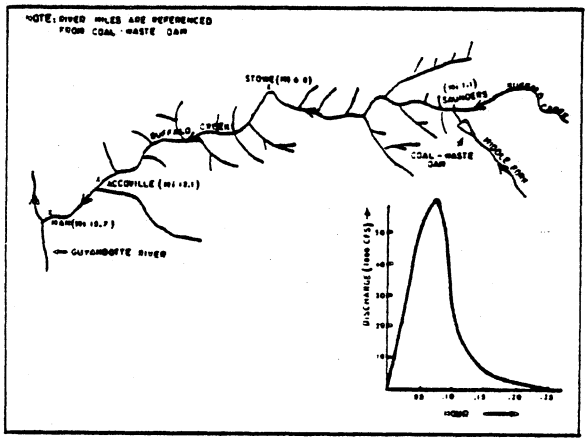

Fig. 9 — OUTFLOW HYDROGRAPH FROM COAL-WASTE DAM AND LOCATION PLAN OF BUFFALO CREEK

500 acre-feet of impounded waters into Buffalo Creek valley, causing the most catastrophic flood in the state's history with the loss of 118 lives, 500 homes, and property damage exceeding $50 million. Observations were available on the approximate development sequence of the breach, the time required to empty the reservoir, indirect peak discharge measurements at four sites, approximate flood-peak travel times, and flood-peak elevations (Davies, et al., 1972). Cross-sections and estimates of the Manning roughness coefficients were taken from a report on routing dam-break floods by McQuivey and Keefer (1975).

The time of failure was estimated to be in the range of 5 minutes and the reservoir took only 15 minutes to empty according to eyewitnesses' reports. The following breach parameters were used: τ = 0.083 hours, b = 170 feet, z = 2.6 feet, h_{bm} = 0.0 feet, $h_f = h_d = h_o$ = 40.0 feet. Cross-sectional properties were specified for eight locations along the 15.7 mile reach from the coal-waste dam to below Man at

the confluence of Buffalo Creek with the Guyandotte River as shown in Fig. 9. The downstream valley widened from the narrow width (approximately 100 ft) of Middle Fork to about 400-600 feet width of Buffalo Creek Valley. Minimum Δx (DXM) values were gradually increased from 0.2 mile near the dam to 0.4 mile near Man at the downstream boundary. The reservoir area-elevation values were obtained from Davies, et al., (1972).

The 15.7 mile reach was divided into two reaches; one was approximately 4 miles long, in which the very steep channel bottom slope (84 ft/mi) produced supercritical flows, and the second extended on downstream approximately 12 miles, with an average bottom slope of 40 ft/mi, in which subcritical flow prevailed. The computations were unstable when the supercritical reach was modeled using the same type of boundary conditions as used with subcritical flows. This computational problem was eliminated when the supercritical boundary condition, Eq. (62), was used.

The reservoir storage routing option was used to generate the outflow hydrograph shown in Fig. 9. The computations indicated the reservoir was drained of its contents in approximately 15 minutes, which agreed with the observed time to completely empty its contents. The indirect measurements of peak discharge at miles 1.1, 6.8, 12.1, and 15.7 downstream of the dam are shown in Fig. 10. Again, as in the Teton

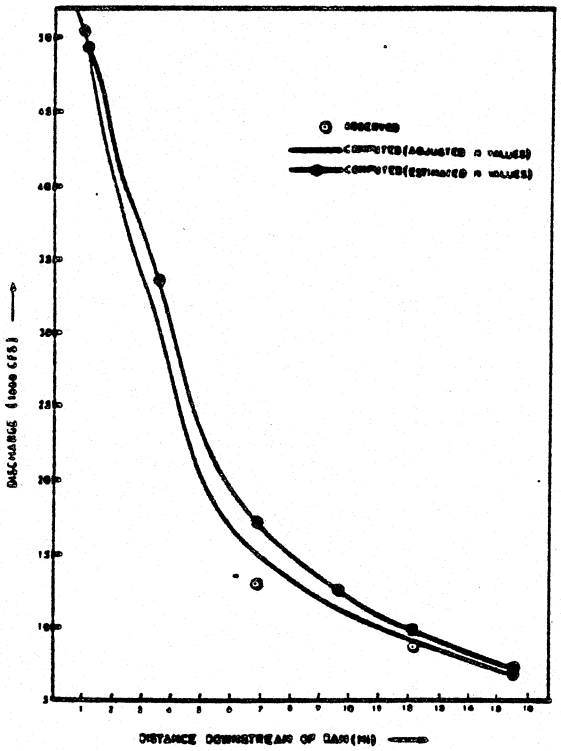

Fig. 10 — PROFILE OF PEAK DISCHARGE FROM BUFFALO CRK. FAILURE

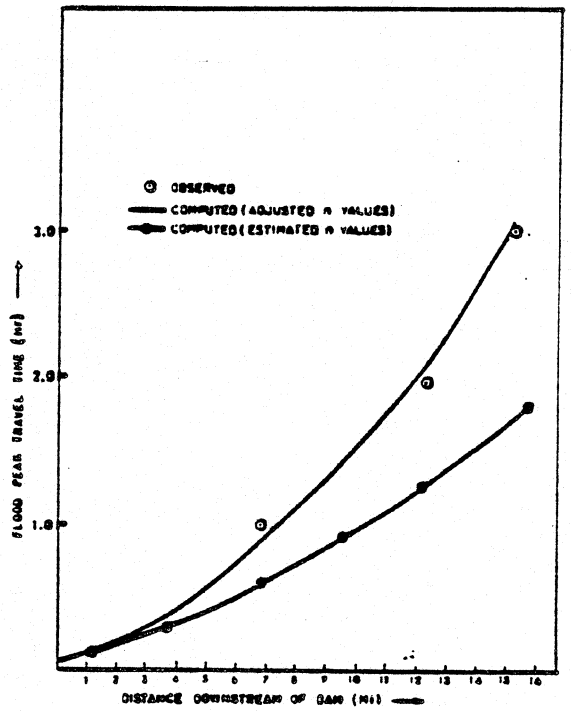

Fig. 11 — TRAVEL TIME OF FLOOD PEAK FROM BUFFALO CREEK FAILURE

Dam flood, the flood peak was greatly attenuated as it advanced downstream. Whereas the Teton flood was attenuated by a factor of 0.69 in the first 16 miles of which 11 miles included the wide, flat valley

below the Teton Canyon, the Buffalo Creek flood was confined to a relatively narrow valley, but was attenuated by a factor of 0.88 in the same distance. The attenuation of the Buffalo Creek flood was due to the much smaller volume of its outflow hydrograph compared with that of the Teton flood.

In Fig. 10, the computed discharges agree favorably with the observed. There are two curves of the computed peak discharge in Fig. 10; one is associated with n values of 0.040. In the former, the n values are reresentative of field estimates, while the latter results from adjustments in the n values such that computed flood travel times compare favorably with the observed. (Comparison of computed flood travel times with the observed are shown in Fig. 11 for estimated n values and for the final adjusted n values.) It should be noted that the two computed curves in Fig. 10 are not significantly different, although the n values differ by a factor of 1.75. Again, as in the Teton application, the n values influence the time of travel much more than the peak discharge. The large adjusted n values appear to be appropriate for dam-break waves in the near vicinity of the breached dam where extremely high flow velocities uproot trees and transport considerable sediment and boulders (if present), and generally result in large energy losses.

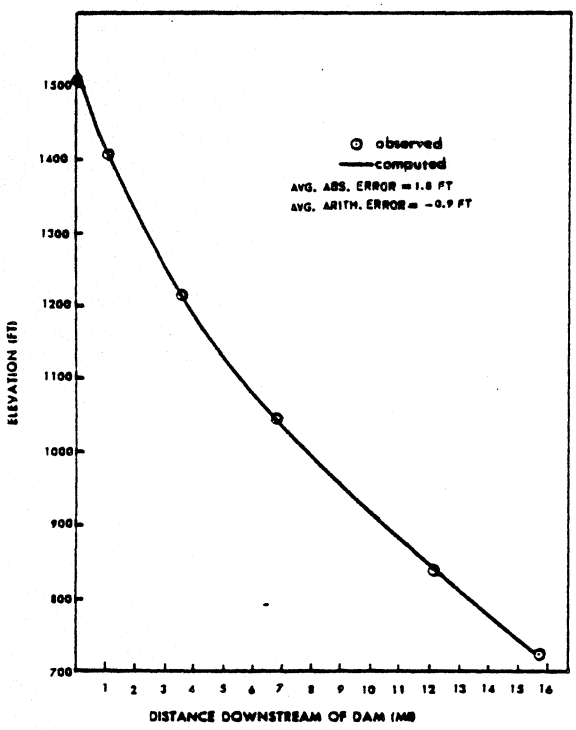

Fig. 12 — PROFILE OF PEAK FLOOD ELEVATION FROM BUFFALO CREEK FAILURE

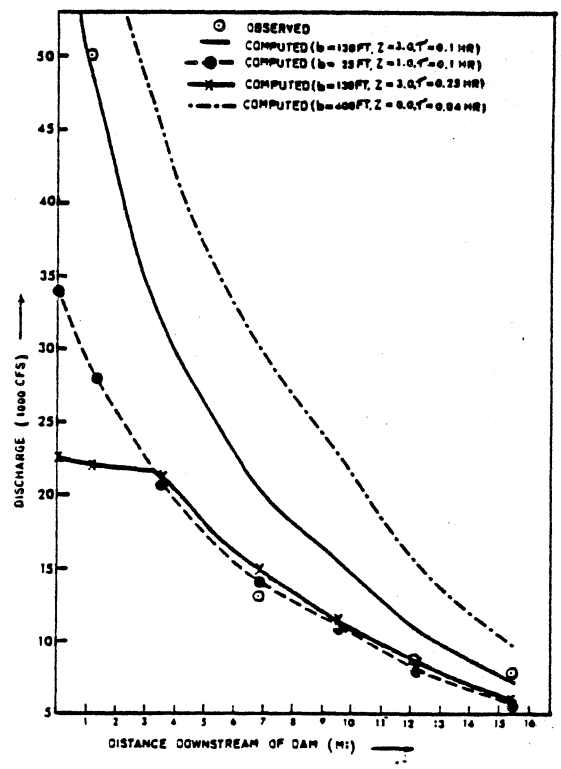

Fig. 13 — PROFILE OF PEAK DISCHARGE FROM BUFFALO CRK. FAILURE SHOWING SENSITIVITY OF VARIOUS INPUT PARAMETERS

A profile of the observed peak flood elevations downstream of the Buffalo Creek coal-waste dam is shown in Fig. 12, along with the computed elevations using adjusted n values. The average absolute error is 1.8 feet and the average arithmetic error is -0.9 foot.

Sensitivities of the computed downstream peak discharges to reasonable variations in the selection of breach parameters (τ, b, and z) are shown in Fig. 13. The resulting differences in the computed discharges diminish in the downstream direction. Like the Teton dam-break flood wave, errors in forecasting the breach are damped-out as the flood advances downstream.

A typical simulation of the Buffalo Creek flood involved 63 Δx reaches, 3.0 hours of prototype time, use of the reservoir storage routing option, and initial time step of 0.002 and 0.005 hour for the supercritical and subcritical downstream reaches, respectively. Computation time for a typical simulation run was 18 seconds (IBM 360/195).

5. FLOOD INUNDATION APPLICATIONS

The NWS DAMBRK model is suitable for the following two types of dam-break flood inundation applications: 1) pre-computation of flood peak elevations and travel times prior to a dam failure, and 2) real-time computation of the downstream flooding when a dam failure is imminent or has immediately occurred.

Pre-computations of dam failures enable the preparation of concise graphs or flash flood tables for use by those responsible for community preparedness downstream of critically located dams. The graphs provide information on flood peak elevations and travel times throughout the critical reach of the downstream valley. The variations in the precomputed values due to uncertainty in the breach parameters (τ and $\bar{b}$) can be included in the graph. Results obtained using a maximum probable estimate of $\bar{b}$ and a minimum probable estimate of τ would define the upper envelope of probable flood peak elevations and minimum travel times. Similarly, the use of a minimum probable estimated $\bar{b}$, would define the lower limit of the envelope of probable peak elevations and maximum travel times. In the precomputation mode, the forecaster can use as much of the capabilities of the DAMBRK model as time and data availability warrant.

Real-time computation is also possible in certain situations where the total response time for a dam-break flood warning exceeds a few hours. An abbreviated data input to DAMBRK can be used to quickly compute an approximate crest profile and arrival times. Computer coding forms have been prepared by the NWS Ft. Worth River Forecast Center with invariable parameters delineated and essential input data flagged. Using available topo maps and a minimum of information on the dam such as its height and storage volume, a forecast can be made within approximately 30 minutes.

In some cases it may be possible to make a revised forecast in real-time to update a pre-computed forecast when observations of the extent of the breach are made available to the forecaster. This would be valuable in refining the forecast for communities located far downstream where the possibility of flood inundation is questionable and the need for eventual evacuation can be more accurately defined by utilizing

observations at the dam or actual flood elevations observed a few miles below the dam. The data set used to make the real-time update of the pre-computed forecast would have been retrieved from a data storage system and the critical parameters therein changed.

The DAMBRK model can also be used to route any specified flow through a river valley. In such applications of the model, the dam breach and reservoir routing data input and computational components are not used.

6. SUMMARY AND CONCLUSIONS

A dam-break flood forecasting model (DAMBRK) is described and applied to some actual dam-break flood waves. The model consists of a breach component which utilizes simple parameters to provide a temporal and geometrical description of the breach. A second component computes the reservoir outflow hydrograph resulting from the breach via a broad-crested weir-flow approximation, which includes effects of submergence from downstream tailwater depths and corrections for approach velocities. Also, the effects of storage depletion and upstream inflows on the computed outflow hydrograph are accounted for through storage routing within the reservoir. The third component consists of a dynamic routing technique for determining the modifications to the dam-break flood wave as it advances through the downstream valley, including its travel time and resulting water surface elevations. The dynamic routing component is based on a weighted, four-point non-linear finite difference solution of the one-dimensional equations of unsteady flow which allows variable time and distance steps to be used in the solution procedure. Provisions are included for routing supercritical flows as well as subcritical flows, and incorporating the effects of downstream obstructions such as road-bridge embankments and/or other dams.

Model data requirements are flexible, allowing minimal data input when it is not available while permitting extensive data to be used when appropriate.

The model was tested on the Teton Dam failure and the Buffalo Creek coal-waste dam collapse. Computed outflow volumes through the breaches coincided with the observed values in magnitude and timing. Observed peak discharges along the downstream valleys were satisfactorily reproduced by the model even though the flood waves were severely attenuated as they advanced downstream. The computed peak flood elevations were within an average of 1.5 ft and 1.8 ft of the observed maximum elevations for Teton and Buffalo Creek, respectively. Both the Teton and Buffalo Creek simulations indicated an important lack of sensitivity of downstream discharge to errors in the forecast of the breach size and timing. Such errors produced significant differences in the peak discharge in the vicinity of the dams; however, the differences were rapidly reduced as the waves advanced downstream. Computational requirements of the model are quite feasible; CPU time (IBM 360/195) was 0.005 second per hr per mile of prototype dimensions for the Teton Dam simulation, and 0.095 second per hr per mile for the Buffalo Creek

simulation. The more rapidly rising Buffalo Creek wave (τ = 0.008hr as compared to Teton where τ = 1.25 hr) required smaller Δt and Δx computational steps; however, total computation times (Buffalo: 19 sec and Teton: 18 sec) were similar since the Buffalo Creek wave attenuated to insignificant values in a shorter distance downstream and in less time than the Teton flood wave.

Suggested ways for using the DAMBRK model in preparation of pre-computed flood information and in real-time forecasting were presented.

REFERENCES

Amein, M., and C. S. Fang, 1970: Implicit flood routing in natural channels. Journ. Hydraulic. Div., ASCE, 96, HY12, Dec., pp. 2481-2500.

Balloffet, A., 1977: Simulation of dam break flooding under normal and probable maximum flood conditions, Proceedings, Dam-Break Flood Modeling Workshop, U. S. Water Resources Council, Washington, D.C., pp. 384-401.

Balloffet, A., E. Cole, and A. F. Balloffet, 1974: Dam collapse wave in a river, Journ. Hydraul. Div., ASCE, 100, HY5, May, pp. 645-665.

Baltzer, R., and C. Lai, 1969: Computer simulation of unsteady flows in waterways. Journ. Hydraul. Div., ASCE, 94, HY4, July, pp. 1083-1117.

Brater, E., 1959: Hydraulics. Civil Engineering Handbook, edited by L. C. Urquhart, Sect. 4, McGraw-Hill Book Co., New York, pp. 4.44-4.60.

Brevard, J. A., and F. D. Theurer, 1979: Simplified dam-break routing procedure, Technical Release Number 66, U. S. Dept. of Agriculture, Soil Conservation Service, Engr. Div., 35 pp.

Brown, R. J., and D. C. Rogers, 1977: A simulation of the hydraulic events during and following the Teton Dam failure, Proceedings, Dam-Break Flood Modeling Workshop, U. S. Water Resources Council, Washington, D. C. pp.131-163.

Chaudhry, Y. M., and D. N. Contractor, 1973: Application of the implicit method to surges in open channels. Water Resour. Res., 9, No. 6, Dec., pp. 1605-1612.

Chen, C., and L. A. Druffel, 1977: Dam-break flood wave computation by method of characteristics and linearized implicit schemes, Proceedings, Dam-Break Flood Modeling Workshop, U. S. Water Resources Council, Washington, D. C., pp. 312-345.

Chow, V. T., 1959: Open-channel Hydraulics, McGraw-Hill Co., New York, pp. 476-481.

Cristofano, E. A., 1965: Method of computing rate for failure of earth fill dams. Bureau of Reclamation, Denver, Colo., April.

Cunge, J. A., 1975: Rapidly varying flow in power and pumping canals. Unsteady Flow in Open Channels, edited by K. Mahmood and V. Yevjevich, Vol. II, Chapt. 14, Water Resour. Pub., Ft. Collins, Colo., pp. 539-586.

Davidson, D. D., and B. L. McCartney, 1975; Water waves generated by landslides in reservoirs. Journ. Hydraul. Div., ASCE, 101, HY12, Dec., pp. 1489-1501.

Davies, W. E., J. F. Bailey, and D. B. Kelly, 1972: West Virginia's Buffalo Creek flood: a study of the hydrology and engineering geology. Geological Survey Circular 667, U. S. Geological Survey, 32 pp.

De Saint-Venant, Barre, 1871: Theory of unsteady water flow, with application to river floods and to propagation of tides in river channels. Acad. Sci. (Paris) Comptes rendus, 73, pp. 237-240.

Dressler, R. F., 1954: Comparison of theories and experiments for the hydraulic dam-break wave. Internat. Assoc. Sci. Pubs., 3, No. 38, pp. 319-328.

Fread, D. L., 1971: Discussion of implicit flood routing in natural channels. M. Amein and C. S. Fang. Journ. Hydraul. Div., ASCE, 97, HY7, July, pp.1156-1159.

Fread, D. L., and T. E. Harbaugh, 1973" Transient hydraulic simulation of breached earth dams, Journ. Hydraul. Div., ASCE, 99, HY1, Jan., pp 139-154.

Fread, D. L., 1974a: Numerical properties of implicit four-point finite difference equations of unsteady flow. NOAA Tech. Memo. NWS HYDRO-18, U. S. Dept of Commerce, NOAA, National Weather Service, 38 pp.

Fread, D. L., 1974b: Implicit dynamic routing of floods and surges in the Lower Mississippi. Presented at AGU Natl. Mtg., Wash., D. C., April, 26 pp.

Fread, D. L., 1975: Discussion of comparison of four numerical methods for flood routing, R. K. Price, Journ. Hydraul. Div., ASCE, 101, HY3, March, pp.565-567.

Fread, D. L., 1976: Flood routing in meandering rivers with flood plains, Proceedings, Rivers '76, Third Ann. Symp. of Waterways, Harbors and Coastal Eng. Div., ASCE, Vol. I, Aug., pp. 16-35.

Fread, D. L., 1977: The development and testing of a dam-break flood forecasting model, Proceedings, Dam-Break Flood Modeling Workshop, U. S. Water Resources Council, Washington, D. C., 1977, pp. 164-197.

Fread, D. L., 1978: NWS operational dynamic wave model, Verification of Mathematical and Physical Models in Hydraulic Engineering, Proceedings, 26th Annual Hydraulics Div. Specialty Conf., College Park, Md., Aug., pp.455-464.

Gundlach, D. L., and W. A. Thomas, 1977: Guidelines for calculating and routing a dam-break flood, Research Note No. 5, Corps of Engineers, U. S. Army, The Hydrologic Engr. Center, 50 pp.

Harris, G. W., and D. A. Wagner, 1967: Outflow from breached dams, Univ. of Utah.

Johnson, F. A., and P. Illes, 1976: A classification of dam failures, Water Power and Dam Construction, Dec., pp. 43-45.

Keefer, T. N., and R. K. Simons, 1977: Qualitative comparison of three dam-break routing models, Proceedings, Dam-Break Flood Modeling Workshop, U. S. Water Resources Council, Washington, D. C., pp.292-311.

Koutitas, C.G., 1977: Finite element approach to waves due to landslides, Journ. Hydraul. Div., ASCE, 103, HY9, Sept., pp. 1021-1029.

Liggett, J., and J. A. Cunge, 1975: Numerical methods of solution of the unsteady flow equations. Unsteady Flow in Open Channels, edited by K. Mahmood and V. Yevjevich, Vol. I, Chapt. 4, Water Resour. Pub., Ft. Collins, Colo., pp. 89-182.

Martin, C. S., and J. J. Zovne, 1971: Finite-difference simulation of bore propagation. Journal. Hydraul. Div. ASCE, 97, HY7, July, pp. 993-1010.

McQuivey, R. S., and T. N. Keefer, 1976: Application of simple dam break routing model. Proceedings, 16th Congress, IAHR, Sao Paulo, Brazil, July 27-August 1, 1975, Vol. 2, pp. 315-324.

Middlebrooks, T. A., 1952: Earth-dam practice in the United States, Centennial Transactions, ASCE, Paper No. 2620, pp. 697-722.

Morris, H. M., and J. M. Wiggert, 1972: Applied Hydraulics in Engineering, The Ronald Press Co., New York, pp. 570-573.

Preissmann, A., 1961: Propagatin of translatory waves in channels and rivers. Paper presented at First Congress of French Assoc. for Computation, Grenoble, Sept. 14-16, Proceedings, AFCAL, pp. 433-442.

Price, J. T., G. W. Lowe, and J. M. Garrison, 1977: Unsteady flow modeling of dam-break waves, Proceedings, Dam-Break Flood Modeling Workshop, U. S. Water Resources Council, Washington, D. C., pp. 90-130.

Rajar, R., 1978: Mathematical Simulation of dam-break flow, Journ. Hydraul. Div., ASCE, 104, HY7, July, pp. 1011-1026.

Ray, H. A., L. C. Kjelstrom, E. G. Crosthwaite, and W. H. Low, 1976: The flood in southeastern Idaho from the Teton Dam failure of June 5, 1976. Unpublished open file report, U. S. Geological Survey, Boise, Idaho.

Re, R., 1946: A study of sudden water release from a body of water to canal by the graphical method. Houille Blanche (France), No. 3, pp. 181-187.

Ritter, A., 1892: The propagation of water waves. Ver. Deutsch Ingenieure Zeitschr. (Berlin), 36, Pt. 2, No. 33, pp. 947-954.

Sakkas, J. G., and T. Strelkoff, 1973: Dam break flood in a prismatic dry channel, Journ. Hydraul. Div., ASCE, 99, HY12, Dec., pp. 2195-2216.

Schocklitsch, A., 1917: On waves created by dam breaches. Akad. Wiss. (Vienna) Proc., 126, Pt. 2A, pp. 1489-1514.

Smith, R. H., 1978: Development of a dynamic flood routing model for small meandering rivers. Ph.D. dissertation, Univ. Missouri-Rolla, 159 pp.

Stoker, J. J., 1957: Water Waves, Inter-Science Pub., New York, pp. 333-341.

Strelkoff, T., 1970: Numerical solution of Saint-Venant equations. Journ. Hydraul. Div., ASCE, 96, HY1, Jan., pp. 223-252.

Su, S. T., and A. H. Barnes, 1970: Geometric and frictional effects on sudden releases. Journ. Hydraul. Div., ASCE, 96, HY11, Nov., pp. 2185-2200.

Terzidis, G., and T. Strelkoff, 1970: Computation of open channel surges and shocks. Journ. Hydraul. Div., ASCE, 96, HY12, Dec., pp. 2581-2610.

Thomas, W. A., 1977: Calculating and routing of the Teton dam-break flood, Proceedings, Dam-Break Flood Modeling Workshop, U. S. Water Resources Council, Washington, D. C., pp. 198-227.

U. S. Army Corps of Engineers, 1960: Floods resulting from suddenly breached dams--conditions of minimum resistance, hydraulic model investigation. Misc. Paper 2-374, Report 1, WES, Feb., 176 pp.

U. S. Army Corps of Engineers, 1961: Floods resulting from suddenly breached dams--conditions of high resistance, hydraulic model investigation. Misc. Paper 2-374, Report 2, WES, Nov., 121 pp.

U. S. Army Corps of Engineers, 1975, National Program of Inspection of Dams, Bol. I-4, Dept. of the Army, Office of Chief of Engineers, Washington, D. C.

U. S. Dept. Transportation/Federal Highway Administration, 1978: Hydraulics of Bridge Waterways, Hydraulic Design Series No. 1, Washington, D. C., pp. 45-46.

Venard, J. K., 1954: Elementary Fluid Mechanics, John Wiley and Sons, New York, pp. 312-325.

APPENDIX A

INPUT DATA STRUCTURE FOR DAM-BREAK (DAMBRK): 07/18/84

Input card group no.

(1) MDAM, MRVR, MNAME - 20 A 4 Format

MDAM	Name of dam (col. 1-20).
MRVR	Name of reservoir (col. 21-40).
MNAME	Agency name (col. 41-60).

MESAGE - 20 A 4 Format

MESAGE	Agency address--street, room (col. 1-40). Agency Address--city, state, zip code (col. 41-72).

(2) KKN, KUI, MULDAM, KDMP, ITEH, NPRT, KFLP, KSL - 8 I 10 Format

KKN	Parameter which is associated with KSUPC on card (16). If KSUPC=0, KKN=1; if KSUPC=1, KKN should be given a value of 1 if the downstream channel valley below the dam is entirely supercritical flow or KKN should be given a value of 2 if the downstream reach is divided into two reaches (an upstream reach having supercritical flow and a downstream reach having subcritical flow). If KKN=9, a hydrograph is read in and then routed through the downstream valley.
KUI	Parameter used to select type of reservoir routing for determining outflow hydrograph; if KUI=0, storage routing is used; if KUI=1, dynamic routing is used.
MULDAM	Parameter used to select option for routing through multiple reservoirs sequentially located downstream of first dam. If one or more dams are located downstream of first dam, MULDAM=1, if no dams are downstream of first dam, then MULDAM=0. Any number of downstream sequentially located dams may be simulated by letting KKN=1 + no. of downstream dams.
KDMP	Parameter for printing; users outside of the National Weather Service set KDMP=3. KDMP=0, print only title page; KDMP=1, title page, abstract, variable descriptions; KDMP=2, same as KDMP=1 plus input data; KDMP=3, title page plus input data; KDMP=4, same as KDMP=2, then stop; if KDMP=5, IOPUT on card (4) allowing selective printout of computations is read-in and KDMP is reset to 3.

ITEH — Parameter denoting number of hydrograph ordinates of inflow hydrograph to reservoir; maximum value of 50 is allowed; if ITEH=0, the inflow hydrograph is generated via a mathematical function.

NPRT — Parameter to control print output for JNK=9, NPRT is the total number of cross-sections at which hydraulic information is printed-out during dynamic routing; if NPRT=0, the program uses a variable NPRT computed by the program and prints-out hydraulic information at NPRT intervals of cross-sections along the routing reach.

KFLP — Parameter denoting the use of the special flood-plain routing feature; if KFLP=0, the special flood-plain feature is <u>not</u> used; if KFLP=1, the special flood-plain routing is used.

KSL — Parameter denoting simulation of landslide; if KSL=0, <u>no</u> landslide; if KSL=1, a landslide occurring along one bank of the reservoir is simulated; if KSL=2, the landslide occurs along both banks of reservoir.

(3) NPT(K) - 8 I 10 Format

NPT(K) — Sequential number of cross-section at which hydraulic information is printed-out; this card is omitted if NPRT=0; K index goes from 1 to NPRT where NPRT $\leq$ 30.

(4) IOPUT(K) - 10 I 1, 2 I 2 Format

IOPUT(K) — Optional print parameter that may override the JNK parameter, (card 16). K index goes from 1 to 12. If IOPUT(K)=0, allow the output to be printed; if IOPUT(K)=1, suppress the output. The following output can be controlled:

Col	
1	Slope profile plot
2	Summary tables of input x.s. and reaches
3	Initial conditions table - flow and "L" tables (reversed)
4	Initial conditions table - backwater elevation table (forward)
5	Dynamic routing - at upstream and downstream boundaries
6	Dynamic routing - at each multiple dam site (similar to depletion table)
7	Summary plots - peak elevation, discharge, time to peak, and time to flood elevation
8	Arrays for selected hydrograph plots
9	List of input cross-sectional information
10	Reservoir depletion table

Col	
11-12	This value reperesents the time at which printing of output will commence. All output will be suppressed until this time is reach.
13-14	The interval at which the output will be printed.

Note: This information can only be controlled if the JNK parameter allowed it to be printed originally.

(5) IDAM(K) - 8 I 10 Format

IDAM(K) Number of cross-section coincident with the upstream face of each dam; K index goes from 1 to MULDAM. This parameter is only read-in when the simultaneous computation of the complete system is desired (see note on page A-21 for further information on the use of this computational option).

(6) SA(K) - 8 F 10.0 Format

SA(K) Surface area (acres) or volume (acre-ft) of reservoir at elevation HSA(K). If KUI=1 and KKN≠1 or KKN=9, omit card (6). Maximum of 8 values allowed.

(7) HSA(K) - 8 F 10.0 Format

HSA(K) Elevation (ft) at which reservoir surface area SA(K) is defined; elevation is referenced to a datum plane corresponding to mean sea level (m.s.l.). If KUI=1 and KKN≠1 or KKN=9, omit card (7). Elevations start at highest and proceed to lowest. Maximum of 8 values allowed. Lowest elevation must be YBMIN as defined on card (8).

(8) RLM, YO, Z, YBMIN, BB, TFH, DATUM, VOL - 8 F 10.0 Format

RLM Length (mi) of reservoir.

YO Elevation (ft) of water surface in reservoir when computation commences; elevation is referenced to m.s.l. datum.

Z Side slope (1:vertical to z:horizontal) of breach.

YBMIN Lowest elevation (ft) that bottom of breach reaches; elevation is referenced to m.s.l. datum.

BB	Width (ft) of base of breach.
TFH	Time (hr) from beginning of breach formation until it reached its maximum size.
DATUM	Elevation (m.s.l.) of bottom of dam.
VOL	Parameter indicating if SA(K) is surface area (acres) or volume (acre-ft); if VOL=0.0, SA(K) is acres; if VOL=1.0, SA(K) is acre-ft.

(9) HF, HD, HSP, HGT, CS, CG, CDO, QT - 8 F 10.0 Format

HF	Elevation (ft) of water when failure of dam commences; elevation is referenced to m.s.l. datum; if HF is less than HD, the breach is formed by "piping."
HD	Elevation (ft) of top of dam; elevation is referenced to m.s.l. datum.
HSP	Elevation (ft) of uncontrolled spillway crest; elevation is referenced to m.s.l. datum.
HGT	Elevation (ft) of center of gate openings; elevation is referenced to m.s.l. datum.
CS	Discharge coefficient for uncontrolled spillway; it is equal to the coefficient of discharge (2.6-3.2) times the length (ft) of the spillway.
CG	Discharge coefficient for gate flow; it is equal to the coefficient of discharge (0.60-0.80) times the area of gates.
CDO	Discharge coefficient for uncontrolled weir flow over the top of the dam; it is equal to the coefficient of discharge (2.6-3.2) times the length of the dam crest (ft) less the length of the uncontrolled spillway and gates.
QT	Discharge (cfs) through turbines; this flow is assumed constant from start of computations until the dam is completely breached; thereafter, QT is assumed to be zero. QT may also be considered leaking or constant spillway flow.

<u>Note</u>: Omit cards (8) and (9) if KKN=9.

(10) QSPILL(K,L) - 8 F 10.0 Format

QSPILL(K,L)	Flow (cfs) of spillway or gate rating curve; K goes from 1 to maximum of 8; L goes from 1 to MULDAM (card (2)) which may be a maximum of 10; if MULDAM=0, L goes from 1 to 1.

(11) HEAD(K,L) - 8 F 10.0 Format

HEAD(K,L) Head (ft) above spillway crest or gate center; head is associated with spillway flow or gate flow in rating curve; K goes from 1 to maximum of 8; L goes from 1 to MULDAM.

Note: Repeat cards 10-11 as L index goes from 1 to MULDAM. If MULDAM=0, L index goes from 1 to 1.

Note: Cards (10) and (11) are read-in only if either HSP is non-zero and CS is zero, or HGT is non-zero and CG is zero. This option allows a rating curve to be used for either the uncontrolled spillway or submerged gate rather than an equation for each using a constant discharge coefficient as in Eq. (17).

(12) DHF, TEH - 2 F 10.0 Format

DHF Interval (hr) between QI(K) input hydrograph ordinates; enter 0.0 if intervals are not equal.

TEH Time (hrs) from beginning of routing until routing is terminated.

(13) QO, RHO, GAMA, TPG - 4 F 10.0 Format

QO Initial steady discharge (cfs).

RHO Ratio of peak flow to initial flow of inflow hydrograph.

GAMA Ratio of time from initial steady flow to center of gravity of inflow hydrograph to time to peak of inflow hydrograph.

TPG Time from initial flow to peak flow of inflow (hr).

Note: Omit card 13 if ITEH (card 2) is nonzero.
If card 13 is included, then omit cards (14) and (15).

(14) QI(K) - 8 F 10.0 Format

QI(K) Inflow (cfs) at upstream end of reservoir for each interval of time during the failure and until time TEH is reached; K goes from 1 to ITEH which can assume a maximum value of 50; if ITEH=0, omit this card.

(15) TI(K) - 8 F 10.0 Format

TI(K) Time associated with QI(K) inflows; if DHF (card 12) is non-zero, or if ITEH (card 2) is equal to zero, omit this card, K goes from 1 to ITEH.

(16) NS, NCS, NTT, JNK, KSA, KSUPC, LQ, KCG - 8 I 10 Format

NS Number of cross-sections used to describe the channel and valley downstream of dam; first cross-section should be immediately downstream of dam; last cross-section should be at farthest point downstream of dam where flood information is desired; other cross-sections can be located as desired by user; maximum of 90 and minimum of 2 cross-sections can be used to describe the downstream channel valley.

NCS Maximum numer of top widths used to describe a cross-section.

NTT Total number of cross-sections at which discharge hydrographs will be plotted; maximum number is limited to 6. The location of the cross-sections at which plots are provided is specified by the parameter NT(K), which is on card (17). If NTT=0, no plots are provided. If NTT=a negative value between 1 and 6, the profile plots are suppressed.

JNK Parameter to specify the type of output other than plots which will be provided; if JNK=0, a minimum of output is provided—this includes all input data and hydrograph plots; if NTT=0, no hydrographs or other output printed; if JNK=1, reservoir depletion table printed, profile of downstream crests and times, and designated hydrographs; if JNK=4, additional information is printed at each time step for debugging; if JNK=9, information is printed for debugging.

KSA Parameter to enable downstream channel-valley cross-sections to be specified by a surface area vs. elevation table similar to the SA(K) and HSA(K) values described above; if KSA=1, downstream channel-valley cross-sections will be described by input data consisting of a single table of surface area vs. elevations as indicated for cards (24) and (25); if KSA=0, this option is not used.

Also, a parameter to indicate type of cross section smoothing. If KSA<0, then smoothing of cross sections will be automatically performed. Type of smoothing is specified on card (18).

KSUPC — Parameter to indicate if flow is supercritical. If KSUPC=0, flow through entire downstream channel-valley reach is subcritical and no special treatment is required; if KSUPC=1, the flow is known to be supercritical in either an upstream portion of the downstream channel-valley or throughout the entire downstream reach. When flow is supercritical, special computational procedures are used within the program. If only the upstream portion of the reach has supercritical flow, two sets of downstream channel-valley inputs commencing with card no. (16) are read in.

LQ — Parameter denoting the total number of lateral inflow hydrographs along the downstream channel-valley; a maximum of 10 hydrographs, each with 50 ordinates, are allowed.

KCG — Number of ordinates in spillway gate control curve of gate coefficient (CGCG) vs. time (TCG) described on cards (43) and (46). If KCG is negative, it is the total number of floodplain compartments. Maximum of 16 allowed.

Note: For debugging, JNK=4 or 9 is preferred.

(17) NT(K) - 6 I 10 Format

NT(K) — Number of cross-section (1 through NS) at which hydrograph plots are desired; K goes from 1 to NTT: if NTT=0, card no. (17) is omitted.

(18) SMF, NTSM, NSMR - F10.2, 2 I 10

SMF — Smoothing factor, $0.5 \leq SMF \leq 0.9$.

NTSM — Parameter indicating type of smoothing. If NTSM=1, smoothing of widths along x-axis; if NTSM=2, smoothing of widths in vertical where maximum width/ft change is |KSA|*50; if NTSM=3, smoothing of elevations along x-axis; NTSM=4, type 1 and type 2 smoothing; if NTSM=5, type 1, 2, and 3 smoothing.

NSMR — Number of separate smoothing reaches within the total routing reach.

(19) NUSM(K), NDSM(K) - 2 I 10

NUSM(K) — Upstream cross section number of Kth smoothing reach.

NDSM(K) — Downstream cross section number of Kth smoothing reach.

Note: Card (19) is read-in for each Kth smoothing reach as K goes from 1 to NSMR.

Note: Omit cards 18 and 19 if KSA $\geq$ 0 (card 16)

(20) XS(I), FSTG(I), XSL(I), XSR(I) - 4 F 10.0 Format

XS(I)	Location (mi) of cross-sections used to describe downstream channel-valley; mileage must increase in the downstream direction from dam. If KFLP=1 (card (2)), XS(I) is mileage measured along center of channel.
FSTG(I)	Elevation (m.s.l.) at which flooding commences; may be left blank.
XSL(I)	If KFLP=0, leave blank; if KFLP=1, XSL(I) is the mileage (location) of the Ith cross-section along the left (looking upstream) flood-plain.
XSR(I)	If KFLP=0, leave blank; if KFLP=1, XSR(I) is the mileage (location) of the Ith cross-section along the right flood-plain.

(21) HS(K,I) - 8 F 10.0 Format

HS(K,I)	Elevation (ft), referenced to m.s.l. datum, corresponding to each top width (BS(K,I)) on card (22) used to describe cross-section; K goes from 1 to NCS; NCS values of HS(K,I) are punched on a single card. NCS is limited to a maximum of 8. Start with lowest HS and proceed to highest value of HS.

(22) BS(K,I) - 8 F 10.0 Format

BS(K,I)	Top width (ft) of active flow portion of channel-valley cross-section corresponding to each elevation HS(K,I); K goes from 1 to NCS; NCS values of BS(K,I) are punched on a single card; NCS is limited to maximum of 8. This card is omitted if KSA=1.

(23) BSL(K,I) - 8 F 10.0 Format

BSL(K,I)	Top width (ft) of active flow portion of left flood-plain corresponding to each elevation HS(K,I); K goes from 1 to NCS; NCS values of BSL(K,I) are punched on a single card; NCS is limited to a maximum of 8. This card is omitted if KFLP=0 (card (2)).

(24) BSR(K,I) - 8 F 10.0 Format

BSR(K,I) Top width (ft) of active flow portion of right flood-plain corresponding to each elevation HS(K,I). This card is omitted if KFLP=0.

(25) BSS(K,I) - 8 F 10.0 Format

BSS(K,I) Top width (ft) of off-channel storage portion of channel-valley cross-section corresponding to each elevation HS(K,I); K goes from 1 to NCS; NCS values of BSS(K,I) are punched on a single card; NCS is limited to maximum of 8; this card is omitted if KSA=1 (card (16)).

(26) DSA(K,I) - 8 F 10.0 Format

DSA(K,I) Surface area (acres) of active flow portion of down-stream channel-valley cross-section corresponding to each elevation HS(K,I); K goes from 1 to NCS; NCS values of DSA(K,I) are punched on a single card; NCS is limited to maximum of 8; this card is omitted if KSA < 0.

(27) SSA(K,I) - 8 F 10.0 Format

SSA(K,I) Surface area (acres) of off-channel storage portion of channel valley cross-section corresponding to each elevation HS(K,I); K goes from 1 to NCS; NCS values of SSA(K,I) are punched on a single card; NCS is limited to maximum of 8; this card is omitted if KSA=0.

Note: Cards (20)-(25) are repeated for each cross-section as in the index I goes from 1 to NS.
When KSA=1, the cards are read-in as follows: (20), (21), (26), (27), (20), (21); this option is limited to the case of NS=2.

(28) CM(K,I) - 8 F 10.0 Format

CM(K,I) Manning n for channel corresponding to each elevation HS(K,I); K goes from 1 to NCS: NCS values of CM(K,I) are punched on a single card; NCS is limited to maximum of 8; the Manning n represents the roughness enountered by the flow through the reach bounded by cross-sections at locations I and I+1.

(29) CML(K,I) - 8 F 10.0 Format

CML(K,I) Manning n for left flood-plain corresponding to each elevation HS(K,I); K goes from 1 to NCS; NCS values of CM(K,I) are punched on a single card; NCS is limited to a maximum of 8. This card is omitted if KFLP=0 (card 2).

(30) CMR(K,I) - 8 F 10.0 Format

CMR(K,I) Manning n for right flood-plain corresponding to each elevation HS(K,I). This card is omitted if KFLP=0.

Note: Cards (28, 29, 30) are repeated for (NS-1) reaches.

(31) DXM(I) - 8 F 10.0 Format

DXM(I) Minimum Δx distance (mi) between cross-sections used in the computations. If DXM(I) is less than the distance between two adjacent cross-sections among the NS cross-sections read in, then intermediate cross-sections are created within the program via an interpolation procedure. (NS-1) values of DXM(I) are punched on one or more cards (8 values to a card); maximum no. of DXM(I) values is limited to 89; values assigned to DXM(I) should not result in more than 200 cross-sections produced by the interpolation procedure. (DXM values should be determined by the relationship C times Δt, where C is the approximate speed of the flood wave.)

(32) FKC(I) - 8 F 10.0 Format

FKC(I) Contraction-expansion coefficient; contraction values vary from 0.1 to 0.3, expansion values vary from -0.5 to -1.0; if contraction-expansion effects are negligible, enter 0.0 for FKC(I); (NS-1) values of FKC(I) are punched on one or more cards (8 values to a card); maximum no. of FKC(I) values is limited to 89.

(33) QMAXD, QLL, DTHM, YDN, SOM, F1I, EPSY, TFI - 8 F 10.0 Format

QMAXD	Estimated maximum discharge (cfs) at downstream extremity of channel-valley reach; can be read in as 0.0 for initial run; subsequent runs can have a value of QMAXD as determined by the routing computations during the initial run. Only required when QLL is non-zero.
QLL	Maximum lateral outflow (cfs/ft) producing the volume losses experienced by the passage of the dam-break flood wave through the downstream valley; QLL has a negative sign and is computed by Eq. (63) in paper.
DTHM	Initial Δt time step size (hr); if 0.0 is read in, the value of DTHM is computed by the program; if DTHM<0.0, DTHM represents the divisor MDT for determining the time step (DTH=TFH/MDT) and DTHM is reset to zero. See note on page A-23.
YDN	Initial elevation of water surface at downstream end of routing reach; if channel control exists at this location, enter 0.0; YDN is non-zero if a dam or other control structure exists at the downstream end of the routing reach; if YDN=0.25, a single value rating curve of water surface elevation (m.s.l.) vs. discharge exists at downstream end; if YDN=0.5, critical flow such as waterfall exists at downstream end; if YDN=0.75, a specified water surface elevation (m.s.l.) such as a tide exists at the downstream end; if YDN=1.0, channel control exists at downstream end, but this signals the program that initial water surface elevations will be read-in at the NS cross-sections via card (48).
SOM	Slope of downstream channel (ft/mi) for first mile below dam.
F1I	Theta (Θ) weighting factor in finite difference solution; if left blank, a value of 0.60 is used in program; if 0.5 is used, Θ is set internally to 0.60 and the model is capable of allowing negative flows to occur; if 0.51 is used, Θ is set internally to 0.60 and the model routing is done by the diffusion method instead of dynamic routing.
EPSY	Convergence criterion for stage (ft) in Newton-Raphson iterative solution of finite difference unsteady flow equations; varies from .01 to .1 ft; if left blank, program use 0.01 ft. Also, can be used to specify the exponent m used in Eq. 65 in the paper; if EPSY<0.50, m=4; if EPSY>0.5, m=EPSY and EPSY is automatically set to 0.01.
TFI	Time (hr) when time step changes from DTHM to TFH/MDT. See time step note on page A-23.

(34) NPLD - I 10

NPLD	Number of last floodplain compartment on same side of river where first floodplain compartment (FPC) is located; if no flow is transferred from one FPC to an adjacent FPC, let NPLD=0. Omit this card if KCG=0.

(35) NPXI(K), NQLP(K), PWELV(K), PCWR(K), PEO(K), QMINP(K) - 2 I 10, 4 F 10.0

NPXI(K)	Number of cross section immediately upstream of Δx reach where inflow to K^{th} FPC occurs.
NQLP(K)	Parameter indicating if pump discharge within the Kth FPC will be specified by a discharge hydrograph; 0 if no, 1 if yes.
PWELV(K)	Average elevation (ft. msl) of crest of weir (levee) along Δx reach where inflow to K^{th} FPC occurs.
PCWR(K)	Coefficient of discharge for weir flow along Δx reach where inflow to K^{th} FPC occurs; ranges in value from 2.6 to 3.2.
PEO(K)	Initial elevation (ft. msl) of water surface in K^{th} FPC at time = 0.
QMINP(K)	Minimum discharge (cfs) of total number of pumps in K^{th} FPC at all times.

(36) PSA(I,K) - 8 F 10.0

PSA(I,K)	Total volume (acre-ft) of Kth FPC below each elevation (PEL(I,K)); I index goes from 1 to 8.

(37) PEL(I,K) - 8 F 10.0

PEL(I,K)	Elevation (ft. msl) associated with each volume (PSA(I,K); elevations start at the lowest and proceed to the highest; I index goes from 1 to 8; last specified elevation should be greater than any expected water elevation within the FPC.

(38) QPU(I,K) - 8 F 10.0

QPU(I,K)	Inflow (cfs) to K^{th} FPC other than that transmitted over the weir (levee) from the main river; I index goes from 1 to ITEH (card no. 2).

(39) QLP(I,K) - 8 F 10.0

QLP(I,K) Specified total pump discharge (cfs) for K^{th} FPC; I index goes from 1 to ITEH (card no. 2); omit this card if NQLP(K)=0.

(40) COFF(I,K) - 8 F 10.0

COFF(I,K) Coefficient of discharge for flow over levee separating the Kth and K^{th}+1 FPC; coefficient is product of the broad-crested weir coefficient (2.6 to 3.2) and the length (ft) of the weir crest; the coefficient varies with elevation (HCFF(I,K)); I index goes from 1 to 8; omit this card if NPLD=0.

(41) HCFF(I,K) - 8 F 10.0

HCFF(I,K) Elevation (ft. msl) associated with the discharge coefficients (COFF(I,K)); elevations start at the lowest point along the levee crest and proceed upward; I index goes from 1 to 8; omit this card if NPLD=0.

Note Omit card no. 34 to 45 if KCG$\geq$0; otherwise repeat card no. 33 to 41 as K index goes from 1 to ABS(KCG).

(42) NPM - I 10

NPM Total number of pumps in all the FPC.

Note> Omit card no. 43 to 45 if NPM=0.

(43) IPMPL(L), NXPO(L), PEMN(L), PEMX(L) - 2 I 10, 2 F 10.0

IPMPL(L) Number of the Kth FPC in which the Lth pump is located.

NXPO(L) Number of the cross section immediately upstream of Δx reach where the Lth pump discharges into main river.

PEMN(L) Elevation (ft. msl) of water in K^{th} FPC when L^{th} pump starts pumping.

PEMX(L) Elevation (ft. msl) of water in K^{th} FPC when Lth pump stops pumping.

(44) DHP(I,L) - 8 F 10.0

DHP(I,L) Head (ft) associated with L^{th} pump rating curve; I index goes from 1 to 8; head starts at smallest and proceeds to greatest; negative head may be specified. Omit this card if NQLP(K)=0.

(45) OP(I,L) - 8 F 10.0

OP(I,L) Pump discharge (cfs) associated with L^{th} pump rating curve; I index goes from 1 to 8; each value is associated with its corresponding DHP(I,L) value. Omit this card if NQLP(K)=0.

Note Repeat card no. 43 to 45 as L index goes from 1 to NPM.

(46) LQX(K) - 8 I 10 Format

LQX(K) Number of cross-section immediately upstream of lateral inflow/outflow; K goes from 1 to LQ (card (16)). If LQX(K) is specified as a negative number, this indicates that the reach may have outflow via broad-crested weir flow.

(47) QL(L,K) - 8 F 10.0 Format

QL(L,K) Lateral inflow (cfs) for k^{th} lateral inflow point; L index goes from 1 to ITEH (card (2)); ordinates of lateral inflow hydrograph have same times as those of reservoir inflow hydrograph (QI(L)) on card (14)); K index goes from 1 to LQ.

If LQX(K) is negative, two values only are specified on card (47) according to a 2 F 10.2 format. The first (WELV(K)) is the crest elevation (msl) at which overflow occurs (this represents the average crest elevation along the reach). The second (CWR(K)) is the discharge coefficient ranging in value from 2.6 to 3.2 with 3.0 a most common value.

Note: Omit cards (46) and (47) if LQ=0 (on card no. 16).

(48) YD(I) - 8 F 10.0 Format

YD(I) Initial water surface elevations (m.s.l.) along routing reach; this is used only if YDN=1.0; if YDN≠1.0, omit this card and program computes the initial water surface elevations.

(49) RH(K) - 8 F 10.0 Format

RH(K) Elevation (m.s.l.) points on single value rating curve for downstream boundary, read in only if YDN (card no. 33) = 0.25; K index goes from 1 to maximum of 8.

(50) RQ(K) - 8 F 10.0 Format

RQ(K) Discharge (cfs) associated with elevation points on single value rating curve for downstream boundary, read in only if YDN=0.25.

(51) STN(K) - 8 F 10.0 Format

STN(K) Specified water surface elevation (m.s.l.) at downstream boundary such as a tide; K goes from 1 to ITEH, read in only if YDN=0.75.

(52) TTN(K) - 8 F 10.0 Format

TTN(K) Time (hrs) associated with STN(K); K goes from 1 to ITEH, read in only if YDN=0.75.

(53) NSLI - I 10 Format

NSLI Total no. of cross-sections (read-in) where landslide occurs; maximum no. allowed is 6; also maximum total cross-sections (including interpolated ones created by DXM values on card (31)) is limited to 31; omit if KSL=0 (card (2)).

(54) NXSLI(K), TSL, HSL(K), HSM(K), HSU(K), THKSL(K), ALPHA, POR - I 10, 7 F 10.2 Format

NXSLI(K)	Sequential number of cross-section where landslide occurs; K index goes from 1 to NSLI.
TSL	Time of duration for landslide (usually in the range of 15 seconds to a few minutes); unit must be in hrs.
HSL(K)	Elevation (ft above m.s.l.) of lowest portion of landslide mass; K goes from 1 to NSLI.
HSM(K)	Elevation (ft above m.s.l.) of middle portion of landslide mass--at this elevation, the landslide mass has the greatest thickness into the bank; K goes from 1 to NSLI.
HSU(K)	Elevation (ft above m.s.l.) of highest portion of landslide mass, K goes from 1 to NSLI.
THKSL(K)	Greatest thickness (depth into the bank) in ft of the landslide mass at elevation HSM(K); K goes from 1 to NSLI.
ALPHA	Angle of repose that deposited material from the landslide assumes in the bottom of the reservoir, in degrees.
POR	Porosity of landslide material, decimal fraction.

Note: Omit cards (53) and (54) if KSL=0.

Note: Card (54) is repeated for each K as it goes from 1 to NSLI.

(55) ICG(K) - 8 I 10 Format

ICG(K)	Parameter indicating if a dam has time-dependent gate flow; if yes, ICG(K)=1; if no, ICG(K)=0; K goes from 1 to M, where M=MULDAM if MULDAM$\geq$1 and M=1 if MULDAM=0.

(56) CGCG(L,K) - 8 F 10.0 Format

CGCG(L,K)	Spillway gate coefficient equal to area of gates (opened at time TCG(L,K)) x coefficient of discharge; L goes from 1 to KCG (see card 16); and K goes from 1 to the total number of dams having time-dependent gate control.

(57) GBL(L,K) - 8 F 10.0 Format

GBL(L,K)	Distance (ft) from bottom of gate to gate sill (HGT-card(9)); This distance is time dependent and is associated with the time array TCG(L,K); L and K index are same as described on card (56).

(58) TCG(L,K) - 8 F 10.0 Format

TCG(L,K)	Time (hrs) associated with CGCG(L,K); L goes from 1 to KCG; and K goes from 1 to the total number of dams having time-dependent gate control.

Note: Omit cards (55), (56, (57), and (58) if KCG=0 (on card no. 16).

(59) Z, YBMIN, BB, TFH - 4 F 10.0 Format

Z	Side slope (1:vertical to z:horizontal) of breach of downstream dam.
YBMIN	Lowest elevation (ft) that bottom of breach reaches; elevation is referenced to m.s.l. datum.
BB	Width (ft) of base of breach of downstream dam.
TFH	Time (hr) from beginning of breach formation of downstream dam until it reaches its maximum size.

(60) HF, HD, HSP, HGT, CS, CG, CDO, QT - 8 F 10.0 Format

HF	Elevation (ft) of water when failure of downstream dam commences; elevation is referenced to m.s.l. datum.
HD	Elevation (ft) of top of downstream dam; elevation is referenced to m.s.l. datum.
HSP	Elevation (ft) of uncontrolled spillway crest; elevation is referenced to m.s.l. datum.
HGT	Elevation (ft) of center of gate openings; elevation is referenced to m.s.l. datum.
CS	Discharge coefficient for uncontrolled spillway; it is equal to the coefficient of discharge (2.6-3.2) times the length (ft) of the spillway.
CG	Discharge coefficient for gate flow; it is equal to the coefficient of discharge (0.10-0.80) times the area of gates.
CDO	Discharge coefficient for uncontrolled weir flow over the top of the downstream dam; it is equal to the coefficient of discharge (2.6-3.2) times the length of the downstream dam crest (ft) less the length of the uncontrolled spillway and gates.

QT — Discharges (cfs) through turbines; this flow is assumed constant from start of computations until the downstream dam is completely breached; thereafter QT is assumed to be zero.

(61) QSPILL(K,1) - 8 F 10.0 Format

QSPILL(K,1) — Flow (cfs) of spillway or gate rating curve; k goes from 1 to maximum of 8.

(62) HEAD(K,1) - 8 F 10.0 Format

HEAD(K,1) — Head (ft) above spillway crest or gate center; head is associated with spillway flow or gate flow in rating curve.

Note: Cards (61) and (62) are read-in only if either HSP is non-zero and CS is zero or HGT is non-zero and CG is zero. This option allows a rating curve to be used for either the uncontrolled spillway or submerged gate rather than an equation for each using a constant discharge coefficient as in Eq. (17).

(63) UPSH, SOM, CMN - 3 F 10.0 Format

UPSH — Dummy variable, leave blank.
SOM — Slope of downstream channel (ft/mi) for first few miles below dam.
CMN — Average Manning's n for downstream channel for first few miles below dam.

Note: Cards (59-63) are omitted if KUI=0 and MULDAM=0 or if KKN=9.

Note: If KUI=1 and dynamic routing is used for the reservoir routing procedure, cards (6) and (7) are omitted and cards (8)-(58) and (51) apply to the reservoir characteristics. Then, cards (16)-(58) are read in again; this time they apply to the downstream channel and valley.

Note: If KKN=9, only a downstream routing is used to route a read-in hydrograph (cards (12)-(15)). Also, cards (16)-(25) and (28)-(58) are required.

<u>Note</u>: The program has the capability of simulating a total of 12 different cases. These are outlined as follows:

Option 1: Reservoir storage routing to compute outflow hydrograph from reservoir with subcritical dynamic routing of outflow hydrograph through entire length of downstream valley--KUI=0, KKN=1, KSUPC=0, MULDAM=0.
Input data cards--1-4, 6-58.

Option 2: Reservoir storage routing to compute outflow hydrograph from reservoir with supercritical dynamic routing of outflow hydrograph through entire length of downstream valley--KUI=0, KKN=1, KSUPC=1, MULDAM=0.
Input data cards--1-4, 6-58.

Option 3: Reservoir storage routing to compute outflow hydrograph from reservoir with supercritical dynamic routing of outflow hydrograph through upstream portion of downstream valley and subcritical dynamic routing through downstream portion of downstream valley--KUI=0, KKN=2, KSUPC=1, MULDAM=0.
Input data cards--1-4, 6-52, 16-58.

Option 4: Same as Option 1 except reservoir dynamic routing to compute outflow hydrograph from reservoir--KUI=1, KKN=2, KSUPC=0, MULDAM=0.
Input data cards--1-4, 8-58, 63, 16-52.

Option 5: Same as Option 2 except reservoir dynamic routing to compute outflow hydrograph from reservoir--KUI=1, KKN=2, KSUPC=1, MULDAM=0.
Input data cards--1-4, 8-58, 63, 16-52

Option 6: Same as Option 3 except reservoir dynamic routing to compute outflow hydrograph from reservoir--KUI=1, KKN=3, KSUPC=1, MULDAM=0.
Input data cards--1-4, 8-58, 63, 16-52, 16-52.

Option 7: Subcritical dynamic routing of input hydrograph through a channel-valley--KUI=0, KKN=9, KSUPC=0, MULDAM=0.
Input data cards--1-4, 12-52. (See note on page A-20.)

Option 8: Supercritical dynamic routing of input hydrograph through a channel-valley--KUI=0, KKN=9, KSUPC=1, MULDAM=0.
Input data cards--1-4, 12-52. (See note on page A-20.)

Option 9: "Sequential Method" Reservoir storage routing to compute outflow hydrograph from reservoir with subcritical dynamic routing of outflow hydrograph through downstream channel-reservoir having a dam which may fail--KUI=0, KKN=2, KSUPC=0, MULDAM=1.
Input data cards--1-4, 6-63, 16-63, ... 16-52.

Option 10: "Sequential Method" Reservoir dynamic routing to compute outflow hydrograph from reservoir with subcritical dynamic routing of outflow hydrograph through downstream channel-reservoir having a dam which may fail--KUI=1, KKN=3, KSUPC=0, MULDAM=1.
Input data cards--1-4, 8-58, 63, 16-63, ... 16-52.

Option 11: "Simultaneous Method" Simultaneous computation method for single dam or bridge (structure) using dynamic routing in the reach upstream of the structure and downstream of the structure with special internal boundary conditions for flow thru the structure--KUI=1, KKN=1, MULDAM=1, KSUPC=0.
Input data cards--1-5, 8-11, 12-58. See note on page A-21 for input variables for bridge and embankment.

Option 12: "Simultaneous Method" Simultaneous computation method for multiple dams and/or bridges (structures) using dynamic routing for all reaches with special internal boundary conditions for flow thru each structure--KUI=1, KKN=1, MULDAM=no. of dams and/or bridges, KSUPC=0.
Input data cards--1-5, 8-11, 8-11, 8-11, ... 12-58. See note on page A-21 for input variables and embankments.

"SIMULTANEOUS METHOD" OF COMPUTATION OF COMPLETE SYSTEM:

This option treats the upstream reservoir, any intermediate reservoir, and the downstream channel as one system. Cross sections are numbered consecutively from the very upstream end of the most upstream reservoir to the downstream extremity of the downstream channel. Cross sections are specified for the upstream and downstream sides of each dam. This option is most useful for problems in which the tailwater below a dam is affected by backwater from downstream dams or other constrictions. It is necessary when using this option to specify KKN=1, KUI=1, MULDAM $\geq$ 1 to read-in card (5). Also, cards (6) and (7) are omitted, and cards (8) and (9) are repeated for each dam in

the system. Cards (59), (60), (61), (62), and (63) are not applicable for this option. MULDAM is defined as the number of dams in the system.

BRIDGE COMPUTATION

The simultaneous method can be used for either multiple dams or bridges. Cards (8) and (9) are used to describe the flow thru and across the bridge and embankment. The bridge embankment may be allowed to breach. If breaching is not considered possible, HF on card (9) is set to a very large value so that the water surface will not reach it. On card (8), RLM must be left blank as well as YO; other variables on card (8) are associated with the breach of the embankment and are defined essentially the same as shown on page A-4. The variables other than HF on card (9) are defined as follows: HD--height (ft m.s.l.) of crest of uppermost portion of road embankment; HSPD--length (ft) of crest of uppermost portion of road embankment measured across valley and perpendicular to flow; HGTD--height (ft m.s.l.) of crest of lower portion (emergency overflow) of road embankment (if non-existent, leave blank); CSD--length (ft) of crest of lower portion of road embankment measured across valley and perpendicular to flow; CGD--width of top of road embankment as measured parallel to flow; CDOD--coefficient of discharge of flow thru bridge opening (see: Chow, "Open-Channel Hydraulics" pp. 476-490); QT--time step to be used when the upper road embankment is overtopped. QT is only needed when the first structure in the routing reach is a bridge and when the inflow hydrograph is a slowly rising hydrograph. It should be left blank at all other times. If it is left blank when needed, the default value is 0.5 hr. Instead of reading in the length of the upper road embankment, a table of length of embankment (ft) vs. water surface elevation (ft msl) may be read in on cards (9) and (10) respectively. HSPD is then read in as zero.

ROUTING SPECIFIED INFLOW HYDROGRAPH (Options 7 and 8)

Options (7) and (8) are for routing a specified inflow hydrograph through the downstream valley, i.e., there is no upstream reservoir and associated outflow hydrograph as computed by DAMBRK. These options do not enable the treatment of bridges or dams located along the downstream valley.

LEVEL POOL ROUTING USING OPTIONS 11 AND 12

The storage routing (level pool) technique based on Eq. (18) may also be used simultaneously with the dynamic routing technique for simulating the unsteady flow through the downstream channel-valley. Eq. (18) is combined with Eq. (65) to form the upstream boundary condition and the dam is treated as an internal boundary via Eqs. (51-52). The advantages of this combination of the two routing techniques within a simultaneous computation method are: (1) simple routing technique for reservoir, (2) dynamic routing for downstream dam-break hydrograph, and (3) more accurate computation of tail-water elevation than via Eq. (11).

Level pool routing may be used with options 11 and 12 by: (1) including cards (6) and (7) after card (5); (2) IDAM(1) will always be 1, i.e., the first cross-section represents the upstream face of the first dam (level pool routing can only be used for the first or upstream reservoir).

FLOODPLAIN COMPARTMENTS (FPC)

Each FPC may have only one Δx-reach in which flow from the river enters the FPC or, if the differential head favors the FPC, the flow goes from the FPC to the river. This Δx-reach is designated by NXPI(K), where the K index goes from 1 to the total number of FPC's (KCG).

Each FPC may have only one Δx-reach in which the FPC pump(s) return water to the river. The Δx-reach is designated by NXPO(L), where the L index goes from 1 to the total number of pumps (NPM).

A particular Δx-reach cannot be used for more than one FPC; thus, NXPI(1)≠NXPI(2).

A particular Δx-reach cannot be used for both types of flow exchange (weir flow or pump flow); thus, NXPI(K)≠NXPO(L).

An FPC may pass flow to an adjacent FPC via broad-crested weir flow with submergence correction. Also, the most downstream FPC may pass flow on downstream via overtopping weir flow. FPC's are numbered from upstream to downstream, commencing on one side of the river and then the other side of the river.

TIME STEP SELECTION

The time step size used to route the hydrograph through the downstream channel-valley can be user controlled with the DTHM and TFI parameters on card (33). If a constant time step is desired, the user reads in DTHM (time step size) and leaves TFI blank.

If DTHM and TFI are both read in as zero, the model will generate an initial time step size based on the inflow hydrograph - TP/MDT where TP is the time from start of rise to peak of the hydrograph and MDT is the assumed to be 20 unless specified differently by reading in a negative DTHM value. This time step is used until time TFI (the time just prior to dam failure) is exceeded. If KUI=0 (card 2), this value is computed as the time to peak of the outflow hydrograph minus the time to failure. If KUI=1, TFI is set equal to TEH (card 12). If the time exceeds TFI or if the dam fails, the time step is cut back to TFH/MDT. If DTHM and TFI are read in as nonzero values, the DTHM is used until time TFI is exceeded and then the time step is cut back to TFH/MDT.

If TFI is read in as a nonzero value and DTHM is read in as zero, the model will compute DTHM=TP/MDT and use that time step until TFI is exceeded and then cut back to TFH/MDT.

UPDATE FEATURE:

If the parameters (BB, Z, TFH, HD, YO, HF) are the only ones that may have a different value than contained on all input data cards (1)-(63), the following UPDATE procedure can be used:

Place the following two cards immediately before card (1):

UPDATE (with U starting in column 1)
BB, Z, TFH, HD, YO, HF — 6F10.0

where BB, Z, etc., are defined as described previously on cards (8)-(9). If any of these values do not change, leave the appropriate space blank. The update feature is only applicable for Options 1-6.

1/20

Parameter Selection

1. Area (A)

2. Manning n

DEFAULT OPTION OF DTHM:

WAVE SPEED

time to peak of failure

$$\Delta X \leq C\,\Delta t \qquad \Delta t = \frac{T_p}{20} \quad \text{if} \quad DTHM = 0.0$$

computational method for Δx and Δt steps

if DXM > X-SEC. DXM IS IGNORED.

To ESTIMATE/CALCULATE $C = \frac{L}{T_p}$ for hydrographs at 2 x-sections

$$C \approx 2\sqrt{S_m\,(ft./mi)}$$ results in m.p.h.

WAVE SPEED

To ACCOUNT FOR BROAD FLOODPLAINS:

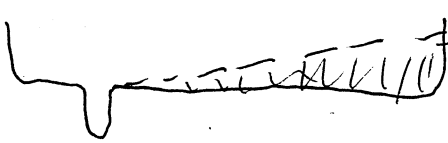

A FALSE BOTTOM NEEDS TO BE INSERTED AND DEAD STORAGE CALCULATED TO ACCOMPLISH THIS USE TYPE 2 SMOOTHING FACTOR

Cross sections need to be located closely enough to accurately reflect the hydraulic characteristics of a channel and its adjacent overbanks between the cross sections. The sections need to extend across the entire flood plain and need to be at right angles to the anticipated direction of flow in both the main channel and overbanks. This may indicate the need for curved or angled sections at some locations. The location of the sections needs to ensure an accurate evaluation of energy losses between sections. For each reach, the energy gradient, water-surface slope, and streambed slope need to be as nearly parallel as possible. If any channel condition causes one of these profiles not to be parallel, it is an indication that additional cross sections are needed. A sufficient number of cross sections are needed to accurately reflect flood-plain geometry.

Some general criteria for locating cross sections are listed below. These criteria help satisfy the assumption of steady uniform flow in individual subreaches.

1. The cross sections need to be located at major changes in bed or water-surface profiles. If old flood profiles are available, they can be used to locate the breaks in water-surface profiles.
2. The cross sections need to be placed at points of minimum and maximum cross-sectional area, width, or depth. The number of cross sections needs to be greater in expanding reaches and in bends to minimize the relative degree of expansion between cross sections and leave the individual subreaches more nearly uniform.
3. The number of cross sections needs to be greater in reaches that have moderate to severe changes in cross-section shape, even though the total areas may differ only slightly from each other. An example would be sections that change shape from just a main channel to main channel with overbank flow.
4. The cross sections need to be located at abrupt changes in roughness characteristics, for example, where the flood plain is heavily vegetated in one subreach, but has been cleared and cultivated in the adjacent subreach. The use of a cross section twice, in close proximity and with different roughness values, must suffice for the present to evaluate the frictional losses.
5. The cross sections need to be located at control sections if critical or *supercritical flow* conditions exist. These controls include natural and manmade weirs, check dams, rock walls, fences, and severe obstructions.
6. The cross sections need to be located at tributaries where changes in discharge are anticipated. The exact placement of the cross sections varies, depending on the method of analysis and program requirements.

Where abrupt channel changes occur, several cross sections need to be established to accurately indicate the changes, regardless of the distance between the sections. At bridges and other hydraulic structures, a sufficient number of cross sections are needed to define the approach and outlet conditions as well as the geometry of the structure, but these conditions are not discussed in this report.

LAST RESORT

CROSS SECTION SMOOTHING

USING THIS AS AN EXAMPLE

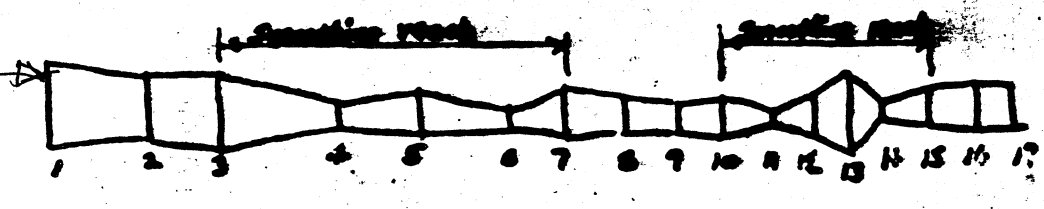

KSA —— 0 ..... No smoothing

< 0 ..... Smoothing

SMF —— Smoothing factor ..... $0.5 \le SMF \le 0.9$ significant to slight smoothing effect.

NTSM —— Type of Smoothing

1 ..... width along x-direction

2 ..... width in vertical direction

3 ..... bottom elevation along x-direction

4 ..... 1 and 2

5 ..... 1 and 2 and 3

(2) NSMR —— Number of smoothing reaches

(3)(10) NUSM(K) —— Upstream cross section number of smoothing reach (K)

(7)(15) NDSM(K) —— Downstream cross section number of smoothing reach (K)

Smoothing function TYPE 1

Smoothing function — TYPE 1

$B_L = \left(\frac{1-SMF}{2}\right) B_{L-1} + (SMF)\, B_L + \left(\frac{1-SMF}{2}\right) B_{L+1}$ .... NUSM(K) < L < NDSM(K)

TYPE 2

Smoothing function — TYPE 2

$B_L = |KSA| \cdot 50$

if $B_L > B_L$ ..... $B_L = B_L + B_L$ .... NUSM(K) ≤ L ≤ NDSM(K)

$BS_L = BS_L + (\text{[illegible]})$

to create dead storage automatically try to get greatest KSA to minimize angle of false bottom

TYPE 3

Smoothing function — TYPE 3

$h_{0L} = \left(\frac{1-SMF}{2}\right) h_{0L-1} + (SMF)\, h_{0L} + \left(\frac{1-SMF}{2}\right) h_{0L+1}$ ..... NUSM(K) ≤ L ≤ NDSM(K)

(4) CROSS-SECTION AREA OF CHANNEL - VALLEY

Errors due to :

1) field measurements
2) sampling interval
3) linear variation of contour interval of topographic maps

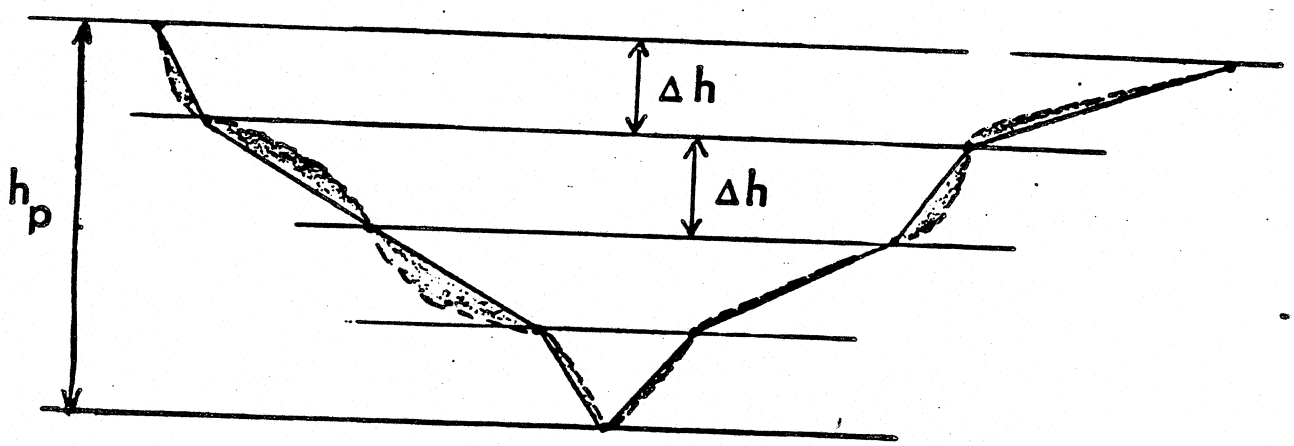

$$\frac{A_e}{A} \propto \underbrace{(m+1)}_{\text{SHAPE FACTOR}} \left(\frac{\Delta h}{h_p}\right)^{m+1}$$

expected peak elevation

$$\frac{h_e}{h} = \left(\frac{A_e}{A}\right)^{\frac{5}{3m+5}}$$

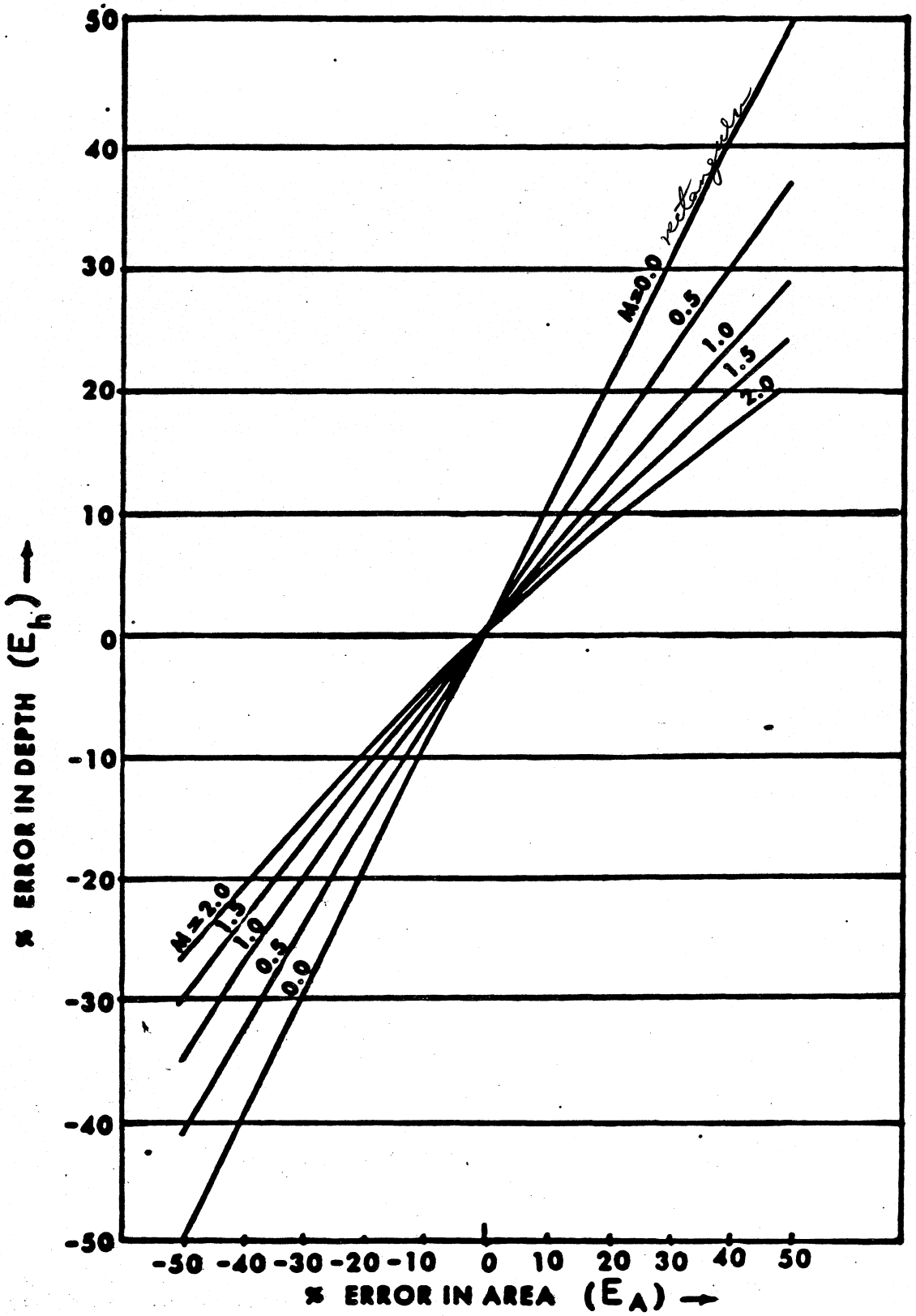

FIG.4-ERROR IN FLOOD DEPTH CAUSED BY ERROR IN CROSS-SECTIONAL AREA FOR VARIOUS SHAPED SECTIONS HAVING STEADY FLOW

FYI

Estimation of Manning n — Steep Gradient Streams

$S_m > 10$ ft/mi $\qquad S > .002$ ft/ft

$$n \approx (0.4)\frac{S^{0.4}}{R^{0.16}}$$

R. D. Jarrett
USGS
ASCE J. Hydraulics
Nov. 1984

Composite n: for DAMBRK

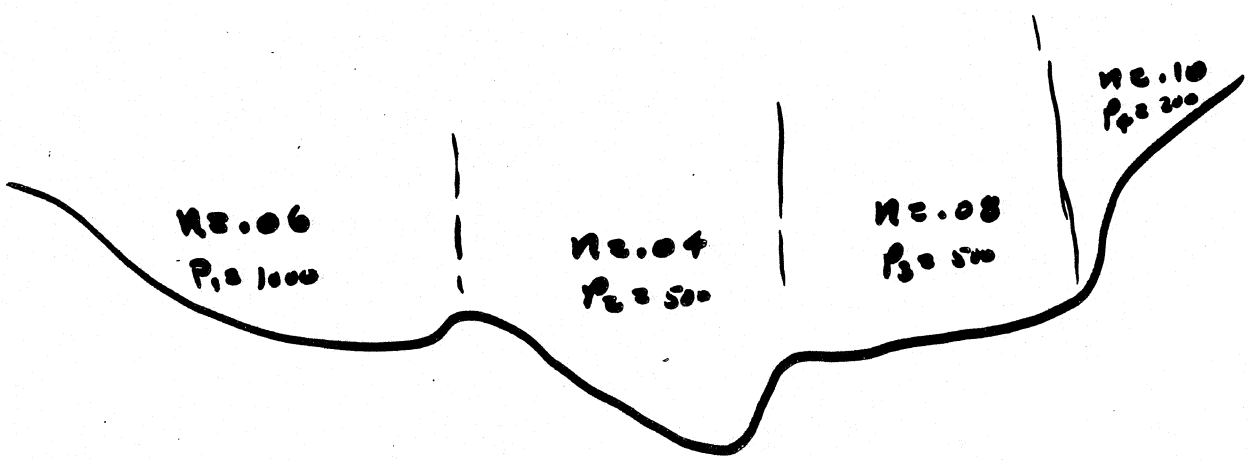

$$\bar{n} = \frac{n_1 P_1 + n_2 P_2 + n_3 P_3 + n_4 P_4}{P_1 + P_2 + P_3 + P_4}$$

PREDICTION OF MANNING n FOR INUNDATED OVERBANK AREAS

$$\boxed{n = 0.0926\sqrt{f}\,(d)^{1/6}}$$

WHERE:

$$f = \overbrace{\frac{0.32\left[1 - 1.3\left(\frac{\phi}{s}\right)^2\right]}{\left[\ln\left(10.94\frac{d}{k} + 1\right)\right]^2}}^{\text{BOTTOM FRICTION (SUBMERGED)}} + \overbrace{6.6\, C_D\left(\frac{\phi}{s}\right)\left(\frac{d}{s}\right)}^{\text{DRAG FROM PARTIALLY SUBMERGED OBSTRUCTIONS}}$$

WHERE:
- d — AVG. DEPTH OF FLOW, ft.
- ϕ — AVG. DIAMETER OF OBSTRUCTION, ft.
- s — AVG. SPACING BETWEEN OBSTRUCTIONS, ft.
- K — NIKURADSES EQUIVALENT SAND ROUGHNESS, ft.

	K (FT)
BERMUDA GRASS	3.75
SWAMP GRASS	12.0
NORMAL GROUND (LAWNS, ETC.)	1.5
COMPLETELY SUBMERGED HOUSES	.36.

C_D - DRAG COEFFICIENT, DIMENSIONLESS

	C_D
TREES	0.4 → 0.8
HOUSES	1.0

ADVANTAGES:
1) ACCOUNTS FOR DRAG FRICTION WHEN FLOW PARTIALLY SUBMERGES TREES, HOUSES, OTHER OBSTRUCTIONS
2) n IS SOMEWHAT INSENSITIVE TO ACCURACY OF K SINCE $n \propto K^{1/6}$

ΔK	Δn
5	1.3
20	1.64

REFERENCES:
1. "FRICTION FACTORS IN FLOODING DUE TO HURRICANES", B.A. CHRISTENSEN & R. WALTON, URBAN STORM WATER MANAGEMENT IN COASTAL AREAS, VIRGINIA TECH., JUNE 19-20, 1980 P265-274
2. "FRICTION FACTORS IN STORM SURGES OVER INLAND AREAS", R. WALTON & B.A. CHRISTENSON, JOURNAL OF WATERWAY, PORT, COASTAL AND OCEAN DIV. ASCE, MAY 1980, VOL. 106, WW2, P261-271.

(4) FRICTIONAL RESISTANCE TO FLOW :

errors due to :

1) flows occurs in previously unflooded areas

2) this new flooded area may often have large flow resistance

3) short- circuiting of flood-plain flow across a meandering river

4) impinged debris

5) sediment trapped behind dam

$$\frac{h_e}{h} = \left(\frac{n_e}{n}\right)^{\frac{3}{3m+5}}$$

$$\frac{C_e}{C} = \left(\frac{n_e}{n}\right)^{\frac{2}{3m+5}-1}$$

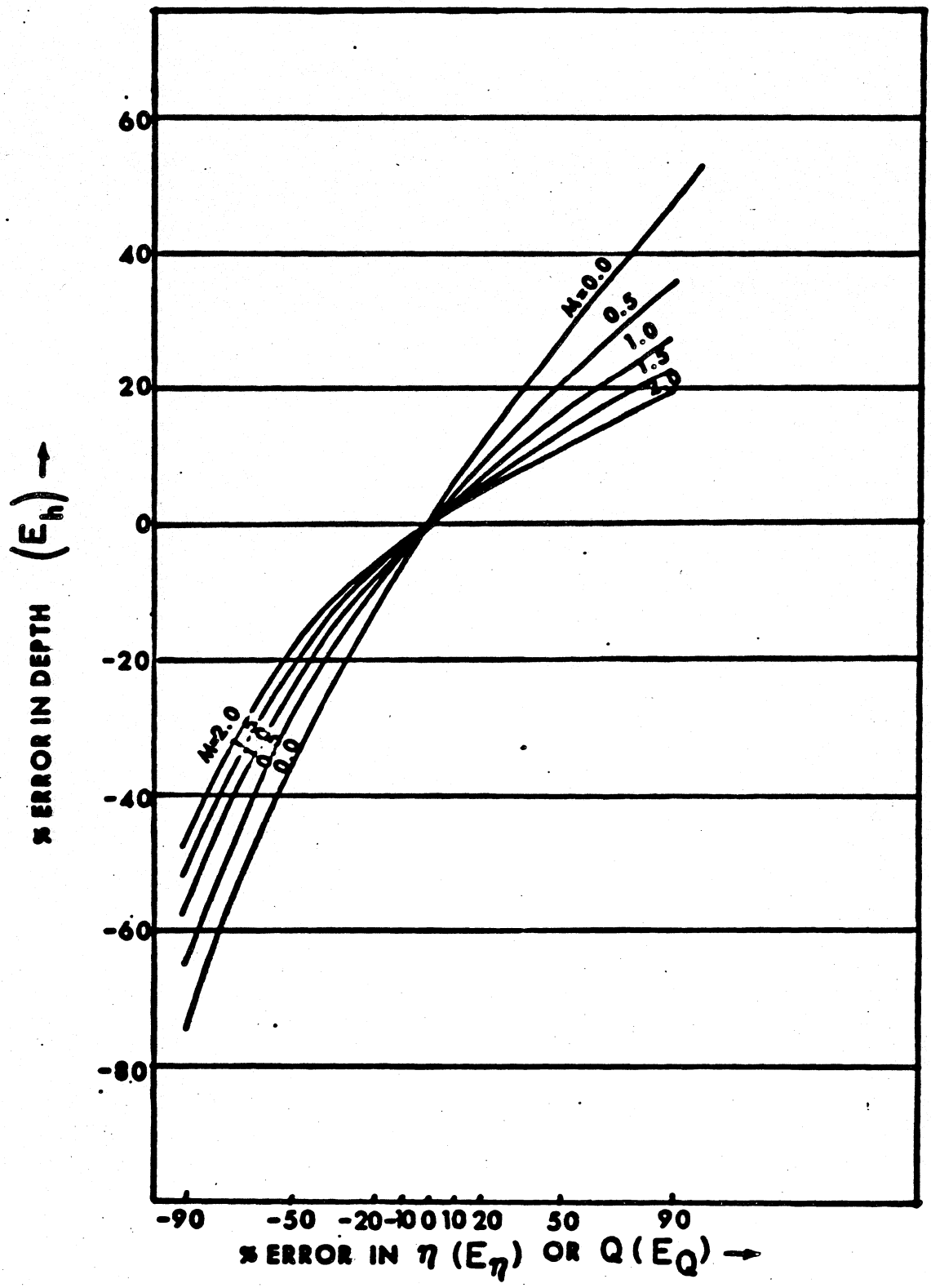

FIG.2-ERROR IN FLOOD DEPTH CAUSED BY ERROR IN ROUGHNESS (η) OR FLOW (Q) FOR VARIOUS SHAPED SECTIONS HAVING STEADY FLOW

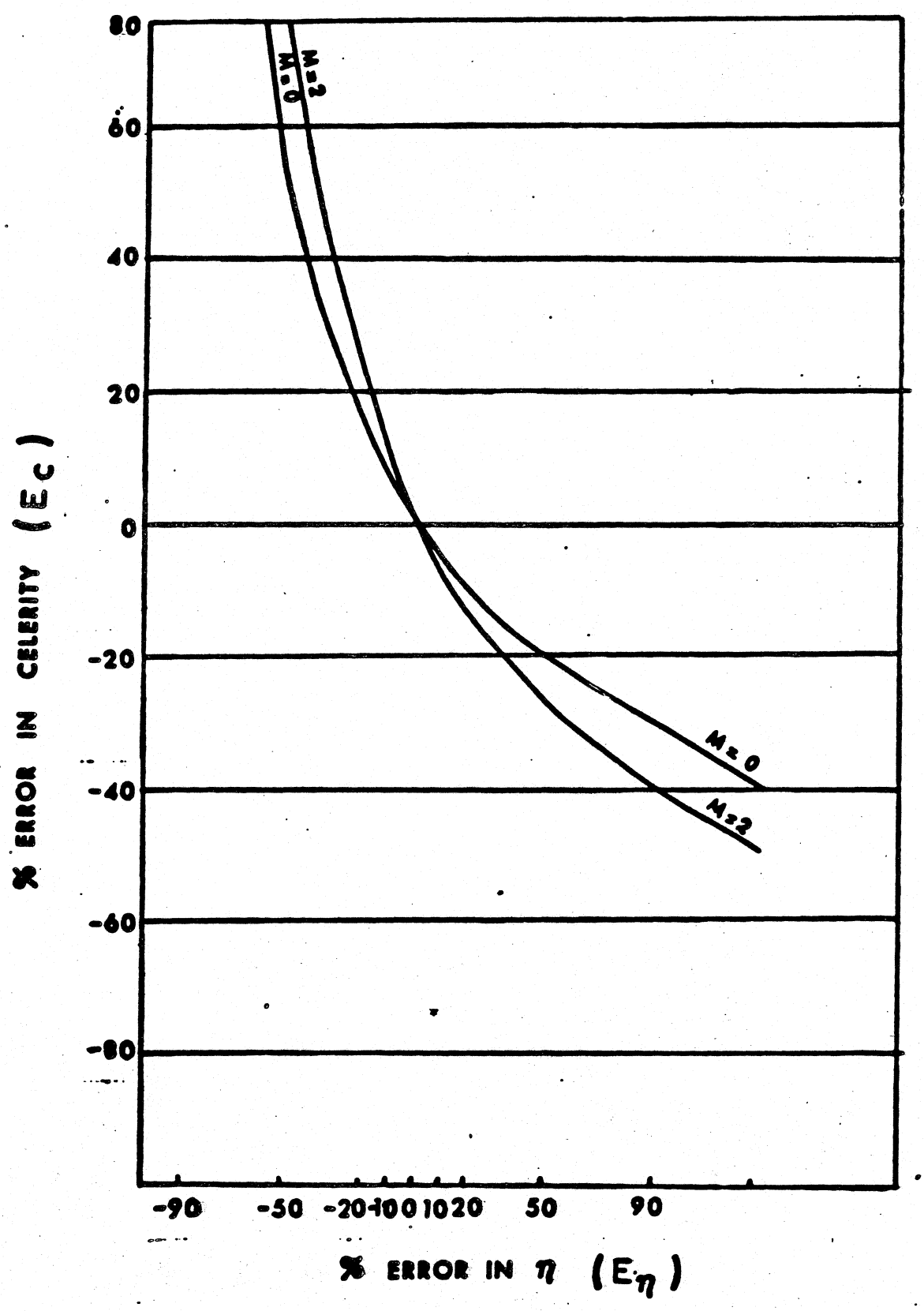

FIG. 5- ERROR IN FLOOD CELERITY CAUSED BY ERROR IN ROUGHNESS FOR VARIOUS SHAPED SECTIONS

OFF-CHANNEL STORAGE AT A POINT

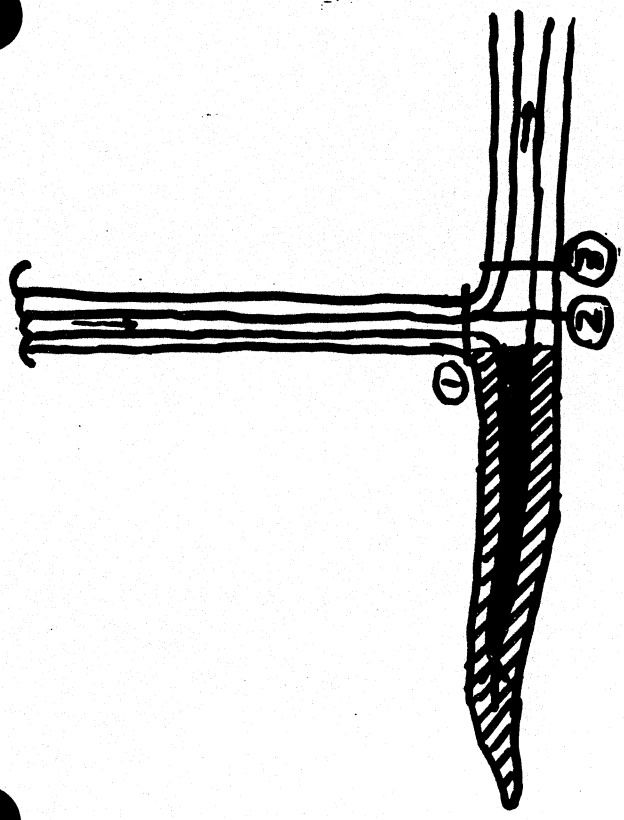

AREA AT ELEV. 52.

AREA AT ELEV. 45.

USE TRIANGULAR DISTRIBUTION BETWEEN 1 AND 3

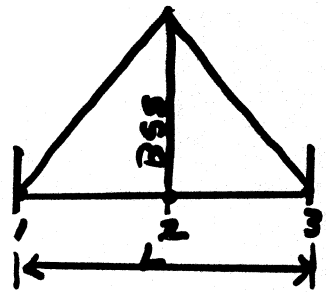

$$SA = \frac{BSS}{2} L \quad (ft^2,\ ft,\ ft)$$

$$\therefore BSS = \frac{2\,SA}{L}$$

SAY $L = 1/2$ mi $= 2640$ ft

IF $SA = 456{,}000\ ft^2$ @ ELEV. 52.

$$BSS = \frac{(2)\,456000}{2640} = 345.\ ft$$

IF $SA = 100{,}200\ ft^2$ @ ELEV. 45.

$$BSS = \frac{(2)\,102000}{2640} = 77.\ ft$$

input card 46-47

Computed Lateral Outflow :

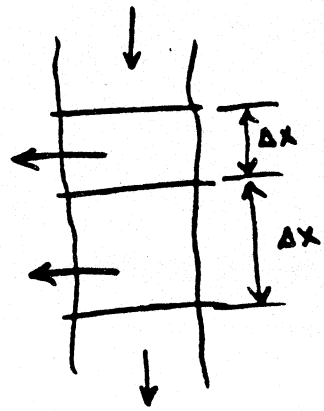

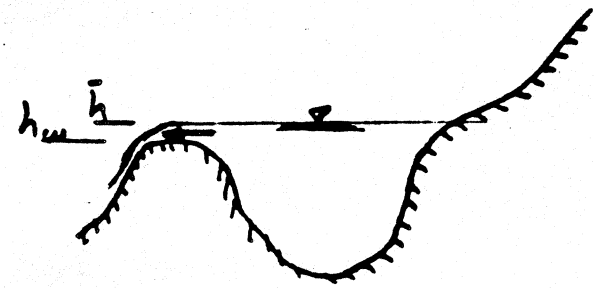

$$q_i = -c_i\left(\bar{h}_i - h_{w_i}\right)^{3/2}$$

c_i = coefficient of discharge for Δx_i reach (input)

$\bar{h}_i = \left(h_i^{j+1} + h_{i+1}^{j+1}\right)/2$

h_w = avg. crest elev. for Δx_i reach (input)

input card 42-45

card 16 KCG signals this option and is negative

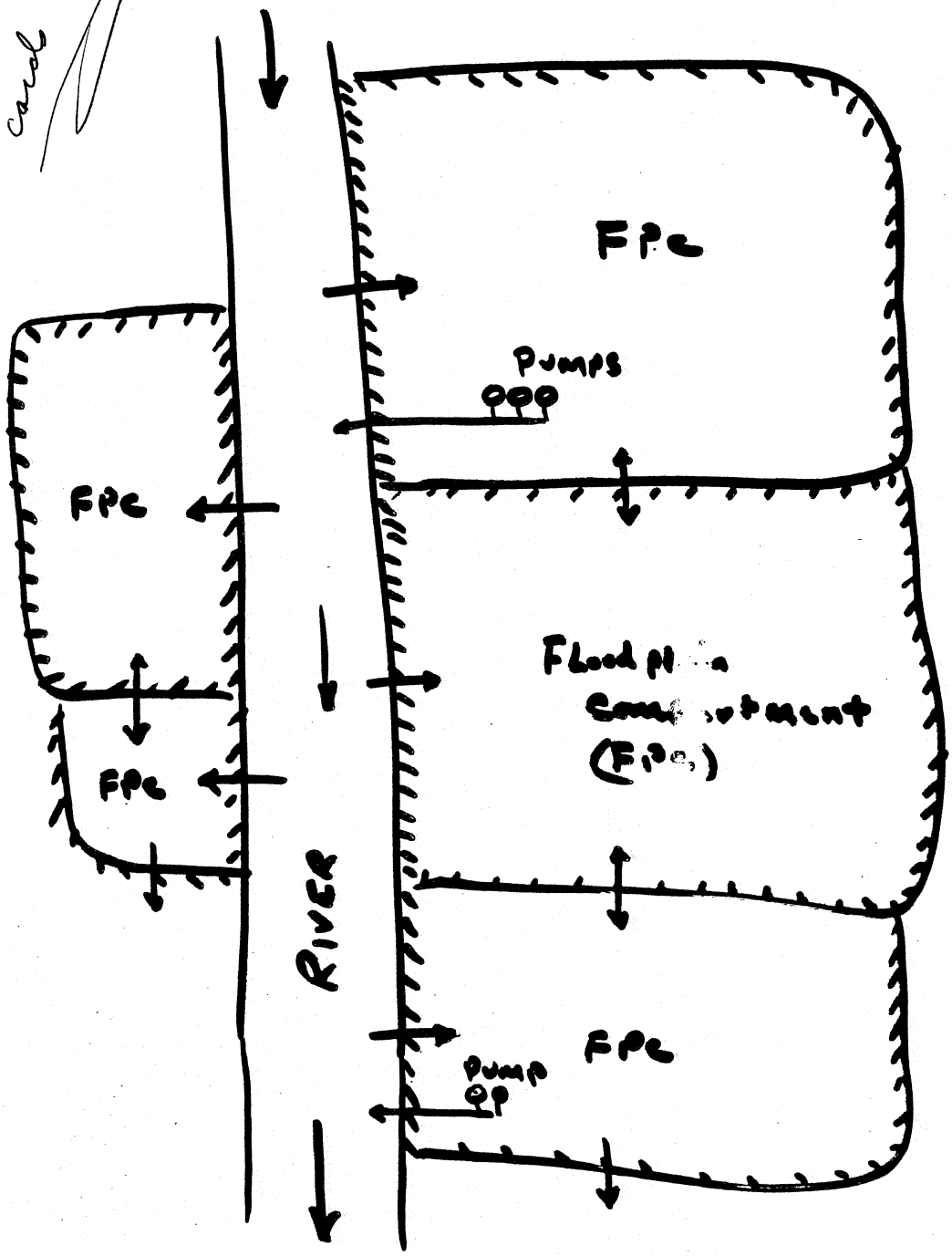

Floodplain Compartment Option

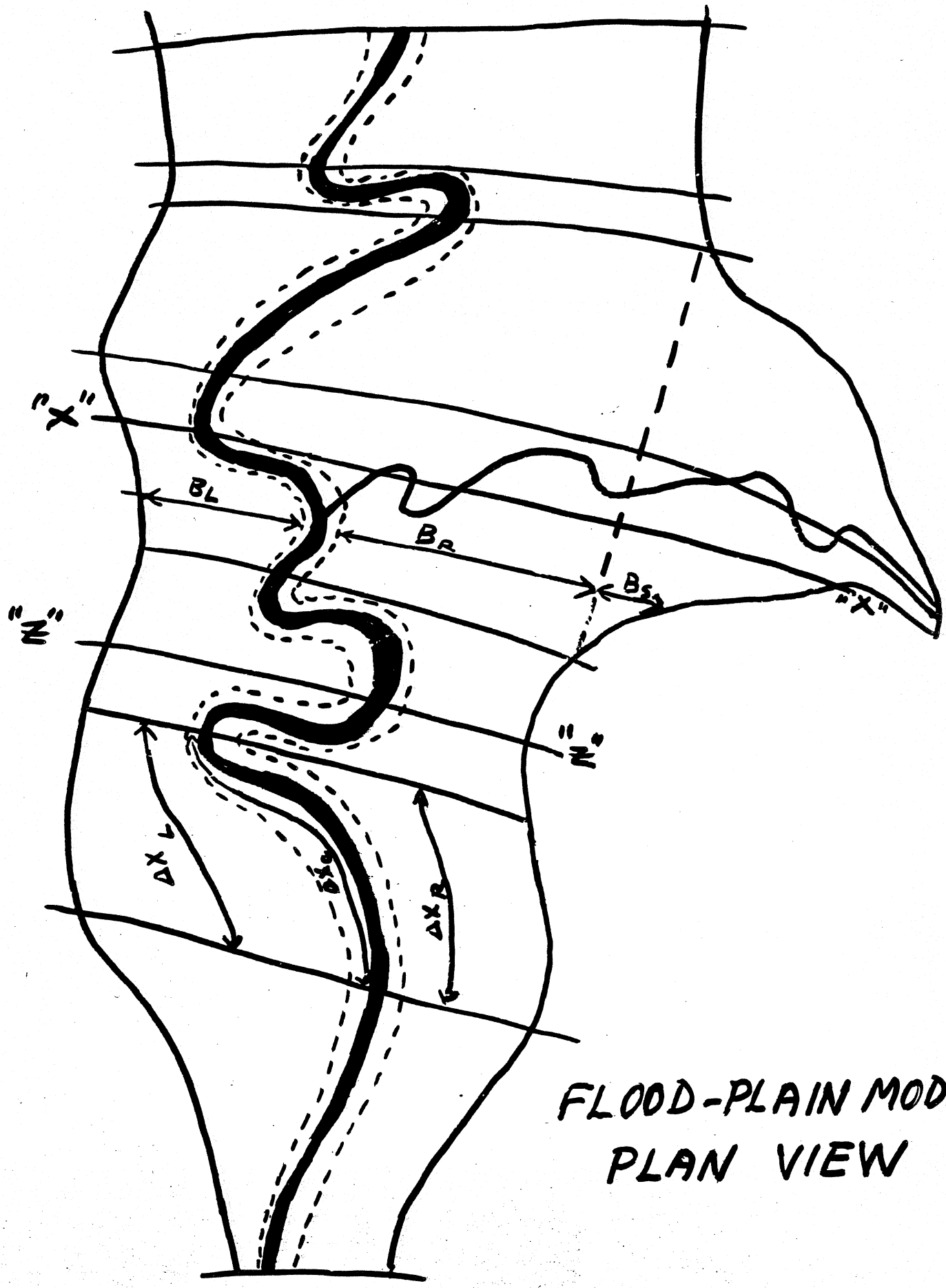

FLOOD-PLAIN MODEL
PLAN VIEW

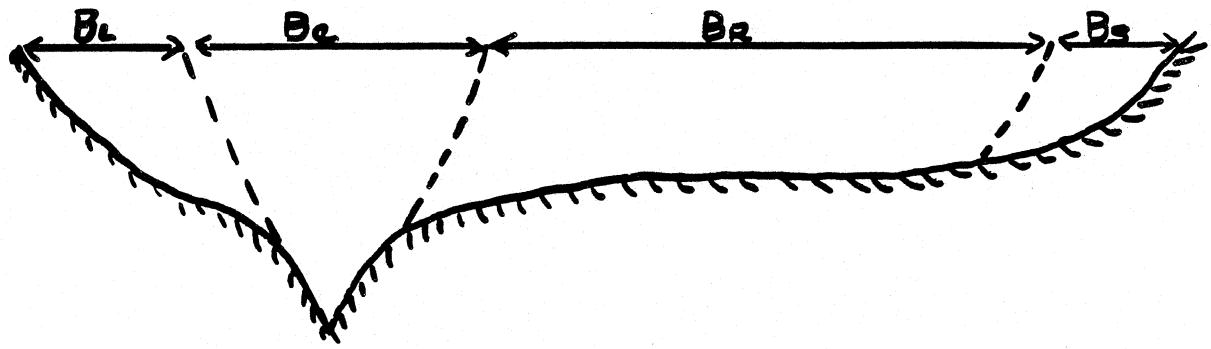

SEC "X"-"X"

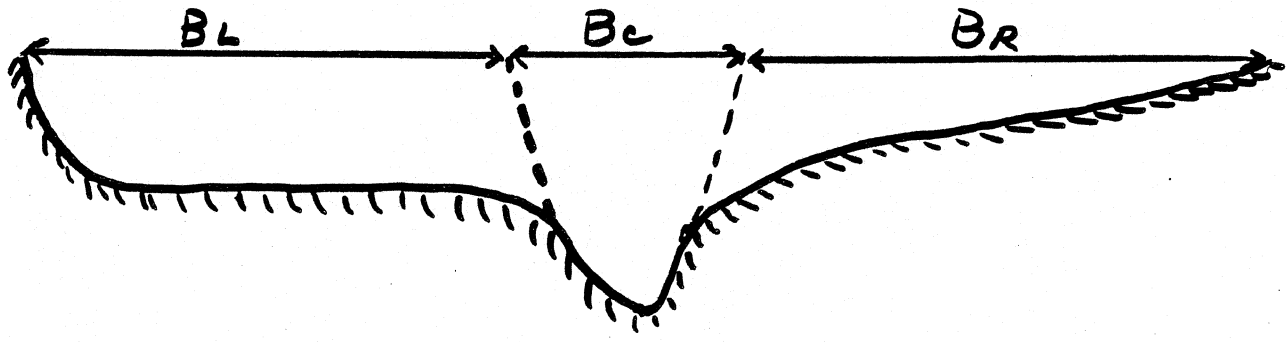

SEC "Z"-"Z"

FLOOD-PLAIN MODEL
CROSS-SECTIONS

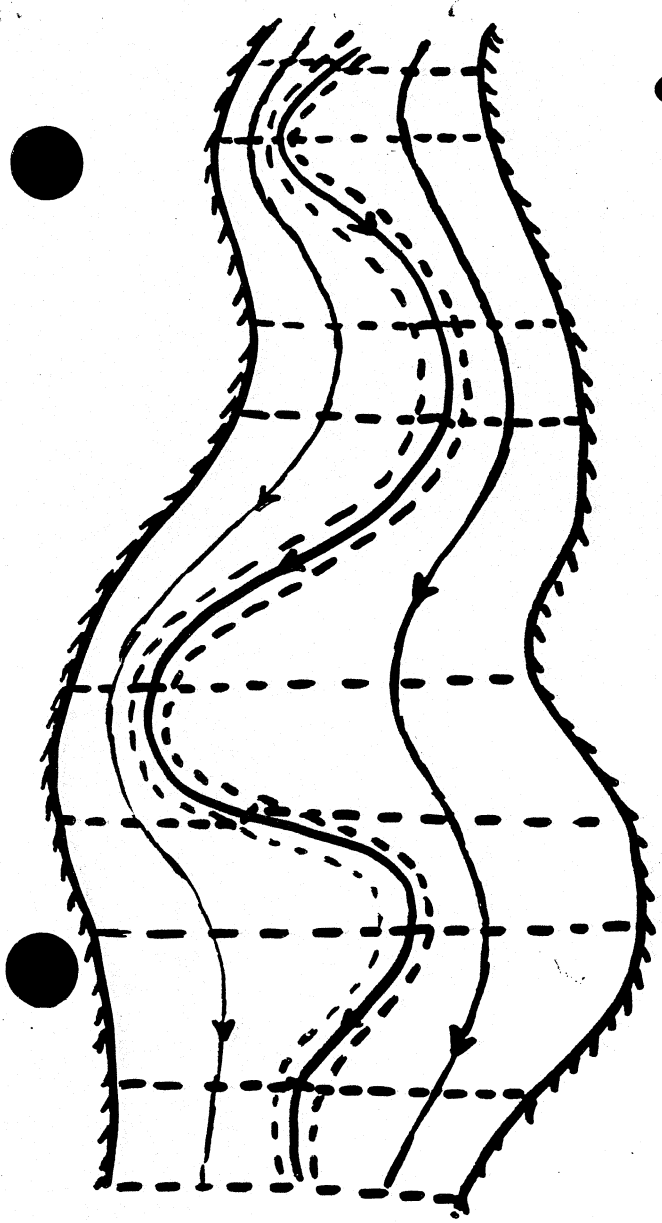

CHANNEL - LEFT/RIGHT FLOODPLAIN

$$A = A_c + A_L + A_R + A_s$$

$$) \frac{\partial K_c Q}{\partial x_c} + \frac{\partial K_L Q}{\partial x_L} + \frac{\partial K_R Q}{\partial x_R} + \frac{\partial A}{\partial t} - q = 0$$

$$) \frac{\partial Q}{\partial t} + \frac{\partial (K_c^2 Q^2 / A_c)}{\partial x_c} + \frac{\partial (K_L^2 Q^2 / A_L)}{\partial x_L} + \frac{\partial (K_R^2 Q^2 / A_R)}{\partial x_R}$$

$$+ g A_c \left(\frac{\partial h}{\partial x_c} + S_{fc} + S_c \right) + g A_L \left(\frac{\partial h}{\partial x_L} + S_{fL} \right) + g A_R \left(\frac{\partial h}{\partial x_R} + S_{fR} \right) - q v_x = 0$$

$$K_c = \frac{1}{1 + k_L + k_R} = K_c$$

$$K_L = \frac{k_L}{1 + k_L + k_R}$$

$$K_R = \frac{k_R}{1 + k_L + k_R}$$

$$k_L = \frac{Q_L}{Q_c} = \frac{n_c A_L}{n_L A_c} \left(\frac{R_L}{R_c} \right)^{2/3} \left(\frac{\Delta x_c}{\Delta x_L} \right)^{1/2}$$

$$k_R = \frac{Q_R}{Q_c} = \frac{n_c A_R}{n_R A_c} \left(\frac{R_R}{R_c} \right)^{2/3} \left(\frac{\Delta x_c}{\Delta x_R} \right)^{1/2}$$

VOLUME LOSSES DURING DOWNSTREAM ROUTING

USE LATERAL OUTFLOW q IN CONSERVATION OF MASS EQUATION TO MODEL LOSSES DUE TO:

1) INFILRATION 2) DETENTION LOSSES 3) SHORT-CIRCUITING VIA CANALS OR OVER TOPPING OF VALLEY RIDGES

$$\boxed{q_m = -0.00458 \frac{V_L \; P}{L \; \bar{T}}}$$

q_m = MAXIMUM LATERAL OUTFLOW

V_L = VOLUME (ACRE-FT) OF OUTFLOW HYDROGRAPH

= VOLUME OF RESERVOIR IF BREACH FORMS TO BOTTOM OF DAM

$$P = \frac{\text{ESTIMATED VOLUME LOSS}}{V_L}$$

TETON: $P = .25$ { WIDE VALL IRRIGATION-LEVEL CANALS

BUFFALO CRK: $P = .25$ - SLUDGE

$$0 < P < .30$$

L = LENGTH (MI) OF DOWNSTREAM VALLEY

$\bar{T}$ = AVERAGE DURATION OF FLOOD WAVE THROUGH THE DOWNSTREAM VALLEY

*VOLUME LOSSES DURING DOWNSTREAM ROUTING

$$q_m = -0.00458 \frac{V_L P}{L \bar{T}}$$

$$\bar{T} = \frac{T_1 + T_2}{2}$$

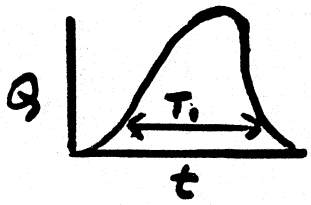

UPSTREAM

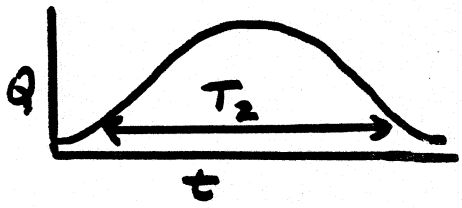

DOWNSTREAM

P: $0 < P < .3$

TETON —— $P = .25$ { WIDE VALLEY (10 MI.) IRRIGATION LEVELS CANALS

BUFFALO CRK. — $P = .25$ - SLUDGE

NARROW VALLEY - SILT, LOAM $0 < P < .05$

WIDE VALLEY - SAND, LOAM $.05 < P < .10$

TIME DISTRIBUTION: $q_i^j = \left(\frac{Q_i^j - Q_i^1}{Q_{max_i} - Q_i^1} \right) q_m$

Q_{max_i} OBTAINED FROM LINEAR INTERPOLATION BETWEEN MAX FLOW AT DAM AND MAX FLOW AT DOWNSTREAM EXTREMITY OF VALLEY (QMAXD)

USUALLY, SIMULATE DAM-BREAK FIRST WITH $q_m = QLL = 0$. QMAXD = 0.

THEN, SIMULATE WITH QMAXD OBTAINED FROM 1ST SIMUATION

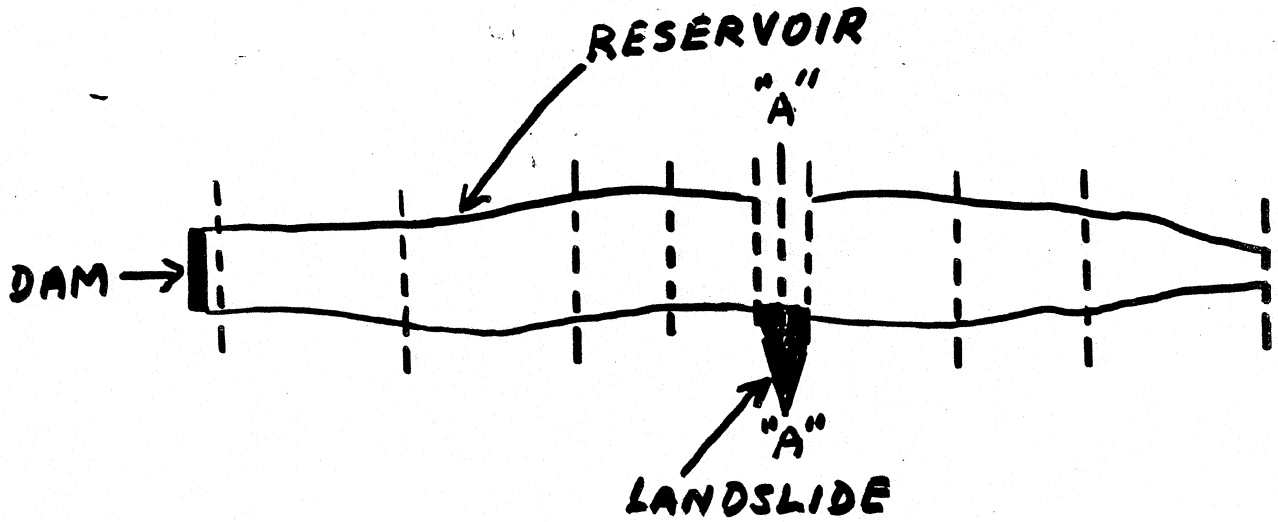

— PLAN —

LANDSLIDE

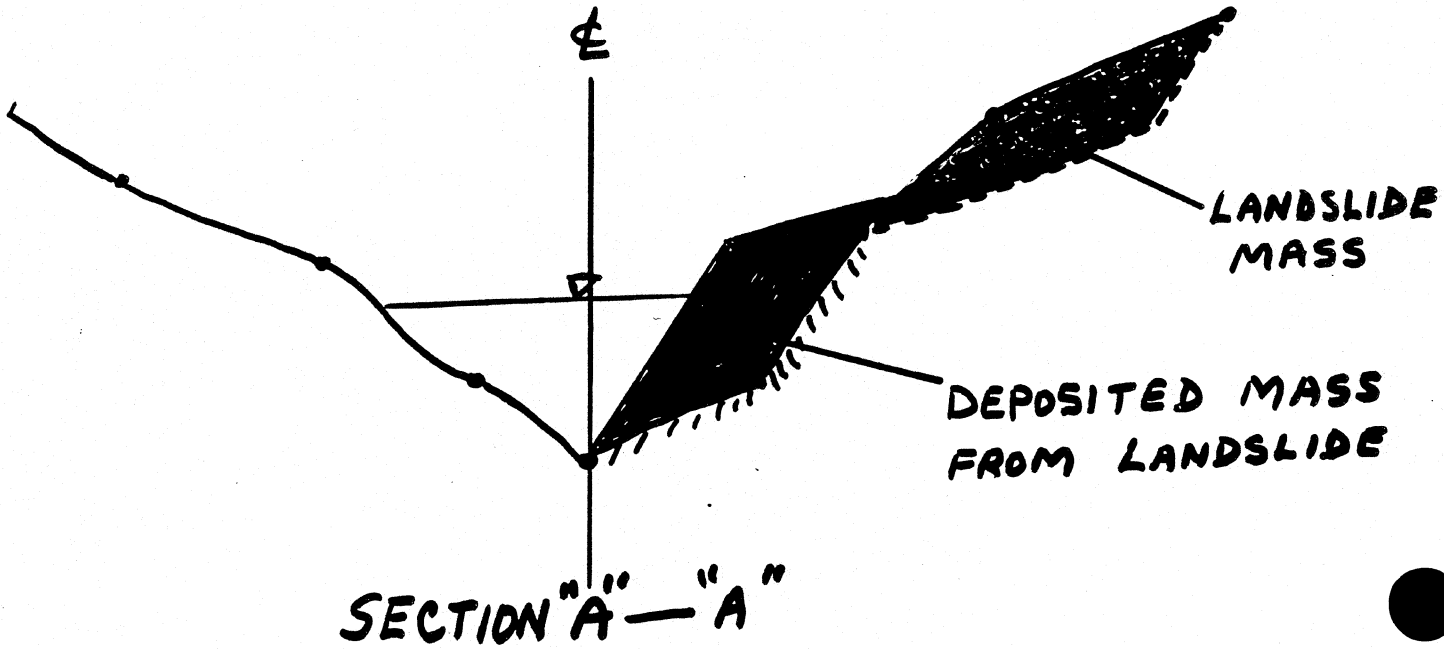

LANDSLIDE

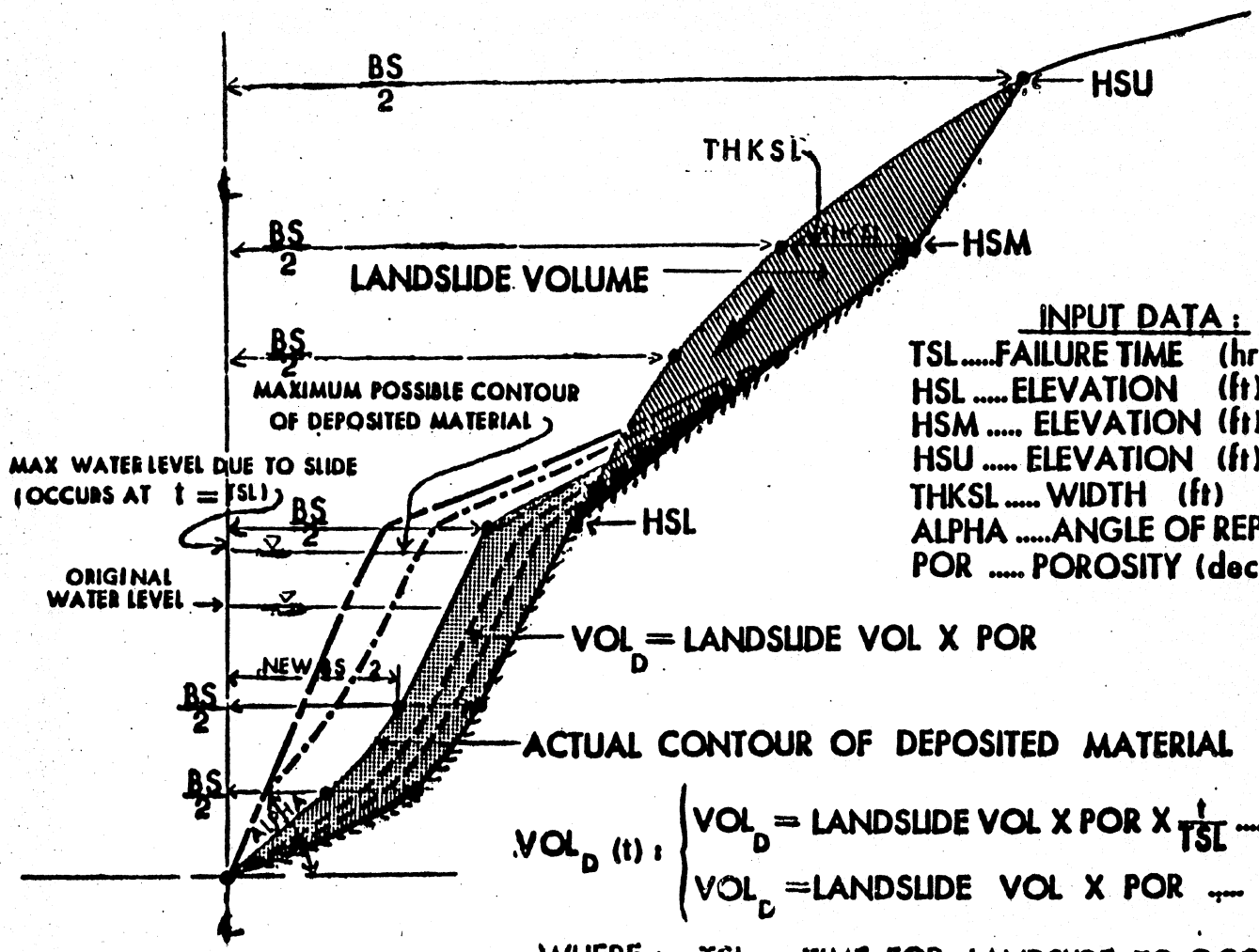

INPUT DATA :

TSL.....FAILURE TIME (hrs)
HSL .....ELEVATION (ft)
HSM ..... ELEVATION (ft)
HSU ..... ELEVATION (ft)
THKSL ..... WIDTH (ft)
ALPHA .....ANGLE OF REPOSE (deg)
POR ..... POROSITY (decimal ratio)

VOL_D = LANDSLIDE VOL X POR

ACTUAL CONTOUR OF DEPOSITED MATERIAL

$$VOL_D(t) : \begin{cases} VOL_D = \text{LANDSLIDE VOL X POR X } \frac{t}{TSL} \text{ ---} 0 \le t \le TSL \\ VOL_D = \text{LANDSLIDE VOL X POR ....} \ t > TSL \end{cases}$$

WHERE : TSL = TIME FOR LANDSLIDE TO OCCUR (hrs)

POR = POROSITY OF LANDSLIDE VOLUME $\left(\frac{\text{solids vol}}{\text{total vol}}\right)$

ASSUMPTIONS : 1) FILLING FROM SIDE TO CENTER

2) VERTICAL DAM FACE

IF SLOPING FACE : WAVE RUNUP $\simeq$ 2.5 Ht. of WAVE

Comparison of "NWS DAMBRK" and "HEC-1 DB"

Outflow Hydrograph :

1. Initial breach width is the same as the final breach width in HEC-1 DB but in DAMBRK initial width is zero.

2. Tailwater submergence effects are considered in DAMBRK but neglected in HEC-1 DB.

3. DAMBRK uses either level pool (storage routing) or the St. Venant unsteady flow equations for reservoir routing while HEC-1 DB uses only level pool routing.

Downstream Routing :

1. DAMBRK uses St. Venant equations while HEC-1 DB uses Modified Puls (storage routing).

2. HEC-1 DB does not consider the effects of
   a. multiple dams
   b. bridges/embankments
   c. flow losses
   d. dead storage areas
   e. special treatment of floodplains
   f. landslides

DAMBRK Application

" Buffalo Crk. Flood"

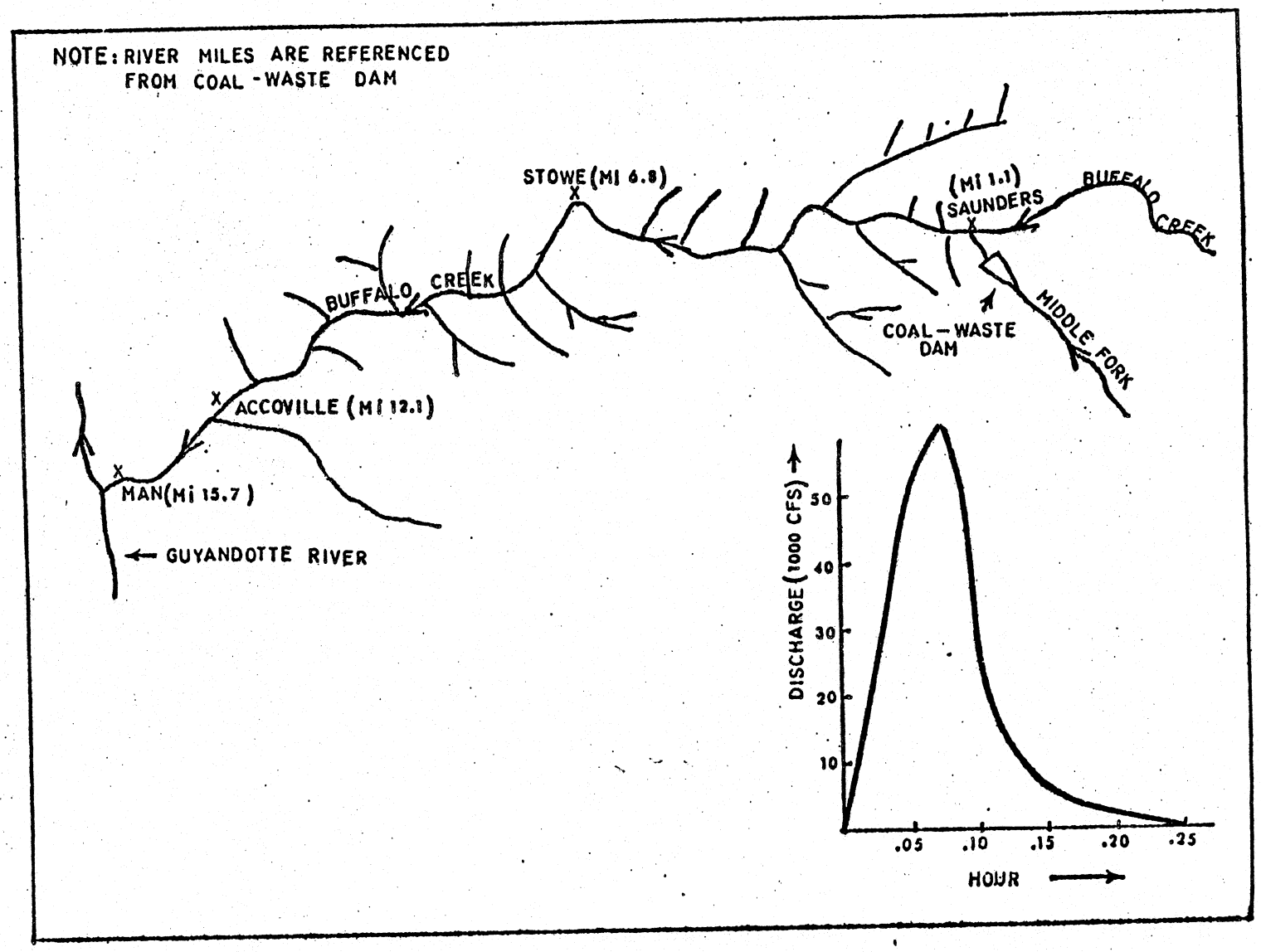

Fig. 9 — OUTFLOW HYDROGRAPH FROM COAL-WASTE DAM AND LOCATION PLAN OF BUFFALO CREEK

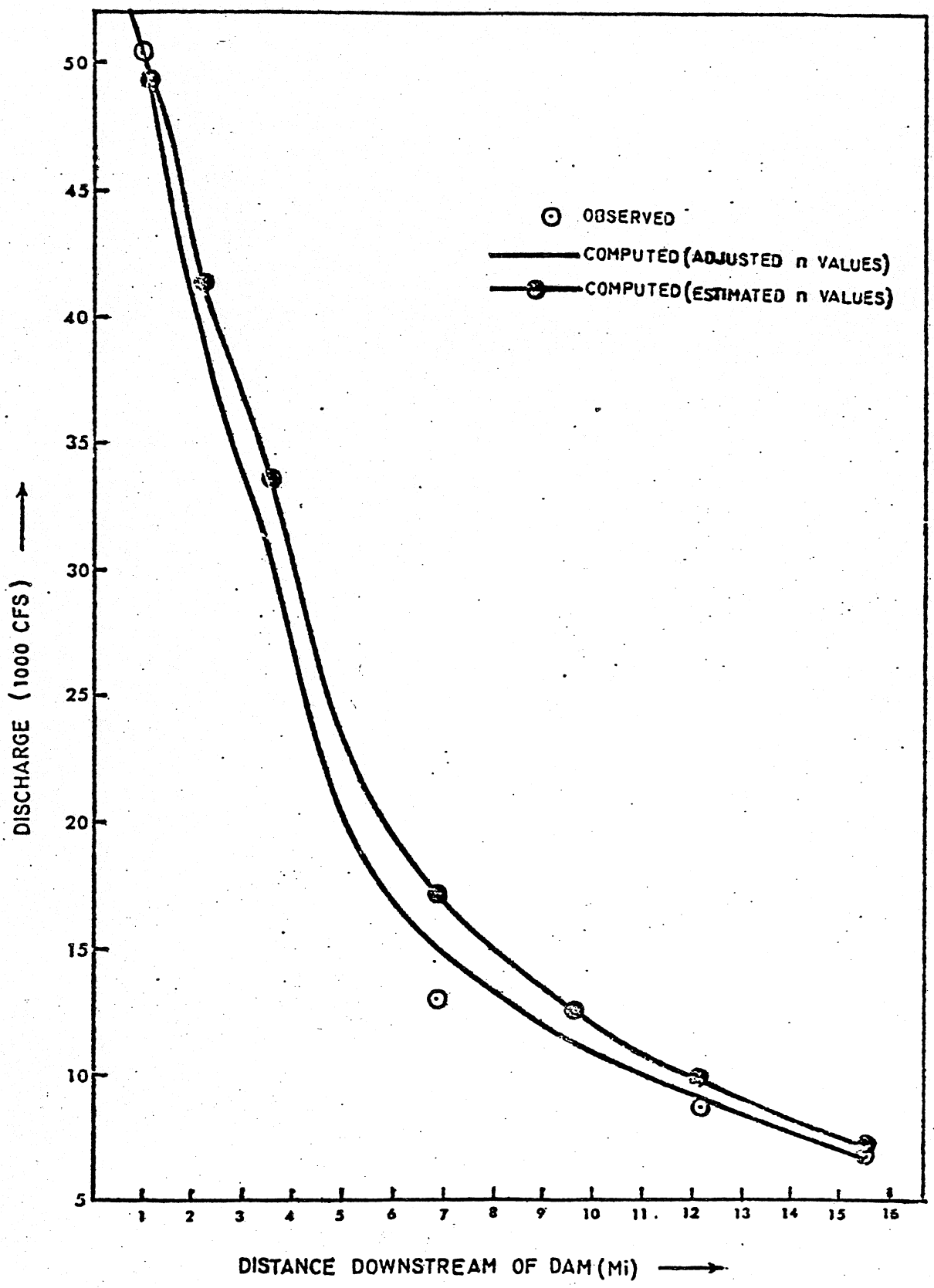

Fig. 10 — PROFILE OF PEAK DISCHARGE FROM BUFFALO CRK. FAILURE

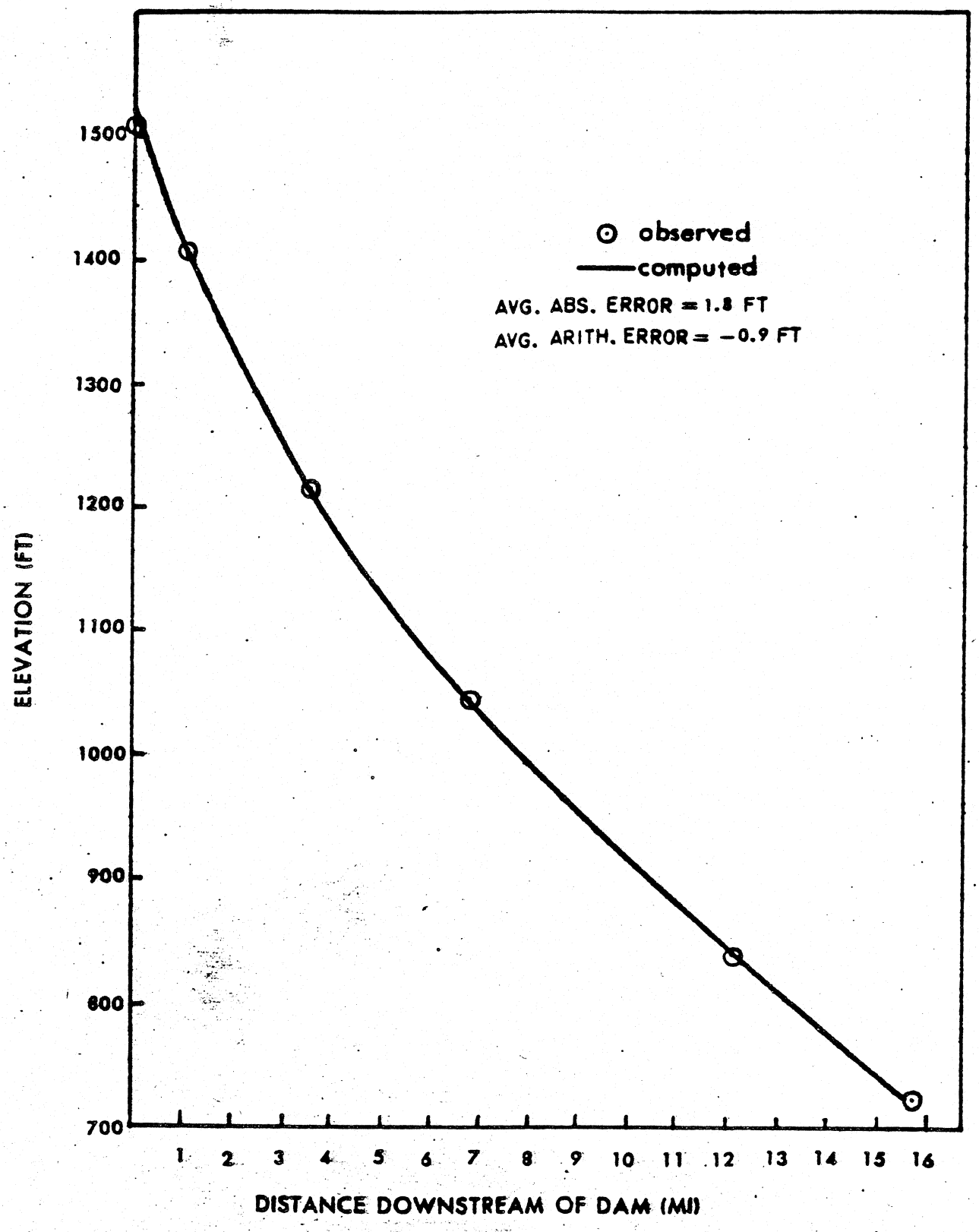

Fig. 12—PROFILE OF PEAK FLOOD ELEVATION FROM BUFFALO CREEK FAILURE

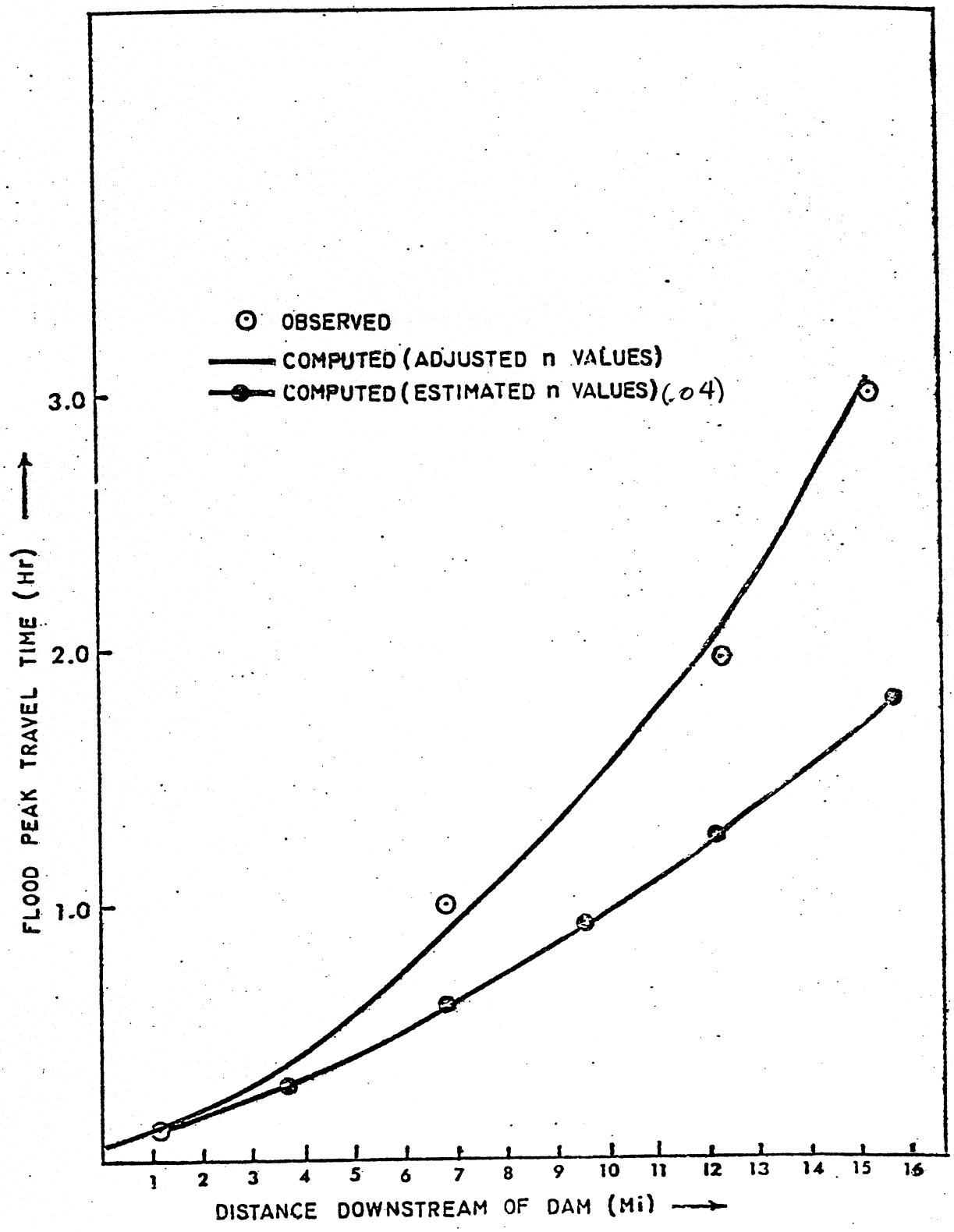

Fig. 11 — TRAVEL TIME OF FLOOD PEAK FROM BUFFALO CREEK FAILURE

Typical Difficulties using DWOPER/DAMBRE

1. Data errors
2. Data not entered correctly
3. Model Parameters not understood
4. Starting with too complex of a problem
5. Subcritical/Supercritical flow
6. Expanding/Contracting cross-sections
7. Wide, flat overbank (floodplain)
8. Δx, Δt too large

INTERPOLATION OF CROSS-SECTION

EXAMPLE OF INCORRECT DATA (BS TOP WIDTHS)

CROSS-SECT "1"	0.	100.	1000	1200.				
CROSS-SECT "2"	0.	60.	95.	400.	450.	950.	1075.	

INCORRECT BECAUSE OF: 1) UNEQUAL NUMBER OF TOP WIDTHS
2) LACK OF GEOMETRIC SIMILARITY

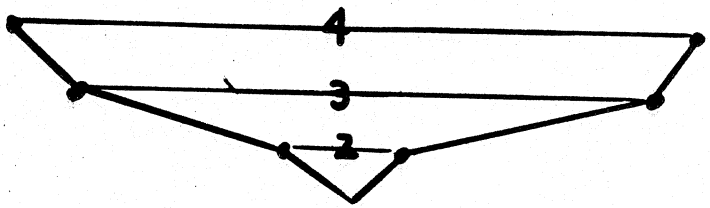

CROSS-SECT "1"

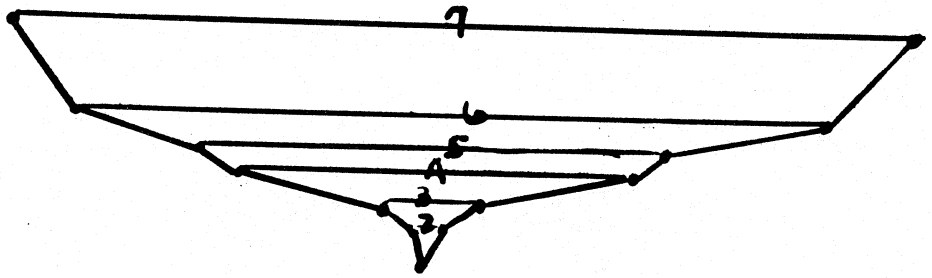

CROSS-SECT "2"

INTERPOLATION OF CROSS-SECTIONS

EXAMPLE OF INCORRECT DATA (BS TOP WIDTHS)

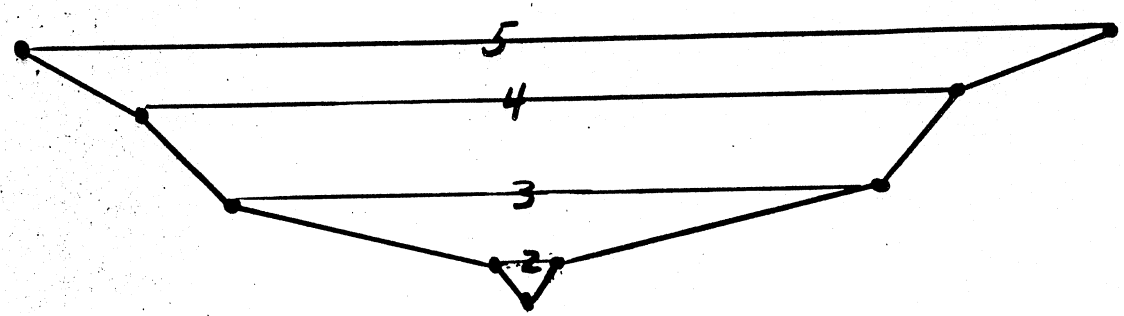

CROSS-SECTION "1"

CROSS-SECT "1"	0.	100.	600.	700.	850.
CROSS-SECT "2"	0.	60.	105.	750.	830.

INCORRECT BECAUSE OF: 1) LACK OF GEOMETRIC SIMILARITY

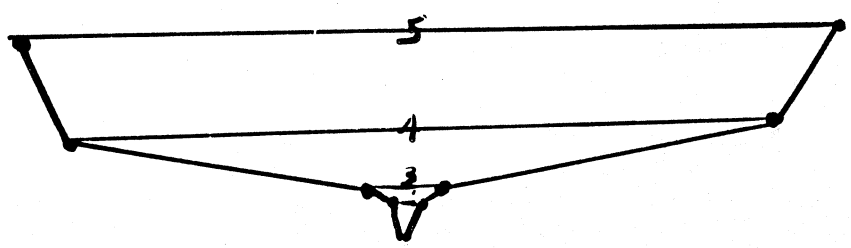

CROSS-SECTION "2"

Simplify the problem to start.

Then, add complexities one or two at a time.

Example: Variable geometry & roughness
2 bridges
levees along both sides

1. Prismatic geometry, constant roughness
2. variable geometry, variable roughness
3. add 1 bridge, then the other
4. add levees

Subcritical / Supercritical Flow

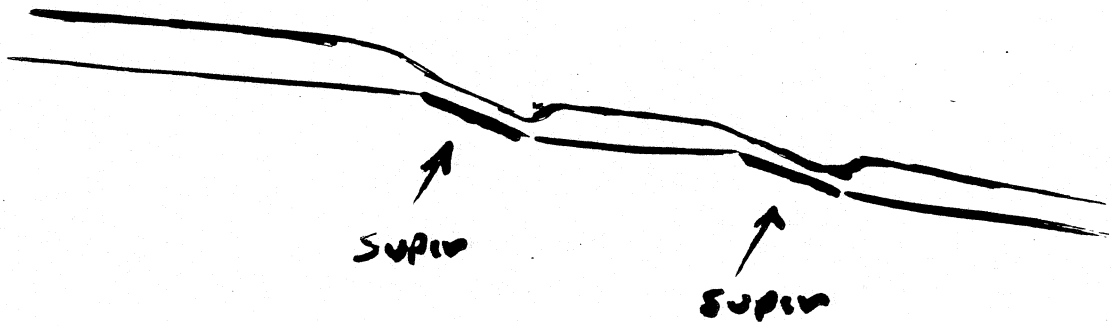

1. Adjust Manning n so that flow is subcritical or supercritical throughout the reach

$$S_c = 77000 \frac{n^2}{D^{1/3}}$$

S_c = critical slope, ft/mi
n = Manning n
$D = A/B$ = Hydraulic Depth, ft

2. Use internal boundary condition for short reach through rapids
   a. rating curve
   b. critical flow/depth relation

3. Split the total reach into separate reaches of only subcritical or supercritical

4. New algorithm may be the approach to use.

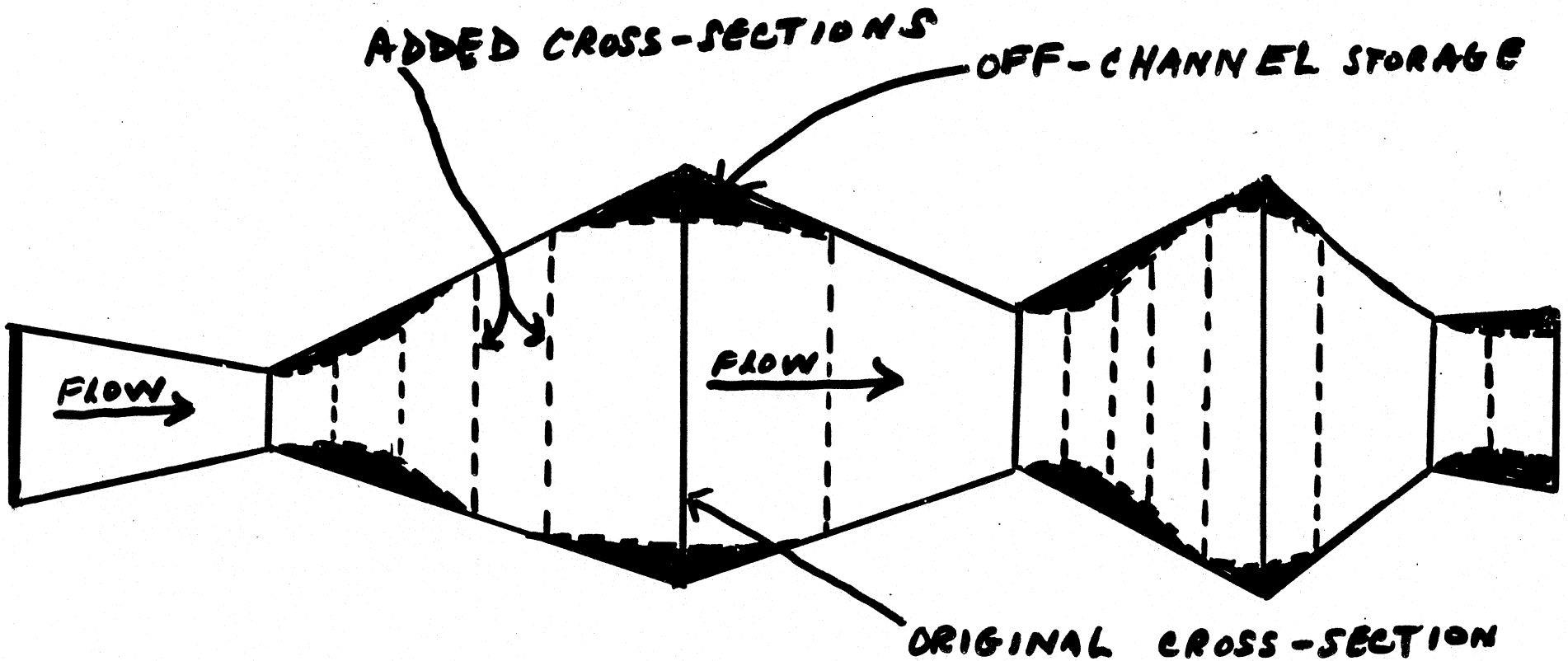

NONLINEAR CROSS-SECTIONS ALONG FLOW AXIS

SMOOTHING NONLINEARITIES ALONG FLOW

Numerical Problems with Very Wide, Flat Flood Plains

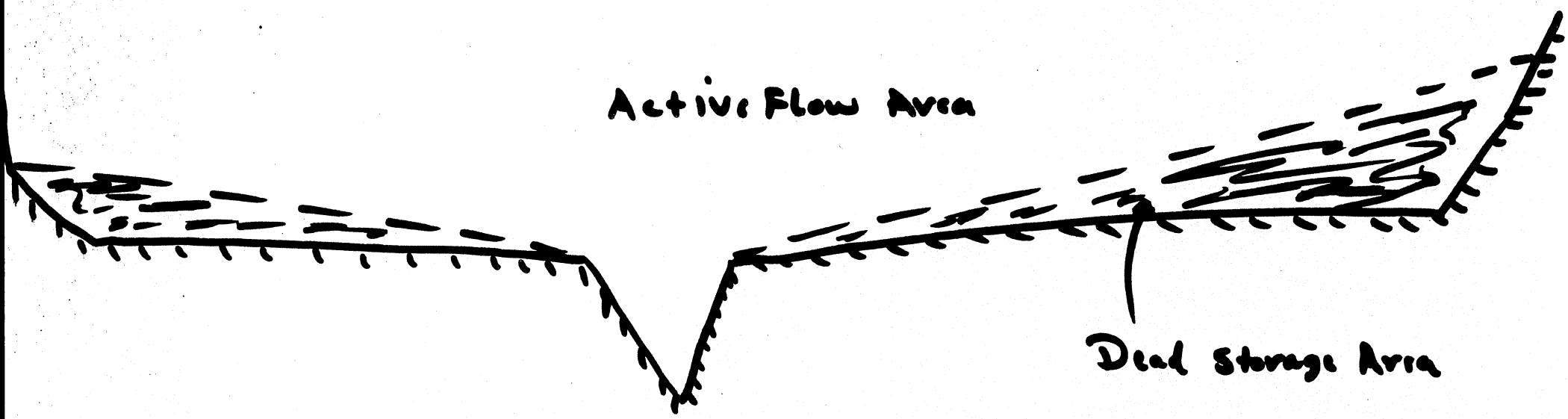

Time Step Selection :

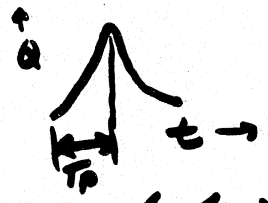

$$\Delta t \le \frac{T_p}{M}$$

$6 \le M \le 40$

usually $M \approx 20$

$$\Delta t \le 0.11\, c\, \frac{z\, T_p}{\sqrt{D_o}}$$

$$z = \left(\frac{1-\epsilon^2}{\theta^2 \epsilon^2 - (2\theta - 2)^2} \right)^{1/2}$$

$0.85 \le \epsilon \le 0.99$

D_o = Initial Hydraulic Depth

ϵ = 1 - error

θ = wt. factor

$0.5 \le \theta < 1$

$$c = K V$$

$$K = 5/3 - 2/3 \frac{m}{m+1}$$

$1.2 \le K \le 1.67$

$$V = \frac{\bar{Q}}{A}$$

Distance Step Selection :

$$\Delta x \le c\, \Delta t$$

$c = .68\, c$

DAMBRK Review

- Complete 1-D St. Venant Eqs (Dynamic Routing)

  Conservation Form of Eqs.

  4-pt. Nonlinear Finite Difference (Implicit) Solution

  Newton-Raphson Iteration with Extrapolation

  Automatic Numerical Fix-up via Δt and/or θ

  Unequal Δx

* Additional cross-sections created by Linear Interpolation

Upstream Boundary : $Q(t)$

- Downstream Boundary : $Q(h)$ < rating curve / loop rating / critical flow ; $h(t)$

  Dam (Spillway flow; Breach flow)

Initial Conditions : Steady flow Q
h computed via backwater solution

Manning n : $n(h, x)$

Lateral Inflow/outflow : Specified $q(t)$

Cross sections : Tabular $B(h)$

* Variable Δt or Constant Δt

- Expansion-Contraction Loss

  Off channel (Dead) storage

* This feature not in DWOPER

DAMBRK Review

Single channel

Two-step Application for: 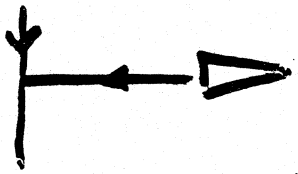

* Upstream Reservoir: 1) Dynamic Routing
  2) Level Pool Storage Routing

* Breach: Time dependent, variable size & shape

* Breach flow corrected for tailwater Submergence

* Spillway Flows: Uncontrolled, time-dependent gate, constant gate, dam crest overflow, rating curve, constant flow

* Multiple Dams treated as Internal Boundaries

* Bridge-Embankment: Overtopping/failure

* Channel-Left/Right Floodplain Dynamic Routing

* Supercritical Flow

* Landslide Wave

* Line Plot of $Q(t)$; $Q_m(x)$; $h_m(x)$; $t_m(x)$

Selective Print-Output

$$\text{CPU} \frac{\text{sec}}{\Delta x \, \Delta t} \approx 0.001$$

HRL Supported, Documented, Training Seminars — NWS, HEC, UNIV.

A Synopsis of NWS Models for Predicting the Flooding Due to Dam Failures

by D.L. Fread*

April 3,1985

1. INTRODUCTION

Catastrophic flooding occurs when a dam is breached and the impounded water escapes through the breach into the downstream valley. Usually the response time available for warning is much shorter than for precipitation-runoff floods. Dam failures are often caused by overtopping of the dam due to inadequate spillway capacity during large inflows to the reservoir from heavy precipitation runoff. Dam failures may also be caused by seepage or piping through the dam or along internal conduits, slope embankment slides, embankment cracks or liquefaction of earthen dams from earthquakes, and landslide-generated waves within the reservoir. Middlebrooks (1952) describes earthen dam failures occurring within the U.S. prior to 1951. Johnson and Illes (1976) summarize 300 dam failures throughout the world.

During the last decade some major improvements were made in models which predict the changing celerity and magnitude of a flood wave emanating from a breached (failed) dam and propagating through the downstream valley. Such improvements included consideration of the breach dynamics, use of the one-dimensional equations of unsteady flow to route the flood wave through the downstream valley, and consideration of the effects of downstream bridge-embankments, dams, and dead storage areas on the propagating wave.

The National Weather Service (NWS), having the responsibility to advise the public of downstream flooding when there is a failure of a dam, has developed three models to aid NWS hydrologists who are called upon to forecast the extent of flood inundation and available evacuation time. This paper briefly describes the three models (BREACH, DAMBRK, SMPDBK) used to forecast dam-break floods. These models are also used extensively for a multitude of purposes by planners, designers, and analysts who are concerned with possible future flood inundation due to dam-break floods and/or reservoir spillway floods, or any specified flood hydrograph.

Essentially, BREACH can be used to predict the size and timing of the development of the breach in earthen dams. DAMBRK can be used to develop the outflow hydrograph due to a breached dam (earthen or concrete) and determine the extent and timing of the flooding that occurs at various locations downstream of the dam. SMPDBK can do the same thing as DAMBRK except in a relatively simple manner which usually yields more approximate results.

---

*Senior Research Hydrologist, Hydrologic Research Laboratory, National Weather Service, NOAA, 8060 13th Street, Silver Spring, Maryland 20910.

2. BREACH

An earthen dam is subject to possible failure from either overtopping or piping waters which erode a passage (breach) through the dam. The breach formation is gradual with respect to time and its width as measured along the crest of the dam usually encompasses only a portion of the dam's crest length. In many instances, the bottom of the breach progressively erodes downward until it reaches the bottom of the dam; however, in some cases, it may cease its downward progression at some intermediate elevation between the top and bottom of the dam. The size of the breach, as constituted by its depth and its width (which may be a function of the depth), and the rate of the breach formation determine the magnitude and shape of the resulting breach outflow hydrograph. This is of vital interest to hydrologists and engineers concerned with real-time forecasting or evacuation planning for floods produced by dam failures.

BREACH is an enhanced version of a mathematical model (Fread, 1984b) for predicting the breach characteristics (size, shape, time of formation) and the breach outflow hydrograph. The model is physically based on the principles of hydraulics, sediment transport, soil mechanics, the geometric and material properties of the dam, and the reservoir properties (storage volume, spillway characteristics, and time dependent reservoir inflow rate). The dam may be either man-made or naturally formed as a consequence of a landslide. In either, the mechanics of breach formation are very similar, the principal difference being one of scale. The landslide-formed dam is often much larger than even the largest of man-made earthen dams. The critical material properties of the dam are the internal friction angle, cohesion strength, and average grain size diameter (D_{50}).

The BREACH model differs from the parametric approach which the author has used in the NWS DAMBRK Model (Fread, 1977, 1984a). The parametric model uses empirical observations of previous dam failures such as the breach width-depth relation, time of breach formation, and depth of breach to develop the outflow hydrograph. The breach erosion model can provide some advantages over the parametric breach model for application to man-made dams since the critical properties used by the model are measurable or can be estimated within a reasonable range from a qualitative description of the dam materials. However, it should be emphasized that even if the properties can be measured there is a range for their probable value and within this range outflow hydrographs of varying magnitude and shape will be produced by the model. The hydrologist or engineer should investigate the most critical combination of values for the dam's material properties. It is considered essential when predicting breach outflows of landslide dams to utilize a physically based model since observations of such are essentially non-existent, rendering the parametric approach infeasible.

2.1 General Description

The breach erosion model (BREACH) simulates the failure of an earthen dam as shown in Fig. 1. The dam may be homogeneous or it may consist of two materials, an outer zone with distinct material properties (ϕ - friction angle, C - cohesion, D_{50} - average grain size (mm), and γ - unit weight) and an inner core with its ϕ, C, D_{50}, and γ values. Also, the downstream face

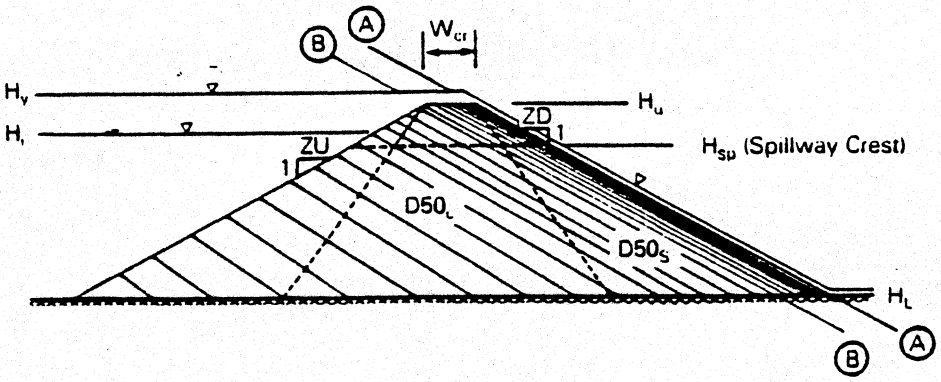

Figure 1. Side View of Dam Showing Conceptualized Overtopping Failure Sequence.

of the dam may be specified as having: 1) a grass cover with specified length of either good or fair stand, 2) material identical to the outer portion of the dam, or 3) material of larger grain size than the outer portion. The geometry of the downstream face of the dam is described by specifying the top of the dam (H_u), the bottom elevation of the dam (H_ℓ) which can also denote the original streambed elevation or the lowest level that the breach will form, and its slope as given by the ratio 1 (vertical) : ZD (horizontal). Then, the geometry of the upstream face of the dam is described by specifying its slope as the ratio 1 (vertical) : ZU (horizontal). If the dam is man-made it is further described by specifying a flat crest width (W_{cr}) and a spillway rating table of spillway flow vs. water elevation, in which the first elevation represents the spillway crest. Naturally formed landslide dams are assumed to <u>not</u> have a flat crest or, of course, a spillway.

The storage characteristics of the reservoir are described by specifying a table of surface area (S_a) in units of acre-ft vs. water elevation, the initial water surface elevation (H_i) at the beginning of the simulation, and a table of reservoir inflows (Q_i) in cfs vs. the hour of their occurrence (T_i).

If an overtopping failure is simulated, the water level (H) in the reservoir must exceed the top of the dam before any erosion occurs. The first stages of the erosion are only along the downstream face of the dam as denoted by the line A-A in Fig. 1 where, initially if no grass cover exists, a small rectangular-shaped rivulet is assumed to exist along the face. An erosion channel of depth-dependent width is gradually cut into the downstream face of the dam. The flow into the channel is determined by the broad-crested weir relationship:

$$Q_b = 3\ B_o(H-H_c)^{1.5} \qquad (1)$$

in which Q_b is the flow into the breach channel, B_o is the instantaneous

width of the initially rectangular-shaped channel, and H_c is the elevation of the breach bottom. As the breach erodes into the downstream face of the dam, the breach bottom elevation (H_c) remains at the top of the dam (H_u), and the most upstream point of the breach channel moves across the crest of the dam towards the dam's upstream face. When the bottom of the erosion channel has attained the position of line B-B in Fig. 1, the breach bottom (H_c) starts to erode vertically downward. The breach bottom is allowed to progress downward until it reaches the bottom elevation of the dam (H_ℓ) or in unusual circumstances to an elevation that may be specified as lower than the bottom of the dam.

If the downstream face of the dam (line A-A in Fig. 1) has a grass cover, the velocity of the overtopping flow along the grassed downstream face is computed at each time step by the Manning equation. This velocity is compared with a specified maximum permissible velocity for grass-lined channels (see Chow, 1959). Failure of the downstream face via erosion is initiated at the time when the permissible velocity is exceeded. At that time a single rivulet having dimensions of one (ft) depth x two width is instantly created along the downstream face. Erosion within the rivulet is allowed to proceed as in the case where a grass cover does not exist. The velocity (v) along the downstream face is computed as follows:

$$q = 3(H-Hc)^{1.5} \tag{2}$$

$$y = \left[\frac{qn'}{1.49(1/ZD)^{0.5}}\right]^{0.6} \tag{3}$$

$$n' = aq^b \tag{4}$$

$$v = q/y \tag{5}$$

in which q is the overtopping flow per foot of crest length, (H-Hc) is the hydrostatic head (ft) over the crest, n' is the Manning coefficient for grass-lined channels (Chow, 1959), a and b are fitting coefficients required to represent in mathematical form the graphical curves given in Chow.

If a piping breach is simulated, the initial water level (H) in the reservoir must be greater than the assumed center-line elevation (H_p) of the initially rectangular-shaped piping channel before the size of the pipe starts to increase via erosion. The bottom of the pipe is eroded vertically downward while its top erodes at the same rate vertically upwards. The flow into the pipe is controlled by orifice flow, i.e.,

$$Q_b = A\left[2g(H-Hp)/(1 + fL/D)\right]^{0.5} \tag{6}$$

in which Q_b is the flow (cfs) through the pipe, g is the gravity acceleration constant, A is the cross-sectional area (ft^2) of the pipe channel, (H-Hp) is the hydrostatic head (ft) on the pipe, L is the length (ft) of the

pipe channel, D is the diameter or width (ft) of the pipe, and f is the Darcy friction factor computed from a mathematical representation of the Moody curves (Morris and Wiggert, 1972) and the breach material average grain size (D50). As the top elevation (H_{pu}) of the pipe erodes vertically upward, a point is reached when the flow changes from orifice-control to weir-control. The transition is assumed to occur when the following inequality is satisfied:

$$H < H_{pu} + 2(H_{pu} - H_p) \tag{7}$$

The weir flow is then governed by Eq. (1) in which H_c is equivalent to the bottom elevation of the pipe and B_o is the width of the pipe at the instant of transition. Upon reaching the instant of flow transition from orifice to weir, the remaining material above the top of the pipe and below the top of the dam is assumed to collapse and is transported along the breach channel at the current rate of sediment transport before further erosion occurs. The erosion then proceeds to cut a channel parallel to and along the remaining portion of the downstream face of the dam between the elevation of the bottom of the pipe and the bottom of the dam. The remaining erosion process is quite similar to that described for the overtopping type of failure with the breach channel now in a position similar to line A-A in Fig. 1.

The preceding general description of the erosion process was for a man-made dam. If a landslide dam is simulated the process is identical except, due to the assumption that the landslide dam has no crest width (W_{cr}), the erosion initially commences with the breach channel in the position of line B-B in Fig. 1. A failure mode of overtopping or piping may be initiated for a landslide-formed dam.

2.2 Breach Width

The method of determining the width of the breach channel is a critical component of the breach model. In this model the width of the breach is dynamically controlled by two mechanisms. The first, assumes the breach has an initial rectangular shape as shown in Fig. 2. The width of the breach (B_o) is governed by the following relation:

$$B_o = B_r\, y \tag{8}$$

in which B_r is a factor based on optimum channel hydraulic efficiency and y is the depth of flow in the breach channel. The parameter B_r has a value of 2 for overtopping failures while for piping failures, B_r is set to 1.0. The model assumes that y is the critical depth at the entrance to the breach channel, i.e.,

$$y = 2/3(H-H_c). \tag{9}$$

The second mechanism controlling the breach width is derived from the stability of soil slopes (Spangler, 1951). The initial rectangular-shaped

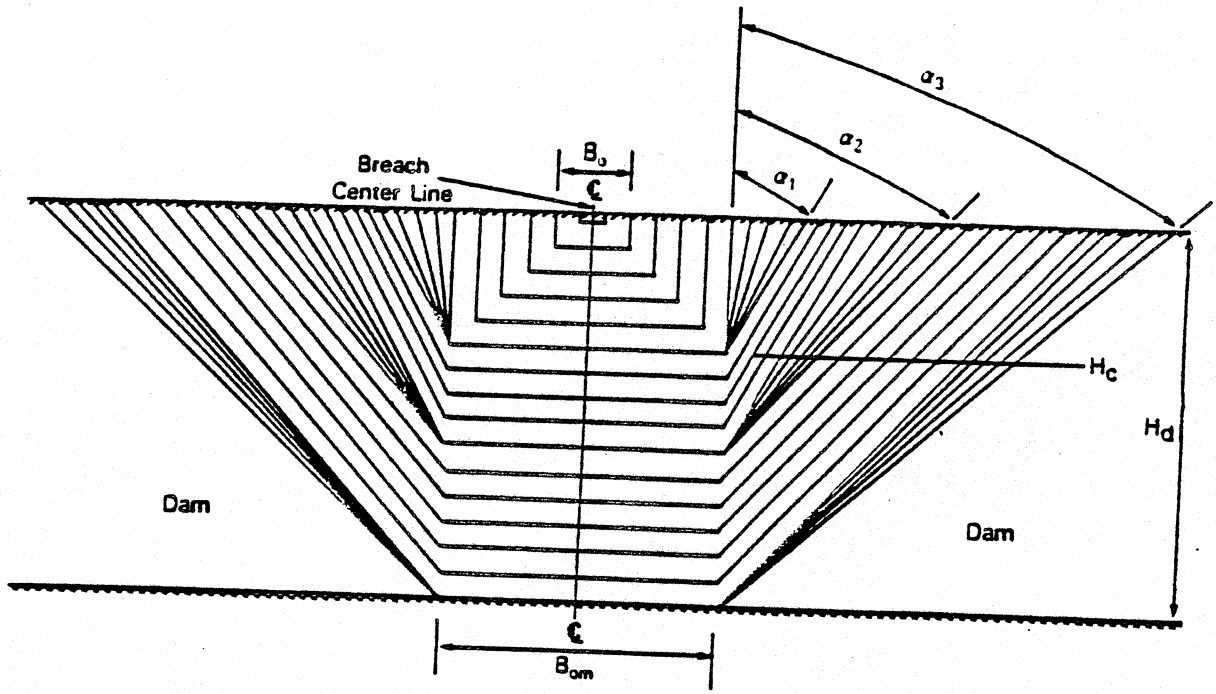

Figure 2. Front View of Dam with Breach Formation Sequence.

channel changes to a trapezoidal channel when the sides of the breach channel collapse, forming an angle (α) with the vertical. The collapse occurs when the depth of the breach cut (H_c') reaches the critical depth (H') which is a function of the dam's material properties of internal friction (ϕ), cohesion (C), and unit weight (γ), i.e.,

$$H_k' = \frac{4\ C \cos\phi\ \sin\theta_{k-1}'}{\gamma\ [1 - \cos(\theta_{k-1}' - \phi)]} \quad . . . \ k = 1,2,3 \tag{10}$$

in which the subscript k denotes one of three successive collapse conditions as shown in Fig. 2, and θ is the angle that the side of the breach channel makes with the horizontal. Angles (θ) and (α) are computed as follows:

$$\theta = (\theta'_{k-1} + \phi)/2 \tag{11}$$

$$\alpha = \Pi/2 - \theta \tag{12}$$

The subscript (k) is incremented by 1 at the instant when

$$H_k > H_k'. \tag{13}$$

where: $H_k = H_c' - y/3$ (14)

The term (y/3) is subtracted from H_c' to give the actual free-standing depth of breach cut in which the supporting influence of the water on the stability of the sides of the breach is taken into account. Through this mechanism, it is possible for the breach to widen after the peak outflow through the breach has occurred since the flow depth (y) diminishes during the receding flow.

Erosion is assumed to occur equally along the bottom and sides of the breach channel except when the sides of the breach channel collapse. Thereupon the breach bottom is assumed not to continue to erode downward until the volume of collapsed material along the breach is removed at the rate of the sediment transport capacity of the breach channel at the instant of collapse. After this characteristically short pause, the breach bottom and sides continue to erode.

2.3 Reservoir Level Determination

Conservation of mass is used to compute the change in the reservoir water surface elevation (H) due to the influence of reservoir inflow (Q_i), spillway outflow (Q_{sp}), crest overflow (Q_o), breach outflow (Q_b), and the reservoir storage characteristics. The conservation of mass over a time step (Δt) in hours is represented by the following:

$$\bar{Q}_i - (\bar{Q}_b + \bar{Q}_{sp} + \bar{Q}_o) = S_a \frac{\Delta H}{\Delta t} \frac{43560}{3600} \tag{15}$$

in which ΔH is the change in water surface elevation during the time interval (Δt), and S_a is the surface area in acres at elevation H. All flows are expressed in units of cfs and the bar (-) indicates the flow is averaged over the time step. Rearranging Eq. (15) yields the following expression for the change in the reservoir water surface:

$$\Delta H = \frac{0.0826 \Delta t}{S_a} (\bar{Q}_i - \bar{Q}_b - \bar{Q}_{sp} - \bar{Q}_o) \tag{16}$$

The reservoir elevation (H) at time (t) can easily be obtained from the relation,

$$H = H' + \Delta H \tag{17}$$

in which H' is the reservoir elevation at time $t-\Delta t$.

The reservoir inflow ($\bar{Q}_i$) is determined from the specified table of inflows (Q_i) vs. time (T_i). The spillway flow ($\bar{Q}_s$) is determined from the specified table of spillway flows (Q_s) vs. reservoir elevation (H). The breach flow (Q_b) is computed from Eq. (6) for piping flow. When the breach flow is weir-type, Eq. (1) is used when $H_c = H_u$; however, when $H_c < H_u$, the following broad-crested weir equation is used:

$$Q_b = 3\ B_o\ (H - H_c)^{1.5} + 2\ \tan(\alpha)\ (H - H_c)^{2.5} \tag{18}$$

in which B_o is the bottom width and α is given by Eq. (12). The crest overflow is computed as broad-crested weir flow from Eq. (1), where B_o is replaced by the crest length of the dam and H_c is replaced by H_u.

2.4 Breach Channel Hydraulics

The breach flow is assumed to be adequately described by quasi-steady uniform flow as determined by applying the Manning open channel flow equation at each Δt time step, i.e.,

$$Q_b = \frac{1.49\ S^{0.5}\ A^{1.67}}{n\ \ P^{0.67}} \tag{19}$$

in which $S = 1/ZD$, A is the channel cross-section area, P is the wetted perimeter of the channel, and n is the Manning coefficient. In this model, n is computed using the Strickler relation which is based on the average grain size of the material forming the breach channel, i.e.,

$$n = 0.013\ D_{50}^{\ 0.167} \tag{20}$$

in which D_{50} represents the average grain size diameter expressed in mm.

The use of quasi-steady uniform flow is considered appropriate because the extremely short reach of breach channel, very steep channel slopes (1/ZD) for man-made dams, and even in the case of landslide dams where the channel length is greater and the slope is smaller, contribute to produce extremely small variation in flow with distance along the breach channel. The use of quasi-steady uniform flow in contrast to the unsteady flow equations as used by Ponce and Tsivoglou (1981) in their breach erosion model greatly simplifies the hydraulics and computational algorithm. Such simplification is considered commensurate with the other simplifications inherent in the treatment of the breach development in dams for which precise measurements of material properties are lacking or impossible to obtain and the wide variance which exists in such properties in many dams. The simplified hydraulics eliminates troublesome numerical computation problems and enables the breach model to require only minimal computational resources.

2.5 Sediment Transport

The rate at which the breach is eroded depends on the capacity of the flowing water to transport the eroded material. The Meyer-Peter and Muller sediment transport relation as modified by Smart (1984) for steep channels is used, i.e.,

$$Q_s = 3.64\ (D_{90}/D_{30})^{0.2}\ \ \frac{D^{2/3}}{n}\ \ S^{1.1}\ (DS - 0.0054\ D_{50}\ \tau_c) \tag{21}$$

where:

$$\tau_c = a' \tau_c' \tag{22}$$

$$a' = \cos \Theta (1. - 1.54 \tan \Theta) \tag{23}$$

$$\Theta = \tan^{-1} S \tag{24}$$

$$\tau_c' = 10^{-1.21 - .19 \log R^*} \quad \ldots\ldots\ldots\ldots R^* < 30 \tag{25}$$

$$\tau_c' = 10^{-1.49 + .35(\log R^* - 1.48)} \quad \ldots\ldots\ldots 30 \leq R^* \leq 200 \tag{26}$$

$$\tau_c' = 0.062 \quad \ldots\ldots\ldots 200 < R^* < 25000 \tag{27}$$

$$S = \frac{1}{ZD} \tag{28}$$

$$R^* = 1524 \; D_{50} \; (DS)^{0.5} \tag{29}$$

in which Q_s is the sediment transport rate (cfs); D_{30}, D_{50}, D_{90} (mm) are grain sizes at which 30, 50, and 90 percent of the total weight is finer; D is the hydraulic depth of flow (ft), S is the slope of the downstream face of the dam; and τ_c' is the Shields' critical shear stress.

2.6 Breach Enlargement By Sudden Collapse

It is possible for the breach to be enlarged by a rather sudden collapse failure of the upper portions of dam in the vicinity of the breach development. Such a collapse would consist of a wedge-shaped portion of the dam having a vertical dimension (Y_c). The collapse would be due to the pressure of the water on the upstream face of the dam exceeding the resistive forces due to shear and cohesion which keep the wedge in place. When this occurs the wedge is pushed into the breach and then transported by the escaping water through the now enlarged breach. When collapse occurs, the erosion of the breach ceases until the volume of the collapsed wedge is transported through the breach channel at the transport rate of the water escaping through the suddenly enlarged breach. A check for collapse is made at each Δt time step during the simulation. The collapse check consists of summing the forces acting on the wedge of height, Y_c. The forces are those due to the water pressure and the resisting forces which are the shear force acting along the bottom of the wedge, the shear force acting along both sides of the wedge, the force due to cohesion along the sides and bottom of the wedge.

2.7 Computational Algorithm

The sequence of computations in the model are iterative since the flow into the breach, is dependent on the bottom elevation of the breach and its width while the breach properties are dependent on the sediment transport capacity of the breach flow; the transport capacity is dependent on the breach size and flow. A simple iterative algorithm is used to account for the mutual dependence of the flow, erosion, and breach properties. An estimated incremental erosion depth ($\Delta H'_c$) is used at each time step to start the iterative computation. This estimated value can be extrapolated from previously computed incremental erosion depths after the first few time steps. The computational algorithm is described elsewhere (Fread, 1984b).

2.8 Computational Requirements

The basic time step (Δt) is specified; however when rapid erosion takes place the basic time step is automatically reduced to $\Delta t/20$. The specified value for the basic time step is usually about 0.02 hrs with slightly larger values acceptable for landslide dams. For typical applications, the BREACH model requires less than 10 seconds of CPU time on a Prime 750 computer and less than 2 seconds on an IBM 360/195 computer, both of which are mainframe computers. Although it has not been used on microcomputers, it would be quite amenable to such applications.

The model has displayed a lack of numerical instability or convergence problems. The computations show very little sensitivity to a reasonable variation in basic time step size. Numerical experimentation indicates that as the time step is increased by a factor of 4, the computed peak flow (Q_p), time of peak (T_p), and final breach dimensions vary by less than 10, 4, and 0.5 percent, respectively.

2.9 Model Applications

The BREACH model was applied to two earthen dams to determine the outflow hydrograph produced by a gradual breach of each. The first was the piping failure of the man-made Teton dam in Idaho, and the second was an overtopping failure of the landslide-formed dam which blocked the Mantaro River in Peru.

2.9.1 Teton Dam

The Teton Dam, a 300 ft high earthen dam with a 3000 ft long crest and 262 ft depth of stored water amounting to about 250,000 acre-ft, failed on June 5, 1976. According to a report by Ray, et. al (1976) the failure started as a piping failure about 10:00 AM and slowly increased the rate of outflow until about 12:00 noon when the portion of the dam above the piping hole collapsed and in the next few minutes (about 12 minutes according to Blanton (1977)) the breach became fully developed allowing an estimated 1.6 to 2.8 million cfs (best estimate of 2.3) peak flow (Brown and Rogers, 1977) to be discharged into the valley below. At the time of peak flow the breach was estimated from photographs to be trapezoidal shape having a top width at

the original water surface elevation of about 500 ft and side slopes of about 1 vertical to 0.5 horizontal. After the peak outflow the outflow gradually decreased to a comparatively low flow in about five hours as the reservoir volume was depleted and the surface elevation receded. The downstream face of the dam had a slope of 1:2 and the upstream face 1:2.5. The crest width was 35 ft and the bulk of the breach material was a D_{50} size of 0.03 mm. The inflow to the reservoir during failure was insignificant and the reservoir surface area at time of failure was about 1950 acre-ft.

The BREACH model was applied to the piping generated failure of the Teton Dam. The center-line elevation for the piping breach was 160 ft above the bottom of the dam, and an initial width of 0.1 ft was used for the assumed square-shaped pipe. The material properties of the breach were assumed as follows: ϕ = 40 deg, C = 250 lb/ft^2, and γ = 100 lb/ft^3. The Strickler equation was judged not to be applicable for the extremely fine breach material, and the n value was computed as 0.013 from a Darcy friction factor based on the D_{50} grain size and the Moody curves. The computed outflow hydrograph is shown in Fig. 3. The timing, shape, and magnitude of the hydrograph compares quite well with the estimated actual values. The computed peak outflow of 2.3 million cfs agrees with the best estimate made by the U.S. Geological Survey and the time of occurrence is also the same. The computed breach width of 460 ft agrees closely with the estimated value

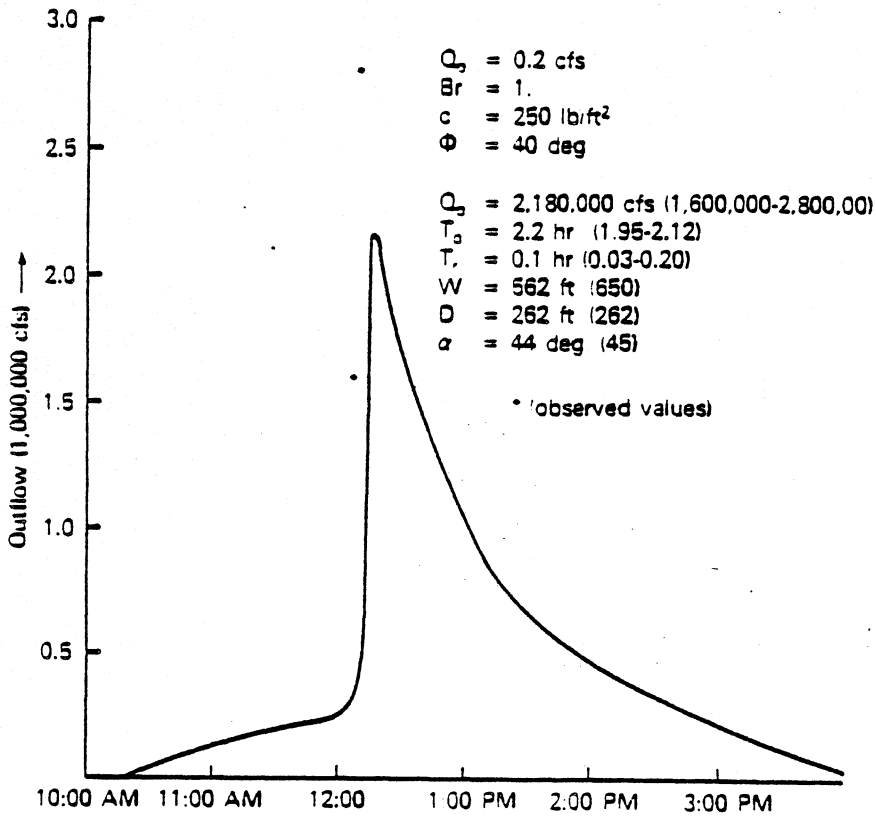

Figure 3. Teton Dam: Predicted and Observed Breach Outflow Hydrograph and Breach Properties.

of 500 ft at the elevation of the initial reservoir water surface. A larger estimated actual breach width of 650 ft breach width was reported by Brown and Rogers (1977); however this was the final breach width after additional enlargement of the breach occurred. The (BREACH) model produced a final width of 560 ft when the reservoir water elevation had receded to near the reservoir bottom; the additional widening of the breach during the recession of the outflow is due to the influence of the depth (y) in Eq. (14).

Sensitivities of the peak breach outflow (Q_p), time of peak flow (T_p) and the top width (W) of the trapezoidal-shaped breach to variations in the specified breach material properties, cohesive strength (C) and internal friction angle (ϕ), are shown in Fig. 4. The dashed lines apply to the Teton simulation. Peak outflow is moderately affected by the cohesion; however it is sensitive to the ϕ value which mostly controls the enlargement of the breach width. Q_p is sensitive to a full range of ϕ values, however the ϕ value may vary by ± 10 degrees with less than 20% variation in Q_p. The breach width (W) was moderately sensitive to variations in the cohesion (C), and somewhat more sensitive to the ϕ value. The time to peak outflow (T_p) was almost insensitive to variations in C and ϕ.

2.9.2 Mantaro Landslide Dam

A massive landslide occurred in the valley of the Mantaro River in the mountainous area of central Peru on April 25, 1974. The slide, with a volume of approximately 5.6×10^{10} ft^3, dammed the Mantaro River and formed

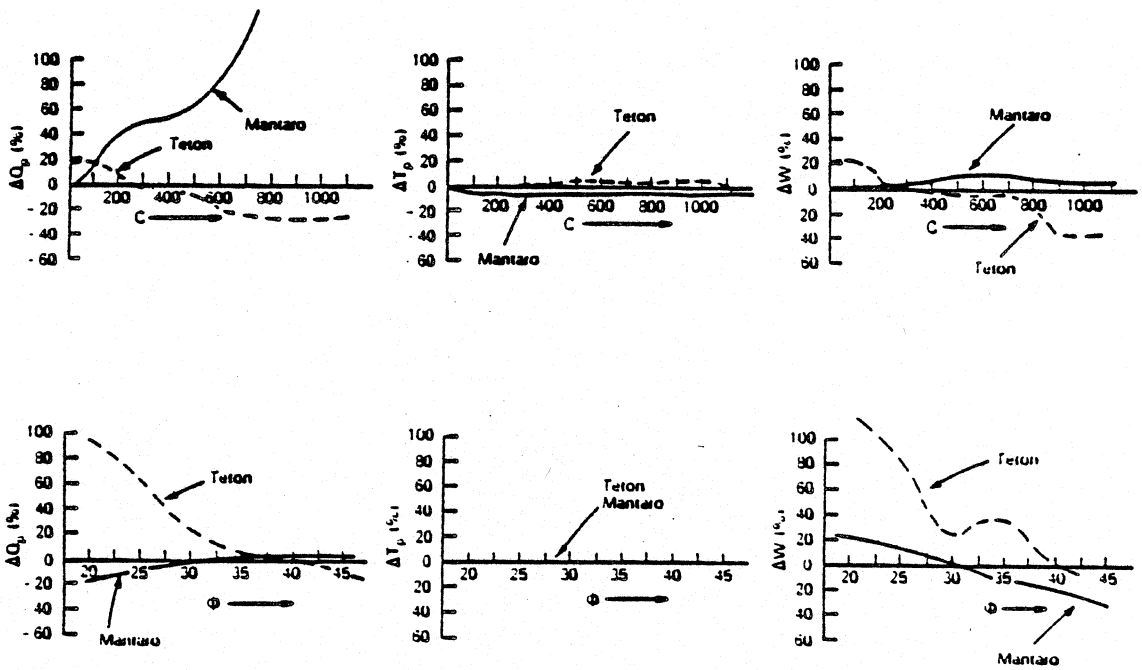

Figure 4. Sensitivity of Mantaro and Teton Predictions of Peak Outflow (Q_p), Time to Peak (T_p), and Breach Width (W) to Changes in the Material Properties of the Dam: Cohesion (C) and Internal Friction Angle (ϕ).

a lake which reached a depth of about 560 ft before overtopping during the period June 6-8, 1974 (Lee and Duncan, 1975). The overtopping flow very gradually eroded a small channel along the approximately 1-mile long downstream face of the slide during the first two days of overtopping. Then a dramatic increase in the breach channel occurred during the next 6-10 hrs resulting in a final trapezoidal-shaped breach channel approximately 350 ft in depth, a top width of some 800 ft, and side slopes of about 1:1. The peak flow was estimated at 353,000 cfs as reported by Lee and Duncan (1975), although Ponce and Tsivoglou (1981) later reported an estimated value of 484,000 cfs. The breach did not erode down to the original river bed; this caused a rather large lake to remain after the breaching had subsided some 24 hrs after the peak had occurred. The slide material was mostly a mixture of silty sand with some clay resulting in a D_{50} size of about 11 mm with some material ranging in size up to 3-ft boulders.

The BREACH model was applied to the Mantaro landslide-formed dam using the following parameters: ZU = 17, ZD = 8.0, H_u = 560 ft, D_{50} = 11 mm, P_{or} = 0.5, S_a = 1200 acres, C = 30 lb/ft^2, ϕ = 30 deg, γ = 100 lb/ft^3 B_r = 2, and Δt = 0.1 hr. The Manning n was estimated by Eq. (20) as 0.020 and the initial breach depth was assumed to be 0.3 ft. The computed breach outflow is shown in Fig. 5 along with the estimated actual values. The timing of the peak outflow and its magnitude are very similar except for a somewhat more gradual rising limb of 10 hr compared to the estimated actual of 6 hr. The dimensions of the gorge eroded through the dam are similar as shown by the values of D, W, and α in Fig. 5.

The sensitivities of Q_p, T_p and W for variations in C and ϕ are shown in Fig. 4. The solid line denotes the Mantaro application. Most notably, Q_p is very sensitive to the cohesion (C) while much less sensitive to the internal friction angle (ϕ). T_p is almost insensitive to the value of C and quite insensitive to ϕ. W is not very sensitive to C and moderately sensitive to ϕ; a variation of ± 10 degrees in ϕ results in a change in W of less than 20%.

3. DAMBRK

The DAMBRK model represents the current state-of-the-art in understanding of dam failures and the utilization of hydrodynamic theory to predict the dam-break wave formation and downstream progression. The model has wide applicability; it can function with various levels of input data ranging from rough estimates to complete data specification; the required data is readily accessible; and it is economically feasible to use, i.e., it requires a minimal computation effort on mainframe computing facilities and can be used with microcomputers.

The model consists of three functional parts, namely: (1) description of the dam failure mode, i.e., the temporal and geometrical description of the breach; (2) computation of the time history (hydrograph) of the outflow through the breach as affected by the breach description, reservoir inflow, reservoir storage characteristics, spillway outflows, and downstream

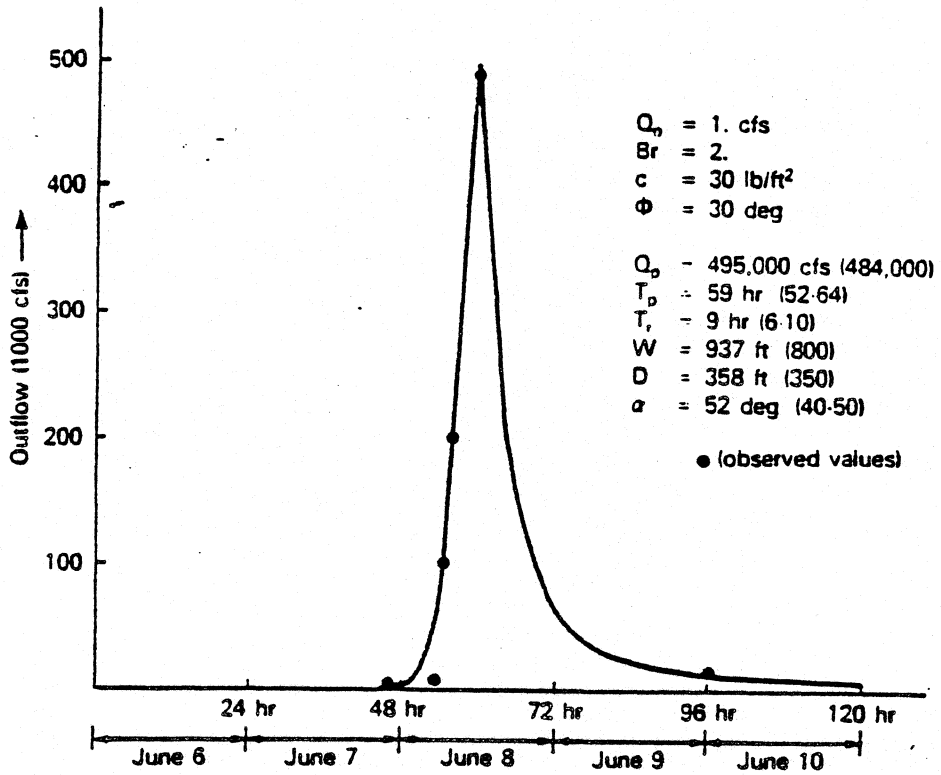

Figure 5. Mantaro Landslide Dam: Predicted and Observed Breach Outflow Hydrograph and Breach Properties.

tailwater elevations; and (3) routing of the outflow hydrograph through the downstream valley in order to determine the changes in the hydrograph due to valley storage, frictional resistance, downstream bridges or dams, and to determine the resulting water surface elevations (stages) and flood-wave travel times.

DAMBRK is an expanded version of a practical operational model first presented in 1977 by the author (Fread, 1977). That model was based on previous work by the author on modeling breached dams (Fread and Harbaugh, 1973) and routing of flood waves (Fread, 1974a, 1976).

3.1 Breach Description

The breach is the opening formed in the dam as it fails. Earthen dams which exceedingly outnumber all other types of dams do not tend to completely fail, nor do they fail instantaneously. The fully formed breach in earthen dams tends to have an average width ($\bar{b}$) in the range ($h_d < \bar{b} < 4h_d$) where h_d is the height of the dam. The middle portion of this range for $\bar{b}$ is supported by the summary report of Johnson and Illes (1976). Breach widths for earthen dams are therefore usually much less than the total length of the dam as measured across the valley. Also, the breach requires a finite interval of time for its formation through erosion of the dam materials by the escaping water. Total time of failure may be in the range of a few minutes to a few hours, depending on the height of the dam, the type materials used in construction, the extent of compaction of the

materials, and the extent (magnitude and duration) of the overtopping flow of the escaping water. Piping failures occur when initial breach formation takes place at some point below the top of the dam due to erosion of an internal channel through the dam by escaping water. As the erosion proceeds, a larger and larger opening is formed; this is eventually hastened by caving-in of the top portion of the dam.

Concrete gravity dams also tend to have a partial breach as one or more monolith sections formed during the construction of the dam are forced apart by the escaping water. The time for breach formation is in the range of a few minutes.

Poorly constructed earthen dams and coal-waste slag piles which impound water tend to fail within a few minutes, and have average breach widths in the upper range or even greater than those for the earthen dams mentioned above.

In DAMBRK, the failure time (τ) and the size and shape of the breach are selected as input parameters similar to the approach used by Fread and Harbaugh (1973). The shape (see Fig. 6) is specified by a parameter (z) identifying the side slope of the breach, i.e., 1 vertical: z horizontal slope. The range of z values is: $0 < z < 2$. Rectangular triangular, or trapezoidal shapes may be specified in this way. For example, z=0 and b>0 produces a trapezoidal shape. The final breach size is controlled by the z parameter and another parameter (b) which is the terminal width of the bottom of the breach. As shown in Fig. 6, the model assumes the breach bottom width starts at a point and enlarges at a linear rate over the failure time interval (τ) until the terminal width is attained and the breach bottom has eroded to the elevation h_{bm} which is usually, but not necessarily, the bottom of the reservoir or outlet channel bottom. If τ is less than 10 minutes, the width of the breach bottom starts at a value of b rather than at a point. This represents more of a collapse failure than an erosion failure.

During the simulation of a dam failure, the actual breach formation commences when the reservoir water surface elevation (h) exceeds a specified value, h_f. This feature permits the simulation of an overtopping of a dam in which the breach does not form until a sufficient amount of water is flowing over the crest of the dam. A piping failure may be simulated when h_f is specified less than the height of the dam, h_d.

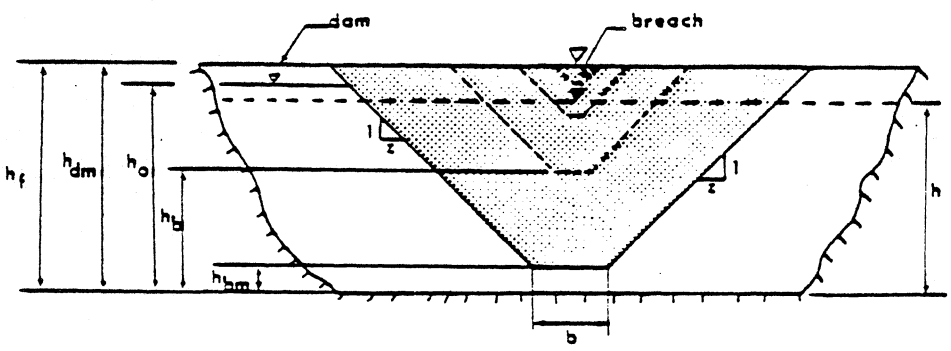

Figure 6. Front View of Dam Showing Formation of Breach

Selection of breach parameters before a breach forms, or in the absence of observations, introduces a varying degree of uncertainty in the model results; however, errors in the breach description and thence in the resulting time rate of volume outflow are rapidly damped-out as the flood wave advances downstream. For conservative forecasts which err on the side of larger flood waves, values for b and z should produce an average breach width ($\bar{b}$) in the uppermost range for a certain type of dam. Failure time (τ) should be selected in the lower range to produce a maximum outflow.

3.2 Reservoir Outflow Hydrograph

The total reservoir outflow consists of broad-crested weir flow through the breach and flow through any spillway outlets, i.e.,

$$Q = Q_b + Q_s \tag{30}$$

The breach outflow (Q_b) is computed as:

$$Q_b = c_1(h-h_b)^{1.5} + c_2(h-h_b)^{2.5} \tag{31}$$

where:

$$c_1 = 3.1\ b_i\ c_v\ k_s \tag{32}$$

$$c_2 = 2.45\ z\ c_v\ k_s \tag{33}$$

$$h_b = h_d - (h_d - h_{bm})\frac{t_b}{\tau} \qquad \text{if} \qquad t_b < \tau \tag{34}$$

$$h_b = h_{bm} \qquad \text{if} \qquad t_b > \tau \tag{35}$$

$$b_i = b\ t_b/\tau \qquad \text{if} \qquad t_b < \tau \tag{36}$$

$$c_v = 1.0 + 0.023\ Q^2/[B_d^2\ (h-h_{bm})^2\ (h-h_b)] \tag{37}$$

$$k_s = 1.0 \qquad \text{if} \qquad \frac{h_t - h_b}{h-h_b} < 0.67 \tag{38}$$

otherwise:

$$k_s = 1.0 - 27.8\ \left[\frac{h_t - h_b}{h-h_b} - 0.67\right]^3 \tag{39}$$

in which h_b is the elevation of the breach bottom, h is the reservoir water surface elevation, b_i is the instantaneous breach bottom width, t_b is time

interval since breach started forming, c_v is correction for velocity of approach, Q is the total outflow from the reservoir, B_d is width of the reservoir at the dam, k_s is the submergence correction for tailwater effects on weir outflow (Venard, 1954), and h_t is the tailwater elevation (water surface elevation immediately downstream of dam).

The tailwater elevation (h_t) is computed from Manning's equation, i.e.,

$$Q = \frac{1.49}{n} S^{1/2} \frac{A^{5/3}}{B^{2/3}} \tag{40}$$

in which n is the Manning roughness coefficient, A is the cross-sectional area of flow, B is the top width of the wetted cross-sectional area, and S is the energy slope. Each term in Eq. (40) applies to a representative channel reach immediately downstream of the dam. The S parameter can be specified by the user; it does not change with time; if it is not specified, the model uses the channel bottom slope of the first third of the downstream valley reach. Since A and B are functions of h_t and Q is the total discharge given by Eq. (30), Eq. (40) provides a sufficiently accurate value for h_t if there are no backwater effects immediately below the dam due to downstream constrictions, dams, bridges, or significant tributary inflows. When these affect the tailwater, Eq. (40) is not used and the dam is treated as an internal boundary which is described in a following section on multiple dams and bridges.

If the breach is formed by piping, Eq. (31)-(39) are replaced by the following orifice flow equation:

$$Q_b = 4.8\ A_p(h-\bar{h})^{1/2} \tag{41}$$

where:

$$A_p = [2b_i+4z(h_f-h_b)]\ (h_f-h_b) \tag{42}$$

$$\bar{h} = h_f \qquad \text{if} \qquad h_t < 2h_f - h_b \tag{43}$$

$$\bar{h} = h_t \qquad \text{if} \qquad h_t > 2h_f - h_b \tag{44}$$

and h_d is replaced by h_f in Eq. (34) to compute h_b. However, if $\bar{h} = h_f$ and

$$h - h_b < 2.2(h_f-h_b) \tag{45}$$

the flow ceases to be orifice flow and the broad-crested weir flow, Eq. (31), is used.

The spillway outflow (Q_s) is computed as:

$$Q_s = c_s L_s (h-h_s)^{1.5} + c_g A_g (h-h_g)^{0.5} + c_d L_d (h-h_d)^{1.5} + Q_t \qquad (46)$$

in which c_s is the uncontrolled spillway discharge coefficient, h_s is the uncontrolled spillway crest elevation, c_g is the gated spillway discharge coefficient, h_g is the center-line elevation of the gated spillway, c_d is the discharge coefficient for flow over the crest of the dam L_s is the spillway length, A_g is the gate flow area, L_d is the length of the dam crest less L_s, and Q_t is a constant outflow term which is head independent. The uncontrolled spillway flow or the gated spillway flow can also be represented as a table of head-discharge values. The gate flow may also be specified as a function of time.

The total outflow is a function of the water surface elevation (h). Depletion of the reservoir storage volume by the outflow causes a decrease in h which then causes a decrease in Q. However, any inflow to the reservoir tends to increase h and Q. In order to determine the total outflow (Q) as function of time, the simultaneous effects of reservoir storage characteristics and reservoir inflow require the use of a reservoir routing technique. DAMBRK utilizes a hydrologic storage routing technique based on the law of conservation of mass, i.e.,

$$I - Q = dS/dt \qquad (47)$$

in which I is the reservoir inflow, Q is the total reservoir outflow, and dS/dt is the time rate of change of reservoir storage volume. Eq. (47) may be expressed in finite difference form as:

$$(I+I')/2 - (Q+Q')/2 = \Delta S/\Delta t \qquad (48)$$

in which the prime (') superscript denotes values at the time $t-\Delta t$ and the Δ approximates the differential. The term ΔS may be expressed as:

$$\Delta S = (A_s+A_s') \ (h-h')/2 \qquad (49)$$

in which A_s is the reservoir surface area coincident with the elevation (h).

Combining Eqs. (30), (31), (46), (48) and (49) result in the following expression:

$$(A_s+A_s') \ (h-h')/\Delta t + c_1(h-h_b)^{1.5} + c_2(h-h_b)^{2.5} + c_s(h-h_b)^{1.5}$$

$$+ c_g(h-h_g)^{0.5} + c_d(h-h_d)^{1.5} + Q_t + Q' - I - I' = 0 \qquad (50)$$

Since A_s is a function of h and all other terms except h are known, Eq. (50) can be solved for the unknown h using Newton-Raphson iteration. Once h is

obtained, Eqs. (31) and (46) can be used to obtain the total outflow (Q) at time (t). In this way the outflow hydrograph Q(t) can be developed for each time (t) as to goes from zero to some terminating value (t_e) sufficiently large for the reservoir to be drained. In Eq. (50) the time step (Δt) is chosen sufficiently small to incur minimal numerical integration error. This value is preset in the model to $\tau/50$.

3.3 Downstream Routing

After computing the hydrograph of the reservoir outflow, the extent of and time of occurrence of flooding in the downstream valley is determined by routing the outflow hydrograph though the valley. The hydrograph is modified (attenuated, lagged, and distorted) as it is routed through the valley due to the effects of valley storage, frictional resistance to flow, and downstream obstructions and/or flow control structures. Modifications to the dam-break flood wave are manifested as attenuation of the flood peak elevation, spreading-out or dispersion of the flood wave volume, and changes in the celerity (translation speed) or travel time of the flood wave. If the downstream valley contains significant storage volume such as a wide flood plain, the flood wave can be extensively attenuated and its time of travel greatly increased. Even when the downstream valley approaches that of a uniform rectangular-shaped section, there is appreciable attenuation of flood peak and reduction in wave celerity as the wave progresses through the valley.

A distinguishing feature of dam-break waves is the great magnitude of peak discharge when compared to runoff-generated flood waves having occurred in the past in the same valley. The dam-break flood is usually many times greater than the runoff flood of record. The above-record discharges make it necessary to extrapolate certain coefficients used in various flood routing techniques and make it impossible to fully calibrate the routing technique.

Another distinguishing characteristic of dam-break floods is the very short duration time, and particularly the extremely short time from beginning of rise until the occurrence of the peak. The time to peak is in almost all instances synonymous with the breach formation time (τ) and, therefore, is in the range of a few minutes to a few hours. This feature, coupled with the great magnitude of the peak discharge, causes the dam-break flood wave to have acceleration components of a far greater significance than those associated with a runoff-generated flood wave.

A hydraulic routing technique (dynamic routing) based on the complete equations of unsteady flow is used to route the dam-break flood hydrograph through the downstream valley. This method is derived from the original equations developed by Barre De Saint-Venant (1871). In this method the important acceleration effects are properly considered. Also, the only coefficient that must be extrapolated beyond the range of past experience is the coefficient of flow resistance. It so happens that this is usually not a sensitive parameter in effecting the modifications of the flood wave due to its progression through the downstream valley. The dynamic routing technique properly considers the effect of downstream constrictions and flow control structures such as bridge-road embankments or dams.

The Saint-Venant unsteady flow equations consist of a conservation of mass equation, i.e.,

$$\frac{\partial Q}{\partial x} + \frac{\partial(A+A_o)}{\partial t} - q = 0 \tag{51}$$

and a conservation of momentum equation, i.e.,

$$\frac{\partial Q}{\partial t} + \frac{\partial(Q^2/A)}{\partial x} + gA(\frac{\partial h}{\partial x} + S_f + S_e) + L = 0 \tag{52}$$

where A is the active cross-sectional area of flow, A_o is the inactive (off-channel storage) cross-sectional area, x is the longitudinal distance along the channel (valley), t is the time, q is the lateral inflow or outflow per linear distance along the channel (inflow is positive and outflow is negative in sign), g is the acceleration due to gravity, S_f is the friction slope, and S_e is the expansion-contraction slope. The friction slope is evaluated from Manning's equation for uniform, steady flow, i.e.,

$$S_f = \frac{n^2|Q|Q}{2.21\ A^2\ R^{4/3}} \tag{53}$$

in which n is the Manning coefficient of frictional resistance and R is the hydraulic radius defined as A/B where B is the top width of the active cross-sectional area. The term (S_e) is defined as follows:

$$S_e = \frac{k\ \Delta(Q/A)^2}{2g\ \Delta x} \tag{54}$$

in which k (Morris and Wiggert, 1972) is the expansion-contraction coefficient varying from 0.0 to ±1.0 (+ if contraction, - if expansion), and $\Delta(Q/A)^2$ is the difference in the term $(Q/A)^2$ at two adjacent cross-sections separated by a distance Δx. L is the momentum effect of lateral flow assumed herein to enter or exit perpendicular to the direction of the main flow. This term has the following form: 1) lateral inflow, L = 0; 2) seepage lateral outflow, L = -0.5qQ/A; and 3) bulk lateral outflow, L = -qQ/A.

Eqs. (51)-(52) which are nonlinear partial differential equations, must be solved by numerical techniques. An implicit 4-pt. finite difference technique is used to obtain a solution to either set of equations. This particular technique (Fread, 1974) is used for its computational efficiency, flexibility, and convenience in the application of the equations to flow in complex channels existing in nature. In essence, the technique determines the unknown quantities (Q and h at all specified cross-sections along the downstream channel-valley at various times into the future; the solution is advanced from one time to a future time by a finite time interval (time step) of magnitude Δt. The flow equations are expressed in finite difference form for all cross-sections along the valley and then solved simultaneously for the unknowns (Q and h) at each cross-section. Due to the nonlinearity of the partial differential equations and their finite difference

representations, the solution is iterative and a highly efficient quadratic iterative technique known as the Newton-Raphson method is used. Convergence of the iterative technique is attained when the difference between successive iterative solutions for each unknown is less than a relatively small prescribed tolerance. Usually, one to three iterations at each time step are sufficient for convergence to be attained for each unknown at all cross-sections. A more complete description of the solution technique may be found elsewhere (Amein and Fang, 1970; Fread, 1974a, Fread, 1977).

3.4 Tributary Inflows/Outflows

Unsteady flows associated with tributaries downstream of the dam can be added to the unsteady flow resulting from the dam failure. This is accomplished via the term q in Eq. (51). The tributary flow is distributed along a single Δx reach. Backwater effects of the dam-break flow on the tributary flow are ignored, and the tributary flow is assumed to enter perpendicular to the dam-break flow. Outflows are assigned negative values. Outflows which occur as broad-crested weir flow over a levee or natural crest may be simulated. The crest elevation, discharge coefficient, and location along the river-valley must be specified. The head is computed as the average water surface elevation, along the length of the crest, less the crest elevation.

3.5 Multiple Dams and Bridges

The dam-break flood forecasting model can simulate the progression of a dam-break wave through a downstream valley containing a reservoir created by another downstream dam, which itself may fail due to being sufficiently overtopped by the wave produced by the failure of the upstream dam. In fact, an unlimited number of reservoirs located sequentially along the valley can be simulated. When the tailwater below a dam is affected by flow conditions downstream of the tailwater section (e.g., backwater produced by a downstream dam, flow constriction, bridge, and/or tributary inflow), the flow occurring at the dam is computed by using an internal boundary condition at the dam. In this method the dam is treated as a short Δx reach in which the flow through the reach is governed by the following two equations rather than either Eqs. (51)-(52):

$$Q_i = Q_{i+1} \tag{55}$$

$$Q_i = Q_b + Q_s \tag{56}$$

in which Q_b and Q_s are breach flow and spillway flow. In this way, the flows Q_i and Q_{i+1} and the elevations h_i and h_{i+1} are in balance with the other flows and elevations occurring simultaneously throughout the entire flow system which may consist of additional dams which are treated as additional internal boundary conditions via Eqs. (55)-(56).

Highway/railway bridges and their associated earthen embankments which are located at points downstream of a dam may also be treated as internal boundary conditions. Eqs. (55)-(56) are used at each bridge; the term Q_s in Eq. (56) is computed by the following expression:

$$Q_s = C\sqrt{2g}\, A_{i+1}(h_i - h_{i+1})^{1/2} + C_d k_s (h - h_c)^{3/2} \tag{57}$$

in which C is a coefficient of bridge flow, C_d is the coefficient of flow over the crest of the road embankment, h_c is the crest elevation of the embankment, and k_s is similar to Eqs. (38)-(39).

3.6 Supercritical Flow

The DAMBRK model can simulate the flow through the downstream valley when the flow is supercritical. This type of flow occurs when the slope of the downstream valley exceeds about 50 ft/mi. Slopes less than this usually result in the flow being subcritical to which all preceding comments pertaining to the downstream routing apply. When the flow is supercritical, any flow disturbances cannot travel back upstream; therefore, the downstream boundary becomes superfluous. Thus, for supercritical flow, a downstream boundary condition is not required; however, an additional equation other than the reservoir outflow hydrograph is needed. To satisfy this requirement, an equation similar to Eq. (40) but with a time-dependent energy slope, is used at the upstream boundary. Multiple reservoirs on supercritical valley slopes must be treated using a storage routing technique such as Eq. (50) rather than the dynamic routing technique.

3.7 Floodplain Compartments

The DAMBRK model can simulate the exchange of flow between the river and floodplain compartments. The floodplain compartments are formed by one or two levees which run parallel to the river on either or both sides of the river, and other levees or road embankments which run perpendicular to the river. Flow transfer between a floodplain compartment and the river is assumed to occur along one Δx reach and is controlled by broad-crested weir flow with submergence correction. Flow can be either away from the river or into the river, depending on the relative water surface elevations of the river and the floodplain compartment. The river elevations are computed via Eqs. (51)-(52), and the floodplain water surface elevations are computed by a simple storage routing relation, i.e.,

$$V_\ell^{\,t} = V_\ell^{\,t-\Delta t} + \left(I^t - O^t\right) \Delta t/43560 \tag{58}$$

in which V_ℓ is the volume (acre-ft) in the floodplain compartment at time t or $t-\Delta t$ referenced to the water elevation, I is the inflow from the river or adjacent floodplain compartments, and O is the outflow from the floodplain compartment to the river and/or to adjacent floodplain compartments. Flow transfer between adjacent floodplain compartments is also controlled by broad-crested weir flow with submergence correction. The broad-crested weir flow is according to the following:

$$I = c\, s_b \left(h_r - h_{fp}\right)^{3/2} \tag{59}$$

$$O = c\, s_b \left(h_{fp} - h_r\right)^{3/2} \tag{60}$$

in which c is a specified discharge coefficient, h_r is the river elevation, h_{fp} is the water surface elevation of the floodplain, and s_b is the submergence correction factor, i.e.

$$s_b = 1.0 \qquad h_r < 0.67 \tag{61}$$

$$s_b = 1.0 - 27.8\left(H_r - 0.67\right)^3 \qquad h_r > 0.67 \tag{62}$$

$$H_r = \left(h_r - h_w\right)/\left(h_{fp} - h_w\right) \tag{63}$$

and h_w is the specified elevation of the crest of the levee. The floodplain elevation $\left(h_{fp}\right)$ is obtained iteratively via a table look-up algorithm from the specified table of volume-elevation values. The outflow from a floodplain compartment may also include that from one or more pumps associated with each floodplain compartment. Each pump has a specified discharge-head relation given in tabular form along with start-up and shut-off operation instructions depending on specified water surface elevations. The pumps discharge to the river.

3.8 Routing Losses

Often in the case of dam-break floods, where the extremely high flows inundate considerable portions of channel overbank or valley flood plain, a measurable loss of flow volume occurs. This is due to infiltration into the relatively dry overbank material, detention storage losses, and sometimes short-circuiting of flows from the main valley into other drainage basins via canals. Such losses of flow may be taken into account via the term q in Eq. (51). An expression describing the loss is given by the following:

$$q_m = -0.00458\, V_L\, P/(L\, \bar{T}) \tag{64}$$

in which V_L is the outflow volume (acre-ft) from the reservoir; P is the volume loss ratio which may range from 0 to as high as 0.3; L is the length (mi) of downstream channel through which the loss occurs; and T is the average duration (hr) of the flood wave throughout the reach length L; and q_m is the maximum lateral outflow (cfs/ft) occurring along the reach L throughout the duration of flow. The mean lateral outflow is proportioned in time and distance along the reach L.

3.9 Landslide Generated Waves

Reservoirs are sometimes subject to landslides which rush into the reservoir displacing a portion of the reservoir contents, and thereby

creating a very steep water wave which travels up and down the length of the reservoir. This wave may have sufficient amplitude to overtop the dam and precipitate a failure of the dam, or the wave by itself may be large enough to cause catastrophic flooding downstream of the dam without resulting in the failure of the dam as perhaps in the case of a concrete dam.

The capability to generate waves produced by landslides is provided within DAMBRK. The volume of the landslide mass, its porosity, and time interval over which the landslide occurs, are input to the model. Within the model, the landslide mass is deposited within the reservoir in layers during small computational time steps, and simultaneously the original dimensions of the reservoir are reduced accordingly. The time rate of reduction in the reservoir cross-sectional area creates the wave during the solution of the unsteady flow Eqs. (51)-(52), which are applied to he cross-sections describing the reservoir characteristics.

3.10 Model Testing

The DAMBRK model has been tested on five historical dam-break floods to determine its ability to reconstitute observed downstream peak stages, discharges, and travel times. Those floods that have been used in the testing are: 1976 Teton Dam, 1972 Buffalo Creek Coal-Waste Dam, 1889 Johnstown Dam, 1977 Toccoa (Kelly Barnes) Dam, and the 1977 Laurel Run Dam floods. However, only the Teton flood will be presented herein.

The Teton Dam, a 300 ft. high earthen dam with a 3,000 ft. long crest, failed on June 5, 1976, killing 11 people making 25,000 homeless, and inflicting about $400 million in damages to the downstream Teton-Snake River Valley. Data from a Geological Survey Report by Ray, et al. (1977) provided observations on the approximate development of the breach, description of the reservoir storage, downstream cross-sections and estimates of Manning's n approximately every 5 miles, indirect peak discharge measurements at three sites, flood peak travel times, and flood peak elevations. The inundated area is shown in Fig. 7.

The following breach parameters were used in DAMBRK to reconstitute the downstream flooding the downstream flooding due to the failure of Teton Dam: τ = 1.25 hrs, BB = 150 ft, z = 0, h_{bm} = 0.0, $h_f = h_d = h_o$ = 261.5 ft. Cross-sectional properties at 12 locations shown in Fig. 7 along the 60 mile reach of the Teton-Snake River Valley below the dam were used. Five top widths were used to describe each cross-section. The downstream valley consisted of a narrow canyon (approx. 1,000 ft. wide) for the first 5 miles and thereafter a wide valley which was inundated to a width of about 9 miles. Manning's n values ranging from 0.028 to 0.047 were provided from field estimates by the Geological Survey. Values of Δx between cross-sections gradually increased from 0.5 miles near the dam, to 1.5 miles near the downstream boundary at the Shelly gaging station (valley mile 59.5 downstream from the dam). The reservoir surface area-elevation values were obtained from Geological Survey topo maps. The downstream boundary was assumed to he channel flow control as represented by a loop rating curve given by Eq. (40).

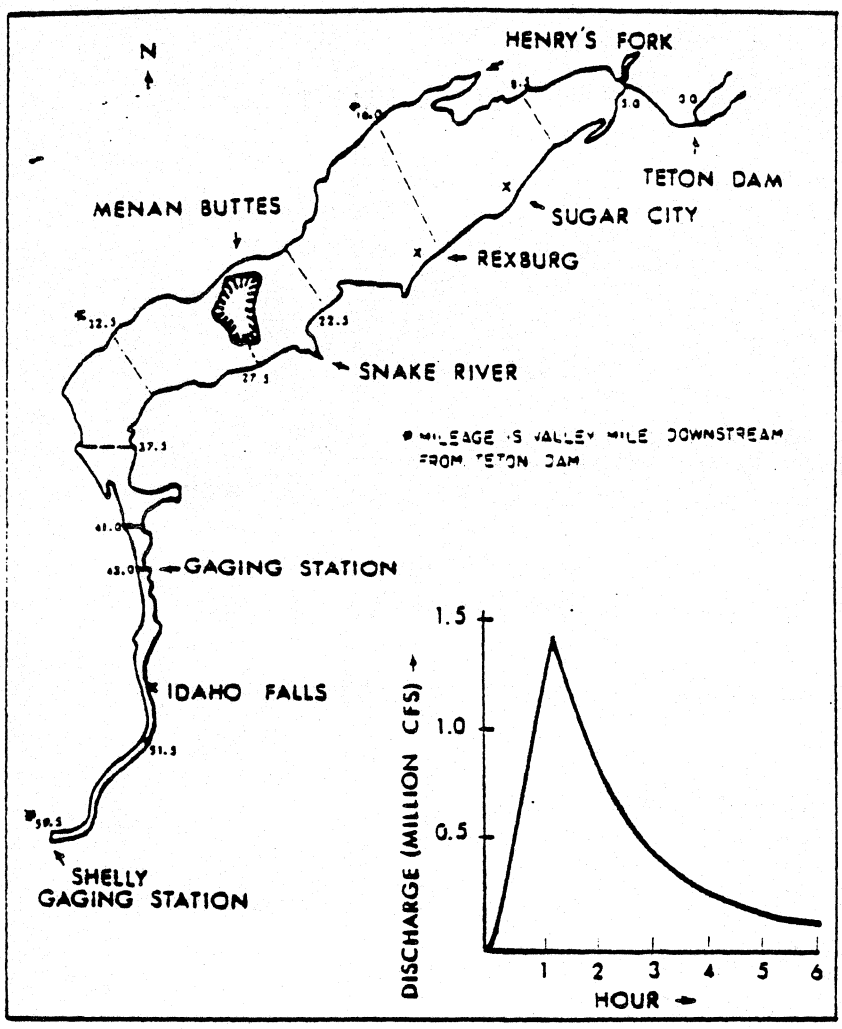

Figure 7. Outflow Hydrograph and Flooded Area Downstream of Teton Dam

The computed outflow hydrograph is shown in Fig. 7. It has a peak value of 1,652,300 cfs (cubic feet per second), a time to peak of 1.25 hrs, and a total duration of about 6 hrs. The peak is about 20 times greater than the flood of record. The temporal variation of the computed outflow volume compared within 5 percent of observed values. The computed peak discharge values along the 60-mile downstream valley are shown in Fig. 8 along with three observed (indirect measurement) values at miles 8.5, 43.0, and 59.5. The average difference between the computed and observed values is 4.8 percent. Most apparent is the extreme attenuation of the peak discharge as the flood wave progresses though the valley. Two computed curves were assumed, i.e., $q_m = 0$; and a second in which the losses were assumed to be uniform along the valley. The losses were assumed to vary from 0 to a maximum of $q_m = -0.30$ and were accounted for in the model through the q term in Eq. (51). Losses were due to infiltration and detention storage behind irrigation levees.

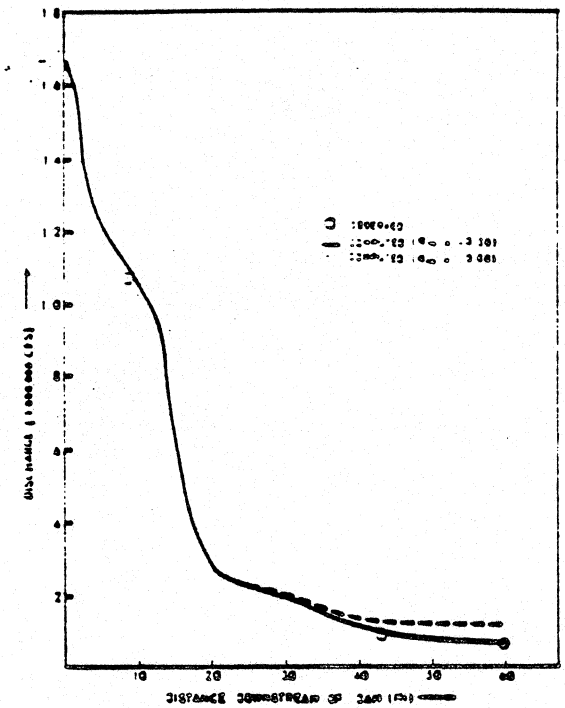

Figure 8. Profile of Peak Discharge from Teton Dam Failure

The a priori selection of the breach parameters (τ and BB) causes the greatest uncertainty in forecasting dam-break flood waves. The sensitivity of downstream peak discharges to reasonable variations in τ and $\bar{b}$ is shown in Fig. 9.

Although there are large differences in the discharges (+45 to -25 percent) near the dam, these rapidly diminish in the downstream direction. After 10 miles the variation is +20 to -14 percent, and after 15 miles the variation has further diminished (+15 to -8 percent). The tendency for extreme peak attenuation and rapid damping of differences in the peak discharge is accentuated in the case of Teton Dam due to the presence of the very wide valley. Had the narrow canyon extended all along the 60-mile reach to Shelly, the peak discharge would not have attenuated as much as the differences in peak discharges due to variations in τ and $\bar{b}$ would be more persistent. In this instance, the peak discharge would have attenuated to about 350,000 rather than 67,000 as shown in Fig. 9, and the differences in peak discharges at mile 59.5 would have been about 27 percent as opposed to less than 5 percent as shown in Fig. 9.

Computed peak elevations compared favorably with observed values. The average absolute error was 1.5 ft, while the average arithmetic error was only -0.2 ft.

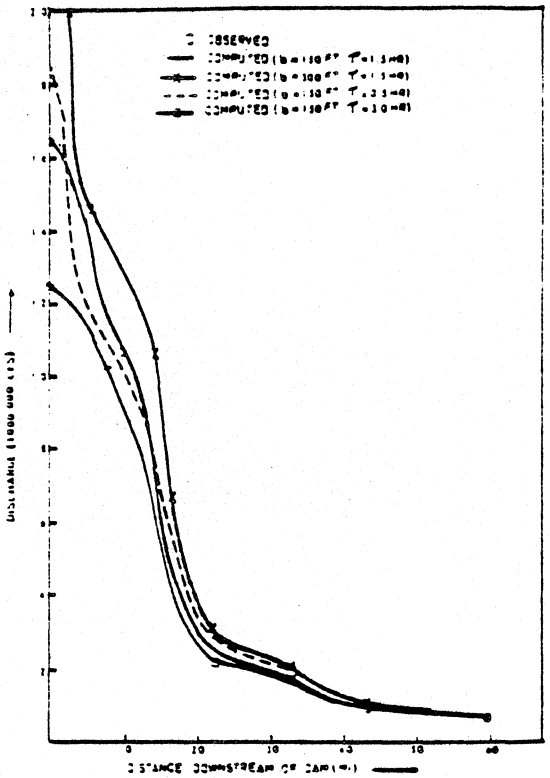

Figure 9. Profile of Peak Discharge from Teton Dam Failure Showing Sensitivity of Various Input Parameters.

The computed flood peak travel times and three observed values are shown in Fig. 10. The differences between the computed and observed are about 10 percent for the case of using the estimated Manning's n values and about 1 percent if the n values are slightly increased by 7 percent.

As mentioned previously, the Manning's n must be estimated, especially for the flows above the flood of record. The sensitivity of the computed stages and discharges of the Teton flood due to a substantial change (20 percent) in the Manning's n was found to be as follows: 1) 0.5 ft. in computed peak water surface elevations or about 2 percent of the maximum flow depths, 2) 16 percent deviation in the computed peak discharges, 3) 0.8 percent change in the total attenuation of peak discharge incurred in the 60-mile reach from Teton Dam to Shelly, and 4) 15 percent change in the flood peak travel time to Shelly. These results indicate that Manning's n has little effect on peak elevations or depths; however, the travel time is affected by nearly the same percent that the n values are changed.

A typical simulation of the Teton flood as described above involved 73 Δx reaches, 55 hrs of prototype time, and an initial time step (Δt) of 0.06 hrs. Such a simulation run required only 19 seconds of CPU time on an IBM 360/196 computer system; the associated cost was less than $5 per run. Microcomputer runs require about 10 min for the Teton simulation.

Information on similar testing of DAMBRK on the Buffalo Creek flood can be found in Fread (1977, 1984a). The results showed a similar degree of comparison between computed and observed values.

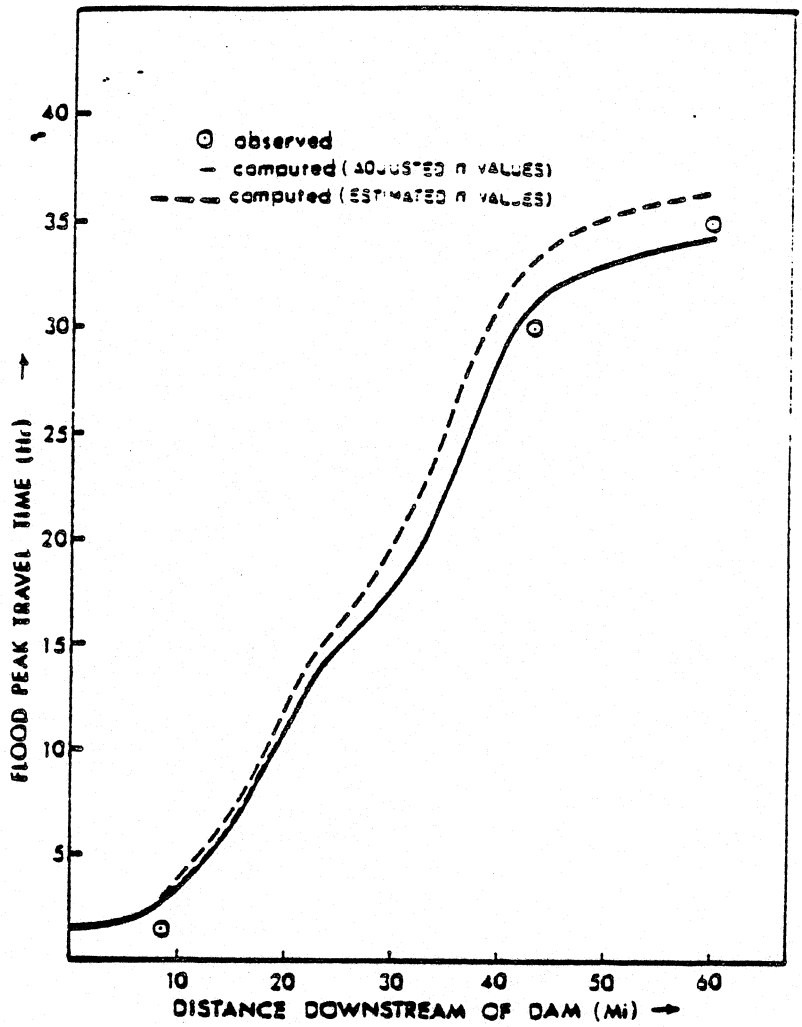

Figure 10. Travel Time of Flood Peak from Teton Dam Failure.

4. SMPDBK

SMPDBK is a simple model for predicting the characteristics of the floodwave peak produced by a breached dam (Wetmore and Fread, 1984). It will, with minimal computational resources (hand-held computers, micro-computers), determine the peak flow, depth, and time of occurrence at selected locations downstream of a breached dam. SMPDBK first computes the peak outflow at the dam, based on the reservoir size and the temporal and geometrical description of the breach. The computed floodwave and channel properties are used in conjunction with routing curves to determine how the peak flow will be diminished as it moves downstream. Based on this predicted floodwave reduction, the model computes the peak flows at specified downstream points. The model then computes the depth reached by the peak flow based on the channel geometry, slope, and roughness at these downstream points. The model also computes the time required for the peak to reach each forecast point and, if a flood depth is entered for the point, the time at which that depth is reached as well as when the floodwave

recedes below that depth, thus providing a time frame for evacuation and fortification on which a preparedness plan may be based. The SMPDBK Model neglects backwater effects created by downstream dams or bridge embankments, the presence of which can substantially reduce the model's accuracy. However, its speed and ease of use together with its small computational requirement make it a attractive tool for use in cases where limited time and resources preclude the use of the DAMBRK Model. In such instances planners, designers, emergency managers, and consulting engineers responsible for predicting the potential effects of a dam failure may employ the model in situations where backwater effects are not significant for pre-event delineation of areas facing danger should a particular dam fail.

4.1 General Description

The SMPDBK model retains the critical deterministic components of the numerical DAMBRK model while eliminating the need for large computer facilities. SMPDBK accomplishes this by approximating the downstream channel as a prism, neglecting the effects of off-channel storage, concerning itself with only the peak flows, stage, and travel times, neglecting the effects of backwater from downstream bridges and dams, and utilizing dimensionless peak-flow routing graphs developed using the NWS DAMBRK model. The applicability of the SMPDBK model is further enhanced by its minimal data requirements; the peak flow at the dam may be calculated with only four readily accessible data values and the downstream channel may be defined by a single "average" cross-section, although prediction accuracy increases with the number of cross-sections specified.

Three steps make up the procedure used in the SMPDBK model. These are: (1) calculation of the peak outflow at the dam using the temporal and geometrical description of the breach and the reservoir volume; (2) approximation of the channel downstream of the dam as a prismatic channel; and (3) calculation of dimensionless routing parameters used with dimensionless routing curves to determine the peak flow at specified cross sections downstream of the dam.

4.2 Breach Description and Peak Outflow Computation

Since earthen dams generally do not fail completely nor instantaneously, the SMPDBK model allows for the investigation of partial failures occurring over a finite interval of time. And, although the model assumes a rectangular-shaped breach, a trapezoidal breach may be analyzed by specifying a rectangular breach width that is equal to the average width of the trapezoidal breach. Failures due to overtopping of the dam and/or failures in which the breach bottom does not erode to the bottom of the reservoir may also be analyzed by specifying an appropriate "H" parameter which is the elevation of the reservoir water surface elevation when breach formation commences minus the final breach bottom elevation (i.e., "H" is the depth to which the breach cuts).

The model uses a single equation to determine the maximum breach outflow and the user is required to supply the values of four variables for this equation. These variables are: 1) the surface area (A_s, acres) of the

reservoir; 2) the depth (H, ft) to which the breach cuts; 3) the time (t_f, minutes) required for breach formation; and 4) the final width (B_r, ft) of the breach. These parameters are substituted into a broad-crested weir flow equation to yield the maximum breach outflow (Q_{bmax}) in cfs, i.e.

$$Q_{bmax} = Q_o + 3.1\ B_r \left(\frac{C}{\frac{t_f}{60} + \frac{C}{\sqrt{H}}}\right)^3 \tag{65}$$

where: $$C = \frac{23.4\ A_S}{B_r} \tag{66}$$

and Q_o is the spillway flow and overtopping crest flow which is estimated to occur simultaneously with the peak breach outflow.

Once the maximum outflow at the dam has been computed, the depth of flow produced by this discharge may be determined based on the geometry of the channel immediately downstream of the dam, the Manning "n" (roughness coefficient) of the channel and the slope of the downstream channel. This depth is then compared to the depth of water in the reservoir to find whether it is necessary to include a submergence correction factor for tailwater effects on the breach outflow (i.e., to find whether the water downstream is restricting the free flow through the breach). This comparison and (if necessary) correction allows the model to provide the most accurate prediction of maximum breach outflow which properly accounts for the effects of tailwater depth downstream of the dam.

The maximum breach outflow must be corrected iteratively for submergence resulting from tailwater effects if the computed maximum outflow stage (h_{max}) is greater than ($0.67\ h_{weir}$) where h_{weir} is the head over the weir (breach) at time t_f as expressed by the following relation:

$$h_{weir} = \left(\frac{C}{\frac{t_f}{60} + \frac{C}{\sqrt{H}}}\right)^2 \tag{67}$$

where C is defined by Eq. (66).

If the ratio of (h_{max}/h_{weir}) is greater than 0.67, a submergence correction factor must be computed as follows:

$$K_s^* = 1 - 27.8 \left[\frac{h_{max}}{h_{weir}} - 0.67\right]^3 \tag{68}$$

This value for K_s^* is substituted into Eq. (69) to obtain an <u>averaged</u> submergence correction factor given by the following:

$$K_s^{\,k} = \frac{K_s^{\,*} + K_s^{\,k-1}}{2} \tag{69}$$

where the k superscript is the iteration counter and the first iteration value for $K_s^{\,o}$ is 1. This correction factor is applied to the breach outflow as follows

$$Q_b^{\,k} = K_s^{\,k} \; Q_b^{\,k-1} \tag{70}$$

where: $Q_b^{\,k-1} = Q_{bmax}$ is the first iteration. The corrected breach outflow ($Q_b^{\,k}$) is then used to compute an outflow depth ($h_{max}^{\,k}$). The computation of h_{max} is described later via Eq. (75). Also, because there is decreased flow through the breach, there is less drawdown. Thus, the head over the weir (h_{weir}) must be recalculated using the relation:

$$h_{weir}^{\,k} = h_{weir}^{\,k-1} + \left(Q_b^{\,k-1} - Q_b^{\,k}\right) \frac{t_f \;\; (\text{sec.})}{2A_s \;\; (\text{sq.ft.})} \tag{71}$$

Now the ratio of the two new values, $h_{max}^{\,k}/h_{weir}^{\,k}$ is used in Eq. (68) to compute a new submergence correction factor. If the new maximum breach outflow computed via Eq. (70) is significantly different (± 5%) from that computed in the previous iteration, the procedure is repeated. Generally, within two or three iterations the K_s value will converge and a suitable value for the maximum breach outflow (Q_b) is achieved which properly accounts for the effects of submergence.

4.3 Channel Description

The river channel downstream of the dam to the specified routing point is approximated as a prismatic channel by defining a single cross-section (an average section that incorporates the geometric properties of all intervening sections via a distance weighting technique) and fitting a mathematical function that relates the section's width to depth. This prismatic representation of the channel allows easy calculation of flow area and volume in the downstream channel which is required to accurately predict the amount of peak flow attenuation.

Approximating the channel as a prism requires three steps. First, topwidth vs. depth data must be obtained from topographic maps or survey notes. For each depth (h_i), a distance weighted topwidth $\bar{B}_i$ is defined producing a table of values that may be used for fitting (using least-squares or a log-log plot) a single equation of the form $\bar{B} = \bar{K}h^{\bar{m}}$ to define the prismatic channel geometry. The fitting coefficients ($\bar{K}$ and $\bar{m}$) are computed using the following least squares algorithm:

$$\bar{m} = \frac{\sum \left[(\log h_i)\ (\log \bar{B}_i)\right] - \dfrac{(\sum \log h_i)\ (\sum \log \bar{B}_i)}{I}}{\sum (\log h_i)^2 - \dfrac{(\sum \log h_i)^2}{I}} \tag{72}$$

$$\log \bar{K} = \frac{\sum \log \bar{B}_i}{I} - \bar{m}\ \frac{\sum \log h_i}{I} \tag{73}$$

$$\bar{K} = 10^{(\log \bar{K})} \tag{74}$$

After computing $\bar{K}$ and $\bar{m}$, the depth (h) may be computed for a given discharge (Q) by using the Manning equation, i.e.,

$$h = (Q/a)^b \tag{75}$$

where: $$a = \frac{1.49}{n}\ S^{1/2}\ \frac{\bar{K}}{(\bar{m}+1)^{5/3}} \tag{76}$$

$$b = 3/(3\bar{m}+5) \tag{77}$$

Also, S is the channel bottom slope (ft/ft), and n is the Manning n appropriate for the section of river-valley associated with the computed depth (h). In this manner h_{max} of Eq. (68) can be computed if Q_{bmax} is substituted for Q and the fitting coefficients $\bar{K}$ and $\bar{m}$ apply only to the tailwater section.

4.4 Downstream Routing

The peak outflow discharge determined in the preceding step may be routed downstream using the dimensionless routing curves. (See Fig. 11-13.) These curves were developed from numerous executions of the NWS DAMBRK Model and they are grouped into families based on the Froude number associated with the floodwave peak, and have as their X-coordinate the ratio of the downstream distance (from the dam to a selected cross-section) to a distance parameter (X_c). The Y-coordinate of the curves used in predicting peak downstream flows is the ratio of the peak flow at the selected cross section to the computed peak flow at the dam. To determine the correct family and member curve that most accurately predicts the attenuation of the flood, certain routing parameters must be defined.

The distinguishing characteristic of each curve family is the Froude number developed as the floodwave moves downstream. The distinguishing characteristic of each member of a family is the ratio of the volume in the reservoir to the average flow volume in the downstream channel. Thus it may be seen that to predict the peak flow of the floodwave at a downstream

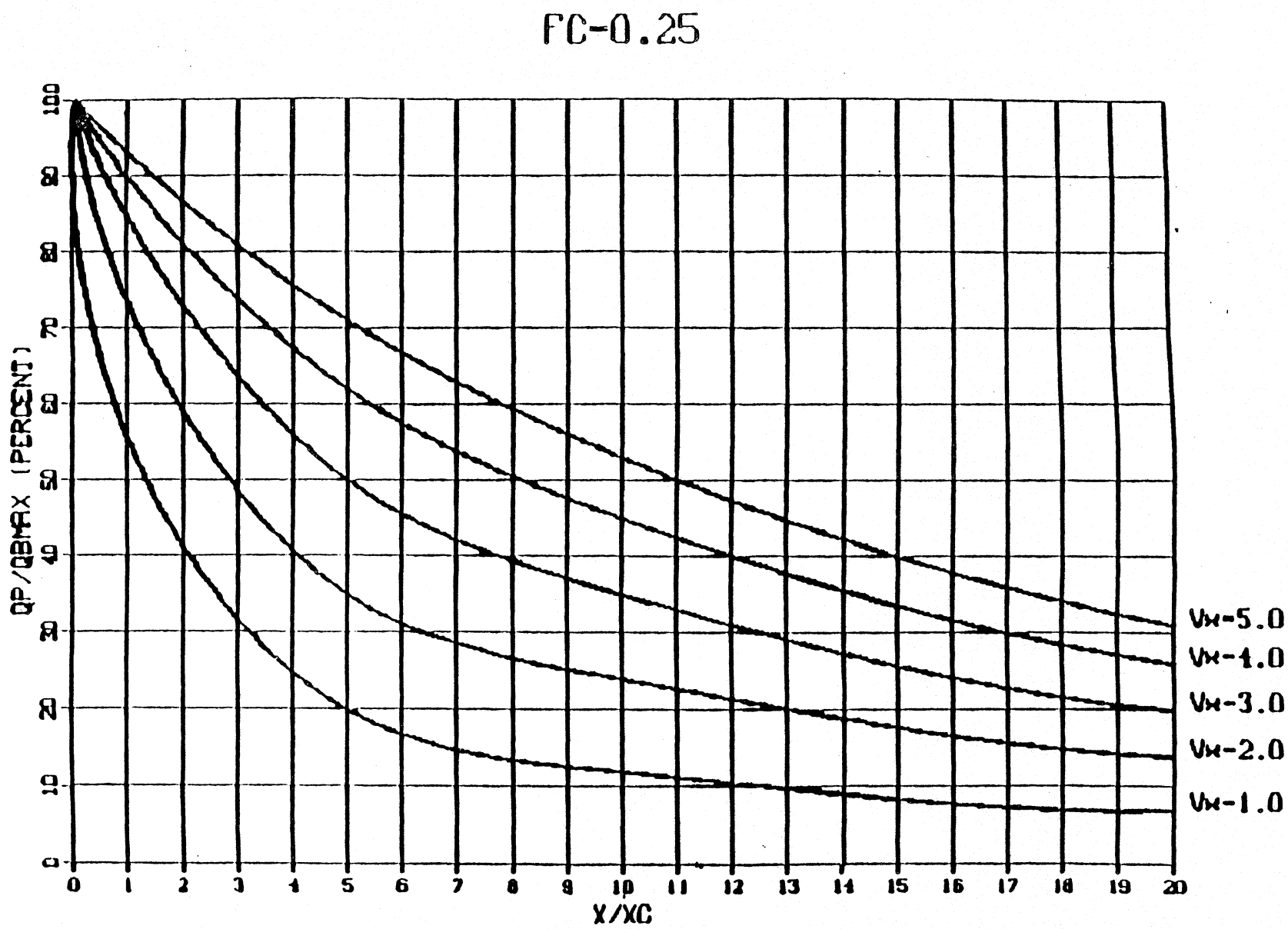

Figure 11. Simplified Routing Curves for F_c = 0.25.

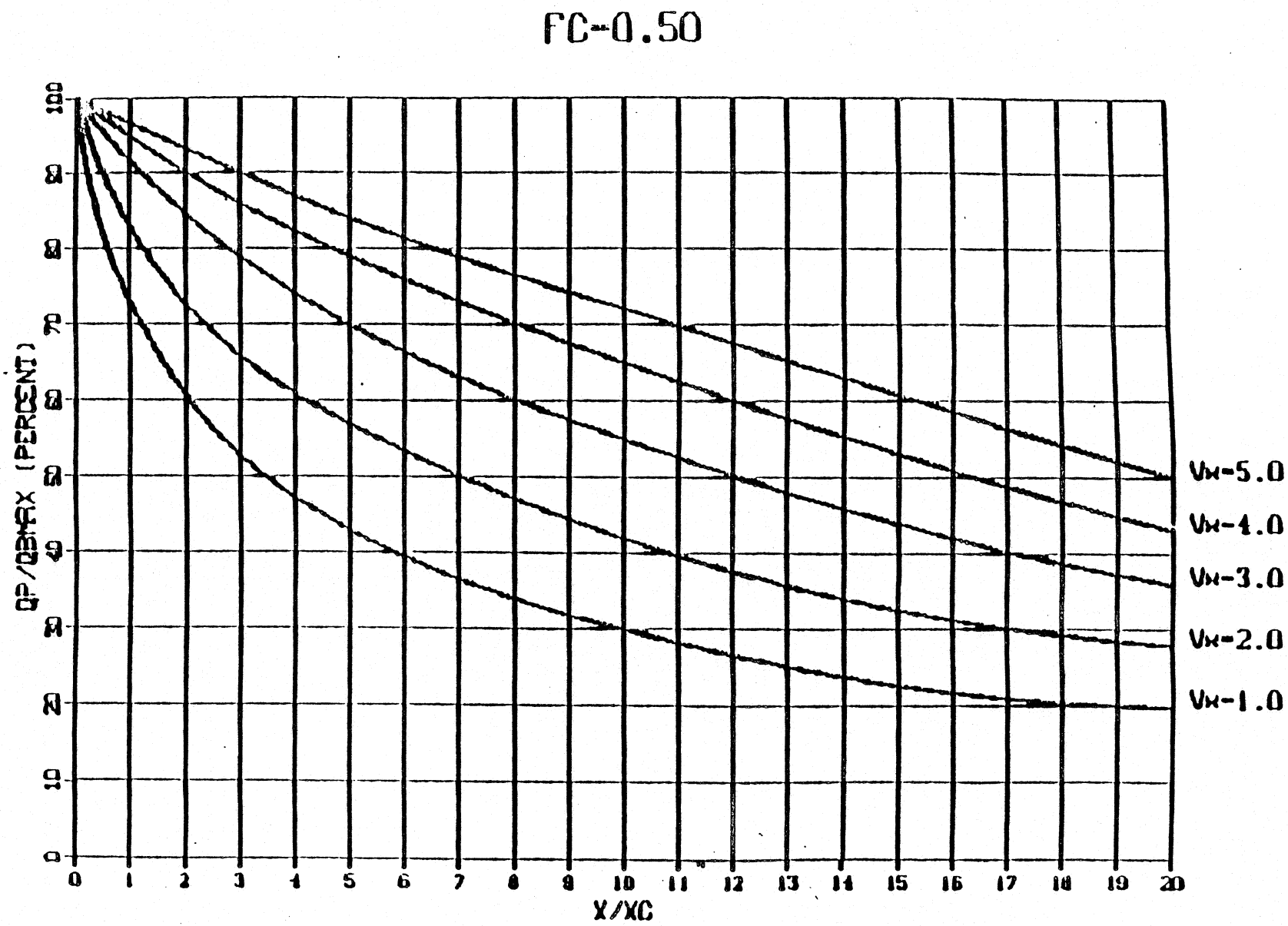

Figure 12. Simplified Routing Curves for F_c = 0.50.

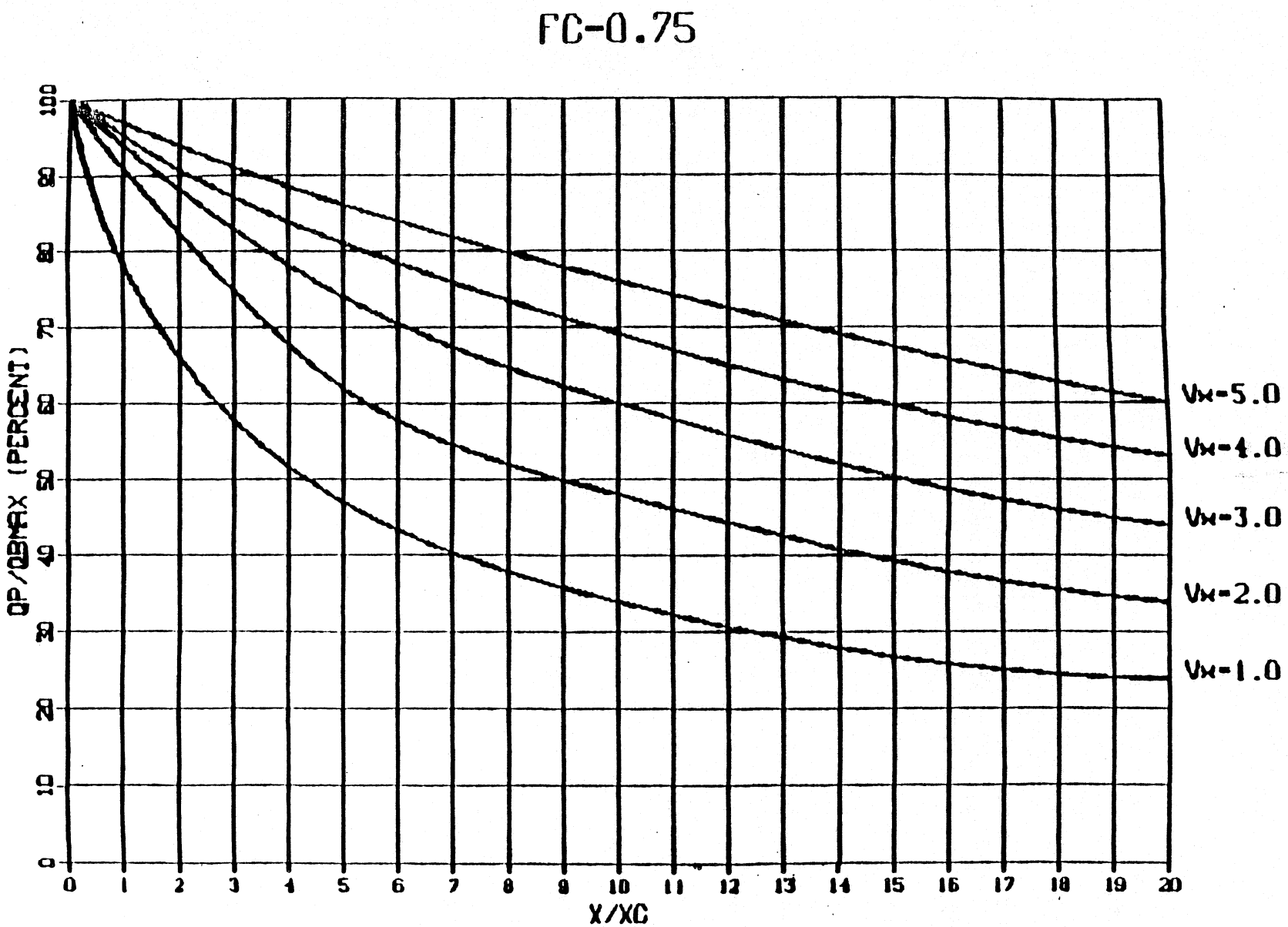

Figure 13. Simplified Routing Curves for F_c = 0.75.

point, the desired distinguishing characteristic of the curve family and member must be determined. This determination is based on the calculation of the Froude number and the volume ratio parameter. To specify the distance in dimensionless form, the distance parameter must also be computed.

The distance parameter (X_c) is calculated using Eq. (78) as follows:

$$X_c \text{ (ft)} = \frac{(\bar{m}+1)}{\bar{K}} \frac{VOL_r}{H_d^{\bar{m}+1}} \frac{6}{1 + 4\,(0.5)^{\bar{m}+1}} \tag{78}$$

where: VOL_r = volume in reservoir (cubic ft)

$\bar{K}$ & $\bar{m}$ = average channel geometry fitting coefficients

H_d = height of dam (ft)

Within the distance (X_c) in the downstream reach, the floodwave attenuates such that the depth at point X_c is h_x (see Fig. 14), which is a function of the maximum depth (h_{max}). The average depth ($\bar{h}$) in this reach is:

$$\bar{h} = \frac{h_{max} + h_x}{2} = \theta\, h_{max} \tag{79}$$

where θ is an empirical weighting factor that must be determined iteratively. The starting estimate for θ is 0.95.

The average hydraulic depth (D_c) in the reach is given by Eq. (80) as follows:

$$D_c = \frac{\theta\, h_{max}}{m+1} \tag{80}$$

The average velocity in the reach is given by the Manning equation, i.e.,

$$V_c = \frac{1.49}{n} S^{1/2} \left(D_c\right)^{2/3} \tag{81}$$

where S is the slope of the channel from the dam to the routing point.

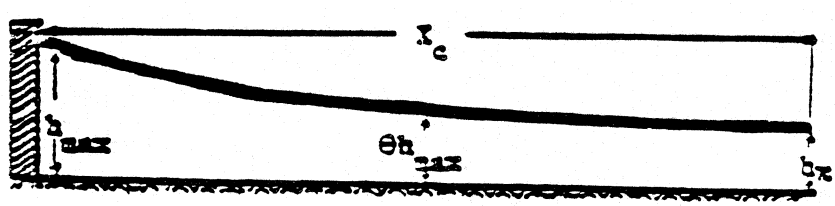

Figure 14. Attenuation of depth downstream of dam.

The average velocity (V_c) and hydraulic depth (D_c) are substituted into Eq. (82) to determine the average Froude number (F_c) in the reach as follows:

$$F_c = \frac{\bar{V}_c}{\sqrt{gD_c}} \tag{82}$$

where: $g = 32.2$ ft/sec^2 (acceleration of gravity).

The dimensionless volume parameter (V^*) that identifies the specific member of the curve family for the computed Froude number is the ratio of the reservoir storage volume to the average flow volume within the X_c reach. The average cross-sectional area of flow (A_c) is given by Eq. (83) as follows:

$$A_c = \bar{K}(\theta h_{max})^{\bar{m}} D_c \tag{83}$$

The volume parameter (V^*) is determined by dividing the average flow volume (A_cX_c) into the reservoir storage volume (VOL_r), i.e.,

$$V^* = \frac{VOL_r}{A_cX_c} \tag{84}$$

With the values of F_c and V^*, the specific curve (Fig. 11-13) can be used (interpolation may be necessary) to determine the routed discharge. The ordinate of the routing curve at $X^* = 1$ is the ratio of the peak flow (Q_p) at X_c to $Q_{b_{max}}$. Knowing Q_p, the stage (h_x) at X_c may be determined using Eq. (75) with the average channel fitting coefficients. The value of θ is checked by rearranging Eq. (79), i.e.,

$$\Theta = \frac{h_{max} + h_x}{2\ h_{max}} \tag{85}$$

If there is a significant difference in the new value of θ from the initial estimate of θ (e.g., ±5%), Eqs. (80)-(84) are recalculated and the new value of θ rechecked. Generally, within two iterations the value for θ will converge.

The distance(s) downstream to the forecast point(s) are non-dimensionalized using the following:

$$X_i^* = \frac{X_i}{X_c} \tag{86}$$

where X_i is the downstream distance to the ith forecast point, $i = 1,2,3,\ldots$ The peak flow at X_i is determined from the proper family of routing curves and the ordinate of the specific V^* curve at X_i^*. Multiplying the

value of this ordinate by $Q_{b_{max}}$ produces the peak flow (Q_p) at X_i miles downstream of the dam.

The time of occurrence of the peak flow at a selected cross section is determined by adding the time of failure to the peak travel time from the dam to that cross-section. The travel time is computed using the kinematic wave velocity which is a known function of the average flow velocity throughout the routing reach. The times of first flooding and "de-flooding" of a particular elevation at the cross section may also be determined.

The time of travel for the floodwave to X_i is computed by first calculating the reference flow velocity at the midpoint between the dam and X_i. The user must determine, from the routing curve, the peak flow ($Q_{x/2}$) at ($X_i/2$) miles downstream of the dam. This flow is multiplied by the factor ($0.3 + \bar{m}/10$) and substituted into Eq. (87) to find the reference depth (h_{ref}). Thus,

$$h_{ref} = \left(\frac{Q}{a}\right)^b \tag{87}$$

The reference hydraulic depth is given by Eq. (88), i.e.,

$$D_{x_i} = \frac{h_{ref}}{m+1} \tag{88}$$

The reference flow velocity (V_{x_i}) in ft/sec is given by the Manning equation, i.e.,

$$V_{x_i} = \frac{1.49}{n} S^{1/2} \; D_{x_i}^{2/3} \tag{89}$$

This value for V_{x_i} is substituted into the wave celerity equation (Eq. (90)) to find the wave speed (c) in mi/hr, i.e.,

$$C = 0.682 \; V_{x_i} \left[5/3 - 2/3 \left(\frac{\bar{m}}{\bar{m}+1}\right)\right] \tag{90}$$

The time to peak is then given by Eq. (91) as follows:

$$t_{p_i} = t_f + \frac{X_i}{C} \tag{91}$$

where: t_p = time (hr) of peak occurrences

t_f = time (hr) of failure for dam

To compute the peak depth at mile X_i, K and m coefficients are fitted for that cross-section by substituting the specific depths and topwidths at

mile X_i into Eqs. (72)-(74). Eq. (75) is used to find the peak depth (h_{x_i}) at mile X_i.

The SMPDBK allows the option to determine the time at which flooding commences and/or the time at which it ceases. To do this, a flow rate (Q_f) that corresponds with flood depth at the cross-section is computed as follows:

$$Q_f = a\ h_f^{\ b} \tag{92}$$

where: h_f = flood depth
and a and b are defined by Eqs. (76)-(77) using the K and m coefficients fitted for the cross-section at mile X_i.

This value for Q_f is substituted into Eq. (93) to determine the time to flooding (t_{fld}) as follows:

$$t_{fld} = t_{p_i} - \left(\frac{Q_{p_i} - Q_f}{Q_{p_i} - Q_o}\right) t_f \tag{93}$$

where: t_{p_i} = the time (hr) to peak calculated in Eq. (91)
t_f = the time (hr) of failure for the dam, and
Q_o = the flow (spillway/turbine/overtopping) other than flow.

To determine the time flooding ceases, t_d, the value of Q_f is substituted into the following relation:

$$t_d = t_{p_i} + \left(\frac{24.2\ VOL_r}{Q_{p_i} - Q_o} - t_f\right) \left(\frac{Q_{p_i} - Q_f}{Q_{p_i} - Q_o}\right) \tag{94}$$

where: VOL_r = the reservoir storage volume (ac-ft).

To route the peak flow downstream to cross-sections 3,4,..., the <u>distance-weighted</u> average cross-section must be determined between the dam and the routing point and new $\bar{K}$ and $\bar{m}$ parameters must be fitted to this average cross section. The distance-weighted average cross section may be determined as follows:

For each depth (h_i), the distance weighted topwidth ($\bar{B}_i$) is given by the relation:

$$\bar{B}_i = \frac{\frac{(B_{i,1} + B_{i,2})}{2}(X_2 - X_1) + \ldots + \frac{(B_{i,J-1} + B_{i,J})}{}(X_J - X_{J-1})}{(X_J - X_1)} \tag{95}$$

where: h_i = the ith depth, $i = 1,2,3 \ldots I$ (number of topwidths per cross-section

$B_{i,j}$ = the ith topwidth (corresponding to the ith depth h_i) at the jth cross-section where $j = 1,2,3, \ldots J$ (number of cross-sections)

$\bar{B}_i$ = the weighted i^{th} topwidth

X_j = the downstream distance to the jth cross-section.

The table of values produced by defining a distance-weighted topwidth ($\bar{B}_i$) for each depth (h_i) may then be used for fitting a single equation of the form $B = \bar{K}h^{\bar{m}}$ to define the prismatic channel geometry. The fitting coefficients $\bar{K}$ and $\bar{m}$ may be computed using the least squares algorithm given in Eqs. (72)-(74).

With these weighted average $\bar{K}$ and $\bar{m}$ coefficients, the peak depth is recomputed at the dam using new routing parameters from Eqs. (79)-(84). The flow may then be routed to cross-section 3,4,.... by following the procedure given above.

4.5 Model Testing and Limitations

In both real-time forecasting and disaster preparedness planning, there is a clear need for a fast and economical method of predicting dam-break floodwave peak stages and travel times. The SMPDBK model fills this need, producing such predictions quickly, inexpensively and with reasonable accuracy. For example, in test analyses of the Teton and Buffalo Creek dam failures where the progression of the floodwave was not affected by backwater, approximating the channel as a prism, calculating the maximum breach outflow and stage at the dam, defining the routing parameters, and evaluating the peak stage and travel time to the forecast points required less than 20 minutes of time with the aid of a non-programable hand-held calculator while the average error in forecasted peak flow and travel time was 10-20% with stage errors of approximately 1 ft. Furthermore, comparisons of SMPDBK model results with DAMBRK model results from test runs of theoretical dam breaks show the simplified model produces average errors of 10% or less. The authors had the advantages, however, of prior experience with the model and possession of all required input data, the collection of which consumes precious warning response time in a dam-break emergency.

The SMPDBK Model can be a very useful tool in preparing for and during a dam failure event, however, the user must keep in mind the model's limitations (Fread 1981). First of all, as with all dam breach flood routing models, the validity of the SMPDBK model's prediction depends upon the accuracy of the required input data. To produce the most reliable results, the user should endeavor to obtain the best estimates of the various input parameters that time and resources allow. Secondly, because the model assumes normal, steady flow at the peak, the backwater effects created by downstream channel constrictions such as bridge embankments or

dams cannot be accounted for and the model will predict peak depths upstream of the constriction that may be substantially lower than those actually encountered, while peak depths downstream of the constriction may be over predicted. Finally, because the "slowing down" of the floodwave caused by temporary off-channel dead storage is not accounted for by the model, the predicted time to peak at a certain point may be somewhat shorter than the actual time to peak. Recognizing these limitations and exercising good engineering judgment, the SMPDBK model may provide useful dam break flood inundation information with relatively small expense of time and computing resources.

5. SUMMARY AND CONCLUSIONS

Three NWS models for predicting the flooding due to dam failures were presented. The Breach Model can aid the hydrologist/engineer in determining the properties of the piping or overtopping initiated breach of an earthen dam. This information can be used in conjunction with historical breach data to create the dam breach hydrograph and route it through the downstream channel-valley using the complex DAMBRK Model or the simplified SMPDBK Model. The choice of either the DAMBRK or SMPDBK model is influenced by the available time, data, computer facilities, modeling experience, and required accuracy for each dam break analysis. Complexities in the downstream channel valley such as highway/railway embankment-bridges, significant channel constrictions, levee overtopping, flow volume losses, downstream dams, weirs, lakes require the DAMBRK Model to be used rather than the SMPDBK Model since latter model ignores such factors.

Notwithstanding the capabilities of state-of-the-art models (BREACH, DAMBRK, SMPDBK) the accuracy of the predicted magnitude and timing of downstream flood inundation can be subject to significant error (two feet or more in the crest profile) due to inaccuracies in the following: 1) the reservoir inflow computed from hydrologic precipitation-runoff models; 2) the breach characteristics; 3) the downstream cross-section properties; 4) the estimated flow resistance coefficients; 5) the neglected effects of transported debris of flow resistance and blockage of constricted cross sections; 6) the neglected infiltration and detention storage losses of flood volume; 7) the neglected sediment transport effects on bottom elevation and flow resistance of the downstream channel-flood plain and 8) the highly turbulent flows and complex flow patterns not adequately described by one-dimensional flow equations.

6. REFERENCES

Amein, M., and C.S. Fang, 1970. Implicit flood routing in natural channels. Journal of Hydraulics Division, ASCE, 96, HY12, December, pp. 2481-2500.

Blanton, J.O. III, 1977. Flood plain inundation caused by dam failure. Proceedings of the Dam-Break Flood Routing Workshop, Water Resources Council, pp. 47-64.

Brown, R.J., and D.C. Rogers, 1977. A simulation of the hydraulic events during and following the Teton Dam failure. Proceedings of the Dam-Break Flood Routing Workshop, Water Resources Council, pp. 131-163.

Chow, V.T., 1959. Open-Channel Hydraulics. McGraw-Hill Book Co., New York, pp. 179-188.

De Saint-Venant, Barre, 1871. Theory of unsteady water flow, with application to river floods and to propagation of tides in river channels. Acad. Sci. (Paris) Comptes rendus, 73, pp. 237-240.

Fread, D.L., and T.E. Harbaugh, 1973. Transient hydraulic simulation of breached earth dams. Journal of Hydraulics Division, ASCE, 99, HY1, January, pp 139-154.

Fread, D.L., 1974a. Numerical properties of implicit four-point finite difference equations of unsteady flow. NOAA Tech. Memo. NWS HYDRO-18, U. S. Dept of Commerce, NOAA, National Weather Service, 38 pp.

Fread, D.L., 1974b. Implicit dynamic routing of floods and surges in the Lower Mississippi. Presented at AGU National Meeting, Washington, D. C., April, 26 pp.

Fread, D.L., 1976. Flood routing in meandering rivers with flood plains. Proceedings, Rivers '76, Third Annual Symposium of Waterways, Harbors and Coastal Eng. Div., ASCE, Vol. I, August, pp. 16-35.

Fread, D.L., 1977. The development and testing of a dam-break flood forecasting model. Proceedings of the Dam-Break Flood Routing Workshop, Water Resources Council, pp. 164-197.

Fread, D.L., 1980. Capabilities of NWS model to forecast flash floods caused by dam failures. Proceedings of the Second Conference on Flash Floods, American Meteorological Society, pp. 171-178.

Fread, D.L., 1981. Some limitations of dam breach flood routing models. Preprint, ASCE Fall Convention, St. Louis, Missouri, October 26-30, 1981.

Fread, D.L., 1984a. DAMBRK: The NWS dam-break flood forecasting model. Hydrologic Research Laboratory, National Weather Service, Silver Spring, Maryland, 56 pp.

Fread, D.L., 1984b. A breach erosion model for earthen dams. Proceedings of the Specialty Conference on Delineation of Landslide, Flash Flood, and Debris Flow Hazards in Utah, 30 pp., Utah State University, Logan, Utah.

Johnson, F.A., and P. Illes, 1976. A classification of dam failures. Water Power and Dam Construction, December, pp. 43-45.

Lee, K.L., and J.M. Duncan, 1975. Landslide of April 25, 1974 on the Mantaro River, Peru. National Academy of Sciences, Washington, D.C., 72 pp.

Middlebrooks, T.A., 1952. Earth-dam practice in the United States. Centennial Transactions, ASCE, Paper No. 2620, pp. 697-722.

Morris, H.M., and J.M. Wiggert, 1972. Applied Hydraulics in Engineering. The Ronald Press Co., New York, pp. 69-70, 290, 451-452, 460.

Ponce, V.M., and A.J. Tsivoglou, 1981. Modeling of gradual dam-breaches. Journal of Hydraulics Division, American Society of Civil Engineers, 107(HY6), pp. 829-838.

Ray, H.A., L.C. Kjelstrom, E.G. Crosthwaite, and W.H. Low, 1976. The flood in southeastern Idaho from Teton Dam failure of June 5, 1976. Open File Report, U.S. Geological Survey, Boise, Idaho.

Smart, G.M., 1984. Sediment transport formula for steep channels. Journal of Hydraulics Division, American Society of Civil Engineers, 110 (No. 3), pp. 267-276.

Spangler, M.G., 1951. Soil Engineering. International Textbook Co., Scranton, Pennsylvania, pp. 321-323.

Venard, J.K., 1954. Elementary Fluid Mechanics. John Wiley and Sons, New York, pp. 312-325.

Wetmore, J.N. and D.L. Fread, 1984. The Simplified Dam Break Flood Forecasting Model for Desk-Top and Hand-Held Microcomputers. Office of Hydrology, National Weather Service, Silver Spring, Maryland.

SOME LIMITATIONS OF DAM-BREACH FLOOD ROUTING MODELS

KEY WORDS: Breach, Dams, Failure, Floods, Flood routing, Forecasting, Models, Reservoirs, Rivers

ABSTRACT: During the last decade some major improvements were made in models which predict the changing celerity and magnitude of a flood wave emanating from a breached (failed) dam and propagating through the downstream valley. Such improvements included consideration of the breach dynamics, use of the one-dimensional equations of unsteady flow to route the flood wave through the downstream valley, and consideration of the effects of downstream bridge-embankments, dams, and dead storage areas on the propagating wave. Notwithstanding this, the predictive accuracy of such models can be subject to significant error (two feet or more in the crest profile) due to inaccuracies in the following: 1) the reservoir inflow computed from hydrologic precipitation-runoff models; 2) the breach dynamics which are estimated from previous dam failures; 3) the downstream cross-section properties; 4) the estimated flow resistance coefficients; 5) the neglected effects of transported debris on flow resistance and blockage of constricted cross sections; 6) the neglected infiltration and detention storage losses of flood volume; 7) the neglected sediment transport effects on bottom elevation and flow resistance of the downstream channel-flood plain; and 8) the highly turbulent flows and complex flow patterns not adequately described by one-dimensional flow equations.

REFERENCE: Fread, Danny L., "Some Limitations of Dam-Breach Flood Routing Models," Preprint, ASCE Fall Convention, St. Louis, Missouri, October 26-30, 1981.

SOME LIMITATIONS OF DAM-BREACH FLOOD ROUTING MODELS[a]

By Danny L. Fread[1], M. ASCE

INTRODUCTION

A flood which is caused by the failure (breach) of a dam is much larger than any of the previous floods that originated from the runoff of rainfall and/or snowmelt; and, its consequences are often catastrophic if human development exists downstream of the dam. Our ability to predict the magnitude and timing of the dam-breach flood is of paramount importance for purposes of: 1) planning and decision making concerning dam safety, 2) contingency evacuation planning, and 3) real-time flood forecasting.

During the last decade some major improvements were made in the mathematical techniques (models) used to predict the continually changing magnitude and velocity of the dam-breach flood wave. Advancing beyond the simple, classical mathematical treatment of dam-breach waves of St. Venant (7), Ritter (22), and Schoklitsch (24), models were developed which by using simple storage routing concepts considered the effects of the downstream valley friction and storage volume on the wave's propagation, e.g., HEC (11), Snyder (25), Keefer and McQuivey (14), Keefer and Simons (15), and Brevard and Theurer (2).

Other models requiring large, high-speed computers were developed which utilized the more complex and accurate one-dimensional equations of unsteady flow for routing the dam-breach flood wave through the downstream valley. Included among these were Cunge (6), Balloffet, et al. (1), Price and Garrison (19), Price, et al. (20), Thomas (26), Fread (8,9), Rajar (21), and Chen and Armbruster (3). Also, models of this type but considerably simplified for use with desk calculators were developed by Sakkas and Strelkoff (23) and Wetmore and Fread (28). Some models (9,15) also considered the effects of other dams and/or bridge-embankments in the downstream valley.

---

[a]Presented at the October 26-30, 1981 ASCE Fall Convention, St. Louis, Missouri.

[1]Senior Research Hydrologist, Hydrologic Research Laboratory, National Weather Service, NOAA, 8060 13th St., Silver Spring, MD.

Most of the models relied on the classical methods of St. Venant and Schoklitsch to determine the magnitude of the wave at its point of origin, the breached dam. Simple storage concepts were used to determine its assumed triangular shape, and the formation of the breach was assumed to take place instantaneously. The models of HEC (11), Price and Garrison (19), Fread (8,9), and Wetmore and Fread (28) attempted to treat the breach formation for an earthen dam more realistically by approximating its dynamic development. Also, the integrated effects of reservoir inflow and storage characteristics and the downstream valley backwater on the magnitude and shape of the dam-breach wave were considered by Fread (8,9) and HEC (11).

Notwithstanding the improvements in the dam-breach flood models that have evolved over the last decade, several sources of error still limit the accuracy of the most advanced models to predict the magnitude and time of occurence of the flooding at any specified location downstream of the dam. The errors are due to our inability at the present time to accurately answer the following questions: When will a dam fail? When and to what extent will a dam be overtopped? What is the size, shape, and time of formation of the breach? What is the storage volume and hydraulic resistance of the downstream channel-valley? Will debris (uprooted trees, etc.) and sediment (entrapped behind the dam and in the stream channel) transported by the flood wave significantly affect its propagation? Can the wave be approximated adequately by the one-dimensional flow equations?

MODEL LIMITATIONS

Comparisons have been made of several dam-breach flood routing models (3,8,9,14,16,21,26,28) with observations from some actual dam-breach floods, e.g., the Teton, Toccoa, Laurel Run, Buffalo Creek floods. The comparisons indicate that even the most advanced models have limitations in the accuracy of the predicted flood crest profiles. Errors are usually one to two feet or more for all of the models, even when the actual breach geometry is specified as input to the models. The factors which can cause errors in the prediction accuracy of the most advanced dam-breach flood models are several.

Dam Failure. - Many times the most difficult prediction is whether or not the dam will fail. Certainly in cases where dam failure is caused by piping, seepage, slides, or seismic disturbances prediction of if and when a dam will fail is not within the capability of the models. Such causes of failure constitute somewhere between 40 and 50 percent of the total number recorded failures (12,17). Failures caused by overtopping of the dam due to inadequate spillway capacity total about 30 to 35 percent of the dam failures with the remaining 15 to 30 percent classified as miscellaneous causes.

Although overtopping can be predicted it is subject to error due to the limitations of the hydrologic model chosen to predict the inflow to the reservoir from rainfall and/or snowmelt. Errors in observed or predicted areal precipitation (the primary input to hydrologic models) is considerable. Also, the use of statistically generated probable maximum precipitation or probable maximum runoff is beset with considerable uncertainties.

Notwithstanding the errors in the inflow to the reservoir, the determination of the extent of overtopping (depth of flow over the crest and the duration of the overtopping flow) which is required for breaching to occur is not an inherent feature of the dam-breach flood models. Some attempts were made to develop erosion models for earthen dams (5,10) however, these were not very adequate. A recent effort by Ponce and Tsivoglou (18) may hold some promise although the difficulties of nonhomogeneity and lack of detailed data for most earthen dams may limit the applicability of this approach. Almost all of the dam-breach models do not address the question of when failure from overtopping commences although a few (8,9,11) utilize a specified depth of overtopping flow to start the formation of the breach.

Breach Characteristics. - A significant source of error is the size, shape, and time of formation of the breach. The few models (8,9,11) which attempt to include the dynamic characteristics of the breach require the user to specify the terminal width, shape and a time of formation which is assumed linear. This information must be obtained from historical dam failures and then applied to the dam being modeled using sound engineering judgement by considering the type of dam (earthfill, rockfill, concrete gravity or arch), the dam's material properties, the cause of failure, the height of the dam, the reservoir volume, and any other special characteristics which might affect the breach formation. An erosion model (18) may in certain instances increase the accuracy of the breach prediction.

Of the three breach characteristics, the shape is least important. Time of formation becomes increasingly insignificant as the reservoir volume becomes very large. The peak discharge (Q_p) emanating from a time-dependent breach can be approximated (28) as:

$$Q_p = 3.1\ W\ [C/(\tau + C/\sqrt{H})]^3 \qquad (1)$$

where: $C = 23.4\ S_a/W$ (2)

in which W is the average breach width (ft), τ is the time (hrs) of breach formation (the time in which the flow passage is enlarging), H is the height (ft) of the dam, and S_a is the reservoir surface area (acres) at the dam crest. Using Eq (1) the peak discharge can be determined for various values of τ, and the sensitivity of Q_p to errors in the time of failure can be determined readily. For example

if, τ=1.5 hr, W=150 ft, S_a=1936 acres, H=262 ft which approximates the Teton dam failure, values of Q_p as a function, of τ are given in Table 1.

Table 1. - Peak Discharge (Q_p) Variations with Time of Failure (τ)

Q_p(cfs)	τ (hr)	Error(%)
1,977,589	0.0	+ 26.1
1,756,766	0.75	+ 12.1
1,567,817	1.5	0.0
1,263,868	3.0	- 19.3

If S_a were 193,600 acres, the error for τ=0. would only be +.2%; whereas, if S_a were only 193.6 acres, a τ=0. would produce a much larger error in Q_p of +487.5%.

Eq (1) can also be used in a similar manner to acertain the effect of error in the average breach width (W). This is a most important source of error. It is most difficult to determine for concrete gravity dams, while its probable value for concrete arch dams is near the full width of the dam. For earthfill dams there is evidence (9,12) that W is somewhat correlated to the dam height (H), i.e.,

$$0.5\ H \leq W \leq 3\ H \qquad (3)$$

At this time the best analysis that can be achieved with such uncertainties in the breach properties is to make two predictions, first using a maximum probable W and minimum probable τ and then using a minimum probable W and maximum probable τ. The first produces a maximum expected downstream flooding while the second produces a minimum expected flooding. This is illustrated in Fig. 1 in which the peak discharge profile is shown for four different conditions. The two lower profiles are associated with the approximated actual downstream valley (Teton-Snake River) dimensions while the two upper profiles are for a narrow canyon (approx. 1100 ft wide) extending throughout the 60 mile downstream reach.

Four properties of dam-breach floods are illustrated by the profiles shown in Fig 1. First, in each case significant differences in the predicted peak flow in the vicinity of the dam are significantly reduced as the flood propagates downstream. Second, the differences are more rapidly reduced for the actual valley (which is very wide and flat having a maximum inundated width of about nine miles) than for the narrow canyon. Third, the peak discharge is rapidly attenuated as the flood advances downstream, and fourth, the peak flow is attenuated more in the wide valley than in the narrow canyon. These general properties are applicable to dam-failure floods; however, the degree of trend of the first three becomes less

as the reservoir volume increases. This is due to the fact that attenuation of the peak discharge becomes less as the volume of the flood wave increases in relation to a fixed storage volume of the downstream valley.

The first principle, the dampening of initial differences in the peak discharge as the flood propagates downstream, enables prediction accuracy to increase in the downstream direction.

The errors in the routed discharge may be transformed into errors in flow depth (h), which are more meaningful, by either using actual depth-discharge rating curves or in the following way. Let the average cross section of the downstream channel-valley be described as:

$$B = kh^m \tag{4}$$

$$A = \frac{kh^{m+1}}{m+1} \tag{5}$$

in which B is the width, A is the cross-sectional area, and k and m are fitting coefficients (see Fig. 1). Then from the Manning Equation,

$$h = (Q/a)^b \tag{6}$$

where: $$a = 1.49\ S^{1/2}\ k/[n(m+1)^{5/3}] \tag{7}$$

$$b = 3/(3m + 5) \tag{8}$$

in which S is the channel-valley slope and n is the Manning roughness coefficient. Using Eq (6), the following ratio may be developed:

$$h_e/h = (Q_e/Q)^b \tag{9}$$

in which the subscript (e) designates quantities possessing some error. Since the fitting coefficient m is present in Eq (9), the general shape of the cross section as determined by m as shown in Fig 1. must be considered. An expression for the percent error in depth (E_h) may be developed in terms of the ratio h_e/h, i.e.,

$$E_h = 100\ (h_e/h - 1) \tag{10}$$

and a similar expression for the percent error in discharge (E_Q), i.e.,

$$E_Q = 100\ (Q_e/Q - 1) \tag{11}$$

Furthermore, the error term (E_h) may be plotted as shown in Fig. 2 against the percent error in the discharge (E_Q) for a range of cross-sectional shapes. Fig. 2 shows that the relationship between E_h and

E_Q is nonlinear. For example, if E_Q = +50% and m=2.0, E_h is determined from Fig. 2 to be about 9.5%. The tendency for an error in flow to yield a smaller error in depth is characteristic of all curves in Fig. 2; this is helpful in promoting prediction accuracy of dam-breach flood routing models. Fig. 2 is based on steady flow, therefore it is strictly applicable only for discharge errors existing after flood routing computations have been performed.

Cross-Sectional Area. - Errors to some extent are always present in the description of the cross-sectional properties (width and area as a function of flow depth) of the downstream channel-valley. These are: errors in sampling, errors in field measurements, and errors inherent in the assumed linear variation between contour intervals of topographic maps. The first two errors are associated with the use of field measured cross-sections while all three errors can occur when using topographic maps for determing cross-sections for a dam-breach flood routing model.

The cross-sectional volume error due to the sampling interval can be eleminated if planmetered surface areas between two selected cross-sections are used to compute the properties of an average section placed between the selected sections. The width ($\bar{B}$) of the average section can be determined from a distance-weighting relationship, e.g.,

$$\bar{B} = (2\ S_c - B_1 \Delta x_1 - B_2 \Delta x_2)/(\Delta x_1 + \Delta x_2) \qquad (12)$$

in which S_c is the surface area contained between contour lines of the same elevation and located on opposite sides of the valley and bounded on the ends by the selected sections designated by subscripts 1 and 2. Also, Δx_1 and Δx_2 are the respective distances (ft) from the first end section to the location of the average section, and from the average section to the second end section. Field measured properties of the cross section within the banks of the channel are needed to reduce errors in this portion of the cross-section since topographic maps do not extend below the typical water level. However, in many cases peak dam-breach flows would have small errors since the in-bank area is a small percentage of the flooded over-bank area.

The error associated with the assumed linear variation between contour intervals (Δh) is illustrated in Fig. 3. An approximate expression for the ratio of A_e/A is given by the following:

$$A_e/A = 1.0 + 0.5\ \bar{P}\ I(m+1)\ (\Delta h/h_p)^{m+1} \qquad (13)$$

where: $$\bar{P} = \frac{1}{2N} \sum_{i=1}^{N} e_i = \frac{1}{2N} \sum_{i=1}^{N} \Delta A_i / A_i' \qquad (14)$$

$$I = \sum_{i=1}^{N} [i^m - (i-1)^m] \tag{15}$$

$$N \cong h_p/\Delta h \tag{16}$$

in which Δh is the contour interval, h_p is the maximum depth in the section from Eqs (1) and (6), ΔA_i and A'_i are defined in Fig. 3, and m is defined in Eq (4). A realistic maximum value for the ratio (A_e/A) can be obtained from Eq (13) by using $\overline{P} = 0.4$. From Eq (13) it is seen that larger values of A_e/A and therefore larger errors in the cross-sectional area are directly proportional to m and to the term $(\Delta h/h_p)^{m+1}$. The latter term represents the ratio of contour interval to peak depth. Therefore as the contour interval increases, the error increases. Also, the error increases as the ratio $(\Delta h/h_p)$ increases and since h_p is related to the dam height (H) through Eqs (1) and (16), the error increases as the ratio $\Delta h/H$ increases. The error is related to the cross-sectional shape by the exponent m in the term $(\Delta h/h_p)^{m+1}$.

Using Eq (6), the following ratio may be developed:

$$h_e/h = (A_e/A)^{5b/3} \tag{17}$$

and an expression for percent error in the cross-sectional area (E_A) is given by:

$$E_A = 100\ (A_e/A - 1) \tag{18}$$

The error term E_A may be plotted as shown in Fig 4. against the percent error (E_A) for a range of channel shapes. The relationship is linear for m=0 and becomes more nonlinear as m increases. As m increases the errors become more damped, i.e., if E_A = +50% and m = 2.0, E_h is only +20%.

Flow Resistance Coefficients. - Errors in the flow resistance coefficients are due to such factors as: (1) dam-breach flows which are relatively large occur in previously unflooded areas; thus previous flows are not very useful in computing the flow resistance coefficients; (2) the inundated area often contains more flow resistance in the form of trees, houses, etc. which are not typical of the resistance encountered by most normal floods; (3) the flood-plain flow short-circuits across a meandering channel (4) causing some additional flow resistance; (4) debris (trees, etc.) uplifted and transported by the flood may become impinged on permanent obstructions causing additional undefined flow resistance; and (5) sediment entrapped behind the dam and released during the failure may slightly reduce the flow resistance when it is deposited on the flood plain (4).

The errors associated with the first two factors may be reduced by using a type of Colebrook-White frictional expression which separately approximates effects of submerged and partially submerged objects on the flow resistance (27). The computed Darcy friction factor (f) can then be changed to the more popular Manning n coefficient by using the relation,

$$n = f^{1/2} h^{1/6} / 10.8 \tag{19}$$

The effect that the total error in the frictional resistance (expressed in terms of the Manning n) has on the flood depth can be obtained by using Eq (6). Thus,

$$h_e/h = (n_e/n)^b \tag{20}$$

An expression for the percent error in the Manning n (E_n) may be developed, i.e.,

$$E_n = 100\ (n_e/n - 1) \tag{21}$$

If E_n is plotted against E_h as shown in Fig. 2 it is apparent that the relationship is nonlinear and that errors in the Manning n (E_n) are dampened when transformed into errors in flow depth (E_h) as was also the case with the errors in flow (E_Q). The extent of dampening is directly proportional to the channel shape or the m coefficient of Eq (9). The error dampening characteristic is beneficial for the prediction accuracy of computed depths.

Errors in the Manning n will also have a significant effect on the kinematic celerity (approximate propagation speed) of the flood wave. Using Eq (20), the following celerity ratio can be developed:

$$c_e/c = (n_e/n)^{2b/3 - 1} \tag{22}$$

Eq (22) indicates that errors in the Manning n will produce damped errors in the wave celerity. For example, if E_n = +50% and m = 1.0 the error in the wave celerity would be only -25%. Also, the influence of the cross-section shape factor(m) is very weak in Eq (22). The error in celerity (E_c) is plotted against the error in the friction (E_n) in Fig. 5.

Debris. - Uprooted trees, demolished houses, cars, fences, and other debris transported by the high velocity flow associated with the dam-breach flood cause unpredictable errors. The debris can increase the frictional resistance coefficients. It may also accumulate at constricted cross sections such as bridge openings where it partially or completely restricts the flow as a temporary dam. This occured during the infamous Johnstown dam-breach flood of 1889. At best, the maximum magnitude of this effect can only be approximated by a dam-breach model (9) which treats the blocked constriction as another downstream dam having an estimated head-

discharge rating which somewhat approximates the gradual flow stoppage and the later possible rapid increase if the debris dam is breached. The errors in dam-breach flow predictions caused by debris dams are not predictable since the occurrance, itself, cannot be predicted.

Volume Losses. - Often in dam-breach floods, where the extremely high flows inundate considerable portions of channel overbank or valley flood plain, a measurable loss of flow volume occurs. This is due to infiltration into the relatively dry overbank material, detention storage losses, and sometimes short-circuiting of flows from the main valley into other drainage basins via canals or overtopping natural ridges separating the drainage basins. Such losses of flow are most difficult to predict; usually they are neglected in the dam-breach models, although the losses can be significant. In the case of the Teton flood where the measured losses amounted to about 25% of the reservoir volume, consideration of the losses (8) decreased the routed peak discharge and depth by 50% and 31%, respectively, at a cross-section which had a shape factor(m) of 0.5 and located 60 miles downstream. The average decrease in peak discharge and depth along the 60 mile reach were about 18% and 7%, respectively.

Sediment Transport. - Sediment entrapped behind a breached dam may be transported along with the breach flow and deposited in the downstream valley. In some cases (4) this can reduce the flow resistance coefficient. Also, degradation of the channel bottom may occur due to the high velocity flow emanating from a breached dam. Degradation increases the cross-sectional area of the channel; however, since the channel area is usually small compared to the flooded overbank area the effect on the total flow would be small.

Complex Flow. - The highly turbulent flow in the reach just downstream of the breached dam may not be adequately described by the equations of one-dimensional flow. Also, dam-breach flow that spreads onto a very wide, flat flood plain is subject to some computational error when treated with one-dimensional routing models. In this case, two-dimensional models (13,29) may provide more accuracy; however, at the present time such models are not sufficiently developed for practical and general application, and are functional primarily as research tools.

CONCLUSIONS

In recent years, significant developments have been made in one-dimensional models to predict the flooding due to breached dams; nevertheless, even the more advanced models are limited in their prediction accuracy. The models, when used to reproduce historical dam-failure floods (3,9,16) in which the breach characteristics (shape, size, time of formation) and/or the breach outflow could be adequately approximated, produced errors of about two feet or more in the profile of the flood crest. When the models are used to predict future dam-breach floods, additional significant errors are introduced through the prediction of the breach characteristics and/or the

breach outflow. Perhaps the greatest error in many applications is determining if indeed a dam will be breached. Other errors in the predicted downstream flooding are due to errors in the downstream cross-sectional volume, estimated flow resistance coefficients, undefined effects of transported debris and sediment, undefined flow volume losses, and complex flows that are not well-suited for one-dimensional flow computations.

The errors associated with the breach characteristics do dampen as the flood propagates downstream, and the degree of dampening depends on the cross-sectional shape and the reservoir volume. Also, the percent error in the computed flow depth is less than the percent error in routed discharge, cross-sectional area, and/or flow resistance. Also, there is a dampening of the error in the wave celerity caused by error in the resistance coefficient. These error properties aid in producing the accuracy that is now achievable with dam-breach flood routing models.

APPENDIX 1. - REFERENCES

1. Balloffet, A., Cole, E. and Balloffet, A.F., "Dam Collapse Wave in a River", Journal of the Hydraulics Division, ASCE, Vol. 100, HY5, pp. 645-665, May 1974.
2. Brevard, J.A., and Theurer, F.D., "Simplified Dam-Break Routing Procedure", Technical Release Number 66, U.S. Dept. of Agriculture, Soil Conservation Service, Engr. Div., 35 pp., 1979.
3. Chen, C. and Armbruster, J.T., "Dam-Break Wave Model: Formulation and Verification", Journal of the Hydraulics Division, ASCE, Vol. 106, HY5, pp. 747-767, May 1980.
4. Chen, Y.H. and Simons, D.B., "An Experimental Study of Hydraulic and Geomorphic Changes in an Alluvial Channel Induced by Failure of a Dam", Water Resources Research, Vol. 15, No. 5, pp. 1183-1188, October 1979.
5. Cristofano, E.A., "Method of Computing Rate for Failure of Earthfill Dams". Bureau of Reclamation, Denver, Colo., April, 1965.
6. Cunge, J.A., "Calcul de Propagation des Ondes de Rupture de Barrage (Computation of Dam-Break Waves)", La Houille Blanche, No. 1, 1970.
7. De Saint-Venant, Barre, "Theory of Unsteady Water Flow, with Application to River Floods and to Propagation of Tides in River Channels", Acad. Science (Paris) Comptes rendus, Vol. 73, pp. 237-240, 1871.
8. Fread, D.L., "The Development and Testing of a Dam-Break Flood Forecasting Model", Proceedings, Dam-Break Flood Modeling Workshop, U.S. Water Resources Council, Washington, D.C., pp. 164-197, 1977.
9. Fread, D.L., "Capabilities of NWS Model to Forecast Flash Floods Caused by Dam Failures", Preprint Volume, Second Conference on Flash Floods, March 18-20, Amer. Meteorological Soc., Boston, Mass., pp. 171-178, 1980.
10. Harris, G.W., and Wagner, D.A., "Outflow from Breached Dams", University of Utah, 1967.

11. Hydrologic Engineering Center (HEC), "Flood Hydrograph Package (HEC-1): Users Manual for Dam Safety Investigation", The Hydrologic Engineering Center, Corps of Engineers, U.S. Army, Davis, Cal., 88 pp., Sept. 1978.
12. Johnson, F.A., and Illes, D.A., "A Classification of Dam Failures", Water Power and Dam Construction, pp. 43-45, Dec., 1976.
13. Katapodes, N., and Strelkoff, T., "Two-Dimensional Shallow Water-Wave Models", Journal of the Engineering Mechanics Division, ASCE, Vol. 105, EM2, pp. 317-334, April 1979.
14. Keefer, T.N., and McQuivey, R.S., "Simplified Routing of Dam Break Waves", Proceedings, IAHR, Vol. 2, San Paulo, Brazil, pp. 325-329, 1975.
15. Keefer, T.N., and Simons, R.K., "Qualitative Comparison of Three Dam-Break Routing Models", Proceedings, Dam-Break Flood Modeling Workshop, U.S. Water Resources Council, Washington, D.C., pp. 292-311, 1977.
16. Land, L.F., "Evaluation of Selected Dam-Break Flood-Wave Models by Using Field Data", U.S. Geological Survey Gulf Coast Hydro Science Center, NSTL Station, Miss., Water-Resources Investigations 80-44, 54 pp., July 1980.
17. Middlebrooks, T.A., "Earth-Dam Practice in the United States", Centennial Transactions, ASCE, Paper No. 2620, pp. 697-722, 1952.
18. Ponce, V.M., and Tsivoglou, A.J., "Modeling Gradual Dam Breaches", Journal of the Hydraulics Division, ASCE, Vol. 107, HY6, Paper No. 16371, June 1981.
19. Price, J.T. and Garrison, J.M., "Floodwaves from Hydrologic and Seismic Dam Failures", Paper presented at ASCE National Water Resources Meeting, January 1973.
20. Price, J.T., Lowe, G.W., and Garrison, J.M. "Unsteady Flow Modeling of Dam-Break Waves", Proceedings, Dam-Break Flood Modeling Workshop, U.S. Water Resources Council, Washington, D.C., pp. 90-130.
21. Rajar, R., "Mathematical Simulation of Dam-Break Flow", Journal of the Hydraulics Division, ASCE, Vol. 104, HY7, pp. 1011-1026, July 1978.
22. Ritter, A., "The Propagation of Water Waves", Ver. Deutsch Ingenieure Zeitschr. (Berlin), Vol. 36, Pt. 2, No. 33, pp. 947-954, 1892.
23. Sakkas, J.G., and Strelkoff, T. "Dam Break Flood in a Prismatic Dry Channel", Journal of the Hydraulics Division, ASCE, Vol. 99, HY12, pp. 2195-2216, Dec., 1973.
24. Schoklitsch, A., "On Waves Created by Dam Breaches", Akad. Wiss. (Vienna) Proc., 126, Pt. 2A, pp. 1489-1514, 1917.
25. Snyder, F.F., "Floods from Breaching of Dams". Proceedings, Dam-Break Flood Modelling Workshop, U.S. Water Resources Council, Washington, D.C., pp. 75-85, 1977.
26. Thomas, W.A., "Calculating and Routing of the Teton Dam-Break Flood", Proceedings, Dam-Break Flood Modeling Workshop, U.S. Water Resources Council, Washington, D.C., pp. 198-227, 1977.
27. Walton, R. and Christensen, B.A., "Friction Factors in Storm Surges Over Inland Areas", Journal of Waterway, Port, Coastal and Ocean Division, ASCE, Vol. 106, WW2, pp. 261-271, May 1980.

28. Wetmore, J.N., and Fread, D.L., "The NWS Simplified Dam-Break Flood Forecasting Model", Proceedings, 5th Canadian Hydrotechnical Conference, Fredericton, Canada, 24 pp., May 1981.
29. Xanthopoulous, T., and Koutitas, C., "Numerical Simulation of a Two-Dimensional Flood Wave Propagation Due to Dam Failure", Journal of Hydraulic Research, IAHR, Vol. 14, No. 4, pp. 321-331, 1976.

APPENDIX 2. - NOTATION

The following symbols are used in this paper:

A = cross-sectional area
A_e = cross-sectional area with error
A_i = cross-sectional area defined in Fig. 3
a = coefficient defined by Eq (7)
B = cross-sectional top width
$\bar{B}$ = cross-sectional top width for average section between two end sections
b = coefficient defined by Eq (8)
C = coefficient defined by Eq (2)
c = kinematic wave celerity
c_e = kinematic wave celerity with error
E_A = percent error in cross-sectional area
E_h = percent error in flow depth
E_n = percent error in Manning n
E_Q = percent error in flow
e_i = error in cross-section
f = Darcy friction factor
H = dam height
h = depth of flow
h_e = depth with error
h_p = depth associated with peak flow at a section
k = fitting coefficient for cross-section (scale factor)
m = fitting coefficient for cross-section (shape factor)
N = integer defined by Eq (15)
n = Manning n
n_e = Manning n with error
$\bar{P}$ = cumulative error ratio for cross-section area
Q = flow
Q_e = flow with error
Q_p = peak flow emanating from breached dam
S = channel-valley slope
S_a = surface area of reservoir at height of dam
S_c = surface area of downstream valley reach between two end sections
W = average width of breach
ΔA_i = cross-sectional area (error)
Δh = contour interval
Δx = distance between end section and average section
τ = time for breach formation

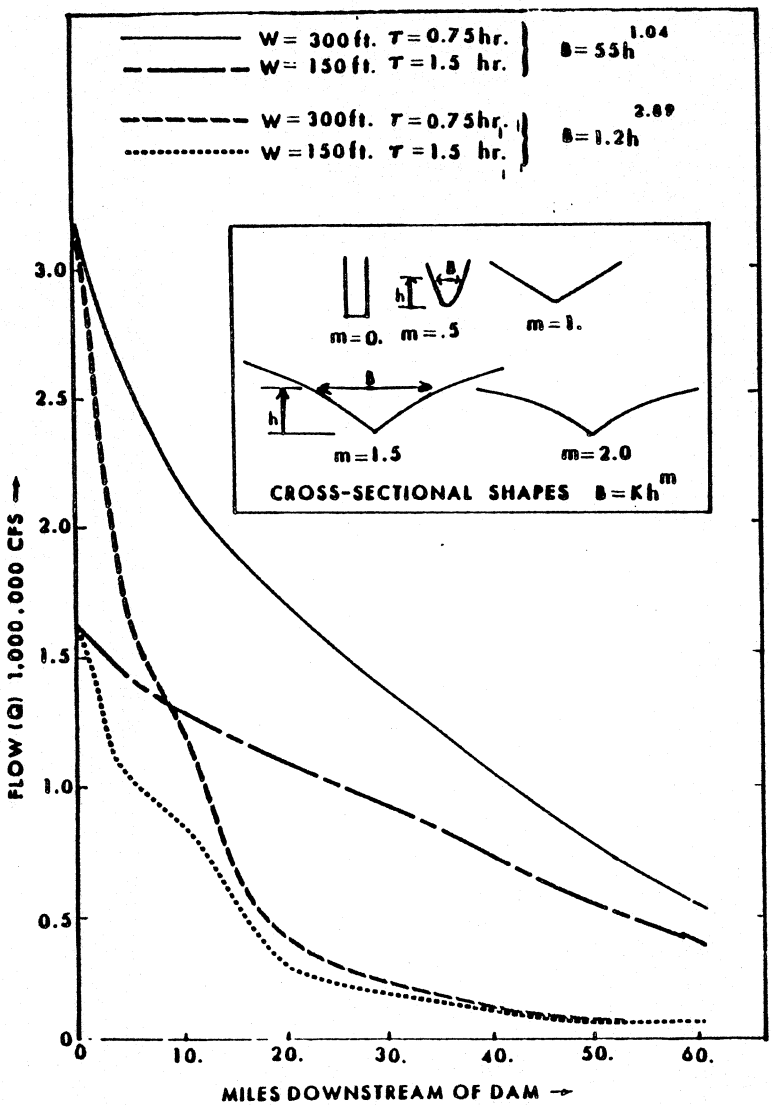

FIG. 1 - VARIATION OF PEAK FLOW DOWNSTREAM OF DAM

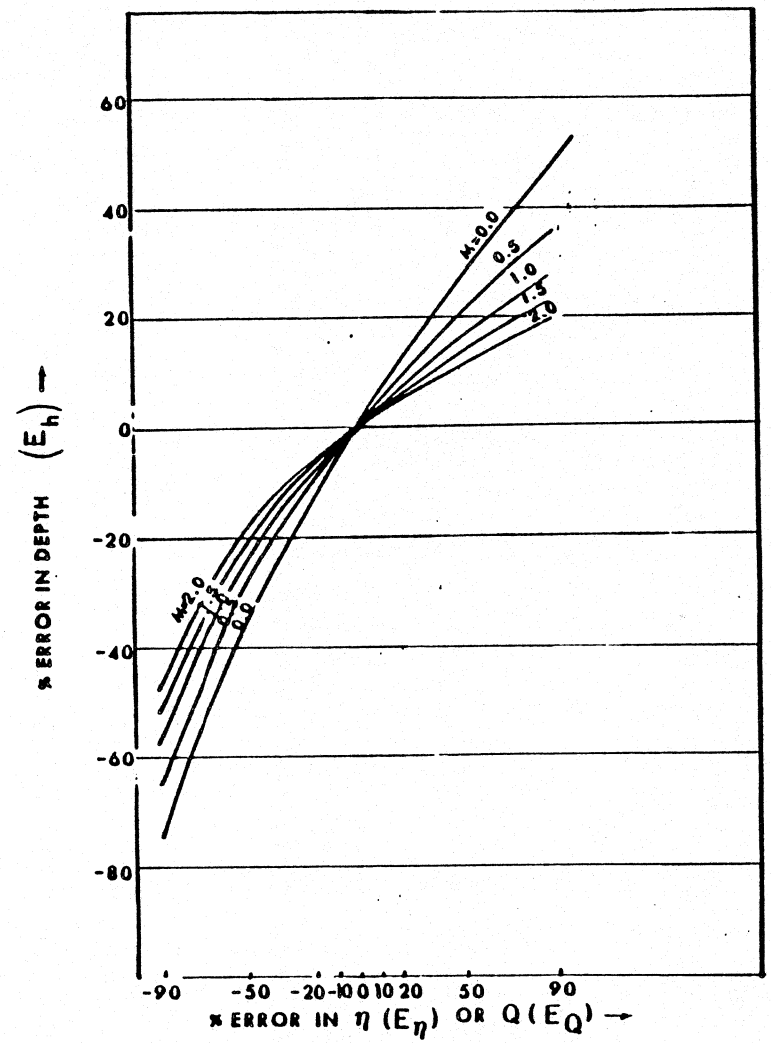

FIG. 2 - ERROR IN FLOOD DEPTH CAUSED BY ERROR IN ROUGHNESS (η) OR FLOW (Q) FOR VARIOUS SHAPED SECTIONS HAVING STEADY FLOW

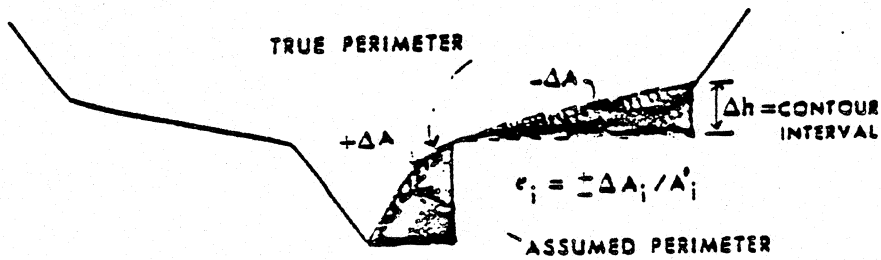

FIG.3-CROSS SECTION SHOWING ERROR $\left(e_i = \pm \Delta A / A'_i\right)$ DUE TO ASSUMED STRAIGHT-LINE VARIATION BETWEEN CONTOUR INTERVALS

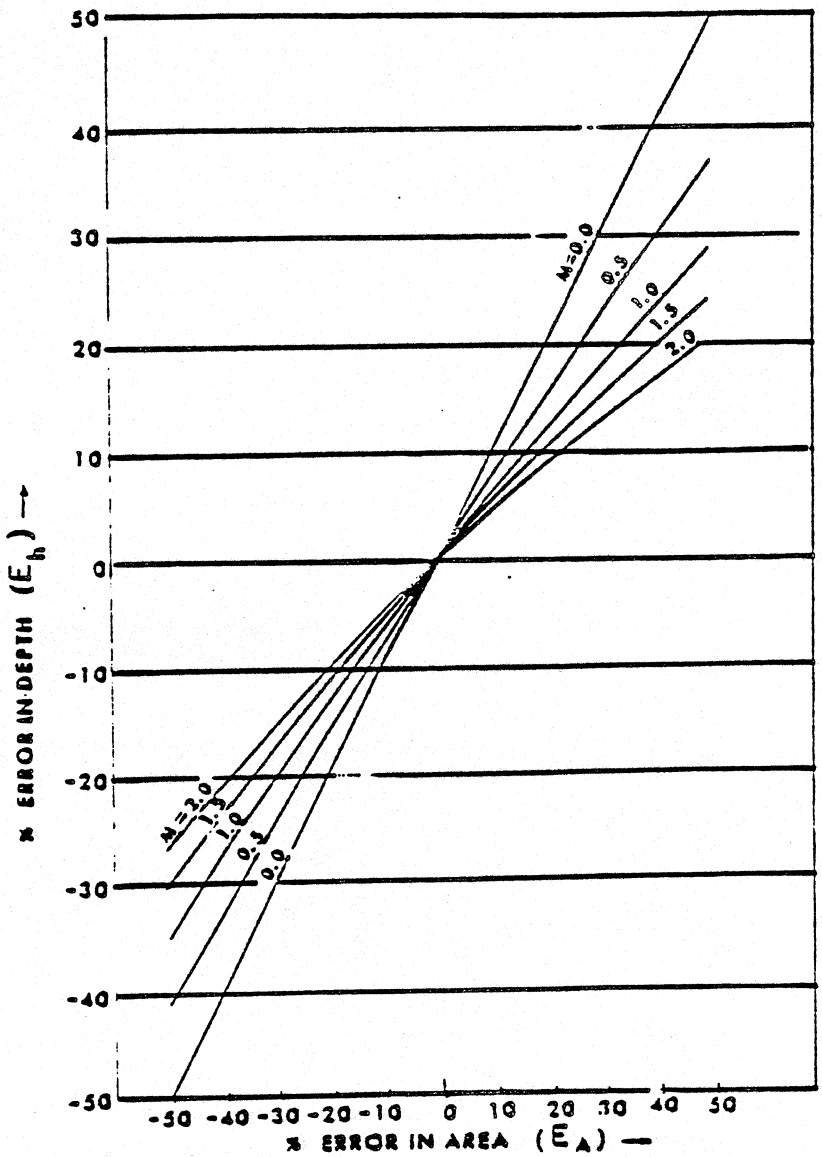

FIG.4-ERROR IN FLOOD DEPTH CAUSED BY ERROR IN CROSS-SECTIONAL AREA FOR VARIOUS SHAPED SECTIONS HAVING STEADY FLOW

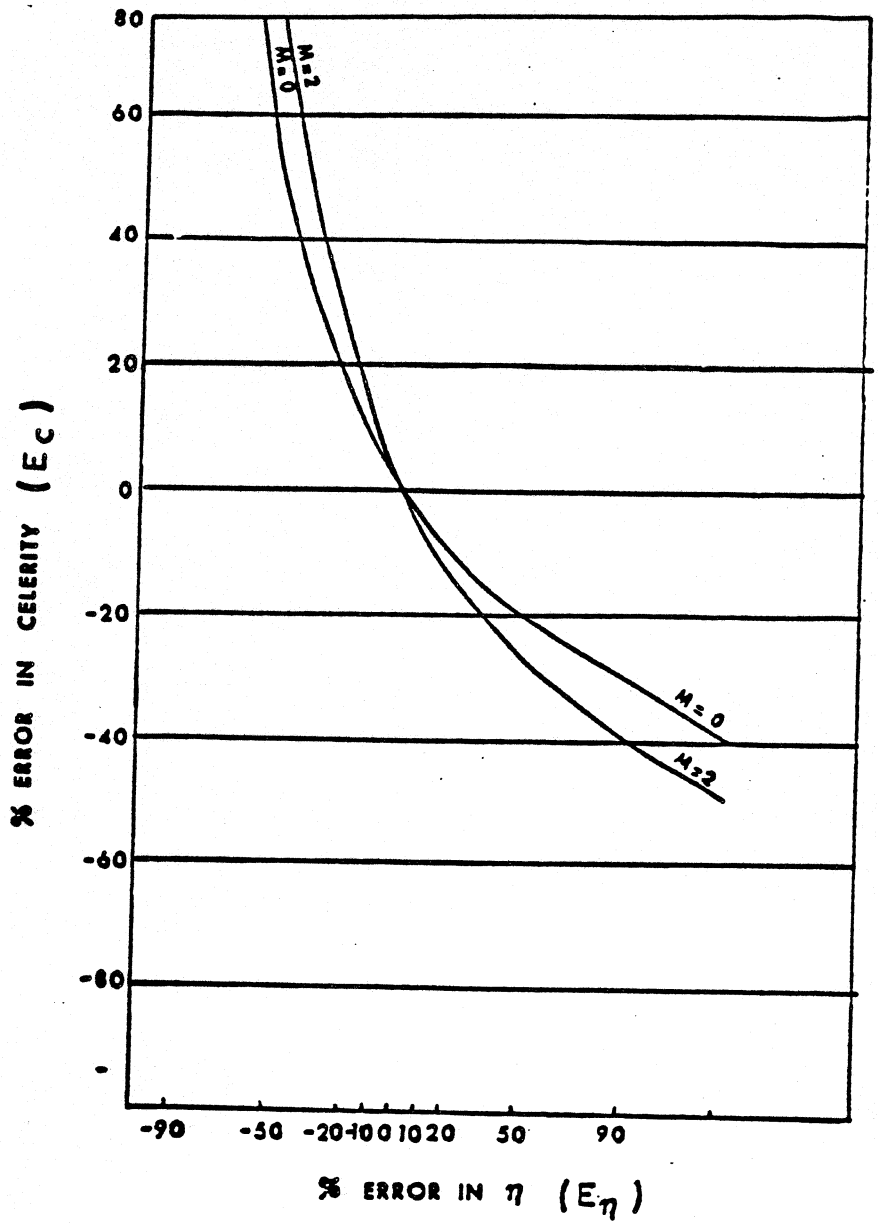

FIG. 5- ERROR IN FLOOD CELERITY CAUSED BY ERROR IN ROUGHNESS FOR VARIOUS SHAPED SECTIONS

The NWS Simplified Dambreak Model

"SMPDBK"

Objectives of SMPDBK

1. need very small computer resources
   a. hand-held non-programmable
   b. hand-held programmable
   c. micro
   d. mini
   e. main-frame

2. predict peak conditions (flow, depth, timing)

3. simple data requirements

4. numerical stability

$$Q_{max} = Q_o + 3.1\, B_v \left(\frac{C}{t_f + \frac{C}{\sqrt{H}}} \right)^3$$

$$C = \frac{23.4\, A_s}{B_v}$$

Q_o = crest overflow + Spillway flow when breach occurs, cfs

B_v = width of Breach, ft

t_f = time for breach development, hr.

H = Height of dam, ft

A_s = Surface Area (acres) of reservoir

Cross-Section Parameters (k, m)

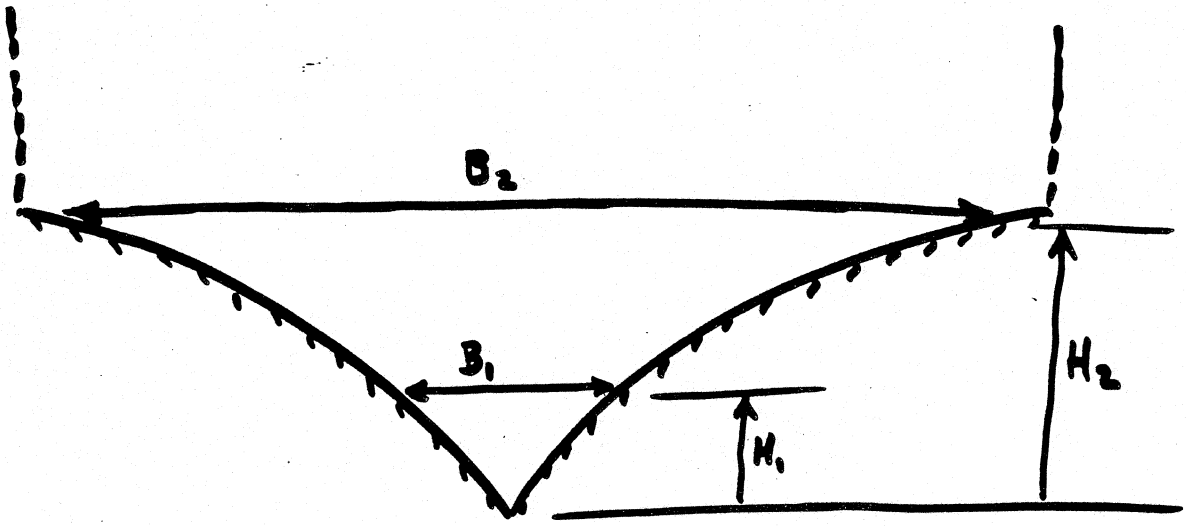

$$m = \frac{\log B_1 - \log B_2}{\log H_1 - \log H_2}$$

$$K = 10^{[\log B_1 - m \log H_1]}$$

Say: $B_1 = 200$ $B_2 = 1000$ $m = \dfrac{\log 200 - \log 1000}{\log 10 - \log 20} = 2.32$

$H_1 = 10$ $H_2 = 20$

$K = 10^{[\log 200 - 2.32 \log 10]} = 10^{-.0189} = 0.96$

$\therefore B = K h^m = 0.96\, h^{2.32}$

m=0. m=.5 m=1. m=1.5 m=2.

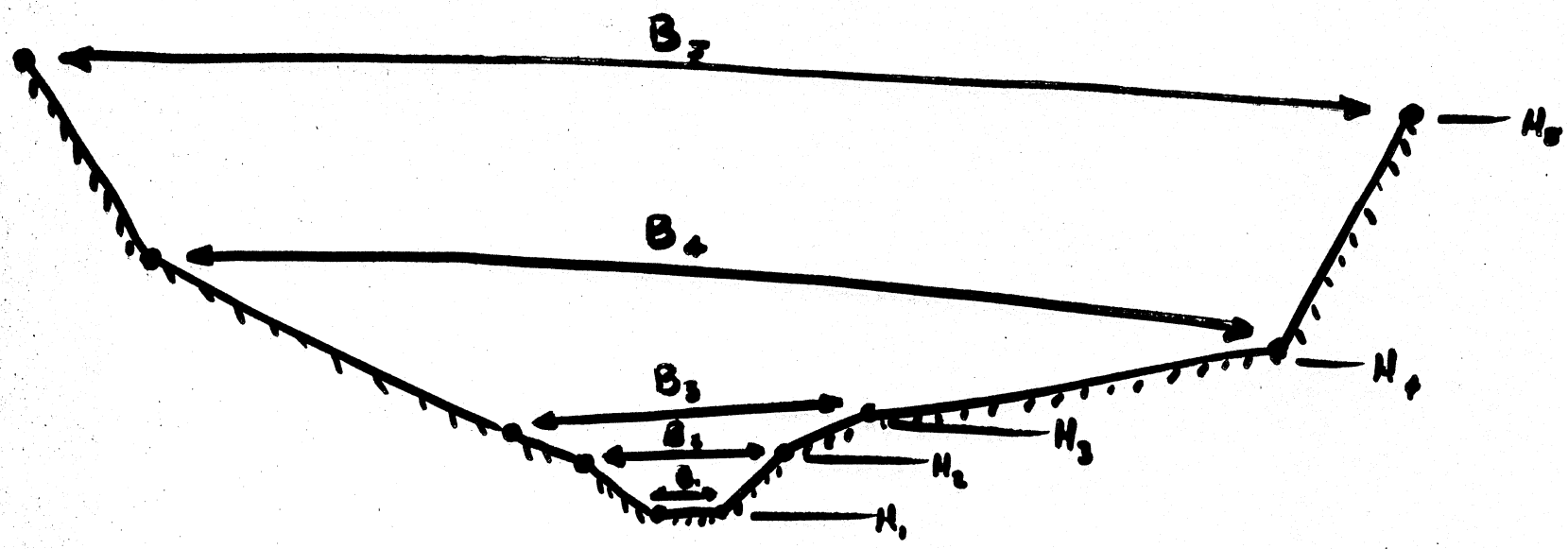

CROSS-SECTION DATA

Maximum Depth Calculation

Once the maximum outflow has been calculated, the maximum depth (h_{max}) at the downstream face of the dam must be determined. To do this, the cross section (X-section) at the downstream face of the dam must first be "fitted" (approximated) with an equation of the form $B = Kh^m$ (topwidth = K * depth^m) where K and m are the fitting coefficients computed using the following least squares algorithm:

$$m = \frac{\sum \left[(\log h_i)\ (\log \bar{B}_i)\right] - \dfrac{(\sum \log h_i)\ (\sum \log \bar{B}_i)}{I}}{\sum (\log h_i)^2 - \dfrac{(\sum \log h_i)^2}{I}} \qquad (5)$$

$$\log K = \frac{\sum \log \bar{B}_i}{I} - m\left(\frac{\sum \log h_i}{I}\right) \qquad (6)$$

$$K = 10^{(\log K)} \qquad (6a)$$

where: B_i is the topwidth associated with depth h_i, $i = 1,2,3,\ldots I$ (total number of topwidths)

For rivers with very steep valley side-walls adjacent to the channel (see figure 1a), an additional parameter (h_v) may be specified to indicate the depth at which the channel geometry no longer follows the $B = Kh^m$ relation. As can be seen in Figure 1b, this feature allows for a more accurate representation of the true channel-valley shape.

$$Q_{max}^{k} = K_s^{k} \, Q_{max}^{k-1}$$

$$K_s^{k} = \frac{K_s^{*} + K_s^{k-1}}{2} \qquad k = 1, 2, \ldots$$

$$K_s^{*} = 1 - 27.8 \left(\frac{h}{h_{weir}} - 0.67 \right)^3$$

$$h_{weir} = \left(\frac{c}{t_f + \frac{c}{\sqrt{H}}} \right)^2$$

$$K_s^{0} = 1$$

a iterative to account for submergence

Depth Computation:

$$h = \left(\frac{Q}{a}\right)^b$$

$$a = \frac{1.49}{n} S^{1/2} \frac{K}{(m+1)^{5/3}}$$

$$b = \frac{3}{3m+5}$$

Discharge Computation
at Points downstream of dam:

$$Q_p = \left(\frac{Q_p}{Q_{max}}\right) Q_{max}$$

from routing curves

SIMPLIFIED DAMBREAK ROUTING CURVES

FROUDE NUMBER → FC=0.25

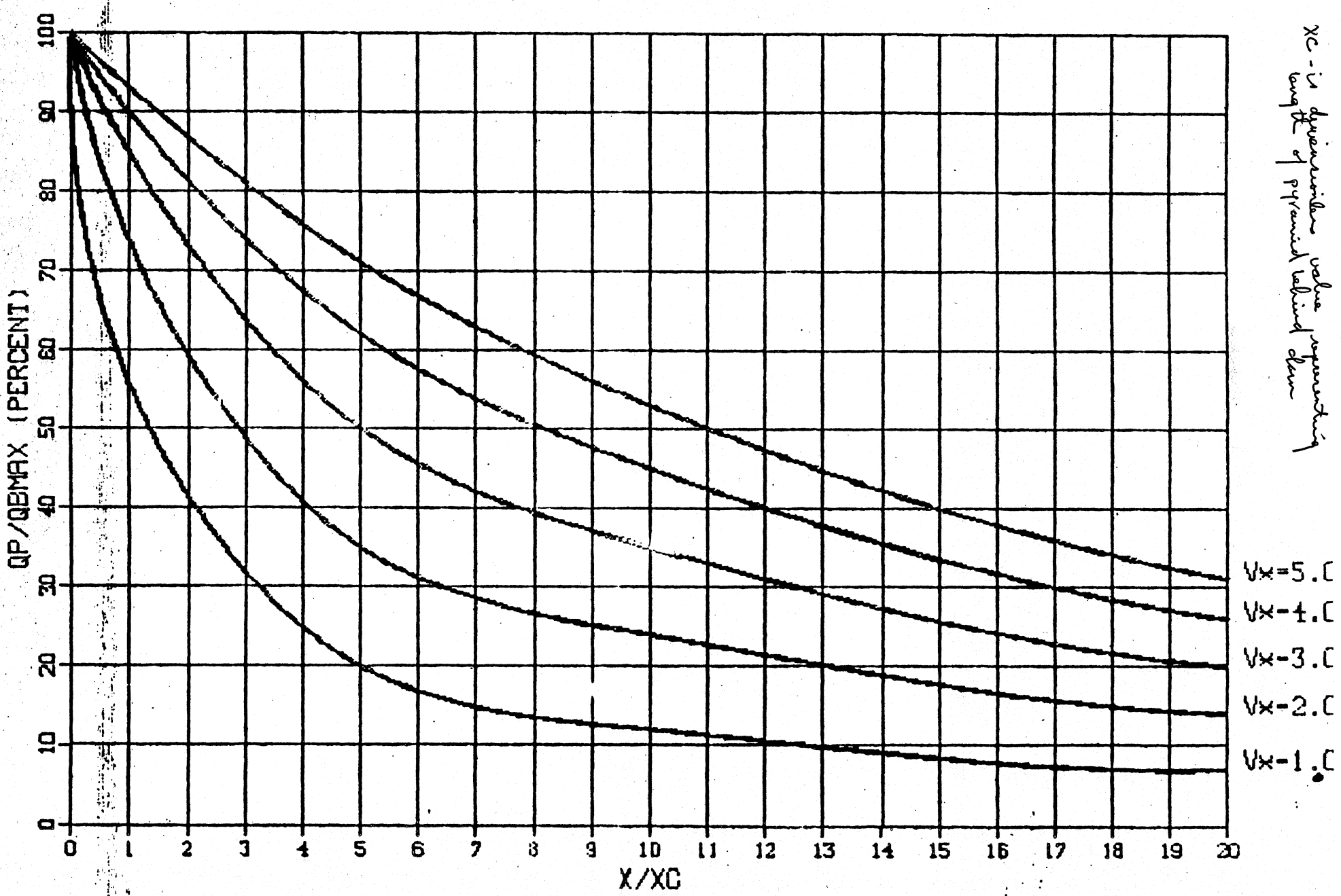

XC - is dimensionless value representing length of pyramid behind dam

$$\rightarrow X^* = \frac{x}{X_c}$$

$$X_c = \frac{m+1}{K} \frac{Vol_r}{H_d^{m+1}} \left(\frac{6}{1+4(0.5)^{m+1}} \right)$$

$$\rightarrow V^* = \frac{Vol_r}{A_c X_c}$$

$$A_c = K(\theta h_{max})^m D_c$$

$$D_c = \frac{\theta h_{max}}{m+1}$$

$$\theta = \frac{h_{max} + h_x}{2 h_{max}}$$

$$\rightarrow F_c = \frac{V_c}{\sqrt{g D_c}}$$

$$V_c = \frac{1.49}{n} S^{1/2} D_c^{2/3}$$

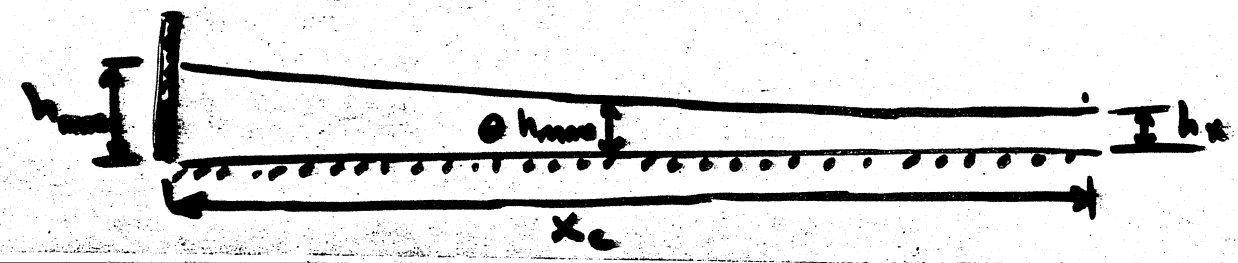

time of peak occurence :

$$t_p = t_f + \frac{X}{c} \quad \frac{\text{miles}}{\text{m.p.h.}}$$

time of failure

$$c = 0.682\, V_{x_i} \left[\frac{5}{3} - \frac{2}{3}\left(\frac{m}{m+1}\right)\right]$$

$$V_{x_i} = \frac{1.49}{n} S^{1/2} D_{x_i}^{2/3}$$

$$D_{x_i} = \frac{h_{ref}}{m+1}$$

$$h_{ref} = \left(\frac{Q^*}{a}\right)^b$$

$$Q^* = Q_{\frac{1}{2}} \left(0.3 + \frac{m}{10}\right)$$

time of flooding and deflooding of elevation h_f :

$$Q_f = a\, h_f^{\,b}$$

$$t_{fld} = t_p - \left(\frac{Q_p - Q_f}{Q_p - Q_o} \right) t_f$$

$$t_d = t_p + \left(\frac{24.2\ Vol_v}{Q_p - Q_o} - t_f \right) \left(\frac{Q_p - Q_f}{Q_p - Q_o} \right)$$

1.) errors in shape of hydrograph reason kinds of

2.) Δ in time to peak are not accounted for

Limitations of SMPDBK :

1. no significant backwater from downstream dams or constrictions or bridges

2. 5—10 % error relative to DAMBRK
   with no errors in fitting of x-sections and backwater effects

3. try to minimize cross-section fitting error for K and m

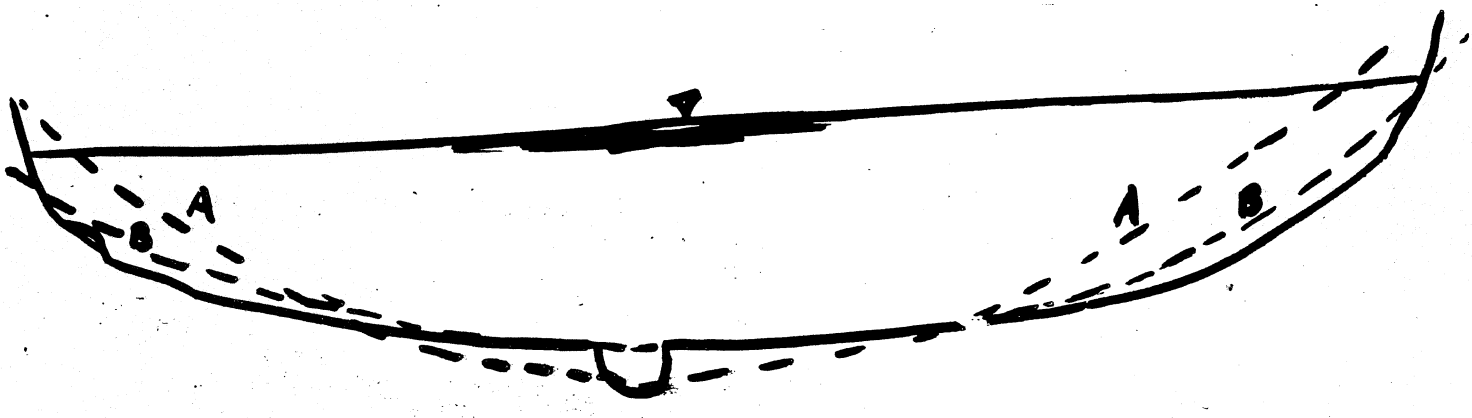

BREACH

An Erosion Model for Earthen Dams

overtopping
Piping } failure mode

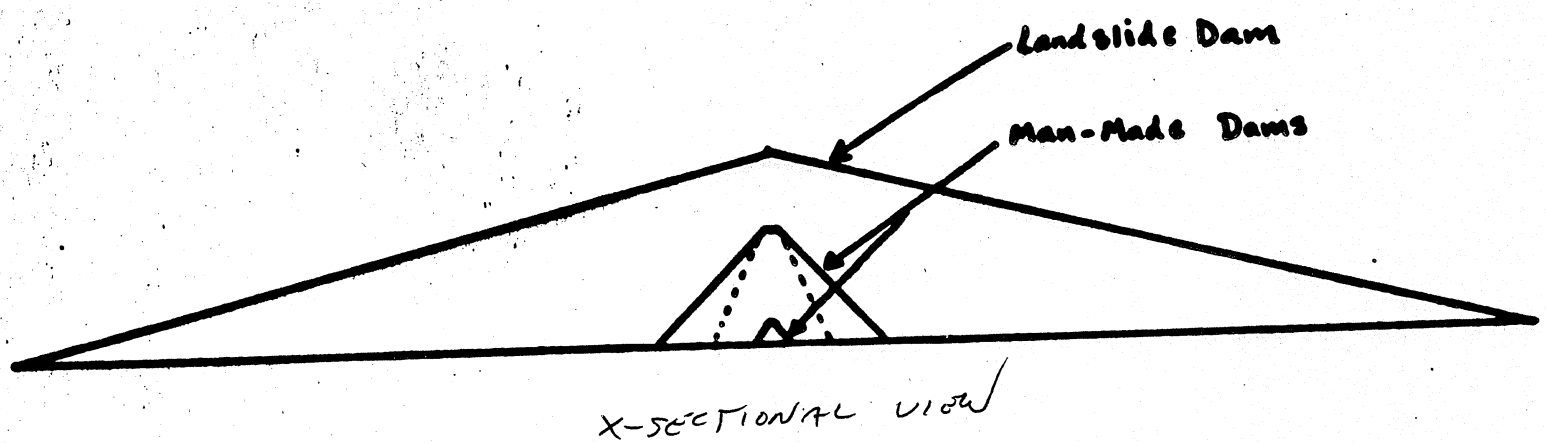

Figure 1 - Comparative View of Natural Landslide Dams and Man-Made Dams.

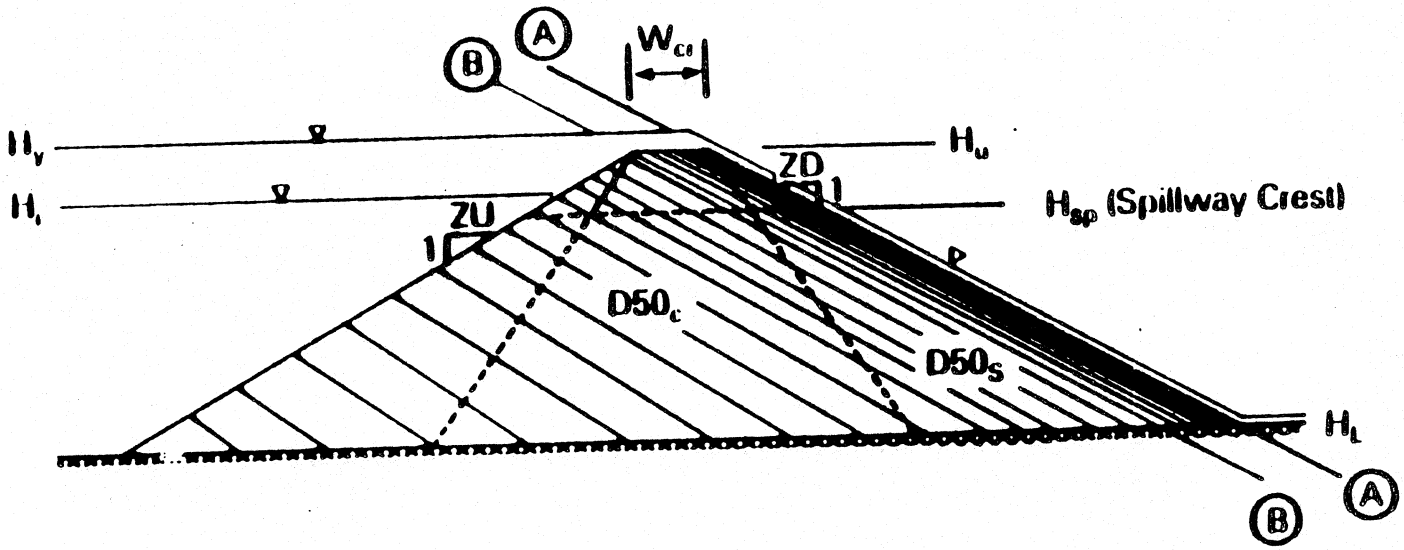

Figure 2. Side View of Dam Showing Conceptualized Overtopping Failure Sequence.

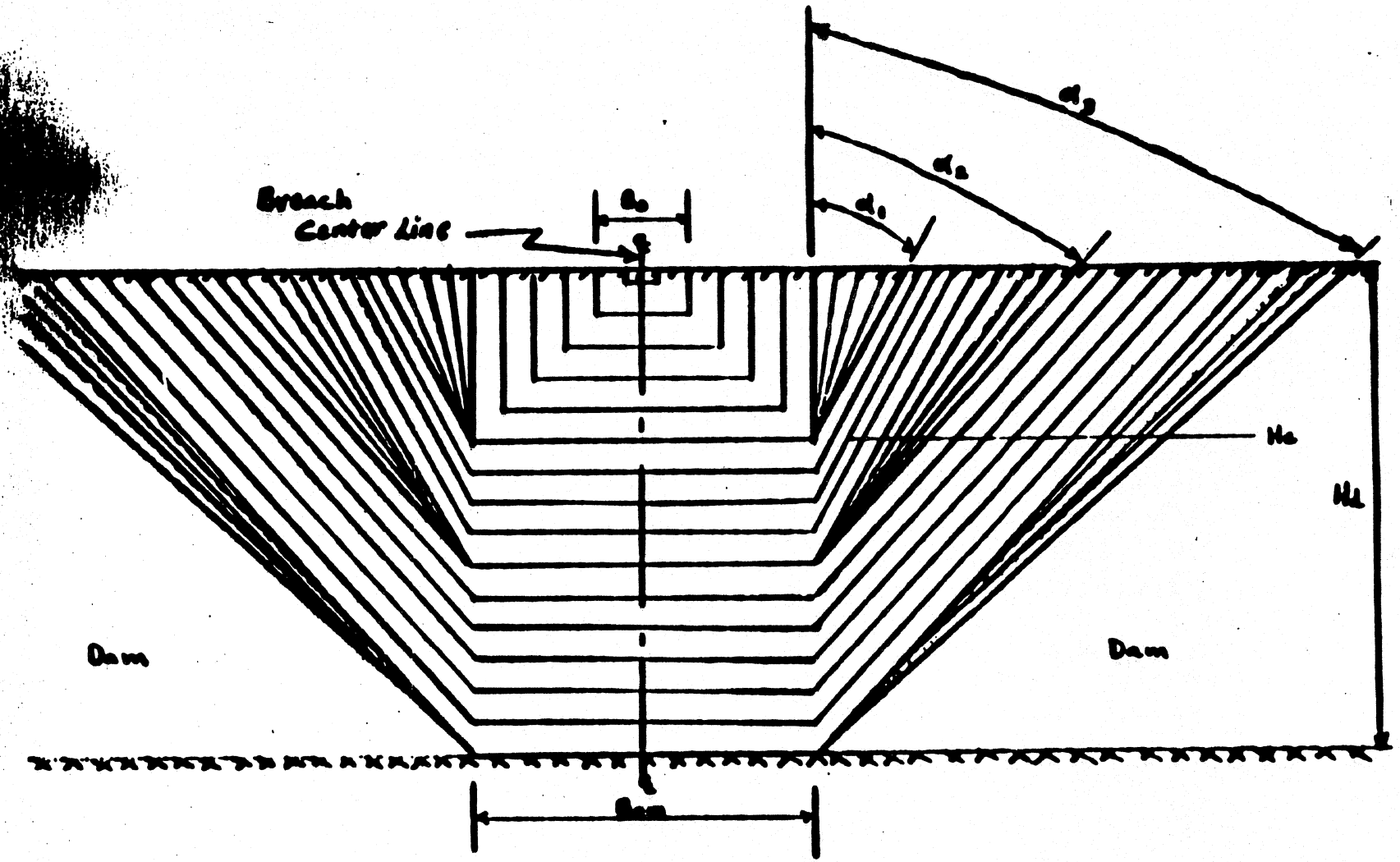

Figure 3 - Front View of Dam with Breach Formation Sequence.

Breach Enlargement:

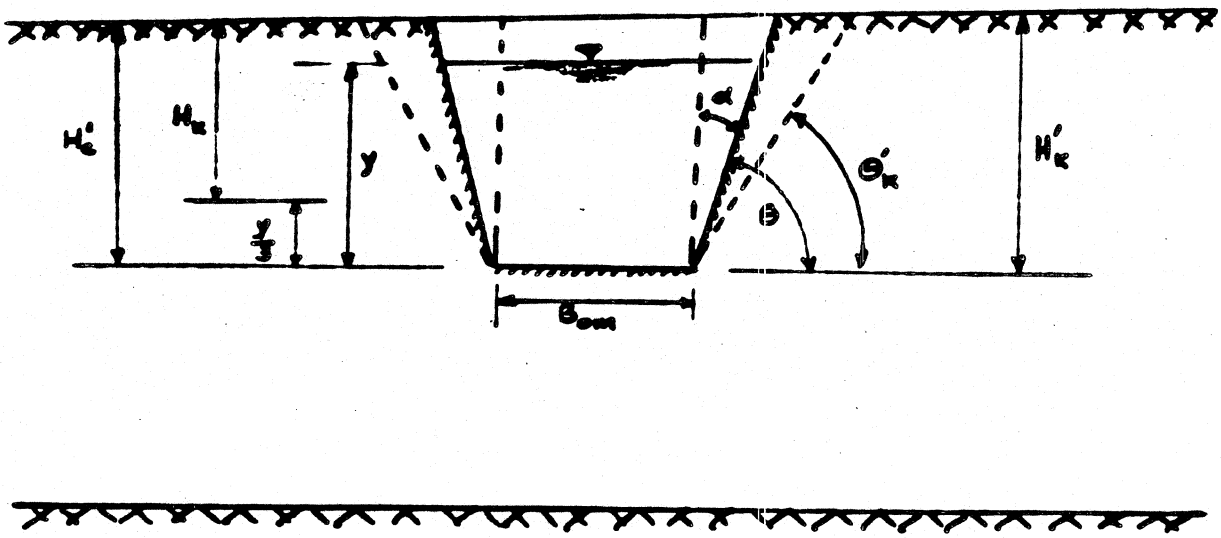

$$\theta = \theta'_{k-1} \quad \ldots\ldots \quad H_k \le H'_k$$

$$\theta = \theta'_k \quad \ldots\ldots\ldots \quad H_k > H'_k$$

$$k = k+1$$

$$\alpha = \frac{\pi}{2} - \theta$$

$$B_o = B_r\, y \quad \ldots\ldots\ldots \quad k=1$$

$$B_o = B_{om} \quad \ldots\ldots\ldots \quad k>1$$

$$B_{om} = B_r\, y \quad \ldots\ldots \text{ when } H_1 = H'_1$$

where:

$$\theta'_o = \frac{\pi}{2}$$

$$\theta'_k = (\theta'_{k-1} + \phi)/2$$

$$H_k = H'_k - y/3$$

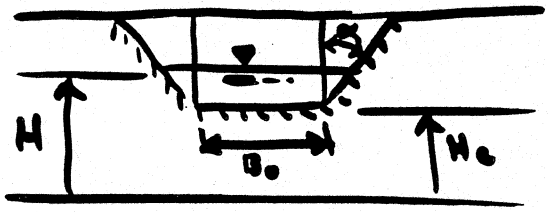

Breach Flow :

$$Q = 3 B_o (H - H_c)^{3/2} + 2 \tan\alpha \, (H - H_c)^{5/2}$$

Piping :

$$Q = A \sqrt{\frac{2g(H - H_p)}{1 + f/LD}}$$

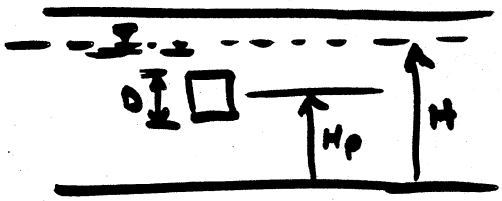

Breach Channel Hydraulics:

$$Q_b = \frac{1.49\, S^{0.5} A^{1.67}}{n\, P^{0.67}}$$

$$S = \frac{1}{20}$$

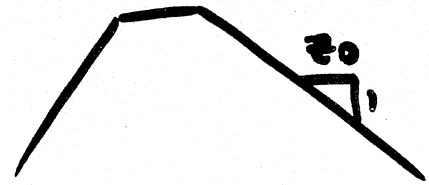

$$n = 0.013\, D_{50}^{0.167}$$

is this the same

WHY BOTHER WITH A SED. REGN'S.

Sediment Transport:

$$Q_s = 3.64 \left(\frac{D_{90}}{D_{30}}\right)^{0.2} \frac{D^{2/3}}{n} S^{1.1} \left(DS - 0.0054\, D_{50}\, \tau_c\right)$$

τ_c = critical Shear Stress from Shield's Curve →

$$\tau_c = f(R^*)$$

$$R^* = 15.14\, D_{50} \sqrt{DS}$$

no calibration

how can you route a dynamic wave over a breach with a sed. transport function based on uniform steady flow?

Hydraulics :

$$\Delta H = \frac{0.0826\,\Delta t}{S_a}\left(\bar{Q}_i - \bar{Q}_b - \bar{Q}_{sp} - \bar{Q}_o\right)$$

ΔH = change in reservoir elev.

Δt = time step, hr

S_a = reservoir surface area, acre-ft

$\bar{Q}_i$ = avg. reservoir inflow during Δt, cfs

$\bar{Q}_b$ = avg. breach outflow during Δt, cfs

$\bar{Q}_{sp}$ = avg. spillway outflow during Δt, cfs

$\bar{Q}_o$ = avg. crest overflow during Δt, cfs

iterative

$$Q_b = 3\,B_o\,(H-H_c)^{1.5}$$ ..... weir flow (rectangular)

$$Q_b = 3\,B_{om}(H-H_c)^{1.5} + 2\tan\alpha\,(H-H_c)^{2.5}$$ ... weir flow (trapezoidal)

$$Q_b = 7.85\,A\,(H-H_p)^{0.5}$$ .... pipe flow

$$H < H_{pu} + 2\,(H_{pu}-H_p)$$ .... pipe flow changes to weir flow

$$Q_b = \frac{1.49\,S^{0.5}\,A^{1.67}}{n\;P^{0.67}}$$ .... Manning Eq.

$$n = 0.034\left(\frac{D_{50}}{3.05}\right)^{0.167}$$ .... Strickler Eq.

the development of this equation aren't applicable to its use here.

Computational Algorithm :

1. $t = t + \Delta t$

2. $H_c = H_c' - \Delta H_c'$

3. $H = H' + \Delta H$

4. compute $\bar{Q}_i$, $\bar{Q}_{sp}$, $\bar{Q}_o$

5. $\Delta H = \frac{0.0626\,\Delta t}{S_a} \left(\bar{Q}_i - Q_{\parallel}' - \bar{Q}_{sp} - \bar{Q}_o \right)$

6. $H = H' + \Delta H$

7. compute Q_b

8. correct Q_b for tailwater submergence

9. Compute breach channel properties $(B_b, \theta_k, \alpha_k, B, P, R)$

10. Compute Q_s

11. $\Delta H_c = \frac{3600\,\Delta t\, Q_s}{P_b\, L\,(1 - P_{or})}$ how do you calibrate porosity

12. if $100\left(\frac{\Delta H_c' - \Delta H_c}{\Delta H_c}\right) > E$ return to (2) with $\Delta H_c' = \Delta H_c$

13. Check for collapse

14. extrapolate estimates : $\Delta H_c'$, $\Delta H'$

15. if $t < t_e$ return to (1)

16. Plot outflow hydrograph

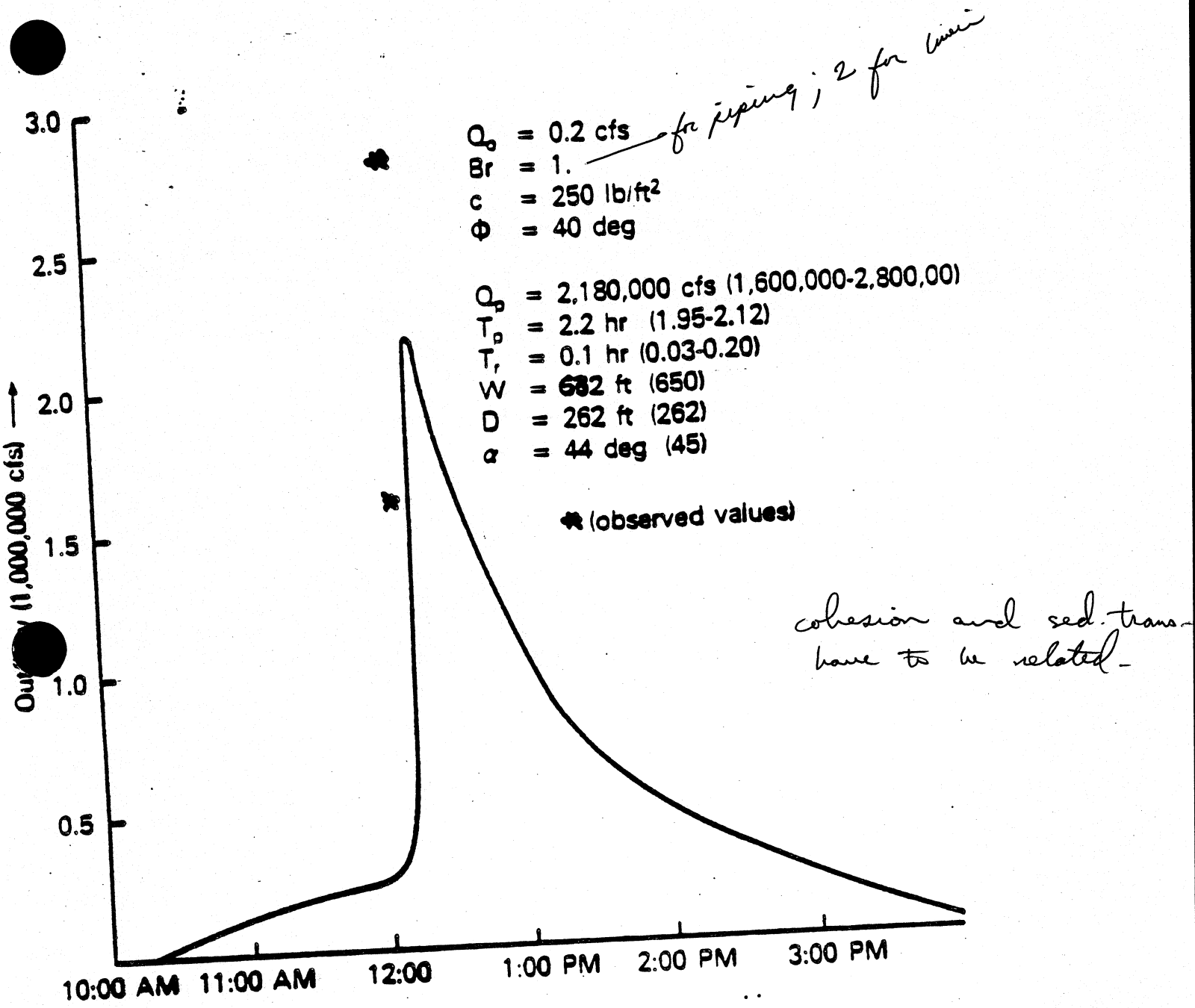

Figure 6. Teton Dam: Predicted and Observed Breach Outflow Hydrograph and Breach Properties.

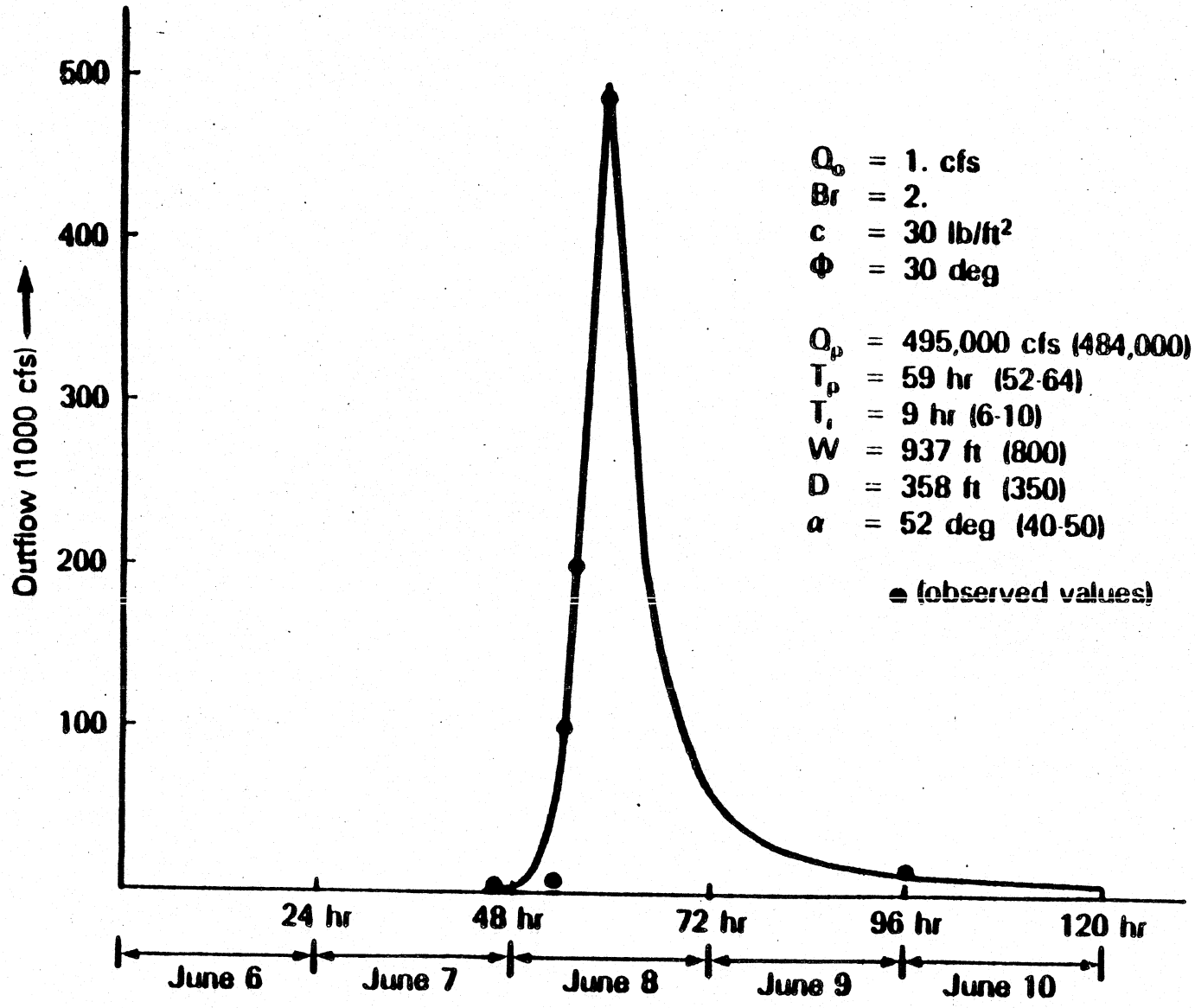

Figure 8. Mantaro Landslide Dam: Predicted and Observed Breach Outflow Hydrograph and Breach Properties.

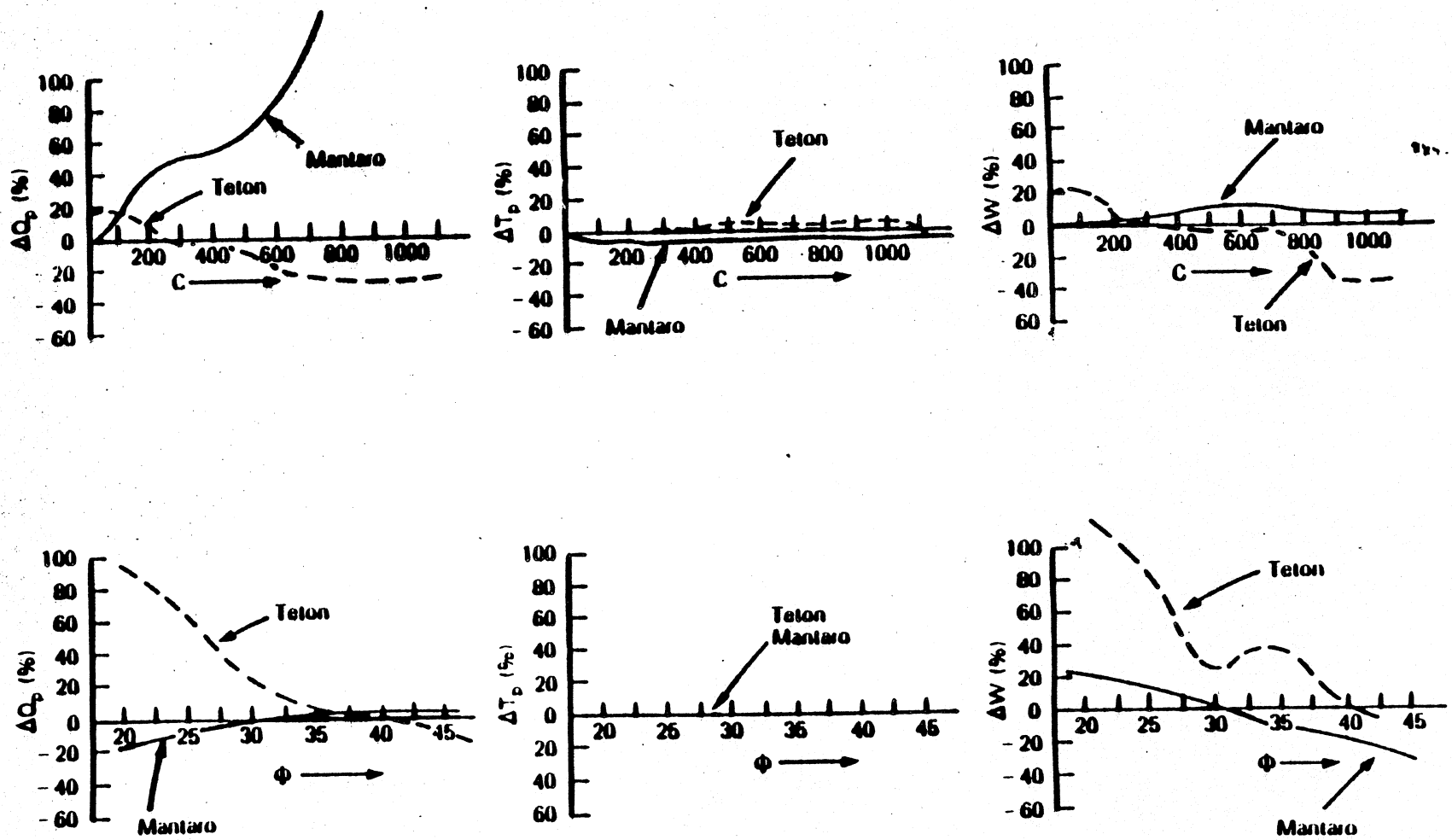

Figure 7. Sensitivity of Mantaro and Teton Predictions of Peak Outflow (Qp), Time to Peak (Tp), and Breach Width (W) to Changes in the Material Properties of the Dam: Cohesion (C) and Internal Friction Angle (Φ).

APPENDIX A

INPUT DATA FOR BREACH EROSION MODEL (BREACH): VERSION 1/2/85

Card No.	Data Description and Input Form	
(1)	MESSAGE - 20A4	
	MESSAGE	Any message such as name of dam, message may be < 80 characters.
(2)	HI, HU, HL, HPI, HSP, - 5F10.2	
	HI	Initial elevation (ft) of water surface in reservoir at t = 0.
	HU	Elevation of top of dam.
	HL	Elevation of bottom of dam (usually original stream-bed elevation).
	HPI	Elevation at which piping failure commences (if no piping failure is simulated, leave blank).
	HSP	Elevation of spillway crest (if no spillway, leave blank).
(3)	QIN(I) - 8F10.2	
	QIN	Inflow (cfs) to reservoir. I subscript goes from 1 to 8. Inflow hydrograph may be defined with from 2 to 8 values.
(4)	TIN(I) - 8F10.2	
	TIN(I)	Time (hrs) associated with QIN(I) reservoir inflow.
(5)	RSA(I) - 8F10.2	
	RSA(I)	Surface area (acres) of reservoir. I subscript goes from 1 to 8. Surface area is defined at from 2 to 8 elevations starting at the highest elevation and proceeding to the reservoir bottom.
(6)	HSA(I) - 8F10.2	
	HSA(I)	Elevation (ft) associated with RSA(I) surface area.

Card No.	Data Description and Input Format

(7) ZU, ZD, ZC, PORW, GL, GS, VMP - 7F10.2

ZU	Slope of upstream face of dam [1 (vertical) : ZU (horizontal)]
ZD	Slope of downstream face of dam (1 (vertical) : ZD (horizontal)]
ZC	Average slope of upstream and downstream faces of inner core of dam [1 (vertical) : ZC (horiz.)]. If no inner core, leave blank.
PORW	Ratio of total pore space of dam material which contains water (0.0 to 1.0)
GL	Average length of grass (inches). If no grass, leave blank.
GS	Condition of stand of grass. If good, GS=1.0; if poor stand or no grass exists, GS=0.0.
VMP	Maximum permissible velocity (ft/sec) for grass-lined channel before grass cover is eroded away. Can vary from 3 to 6 ft/sec. If no grass, leave blank.

(8) D50C, PORC, UWC, CNC, AFRC, COHC, UNFCC - 3F10.2, F10.4, 3F10.2

D50C	D50 (mm) grain size of inner core material (50% finer). If no core, leave blank.
PORC	Porosity ratio of inner core material. If no core, leave blank.
UWC	Unit weight (lb/ft^3) of inner core material. If no core, leave blank.
CNC	Manning n of inner core material. If left blank, it will be computed from the Strickler Equation which is a function of the grain size. If a value greater than 0.99 is entered, it will be computed from a Moody diagram (Darcy f vs. D50 relationship). If no core, leave blank.
AFRC	Internal friction angle (degree) of inner core material. If no core, leave blank.
COHC	Cohesive strength (lb/ft^2) of inner core material. If no core, leave blank.
UNFCC	Ratio of D90 to D30 grain sizes of inner core material. If no core, leave blank. If core exists and left blank, default value is 10.

Card No.	Data Description and Input Format

(9) D50S, PORS, UWS, CNS, AFRS, COHS, UNFCS - 3F10.2, F10.4, 3F10.2

D50S	D50(mm) of outer material of dam (50% finer).
PORS	Porosity ratio of outer material.
UWS	Unit weight (lb/ft^3) of outer material.
CNS	Manning n of outer material. If left blank, it will be computed from the Strickler Equation which is a function of the grain size. If a value greater than 0.99 is entered, it will be computed from a Moody diagram (Darcy f vs. D50 relationship).
AFRS	Internal friction angle (degree) of outer material.
COHS	Cohesive strength (lb/ft^2) of outer material.
UNFCS	Ratio of D90 to D30 grain size of outer material. If left blank, default value is 10.

Note: If dam material is homogeneous, use the outer layer to represent the entire homogenous dam material.

(10) BR, WC, CRL, SM, WV, CNV, D50DF, UNFCDF - 5F10.2, F10.4

BR	Ratio of breach width to flow depth for initial rectangular-shaped breach. Range of values are: $1 < B_r < 2$. Usually use 2.0 for overtopping failure and 1.0 for a piping failure. If left blank, BR = 2.
WC	Width (ft) of crest of dam (can be zero).
CRL	Length (ft) of crest of dam.
SM	Bottom slope (ft/mile) of downstream river for first few thousand feet below the dam.
WV	Width (ft) of valley for which SM is applicable.
CNV	Manning n of valley for which SM is applicable.
D50DF	D50 (mm) grain size of material composing the top one-foot of the downstream face of the dam. If left blank, D50DF=D50S.
UNFCDF	Ratio of D90 to D30 grain size of material of downstream face. If left blank, UNFCDF=3.0 when D50DF>0.0, or UNFCDF=UNFCS when D50DF=0.0.

Card No.	Data Description and Input Format

(11) DTH, DBG, H, TEH, ERR, FPT - 2F10.3, 4F10.2

DTH	Basic time step size (hr). 0.02 < DTH < 0.20, lower values for man-made dams, larger values for large landslide dams. If left blank, DTH = 0.05.
DBG	Output control parameter. DBG = 0.0, minimal output of discharge hydrograph only. DBG = 0.001, output at each time step + hydrograph. DBG = 0.002, output at each iteration of each time step + hydrograph. DBG = 0.003, maximum output.
H	Initial depth (ft) of breach along the downstream face of dam for overtopping failure. Initial width of piping breach. Usually, 0.1 < H < 1.0. If left blank, H = 0.10.
TEH	Duration (hrs) of simulation.
ERR	Error tolerance in iterative solution, expressed as a percentage ratio (0.1 < ERR < 1.0). If left blank, ERR = 0.10.
FPT	Interval of time steps at which computed discharges are plotted. (1. < FPT < 10.) If left blank, FPT = 1.0.

Note: Omit cards no. (12) and (13) if spillway crest elev., HSP, (card no. 2) is blank or zero.

(12) SPQ(I) - 8F10.2

SPQ(I)	Spillway flow (cfs). I subscript goes from 1 to 8. Spillway flow is defined for from 2 to 8 elevations starting at the spillway crest elev. and proceeding upwards until maximum spillway discharge is specified.

(13) SPH(I) - 8F10.2

SPH(I)	Elevation (ft) associated with SPQ(I) spillway flow.

OUTPUT PARAMETERS FOR "BREACH" MODEL ,VERSION 7/2/84

I	COUNTER
T	TIME,HR
DTH	TIME STEP,HR
KG	CODE FOR REGION OF FAILURE : 1 EROSION OF DOWNSTREAM FACE 2 EROSION OF UPSTREAM FACE 3 DRAINING OF RESERVOIR WITH BREACH SIZE FIXED AT MAX DIMENSIONS 4 PIPING MODE 5 COLLAPSE MODE
KC	COLLAPSE HEIGHT
QTOT	TOTAL OUTFLOW,CFS
QTS	SPILLWAY OUTFLOW,CFS
QB	BREACH OUTFLOW,CFS
SUB	SUBMERGENCE CORRECTION FACTOR
BT	TOP WIDTH OF BREACH,FT
HY	ELEV OF RESERVOIR WATER SURFACE,FT
HC	ELEV OF BOTTOM OF BREACH,FT
BO	BOTTOM WIDTH OF BREACH,FT
PPP	PIPING LENGTH(FT) WHEN KG=4; MAX DEPTH ALLOWABLE PRIOR TO SIDE SLOPE FAILURE WHEN KG=2; REMAINING CREST WIDTH (FT) TO BE ERODED WHEN KG=1
HP	TOP OF PIPING BREACH OR DEPTH OF BREACH,FT
YN	NORMAL DEPTH OF FLOW IN BREACH CHANNEL,FT
DH	ESTIMATED EROSION DEPTH(FT) DURING TIME STEP
DHR	COMPUTED EROSION DEPTH(FT) DURING TIME STEP
KIT	ITERATION COUNTER
TH	ACUTE ANGLE(DEG) THAT BREACH SIDE MAKES WITH VERTICAL

OTHER OUTPUT CONSISTS OF A HYDROGRAPH OF TOTAL OUTFLOW

THE FOLLOWING SUMMARY INFORMATION IS ALSO PRINTED OUT:

TF	TIME(HR) AT WHICH FAILURE MODE 2 STARTS
QTF	FLOW(CFS) AT TIME TF
TP	TIME(HR) AT WHICH PEAK OUTFLOW OCCURS
QP	MAX OUTFLOW(CFS) OCCURRING AT TIME TP
TRS	DURATION(HR) OF RISING LIMB OF HYDROGRAPH
TB	TIME(HR) AT WHICH SIGNIFICANT RISE IN OUTFLOW STARTS
TRSB	TP-TB
BRD	FINAL DEPTH(FT) OF BREACH
BRW	FINAL TOP WIDTH(FT) OF BREACH
HU	ELEV (FT) OF TOP OF DAM
HY	FINAL ELEV (FT) OF RESERVOIR WATER SURFACE
HC	FINAL ELEV (FT) OF BOTTOM OF BREACH
THETA	FINAL ACUTE ANGLE THAT BREACH SIDE MAKES WITH VERTICAL
QO	OUTFLOW (CFS) AT T=0.0
YNM	MAX NORMAL FLOW DEPTH (FT) IN BREACH CHANNEL
HMC	MAX CRITICAL FLOW DEPTH (FT) IN BREACH CHANNEL
DTC	DURATION (HR) TO REMOVE COLLAPSED MATERIAL
Z	FINAL SIDE SLOPE OF BREACH (FT/FT)
TFH	TIME OF FAILURE (HR) WHICH IS SAME AS TRS
BO	BOTTOM WIDTH (FT) OF BREACH

THE NWS SIMPLIFIED DAM BREAK FLOOD FORECASTING MODEL FOR DESK-TOP AND HAND-HELD MICROCOMPUTERS

Jonathan N. Wetmore and Danny L. Fread[1]

SYNOPSIS

The National Weather Service (NWS) has developed a simplified procedure that utilizes desk-top or hand-held microcomputers for predicting downstream flooding produced by a dam failure. This procedure, known as the Simplified Dam Break (SMPDBK) Flood Forecasting Model, produces information needed for delineating areas endangered by dam break floodwaters while substantially reducing the amount of time, data, computer facilities, and technical expertise required in employing more highly sophisticated unsteady flow routing models. With only an inexpensive microcomputer and a minimal amount of data, the user may within minutes predict the dam break floodwave peak flows, depths, and travel times at selected downstream points. This capacity for providing results quickly and efficiently should make the SMPDBK model a useful forecasting tool in a dam failure emergency when warning response time is short, little data are available, and large computer facilities are inaccessible. However, the SMPDBK model should prove even more useful for "pre-event" dam failure analysis by emergency management personnel engaged in preparing disaster contingency plans when the use of other flood routing models is precluded by limited resources.

The SMPDBK model is designed for interactive use (i.e., the computer prompts the user for information on the dam, reservoir, and downstream channel and the user responds by entering the appropriate data values), and it allows the user to enter as much or as little data as are available, automatically using preprogrammed defaults when the response to a prompt indicates the data is not available. Using the internally set default values, SMPDBK is capable of producing approximate flood forecasts after reading in only the dam height, reservoir storage volume, and depth-vs.-width data for one cross-section of the downstream river valley (determined from on-site inspection or topographic maps). If however, the user has access to additional information (i.e., the reservoir surface area, estimates of the final width and depth of the breach, the time required for breach formation, the turbine/spillway/overtopping flow, the slope of the channel and the Manning roughness coefficient, flood depth (depth where flooding becomes a problem), and elevation-vs.-width data for up to five downstream channel cross-sections), the model will utilize this information to enhance the accuracy of the forecast.

---

[1]Research Hydrologist and Senior Research Hydrologist, Hydrologic Research Laboratory, Office of Hydrology, National Weather Service, NOAA, 8060 13th Street, Silver Spring, Maryland.

In producing the dam break flood forecast, the SMPDBK model first computes the peak outflow at the dam, based on the reservoir size and the temporal and geometrical description of the breach. The computed floodwave and channel properties are used in conjunction with routing curves to determine how the peak flow will be diminished as it moves downstream. Based on this predicted floodwave reduction, the model computes the peak flows at specified downstream points with an average error of +10 percent or less. The model then computes the depth reached by the peak flow based on the channel geometry, slope, and roughness at these downstream points. The model also computes the time required for the peak to reach each forecast point and, if the user entered a flood depth for the point, the time at which that depth is reached as well as when the floodwave recedes below that depth, thus providing the user with a time frame for evacuation and fortification on which the preparedness plan may be based.

The SMPDBK model has performed well in test simulations of the flooding produced by the failure of Teton Dam and the Buffalo Creek "coal waste" Dam, as well as in numerous theoretical dam failure simulations where the progression of the floodwave was not significantly altered by backwater effects created by downstream dams or bridge embankments, the presence of which can substantially reduce the model's accuracy. Its speed and ease of use recommend it well for use in emergencies. However, emergencies are not the only situations where it can be useful: planners, designers, emergency managers, and consulting engineers responsible for predicting the potential effects of a dam failure may employ the model in situations where backwater effects are not significant for pre-event delineation of areas facing danger should a particular dam fail.

I. INTRODUCTION

The devastation that occurs as impounded reservoir water escapes through the breach of a failed dam and rushes downstream is quick and deadly. This potential for disastrous flash flooding poses a grave threat to many communities located downstream of dams. Indeed, a report by the U.S. Army (1975) indicates 20,000 dams in the U.S. are "so located that failure of the dam could result in loss of human life and appreciable property damage ..." This report, as well as the tragic destruction resulting from the failures of the Buffalo Creek coal-waste dam, the Toccoa Dam, the Teton Dam, and the Laurel Run Dam, underscores the real need for accurate and prompt forecasting of dam-break flooding.

Advising the public of downstream flooding during a dam failure emergency is the responsibility of the National Weather Service (NWS). To aid NWS flash flood hydrologists in forecasting the inundation resulting from dam-failures, the numerical NWS Dam-Break Flood Forecasting Model (DAMBRK) (Fread 1977,1980) was developed for use with large, high-speed computers to model the outflow hydrograph produced by a time-dependent, partial dam breach, and route this hydrograph downstream using the complete one-dimensional unsteady flow equations while accounting for the effects of downstream dams, bridges, and off-channel storage. However, in some situations the real-time use of the DAMBRK model may be precluded because warning-response time is extremely short or adequate computing facilities are not available.

To alleviate this potential problem and attempt to improve upon the accuracy and versatility of existing simplified dam breach modelling procedures, the NWS has developed the Simplified Dam-Break (SMPDBK) Flood Forecasting Model. With this model, the user may within minutes produce forecasts of the dam-break floodwave peak discharges, stages, and travel times. It should be noted, however, that the use of the NWS SMPDBK model is not limited to NWS flash flood hydrologists. Planners, designers, civil defense officials, and consulting engineers who are concerned with the potential effects of a dam failure and who have limited time, resources, data, computer facilities, and/or experience with unsteady flow models may also wish to employ the model to delineate the areas facing danger in a dam-break emergency.

This document presents an outline of the NWS SMPDBK model's conceptual basis. Appendix I gives a step-by-step guide and example of the computations involved in the model. Appendix II presents the FORTRAN computer code for the automated (mini/micro-computer) version of the model and an example run of that version. Appendix III presents the BASIC computer code for the microcomputer or programmable hand-held computer version of the model. Appendix IV presents the HP41C hand-held computer version of the model.

II. MODEL DEVELOPMENT

The SMPDBK model retains the critical deterministic components of the numerical DAMBRK model while eliminating the need for large computer facilities. SMPDBK accomplishes this by approximating the downstream channel as a prism, neglecting the effects of off-channel storage, concerning itself with only the peak flows, stage, and travel times, neglecting the effects of backwater from downstream bridges and dams, and utilizing dimensionless peak-flow routing graphs developed using the NWS DAMBRK model. The applicability of the SMPDBK model is further enhanced by its minimal data requirements; the peak flow at the dam may be calculated with only four readily accessible data values and the downstream channel may be defined by a single "average" cross-section, although prediction accuracy increases with the number of cross-sections specified.

Three steps make up the procedure used in the SMPDBK model. These are: (1) calculation of the peak outflow at the dam using the temporal and geometrical description of the breach and the reservoir volume; (2) approximation of the channel downstream of the dam as a prismatic channel; and (3) calculation of dimensionless routing parameters used with dimensionless routing curves to determine the peak flow at specified cross sections downstream of the dam.

2.1 Breach Description

Most investigators of dam-break flood waves have assumed that the breach or opening formed in a failing dam encompassed the entire dam and occurred instantaneously. While this assumption may be valid for a few concrete arch dams, it is not valid for the exceedingly large number of earth dams. Because earthen dams generally do not fail completely nor instantaneously, the SMPDBK model allows for the investigation of partial failures occurring over a finite interval of time. And, although the model assumes a rectangular-shaped breach, a trapezoidal breach may be analyzed by specifying a rectangular breach width that is equal to the average width of

the trapezoidal breach. Failures due to overtopping of the dam and/or failures in which the breach bottom does not erode to the bottom of the reservoir may also be analyzed by specifying an appropriate "H" parameter which is the elevation of the reservoir water surface elevation when breach formation commences minus the final breach bottom elevation (i.e., "H" is the depth to which the breach cuts).

The model uses a single equation to determine the maximum breach outflow and the user is required to supply the values of four variables for this equation. These variables are: 1) the surface area of the reservoir; 2) the depth to which the breach cuts; 3) the time required for breach formation; and 4) the final width of the breach. (Note: For "pre-event" analyses, the user must estimate the last three variables above. To assist in this estimation, the following table of default values is provided.)

Table 1—Default Values for Breach Description

Value	Units	Description	Default
H	ft	Depth to which breach cuts	Height of dam
B_f	ft	Final breach width	3 x breach depth (earth dams) 1/4 - 1/2 dam width (concrete gravity dams) Entire dam width (concrete arch dams)
t_f	minutes	Time of failure	H/3 (earth dams) H/1000 (concrete dams)

Once the maximum outflow at the dam has been computed, the depth of flow produced by this discharge may be determined based on the geometry of the channel immediately downstream of the dam, the Manning "n" (roughness coefficient) of the channel and the slope of the downstream channel. This depth is then compared to the depth of water in the reservoir to find whether it is necessary to include a submergence correction factor for tailwater effects on the breach outflow (i.e., to find whether the water downstream is restricting the free flow through the breach). This comparison and (if necessary) correction allows the model to provide the most accurate prediction of maximum breach outflow which properly accounts for the effects of tailwater depth downstream of the dam.

2.2 Channel Description

The river channel downstream of the dam to the specified routing point is approximated as a prismatic channel by defining a single cross section (an average section that incorporates the geometric properties of all intervening sections via a distance weighting technique) and fitting a mathematical function that relates the section's width to depth. This prismatic representation of the channel allows easy calculation of flow area and volume in the downstream channel which is required to accurately predict the amount of peak flow attenuation.

Approximating the channel as a prism requires three steps. First, topwidth vs. depth data must be obtained from topographic maps or survey

notes. For each depth (h_i), a distance weighted topwidth $\bar{B}_i$ is defined producing a table of values that may be used for fitting (using least-squares or a log-log plot) a single equation of the form $B = Kh^m$ to define the prismatic channel geometry.

For rivers with very steep valley side-walls adjacent to the channel (see Fig. 1a), an additional parameter (h_v) may be specified to indicate the depth at which the channel geometry no longer follows the $B = Kh^m$ relation. As can be seen in Fig. 1b, this feature allows for a more accurate representation of the true channel-valley shape.

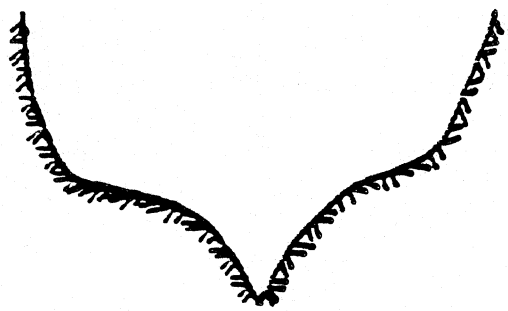

Fig. 1a. Typical Downstream Cross-Section

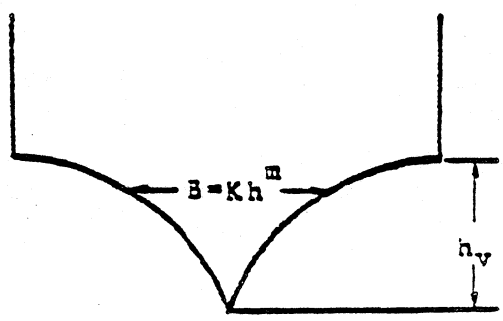

Fig. 1b. Approximated Prismatic Downstream Cross-Section

2.3 Downstream Routing

After the maximum breach outflow and stage have been calculated, it is necessary to route the flow downstream. This routing is achieved by employing dimensionless curves developed using the NWS DAMBRK model. These dimensionless curves are grouped into families (see Appendix Ia) and have as their X-coordinate the ratio of the downstream distance (from the dam to a selected cross section) to a distance parameter computed using the equations given in Appendix I. The Y-coordinate of the curves used in predicting peak downstream flows is the ratio of the peak flow at the selected cross section to the computed peak flow at the dam.

The distinguishing characteristic of each curve family is the Froude number developed as the floodwave moves downstream. The distinguishing characteristic of each member of a family is the ratio of the volume in the reservoir to the average flow volume in the downstream channel. Thus it may be seen that to predict the peak flow of the floodwave at a downstream point the user must first determine the desired distinguishing characteristic of the curve family and member. This determination is based on the calculation of the Froude number and the volume ratio parameter. To specify the distance in dimensionless form, the distance parameter must also be computed. The equations required for these computations, as well as the equations for determining the peak stage at forecast points are presented in Appendix I.

The time of occurrence of the peak flow at a selected cross section is determined by adding the time of failure to the peak travel time from the dam to that cross section. The travel time is computed using the kinematic wave velocity which is a known function of the average flow velocity throughout the routing reach. The times of first flooding and "de-flooding" of a particular elevation at the cross section may also be determined when the user provides the selected elevation.

III. MODEL CONFIGURATIONS

The SMPDBK model was developed for use in dam failure analyses when time is short or where main frame (large) computer facilities are unavailable to the user. For the first reason above, the model's data requirements have been kept to a minimum. For the second reason, the model's computational requirements have also been kept to a minimum such that it can be employed with small (mini- or micro-) computer systems or even with a simple, non-programmable, hand-held calculator. To allow for these three applications, the model has three versions. The first version, known as the "manual" version, allows the user, employing only an inexpensive calculator and the routing curves provided in Appendix Ia, to produce forecasts of the dam-break floodwave peak discharges, stages, and travel times at selected downstream points. To accomplish this, the user simply follows the step-by-step guide provided in Appendix I for making the required calculations, providing data input where necessary, and selects the indicated values from the routing curves.

The second version, known as the "FORTRAN Mini/Micro-computer" version has been, as its name implies, developed for use on mini-computers or micro-computers with a FORTRAN compiler. The computational procedure followed by this verion is the same as that followed in the manual version; however, the computations are made by the computer rather than the user, thus significantly reducing the time required to prepare a forecast. This version was developed for interactive use and prompts the user for information (data) as it is needed, automatically using default values (where applicable) when the user is unable to provide them. Included in this version is a "short" option that may be employed when the only channel cross-section data available is that describing the dam face; the model assumes a constant channel configuration and provides forecast information at seven user-specified points downstream. A copy of the FORTRAN code for this version and an example run are provided in Appendix II.

The third version of the model, or the "micro-BASIC" version, has been developed for use on micro-computers with BASIC compilers. This version performs the same computations and requires the same data input as the FORTRAN version and its storage requirements are small enough for it to fit on most micro-computers. The "short" option available in the FORTRAN version is provided in this version as well. Also, a hybrid of this version has been developed for use on a hand-held, programmable computer (See Appendices IIIa and IV). A listing of the BASIC code and an example run is included in Appendix III.

IV. CONCLUDING REMARKS

In both real-time forcasting and disaster preparedness planning, there is a clear need for a fast and economical method of predicting dam-break floodwave peak stages and travel times. The SMPDBK model fills this need, producing such predictions quickly, inexpensively and with reasonable accuracy. For example, in test analyses of the Teton and Buffalo Creek dam failures, approximating the channel as a prism, calculating the maximum breach outflow and stage at the dam, defining the routing parameters, and evaluating the peak stage and travel time to the forecast points required less than 20 minutes of time with the aid of a non-programable hand-held calculator while the average error in forecasted peak flow and travel time was 10-20% with stage errors of approximately 1 ft. Furthermore, comparisons of SMPDBK model results with DAMBRK model results from test runs of theoretical dam breaks show the simplified model produces average errors of 10% or less. The authors had the advantages, however, of prior experience with the model and possession of all required input data, the collection of which consumes precious warning response time in a dam-break emergency.

To help reduce the time required for data collection, default values for some of the input data are presented in Appendix I. These default values may be used by dam-break flood forecasters when time is short and reliable data are unavailable. Additionally, to help further reduce the time needed to employ the model, computerized versions of the model have been developed for FORTRAN-compatible mini-computers and for BASIC language micro-computers and programmable hand-held computers (see Appendices II and III.)

The SMPDBK model is not only useful in a dam-break emergency, it is also suitable for pre-computation of flood peak elevations and travel times prior to a dam failure. Pre-computation of dam failures allows those responsible for community preparedness to delineate danger areas downstream should the dam fail. Ideally, to obtain the most reliable estimate of probable flood elevations and travel times, the sophisticated NWS DAMBRK model would be used in a long-term disaster preparedness study where sufficient computer resources are available. However, for short term studies with limited resources, the SMPDBK model will be most helpful in defining approximate peak stages, discharges, and travel times.

In closing, the authors would like to stress that while the SMPDBK model can be a very useful tool in preparing for and during a dam failure event, the user must keep in mind the model's limitations (Fread 1981). First of all, as with all dam breach flood routing models, the validity of the SMPDBK model's prediction depends upon the accuracy of the required

input data, whether these data be supplied by the user or provided as default "most probable" values by the model. To produce the most reliable results, the user should endeavor to obtain the best estimates of the various input parameters that time and resources allow. Secondly, because the model assumes normal, steady flow at the peak, the backwater effects created by downstream channel constrictions such as bridge embankments or dams cannot be accounted for and the model will predict peak depths upstream of the constriction that may be substantially lower than those actually encountered, while peak depths downstream of the constriction may be over predicted. Finally, because the "slowing down" of the floodwave caused by temporary off-channel dead storage is not accounted for by the model, the predicted time to peak at a certain point may be somewhat shorter than the actual time to peak. Recognizing these limitations and exercising good engineering judgement, the SMPDBK model user may obtain useful dam break flood inundation information with relatively small expense of time and computing resources.

V. BIBLIOGRAPHY

Davies, W.E., J.F. Bailey, and D.B. Kelly, 1972: "West Virginia's Buffalo Creek Flood: A Study of the Hydrology and Engineering Geology." Geological Survey, Circular 667, U.S. Geological Survey, Washington, D.C., 1972, 32 pp.

Fread, D.L., 1977: "The Development and Testing of a Dam-Break Flood Forecasting Model." Proceedings, Dam-Break Flood Modelling Workshop, U.S. Water Resources Council, Washington, D.C., 1977, pp. 164-197.

Fread, D.L., 1980: "DAMBRK: The NWS Dam-Break Flood Forecasting Model." Office of Hydrology, National Weather Service (NWS), Silver Spring, Md., 1980, 37 pp.

Fread, D.L., 1981: "Some Limitations of Dam Breach Flood Routing Models," Preprint, ASCE Fall Convention, St. Louis Missouri, Oct 26-30, 1981.

McQuivey, R.S. and T.N. Keefer, 1975: "Application of a Simple Dambreak Routing Model." Proceedings, 16th Congress IAHR, Vol. II, Sao Paulo, Brazil, 1975, pp. 315-324.

Ray, H.A., L.C. Kjelstrom, E.G. Crosthwaite, and W.H. Low, 1976: "The Flood in Southeastern Idaho from the Teton Dam Failure of June 5, 1976." Unpublished open file report, U.S. Geological Survey, Boise, Idaho.

Saakas, J.G., and T. Strelkoff, 1973: "Dam-Break Flood in a Prismatic Dry Channel." Journal of the Hydraulics Division, ASCE, Vol. 99, No. HY12, Proc. Paper 10233, Dec. 1973, pp. 2195-2216.

SCS, 1979: "Simplified Dam-Breach Flood Routing Procedure." Technical Release No. 66, Engineering Division, USDA Soil Conservation Service, 1979, 23 pp.

U.S. Army Corps of Engineers, 1975: National Program of Inspection of Dams, Vol. I-V, Dept. of the Army, Office of Chief of Engineers, Washington, D.C.

APPENDIX I

THE NWS SIMPLIFIED DAM BREAK MODEL
PROGRAM DOCUMENTATION AND USERS' GUIDE
WITH EXAMPLE PROBLEM

The following User Guide is intended to familiarize the user with the Simplified Dam Break Model's data requirements and the computations it performs in producing the information necessary for delineating endangered areas downstream of a failed dam. Briefly stated the model calculates the maximum outflow at the dam, evaluates how this flow will be reduced as it moves from the dam to the downstream point(s) specified by the user, determines the depth attained by this flow at the point(s) and finally computes the time required for the flow to reach the point(s). All of these calculations utilize information (data) supplied by the user, a summary of which is given below. The user should note that while the model supplies default values for many of these input variables, the most accurate results are produced when the most accurate data is entered and the authors strongly urge the use of the best possible estimates of variable values for each study case.

Table A. Simplified Dam Break Model Input Variables

Dam Crest Elevation (Top of Dam)

Final Breach Bottom Elevation

Reservoir Storage Volume

Reservoir Surface Area

Final Breach Width

Time Required for Breach Formation

Turbine / Spillway / Overtopping Flow (at time of failure)

Topwidth (distance between equal contours) vs. (contour) Elevation data for one or more downstream river valley cross-sections

Manning Roughness Cofficient (estimate for each given cross-section)

Flood Depth (depth at which flooding becomes a problem) at each cross-section

Height of Valley Wall (required for routing through canyons)

Channel Bottom Slope (required if only one downstream cross-section given)

MAXIMUM BREACH OUTFLOW DISCHARGE AND DEPTH CALCULATION

To determine the maximum breach outflow (Q_{bmax}) from the dam the user must first obtain the following data values:

A_s - Reservoir surface area (acres) at maximum pool level
H - Depth (ft) of maximum pool level above final breach elevation
B_r - Average final breach width (ft)
t_f - Time of failure (minutes)
Q_o - Additional (non-breach) outflow (cfs) at time t_f (i.e., spillway flow, turbine flow, and/or crest overflow) (optional data value, may be set to 0.)

Defaults: The reservoir surface area may be estimated to be equal to twice the reservoir volume divided by the dam height. The breach depth, H, may be set equal to the height of the dam. The average final breach width may be estimated to be one to three times the height of the earth dam and the entire width of a concrete arch dam. The time of failure may be estimated to be near zero for a concrete arch dam (see following subsection on instantaneous failure) while the breach erosion rate for earth dams is generally around 2 feet per minute (i.e., t_f minutes = H/3).

These values are substituted into the broad-crested weir flow equation to yield the maximum breach outflow (Q_{bmax}) in cfs, i.e.

$$Q_{bmax} = Q_o + 3.1\, B_r \left(\frac{C}{\frac{t_f}{60} + \frac{C}{\sqrt{H}}} \right)^3 \qquad (1)$$

$$\text{where } C = \frac{23.4\, A_S}{B_r} \qquad (2)$$

Instantaneous Failure

In some situations where a dam fails very rapidly, the negative wave that forms in the reservoir may significantly affect the outflow from the dam. In such cases, a special equation (Eq. (1a)) must be used to compute the maximum breach outflow. The constraint that indicates whether Eq. (1a) should be used is as follows:

If time of failure in min. $(t_f) < 0.001$ * Height of dam in feet (H_d), then:

$$Q_{bmax} = 3.1\ B_r\ (I_v\ I_a)\ H_d^{3/2} \tag{1a}$$

where:

$$I_v = \left[1.0 + 0.148 \left(\frac{B_r}{B}\right)^2 (m+1)^2 - 0.083 \left(\frac{B_r}{B}\right)^3 (m+1)^{5/2}\right]^{3/2} \tag{3}$$

$$I_a = \left[1.0 - 0.5467 \left(\frac{B_r}{B}\right) (m+1)^{1/2} + 0.2989 \left(\frac{B_r}{B}\right)^2 (m+1)^{1/4} - 0.1634 \left(\frac{B_r}{B}\right)^3 (m+1)^{1/8} + 0.0893 \left(\frac{B_r}{B}\right)^4 (m+1)^{1/16} - 0.0486 \left(\frac{B_r}{B}\right)^5 (m+1)^{1/32}\right]^{3/2} \tag{4}$$

where: B_r = Breach width

B = Valley topwidth at dam crest

H_d = Height of dam

m = Channel fitting coefficient

Maximum Depth Calculation

Once the maximum outflow has been calculated, the maximum depth (h_{max}) at the downstream face of the dam must be determined. To do this, the cross section (X-section) at the downstream face of the dam must first be "fitted" (approximated) with an equation of the form $B = Kh^m$ (topwidth = K * depth^m) where K and m are the fitting coefficients computed using the following least squares algorithm:

$$m = \frac{\sum \left[(\log h_i)\ (\log \bar{B}_i)\right] - \dfrac{(\sum \log h_i)\ (\sum \log \bar{B}_i)}{I}}{\sum (\log h_i)^2 - \dfrac{(\sum \log h_i)^2}{I}} \qquad (5)$$

$$\log K = \frac{\sum \log \bar{B}_i}{I} - m\left(\frac{\sum \log h_i}{I}\right) \qquad (6)$$

$$K = 10^{(\log K)} \qquad (6a)$$

where: B_i is the topwidth associated with depth h_i, $i = 1,2,3,\ldots I$ (total number of topwidths)

For rivers with very steep valley side-walls adjacent to the channel (see figure 1a), an additional parameter (h_v) may be specified to indicate the depth at which the channel geometry no longer follows the $B = Kh^m$ relation. As can be seen in Figure 1b, this feature allows for a more accurate representation of the true channel-valley shape.

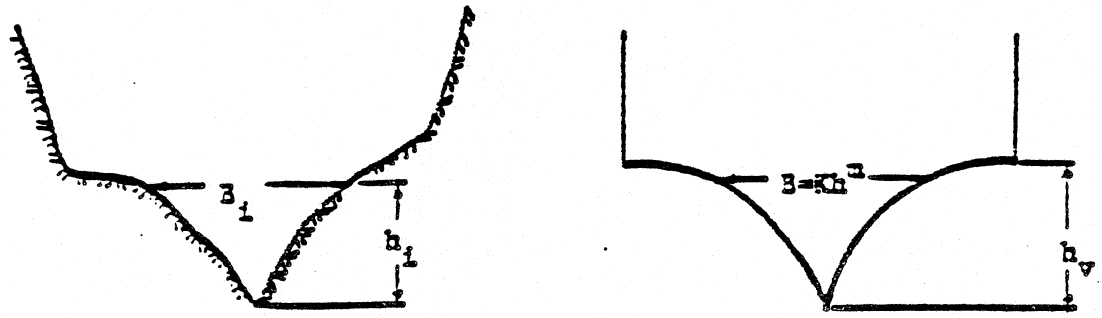

Figure 1 (a) and (b)

Once the K and m parameters have been computed for the dam face cross section, the flow (Q_v) that produces the depth (h_v) (shown above) must be evaluated and compared with Q_{bmax} to determine whether the maximum depth is above or below h_v. The flow Q_v is evaluated using the Manning equation, i.e.,

$$Q_v = \frac{1.49}{n} \; S^{1/2} \left(\frac{K}{(m+1)^{5/3}} \right) \; h_v^{(m + 5/3)} \tag{7}$$

where: n = Manning roughness coefficient

S = Channel bottom slope immediately downstream of dam

K & m = Channel fitting coefficients

Note: The Manning roughness coefficient may be estimated to be 0.04 for a cross-section located in an area of pastureland, .07 for a moderately wooded area and 0.10-0.15 for a heavily wooded area (use the higher value to account for effects caused by significant amounts of debris in the downstream valley).

If Q_v is found to be <u>greater</u> than Q_{bmax}, then h_v must be greater than h_{max}, and h_{max} is determined using the relation:

$$h_{max} = \left(\frac{Q_{bmax}}{a} \right)^{1/b} \tag{8}$$

where

$$a = \frac{1.49}{n} \; S^{1/2} \; \frac{K}{(m+1)^{5/3}} \tag{9}$$

$$b = m + 5/3 \tag{10}$$

If however, Q_v is found to be <u>less</u> than Q_{bmax} then h_v must be less than h_{max}, and h_{max} is calculated as follows:

$$h_{max} = \rho\left(Q_{bmax}\right)^{3/5} + \gamma\ h_v \tag{11}$$

where:

$$\rho = \left[\frac{1}{a(m+1)^{5/3}\ h_v^{\ m}}\right]^{3/5} \tag{12}$$

$$\gamma = \frac{m}{m+1} \tag{13}$$

and a is defined by Eq. (9).

Submergence Correction[1]

The maximum breach outflow must be corrected iteratively for submergence resulting from tailwater effects if the computed maximum outflow stage (h_{max}) is greater than (0.67 h_{weir}) where h_{weir} is the head over the weir (breach) at time t_f as expressed by the following relation:

$$h_{weir} = \left(\frac{C}{t_f + \frac{C}{\sqrt{H}}}\right)^2 \tag{14}$$

where C is defined by Eq. (2).

If the ratio of (h_{max}/h_{weir}) is greater than 0.67, a sumbergence correction factor must be computed as follows:

$$K_s^{\ *} = 1 - 27.8\left[\frac{h_{max}}{h_{weir}} - 0.67\right]^3 \tag{15}$$

---

[1] Note: Submergence correction need not be made in the event of an instantaneous failure.

This value for K_s^* is substituted into Eq. (15a) to obtain an <u>averaged</u> submergence correction factor given by the following:

$$K_s^k = \frac{K_s^* + K_s^{k-1}}{2} \tag{15a}$$

where the k superscript is the iteration counter and the first iteration value for K_s^0 is 1.

Note: In some situations, the correction factor K_s^*, may be computed to be less than 0.8, in which case it should be reset to 0.8 to prevent over-compensating for submergence in the first iteration.

This correction factor is applied to the breach outflow to compute the corrected breach outflow as follows:

$$Q_b^k = K_s^k \cdot Q_b^{k-1} \tag{16}$$

where: $Q_b^{k-1} = Q_{bmax}$ in the first iteration

The corrected breach outflow (Q_b^k) is then compared with Q_v, and a new outflow depth (h_{max}^k) is calculated using Eq. (8) or (11). Also, because there is decreased flow through the breach, there is less drawdown. Thus, the head over the weir (h_{weir}) must be recalculated using the relation:

$$h_{weir}^k = h_{weir}^{k-1} + Q_b^{k-1} - Q_b^k \frac{t_f \text{ (sec.)}}{2A_s \text{ (sq.ft.)}} \tag{17}$$

Now the ratio of the two new values, h_{max}^k/h_{weir}^k is used in Eq. (15) to compute a new submergence correction factor.

If the new maximum breach outflow computed via Eq. (16) is significantly different (± 5%) from that computed in the previous iteration, the procedure is repeated. Generally, within two or three iterations the K_s value will converge and a suitable value for the maximum breach outflow (Q_b) is achieved which properly accounts for the effects of submergence.

EXAMPLE MAXIMUM BREACH OUTFLOW DISCHARGE AND DEPTH CALCULATION

The following data on the reservoir and breach are gathered:

Reservoir surface area at max pool level,	A_s, = 350 acres
Height of max pool level above final breach elevation	H, = 50 ft
Average final breach width (estimated),	B_r, = 100 ft
Time to maximum breach size (time of failure),	t_f, = 45 minutes
Additional outflow at time t_f,	Q_o, = 5000 cfs

These values are substituted into Eqs. (1) and (2) to determine the maximum breach outflow, i.e.

$$C = \frac{23.4\ (350)}{100} = 81.9$$

$$Q_{bmax} = 3.1(100)\left(\frac{81.9}{\frac{45}{60} + \frac{81.9}{\sqrt{50}}}\right)^3 + 5000 = \underline{\underline{95800\text{cfs}}}$$

From a topographic map the following cross-sectional data is obtained:

Table 1 — X-SECTION DATA FOR EXAMPLE PROBLEM

Mile 0.0		Mile 12.3		Mile 40.5	
Elev	Topwidth	Elev	Topwidth	Elev	Topwidth
5532	0	5483	0	5370	0
5540	480	5490	400	5380	590
5550	900	5500	770	5390	930
5560	1300	5510	1330	5400	1440
5570	1350	5520	1400	5410	1460

To compute the K and m fitting coefficients for the X-section at the downstream face of the dam, the X-sectional data at mile 0.0 is reduced by subtracting the channel invert elevation from the elevation associated with each topwidth, producing table 2.

Table 2 — TOPWIDTH VS. DEPTH AT DAM FOR EXAMPLE PROBLEM

Depth	Topwidth
0	0
8	480
18	900
28	1300
38	1350

Examination of this reduced data indicates that, because the topwidths increase very slowly above a depth of approximately 30 feet, a reasonable value for h_y is 30.

This reduced data is used in Eqs. (5)-(6a) to determine the K and m coefficients of the equation $B = Kh^m$.

Table 3 — VALUES USED IN LEAST SQUARES COMPUTATION OF K AND M COEFFICIENTS AT DAM

i	h_i	$\log h_i$	$(\log h_i)^2$	B_i	$\log B_i$	$(\log h_i)(\log B_i)$
1	8	0.90	0.82	480	2.68	2.42
2	18	1.26	1.58	900	2.95	3.71
3	28	1.45	2.09	1300	3.11	4.51
-	h_y	-	-	-	-	-
4	30	1.48	2.18	1310*	3.12	4.60
	=	5.08	6.67		11.87	15.24

*Linearly interpolated.

$$m = \frac{15.24 - \frac{(5.08)(11.87)}{4}}{6.67 - \frac{(5.08)^2}{4}} = 0.78$$

$$\text{Log } K = \frac{11.87}{4} - 0.78 \left(\frac{5.08}{4}\right) = 1.98$$

$$K = 10^{\log K} = 95.76$$

To calculate the maximum depth at the dam, the value of Q_v must first be determined using Eq. (7). The channel bottom slope immediately downstream of the dam, S, is determined from the X-sectional data, i.e.,

$$S = \frac{(5532 - 5483)}{(12.3)\ (5280)} = 0.0008$$

and the Manning roughness coefficient, n, for the downstream channel is estimated to be 0.045.

Thus Q_v is calculated as follows:

$$Q_v = \frac{1.49}{.045} (.0008)^{1/2} \left(\frac{95.76}{(0.78 + 1)^{5/3}}\right) (30)^{(0.78 + 5/3)} = 136976 \text{ cfs}$$

Because Q_v is greater than Q_{bmax} (95800 cfs), Eq. (8) is used to determine h_{max}, i.e.,

$$a = \frac{1.49}{.045} (.0008)^{1/2} \left(\frac{95.76}{(0.78 + 1)^{5/3}}\right) = 33.31$$

$$b = 0.78 + 5/3 = 2.45$$

$$h_{max} = \frac{95800}{33.31}^{(1/2.45)}$$

$$\underline{h_{max} = 25.81 \text{ ft}}$$

To check for submergence, the head over the weir (breach), h_{weir}, is calculated using Eq. (14), i.e.,

$$h_{weir} = \left(\frac{81.9}{\frac{45}{60} + \frac{81.9}{\sqrt{50}}} \right)^2 = 44.1 \text{ ft}$$

Then the ratio of h_{max} to h_{weir} is checked as follows:

$$\frac{h_{max}}{h_{weir}} = \frac{25.81}{44.10} = 0.59$$

Because the ratio is less than 0.67, the tailwater does not affect breach outflow.

DOWNSTREAM ROUTING

The peak outflow discharge determined in the preceding step may be routed downstream using the dimensionless routing curves in Appendix Ia. These curves were developed from numerous executions of the NWS DAMBRK Model and they are grouped into families based on the Froude number associated with the floodwave peak. To determine the correct family and member curve that most accurately predicts the attenuation of the flood, the user must first define certain routing parameters.

Prior to defining the routing parameters, however, the user must first describe the river channel downstream from the dam to the first routing point as a prism. To describe the river channel downstream of the dam as a prismatic channel the user must reduce the topwidth vs. elevation data (see table 1) for the first two cross-sections. This cross-section data is reduced (see table 4, p. I-24) to depth (h) vs. topwidth (B) data by subtracting the channel invert elevation from the elevation associated with each topwidth at a given cross-section. From this reduced data, an average cross section may be determined using the following algorithm.

For each depth (h_i), the average topwidth ($\bar{B}_i$) is given by the relation:

$$\bar{B}_i = \frac{(B_{i,1} + B_{i,2})}{2} \qquad (18)$$

Where: h_i is the ith depth, $i = 1,2,3 \ldots I$ (number of topwidths per X-Section)

$B_{i,j}$ is the ith topwidth (corresponding to the ith depth h_i) at the jth X-section where $j = 1,2$

$\bar{B}_i$ is the average i^{th} topwidth

Note: The preceding calculation is unnecessary when depth vs. topwidth data is available for only <u>one</u> X-section.

The table of values produced by defining an average topwidth ($\bar{B}_i$) for each depth (h_i) may then be used for fitting (using least squares or a log-log plot) a single equation of the form $B = Kh^m$ to define the prismatic channel geometry. The fitting coefficients K and m may be computed using the following least squares algorithms:

$$\bar{m} = \frac{\sum \left[(\log h_i)(\log \bar{B}_i) \right] - \frac{\left(\sum \log h_i\right)\left(\sum \log \bar{B}_i\right)}{I}}{\sum (\log h_i)^2 - \frac{\left(\sum \log h_i\right)^2}{I}} \tag{5a}$$

$$\log \bar{K} = \frac{\sum \log \bar{B}_i}{I} - m\left(\frac{\sum \log h_i}{I}\right) \tag{6b}$$

$$\bar{K} = 10^{(\log K)} \tag{6c}$$

Using these average cross-section fitting coefficients, the user must recompute the maximum depth at the dam using Eq. (8) or (11). Note, however, that a new check for submergence need not be made. This redefined value for h_{max} will be used in computing the routing parameters given in the following section.

Routing Parameters

The distance parameter (X_c) is calculated using either Eq. (19) or (19a). If the height (H_d) of the dam is less than h_v (defined earlier), the distance parameter is computed as follows:

$$X_c \text{ (ft)} = \frac{(\bar{m}+1)}{\bar{K}} \left(\frac{VOL_r}{H_d^{\bar{m}+1}}\right) \left(\frac{6}{1 + 4\,(0.5)^{\bar{m}+1}}\right) \tag{19}$$

where: VOL_r = volume in reservoir (cubic ft)

$\bar{K}$ & $\bar{m}$ = average channel geometry fitting coefficients

H_d = height of dam (ft)

If the height (H_d) of the dam is greater than h_v, the equation for X_c is given by the following:

$$X_c \text{ (ft)} = \frac{6\ VOL_r}{\bar{K}h_v^{\bar{m}}\left(3H_d - 5\dfrac{\bar{m}h_v}{\bar{m}+1}\right)} \tag{19a}$$

Within the distance (X_c) in the downstream reach, the floodwave attenuates such that the depth at point X_c is h_x (see figure 2), which is a function of the maximum depth (h_{max}). The average depth ($\bar{h}$) in this reach is:

$$\bar{h} = \frac{h_{max} + h_x}{2} = \theta\ h_{max} \tag{20}$$

where θ is an empirical weighting factor that must be determined iteratively. The starting estimate for θ is 0.95.

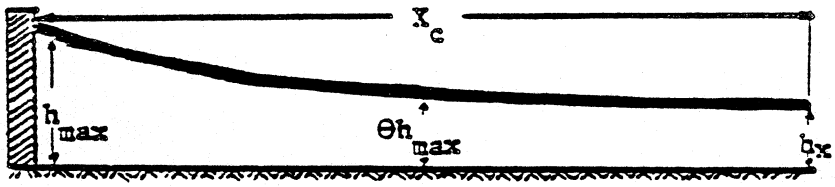

Figure 2

The average <u>hydraulic</u> depth (D_c) in the reach is given by Eq. (21) or (22) as follows:

CASE I: If ($Q_{b_{max}} < Q_v$), then $$D_c = \frac{\theta\ h_{max}}{m+1} \tag{21}$$

CASE II: If ($Q_{b_{max}} > Q_v$), then $$D_c = \theta\ h_{max} - h_v + \frac{h_v}{m+1} \tag{22}$$

The average velocity in the reach is given by the Manning equation, i.e.:

$$V_c = \frac{1.49}{n} S^{1/2} \left(D_c\right)^{2/3} \tag{23}$$

where S is the slope of the channel from the dam to the routing point.

The average velocity (V_c) and hydraulic depth (D_c) are substituted into Eq. (24) to determine the average Froude number (F_c) in the reach as follows:

$$F_c = \frac{V_c}{\sqrt{gD_c}} \tag{24}$$

where: $g = 32.2$ ft/sec^2 (acceleration of gravity)

The dimensionless volume parameter (V^*) that identifies the specific member of the curve family for the computed Froude number is the ratio of the reservoir storage volume to the average flow volume within the X_c reach. The average cross sectional area of flow (A_c) is given by Eq. (25) or (26) as follows:

CASE I: if ($Q_{b_{max}} < Q_v$), then $$A_c = \bar{K}(\theta\, h_{max})^{\bar{m}}\, D_c \tag{25}$$

CASE II: if ($Q_{b_{max}} > Q_v$), then $$A_c = \bar{K} h_v^{\bar{m}}\, D_c \tag{26}$$

The volume parameter (V^*) is determined by dividing the average flow volume ($A_c X_c$) into the reservoir storage volume (VOL_r), i.e.:

$$V^* = \frac{VOL_r}{A_c X_c} \tag{27}$$

To summarize this section on routing parameter calculation and to allow for quick reference, the following table of equations is presented.

SIMPLIFIED DAMBREAK ROUTING PARAMETER EQUATIONS

Parameter	Case I	Equation	Eq. No.	Case II	Equation	Eq. No.
X_c (ft)	$H_d < h_v$	$X_c = \frac{\bar{m}+1}{\bar{K}} \frac{VOL._r}{H_d^{\bar{m}+1}} \left[\frac{6}{1+4(0.5)^{\bar{m}+1}}\right]$	(19)	$H_d > h_v$	$X_c = \left[\frac{VOL._r}{\bar{K} h_v^{\bar{m}}}\right]\left[\frac{6}{3H_d - 5\frac{\bar{m}h_v}{\bar{m}+1}}\right]$	(19a)
θ	all cases	$\theta = 0.95^*$				
D_c (ft)	$Q_{b_{max}} < Q_v$	$D_c = \frac{\theta\, h_{max}}{\bar{m}+1}$	(21)	$Q_{b_{max}} > Q_v$	$D_c = \theta\, h_{max} - h_v + \frac{h_v}{\bar{m}+1}$	(22)
V_c (ft/s)	all cases	$V_c = \frac{1.49}{n} S^{1/2} (D_c)^{2/3}$	(23)			
F_c	all cases	$F_c = \frac{V_c}{\sqrt{g\, D_c}}$	(24)			
A_c (ft^2)	$Q_{b_{max}} < Q_v$	$A_c = \bar{K} (\theta\, h_{max})^{\bar{m}} D_c$	(25)	$Q_{b_{max}} > Q_v$	$A_c = \bar{K}\, h_v^{\bar{m}} D_c$	(26)
V^*	all cases	$V^* = \frac{VOL._r}{A_c X_c}$	(27)			

*Note: Further discussion of the value of θ follows.

Routing Curves

Knowing the value of F_c and V^*, the user may consult the specific curve (see Appendix Ia) defined for these values (interpolation may be necessary) and check the original estimate of the value of θ used in Eq. (21)-(27). The ordinate of the routing curve at $X^* = 1$ is the ratio of the peak flow (Q_p) at X_c to $Q_{b_{max}}$. Knowing Q_p, the user may determine the stage (h_x) at X_c using Eq. (8) or (11) with the average channel fitting coefficients. The value of θ is checked by rearranging Eq. (20), i.e.:

$$\theta = \frac{h_{max} + h_x}{2\, h_{max}} \tag{28}$$

If there is a significant difference in the new value of θ from the initial estimate of θ (e.g., ±5%), Eqs. (21)-(27) should be recalculated and the new value of θ rechecked. Generally, within two passes the value for θ will converge.

Knowing the proper routing curve for predicting peak flow attenuation, the user may then non-dimensionalize the distance(s) downstream to the forecast point(s) using the relation.

$$X_i^* = \frac{X_i}{X_c} \tag{29}$$

where X_i is the downstream distance to the ith forecast point, $i = 1,2,3,\ldots$

To find the peak flow at X_i, the user consults the proper family of routing curves and finds the ordinate of the specific V^* curve at X_i^*. Multiplying the value of this ordinate by $Q_{b_{max}}$ produces the peak flow (Q_p) at X_i miles downstream of the dam.

The time of travel for the floodwave to X_i is computed by first calculating the reference flow velocity at the midpoint between the dam and X_i. The user must determine, from the routing curve, the peak flow ($Q_{x/2}$)

at $(X_i/2)$ miles downstream of the dam. This flow is multiplied by the factor $(0.3 + \bar{m}/10)$ and substituted into Eq. (30) or (31) to find the reference depth (h_{ref}).

$$\text{If } Q < Q_v, \text{ then } \ldots\ h = \left(\frac{Q}{a}\right)^{1/b} \tag{30}$$

where a and b are defined by Eqs. (9 and 10).

$$\text{If } Q > Q_v, \text{ then } \ldots\ h = \rho\ Q^{3/5} + \gamma\ h_v \tag{31}$$

where ρ and γ are defined by Eq. (12) and (13).

The reference hydraulic depth is given by Eq. (32) or Eq. (33) i.e.:

$$\text{CASE I:} \quad \text{If } h_{ref} < h_v, \text{ then } D_{x_i} = \frac{h_{ref}}{m+1} \tag{32}$$

$$\text{CASE II:} \quad \text{If } h_{ref} > h_v, \text{ then } D_{x_i} = h_{ref} - h_v + \frac{h_v}{m+1} \tag{33}$$

The reference flow velocity is given by the Manning equation, i.e.:

$$V_{x_i}(ft/s) = \frac{1.49}{n} S^{1/2}\ D_{x_i}^{2/3} \tag{34}$$

This value for V_{x_i} is substituted into the wave celerity equation (Eq. (35)) to find the wave speed.

$$C(mi/hr) = 0.682\ V_{x_i}\left[5/3 - 2/3\left(\frac{\bar{m}}{\bar{m}+1}\right)\right] \tag{35}$$

The time to peak is then given by Eq. (36) as follows:

$$t_{p_i}(hr) = t_f(hr) + \frac{X_i(mi)}{C\ (mi/hr)} \tag{36}$$

where: t_f (hr) = time of failure for dam (minutes)/60

To compute the peak depth at mile X_i, the user must fit K and m coefficients for that X-section by substituting the specific depths and topwidths at mile X_i into Eqs. (5)-(6a). The peak flow at mile X_i is then compared with Q_v (Eq. (7)) and Eq. (30) or (31) is used to find the peak depth (h_{x_i}) at mile X_i.

The user may wish to determine the time at which flooding commences and/or the time at which it ceases. To do this, the user must first specify a flow rate, Q_f that corresponds with flood depth at the X-section.

$$Q_f = a\ h_f^{\ b} \tag{37}$$

where h_f = flood depth

and a and b are defined by Eqs. (9)-(10) using the K and m coefficients fitted for the X-section at mile X_i.

This value for Q_f is substituted into Eq. (38) to determine the time to flooding, t_{fld}, as follows:

$$t_{fld}(hr) = t_{p_i}(hr) - \left(\frac{Q_{p_i} - Q_f}{Q_{p_i} - Q_o}\right) t_f(hr) \tag{38}$$

where t_{p_i} is the time to peak calculated in Eq. (36)

t_f is the time of failure for the dam, and

Q_o is the nonbreach (spillway/turbine/overtopping) flow.

To determine the time flooding ceases, t_d, the value of Q_f is substituted into the following relation:

$$t_d(hr) = t_{p_i}(hr) + \left[\frac{24.2\ VOL_r}{Q_{p_i} - Q_o} - t_f(hr)\right]\left(\frac{Q_{p_i} - Q_f}{Q_{p_i} - Q_o}\right) \tag{39}$$

where VOL_r is the reservoir storage volume (ac-ft).

To route the peak flow downstream to cross sections 3,4,..., the user must determine the <u>distance weighted</u> average cross section between the dam and the routing point and fit new $\bar{K}$ and $\bar{m}$ parameters to this cross section. From the reduced data, a distance weighted average cross section may be determined using the following algorithm.

For each depth (h_i), the distance weighted topwidth ($\bar{B}_i$) is given by the relation:

$$\bar{B}_i = \frac{\frac{(B_{i,1} + B_{i,2})}{2}(X_2 - X_1) + \ldots + \frac{(B_{i,J-1} + B_{i,J})}{2}(X_J - X_{J-1})}{(X_J - X_1)} \tag{40}$$

Where: h_i is the ith depth, $i = 1,2,3 \ldots I$ (number of topwidths per X-section

$B_{i,j}$ is the ith topwidth (corresponding to the ith depth h_i) at the jth X-section where $j = 1,2,3, \ldots J$ (number of X-sections)

$\bar{B}_i$ is the <u>weighted</u> i^{th} topwidth

X_j is the downstream distance to the jth X-section.

The table of values produced by defining a distance weighted topwidth ($\bar{B}_i$) for each depth (h_i) may then be used for fitting a single equation of the form $B = Kh^m$ to define the prismatic channel geometry. The fitting coefficients $\bar{K}$ and $\bar{m}$ may be computed using the least squares algorithm given in Eqs. (5a)-(6c).

With these weighted average $\bar{K}$ and $\bar{m}$ coefficients, the user must then recompute a peak depth at the dam and new routing parameters using Eqs. (20)-(27). The user may then route the flow to cross-section 3,4, ... J by following the procedure given above.

EXAMPLE SIMPLIFIED DAMBREAK DOWNSTREAM ROUTING

To route the flow from the dam to the cross section at mile 12.3, the user must first define an average cross section for the reach and then fit $\bar{K}$ and $\bar{m}$ coefficients. Reducing the data given in Table 1 produces the following table.

Table 4.—TOPWIDTH VS. DEPTH FOR EXAMPLE PROBLEM

Mile 0.0		Mile 12.3	
Depth	Topwidth	Depth	Topwidth*
0	0	0	0
8	480	8	437
18	900	18	826
28	1300	28	1337
38	1350	38	1407

*Linearly interpolated to agree with depth value at mile zero.

To determine the average K-section, the depth vs. topwidth data is substituted into the relation given in Eq. (18), i.e.,

for $h_1 = 8$,

$$B_1 = \frac{480 + 437}{2} = 458.5$$

for $h_2 = 18$;

$$B_2 = \frac{900 + 826}{2} = 863$$

for $h_3 = 28$,

$$B_3 = \frac{1300 + 1337}{2} = 1318.5$$

The average cross section data is used in Eqs. (5a)-(6c) to determine the average $\bar{K}$ and $\bar{m}$ coefficients for the reach.

Table 5.— VAUES USED IN LEAST SQUARES COMPUTATION OF K AND M

i	h_i	$\log h_i$	$(\log h_i)^2$	B_i	$\log B_i$	$(\log h_i)(\log B_i)$
1	8	0.90	0.82	458	2.66	2.40
2	18	1.26	1.58	863	2.94	3.69
3	28	1.45	2.09	1318.5	3.12	4.52
-	h_v	-	-			
4	30	1.48	2.18	1330.5	3.12	4.61
		5.08	6.67		11.84	15.22

$$\bar{m} = \frac{15.22 - \frac{(508)\ (11.84)}{4}}{6.67 - \frac{(5.08)^2}{4}} = 0.82$$

$$\log \bar{K} = \frac{11.84}{4} - .82 \left(\frac{5.08}{4}\right) = 1.91$$

$$\bar{K} = 10^{\log \bar{K}} = 81.75$$

With these average $\bar{K}$ and $\bar{m}$ coefficients, the max depth at the dam may be recomputed using Eq. (8) as follows:

$$a = \frac{1.49}{0.45} (.0008)^{1/2} \left(\frac{81.75}{(0.82 + 1)^{5/3}}\right) = 27.29$$

$$b = 0.82 + 5/3 = 2.49$$

$$h_{max} = \frac{95800}{27.29}^{(1/2.49)} = 26.49$$

The data required for the flow routing computations are as follows:

VOL_r	= 8750 ac-ft	(reservoir volume)
H_d	= 50 ft	(height of dam)
$Q_{b_{max}}$	= 95800 cfs	(max breach outflow)
h_{max}	= 26.49 ft	(recomputed max stage at dam)
h_v	= 30 ft	(height of valley wall)
$\bar{m}$	= 0.82	(fitting coefficient for average cross section)
$\bar{K}$	= 81.75	(fitting coefficient for average cross section)
S	= 0.0008	(channel bottom slope from mile 0.0 to mile 12.3)
n	= 0.045	(Manning roughness coefficient)
h_f	= 10 ft	(flood stage at mile 12.3)
Q_o	= 5000 cfs	(initial flow)

Because ($H_d > h_v$), Eq. (19) is used to compute X_c.

$$X_c(ft) = \frac{6\ VOL_r}{\bar{K}\ h_v^{\bar{m}} \left(3H_d - 5\ \frac{\bar{m}h_v}{\bar{m}+1}\right)}$$

$$= \frac{6\ (8750) \times 43560\ (ft^3/ac\text{-}ft)}{81.75(30)^{0.82}\left(3(50) - 5\ \frac{.82(30)}{1.82}\right)} = 20600\ ft\ (3.9\ mi)$$

The first estimate for θ is 0.95.

Because ($Q_{b_{max}} < Q_v$) the hydraulic depth (D_c) is given by Eq. (21), i.e.:

$$D_c = \frac{\theta\ h_{max}}{m+1} = \frac{0.95\ (26.49)}{1.82} = 13.83$$

The average particle velocity in the X_c reach is as follows (Eq. (24)):

$$V_c = \frac{1.49}{n} S^{1/2} \quad (D_c)^{2/3} = \frac{1.49}{0.045} (0.0008)^{1/2} \ (13.83)^{2/3} = 5.24 \text{ ft/s}$$

The Froude number developed by the floodwave is determined by the following equation (Eq. (24)):

$$F_c = \frac{V_c}{\sqrt{g\ D_c}} = \frac{5.24}{\sqrt{32.2\ (13.83)}} = 0.25$$

Because ($Q_{b_{max}} < Q_v$), the average cross-sectional area (A_c) of the wave is given by Eq. (25), i.e.:

$$A_c = K(\theta h_m)^m D_c = 81.75\ (0.95(26.49))^{0.82} \quad (13.83) = 16158\ (ft^2)$$

The volume parameter (V^*)is as follows (Eq. (27)):

$$V^* = \frac{VOL_r}{A_c\ X_c} = \frac{8750\ (43560)}{(16158)\ (20600)} = 1.15$$

To check the original estimate for θ, the family of curves for $F_c = 0.25$ is examined to find by interpolation the ratio of Q_p/Q_{max} for ($V^* = 1.15$) at ($X^* = 1$). This ratio is found to be approximately 0.60, indicating that the peak flow at X_c is

$$Q_p \text{ at } X_c = (Q_p/Q_{b_{max}})\ (Q_{b_{max}}) = 0.60\ (95800) = 57480 \text{ cfs}$$

Because this peak flow is less than Q_v (Eq. (7)), the depth reached by the floodwave at X_c is given by Eq. (8) as follows:

$$h_{x_c} = \left(\frac{Q_p}{a}\right)^{1/b}$$

$$a = \frac{1.49}{n} S^{1/2}\left(\frac{\bar{R}}{(\bar{m} + 1)^{5/3}}\right) = 27.29$$

$$b = \bar{m} + 5/3 = 2.49$$

$$h_{x_c} = \left(\frac{57480}{27.29}\right)^{1/2.49}$$

$$h_{x_c} = 21.61$$

This value of h_x is substituted into Eq. (28) to re-evaluate the original estimate for θ :

$$\theta = \frac{h_{max} + h_x}{2\ h_{max}} = \frac{26.49 + 21.61}{2\ (26.49)} = 0.91$$

Because the re-evaluated θ is within (±5%) of the original estimate for θ, the initial calculations are acceptable and the attenuation of the flood peak may be predicted using the curves for $F_c = 0.25$ and interpolating $V^* = 1.15$.

The dimensionless distances (X_1^*) to at mile 12.3 is as follows:

$$X_1^* = \frac{12.3}{X_c} = \frac{12.3}{\left(\frac{20600}{5230}\right)} = 3.15$$

The ratio of $(Q_p/Q_{b_{max}})$ at $X^* = 3.15$ is found by interpolation to be 0.34, indicating the peak flow at mile 12.3 to be (0.34) (95800) = 32572 cfs.

To determine the time to peak at the forecast point, the velocity of flow at the midpoint between the dam and the forecast point must be determined The ratio of the average peak flow $(Q_{X/2})$ to $Q_{b_{max}}$ in the 12.3 mile reach is found on the curve at $X^* = 1.58$.

$$X_i^*/2 = X_i/2X_c = 12.3/2(3.9) = 1.58$$

This ratio is approximately 0.5, indicating the midpoint peak flow to be (0.5 x 95800) = 47900 cfs. This flow is multiplied by the factor $(0.3 + \bar{m}/10)$ to compute the reference flow $Q_{ref} = (.3 + .82/10)\ 47900 = 18297$.

Because this flow is less than Q_v, Eq. (30) is used to determine the reference peak depth in the reach as follows:

$$h_{ref} = \left(\frac{Q_{ref}}{a}\right)^{1/b} = \left(\frac{18297}{27.29}\right)^{1/2.49} = 13.65 \text{ ft}$$

The midpoint reference hydraulic depth in the reach is found using Eq. (32), i.e.:

$$D_{ref} = \frac{h_{ref}}{m+1} = \frac{13.65}{1.82} = 7.50$$

The average particle velocity is determined by substituting this value of D_{x_i} into Eq. (34) as follows:

$$V_{x_i} = \frac{1.49}{n} S^{1/2} \left(D_{x_i}\right)^{2/3} = \frac{1.49}{0.045} (.0008)^{1/2} (7.50)^{2/3}$$

$$V_{x_i} = 3.48 \text{ ft/sec}$$

Thus, the wave celerity as determined with Eq. (35) is:

$$C = 0.682\ (3.48) \left[5/3 - 2/3 \left(\frac{.82}{1.82} \right) \right] = 3.25 \text{ mi/hr}$$

The time of travel for the flood peak to the forecast point at mile 12.3 is given by Eq. (36) as follows:

$$t_p\ (X=12.3) = T_r + \frac{12.3}{C} = 0.75 + \frac{12.3}{3.25}$$

$$t_p = 4.54 \text{ hrs}$$

To compute the peak stage at mile 12.3, the user must first compute the K and m coefficients for that cross section. This is done by first reducing the X-sectional data at mile 12.3 from table 1 as follows:

Table 6 — TOPWIDTH VS. DEPTH DATA AT MILE 12.3

Depth	Topwidth
7	400
17	770
27	1330
37	1400

Substituting this reduced data into Eqs. (5)-(6a) produces a K value of 71.96 and an m value of 0.87. These values are substituted with the peak flow into Eq. (8) to compute the peak depth at mile 12.3 as follows:

$$a = \frac{1.49}{.045} (.008)^{1/2} \quad \frac{71.96}{(0.87 + 1)^{5/3}} = 23.12$$

$$b = 0.87 + 5/3 = 2.53$$

$$h_{12.3} = \left(\frac{32572}{23.12}\right)^{1/2.53} = 17.49$$

To determine the time to flooding (floodwave reaching flood stage), the flow, Q_f, associated with the flood stage, h_f, (10 ft) must be computed.

$$Q_f = a\left(h_f\right)^b = 23.12\ (10)^{2.53}$$

$$Q_f = 7834 \text{ cfs}$$

This value for Q_f is substituted into Eq. (38) to calculate time to flooding, t_{fld}, as follows

$$t_{fld} = t_p - \left(\frac{Q_p - Q_f}{Q_p - Q_o}\right) t_f$$

$$= 4.54 - \left(\frac{32572 - 7834}{32572 - 5000}\right) (0.75)$$

$$t_{fld} = 3.87 \text{ hours}$$

The time at which the flooding ceases (floodwave drops below flood stage is calculated using Eq. (39), i.e.,

$$td = t_p + \left[\frac{24.2\ VOL_R}{Q_p - Q_o} - t_f\right] \left(\frac{Q_p - Q_f}{Q_p - Q_o}\right)$$

$$= 3.54 + \left[\frac{24.2\ (8750)}{(32572 - 5000)} - 0.75\right] \left(\frac{32572 - 7834}{(32572 - 5000)}\right)$$

$$t_d = 10.76 \text{ hours}$$

Routing the flow to mile 40.5 requires the fitting of $\bar{K}$ and $\bar{m}$ parameters to the <u>distance weighted</u> average cross section for the reach. The reduced cross-sectional data for the reach is given in table 6.

Table 6 — TOPWIDTH VS. DEPTH FOR EXAMPLE CHANNEL DESCRIPTION

Mile 0.0		Mile 12.3		Mile 40.5	
Depth	Topwidth	Depth	Topwidth*	Depth	Topwidth*
0	0	0	0	0	0
8	480	8	437	8	472
18	900	18	826	18	862
28	1300	28	1337	28	1338
38	1350	38	1407	38	1456

*Linearly interpolated to agree with depth value at mile zero.

To determine the distance weighted average X-section, the depth vs. topwidth data is substituted into the relation given in (Eq. (40)), i.e., for $h_1 = 8$,

$$\bar{B}_1 = \frac{\frac{480 + 437}{2}(12.3 - 0.0) + \frac{437 + 472}{2}(40.5 - 12.3)}{(40.5 - 0.0)} = 455.7$$

for $h_2 = 18$;

$$\bar{B}_2 = \frac{\frac{900 + 826}{2}(12.3 - 0.0) + \frac{826 + 862}{2}(40.5 - 12.3)}{(40.5 - 0.0)} = 849.8$$

for $h_3 = 23$,

$$\bar{B}_3 = \frac{\frac{1300 + 1337}{2}(12.3 - 0.0) + \frac{1337 + 1338}{2}(40.5 - 12.3)}{(40.5 - 0.0)} = 1331.7$$

Examination of the X-sectional data indicates that, because the topwidths increase very slowly above a depth of approximately 30 ft, a reasonable value for h_v is 30.

The distance weighted average cross-section data is used in Eqs. (5a)-(6c) to determine the K and m parameters of the equation $B = Kh^m$.

Table 7 — VALUES USED IN LEAST SQUARES COMPUTATION OF $\bar{K}$ and $\bar{m}$ PARAMETERS

i	h_i	$\log h_i$	$(\log h_i)^2$	B_i	$\log B_i$	$(\log h_i)(\log B_i)$
1	8	0.90	0.82	455.7	2.66	2.39
2	18	1.26	1.58	849.8	2.93	3.67
3	28	1.45	2.09	1331	3.12	4.51
-	h_v	-	-	-	-	-
4	30	1.48	2.18	1383	3.14	4.64
		5.08	6.67		11.85	15.23

$$\bar{m} = \frac{15.23 - \frac{(5.08)\ (11.85)}{4}}{6.67 - \frac{(5.08)^2}{4}} = 0.84$$

$$\text{Log } \bar{K} = \frac{11.84}{4} - 0.84 \left(\frac{5.08}{4}\right) = 1.89$$

$$\bar{K} = 10^{\log \bar{K}} = 78.2$$

With these distance weighted average $\bar{K}$ and $\bar{m}$ parameters, the new peak depth at the dam is found to be 26.53 feet. This value is used in Eqs. (19)-(27) to compute the following routing parameters.

X_c = 20605.6 = 3.9 mi

θh_{max} = 25.20

D_c = 13.70

V_c = 5.22

F_c = 0.25

A_c = 16110

V^* = 1.15

The dimensionless distance to mile 40.5 is (40.5/3.9) = 10.4. The ordinate of the Q_p/Q_{bmax} curve at V^* = 1.15 and X^* = 10.4 is interpolated to be approximately 0.15 indicating the peak flow at mile 40.5 is 95800 x 0.15 = 14400 cfs. The midpoint flow (at mile 40.5/2) is found to be 21737.5. The reference flow is (.3 + 0.1 * 0.84) x 21737.4 = 8347.16 which produces a reference depth of 10.05. This value is used Eqs. (32)-(36) to find a time to peak at mile 40.5 of 16.21 hours.

The true K and n coefficients at mile 40.5 are 92.1 and 0.80, respectively. These values and the peak flow value are substituted into Eq. (30) to compute a peak depth at mile 40.5 of 11.98 feet. Finally, the time of flooding is found to be 15.85 hours and the time to "deflooding" is found to be 28.48 hours.

APPENDIX I (a)

THE NWS SIMPLIFIED DAM BREAK MODEL

FLOW ROUTING CURVES

SIMPLIFIED DAMBREAK ROUTING CURVES

FC=0.25

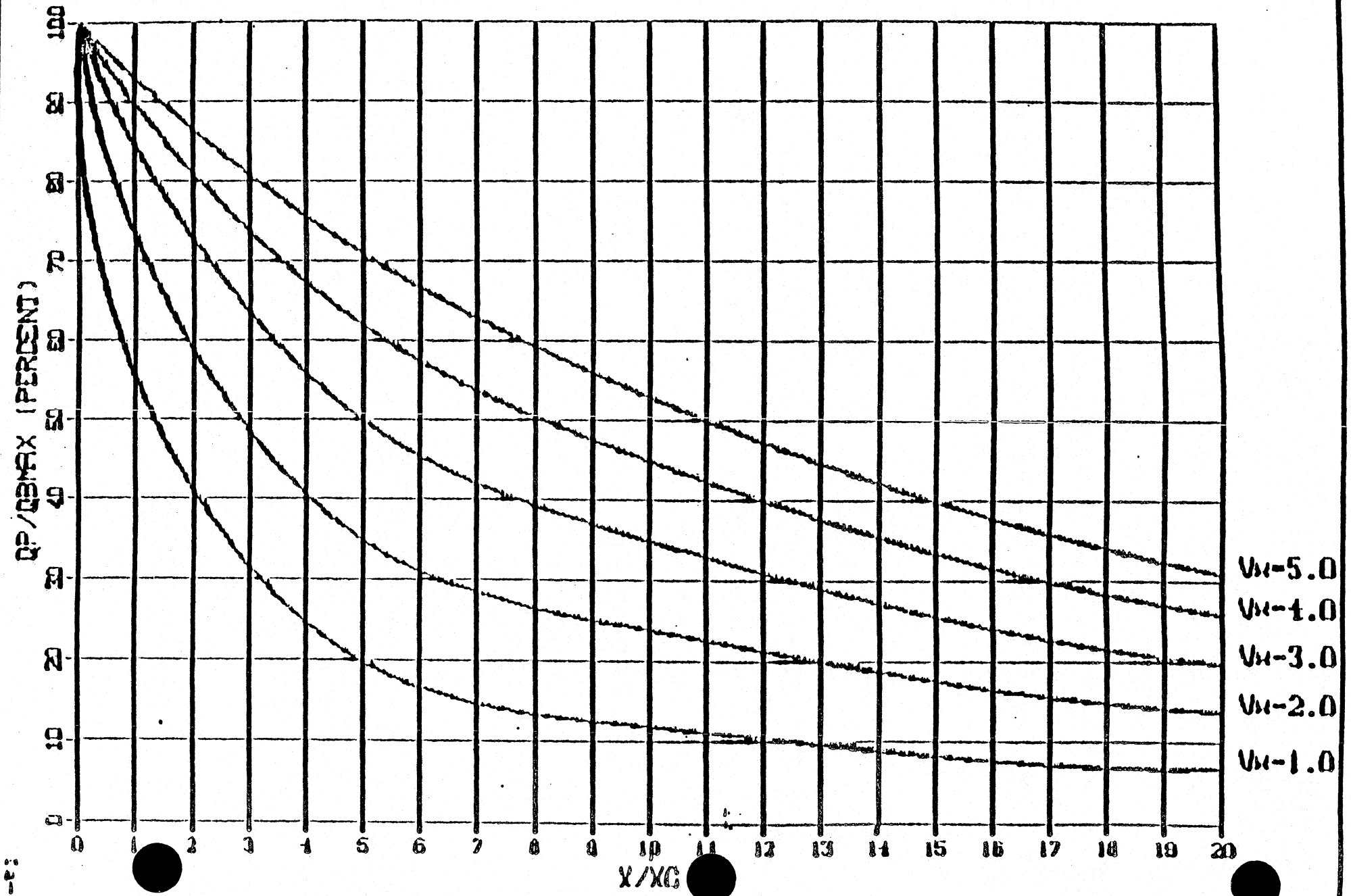

SIMPLIFIED DAMBREAK ROUTING CURVES

FC=0.50

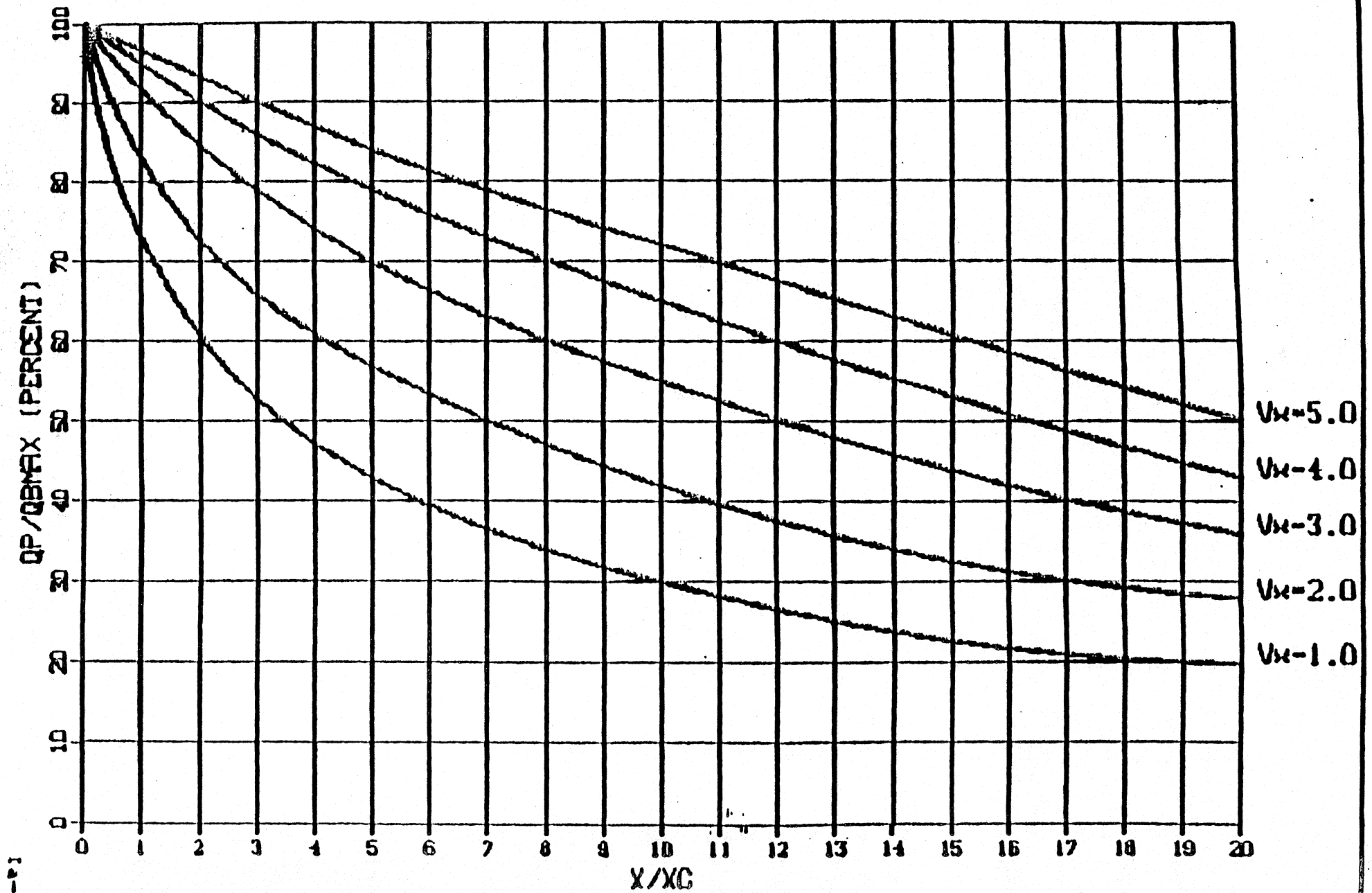

SIMPLIFIED DAMBREAK ROUTING CURVES

FC-0.75

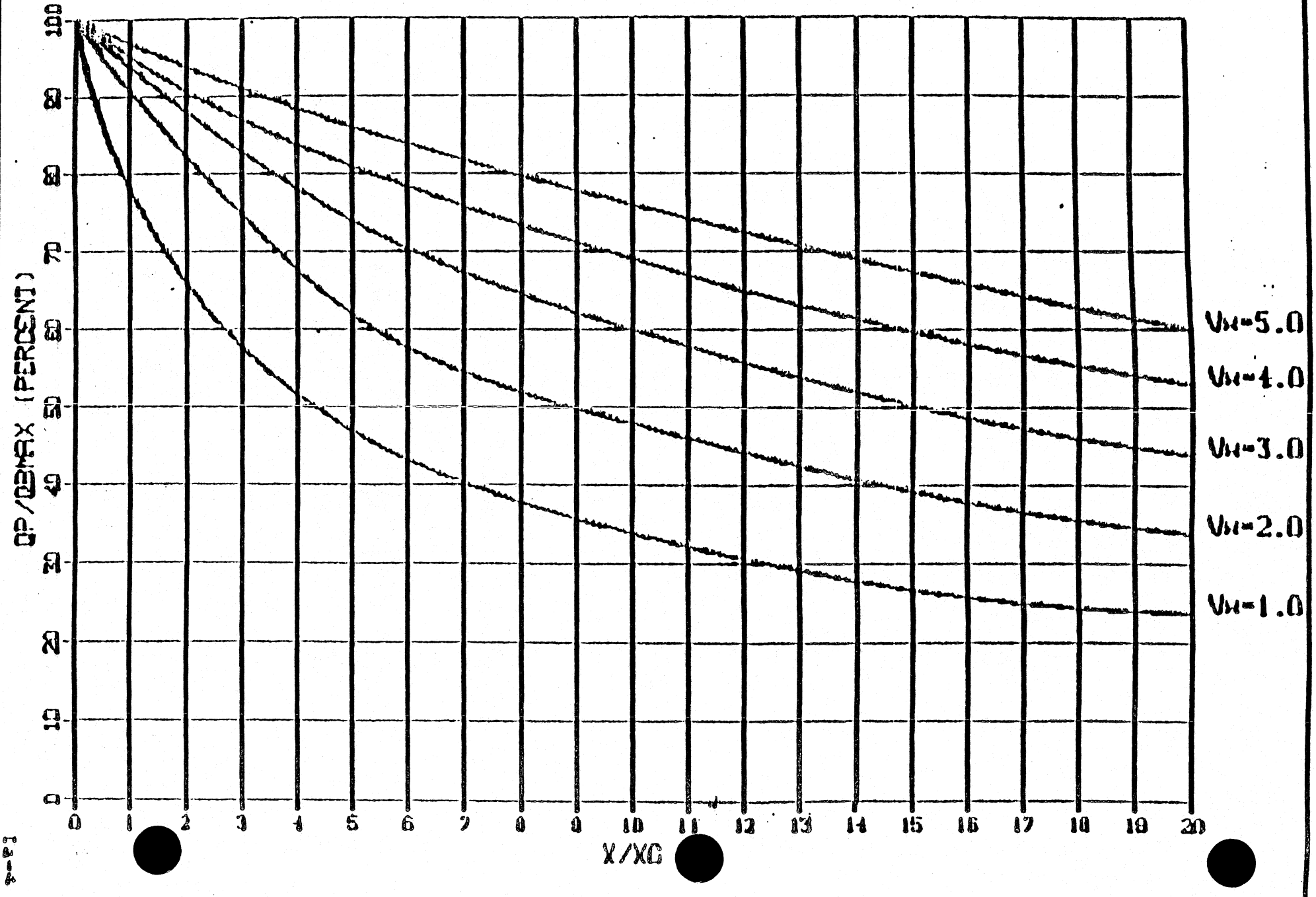

APPENDIX II

THE NWS SIMPLIFIED DAM BREAK MODEL

FORTRAN VERSION LISTING
WITH EXAMPLE RUNS

```
C
C
C     SIMPLIFIED DAMBREAK MODEL
C     FORTRAN LANGUAGE INTERACTIVE VERSION
C     WRITTEN BY JONATHAN WETMORE  5/3/83
C     UPDATED 8/30/83 FOR DEFAULT TFAIL=H2/3 AND BREACH WIDTH =3*H2
C
      REAL K,K0,K1,M,M0,M1,N
      COMMON/ARAY/ F(15,6),X(6),D(8),E(8,8),T(8,8),C(3,8),H(2,8),B(4,8),
     1P(8,5)
      COMMON/SCALAR/ C0,B0,V0,A0,W0,T0,Q0,N0,N1,S0
      DIMENSION DAMNAM(5),RIVNAM(5),FTMSL(2),FEET(2)
      DATA YES,SH,STG,ELEV/4HYES ,4HSHOR,4HDEPT,4HELEV/
      DATA FTMSL/4H(FT ,4HMSL)/
      DATA FEET/4H (F,4HEET)/
C
C
C     ********** SUMMARY OF INPUT DATA VARIABLES **********
C
C       C0      =  RES. DAM CREST ELEVATION (FT. MSL)
C       B0      =  FINAL BREACH ELEV (FT. MSL)
C       V0      =  VOLUME OF RESERVOIR (AC-FT)
C       A0      =  RES. SURF. AREA (ACRES)
C       W0      =  FINAL BREACH WIDTH
C       T0      =  TIME OF FAILURE (MINUTES)
C       Q0      =  SPILLWAY/TURBINE/SURCHARGE FLOW (CFS)
C       N0      =  NO. OF X-SECTIONS TO BE READ IN
C       N1      =  NO. OF ELEV-TOPW PAIRS
C       D(I)    =  DOWNSTREAM DIST TO X-S (I)
C       E(I,J)  =  ELEV(J) CORRESPONDING TO TOPW(J) AT X-S (I)
C       T(I,J)  =  TOPW(J) CORRESPONDING TO ELEV(J) AT X-S (I)
C       C(1,I)  =  MANNING 'N' AT X-S (I)
C       C(2,I)  =  'HV' DEPTH AT X-S (I)
C       C(3,I)  =  FLOOD DEPTH AT X-S (I)
C       S0      =  DOWNSTREAM SLOPE (READ IN IF ONLY 1 X-S GIVEN)
C
C     ***********************************************************
C
C     ********** SUMMARY OF INTERNAL ARRAYS **********
C
C       X(I)    =  X-ORDINATES OF FC CURVE FAMILY MATRICES
C       F(I,J)  =  Y-ORDINATES OF FC CURVE FAMILY MATRICES
C       H(1,J)  =  GIVEN X-S HEIGHT J ABOVE INVERT AT X-S (I)
C       H(2,J)  =  GIVEN X-S HEIGHT ABOVE INVERT AT FIRST X-S
C       B(1,J)  =  INTERP. TW AT CURRENT X-S CORRESPONDING TO H(2,J)
C       B(2,J)  =  TOPW AT PREVIOUS X-S CORRESPONDIG TO H(2,J)
C       B(3,J)  =  WEIGHTED TOPW CORRESPONDING TO H(2,J)
C       B(4,J)  =  DISTANCE WEIGHTED TOPW (J) AT CURRENT X-S
C       P(I,1)  =  Q PEAK AT X-S (I)
C       P(I,2)  =  PEAK DEPTH AT X-S (I)
C       P(I,3)  =  TIME TO PEAK AT X-S (I)
C       P(I,4)  =  TIME OF FLOODING AT X-S (I)
C       P(I,5)  =  TIME OF DEFLOODING AT X-S (I)
C
C*************************************************************
C
C
C     INITIALIZE VARIABLES
C
C     "IN" IS THE LOGICAL UNIT NUMBER FOR THE INPUT DEVICE
C     "IOUT" IS THE LOGICAL UNIT NUMBER FOR THE OUTPUT DEVICE
      IN=5
      IOUT=6
      W0=0.
      N0=1
      A0=0.
H(1,I)=0.  DO 10 I=1,8
      B(3,I)=0.0
      C(3,I)=0.0
   10 CONTINUE
      WRITE(IOUT,900)
  900  FORMAT(/1X,' SIMPLIFIED DAMBREAK MODEL',
     1/2X,' FORTRAN LANGUAGE INTERACTIVE VERSION',/1X,
     1' WRITTEN BY JONATHAN N. WETMORE  HRL  MAY, 1983',/)
C
```

```
      WRITE(IOUT,901)
 901  FORMAT(/1X,'INPUT "SHORT" FOR SHORT VERSION, "LONG" FOR FULL',
     1' MODEL')
      READ(IN,705) VERS
      IF(VERS.NE.SH) GO TO 20
      WRITE(IOUT,9010)
 9010 FORMAT(/1X,'INPUT HEIGHT (FEET) OF DAM')
      READ(IN,702) H2
      GO TO 120
 20   WRITE(IOUT,902)
 902   FORMAT(/1X, 'INPUT NAME OF DAM')
      READ(IN,701) DAMNAM
C
      WRITE(IOUT,903)
 903   FORMAT(/1X, 'INPUT RIVER NAME')
      READ(IN,701) RIVNAM
C
 100  WRITE(IOUT,904)
 904   FORMAT(/1X, 'INPUT DAM CREST ELEVATION (FT. MSL)')
      READ(IN,702) CO
      IF(CO.LT.0.1) GO TO 100
C
 110  WRITE(IOUT,905)
 905   FORMAT(/1X, 'INPUT FINAL BREACH BOTTOM ELEVATION (FT. MSL)')
      READ(IN,702) BO
      IF(BO.LT.0.01 ) GO TO 110
C
C H2 IS THE DEPTH OF BREACH
      H2=CO-BO
 120  WRITE(IOUT,906)
 906   FORMAT(/1X, 'INPUT VOLUME OF RESERVOIR (AC-FT) AT MAX POOL ELEV')
      IF(VERS.NE.SH) WRITE(IOUT,9060)
 9060 FORMAT(1X,'IF N/A ENTER 0. AND VOL WILL BE EST. FROM SURF. AREA')
      READ(IN,702) VO
      IF(VERS.EQ.SH) GO TO 130
C
      WRITE(IOUT,907)
 907  FORMAT(/1X,'INPUT RESERVOIR SURFACE AREA (ACRES) AT MAX POOL ELEV',
     1/1X, 'IF N/A ENTER 0. AND S.A. WILL BE EST. FROM VOLUME.')
      READ(IN,702) AO
      IF(VO.GT.0.1 ) GO TO 130
      IF(AO.GT.0.1 ) GO TO 130
      WRITE(IOUT,908)
 908  FORMAT(/1X, 'A VALUE FOR EITHER VOLUME OR SURFACE AREA MUST BE',
     1' ENTERED')
      GO TO 120
C
 130  WRITE(IOUT,909)
 909   FORMAT(/1X, 'INPUT FINAL BREACH WIDTH (FT)',
     1/1X, 'IF N/A ENTER 0.  DEFAULT USED = 3 * BREACH DEPTH')
      READ(IN,702) WO
 135  IF(WO.LT.0.1)  WO=3.*H2
C
      WRITE(IOUT,910)
 910   FORMAT(/1X, 'INPUT TIME (MINUTES) REQUIRED FOR BREACH FORMATION',
     1/1X, 'IF N/A , ENTER 0.')
      READ(IN,702) TO
      IF(TO.GT.0.00001 ) GO TO 140
C TIME OF FAILURE NOT GIVEN...MAKE ESTIMATE
      WRITE(IOUT,911)
 911   FORMAT(1X, 'ENTER TYPE OF DAM...0 FOR EARTH DAM, 1 FOR CONCRETE',
     1' DAM')
      READ(IN,703) IT1
      IF(IT1.GT.0)  WRITE(IOUT,9111)
 9111 FORMAT(/1X, 'IS THIS AN INSTANTANEOUS FAILURE?')
      IF(IT1.GT.0) READ(IN,705) ANS
      IF(IT1.GT.0.AND.ANS.EQ.YES) TO=H2/1500.
      IF(IT1.LT.1)  TO=H2/3.
      WRITE(IOUT,9110) TO
 9110 FORMAT(1X,'ESTIMATED TIME OF FAILURE =',F8.2,' MINUTES')
 140  IF(VERS.EQ.SH) GO TO 160
C
      WRITE(IOUT,912)
 912   FORMAT(/1X, 'INPUT TURBINE/SPILLWAY/OVERTOPPING FLOW (CFS). ',
     1/1X, 'IF N/A, ENTER 0.0.  DEFAULT = 0.0')
```

```
      READ(IN,702) QO
C
 150  WRITE(IOUT,913)
 913  FORMAT(/1X,'INPUT NUMBER OF X-SECTIONS (STARTING AT DAM) USED TO',
     1/1X, 'DESCRIBE ROUTING REACH.  (MIN=1, MAX=8)')
      READ(IN,703) NO
      IF(NO.LT.1 ) GO TO 150
C
 160  WRITE(IOUT,914)
 914  FORMAT(/1X, 'INPUT NUMBER OF PAIRS OF ELEV-TOPWIDTHS USED TO',
     1/1X, 'DESCRIBE EACH X-SECTION (MIN=2, MAX=8)')
      IF(VERS.EQ.SH) WRITE(IOUT,9140)
 9140 FORMAT(1X,'MODEL ASSUMES DEPTH #1 = 0. AND TOPW #1 = 0.')
      READ(IN,703) N1
      IF(N1.LT.2 ) GO TO 160
C
C BEGIN READING IN X-SECTION INFORMATION
C
      D(1)=0.
      DO 400 I=1,NO
      T(I,1)=0.
C
      IF(I.GT.1)  WRITE(IOUT,915) I
 915  FORMAT(/1X,'INPUT DISTANCE DOWNSTREAM (MILES) TO X-SECTION #',I2)
      IF(I.GT.1)  READ(IN,702) D(I)
      IF(VERS.NE.SH) GO TO 165
      E(1,1)=0.
      CO=H2
      BO=0.
      ELEV=STG
      FTMSL(1)=FEET(1)
      FTMSL(2)=FEET(2)
      GO TO 167
C
 165  WRITE(IOUT,916) I
 916  FORMAT(/1X,'INPUT LOWEST CHANNEL ELEV.(FT.MSL) AT X-SECTION #',I2)
      IF(I .EQ. 1)  WRITE(IOUT,917)
 917  FORMAT(1X, '(ELEVATION OF BASE OF DAM (FT. MSL))')
      READ(IN,702) E(I,1)
 167  IF(I .GT. 1 ) GO TO 170
C
C  IF SURFACE AREA NOT GIVEN, ESTIMATE AO USING VO
      IF(AO .LT. 0.01) AO=2.*VO/(CO-E(1,1))
C  IF VOLUME NOT GIVEN, ESTIMATE VO USING AO
      IF(VO .LT. 0.01) VO=(AO/2.)*(CO-E(1,1))
C
      IF(BO .LE. (E(1,1)+5.))  GO TO 170
C  PERCHED BREACH...RECOMPUTE VO BASED ON AVAILABLE VOLUME
      VO=H2/2.*AO*(1.+((BO-E(1,1))/(CO-E(1,1)))**2.)
C
C ONCE FIRST X-S HAS BEEN READ IN & FITTED & SLOPE FOUND COMPUTE PEAK
 170  IF(I .NE. 2 ) GO TO 180
 175  M=MO
      K=KO
      N=C(1,1)
      H3=C(2,1)
      H4=C(3,1)
      CALL DAMBRK(K,M,N,S2,H2,H3,H4,Q3,Q,H1)
C SAVE FLOW,DEPTH AND TPEAK AT DAM
      P(1,1)=Q
      P(1,2)=H1
      P(1,3)=TO/60.
      T1=TO/60.
      CALL TIMFLD(K,M,N,S2,H3,H4,Q,Q3,T1,T4,T5)
C  SAVE TIMES OF FLOODING AND DEFLOODING AT DAM
      P(1,4)=T4
      P(1,5)=T5
      IF(NO .LT. 2) GO TO 400
C
 180  DO 190 J=2,N1
C
      WRITE(IOUT,918) ELEV,FTMSL(1),FTMSL(2),J,I
 918  FORMAT(/1X,'INPUT ',3A4,' #',I2,' AND ASSOC. TOPWIDTH FOR X-S ',
     1' #',I2)
      READ(IN,702) E(I,J)
```

```
      READ(IN,702) T(I,J)
 190  CONTINUE
C
      WRITE(IOUT,919) I
 919  FORMAT(/1X,'INPUT MANNING N AT X-S #',I2,' (DEFAULT = 0.050)')
      READ(IN,704) C(1,I)
      IF(C(1,I) .LT. 0.0001) C(1,I) = 0.050
C
      IF(VERS.NE.SH) GO TO 195
      C(2,1)=H2
      C(3,1)=0.
      GO TO 197
C
 195  WRITE(IOUT,920) I
 920   FORMAT(/1X, 'INPUT VALLEY WALL HEIGHT ABOVE CHANNEL BOTTOM AT ',
     1'X-S #',I2,/1X, 'IF N/A INPUT 0.')
      READ(IN,702) C(2,I)
      IF(C(2,I) .LT. 0.01)  C(2,I) = (E(I,N1)-E(I,1)) + H2
C
      WRITE(IOUT,921) I
 921   FORMAT(/1X, 'INPUT FLOOD DEPTH AT X-S #',I2,
     1/1X, 'IF N/A ENTER 0.')
      READ(IN,702) C(3,I)
C
 197  IF(NO .LT. 2) WRITE(IOUT,922)
 922   FORMAT(/1X,'INPUT CHANNEL SLOPE (FT/MI) BELOW DAM')
      IF(NO .LT. 2)  READ(IN,702) SO
      IF(SO.EQ.0) SO=H2**2*(T(1,N1)/(24.75*VO))
C
C  FIT X-SECTION W/ K & M PARMS
      IF(N1 .GT. 2) GO TO 200
C ONLY 2 X-S POINTS GIVEN.  SET M = 1
      MO=1.0
      KO=T(I,N1)/(E(I,N1)-E(I,1))
      IF(I .LT. 2)  H(2,N1)=E(I,N1)-E(I,1)
      IF(I .LT. 2)  B(2,N1)=T(I,N1)
      N4=N1
      GO TO 250
C  INITIALIZE LEAST SQUARES ALGORITHM
 200  U1=0.
      U2=0.
      U3=0.
      U4=0.
      N2=N1
      DO 230 J1=2,N1
      H(1,J1)=E(I,J1)-E(I,1)
C SAVE H'S OF FIRST X-S FOR WEIGHTED X-S ROUTINE
      IF(I .GT. 1) GO TO 210
        H(2,J1)=H(1,J1)
        IF(H(1,J1) .GE. C(2,1)) H(2,J1)=C(2,1)
        B(2,J1)=T(I,J1)
C SEE IF HV IS EXCEEDED
 210   IF(H(1,J1-1) .GE. C(2,I))  N2=J1-1
      IF(H(1,J1) .GE. C(2,I)) H(1,J1)=C(2,I)
      IF(H(1,J1-1) .GE. C(2,I)) GO TO 240
      U1=U1+LOG(H(1,J1))
      U2=U2+(LOG(H(1,J1)))**2.
      IF(H(1,J1) .LT. C(2,I)) GO TO 220
C HV MET OR EXCEEDED, COMPUTE TW ASSOC. W/ HV
      DO=(T(I,J1)-T(I,J1-1))/(E(I,J1)-E(I,J1-1))
      T(I,J1)=T(I,J1-1)+(H(1,J1)+E(I,1)-E(I,J1-1))*DO
      IF(I .EQ. 1) B(2,J1)=T(I,J1)
 220   U3=U3+LOG(T(I,J1))
      U4=U4+LOG(H(1,J1))*LOG(T(I,J1))
 230  CONTINUE
 240   N3=N2-1
      IF(I .EQ. 1)  N4=N2
      IF(N2 .GT. 2) GO TO 242
C ONLY 2 X-S POINTS BELOW HV. SET M = 1
      MO=1.0
      KO=T(I,N2)/H(1,N2)
      GO TO 250
 242  MO=U4-U1*U3/N3
      MO=MO/(U2-(U1**2.)/N3)
      IF(MO .LE. 0.0)  MO = 0.01
```

```
      K0=U3/N3-M0*U1/N3
      K0=EXP(K0)
C
C  CHECK GOODNESS OF FIT BETWEEN GIVEN AND FITTED X-SECTION
      IU8=0
      IU7=0
 245  IF(IU8.GT.1) WRITE(IOUT,9220) K0,M0
 9220 FORMAT(/1X,'DEPTH',4X,'GIVEN TW',4X,'FIT TW',4X,'K =',F6.2,
     13X,'M =',F6.2)
      DO 248 J1=2,N2
      T4=K0*H(1,J1)**M0
      IF(IU8.GT.1) WRITE(IOUT,9221) H(1,J1),T(I,J1),T4
 9221 FORMAT(/1X,F6.2,3X,F8.2,3X,F8.2)
      IF(ABS((T(I,J1)-T4))/T(I,J1).GT.0.5) IU7=N2-1
 248  CONTINUE
      IF (IU8.GT.1) GO TO 250
      IF(IU7.LT.1) GO TO 250
      WRITE(IOUT,9222) D(I)
 9222 FORMAT(/1X, '*** WARNING *** X-SECTION FIT IS OFF AT MILE',F6.2,
     1/1X,'DEPTH ERRORS MAY OCCUR...USER SHOULD PLOT THE X-S,',/1X,
     1'DRAW A SMOOTH CURVE THRU POINTS, AND RERUN WITH SMOOTHED POINTS')
      IU8=2
      GO TO 245
 250   IF(NO .LT. 2 ) GO TO 175
      IF(I .EQ. 1) GO TO 400
C
C COMPUT DISTANCE WEIGHTED X-SECTION
C
      DO 280 J1=2,N4
C
C INTERP H(2,J1) INTO ELEV TABLE TO FIND ASSOC TOPW @ X-S(I)
      IF(H(2,J1).GT.(E(I,N1)-E(I,1)))  J0=N1
      IF(H(2,J1) .GT. (E(I,N1)-E(I,1))) GO TO 270
      DO 260 J2=2,N1
      J0=J2
      IF((H(2,J1) - (E(I,J2)-E(I,1))) .LE. 0.0) GO TO 270
 260  CONTINUE
C  BRACKETING ELEVS FOUND...COMPUTE DB/DH
 270   J3=J0-1
      D0=(T(I,J0)-T(I,J3))/(E(I,J0)-E(I,J3))
C
C DET. ASSOC TOPW @ X-S I
      B(1,J1)=T(I,J3)+(E(I,1)+H(2,J1)-E(I,J3))*D0
C  CHECK IF HV IS EXCEEDED
      IF(H(2,J1) .GE. C(2,I))  B(1,J1) = T(I,N2)
C B(3,J1) IS THE WEIGHTED TOPWIDTH
      B(3,J1)=B(3,J1)+((B(2,J1)+B(1,J1))/2.)*(D(I)-D(I-1))
C SAVE INTERPOLATED TOPW AS B(2,J1)
      B(2,J1)=B(1,J1)
 280  CONTINUE
C
C DIVIDE WEIGHTED TOPW BY DISTANCE
      DO 290 J1=2,N4
      B(4,J1)=B(3,J1)/(D(I)-D(1))
 290  CONTINUE
C
C COMPUTE DISTANCE WEIGHTED MANNING N
      N=0.
      DO 300 J1=2,I
      N=N+((C(1,J1)+C(1,J1-1))/2)*(D(J1)-D(J1-1))
 300  CONTINUE
      N = N/(D(I)-D(1))
C
C  FIT K & M PARMS TO DIST WEIGHTED X-S
C
C
      IF(N1 .GT. 2) GO TO 310
C ONLY 2 X-S POINTS GIVEN.  SET M = 1
      M1=1.0
      K1=B(4,N1)/H(2,N1)
      GO TO 330
C  INITIALIZE LEAST SQUARES ALGORITHM
 310  U1=0
      U2=0.
      U3=0.
```

```
      U4=0.
      DO 320 J1=2,N4
      U1=U1+LOG(H(2,J1))
      U2=U2+(LOG(H(2,J1)))**2.
      U3=U3+LOG(B(4,J1))
      U4=U4+LOG(H(2,J1))*LOG(B(4,J1))
 320  CONTINUE
      N3=N4-1
      IF(N4 .GT. 2) GO TO 322
C ONLY 2 X-S POINTS GIVEN.  SET M = 1
      M1=1.0
      K1=B(4,N4)/H(2,N4)
      GO TO 330
 322  M1=U4-U1*U3/N3
      M1=M1/(U2-(U1**2.)/N3)
      IF(M1 .LE. 0.0)  M1 = 0.01
      K1=U3/N3-M1*U1/N3
      K1=EXP(K1)
C
C  CHECK GOODNESS OF FIT OF WEIGHTED X-SECTION
      IU8=0
      IU7=0
 325  IF(IU8.GT.1) WRITE(IOUT,9230) K1,M1
 9230 FORMAT(/1X,'DEPTH',4X,'WEIGHTED TW',4X,'FIT TW',4X,'K =',F6.2,
     13X,'M =',F6.2)
      DO 328 J1=2,N4
      T4=K1*H(2,J1)**M1
      IF(IU8.GT.1) WRITE(IOUT,9231) H(1,J1),B(4,J1),T4
 9231 FORMAT(/1X,F6.2,6X,F8.2,3X,F8.2)
      IF (ABS((B(4,J1)-T4))/B(4,J1).GT.0.5) IU7=N4-1
 328  CONTINUE
      IF (IU8.GT.1) GO TO 330
      IF (IU7.LT.1) GO TO 330
      WRITE(IOUT,9232) D(I)
 9232 FORMAT(/1X,'*WARNING* WEIGHTED X-SECTION FIT IS OFF AT MILE',F6.2,
     1/1X,'ROUTING ERRORS MAY OCCUR...USER SHOULD PLOT THE X-S,',/1X,
     1'DRAW A SMOOTH CURVE THRU POINTS, AND RERUN WITH SMOOTHED POINTS')
      IU8=2
      GO TO 325
C
C RECOMPUTE DEPTH AT DAM USING WIGHTED X-S PROPERTIES
 330   S2=(E(1,1)-E(I,1))/((D(I)-D(1))*5280.)
      K=K1
      M=M1
      Q=P(1,1)
      CALL COMPHV(I,H3)
      CALL COMPQV(K,M,N,S2,H3,Q3)
      CALL STAGE(K,M,N,S2,Q,H3,Q3,H1)
      H0=H1
C F1 IS THETA
      F1=0.95
      I9=0
 340   I8=I9
      Q=P(1,1)
      CALL STAGE(K,M,N,S2,Q,H3,Q3,H1)
      CALL RPARMS(K,M,N,S2,Q,F1,H1,H3,F7,V7,X1)
      X5=X1
 350   IF(I9 .GT. 0)  X5=D(I)
      Q=P(1,1)
      CALL ROUTE(F7,V7,X1,X5,Q,Q7)
C
      IF(I9 .GT. 0) GO TO 360
C  CHECK THETA VALUE
      Q=Q7
      CALL STAGE(K,M,N,S2,Q,H3,Q3,H1)
      F2=(H0+H1)/(2.*H0)
      IF((ABS(F1-F2)/F1) .LE. 0.02)  I9=1
      IF(I9 .NE. I8) GO TO 350
C  NEW THETA MUST BE COMPUTED
      F1=(F1+F2)/2.
      GO TO 340
C
C
C SAVE PEAK FLOW  AT X-S (I)
 360   P(I,1)= Q7
```

```
      IF(P(I-1,1).LT.P(I,1)) P(I,1)=.99*P(I-1,1)
C COMPUTE TIME TO PEAK
      XS=D(I)/2
      CALL ROUTE(F7,V7,X1,XS,Q,Q7)
      Q=(.3+.1*M)*Q7
      CALL STAGE(K,M,N,S2,Q,H3,Q3,H1)
      D9=H1/(M+1.)
      IF(H1 .GT. H3)  D9=H1-H3+H3/(M+1.)
      V6=(1.49/N)*(S2**0.5)*D9**0.667
      C9=0.682*V6*(1.667-(.667*(M/(M+1.))))
      P(I,3)=(TO/60.)+D(I)/C9
      IF(P(I,3).LT.P(I-1,3)) P(I,3)=1.01*P(I-1,3)
C
C  COMPUTE AND SAVE PEAK DEPTH AT X-S (I)
      K=KO
      M=MO
      S2=(E(I-1,1)-E(I,1))/((D(I)-D(I-1))*5280.)
      N=C(1,I)
      H3=C(2,I)
      Q=P(I,1)
      CALL COMPQV(K,M,N,S2,H3,Q3)
      CALL STAGE(K,M,N,S2,Q,H3,Q3,H1)
      P(I,2)=H1
C  DET TIME FLOODING AND DEFLOODING
      T1=P(I,3)
      H4=C(3,I)
      CALL TIMFLD(K,M,N,S2,H3,H4,Q,Q3,T1,T4,T5)
      P(I,4)=T4
      P(I,5)=T5
C
C
 400  CONTINUE
      IF(NO .GT. 1) GO TO 455
 703  FORMAT(A4)
C  SET UP FORECAST POINT PROFILE DISTANCES
      WRITE(IOUT,9260)
9260  FORMAT(/2X,'ENTER NUMBER OF FORECAST POINTS BELOW DAM (MAX = 7)')
      READ(IN,703) NO
      NO=NO+1
      IF(NO .LT. 2) GO TO 455
      HO = P(1,2)
C F1 IS THETA
      F1=0.95
      I9=0
 420   I8=I9
      Q=P(1,1)
      CALL STAGE(K,M,N,S2,Q,H3,Q3,H1)
      CALL RPARMS(K,M,N,S2,Q,F1,H1,H3,F7,V7,X1)
      XS=K1
      CALL ROUTE(F7,V7,X1,XS,Q,Q7)
C  CHECK THETA VALUE
      Q=Q7
      CALL STAGE(K,M,N,S2,Q,H3,Q3,H1)
      F2=(HO+H1)/(2.*HO)
      IF((ABS(F1-F2)/F1) .LE. 0.02)  I9=1
      IF(I9 .GT. 0) GO TO 430
C  NEW THETA MUST BE COMPUTED
      F1=(F1+F2)/2.
      GO TO 420
C
 430   DO 450 I = 2,NO
      IM=I-1
      WRITE(IOUT,926) IM
 926  FORMAT(/1X,'INPUT DIST DOWNSTREAM (MILES) TO FORECAST PT. NO.',I2)
      READ (IN,702) D(I)
      XS = D(I)
      Q=P(1,1)
      CALL ROUTE(F7,V7,X1,XS,Q,Q7)
C
C SAVE PEAK FLOW  AT X-S (I)
      P(I,1)= Q7
C COMPUTE TIME TO PEAK
      XS=D(I)/2
      CALL ROUTE(F7,V7,X1,XS,Q,Q7)
      Q=(.3+.1*M)*Q7
```

```
      CALL STAGE(K,M,N,S2,Q,H3,Q3,H1)
      D9=H1/(M+1.)
      IF(H1 .GT. H3)  D9=H1-H3+H3/(M+1.)
      V6=(1.49/N)*(S2**0.5)*D9**0.667
      C9=0.682*V6*(1.667-(.667*(M/(M+1.))))
      P(I,3)=(T0/60.)+D(I)/C9
C
C  COMPUTE AND SAVE PEAK DEPTH AT X-S (I)
      Q=P(I,1)
      CALL STAGE(K,M,N,S2,Q,H3,Q3,H1)
      P(I,2)=H1
C  DET TIME FLOODING AND DEFLOODING
      T1=P(I,3)
      H4=C(3,I)
      CALL TIMFLD(K,M,N,S2,H3,H4,Q,Q3,T1,T4,T5)
      P(I,4)=T4
      P(I,5)=T5
C
 450  CONTINUE
C
C
C PRINT HEADING
 455  WRITE(IOUT,924) DAMNAM,RIVNAM
 924  FORMAT(//1X,'      PROFILE OF CRESTS AND TIMES FOR ',5A4,' DAM',
     1/20X,' ON ',5A4,' RIVER'//1X,' DISTANCE',
     11X,'  PEAK      PEAK      FLOOD      TIME       TIME      TIME',
     1/1X,'DOWNSTREAM   FLOW      DEPTH      DEPTH      FLOOD      PEAK ',
     1'    DEFLOOD',
     1/1X,' (MILES)     CFS       FEET       FEET       HR         HR   ',
     1'      HR',/)
C
      DO 460 I = 1,NO
      WRITE(IOUT,925) D(I),P(I,1),P(I,2),C(3,I),P(I,4),P(I,3),P(I,5)
 460  CONTINUE
 925  FORMAT(F8.2,F12.2,F8.2,4F10.2)
C
   1  FORMAT(/)
 701  FORMAT(5A4)
 702  FORMAT(F10.2)
 703  FORMAT(I1)
 704  FORMAT(F10.3)
 500  STOP
      END
C
      BLOCK DATA
      COMMON/ARAY/ F(15,6),X(6),D(8),E(8,8),T(8,8),C(3,8),H(2,8),B(4,8),
     1P(8,5)
C X(I) IS THE X* DISTANCE (10X)
C  F(1,I) IS FC25(1,I), F(2,I) IS FC25(2,I), ETC, I=X* POINTER
C  F(6,I) IS FC50(1,I), F(7,I) IS FC50(2,I), ETC, I=X* POINTER
C  F(11,I) IS FC75(1,I), F(12,I) IS FC75(2,I), ETC, I=X* POINTER
C
      DATA X(1),X(2),X(3),X(4),X(5),X(6)
     1/0.0001,10.00,30.00,50.00,100.00,200.00/
      DATA F(1,1),F(1,2),F(1,3),F(1,4),F(1,5),F(1,6)
     1/100.,56.,32.,20.,12.,7./
      DATA F(2,1),F(2,2),F(2,3),F(2,4),F(2,5),F(2,6)
     1/100.,74.,49.,35.,24.,13./
      DATA F(3,1),F(3,2),F(3,3),F(3,4),F(3,5),F(3,6)
     1/100.,85.,64.,50.,35.,20./
      DATA F(4,1),F(4,2),F(4,3),F(4,4),F(4,5),F(4,6)
     1/100.,90.,74.,62.,45.,26./
      DATA F(5,1),F(5,2),F(5,3),F(5,4),F(5,5),F(5,6)
     1/100.,93.,81.,71.,53.,31./
      DATA F(6,1),F(6,2),F(6,3),F(6,4),F(6,5),F(6,6)
     1/100.,73.,53.,43.,30.,20./
      DATA F(7,1),F(7,2),F(7,3),F(7,4),F(7,5),F(7,6)
     1/100.,83.,66.,57.,42.,28./
      DATA F(8,1),F(8,2),F(8,3),F(8,4),F(8,5),F(8,6)
     1/100.,92.,79.,70.,54.,36./
      DATA F(9,1),F(9,2),F(9,3),F(9,4),F(9,5),F(9,6)
     1/100.,95.,86.,79.,64.,43./
      DATA F(10,1),F(10,2),F(10,3),F(10,4),F(10,5),F(10,6)
     1/100.,97.,90.,84.,71.,50./
      DATA F(11,1),F(11,2),F(11,3),F(11,4),F(11,5),F(11,6)
```

```
     1/100.,78.,58.,47.,34.,24./
      DATA F(12,1),F(12,2),F(12,3),F(12,4),F(12,5),F(12,6)
     1/100.,91.,75.,62.,48.,34./
      DATA F(13,1),F(13,2),F(13,3),F(13,4),F(13,5),F(13,6)
     1/100.,94.,83.,74.,60.,44./
      DATA F(14,1),F(14,2),F(14,3),F(14,4),F(14,5),F(14,6)
     1/100.,95.,87.,81.,69.,53./
      DATA F(15,1),F(15,2),F(15,3),F(15,4),F(15,5),F(15,6)
     1/100.,97.,91.,86.,76.,60./
      END
C*****************************************************************
C ************************* SUBROUTINES ************************
C*****************************************************************
C
C
C
C
C*************************************************** DEPTH CALCULATION ROUTINE
      SUBROUTINE STAGE(K,M,N,S2,Q,H3,Q3,H1)
C  INPUT PARMS ARE:
C  K,M =CHNL. FIT PARMS, Q3=QV, Q=FLOW, S2=SLOPE, N=MANNING N
C
      REAL K,K0,K1,M,M0,M1,N
      COMMON/ARAY/ F(15,6),X(6),D(8),E(8,8),T(8,8),C(3,8),H(2,8),B(4,8),
     1P(8,5)
      COMMON/SCALAR/ C0,B0,V0,A0,W0,T0,Q0,N0,N1,S0
      A1 = (1.49/N)*(S2**0.5)*K/((M+1.)**1.667)
      B1=1.667+M
      IF(Q .GT. Q3) GO TO 50
C                                                  CASE 1 STG < HV
      H1=(Q/A1)**(1./B1)
      GO TO 100
C                                                  CASE 2 STG > HV
 50    R1=A1*((M+1.)**1.667)*(H3**M)
      R1=(1/R1)**.6
      H1=(Q**.6)*R1+H3*(M/(M+1.))
 100  RETURN
      END
C
C*************************************************** HV CALCULATION ROUTINE
      SUBROUTINE COMPHV(I,H3)
C THIS ROUTINE COMPUTES THE WEIGHTED AVERAGE HV ELEVATION OF REACH
      REAL K,K0,K1,M,M0,M1,N
      COMMON/ARAY/ F(15,6),X(6),D(8),E(8,8),T(8,8),C(3,8),H(2,8),B(4,8),
     1P(8,5)
      COMMON/SCALAR/ C0,B0,V0,A0,W0,T0,Q0,N0,N1,S0
      H3=0
      DO 100 J1 = 2,I
      H3 = H3+((C(2,J1-1)+C(2,J1))/2.)*(D(J1)-D(J1-1))
 100  CONTINUE
      H3=H3/(D(I)-D(1))
      RETURN
      END
C
C*************************************************** QV CALCULATION ROUTINE
      SUBROUTINE COMPQV(K,M,N,S2,H3,Q3)
C  THIS ROUTINE COMPUTES THE FLOW QV ASSOC. WITH HV
      REAL K,K0,K1,M,M0,M1,N
      COMMON/ARAY/ F(15,6),X(6),D(8),E(8,8),T(8,8),C(3,8),H(2,8),B(4,8),
     1P(8,5)
      COMMON/SCALAR/ C0,B0,V0,A0,W0,T0,Q0,N0,N1,S0
C  INPUT PARMS ARE:
C  K,M =CHNL. FIT PARMS,  S2=SLOPE, N=MANNING N, H3=HV
      A1=(1.49/N)*(S2**.5)*K/((M+1.)**1.667)
      B1=1.667+M
      Q3=A1*(H3**B1)
      RETURN
      END
C
C*************************************************BREACH ROUTINE
      SUBROUTINE DAMBRK(K,M,N,S2,H2,H3,H4,Q3,Q,H1)
C THIS ROUTINE DET. THE MAX OUTFLOW AT DAM, ACCTNG FOR SUBMERGENCE
      REAL K,K0,K1,M,M0,M1,N
      COMMON/ARAY/ F(15,6),X(6),D(8),E(8,8),T(8,8),C(3,8),H(2,8),B(4,8),
```

```
     1P(8,5)
      COMMON/SCALAR/ CO,BO,VO,AO,WO,TO,QO,NO,N1,SO
C   CHECK FOR INSTANTANEOUS FAILURE
      IF(TO.LT.(H2/1000)) GO TO 125
      C1=(73.4*AO)/WO
C H8 IS HEAD OVER WEIR
      H8=(C1/((TO/60.)+C1/(H2**.5)))**2.
      Q=QO+3.1*WO*H8**1.5
C COMPUTE QV AT DAM
      IF(NO .LT. 2)  S2=SO/5280.
      IF(NO .LT. 2)  GO TO 50
      S2=(E(1,1)-E(2,1))/((D(2)-D(1))*5280.)
 50   CALL COMPQV(K,M,N,S2,H3,Q3)
C COMPUTE DEPTH AT DAM
      CALL STAGE(K,M,N,S2,Q,H3,Q3,H1)
C CHECK FOR SUBMERGENCE
C  NO CHECK IF FLOW AT DAM IS SUPERCRITICAL
      D1=H1/(M+1.)
      IF(H1.GT.H3) D1=H1-H3+H3/(M+1.)
      V9=(1.49/N)*SQRT(S2)*D1**(2./3.)
      FRD=V9/(32.2*D1)**0.5
      IF(FRD.GE.1.) GO TO 150
      IF(((H1+E(1,1)-BO)/H8) .LT. 0.67) GO TO 150
C
      C6=1.
      DO 100 I1=1,10
      C7=1-27.8*(((H1+E(1,1)-BO)/H8)-0.67)**3.
      IF(C7 .LT. .8)  C7 = .8
      C7=(C6+C7)/2.
      C6=C7
      Q6=Q
      Q=C7*Q
      IF(ABS(Q6-Q) .LT. Q6/20.) GO TO 150
C RECOMPUTE DEPTH AND HEAD WITH NEW FLOW
      CALL STAGE(K,M,N,S2,Q,H3,Q3,H1)
      H8=H8+((Q6-Q)*(60.*TO)/(43560.*2.*AO))
 100  CONTINUE
       GOTO 150
C
C  INSTANTANEOUS FAILURE CALCULATION
 125   M1=M+1.
       B1=WO/T(1,N1)
       C6=(1.0+0.148*(B1**2.)*(M1**2.)-0.083*(B1**3.)*(M1**2.5))**1.5
       C7=1.-.5467*B1*M1**.5+.2989*(B1**2.)*M1**.25
       C7=C7-.1634*(B1**3.)*M1**.125
       C7=C7+.0893*(B1**4.)*M1**.0625-.0486*(B1**5.)*M1**.03125
       C7=C7**1.5
       Q=QO+3.1*WO*(C6*C7)*H2**1.5
       S2=SO/5280
       IF(NO.GT.1) S2=(E(1,1)-E(2,1))/((D(2)-D(1))*5280)
      CALL COMPQV(K,M,N,S2,H3,Q3)
      CALL STAGE(K,M,N,S2,Q,H3,Q3,H1)
 150  RETURN
      END
C
C***************************************** TIME OF FLOOD ROUTINE
      SUBROUTINE TIMFLD(K,M,N,S2,H3,H4,Q,Q3,T1,T4,T5)
C  THIS SUBROUTINE COMPUTES THE TIME OF FLOOD AND DEFLOOD
C  INPUT PARMS ARE
C K,M = CHNL FIT PARMS, S2=SLOPE, Q=FLOW, H4=FLOOD DEPTH, Q3=QV, H3=HV
C
      REAL K,KO,K1,M,MO,M1,N
      COMMON/ARAY/ F(15,6),X(6),D(8),E(8,8),T(8,8),C(3,8),H(2,8),B(4,8),
     1P(8,5)
      COMMON/SCALAR/ CO,BO,VO,AO,WO,TO,QO,NO,N1,SO
      Q4=-999.
      T4=-999.
      T5=-999.
      IF(H4 .LT. 0.01) GO TO 100
      IF(H4 .GT. H3) GO TO 25
      B1=K*H4**M
      A1=(K/(M+1.))*H4**(M+1.)
      GO TO 50
 25    B1=K*H3**M
      A1=(K/(M+1.))*H3**(M+1.)+(H4-H3)*B1
```

```
 50    Q4=(1.49/N)*(S2**.5)*(A1**1.667)/(B1**.667)
       IF(Q .LT. Q4) GO TO 100
       IF(Q0.GT.Q4) GO TO 100
C COMPUTE TIME OF FLOOD
       T4=T1-((Q-Q4)/(Q-Q0))*T0/60.
C COMPUTE TIME OF DEFLOOD
       T5=T1+(((Q-Q4)/(Q-Q0))*((87120.*V0/(Q-Q0))-T0*60.))/3600.
 100   RETURN
       END
C
C*************************************SUBROUTINE RPARMS
       SUBROUTINE RPARMS(K,M,N,S2,Q,F1,H1,H3,F7,V7,X1)
C THIS ROUTINE COMPUTES THE ROUTINE PARAMETERS XC, FC, AND V*
C
C  INPUT PARMS ARE
C  KGM=CHNL FIT PARMS,V0=RES.VOL.,C0=DAM CREST ELEV, E(1,1)=DAM BASE EL.
C  H1=DEPTH AT DAM, H3=HV, F1=THETA, S2=SLOPE, N=MANNING N
C  OUTPUT PARMS ARE
C  F7=FC, V7=V*, X1=XC
C
       REAL K,K0,K1,M,M0,M1,N
       COMMON/ARAY/ F(15,6),X(6),D(8),E(8,8),T(8,8),C(3,8),H(2,8),B(4,8),
      1P(8,5)
       COMMON/SCALAR/ C0,B0,V0,A0,W0,T0,Q0,N0,N1,S0
C D8 IS THE DAM HEIGHT
       D8=C0-E(1,1)
       X1=((V0*43560.*(M+1.))/(K*D8**(M+1.)))*(6./(1.+4.*(.5**(M+1.))))
       V064=6.*V0*43560.
       IF(D8.GT.H3) X1=V064/((K*H3**M)*(3.*D8-5.*(M*H3)/(M+1.)))
       IF(D8.LT.H3.OR.(D8/2.).GT.H3) GO TO 50
       X1=V064/((K*H3**M)*(H3/(M+1)+D8-H3)+4*(K/(M+1))*(D8/2)**(M+1))
 50    IF(F1.LE.0.01)  F1=0.95
       D1=F1*H1/(M+1.)
       IF((F1*H1) .GT. H3)  D1 = F1*H1-H3+(H3/(M+1.))
       V1 = (1.49/N)*(S2**.5)*(D1**0.667)
       F7=V1/((32.2*D1)**.5)
       A2=K*((F1*H1)**M)*D1
       IF(H1 .GT. H3)  A2=K*(H3**M)*D1
       V7=(V0*43560.)/(A2*X1)
       X1=X1/5280.
       RETURN
       END
C
C*************************************** SUBROUTINE ROUTE
       SUBROUTINE ROUTE(F7,V7,X1,X5,Q,Q7)
C  THIS SUBROUTINE COMPUTES THE PEAK FLOW AT A GIVEN X-S
C
C INPUT PARMS ARE:
C F7 = FC, V7 = V*, X5 = DIST TO X-S, X1 = XC,
C
C  RETURNED VALUE IS Q7
       REAL K,K0,K1,M,M0,M1,N
       INTEGER V8,V9,F8,F9,F0,V5
       COMMON/ARAY/ F(15,6),X(6),D(8),E(8,8),T(8,8),C(3,8),H(2,8),B(4,8),
      1P(8,5)
       COMMON/SCALAR/ C0,B0,V0,A0,W0,T0,Q0,N0,N1,S0
C SET X* VALUE
       X2=X5/X1
C
C SET V* POINTER
       V8=IFIX(V7)
       V9=IFIX(V7+1)
       IF(V7 .LE. 1)  V8=1
       IF(V7 .GT. 5)  V8=5
       IF(V7 .GT. 5)  V9=5
C
C SET FC POINTERS
       F8=IFIX(4.*F7)
       F9=IFIX((4.*F7)+1.)
       IF(F7 .LE. 0.25)  F8=F9
C  ***NOTE: WHEN FC=1.5 CURVES AVAILABLE, CHANGE FOLLOWING TWO LINES
       IF(F7 .GT. 0.75)  F8=3
       IF(F7 .GT. 0.75)  F9=3
       D0=(F7-FLOAT(F8)/4.)/0.25
      IF(F8 .EQ. F9)  D0=0.
```

```
      IF(F8 .EQ. 3)  DO=DO/3.
C
C CALL ROUTINE FOR DOWNSTREAM PEAK FLOWS
      F0=F8
      V5=V8
      CALL PREDIC(X2,F0,V5,Q,Q8)
      Q1=Q8
      F0=F9
      CALL PREDIC(X2,F0,V5,Q,Q8)
      Q2=Q8
C INTERPOL FOR SPEC FC AND LOWER V*
      Q4=Q1+(Q2-Q1)*DO
      F0=F8
      V5=V9
      CALL PREDIC(X2,F0,V5,Q,Q8)
      Q1=Q8
      F0=F9
      CALL PREDIC(X2,F0,V5,Q,Q8)
      Q2=Q8
C INTERP FOR SPEC FC AND UPPER V*
      Q5=Q1+(Q2-Q1)*DO
C INTERP FOR SPECIFIC V*
      Q7=Q4+(Q5-Q4)*(V7-FLOAT(V8))
      IF(V7 .LT. 1.0)  Q7=Q4
C
      RETURN
      END
C
C*****************************************SUBROUTINE PREDIC
C
      SUBROUTINE PREDIC(X2,F0,V5,Q,Q8)
C  THIS ROUTINE INTERPOLATES WITHIN THE ROUTING CURVES TO
C  FIND THE RATIO OF QP TO QBMAX FOR A SPECIFIC (INTEGER)
C  VALUE OF V* AND AN FC OF 0.25, 0.50, OR 0.75.
C
C  INPUT VARIABLES ARE:
C  F0 = FC POINTER, V5 = V* POINTER, X2 = X*, Q = PEAK FLOW AT DAM
C  RETURN VALUE IS Q8
C
      INTEGER V5,F0
      COMMON/ARAY/ F(15,6),X(6),D(8),E(8,8),T(8,8),C(3,8),H(2,8),B(4,8),
     1P(8,5)
      COMMON/SCALAR/ CO,BO,VO,AO,WO,TO,QO,NO,N1,SO
      DO 50 I1 = 1,6
      I2=I1
      X3=X(I1)/10.
      IF((X2-X3) .LE. 0.00) GO TO 100
 50   CONTINUE
C BRACKETING X'S FOUND
 100   I3=I2-1
      J0=0
      IF(F0 .GT. 1)  J0=J0+5
      IF(F0 .GT. 2)  J0=J0+5
      J3=J0+V5
      RL1=ALOG(F(J3,I3))
      RL2=ALOG(F(J3,I2))
      RL3=ALOG(X(I3))
      RL4=ALOG(X(I2))
      RL5=ALOG(X2*10.)
      D3=(RL2-RL1)/(RL4-RL3)
      RL6=(RL5-RL3)*D3 + RL1
      IF((X2*10.) .GT. X(6))  RL6 = (RL5-RL4)*D3 + RL2
      IF(RL6 .LT. -3.0)  RL6 = -3.0
      Q8 = (EXP(RL6)/100.) * Q
C
      RETURN
      END
```

```
SIMPLIFIED DAMBREAK MODEL
FORTRAN LANGUAGE INTERACTIVE VERSION
WRITTEN BY JONATHAN N. WELMORE  HRL  MAY, 1983

INPUT "SHORT" FOR SHORT VERSION, "LONG" FOR FULL MODEL
SHORT

INPUT HEIGHT (FEET) OF DAM
  100.00

INPUT VOLUME OF RESERVOIR (AC-FT) AT MAX POOL ELEV
25000.00

INPUT FINAL BREACH WIDTH (FT)
IF N/A ENTER 0.  DEFAULT USED = 3 * BREACH DEPTH
    0.00

INPUT TIME (MINUTES) REQUIRED FOR BREACH FORMATION
IF N/A , ENTER 0.
    0.00
ENTER TYPE OF DAM...0 FOR EARTH DAM, 1 FOR CONCRETE DAM
0
ESTIMATED TIME OF FAILURE =   33.33 MINUTES

INPUT NUMBER OF PAIRS OF ELEV-TOPWIDTHS USED TO
DESCRIBE EACH X-SECTION (MIN=2, MAX=8)
MODEL ASSUMES DEPTH #1 = 0. AND TOPW #1 = 0.
2

INPUT DEPTH (FEET) # 2 AND ASSOC. TOPWIDTH FOR X-S  # 1
  100.00
 1000.00

INPUT MANNING N AT X-S # 1 (DEFAULT = 0.050)
0.000

INPUT CHANNEL SLOPE (FT/MI) BELOW DAM
    0.00

 ENTER NUMBER OF FORECAST POINTS BELOW DAM (MAX = 7)
7

INPUT DIST DOWNSTREAM (MILES) TO FORECAST PT. NO. 1
   10.00
INPUT DIST DOWNSTREAM (MILES) TO FORECAST PT. NO. 2
   20.00
INPUT DIST DOWNSTREAM (MILES) TO FORECAST PT. NO. 3
   30.00
INPUT DIST DOWNSTREAM (MILES) TO FORECAST PT. NO. 4
   40.00
INPUT DIST DOWNSTREAM (MILES) TO FORECAST PT. NO. 5
   50.00
INPUT DIST DOWNSTREAM (MILES) TO FORECAST PT. NO. 6
   60.00
INPUT DIST DOWNSTREAM (MILES) TO FORECAST PT. NO. 7
   70.00
```

PROFILE OF CRESTS AND TIMES FOR ON RIVER DAM

DISTANCE DOWNSTREAM (MILES)	PEAK FLOW CFS	PEAK DEPTH FEET	FLOOD DEPTH FEET	TIME FLOOD HR	TIME PEAK HR	TIME DEFLOOD HR
0.00	324314.38	63.50	0.00	-999.00	0.56	-999.00
10.00	238917.97	56.02	0.00	-999.00	1.46	-999.00
20.00	206646.09	53.06	0.00	-999.00	2.37	-999.00
30.00	183701.38	50.77	0.00	-999.00	3.32	-999.00
40.00	167489.13	49.04	0.00	-999.00	4.32	-999.00
50.00	152864.66	47.39	0.00	-999.00	5.34	-999.00
60.00	141868.66	46.08	0.00	-999.00	6.38	-999.00
70.00	131442.41	44.78	0.00	-999.00	7.42	-999.00

```
  SIMPLIFIED DAMBREAK MODEL
  FORTRANE LANGUAGE INTERACTIVE VERSION
  WRITTEN BY JONATHAN N. WEIMORE  HRL  MAY, 1983

INPUT "SHORT" FOR SHORT VERSION, "LONG" FOR FULL MODEL
LONG

INPUT NAME OF DAM
TEST4

INPUT RIVER NAME
NON-PRISMATIC #4

INPUT DAM CREST ELEVATION (FT. MSL)
 1100.00

INPUT FINAL BREACH BOTTOM ELEVATION (FT. MSL)
 1000.00

INPUT VOLUME OF RESERVOIR (AC-FT) AT MAX POOL ELEV
IF N/A ENTER 0. AND VOL WILL BE EST. FROM SURF. AREA
    0.00

INPUT RESERVOIR SURFACE AREA (ACRES) AT MAX POOL ELEV
IF N/A ENTER 0. AND S.A. WILL BE EST. FROM VOLUME.
  500.00

INPUT FINAL BREACH WIDTH (FT)
IF N/A ENTER 0.  DEFAULT USED = 2 * BREACH DEPTH
  100.00

INPUT TIME (MINUTES) REQUIRED FOR BREACH FORMATION
IF N/A , ENTER 0.
   90.00

INPUT TURBINE/SPILLWAY/OVERTOPPING FLOW (CFS).
IF N/A, ENTER 0.0.  DEFAULT = 0.0
 1500.00

INPUT NUMBER OF X-SECTIONS (STARTING AT DAM) USED TO
DESCRIBE ROUTING REACH.  (MIN=1, MAX=8)
5

INPUT NUMBER OF PAIRS OF ELEV-TOPWIDTHS USED TO
DESCRIBE EACH X-SECTION (MIN=2, MAX=8)
5

INPUT LOWEST CHANNEL ELEV.(FT.MSL) AT X-SECTION # 1
(ELEVATION OF BASE OF DAM (FT. MSL))
 1000.00

INPUT ELEV(FT MSL) # 2 AND ASSOC. TOPWIDTH FOR X-S  # 1
 1025.00
  250.00

INPUT ELEV(FT MSL) # 3 AND ASSOC. TOPWIDTH FOR X-S  # 1
 1050.00
  500.00

INPUT ELEV(FT MSL) # 4 AND ASSOC. TOPWIDTH FOR X-S  # 1
 1075.00
  750.00

INPUT ELEV(FT MSL) # 5 AND ASSOC. TOPWIDTH FOR X-S  # 1
 1100.00
 1000.00

INPUT MANNING N AT X-S # 1 (DEFAULT = 0.050)
0.000

INPUT VALLEY WALL HEIGHT ABOVE CHANNEL BOTTOM AT X-S # 1
IF N/A INPUT 0.
    0.00
```

```
INPUT FLOOD DEPTH AT X-S # 1
IF N/A ENTER 0.
   30.00

INPUT DISTANCE DOWNSTREAM (MILES) TO X-SECTION # 2
   10.00

INPUT LOWEST CHANNEL ELEV.(FT.MSL) AT X-SECTION # 2
  850.00

INPUT ELEV(FT MSL) # 2 AND ASSOC. TOPWIDTH FOR X-S  # 2
  875.00
  400.00

INPUT ELEV(FT MSL) # 3 AND ASSOC. TOPWIDTH FOR X-S  # 2
  900.00
  750.00

INPUT ELEV(FT MSL) # 4 AND ASSOC. TOPWIDTH FOR X-S  # 2
  925.00
 1125.00

INPUT ELEV(FT MSL) # 5 AND ASSOC. TOPWIDTH FOR X-S  # 2
  950.00
 1500.00

INPUT MANNING N AT X-S # 2 (DEFAULT = 0.050)
0.000

INPUT VALLEY WALL HEIGHT ABOVE CHANNEL BOTTOM AT X-S # 2
IF N/A INPUT 0.
    0.00

INPUT FLOOD DEPTH AT X-S # 2
IF N/A ENTER 0.
   20.00

INPUT DISTANCE DOWNSTREAM (MILES) TO X-SECTION # 3
   20.00

INPUT LOWEST CHANNEL ELEV.(FT.MSL) AT X-SECTION # 3
  700.00

INPUT ELEV(FT MSL) # 2 AND ASSOC. TOPWIDTH FOR X-S  # 3
  725.00
  200.00

INPUT ELEV(FT MSL) # 3 AND ASSOC. TOPWIDTH FOR X-S  # 3
  750.00
  400.00

INPUT ELEV(FT MSL) # 4 AND ASSOC. TOPWIDTH FOR X-S  # 3
  775.00
  600.00

INPUT ELEV(FT MSL) # 5 AND ASSOC. TOPWIDTH FOR X-S  # 3
  800.00
  800.00

INPUT MANNING N AT X-S # 3 (DEFAULT = 0.050)
0.000

INPUT VALLEY WALL HEIGHT ABOVE CHANNEL BOTTOM AT X-S # 3
IF N/A INPUT 0.
    0.00

INPUT FLOOD DEPTH AT X-S # 3
IF N/A ENTER 0.
   20.00

INPUT DISTANCE DOWNSTREAM (MILES) TO X-SECTION # 4
   30.00
```

```
INPUT LOWEST CHANNEL ELEV.(FT.MSL) AT X-SECTION # 4
  550.00

INPUT ELEV(FT MSL) # 2 AND ASSOC. TOPWIDTH FOR X-S  # 4
  575.00
  500.00

INPUT ELEV(FT MSL) # 3 AND ASSOC. TOPWIDTH FOR X-S  # 4
  600.00
 1000.00

INPUT ELEV(FT MSL) # 4 AND ASSOC. TOPWIDTH FOR X-S  # 4
  625.00
 1500.00

INPUT ELEV(FT MSL) # 5 AND ASSOC. TOPWIDTH FOR X-S  # 4
  650.00
 2000.00

INPUT MANNING N AT X-S # 4 (DEFAULT = 0.050)
0.000

INPUT VALLEY WALL HEIGHT ABOVE CHANNEL BOTTOM AT X-S # 4
IF N/A INPUT 0.
    0.00

INPUT FLOOD DEPTH AT X-S # 4
IF N/A ENTER 0.
   10.00

INPUT DISTANCE DOWNSTREAM (MILES) TO X-SECTION # 5
   40.00

INPUT LOWEST CHANNEL ELEV.(FT.MSL) AT X-SECTION # 5
  400.00

INPUT ELEV(FT MSL) # 2 AND ASSOC. TOPWIDTH FOR X-S  # 5
  425.00
  250.00

INPUT ELEV(FT MSL) # 3 AND ASSOC. TOPWIDTH FOR X-S  # 5
  450.00
  500.00

INPUT ELEV(FT MSL) # 4 AND ASSOC. TOPWIDTH FOR X-S  # 5
  475.00
  750.00

INPUT ELEV(FT MSL) # 5 AND ASSOC. TOPWIDTH FOR X-S  # 5
  500.00
 1000.00

INPUT MANNING N AT X-S # 5 (DEFAULT = 0.050)
0.000

INPUT VALLEY WALL HEIGHT ABOVE CHANNEL BOTTOM AT X-S # 5
IF N/A INPUT 0.
    0.00

INPUT FLOOD DEPTH AT X-S # 5
IF N/A ENTER 0.
   10.00
```

PROFILE OF CRESTS AND TIMES FOR TEST4 DAM
ON NON-PRISMATIC #4 RIVER

DISTANCE DOWNSTREAM (MILES)	PEAK FLOW CFS	PEAK DEPTH FEET	FLOOD DEPTH FEET	TIME FLOOD HR	TIME PEAK HR	TIME DEFLOOD HR
0.00	217304.78	54.83	30.00	0.29	1.50	2.55
10.00	165005.25	41.38	20.00	1.29	2.58	4.47
20.00	137956.94	50.28	20.00	2.26	3.65	6.36
30.00	123123.34	34.17	10.00	3.39	4.85	8.24
40.00	110151.70	42.50	10.00	4.62	6.11	10.15

****

FULL DAMBRK RESULTS

****

PROFILE OF CRESTS AND TIMES FOR TEST NO. 4 OF NON-PR
BELOW SIMPLIFIED DAMBREAK

RVR MILE FROM DAM	MAX ELEV (FT)	MAX FLOW (CFS)	TIME MAX ELEV(HR)	FLOOD ELEV (FT)	TIME FLOOD (HR)
0.000	53.75	224206	1.500	30.00	0.75
10.000	42.51	173374	2.400	20.00	1.80
20.000	49.40	143972	3.450	20.00	2.85
30.000	34.73	126714	4.575	10.00	3.90
40.000	40.10	108592	5.310	10.00	5.10

APPENDIX III

THE NWS SIMPLIFIED DAM BREAK MODEL

BASIC VERSION LISTING WITH EXAMPLE RUNS

```
 10 REM#
 20 REM#
 30 REM#  SIMPLIFIED DAMBREAK MODEL
 40 REM#  BASIC LANGUAGE INTERACTIVE VERSION
 50 REM#  WRITTEN BY JONATHAN WEIMORE  5/3/83
 60 REM#
 70 DIM F(15,6),X(6),D(8),E(8,8),T(8,8),C(3,8),H(2,8),B(4,8),P(8,5)
 80 REM#
 90 REM#
100 REM#  ************ SUMMARY OF INPUT DATA VARIABLES *************
110 REM#
120 REM#    CO      =  DAM CREST ELEVATION (FT. MSL)
130 REM#    BO      =  FINAL BREACH ELEV (FT. MSL)
140 REM#    VO      =  VOLUME OF RESERVOIR (AC-FT)
150 REM#    AO      =  RES. SURF. AREA (ACRES)
160 REM#    WO      =  FINAL BREACH WIDTH
170 REM#    TO      =  TIME OF FAILURE (MINUTES)
180 REM#    QO      =  SPILLWAY/TURBINE/SURCHARGE FLOW (CFS)
190 REM#    NO      =  NO. OF X-SECTIONS TO BE READ IN
200 REM#    N1      =  NO. OF ELEV-TOPW PAIRS
210 REM#    D(I)    =  DOWNSTREAM DIST TO X-S (I)
220 REM#    E(I,J)  =  ELEV(J) CORRESPONDING TO TOPW(J) AT X-S (I)
230 REM#    T(I,J)  =  TOPW(J) CORRESPONDING TO ELEV(J) AT X-S (I)
240 REM#    C(1,I)  =  MANNING 'N' AT X-S (I)
250 REM#    C(2,I)  =  'HV' DEPTH AT X-S (I)
260 REM#    C(3,I)  =  FLOOD DEPTH AT X-S (I)
270 REM#    SO      =  DOWNSTREAM SLOPE (READ IN IF ONLY 1 X-S GIVEN)
280 REM#
290 REM#*****************************************************************
300 REM#
310 REM# ************** SUMMARY OF INTERNAL ARRAYS ********************
320 REM#
330 REM#   X(I)     =  X-ORDINATES OF FC CURVE FAMILY MATRICES
340 REM#   F(I,J)   =  Y-ORDINATES OF FC CURVE FAMILY MATRICES
350 REM#   H(1,J)   =  GIVEN X-S HEIGHT J ABOVE INVERT AT X-S (I)
360 REM#   H(2,J)   =  GIVEN X-S HEIGHT ABOVE INVERT AT FIRST X-S
370 REM#   B(1,J)   =  INTERP. TW AT CURRENT X-S CORRESPONDING TO H(2,J)
380 REM#   B(2,J)   =  TOPW AT PREVIOUS X-S CORRESPONDIG TO H(2,J)
390 REM#   B(3,J)   =  WEIGHTED TOPW CORRESPONDING TO H(2,J)
400 REM#   B(4,J)   =  DISTANCE WEIGHTED TOPW (J) AT CURRENT X-S
410 REM#   P(I,1)   =  Q PEAK AT X-S (I)
420 REM#   P(I,2)   =  PEAK DEPTH AT X-S (I)
430 REM#   P(I,3)   =  TIME TO PEAK AT X-S (I)
440 REM#   P(I,4)   =  TIME OF FLOODING AT X-S (I)
450 REM#   P(I,5)   =  TIME OF DEFLOODING AT X-S (I)
460 REM#
470 REM# *****************************************************************
480 REM#  INITIALIZE VARIABLES
482 WO=0
484 NO=1
486 AO=0
500 FOR I=1 TO 8
510 B(3,I)=0
520 NEXT I
530 REM# SET UP CURVE MATRICES
540 REM# X(I) IS THE X* DISTANCE (10X)
550 READ X(1),X(2),X(3),X(4),X(5),X(6)
560 DATA 1.E-05,10,30,50,100,200
570 REM#
580 REM#  SET UP CURVE ORDINATES FOR FC = 0.25, V* = 1-5)
590 REM#  SET UP CURVE ORDINATES FOR FC = 0.50, V* = 1-5)
600 REM#  SET UP CURVE ORDINATES FOR FC = 0.75, V* = 1-5)
610 REM#  F(1,I) IS FC25(1,I), F(2,I) IS FC25(2,I), ETC, I=X* POINTER
620 REM#  F(6,I) IS FC50(1,I), F(7,I) IS FC50(2,I), ETC, I=X* POINTER
630 REM#  F(11,I) IS FC75(1,I), F(12,I) IS FC75(2,I), ETC, I=X* POINTER
640 REM#
650 FOR J=1 TO 6
660 FOR I=1 TO 15
670 READ F(I,J)
680 NEXT I
690 NEXT J
700 REM#
710 DATA 100,100,100,100,100
720 DATA 100,100,100,100,100
```

```
730 DATA 100,100,100,100,100
740 DATA 56,74,85,90,93
750 DATA 73,83,92,95,97
760 DATA 78,91,94,95,97
770 DATA 32,49,64,74,81
780 DATA 53,66,79,86,90
790 DATA 58,75,83,87,91
800 DATA 20,35,50,62,71
810 DATA 43,57,70,79,84
820 DATA 47,62,74,81,86
830 DATA 12,24,35,45,53
840 DATA 30,42,54,64,71
850 DATA 34,48,60,69,76
860 DATA 7,13,20,26,31
870 DATA 20,28,36,43,50
880 DATA 24,34,44,53,60
882 READ S$,E$,F$,M$,N$
884 DATA 'SHORT','ELEV.','DEPTH','(FT. MSL)','(FEET)'
888 PRINT
890 PRINT '  SIMPLIFIED DAMBREAK MODEL'
900 PRINT '  BASIC LANGUAGE INTERACTIVE VERSION'
910 PRINT '  WRITTEN BY JONATHAN N. WETMORE  HRL  MAY, 1983'
920 PRINT
921 PRINT 'INPUT "SHORT" FOR SHORTENED VERSION, "LONG" FOR FULL MODEL'
922 INPUT V$
924 IF V$<>S$ THEN 930
925 PRINT
926 PRINT 'INPUT HEIGHT OF DAM (FEET)'
927 INPUT H2
929 GOTO 1090
930 PRINT
935 PRINT 'INPUT NAME OF DAM'
940 INPUT D$
950 PRINT
960 PRINT 'INPUT RIVER NAME'
970 INPUT R$
980 PRINT
990 PRINT 'INPUT DAM CREST ELEVATION (FT. MSL)'
1000 INPUT C0
1010 IF C0<.1 THEN 990
1020 PRINT
1030 PRINT 'INPUT FINAL BREACH BOTTOM ELEVATION (FT. MSL)'
1040 INPUT B0
1050 IF B0<.01 THEN 1030
1070 REM# H2 IS THE DEPTH OF BREACH
1080 H2=C0-B0
1090 PRINT
1093 PRINT 'INPUT VOLUME OF RESERVOIR (AC-FT) AT MAX POOL ELEV'
1095 IF V$=S$ THEN 1110
1100 PRINT 'IF N/A ENTER 0. AND VOL WILL BE EST. FROM SURF. AREA'
1110 INPUT V0
1115 IF V$=S$ THEN 1200
1120 PRINT
1130 PRINT 'INPUT RESERVOIR SURFACE AREA (ACRES) AT MAX POOL ELEV'
1140 PRINT 'IF N/A ENTER 0. AND S.A. WILL BE EST. FROM VOLUME.'
1150 INPUT A0
1160 IF V0>.1 THEN 1200
1170 IF A0>.1 THEN 1200
1180 PRINT 'A VALUE FOR EITHER VOLUME OR SURFACE AREA MUST BE ENTERED'
1190 GOTO 1090
1200 PRINT
1210 PRINT 'INPUT FINAL BREACH WIDTH (FT)'
1220 PRINT 'IF N/A ENTER 0.  DEFAULT USED = 3 * BREACH DEPTH'
1230 INPUT W0
1240 IF W0>0 THEN 1250
1245 W0=3*H2
1250 PRINT
1260 PRINT 'INPUT TIME (MINUTES) REQUIRED FOR BREACH FORMATION'
1270 PRINT 'IF N/A , ENTER 0.'
1280 INPUT T0
1290 IF T0>.00001 THEN 1350
1295 T0=H2/3
1300 REM# TIME OF FAILURE NOT GIVEN...MAKE ESTIMATE
1310 PRINT 'ENTER TYPE OF DAM...0 FOR EARTH DAM, 1 FOR CONCRETE DAM'
1320 INPUT T1
```

```
1324 IF T1<1 THEN  1340
1326 PRINT 'IS THIS AN INSTANTANEOUS FAILURE?'
1328 INPUT L$
1330 T0=5
1332 IF L$<>'YES' THEN 1340
1334 T0=H2/1500
1340 PRINT 'ESTIMATED TIME OF FAILURE =':T0:'MINUTES'
1350 IF V$=S$ THEN 1440
1355 PRINT
1360 PRINT 'INPUT TURBINE/SPILLWAY/OVERTOPPING FLOW (CFS). '
1370 PRINT 'IF N/A, ENTER 0.0.  DEFAULT = 0.0'
1380 INPUT Q0
1390 PRINT
1400 PRINT 'INPUT NUMBER OF X-SECTIONS (STARTING AT DAM) USED TO'
1410 PRINT 'DESCRIBE ROUTING REACH.  (MIN=1, MAX=8)'
1420 INPUT N0
1430 IF N0<1 THEN 1390
1440 PRINT
1450 PRINT 'INPUT NUMBER OF PAIRS OF ELEV-TOPWIDTHS USED TO'
1460 PRINT 'DESCRIBE EACH X-SECTION (MIN=2, MAX=8)'
1462 IF V$<>S$ THEN 1470
1464 PRINT 'MODEL ASSUMES DEPTH #1 = 0. AND TOPWIDTH #1 = 0.'
1470 INPUT N1
1480 IF N1<2 THEN 1440
1490 REM#
1500 REM# BEGIN READING IN X-SECTION INFORMATION
1520 D(1)=0
1530 FOR I=1 TO N0
1540 T(I,1)=0
1550 IF I=1 THEN 1580
1555 PRINT
1560 PRINT 'INPUT DISTANCE DOWNSTREAM FROM DAM (MILES) TO X-SECTION #':I
1570 INPUT D(I)
1580 IF V$<>S$ THEN 1590
1581 E(1,1)=0
1582 C0=H2
1584 B0=0
1585 E$=F$
1586 M$=N$
1587 GOTO 1625
1590 PRINT
1600 PRINT 'INPUT LOWEST CHANNEL ELEV. (FT. MSL) AT X-SECTION #':I
1610 IF I>1 THEN 1620
1615 PRINT '(ELEVATION OF BASE OF DAM (FT. MSL))'
1620 INPUT E(I,1)
1625 IF I>1 THEN 1720
1630 REM#
1640 REM#  IF SURFACE AREA NOT GIVEN, ESTIMATE A0 USING V0
1645 IF A0>0 THEN 1655
1647 A0=2*V0/(C0-E(1,1))
1650 REM#  IF VOLUME NOT GIVEN, ESTIMATE V0 USING A0
1655 IF V0>0 THEN 1670
1657 V0=(A0/2)*(C0-E(1,1))
1660 REM#
1670 IF B0<=(E(1,1)+5) THEN 1720
1680 REM#  PERCHED BREACH...RECOMPUTE V0 BASED ON AVAILABLE VOLUME
1690 V0=H2/2*A0*(1+((B0-E(1,1))/(C0-E(1,1)))^2)
1700 REM#
1710 REM# ONCE 1ST X-S HAS BEEN READ IN & FITTED & SLOPE FOUND COMPUTE PEAK
1720 IF I<>2 THEN 1915
1750 M=M0
1760 K=K0
1770 N=C(1,1)
1780 H3=C(2,1)
1790 H4=C(3,1)
1800 GOSUB 4970
1810 REM# SAVE FLOW,DEPTH AND TPEAK AT DAM
1820 P(1,1)=Q
1830 P(1,2)=H1
1840 P(1,3)=T0/60
1850 T1=T0/60
1860 GOSUB 5320
1870 REM#  SAVE TIMES OF FLOODING AND DEFLOODING AT DAM
1880 P(1,4)=T4
1890 P(1,5)=T5
```

```
1900 IF NO<2 THEN 3740
1910 REM#
1915 FOR J=2 TO N1
1920 PRINT
1930 PRINT 'INPUT':E$:M$:'#':J:'AND ASSOC. TOPWIDTH FOR X-S #':I
1940 INPUT E(I,J),T(I,J)
1950 NEXT J
1951 IF V$<>S$ THEN 1960
1953 C(2,I)=H2+5
1954 C(3,I)=0
1960 PRINT
1970 PRINT 'INPUT MANNING N AT X-S #':I:'(DEFAULT = 0.050)'
1980 INPUT C(1,I)
1990 IF C(1,I)>0 THEN 1995
1992 C(1,I)=.05
1995 IF V$=S$ THEN 2090
2000 PRINT
2010 PRINT 'INPUT VALLEY WALL HEIGHT ABOVE CHANNEL BOTTOM AT X-S #':I
2020 PRINT 'IF N/A INPUT 0.'
2030 INPUT C(2,I)
2040 IF C(2,I)>0 THEN 2050
2045 C(2,I)=H2+5
2050 PRINT
2060 PRINT 'INPUT FLOOD DEPTH AT X-S #':I
2070 PRINT 'IF N/A ENTER 0.'
2080 INPUT C(3,I)
2090 PRINT
2100 IF NO>1 THEN  2140
2105 PRINT 'INPUT CHANNEL SLOPE (FT/MI) BELOW DAM'
2110 INPUT S0
2112 IF S0>0 THEN 2140
2114 S0=H2^2*(T(1,N1)/(24.75*V0))
2120 REM#
2130 REM#  FIT X-SECTION W/ K & M PARMS
2140 IF N1>2 THEN 2230
2150 REM# ONLY 2 X-S POINTS GIVEN.  SET M = 1
2160 M0=1
2170 K0=T(I,N1)/(E(I,N1)-E(I,1))
2180 IF I>1 THEN 2200
2185 H(2,N1)=E(I,N1)-E(I,1)
2190 B(2,N1)=T(I,N1)
2200 N4=N1
2210 GOTO 2485
2220 REM#  INITIALIZE LEAST SQUARES ALGORITHM
2230 U1=0
2240 U2=0
2250 U3=0
2260 U4=0
2270 N2=N1
2280 FOR J1=2 TO N1
2290 H(1,J1)=E(I,J1)-E(I,1)
2300 REM# SAVE H'S OF FIRST X-S FOR WEIGHTED X-S ROUTINE
2305 IF I>1 THEN 2340
2310 H(2,J1)=H(1,J1)
2315 IF H(1,J1)<C(2,1) THEN 2320
2317 H(2,J1)=C(2,1)
2320 B(2,J1)=T(I,J1)
2330 REM# SEE IF HV IS EXCEEDED
2340 IF H(1,J1)<C(2,I) THEN 2342
2341 H(1,J1)=C(2,I)
2342 IF H(1,J1-1)<C(2,I) THEN 2360
2343 N2=J1-1
2344 GO TO 2410
2360 U1=U1+LOG(H(1,J1))
2370 U2=U2+(LOG(H(1,J1)))^2
2372 IF H(1,J1)<C(2,I) THEN 2380
2375 D0=(T(I,J1)-T(I,J1-1))/(E(I,J1)-E(I,J1-1))
2376 T(I,J1)=T(I,J1-1)+(H(1,J1)+E(I,1)-E(I,J1-1))*D0
2377 IF I>1 THEN  2380
2378 B(2,J1)=T(I,J1)
2380 U3=U3+LOG(T(I,J1))
2390 U4=U4+LOG(H(1,J1))*LOG(T(I,J1))
2400 NEXT J1
2410 N3=N2-1
2420 IF I>1 THEN 2426
```

```
2425 N4=N2
2426 IF N2>2 THEN 2430
2427 M0=1
2428 K0=T(I,N2)/H(1,N2)
2429 GO TO 2470
2430 M0=U4-U1*U3/N3
2440 M0=M0/(U2-(U1^2)/N3)
2450 IF M0>0 THEN  2460
2455 M0=.01
2460 K0=U3/N3-M0*U1/N3
2465 K0=EXP(K0)
2467 REM#
2468 REM# CHECK GOODNESS OF FIT BETW GIVEN AND FITTED X-S
2470 U8=0
2471 U7=0
2472 IF U8>1 THEN  PRINT "DEPTH","GIVEN TW","FIT TW","K =":K0:"M =":M0
2473 FOR J1=2 TO N2
2474 IF U8>1 THEN  PRINT H(1,J1),T(I,J1),K0*H(1,J1)^M0
2475 IF ABS((T(I,J1)-K0*H(1,J1)^M0))/T(I,J1)<=.5 THEN  2477
2476 U7=N2-1
2477 NEXT J1
2478 IF U8>1 THEN 2485
2479 IF U7<1 THEN 2485
2480 PRINT "*** WARNING *** X-SECTION FIT IS OFF AT MILE":D(I)
2481 PRINT "DEPTH ERRORS MAY OCCUR...TO FIX, USER SHOULD PLOT THE X-SECTION,"
2482 PRINT "DRAW A SMOOTH CURVE THRU THE POINTS, AND RERUN WITH SMOOTHED POINTS"
2483 U8=2
2484 GOTO 2472
2485 IF N0<2 THEN 1750
2490 IF I=1 THEN 3740
2500 REM#
2510 REM# COMPUT DISTANCE WEIGHTED X-SECTION
2520 REM#
2530 FOR J1=2 TO N4
2540 REM#
2550 REM# INTERP H(2,J1) INTO ELEV TABLE TO FIND ASSOC TOPW @ X-S(I)
2560 IF H(2,J1)<=(E(I,N1)-E(I,1)) THEN 2580
2570 J0=N1
2575 GO TO 2630
2580 FOR J2=2 TO N1
2590 J0=J2
2600 IF (H(2,J1)-(E(I,J2)-E(I,1)))<=0 THEN 2630
2610 NEXT J2
2620 REM#  BRACKETING ELEVS FOUND...COMPUTE DB/DH
2630 J3=J0-1
2640 D0=(T(I,J0)-T(I,J3))/(E(I,J0)-E(I,J3))
2650 REM#
2660 REM# DET. ASSOC TOPW @ X-S I
2670 B(1,J1)=T(I,J3)+(E(I,1)+H(2,J1)-E(I,J3))*D0
2680 REM#  CHECK IF HV IS EXCEEDED
2690 IF H(2,J1)<C(2,I) THEN  2710
2695 B(1,J1)=T(I,N2)
2700 REM# B(3,J1) IS THE WEIGHTED TOPWIDTH
2710 B(3,J1)=B(3,J1)+((B(2,J1)+B(1,J1))/2)*(D(I)-D(I-1))
2720 REM# SAVE INTERPOLATED TOPW AS B(2,J1)
2730 B(2,J1)=B(1,J1)
2740 NEXT J1
2750 REM#
2760 REM# DIVIDE WEIGHTED TOPW BY DISTANCE
2770 FOR J1=2 TO N4
2780 B(4,J1)=B(3,J1)/(D(I)-D(1))
2790 NEXT J1
2800 REM#
2810 REM# COMPUTE DISTANCE WEIGHTED MANNING N
2820 N=0
2830 FOR J1=2 TO I
2840 N=N+((C(1,J1)+C(1,J1-1))/2)*(D(J1)-D(J1-1))
2850 NEXT J1
2860 N=N/(D(I)-D(1))
2870 REM#
2880 REM#  FIT K & M PARMS TO DIST WEIGHTED X-S
2890 REM#
2900 REM#
2910 IF N4>2 THEN 2970
2920 REM# ONLY 2 X-S POINTS GIVEN.  SET M = 1
```

```
2930 M1=1
2940 K1=B(4,N4)/H(2,N4)
2950 GOTO 3150
2960 REM#  INITIALIZE LEAST SQUARES ALGORITHM
2970 U1=0
2980 U2=0
2990 U3=0
3000 U4=0
3010 FOR J1=2 TO N4
3020 U1=U1+LOG(H(2,J1))
3030 U2=U2+(LOG(H(2,J1)))^2
3040 U3=U3+LOG(B(4,J1))
3050 U4=U4+LOG(H(2,J1))*LOG(B(4,J1))
3060 NEXT J1
3070 N3=N4-1
3080 M1=U4-U1*U3/N3
3090 M1=M1/(U2-(U1^2)/N3)
3100 IF M1>0 THEN  3110
3105 M1=.01
3110 K1=U3/N3-M1*U1/N3
3115 K1=EXP(K1)
3117 REM#
3118 REM# CHECK GOODNESS OF FIT OF WEIGHTED X-S
3120 U8=0
3121 U7=0
3122 IF U8>1 THEN  PRINT 'DEPTH','WEIGHTED TW','FIT TW','K =':K1:'M =':M1
3123 FOR J1=2 TO N4
3124 IF U8>1 THEN  PRINT H(2,J1),B(4,J1),K1*H(2,J1)^M1
3125 IF ABS((B(4,J1)-K1*H(2,J1)^M1))/B(4,J1)<=.5 THEN  3127
3126 U7=N4-1
3127 NEXT J1
3128 IF U8>1 THEN 3150
3129 IF U7<1 THEN 3150
3130 PRINT 'WARNING - X-S FIT IS OFF FOR AVG REACH FROM DAM TO MILE':D(I)
3131 ~~3131~~ PRINT 'ROUTING ERRORS MAY OCCUR...TO FIX, USER SHOULD PLOT THE X-SECTION,'
3132 ~~3132~~ PRINT 'DRAW A SMOOTH CURVE THRU THE POINTS, AND RERUN WITH SMOOTHED POINTS'
3133 U8=2
3134 GOTO 3122
3140 REM# RECOMPUTE DEPTH AT DAM USING WIGHTED X-S PROPERTIES
3150 S2=(E(1,1)-E(I,1))/((D(I)-D(1))*5280)
3160 K=K1
3170 M=M1
3180 Q=P(1,1)
3190 GOSUB 4770
3200 GOSUB 4870
3210 GOSUB 4630
3220 H0=H1
3230 REM# F1 IS THETA
3240 F1=.95
3243 I9=0
3250 I8=I9
3255 Q=P(1,1)
3257 GOSUB 4630
3260 GOSUB 5590
3270 X5=X1
3280 IF I9<1 THEN  3285
3282 X5=D(I)
3285 Q=P(1,1)
3290 GOSUB 5810
3300 REM#
3310 IF I9>0 THEN 3440
3320 REM#  CHECK THETA VALUE
3330 Q=Q7
3340 GOSUB 4630
3350 F2=(H0+H1)/(2*H0)
3360 IF (ABS(F1-F2)/F1)>.02 THEN  3370
3365 I9=1
3370 IF I9<>I8 THEN 3280
3380 REM#  NEW THETA MUST BE COMPUTED
3390 F1=(F1+F2)/2
3400 GOTO 3250
3410 REM#
3420 REM#
3430 REM# SAVE PEAK FLOW  AT X-S (I)
3440 P(I,1)=Q7
```

```
3445 IF P(I-1,1)>P(I,1) THEN 3450
3447 P(I,1)=.99*P(I-1,1)
3450 REM# COMPUTE TIME TO PEAK
3460 XS=D(I)/2
3470 GOSUB 5810
3480 Q=(.3+.1*M)*Q7
3490 GOSUB 4630
3500 D9=H1/(M+1)
3510 IF H1<=H3 THEN  3520
3515 D9=H1-H3+H3/(M+1)
3520 V9=(1.49/N)*(S2^.5)*D9^.667
3530 C9=.682*V9*(1.667-(.667*(M/(M+1))))
3540 P(I,3)=(T0/60)+D(I)/C9
3545 IF P(I,3)>P(I-1,3) THEN 3570
3547 P(I,3)=1.01*P(I-1,3)
3560 REM#  COMPUTE AND SAVE PEAK DEPTH AT X-S (I)
3570 K=K0
3580 M=M0
3590 S2=(E(I-1,1)-E(I,1))/((D(I)-D(I-1))*5280)
3592 N=C(1,I)
3600 H3=C(2,I)
3610 Q=P(I,1)
3620 GOSUB 4870
3630 GOSUB 4630
3640 P(I,2)=H1
3650 REM#  DET TIME FLOODING AND DEFLOODING
3660 T1=P(I,3)
3670 H4=C(3,I)
3680 GOSUB 5320
3690 P(I,4)=T4
3700 P(I,5)=T5
3710 REM#
3740 NEXT I
3370 REM#
3880 IF NO>1 THEN 4470
3890 PRINT 'ENTER NUMBER OF FORECAST POINTS BELOW DAM (MAX = 7)'
3900 INPUT NO
3910 NO=NO+1
3920 IF NO < 2 THEN 4470
3960 H0=P(1,2)
3970 REM# F1 IS THETA
3980 F1=.95
3982 I9=0
3990 I8=I9
3995 Q=P(1,1)
3997 GOSUB 4630
4000 GOSUB 5590
4010 XS=X1
4020 GOSUB 5810
4030 REM#
4040 REM#  CHECK THETA VALUE
4050 Q=Q7
4060 GOSUB 4630
4070 F2=(H0+H1)/(2*H0)
4080 IF (ABS(F1-F2)/F1)>.02 THEN  4090
4085 I9=1
4090 IF I9>0 THEN 4140
4100 REM#  NEW THETA MUST BE COMPUTED
4110 F1=(F1+F2)/2
4120 GOTO 3990
4130 REM#
4140 PRINT
4145 FOR I=2 TO NO
4150 PRINT 'INPUT DISTANCE (MI.) FROM DAM TO FORECAST POINT #':I-1
4152 INPUT D(I)
4160 XS=D(I)
4165 Q=P(1,1)
4170 GOSUB 5810
4180 REM#
4190 REM# SAVE PEAK FLOW  AT X-S (I)
4200 P(I,1)=Q7
4210 REM# COMPUTE TIME TO PEAK
4220 XS=D(I)/2
4230 GOSUB 5810
4240 Q=(.3+.1*M)*Q7
```

```
4250 GOSUB 4630
4260 D9=H1/(M+1)
4270 IF H1<=H3 THEN  4280
4275 D9=H1-H3+H3/(M+1)
4280 V9=(1.49/N)*(S2^.5)*D9^.667
4290 C9=.682*V9*(1.667-(.667*(M/(M+1))))
4300 P(I,3)=(T0/60)+D(I)/C9
4310 REM#
4320 REM#  COMPUTE AND SAVE PEAK DEPTH AT X-S (I)
4330 Q=P(I,1)
4340 GOSUB 4630
4350 P(I,2)=H1
4360 REM#  DET TIME FLOODING AND DEFLOODING
4370 T1=P(I,3)
4380 H4=C(3,I)
4390 GOSUB 5320
4400 P(I,4)=T4
4410 P(I,5)=T5
4420 REM#
4430 NEXT I
4440 REM#
4450 REM#
4460 REM# PRINT HEADING
4470 PRINT
4472 PRINT
4475 PRINT '        PROFILE OF CRESTS AND TIMES FOR':D$:'DAM'
4480 PRINT '                          ON':R$:'RIVER'
4490 PRINT
4500 PRINT ' DISTANCE    PEAK      PEAK      FLOOD     TIME      TIME      TIME'
4510 PRINT 'DOWNSTREAM   FLOW      DEPTH     STAGE     FLOOD     PEAK    DEFLOOD'
4512 PRINT '  (MILES)    CFS       FEET      FEET      HR        HR        HR'
4520 PRINT
4530 REM#
4540 FOR I=1 TO NO
4550 REM# ROUND OFF PRINT VALUES TO TWO PLACES AFTER DECIMAL POINT
4551 FOR J=2 TO 5
4552 P(I,J)=INT(P(I,J)*100+.5)/100
4553 NEXT J
4554 D(I)=INT(D(I)*100+.5)/100
4555 C(3,I)=INT(C(3,I)*100+.5)/100
4556 PRINT TAB(3):D(I):TAB(11):P(I,1):TAB(23):P(I,2):TAB(33):C(3,I):TAB(43):
4557 PRINT P(I,4):TAB(53):P(I,3):TAB(63):P(I,5)
4560 NEXT I
4570 STOP
4580 END
4581 REM#
4582 REM# ******************************************************************
4583 REM# *************                SUBROUTINES              *************
4584 REM# ******************************************************************
4585 REM#
4590 REM# ********************************** DEPTH CALCULATION ROUTINE
4600 REM#  INPUT PARMS ARE:
4610 REM#  K,M =CHNL. FIT PARMS, Q3=QV, Q=FLOW, S2=SLOPE, N=MANNING N
4620 REM#
4630 A1=(1.49/N)*(S2^.5)*K/((M+1)^1.667)
4640 B1=1.667+M
4650 IF Q>Q3 THEN 4700
4660 REM#                                                  CASE 1 STG < HV
4670 H1=(Q/A1)^(1/B1)
4680 GOTO 4730
4690 REM#                                                  CASE 2 STG > HV
4700 R1=A1*((M+1)^1.667)*(H3^M)
4710 R1=(1/R1)^.6
4720 H1=(Q^.6)*R1+H3*(M/(M+1))
4730 RETURN
4740 REM#
4750 REM# ********************************** HV CALCULATION ROUTINE
4760 REM# THIS ROUTINE COMPUTES THE WEIGHTED AVERAGE HV ELEVATION OF REACH
4770 H3=0
4780 FOR J1=2 TO I
4790 H3=H3+((C(2,J1-1)+C(2,J1))/2)*(D(J1)-D(J1-1))
4800 NEXT J1
4810 H3=H3/(D(I)-D(1))
4820 RETURN
4830 REM#
```

```
4840 REM# ********************************** QV CALCULATION ROUTINE
4850 REM#  INPUT PARMS ARE:
4860 REM#  K,M =CHNL. FIT PARMS,  S2=SLOPE, N=MANNING N, H3=HV
4870 A1=(1.49/N)*(S2^.5)*K/((M+1)^1.667)
4880 B1=1.667+M
4890 Q3=A1*(H3^B1)
4900 RETURN
4910 REM#
4920 REM# ********************************** BREACH ROUTINE
4930 REM# THIS ROUTINE DET. THE MAX FLOW AT DAM, ACCTNG FOR SUBMERGENCE
4940 REM# INPUT PARMS ARE
4950 REM# A0=SURF AREA, W0=BREACH WIDTH, T0 = TF(MIN) H2=DEPTH OF BREACH,
4960 REM# Q0=INFLOW PEAK,
4964 REM#  CHECK FOR INSTANTANEOUS FAILURE
4970 IF T0 < (H2/1000) THEN 5242
4976 C1=(23.4*A0)/W0
4980 REM# H8 IS HEAD OVER WEIR
4990 H8=(C1/((T0/60)+C1/(H2^.5)))^2
5000 Q=Q0+3.1*W0*H8^1.5
5010 REM# COMPUTE QV AT DAM
5020 IF N0>1 THEN  5040
5025 S2=S0/5280
5030 GO TO 5050
5040 S2=(E(1,1)-E(2,1))/((D(2)-D(1))*5280)
5050 GOSUB 4870
5060 REM# COMPUTE DEPTH AT DAM
5070 GOSUB 4630
5080 REM# CHECK FOR SUBMERGENCE
5081 REM#   NO CHECK IF FLOW AT DAM IS SUPERCRITICAL
5082 D1=H1/(M+1.)
5083 IF H1 <= H3 THEN 5087
5085 D1=H1-H3+H3/(M+1.)
5087 F6=((1.49/N)*(S2^.5)*D1^(2./3.))/((32.2*D1)^.5)
5088 IF F6>= 1.0 THEN 5260
5090 IF ((H1+E(1,1)-B0)/H8)<.67 THEN 5260
5100 REM#
5110 REM#  SUBMERGENCE CORRECTION NEEDED
5120 C6=1
5130 FOR I1=1 TO 10
5140 C7=1-27.8*(((H1+E(1,1)-B0)/H8)-.67)^3
5150 IF C7>.80 THEN 5160
5155 C7=.80
5160 C7=(C6+C7)/2
5170 C6=C7
5180 Q6=Q
5190 Q=C7*Q
5200 IF ABS(Q6-Q)<Q6/20 THEN 5260
5210 REM# RECOMPUTE DEPTH AND HEAD WITH NEW FLOW
5220 GOSUB 4630
5230 H8=H8+((Q6-Q)*(60*T0)/(43560*2*A0))
5240 NEXT I1
5241 GOTO 5260
5242 M2=M+1.
5243 B1=W0/T(1,N1)
5244 C6=(1.0+0.148*(B1^2.)*(M2^2.)-0.083*(B1^3.)*(M2^2.5))^1.5
5245 C7=1.-.5467*B1*M2^.5+.2989*(B1^2.)*M2^.25-.1634*(B1^3.)*M2^.125
5246 C7=C7+.0893*(B1^4.)*M2^.0625-.0486*(B1^5.)*M2^.03125
5247 C7=C7^1.5
5248 Q=Q0+3.1*W0*(C6*C7)*H2^1.5
5249 IF N0>1 THEN  5254
5250 S2=S0/5280
5252 GO TO 5256
5254 S2=(E(1,1)-E(2,1))/((D(2)-D(1))*5280)
5256 GOSUB 4870
5259 GOSUB 4630
5260 RETURN
5270 REM# ********************************** TIME OF FLOOD ROUTINE
5280 REM#  THIS SUBROUTINE COMPUTES THE TIME OF FLOOD AND DEFLOOD
5290 REM#  INPUT PARMS ARE
5300 REM# K,M = CHNL FIT PARMS,S2=SLOPE,Q=FLOW,H4=FLD DEPTH,Q3=QV,H3=HV
5310 REM#
5320 Q4=-999
5330 T4=-999
5340 T5=-999
5350 IF H4<.01 THEN 5470
```

```
5360 IF H4>H3 THEN 5400
5370 B1=K*H4^M
5380 A1=(K/(M+1))*H4^(M+1)
5390 GOTO 5420
5400 B1=K*H3^M
5410 A1=(K/(M+1))*H3^(M+1)+(H4-H3)*B1
5420 Q4=(1.49/N)*(S2^.5)*(A1^1.667)/(B1^.667)
5430 IF Q<Q4 THEN 5470
5435 IF Q0>Q4 THEN 5470
5440 REM# COMPUTE TIME OF FLOOD
5450 T4=T1-((Q-Q4)/(Q-Q0))*T0/60
5460 T5=T1+(((Q-Q4)/(Q-Q0))*((2*V0*43560/(Q-Q0))-T0*60))/3600
5470 RETURN
5480 REM#
5490 REM# ***********************************SUBROUTINE RPARMS
5500 REM# THIS ROUTINE COMPUTES THE ROUTINE PARAMETERS XC, FC, AND V*
5510 REM#
5520 REM#  INPUT PARMS ARE
5530 REM#  K&M=CHNL PARMS,V0=RES.VOL.,C0=DAM CREST ELEV,E(1,1)=BASE OF DAM
5540 REM#  H1=DEPTH AT DAM, H3=HV, F1=THETA, S2=SLOPE, N=MANNING N
5550 REM#  OUTPUT PARMS ARE
5560 REM#  F7=FC, V7=V*, X1=XC
5570 REM#
5580 REM# D8 IS THE DAM HEIGHT
5590 D8=C0-E(1,1)
5600 X1=((V0*43560*(M+1))/(K*D8^(M+1)))*(6/(1+4*(.5^(M+1))))
5610 IF D8<=H3 THEN  5620
5615 X1=(6*V0*43560)/((K*H3^M)*(3*D8-5*(M*H3)/(M+1)))
5617 IF (D8/2)>H3 THEN 5620
5618 X1=(6*V0*43560)/((K*H3^M)*(H3/(M+1)+D8-H3)+4*(K/(M+1))*(D8/2)^(M+1))
5620 IF F1>0 THEN 5630
5625 F1=.95
5630 D1=F1*H1/(M+1)
5640 IF (F1*H1)<=H3 THEN  5650
5645 D1=F1*H1-H3+(H3/(M+1))
5650 V1=(1.49/N)*(S2^.5)*(D1^.667)
5660 F7=V1/((32.2*D1)^.5)
5670 A2=K*((F1*H1)^M)*D1
5680 IF H1<=H3 THEN  5690
5685 A2=K*(H3^M)*D1
5690 V7=(V0*43560)/(A2*X1)
5700 X1=X1/5280
5710 RETURN
5720 REM#
5730 REM# ************************************** SUBROUTINE ROUTE
5740 REM#  THIS SUBROUTINE COMPUTES THE PEAK FLOW AT A GIVEN X-S
5750 REM#
5760 REM# INPUT PARMS ARE:
5770 REM# F7 = FC, V7 = V*, X5 = DIST TO X-S, X1 = XC,
5780 REM#
5790 REM#  RETURNED VALUE IS Q7
5800 REM# SET X* VALUE
5810 X2=X5/X1
5820 REM#
5830 REM# SET V* POINTER
5840 V8=INT(V7)
5850 V9=INT(V7+1)
5860 IF V7>1 THEN  5870
5865 V8=1
5870 IF V7<5 THEN 5910
5875 V8=5
5880 V9=5
5890 REM#
5900 REM# SET FC POINTERS
5910 F8=INT(4*F7)
5920 F9=INT((4*F7)+1)
5930 IF F7>=.25 THEN 5950
5935 F8=F9
5940 REM#  ***NOTE: WHEN FC=1.5 CURVES AVAILABLE, CHANGE NEXT TWO LINES
5950 IF F7<.75 THEN 5970
5955 F8=3
5960 F9=3
5970 D0=(F7-(F8/4))/.25
5980 IF F8<>F9 THEN  6020
5990 D0=0
```

```
6000 REM#
6010 REM# CALL ROUTINE FOR DOWNSTREAM PEAK FLOWS
6020 F0=F8
6030 V5=V8
6040 GOSUB 6360
6050 Q1=Q8
6060 F0=F9
6070 GOSUB 6360
6080 Q2=Q8
6090 REM# INTERPOL FOR SPEC FC AND LOWER V*
6100 Q4=Q1+(Q2-Q1)*D0
6110 F0=F8
6120 V5=V9
6130 GOSUB 6360
6140 Q1=Q8
6150 F0=F9
6160 GOSUB 6360
6170 Q2=Q8
6180 REM# INTERP FOR SPEC FC AND UPPER V*
6190 Q5=Q1+(Q2-Q1)*D0
6200 REM# INTERP FOR SPECIFIC V*
6210 Q7=Q4+(Q5-Q4)*(V7-V8)
6230 REM#
6240 RETURN
6250 REM#
6260 REM#      ***********************************SUBROUTINE PREDIC
6270 REM#
6280 REM#  THIS ROUTINE INTERPOLATES WITHIN THE ROUTING CURVES TO
6290 REM#  FIND THE RATIO OF QP TO QBMAX FOR A SPECIFIC (INTEGER)
6300 REM#  VALUE OF V* AND AN FC OF 0.25, 0.50, OR 0.75.
6310 REM#
6320 REM#  INPUT VARIABLES ARE:
6330 REM#  F0 = FC POINTER, V5 = V* POINTER, X2 = X*, Q =  FLOW AT DAM
6340 REM#  RETURN VALUE IS Q8
6350 REM#
6360 FOR I1=1 TO 6
6370 I2=I1
6372 X3=K(I1)/10
6380 IF (X2-X3)<=0 THEN 6410
6390 NEXT I1
6400 REM# BRACKETING X'S FOUND
6410 I3=I2-1
6420 J3=(F0-1)*5+V5
6460 L1=LOG(F(J3,I3))
6470 L2=LOG(F(J3,I2))
6480 L3=LOG(X(I3))
6490 L4=LOG(X(I2))
6500 L5=LOG(X2*10)
6510 D3=(L2-L1)/(L4-L3)
6520 L6=(L5-L3)*D3+L1
6530 IF (X2*10)<=X(6) THEN 6540
6535 L6=(L5-L4)*D3+L2
6540 IF L6>-3 THEN 6550
6545 L6=-3
6550 Q8=(EXP(L6)/100)*Q
6560 REM#
6570 RETURN
```

```
SIMPLIFIED DAMBREAK MODEL
BASIC LANGUAGE INTERACTIVE VERSION
WRITTEN BY JONATHAN N. WETMORE  HRL  MAY, 1983

INPUT "SHORT" FOR SHORTENED VERSION, "LONG" FOR FULL MODEL
!SHORT

INPUT HEIGHT OF DAM (FEET)
!100

INPUT VOLUME OF RESERVOIR (AC-FT) AT MAX POOL ELEV
!25000

INPUT FINAL BREACH WIDTH (FT)
IF N/A ENTER 0.  DEFAULT USED = 3 * BREACH DEPTH
!0

INPUT TIME (MINUTES) REQUIRED FOR BREACH FORMATION
IF N/A , ENTER 0.
!0
ENTER TYPE OF DAM...0 FOR EARTH DAM, 1 FOR CONCRETE DAM
0
ESTIMATED TIME OF FAILURE = 33.3333 MINUTES

INPUT NUMBER OF PAIRS OF ELEV-TOPWIDTHS USED TO
DESCRIBE EACH X-SECTION (MIN=2, MAX=8)
MODEL ASSUMES DEPTH #1 = 0. AND TOPWIDTH #1 = 0.
!2

INPUT DEPTH (FEET) # 2 AND ASSOC. TOPWIDTH FOR X-S # 1
!100
!1000

INPUT MANNING N AT X-S # 1 (DEFAULT = 0.050)
!0

INPUT CHANNEL SLOPE (FT/MI) BELOW DAM
!0

ENTER NUMBER OF FORECAST POINTS BELOW DAM (MAX = 7)
!7
INPUT DISTANCE (MI.) FROM DAM TO FORECAST POINT # 1
!10
INPUT DISTANCE (MI.) FROM DAM TO FORECAST POINT # 2
!20
INPUT DISTANCE (MI.) FROM DAM TO FORECAST POINT # 3
!30
INPUT DISTANCE (MI.) FROM DAM TO FORECAST POINT # 4
!40
INPUT DISTANCE (MI.) FROM DAM TO FORECAST POINT # 5
!50
INPUT DISTANCE (MI.) FROM DAM TO FORECAST POINT # 6
!60
INPUT DISTANCE (MI.) FROM DAM TO FORECAST POINT # 7
!70
```

PROFILE OF CRESTS AND TIMES FOR DAM
ON RIVER

DISTANCE DOWNSTREAM (MILES)	PEAK FLOW CFS	PEAK DEPTH FEET	FLOOD STAGE FEET	TIME FLOOD HR	TIME PEAK HR	TIME DEFLOOD HR
0	324314	63.5	0	-998.99	.56	-998.99
10	238688	56	0	-998.99	1.46	-998.99
20	206646	53.06	0	-998.99	2.37	-998.99
30	183701	50.77	0	-998.99	3.32	-998.99
40	167489	49.04	0	-998.99	4.32	-998.99
50	152864	47.39	0	-998.99	5.34	-998.99
60	141869	46.08	0	-998.99	6.38	-998.99
70	131442	44.78	0	-998.99	7.42	-998.99

```
SIMPLIFIED DAMBREAK MODEL
BASIC LANGUAGE INTERACTIVE VERSION
WRITTEN BY JONATHAN N. WEIMORE  HRL  MAY, 1983

INPUT "SHORT" FOR SHORTENED VERSION, "LONG" FOR FULL MODEL
LONG

INPUT NAME OF DAM
TEST4

INPUT RIVER NAME
NON-PRISMATIC #4

INPUT DAM CREST ELEVATION (FT. MSL)
1100

INPUT FINAL BREACH BOTTOM ELEVATION (FT. MSL)
1000

INPUT VOLUME OF RESERVOIR (AC-FT) AT MAX POOL ELEV
IF N/A ENTER 0. AND VOL WILL BE EST. FROM SURF. AREA
0

INPUT RESERVOIR SURFACE AREA (ACRES) AT MAX POOL ELEV
IF N/A ENTER 0. AND S.A. WILL BE EST. FROM VOLUME.
500

INPUT FINAL BREACH WIDTH (FT)
IF N/A ENTER 0.  DEFAULT USED = 3 * BREACH DEPTH
100

INPUT TIME (MINUTES) REQUIRED FOR BREACH FORMATION
IF N/A , ENTER 0.
90

INPUT TURBINE/SPILLWAY/OVERTOPPING FLOW (CFS).
IF N/A, ENTER 0.0.  DEFAULT = 0.0
1500

INPUT NUMBER OF X-SECTIONS (STARTING AT DAM) USED TO
DESCRIBE ROUTING REACH.  (MIN=1, MAX=8)
5

INPUT NUMBER OF PAIRS OF ELEV-TOPWIDTHS USED TO
DESCRIBE EACH X-SECTION (MIN=2, MAX=8)
5

INPUT LOWEST CHANNEL ELEV. (FT. MSL) AT X-SECTION # 1
(ELEVATION OF BASE OF DAM (FT. MSL))
1000

INPUT ELEV. (FT. MSL) # 2 AND ASSOC. TOPWIDTH FOR X-S # 1
1025
250

INPUT ELEV. (FT. MSL) # 3 AND ASSOC. TOPWIDTH FOR X-S # 1
1050
500

INPUT ELEV. (FT. MSL) # 4 AND ASSOC. TOPWIDTH FOR X-S # 1
1075
750

INPUT ELEV. (FT. MSL) # 5 AND ASSOC. TOPWIDTH FOR X-S # 1
1100
1000

INPUT MANNING N AT X-S # 1 (DEFAULT = 0.050)
0
```

```
INPUT VALLEY WALL HEIGHT ABOVE CHANNEL BOTTOM AT X-S # 1
IF N/A INPUT 0.
0

INPUT FLOOD DEPTH AT X-S # 1
IF N/A ENTER 0.
30

INPUT DISTANCE DOWNSTREAM FROM DAM (MILES) TO X-SECTION # 2
10

INPUT LOWEST CHANNEL ELEV. (FT. MSL) AT X-SECTION # 2
850

INPUT ELEV. (FT. MSL) # 2 AND ASSOC. TOPWIDTH FOR X-S # 2
875
400

INPUT ELEV. (FT. MSL) # 3 AND ASSOC. TOPWIDTH FOR X-S # 2
900
750

INPUT ELEV. (FT. MSL) # 4 AND ASSOC. TOPWIDTH FOR X-S # 2
925
1125

INPUT ELEV. (FT. MSL) # 5 AND ASSOC. TOPWIDTH FOR X-S # 2
950
1500

INPUT MANNING N AT X-S # 2 (DEFAULT = 0.050)
0

INPUT VALLEY WALL HEIGHT ABOVE CHANNEL BOTTOM AT X-S # 2
IF N/A INPUT 0.
0

INPUT FLOOD DEPTH AT X-S # 2
IF N/A ENTER 0.
20

INPUT DISTANCE DOWNSTREAM FROM DAM (MILES) TO X-SECTION # 3
20

INPUT LOWEST CHANNEL ELEV. (FT. MSL) AT X-SECTION # 3
700

INPUT ELEV. (FT. MSL) # 2 AND ASSOC. TOPWIDTH FOR X-S # 3
725
200

INPUT ELEV. (FT. MSL) # 3 AND ASSOC. TOPWIDTH FOR X-S # 3
750
400

INPUT ELEV. (FT. MSL) # 4 AND ASSOC. TOPWIDTH FOR X-S # 3
775
600

INPUT ELEV. (FT. MSL) # 5 AND ASSOC. TOPWIDTH FOR X-S # 3
800
800

INPUT MANNING N AT X-S # 3 (DEFAULT = 0.050)
0

INPUT VALLEY WALL HEIGHT ABOVE CHANNEL BOTTOM AT X-S # 3
IF N/A INPUT 0.
0

INPUT FLOOD DEPTH AT X-S # 3
IF N/A ENTER 0.
20
```

```
INPUT DISTANCE DOWNSTREAM FROM DAM (MILES) TO X-SECTION # 4
30

INPUT LOWEST CHANNEL ELEV. (FT. MSL) AT X-SECTION # 4
530

INPUT ELEV. (FT. MSL) # 2 AND ASSOC. TOPWIDTH FOR X-S # 4
575
500

INPUT ELEV. (FT. MSL) # 3 AND ASSOC. TOPWIDTH FOR X-S # 4
600
1000

INPUT ELEV. (FT. MSL) # 4 AND ASSOC. TOPWIDTH FOR X-S # 4
625
1500

INPUT ELEV. (FT. MSL) # 5 AND ASSOC. TOPWIDTH FOR X-S # 4
650
2000

INPUT MANNING N AT X-S # 4 (DEFAULT = 0.050)
0

INPUT VALLEY WALL HEIGHT ABOVE CHANNEL BOTTOM AT X-S # 4
IF N/A INPUT 0.
0

INPUT FLOOD DEPTH AT X-S # 4
IF N/A ENTER 0.
10

INPUT DISTANCE DOWNSTREAM FROM DAM (MILES) TO X-SECTION # 5
40

INPUT LOWEST CHANNEL ELEV. (FT. MSL) AT X-SECTION # 5
400

INPUT ELEV. (FT. MSL) # 2 AND ASSOC. TOPWIDTH FOR X-S # 5
425
250

INPUT ELEV. (FT. MSL) # 3 AND ASSOC. TOPWIDTH FOR X-S # 5
450
500

INPUT ELEV. (FT. MSL) # 4 AND ASSOC. TOPWIDTH FOR X-S # 5
475
750

INPUT ELEV. (FT. MSL) # 5 AND ASSOC. TOPWIDTH FOR X-S # 5
500
1000

INPUT MANNING N AT X-S # 5 (DEFAULT = 0.050)
0

INPUT VALLEY WALL HEIGHT ABOVE CHANNEL BOTTOM AT X-S # 5
IF N/A INPUT 0.
0

INPUT FLOOD DEPTH AT X-S # 5
IF N/A ENTER 0.
10
```

PROFILE OF CRESTS AND TIMES FOR TEST4 DAM
ON NON-PRISMATIC #4 RIVER

DISTANCE DOWNSTREAM (MILES)	PEAK FLOW CFS	PEAK DEPTH FEET	FLOOD STAGE FEET	TIME FLOOD HR	TIME PEAK HR	TIME DEFLOOD HR
0	217305	54.83	30	.29	1.5	2.55
10	165006	41.38	20	1.29	2.58	4.47
20	137957	50.28	20	2.26	3.65	6.36
30	123124	34.17	10	3.39	4.85	8.24
40	110152	42.5	10	4.62	6.11	10.15

****
FULL DAMBRK RESULTS
****

PROFILE OF CRESTS AND TIMES FOR TEST NO. 4 OF NON-PR
BELOW SIMPLIFIED DAMBREAK

RVR MILE FROM DAM	MAX ELEV (FT)	MAX FLOW (CFS)	TIME MAX ELEV(HR)	FLOOD ELEV (FT)	TIME FLOOD (HR)
0.000	53.75	224206	1.500	30.00	0.75
10.000	42.51	173374	2.400	20.00	1.80
20.000	49.40	143972	3.450	20.00	2.85
30.000	34.73	126714	4.575	10.00	3.90
40.000	40.10	108592	5.810	10.00	5.10

APPENDIX III (a)

THE NWS SIMPLIFIED DAM BREAK MODEL

RADIO SHACK TRS80 MODEL PC2 VERSION LISTING WITH EXAMPLE RUNS

```
  69 "?"
  70 DIM F(15,5),X(5),D(5),G(5),E(5),T(5),C(3,5),H(2,5),B(4,5),P(5,5)
 500 WO=0:QO=0:NO=1:D(1)=0:AO=0:FOR I=1 TO 5:C(3,I)=0:B(3,I)=0:NEXT I:SO=1
 560 X(1)=1.E-05:X(2)=10:X(3)=30:X(4)=50:X(5)=200
 660 FOR J=2 TO 5:FOR I=1 TO 15:F(I,1)=100:READ F(I,J):NEXT I:NEXT J
 740 DATA 56,74,85,90,93,73,83,92,95,97,78,91,94,95,97,32,49,64,74,81,53,66,79
 800 DATA 86,90,58,75,83,87,91,20,35,50,62,71,43,57,70,79,84,47,62,74,81,86
 860 DATA 7,13,20,26,31,20,28,36,43,50,24,34,44,54,60
 884 SS="YES":ES="ELEV.":FS="DEPTH"
 922 PRINT "SHORT VERSION?":INPUT VS:IF VS<>SS THEN 990
 926 PRINT "HEIGHT OF DAM = ?":INPUT HZ:GOTO 1093
 990 PRINT "CREST EL. = ?":INPUT CO:IF CO<.1 THEN 990
1030 PRINT "FINAL BREACH EL. = ?":INPUT BO:IF BO<.1 THEN 1030
1040 HZ=CO-BO
1093 PRINT "RES. VOLUME = ?":INPUT VO:IF VS=SS THEN 1210
1130 PRINT "RES. SURF AREA = ?":INPUT AO:IF VO>.1 THEN 1210
1140 IF AO>.1 THEN 1210
1180 PRINT "MUST GIVE EITHER VOL OR S.A.":GOTO 1093
1210 PRINT "FINAL BREACH WIDTH = ?":INPUT WO
1240 IF WO>.1 THEN 1250
1245 WO=3*HZ
1250 PRINT "TIME (MIN.) OF FAILURE = ?":INPUT TO:IF TO>.0001 THEN 1290
1255 TO=HZ/3
1290 IF VS=SS THEN 1450
1300 PRINT "NONBREACH FLOW =?":INPUT QO
1400 PRINT "NO. X-S = ?":INPUT NO:IF NO<1 THEN 1400
1450 PRINT "NO. PAIRS EL-TW = ?":INPUT N1:IF N1<2 THEN 1450
1530 FOR I=1 TO NO:T(1)=0
1560 IF I>1 THEN  PRINT "DIST TO X-S #";I;" = ?":IF I>1 THEN INPUT D(I)
1581 IF VS<>SS THEN 1600
1582 G(1)=0:CO=HZ:BO=0:ES=FS:GOTO 1645
1600 PRINT "INVERT EL. AT X-S #";I;"= ?":INPUT E(1):G(I)=E(1):IF I>1 THEN 1720
1645 IF VO>.1 THEN 1647
1646 VO=(AO/2)*(CO-G(1))
1647 IF AO>.01 THEN 1690
1648 AO=2*VO/(CO-G(1))
1690 IF BO<(G(1)+5) THEN 1720
1691 VO=(HZ/2)*AO*(1+((BO-G(1))/(CO-G(1)))^2)
1720 IF I<>2 THEN 1915
1750 M=MO:K=KO:N=C(1,1):H3=C(2,1)
1800 GOSUB 4970:P(1,1)=Q:P(1,2)=H1:P(1,3)=TO/60:I=1:GOSUB 6520:IF NO<2 THEN 3740
1801 I=2
1915 FOR J=2 TO N1:PRINT ES;"#";J;"FOR X-S #";I;"= ?":INPUT E(J)
1936 PRINT "TW #";J;"FOR X-S #";I;"= ?":INPUT T(J):NEXT J
1970 PRINT "MANNING N AT X-S #";I;"= ?":INPUT C(1,I)
1990 IF C(1,I)>.0001 THEN  2010
1991 C(1,I)=.05
2010 IF VS<>SS THEN 2015
2012 C(2,1)=HZ:GOTO 2105
2015 PRINT "HV AT X-S #";I;"= ?":INPUT C(2,I)
2040 IF C(2,I)>.01 THEN  2100
2041 C(2,I)=HZ
2000 PRINT "FLD DEPTH AT X-S #";I;"= ?":INPUT C(3,I)
2105 IF NO>1THEN 2230
2110 PRINT "SLOPE (FT/MI) BELOW DAM = ?":INPUT SO:IF SO>0 THEN 2230
2115 SO=HZ*(T(N1)/(24.75*VO))
2230 U1=0:U2=0:U3=0:U4=0:N2=N1
2280 FOR J1=2 TO N1:H(1,J1)=E(J1)-E(1):IF I>1 THEN 2340
2310 H(2,J1)=H(1,J1):B(2,J1)=T(J1).
2315 IF H(1,J1)<C(2,1) THEN   2340
2320 H(2,J1)=C(2,1)
2340 IF H(1,J1)<C(2,I) THEN 2342
2341 H(1,J1)=C(2,I)
2342 IF H(1,J1-1)<C(2,I) THEN 2360
2343 N2=J1-1:GO TO 2410
2360 U1=U1+LOG(H(1,J1)):U2=U2+(LOG(H(1,J1)))^2
2374 IF H(1,J1)<C(2,I) THEN 2380
2375 DO=(T(J1)-T(J1-1))/(E(J1)-E(J1-1))
2376 T(J1)=T(J1-1)+(H(1,J1)+E(1)-E(J1-1))*DO
2377 IF I>1 THEN  2380
2378 B(2,J1)=T(J1)
2380 U3=U3+LOG(T(J1)):U4=U4+LOG(H(1,J1))*LOG(T(J1)):NEXT J1
2410 N3=N2-1:IF I>1 THEN  2430
2420 N4=N2
```

```
2430 IF N1>2 THEN 2450
2440 M0=1:K0=T(N1)/H(1,N1):GOTO 2480
2450 M0=(U4-U1*U3/N3)/(U2-(U1^2)/N3)
2460 K0=10^(U3/N3-M0*U1/N3)
2480 IF N0<2 THEN 1750
2481 IF I=1 THEN 3740
2482 FOR J1=2 TO N4
2580 FOR J2=2 TO N1:J0=J2
2600 IF (H(2,J1)-(E(J2)-E(1)))<=0 THEN 2630
2610 NEXT J2
2630 J3=J0-1:D0=(T(J0)-T(J3))/(E(J0)-E(J3))
2670 B(1,J1)=T(J3)+(E(1)+H(2,J1)-E(J3))*D0
2690 IF H(2,J1)<C(2,I) THEN  2710
2695 B(1,J1)=T(N2)
2710 B(3,J1)=B(3,J1)+((B(2,J1)+B(1,J1))/2)*(D(I)-D(I-1))
2730 B(2,J1)=B(1,J1):NEXT J1
2770 FOR J1=2 TO N4:B(4,J1)=B(3,J1)/(D(I)-D(1)):NEXT J1
2820 N=0:FOR J1=2 TO I:N=N+((C(1,J1)+C(1,J1-1))/2)*(D(J1)-D(J1-1)):NEXT J1
2860 N=N/(D(I)-D(1)):U1=0:U2=0:U3=0:U4=0:FOR J1=2 TO N4
3020 U1=U1+LOG(H(2,J1)):U2=U2+(LOG(H(2,J1)))^2
3040 U3=U3+LOG(B(4,J1)):U4=U4+LOG(H(2,J1))*LOG(B(4,J1)):NEXT J1
3070 N3=N4-1:IF N4>2 THEN 3075
3072 M1=1:K1=B(4,N4)/H(2,N4):GO TO 3150
3075 M1=(U4-U1*U3/N3)/(U2-(U1^2)/N3)
3110 K1=10^(U3/N3-M1*U1/N3)
3150 S2=(G(1)-G(I))/((D(I)-D(1))*5280)
3190 K=K1:M=M1:Q=P(1,1):GOSUB 4770:GOSUB 4870:GOSUB 4630
3220 H0=H1:F1=.95:I9=0
3250 I8=I9:Q=P(1,1):GOSUB 4630: GOSUB 5590
3270 Q=P(1,1):X5=X1:IF I9<1 THEN 3275
3272 X5=D(I)
3275 GOSUB 5810:IF I9>0 THEN 3440
3330 Q=Q7:GOSUB 4630
3360 F2=(H0+H1)/(2*H0):IF (ABS(F1-F2)/F1)>.02 THEN 3370
3365 I9=1
3370 IF I9<>I8 THEN 3270
3375 F1=(F1+F2)/2:GOTO 3250
3440 P(I,1)=Q7:IF P(I,1)<P(I-1,1) THEN 3445
3442 P(I,1)=.99*P(I-1,1)
3445 X5=D(I)/2:GOSUB 5810:Q=(.3+.1*M)*Q7:GOSUB 4630
3510 D9=H1/(M+1):IF H1<=H3 THEN 3520
3515 D9=H1-H3+H3/(M+1)
3520 C9=.682*((1.49/N)*(S2^.5)*D9^.667)*(1.667-(.667*(M/M+1))))
3570 P(I,3)=(T0/60)+D(I)/C9:K=K0:M=M0:N=C(1,I):H3=C(2,I):Q=P(I,1)
3575 IF P(I,3)>P(I-1,3) THEN 3590
3580 P(I,3)=1.01*P(I-1,3)
3590 S2=(G(I-1)-G(1))/((D(I)-D(I-1))*5280)
3620 GOSUB 4870:GOSUB 4630:P(I,2)=H1:GOSUB 6520
3740 NEXT I
3900 IF N0>1 THEN 4450
3960 N0=5:H0=P(1,2):F1=.95
3995 I9=0:Q=P(1,1):GOSUB 4630: GOSUB 5590:X5=X1:GOSUB 5810:Q=Q7:GOSUB 4630
4080 F2=(H0+H1)/(2*H0):IF (ABS(F1-F2)/F1)>.02 THEN   4085
4082 I9=1
4085 IF I9>0 THEN 4140
4110 F1=(F1+F2)/2:GOTO 3995
4140 I=I+1:C(3,I)=C(3,1)
4141 PRINT "DIST. TO FCST PT #";I;" = ?":INPUT D(I):X5=D(I):Q=P(1,1):GOSUB 5810
4220 P(I,1)=Q7:X5=D(I)/2:GOSUB 5810:Q=(.3+.1*M)*Q7:GOSUB 4630
4260 D9=H1/(M+1):IF H1<=H3 THEN 4290
4265 D9=H1-H3+H3/(M+1)
4290 C9=.682*((1.49/N)*(S2^.5)*D9^.667)*(1.667-(.667*(M/(M+1))))
4300 P(I,3)=(T0/60)+D(I)/C9:Q=P(I,1):GOSUB 4630:P(I,2)=H1:GOSUB 6520
4449 IF I<N0 THEN 4140
4450 FOR I=1 TO N0:PRINT"Q (CFS) AT MI. ";D(I);"=";P(I,1)
4451 PRINT "DEPTH (FT) AT MI.";D(I);"=";INT (P(I,2)*100+.5)/100
4454 PRINT "TPEAK(HR) AT MI";D(I);"=";INT (P(I,3)*100+.5)/100:IF P(I,5)=0THEN 4460
4455 PRINT "T (HR) FLD AT MI.";D(I);"=";INT (P(I,4)*100+.5)/100
4457 PRINT "T(HR) DEFLD =";P(I,5)
4460 NEXT I:END
4630 A1=(1.49/N)*(S2^.5)*K/((M+1)^1.667):H1=(Q/A1)^(1/(1.667+M)):IF Q<Q3THEN 4730
4720 H1=(Q^.6)*(1/(A1*((M+1)^1.667)*(H3^M))^.6)+H3*(M/(M+1))
4730 RETURN
4770 H3=0:FOR J1=2 TO I:H3=H3+((C(2,J1-1)+C(2,J1))/2)*(D(J1)-D(J1-1))
4810 NEXT J1:H3=H3/(D(I)-D(1))):RETURN
```

```
4870 A1=(1.49/N)*(S2^.5)*K/((M+1)^1.667):B1=1.667+M:Q3=A1*(H3^B1):RETURN
4970 S2=S0/5280:IF N0<2 THEN 4985
4980 S2=(G(1)-G(2))/((D(2)-D(1))*5280)
4985 IF T0<(H2/1000) THEN 5242
4990 C1=(23.4*A0)/W0:H8=(C1/((T0/60)+C1/(H2^.5)))^2:Q=Q0+3.1*W0*H8^1.5
5090 GOSUB 4870:GOSUB 4630:D1=H1/(M+1):IF H1<=H3 THEN 5100
5095 D1=H1-H3+H3/(M+1)
5100 IF ((1.49/N)*(S2^.5)*D1^(2/3))/((32.2*D1)^.5) >= 1 THEN 5250
5110 IF ((H1+G(1)-B0)/H8)<.67 THEN 5250
5120 C6=1:FOR I1=1 TO 10:C7=1-27.8*(((H1+G(1)-B0)/H8)-.67)^3
5150 IF C7>.8 THEN 5155
5152 C7=.8
5155 C7=(C6+C7)/2:C6=C7:Q6=Q:Q=C7*Q
5200 IF ABS(Q6-Q)<Q6/20 THEN 5250
5220 GOSUB 4630:H8=H8+((Q6-Q)*(60*T0)/(43560*2*A0)):NEXT I1:GOTO 5250
5242 M2=M+1:B1=W0/T(N1):C5=(1+.148*(B1^2)*(M2^2)-.083*(B1^3)*(M2^2.5))^1.5
5243 C7=1.-.5467*B1*M2^.5+.2989*(B1^2.)*M2^.25-.1634*(B1^3.)*M2^.125
5244 C7=(C7+.0893*(B1^4)*M2^.0625-.0486*(B1^5)*M2^.03125)^1.5
5245 Q=Q0+3.1*W0*(C5*C7)*H2^1.5:GOSUB 4870:GOSUB 4630
5250 RETURN
5590 D8=C0-G(1):X1=((V0*43560*(M+1))/(K*D8^(M+1)))*(6/(1+4*(.5^(M+1))))
5610 IF D8<=H3 THEN  5640
5615 X1=(6*V0*43560)/((K*H3^M)*(3*D8-5*(M*H3)/(M+1)))
5640 D1=F1*H1/(M+1):IF (F1*H1)<=H3 THEN 5650
5645 D1=F1*H1-H3+(H3/(M+1))
5650 F7=((1.49/N)*(S2^.5)*(D1^.667))/((32.2*D1)^.5)
5680 A2=K*((F1*H1)^M)*D1:IF H1<=H3 THEN 5690
5685 A2=K*(H3^M)*D1
5690 V7=(V0*43560)/(A2*X1):X1=X1/5280:RETURN
5810 X2=X3/X1:V8=INT(V7):V9=INT(V7+1):IF V7>1 THEN 5880
5817 V8=1
5880 IF V7<= 5 THEN 5885
5882 V8=5:V9=5
5885 F8=INT(4*F7):F9=INT((4*F7)+1)
5930 IF F7>.25 THEN  5935
5933 F8=F9
5935 IF F7<=.75 THEN 5970
5936 F8=3:F9=3
5970 D0=(F7-(F8/4))/.25:IF F8<>F9 THEN 6020
5975 D0=0
6020 F0=F8:V5=V8:GOSUB 6360:Q1=Q8:F0=F9:GOSUB 6360:Q2=Q8
6100 Q4=Q1+(Q2-Q1)*D0
6110 F0=F8:V5=V9:GOSUB 6360:Q1=Q8:F0=F9:GOSUB 6360:Q2=Q8
6190 Q5=Q1+(Q2-Q1)*D0
6210 Q7=Q4+(Q5-Q4)*(V7-V8):RETURN
6360 FOR I3=1 TO 5
6370 I2=I3:IF (X2-X(I3)/10)<=0 THEN 6410
6375 NEXT I3
6410 I3=I2-1:J3=(F0-1)*5+V5:D3=(LN(F(J3,I2))-LN(F(J3,I3)))/(LN(X(I2))-LN(X(I3)))
6500 Q8=EXP(((LN(X2*10)-LN(X(I3)))*D3+LN(F(J3,I3))))*Q/100
6510 RETURN
6520 IF C(3,I)<.01 THEN 6600
6530 IF C(3,I)>H3 THEN 6550
6540 B1=K*C(3,I)^M:A1=(K/(M+1))*C(3,I)^(M+1):GOTO 6580
6550 B1=K*H3^M:A1=(K/(M+1))*H3^(M+1)+(C(3,I)-H3)*B1
6580 Q4=(1.49/N)*(S2^.5)*(A1^1.667)/(B1^.667):IF Q<Q4 THEN 6600
6585 IF Q0>Q4 THEN 6600
6590 P(I,4)=P(I,3)-((Q-Q4)/(Q-Q0))*T0/60
6595 P(I,5)=P(I,3)+(((Q-Q4)/(Q-Q0))*((87120*V0/(Q-Q0))-T0*60))/3600
6600 RETURN
```

SIMPLIFIED DAMBREAK MODEL
TRS80 MODEL PC2 VERSION INPUT VARIABLE DEFINITIONS/SUMMARY*

SHORT OPTION

Prompt	Description
SHORT VERSION? ? YES	Input "YES" for shortened version, "NO" for full model
HEIGHT OF DAM = ? ?	Input height of dam (feet) (no default)
RES. VOLUME = ? ?	Input volume of reservoir (ac-ft) at max pool elev. (no default)
FINAL BREACH WIDTH = ? ?	Input final breach width (ft) If N/A, enter 0. Default used = 2 * breach depth
TIME (MIN.) OF FAILURE = ? ?	Input time (minutes) required for breach formation If N/A, enter 0. Default = 1/2 height of dam
NO. PAIRS EL-TW = ? ?	Input number of pairs of elev.-vs.-topwidth used to describe each X-section (min=2, max=5) Model assumes depth #1 = 0 and topwidth #1 = 0
DEPTH # 2 FOR X-S # 1 = ? ?	Input depth (feet) #2 for X-S #1
TW # 2 FOR X-S # 1 = ? ?	Input topwidth assoc. with depth #2 for X-S #1
MANNING N AT X-S # 1 = ? ?	Input Manning "n" at X-S #1 (roughness coefficient) (default = 0.050)
SLOPE (FT/MI) BELOW DAM = ? ?	Input channel slope (ft/mi) below dam Should be entered if possible. If 0 is entered, value will be estimated based on dam height and reservoir volume
DIST. TO FCST PT # 2 = ? ?	Input distance (mi.) from dam to forecast point #2
DIST. TO FCST PT # 3 = ? ?	Input distance (mi.) from dam to forecast point #3
DIST. TO FCST PT # 4 = ? ?	Input distance (mi.) from dam to forecast point #4
DIST. TO FCST PT # 5 = ?	Input distance (mi.) from dam to forecast point #5

*Note: To execute program, enter CLEAR, enter RUN, then, after every prompt hit ENTER, key in the response to the prompt, and hit ENTER again.

LONG OPTION

Prompt	Description
SHORT VERSION? ? NO	Input "YES" for shortened version, "NO" for full model
CREST EL. = ? ?	Input dam crest elevation (ft. msl) (no default)
FINAL BREACH EL. = ? ?	Input final breach bottom elevation (ft. msl) (no default)
RES. VOLUME = ? ?	Input volume of reservoir (ac-ft) at max pool elev. If N/A, enter 0. and volume will be estimated from surface area
RES. SURF AREA = ? ?	Input reservoir surface area (acres) at max pool elev If N/A, enter 0. and S.A. will be est. from volume
FINAL BREACH WIDTH = ? ?	Input final breach width (ft) If N/A, enter 0. Default used = 2 * breach depth
TIME (MIN.) OF FAILURE = ? ?	Input time (minutes) required for breach formation If N/A, enter 0. Default used = 1/2 height of dam
NONBREACH FLOW = ? ?	Input turbine/spillway/overtopping flow (CFS) If N/A, enter 0.0. Default = 0.0
NO. X-S = ? ?	Input number of X-sections (starting at dam) used to describe routing reach (min=1, max=5)
NO. PAIRS EL-TW = ? ?	Input number of pairs of elev-topwidths used to describe each X-section (min=2, max=5)
INVERT EL. AT X-S # 1 = ? ?	Input lowest channel elev. (ft. msl) at X-section #1 (elevation of base of dam (ft. msl)). Model assumes topwidth at invert=0
ELEV. # 2 FOR X-S # 1 = ? ?	Input elev. (ft. msl) #2 and assoc. topwidth for X-S #1
TW # 2 for X-S # 1 = ? ?	
ELEV. # 3 FOR X-S # 1 = ? ?	Input elev. (ft. msl) #3 and assoc. topwidth for X-S #1
TW # 3 for X-S # 1 = ? ?	

LONG OPTION (continued)

Prompt	Description
ELEV. # 4 FOR X-S # 1 = ? ?	Input elev. (ft. msl) #4 and assoc. topwidth for X-S #1
TW # 4 for X-S # 1 = ? ?	
ELEV. # 5 FOR X-S # 1 = ? ?	Input elev. (ft. msl) #5 and assoc. topwidth for X-S #1
TW # 5 for X-S # 1 = ? ?	
MANNING N AT X-S # 1 = ? ?	Input Manning n at X-S #1 (default = 0.050)
HV AT X-S # 1 = ? ?	Input valley wall height above channel bottom at X-S #1 If N/A, input 0.
FLD DEPTH AT X-S # 1 = ? ?	Input flood depth (ft) at X-S #1 If N/A, enter 0.
DIST TO X-S # 2 = ? ?	Input distance downstream from dam (miles) to X-section #2

The prompts for X-sectional information repeat for the number of X-sections specified.

```
SHORT VERSION?
!YES
HEIGHT OF DAM = ?
!100
RES. VOLUME = ?
!25000
FINAL BREACH WIDTH = ?
!0
TIME (MIN.) OF FAILURE = ?
!0
NO. PAIRS EL-TW = ?
!2
DEPTH # 2 FOR X-S # 1 = ?
!100
TW # 2 FOR X-S # 1 = ?
!1000
MANNING N AT X-S # 1 = ?
!0
SLOPE (FT/MI) BELOW DAM = ?
!0
DIST. TO FCST PT # 2  = ?
!10
DIST. TO FCST PT # 3  = ?
!20
DIST. TO FCST PT # 4  = ?
!30
DIST. TO FCST PT # 5  = ?
!40

Q (CFS) AT MI. 0 = 324316.1
DEPTH (FT) AT MI. 0 = 63.5
TPEAK(HR) AT MI 0 = .56

Q (CFS) AT MI. 10 = 238748
DEPTH (FT) AT MI. 10 = 56.0
TPEAK(HR) AT MI 10 = 1.46

Q (CFS) AT MI. 20 = 206707
DEPTH (FT) AT MI. 20 = 53.0
TPEAK(HR) AT MI 20 = 2.37

Q (CFS) AT MI. 30 = 183762
DEPTH (FT) AT MI. 30 = 50.7
TPEAK(HR) AT MI 30 = 3.32

Q (CFS) AT MI. 40 = 167547
DEPTH (FT) AT MI. 40 = 49.0
TPEAK(HR) AT MI 40 = 4.32
```

```
SHORT VERSION?
NO
CREST EL. = ?
1100
FINAL BREACH EL. = ?
1000
RES. VOLUME = ?
0
RES. SURF AREA = ?
500
FINAL BREACH WIDTH = ?
100
TIME (MIN.) OF FAILURE = ?
90
NONBREACH FLOW = ?
1500
NO. X-S = ?
5
NO. PAIRS EL-TW = ?
5
INVERT EL. AT X-S # 1 = ?
1000
ELEV. # 2 FOR X-S # 1 = ?
1025
TW # 2 FOR X-S # 1 = ?
250
ELEV. # 3 FOR X-S # 1 = ?
1050
TW # 3 FOR X-S # 1 = ?
500
ELEV. # 4 FOR X-S # 1 = ?
1075
TW # 4 FOR X-S # 1 = ?
750
ELEV. # 5 FOR X-S # 1 = ?
1100
TW # 5 FOR X-S # 1 = ?
1000
MANNING N AT X-S # 1 = ?
0
HV AT X-S # 1 = ?
0
FLD DEPTH AT X-S # 1 = ?
30
DIST TO X-S # 2  = ?
10
INVERT EL. AT X-S # 2 = ?
850
ELEV. # 2 FOR X-S # 2 = ?
875
TW # 2 FOR X-S # 2 = ?
400
ELEV. # 3 FOR X-S # 2 = ?
900
TW # 3 FOR X-S # 2 = ?
750
ELEV. # 4 FOR X-S # 2 = ?
925
TW # 4 FOR X-S # 2 = ?
1125
ELEV. # 5 FOR X-S # 2 = ?
950
TW # 5 FOR X-S # 2 = ?
1500
MANNING N AT X-S # 2 = ?
0
HV AT X-S # 2 = ?
0
FLD DEPTH AT X-S # 2 = ?
20
DIST TO X-S # 3  = ?
20
INVERT EL. AT X-S # 3 = ?
700
```

```
ELEV. # 2 FOR X-S # 3 = ?
725
TW # 2 FOR X-S # 3 = ?
200
ELEV. # 3 FOR X-S # 3 = ?
750
TW # 3 FOR X-S # 3 = ?
400
ELEV. # 4 FOR X-S # 3 = ?
775
TW # 4 FOR X-S # 3 = ?
600
ELEV. # 5 FOR X-S # 3 = ?
800
TW # 5 FOR X-S # 3 = ?
800
MANNING N AT X-S # 3 = ?
0
HV AT X-S # 3 = ?
0
FLD DEPTH AT X-S # 3 = ?
20
DIST TO X-S # 4  = ?
30
INVERT EL. AT X-S # 4 = ?
550
ELEV. # 2 FOR X-S # 4 = ?
575
TW # 2 FOR X-S # 4 = ?
500
ELEV. # 3 FOR X-S # 4 = ?
600
TW # 3 FOR X-S # 4 = ?
1000
ELEV. # 4 FOR X-S # 4 = ?
625
TW # 4 FOR X-S # 4 = ?
1500
ELEV. # 5 FOR X-S # 4 = ?
650
TW # 5 FOR X-S # 4 = ?
2000
MANNING N AT X-S # 4 = ?
0
HV AT X-S # 4 = ?
0
FLD DEPTH AT X-S # 4 = ?
10
DIST TO X-S # 5  = ?
40
INVERT EL. AT X-S # 5 = ?
400
ELEV. # 2 FOR X-S # 5 = ?
425
TW # 2 FOR X-S # 5 = ?
250
ELEV. # 3 FOR X-S # 5 = ?
450
TW # 3 FOR X-S # 5 = ?
500
ELEV. # 4 FOR X-S # 5 = ?
475
TW # 4 FOR X-S # 5 = ?
750
ELEV. # 5 FOR X-S # 5 = ?
500
TW # 5 FOR X-S # 5 = ?
1000
MANNING N AT X-S # 5 = ?
0
HV AT X-S # 5 = ?
0
FLD DEPTH AT X-S # 5 = ?
10
```

Q (CFS) AT MI. 0 = 217306.4
DEPTH (FT) AT MI. 0 = 54.84
TPEAK(HR) AT MI 0 = 1.5
T (HR) FLD AT MI. 0 = .29
T(HR) DEFLD = 2.549

Q (CFS) AT MI. 10 = 165006
DEPTH (FT) AT MI. 10 = 41.3
TPEAK(HR) AT MI 10 = 2.52
T (HR) FLD AT MI. 10 = 1.23
T(HR) DEFLD = 4.40

Q (CFS) AT MI. 20 = 137958
DEPTH (FT) AT MI. 20 = 50.2
TPEAK(HR) AT MI 20 = 3.52
T (HR) FLD AT MI. 20 = 2.14
T(HR) DEFLD = 6.23

Q (CFS) AT MI. 30 = 123124
DEPTH (FT) AT MI. 30 = 34.1
TPEAK(HR) AT MI 30 = 4.67
T (HR) FLD AT MI. 30 = 3.21
T(HR) DEFLD = 8.05

Q (CFS) AT MI. 40 = 110152
DEPTH (FT) AT MI. 40 = 42.5
TPEAK(HR) AT MI 40 = 5.86
T (HR) FLD AT MI. 40 = 4.37
T(HR) DEFLD = 9.89

****

FULL DAMBRK RESULTS

****

PROFILE OF CRESTS AND TIMES FOR TEST NO. 4 OF NON-PR
BELOW SIMPLIFIED DAMBREAK

RVR MILE FROM DAM	MAX ELEV (FT)	MAX FLOW (CFS)	TIME MAX ELEV(HR)	FLOOD ELEV (FT)	TIME FLOOD (HR)
0.000	53.75	224206	1.500	30.00	0.75
10.000	42.51	173374	2.400	20.00	1.80
20.000	49.40	143972	3.450	20.00	2.85
30.000	34.73	126714	4.575	10.00	3.90
40.000	40.10	108592	5.810	10.00	5.10

```
SHORT VERSION?
NO
CREST EL. = ?
5288
FINAL BREACH EL. = ?
5027
RES. VOLUME = ?
230473
RES. SURF AREA = ?
1937
FINAL BREACH WIDTH = ?
150
TIME (MIN.) OF FAILURE = ?
75
NONBREACH FLOW = ?
13000
NO. X-S = ?
3
NO. PAIRS EL-TW = ?
5
INVERT EL. AT X-S # 1 = ?
5027
ELEV. # 2 FOR X-S # 1 = ?
5037
TW # 2 FOR X-S # 1 = ?
590
ELEV. # 3 FOR X-S # 1 = ?
5051
TW # 3 FOR X-S # 1 = ?
820
ELEV. # 4 FOR X-S # 1 = ?
5107
TW # 4 FOR X-S # 1 = ?
1130
ELEV. # 5 FOR X-S # 1 = ?
5125
TW # 5 FOR X-S # 1 = ?
1200
MANNING N AT X-S # 1 = ?
.08
HV AT X-S # 1 = ?
24
FLD DEPTH AT X-S # 1 = ?
20
DIST TO X-S # 2  = ?
5
INVERT EL. AT X-S # 2 = ?
4965
ELEV. # 2 FOR X-S # 2 = ?
4980
TW # 2 FOR X-S # 2 = ?
850
ELEV. # 3 FOR X-S # 2 = ?
5015
TW # 3 FOR X-S # 2 = ?
4600
ELEV. # 4 FOR X-S # 2 = ?
5025
TW # 4 FOR X-S # 2 = ?
5500
ELEV. # 5 FOR X-S # 2 = ?
5030
TW # 5 FOR X-S # 2 = ?
6800
MANNING N AT X-S # 2 = ?
.065
HV AT X-S # 2 = ?
70
FLD DEPTH AT X-S # 2 = ?
20
DIST TO X-S # 3  = ?
8.5
INVERT EL. AT X-S # 3 = ?
4920
```

```
ELEV. # 2 FOR X-S # 3 = ?
4930
TW # 2 FOR X-S # 3 = ?
800
ELEV. # 3 FOR X-S # 3 = ?
4942
TW # 3 FOR X-S # 3 = ?
4000
ELEV. # 4 FOR X-S # 3 = ?
4953
TW # 4 FOR X-S # 3 = ?
18000
ELEV. # 5 FOR X-S # 3 = ?
4958
TW # 5 FOR X-S # 3 = ?
25000
MANNING N AT X-S # 3 = ?
.04
HV AT X-S # 3 = ?
0
FLD DEPTH AT X-S # 3 = ?
26

Q (CFS) AT MI. 0 = 1627831.
DEPTH (FT) AT MI. 0 = 107.8
TPEAK(HR) AT MI 0 = 1.25
T (HR) FLD AT MI. 0 = 0.04
T(HR) DEFLD = 3.389909566

Q (CFS) AT MI. 5 = 1334272.
DEPTH (FT) AT MI. 5 = 59.11
TPEAK(HR) AT MI 5 = 1.83
T (HR) FLD AT MI. 5 = 0.61
T(HR) DEFLD = 4.721429949

Q (CFS) AT MI. 8.5 = 949225
DEPTH (FT) AT MI. 8.5 = 31.
TPEAK(HR) AT MI 8.5 = 2.65
T (HR) FLD AT MI. 8.5 = 1.97
T(HR) DEFLD = 5.289432199
```

****

FULL DAMBRK RESULTS

****

PROFILE OF CRESTS AND TIMES FOR TETON-SNAKE RIVER BELOW TETON DAM

RVR MILE FROM DAM	MAX ELEV (FT)	MAX FLOW (CFS)	TIME MAX ELEV(HR)	FLOOD ELEV (FT)	TIME FLOOD (HR)
0.000	94.75	1646490	1.375	5047.00	0.31
5.000	58.96	1015458	2.438	4985.00	1.31
8.500	30.07	926998	3.212	4946.00	2.44

APPENDIX IV

THE NWS SIMPLIFIED DAM BREAK MODEL

HP41CV OR HP41C W/QUAD MEMORY MODULE VERSION LISTING WITH EXAMPLE RUNS

SIMPLIFIED DAM BREAK FLOOD FORECASTING MODEL

HP 41CV VERSION

STORAGE REGISTER LOCATION SUMMARY ("SIZE"=073)

LOCATION	VALUE HELD
00	X-section counter
01	X-S Depth(1)
02	X-S Depth(2)
03	X-S Depth(3)
04	X-S Depth(4)
05	No. elev-topw counter
06	Routing counter
07	Reservoir pool crest elev.
08	Final breach elev.
09	Depth of breach
10	Sum LOG(depth) — Statistical Registers 10 - 15 used by Least Squares Routine
11	Sum LOG(depth)^2
12	Sum LOG(topw)
13	Sum LOG(topw)^2
14	Sum LOG(depth) * LOG(topw)
15	No. of values
16	Reservoir storage volume (ac-ft)
17	Res. surf. area (ac) for routines DB and CK; Dist for rtn RT
18	Final breach width (ft)
19	Time of failure (minutes)
20	Non-breach flow (cfs) for routine DB; Reit theta for routine RP
21	Total number of X-S to be read in
22	No. pairs elev-topw to be given
23	Invert at dam
24	Distance from dam to "current XS"
25	Distance from dam to "previous XS"
26	Invert at "current XS"
27	Invert at "previous XS"
28	"True" K fitting coeff. at "current XS"
29	"True" K fitting coeff. at "previous XS"
30	"True" m fitting coeff. at "current XS"
31	"True" m fitting coeff. at "previous XS"
32	Manning "n" at "current XS"
33	Manning "n" at "previous XS"
34	Temporary K fitting coefficient (produced by routine LS)
35	Average K fitting coefficient for entire routing reach
36	Temporary m fitting coefficient (produced by routine LS)
37	Average m fitting coefficient for entire routing reach
38	Channel slope at "current XS"
39	Channel slope from dam to "current XS"
40	Average Manning "n" for entire routing reach
41	Peak flow at dam
42	Peak stage at dam (recomputed with avg. K & m for each "curr XS")
43	Routed flow (produced by routine RT)
44	Routed stage
45	Breach eqn. factor, depth of water over weir (both for routine DB); Theta for routines SD and RP
46	Hydr. depth for routine RP; Dimensionless dist. for routine RT
47	Submergence corr. factor for DB; Tpeak for routine SD
48	Uncorr. flow for routine DB; Routed flow for routine SD
49	Flow for routine ST
50	Manning "n" for routine ST; Counter for routine BK
51	Slope for routine ST
52	Froude parameter
53	Volume parameter
54	Distance for routine RT
55	LOG Q (V*=1,Fc=0.25,0.75)
56	LOG Q (V*=1,Fc=FC(true))
57	Routing curve parameter (=0.357253).
58	Routing curve parameter (=45.05517)
59	Routing curve parameter (=0.5471514)
60	Routing curve parameter (=22.54279)
61	Routing curve parameter (=0.3728797)
62	Routing curve parameter (=7.09253)
63	Routing curve parameter (=0.960861)
64	Routing curve parameter (=3.0458380)

STORAGE REGISTER LOCATION SUMMARY (cont.)

LOCATION	VALUE HELD
65	Routing curve parameter (=0.0971795)
66	Routing curve parameter (=70.3383)
67	Routing curve parameter (=0.2373341)
68	Routing curve parameter (=37.59657)
69	Routing curve parameter (=0.6109883)
70	Routing curve parameter (=11.40695)
71	Routing curve parameter (=0.7631309)
72	Routing curve parameter (=4.101548)

"SD" Routine

This is the "main program" for the simplified dam break model.

```
01  LBL "SD"
02  XEQ "EN"
03  SF 01
04  "NO. SCTNS?
05  PROMPT
06  STO 21
07  1000
08  /
09  2.00001
10  +
11  STO 00
12  "NO. EL-TW?
13  PROMPT
14  1
15  -
16  STO 22
17  XEQ "SZT
18  0
19  STO 24
20  "INVERT?
21  PROMPT
22  STO 23
23  STO 26
24  XEQ "CK
25  XEQ "RX
26  XEQ "TC
27  XEQ "BK
28  RCL 21
29  1
30  -
31  X = 0?
32  GTO 01
33  XEQ "X1
34  SF 05
35  2.00501
36  STO 00
37  LBL 01
38  RCL 00
39  INT
40  "DIST? TO XS
41  ARCL X
42  PROMPT
43  STO 24
44  FS? 05
45  GTO 08
46  "INVERT?
47  PROMPT
48  STO 26
49  XEQ "SO
50  LBL 08
51  FS? 01
52  XEQ "DS
53  CF 01
54  FS? 05
55  GTO 09
56  XEQ "RX
57  XEQ "TC
58  XEQ "AN
59  XEQ "AV
60  LBL 09
61  RCL 41
62  STO 49
63  RCL 40
64  STO 50
65  RCL 39
66  STO 51
67  XEQ "ST
68  STO 42
69  0.95
70  STO 45
71  CF 02
72  LBL 02
73  CF 03
74  FS? 02
75  SF 03
76  XEQ "RP
77  LBL 03
78  RCL 17
79  FS? 02
80  RCL 24
81  STO 54
82  XEQ "RT
83  FS? 02
84  GTO 04
85  RCL 43
86  STO 49
87  XEQ "ST
88  RCL 42
89  +
90  2
91  /
92  RCL 42
93  /
94  STO 20
95  CHS
96  RCL 45
97  +
98  ABS
99  RCL 45
100 /
101 0.02
102 X>Y?
103 SF 02
104 FS? 02
105 FS? 03
106 FS? 02
107 GTO 03
108 RCL 20
109 RCL 45
110 +
111 2
112 /
113 STO 45
114 GTO 02
115 LBL 04
116 RCL 43
117 RCL 48
118 0.99
119 *
120 X>Y?
121 X<>Y
122 STO 48
123 RCL 24
124 2
125 /
126 STO 54
127 XEQ "RT
128 RCL 36
129 0.1
130 *
131 0.3
132 +
133 RCL 43
134 *
135 STO 49
136 XEQ "ST
137 RCL 36
138 1
139 +
140 /
141 0.667
142 Y↑X
143 RCL 39
144 SQRT
145 *
146 1.49
147 *
148 RCL 40
149 /
150 0.682
151 *
152 RCL 36
153 1
154 +
155 1/X
156 RCL 36
157 *
158 0.667
159 *
160 CHS
161 1.667
162 +
163 *
164 1/X
165 RCL 24
166 *
167 RCL 19
168 60
169 /
170 +
171 RCL 47
172 1.01
173 *
174 X<=Y?
175 X<>Y
176 STO 47
177 RCL 28
178 STO 34
179 RCL 30
180 STO 36
181 RCL 32
182 STO 50
183 RCL 38
184 STO 51
185 RCL 48
186 STO 49
187 XEQ "ST
188 STO 44
189 RCL 24
190 "AT MILE
191 ARCL X
192 AVIEW
193 PSE
194 RCL 48
195 "FLOW=
196 ARCL X
197 AVIEW
198 PSE
199 RCL 44
200 "DEPTH=
201 ARCL X
202 AVIEW
203 PSE
204 RCL 47
205 "PEAK=
206 ARCL X
207 AVIEW
208 PSE
209 XEQ "AV
210 XEQ "BK
211 ISG 00
212 GTO 01
213 RTN
214 END
```

"EN" Routine
This subroutine prompts user for reservoir, dam, and breach parms and stores values

```
01  LBL "EN
02  LBL 00
03  "CREST EL?
04  PROMPT
05  X=0?
06  GTO 00
07  STO 07
08  "BRCH EL?
09  PROMPT
10  STO 08
11  -
12  STO 09
13  LBL 01
14  "VOLUME?
15  PROMPT
16  STO 16
17  "SURF AREA?
18  PROMPT
19  STO 17
20  +
21  X=0?
22  GTO 01
23  "BRCH WDTH?
24  PROMPT
25  X ≠ 0?
26  GTO 02
27  RCL 09
28  3
29  *
30  LBL 02
31  STO 18
32  "TIME FAIL?
33  PROMPT
34  X ≠ 0?
35  GTO 03
36  RCL 09
37  3
38  /
39  LBL 03
40  STO 19
41  "NONBR FLO?
42  PROMPT
43  STO 20
44  RTN
45  END
```

"RX" Routine

This subroutine reads in the elev-topw data, takes logs and fills the statistical registers for least squares routine

```
01  LBL "RX
02  LBL 00
03  "ELEV?
04  PROMPT
05  RCL 26
06  -
07  STO IND 05
08  LOG
09  "TOPW?
10  PROMPT
11  LOG
12  X<>Y
13  Σ+ (Sum +)
14  ISG 05
15  GTO 00
16  "MANNING N?
17  PROMPT
18  X ≠ 0?
19  GTO 01
20  0.05
21  LBL 01
22  STO 32
23  XEQ "LS
24  XEQ "SET
25  RTN
26  END
```

"SET" Routine

This subroutine resets the counter for the number of elev-topw pairs given

```
01  LBL "SET
02  RCL 22
03  1000
04  /
05  1.00001
06  +
07  STO 05
08  RTN
09  END
```

"TC" Routine

This saves "temporary" X & m coefficient from LS routine as true "current XS" X & m

```
01  LBL "TC
02  RCL 34
03  STO 28
04  RCL 36
05  STO 30
06  RTN
07  END
```

"LS" Routine

This subroutine computes (via least squares) the K & m channel fitting coefficients using the values stored in statistical regs. 10 - 16

```
01  LBL "LS
02  RCL 14
03  RCL 10
04  RCL 12
05  *
06  RCL 15
07  /
08  -
09  RCL 11
10  RCL 10
11  X^2
12  RCL 15
13  /
14  -
15  /
16  STO 36
17  RCL 12
18  RCL 15
19  /
20  RCL 10
21  RCL 15
22  /
23  RCL 36
24  *
25  -
26  10^X
27  STO 34
28  CLΣ
29  RTN
30  END
```

"DB" Routine

This subroutine computes the peak outflow at the dam

```
01  LBL "DB
02  RCL 17
03  23.4
04  *
05  RCL 18
06  /
07  STO 45
08  RCL 09
09  SQRT
10  /
11  RCL 19
12  60
13  /
14  +
15  RCL 45
16  X<>Y
17  /
18  X^2
19  STO 45
20  1.5
21  Y^X
22  RCL 18
23  *
24  3.1
25  *
26  RCL 20
27  +
28  STO 41
29  STO 48
30  STO 49
31  RCL 32
32  STO 50
33  RCL 38
34  STO 51
35  XEQ "ST
36  STO 42
37  RCL 36
38  1
39  +
40  /
41  STO 46
42  0.6667
43  Y^X
44  RCL 38
45  SQRT
46  *
47  1.49
48  *
49  RCL 32
50  /
51  RCL 46
52  32.2
53  *
54  SQRT
55  /
56  1
57  STO 47
58  X<=Y?
59  GTO 05
60  LBL 01
61  RCL 42
62  RCL 23
63  +
64  RCL 08
65  -
66  RCL 45
67  /
68  0.67
69  X>Y?
70  GTO 05
71  X<>Y
72  0.67
73  -
74  3
75  Y^X
76  27.8
77  *
78  CHS
79  1
80  +
81  0.3
82  X<=Y?
83  X<>Y
84  RCL 47
85  +
86  2
87  /
88  STO 47
89  RCL 41
90  STO 48
91  *
92  STO 49
93  RCL 48
94  -
95  ABS
96  RCL 48
97  20
98  /
99  X>Y?
100 GTO 05
101 RCL 49
102 STO 41
103 CHS
104 RCL 48
105 +
106 RCL 19
107 60
108 *
109 *
110 RCL 17
111 87120
112 *
113 /
114 RCL 45
115 +
116 STO 45
117 XEQ "ST
118 STO 42
119 GTO 01
120 LBL 05
121 RCL 41
122 "DAMFLO=
123 ARCL X
124 AVIEW
125 PSE
126 RCL 42
127 "DEPTH=
128 ARCL X
129 AVIEW
130 PSE
131 RCL 19
132 60
133 /
134 STO 47
135 "PEAK=
136 ARCL X
137 AVIEW
138 RTN
139 END
```

"AV" Routine

This subroutine computes the distance weighted K & m coefficients for reach from dam to XS(I)

```
01  LBL "AV
02  LBL 01
03  RCL IND 05
04  RCL 30
05  Y^X
06  RCL 28
07  *
08  RCL IND 05
09  RCL 31
10  Y^X
11  RCL 29
12  *
13  +
14  2
15  /
16  RCL 24
17  RCL 25
18  -
19  *
20  RCL IND 05
21  RCL 37
22  Y^X
23  RCL 35
24  *
25  RCL 25
26  *
27  +
28  RCL 24
29  /
30  LOG
31  RCL IND 05
32  LOG
33  Σ+ (Sum +)
34  ISG 05
35  GTO 01
36  XEQ "LS
37  XEQ "SET
38  RTN
39  END
```

"CX" Routine

This subroutine computes the default reservoir volume or surface area and checks for perched breach

```
01  LBL "CX
02  RCL 17
03  X = 0?
04  GTO 01
05  RCL 16
06  2
07  *
08  RCL 07
09  RCL 23
10  -
11  /
12  STO 17
13  LBL 01
14  RCL 16
15  X = 0?
16  GTO 02
17  RCL 17
18  2
19  /
20  RCL 07
21  RCL 23
22  -
23  *
24  STO 16
25  LBL 02
26  RCL 23
27  5
28  +
29  RCL 08
30  X<=Y?
31  GTO 03
32  RCL 08
33  RCL 23
34  -
35  RCL 07
36  RCL 23
37  -
38  /
39  X^2
40  1
41  +
42  RCL 17
43  *
44  RCL 09
45  *
46  2
47  /
48  STO 16
49  LBL 03
50  RTN
51  END
```

"SO" Routine

This subroutine computes the channel slope at the "current XS" and the slope from the dam to the "current XS"

```
01  LBL "SO
02  RCL 27
03  RCL 26
04  -
05  RCL 24
06  RCL 25
07  -
08  5280
09  *
10  /
11  STO 38
12  RCL 23
13  RCL 26
14  -
15  RCL 24
16  5280
17  *
18  /
19  STO 39
20  RTN
21  END
```

"ST" Routine

This subroutine computes the stage at a given point

```
01  LBL "ST
02  1.49
03  RCL 50
04  /
05  RCL 51
06  SQRT
07  *
08  RCL 34
09  *
10  RCL 36
11  1
12  +
13  1.667
14  Y^X
15  /
16  1/X
17  RCL 49
18  *
19  RCL 36
20  1.667
21  +
22  1/X
23  Y^X
24  RTN
25  END
```

"AN" Routine

This subroutine computes the distance weighted average Manning "n" for reach

```
01  LBL "AN
02  RCL 32
03  RCL 33
04  +
05  2
06  /
07  RCL 24
08  RCL 25
09  -
10  *
11  RCL 40
12  RCL 25
13  *
14  +
15  RCL 24
16  /
17  STO 40
18  RTN
19  END
```

"BK" Routine

This subroutine saves "current XS" temporary variables as "past XS" variables

```
01  LBL "BK
02  24.03701
03  STO 50
04  LBL 01
05  RCL IND 50
06  ISG 50
07  STO IND 50
08  ISG 50
09  GTO 01
10  RTN
11  END
```

"RP" Routine

This subroutine computes the routing parameters Xc, Fc, and V*

```
01  LBL "RP
02  RCL 16
03  43560
04  *
05  RCL 36
06  1
07  +
08  *
09  RCL 07
10  RCL 23
11  -
12  RCL 36
13  1
14  +
15  Y^X
16  RCL 34
17  *
18  /
19  0.5
20  RCL 36
21  1
22  +
23  Y^X
24  4
25  *
26  1
27  +
28  1/X
29  6
30  *
31  *
32  STO 17
33  RCL 45
34  RCL 42
35  *
36  RCL 36
37  1
38  +
39  /
40  STO 46
41  0.667
42  Y^X
43  RCL 39
44  SQRT
45  *
46  1.49
47  *
48  RCL 40
49  /
50  32.2
51  RCL 46
52  *
53  SQRT
54  /
55  .26
56  X<=Y?
57  X<>Y
58  .75
59  X>Y?
60  X<>Y
61  STO 52
62  RCL 45
63  RCL 42
64  *
65  RCL 36
66  Y^X
67  RCL 34
68  *
69  RCL 46
70  *
71  RCL 17
72  *
73  1/X
74  43560
75  *
76  RCL 16
77  *
78  1
79  X<=Y?
80  X<>Y
81  STO 53
82  5
83  X>Y?
84  X<>Y
85  STO 53
86  RCL 17
87  5280
88  /
89  STO 17
90  RTN
91  END
```

"RT" Routine

This "routing" subroutine computes the peak flow downstream of the dam

```
01  LBL "RT"
02  RCL 54
03  RCL 17
04  /
05  STO 46
06  5
07  X<>Y
08  X>Y?
09  GTO 01
10  57.06401
11  STO 06
12  GTO 02
13  LBL 01
14  65.07201
15  STO 06
16  LBL 02
17  XEQ 07
18  STO 55
19  ISG 06
20  XEQ 07
21  XEQ 08
22  STO 56
23  ISG 06
24  XEQ 07
25  STO 55
26  ISG 06
27  XEQ 07
28  XEQ 08
29  RCL 56
30  -
31  0.6990
32  /
33  RCL 53
34  LOG
35  *
36  RCL 56
37  +
38  10^X
39  100
40  /
41  RCL 41
42  *
43  STO 43
44  RTN
45  LBL 07
46  RCL 46
47  RCL IND 06
48  Y^X
49  ISG 06
50  RCL IND 06
51  *
52  CHS
53  100
54  +
55  5
56  X<=Y?
57  X<>Y
58  LOG
59  RTN
60  LBL 08
61  RCL 55
62  -
63  1.6990
64  /
65  RCL 52
66  100
67  *
68  25
69  -
70  LOG
71  *
72  RCL 55
73  +
74  RTN
75  END
```

"X1" Routine

This subroutine is used when only one X-S is to be read in. It prompts for channel slope and computes default if none given. It also stores "average XS" parameters

```
01  LBL "X1
02  "SLOPE FT/MI?
03  PROMPT
04  X ≠ 0?
05  GTO 01
06  RCL IND 22
07  RCL 30
08  Y^X
09  RCL 28
10  *
11  24.75
12  /
13  RCL 16
14  /
15  RCL 09
16  X^2
17  *
18  LBL 01
19  5280
20  /
21  STO 38
22  STO 39
23  RCL 33
24  STO 40
25  RTN
26  END
```

PROGRAM INITIALIZATION PROCEDURE

SIMPLIFIED DAM BREAK FLOOD FORECASTING MODEL
HP 41CV VERSION

Prior to executing the model code that has been entered into the HP, it is necessary to first initialize various storage registers. The user must XEQ the HP routines "FIX" (= 2), "TREG" (= 10) and "CLX". Then the following values must be stored as shown below (this storing need be done only once after each time the program is entered into the HP). Then key in XEQ SD and the program will run (see example run on following page).

```
0.357253
STO 57
45.05517
STO 58
0.5471514
STO 59
22.54279
STO 60
0.8728797
STO 61
7.09253
STO 62
0.960861
STO 36
3.0458380
STO 64
0.0971795
STO 65
70.3383
STO 66
0.2373341
STO 67
37.59657
STO 68
0.6109883
STO 69
11.40695
STO 70
0.7631309
STO 71
4.101548
STO 72
```

NOTE: Because a new "space saving" algorithm is used for routing the flows in the HP41C version, the results produced by this version will vary somewhat from the results produced by the FORTRAN and BASIC versions. Additionally, because of limited storage space, the "Height of Valley Wall" and the "Flood Depth" (Time of flooding and deflooding) parameters available in the other versions have been eliminated.

SIMPLIFIED DAM BREAK FLOOD FORECASTING MODEL

HP 41CV VERSION

EXAMPLE RUN FOR 1 X-S GIVEN, ALL DEFAULTS USED

Keystrokes	Display	Comments
XEQ SD		Execute SMPDBK Program
1100 R/S	CREST EL? 1,100	Max. pool elev. (ft MSL) prompt
1000 R/S	BRCH EL? 1,000	Final breach elev. (ft MSL) prompt
25000 R/S	VOLUME? 25,000	Reservoir Volume (ac-ft) prompt (If 0 input, compute from Surface Area) (Must enter either Vol. or S.A. or both)
0 R/S	SURF AREA? 0	Reservoir Surface Area (acres) prompt (If 0 input, compute S.A. from Volume)
0 R/S	BRCH WDTH? 0	Final breach width (feet) prompt (If 0 input, BW = 3 * dam height)
0 R/S	TIME FAIL? 0	Time of failure (minutes) prompt (If 0 input, TF = dam height/3)
0 R/S	NONBR FLO? 0	Non-breach flow (cfs) prompt (If 0 input, Q0 = 0)
1 R/S	NO. SCTNS? 1	No. X-S to be specified prompt (Min. = 1, no maximum)
3 R/S	NO. EL-TW? 3	No. pairs of elev-vs-topw data prompt (Min. = 3, Max = 5)
1000 R/S	INVERT? 1,000	Channel invert (ft MSL) at X-S #1 prompt (Elev. of base of dam) (Model assumes invert topwidth = 0)
1050 R/S	ELEV? 1,050	Elevation #2 (ft MSL) at X-S #1 prompt
500 R/S	TOPW? 500	Topwidth #2 (ft) at X-S #1 prompt
1100 R/S	ELEV? 1,100	Elevation #3 (ft MSL) at X-S #1 prompt
1000 R/S	TOPW? 1,000	Topwidth #3 (ft) at X-S #1 prompt
0 R/S	MANNING N? 0	Manning roughness coeff. prompt (If 0 input, default = 0.050)
0 R/S	SLOPE FT/MI 0	Downstream channel slope prompt (Prompts only when one X-S specified) (If 0 input, slope computed internally)

EXAMPLE RUN (cont.) FOR 1 X-S GIVEN, ALL DEFAULTS USED

Keystrokes	Display	Comments
	DIST? TO XS 2.00	Dist.(miles) to forecast point #2 prompt (When only one X-S specified, model allows four additional forecast points)
10 R/S	10	
	DAMFLO=333,627.15 DEPTH=63.50 TPEAK=0.56	Peak outflow (cfs) at dam Peak depth (ft) at dam Time of peak (hours) at dam
	AT MILE 10.00 FLOW=253,200.72 DEPTH=57.26 TPEAK=1.43	 Peak flow (cfs) at forecast point #2 Peak depth (ft) at forecast point #2 Time of peak (hours) at forecast pt. #2
	DIST? TO XS 3.00	Dist.(miles) to forecast point #3 prompt
20 R/S	20	
	AT MILE 20.00 FLOW=220,175.16 DEPTH=54.33 TPEAK=2.35	 Peak flow (cfs) at forecast point #3 Peak depth (ft) at forecast point #3 Time of peak (hours) at forecast pt. #3
	DIST? TO XS 4.00	Dist.(miles) to forecast point #4 prompt
30 R/S	30	
	AT MILE 30.00 FLOW=194,631.49 DEPTH=51.88 TPEAK=3.29	 Peak flow (cfs) at forecast point #4 Peak depth (ft) at forecast point #4 Time of peak (hours) at forecast pt. #4
	DIST? TO XS 5.00	Dist.(miles) to forecast point #5 prompt
40 R/S	40	
	AT MILE 40.00 FLOW=172,925.67 DEPTH=49.63 TPEAK=4.26	 Peak flow (cfs) at forecast point #5 Peak depth (ft) at forecast point #5 Time of peak (hours) at forecast pt. #5

SIMPLIFIED DAM BREAK FLOOD FORECASTING MODEL

HP 41CV VERSION

EXAMPLE RUN

Keystrokes	Display	Comments
XEQ SD		Execute SMPDBK Program
1100 R/S	CREST EL? 1,100	Max. pool elev. (ft MSL) prompt
1000 R/S	BRCH EL? 1,000	Final breach elev. (ft MSL) prompt
0 R/S	VOLUME? 0	Reservoir Volume (ac-ft) prompt (If 0 input, compute from Surface Area) (Must enter either Vol. or S.A. or both)
500 R/S	SURF AREA? 500	Reservoir Surface Area (acres) prompt (If 0 input, compute S.A. from Volume)
100 R/S	BRCH WDTH? 100	Final breach width (feet) prompt (If 0 input, BW = 3 * dam height)
90 R/S	TIME FAIL? 90	Time of failure (minutes) prompt (If 0 input, TF = dam height/3)
1500 R/S	NONBR FLO? 1,500	Non-breach flow (cfs) prompt (If 0 input, QO = 0)
5 R/S	NO. SCTNS? 5	No. X-S to be specified prompt (Min. = 1, no maximum)
5 R/S	NO. EL-TW? 5	No. pairs of elev-vs-topw data prompt (Min. = 3, Max = 5)
1000 R/S	INVERT? 1,000	Channel invert (ft MSL) at X-S #1 prompt (Elev. of base of dam) (Model assumes invert topwidth = 0)
1025 R/S	ELEV? 1,025	Elevation #2 (ft MSL) at X-S #1 prompt
250 R/S	TOPW? 250	Topwidth #2 (ft) at X-S #1 prompt
1050 R/S	ELEV? 1,050	Elevation #3 (ft MSL) at X-S #1 prompt
500 R/S	TOPW? 500	Topwidth #3 (ft) at X-S #1 prompt
1075 R/S	ELEV? 1,075	Elevation #4 (ft MSL) at X-S #1 prompt
750 R/S	TOPW? 750	Topwidth #4 (ft) at X-S #1 prompt
1100 R/S	ELEV? 1,100	Elevation #5 (ft MSL) at X-S #1 prompt

EXAMPLE RUN (cont.)

Keystrokes	Display	Comments
	TOPW?	Topwidth #5 (ft) at X-S #1 prompt
1000 R/S	1,000	
	MANNING N?	Manning roughness coeff. prompt (If 0 input, default = 0.050)
0 R/S	0	
	DIST? TO XS 2.00	Distance (miles) to X-section #2 prompt
10 R/S	10	
	INVERT?	Invert elev. (ft MSL) at X-S #2 prompt (Model assumes invert topwidth = 0)
850 R/S	850	
	DAMFLO=217,372.56	Peak outflow (cfs) at dam
	DEPTH=54.34	Peak depth (ft) at dam
	TPEAK=1.50	Time of peak (hours) at dam
	ELEV?	Elevation #2 (ft MSL) at X-S #2 prompt
875 R/S	875	
	TOPW?	Topwidth #2 (ft) at X-S #2 prompt
400 R/S	400	
	ELEV?	Elevation #3 (ft MSL) at X-S #2 prompt
900 R/S	900	
	TOPW?	Topwidth #3 (ft) at X-S #2 prompt
750 R/S	750	
	ELEV?	Elevation #4 (ft MSL) at X-S #2 prompt
925 R/S	925	
	TOPW?	Topwidth #4 (ft) at X-S #2 prompt
1125 R/S	1,125	
	ELEV?	Elevation #5 (ft MSL) at X-S #2 prompt
950 R/S	950	
	TOPW?	Topwidth #5 (ft) at X-S #2 prompt
1500 R/S	1,500	
	MANNING N?	Manning roughness coeff. prompt (If 0 input, default = 0.050)
0 R/S	0	
	AT MILE 10.00	
	FLOW=167,552.34	Peak flow (cfs) at X-section #2
	DEPTH=41.62	Peak depth (ft) at X-section #2
	TPEAK=2.56	Time of peak (hours) at X-section #2
	DIST? TO XS 3.00	Distance (miles) to X-section #3 prompt
20 R/S	20	
	INVERT?	Invert elev. (ft MSL) at X-S #2 prompt (Model assumes invert topwidth = 0)
700 R/S	700	
	ELEV?	Elevation #2 (ft MSL) at X-S #3 prompt
725 R/S	725	
	TOPW?	Topwidth #2 (ft) at X-S #3 prompt
200 R/S	200	
	ELEV?	Elevation #3 (ft MSL) at X-S #3 prompt
750 R/S	750	
	TOPW?	Topwidth #3 (ft) at X-S #3 prompt
400 R/S	400	

EXAMPLE RUN (cont.)

Keystrokes	Display	Comments
	ELEV?	Elevation #4 (ft MSL) at X-S #3 prompt
775 R/S	775	
	TOPW?	Topwidth #4 (ft) at X-S #3 prompt
600 R/S	600	
	ELEV?	Elevation #5 (ft MSL) at X-S #3 prompt
800 R/S	800	
	TOPW?	Topwidth #5 (ft) at X-S #3 prompt
800 R/S	800	
	MANNING N?	Manning roughness coeff. prompt (If 0 input, default = 0.050)
0 R/S	0	
	AT MILE 20.00	
	FLOW=145,071.20	Peak flow (cfs) at X-section #3
	DEPTH=51.23	Peak depth (ft) at X-section #3
	TPEAK=3.69	Time of peak (hours) at X-section #3
	DIST? TO XS 4.00	Distance (miles) to X-section #4 prompt
30 R/S	30	
	INVERT?	Invert elev. (ft MSL) at X-S #4 prompt (Model assumes invert topwidth = 0)
550 R/S	550	
	ELEV?	Elevation #2 (ft MSL) at X-S #4 prompt
575 R/S	575	
	TOPW?	Topwidth #2 (ft) at X-S #4 prompt
500 R/S	500	
	ELEV?	Elevation #3 (ft MSL) at X-S #4 prompt
600 R/S	600	
	TOPW?	Topwidth #3 (ft) at X-S #4 prompt
1000 R/S	1,000	
	ELEV?	Elevation #4 (ft MSL) at X-S #4 prompt
625 R/S	625	
	TOPW?	Topwidth #4 (ft) at X-S #4 prompt
1500 R/S	1,500	
	ELEV?	Elevation #5 (ft MSL) at X-S #4 prompt
650 R/S	650	
	TOPW?	Topwidth #5 (ft) at X-S #4 prompt
2000 R/S	2,000	
	MANNING N?	Manning roughness coeff. prompt (If 0 input, default = 0.050)
0 R/S	0	
	AT MILE 30.00	
	FLOW=132,385.11	Peak flow (cfs) at X-section #4
	DEPTH=35.11	Peak depth (ft) at X-section #4
	TPEAK=4.61	Time of peak (hours) at X-section #4
	DIST? TO XS 5.00	Distance (miles) to X-section #5 prompt
40 R/S	40	
	INVERT?	Invert elev. (ft MSL) at X-S #5 prompt (Model assumes invert topwidth = 0)
400 R/S	400	

EXAMPLE RUN (cont.)

Keystrokes	Display	Comments
	ELEV?	Elevation #2 (ft MSL) at X-S #5 prompt
425 R/S	425	
	TOPW?	Topwidth #2 (ft) at X-S #5 prompt
250 R/S	250	
	ELEV?	Elevation #3 (ft MSL) at X-S #5 prompt
450 R/S	450	
	TOPW?	Topwidth #3 (ft) at X-S #5 prompt
500 R/S	500	
	ELEV?	Elevation #4 (ft MSL) at X-S #5 prompt
475 R/S	475	
	TOPW?	Topwidth #4 (ft) at X-S #5 prompt
750 R/S	750	
	ELEV?	Elevation #5 (ft MSL) at X-S #5 prompt
500 R/S	500	
	TOPW?	Topwidth #5 (ft) at X-S #5 prompt
1000 R/S	1,000	
	MANNING N?	Manning roughness coeff. prompt (IF C input, default = 0.050)
0 R/S	C	
	AT MILE 40.00	
	FLOW=106,292.79	Peak flow (cfs) at X-section #5
	DEPTH=41.93	Peak depth (ft) at X-section #5
	TPEAK=6.49	Time of peak (hours) at X-section #5

FULL DAMBRK RESULTS

PROFILE OF CRESTS AND TIMES FOR TEST NO. 4 OF NON-PR
BELOW SIMPLIFIED DAMBREAK

AVR MILE FROM DAM	MAX ELEV (FT)	MAX FLOW (CFS)	TIME MAX ELEV(HR)	FLOOD ELEV (FT)	TIME FLOOD (HR)
0.000	53.75	224206	1.500	30.00	0.75
10.000	42.51	173374	2.400	20.00	1.80
20.000	49.40	143972	3.450	20.00	2.85
30.000	34.73	126714	4.575	10.00	3.90
40.000	40.10	108592	5.310	10.00	5.10

BREACH: AN EROSION MODEL FOR EARTHEN DAM FAILURES

by D.L. Fread*

January, 1985

ABSTRACT. A physically based mathematical model (BREACH) to predict the breach characteristics (size, time of formation) and the discharge hydrograph emanating from a breached earthen dam is presented. The earthen dam may be man-made or naturally formed by a landslide. The model is developed by coupling the conservation of mass of the reservoir inflow, spillway outflow, and breach outflow with the sediment transport capacity of the unsteady uniform flow along an erosion-formed breach channel. The bottom slope of the breach channel is assumed to be essentially that of the downstream face of the dam. The growth of the breach channel is dependent on the dam's material properties (D_{50} size, unit weight, friction angle, cohesive strength). The model considers the possible existence of the following complexities: 1) core material having properties which differ from those of the outer portions of the dam; 2) the necessity of forming an eroded ditch along the downstream face of the dam prior to the actual breach formation by the overtopping water; 3) the downstream face of the dam can have a grass cover or be composed of a material of larger grain size than the outer portion of the dam; 5) enlargement of the breach through the mechanism of one or more sudden structural collapses due to the hydrostatic pressure force exceeding the resisting shear and cohesive forces; 5) enlargement of the breach width by slope stability theory; and 6) initiation of the breach via piping with subsequent progression to a free surface breach flow. The outflow hydrograph is obtained through a time-stepping iterative solution that requires only a few seconds for computation on a main-frame computer. The model is not subject to numerical stability or convergence difficulties. The model's predictions are compared with observations of a piping failure in the man-made Teton Dam in Idaho and a breached landslide-formed dam in Peru. Also, the model has been used to predict possible downstream flooding from a potential breach of the landslide blockage of Spirit Lake in the aftermath of the eruption of Mount St. Helens in Washington. Model sensitivity to numerical parameters is minimal; however, it is sensitive to the dam's material internal friction angle and the extent of grass cover when simulating man-made dams and to the cohesive strength of the material composing landslide-formed dams.

*D. L. Fread is a Senior Research Hydrologist with the Hydrologic Research Laboratory, National Weather Service, NOAA, Silver Spring, Maryland 20910.

INTRODUCTION

Earthen dams are subject to possible failure from either overtopping or piping water which erode a trench (breach) through the dam. The breach formation is gradual with respect to time and its width as measured along the crest of the dam usually encompasses only a portion of the dam's crest length. In many instances, the bottom of the breach progressively erodes downward until it reaches the bottom of the dam; however, in some cases, it may cease its downward progression at some intermediate elevation between the top and bottom of the dam. The size of the breach, as constituted by its depth and its width (which may be a function of the depth), and the rate of the breach formation determine the magnitude and shape of the resulting breach outflow hydrograph. This is of vital interest to hydrologists and engineers concerned with real-time forecasting or evacuation planning for floods produced by dam failures.

This paper presents a mathematical model (BREACH) for predicting the breach characteristics (size, shape, time of formation) and the breach outflow hydrograph. The model is physically based on the principles of hydraulics, sediment transport, soil mechanics, the geometric and material properties of the dam, and the reservoir properties (storage volume, spillway characteristics, and time dependent reservoir inflow rate). The dam may be either man-made or naturally formed as a consequence of a landslide. In either, the mechanics of breach formation are very similar, the principal difference being one of scale. The landslide-formed dam is often much larger than even the largest of man-made earthen dams as illustrated in Fig. 1. The critical material properties of the dam are the internal friction angle, cohesion strength, and average grain size diameter (D_{50}).

The breach erosion model presented herein is a modification of an earlier version first reported by the author (Fread, 1984). The BREACH Model predicts a dam-breach outflow hydrograph. It differs from the parametric approach which the author has used in the NWS DAMBRK Model (Fread, 1977, 1981, 1983). The parametric model uses empirical observations of previous dam failures such as the breach width-depth relation, time of breach formation, and depth of breach to develop the outflow hydrograph. The breach erosion model presented herein can provide some advantages over the parametric breach model for application to man-made dams since the critical properties used by the model are measurable or can be estimated within a reasonable range from a qualitative description of the dam materials. However, it should be emphasized that even if the properties can be measured there is a range for their probable value and within this range outflow hydrographs of varying magnitude and shape will be produced by the model. The hydrologist or engineer should investigate the most critical combination of values for the dam's material properties. It is considered essential when predicting breach outflows of landslide dams to utilize a physically based model since observations of such are essentially non-existent, rendering the parametric approach infeasible.

In this paper, the breach erosion model is applied to the piping initiated failure of the man-made Teton Dam in Idaho, the overtopping

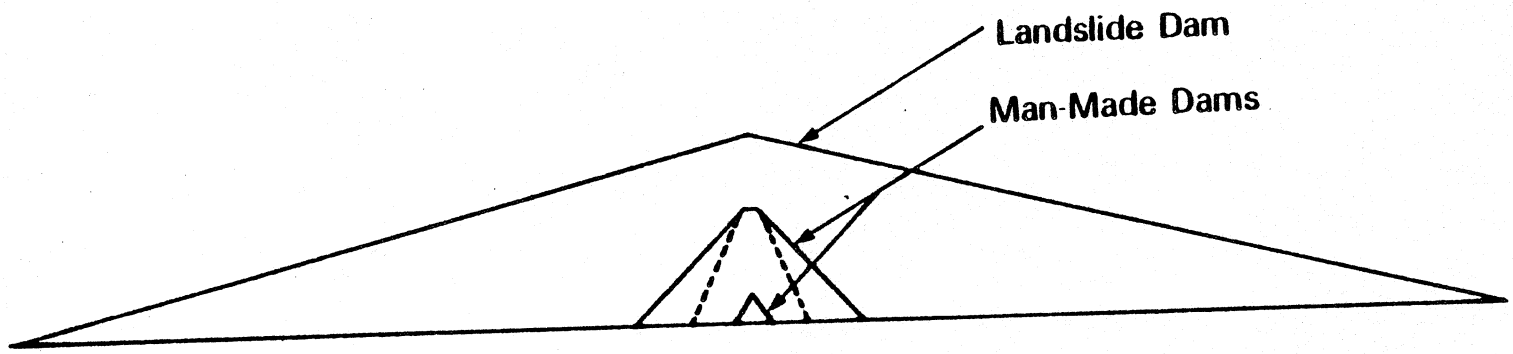

Figure 1. Comparative View of Natural Landslide Dams and Man-Made Dams.

failure of the Mantaro landslide-formed dam in Peru, and the possible failure of the recently formed landslide blockage of Spirit Lake, near Mount St. Helens in Washington.

PREVIOUS RESEARCH

Other investigators of dam breach outflows have developed physically based models.

The first was Cristofano (1965) who derived an equation which related the force of the flowing water through the breach to the shear strength of the soil particles on the bottom of the breach and in this manner developed the rate of erosion of the breach channel as a function of the rate of change of water flowing through the breach. He assumed the breach bottom width to be constant with time and always of trapezoidal shape in which the side slopes of the trapezoid were determine by the angle of repose of the breach material, and the bottom slope of the breach channel was equal to the internal friction angle of the breach material. An arbitrary empirical coefficient which was critical to the model's prediction was also utilized.

Harris and Wagner (1967) used the Schoklitsch sediment transport equation and considered the breach to commence its downward progession immediately upon overtopping, and the erosion of the breach was assumed to progress to the bottom of the dam. Brown and Rogers (1977) presented a breach model which was based on the work of Harris and Wagner.

Most recently Ponce and Tsivoglou (1981) presented a rather computationally complex breach erosion model which coupled the Meyer-Peter and Muller sediment transport equation to the one-dimensional differential equations of unsteady flow and sediment conservation. Reservoir storage depletion was included in the upstream boundary equation used in conjunction with the unsteady flow equations. The set of differential equations was solved with a four-point implicit finite difference scheme. Flow resistance was represented through use of the Manning n. Breach width was empirically related to the rate of breach flow. A small rivulet was assumed to be initially present along the flow path. "Outflow at start of the computation is a function of the assumed initial size of the rivulet. Progressive erosion widens and deepens the rivulet, increasing outflow and erosion rate in a self-generating manner. The upper cross-section on the sloping downstream face creeps upstream across the dam top until it reaches the upstream face, whereby rate of flow and erosion increase at a faster rate. If outflow increases enough to lower the reservoir level faster than the channel bed erodes, both outflow and erosion gradually diminish. Of course, outflow will eventually decrease even if the breach bed erodes all the way down to the stream bed. This mode of failure creates the outflow hydrograph in the shape of a sharp but nevertheless gradual flood wave." Ponce and Tsivoglou compared the model's predictions with observations of a breached landslide-formed dam on the Mantaro River in Peru. The results were considered good. However, they were influenced by the judicious selection of the Manning n, the breach width-flow relation parameter, and a coefficient in the sediment transport equation, although Ponce and Tsivoglou

stated that the selected values were within each one's reasonable range of variation. Also, problems of a numerical computational nature were alluded to in connection with solving the implicit finite difference unsteady flow equations. They also implied that further work was needed to improve the breach width-flow relation and in developing a relation between the Manning n and the hydraulic/sediment characteristics of the breach channel.

The breach erosion model presented in this paper differs substantially from those previously reported. A summation of the important differences will be given after the model has been completely described in the next section.

MODEL DESCRIPTION

General

The breach erosion model (BREACH) simulates the failure of an earthen dam as shown in Fig. 2. The dam may be homogeneous or it may consist of two materials, an outer zone with distinct material properties (ϕ - friction angle, C - cohesion, D_{50} - average grain size (mm), and γ - unit weight) and an inner core with its ϕ, C, D_{50}, and γ values. Also, the downstream face of the dam may be specified as having: 1) a grass cover with specified length of either good or fair stand, 2) material identical to the outer portion of the dam, or 3) material of larger grain size than the outer portion. The geometry of the downstream face of the dam is described by specifying the top of the dam (H_u), the bottom elevation of the dam (H_ℓ) or original streambed elevation, and its slope as given by the ratio 1 (vertical) : ZD (horizontal). Then, the geometry of the upstream face of the dam is described by specifying its slope as the ratio 1 (vertical) : ZU (horizontal). If the dam is man-made it is further described by specifying a flat crest width (W_{cr}) and a spillway rating table of spillway flow vs. water elevation, in which the first elevation represents the spillway crest. Naturally formed landslide dams are assumed to <u>not</u> have a flat crest or, of course, a spillway.

The storage characteristics of the reservoir are described by specifying a table of surface area (S_a) in units of acre-ft vs. water elevation, the initial water surface elevation (H_i) at the beginning of the simulation, and a table of reservoir inflows (Q_i) in cfs vs. the hour of their occurrence (T_i).

If an overtopping failure is simulated, the water level (H) in the reservoir must exceed the top of the dam before any erosion occurs. The first stages of the erosion are only along the downstream face of the dam as denoted by the line A-A in Fig. 2 where, initially if no grass cover exists, a small rectangular-shaped rivelet is assumed to exist along the face. An erosion channel of depth-dependent width is gradually cut into the downstream face of the dam. The flow into the channel is determined by the broad-crested weir relationship:

$$Q_b = 3\ B_o(H-H_c)^{1.5} \qquad (1)$$

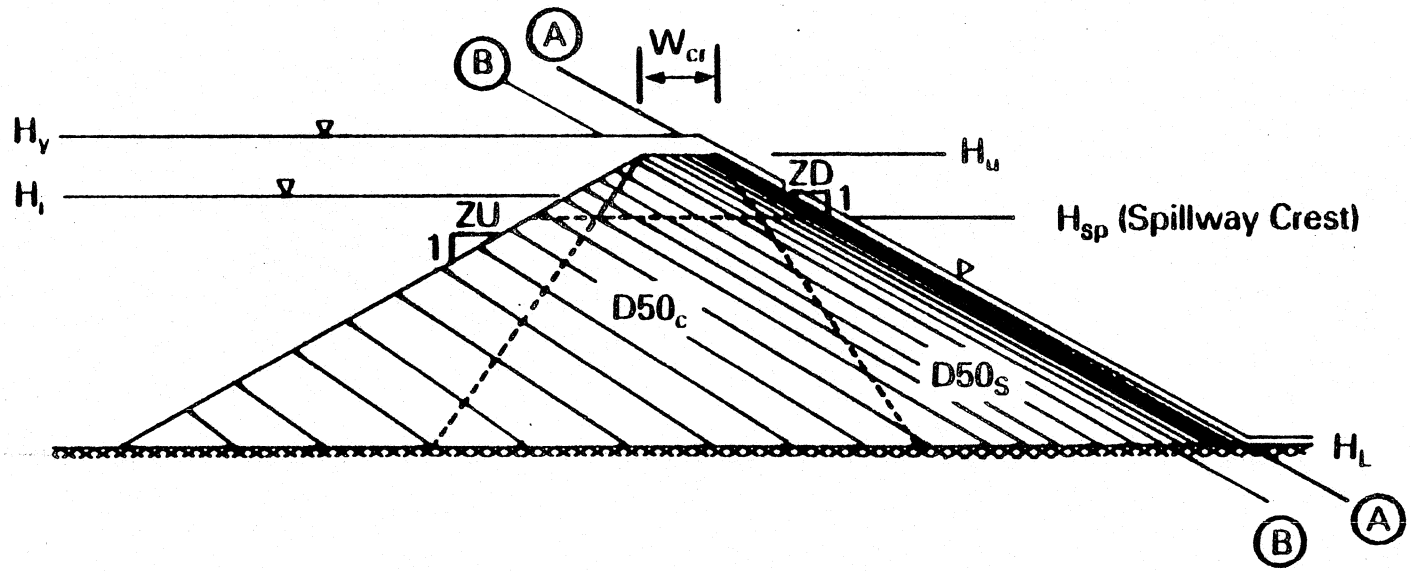

Figure 2. Side View of Dam Showing Conceptualized Overtopping Failure Sequence.

in which Q_b is the flow into the breach channel, B_o is the instantaneous width of the initially rectangular-shaped channel, and H_c is the elevation of the breach bottom. As the breach erodes into the downstream face of the dam, the breach bottom elevation (H_c) remains at the top of the dam (H_u), and the most upstream point of the breach channel moves across the crest of the dam towards the dam's upstream face. When the bottom of the erosion channel has attained the position of line B-B in Fig. 2, the breach bottom (H_c) starts to erode vertically downward. The breach bottom is allowed to progress downward until it reaches the bottom elevation of the dam (H_c) or in unusual circumstances to an elevation (H_m) that may be specified as lower than the bottom of the dam.

If the downstream face of the dam (line A-A in Fig. 2) has a grass cover, the velocity of the overtopping flow along the grassed downstream face is computed at each time step by the Manning equation. This velocity is compared with a specified maximum permissible velocity for grass-lined channels (see Chow, 1959). Failure of the downstream face via erosion is initiated at the time when the permissible velocity is exceeded. At that time a single rivulet having dimensions of one (ft) depth x two width is instantly created along the downstream face. Erosion within the rivulet is allowed to proceed as in the case where a grass cover does not exist. The velocity (v) along the downstream face is computed as follows:

$$q = 3(H-Hc)^{1.5} \tag{2}$$

$$y = \left[\frac{qn'}{1.49(1/ZD)^{0.5}}\right]^{0.6} \tag{3}$$

$$n' = aq^b \tag{4}$$

$$v = q/y \tag{5}$$

in which q is the overtopping flow per foot of crest length, (H-Hc) is the hydrostatic head (ft) over the crest, n' is the Manning coefficient for grass-lined channels (Chow, 1959), a and b are fitting coefficients required to represent in mathematical form the graphical curves given in Chow.

If a piping breach is simulated, the water level (H) in the reservoir must be greater than the assumed center-line elevation (H_p) of the initially rectangular-shaped piping channel before the size of the pipe starts to increase via erosion. The bottom of the pipe is eroded vertically downward while its top erodes at the same rate vertically upwards. The flow into the pipe is controlled by orifice flow, i.e.,

$$Q_b = A\left[2g(H-Hp)/(1 + fL/D)\right]^{0.5} \tag{6}$$

in which Q_b is the flow (cfs) through the pipe, g is the gravity acceleration constant, A is the cross-sectional area (ft^2) of the pipe channel, (H-Hp) is the hydrostatic head (ft) on the pipe, L is the length (ft) of the pipe channel, D is the diameter or width (ft) of the pipe, and f is the Darcy friction factor computed from the following mathematical representation of the Moody curves (Morris and Wiggert, 1972):

$$f = 64/N_R \quad \ldots\ldots\ldots\ldots N_R < 2000 \tag{7}$$

$$f = 0.105 \left(\frac{D_{50}}{D}\right)^{0.167} \quad \ldots\ldots N_R > 2000 \tag{8}$$

$$N_R = 83333\ Q_b\ D/A \tag{9}$$

in which f is the Darcy friction factor and N_R is the Reynolds number. As the top elevation (H_{pu}) of the pipe erodes vertically upward, a point is reached when the flow changes from orifice-control to weir-control. The transition is assumed to occur when the following inequality is satisfied:

$$H < H_{pu} + 2(H_{pu} - H_p) \tag{10}$$

The weir flow is then governed by Eq. (1) in which H_c is equivalent to the bottom elevation of the pipe and B_o is the width of the pipe at the instant of transition. Upon reaching the instant of flow transition from orifice to weir, the remaining material above the top of the pipe and below the top of the dam is assumed to collapse and is transported along the breach channel at the current rate of sediment transport before further erosion occurs. The erosion then proceeds to cut a channel parallel to and along the remaining portion of the downstream face of the dam between the elevation of the bottom of the pipe and the bottom of the dam. The remaining erosion process is quite similar to that described for the overtopping type of failure with the breach channel now in a position similar to line A-A in Fig. 2.

The preceding general description of the erosion process was for a man-made dam. If a landslide dam is simulated the process is identical except, due to the assumption that the landslide dam has no crest width (W_{cr}), the erosion initially commences with the breach channel in the position of line B-B in Fig. 2. A failure mode of overtopping or piping may be initiated for a landslide-formed dam.

Breach Width

The method of determining the width of the breach channel is a critical component of any breach model. In this model the width of the breach is dynamically controlled by two mechanisms. The first, assumes the breach has an initial rectangular shape as shown in Fig. 3. The width of the breach (B_o) is governed by the following relation

$$B_o = B_r\ y \tag{11}$$

in which B_r is a factor based on optimum channel hydraulic efficiency and y

is the depth of flow in the breach channel. The parameter B_r has a value of 2 for overtopping failures while for piping failures, B_r is set to 1.0. The model assumes that y is the critical depth at the entrance to the breach channel, i.e.,

$$y = 2/3(H-H_c). \tag{12}$$

The second mechanism controlling the breach width is derived from the stability of soil slopes (Spangler, 1951). The initial rectangular-shaped channel changes to a trapezoidal channel when the sides of the breach channel collapse, forming an angle (α) with the vertical. The collapse occurs when the depth of the breach cut (H_c') reaches the critical depth (H') which is a function of the dam's material properties of internal friction (ϕ), cohesion (C), and unit weight (γ), i.e.,

$$H_k' = \frac{4\ C \cos \phi \ \sin \theta_{k-1}'}{\gamma\ [1 - \cos\ (\theta_{k-1}' - \phi)]} \quad . \ . \ . \ k = 1,2,3 \tag{13}$$

in which the subscript k denotes one of three successive collapse conditions as shown in Fig. 3, and θ is the angle that the side of the breach channel makes with the horizontal as shown in Fig. 4. Thus, the angle (θ) or (α) at any time during the breach formation is given as follows:

$$\theta = \theta_{k-1}' \quad \ldots\ldots \quad H_k < H_k' \tag{14}$$

$$\theta = \theta_k' \quad \ldots\ldots \quad H_k > H_k' \tag{15}$$

$$B_o = B_r\ y \quad \ldots\ldots \quad k = 1 \tag{16}$$

$$B_o = B_{om} \quad \ldots\ldots \quad k > 1 \tag{17}$$

$$B_{om} = B_r\ y \quad \ldots\ldots \quad \text{when } H_1 = H_1' \tag{18}$$

$$\alpha = 0.5\pi - \theta \tag{19}$$

where:

$$\theta_o' = 0.5\pi \tag{20}$$

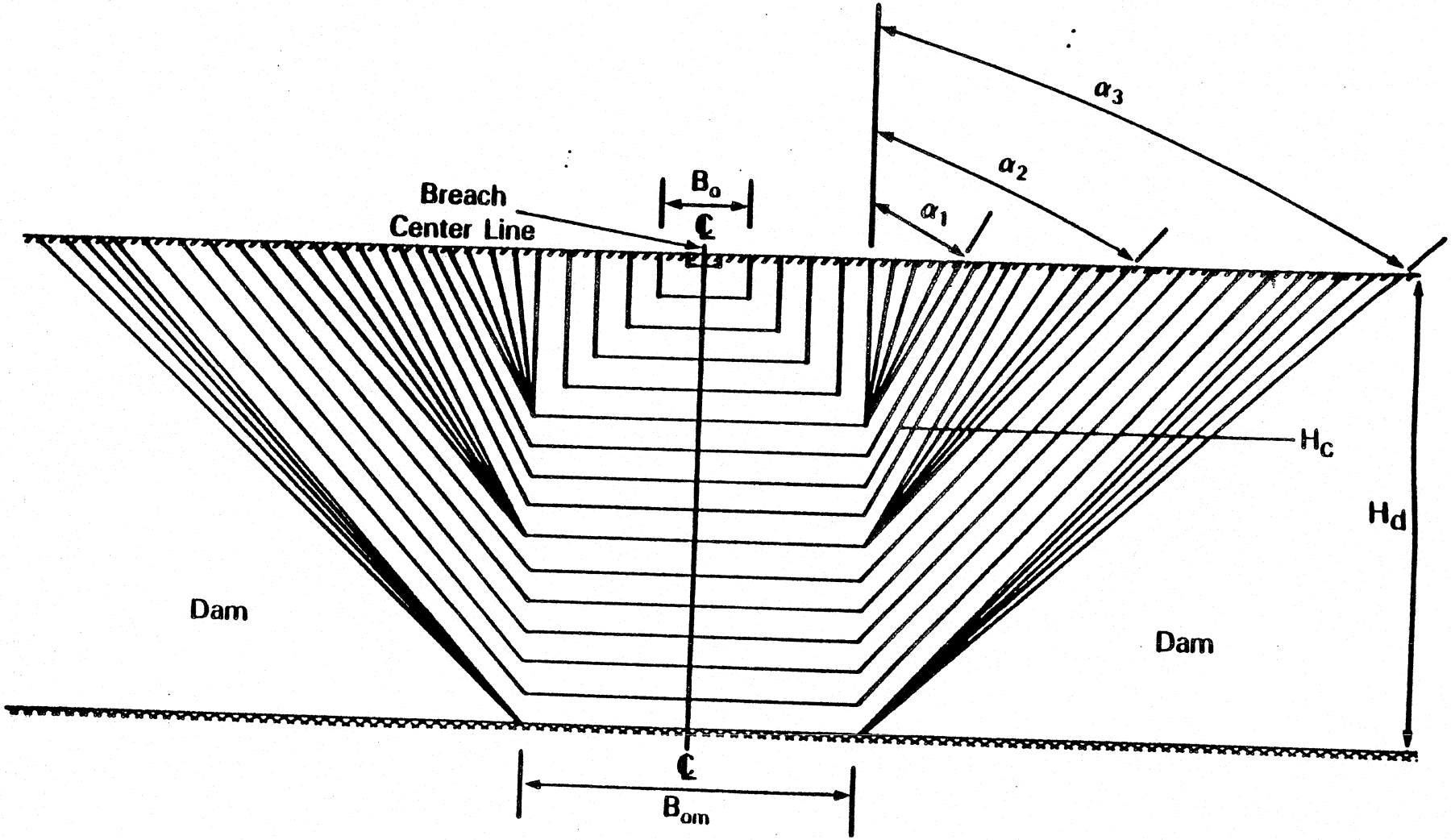

Figure 3. Front View of Dam with Breach Formation Sequence.

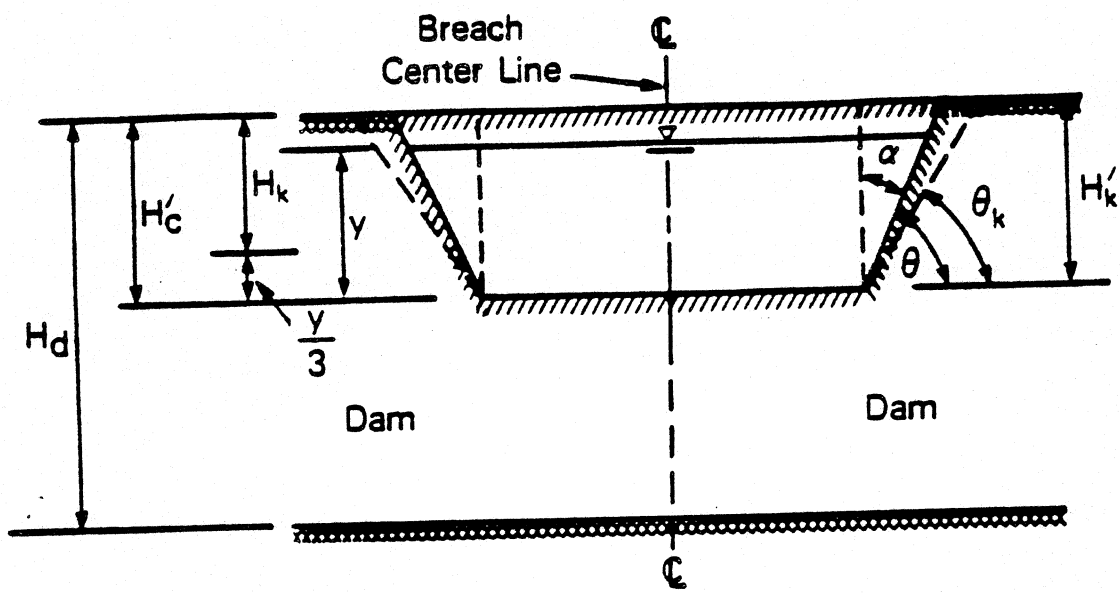

Figure 4. Front View of Dam with Breach.

$$A'_k = (A'_{k-1} + \phi)/2 \quad . \; . \; . \; . \; . \quad k = 1,2,3 \tag{21}$$

$$H_k = H'_c - y/3 \tag{22}$$

The subscript (k) is incremented by 1 at the instant when $H_k > H'_k$. In Eq. (22), the term (y/3) is subtracted from H'_c to give the actual free-standing depth of breach cut in which the supporting influence of the water on the stability of the sides of the breach is taken into account. Through this mechanism, it is possible for the breach to widen after the peak outflow through the breach has occurred since the flow depth (y) diminishes during the receding flow.

Erosion is assumed to occur equally along the bottom and sides of the breach channel except when the sides of the breach channel collapse. Thereupon the breach bottom is assumed not to continue to erode downward until the volume of collapsed material along the breach is removed at the rate of the sediment transport capacity of the breach channel at the instant of collapse. After this characteristically short pause, the breach bottom and sides continue to erode.

When landslide dams are simulated, the relatively long breach channel lengths compared to those of man-made dams suggest that the width for the channel be computed apart from the entrance width of the breach. In this case, y in Eq. (11), (16), (18), and (22) is computed as the normal uniform depth (y_n) in the breach channel rather than the critical depth given by Eq. (12). Equations for computing the normal channel depth are presented in a subsequent section.

Reservoir Level Determination

Conservation of mass is used to compute the change in the reservoir water surface elevation (H) due to the influence of reservoir inflow (Q_i), spillway outflow (Q_{sp}), crest overflow (Q_o), breach outflow (Q_b), and the reservoir storage characteristics. The conservation of mass over a time step (Δt) in hours is represented by the following:

$$\bar{Q}_i - (\bar{Q}_b + \bar{Q}_{sp} + \bar{Q}_o) = S_a \frac{\Delta H}{\Delta t} \frac{43560}{3600} \tag{23}$$

in which ΔH is the change in water surface elevation during the time interval (Δt), and S_a is the surface area in acres at elevation H. All flows are expressed in units of cfs and the bar (-) indicates the flow is averaged over the time step. Rearranging Eq. (23) yields the following expression for the change in the reservoir water surface:

$$\Delta H = \frac{0.0826 \Delta t}{S_a} (\bar{Q}_i - \bar{Q}_b - \bar{Q}_{sp} - \bar{Q}_o) \tag{24}$$

The reservoir elevation (H) at time (t) can easily be obtained from the relation,

$$H = H' + \Delta H \tag{25}$$

in which H' is the reservoir elevation at time $t-\Delta t$.

The reservoir inflow ($\bar{Q}_i$) is determined from the specified table of inflows (Q_i) vs. time (T_i). The spillway flow ($\bar{Q}_s$) is determined from the specified table of spillway flows (Q_s) vs. reservoir elevation (H). The breach flow (Q_b) is computed from Eq. (2) for piping flow. When the breach flow is weir-type, Eq. (1) is used when $H_c = H_u$; however, when $H_c < H_u$, the following broad-crested weir equation is used:

$$Q_b = 3\ B_o\ (H - H_c)^{1.5} + 2\ \tan(\alpha)\ (H - H_c)^{2.5} \tag{26}$$

in which B_o is given by Eq. (16) or Eq. (17) and α is given by Eq. (19). The crest overflow is computed as broad-crested weir flow from Eq. (1), where B_o is replaced by the crest length of the dam and H_c is replaced by H_u.

Breach Channel Hydraulics

The breach flow is assumed to be adequately described by quasi-steady uniform flow as determined by applying the Manning open channel flow equation at each Δt time step, i.e.,

$$Q_b = \frac{1.49\ S^{0.5}\ A^{1.67}}{n\ \ P^{0.67}} \tag{27}$$

in which S = 1/ZD, A is the channel cross-section area, P is the wetted perimeter of the channel, and n is the Manning coefficient. In this model, n is computed using the Strickler relation which is based on the average grain size of the material forming the breach channel, i.e.,

$$n = 0.013\ D_{50}^{\ 0.167} \tag{28}$$

in which D_{50} represents the average grain size diameter expressed in mm.

The use of quasi-steady uniform flow is considered appropriate because the extremely short reach of breach channel, very steep channel slopes (1/ZD) for man-made dams, and even in the case of landslide dams where the channel length is greater and the slope is smaller, contribute to produce extremely small variation in flow with distance along the breach channel. The use of quasi-steady uniform flow in contrast to the unsteady flow

equations as used by Ponce and Tsivoglou (1981) greatly simplifies the hydraulics and computational algorithm. Such simplification is considered commensurate with the other simplifications inherent in the treatment of the breach development in dams for which precise measurements of material properties are lacking or impossible to obtain and the wide variance which exists in such properties in many dams. The simplified hydraulics eliminates troublesome numerical computation problems and enables the breach model to require only minimal computational resources.

When the breach channel is rectangular, the following relations exist between depth of flow (y_n) and discharge (Q_b):

$$y_n = \left(\frac{Q_b\ n}{1.49\ B_o\ S^{0.5}}\right)^{0.6} \tag{29}$$

in which B_o is defined by Eqs. (16-18).

When the breach channel is trapezoidal, the following algorithm based on Newton-Raphson iteration is used to compute the depth of flow (y_n):

$$y_n^{k+1} = y_n^k - \frac{f(y_n^k)}{f'(y_n^k)} \tag{30}$$

$$f(y_n^k) = Q_b P^{0.67} - 1.49\ S^{0.5}\ A^{1.67} \tag{31}$$

in which

$$A = 0.5(B_o + B)\ y_n^k \tag{32}$$

$$B = B_{om} + y_n \tan(\alpha) \tag{33}$$

$$P = B_{om} + y_n/\cos(\alpha) \tag{34}$$

$$f'(y_n^k) = 0.67\ Q_b \frac{P'}{P^{1/3}} - 1.67\ \frac{1.49}{n} S^{0.5} B\ A^{0.67} \tag{35}$$

in which

$$P' = 1/\cos(\alpha). \tag{36}$$

The superscript (k) is an iteration counter; the iteration continues until

$$|y_n^{k+1} - y_n^k| < \varepsilon \qquad \varepsilon \leq 0.01 \tag{37}$$

The first estimate for y_n is obtained from the following:

$$y_n^1 = \left(\frac{Q_b n}{1.49\ \bar{B}\ S^{0.5}}\right)^{0.6} \tag{38}$$

where:

$$\bar{B} = 0.5(B_{om} + B') \tag{39}$$

in which B' is the breach channel top width at the water depth (y_n) at ($t-\Delta t$).

Sediment Transport

The rate at which the breach is eroded depends on the capacity of the flowing water to transport the eroded material. The Meyer-Peter and Muller sediment transport relation as modified by Smart (1984) for steep channels is used, i.e.,

$$Q_s = 3.64\ (D_{90}/D_{30})^{0.2}\ \frac{D^{2/3}}{n}\ S^{1.1}\ (DS-0.0054\ D_{50}\ \tau_c) \tag{40}$$

where:

$$\tau_c = a'\ \tau_c' \tag{41}$$

$$a' = \cos\Theta\ (1. - 1.54\tan\Theta) \tag{42}$$

$$\Theta = \tan^{-1} S \tag{43}$$

$$\tau_c' = 0.122/R^{*0.970} \quad \ldots\ldots\ldots\ldots\ldots R^* < 3 \tag{44}$$

$$\tau_c' = 0.056/R^{*0.266} \quad \ldots\ldots\ldots\ldots\ldots 3 < R^* < 10 \tag{45}$$

$$\tau_c' = 0.0205\ R^{*\ 0.173} \quad \ldots\ldots\ldots\ldots\ldots R^* > 10 \tag{46}$$

$$S = \frac{1}{ZD} \tag{47}$$

$$R^* = 1524\ D_{50}\ (DS)^{0.5} \tag{48}$$

in which Q_s is the sediment transport rate (cfs); D_{30}, D_{50}, D_{90} (mm) are grain sizes at which 30, 50, and 90 percent of the total weight is finer; D is the hydraulic depth of flow (ft), S is the slope of the downstream face of the dam; and τ_c' is the Shields' critical shear stress.

Breach Enlargement By Sudden Collapse

It is possible for the breach to be enlarged by a rather sudden collapse failure of the upper portions of dam in the vicinity of the breach development. Such a collapse would consist of a wedge-shaped portion of the

dam having a vertical dimension (Y_c) as shown in Fig. 5. The collapse would be due to the pressure of the water on the upstream face of the dam exceeding the resistive forces due to shear and cohesion which keep the wedge in place. When this occurs the wedge is pushed to the right in Fig. 6 and is then transported by the escaping water through the now enlarged breach. When collapse occurs, the erosion of the breach ceases until the volume of the collapsed wedge is transported through the breach channel at the transport rate of the water escaping through the suddenly enlarged breach. A check for collapse is made at each Δt time step during the simulation. The collapse check consists of assuming an initial value for Y_c of 10 and then summing the forces acting on the wedge of height, Y_c. The forces are those due to the water pressure (F_w) and the resisting forces which are the shear force (F_{sb}) acting along the bottom of the wedge, the shear force (F_{ss}) acting along both sides of the wedge, the force (F_{cb}) due to cohesion along the wedge bottom and (F_{cs}), the force due to cohesion acting along the sides of the wedge. Thus, collapse occurs if

$$F_w > F_{sb} + F_{ss} + F_{cb} + F_{cs} \tag{49}$$

where:

$$F_w = 0.5\ 62.4\ \bar{B}\ (Y_c + 2\ h_d) \tag{50}$$

$$F_{sb} = \tan\phi\left[(\gamma - 62.4)0.5\ ZU\ \bar{B}\ Y_c^2 + \gamma\ B\ W_{cc}\ Y_c + \right.$$

$$\left.\gamma\ 0.5\ ZD\ \bar{B}\ Y_c^{\ 2} + 0.67\ 62.4\ h_d\ W_{cc} \cdot B + 62.4\ ZD'\ B\ y_n\ Y_c\right] \tag{51}$$

$$F_{ss} = \gamma K \tan\phi\ Y_c^{\ 2}\left[W_{cc} + (ZU + ZD)Y_c\right] \tag{52}$$

$$F_{cb} = CB_o\left[W_{cc} + (ZU + ZD)\ Y_c\right] \tag{53}$$

$$F_{cs} = 2C\left[W_{cc} + (ZU + ZD)Y_c(B_o + 2Y_c/\cos\alpha)\right] \tag{54}$$

in which

$$K = (1 - \sin\phi)/(1 + \sin\phi) \tag{55}$$

$$\bar{B} = B_o + H_c \sin\alpha \tag{56}$$

$$ZD' = (1 + ZD^2)^{0.5} \tag{57}$$

and Y_c, h_d, ZU, ZD, Wcc, y_n are defined in Fig. 5. The top width (B) of the water surface in the breach channel is defined by Eq. (11) or Eq. (33), and α is defined in Fig. 4 and Eq. (19).

If the inequality of Eq. (49) is not satisfied with the first trial Y_c, then no collapse occurs at this time. If it is satisfied, Y_c is increased by 2 ft and Eq. (49) is again evaluated. This cycle continues until the inequality is not satisfied. Then the final value for Y_c is assumed to be Y_c-1.

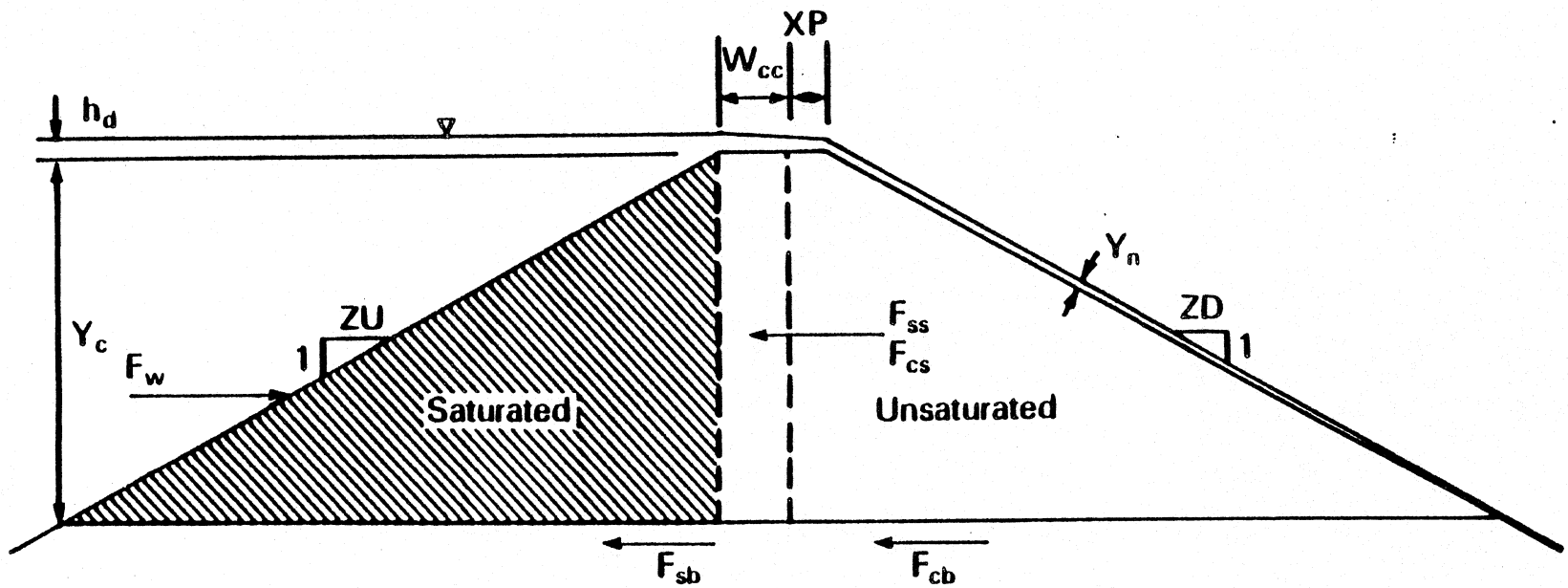

Figure 5. Side View of Dam Showing the Forces which Determine the Possible Collapse of the Upper Portion (Y_c) of the Dam.

Computational Algorithm

The sequence of computations in the model are iterative since the flow into the breach is dependent on the bottom elevation of the breach and its width while the breach properties are dependent on the sediment transport capacity of the breach flow, and the transport capacity is dependent on the breach size and flow. A simple iterative algorithm is used to account for the mutual dependence of the flow, erosion, and breach properties. An estimated incremental erosion depth ($\Delta H_c'$) is used at each time step to start the iterative computation. This estimated value can be extrapolated from previously computed incremental erosion depths after the first few time steps. The computational algorithm follows:

1. increment the time: $t = t' + \Delta t$;

2. compute H_c using estimated $\Delta H_c'$: $H_c = H_c' - \Delta H_c'$;

3. compute reservoir elevation: $H = H' + \Delta H'$, where $\Delta H'$ is an estimated incremental change in the reservoir elevation as obtained by extrapolation from previous changes and H' is the reservoir elevation at time (t');

4. compute $\bar{Q}_{sp}$, $\bar{Q}_i$, $\bar{Q}_o$ associated with elevation H;

5. compute ΔH from Eq. (24) using the previously computed breach flow (Q_b);

6. compute reservoir elevation: $H = H' + \Delta H$;

7. compute breach flow (Q_b) using Eq. (1), Eq. (2), or Eq. (26);

8. correct breach flow for downstream submergence:

   $Q_b = S_b Q_b$, where $S_b = 1.0 - \left(\frac{Y_t - H_c}{H - H_c} - 0.67\right)^3$ in which y_t is the tailwater depth due to the total outflow ($Q_b + Q_{sp} + Q_o$), and is computed from the Manning equation applied to the tailwater cross-section;

9. compute B_o, α, B, P, and R for the breach channel using Eqs. (16-19) 33-34);

10. compute sediment transport rate (Q_s) from Eq. (40);

11. compute ΔH_c as follows: $\Delta H_c = 3600\ \Delta t\ Q_s/[P_o\ L\ (1 - P_{or})]$

    in which L is the length of the breach channel which may be easily computed from the geometric relations shown in Fig. 2, P_{or} is the porosity of the breach material, and P_o is the total perimeter of the breach, $P_o = B_o + 2(H_u - H_c)/\cos\alpha$;

12. compute ΔH_c with the estimated value $\Delta H_c'$:

    if $100(\Delta H_c' - \Delta H_c)/\Delta H_c < E$, where E is an error tolerance in percent (an input to the model having a value between 0.1 and 1.0), then the solution for ΔH_c and the associated outflows Q_b, Q_s and Q_o are considered acceptable; if the above inequality is not satisfied step (2) is returned to with the recently computed ΔH_c replacing ΔH_c; this cycle is repeated until convergence is attained, usually within 1 or 2 iterations.

13. check for collapse;

14. extrapolate estimates for $\Delta H_c'$ and $\Delta H'$;

15. if t is less than the specified duration of the computation (t_e) return to step 1; and

16. plot the outflow hydrograph consisting of the total flow ($Q_b+Q_s+Q_o$) computed at each time step.

Computational Requirements

The basic time step (Δt) is specified; however when rapid erosion takes place the basic time step is automatically reduced to $\Delta t/20$. The specified value for the basic time step is usually about 0.02 hrs with slightly larger values acceptable for landslide dams. For typical applications, the BREACH model requires less than 10 seconds of CPU time on a Prime 750 computer and less than 2 seconds on an IBM 360/195 computer, both of which are main-frame computers. Although it has not been used on micro-computers, it would be quite amenable to such applications.

The model has displayed a lack of numerical instability or convergence problems. The computations show very little sensitivity to a reasonable variation in basic time step size. Numerical experimentation indicates that as the time step is increased by a factor of 4, the computed peak flow (Q_p), time of peak (T_p), and final breach dimensions vary by less than 10, 4, and 0.5 percent, respectively.

Comparison With Previous Models

The BREACH model differs from the models of Cristofano (1965) and Harris and Wagner (1967) in the following significant ways:

1) The sediment transport algorithm utilized, 2) the method used for changing the breach shape and width, 3) the delay in breach erosion downward until the downstream face has been sufficiently eroded, 4) the introduction of a possible collapse mechanism for breach enlargement, 5) the accomodation of a piping failure mode, and 6) the consideration of possible tailwater submergence effects on the breach flow. Similarities are their simplicity of the computational algorithm, the

use of the D_{50} grain size and internal friction angle (ϕ), and the assumption of quasi-steady uniform flow hydraulics.

The BREACH model differs from the model reported by Ponce and Tsivoglou (1981) in the following significant ways: 1) items 1,2,4,5, and 6 as stated above, 2) the much simpler computational algorithm used in BREACH, 3) the use of the internal friction angle, 4) the use of the D_{50} grain size for determining the Manning n and 5) consideration of spillway flows for man-made dams. Similarities between the two models include the gradual development of the breach channel along the downstream face of the dam prior to its erosion vertically through the dam's crest, the use of the Manning n for the breach channel hydraulics, and the way in which the reservoir hydraulics are included in the development of the breach.

MODEL APPLICATIONS

The BREACH model was applied to three earthen dams to determine the outflow hydrograph produced by a gradual breach of each. The first was an actual piping failure of the man-made Teton dam in Idaho, the second was an actual overtopping failure of the landslide-formed dam which blocked the Mantaro River in Peru, and the third was a hypothetical piping failure of the landslide dam which blocks the natural outlet of Spirit Lake near Mount St. Helens in Washington.

Teton Dam

The Teton Dam, a 300 ft high earthen dam with a 3000 ft long crest and 262 ft depth of stored water amounting to about 250,000 acre-ft, failed on June 5, 1976. According to a report by Ray, et. al (1976) the failure started as a piping failure about 10:00 AM and slowly increased the rate of outflow until about 12:00 noon when the portion of the dam above the piping hole collapsed and in the next few minutes (about 12 minutes according to Blanton (1977)) the breach became fully developed allowing an estimated 1.6 to 2.8 million cfs (best estimate of 2.3) peak flow (Brown and Rogers, 1977) to be discharged into the valley below. At the time of peak flow the breach was estimated from photographs to be trapezoidal shape having a top width at the original water surface elevation of about 500 ft and side slopes of about 1 vertical to 0.5 horizontal. After the peak outflow the outflow gradually decreased to a comparatively low flow in about five hours as the reservoir volume was depleted and the surface elevation receded. The downstream face of the dam had a slope of 1:2 and the upstream face 1:2.5. The crest width was 35 ft and the bulk of the breach material was a D_{50} size of 0.03 mm. The inflow to the reservoir during failure was insignificant and the reservoir surface area at time of failure was about 1950 acre-ft.

The BREACH model was applied to the piping generated failure of the Teton Dam. The centerline elevation for the piping breach was 160 ft above the bottom of the dam, and an initial width of 0.1 ft was used for the assumed square-shaped pipe. The material properties of the breach were assumed as follows: ϕ = 40 deg, C = 250 lb/ft^2, and γ = 100 lb/ft^3. The

Strickler equation was judged not to be applicable for the extremely fine breach material, and the n value was computed as 0.013 from a Darcy friction factor based on the D_{50} grain size and the Moody curves (Morris and Wiggert, 1972). The computed outflow hydrograph is shown in Fig. 6. The timing, shape, and magnitude of the hydrograph compares quite well with the estimated actual values. The computed peak outflow of 2.3 million cfs agrees with the best estimate made by the U.S. Geological Survey and the time of occurrence is also the same. The computed breach width of 460 ft agrees closely with the estimated value of 500 ft at the elevation of the initial reservoir water surface. A larger estimated actual breach width of 650 ft breach width was reported by Brown and Rogers (1977); however this was the final breach width after additional enlargement of the breach occurred. The (BREACH) model produced a final width of 560 ft when the reservoir water elevation has receded to near the reservoir bottom; the additional widening of the breach during the recession of the outflow is due to the influence of the depth (y) in Eq. (15)

Sensitivities of the peak breach outflow (Q_p), time of peak flow (T_p) and the top width (W) of the trapezoidal-shaped breach to variations in the specified breach material properties, cohesive strength (C) and internal friction angle (ϕ), are shown in Fig. 7. The dashed lines apply to the Teton simulation. Peak outflow is moderately affected by the cohesion; however it is sensitive to the ϕ value which mostly controls the enlargement of the breach width. Q_p is sensitive to a full range of ϕ values, however the ϕ value may vary by ± 10 degrees with less than 20% variation in Q_p. The breach width (W) was moderately sensitive to variations in the cohesion (C), and somewhat more sensitive to the ϕ value. The time to peak outflow (Tp) was almost insensitive to variations in C and ϕ.

Mantaro Landslide Dam

A massive landslide occurred in the valley of the Mantaro River in the mountaineous area of central Peru on April 25, 1974. The slide, with a volume of approximately 5.6×10^{10} ft^3, dammed the Mantaro River and formed a lake which reached a depth of about 560 ft before overtopping during the period June 6-8, 1974 (Lee and Duncan, 1975). The overtopping flow very gradually eroded a small channel along the approximately 1 mile long downstream face of the slide during the first two days of overtopping. Then a dramatic increase in the breach channel occurred during the next 6-10 hrs resulting in a final trapezoidal-shaped breach channel approximately 350 ft in depth, a top width of some 800 ft, and side slopes of about 1:1. The peak flow was estimated at 353,000 cfs as reported by Lee and Duncan (1975), although Ponce and Tsivoglou (1981) later reported an estimated value of 484,000 cfs. The breach did not erode down to the original river bed; this caused a rather large lake to remain after the breaching had subsided some 24 hrs after the peak had occurred. The slide material was mostly a mixture of silty sand with some clay resulting in a D_{50} size of about 11 mm with some material ranging in size up to 3 ft boulders.

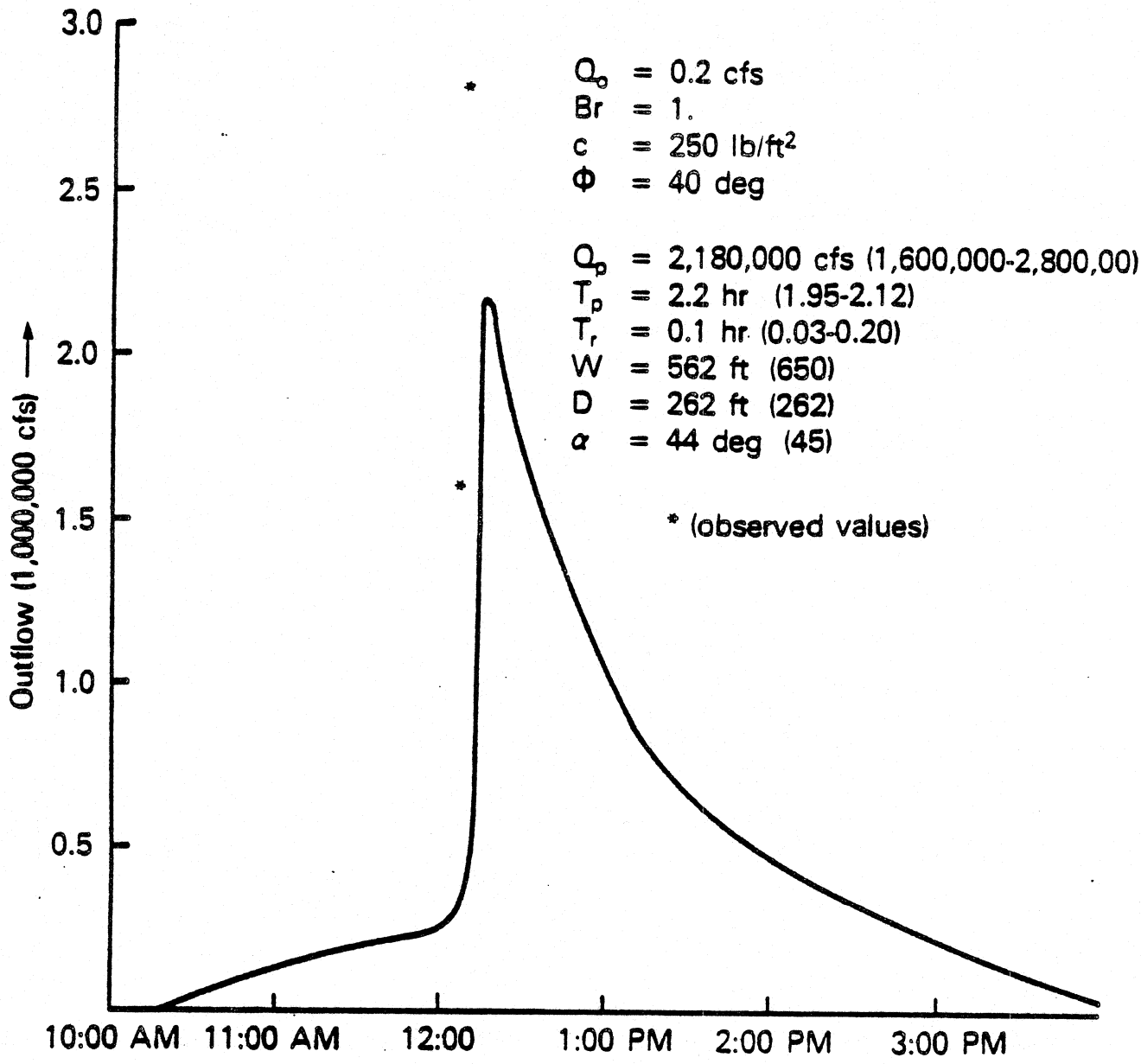

Figure 6. Teton Dam: Predicted and Observed Breach Outflow Hydrograph and Breach Properties.

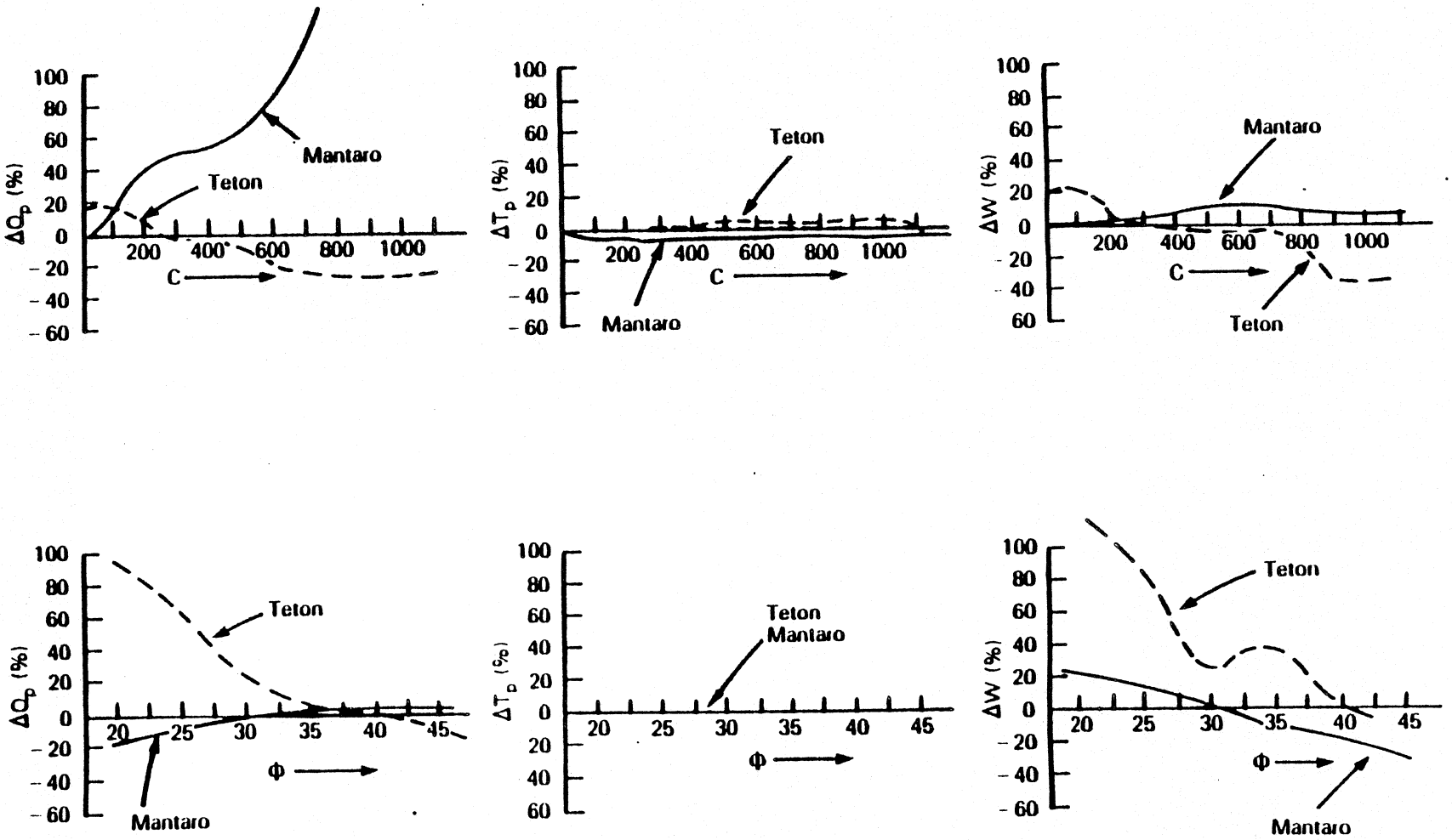

Figure 7. Sensitivity of Mantaro and Teton Predictions of Peak Outflow (Q_p), Time to Peak (T_p), and Breach Width (W) to Changes in the Material Properties of the Dam: Cohesion (C) and Internal Friction Angle (Φ).

The BREACH model was applied to the Mantaro landslide-formed dam using the following parameters: ZU = 17, ZD = 8.0, H_u = 560 ft, D_{50} = 11 mm, P_{or} = 0.5, S_a = 1200 acres, C = 30 lb/ft^2, ϕ = 30 deg, γ = 100 lb/ft^3 B_r = 2, and Δt = 0.1 hr. The Manning n was estimated by Eq. (28) as 0.020 and the initial breach depth was assumed to be 0.3 ft. The computed breach outflow is shown in Fig. 8 along with the estimated actual values. The timing of the peak outflow and its magnitude are very similar except for a somewhat more gradual rising limb of 10 hr compared to the estimated actual of 6 hr. The dimensions of the gorge eroded through the dam are similar as shown by the values of D, W, and α in Fig. 8.

The sensitivities of Q_p, T_p and W for variations in C and ϕ are shown in Fig. 7. The solid line denotes the Mantaro application. Most notably, Q_p is very sensitive to the cohesion (C) while much less sensitive to the internal friction angle (ϕ) . T_p is almost insensitive to the value of C and quite insensitive to ϕ. W is not very sensitive to C and moderately sensitive to ϕ; a variation of ± 10 degrees in ϕ results in a change in W of less than 20%.

Spirit Lake Blockage

The violent eruption of Mount St. Helens on May 18, 1980, in Washington, produced a massive debris avalanche which moved down the north side of the volcano depositing about 105 billion ft^3 of materials in the upper 17 miles of the North Fork of the Toutle River valley and blocking the former outlet channel of Spirit Lake with deposits of up to 500 ft deep (Swift and Kresch, 1983). Spirit Lake, itself was drastically changed by the avalanche; the existing lake has a maximum volume of 314,000 acre-ft at the elevation of 3475 msl when breaching of the debris blockage is anticipated. To avoid this the Corps of Engineers have installed temporary pumps to maintain the lake level at about elevation 3462 (275,000 acre-ft) and are expecting to complete in the near future a permanent outlet channel which will bypass the debris dam and maintain safe lake levels.

Greater than normal precipitation, failure of the pumping system, and/or addition of more avalanche material from another eruption of the volcano could cause the lake level to exceed elevation 3475 and possibly cause the debris dam to fail. Such a hypothetical breach was simulated using the BREACH model.

An initial piping failure was assumed to occur at elevation 3448. The following parameters were determined from physical considerations: H_u = 3475, H_p = 3448, H_ℓ = 3320, ZD = 30, ZU = 22, D_{50} = 7, n = 0.018 from Eq. (28), P_{or} = 0.32, γ = 100, ϕ = 35, C = 150, B_r = 1, an initial pipe of width 0.1 ft, and Δt = 0.20 hr. The simulated outflow hydrograph shown in Fig. 9 has a peak of about 550,000 cfs occurring 15 hrs after the start of failure. The time of rise (T_r) is about 2 hr. The final breach dimensions are: D = 155 ft, W = 420 ft, and α = 50 deg. Sensitivity tests indicate about a 20% variation in the peak flow may occur with expected variation in the internal friction angle and cohesion values. The predicted outflow

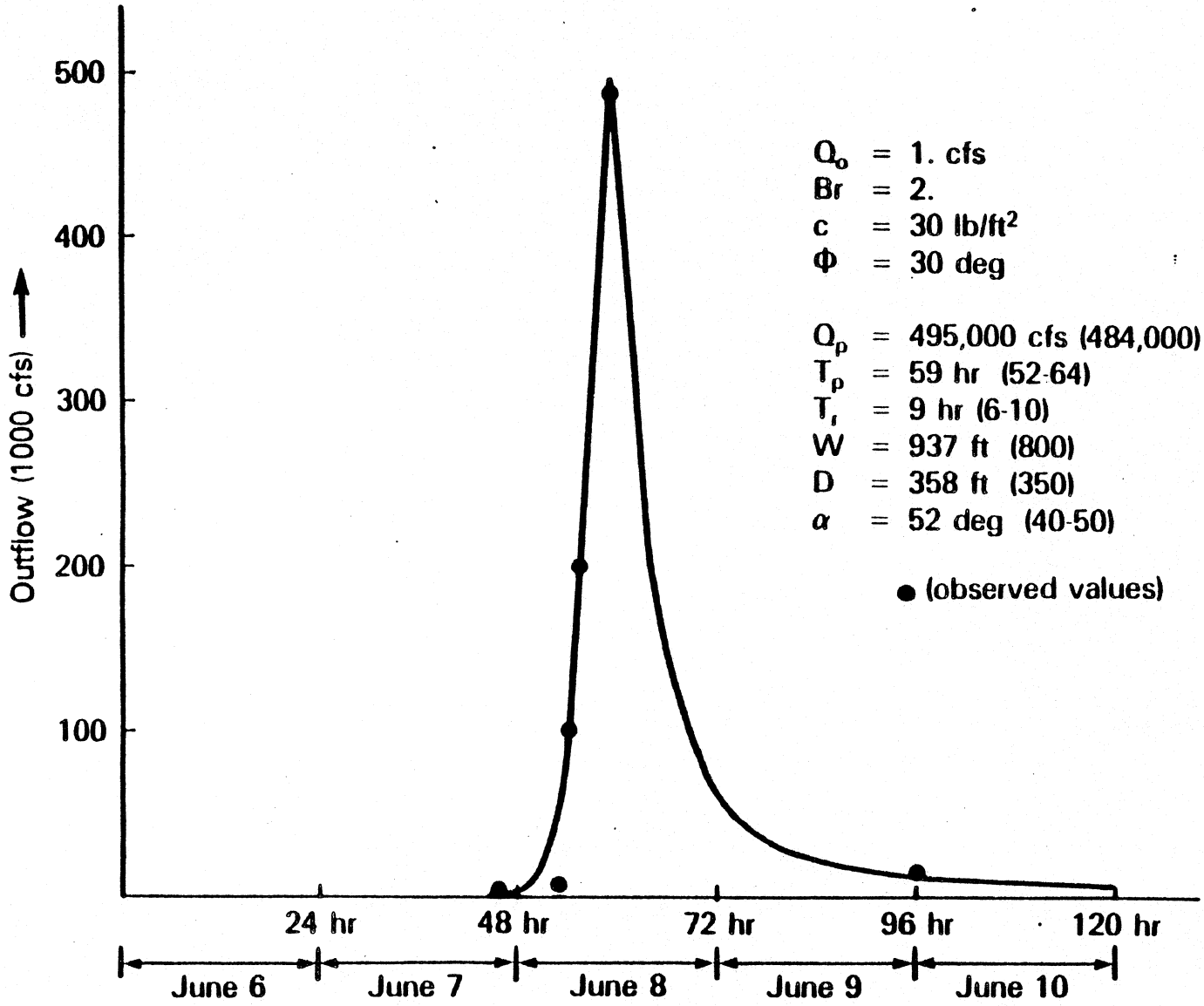

Figure 8. Mantaro Landslide Dam: Predicted and Observed Breach Outflow Hydrograph and Breach Properties.

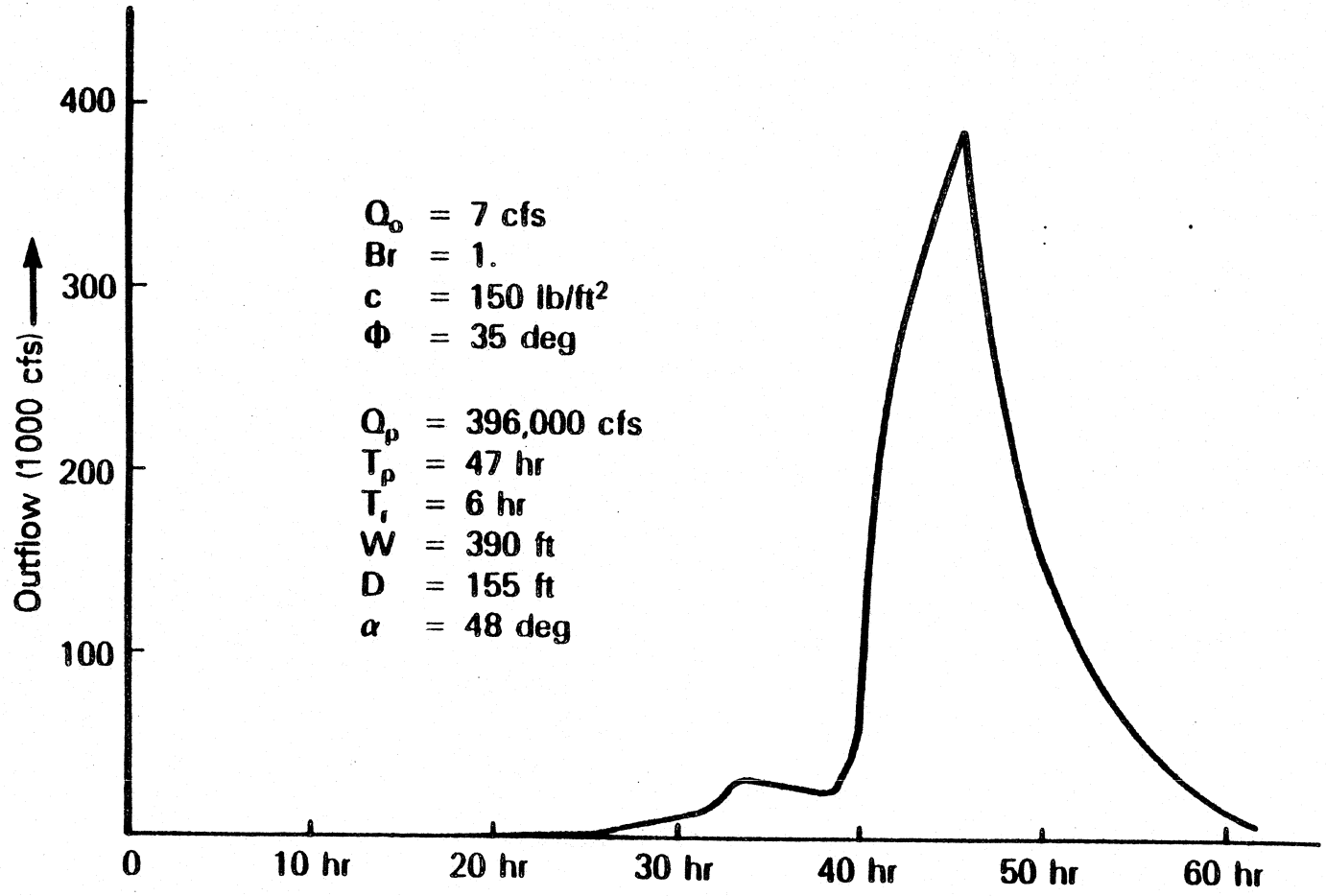

Figure 9. Spirit Lake Landslide Dam: Predicted Breach Outflow Hydrograph.

hydrograph from Spirit Lake was used in a hazard investigation of possible mud flows along the Toutle and Cowlitz Rivers by Swift and Kresch (1983).

SUMMARY

A breach erosion model (BREACH) based on principles of hydraulics, sediment transport, and soil mechanics is described. The model uses equations of weir or orifice flow to simulate the outflow entering a channel that is gradually eroded through an earthen man-made or landslide-formed dam. Conservation of reservoir inflow, storage volume, and outflow (crest overflow, spillway flow, and breach flow) determines the time-dependent reservoir water elevation which along with the predicted breach bottom elevation determines the head controlling the reservoir outflow. A sediment transport relation, the Meyer-Peter and Muller equation modified for steep channels is used to predict the transport capacity of the breach flow whose depth is determined by a quasi-steady uniform flow relation (the Manning equation applied at each Δt time step during the breach simulation). Breach enlargement is governed by the rate of erosion which is a function of the breach bottom slope and depth of flow and by the extent of collapse that occurs to the sides of the breach due to one or more sequential slope failures. The breach material properties (internal friction angle (ϕ) and cohesive strength (C)) are critical in determining the extent of enlargement of the trapezoidal-shaped breach. The Manning n used to compute the flow depth in the breach channel may be predicted on the basis of the grain size of the breach material by the Strickler equation or via the Moody relations. The dam may consist of three different materials, an inner core, an outer portion of the dam, and a thin layer along the downstream face of the dam. The latter is grass covered or of a grain size substantially larger than that of the outer portion of the dam. Piping or overtopping failure modes can be simulated as well as sudden collapses of sections of the breach due to excessive hydrostatic pressure. The model has the potential to determine if a breach will develop sufficiently during an overtopping of the dam to cause a catastrophic release of the reservoir's stored water. The BREACH model has a simple iterative computational structure which has well-behaved and efficient numerical properties. A few seconds of computer time is required for a typical application.

The model is tested on a man-made dam (Teton Dam) which failed by an initial piping which progressed to a weir type free surface breach. The predicted outflow hydrograph and breach size and shape compare favorably with estimated actual values. The predictions are somewhat sensitive to the value of the internal friction angle (ϕ) which was estimated from a grain size and qualitative description of the dam's material composition.

The model is also tested on the naturally formed landslide blockage of the Mantaro River in Peru which was overtopped and developed a large gorge which resulted in the gradual release of three-fourths of its stored water. The model predictions compared well with estimated observed values. The cohesive strength (C) is critical to the prediction of the rate of outflow of massive landslide dams; however if it is selected on the basis

of the breach material's properties, the results are within a reasonable range of variation.

It is considered that further testing of the model to assess its ability to predict overtopping failures of man-made dams is warranted and that its basic structure is suited to the resources (data and computational) which are commonly available to hydrologists/engineers during a detailed investigation of potential dam-failure flooding.

REFERENCES

Blanton, J.O. III. 1977. Flood plain inundation caused by dam failure. Proceedings of the Dam-Break Flood Routing Workshop. Water Resources Council, 47-64.

Brown, R.J., and D.C. Rogers. 1977. A simulation of the hydraulic events during and following the Teton Dam failure. Proceedings of the Dam-Break Flood Routing Workshop. Water Resources Council, 131-163.

Chow, V.T. 1959. Open-channel Hydraulics, McGraw-Hill Book Co., New York, pp. 179-188.

Cristofano, E.A. 1965. Method of computing erosion rate for failure of earthfill dams. United States Bureau of Reclamation, Denver, Colorado.

Fread, D.L. 1977. The development and testing of a dam-break flood forecasting model. Proceedings of the Dam-Break Flood Routing Workshop. Water Resources Council, 164-197.

Fread, D.L. 1980. Capabilities of NWS model to forecast flash floods caused by dam failures. Proceedings of the Second Conference on Flash Floods. American Meteorological Society, 171-178.

Fread, D.L. 1982. DAMBRK: The NWS dam-break flood forecasting model. Hydrologic Research Laboratory, National Weather Service, Silver Spring, MD., 56 p.

Fread, D.L. 1984. A breach erosion model for earthen dams. Proceedings of the Specialty Conference on "Delineation of Landslide, Flash Flood, and Debris Flow Hazards in Utah, 30 pp., Utah State Univ., Logan, Utah.

Harris, G.W. and Wagner, D.A. 1967. Outflow from breached earth dams. University of Utah, Salt Lake City, Utah.

Lee, K.L., and J.M. Duncan. 1975. Landslide of April 25, 1974 on the Mantaro River, Peru. National Academy of Sciences, Washington, D.C., 72 p.

Morris, H.M., and J.M. Wiggert. 1972. Applied Hydraulics in Engineering. The Ronald Press Co., New York, 69-70, 290, 451-452, 460.

Ponce, V.M., and A.J. Tsivoglou. 1981. Modeling of gradual dam-breaches, Journal of Hydraulics Division, American Society of Civil Engineers, 107(HY6):829-838.

Ray, H.A., L.C. Kjelstrom, E.G. Crosthwaite, and W.H. Low. 1976. The flood in southeastern Idaho from Teton Dam failure of June 5, 1976. Open File Report, U.S. Geological Survey, Boise, Idaho.

Smart, G.M. 1984. Sediment transport formula for Steep Channels. Journal of Hydraulics Division, American Society of Civil Engineers, 110(No. 3):267-276.

Spangler, M.G. 1951. Soil Engineering. International Textbook Co., Scranton, PA., 321-323.

Swift, C.H. III and D.L. Kresch. 1983. Mudflow hazards along the Toutle and Cowlitz Rivers from a hypothetical failure of Spirit Lake blockage. Water-Resources Investigations Report 82-4125, U.S. Geological Survey, Tacoma, Washington, 10 p.

APPENDIX A

INPUT DATA FOR BREACH EROSION MODEL (BREACH): VERSION 1/2/85

Card No.	Data Description and Input Form
(1)	MESSAGE - 20A4
	MESSAGE — Any message such as name of dam, message may be < 80 characters.
(2)	HI, HU, HL, HPI, HSP, - 5F10.2
	HI — Initial elevation (ft) of water surface in reservoir at t = 0.
	HU — Elevation of top of dam.
	HL — Elevation of bottom of dam (usually original stream-bed elevation).
	HPI — Elevation at which piping failure commences (if no piping failure is simulated, leave blank).
	HSP — Elevation of spillway crest (if no spillway, leave blank).
(3)	QIN(I) - 8F10.2
	QIN — Inflow (cfs) to reservoir. I subscript goes from 1 to 8. Inflow hydrograph may be defined with from 2 to 8 values.
(4)	TIN(I) - 8F10.2
	TIN(I) — Time (hrs) associated with QIN(I) reservoir inflow.
(5)	RSA(I) - 8F10.2
	RSA(I) — Surface area (acres) of reservoir. I subscript goes from 1 to 8. Surface area is defined at from 2 to 8 elevations starting at the highest elevation and proceeding to the reservoir bottom.
(6)	HSA(I) - 8F10.2
	HSA(I) — Elevation (ft) associated with RSA(I) surface area.

Card No.	Data Description and Input Format

(7) ZU, ZD, ZC, PORW, GL, GS, VMP - 7F10.2

ZU	Slope of upstream face of dam [1 (vertical) : ZU (horizontal)]
ZD	Slope of downstream face of dam (1 (vertical) : ZD (horizontal)]
ZC	Average slope of upstream and downstream faces of inner core of dam [1 (vertical) : ZC (horiz.)]. If no inner core, leave blank.
PORW	Ratio of total pore space of dam material which contains water (0.0 to 1.0)
GL	Average length of grass (inches). If no grass, leave blank.
GS	Condition of stand of grass. If good, GS=1.0; if poor stand or no grass exists, GS=0.0.
VMP	Maximum permissible velocity (ft/sec) for grass-lined channel before grass cover is eroded away. Can vary from 3 to 6 ft/sec. If no grass, leave blank.

(8) D50C, PORC, UWC, CNC, AFRC, COHC, UNFCC - 3F10.2, F10.4, 3F10.2

D50C	D50 (mm) grain size of inner core material (50% finer). If no core, leave blank.
PORC	Porosity ratio of inner core material. If no core, leave blank.
UWC	Unit weight (lb/ft^3) of inner core material. If no core, leave blank.
CNC	Manning n of inner core material. If left blank, it will be computed from the Strickler Equation which is a function of the grain size. If a value greater than 0.99 is entered, it will be computed from a Moody diagram (Darcy f vs. D50 relationship). If no core, leave blank.
AFRC	Internal friction angle (degree) of inner core material. If no core, leave blank.
COHC	Cohesive strength (lb/ft^2) of inner core material. If no core, leave blank.
UNFCC	Ratio of D90 to D30 grain sizes of inner core material. If no core, leave blank. If core exists and left blank, default value is 10.

Card No.	Data Description and Input Format

(9) D50S, PORS, UWS, CNS, AFRS, COHS, UNFCS - 3F10.2, F10.4, 3F10.2

D50S	D50(mm) of outer material of dam (50% finer).
PORS	Porosity ratio of outer material.
UWS	Unit weight (lb/ft^3) of outer material.
CNS	Manning n of outer material. If left blank, it will be computed from the Strickler Equation which is a function of the grain size. If a value greater than 0.99 is entered, it will be computed from a Moody diagram (Darcy f vs. D50 relationship).
AFRS	Internal friction angle (degree) of outer material.
COHS	Cohesive strength (lb/ft^2) of outer material.
UNFCS	Ratio of D90 to D30 grain size of outer material. If left blank, default value is 10.

Note: If dam material is homogeneous, use the outer layer to represent the entire homogenous dam material.

(10) BR, WC, CRL, SM, WV, CNV, D50DF, UNFCDF - 5F10.2, F10.4

BR	Ratio of breach width to flow depth for initial rectangular-shaped breach. Range of values are: $1 < B_r < 2$. Usually use 2.0 for overtopping failure and 1.0 for a piping failure. If left blank, BR = 2.
WC	Width (ft) of crest of dam (can be zero).
CRL	Length (ft) of crest of dam.
SM	Bottom slope (ft/mile) of downstream river for first few thousand feet below the dam.
WV	Width (ft) of valley for which SM is applicable.
CNV	Manning n of valley for which SM is applicable.
D50DF	D50 (mm) grain size of material composing the top one-foot of the downstream face of the dam. If left blank, D50DF=D50S.
UNFCDF	Ratio of D90 to D30 grain size of material of downstream face. If left blank, UNFCDF=3.0 when D50DF>0.0, or UNFCDF=UNFCS when D50DF=0.0.

Card No.	Data Description and Input Format

(11) DTH, DBG, H, TEH, ERR, FPT - 2F10.3, 4F10.2

DTH	Basic time step size (hr). 0.02 < DTH < 0.20, lower values for man-made dams, larger values for large landslide dams. If left blank, DTH = 0.05.
DBG	Output control parameter. DBG = 0.0, minimal output of discharge hydrograph only. DBG = 0.001, output at each time step + hydrograph. DBG = 0.002, output at each iteration of each time step + hydrograph. DBG = 0.003, maximum output.
H	Initial depth (ft) of breach along the downstream face of dam for overtopping failure. Initial width of piping breach. Usually, 0.1 < H < 1.0. If left blank, H = 0.10.
TEH	Duration (hrs) of simulation.
ERR	Error tolerance in iterative solution, expressed as a percentage ratio (0.1 < ERR < 1.0). If left blank, ERR = 0.10.
FPT	Interval of time steps at which computed discharges are plotted. (1. < FPT < 10.) If left blank, FPT = 1.0.

Note: Omit cards no. (12) and (13) if spillway crest elev., HSP, (card no. 2) is blank or zero.

(12) SPQ(I) - 8F10.2

SPQ(I)	Spillway flow (cfs). I subscript goes from 1 to 8. Spillway flow is defined for from 2 to 8 elevations starting at the spillway crest elev. and proceeding upwards until maximum spillway discharge is specified.

(13) SPH(I) - 8F10.2

SPH(I)	Elevation (ft) associated with SPQ(I) spillway flow.

OUTPUT PARAMETERS FOR "BREACH" MODEL ,VERSION 7/2/84

I	COUNTER
T	TIME,HR
DTH	TIME STEP,HR
KG	CODE FOR REGION OF FAILURE : 1 EROSION OF DOWNSTREAM FACE 2 EROSION OF UPSTREAM FACE 3 DRAINING OF RESERVOIR WITH BREACH SIZE FIXED AT MAX DIMENSIONS 4 PIPING MODE 5 COLLAPSE MODE
KC	COLLAPSE HEIGHT
QTOT	TOTAL OUTFLOW,CFS
QTS	SPILLWAY OUTFLOW,CFS
QB	BREACH OUTFLOW,CFS
SUB	SUBMERGENCE CORRECTION FACTOR
BT	TOP WIDTH OF BREACH,FT
HY	ELEV OF RESERVOIR WATER SURFACE,FT
HC	ELEV OF BOTTOM OF BREACH,FT
BO	BOTTOM WIDTH OF BREACH,FT
PPP	PIPING LENGTH(FT) WHEN KG=4; MAX DEPTH ALLOWABLE PRIOR TO SIDE SLOPE FAILURE WHEN KG=2; REMAINING CREST WIDTH (FT) TO BE ERODED WHEN KG=1
HP	TOP OF PIPING BREACH OR DEPTH OF BREACH,FT
YN	NORMAL DEPTH OF FLOW IN BREACH CHANNEL,FT
DH	ESTIMATED EROSION DEPTH(FT) DURING TIME STEP
DHH	COMPUTED EROSION DEPTH(FT) DURING TIME STEP
KIT	ITERATION COUNTER
TH	ACUTE ANGLE(DEG) THAT BREACH SIDE MAKES WITH VERTICAL

OTHER OUTPUT CONSISTS OF A HYDROGRAPH OF TOTAL OUTFLOW

THE FOLLOWING SUMMARY INFORMATION IS ALSO PRINTED OUT:

TF	TIME(HR) AT WHICH FAILURE MODE 2 STARTS
QTF	FLOW(CFS) AT TIME TF
TP	TIME(HR) AT WHICH PEAK OUTFLOW OCCURS
QP	MAX OUTFLOW(CFS) OCCURRING AT TIME TP
TRS	DURATION(HR) OF RISING LIMB OF HYDROGRAPH
TB	TIME(HR) AT WHICH SIGNIFICANT RISE IN OUTFLOW STARTS
TRSB	TP-TB
BRD	FINAL DEPTH(FT) OF BREACH
BRW	FINAL TOP WIDTH(FT) OF BREACH
HU	ELEV (FT) OF TOP OF DAM
HY	FINAL ELEV (FT) OF RESERVOIR WATER SURFACE
HC	FINAL ELEV (FT) OF BOTTOM OF BREACH
THETA	FINAL ACUTE ANGLE THAT BREACH SIDE MAKES WITH VERTICAL
QO	OUTFLOW (CFS) AT T=0.0
YNM	MAX NORMAL FLOW DEPTH (FT) IN BREACH CHANNEL
HMC	MAX CRITICAL FLOW DEPTH (FT) IN BREACH CHANNEL
DTC	DURATION (HR) TO REMOVE COLLAPSED MATERIAL
Z	FINAL SIDE SLOPE OF BREACH (FT/FT)
TFH	TIME OF FAILURE (HR) WHICH IS SAME AS TRS
BO	BOTTOM WIDTH (FT) OF BREACH

NWS Dynamic Wave Operational Model

DWOPER

DWOPER APPLICATIONS

1.* FLAT RIVERS HYDRAULIC SLOPE < 5 ft/mi
NAVIGABLE RIVERS

2.* RIVERS OR ESTUARIES SUBJECT TO TIDES
COLUMBIA

3.* RIVERS OR ESTUARIES SUBJECT TO HURRICANE
STORM SURGES OR TSUNAMI WAVES
MISSISSIPPI - EAST COAST & GULF COAST RIVERS

4. RIVERS WITH TRIBUTARIES WITH MUTUAL BACKWATER
EFFECTS

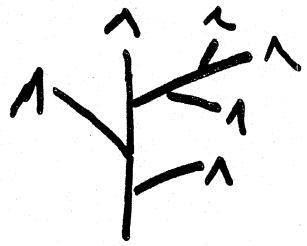

5. RIVERS or Canals WITH LOW DAMS WITH GATE CONTROLLED
POOL ELEVATION OHIO — MISSISSIPPI

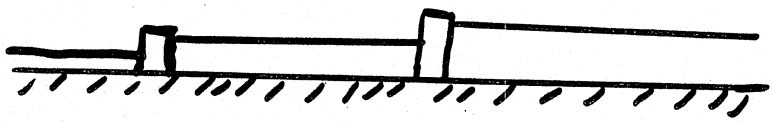

6. FLAT RIVERS WITH IMPORTANT LATERAL INFLOWS

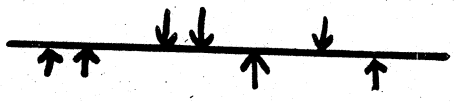

7. RIVERS SUBJECT TO LEVEE OVERTOPPING

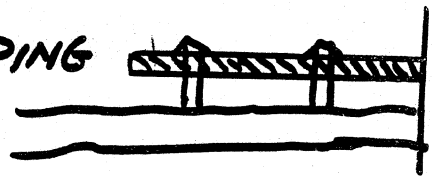

8. COMPLEX RIVER SYSTEMS
ST. JOHN RIVER SYSTEM
RED-OUACHITA-ATCHAFALAYA-MISSISSIPPI SYSTEM

CONT'D.

DWOPER APPLICATIONS — CONT'D.

9.* RESERVOIRS SUBJECT TO WAVES DUE TO RAPID CHANGES IN GATE SETTINGS OR CONTROLS

10. RESERVOIRS WITH SIGNIFICANT BRANCHED INLETS SUBJECT TO LARGE FLOOD WAVES, LAND SLIDE GENERATED WAVES, DAM FAILURES

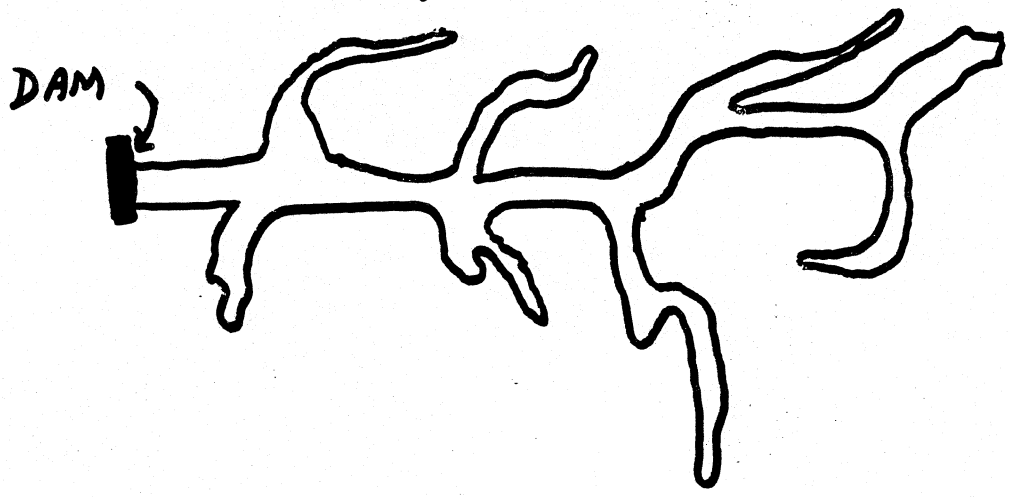

11. FLOW ROUTING DOWNSTREAM OF DAMS WHERE RAPID RELEASES OCCUR DUE TO RESERVOIR OPERATIONS (POWER SURGES AND FLOOD CONTROL RELEASE) OR DAM FAILURE

12.* ANY FLOW ROUTING WHERE HYDRAULIC INFO (ELEV., FLOW, VELOCITIES) ARE REQUIRED AT FREQUENT LOCATIONS FOR ACCURATE STAGE PROFILE DELINEATION

13* PROVIDE HYDRAULIC INFO AT FREQUENT LOCATIONS AS REQUIRED BY OTHER MODELS (e.g., SEDIMENT TRANSPORT, CHEMICAL TRANSPORT, TEMPERATURE TRANSPORT)

* MOST UNSTEADY FLOW MODELS BASED ON ST. VENANT EQUATIONS ARE ALSO APPLICABLE

DWOPER Review

Complete 1-D St. Venant Eqs. (Dynamic Routing)

Conservation Form of Eqs.

* Diffusion Routing Option

4-Pt. Nonlinear Finite Difference (Implicit) Solution

Newton-Raphson Iteration with Extrapolation

Automatic Numerical Fix-up via Δt and/or θ

Unequal Δx

Upstream Boundary: $h(t)$ or $Q(t)$

Downstream Boundary: $h(t)$ $Q(t)$ or $Q(h)$ → Rating Loop Rating

* Initial Conditions: 1) Specified Q and h
2) Steady Flow Q; h computed via a backwater solution

* Manning n : $n(Q)$ or $n(h)$, and $n(x)$

Lateral Inflow/Outflow : Specified $q(t)$

Cross Sections : Tabular $B(h)$

Expansion-Contraction Loss

Off-channel (Dead) Storage

DWOPER Review

- Single River

* Multiple Rivers (1st order Dendritic)

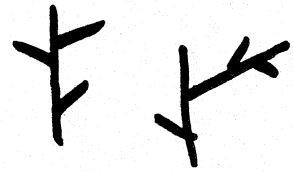

* Levee Overtopping (Failure)

* Automatic Calibration: Unsteady Flow
$n = f(x, h \text{ or } Q)$

* Plot of $Q(t)$ or $h(t)$

- Selective Print-Output

Central Core (IBM): < 250 K

CPU $\frac{\text{sec}}{\Delta x \, \Delta t} \approx 0.004$

* Variable Dimension Array Coding

HRL Supported, Documented, Training Seminars

-

Special Features of DW OPER :

1. River Systems

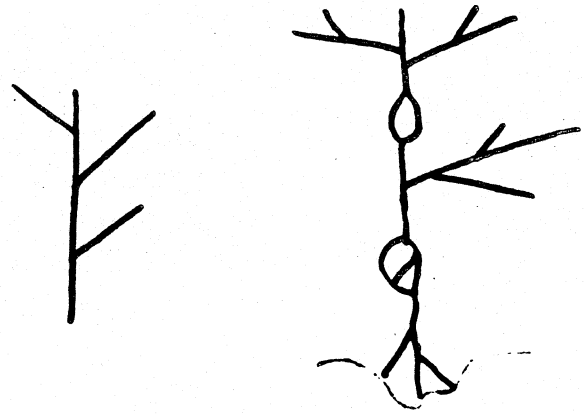

2. Levee Overtopping/Failure

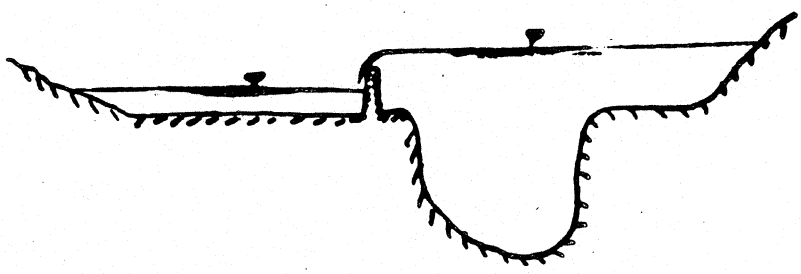

3. Automatic Calibration of n

$$n = f(x, h \text{ or } Q)$$

RIVER SYSTEM : TRIBUTARY ALGORITHM

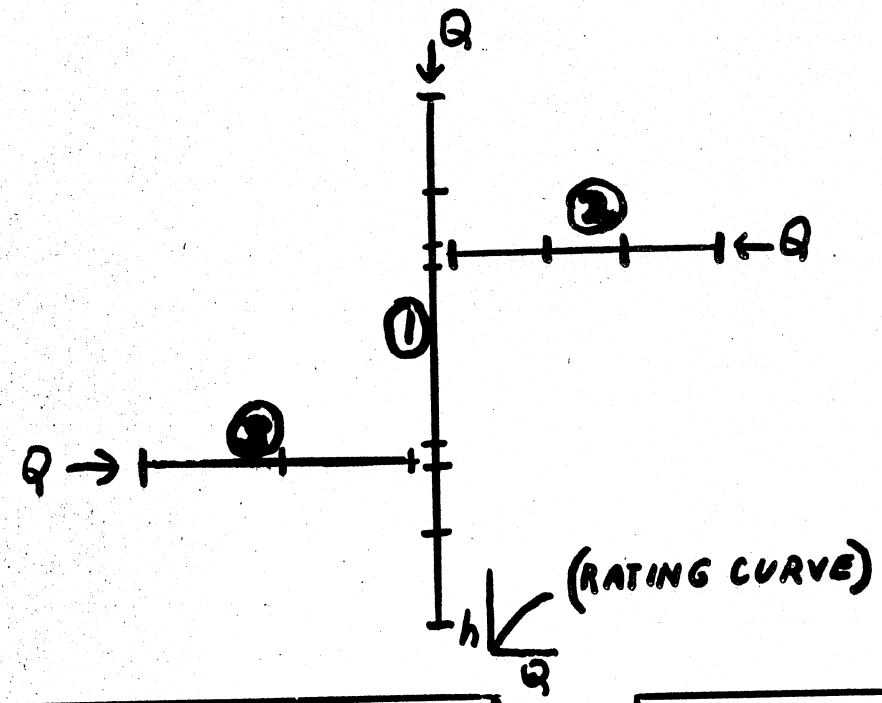

NOTATION:

- Q - BOUNDARY CONDITION
- ΔX - WIDTH AT TRIBUTARY
- Q_L - LATERAL INFLOW FROM TRIBUTARY ALONG ΔX
- Q_e - ESTIMATED Q_L
- h_e - COMPUTED h AT TRIBUTARY JUNCTION
- Q_c - COMPUTED FLOW AT DOWNSTREAM BOUNDARY OF TRIBUTARY
- E - CONVERGENCE TOLERANCE CRITERION
- α - WEIGHTING COEFFICIENT

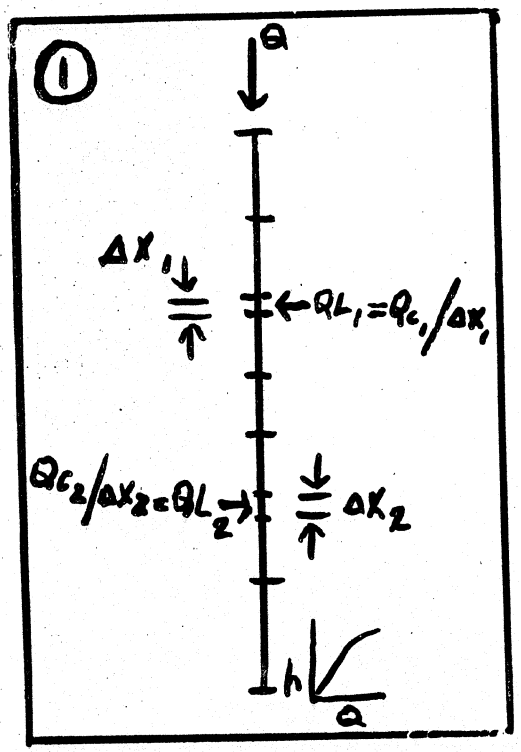

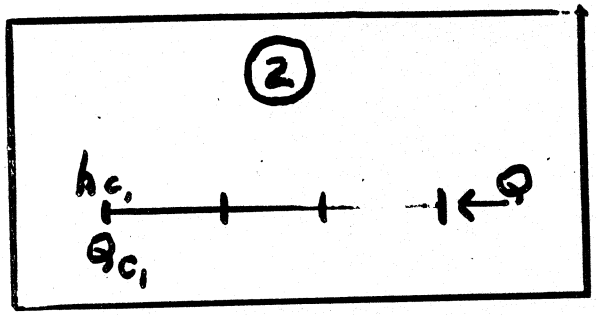

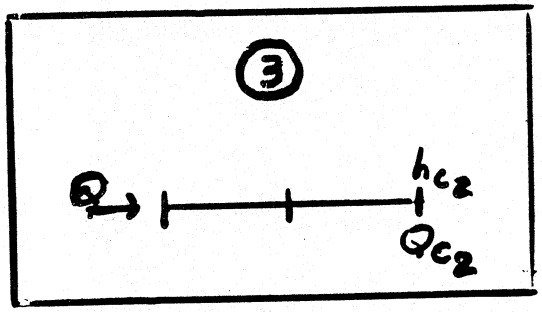

IF: $|Q_{c_1} - Q_{L_1}| > E_Q$ OR $|Q_{c_2} - Q_{L_2}| > E_Q$

REPEAT 1, 2, AND 3

WHERE:

$$\left.\begin{aligned} Q_{e_1} &= \alpha Q_{c_1} + (1-\alpha) Q_{e_1} \\ Q_{e_2} &= \alpha Q_{c_1} + (1-\alpha) Q_{e_1} \end{aligned}\right\} \frac{1}{2} \le \alpha \le 1.$$

(3) LEVEE EFFECTS

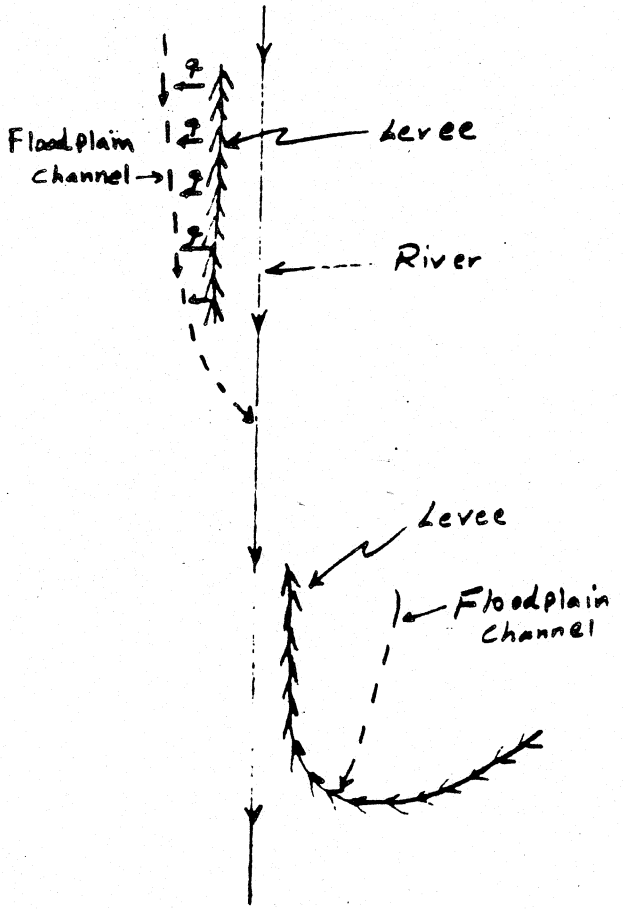

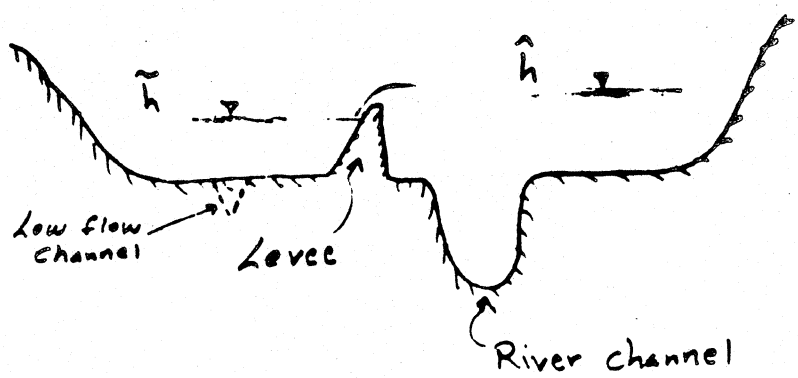

$$q_{\ell e_i} = S_g \, C_{\ell e_i} \, K_{\ell e_i} \, (\hat{h} - h_{\ell e_i})^{3/2} \qquad \ldots\ldots \hat{h} > h_{\ell e_i}$$

where: $$S_g = \frac{(\tilde{h} - \hat{h})}{|\tilde{h} - \hat{h}|}$$

$$K_{\ell e_i} = 1. - 27.8\,(\gamma - 0.67)^3 \quad \ldots\ldots \gamma > 0.67$$

$$\gamma = \frac{\tilde{h} - h_{\ell e_i}}{\hat{h} - h_{\ell e_i}}$$

$$2.6 < C_{\ell e_i} < 3.2$$

AUTOMATIC CALIBRATION THEORY

RIVER SYSTEM :

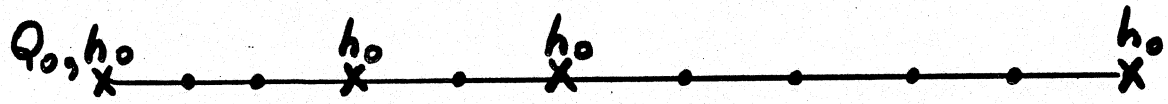

DECOMPOSITION OF SYSTEM :

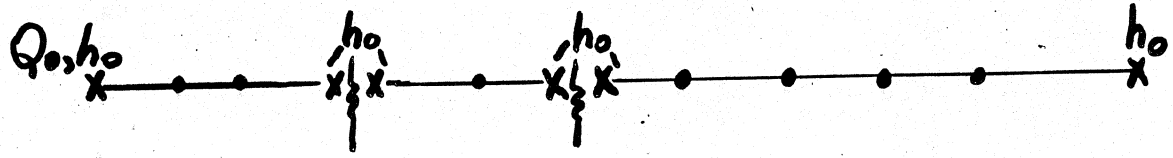

OPTIMAL SOLUTION OF DECOMPOSED SYSTEM:

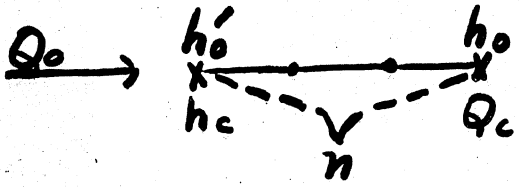

minimize $\left[\sum_{i=1}^{m} (h_c - h_o')_i = f(n(\bar{Q}))\right]$

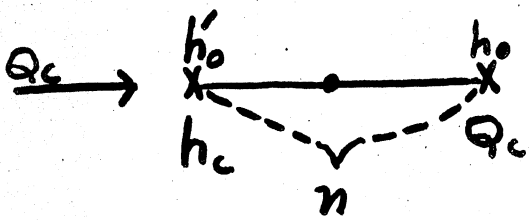

minimize $\left[\sum_{i=1}^{m} (h_c - h_o')_i = f(n(\bar{Q}))\right]$

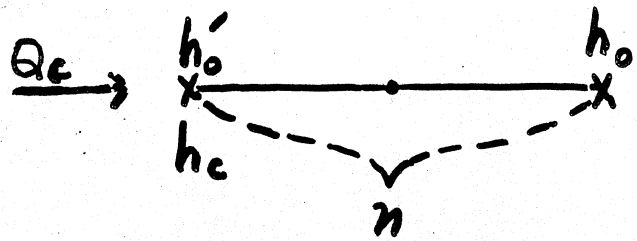

minimize $\left[\sum_{i=1}^{m} (h_c - h_o')_i = f(n(\bar{Q}))\right]$

AUTOMATIC CALIBRATION THEORY

RIVER SYSTEM :

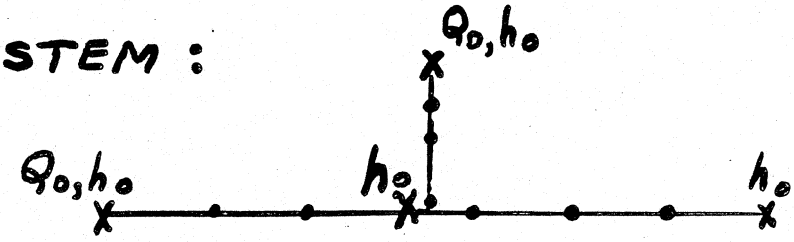

DECOMPOSITION :

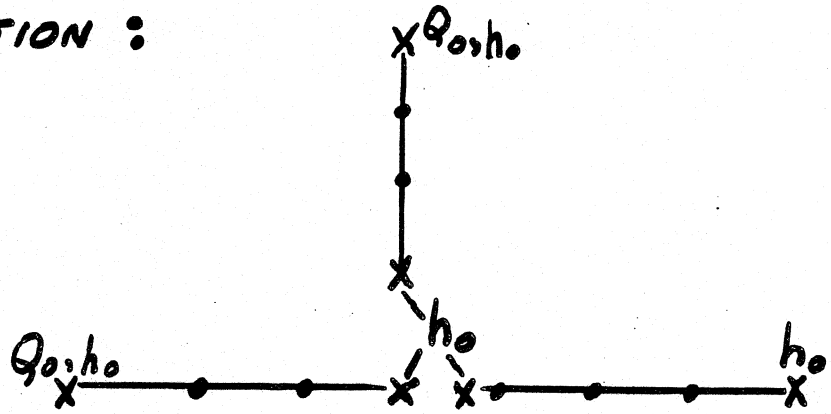

OPTIMAL SOLUTION :

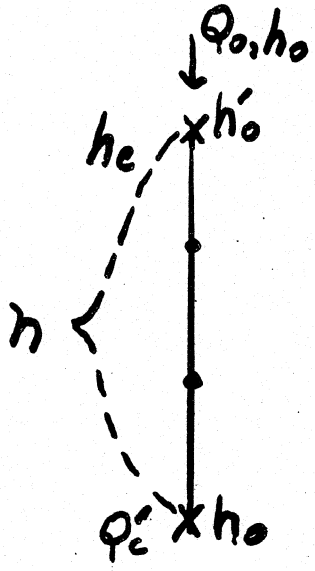

$$\text{minimize}\left[\sum_{i=1}^{m}(h_c-h_o')_i = f(n(\bar{Q}))\right]$$

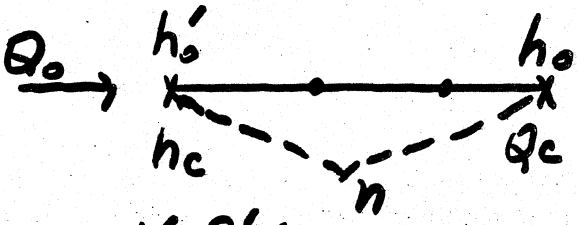

$$\text{minimize}\left[\sum_{i=1}^{m}(h_c-h_o')_i = f(n(\bar{Q}))\right]$$

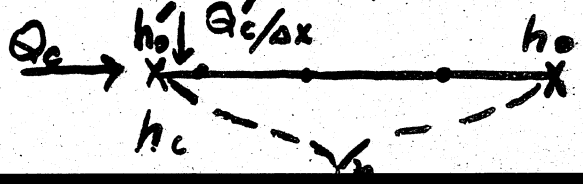

$$\text{minimize}\left[\sum_{i=1}^{m}(h_c-h_o')_i = f(n(\bar{Q}))\right]$$

OPTIMIZATION ALGORITHM FOR AUTOMATIC CALIBRATION PROGRAM

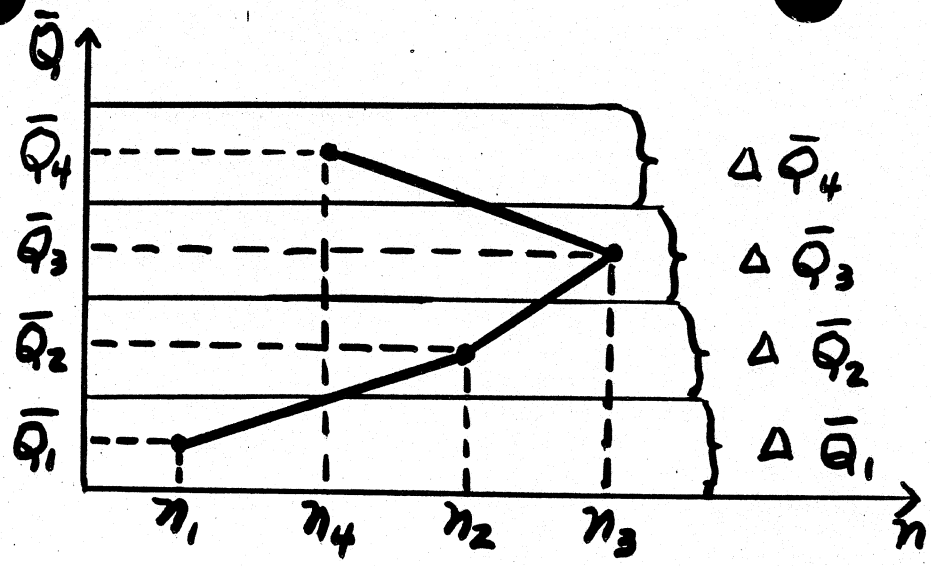

$$\left\langle \text{minimize}\left[\sum_{i=1}^{m}(h_c-h_o)_i = f(h(\bar{Q}))\right]\right\rangle$$

LET: $\sigma_\ell^K = \sum_{i=1}^{m}(h_c-h_o)_i$ WHERE: ℓ DENOTES LEVEL OF $\bar{Q}$ AND $\Delta\bar{Q}$

K DENOTES INTERATION LEVEL IN OPTIMIZATION OF σ

NEWTON-RAPHSON INTERATION ALGORITHM:

$$n_\ell^{K+1} = n_\ell^K - \frac{\sigma_\ell^K}{\dfrac{d(\sigma_\ell)}{d(n_\ell)}}$$

$$\downarrow$$

$$n_\ell^{K+1} = n_\ell^K - \frac{\sigma_\ell^K}{\dfrac{(\sigma_\ell^K-\sigma_\ell^{K-1})}{(n_\ell^K-n_\ell^{K-1})}}$$

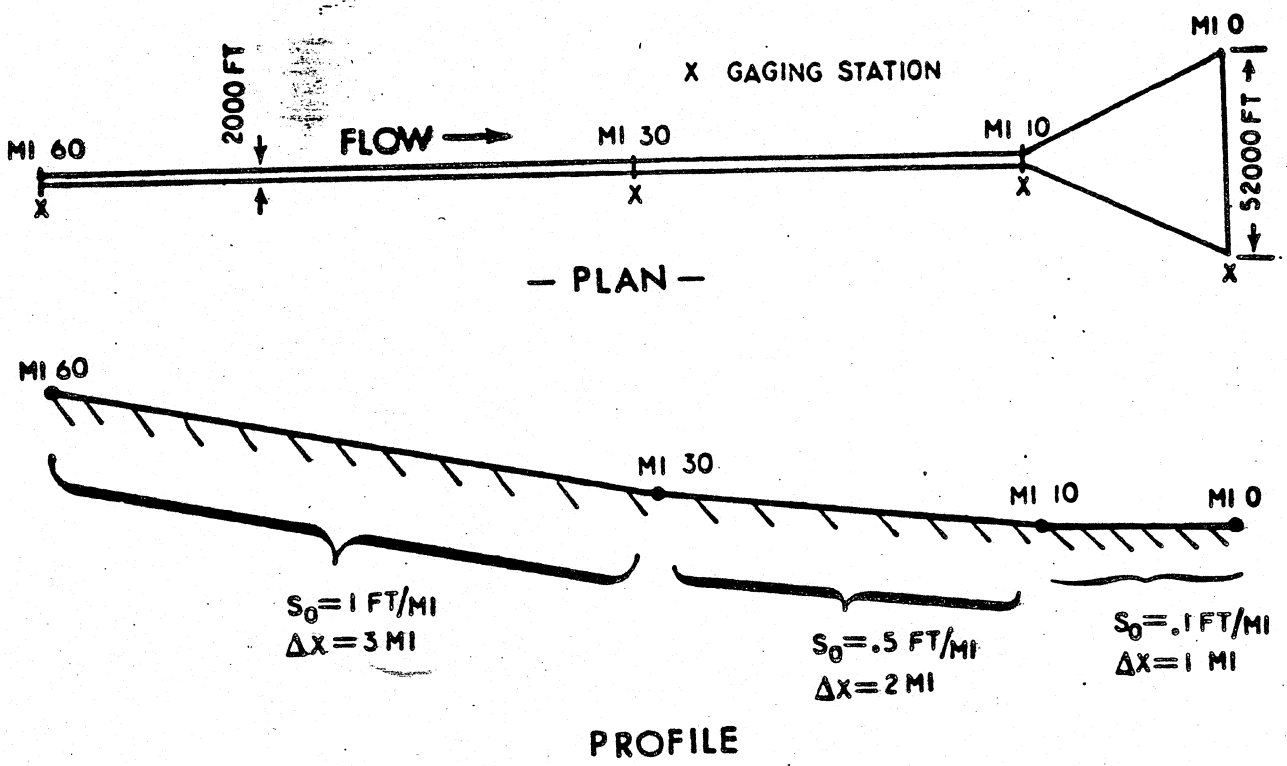

Fig. 5a - Plan and Profile of Multiple-Reach Idealized Channel

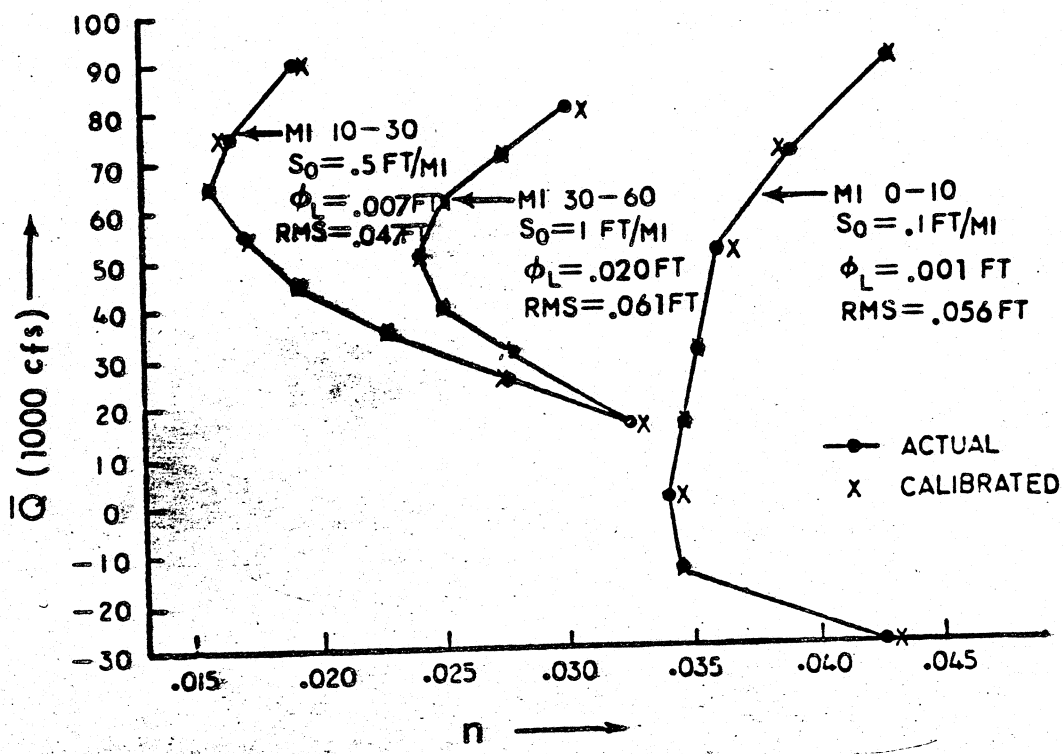

Fig. 5b - Actual and Calibrated n($\bar{Q}$) Functions for Ideal Channel

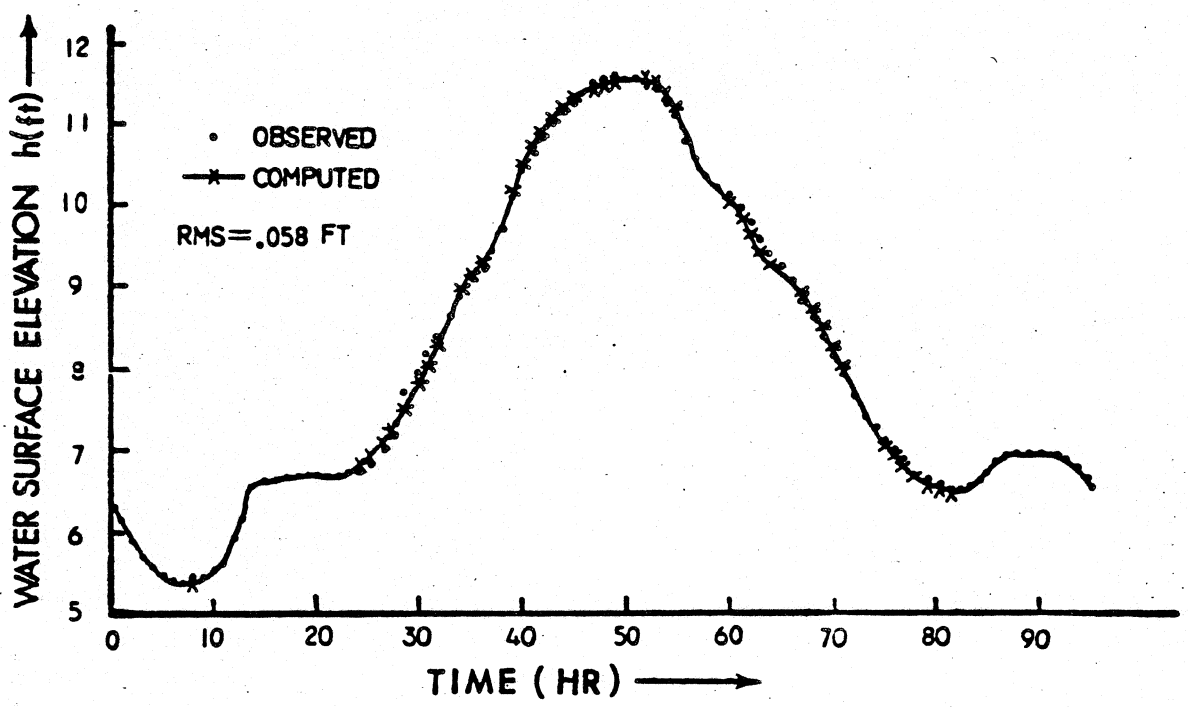

Fig. 6-- Computed and Observed Stages for Mile 10 of Idealized Channel.

SUMMARY OF FLOOD SIMULATIONS

LOWER MISSISSIPPI RIVER (RED RIVER LDG. TO VENICE)

YEAR	AVG. RMS ERROR (FT.)	PEAK DISCHARGE (1,000 CFS)
1959	0.62	750
1960	.31	850
1961	.47	1,220
1962	.61	1,155
1963	.38	950
1964	.51	1,140
1965	.44	1,040
1966	.38	1,090
1967	.38	700
1968	.36	980
1969*	.25	1,065
1970	.91	1,080
1971	.46	940

*CALIBRATED

DWOPER was enhanced with internal boundary selections:

1. Bridges - Embankments
2. Dams with
   a. uncontrolled spillway
   b. gated spillway
      constant
      time-dependent moveable gate
3. tide gates
4. siphons
5. short rapids

Enhanced capability of DWOPER To Model Levee Overtopping

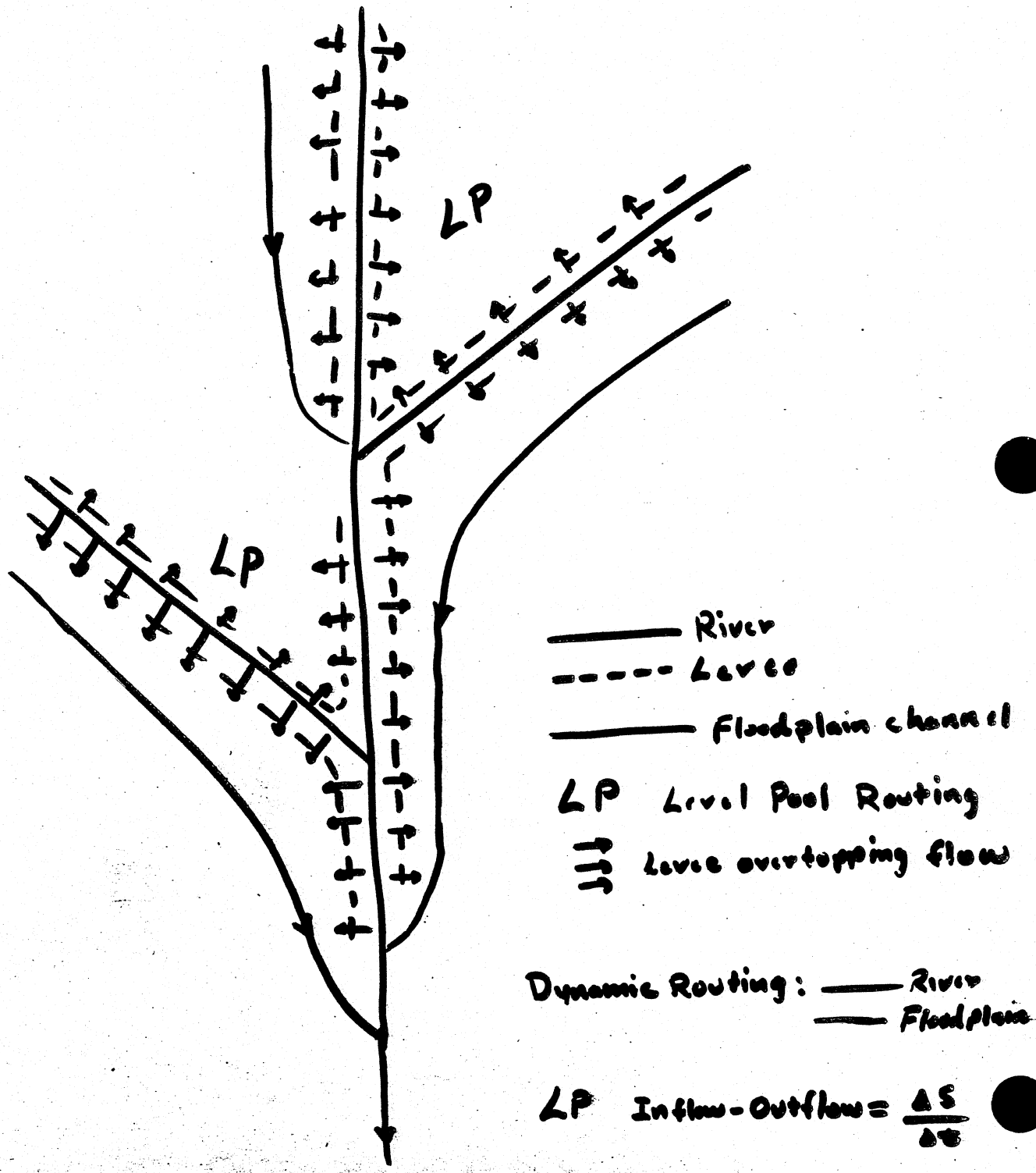

JUNCTION EQUATIONS

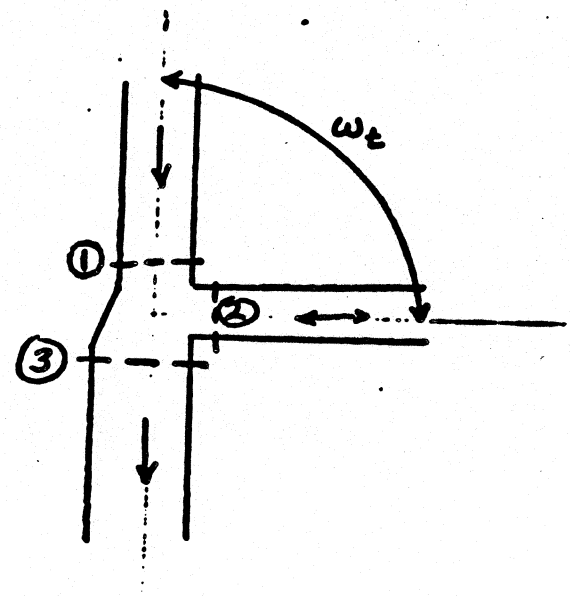

(1) $Q_1 + Q - Q_3 - \frac{\Delta s}{\Delta t} = 0$

where: $\frac{\Delta s}{\Delta t} = \frac{\Delta x}{6\Delta t}\left[B_1^j + B_3^j + B_2^j \cos\omega_t\right]\left[h_1^{j+1} + h_2^{j+1} + h_3^{j+1} - h_1^j - h_2^j - h_3^j\right]$

$$h_1 + \frac{V_1^2}{2g} - h_3 - \frac{V_3^2}{2g} - S_f \Delta x - \frac{C_m V_3^2}{2g} = 0$$

(2) $2g(h_1 - h_3) + V_1^2 - T_1 V_3^2 = 0$

where: $T_1 = 1 + C_m + C_f$

$$C_m = \left(0.1 + 0.83\frac{Q_2}{Q_3}\right)\left(\frac{\omega_t}{90}\right)^M$$

$$C_f = \frac{2g\ \Delta x\ K^2\ n^2}{2.21\ R^{4/3}} \qquad 0 < K < 1$$

(3) $2g\ (h_2 - h_3) + V_2^2 - T_2 V_3^2 = 0$

$T_2 = T_1$

Banded Matrix :

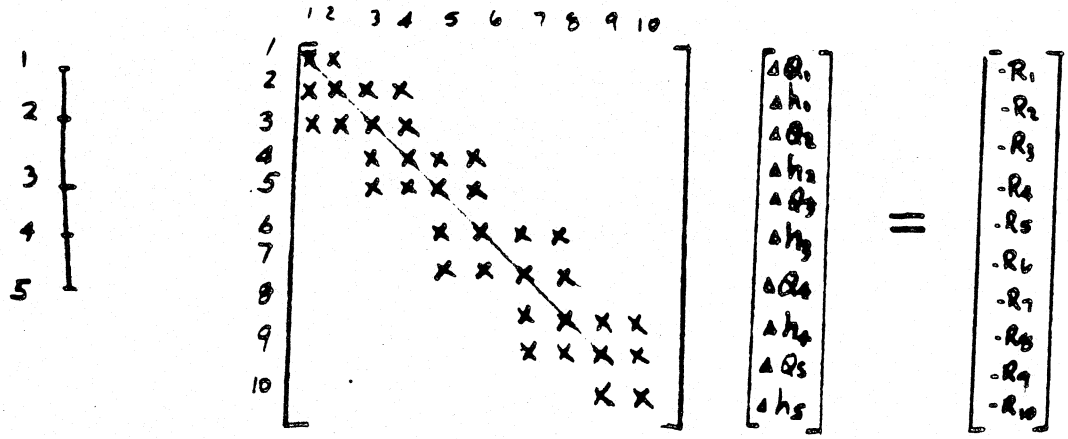

Sparse Matrix :

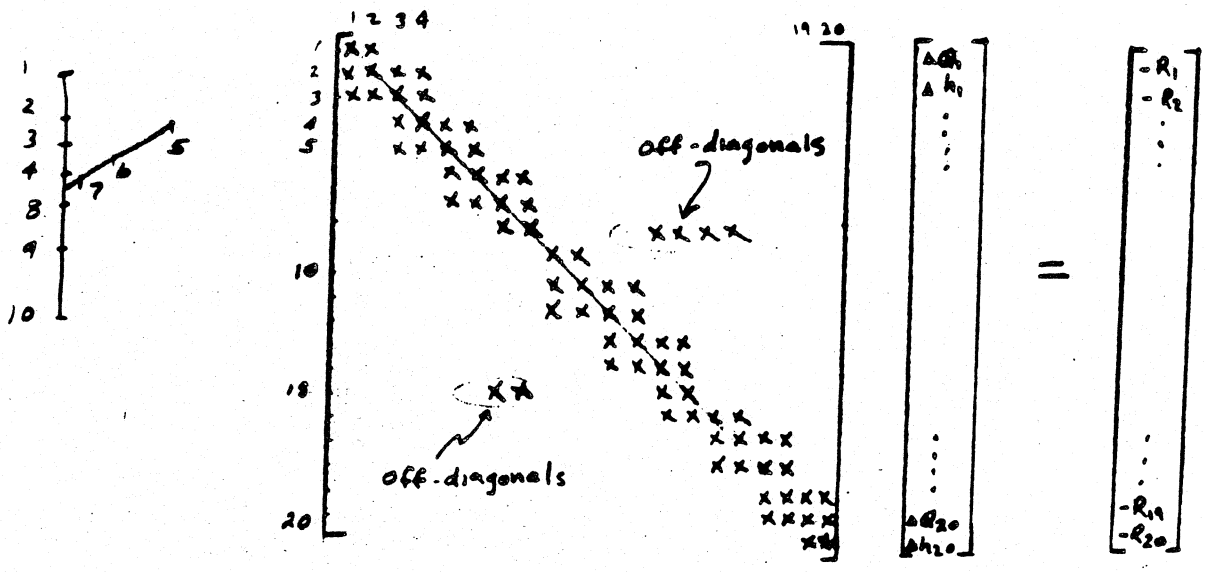

COMPUTATIONAL EFFICIENCY ACHIEVED BY:

(1) MINIMIZING THE NUMBER OF OFF-DIAGONAL ELEMENTS

(2) MINIMIZING THE NUMBER OF NEW OFF-DIAGONAL ELEMENTS CREATED DURING THE MATRIX SOLUTION

(3) USING A SPECIALLY DEVELOPED MATRIX SOLUTION TECHNIQUE WHICH TREATS ONLY NON-ZERO ELEMENTS

A SPECIAL NODE NUMBERING SCHEME IS REQUIRED FOR (1)

A SPECIAL CODE NUMBER IS REQUIRED FOR (2) AND (3)

Node Coding Scheme

Code	Type of Node
1	
2	
3	
4	
5	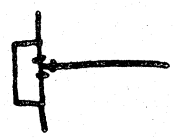
6	
7	
8	OR
9	

Node Numbering Scheme

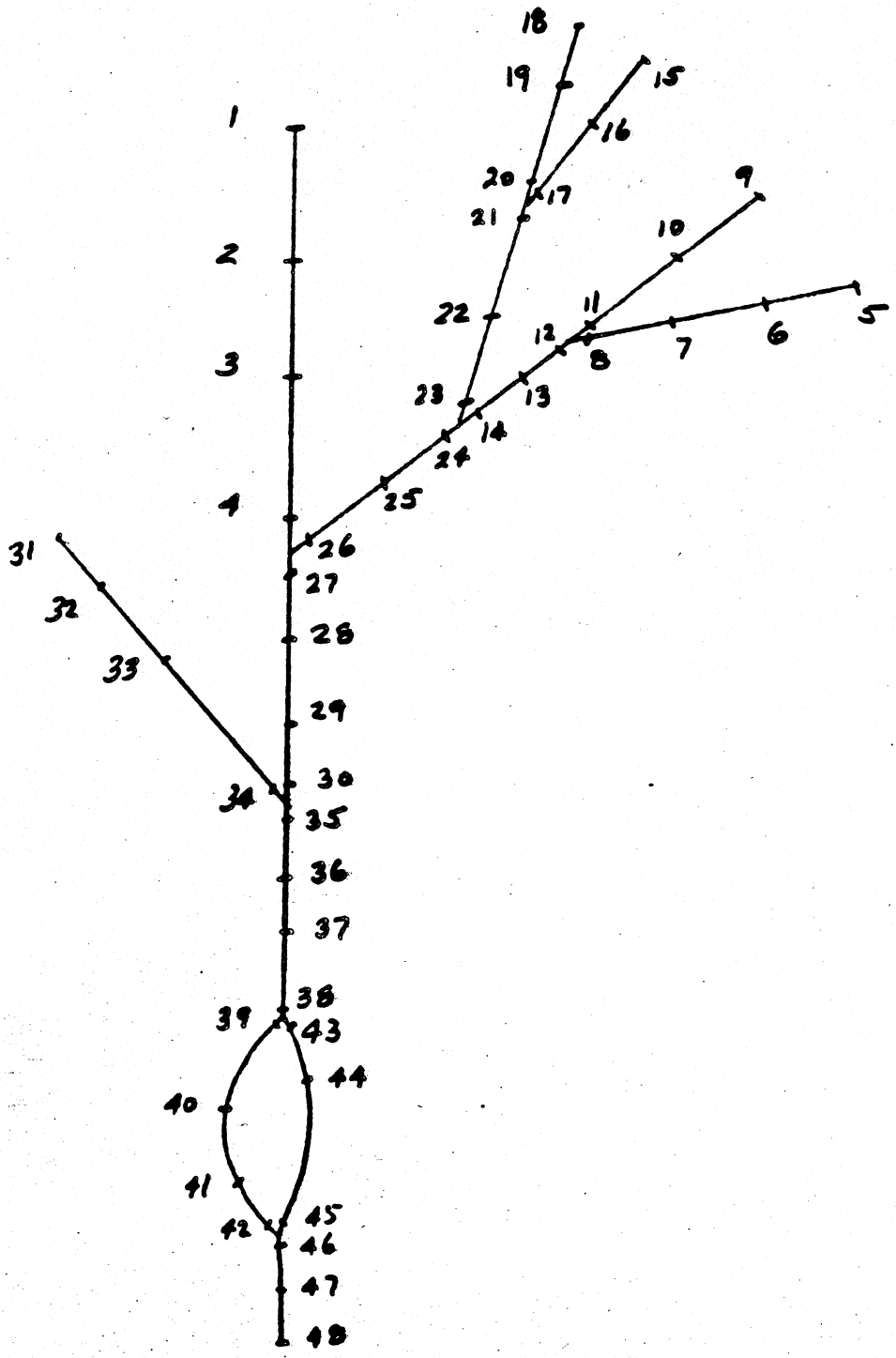

MATRIX SOLUTION EFFORT:

O = NUMBER OF OPERATIONS (+, −, x, ÷)

N = NUMBER OF CROSS SECTIONS

J = NUMBER OF JUNCTIONS

$O \approx 38N - 19$ .....SINGLE CHANNEL

$O \approx 95N - 48$ .....RELAXATION

$O \approx (102 + 46J)N$ .....NETWORK

$O \approx (12 + J^2)\ N^2 + (42 + 11J + J^2/2)\ N$ .....MODIFIED GAUSS

$O \approx 5N^3 + 8N^2 + 5N$ .....STANDARD GAUSS

N/J	O	TYPE OF SOLUTION
100/0	3,781	SINGLE CHANNEL
100/3	9,452	RELAXATION
100/3	24,000	NETWORK
100/3	217,000	MODIFIED GAUSS
100/3	5,080,500	STANDARD GAUSS
200/0	7,581	SINGLE CHANNEL
200/10	18,952	RELAXATION
200/10	112,400	NETWORK
200/10	1,160,400	MODIFIED GAUSS
200/10	40,321,000	STANDARD GAUSS

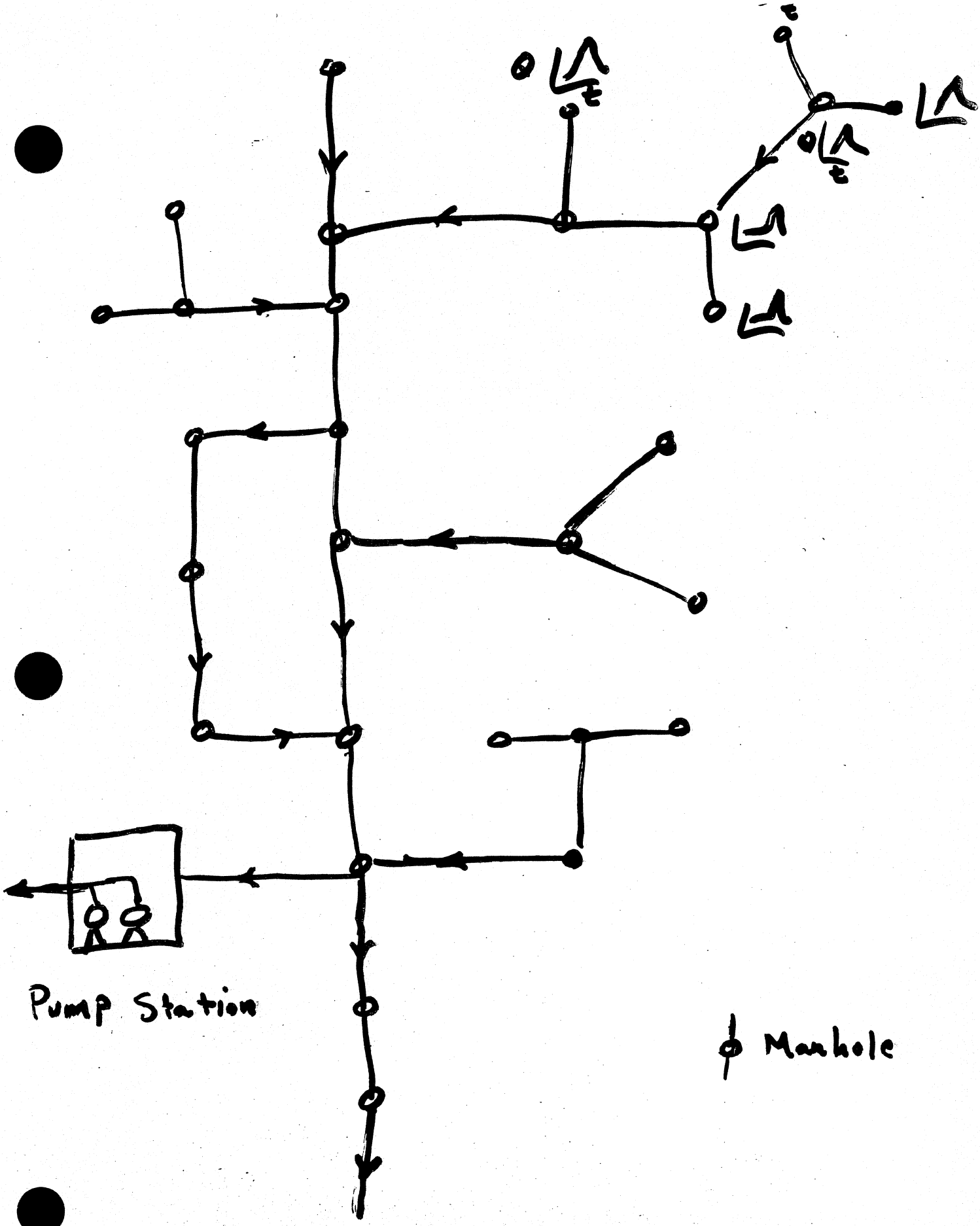

Storm Sewer System

Free Surface/Pressurized Unsteady Flow

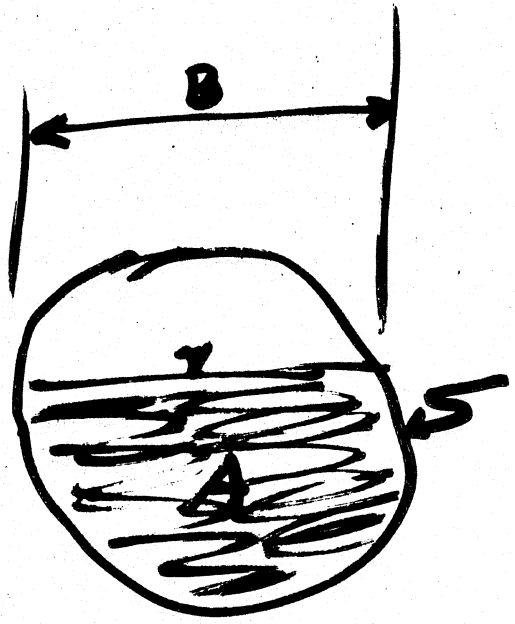

closed conduit

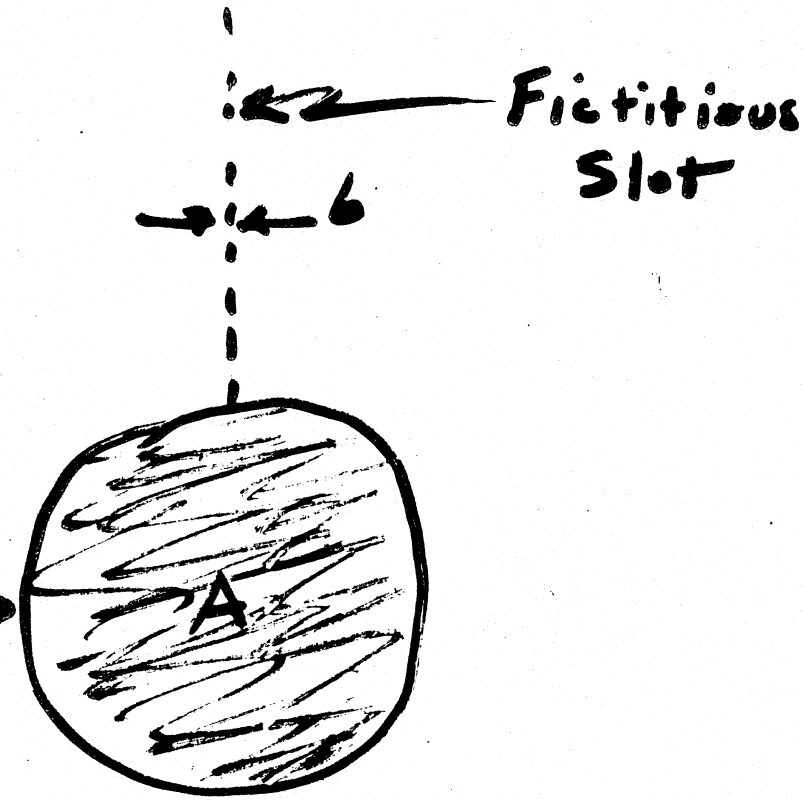

Free Surface Flow

$$c = \sqrt{g\,A/B}$$

Pressure Flow

$$c_p = \sqrt{g\,A/b}$$

$$\therefore\ b = \frac{gA}{c_p^2}$$

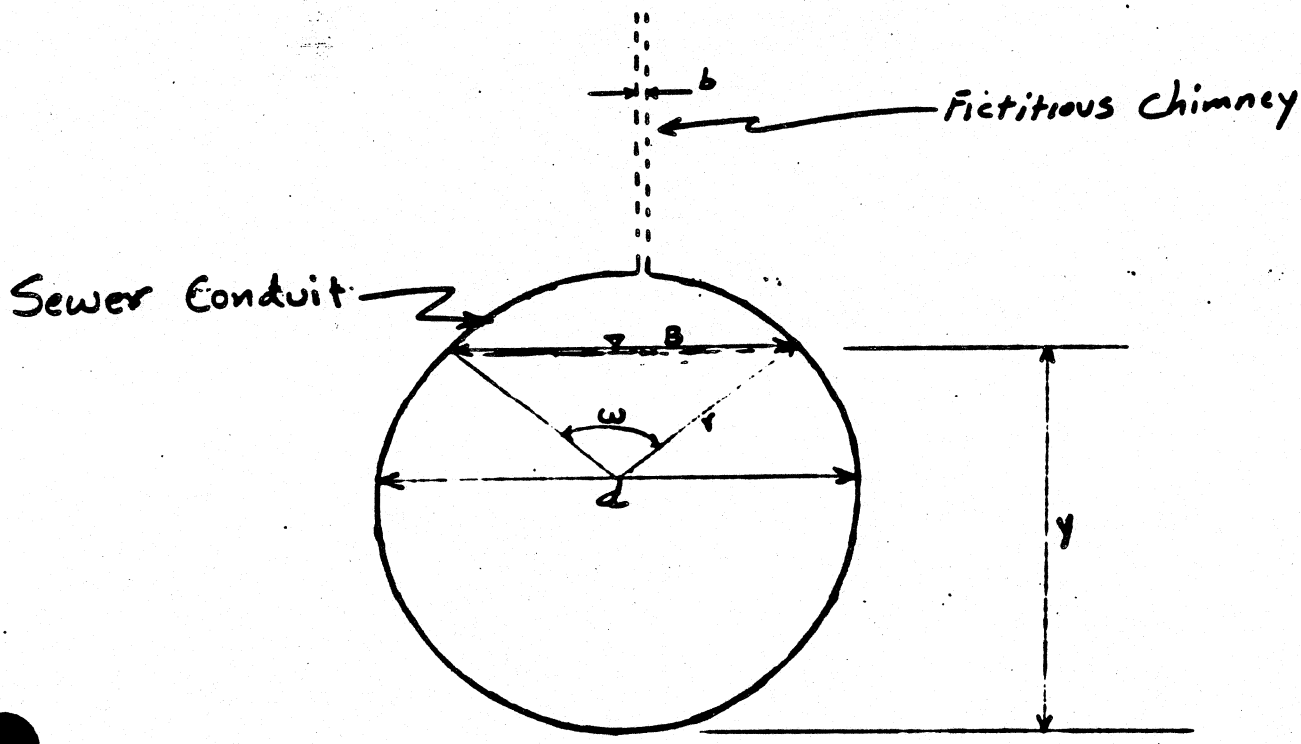

$$\omega = \pi + 2 \sin^{-1}\left(\frac{y-r}{r}\right)$$

$$P = r\,\omega$$

$$A = \frac{d^2}{8}(\omega - \sin\omega) \quad \ldots\ldots \quad y < d$$

$$A = \frac{\pi d^2}{4} \quad \ldots\ldots\ldots\ldots \quad y \geq d$$

$$B = d \sin(\omega/2) \quad \ldots\ldots\ldots \quad y < d$$

$$B = b \quad \ldots\ldots\ldots\ldots \quad y \geq d$$

Arbitrary Shaped Conduits

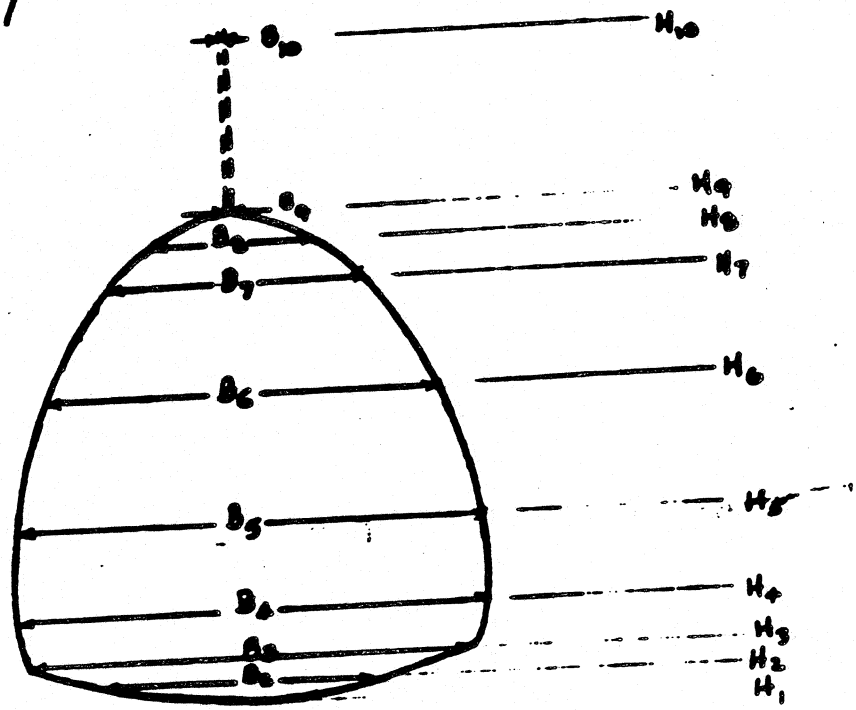

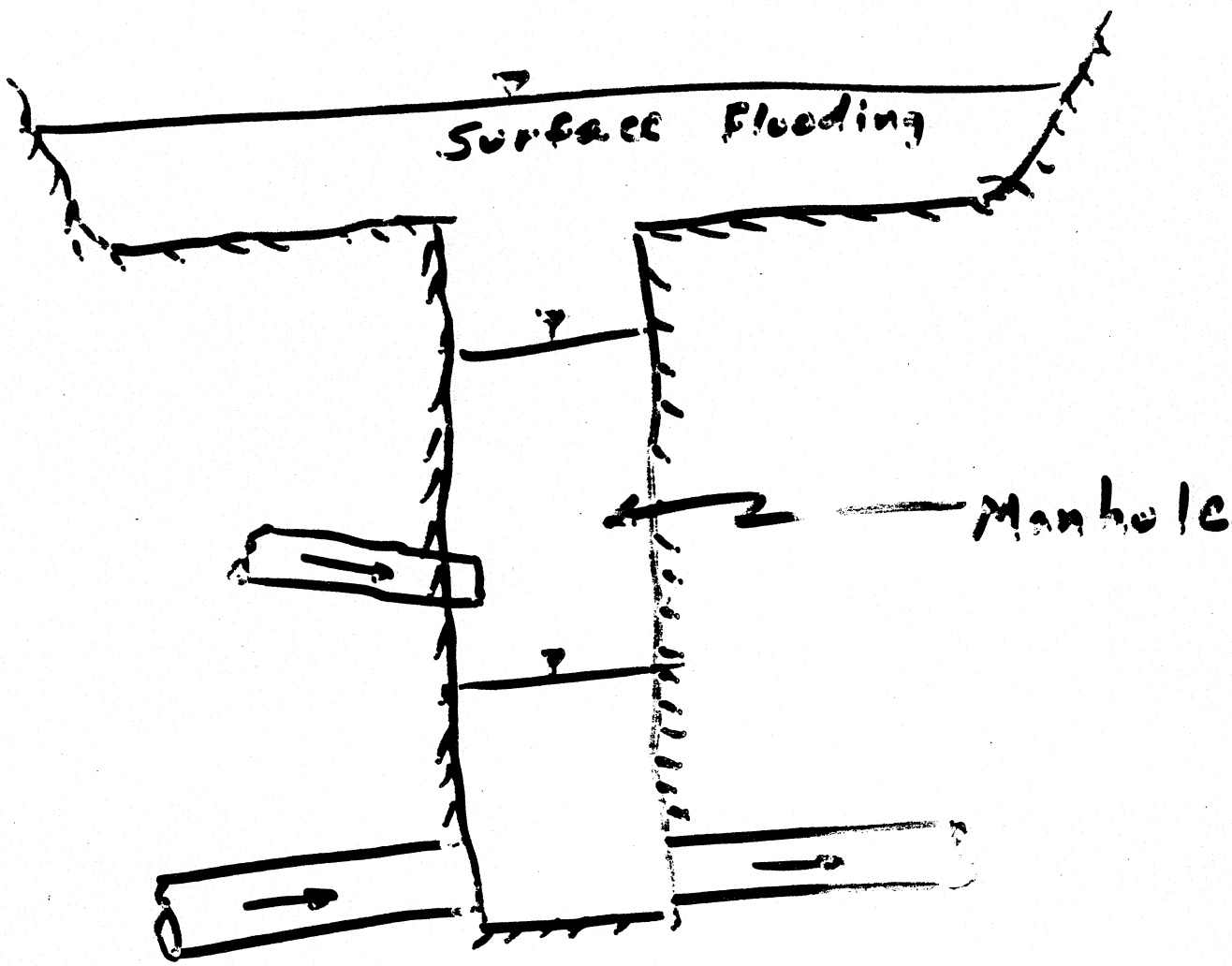

Manhole and Surface Flooding Simulation

Routing Selection Enhancement for DWOPER

1. Dynamic ———
2. Diffusion - - - -
3. Muskingum-Cunge —·—·—
4. Level Pool Reservoir ▷

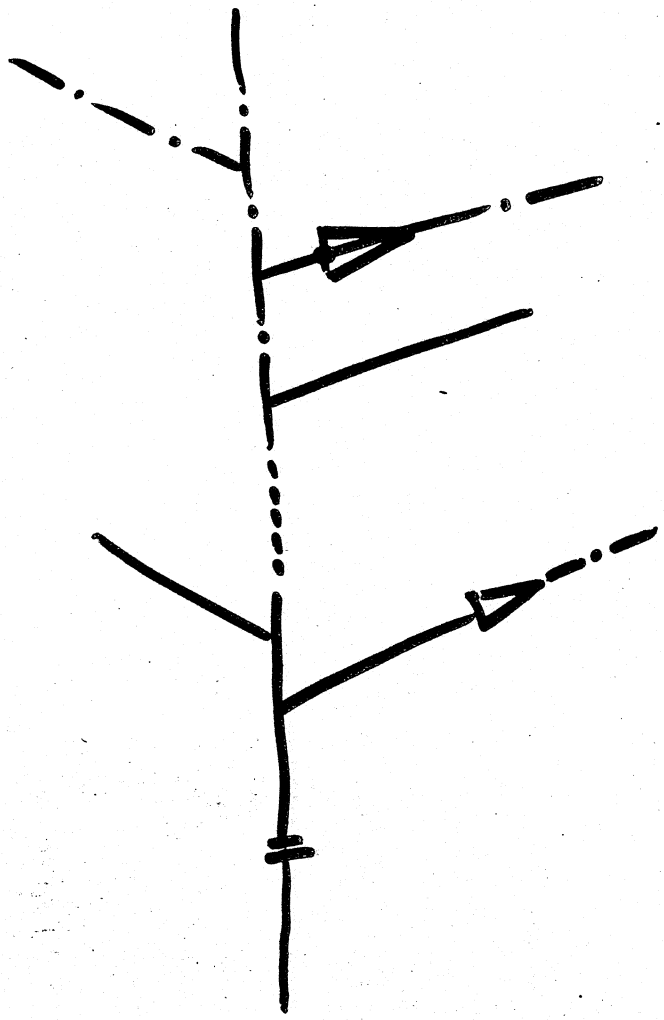

Enhancement to DWOPER

Automatic Calibration of one-Dimensional Unsteady flow model (DWOPER)

with 1. Minimal cross-section info

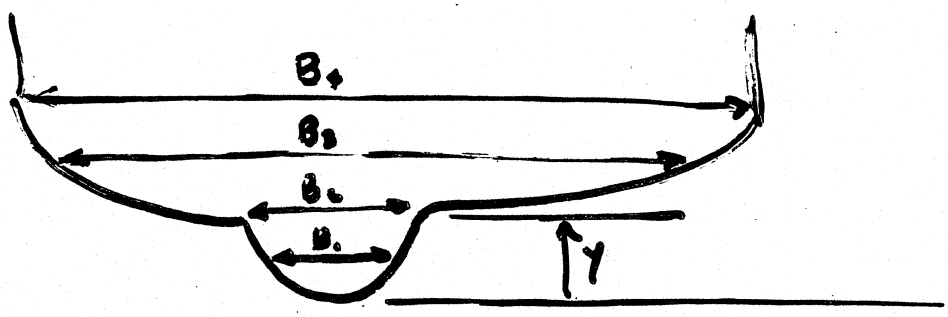

$$B = k y^m$$

a.) B_1, B_2, B_3, B_4

b.) B_2, m_c, B_4, m_f

2. Stage Hydrographs

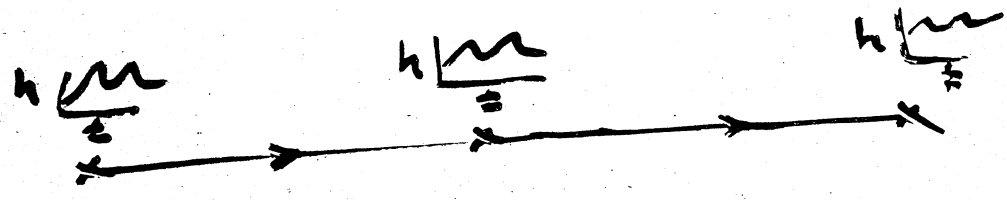

also with constraints on Manning n values

Applications of DWOPER:

Lower Mississippi Surge

Ohio-Miss. Junction Flood

Columbia Tide

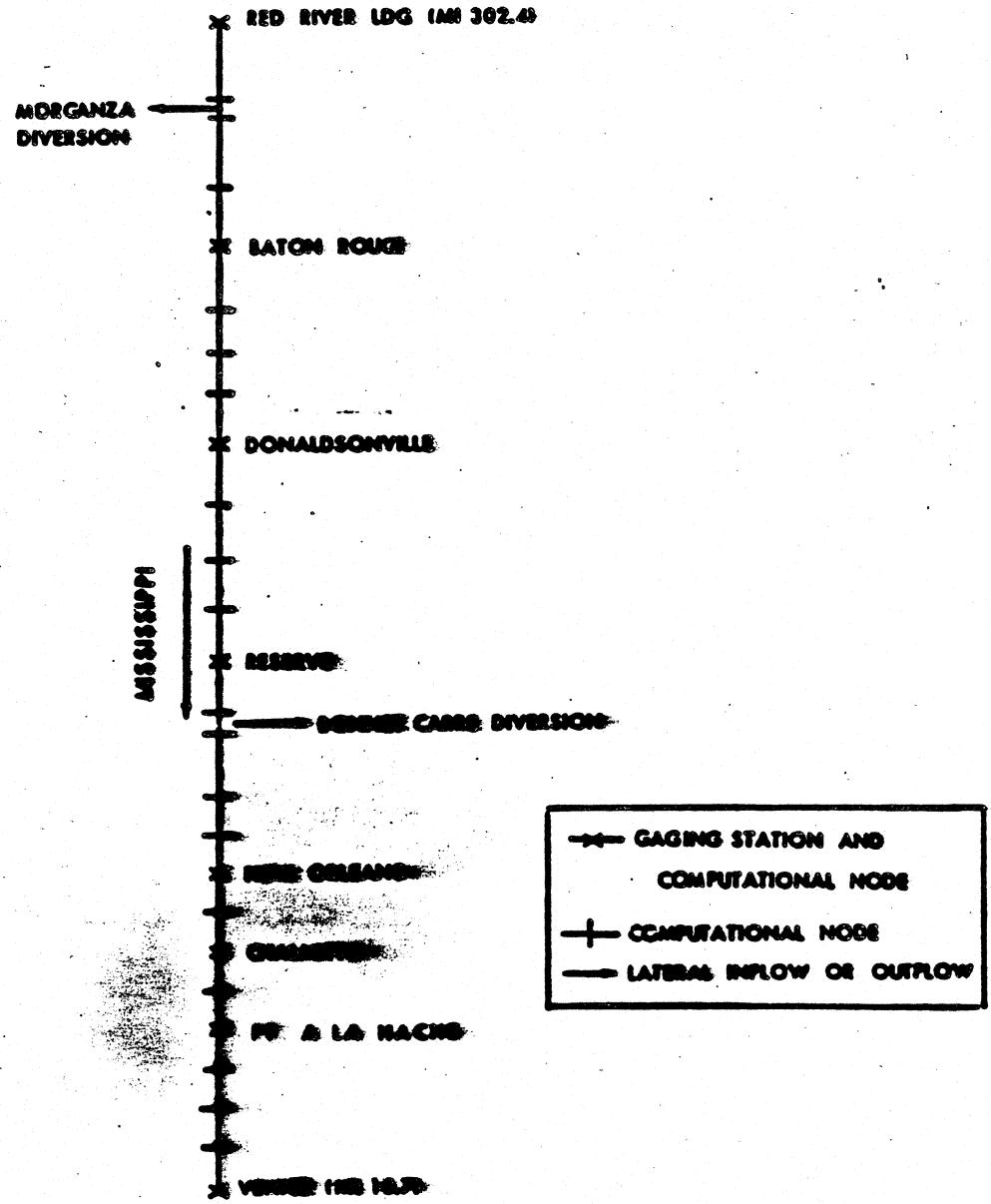

Figure 1. Schematic of Lower Mississippi River.

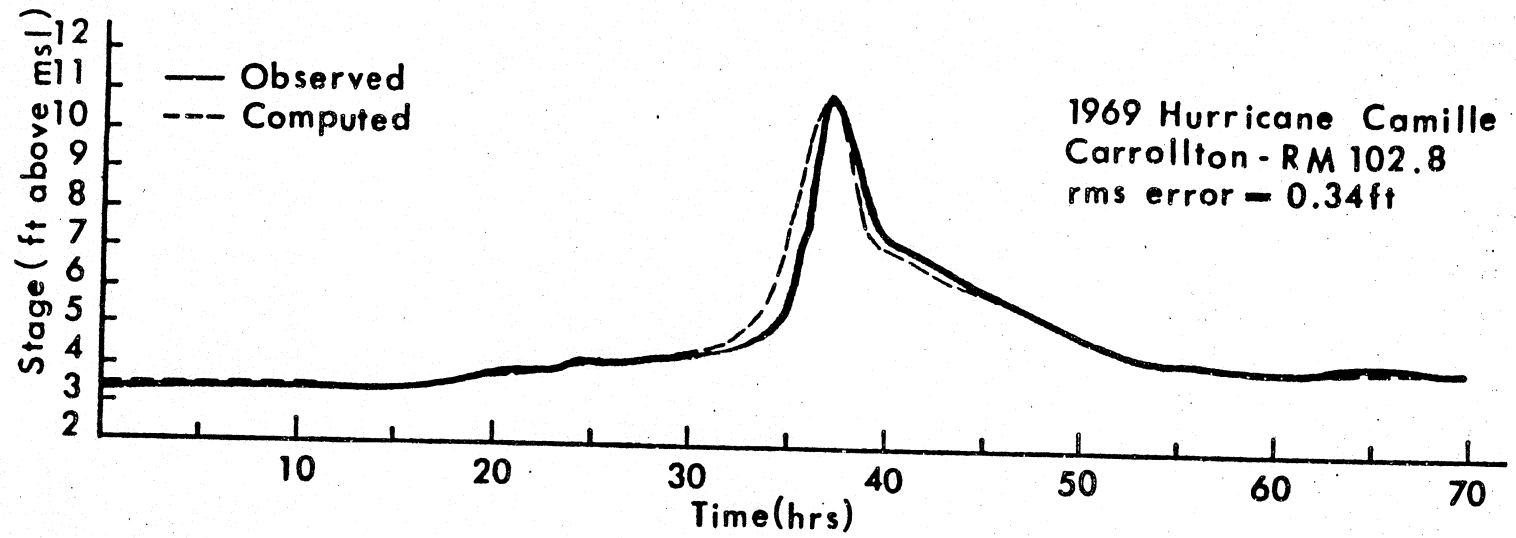

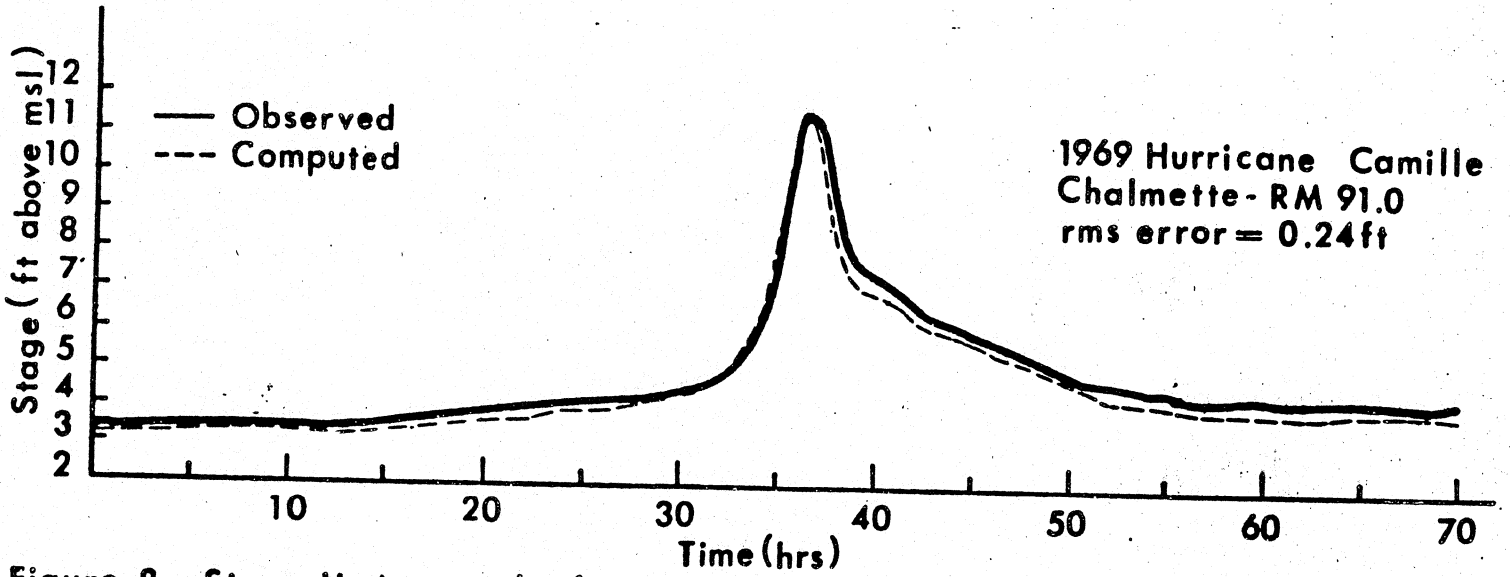

Figure 8. Stage Hydrographs for 1969 Hurricane Camille at Chalmette and Carrollton.

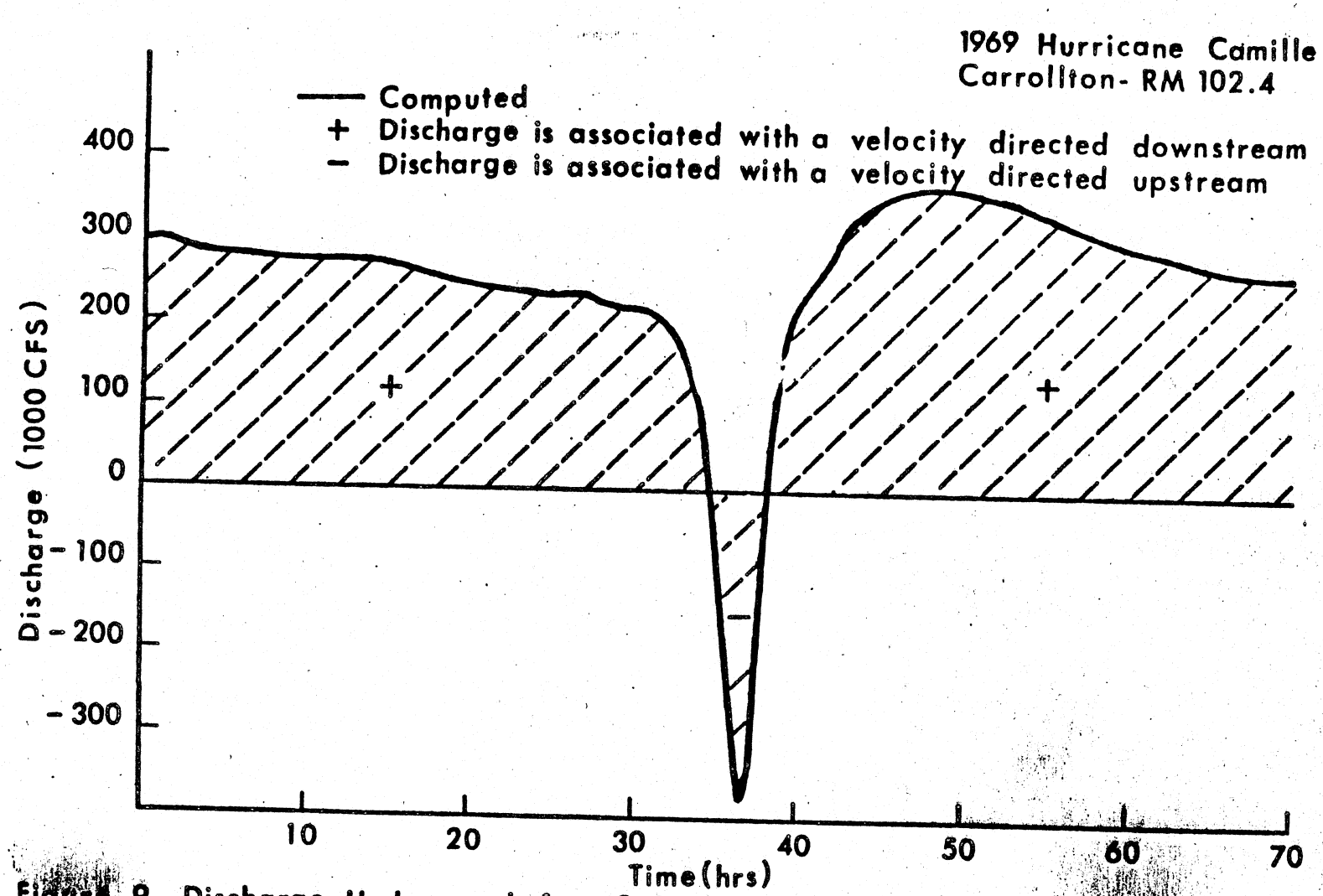

Figure 9. Discharge Hydrograph for 1969 Hurricane Camille at Carrollton.

Unsteady Flows in Lower Mississippi River

Type of Transient	$\frac{\text{Inertia Slope}}{\text{Friction Slope}}$	$\frac{\text{Water Surface}}{\text{Friction Slope}}$
Flood $T_r = 30$ days	0.25	0.80
Surge $T_r = 5$ hrs	2.10	3.25

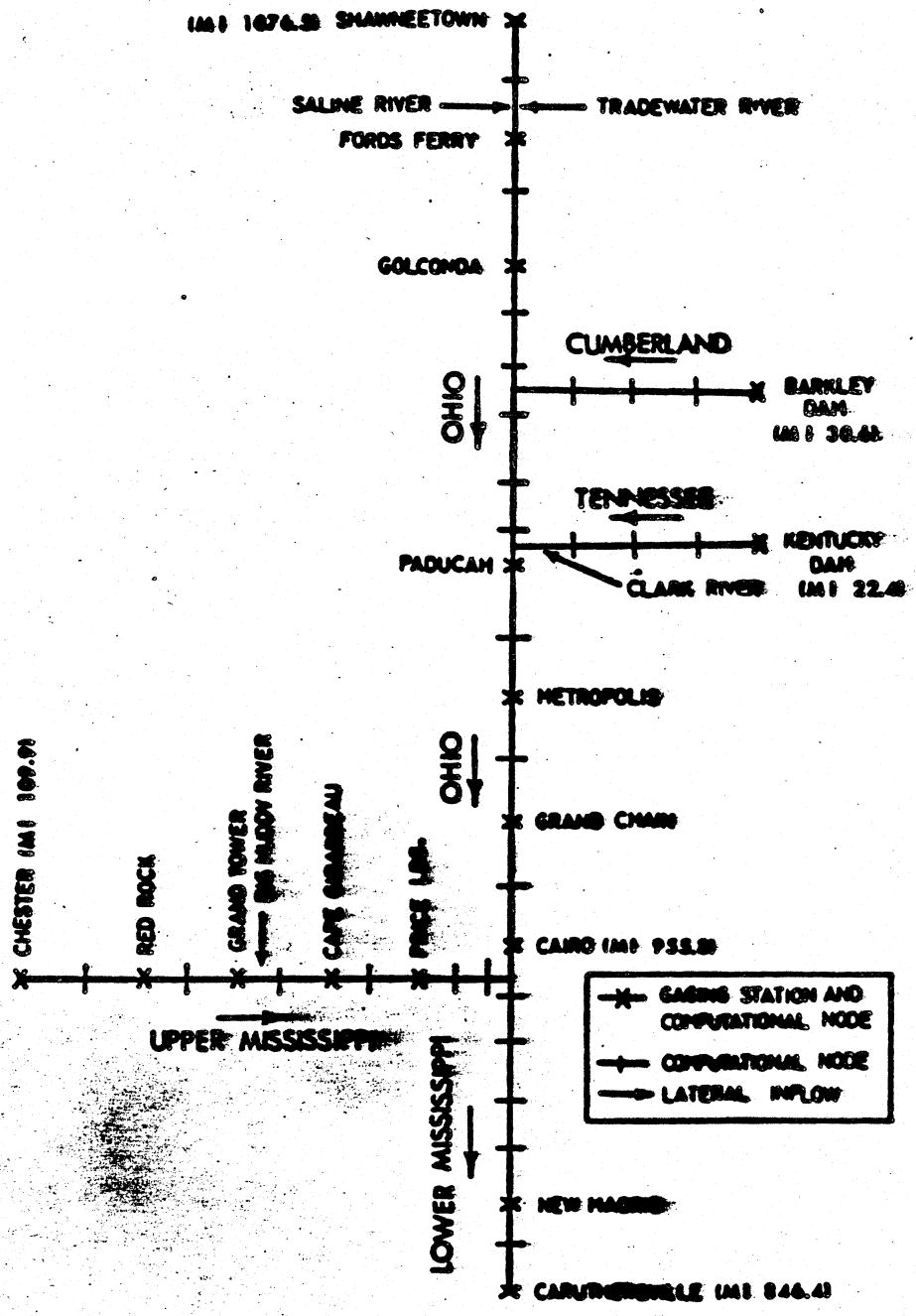

Figure 3. Schematic of Mississippi-Ohio-Cumberland-Tennessee (MOCT) River System.

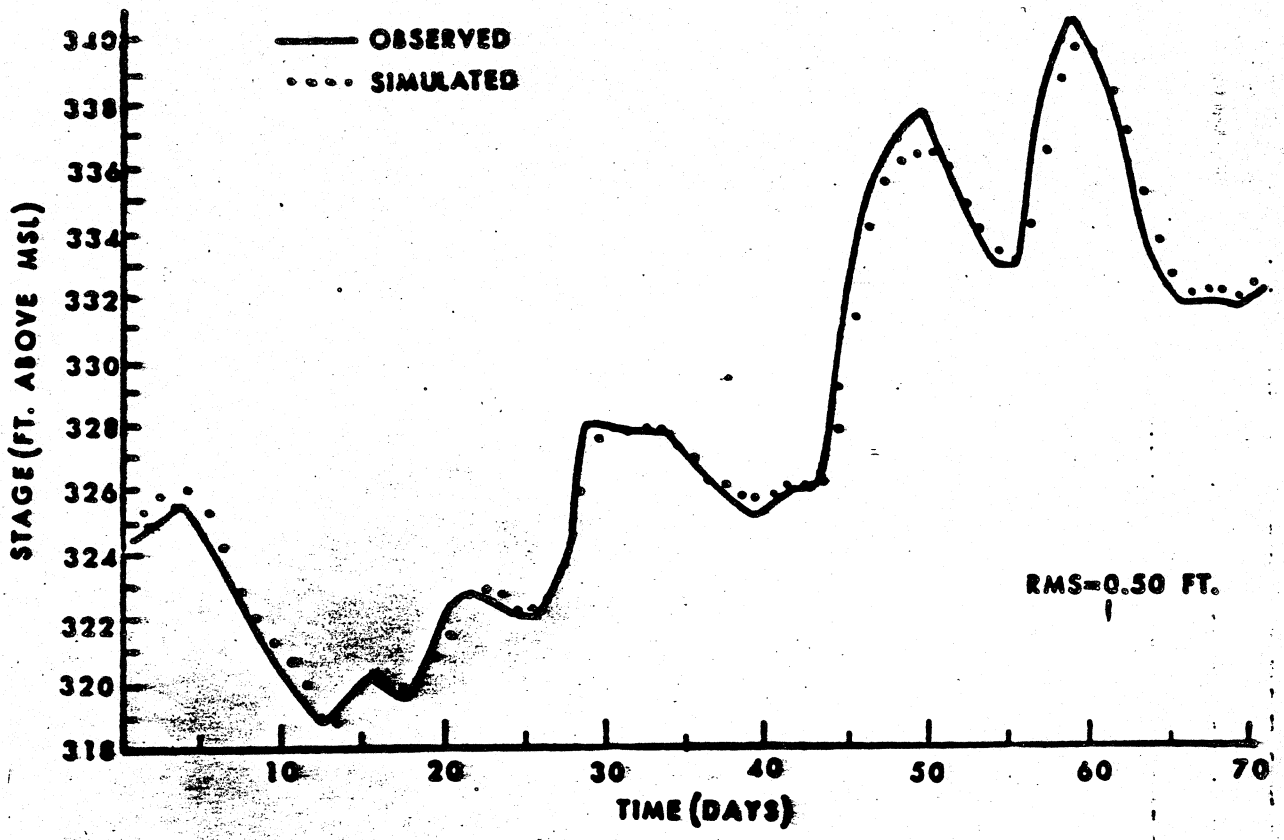

Figure 5. Observed vs. simulated stages at Cape Girardeau for 1970 flood.

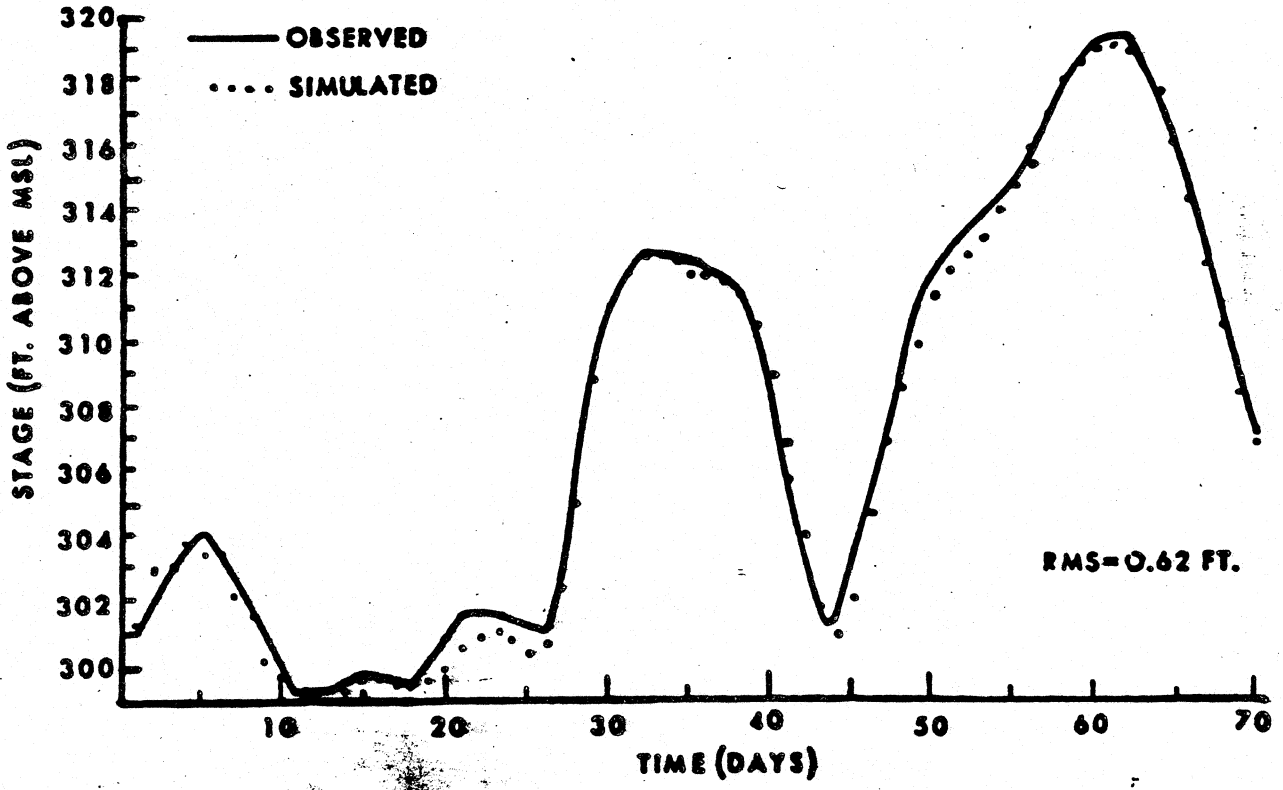

Figure 4. Observed vs. simulated stages at Cairo for 1970 flood.

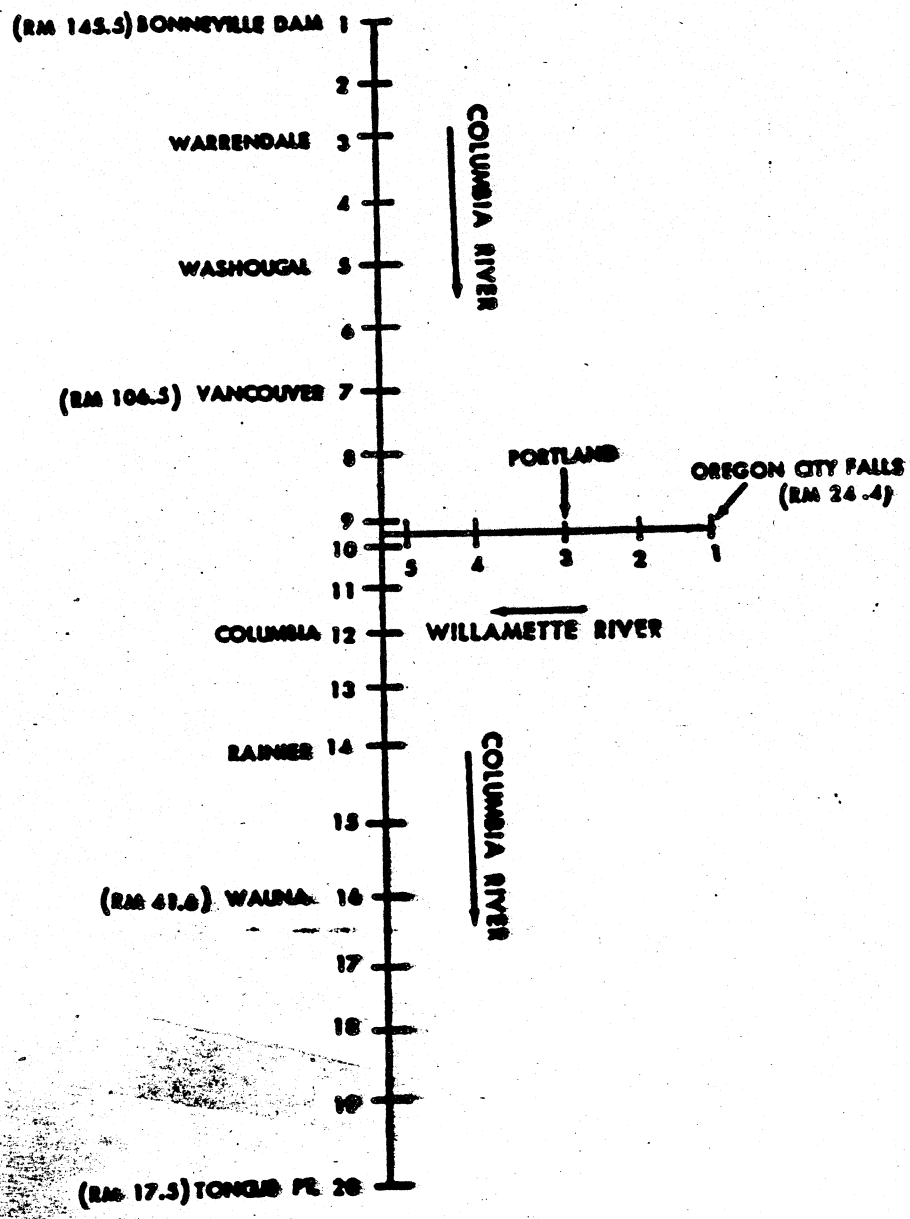

Figure 6. Schematic of lower Columbia-Willamette River System.

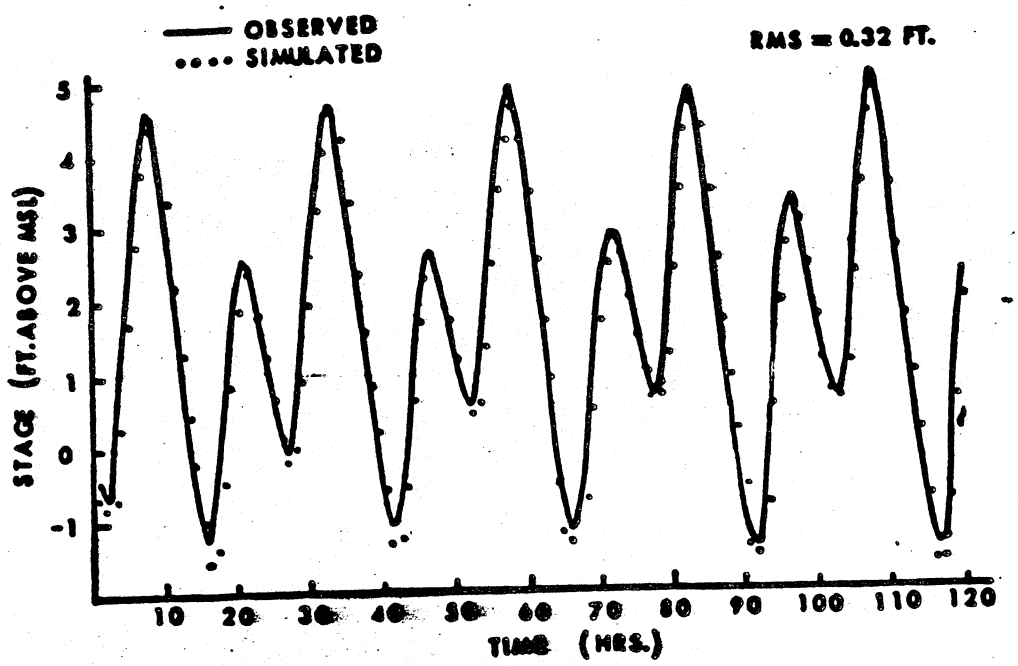

Figure 7. Observed vs. simulated stages at Waunu.

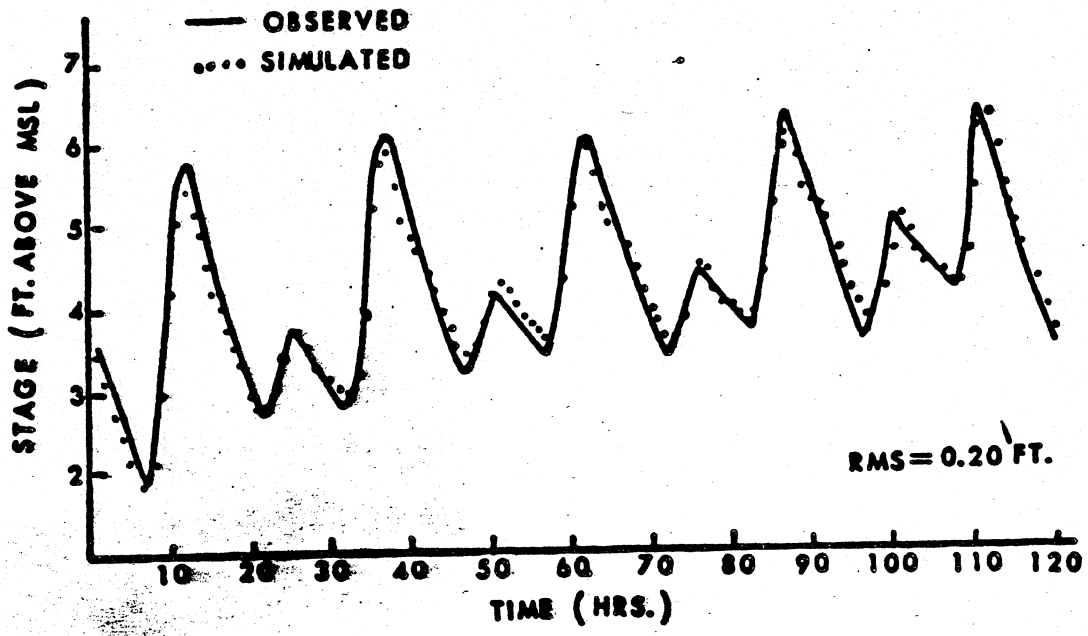

Figure 8. Observed vs. simulated stages at Portland.

NATIONAL WEATHER SERVICE
OPERATIONAL DYNAMIC WAVE MODEL

by D. L. Fread[1]
April 1978
(Reprinted July 1985)

INTRODUCTION

The National Weather Service (NWS) hydrology program is to provide accurate and timely hydrologic information to the general public. This includes flood forecasts, as well as day-to-day river forecasts which are used for water supply, navigation, irrigation, power, reservoir operation, recreation, and water quality interests. Twelve River Forecast Centers prepare the forecasts which are disseminated to the public throughout the United States via local Weather Service Forecast Offices.

In the late 1960's, NWS began moving from an index type catchment runoff model to a continuous conceptual hydrologic model with a strong physical basis (Monro and Anderson, 1974). The new conceptual model is now being implemented throughout the United States.

Where runoff generated from precipitation input to the conceptual model aggregates in fairly large, well-defined channels (rivers), it is transmitted downstream by routing techniques of the hydrologic or storage routing variety, e.g., the lag and K technique (Linsley, et al., 1958). Although the hydrologic routing techniques function adequately in many situations, they have serious shortcomings when the unsteady flows are subjected to backwater effects due to reservoirs, tides, or inflows from large tributaries. When channel bottom slopes are quite mild, the flow inertial effects ignored in the hydrologic technique also become important.

In the early 1970's, the NWS Hydrologic Research Laboratory began developing a dynamic wave routing model based on an implicit finite difference solution of the complete one-dimensional St. Venant equations of unsteady flow. This hydrodynamic model, known as DWOPER (Dynamic Wave Operational Model), has recently begun to be implemented where backwater effects and mild bottom slopes are most troublesome for hydrologic routing methods. It is either in operational service or in the process of being implemented on the Mississippi, Ohio, Columbia, Missouri, Arkansas, Red, Atchafalaya, Cumberland, Tennessee, Willamette, Platte, Kansas, Verdigris, Ouachita, and Yazoo Rivers.

DWOPER features the ability to use large time steps for slowly varying floods and to use cross-sections spaced at irregular intervals along the river system. The model is generalized for wide applicability to rivers of varying physical features, such as irregular geometry, variable roughness parameters, lateral inflows, flow diversions, off-channel storage, local head losses such as bridge contraction-expansions, lock and dam operations, and wind effects. It is suited for efficient application to dendritic river systems or to channel networks consisting of bifurcations with weir-type flow into the bifurcated channel. DWOPER has a highly efficient automatic calibration feature for determining

[1]Research Hydrologist, Hydrologic Research Laboratory, W23, National Weather Service, NOAA, Silver Spring, Md. 20910.

the optimum roughness coefficients for either a single channel or system of interacting channels. Extensive data management programming features allow the model to be used in a day-to-day operational forecasting environment with minimal card coding required. It is also equally applicable for simulating unsteady flows for purposes of engineering planning, design, or analysis.

MODEL DESCRIPTION

Mathematical Basis - The basis for DWOPER is a finite difference solution of the conservation form of the one-dimensional equations of unsteady flow consisting of conservation of mass and momentum equations, i.e.,

$$\frac{\partial Q}{\partial x} + \frac{\partial (A+A_o)}{\partial t} - q = 0 \tag{1}$$

$$\frac{\partial Q}{\partial t} + \frac{\partial (Q^2/A)}{\partial x} + gA\left(\frac{\partial h}{\partial x} + S_f + S_e\right) - qv_x + W_f B = 0 \tag{2}$$

in which Q is discharge, A is cross-sectional area, A_o is off-channel cross-sectional area wherein flow velocity is considered negligible, q is lateral inflow or outflow, x is distance along the channel, t is time, g is gravity acceleration constant, v_x is the velocity of lateral inflow in the x-direction, W_f is the wind term, B is the channel top width and S_f is the friction slope defined as:

$$S_f = \frac{n^2 |Q| Q}{2.2\, A^2 R^{4/3}} \tag{3}$$

in which n is the Manning roughness coefficient and R is the hydraulic radius. The term S_e is defined as:

$$S_e = \frac{K_e \partial (Q/A)^2}{2g \quad \partial x} \tag{4}$$

in which K_e is the expansion-contraction coefficient.

Equations (1) and (2) are nonlinear partial differential equations which may be solved without necessary simplifications by finite differences techniques of explicit or implicit variety. Implicit methods, although simpler in application are not suitable for application of the equations to long-term unsteady flow phenomena such as flood waves because they are restricted by mathematical stability considerations to very small computational time steps (on the order of a few minutes); this causes the explicit techniques to be very inefficient in the use of computer time.

Implicit finite difference techniques, however, have no restrictions on time step size other than accuracy considerations.

The "weighted four-point" implicit scheme first used by Preissmann (1961) and recently by Quinn and Wylie (1973), Chaudry and Contractor (1973), and Fread (1973a, 1974) appears to be the most advantageous of the various implicit schemes which have been proposed from time to time because it can readily be used with unequal distance steps and its stability-convergence properties can be controlled. In the weighted four-point scheme, the continuous x-t region in which solutions of h and Q are sought is represented by rectangular net of discrete points, as shown in Fig. 1 at equal or unequal intervals of Δx and Δt along the x and t axes, respectively. Each point is identified by a subscript (i) which designates the x position and a superscript (j) for time position. The time derivatives are approximated by:

$$\frac{\partial K}{\partial t} = \left(K_i^{j+1} + K_{i+1}^{j+1} - K_i^{j} - K_{i+1}^{j}\right)/2\Delta t \qquad (5)$$

in which K represents any variable. The spatial derivatives are approximated by a finite difference quotient positioned between two adjacent time lines according to weighting factors θ and $1-\theta$, i.e.,

$$\frac{\partial K}{\partial x} = \theta\left(K_{i+1}^{j+1} - K_i^{j+1}\right)/\Delta x + (1-\theta)\left(K_{i+1}^{j} - K_i^{j}\right)/\Delta x \qquad (6)$$

and variables other than derivatives are approximated in a similar manner, i.e.,

$$K = \theta\left(K_i^{j+1} + K_{i+1}^{j+1}\right)/2 + (1-\theta)\left(K_i^{j} + K_{i+1}^{j}\right)/2 \qquad (7)$$

When θ equals 1.0, a fully implicit scheme is formed; this was used by Baltzer and Lai (1968) and Amein and Chu (1975). A box scheme such as used by Amein and Fang (1970) results if θ is fixed at 0.5. The influence of the θ weighting factor on the stability and convergence properties was examined by Fread (1974), who concluded that the accuracy decreases as θ departs from 0.5 and approaches 1.0. This effect becomes more pronounced as the time step size increases. DWOPER allows θ to be an input parameter. A value of 0.55 is often used to minimize loss of accuracy while avoiding weak or pseudo instability as reported by Baltzer and Lai (1968) and Fread (1975) when θ of 0.5 is used.

Substitution of the finite difference quotients defined by Eqs. (5-7) into Eqs. (1) and (2) for the derivatives and non-derivative terms produces two algebraic equations which are nonlinear with respect to the unknowns h and Q at the net points on the j+1 time line. All terms associated with the jth time line are known from either the initial conditions or previous computations. The initial conditions are values of h and Q at

each computational point (node) along the x-axis for the first time line (j+1). They are obtained from a previous unsteady flow solution, or they can be estimated since small errors in the initial conditions dampen out within a few time steps.

The two nonlinear algebraic equations cannot be solved in a direct (explicit) manner since there are four unknowns, h and Q, at points i and i+1 on the j+1 time line and only two equations. However, if similar equations are formed for each of the N-1 Δx reaches between the upstream and downstream boundaries, a total of 2N-2 equations with 2N unknowns results. (N denotes the total number of computational points or cross-sections.) Then prescribed boundary conditions, one at the upstream extremity of the river and one at the downstream extremity, provide the necessary two additional equations required for the system to be determinate. The resulting system of 2N nonlinear equations with 2N unknowns is solved by a functional iterative procedure, the Newton-Raphson method (Amein and Fang, 1970).

In the iterative procedure, trial values obtained via linear or parabolic extrapolation from solutions of h and Q at previous time steps are assigned to the 2N unknowns. Substitution of these into the system of 2N nonlinear equations yields a set of 2N residuals. The Newton-Raphson method seeks to reduce the residuals to an acceptable tolerance level which is usually achieved within one or two iterations. If the Newton-Raphson method is applied only once each time step, the solution procedure degenerates to the equivalent of a quasi-linear finite difference approximation of Eqs. (1) and (2) similar to that used by Chen and Simons (1975) and others. The linear difference solution requires smaller time steps than the nonlinear formulation for the same degree of accuracy. However, for very gradually varying flows, the time step size which may be fixed for reasons of data availability and user requirements can be such that the loss of accuracy using the linear formulation or its equivalent is insignificant.

In the Newton-Raphson method, a system of 2N x 2N linear equations are generated. The coefficient matrix of the system is composed of partial derivatives which are functions of the unknowns; however, the elements in the coefficient matrix can be assigned numerical values by substituting the trial values of unknowns. The coefficient matrix is related to the set of 2N residuals by a set of 2N corrections to the original trial values of the unknowns. It is the 2N corrections that are sought in the solution of the 2N x 2N linear system. The coefficient matrix has a banded structure with at most four elements in any row. This property allows the use of a special modified Gaussian elimination algorithm for solving the system (Fread, 1971). Modification of the elimination algorithm reduces the core storage from $4N^2$ to 3N and the number of computational operations are reduced from the order of $(8/3N^3+4N^2)$ to 18N. The increase in computational efficiency is critical to the feasibility of the implicit solution technique.

Initial Conditions - DWOPER allows initial conditions to be obtained from the following sources:

1) Estimated stages and discharges at each cross-section are read in;
2) Observed stages at each cross-section where a river gage is located are read in; stages at intermediate cross-sections are linearly interpolated within the model; observed discharge at the upstream extremity of the main stem river and each tributary are also read in; all downstream discharges are determined by summation of flows from the upstream to downstream boundaries including tributary inflow to the main stem and lateral inflow occurring along either the main stem or tributaries;
3) Computed stages and discharges which have been saved from a previous unsteady flow simulation; and
4) Assumed steady flow to obtain discharges and backwater computation to obtain stages.

In each case, the unsteady flow equations are solved for several time steps using the initial conditions together with boundary conditions which are held constant during the time steps. This allows the errors in the initial conditions to dampen out which results in the initial conditions being more nearly error free when the actual simulation commences and transient boundary conditions are used.

Boundary Conditions - Boundary conditions must be specified in order to obtain solutions to the St. Venant equations. In fact, in most unsteady flow problems, the unsteady disturbance is introduced into the flow at the boundaries or extremities of the river system. DWOPER can readily accommodate either of the following boundary conditions at the upstream extremities of the river system:

1) known stage (water surface elevation) hydrograph, $h_1(t)$; or
2) known discharge hydrograph, $Q_1(t)$.

Downstream boundary conditions included as options in DWOPER are:

1) known stage hydrograph, $h_N(t)$;
2) known discharge hydrograph, $Q_N(t)$; or
3) a known relationship between stage and discharge such as a rating curve.

With respect to the rating curve boundary condition, the rating may be single-valued and read in as tabular (piece-wise linear) values of stage and discharge with linear interpolation provided internally for intermediate values. The rating may also be a loop rating curve generated internally from cross-section and roughness properties of the downstream extremity and the instantaneous water surface slope at the previous time

step. The rating may also be a weir-type relation of the form $Q_{wr} = C_1 (h_{wr} + h_{wr})^{C2}$ in which the weir coefficients (C_1 and C_2) and the weir crest elevation h_w are read in.

Hydrographs of stage or discharge may be read in at a constant time interval which is also an input to the model or they may be read in at irregular intervals of time, in which case, the interval is also specified each time it changes.

Cross-Sections - Irregular as well as regular geometrical shaped cross-sections are acceptable in DWOPER. Each cross-section is read in as tabular values of channel width and elevation, which together constitute a piece-wise linear relationship. Experience has shown that in almost all instances the cross-section may be sufficiently described with eight or less sets of widths and associated elevations. A low-flow cross-sectional area which can be zero is used to describe the cross-section below the minimum elevation read in. From this input, the cross-sectional area associated with each of the widths is initially computed within the model. During the solution of the unsteady flow equations, any areas or widths associated with a particular water surface elevation are linearly interpolated from the piece-wise linear relationships of width to elevation read in or the area-elevation sets initially generated within the model.

Cross-sections at gaging station locations are always used as computational points in the x-t plane. Cross-sections are also specified at points along the river where significant cross-sectional changes occur or at points where major tributaries enter. Typically, cross-sections for large rivers with slowly varying transients may be spaced as much as 5-20 miles apart. The maximum distance between cross-sections is dependent on the channel properties, duration and rate of rise of the wave, and the computational step size of Δx and Δt. The relation of each to the accuracy of the simulation is defined by Fread (1974). Usually, "average" cross-sections are placed mid-way between cross-sections associated with gaging stations or significant geometry changes. The average cross-section is a weighted average of the cross-sectional properties of the intervening reach. The average cross-section is obtained from a special data processing program in which cross-sections at all sections such as crossings, bends, or other changes in cross-section geometry which violate the assumption of linear variation between adjacent cross-sections are averaged together to obtain a weighted average. The distance between each cross-section is used as the weighting factor.

Off-Channel Storage - Dead storage areas wherein the flow velocity in the x-direction is considered negligible relative to the velocity in the active area of the cross-section is a feature of DWOPER. Such dead or off-channel storage areas can be used to effectively account for embayments, ravines, or tributaries which connect to the flow channel

but do not pass flow and serve only to store the flow. Another effective use of off-channel storage is to model a heavily wooded flood plain which stores a portion of the flood waters passing through the channel. In each of these cases, the use of zero velocity for the portion of the flood waters contained in the dead storage areas results in a more realistic simulation of the actual flow than using an average velocity derived from the main flow channel and the dead storage area. The off-channel storage cross-sectional properties are described in the same way as the active cross-sectional areas, i.e., for each section, a table of top widths and elevations is read in along with the area associated with the lowest elevation. A table of area-elevation is created within DWOPER and intermediate storage top widths or areas are linearly interpolated from the two tables as required.

Roughness Coefficients - Manning's n is used to describe the resistance to flow due to channel roughness caused by bed forms, bank vegetation and obstructions, bend effects, and eddy losses. The Manning n is defined for each channel reach bounded by gaging stations and is specified as a function of either stage or discharge according to a piece-wise linear relation with both n and the independent variable (h or Q) read in to DWOPER in tabular form. Linear interpolation is used to obtain n for values of h or Q intermediate to the tabular values.

Simulation results are often very sensitive to the Manning n. Although in the absence of necessary data (observed stages and discharges), n can be estimated; however, best results are obtained when n is adjusted to reproduce historical observations of stage and discharge. The adjustment process is referred to as calibration. This may be either a trial-error process or an automatic iterative procedure available within DWOPER. The automatic calibration feature is described later.

Lateral Inflows - DWOPER incorporates tributary inflows via the lateral inflow term, q, in Eqs. (1) and (2). The inflows are considered to be independent of flows occurring in the river to which they are added. They are read in as a time series of flows with constant or variable time intervals. They may be specified for any Δx reach along the river. The flow is specified in cfs; it is the sum of all lateral inflow occurring within a particular Δx reach. Outflows may also be simulated by assigning a negative sign to the flow value in the time series. Linear interpolation is used to provide flow values at times other than those of the time series which are determined by the time intervals associated with the flows.

Local Losses - The effects of local head losses incurred at severe contractions and/or expansions such as bridge openings are accounted for by the term S_e as defined by Eq. (4). This necessitates an expansion-contraction coefficient associated with each Δx reach to be read in. The local head loss is in addition to the head losses incurred by the flow resistance due to channel roughness associated with the Manning n.

Wind Effects - The effect of wind resistance on the surface of the flow is accounted for by the term W_f in Eq. (2). W_f is defined as:

$$W_f = C_w(V_r \cos \omega)^2 \tag{8}$$

in which V_r is the velocity of the wind relative to the velocity of the channel flow, ω is the angle between the wind direction and channel flow direction, and C_w is the non-dimensional wind coefficient. C_w may be estimated from empirical studies or it may be assigned a value via a trial-error calibration process.

Lock and Dam Condition - A river system may include small dams with gates to pass the river flow in such a way as to maintain certain water surface elevations on the upstream side of the dam. Usually associated with the dam is a lock for allowing navigation of river craft and barges past the dam. DWOPER can accomodate any number of lock and dam installations within the river system being simulated. A "through" computation scheme is used as opposed to separating the river system into discrete portions because of the lock and dam and specifying external boundary conditions applicable to the lock and dam. The through computation scheme allows the simultaneous simulation of the entire river system including portions with lock and dams. This facilitates data preparation and allows a correct simulation of backwater effects when the tailwater elevation below the dam raises to an elevation such that the pool elevation on the upstream side is no longer controlled by operation of the gates.

In the through computation scheme a specified critical tailwater elevation which is read in for a particular lock and dam is used to determine if the pool elevation is controlled by the gate operation or by channel flow. If the simulated tailwater is less than the critical elevation, the conservation of mass equation, Eq. (1), is replaced by

$$Q_i^{j+1} - Q_{i+1}^{j+1} = 0 \tag{9}$$

and the conservation of momentum equation, Eq. (2), is replaced by

$$h_i^{j+1} - h_t = 0 \tag{10}$$

where h_t is the target pool elevation which the dam tender attempts to maintain via operation of the gates. The target pool elevation may be a constant value or it may be specified as a function of time and read in as a time series.

When the simulated tailwater elevation exceeds the critical tailwater elevation, the flow passes through the dam according to the Eqs. (1) and (2) as in any other Δx reach.

Flow Diversions - Special flow diversions through diversion control structures are accomodated within DWOPER. The model simulates the amount of flow diverted on the basis of the current simulated river elevation on the head water side of the diversion structure, the type and number of diversion gates in operation, and the tailwater elevation on the downstream side of the diversion structure. The latter two must be specified and read in as input data. Currently, DWOPER is programmed for the special flow diversion structures known as Old River Diversion, Morganza Diversion, and Bonnet Carre Diversion; these are all used for diverting flows in the lower Mississippi River. As other diversion structures are encountered in other river systems, they will be added to DWOPER as special subroutines.

Dendritic River Systems - Although the implicit formulation of the unsteady flow equations is well suited for simulating unsteady flows in a system of rivers - in that the response of the system as a whole is determined during each time step - particular care must be given to maintain the necessary solution efficiency as mentioned previously with regards to the matrix solution technique of the Newton-Raphson procedure. An efficient solution technique for dendritic (tree-type) river systems is utilized in DWOPER. This technique, as described by Fread (1973), solves during a time step the unsteady flow equations first for the main stem and then for each tributary of the river system. The tributary flow at the confluence of the tributary and main-stem river is treated as lateral flow q which is first estimated when solving the equations for the main stem.

The tributary flow depends on its upstream boundary condition, lateral inflows along its reach, and the water surface elevation at the confluence which is obtained during the simulation of the main stem. Due to the interdependence of the flows in the main stem and its tributaries, an iterative or relaxation procedure is necessary. Convergence is attained when the estimated tributary flow at the confluence is sufficiently close to the computed flow for the tributary at its downstream boundary using the main stem water surface elevation for the downstream boundary condition. Usually one or two iterations is sufficient for convergence to a suitable tolerance.

DWOPER can accomodate any number of tributaries. Although the iterative algorithm is designed for 1st order tributaries, systems with 2nd order tributaries may sometimes be accomodated by reordering the system, i.e., selecting another branch of the system as the main stem.

Weir-Flow Bifurcations - In DWOPER, any number of Δx reaches along a channel may bypass flow to another channel which connects back into the former channel at some point downstream from the bifurcation. The flow in the bypass channel which may affect the weir flow is accounted for

by a submergence correction to the weir flow. The crest elevation of the overbank section which acts as the weir-flow bypass is specified. Each section has a discharge coefficient which may be estimated or obtained through trial-error calibration. The location along the channel where the bifurcation(s) occur, the average crest elevation of each such dx reach, and the discharge coefficient are read in as input data.

Automatic Calibration - A critical task in the application of one-dimensional hydrodynamic models in natural rivers in dendritic systems is the determination of the roughness parameter in the friction slope term of the momentum equation. The roughness parameter often varies with discharge or stage and with distance along the river. The DWOPER model contains an internal feature which can be accessed to automatically determine the optimum roughness parameter which will minimize the difference between computed and observed values. The automatic calibration feature is a simple and highly efficient optimization technique (Fread and Smith, 1978), for determining the continuous piece-wise linear variation of the roughness parameter with discharge (or stage) for each reach of the river bounded by gaging stations. The optimization technique is based on a decomposition principle which simplifies the treatment of complex river systems of dendritic configuration. Computational requirements are less than twice that required for a normal simulation run in which the roughness parameters are known and calibration is not required.

In the automatic calibration procedure, each reach between gaging stations is calibrated (i.e., a set of optimum roughness coefficients is obtained) sequentially, commencing with the most upstream reach and progressing reach by reach in the downstream direction. Tributaries are calibrated before the main stem river and their flows are added to the main stem as lateral inflows. Discharge is input at the upstream boundary of each river, while observed stages at the downstream gaging station of each reach is used as the downstream boundary condition. Computed stages at the upstream boundary are tested against observed stages at that point. Statistics of bias and root-mean-square (RMS) error are computed for several ranges of discharge or stage so that the roughness coefficient can be calibrated as a function of discharge (stage). For each range of discharge, the adjustment uses the bias to determine the magnitude and whether the change in roughness should be positive or negative. Adjustments are automatically made to the roughness coefficients for the reach and the one reach system is rerun. The cycle is repeated until a minimum RMS error for the reach is found.

The discharges computed at the downstream boundary using the optimum roughness coefficients associated with the minimum RMS error are stored internally and then input as the upstream boundary condition for the next lower reach. An optimum set of roughness coefficients which minimizes RMS errors throughout the river system is determined by proceeding through the river system one reach at a time in a sequence from upstream to downstream and from tributaries to main stem.

Data Management and Display Features - DWOPER consists of three functional elements, each consisting of several subroutines. One element contains the basic algorithms associated with solving the unsteady flow equations for simulating unsteady flows in a river system. The second element is a data management module which provides channel configuration, channel properties such as cross-section geometry and roughness, boundary conditions, and initial conditions for the basic dynamic wave computational element. The third element displays the simulation results in either graphical or tabular form.

Preparation of the data for simulation of a river system requires a substantial amount of work. The river system configuration, cross-sections, etc. must be determined and coded. Stage and discharge data for the boundary and initial conditions must be determined and card coded. This initial work cannot be avoided; however, the data management module does substantially reduce the time and effort required to use the model on a day-to-day operational basis. The data initially card coded to simulate a particular river system are kept on disk, a direct access peripheral mass storage, and only the updated information for boundary conditions need be card coded and read in before a new simulation can be made.

The data stored on disk are of two types: stationary data which does not change with time and stage-discharge data which must be updated as new observations are reported. The stationary data are stored in "carryover" files and stage-discharge data are stored in "hydrograph" files. In order to perform a forecasting run, the river system configuration and physical properties must be determined by retrieving the data in a carryover file and the stage-discharge data must be retrieved from a hydrograph file. After the initial simulation run, the initial conditions which consist of the stages and discharges at every computational point in the river system are available in the carryover file as computed stages and discharges which have been stored from a previous run.

Each carryover and hydrograph file is identified by a unique name. Since any number of carryover and hydrograph files can exist in mass storage, DWOPER searches the carryover files for the name that matches that specified for the current simulation run. With the correct carryover file retrieved, DWOPER then searches the hydrograph files for those hydrographs labeled with the same names as specified in the carryover file. The hydrographs in the file have names which must match the labels in the carryover file. When a match is found, data for the appropriate time period are extracted from the hydrograph file for use in the simulation. The label system allows the two types of data (stationary and hydrograph) to be stored separately and combined properly prior to the computation sequence of a simulation run. Thus, new data which arrive in day-to-day operations need to be added to the hydrograph file.

The data management element, the dynamic wave computational element, and the forecast display element are accessed by commands. Each command causes the program to branch to appropriate subroutines where the desired function is performed. Some of the more significant data management commands are:

1) COINIT - The Carryover file is initialized, i.e., the river configuration, cross-section properties, etc., are read in.
2) HINIT - The Hydrograph file is initialized, i.e., the hydrograph values are read in.
3) COEDIT - Any stationary data contained in the carryover file may be updated by simple reference indicators punched on input cards along with the updated value(s).
4) HEDIT - Any data contained in the hydrograph file may be deleted, replaced, or added to by simple label and time period indicators punched on input cards along with the new hydrograph values.
5) COLIST - List the contents of a particular carryover file.
6) HLIST - List the contents of a particular hydrograph file.

Some of the commands used to activate the dynamic wave computational element are:

1) RUN - Simulates a river system using data from carryover and hydrograph files stored on disk.
2) ICSAVE - A command used concurrently with RUN command. ICSAVE is used to save the water surface elevations and discharges at all computational points at a specified time. These values are retained in peripheral storage for use in subsequent simulation runs as the appropriate and necessary initial conditions.
3) ALONE - Simulates a river system using data (river system configuration, cross-section properties, hydrograph values at boundaries, etc.) read in on cards at the same time as the ALONE command is read in.

One of the commands used to activate the forecast display element is:

1) DISPLAY - A command used concurrently with RUN command. DISPLAY has various options. One of which is: the computed stages, discharges, velocities, and observed stages for all gaging stations within the

river system being simulated will be printed for a single time step. Another option is: the computed stages and observed stages at a single gaging station can be displayed for a selected period up to 12 time steps.

If the DISPLAY command is not used, DWOPER will provide the following output:

1) graphs showing computed and observed values of stage or discharge at selected gaging stations;
2) a list of the stages or discharges which are plotted and;
3) bias and root-mean-square error statistics for computed and observed values at each selected gaging station.

Simulation runs using data from carryover and hydrograph files require essentially the same CPU time as a simulation run using the ALONE command in which the data is read in as cards during the initial stages of the simulation.

Computer Core and Computational Requirements - DWOPER has been created using the programming feature, "variable dimensioning". This enables the size of the arrays of subscripted variables such as observed hydrograph stages, cross-section top widths, computed stages and discharges, etc., to be changed from one simulation run to the next. There is a maximum total size for the sum of all arrays, but within that bound the allocation of core space among the variables is flexible and is specified as a data input which is retained in the carryover file. This flexibility allows maximum use of the core set apart for DWOPER. Actually, three sizes of DWOPER are used in operational forecasting with the smallest version used on all river systems which will fit within its array size. The small version of DWOPER requires 170 K words having 8 bits per word. The medium and large versions require 235 and 300 K words of memory storage, respectively.

Another programming feature known as "overlaying", in which groups of subroutines are loaded into core as needed, is used to reduce the required core to that mentioned above.

The implicit formulation of the basic dynamic wave computational element allows the time step size to be selected according to accuracy requirements rather than numerical stability considerations. This factor makes DWOPER very efficient in the use of computer time. Efficiency due to the implicit formulation compared to computational requirements of explicit finite difference models is greatest for

slowly varying transients in large rivers and decreases as the transient being modeled becomes more rapidly varying. Computational requirements are approximately 0.004 sec/time step/distance step. Some examples of total computational time (IBM 360/195) are:

1) Mississippi-Ohio-Cumberland-Tennessee River system: consisting of 393 miles of river, 45 computational points, 3 months of simulation time, 20 observed and computed hydrographs; slowly varying flood wave simulation using 24 hour time steps required 15 seconds of CPU time.
2) Lower Mississippi River: consisting of 292 miles of river, 25 computational points, 2 months of simulation time, 7 observed and computed hydrographs; slowly varying flood wave simulation using 24 hour time steps required 6 seconds of CPU time.
3) Lower Columbia and Willamette River system: consisting of 155 miles of river, 25 computational points, 9 days of simulation time, 10 observed and computed hydrographs; tidal flows with 12 hour period and 1-hour time steps required 19 seconds of CPU time.

SELECTED APPLICATIONS

Lower Mississippi - DWOPER was applied to a 291.7 mile reach of the Lower Mississippi River from Red River Ldg. to Venice shown schematically in Fig. 2. Six intermediate gaging stations at Baton Rouge, Donaldsonville, Reserve, Carrollton, Chalmette, and Ft. a la Hache were used to evaluate the simulations.

This reach of the Lower Mississippi is contained within levees for most of its length, although some overbank flow occurs along portions of the upper 70 miles. Throughout this reach, the alluvial river meanders between deep bends and relatively shallow crossings; the sinuosity coefficient is 1.6. The low flow depth varies from a minimum of 30 feet at some crossings to a maximum depth of almost 200 feet in some bends. The average channel width is approximately one-half mile. The average channel bottom slope is a very mild 0.034 ft/mi. The discharge varies from low flows of about 100,000 to flood discharges of over 1,200,000 cfs. A total of 25 cross-sections located at unequal intervals ranging from 5-20 miles were used to describe the 291.7 mile reach.

The reach was first automatically calibrated by DWOPER for the 1969 spring flood. Time steps of 24 hours were used. Then, using the calibrated set of Manning n vs. discharge for each reach bounded by

gaging stations, the 1969 flood was simulated using stage hydrographs for upstream and downstream boundaries at Red River Ldg. and Venice, respectively. The simulated stage hydrographs at the six intermediate gaging stations are compared with the observed in Figs. 3-5. The root-mean-square (RMS) error was used as a statistical measure of the accuracy of the calibration. The RMS error varied from 0.17-0.36 feet with an average value of 0.25 feet.

Several historical floods from the period 1959-1971 were then simulated using the calibrated Manning n values obtained from the 1969 flood. An example of simulated vs. observed stages is shown in Figs. 6-8 for the 1966 flood. Average RMS errors for all six stations for each of the simulated floods are shown in Table 1. The average RMS error for all the floods was 0.47 feet. This compares with 0.25 feet for the calibrated flood of 1969, indicating that for this reach of the Mississippi there is not a significant change in the channel roughness from one flood event to another.

Mississippi-Ohio-Cumberland-Tennessee System - A dendritic river system consisting of 393 miles of the Mississippi-Ohio-Cumberland-Tennessee (MOCT) River system was also simulated using DWOPER. A schematic of the river system is shown in Fig. 9. Eleven intermediate gaging stations located at Fords Ferry, Golconda, Paducah, Metropolis, Grand Chain, Cairo, New Madrid, Red Rock, Grand Tower, Cape Girardeau, and Price Ldg. were used to evaluate the simulation.

In applying DWOPER to this system, the main-stem river is considered to be the Ohio-Lower Mississippi segment with the Cumberland, Tennessee, and Upper Mississippi considered as first-order tributaries. The channel bottom slope is mild, varying from about 0.25 to 0.50 ft/mi. Each branch of the river system is influenced by backwater from downstream branches. Total discharge through the system varies from low flows of approximately 120,000 cfs to flood flows of 1,700,000 cfs. A total of 45 cross-sections located at unequal intervals ranging from 0.5-21 miles were used to describe the MOCT river system.

The MOCT system was calibrated to determine the n-Q relationship for each of 15 reaches bounded by gaging stations. Time steps of 24 hours were used. About 25 seconds of IBM 360/195 CPU time were required by DWOPER to perform the calibration. The flood of 1970 was used in the automatic calibration process. The average RMS error for all 15 reaches was 0.60 feet. A typical comparison of observed and simulated stages for the Cairo and Cape Girardeau gaging stations is shown in Fig. 10.

Using the calibrated n-Q relations, the 1969 flood was simulated with DWOPER. Stage hydrographs at Shawneetown and Chester and discharge hydrographs at Barkley Dam and Kentucky Dam were used as upstream boundary conditions, and a rating curve was used as the downstream boundary condition at Caruthersville. Fig. 11 shows the simulated vs. observed

stages for Cairo and Cape Girardeau. The average RMS error for the 11 intermediate gaging stations was 0.56 feet.

Columbia-Willamette System - DWOPER was applied to the 130 mile reach of the lower Columbia River below Bonneville Dam, including the 25-mile tributary reach of the lower Willamette River. A schematic of the river system is shown in Fig. 12.

This reach of the Columbia has a very flat slope (0.06 ft/mi) and the flows are affected by tides from the Pacific Ocean. The tidal effect extends as far upstream as the tailwater of Bonneville Dam during periods of low flow. Reversals in discharge during low flow are possible as far upstream as Vancouver. A total of 25 cross-sections located at unequal distance intervals ranging from 0.5-12 miles were used to describe the river system. One hour time steps were used in the simulations.

The system was first calibrated for a 4-day period in August 1973. Seven intermediate gaging stations at Warrendale, Washougal, Vancouver, Portland, Columbia City, Rainier, and Wauna were used along with the gaging stations at the extremities of the system, i.e., Bonneville, Oregon Falls, and Tongue Pt. Another 5-day period in August 1973 was then simulated using DWOPER and the calibrated n-Q relations. Upstream and downstream boundaries were observed discharges and stages, respectively. The average RMS error for all stations in the simulation run was 0.21 feet. Some examples of simulated and observed stage hydrographs for Warrendale, Vancouver, Portland, and Wauna are shown in Figs. 13 and 14.

SUMMARY AND CONCLUDING REMARKS

An operational hydrodynamic model (DWOPER) developed by the Hydrologic Research Laboratory of the National Weather Service is being placed in operational use by River Forecast Centers on a number of major river systems where storage routing methods are inadequate due to the effects of backwater, tides, and mild channel bottom slopes. The model is based on the complete one-dimensional St. Venant equations and belongs to the category of dynamic wave flood routing models. A weighted four-point nonlinear implicit finite difference scheme is used to obtain solutions to the St. Venant equations via a Newton-Raphson iterative technique.

DWOPER has a number of features which make it applicable to a variety of natural river systems for real-time forecasting. It is designed to accommodate various boundary conditions and irregular cross-sections located at unequal distances along a single multiple-reach river or several such rivers having a dendritic configuration. It allows for

roughness parameters to vary with location and stage or discharge. Temporally varying lateral inflows, wind effects, bridge effects, off-channel storage, weir-flow channel bifurcations are included among its features. Time steps are chosen solely on the basis of desired accuracy since the implicit finite difference technique is not restricted to the very small time steps of explicit techniques due to numerical stability considerations. This enables DWOPER to be very efficient as to computational time for simulating slowly varying floods of several days duration. An efficient automatic calibration procedure for determining optimum Manning n - stage or discharge relationships from observed data is provided as an option in DWOPER. Data handling requirements for day-to-day river forecasting are minimal due to extensive data management features utilizing disk or tape storage. Operationally, card coding is only required to update hydrograph files with the most recent observations.

Applications of DWOPER to several large river systems have demonstrated its operational efficiency, accuracy, and utility. The model is currently being extended to account for effects of channel sinuosity and flood plains (Fread, 1976), sediment transport (Chen and Simons, 1975), and bank storage on unsteady flows in alluvial rivers. Also, it has been coupled to an unsteady temperature transport model (Bowles, et al., 1977) for development as a river temperature forecasting model.

APPENDIX I. - REFERENCES

1. Amein, M., and Fang, C. S., "Implicit Flood Routing in Natural Channels," Journal of the Hydraulics Division, ASCE, Vol. 96, No. HY12, 1970, pp. 2481-2500.

2. Amein, M., and Chu, H. L., "Implicit Numerical Modeling of Unsteady Flows," Journal of the Hydraulics Division, ASCE, Vol. 101, No. HY6, 1975, pp. 717-1431.

3. Baltzer, R. A., and Lai, C., "Computer Simulation of Unsteady Flows in Water-Ways," Journal of the Hydraulics Division, ASCE, Vol. 94, No. HY4, 1968, pp. 1083-1117.

4. Bowles, D. S., Fread, D. L., and Grenney, W. J., "Coupled Dynamic Streamflow Temperature Models," Journal of the Hydraulics Division, ASCE, Vol. 103, No. HY5, 1977, pp. 515-530.

5. Chaudhry, Y. M., and Contractor, D. N., "Application of Implicit Method to Surges in Channels," Water Resources Research, Vol. 9, No. 6, 1975, pp. 1605-1612.

6. Chen, Y. H., and Simons, D. B., "Mathematical Modeling of Alluvial Channels," Modeling 75 Symposium of Modeling Techniques, ASCE, Vol. 1, September 1975, pp. 466-483.

7. Fread, D. L., "Discussion of Implicit Flood Routing in Natural Channels," M. Amein and C. S. Fang, Journal of the Hydraulics Division, ASCE, Vol. 99, No. HY7, 1971, pp. 1156-1159.

8. Fread, D. L., "Effect of Time Step Size in Implicit Dynamic Routing," Water Resources Bulletin, AWRA, Vol. 9, No. 2, 1973a, pp. 338-351.

9. Fread, D. L., "Technique for Implicit Dynamic Routing in Rivers with Major Tributaries," Water Resources Research, Vol. 9, No. 4, 1973b, pp. 918-926.

10. Fread, D. L., "Numerical Properties of Implicit Four-Point Finite Difference Equations of Unsteady Flow," NOAA Technical Memorandum NWS HYDRO 18, NOAA, March 1974, pp. 88.

11. Fread, D. L., "Discussion of Comparison of Four Numerical Methods for Flood Routing," R. K. Price, Journal of the Hydraulics Division, Vol. 101, No. HY3, 1975, pp. 363-367.

12. Fread, D. L., "Flood Routing in Meandering Rivers with Flood Plains," Rivers '75, Vol. I, Symposium on Inland Waterways for Navigation, Flood Control and Water Diversions, Colorado State University, August 10-12, Harbors and Coastal Engineering Division of ASCE, 1976, pp. 16-35.

13. Fread, D. L., and Smith, G. F., "Calibration Technique for One-Dimensional Unsteady Flow Models," Journal of the Hydraulics Division, ASCE, Vol. 104, July 1978 (in press).

14. Linsley, R. K., Kohler, M. A., and Paulhus, J. L., Hydrology for Engineers, McGraw-Hill Book Co., New York, 1958, pp. 216-244.

15. Monro, J. C., and Anderson, E. A., "National Weather Service River Forecasting System, Journal of the Hydraulics Division, ASCE, Vol. 100, No. HY5, 1974, pp. 621-630.

16. Preissmann, A., "Propagation of Translatory Waves in Channels and Rivers," First Congres de l'Assoc. Francaise de Calcul, Grenoble, France, 1961, pp. 433-442.

17. Quinn, F. H., and Wylie, E. B., "Transient Analysis of the Detroit River by the Implicit Method," Water Resources Research, Vol. 8, No. 6, 1972, pp. 1461-1469.

Table 1.—Summary of flood simulations in Lower Mississippi River (Red River Ldg. to Venice) for the years 1959-71

Year	Average RMS error (ft.)	Peak discharge (1,000 cfs)
1959	0.62	750
1960	.31	850
1961	.47	1,220
1962	.61	1,155
1963	.38	950
1964	.51	1,140
1965	.44	1,040
1966	.38	1,090
1967	.38	700
1968	.36	980
1969*	.25	1,065
1970	.91	1,080
1971	.46	940

*Calibrated

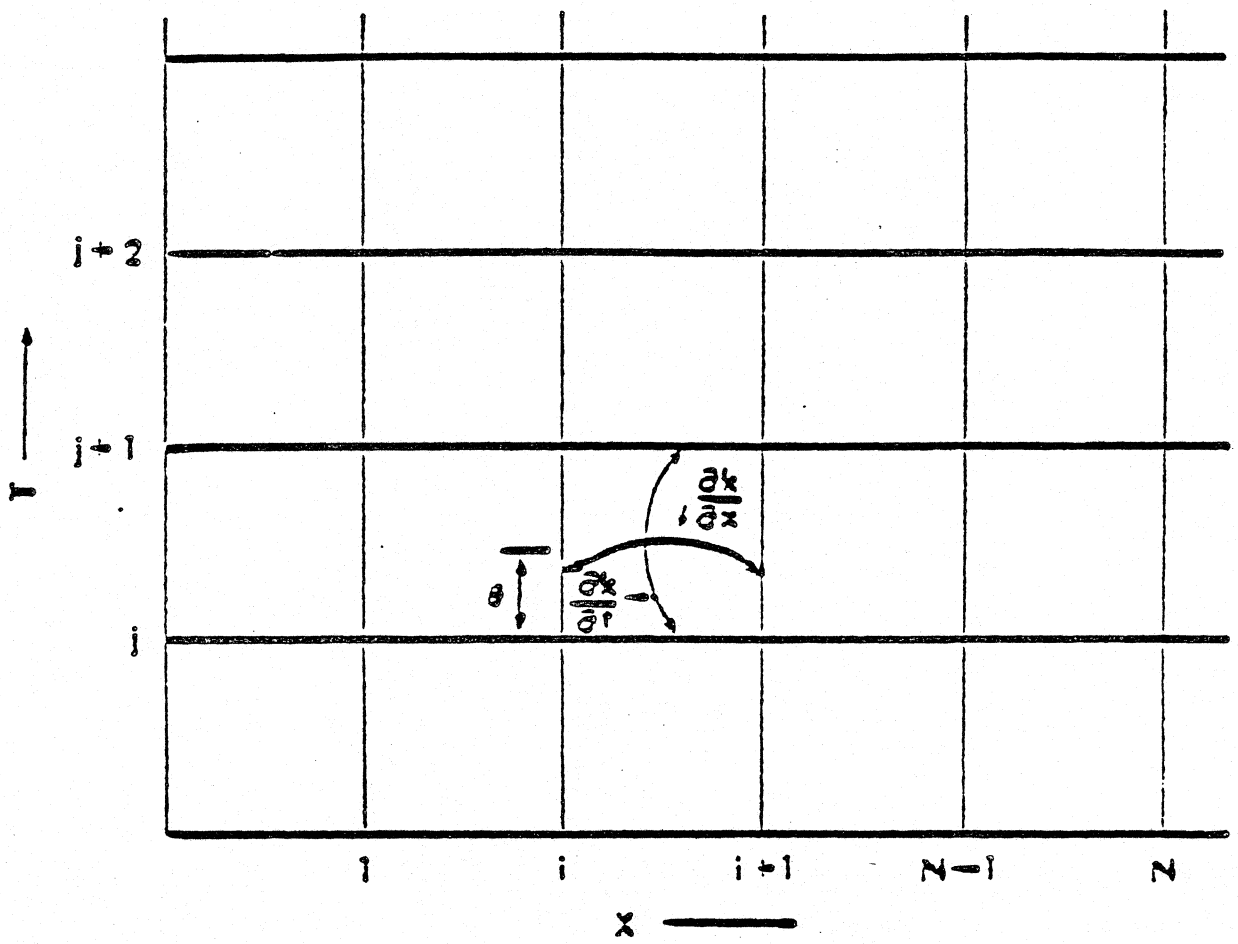

FIG. 1 - DISCRETE X-T SOLUTION DOMAIN

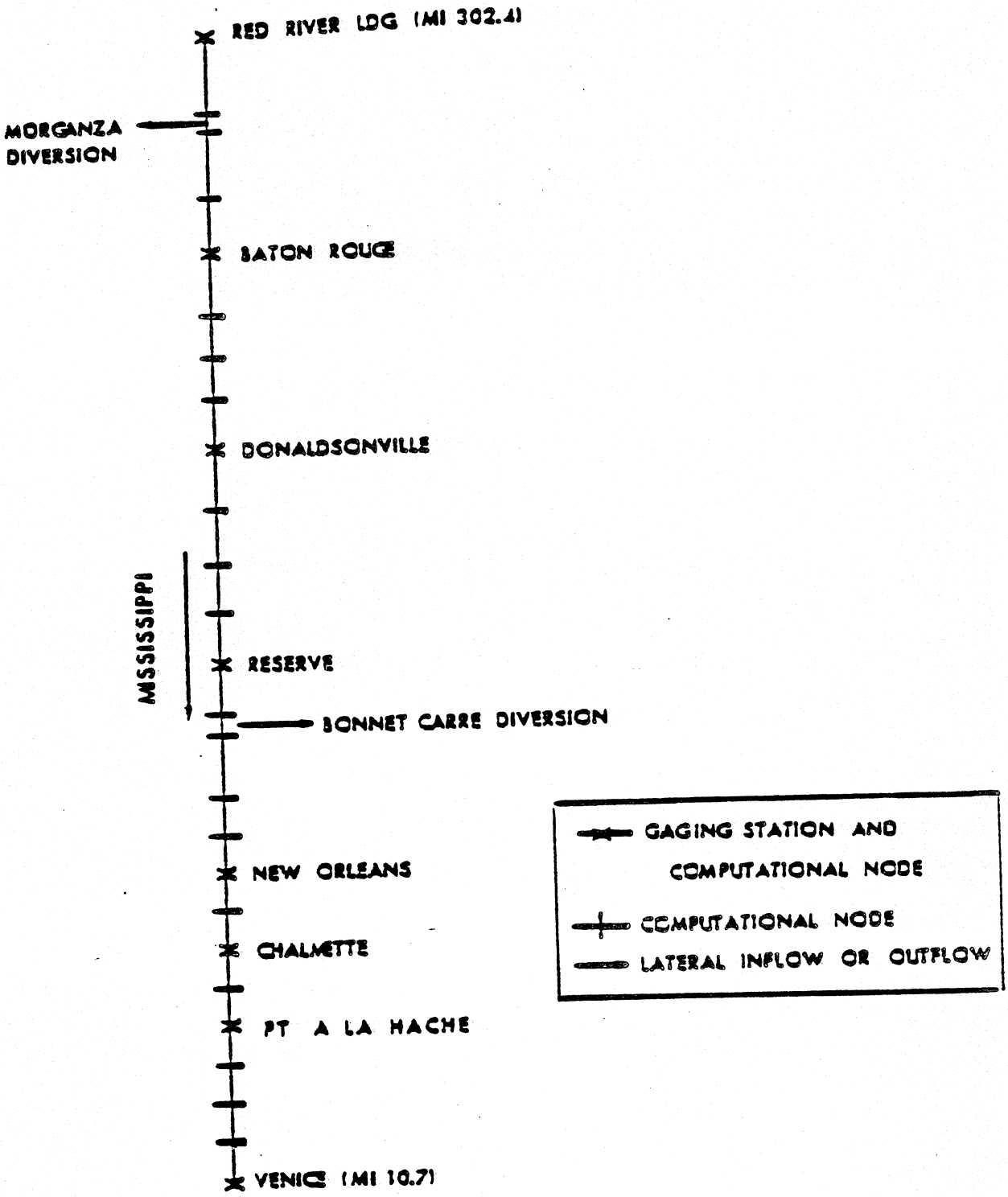

FIG. 2 - SCHEMATIC OF LOWER MISSISSIPPI RIVER

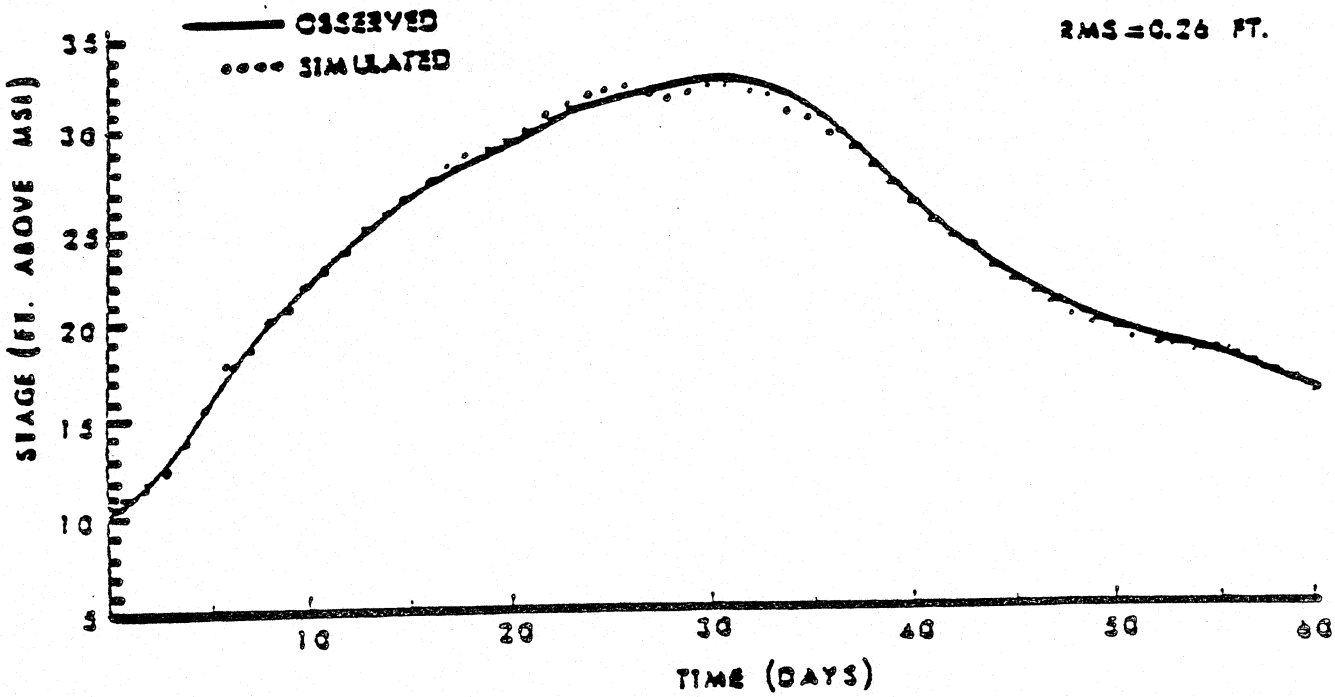

FIG. 3a - OBSERVED VS. SIMULATED STAGES AT BATON ROUGE FOR 1969 FLOOD

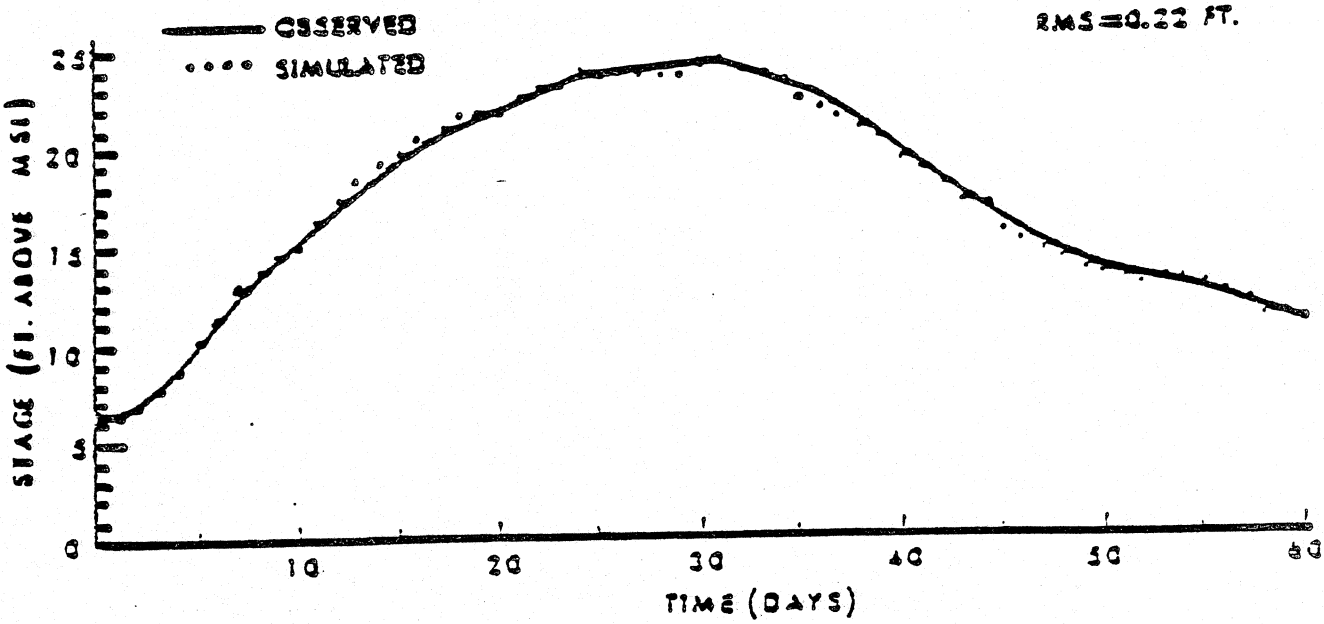

FIG. 3b - OBSERVED VS. SIMULATED STAGES AT DONALDSONVILLE FOR 1969 FLOOD

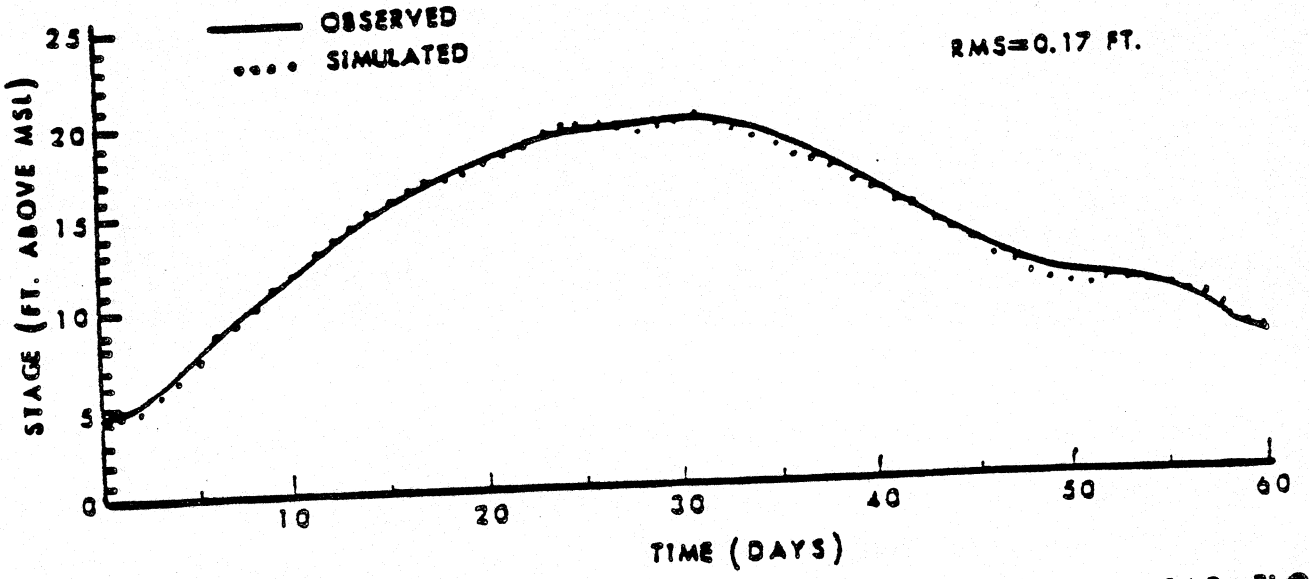

FIG. 4a - OBSERVED VS. SIMULATED STAGES AT RESERVE FOR 1969 FLOOD

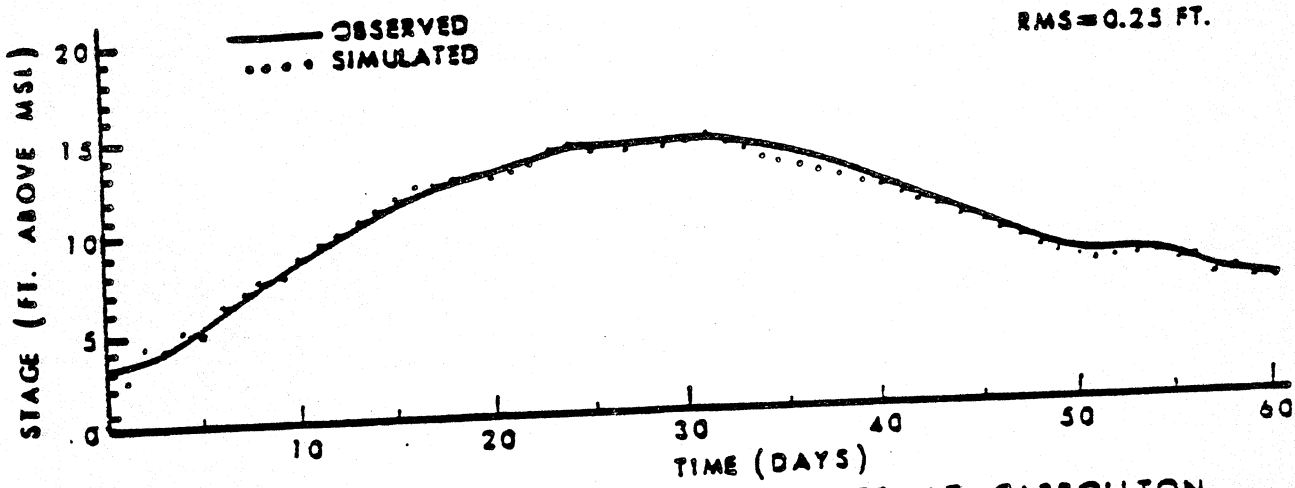

FIG. 4b - OBSERVED VS. SIMULATED STAGES AT CARROLLTON (NEW ORLEANS) FOR 1969 FLOOD

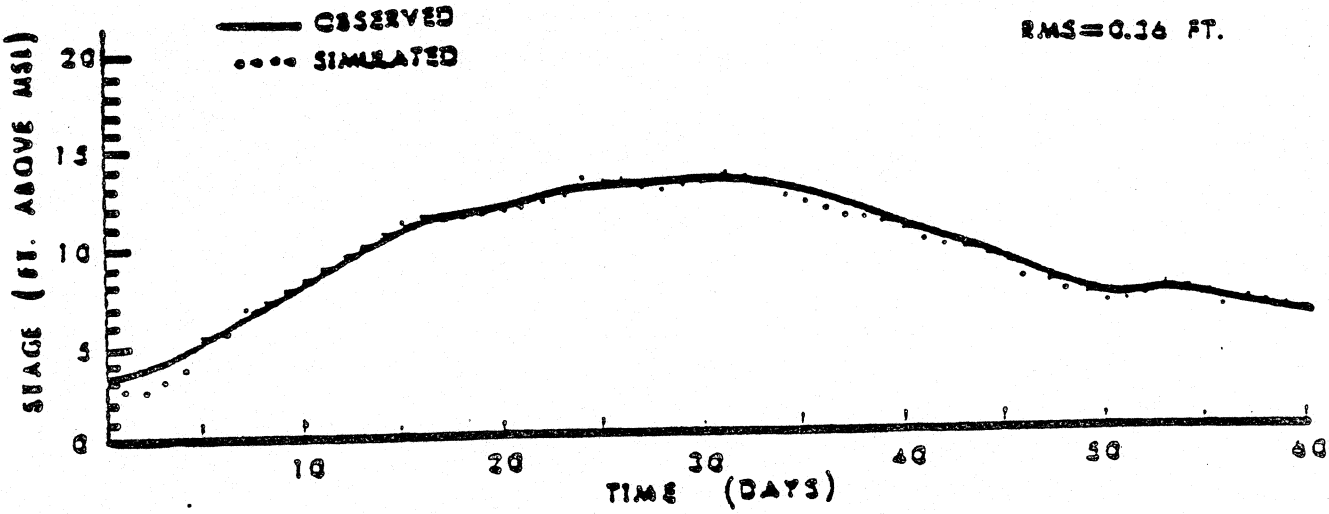

FIG. 5a - OBSERVED VS. SIMULATED STAGES AT CHALMETTE FOR 1969 FLOOD

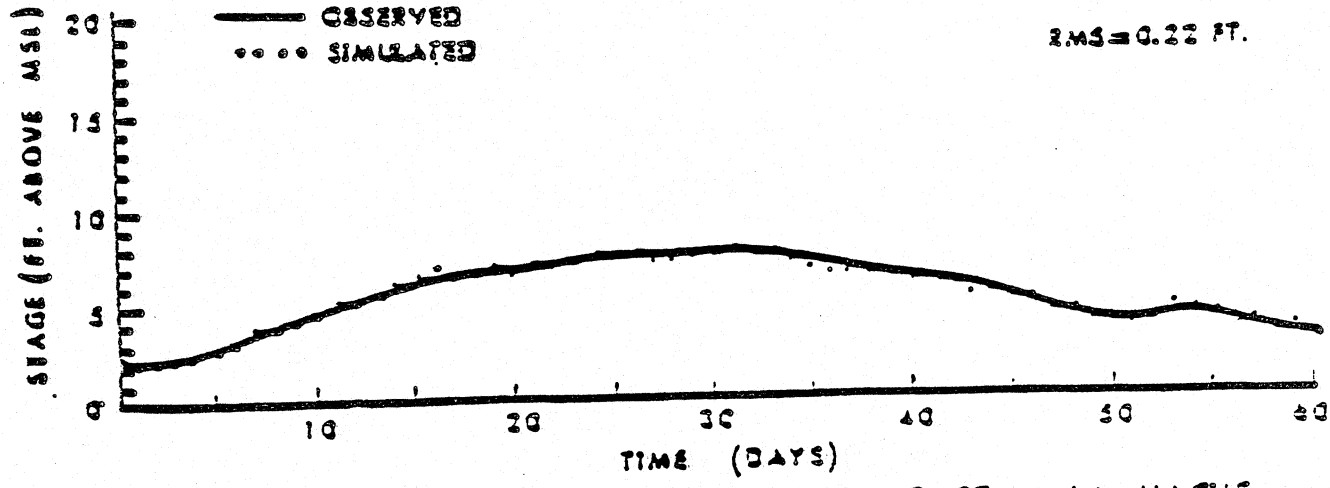

FIG. 5b - OBSERVED VS. SIMULATED STAGES AT PT. A LA HACHE FOR 1969 FLOOD

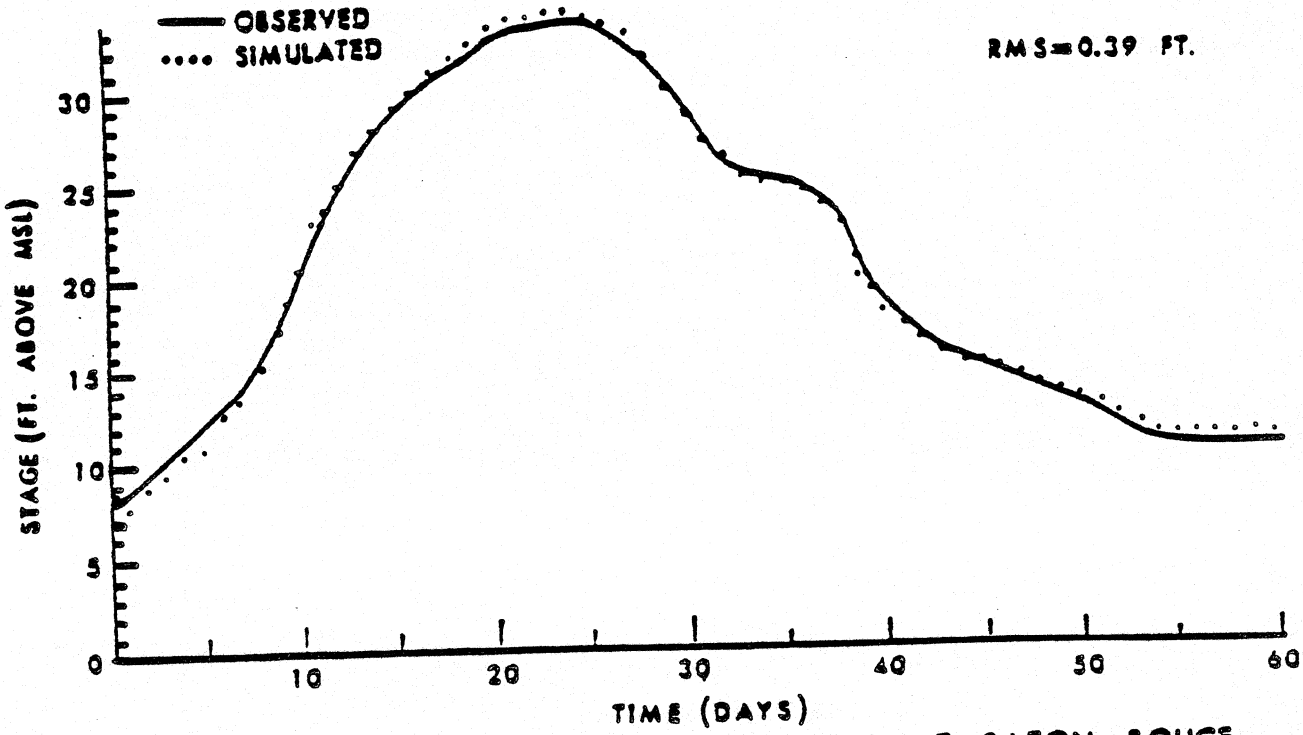

FIG.6a - OBSERVED VS. SIMULATED STAGES AT BATON ROUGE FOR 1966 FLOOD

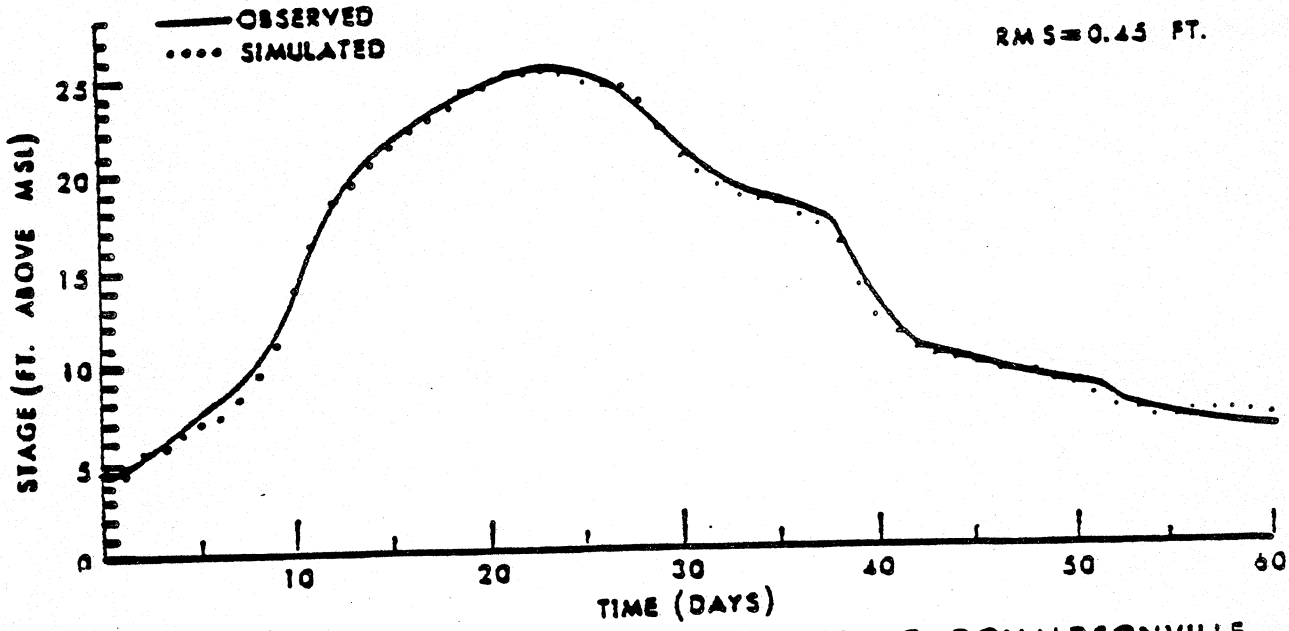

FIG. 6b - OBSERVED VS. SIMULATED STAGES AT DONALDSONVILLE FOR 1966 FLOOD

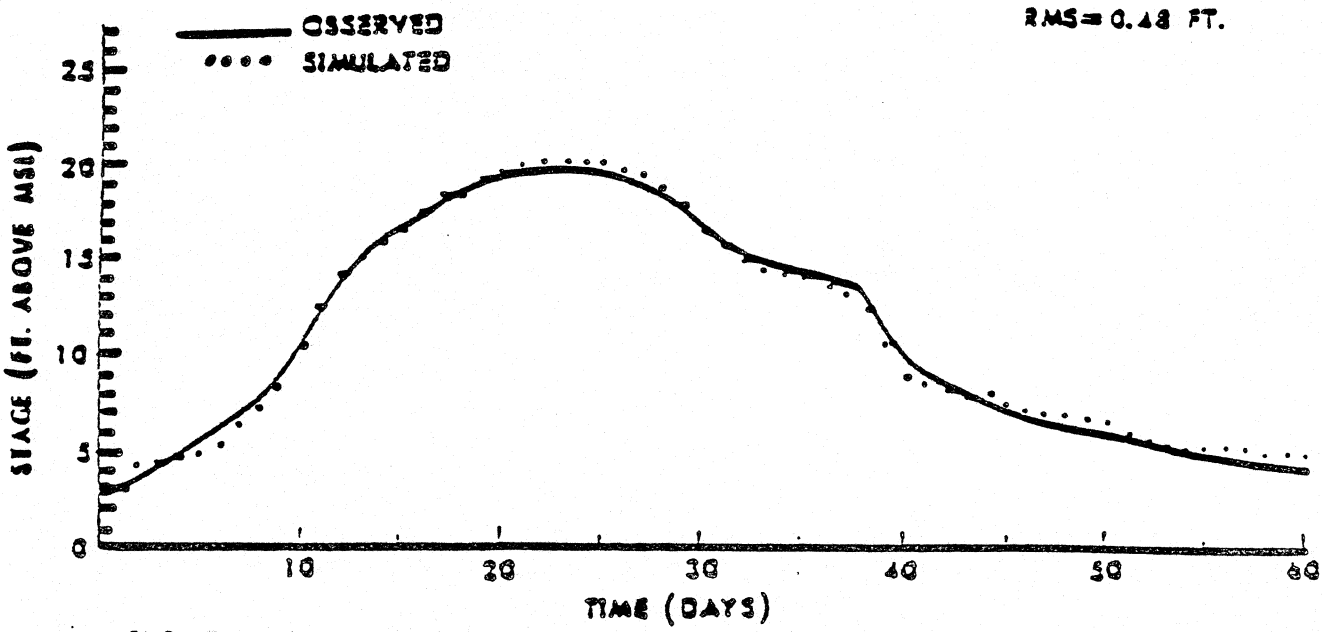

FIG. 7a - OBSERVED VS. SIMULATED STAGES AT RESERVE FOR 1966 FLOOD

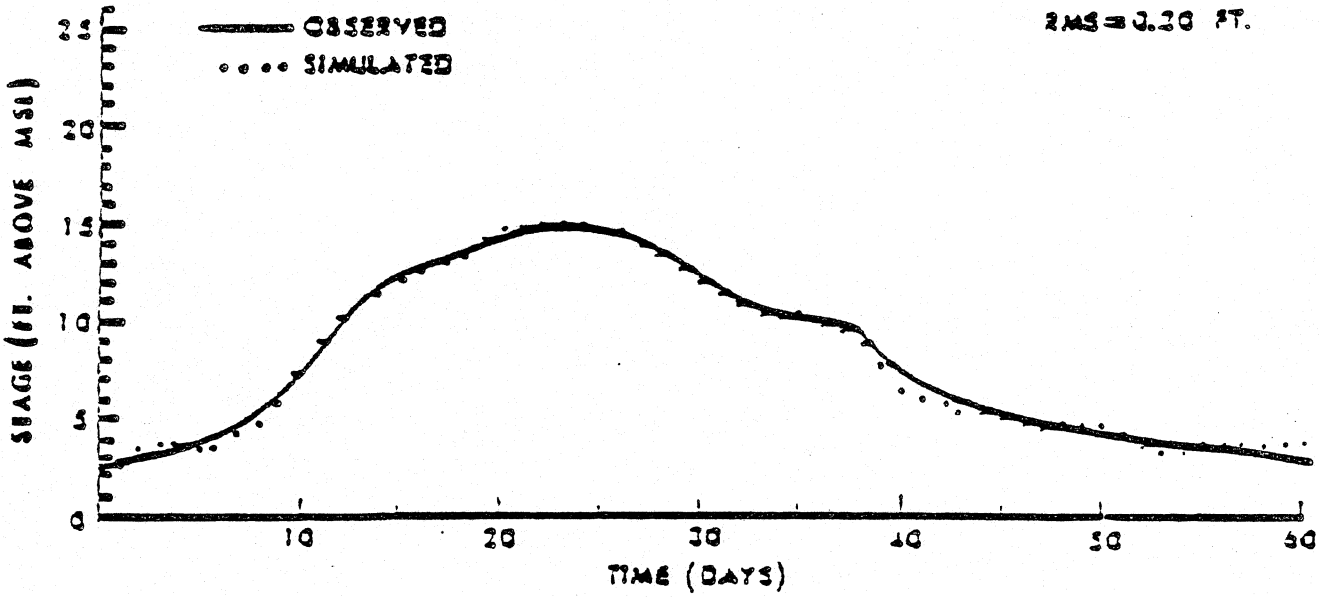

FIG. 7b - OBSERVED VS. SIMULATED STAGES AT CARROLLTON (NEW ORLEANS) FOR 1966 FLOOD

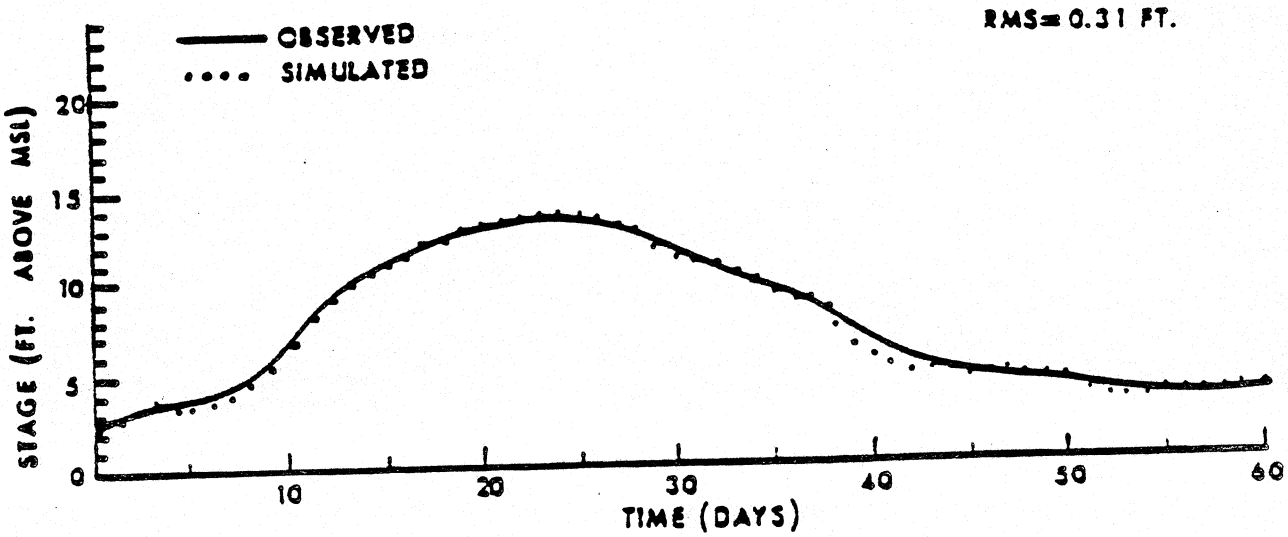

FIG. 8a- OBSERVED VS. SIMULATED STAGES AT CHALMETTE FOR 1966 FLOOD

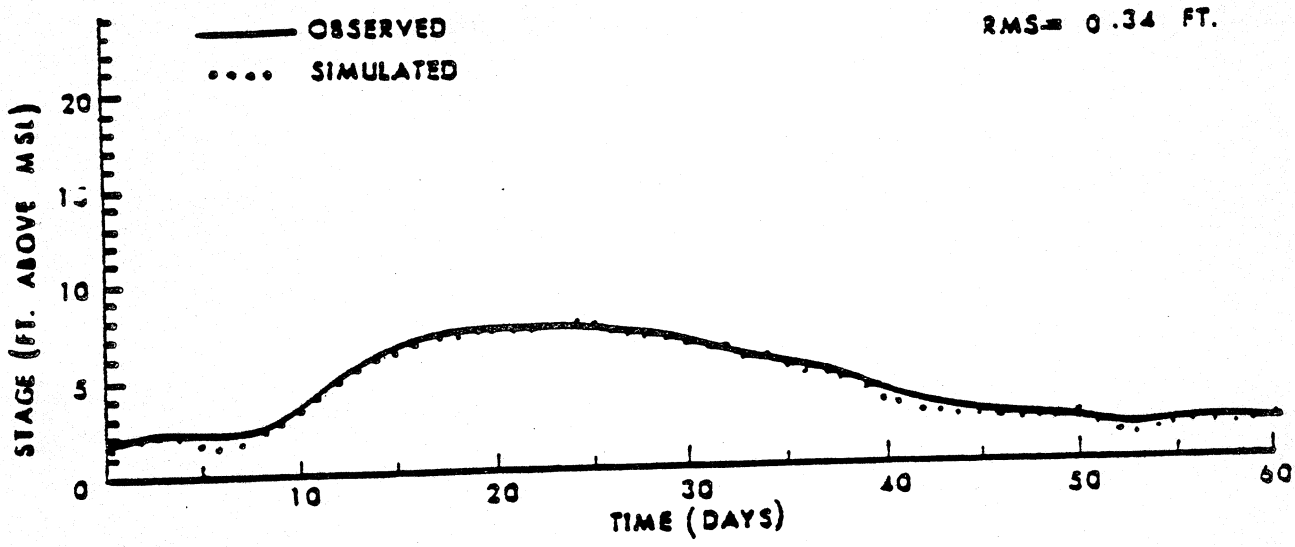

FIG. 8b - OBSERVED VS. SIMULATED STAGES AT PT. A LA HACHE FOR 1966 FLOOD

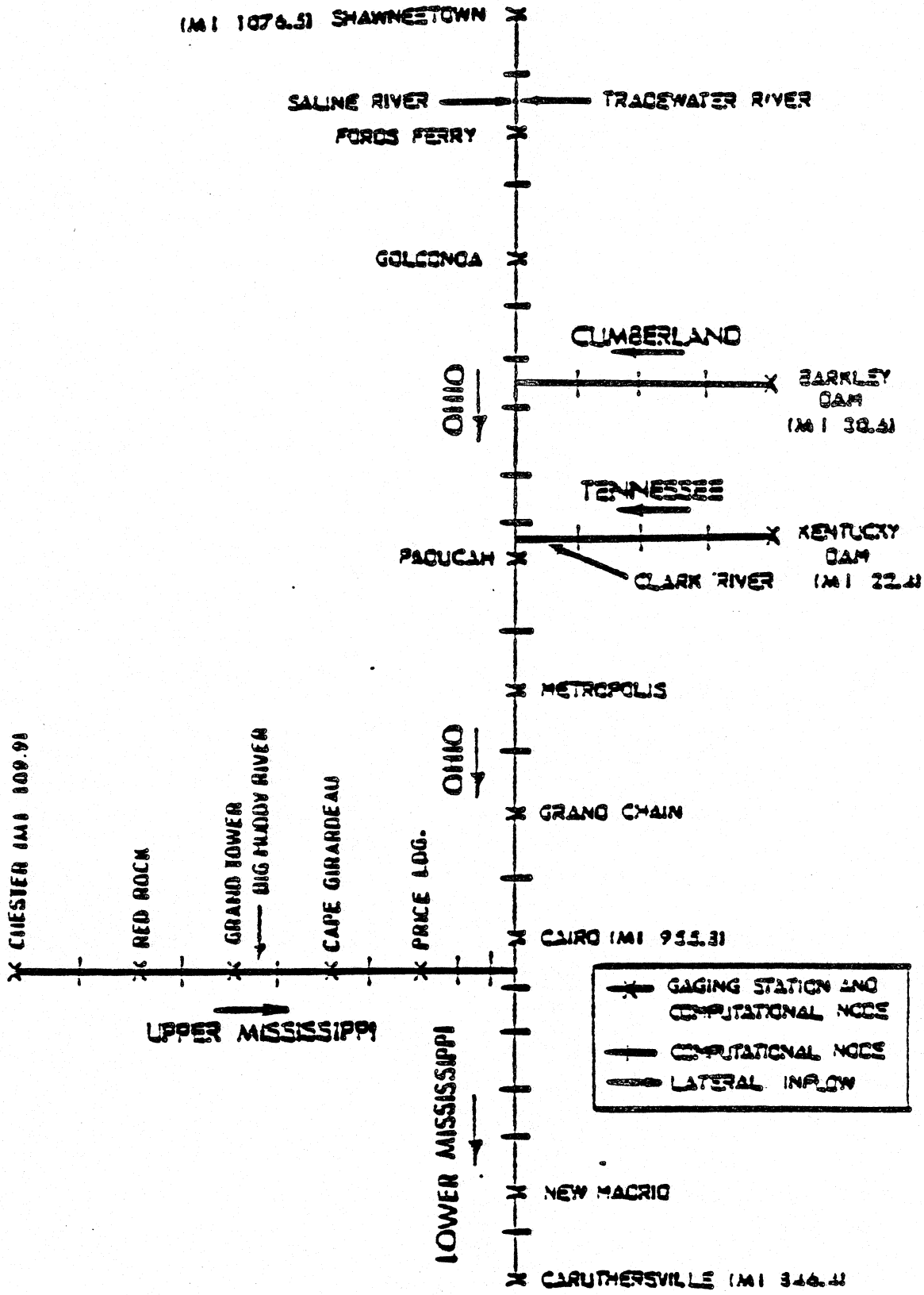

FIG. 9 - SCHEMATIC OF MISSISSIPPI-OHIO-CUMBERLAND-TENNESSEE (MOCT) RIVER SYSTEM

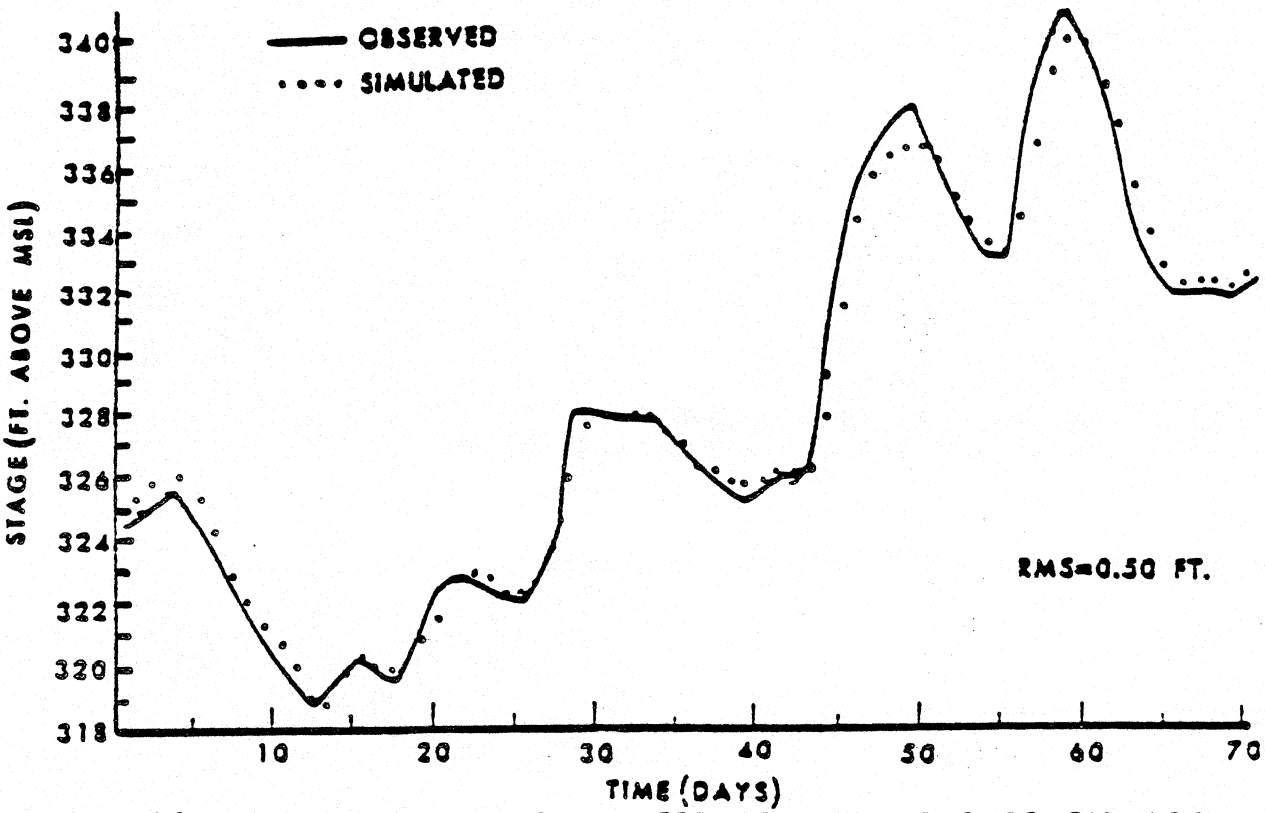

FIG. 10a - OBSERVED VS. SIMULATED STAGES AT CAPE GIRARDEAU FOR 1970 FLOOD

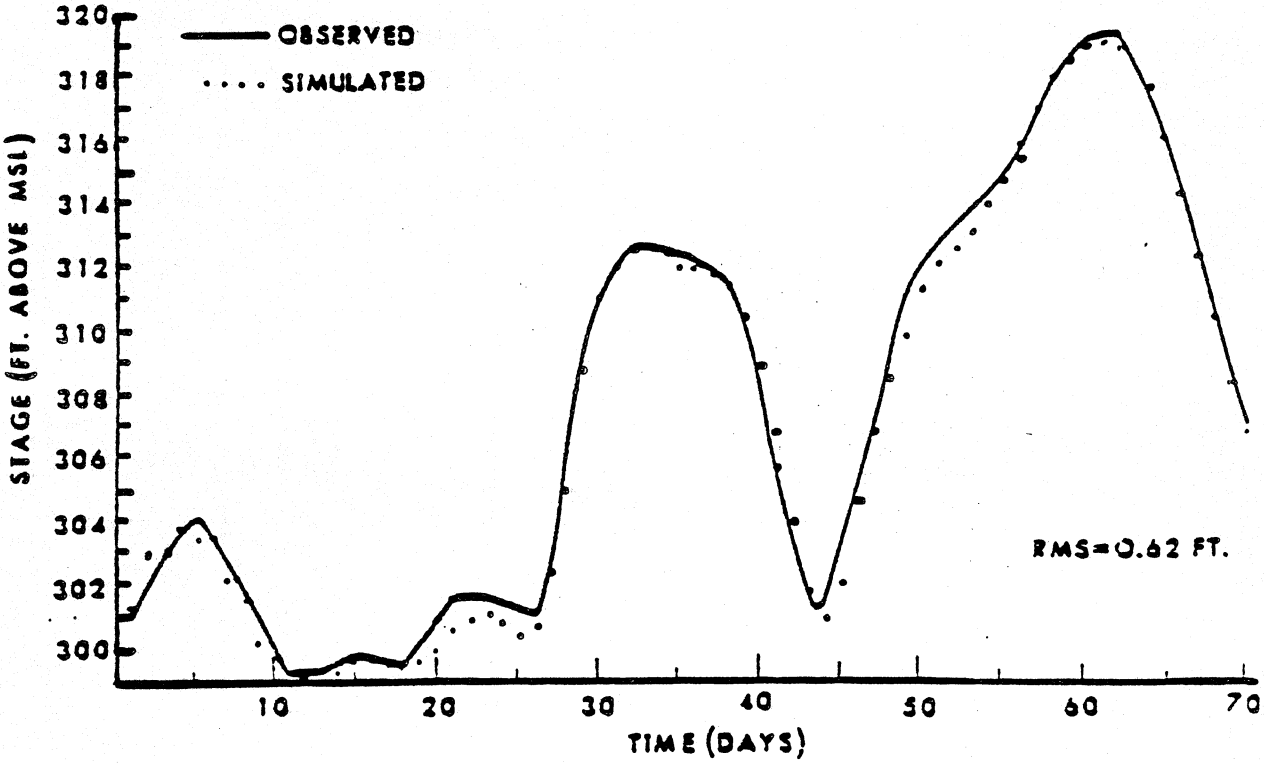

FIG. 10b - OBSERVED VS. SIMULATED STAGES AT CAIRO FOR 1970 FLOOD

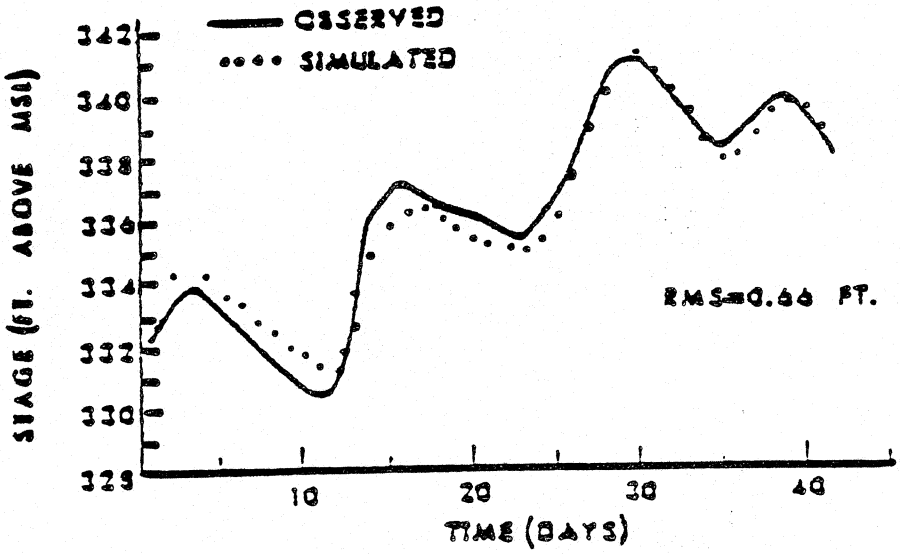

FIG. 11 a - OBSERVED VS. SIMULATED STAGES AT CAPE GIRARDEAU FOR 1969 FLOOD

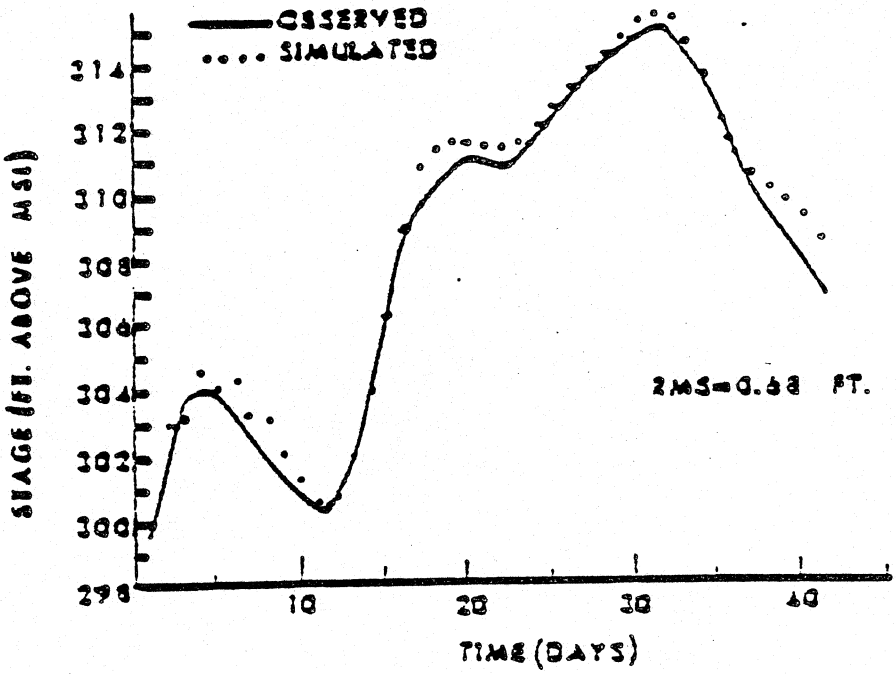

FIG. 11 b - OBSERVED VS. SIMULATED STAGES AT CAIRO FOR 1969 FLOOD

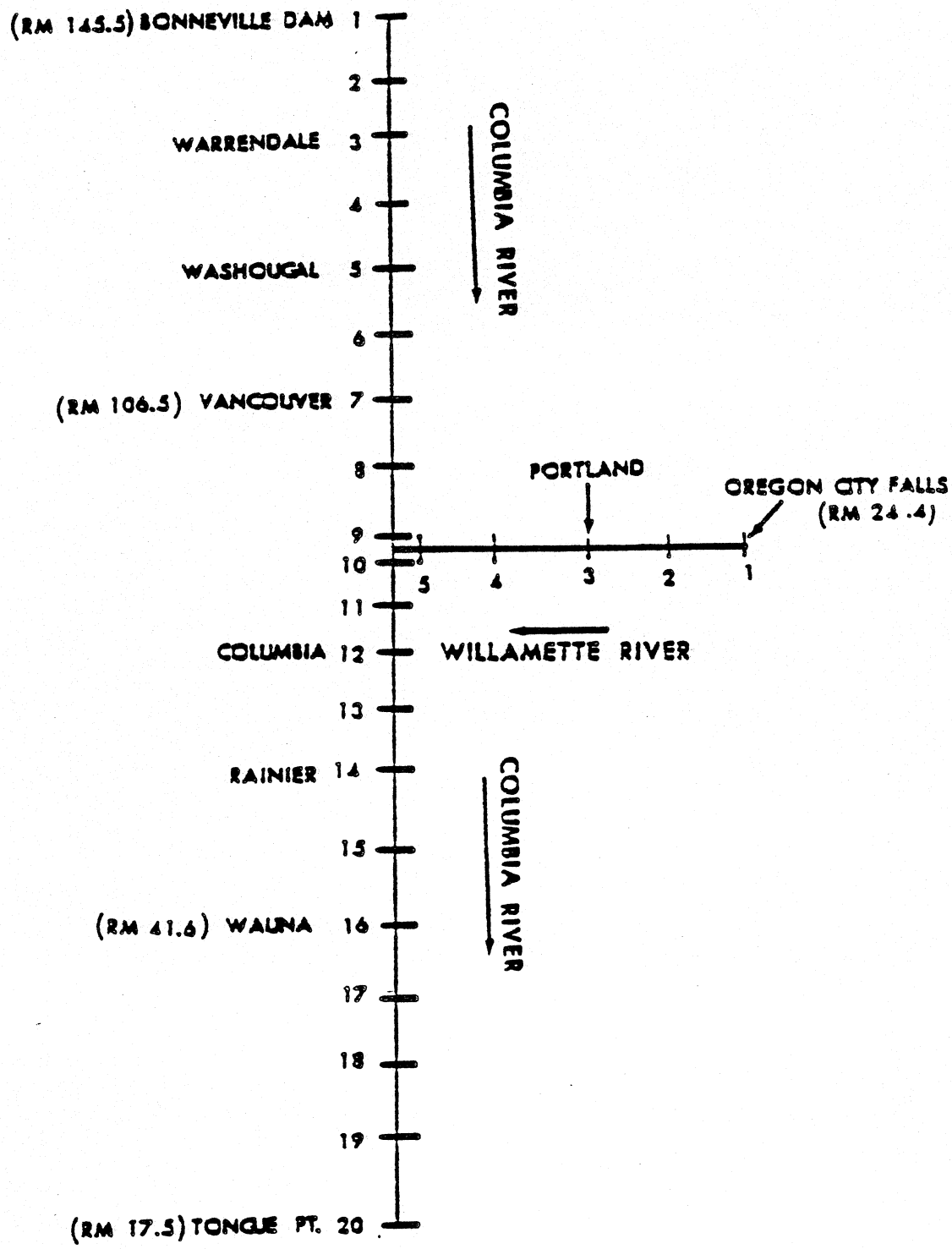

FIG. 12 - SCHEMATIC LOWER COLUMBIA-WILLAMETTE RIVER SYSTEM

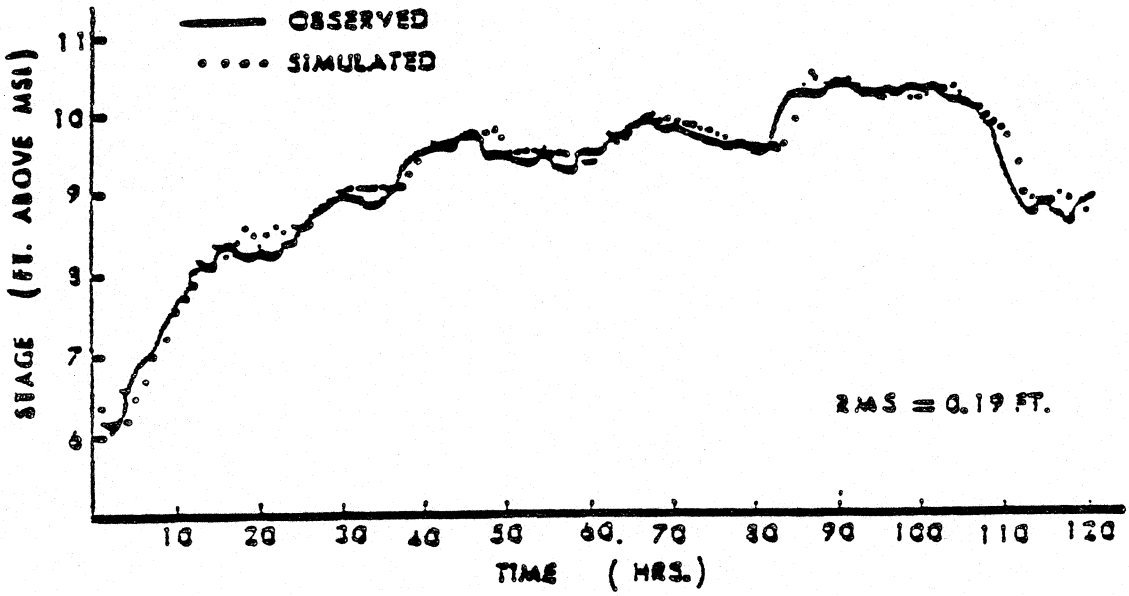

FIG. 13a - OBSERVED VS. SIMULATED STAGES AT WARRENDALE

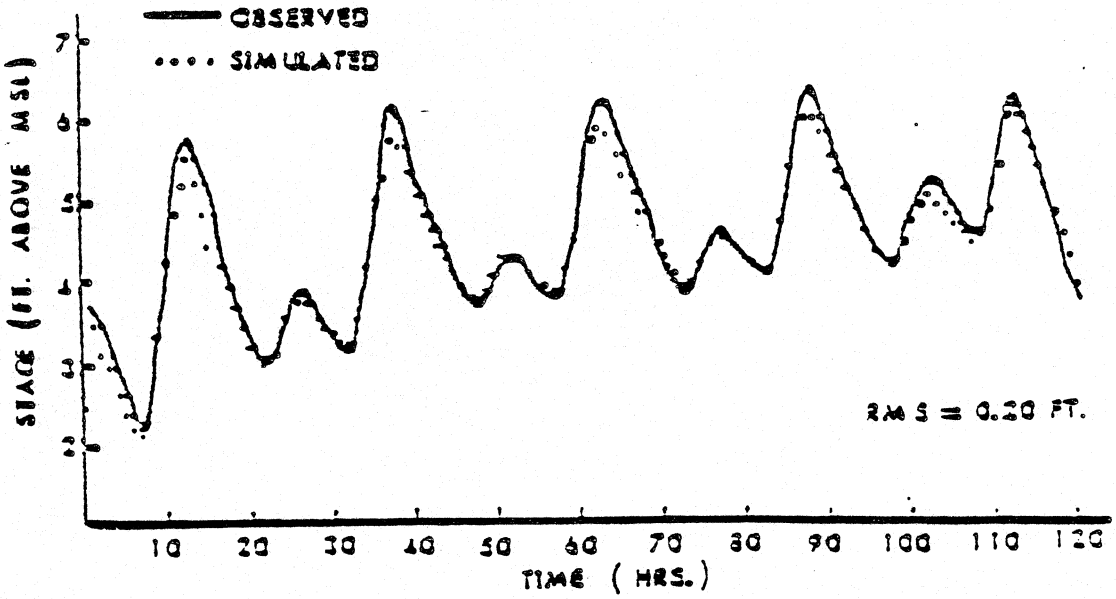

FIG. 13b - OBSERVED VS. SIMULATED STAGES AT VANCOUVER

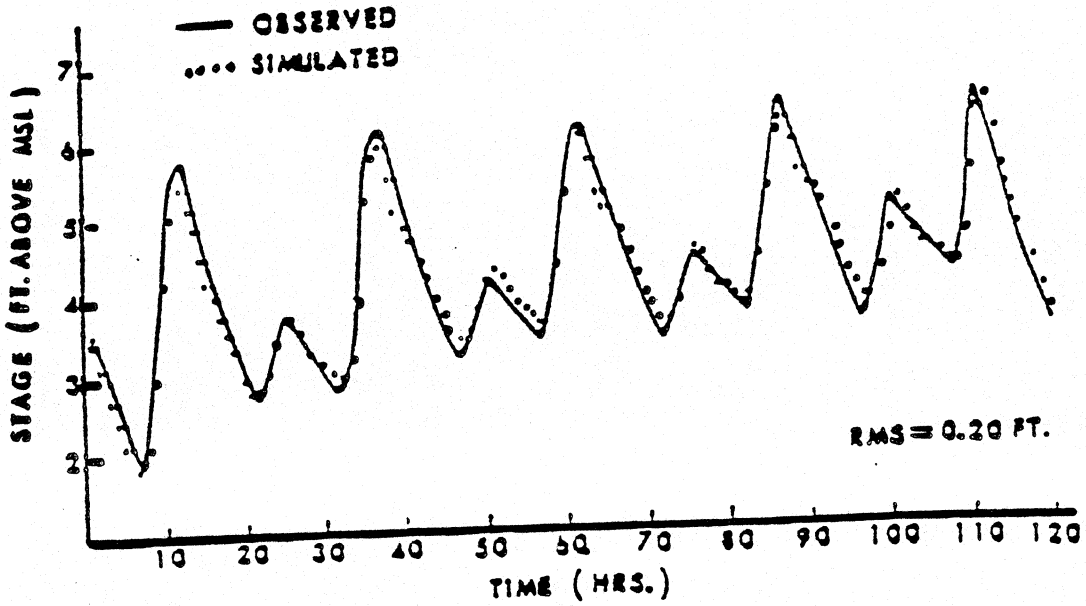

FIG. 14a - OBSERVED VS. SIMULATED STAGES AT PORTLAND

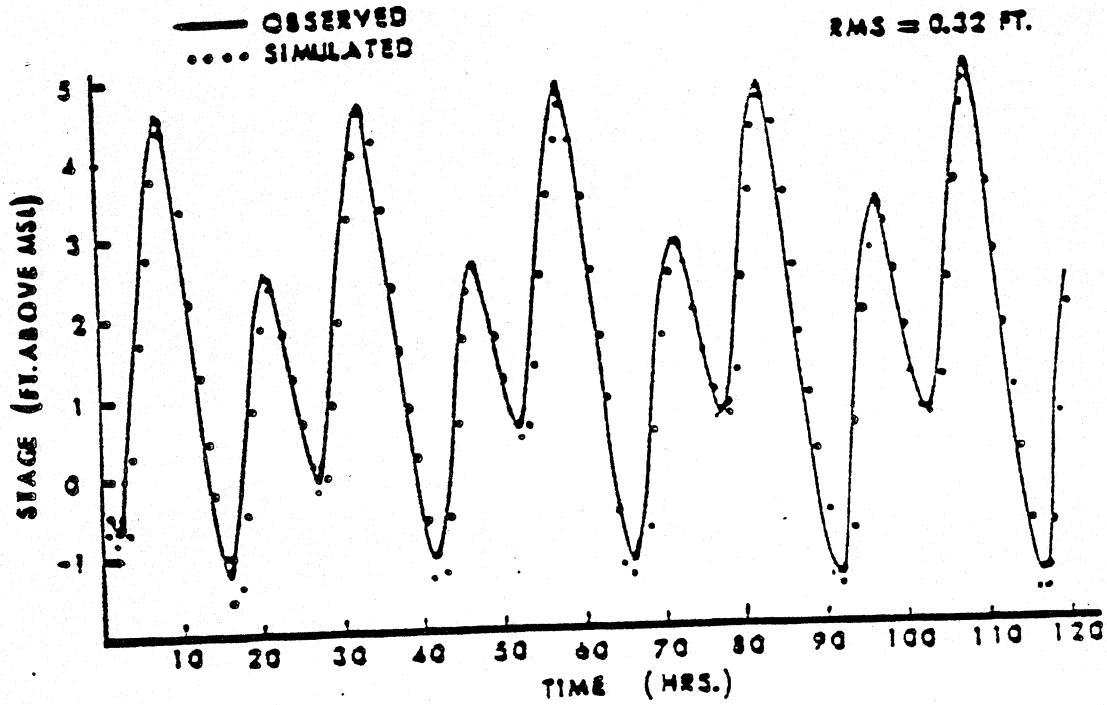

FIG. 14b - OBSERVED VS. SIMULATED STAGES AT WAUNA

APPENDIX A

INPUT DATA STRUCTURE FOR DYNAMIC WAVE MODEL

Version: 07/18/84

Card Input No.	Data Description - Input Format
(1)	K1,K2,K3,K4,K5,K6,K7,K8,K9,K10,K11,K12,K13,K14 - 14I5 (See note at end of Data Input.)
(2)	ALONE (Punch 'ALONE' starting in column 1.)
(3)	EPSY,EPSQ,EPSQJ,THETA,F1,XFACT,DHF,CFNAME - 7F10.0,4X,A4

EPSY	Depth tolerance in Newton Iteration (0.001-1.0 ft). A good value is 0.05 ft.
EPSQ	Discharge tolerance in Newton Iteration (10.-10000. cfs). EPSQ=EPSY x avg. V x avg. width.
EPSQJ	Discharge tolerance in tributary iteration scheme (10.-10000.cfs). EPSQJ=EPSQ.
THETA	Acceleration factor in solving tributary junction problem (0.5-1.0). Varies with each problem with 0.8 a good first choice.
F1	θ weighting factor (normally F1=0.55, but can range from 0.5 to 1.0).
XFACT	Factor to convert units, describing the location of the computation points along the routing reach, to feet; e.g., if units are in miles, XFACT=5280.
DHF	Factor to convert time units associated with specified stage or discharge hydrograph data at the upstream or downstream boundaries into units of hours; e.g., if hydrograph data are read in as daily values, DHF=24.
CFNAME	Name identifying river system which when used in other than the ALONE command identifies carryover file in which this data is stored.

(4) JN,NU,NCT,ICD,NYQD,ITMAX,NCML - 8I10

JN	Number of rivers that are being routed simultaneously (no tributary, JN=1; 1 tributary, JN=2; 2 tributaries, JN=3).
NU	Number of values associated with specified stage or discharge hydrographs; if mathematical function is used to describe the specified hydrographs, NU=0.
NCT	Parameter indicating type of extrapolation used in Newton Iteration to determine estimates of unknowns; if extrapolation is parabolic, NCT=2; if extrapolation is linear, NCT=1; if no extrapolation, NCT=0.
ICD	If any boundary hydrograph changes by more than the value of this parameter (in ft) from the last time step, extrapolation is not used.
NYQD	Number of sets of stage-discharge values in empirical rating curve at downstream boundary.
ITMAX	Maximum number of iterations allowed in the Newton-Raphson Iteration Procedure for solving the system of nonlinear equations; if ITMAX=1, the nonlinear formuation degenerates into a linear formulation and no iterations are required in the Newton-Raphson Iteration Procedure.
NCML	Number of values in Manning's n versus stage or discharge table; this is the same for all Manning's n reaches.

(5) NCS,NCSS,NP,KTERM,KPL,KPL2,JNK,NPEND - 8I10

NCS	Number of values in table of top widths (BS) vs. elevations (HS) referenced to mean sea level (m.s.l.).
NCSS	Number of values in table of top widths of storage sections (BSS) vs. elevations (HSS) referenced to m.s.l.
NP	Parameter indicating if Automatic Calibration option is to be used; if NP=0, no Automatic Calibration will be made; if NP≥1, Automatic Calibration will be used; when using Automatic Calibration, NP also denotes the sequence number of the first computed stage (in the computed stage hydrograph) which will be used in the statistics needed in the automatic calibration for determining the Manning n. (See note at end of Data Input concerning type of data required for using Automatic Calibration option.)
KTERM	Parameter indicating if terms in equation of motion will be computed and printed as special information; if KTERM=1, they will be printed; if KTERM=0, they will <u>not</u> be printed.

KPL	Parameter indicating what information will be plotted; if KPL=0, nothing is plotted; if KPL=1, stage hydrographs are plotted; if KPL=2, discharge hydrographs are plotted.
KPL2	Parameter to denote if observed data are available for plotting at stations for which the computed results are to be plotted; if KPL=0, no data are available; if KPL2=1, observed data are available.
JNK	Parameter indicating if computed water surface elevations, velocities, and discharges will be printed; if JNK=0, they will <u>not</u> be printed; if JNK=1, they will be printed.
NPEND	Parameter indicating the last value in the computed stage hydrograph which will be used in the statistics needed in the Automatic Calibration option to determine the Manning n. If left blank, last value of observed stage hydrograph will be used.

(6) NQL(J) - 8I10

NQL(J)	Parameter for indicating if any lateral inflows are present; NQL(J)=0, if none are present; NQL(J)=K, where K is the number of Δx subreaches where lateral inflows are present; J index goes from 1 to JN.

(7) NWJ(J) - 8I10

NWJ(J)	Number of Δx reaches in J^{th} river where weir-flow (levee overtopping) may occur, J index goes from 1 to JN.

(8) NUMLAD(J) - 8I10

NUMLAD(J)	Number of locks and dams or internal boundaries in J^{th} river, J index goes from 1 to JN.

(9) NCSS1(J) - 8I10

NCSS1(J)	Number of stations that have off-channel storage.

If NCSS1(J)>0 (see card input no. 9), read in NCSSS(K,J)

See note following card 10

(10) NCSSS(K,J) - 8I10

NCSSS(K,J) Station number associated with the computational points or sections along the routing reach which have off-channel storage; computational points or sections are numbered from the upstream boundary toward the downstream boundary; K index goes from 1 to NCSS1(J) (number of stations that have off-channel storage).

Note: Repeat card 10 once for each J, J=1, JN.

(11) NB(1) - I10

NB(1) Number of stations or computational points along the main river.

If JN>1 (see card input no. 4), read in NB(J), NJUN(J), ATF(J).

See note following card 12

(12) NB(J),NJUN(J),ATF(J) - 2I10,F10.0

NB(J) Number of stations along the tributaries, where J is the number of tributary; tributaries are numbered from upstream to downstream along the main river commencing with the number 2.

NJUN(J) Number of station along the main river where tributary J enters (this station coincides with the upstream extremity of the small subreach which is equivalent in length to the tributary width).

ATF(J) Acute angle that the tributary makes with the main river at the confluence; ATF(J) is in degrees.

Note: Repeat card 12 for each J, J=2, JN.

(13) KU(J) - 8I10

KU(J) Parameter indicating the type of upstream boundary condition being specified for the main river or tributaries; if KU(J)=1, a stage hydrograph or if KU(J)=2, a discharge hydrograph is the upstream boundary condition; J index goes from 1 to JN.

(14) KD(J) - 8I10

KD(J) Parameter indicating the type of downstream boundary condition being specified for the main river; if KD(J)=1, a stage hydrograph is the downstream boundary condition (in the case of tributaries, KD(J) where J goes from 2 to JN is always equal to 1) except for levee overtopping simulation in which overflow is ponded beyond levees (in this case KD(J)=2); if KD(1)=2, a discharge hydrograph is the downstream boundary condition; if KD(1)=3, a single value rating curve of discharge as a function of stage is the boundary condition; if KD(1)=4, a loop rating curve is the boundary condition; if KD(1)=5, normal flow computed from Manning's equation (with the channel bottom slope used as the energy slope) is the downstream boundary condition; if KD(1)=1 and NYQD>0, a single value rating curve in which Q is a function of the computed water surface minus the read-in value of STN.

See note following card 16

(15) NRCM1(J),NRT1(J),NNYQ(J) - 3I10

NRCM1(J) Number of different Manning n relationships used in the routing reach (J^{th} river).

NRT1(J) Total number of observed stage hydrographs along J^{th} river (routing reach) which will be compared with computed water surface elevations; maximum number that can be handled by the program is 9; also, denotes total number of stations for which computed values will be plotted.

NNYQ(J) Parameter indicating if Manning's n is a function of water surface elevation or discharge; if NNYQ(J)=0, n is a function of water surface elevation; if NNYQ(J)=1, n is a function of discharge; if n is constant, let NNYQ(J)=0.

Note: If KD(1)=4 or KD(1)=5, add one to NRCM1(1) (for the main river only).

See note following card 16

(16) NCM(K,J) - 8I10

NCM(K,J) Station number of downstream most station in subreach that has the same Manning's n; K index goes from 1 to NRCM1(J).

Note: If KD(1)=4 or KD(1)=5, the last value of NCM for the main river should be one greater than the number of stations on the main river (NB(1)+1).

Note: Repeat card sequence 15 and 16 once for each J, J=1, JN.

If NRT1(J)>0 (see card input no. 15), read in NT(K,J).

See note following card 18

(17) NT(K,J) - 8I10

NT(K,J) Station number of each observed stage hydrograph; K index goes from 1 to NRT1(J).

If NRT1(J)>0 (see card input no. 15), and KPL=1 and KPL2=1 (see card input no. 5), read in GZ(K,J).

See note following card 18

(18) GZ(K,J) - 8I10

GZ(K,J) Gage correction to convert observed stage hydrographs to mean sea level datum; K index goes from 1 to NRT1(J).

Note: Read card sequence 17 and 18 once for each J, J=1, JN.

If NRT1(J)>0 (see card input no. 15), and KPL>0 (see card input no. 5), read in STTNAM(L,I,J).

See note following card 20

(19) STTNAM(L,I,J) - 5A4

STTNAM(L,I,J) 20-character name associated with observed stages (see card 20); L index goes from 1 to 5.

If NRT1(J)>0 (see card input no. 15) and KPL>0 and KPL2=1 (see card input no. 5), read in STT(K,I,J).

See note following card 20

(20) STT(K,I,J) - 8F10.0

STT(K,I,J) Observed stages; K index goes from 1 to NU.

Note: Repeat cards 19 and 20 once for each I, I=1, NRT1(J); and repeat this sequence for each J, J=1, JN.

If NU=0 (see card input no. 4), read in TP, RHO, GAMMA, YI.

(21) TP,RHO,GAMMA,YI - 4F10.0

TP	Time (hours) from initial steady flow to peak of specified upstream boundary hydrograph (used in mathematical function describing the hydrograph).
RHO	Ratio of peak value of specified hydrograph to initial value of hydrograph.
GAMMA	Ratio of time TG to TP, where TG is the time from inital steady flow to the center of gravity of the specified hydrograph (must be greater than 1.)
YI	Initial steady discharge or water surface elevation at upstream boundary.

If NU>0 (see card input no. 4), read in ST1(K,J).

See note following card 23

(22) ST1(K,J) - 8F10.0

ST1(K,J) Observed stages or discharges at upstream boundary of river J; K index goes from 1 to NU.

If NU>0 (see card input no. 4), and KU(J)=1 (see card input no. 13), read in GZ1(J).

See note following card 23

(23) GZ1(J) - 8F10.0

GZ1(J) Gage correction to convert observed stages at upstream boundary of river J to m.s.l. datum.

Note: Repeat card sequence 22, 23 once for each J, J=1, JN.

If KD(J)≤2 (see card input no. 14), read in STN(K,1)

(24) STN(K,1) - 8F10.0

STN(K,1) Observed stages or discharges at downstream boundary of main river; K index goes from 1 to NU with 8 values per data card.

If KD(J)=1 (see card input no. 14), or NYQD>0 (see card input no. 4), read in GZN.

(25) GZN - F10.0

GZN Gage correction to convert stages at downstream boundary of main river to m.s.l. datum.

If NYQD>0 (see card input no. 4), read in YQD(K).

(26) YQD(K) - 8F10.0

YQD(K) Stages used to define empirical rating curve at downstream boundary of main river; K index goes from 1 to NYQD.

If NYQD>0 (see card input no. 4), read in QYQD(K).

(27) QYQD(K) - 8F10.0

QYQD(K) Discharges used to define empirical rating curve at downstream boundary of main river; K index goes from 1 to NYQD.

See note following card 30

(28) BS(K,I,J) - 8F10.0

BS(K,I,J) Top widths of channel cross section at various elevations referenced to m.s.l. datum; K index goes from 1 to NCS; I index goes from 1 to NB(J); i.e., a set of BS top widths are read in for each station along river J.

See note following card 30

(29) HS(K,I,J) - 8F10.0

HS(K,I,J) Elevations (references to m.s.l. datum) corresponding to each top width (BS); K index goes from 1 to NCS; I index goes from 1 to NB(J). Elevations should proceed from bottom to top.

See note following card 30

(30) AS(1,I,J) - 8F10.0

AS(1,I,J) Channel cross sectional areas below HS(1,I,J) or lowest of the HS elevations; I index goes from 1 to NB(J).

Note: Repeat card sequence 28, 29, and 30 once for each J, J=1, JN.

If NCSS>0 (see card input no. 5), and NCSS1(J)>0 (see card input no. 9), read in BSS(K,I,J).

See note following card 33

(31) BSS(K,I,J) - 8F10.0

BSS(K,I,J) Top width of off-channel storage cross sections at various elevations referenced to m.s.l. datum; K index goes from 1 to NCSS.

Note: Only those stations with off-channel storage dimensions are read in; i.e., those stations which do not have any off-channel storage must not be included; a set of BSS top widths is read in for each station that has off-channel storage along the river corresponding to the J index. Stations having off-channel storage are defined by array NCSSS(L,J), where L=1, NCSS1(J).

If NCSS>0 (see card input no. 5), and NCSS1(J)>0 (see card input no. 9), read in HSS(K,I,J).

See note following card 33

(32) HSS(K,I,J) - 8F10.0

HSS(K,I,J) Elevations (references to m.s.l. datum) corresponding to each top width (BSS); K index goes from 1 to NCSS.

If NCSS>0 (see card input no. 5), and NCSS1(J)>0 (see card input no. 9), read n ASS(1,I,J).

See note following card 33

(33) ASS(1,I,J), 8F10.0

ASS(1,I,J) Off-channel storage cross-sectional area below HSS(1,I,J) or lowest of HSS elevations.

Note: Repeat card sequence 31, 32, and 33 for each I, I=1, NCSS(J), and repeat this sequence for each J, J=1, JN.

If KD(1)=5 (see card input no. 14), read in SO.

(34) SO - F10.6

SO	Average bottom slope of main river.

See note following card 37

(35) COFW,VWIND,WINAGL - 3F10.6

COFW	Coefficient of wind stress (1.1×10^{-6} to $3. \times 10^{-6}$).
VWIND	Wind velocity (ft/sec); + if directed upstream; - if directed downstream.
WINAGL	Acute angle (degrees) that wind makes with the channel axis.

See note following card 37

(36) X(I,J) - 8F10.2

X(I,J)	Location of station or cross section where computations are made (units can be anything since XFACT converts these units to ft); I index goes from 1 to NB(J).

See note following card 37

(37) FKC(I,J) - 8F10.0

FKC(I,J)	Expansion or contraction coefficients (expansion coefficients vary from -.30 to -1.00 and contraction coefficients vary from +.10 to +.40, depending on the sharpness of the transition section); if a station has no expansion or contraction, enter 0.0; I index goes from 1 to NB(J).

<u>Note</u>: Repeat card sequence 35, 36, and 37 for each J, J=1, JN.

If NQL(J)>0 (see card input no. 6), read in LQ(I,J).

See note following card 39

(38) LQ(I,J) - 8I10.0

LQ(I,J) Number of station at upstream end of each Δx reach in which lateral inflow is introduced; stations are numbered from upstream to downstream extremities of the routing reach commencing with 1 and going to NB(J); I index goes from 1 to NQL(J).

If NQL(J)>0 (see card input no. 6), read in QL(K,I,J).

See note following card 39

(39) QL(K,I,J) - 8F10.0

QL(K,I,J) Lateral inflow in cfs per Δx reach, either overland flow per Δx reach or tributary inflow per Δx reach; K index goes from 1 to NU; I index goes from 1 to NQL(J).

Note: Repeat card sequence 38 and 39 once for each lateral inflow point and each J, J=1, JN.

If NWJ(J)>0 (see card input no. 7), read in NWJX(K,J)

SEE NOTE FOLLOWING CARD 41

(40) NWJX(K,J) - 8I10.0

NWJX(K,J) Number of station at upstream end of Δx reach in which weir-flow or levee overtopping and/or failure (crevasse) (inflow or outflow) may occur; stations are numbered from upstream to downstream extremities of routing reach commencing with 1 and going to NB(J); K index goes from 1 to NWJ(J).

If NWJ(J)>0 (see card input no.7) read in HWH(K),WC(K),TFL(K),BBL(K), HFL(K),HMINL(K)

See note following card 41

(41) HWH(K),WC(K),TFL(K),BBL(K),HFL(K),HMINL(K) - 6F10.2

HWH(K)	Elevation (ft m.s.l.) of top of levee, ridge line, etc. where weir-flow occurs; elevation is average throughout Δx reach where weir-flow occurs.
WC(K)	Weir-flow discharge coefficient for Δx reach where weir-flow (inflow or outflow) may occur; coefficient ranges from 2.6 to 3.2.
TFL(K)	Time (hr) from start of levee failure (crevasse) until the opening or breach is its maximum size.
BBL(K)	Final width (ft) of levee crevasse which is assumed to have a rectangular shape.
HFL(K)	Elevation (ft m.s.l.) of water surface when levee starts to fail.
HMINL(K)	Final elevation (ft m.s.l.) of bottom of levee crevasse.

Note: Repeat card 41 as K goes from 1 to NWJ(J). Cards 40 and 41 are read-in for main stem river (J=1) if NWJ(1)>0. Thereafter, only card 40 is read-in when NWJ(J)>0 as J goes from 2 to JN. If overtopping may occur and no crevasse is to be simulated, leave TFL,BBL,HFL, and HMINL blank.

(42) LAD(L,J) - 8I10

LAD(L,J)	Number of station at upstream end of Δx reach in which lock and dam or internal boundary is located; stations are numbered from upstream to downstream extremities of routing reach commencing with 1 and going to NB(J); L index goes from 1 to NUMLAD(J). Use (-) integer value to activate internal boundary capability.

(43) POLTAR(L,J) - 8F10.2

POLTAR(L,J)	Elevation (m.s.l.) of water surface in headwater pool at upstream face of lock and dam; this elevation is considered the target pool elevation; the lock-master controls the flow through the dam via gates to maintain the pool elevation at this target elevation; L index goes from 1 to NUMLAD(J). Also, target discharge (cfs) at which gate rating changes to tailwater rating (for Ohio River).

(44) CHCTW(L,J) - 8F10.2

CHCTW(L,J) Elevation (m.s.l.) of water surface in tailwater pool at downstream face of lock and dam; this elevation is considered the elevation at which the lock master can no longer control the flow through the dam and the flow becomes channel control; usually this elevation will be equal or slightly less than the target pool elevation; L index goes from 1 to NUMLAD(J). Also, specifies type of internal boundary condition (See internal boundary note on page A-18 for additional types of internal boundary conditions that can be simulated.)

(45) RHI(K,L,J) - 8F10.2

RHI(K,L,J) Stage (ft m.s.l.) for internal boundary rating curve; omit unless LAD(I,J)<0 and CHCTW(L,J)≤0.05; L goes from 1 to NUMLAD(J); K goes from 1 to 8.

(46) RQI(K,L,J) - 8F10.2

RQI(K,L,J) Discharge (cfs) corresponding to RHI(K,L,J) or bridge embankment flow coefficient if CHCTW(L,J)=0.05. Omit if RHI (K,L,J) is omitted.

(47) GFR(K,L,J) - 8F10.2

GFR(K,L,J) Gate setting (horizontal opening of gate (ft), if CHCTW(L,J)=0.01; differential head if CHCTW(L,J)=0.03); omit unless LAD(I,J)<0 and 0.01≤CHCTW(L,J)≤0.03; L goes from 1 to NUMLAD(J); K goes from 1 to 8.

(48) GQ(K,L,J) - 8F10.2

GQ(K,L,J) Gate discharge (cfs) corresponding to GFR(K,L,J). Omit if GFR(K,L,J) is omitted.

(49) GFT(K,L,J) - 8F10.2

GFT(K,L,J) Gate setting (horizontal ft. of gate opening) time series; L goes from 1 to NUMLAD(J); K goes from 1 to NU. Omit unless GFR(K,L,J) is read-in or unless CHCTW(L,J)=0.05. In the latter, K goes from 1 to 3.

(50) POOLT(K,L,J) - 8F10.2

POOLT(K,L,J) Target pool elevation (same as POLTAR(L,J)) for each time step; if 0.0 or blank is read in, then POLTAR(L,J) is used for POOLT(K,L,J); K index goes from 1 to NU; L index goes from 1 to NUMLAD(J).

(51) ITWT(K,L,J) - 8I10.0

ITWT(K,L,J) Parameter indicating if gates control the flow; if 0 or blank, flow is controlled by gates, if 1, flow is not controlled by gates, e.g., the entire dam is removed as in the case of the low lift dams on the Lower Ohio River and the flow becomes channel controlled; K index goes from 1 to NU; L index goes from 1 to NUMLAD(J).

Note: Cards 42-51 are read in for each river as J goes from 1 to JN if NUMLAD(J)>0.

(52) TE,TM,KITPR - 2F10.2,I10

TE Time (hours) at which routing computations will terminate.

TM Maximum size Δt computational time step (hours).

KITPR Number of Δt time step intervals at which computed values are stored for plotting or printed out. Length of time step times KITPR equals interval at which plots are generated, e.g., if 6-hr time steps are taken and a plot is desired each day, set KITPR=4.

(53) YD1(I,J) - 8F10.0

YDI(I,J) Initial water surface elevations referenced to m.s.l. datum at each station; I index goes from 1 to NB(J); if blank or zeros are used for all the YDI(I,J) values, the program will generate the YDI's via linear interpolation between gaging stations (this is allowed when using the Automatic Calibration option or when gaging stations exist at the upstream extremities of all rivers and the downstream extremity of the main stem); if the upstream extremity does not have an observed hydrograph, this YDI value must be supplied along with all the zeros for the other YDI's; if zeros or blanks are used for all the YDI's except at the downstream extremity of the main stem river when the actual YDI is read in, the program will generate the YDI's via a solution of the steady flow backwater equation.

(54) QDI(I,J) - 8F10.0

QDI(I,J) Initial discharge (cfs) at each station; I index goes from 1 to NB(J); if blank or zeros are used for all the QDI (I,J) values except at the upstream extremity of each river, the program will generate the QDI's by summation of the flows from the upstream to downstream boundaries, including tributary inflow to the main stem and lateral inflow occurring along either the main stem or tributaries.

Note: Repeat card 53 for each J, J=1, JN, and then repeat card 54 for each J, J=1, JN.

See note following card 56

(55) YQCM(L,K,J) - 8F10.0

YQCM(L,K,J) Water surface elevations referenced to m.s.l. datum or discharges associated with n; L index goes from 1 to NCML.

Note: Repeat card 55 for each K, K=1, NRCM1(J); repeat sets of card 55 for each J, J=1, JN.

See note following card 56

(56) CM(L,K,J) - 8F10.0

CM(L,K,J) Manning's n; L index goes from 1 to NCML corresponding to each YQCM(L,K,J) value.

Note: Repeat card 56 for each K, K=1, NRCM1(J); repeat sets of card 56 for each J, J=1, JN.

Note: If KD(1)=4 or KD(1)=5, the values for YQCM(L,NRCM1(1),1) and CM(L,NRCM1(1),1) (the last values for the main river) are used in the loop rating curve or Manning's equation to compute the downstream boundary condition.

(57) MESAGE - 20A4

MESAGE	Up to an 80-character message which will be written at the end of the input data deck.

(58) END (Punch 'END' starting in column 1.)

END	Indicates end of input data deck.

(59) EXIT (Punch 'EXIT' starting in column 1.)

Automatic Calibration Note:

The following data must be included when using the Automatic Calibration option: Upstream boundary condition consisting of a discharge hydrograph for each river, i.e., KU(J)=2; observed stage hydrographs STT(K,I,J) at upstream and downstream ends of each reach wherein the Manning n is to be determined; and a downstream boundary condition consisting of a stage hydrograph, i.e., KD(J)=1; (the stage hydrograph STN(K,I,J) is required for the main stem river, only, since the model can provide the downstream stage hydrograph for each tributary via linear interpolation between observed stage hydrographs along the main stem which are adjacent to the tributary junction).

Plotting Note:

To obtain plots when no observed data are available, set KPL2=0, KPL=1 or 2, NRT1(J)>0, NT(K,J)>0, and enter STTNAM(L,I,J) for each station to be plotted.

Interior Drainage Note:

Overtopping of levees with the resulting flow ponded within the confines of a blocked tributary can be simulated by using cards 40-41 and a value of (2) for KD(2) on card 14. Also required is a tributary having a continuous low flow discharge and a large overbank and off-channel storage area representing the storage in the ponded area outside the levees. Interior drainage back into the river through a gravity-controlled check valve and pipe can also be simulated in the same manner, except HWH (card 41) is the pipe invert elevation and WC (card 41) is computed as 6.4 x pipe cross-sectional area ft^2). Of course, the Δx reach in which the pipe extends through the levee should be a relatively short reach (say 50 to 100 ft). If the receiving tributary of the overtopping levee flow is hydraulically connected to the main river, KD(2) on card 14 should have a value of 1.

INTERNAL BOUNDARY NOTE

Various types of internal boundaries may be simulated by entering a specific value for CHCTW(L,J) on Card No. (44). The types are:

CHCTW(L,J)	REMARKS
0.00	Rating curve, $Q_i=f(h_i)$ where h_i is the water surface elevation at the upstream face of the internal boundary reach.
0.01 (Moveable Gate) (Ohio River)	Rating curve, $Q_i=f(h_{i+1})$ where h_{i+1} is the water surface elevation at the downstream face of the internal boundary reach. This holds as long as Q_{i+1}>POLTAR(L,J); otherwise, a gate rating curve GQ(K,L,J)=f(GFR(K,L,J)) where the value for determining the discharge from the rating curve is obtained from the time series GFT(K,L,J) which is the gate setting vs. time. GFR(K,L,J) is the gate opening in ft. of gate. (This option is for the Ohio River.)
0.03 (Siphon)	Same as for 0.01 except the value for determing the discharge from the rating is the differential head (h_i-h_{i+1}). A siphon rating or other structure with a constant flow area can be simulated by letting GFT(K,L,J)=1.0 and entering zero values for the GQ and GFR arrays with POLTAR(L,J) entered as zero.
0.05 (Bridge)	Bridge internal boundary with contracted flow $[Q_i=\sqrt{2g}c_cA_{i+1}(h_i-h_{i+1})^{1/2}]$ or orifice flow $[Q_i=\sqrt{2g}c_oA_{i+1}(h_i-h_{i+1})^{1/2}]$ and broad-crested weir flow over the road embankment including the bridge deck $[Q_i=S_bc_e(h_i-h_e)^{3/2}]$ where c_c=contracted opening flow coefficient, A_{i+1}=area of flow at downstream end of bridge opening, c_o=orifice flow where $h_i>h_b$ in which h_b=elev. of bridge deck, c_e=coefficient of flow for broad-crested weir multiplied by the length of the weir-crest (c_e is specified via RQI(K,L,J) as a function of h_i or RHI(K,L,J), S_b=submergence correction factor = $1.0-27.8(r-0.67)^3$ where $r=(h_{i+1}-h_e)/(h_i-h_e)$ in which h_e is the weir crest elev. which is specified by RHI(1,L,K). c_c,c_o,h_b are specified by GFT(1,L,J), GFT(2,L,J), GFT(3,L,J), respectively (only 3 values of GFT are read in).
>0.1 (Tide Gate)	Tide gate flow $[Q_i=c(h_i-h_{i+1})^{1/2}]$ where c is the discharge coefficient given by CHCTW(L,J) which is computed as $(2g)^{1/2}$ x discharge loss coef. x max. area of tide gate(s). If $h_{i+1} \geq h_i$, then $Q_i=0$.

K DIMENSIONAL VALUES

DWOPER is programmed with a feature called variable dimensioning. This means that the size of subscripted variables can be changed from one execution of the DWOPER to another. There is a maximum total size for the sum of all arrays, but within that bound the allocation of space among variables is flexible.

For example, when the Ohio-Mississippi Junction (OMJ) is simulated, space must be available for four rivers, with a maximum of 31 computational points on a river. The same space can also be allocated so that for the Lower Mississippi, where only one river is simulated, 36 computational points can be used. Actually, the space for the Lower Mississippi is still less than for the OMJ so, for instance, more time steps could be used.

The dimensions of all arrays are set at the start of each execution of the DWOPER. A single card with 14 values (K1 through K14) sets the maximum dimensions needed. The dimensions which must be set at the start of each execution are:

K1	The number of rivers
K2	The maximum number of computational points on any river
K3	The number of time steps
K4	The maximum number of gaging stations on any river
*K5	The maximum number of HO values on any river
K6	The number of values in the downstream rating curve
K7	The maximum number of Manning n reaches on any river
K8	The maximum number of Manning n values in any Manning n reach
K9	The maximum number of water surface elevation vs. top width values at any cross-section
K10	The maximum number of lateral inflows on any river
*K11	The maximum number of sets of initial conditions to be stored in the carryover file (set to 5)
*K12	The maximum number of computed hydrographs to be saved after simulation
*K13	The total number of stage and discharge hydrographs in any hydrograph file which will be accessed
K14	The maximum number of water surface elevation vs. top width values for any off-channel storage.

*Set these values to one except when using NWS operational program.

APPPENDIX B

ADDITIONAL INPUT DATA FOR "NETWORK, Critical Flow and Time-Dependent Gate" OPTIONS in DWOPER

Version: 1/3/86

Card Input No.	Data Description - Input Format
(1)	K1,K2,K3,K4,K5,K6,K7,K8,K9,K10,K11,K12,K13,K14,K17,K18 - 16I5
	K17 — Total number of upstream boundaries in the system.
	K18 — Total number of junctions in the system.
(1A)	K21,K22 - 2I5 format
	K21 — Maximum number of gates in the system.
	K22 — Maximum number of values in the gate coefficient table.
(3)	EPSY,EPSQ,EPSQJ,THETA,F1,XFACT,DHF,CFNAME - 7F10.2,4X,A4
	CFNAME — If = IMET, the metric option is used. With this option, HGC on card no. 46C and HG on card no. 46D are input in metric; and all output data is printed in metric units.
(4)	JN,NU,NCT,ICD,NYQD,ITMAX,NCML,NET - 8I10
	NET — Parameter indicating if Channel Network option is to be used. If NET=0, this option is not used; if NET≥1, this option is to be used and JN should be set equal to 1. If NET=1, junction losses due to mixing and friction are neglected. These are included if NET=2.
(8A)	NG(J) - 8I10
	NG(J) — Number of gates and/or critical flow sections in J^{th} river, J index goes from 1 to JN.

If NET≥1 (see card input no. 4), read in JCOD(K).

(11A) JCOD(K) - 8I10

JCOD(K)	Code denoting the type node at each cross-section. JCOD(K) can have values of 1,2,3,...,11. K index goes from 1 to NB(J) (See Card 11).

If NET≥1 (see card input no. 4), read in JTN, NUPB

(11B) JTN,NUPB - 2I10

JTN	Total number of junctions in the system.
NUPB	Total number of upstream boundaries in the system.

If NET≥1 (see card input no. 4), read in JU(K), JB(K), JL(K).

See note following card 11C

(11C) JU(K), JB(K), JL(K) - 3I10

JU(K)	Sequence number of cross-section at entry to junction.
JB(K)	Sequence number of cross-section at branch of junction.
JL(K)	Sequence number of cross-section at exit of junction.

Note: Omit card 11C if JTN=0.

Note: Repeat card 11C for each junction.

If NET ≥1 (see card input no. 4) read in KMU(K).

(11D) KMU(K) - 8I10

KMU(K)	Parameter indicating the type of upstream boundary condition: if KMU(K)=1, a stage hydrograph is the boundary condition; if KMU(K)=2, a discharge hydrograph is the boundary condition; or if KMU(K)=4, a depth-discharge relation is the boundary condition. K index goes from 1 to NUPB.

Note: When 11D is used, omit card 13.

(11E) JCPR(K) - 8I10

JCPR(K) Parameter indicating sequential order that cross sections will be listed in output, K index goes from 1 to NB(J).

If NG(J)>0 (see card input no. 8A) read in LGX(K,J), IGT(K,J), NTG(I,K), HGC(K,J).

See note following card 51D

(14) KD(J) - 8I10

KD(J) .....If KD(1)=6, downstream boundary is critical flow equation unless read-in value of (STN+GZN) is greater, in which case the latter is used.

(51A) LGX(K,J),IGT(K,J),NTG(K,J),HGC(K,J) - 3I10,F10.2

LGX(K,J) Sequence number of cross section immediately upstream of gate internal boundary.

IGT(K,J) Parameter indicating the type of gate: if IGT(K,J)=1, the gate has a continuous bottom slope; if IGT(K,J)=2, the gate has a discontinuous bottom slope; if IGT(K,J)=0, the location is a critical flow section.

NTG(K,J) Number of values in the table of gate coefficient (GC) vs. tailwater head (DTW).

HGC(K,J) Gate correction parameter used to correct the height of the gate opening.

If NG(J)>0 (see input no. 8A) read in GC(I,K,J).

See note following card 51D

(51B) GC(I,K,J) - 8F10.2

GC(I,K,J) Gate discharge coefficient; coefficient is determined by multiplying the width of the gate by the loss factor; I index goes from 1 to NTG(K,J).

If NG(J)>0 (see card input no. 8A) read in DTW(I,K,J).

See note following card 51D

(51C) DTW(I,K,J) - 8F10.2

DTW(I,K,J) Tailwater head (tailwater elevation - gate bottom elevation) corresponding to each gate discharge coefficient; I index goes from 1 to NTG(K,J)

If NG(J)>0 (see card input no. 8A) read in HG(I,K,J).

See note following card 51D

(51D) HG(I,K,J) - 8F10.2

HG(I,K,J) Height of gate opening; I index goes from 1 to NU.

Note: Omit card sequence 51B, 51C, and 51D if IGT(K,J) = 0.

Note: Repeat card sequence 51A, 51B, 51C, and 51D once for each K, K=1,NG(J), and repeat this procedure for each river as J goes from 1 to JN.

(54A) NR - I10

NR Number of separate channels or branches or storm sewers in the system.

(54B) NIRB(K) - 8I10

NIRB(K) Number of nodes in each channel or branch; K index goes from 1 to NR; the number of nodes along the main channel or sewer is entered first; then the number of nodes in the most upstream branch is entered with the next most upstream branch following until the most downstream branch is entered.

(54C) IRB(I,K) - 8I10

IRB(I,K) Sequential number of node in each branch; node numbers commence at upstream end of each branch and proceed in the downstream direction until the last node of the branch is reached; I index goes from 1 to NIRB(K).

Note: Repeat card 54C as the K index goes from 1 to NR; branches are ordered from upstream to downstream and the first entry is the main (principal) channel or storm sewer.

Note: Cards 54A,B,C are omitted if NET = 0, or QDI(2,1) not equal to zero and NET ≥ 1.

NODE CODE (JCOD(K), K=1,N)

1 Internal Node

2 Upstream Boundary

3 Downstream Boundary

4 Tributary Junction

5 Tributary Junction on a Bifurcation

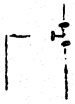

6 Upstream Bifurcation Junction

7 Downstream Bifurcation Junction

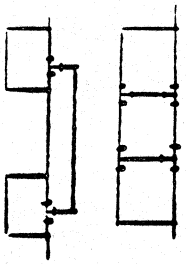

8 Double Bifurcation Junction on a Bifurcation

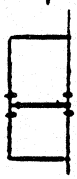

9 Single Bifurcation Junction on a Bifurcation

10 Gate Internal Boundary

11 Critical Flow Internal Boundary

NODE NUMBER SCHEME

Example No. 2:

Junct. No.	Up. Node	Trib. Node	Down. Node
1	3	5	6
2	7	8	12
3	14	11	15
4	17	18	21
5	41	20	42
6	23	38	39
7	26	28	29
8	31	34	35
9	43	44	49
10	46	52	47
11	54	48	55
12	50	51	53
13	56	57	60
14	63	59	64
15	65	66	68
16	71	67	75
17	61	72	62
18	69	74	70
19	78	82	83
20	84	89	90

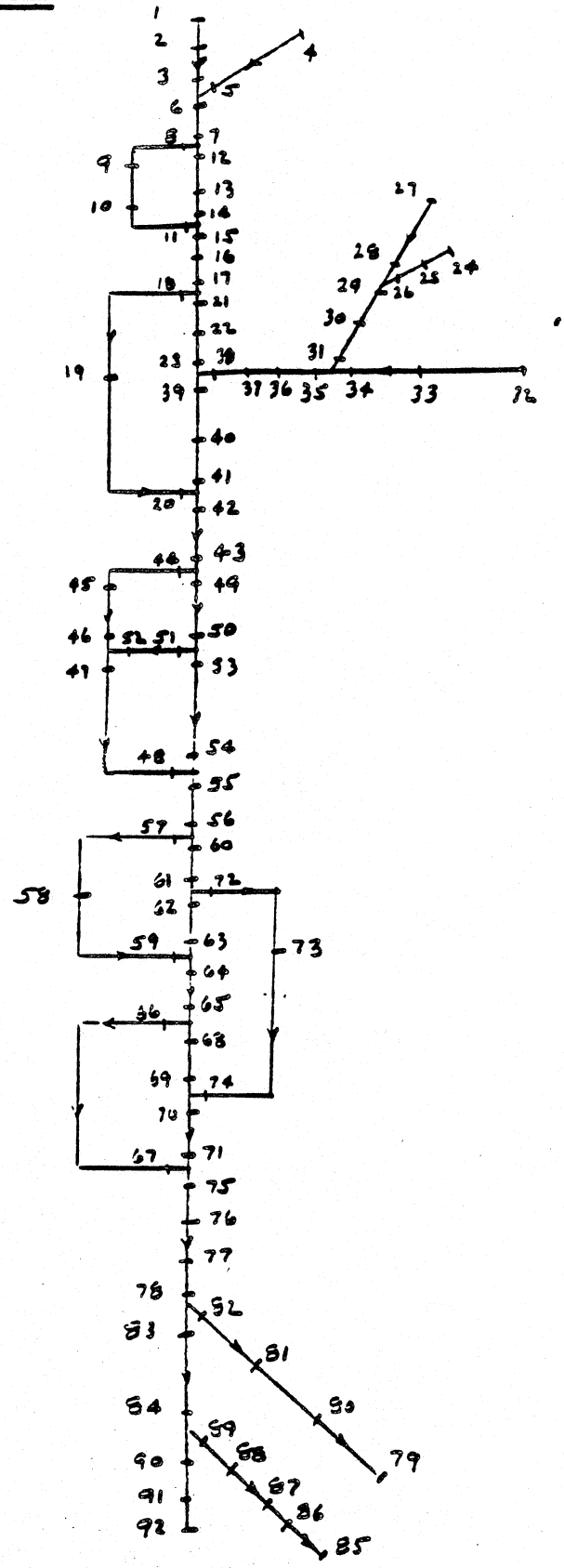

NODE NUMBERING SCHEME

Example No. 1:

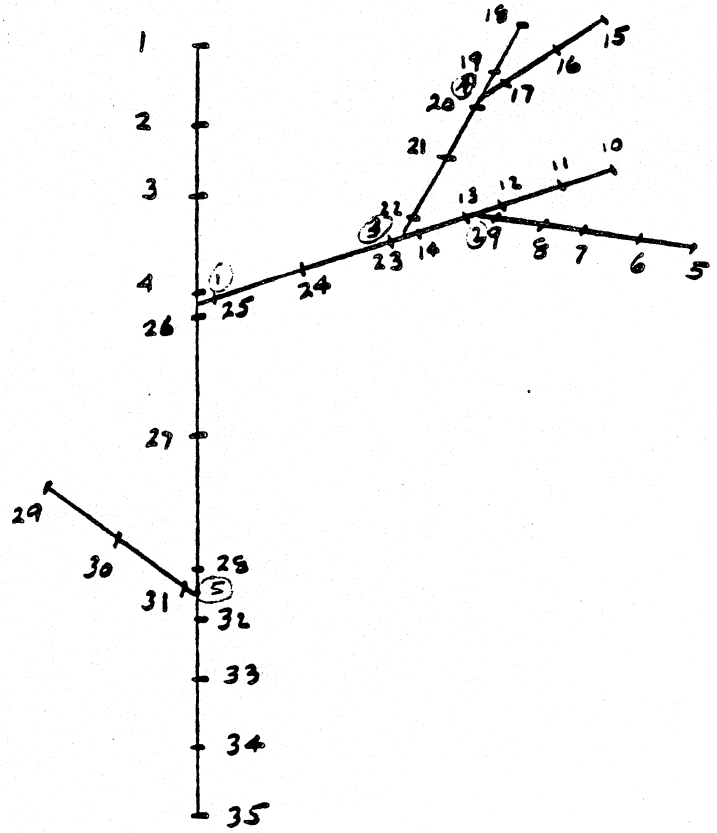

Junction No.	Upstream Node	Tributary Node	Downstream Node
1	4	25	26
2	9	12	13
3	14	22	23
4	17	19	20
5	28	31	32

APPENDIX C

ADDITIONAL INPUT DATA DESCRIPTION FOR "STORM SEWER" OPTION IN DWOPER

Version: 1/3/86

Card Input no.	Data Description - Input Format
(1A)	K21,K22,K23,K24,K25,K26 - 6 I 5
	K23 — Maximum number of manholes.
	K24 — Maximum number of inlet hydrographs other than upstream boundaries.
	K25 — Maximum number of detention or pumping basins
	K26 — Maximum number of pumps.
(5)	NCS,NCSS,NP,KTERM,KPL,KPL2,JNK,NPEND - 8I10
	NPEND — Sequential number indicating the last value in the computed stage hydrograph that will be used in the statistics needed in the Automatic Calibration option to determine the Manning n. If left blank, all computed values will be used. If (-1) or (-2) is entered, the Storm Sewer option can be used. A value of (-2) indicates the storm sewers are circular pipes. A value of (-1) indicates the storm sewers are of arbitrary shape.
(51E)	NMH(J),NQPU(J),NDTB(J),NPM(J) - 4I10
	NMH(J) — Number of manholes in storm sewer system.
	NQPU(J) — Number of inlet hydrographs in storm sewer system.
	NDTB(J) — Number of detention or pumping basins in system.
	NPM(J) — Number of pumps in system.

(51F) NXPI(K,J),DMH(K,J),FKV(K,J),PCWR(K,J),DELVO(K,J),PWELV(K,J) - I10,4F10.2

NXPI(K,J) Sequential number of node (cross-section) which is an entrance to a manhole; if a manhole has two channels entering, use the smallest number to denote this parameter.

DMH(K,J) Diameter (ft) or equivalent diameter of manhole.

FKV(K,J) Head loss coefficient for manhole; varies from about 0.10 to 0.35 (see ASCE J. Hydr., Aug 1984, p. 1150-1154, "Head Losses at Sewer Junction Manholes," by J. Marsalek).

PCWR(K,J) Discharge coefficient for weir flow out of the top of the manhole that is permanently lost from the storm sewer system; varies from 3.1 to 3.3; if the flow out of the top of the manhole returns thru the manhole to the sewer as the flow levels in the system recede, PCWR (K,J) represents the length (ft) of a square area equivalent to the surface area that temporarily stores the water exiting thru the top of the manhole. If PCWR(K,J) is given a value of 10.0, the card (51G) is entered for the surface area.

DELVO(K,J) Elevation interval (ft msl) in table of surface area SAMH(L,K,J) and (51G) vs. elevation.

PWELV(K,J) Elevation (ft) of top of manhole.

(51G) SAMH(L,K,J)

SAMH(L,K,J) Surface area (acres) associated with a manhole where water is temporarily stored as it exits through the top of the manhole; L index goes from 1 to 3; surface area begins at elevation of top of manhole (PWELV) and increments at DELVO(H,J) intervals upward.

<u>Note</u>: (51G) is omitted unless PCWR(K,J) = 10.0.

<u>Note</u>: Repeat card 51 F once for each K, K=1, NMH(J). Omit card 51F if NMH(J) = 0.

(51H) NXQPU(K,J) - I10

NXQPU(K,J) Sequential number of node (cross-section) where an inlet hydrograph occurs.

(51I) QPU(I,K,J) - 8F10.2

QPU(I,K,J) Inflow (cfs) hydrograph ordinate value for K^{th} inlet hydrograph; I index goes from 1 to NU (See card 4).

Note: Repeat cards 51H and 51I once for each K, K=1, NQPU(J). Omit cards 51H and 51I if NQPU(J) = 0.

(51J) NXDTB(K,J),PEO(K,J),DBCW(K,J),DBWELV(K,J),DBCO(K,J) - I10,4F10.2.

NXDTB(K,J) Sequential number of node of inlet to manhole where a connection to a detention or pumping basin is located.

PEO(K,J) Elevation (ft msl) of water surface in detention or pumping basin at t=0.

DBCW(k,J) Weir discharge coefficient for inlet to detention or pumping basin; DBCW(K,J) = (3.1 to 3.3) x length of weir (ft).

DBWELV(K,J) Elevation (ft msl) of weir crest.

DBCO(K,J) Orifice discharge coefficient for inlet to detention or pumping basin; DBCO(K,J) = (0.51 to 0.98) x 8.02 x area of orifice (ft^2).

DBOELV(N,J) Elevation (ft msl) of top of orifice.

(51K) PSA(I,K,J) - 8F10.2

PSA(I,K,J) Volume (ft^3) of Kth detention or pumping basin for a specified elevation within the basin; I index goes from 1 to a minimum value of 2 or a maximum value of 8.

(51L) PEL(I,K,J) - 8F10.2

PEL(I,K,J) Elevation (ft msl) associated with each corresponding value of PSA(I,K,J); elevations start at the bottom of the basin and proceed upwards; I index goes from 1 to a minimum value of 2 or a maximum value of 8.

Note: Repeat cards 51J, 51K, 51L once for each K, K=1, NDTB(J).
Omit cards 51J, 51K, 51L if NBTB(J) = 0.

(51M) NXPO(K,J),NQLP(K,J),PEMN(K,J),PEMX(K,J),PELV(K,J) - 2I10,3F10.2.

NXPO(K,J) Sequential number of node of inlet to manhole where a connection to a basin with pumps is located.

NQLP(K,J) Parameter indicating if pump has a specified discharge hydrograph (NQLP(K,J) =1) or operates according to a specified head-discharge relation (NQLP(K,J) = 0)

PEMN(K,J) Elevation (ft msl) of water surface in pumping basin at which pump stops operating.

PEMX(K,J) Elevation (ft msl) of water surface in pumping basin at which pump starts operating.

PELV(K,J) Elevation (ft msl) at which pump discharges + approximate head loss thru discharge pipe.

(51N) DHP(I,K,J) - 8F10.2

DHP(I,K,J) Head differential (ft) in head-discharge relation; I index goes from 1 to minimum value of 2 or maximum value of 8; head begins at zero and increases.

(51P) OP(I,K,J) - 8F10.2

OP(I,K,J) Pump discharge (cfs) associated with each corresponding DHP(I,K,J) value.

Note: Omit cards 51M and 51N if NQLP(K,J) = 1.

(51Q) QLP(I,K,J) - 8F10.2

QLP(I,K,J) Pump discharge (cfs) hydrograph; or elevation (ft msl) at which pump discharges + approximate heat loss through discharge pipe; if PELV(K,J)=1.0, QLP(I,K,J) is a time-dependent value of PELV(K,J), I index goes from 1 to NU.

Note: Omit card 51Q if NQLP(K,J) = 0 and PELV(K,J) ≠ 1.0.

Note: Repeat cards 51M, 51N and 51P, or 51Q once for each K, K=1, NPM(J).
Omit cards 51M, 51N and 51P, or 51Q if NPM(J) = 0.

Note: Repeat cards 51E thru 51Q once for each J, J=1, JN where JN (card 4) is set to a value of 1 when NET (card 4) is either 1 or 2.

Note: Omit cards 51E thru 51Q if NPEND ≥ 0.

Note: When the storm sewer option is used and the sewers are circular pipes, only two values are required for the BS(K,I,J) top widths on card 28. The first value is the pipe diameter (ft) and the second value represents the diameter or width (ft) of the fictitious chimney emanating from the top of the sewer pipe. The K index goes from 1 to 2. Thus, the value of NCS (card 5) should be entered as a value of 2 when circular pipes comprise the storm sewer system.

Only one value is required for the HS(K,I,J) elevations (card 29). This value represents the invert (bottom) elevation (ft) of the pipe. The K index goes from 1 to 1.

The AS(1,I,J) values on card 30 are entered as zero's for either circular pipes or arbitrary-shaped sewers. Arbitrary-shaped sewers are described by a sufficient number of BS(K,I,J) values and corresponding HS(K,I,J) elevations.

NODE NUMBERING SCHEME

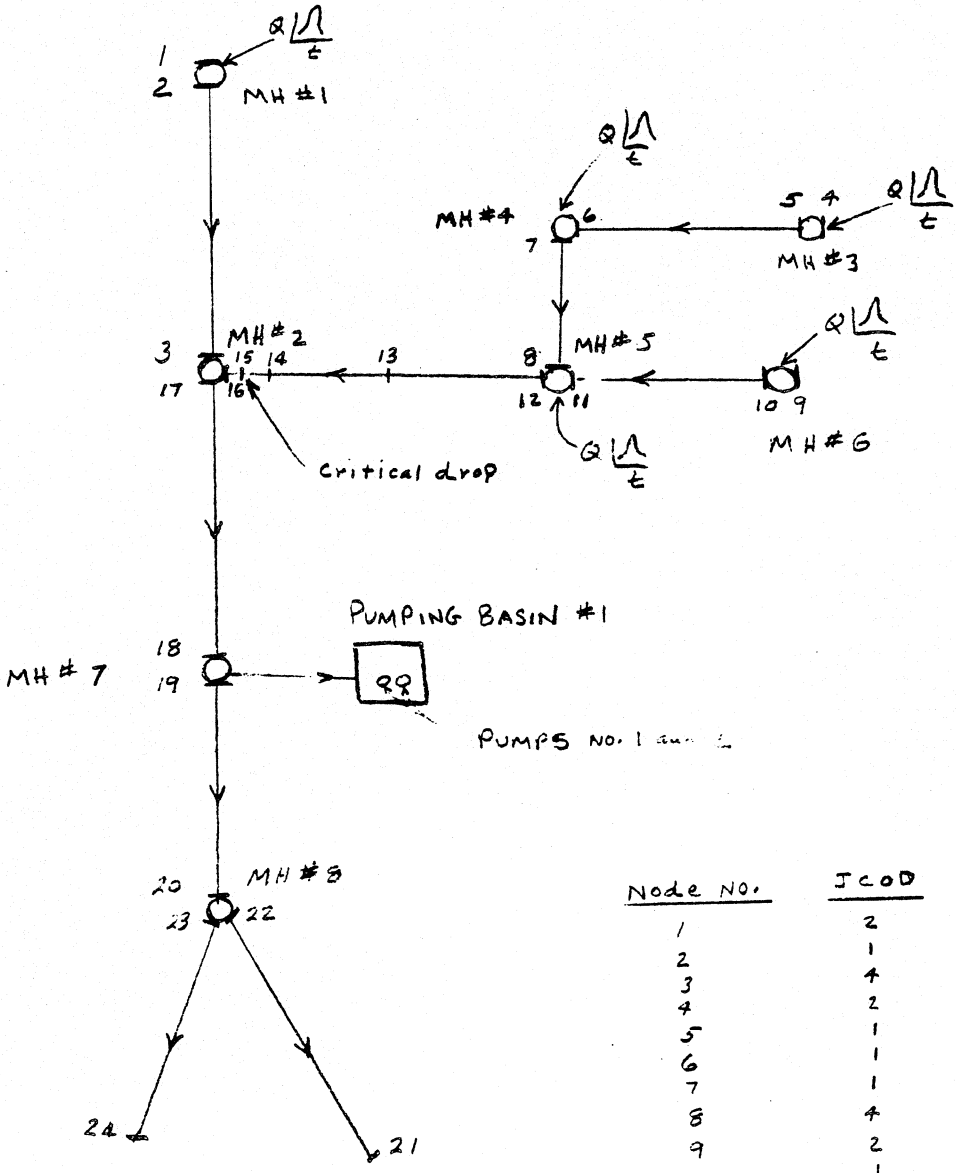

Junction No.	JU	JB	JL
1	3	16	17
2	8	11	12
3	20	22	23

Node No.	JCOD
1	2
2	1
3	4
4	2
5	1
6	1
7	1
8	4
9	2
10	1
11	4
12	4
13	1
14	1
15	11
16	4
17	4
18	1
19	1
20	4
21	2
22	4
23	4
24	3

UNSTEADY FLOW APPLICATIONS IN WATERWAYS[1]

February 1983

Almost all flow in waterways is to some extent unsteady, i.e., it changes with time. Also, the rate of flow and the depth usually vary along the length of the waterway. The extent of flow variation with time and distance may be such that steady flow may be assumed for very limited conditions. Sometimes and in certain applications, the flow may be assumed to be uniform along the length of the waterway. Usually, such simple flow conditions are only approached prior to an unsteady flow disturbance. Indeed, it is usually the unsteady flow disturbance (transient) that is of vital engineering significance. Among the most important causes of transient flows are the following:

(1) Runoff from precipitation (rainfall event and/or snowmelt)
(2) Transient flows released from reservoirs during operations for flood control, hydropower generation, recreation, and wildlife management, etc.
(3) Tidal-generated waves
(4) Dam-break floods
(5) Wind-generated storm surges or seiches
(6) Landslide-generated waves
(7) Earthquake-generated tsunami waves
(8) Irrigation flows affected by gates, pumps, diversions, etc.

The waterway may be naturally formed as in the case of streams, rivers, reservoirs, lakes, and estuaries, in which the cross-sectional geometry and bottom slope may vary from fairly uniform to very irregular. Waterways may be man-made such as canals, ditches, sewers, and flumes in which the cross-sectional geometry and bottom slope are usually uniform with perhaps small discontinuities.

The waterway may be a single channel or a network of connected channels. The network may be dendritic (tree-type) in which the branches (1) function as tributary channels, (2) function as distributary channels such as river deltas or irrigation canals (ditches). The network may consist of bifurcations such as the channels formed by islands; the bifurcations may be associated with bypass channels, sewer systems, or estuarial networks.

Unsteady flow models based on the complete Saint-Venant equations, or some simplified form thereof, provide a means for analyzing the flow of water along various waterways in numerous applications of engineering significance. Some of the applications are listed below:

(1) Flood forecasting for real-time (a) warnings, (b) flood control operations, (c) evacuation, and (d) navigation information.

---

[1]D. L. Fread, Senior Research Hydrologist, Hydrologic Research Laboratory, National Weather Service, Silver Spring, Maryland 20910

(2) Flood prediction for developing (a) flood control systems (man-made reservoirs, bypasses, diversions channels, levees, spillways-uncontrolled, gated), (b) evacuation plans, (c) flood insurance assessments, (d) river improvements, (f) land use analyses, and (g) downstream assessment of reservoir releases (hydropower, flood control, dam-failure).
(3) Design and real-time operation of sewer systems
(4) Design and real-time operation of irrigation systems
(5) Design of highway bridges and culverts
(6) Water quality prediction (temperature, oil spill, BOD, etc.)in conjunction with other transport and reaction models
(7) Prediction of alluvial river bed and roughness changes due to sediment transport in conjunction with sediment transport models
(8) Streamflow-aquifer interactions in conjunction with groundwater models

Four applications are selected for presentation herein. They include: (1) a long, very mild sloping large river with a slow rising flood wave; (2) a dendritic river system consisting of four mild sloping large rivers with moderately rising flood waves and mutual backwater effects among the channels of the network; (3) a large, very mild sloping dendritic river system affected by a large tide at its mouth; and (4) a moderately sloping river subjected to a rapidly rising dam-break flood wave. These applications represent a wide spectrum of wave and channel characteristics for which the dynamic wave model is particularly well-suited and potentially the most accurate of the routing models.

Lower Mississippi. An unsteady flow model (DWOPER) was applied to a 291.7 mile reach of the Lower Mississippi River from Red River Landing to Venice shown schematically in Fig. 1 (Fread, 1978). Six intermediate gaging stations at Baton Rouge, Donaldsonville, Reserve, Carrollton, Chalmette, and Point a la Hache were used to evaluate the simulations. This reach of the Lower Mississippi is contained within levees for most of its length, although some overbank flow occurs along portions of the upper 70 miles. Throughout the reach, the alluvial river meanders between deep bends and relatively shallow crossings; the sinuousity coefficient is 1.6. The low flow depth varies from a minimum of 30 ft at some crossings to a maximum depth of almost 200 ft in some bends. The average channel width is approximately one-half mile. The average channel bottom slope is a very mild 0.0000064. The Manning n varies from about 0.012 to 0.030. The discharge varies from low flows of about 100,000 cfs to flood discharges of over 1,200,000 cfs. A total of 25 cross sections located at unequal intervals ranging from 5-20 miles were used to describe the 291.7 mile reach.

The reach was first automatically calibrated for the 1969 spring flood. Time steps of 24 hours were used. Then, using the calibrated set of Manning n vs. discharge for each reach bounded by gaging stations, the 1969 flood was simulated using water elevation (stage) hydrographs for upstream and downstream boundaries at Red River Landing and Venice, respectively. The simulated stage hydrographs at the six intermediate gaging stations were compared with the observed hydrographs. The root-mean-square (RMS) error was used as a statistical measure of the accuracy of the calibration. The RMS error varied from 0.17 - 0.36 ft with an average value of 0.25 ft.

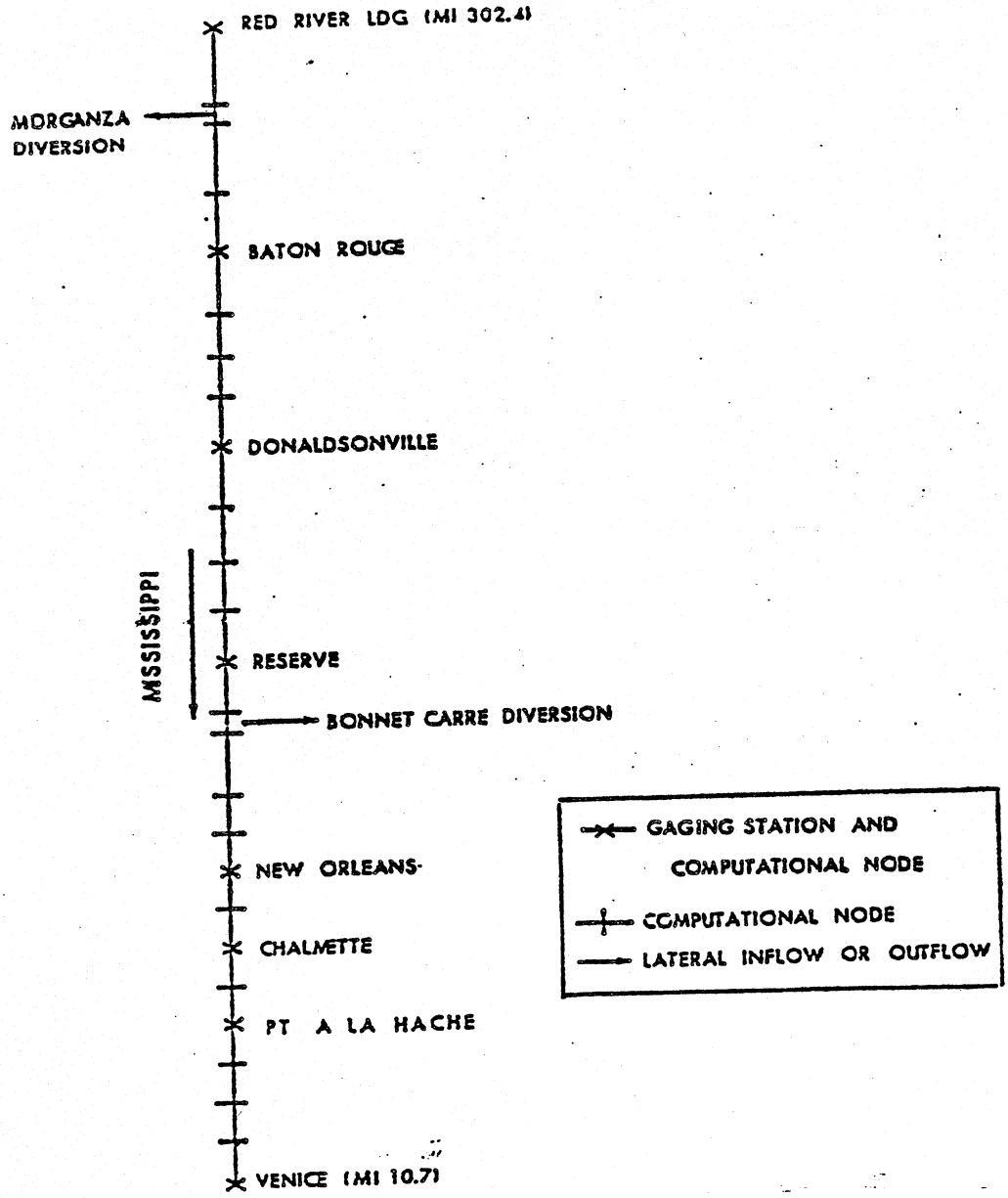

Figure 1. Schematic of Lower Mississippi River.

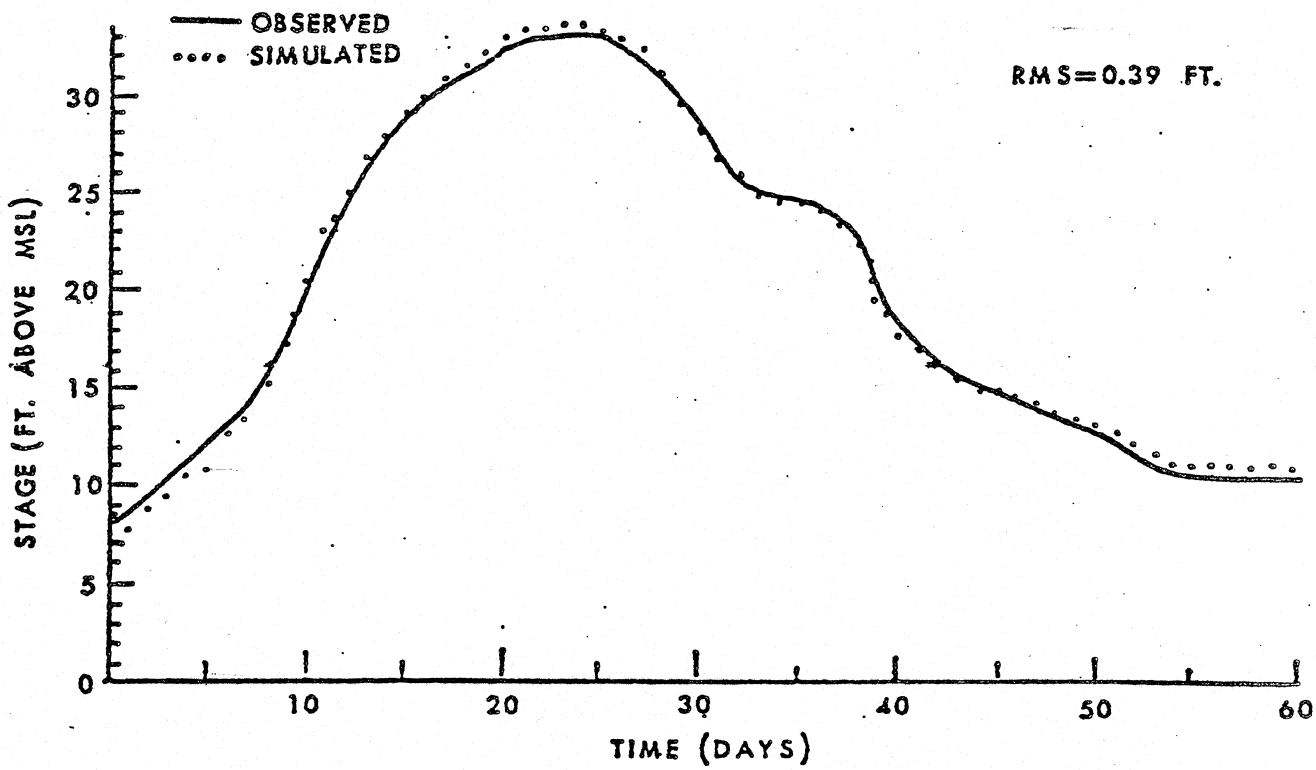

Figure 2. Observed vs. simulated stages at Baton Rouge for 1966 flood.

Several historical floods from the period 1959-1971 were then simulated using the calibrated Manning n values obtained from the 1969 flood. An example of simulated vs. observed stages is shown in Fig. 2 for the 1966 flood. Average RMS errors for all six stations for each of the simulated floods are shown in Table 1. The average RMS error for all the floods was 0.47 ft. This compares with 0.25 ft for the calibrated flood of 1969, indicating that for this reach of the Mississippi there is not a significant change in the channel roughness from one flood event to another. A calibration run required 7 sec on an IBM 360/195 computer system while a normal simulation run required 6 sec.

Mississippi-Ohio-Cumberland-Tennessee System. A dendritic channel system consisting of 393 miles of the Mississippi-Ohio-Cumberland-Tennessee (MOCT) River System was also simulated using DWOPER. A schematic of the river system is shown in Fig. 3. Eleven intermediate gaging stations located at Fords Ferry, Golconda, Paducah, Metropolis, Grand Chain, Cairo, New Madrid, Red Rock, Grand Tower, Cape Girardeau, and Price Landing were used to evaluate the simulation.

In applying DWOPER to this system, the main channel was considered to be the Ohio-Lower Mississippi segment with the Cumberland, Tennessee, and Upper Mississippi considered as first-order tributaries. The channel bottom slope is mild, varying from about 0.000047 to 0.000095. Each branch of the river system is influenced by backwater from downstream branches. Total discharge through the system varies from low flows of approximately 120,000 cfs to flood flows of 1,700,000 cfs. A total of 45 cross sections located at unequal intervals ranging from 0.5 to 20 miles were used to describe the MOCT river system.

The MOCT system was calibrated to determine the n-Q relationship for each of 15 reaches bounded by gaging stations. Time steps of 24 hours were used. About 25 seconds of IBM 360/195 CPU time were required by DWOPER to perform the calibration; a simulation run required only about 15 sec. The flood of 1970 was used in the automatic calibration process. The average RMS error for all 15 reaches was 0.60 ft. Typical comparisons of observed and simulated stages for the Cairo and Cape Girardeau gaging stations are shown in Figs. 4 and 5, respectively.

Using the calibrated n-Q relations, the 1969 flood was simulated. Stage hydrographs at Shawneetown and Chester and discharge hydrographs at Barkely Dam and Kentucky Dam were used as upstream boundary conditions, and a rating curve was used as the downstream boundary condition at Caruthersville. The average RMS error for the 11 intermediate gaging stations was 0.56 ft.

Columbia-Willamette System. DWOPER was applied to the 130-mile reach of the lower Columbia River below Bonneville Dam, including the 25-mile tributary reach of the lower Willamette River. A schematic of the river system is shown in Fig. 6.

This reach of the Columbia has a very flat slope (0.000011) and the flows are affected by the tide from the Pacific Ocean. The tidal effect extends as far upstream as the tailwater of Bonneville Dam during periods of low flow. Reversals in discharge during low flow are possible as far upstream as Vancouver. A total of 25 cross sections located at unequal distance intervals ranging from 0.6 -12 miles were used to describe the river system. One-hour time steps were used in the simulations which required about 11 sec on an IBM 360/195 computer system.

Table 1. Summary of flood simulations in Lower Mississippi River (Red River Landing to Venice) for the years 1959-1971.

Year	Average RMS error (ft.)	Peak discharge (1,000 cfs)
1959	0.62	750
1960	.31	850
1961	.47	1,220
1962	.61	1,155
1963	.38	950
1964	.51	1,140
1965	.44	1,040
1966	.38	1,090
1967	.38	700
1968	.36	980
1969*	.25	1,065
1970	.91	1,080
1971	.41	940

*Calibrated

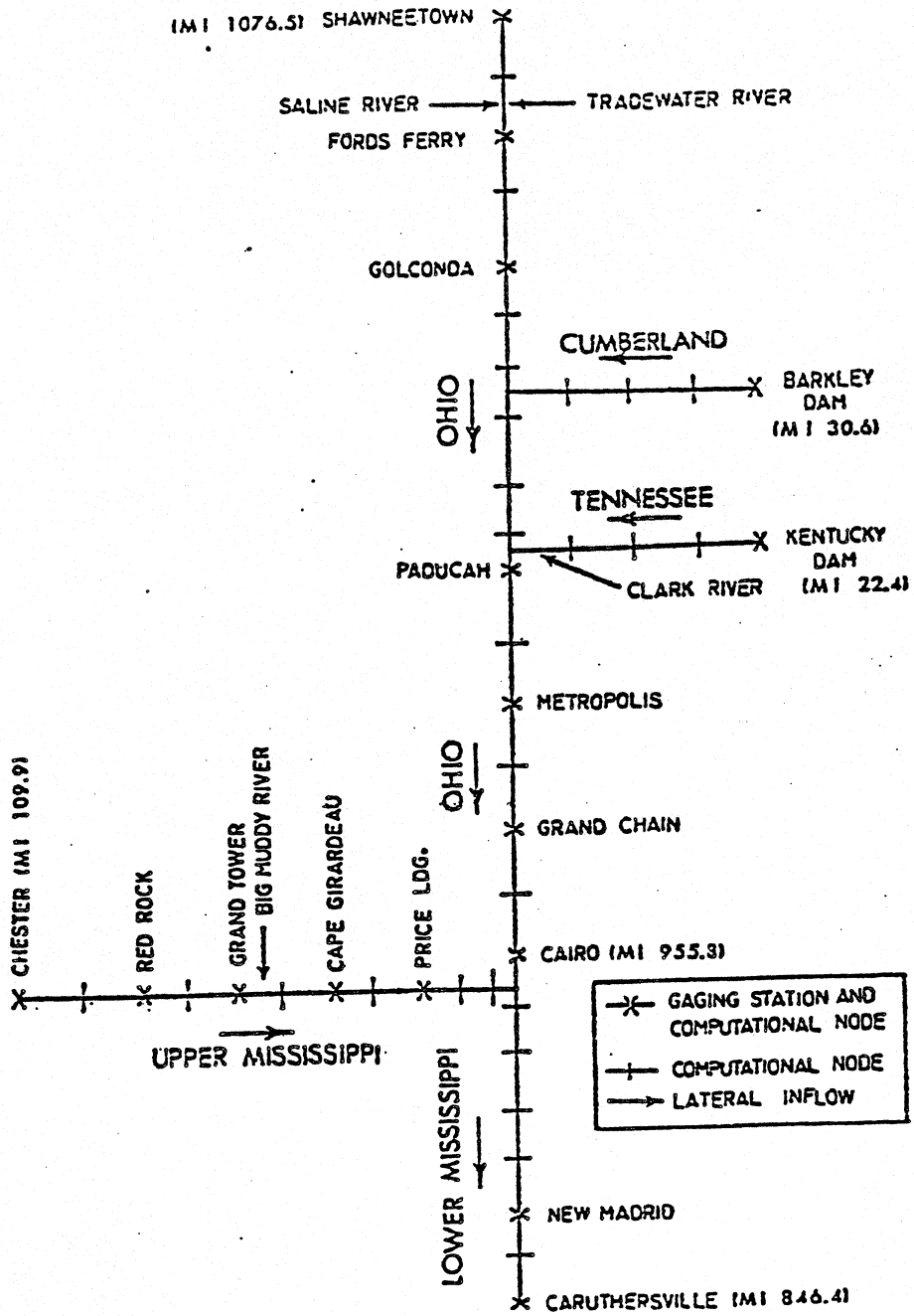

Figure 3. Schematic of Mississippi-Ohio-Cumberland-Tennessee (MOCT) River System.

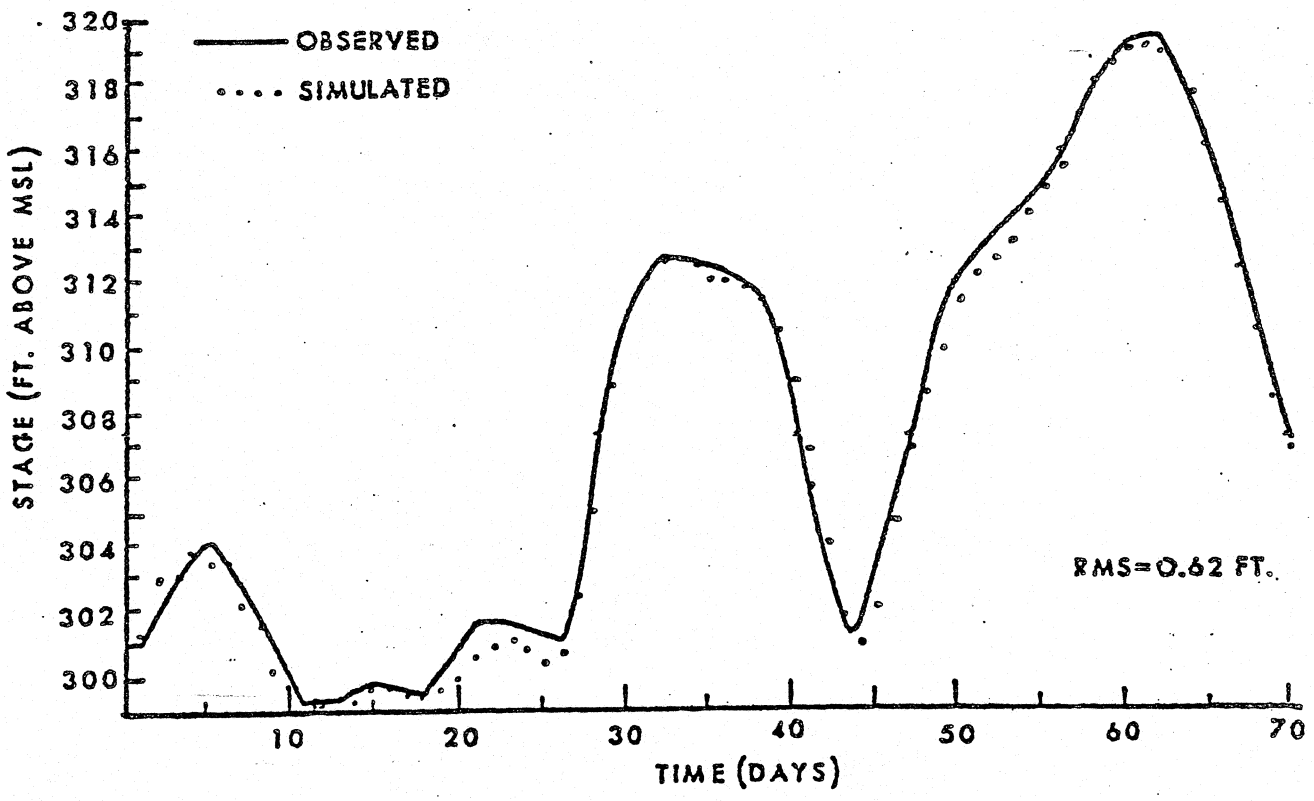

Figure 4. Observed vs. simulated stages at Cairo for 1970 flood.

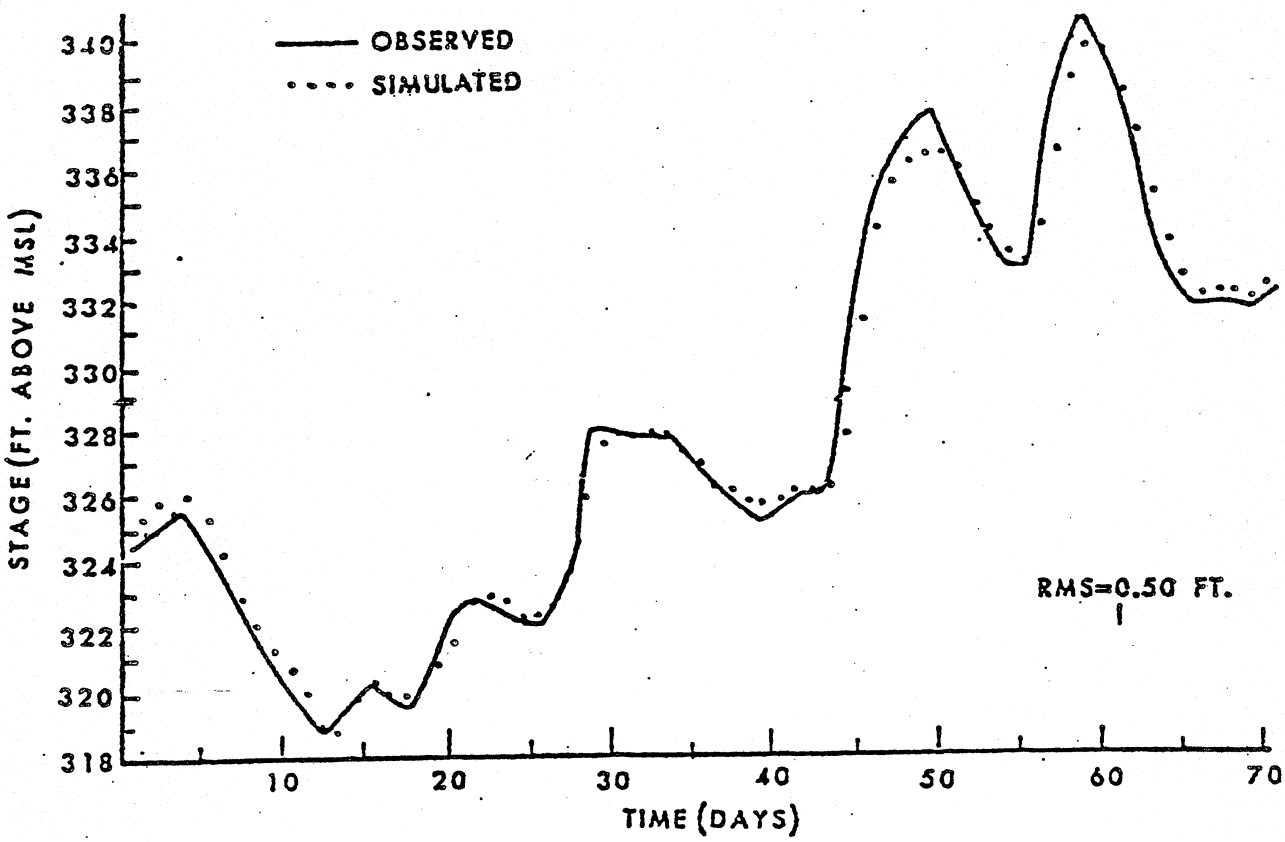

Figure 5. Observed vs. simulated stages at Cape Girardeau for 1970 flood.

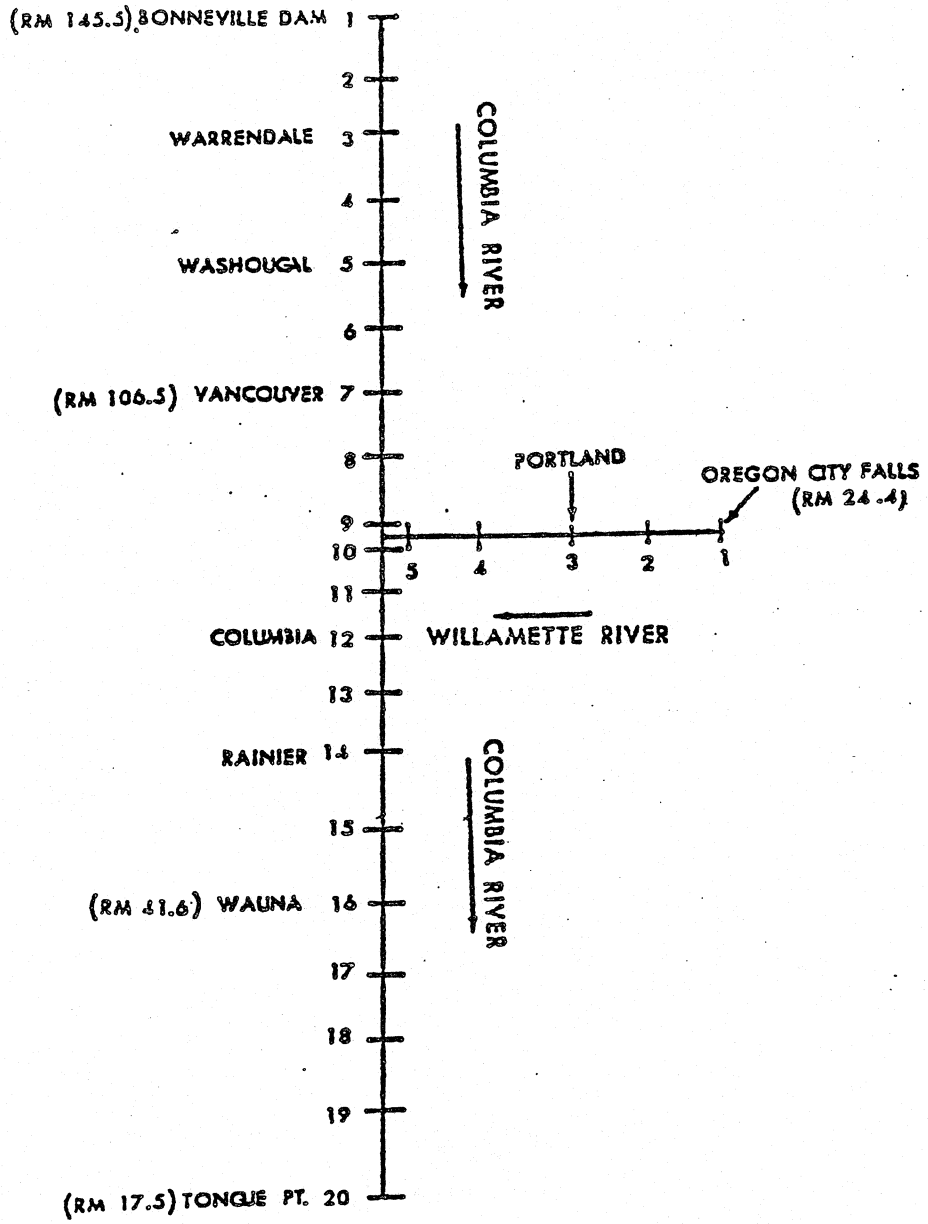

Figure 6. Schematic of lower Columbia-Willamette River System.

The system was first calibrated for a 4-day period in August 1973. Seven intermediate gaging stations at Warrendale, Washougal, Vancouver, Portland, Columbia City, Rainier, and Wauna were used along with the gaging stations at the extremities of the system, i.e., Bonneville, Oregon Falls, and Tongue Point. Another 5-day period in August 1973 was then simulated using the calibrated n-Q relations. Upstream and downstream boundaries were observed discharges and stages, respectively. The average RMS error for all stations in the simulation run was 0.21 ft. Some examples of simulated and observed stage hydrographs for Portland and Wauna are shown in Figs. 7 and 8, respectively.

Teton Dam-Break Flood. The Teton Dam, a 300-ft high earthen dam with a 3,000-ft long crest, failed on June 5, 1976, killing 11 people, making 25,000 people homeless, and inflicting about $400 million in damages to the downstream Teton-Snake River Valley. Data from the U.S. Geological Survey provided observations on the approximate development of the breach, description of the reservoir storage, downstream cross sections and estimated values of the Manning's n approximately every 5 miles, indirect peak discharge measurement at three sites, flood peak travel times, and flood peak elevations. The inundated area is shown in Fig. 9.

The following breach parameters were used in DAMBRK (Fread, 1980) to reconstitute the downstream flooding due to the failure of Teton Dam:

τ_{br} = 1.25 hrs, $\hat{b}$ = 150 ft, z = 0, h_{bm} = 0.0, $h_f = h_d$ = 261.5 ft, Q = 16,000 cfs.

The initial depth of the reservoir was 261.5 ft. Cross sections at 12 locations shown in Fig. 11 along the 60-mile reach of the Teton-Snake River Valley below the dam were used. The average bottom slope of the 60-mile reach is 0.00135. Five top widths were used to describe each cross-section. The downstream valley consists of a narrow canyon (approximately 1,000 ft wide) for the first 5 miles and thereafter a wide valley which was inundated to a width of about 9 miles. The estimated Manning n values vary from 0.028 to 0.047. Additional cross sections were interpolated such that computational reach lengths varied from 0.5 to 1.5 miles. The downstream boundary was assumed to be channel flow control as represented by a loop rating curve.

The computed outflow hydrograph is shown in Fig. 9. It has a peak value of 1,652,300 cfs, a time to peak of 1.25 hrs, and a total duration of about 6 hrs. The peak is about 20 times greater than the flood of record. The temporal variation of the computed outflow volume compared within 5 percent of observed values. The computed peak discharge values along the 60-mile downstream valley are shown in Fig. 10 along with three observed (indirect measurement) values at miles 8.5, 43.0, and 59.5. The average difference between the computed and observed values is 4.8 percent. Most apparent is the extreme attenuation of the peak discharge as the flood wave propagates through the valley. Losses due to infiltration and detention storage behind irrigation levees were assumed to vary from zero to a maximum of -0.30 cfs/ft and were accounted for by the lateral outflow (q).

The a priori selection of the breach parameters (τ_{br} and $\hat{b}$) causes the greatest uncertainty in simulating dam-break flood waves. However, sensitivity studies (Fread, 1980) show that large differences in the discharges near the Teton Dam rapidly diminish in the downstream direction. After 15 miles, the variation diminished to (+15 to -8 percent) for variations in $\hat{b}$

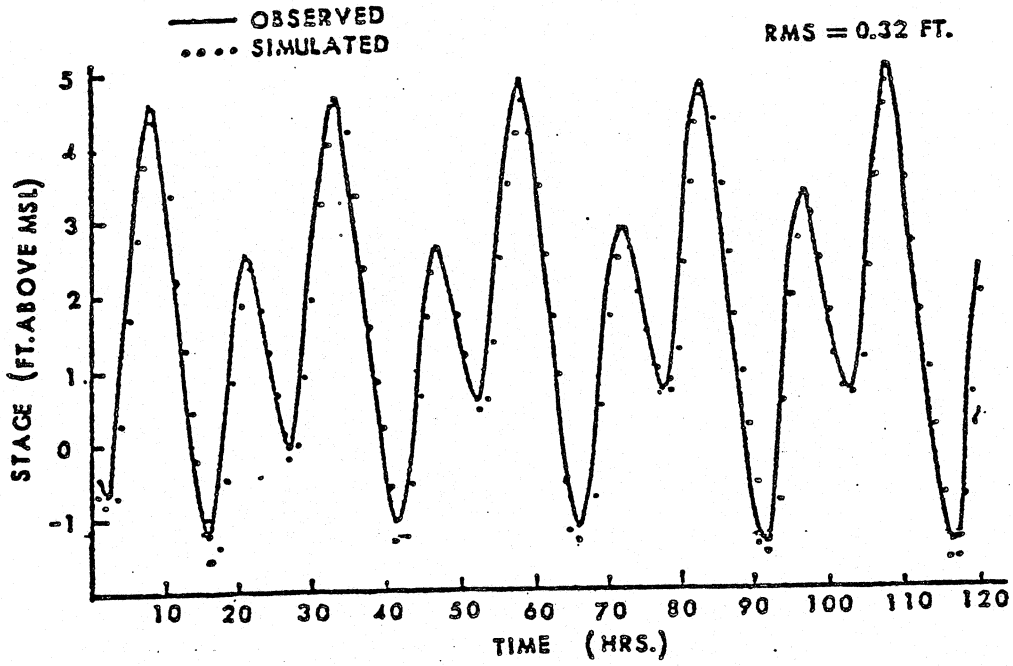

Figure 7. Observed vs. simulated stages at Wauna.

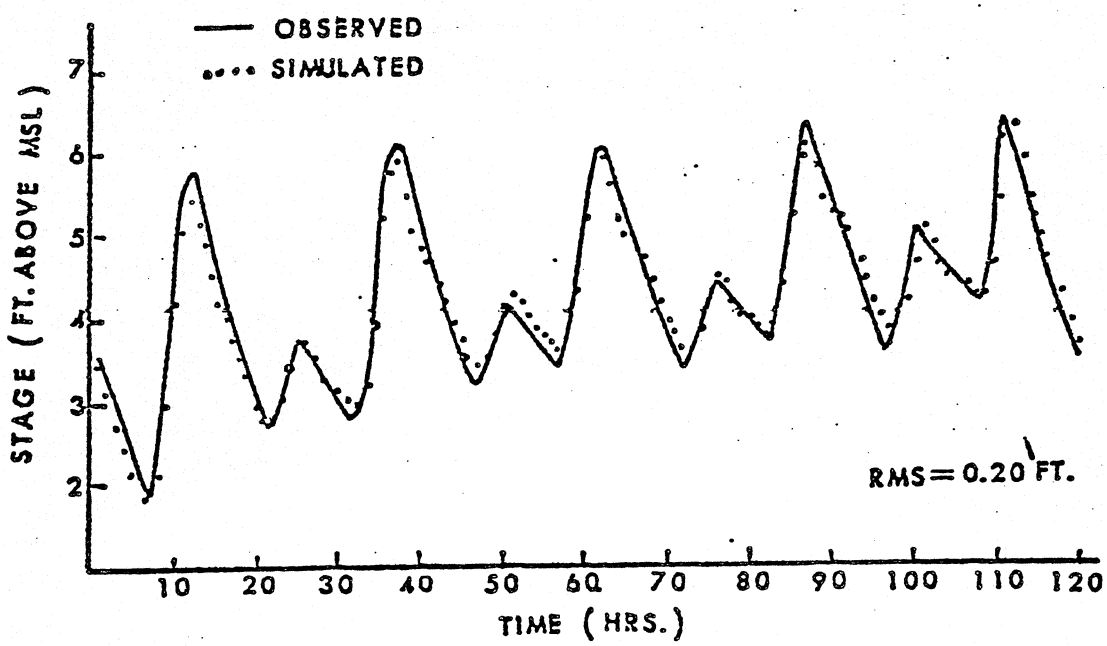

Figure 8. Observed vs. simulated stages at Portland.

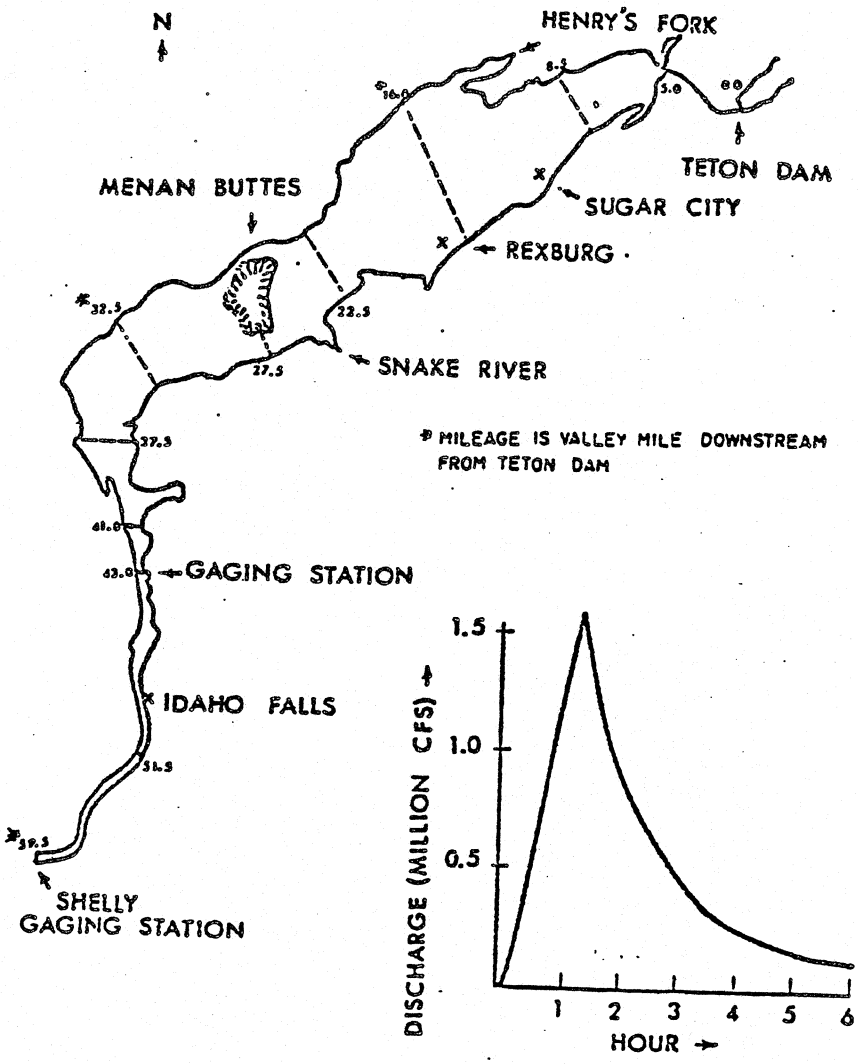

Figure 9. Outflow hydrograph and flood area downstream of Teton Dam.

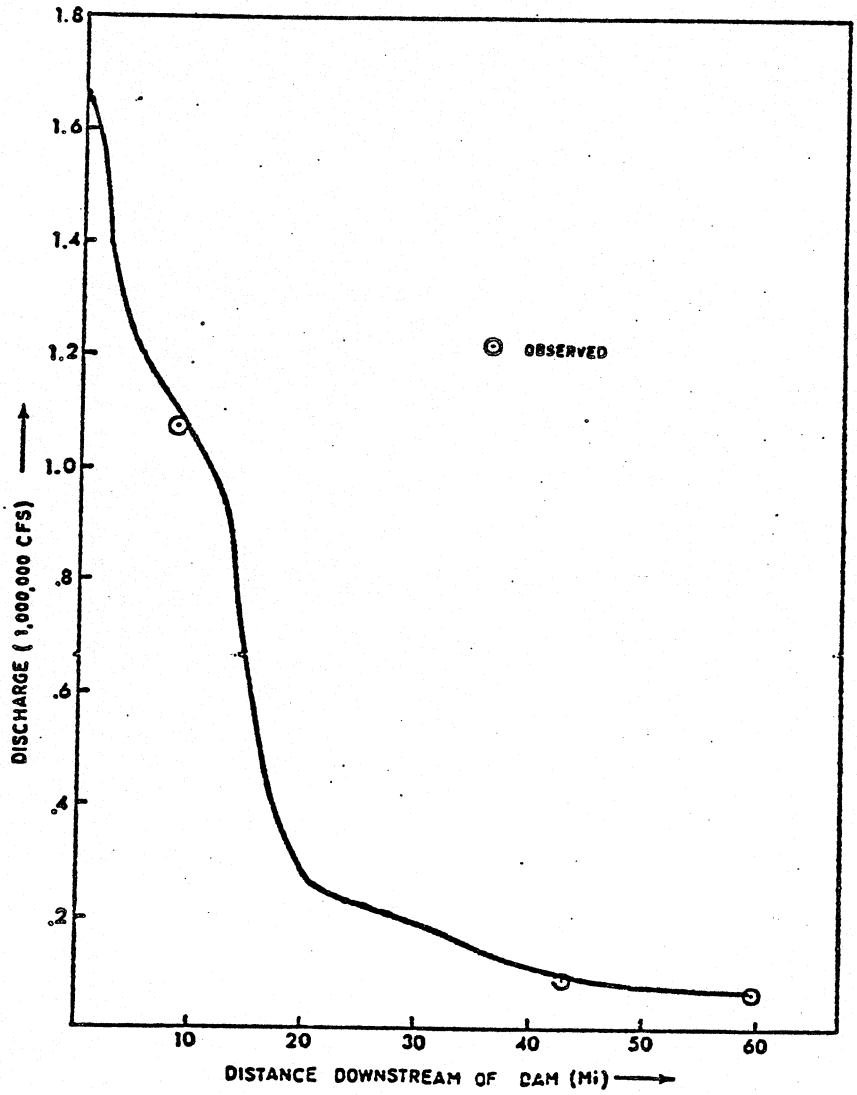

Figure 10. Profile of peak Discharge from Teton Dam failure.

of a factor of 2 and in τ_{br} of a factor from 0.3 to 2. The tendency for extreme peak attenuation and rapid damping of differences in the peak discharge is accentuated in the case of Teton Dam due to the presence of the very wide valley. Had the narrow canyon extended all along the 60-mile reach to the Shelly gage, the peak discharge would not have attenuated as much and the difference in peak discharges due to variations in $\hat{b}$ and τ_{br} would be more persistent. In this instance, the peak discharge (cfs) would have attenuated to about 350,000 rather than 67,000 and the differences in peak discharges at mile 59.5 would have been about 27 percent, as opposed to less than 5 percent for the actual wide valley.

Computed peak elevations compared favorably with observed values. The average absolute error was 1.5 ft, while the average arithmetic error was only -0.2 ft. The computed travel time of the flood wave was compared with observed values at the locations of the discharge measurements; they differed by less than 10 percent.

A typical simulation of the Teton flood involved 78 Δx reaches, 55 hrs of prototype time, and an initial time step (Δt) of 0.06 hrs which was automatically increased gradually to 0.5 hrs as the wave propagated downstream and natural dispersion increased the time of rise. Such a simulation run required only 19 sec on an IBM 360/195 computer system.

REFERENCES

Fread, D.L. (1978). 'NWS operational dynamic wave model", in Verification of Mathematical and Physical Models, Proc. of 26th Annual Hydr. Div., Specialty Conf., ASCE, College Park, Maryland, pp. 455-464.

Fread, D.L. (1980). 'Capabilities of NWS model to forecast flash floods caused by dam failures', in Proc., 2nd Conf. on Flash Floods, Atlanta, Georgia, American Met. Soc., pp. 171-178.

Parameter Optimization of Dynamic Routing Models

D.L. Fread and J.M. Lewis*

Abstract - A methodology has been developed for determining the optimal parameters of dynamic routing models thereby eliminating costly and time-consuming preparation of detailed cross-sectional data. The methodology utilizes (1) approximate cross-sectional properties represented by separate power functions for channel and floodplain, and (2) a very efficient optimization algorithm for determining the Manning n as a function of either stage or discharge. Essential data required for implementing the methodology are stage hydrographs at both ends of each routing reach and a discharge hydrograph at the upstream end of each river. The methodology is applicable to multiple routing reaches along main-stem rivers and their tributaries. Optimal n values may be constrained to fall within a specified min-max range for each routing reach. Specific cross-sectional properties at key locations, e.g., bridges, dams, unusual constrictions, also can be utilized within the optimization methodology. The methodology was tested on 1275 miles (2051 km) of major rivers and their principal tributaries in the U.S. with promising results; the average root-mean-square error was 0.44 ft (0.13 m) or 2.9 percent of the change in stage.

Introduction

Flood routing is an essential tool for flood forecasting and engineering design or analysis of hydraulic structures. Of the many flood routing methods that have been developed, dynamic flood routing based on a four-point implicit finite difference solution of the one-dimensional equations of unsteady flow (Saint-Venant equations) has generally been accepted as the most powerful with feasible computational requirements. Dynamic routing enables the prediction of water elevations (h) and discharges (Q) along a single waterway or a network of interactive waterways. Complex hydraulic phenomena such as reverse flows, backwater effects from tributary inflows and hydraulic structures, flow accelerations, levee overtopping, etc. may be properly accounted for in dynamic routing. However, such phenomena are neglected by the simple hydrologic routing techniques, and yet these are sometimes selected for such applications because data for optimizing their parameters is more readily available than for dynamic routing.

Dynamic routing has been applied when there was a substantial amount of cross-sectional data available to characterize the cross-sectional area (A) and top width (B) as known functions of h. This required the existence of detailed hydrographic survey information and topographical maps, as well as considerable time consuming effort by

*Senior Res. Hydrologist & Res. Hydrologist, National Weather Service Hydrologic Res. Laboratory, 8060 13th St., Silver Spring, MD 20910.

hydrologists to reduce the basic cross-sectional information to the form of A and B as specified tabular functions of h. In order to eliminate the necessity for using such costly and often unavailable detailed data, a very powerful and computationally efficient parameter optimization methodology which utilizes minimal cross-sectional information was developed for application by the National Weather Service hydrologists for flood forecasting. Also, this methodology could be used advantageously by hydrologists/engineers concerned with unsteady flow prediction in waterways of many developing countries where detailed cross-sectional data is prohibitively expensive to obtain because of the remote locations of the waterways and the relative magnitude of the effort required for a single engineering study.

Theory and Background

The Saint-Venant equations of unsteady flow consist of a conservation of mass equation, i.e.

$$\partial Q/\partial x + \partial(A + A_o)/\partial t - q = 0 \qquad (1)$$

and a conservation of momentum equation, i.e.,

$$\partial Q/\partial t + \partial(Q^2/A)/\partial x + gA(\partial h/\partial x + S_f) - qv_x = 0 \qquad (2)$$

where:

$$S_f = n^2 \, |Q|Q/(2.21 \, A^2 \, R^{4/3}) \qquad (3)$$

in which x is the distance along the longitudinal axis of the waterway, t is time, Q is discharge, A is active cross-sectional area, A_o is inactive (off-channel storage) area, q is lateral inflow (positive) or outflow (negative), g is the gravity acceleration constant, h is water surface elevation or stage, v_x is the velocity of the lateral flow in the x-direction, S_f is the friction slope computed by Manning's equation, n is the Manning coefficient, and R is the hydraulic radius.

In this paper, a dynamic routing model, FLDWAV, based on Eqs (1) and (2) which are solved by an implicit 4-point nonlinear finite difference technique described elsewhere (Fread, 1985; Fread and Smith, 1978) is used to implement and test the optimization methodology.

Data normally required to calibrate a dynamic routing model are: 1) cross-sectional area (A) and width (B) as a function of water surface elevation (h) for sections representative of the routing reach, 2) the Manning n which may vary with either elevation or discharge throughout the routing reach, 3) observed discharge and stage hydrographs at the upstream end of the routing reach, and either a stage or discharge hydrograph at the downstream extremity of the routing reach.

To avoid the costly and time-consuming tasks of gathering detailed cross-section data and then reducing the data into tables of top width (B) and water elevation (h), simple approximations are used to represent an average cross-section within each routing reach. A power function, $B_c = k_c Y_c^{m_c}$, is used for the channel and another power function, $B_f = k_f Y_f^{m_f}$, is used for the floodplain. The

parameters k_c, m_c, k_f, m_f are estimated from 1) topographical maps, 2) visual inspection of a few easily accessible cross-sections, and/or 3) a few available cross-sections of the river. The shape parameter (m_c) can be easily computed, i.e.,

$$m_c = (\log B_2 - \log B_1)/(\log Y_2 - \log Y_1) \qquad (4)$$

in which B_2 and Y_2 are the estimated bank-full width and depth and B_1 and Y_1 are estimates of an intermediate width and depth. The scaling parameter (k_c) is computed from the basic power function, i.e., $k_c = B/Y^{m_c}$. Similarly the shape and scaling parameters for the floodplain can be computed from estimates of the floodplain widths and depths. Sometimes it is appropriate simply to estimate the shape parameter, i.e., rectangular-shape (m=0), parabolic shape (m=0.5), triangular shape (m=1.0) or Υ-shapes (m>1). The parameter optimization methodology which has been programmed as an integral option within the FLDWAV routing model allows the k and m parameters to be specified directly or to be computed by the program from the specified B and Y values for each routing reach.

When unusual cross-sections exist in a routing reach, e.g., at a bridge, dam, or some natural constriction, those cross-sections' top width and elevation tables may be specified; they each remain distinct from the average section described by the two power functions.

A parameter optimization algorithm within FLDWAV iteratively determines the best value for the Manning n which is allowed to vary with h or Q for each reach of waterway bounded by water level recorders. An objective function defined as the difference between the computed and observed upstream stage hydrographs for several ranges of flow is minimized by a Newton-Raphson technique (Fread and Smith, 1978; Fread, 1985). A numerical derivative is used in lieu of the analytical derivative for the rate of change of the objective function with respect to the change in the Manning n. With starting values for n based on an assumption of steady flow or simply using a reasonable estimate, convergence to an optimal set of values is obtained in three to four iterations, i.e., the optimal n relation with h or Q for the reach of water bounded by known stage hydrographs can be obtained within three to four evaluations of the objective function; an evaluation consists of routing the flood hydrograph through the reach and comparing computed and observed upstream stage values. An option in FLDWAV allows the hydrologist to estimate a range of minimum and maximum n values within which the optimal n values must reside. When the optimal values are outside the specified min-max range, the cross section is automatically reduced or increased sufficiently to allow the next optimization to yield n values within the allowable range.

The optimization algorithm can be applied to multiple routing reaches, commencing with the most upstream reach and progressing reach-by-reach in the downstream direction. An observed discharge hydrograph is used as an upstream boundary condition for the most upstream reach. Then, the discharges computed at the downstream boundary using the optimal n values are stored internally by the program and used as the upstream boundary condition for the next downstream reach. Dendritic river systems are automatically decomposed into a

series of multiple-reach rivers. Tributaries are optimized before the main-stem river and their flows are added to the main stem as lateral inflow(s).

This parameter optimization methodology offers several advantages over one described by Wormleaton and Karmegam (1984) which required 26 iterations to find the optimal parameters. It was restricted to a trapezoidal shaped cross-section with a constant n value and was for a single routing reach bounded by gaging stations with observed stage and discharge hydrographs from a previous flood.

The optimal n values obtained via the parameter optimization methodology presented herein is limited to expected applications where the maximum discharges do not greatly exceed those used in the optimization. Also, the methodology is best suited for applications where flood predictions are primarily required at locations along the waterway where level recorders exist. Unless detailed cross-sectional information at significant constrictions or expansions is utilized in the optimization methodology, the cross sections throughout each routing reach should be generally uniform.

Applications

The new parameter optimization methodology has been tested on the following four river systems:

Lower Mississippi. This is a 292 mi (470 km) reach of the Lower Mississippi River consisting of eight water level recorders. The discharge is known at the most upstream station. This reach of the Lower Mississippi is contained within levees for most of its length. The average channel slope is an extremely mild 0.0000064. The discharge varies from low flows of about 100,000 cfs (2,832 m/s) to flood discharges of over 1,200,000 cfs (33,985 m/s). A total of 25 cross sections located at unequal intervals including the locations of the level recorders were used in the computations. The results of the parameter optimization are shown in Table 1. The effectiveness of the optimization is represented by the root-mean-square (rms) error between the computed and observed stage hydrographs at each level recorder. The average rms value is 0.37 ft (0.11 m). Also, this is presented as a percentage of the total change in water elevation which is only 2.4 percent. The average number of iterations or times that the flood is routed through each reach is three. Although the n values vary with discharge, the average value is shown for each reach.

Ohio-Mississippi. This is a dendritic river system consisting of 393 miles (633 km) of the Mississippi, Ohio, Cumberland, and Tennessee Rivers with a total of 16 water level recorders and discharge measurements at the most upstream stations on each of the four rivers. The channel bottom slope is mild, varying from about 0.000047 to 0.000095. Each branch of the river system is influenced by backwater from downstream branches. Total discharge through the system varies from about 120,000 cfs (3,398 cms) to flood flows of 1,700,000 cfs (48,145 cms). A total of 45 cross-sections located at unequal intervals were used in the computations. The results of the parameter optimization are shown in Table 1. The average rms error is 0.66 ft. (0.20 m) representing

Table 1. Optimization Results for Four Major River Systems

RIVER SYSTEM River	Station	Root-Mean-Square Error ft (m)	Root-Mean-Square Error Percent	Iterations	n_{avg}
L. MISSISSIPPI					
L. Mississippi	Red River Ldg.	0.11 (.03)	0.5	3	.025
"	Baton Rouge	0.16 (.05)	0.7	3	.018
"	Donaldsonville	0.16 (.05)	0.9	3	.015
"	Carrollton	0.27 (.08)	2.5	2	.014
"	Pt. Hache	0.27 (.08)	4.7	3	.015
		Avg 0.19 (.06)	Avg 1.9	Avg 3	
OHIO-MISSISSIPPI					
Ohio	Shawneetown	0.65 (.20)	2.3	3	.018
"	Golconda	0.67 (.20)	2.4	4	.021
"	Paducah	0.68 (.21)	2.7	3	.023
"	Metropolis	0.59 (.18)	2.8	4	.020
"	Cairo	1.04 (.32)	4.8	6	.026
Cumberland	Berkley Dam T.W.	0.77 (.23)	2.8	4	.016
Tennessee	Kentucky Dam T.W.	0.85 (.26)	3.4	4	.036
U. Mississippi	Chester	0.34 (.10)	1.4	3	.026
"	Grand Tower	0.47 (.14)	2.0	3	.032
"	Cape Girardeau	0.51 (.15)	2.2	2	.024
L. Mississippi	New Madrid	0.72 (.22)	3.8	3	.022
		0.66 (.20)	2.8	3	
ILLINOIS-MISSISSIPPI-MISSOURI					
Illinois	Morris	0.30 (.09)	2.2	2	.025
"	La Salle	0.21 (.06)	1.2	4	.030
"	Henry	0.30 (.09)	2.8	4	.020
"	Peoria	0.21 (.06)	1.6	5	.046
"	Havana	0.63 (.19)	3.3	3	.038
"	Beardstown	0.50 (.15)	2.7	3	.033
"	Meredosia	0.15 (.05)	0.6	3	.022
"	Harding	0.54 (.16)	2.8	3	.017
Mississippi	L&D No. 24 T.W.	0.38 (.12)	1.8	3	.028
"	L&D No. 25 T.W.	0.41 (.13)	1.8	2	.039
"	Dixon Ldg.	0.35 (.11)	1.7	4	.033
"	Alton	0.18 (.05)	0.6	3	.023
"	St. Louis	0.47 (.14)	1.1	4	.024
Missouri	Hermann	0.68 (.21)	2.7	4	.034
		0.38 (.12)	1.9	3	
COLUMBIA					
Columbia	Bonneville	0.22 (.07)	2.4	4	.040
"	Washougal	0.27 (.08)	4.5	3	.032
"	Vancouver	0.31 (.09)	6.2	4	.024
"	Columbia	0.40 (.12)	8.3	4	.016
"	Wauna	0.74 (.23)	11.4	3	.022
Willamette	Portland	0.30 (.09)	5.0	3	.024
		0.37 (.11)	6.3	4	

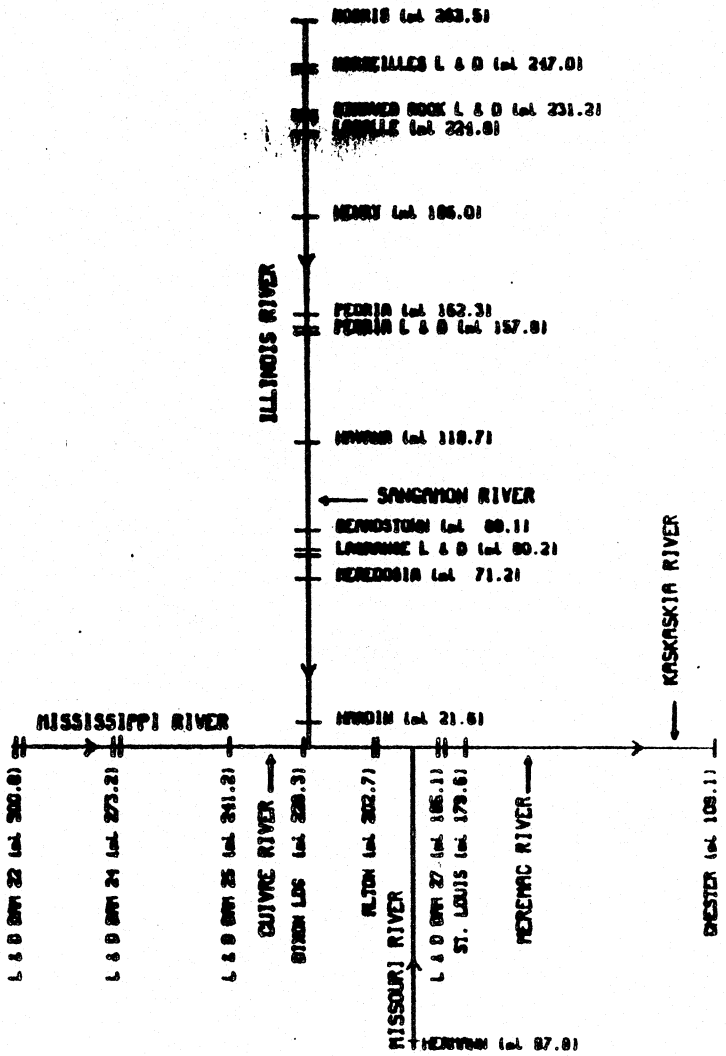

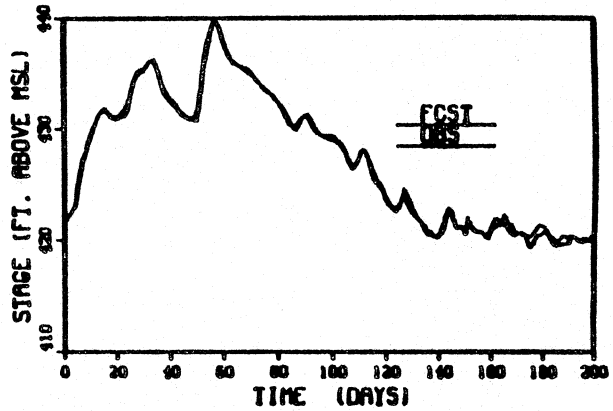

DIXON LDG (mi 228.3)

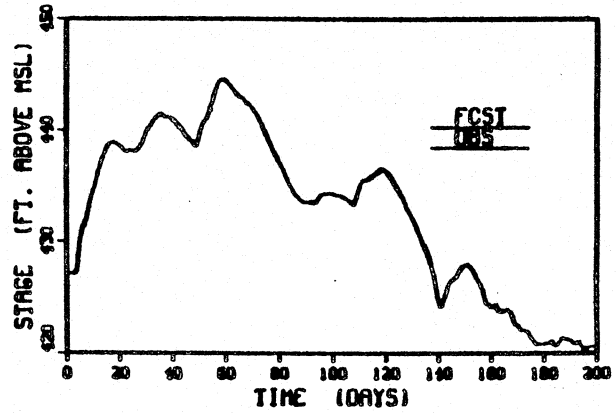

MEREDOSIA (mi 71.2)

Fig. 1 -- Illinois-Mississippi-Missouri River System

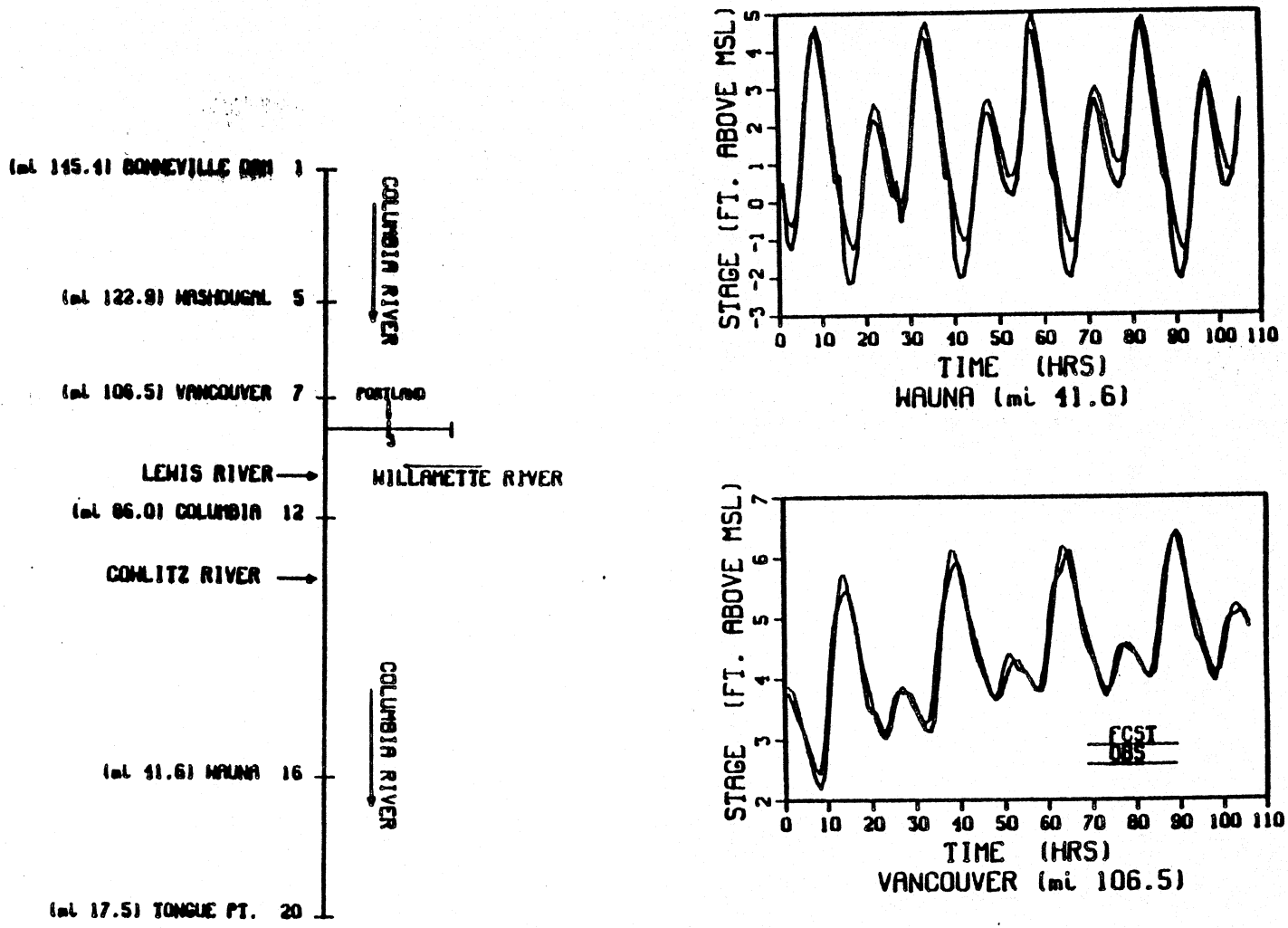

Fig. 2 -- Columbia River System

2.8 percent of the change in water elevation during the flood. An average of only three iterations were required.

Illinois-Mississippi-Missouri. A schematic of this dendritic river system is shown in Figure 1. It consists of 463 miles (741 km) of the Mississippi, Illinois, and Missouri Rivers with a total of 9 lock and dams and 18 level recorders. Discharges are known at the upstream end of each river. The channel bottom slope is mild, varying from 0.00002 to 0.0002. The total discharge through the system varied from 3,600 cfs (102 cms) to 885,000 cfs (25,064 cms). A total of 117 cross sections located at unequal intervals were used in the computations. Results of the parameter optimization are shown in Table 1. The average rms error was 0.38 ft (0.12 m) representing 1.9 percent of the change in water elevation during the flood. About three iterations were required for each reach. Comparisons of computed and observed water elevation at Meredosia and Dixon Landing are shown in Figure 1.

Columbia-Willamette. The lower 128 miles (206 km) of the Columbia River and the lower 24.4 mile (32 km) reach of the Willamette River have a very flat bottom slope (0.000011), and the flows are quite affected by the tide from the Pacific Ocean. A schematic of the reaches modeled are shown in Figure 2. The tidal effect extends as far upstream as the tailwater of Bonneville Dam during periods of low flow. Reverse flows can occur as far upstream as Vancouver. A total of 25 cross sections located at unequal distance intervals were used in the computations. Results of parameter optimization for a 3-day low flow period are shown in Table 1. The average rms error was 0.37 ft. (0.11 m) or 6.9 percent of the change in water elevation. An average of four iterations were required. Comparisons of computed and observed water elevations at Wauna and Vancouver are shown in Figure 2.

Summary

A parameter optimization methodology for dynamic flood routing models has been developed which for some applications can eliminate the need for costly and time-consuming detailed cross-sectional information. The cross sections within a reach are approximated by separate power functions for the channel and the floodplain. A very efficient optimization algorithm determines the optimal Manning n values which may vary with either water elevation or discharge. Minimum-maximum constraints can be imposed on the optimal n values. One or more cross sections within a reach may be specified in detail by a table of top widths and elevations. The methodology has been tested with promising results on several large river systems; the average rms error was 0.44 ft (0.13 m) or 2.9 percent of the change in stage.

Appendix - References

Fread, D.L., "Channel Routing," Chapter 14, Hydrological Forecasting, (Ed: M.G. Anderson and T.P. Burt) John Wiley, 1985, pp. 437-503.

Fread, D.L. and Smith, G.F., "Calibration Technique for 1-D Unsteady Flow Models," ASCE, 104(7), Paper 13892, Jul 1978, pp. 1027-1044.

Wormleaton, P.R. and Karmegam, M.,"Parameter Optimization in Flood Routing," ASCE, 110(12), Paper 19352, Dec. 1984, pp. 1799-1814.

SECTION 6.0

EXAMPLE APPLICATIONS

by

Larry W. Mays

6.0 EXAMPLE APPLICATIONS

This chapter provides example applications to illustrate use of the NETWORK version to simulate unsteady flows in irrigation canals.

6.1 EXAMPLE 1

The first example considers a simple 9,000 ft. long trapezoidal channel (Figure 6.1) with a bottom width of 20 ft. and side slopes of 2:1 (hor:vert). The upstream inflow hydrograph is shown in Figure 6.2. The channel bottom slope is 0.0005 ft/ft with the upstream and bottom elevation at 95.5. The trapezoidal channel has a Manning's roughness factor of n = 0.025. The downstream boundary condition is the rating curve shown in Figure 6.3.

In order to model the channel, cross-sections (station) are used at 1000 ft. intervals as shown in Figure 6.4. The input used for this application are presented in Figure 6.5 and the output is presented in Figure 6.6. This example did not use the channel network option so that NET = 0.

Page _____ of _____

CLIENT _____ PROJECT _____

PROJECT NO. _____ DETAIL _____

PREPARED BY _____ DATE _____ CHECKED BY _____ DATE _____

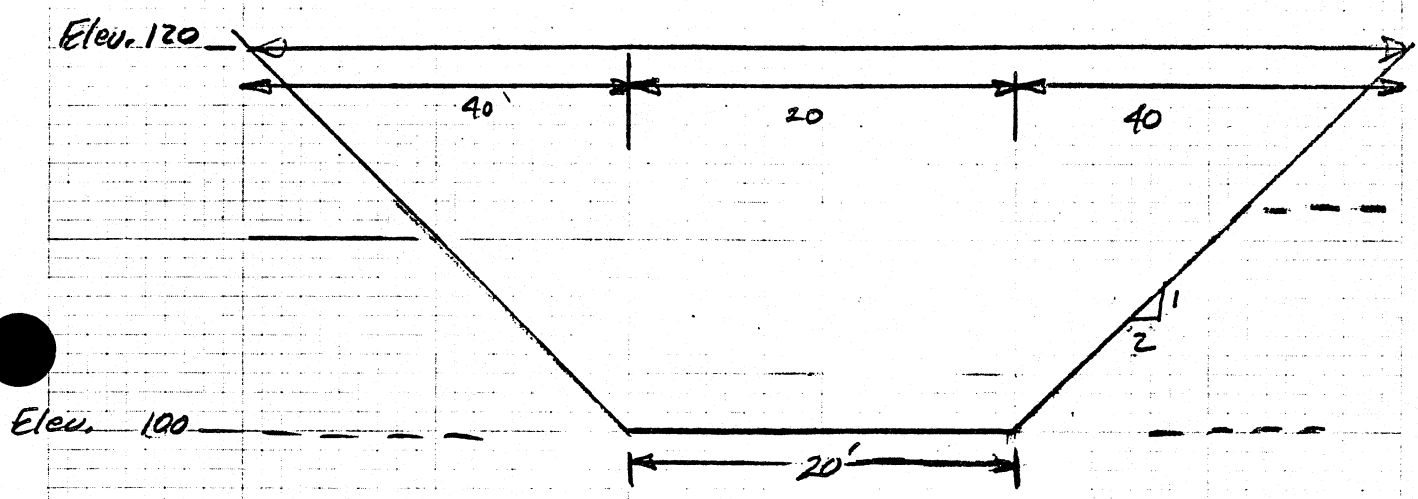

Figure 6.1.

Page ____ of ____

CLIENT ____ PROJECT ____

PROJECT NO. ____ DETAIL ____

PREPARED BY ____ DATE ____ CHECKED BY ____ DATE ____

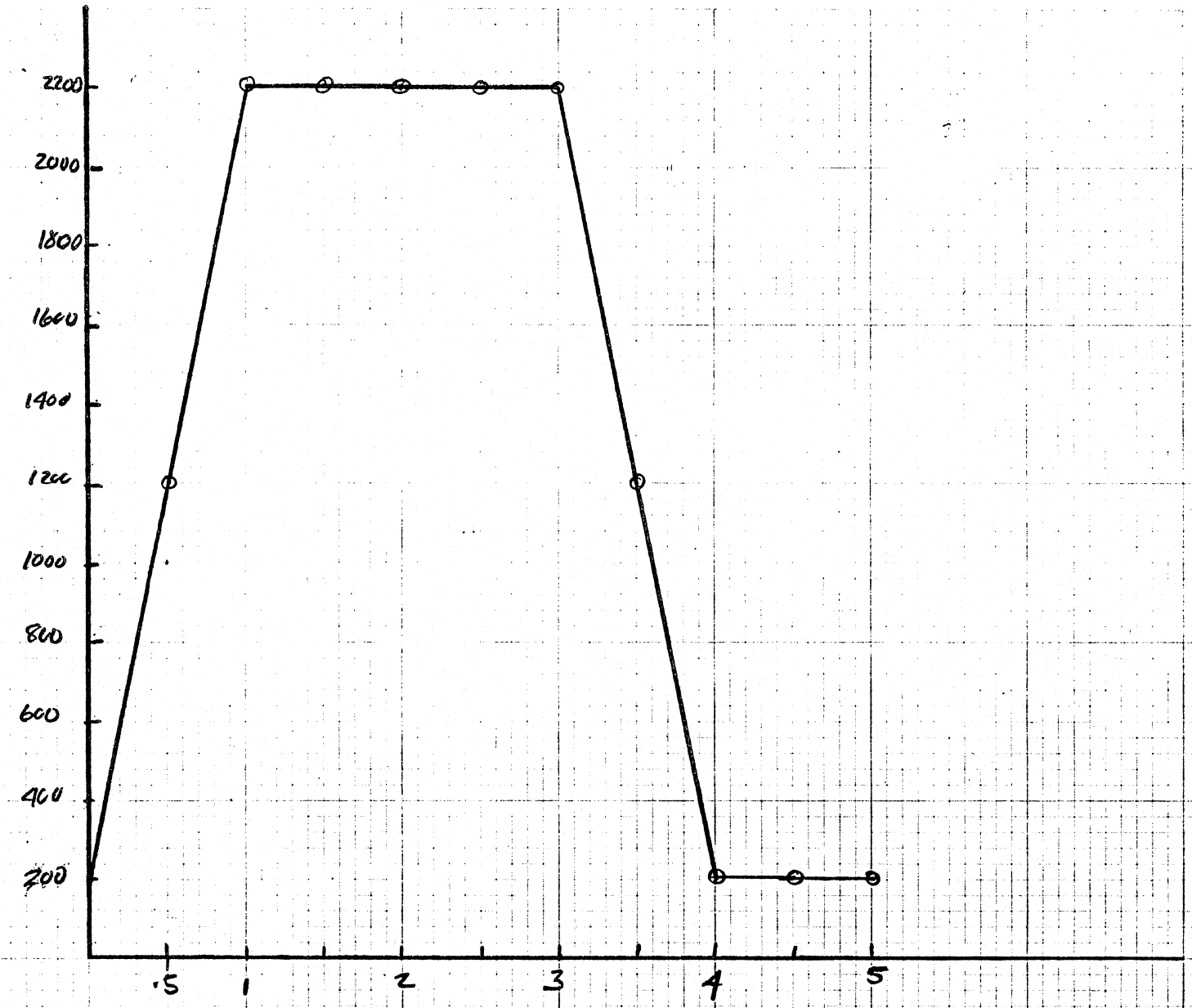

Figure 6.2

Page ____ of ____

CLIENT ____ PROJECT ____

PROJECT NO. ____ DETAIL ____

PREPARED BY ____ DATE ____ CHECKED BY ____ DATE ____

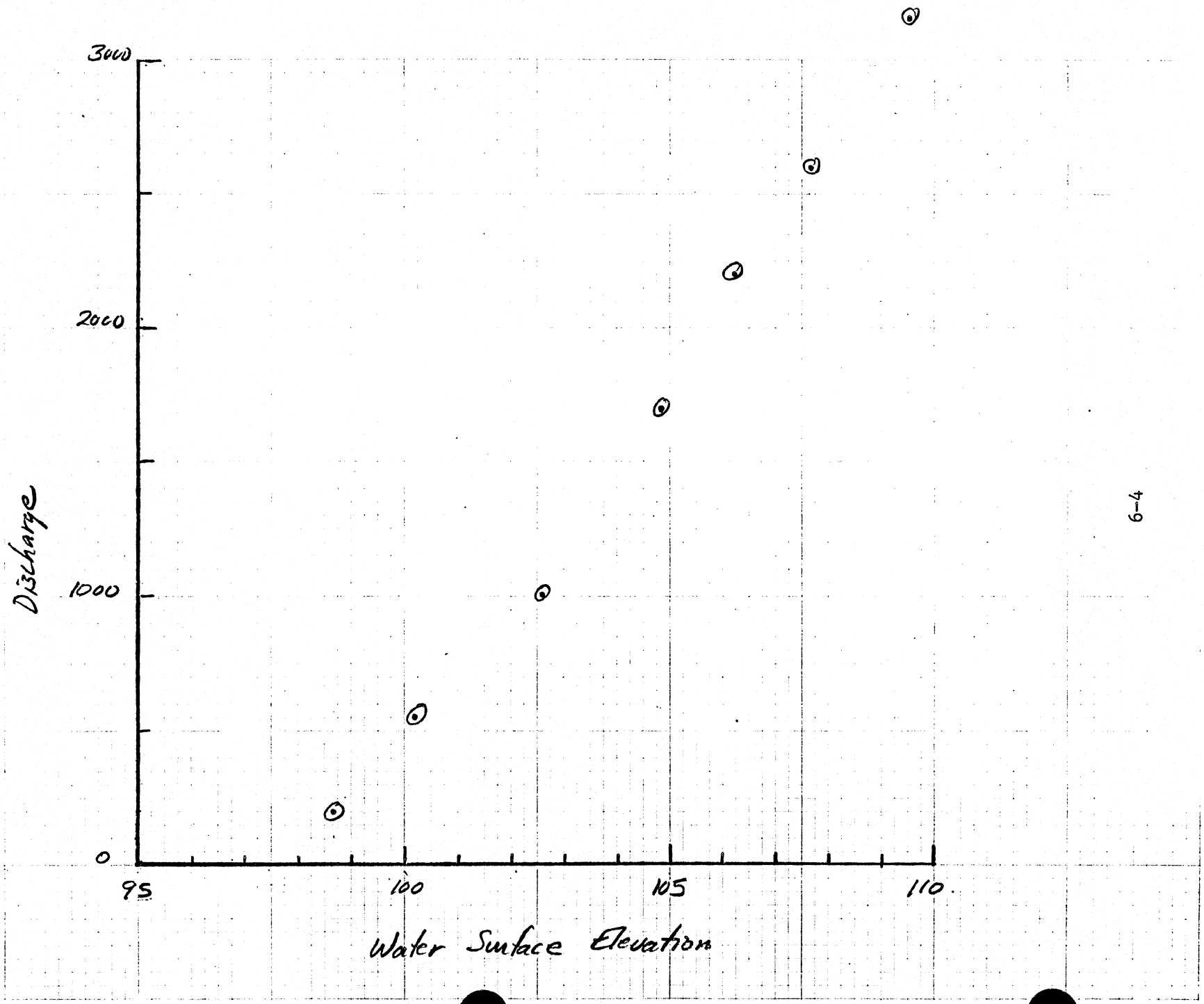

Figure 6.3

Page _____ of _____

CLIENT _____ PROJECT _____

PROJECT NO. _____ DETAIL _____

PREPARED BY _____ DATE _____ CHECKED BY _____ DATE _____

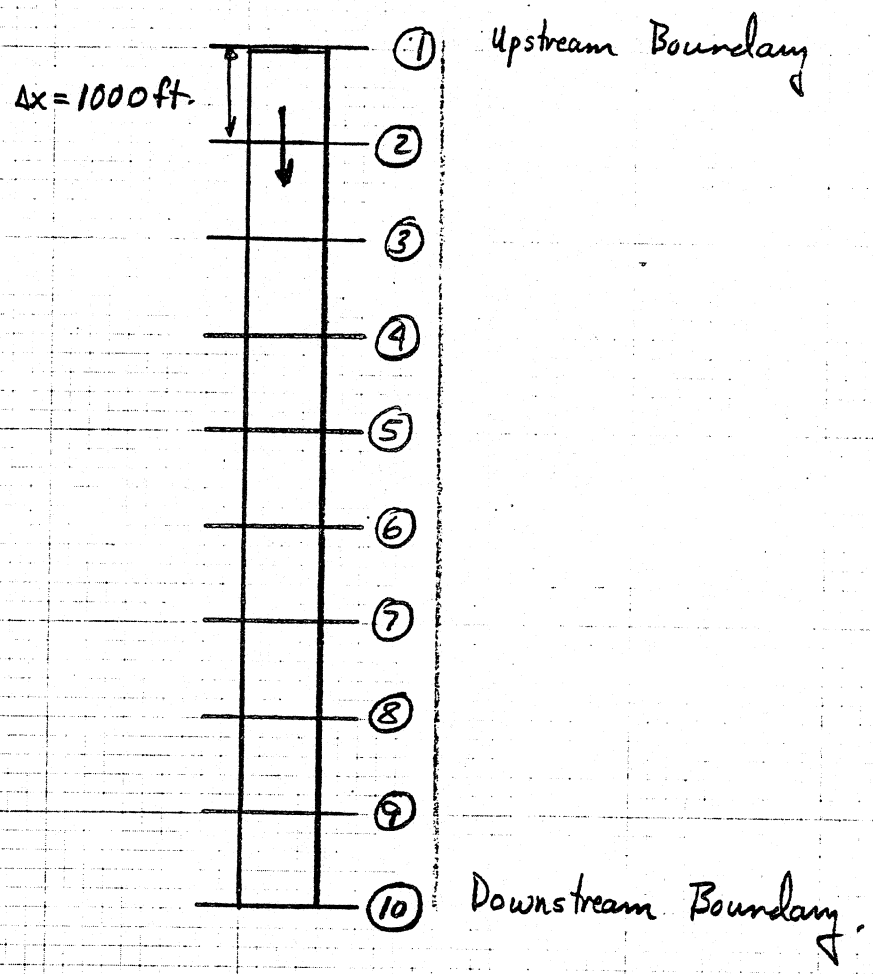

Figure 6.4

Card Example 6.1 Input

Card	1 (1–10)	2 (11–20)	3 (21–30)	4 (31–40)	5 (41–50)	6 (51–60)	7 (61–70)	8 (71–80)
1	1 17	25 1	1 8	1 2	2 1	1 1	1	1 1
1A	1 1	1 1	1 1					
2	ALONE							
3	0.1	50.	50.	0.80	0.55	1.0	0.5	
4	1	10	1	1	7	10	2	0
5	2	0	0	0	0	0	1	
6	0							
7	0							
8	0							
8A	0							
9	0							
11	10							
13	2							
14	3							
15	1	0	1					
16	10							
22	200.	1200.	2200.	2200.	2200.	2200.	2200.	200.
22	200.	200.						
25	1.00							
26	98.6	100.2	102.6	104.3	106.2	107.7	109.5	
27	200.	550.	1000.	1700.	2200.	2600.	3200.	
28	20.	100.						
28	20.	100.						

Card Example 6.1 Input (Cont'd)

Card	1 (10)	2 (20)	3 (30)	4 (40)	5 (50)	6 (60)	7 (70)	8 (80)
28	20.	100.						
28	20.	100.						
28	20.	100.						
28	20.	100.						
28	20.	100.						
28	20.	100.						
28	20.	100.						
28	20.	100.						
29	100.	120.0						
29	99.5	119.5						
29	99.0	119.0						
29	98.5	118.5						
29	98.0	118.0						
29	97.5	117.5						
29	97.0	117.0						
29	96.5	116.5						
29	96.0	116.0						
29	95.5	115.5						
30	0.0	0.0	0.0	0.0	0.0	0.0	0.0	0.0
30	0.0	0.0						
35	0.0	0.0	0.0					
36	9000.	8000.	7000.	6000.	5000.	4000.	3000.	2000.
36	1000.	0.0						

Card Example 6.1 Input (Cont'd)

Card	1 (10)	2 (20)	3 (30)	4 (40)	5 (50)	6 (60)	7 (70)	8 (80)
37	0.0	0.0	0.0	0.0	0.0	0.0	0.0	0.0
37	0.0	0.0						
52	5.00	0.10	5					
53	0.0	0.0	0.0	0.0	0.0	0.0	0.0	0.0
53	0.0	98.6						
54	200.	0.0	0.0	0.0	0.0	0.0	0.0	0.0
54	0.0	0.0						
55	0.0	10000.						
56	0.025	0.025						
57	EXAMPLE TO ILLUSTRATE INPUT FOR A TRAPEZOIDAL SHAPED IRRIGATION CANAL							
58	END							
59	EXIT							

```
TYPE WORLD3.INP
    1   17   25    1    1    8    1    2    2    1    1    1    1    1
    1    1    1    1    1    1
ALONE
       0.1       50.       50.      0.80      0.55       1.0       0.5
         1       10         1         1         7        10         2         0
         2        0         0         0         0         0         1
         0
         0
         0
         0
         0
        10
         2
         3
         1        0         1
        10
      200.     1200.     2200.     2200.     2200.     2200.     2200.      200.
      200.      200.
      1.00
      98.6     100.2     102.6     104.3     106.2     107.7     109.5
      200.      550.     1000.     1700.     2200.     2600.     3200.
       20.      100.
       20.      100.
       20.      100.
       20.      100.
       20.      100.
       20.      100.
       20.      100.
       20.      100.
       20.      100.
       20.      100.
      100.     120.0
      99.5     119.5
      99.0     119.0
      98.5     118.5
      98.0     118.0
      97.5     117.5
      97.0     117.0
      96.5     116.5
      96.0     116.0
      95.5     115.5
       0.0       0.0       0.0       0.0       0.0       0.0       0.0       0.0
       0.0       0.0
       0.0       0.0       0.0
     9000.     8000.     7000.     6000.     5000.     4000.     3000.     2000.
     1000.       0.0
       0.0       0.0       0.0       0.0       0.0       0.0       0.0       0.0
       0.0       0.0
      5.00      0.10         5
       0.0       0.0       0.0       0.0       0.0       0.0       0.0       0.0
       0.0      98.6
      200.       0.0       0.0       0.0       0.0       0.0       0.0       0.0
       0.0       0.0
       0.0     10000.
     0.025     0.025
EXAMPLE TO ILLUSTRATE INPUT FOR A TRAPEZOIDAL SHAPED IRRIGATION CANAL
END
EXIT
```


Figure 6.1

```
$ TYPE FOR006

                    MODIFIED DWOPER PROGRAM (NETWORK) VERSION--7/18/84


                    PROGRAM DEVELOPED BY D.L.FREAD,PHD.
                    NWS HYDROLOGIC RESEARCH LABORATORY, 8060 13 TH ST., SILVER SPRING, MD. 20910, 301-427-7640

  K1   K2   K3   K4   K5   K6   K7   K8   K9  K10  K11  K12  K13  K14  K15  K16  K17  K18  K19  K20  K21  K22  K23  K24  K25  K26
   1   17   25    2    1    8    1    2    2    2    1    1    1    1   34    4    0    0    0    4    1    1    1    1    1    1


*** THE SPACE REQUIRED FOR THESE DIMENSIONS IS      2523  THE SPACE AVAILABLE IN ARRAY A IS   107600 ***

       ALON

 EPSY      EPSQ      EPSQJ     THETA     F1        XFACT     DHF     CFNAME
 0.1000    50.0000   50.0000   0.8000    0.5500    1.0000    0.5000

     JN        NU        NCT       ICD       NYQD      ITMAX     NCML      NET
     [illegible]  10        1         1         7         10        2         0

    NCS       NCSS      NP        KTERM     KPL       KPL2      JNK       NPEND
     2         0         0         0         0         0         1         0

  NQL(J), J = 1, JN
      0

  NWJ(J), J = 1, JN
      0

(NUMLAD(J), J = 1, JN)
      0


(NG(J), J = 1, JN)
      0

  NCSS1(J), J = 1, JN
      0

 NB(1)
     10

  KU(J), J = 1, JN
      2

  [illegible] J = 1, JN
      3

NRCM1(J)  NRT1(J)  NNYQ(J) , J =  1
     1        0        1

  NCM(K,1), K = 1, NCRM1(1)
```

```
    10

  ST1(K,1), K = 1, NU
      200.00       1200.00       2200.00       2200.00       2200.00       2200.00       2200.00       200.00
      200.00       200.00

  GZN
    1.00

  YQD(K), K = 1, NYQD
   98.60    100.20    102.60    104.30    106.20    107.70    109.50

  QYQD(K), K = 1, NYQD
  200.00    550.00   1000.00   1700.00   2200.00   2600.00   3200.00

  BS(K,I,1), K = 1, NCS
I =  1    20.00000 100.00000
I =  2    20.00000 100.00000
I =  3    20.00000 100.00000
I =  4    20.00000 100.00000
I =  5    20.00000 100.00000
I =  6    20.00000 100.00000
I =  7    20.00000 100.00000
I =  8    20.00000 100.00000
I =  9    20.00000 100.00000
I = 10    20.00000 100.00000

  HS(K,I,1), K = 1, NCS
I =  1     100.000   120.000
I =  2      99.500   119.500
I =  3      99.000   119.000
I =  4      98.500   118.500
I =  5      98.000   118.000
I =  6      97.500   117.500
I =  7      97.000   117.000
I =  8      96.500   116.500
I =  9      96.000   116.000
I = 10      95.500   115.500

  AS(1,I,1), I = 1, NB(1)
        0.00          0.00          0.00          0.00          0.00          0.00          0.00          0.00
        0.00          0.00

 COFW      VWIND    WINAGL
   0.00      0.00      0.00

  X(I,1), I = 1, NB(1)
9000.0000 8000.0000 7000.0000 6000.0000 5000.0000 4000.0000 3000.0000 2000.0000
1000.0000    0.0000

  FKC(I,1), I = 1, NS(1)
   0.00      0.00      0.00      0.00      0.00      0.00      0.00      0.00
   0.00      0.00

  TE(HR)    TM(HR)   KITPR
   5.000   0.10000        5      0.00

  YDI(I,1), I = 1, NB(1)
   0.00      0.00      0.00      0.00      0.00      0.00      0.00      0.00
   0.00     98.60
```

```
QDI(I,1), I = 1, NB(1)
      200.0          0.0          0.0          0.0          0.0          0.0          0.0          0.0
        0.0          0.0

YU(L,K,1), K = 1, NRCM1(1)
   0.00  10000.00


CM(L,K,1), K = 1, NRCM1(1)
0.0250    0.0250


      EXAMPLE TO ILLUSTRATE INPUT FOR A TRAPEZOIDAL SHAPED IRRIGATION CANAL


*****WARNING***** TO ROUTE THE SPECIFIED TIME, NU MUST BE SET GREATER THAN OR EQUAL TO    11



 PRECAL


QDI(I,1),I=1,N)
   200.00    200.00    200.00    200.00    200.00    200.00    200.00    200.00
   200.00    200.00
        I= 10    KK= 0    KTR=0    QDI=    200.00    YDI=    98.60    YLLI=    98.60    DEPTH= 3.10    A=    81.22
I=      KK=   1  QB=   200.0  YLLN=    99.1  YLL=    99.1  A=    81.2  B=    32.4  CMM=   0.025  SFB= 0.000504
I=      KK=   2  QB=   200.0  YLLN=    99.1  YLL=    99.1  A=    81.3  B=    32.4  CMM=   0.025  SFB= 0.000503
        I=  9    KK= 2    KTR=0    QDI=    200.00    YDI=    99.10    YLLI=    99.10    DEPTH= 3.10    A=    81.32
I=    8 KK=   1  QB=   200.0  YLLN=    99.6  YLL=    99.6  A=    81.3  B=    32.4  CMM=   0.025  SFB= 0.000502
I=    8 KK=   2  QB=   200.0  YLLN=    99.6  YLL=    99.6  A=    81.4  B=    32.4  CMM=   0.025  SFB= 0.000501
        I=  8    KK= 2    KTR=0    QDI=    200.00    YDI=    99.60    YLLI=    99.60    DEPTH= 3.10    A=    81.36
I=    7 KK=   1  QB=   200.0  YLLN=   100.1  YLL=   100.1  A=    81.3  B=    32.4  CMM=   0.025  SFB= 0.000501
I=    7 KK=   2  QB=   200.0  YLLN=   100.1  YLL=   100.1  A=    81.4  B=    32.4  CMM=   0.025  SFB= 0.000501
        I=  7    KK= 2    KTR=0    QDI=    200.00    YDI=   100.11    YLLI=   100.10    DEPTH= 3.11    A=    81.39
I=    6 KK=   1  QB=   200.0  YLLN=   100.6  YLL=   100.6  A=    81.4  B=    32.4  CMM=   0.025  SFB= 0.000501
        I=  6    KK= 1    KTR=0    QDI=    200.00    YDI=   100.61    YLLI=   100.60    DEPTH= 3.11    A=    81.38
I=    5 KK=   1  QB=   200.0  YLLN=   101.1  YLL=   101.1  A=    81.4  B=    32.4  CMM=   0.025  SFB= 0.000500
        I=  5    KK= 1    KTR=0    QDI=    200.00    YDI=   101.11    YLLI=   101.11    DEPTH= 3.11    A=    81.40
I=    4 KK=   1  QB=   200.0  YLLN=   101.6  YLL=   101.6  A=    81.4  B=    32.4  CMM=   0.025  SFB= 0.000500
        I=  4    KK= 1    KTR=0    QDI=    200.00    YDI=   101.61    YLLI=   101.61    DEPTH= 3.11    A=    81.41
I=    3 KK=   1  QB=   200.0  YLLN=   102.1  YLL=   102.1  A=    81.4  B=    32.4  CMM=   0.025  SFB= 0.000500
        I=  3    KK= 1    KTR=0    QDI=    200.00    YDI=   102.11    YLLI=   102.11    DEPTH= 3.11    A=    81.41
I=    2 KK=   1  QB=   200.0  YLLN=   102.6  YLL=   102.6  A=    81.4  B=    32.4  CMM=   0.025  SFB= 0.000500
        I=  2    KK= 1    KTR=0    QDI=    200.00    YDI=   102.61    YLLI=   102.61    DEPTH= 3.11    A=    81.42
I=    1 KK=   1  QB=   200.0  YLLN=   103.1  YLL=   103.1  A=    81.4  B=    32.4  CMM=   0.025  SFB= 0.000500
        I=  1    KK= 1    KTR=0    QDI=    200.00    YDI=   103.11    YLLI=   103.11    DEPTH= 3.11    A=    81.42

                    INITIAL CONDITIONS AS READ IN

  I   X  (MI)   IC   IG      HHG (FT)      DEP(FT),    YU (FT MSL)      QU (CFS)    VU (FT/SEC)        FR NO   MANN. N


 DT=   0.1000 HRS T=   0.0000 HRS ITER=   0
  I   X  (MI)   IC   IG      HHG (FT)      DEP(FT),    YU (FT MSL)      QU (CFS)    VU (FT/SEC)        FR NO   MANN. N
  1  9000.000    2    0         0.000         3.106       103.106       200.000         2.456         0.273    0.025
```

2	8000.000	1	0	0.000	3.106	102.606	200.000	2.456	0.273	0.025
3	7000.000	1	0	0.000	3.106	102.106	200.000	2.457	0.273	0.025
4	6000.000	1	0	0.000	3.106	101.606	200.000	2.457	0.273	0.025
5	5000.000	1	0	0.000	3.106	101.106	200.000	2.457	0.273	0.025
6	4000.000	1	0	0.000	3.106	100.606	200.000	2.457	0.273	0.025
7	3000.000	1	0	0.000	3.105	100.105	200.000	2.457	0.273	0.025
8	2000.000	1	0	0.000	3.104	99.604	200.000	2.458	0.273	0.025
9	1000.000	1	0	0.000	3.103	99.103	200.000	2.460	0.274	0.025
10	0.000	3	0	0.000	3.100	98.600	200.000	2.462	0.274	0.025

INITIAL CONDITIONS IMPROVED BY SOLVING UNSTEADY FLOW EQUATIONS WITH BOUNDARIES HELD CONSTANT

DT= 0.1000 HRS T= 0.0000 HRS ITER= 0

I	X (MI)	IC	IG	HHG (FT)	DEP(FT),	YU (FT MSL)	QU (CFS)	VU (FT/SEC)	FR NO	MANN. N
1	9000.000	2	0	0.000	3.106	103.106	200.000	2.456	0.273	0.025
2	8000.000	1	0	0.000	3.106	102.606	200.000	2.456	0.273	0.025
3	7000.000	1	0	0.000	3.106	102.106	200.000	2.457	0.273	0.025
4	6000.000	1	0	0.000	3.106	101.606	200.001	2.457	0.273	0.025
5	5000.000	1	0	0.000	3.106	101.106	200.001	2.457	0.273	0.025
6	4000.000	1	0	0.000	3.106	100.606	200.002	2.457	0.273	0.025
7	3000.000	1	0	0.000	3.105	100.105	200.003	2.457	0.273	0.025
8	2000.000	1	0	0.000	3.104	99.604	200.006	2.458	0.273	0.025
9	1000.000	1	0	0.000	3.102	99.102	200.011	2.460	0.274	0.025
10	0.000	3	0	0.000	3.098	98.598	200.020	2.464	0.274	0.025

DT= 0.1000 HRS T= 0.5000 HRS ITER= 1

I	X (MI)	IC	IG	HHG (FT)	DEP(FT),	YU (FT MSL)	QU (CFS)	VU (FT/SEC)	FR NO	MANN. N
1	9000.000	2	0	0.000	7.106	107.106	1200.000	4.936	0.388	0.025
2	8000.000	1	0	0.000	6.795	106.295	1107.474	4.852	0.389	0.025
3	7000.000	1	0	0.000	6.473	105.473	1019.411	4.780	0.391	0.025
4	6000.000	1	0	0.000	6.126	104.626	922.648	4.669	0.391	0.025
5	5000.000	1	0	0.000	5.770	103.770	825.987	4.539	0.389	0.025
6	4000.000	1	0	0.000	5.410	102.910	731.965	4.390	0.387	0.025
7	3000.000	1	0	0.000	5.065	102.065	637.606	4.178	0.378	0.025
8	2000.000	1	0	0.000	4.811	101.311	537.237	3.770	0.349	0.025
9	1000.000	1	0	0.000	4.753	100.753	433.302	3.090	0.287	0.025
10	0.000	3	0	0.000	4.820	100.320	357.425	2.502	0.231	0.025

DT= 0.1000 HRS T= 1.0000 HRS ITER= 1

I	X (MI)	IC	IG	HHG (FT)	DEP(FT),	YU (FT MSL)	QU (CFS)	VU (FT/SEC)	FR NO	MANN. N
1	9000.000	2	0	0.000	9.950	109.950	2200.000	5.542	0.379	0.025
2	8000.000	1	0	0.000	9.752	109.252	2116.837	5.495	0.379	0.025
3	7000.000	1	0	0.000	9.554	108.554	2030.669	5.435	0.378	0.025
4	6000.000	1	0	0.000	9.364	107.864	1943.071	5.358	0.376	0.025
5	5000.000	1	0	0.000	9.190	107.190	1848.529	5.241	0.371	0.025
6	4000.000	1	0	0.000	9.046	106.546	1749.770	5.078	0.361	0.025
7	3000.000	1	0	0.000	8.943	105.943	1650.534	4.872	0.348	0.025
8	2000.000	1	0	0.000	8.903	105.403	1546.618	4.595	0.329	0.025

9	1000.000	1	0	0.000	8.913	104.913	1450.731	4.303	0.308	0.025
10	0.000	3	0	0.000	8.980	104.480	1362.305	3.997	0.285	0.025

DT= 0.1000 HRS T= 1.5000 HRS ITER= 0

I	X (MI)	IC	IG	HHG (FT)	DEP(FT),	YU (FT MSL)	QU (CFS)	VU (FT/SEC)	FR NO	MANN. N
1	9000.000	2	0	0.000	10.642	110.642	2200.000	5.007	0.333	0.025
2	8000.000	1	0	0.000	10.624	110.124	2189.815	4.997	0.333	0.025
3	7000.000	1	0	0.000	10.606	109.606	2170.674	4.966	0.331	0.025
4	6000.000	1	0	0.000	10.598	109.098	2151.680	4.928	0.328	0.025
5	5000.000	1	0	0.000	10.605	108.605	2133.108	4.881	0.325	0.025
6	4000.000	1	0	0.000	10.622	108.122	2113.186	4.823	0.321	0.025
7	3000.000	1	0	0.000	10.659	107.659	2088.193	4.741	0.315	0.025
8	2000.000	1	0	0.000	10.718	107.218	2060.171	4.639	0.308	0.025
9	1000.000	1	0	0.000	10.801	106.801	2029.688	4.517	0.299	0.025
10	0.000	3	0	0.000	10.918	106.418	1994.254	4.366	0.287	0.025

DT= 0.1000 HRS T= 2.0000 HRS ITER= 0

I	X (MI)	IC	IG	HHG (FT)	DEP(FT),	YU (FT MSL)	QU (CFS)	VU (FT/SEC)	FR NO	MANN. N
1	9000.000	2	0	0.000	10.842	110.842	2200.000	4.868	0.321	0.025
2	8000.000	1	0	0.000	10.861	110.361	2195.584	4.846	0.320	0.025
[illegible]	[illegible]0.000	1	0	0.000	10.888	109.888	2191.647	4.819	0.317	0.025
4	[illegible]000.000	1	0	0.000	10.922	109.422	2184.542	4.780	0.314	0.025
5	5000.000	1	0	0.000	10.969	108.969	2177.831	4.735	0.311	0.025
6	4000.000	1	0	0.000	11.030	108.530	2170.965	4.680	0.307	0.025
7	3000.000	1	0	0.000	11.106	108.106	2163.090	4.614	0.301	0.025
8	2000.000	1	0	0.000	11.200	107.700	2154.633	4.537	0.295	0.025
9	1000.000	1	0	0.000	11.314	107.314	2144.938	4.447	0.288	0.025
10	0.000	3	0	0.000	11.451	106.951	2134.540	4.345	0.280	0.025

DT= 0.1000 HRS T= 2.5000 HRS ITER= 0

I	X (MI)	IC	IG	HHG (FT)	DEP(FT),	YU (FT MSL)	QU (CFS)	VU (FT/SEC)	FR NO	MANN. N
1	9000.000	2	0	0.000	10.909	110.909	2200.000	4.823	0.317	0.025
2	8000.000	1	0	0.000	10.940	110.440	2198.617	4.799	0.315	0.025
3	7000.000	1	0	0.000	10.979	109.979	2196.685	4.769	0.313	0.025
4	6000.000	1	0	0.000	11.027	109.527	2195.214	4.734	0.310	0.025
5	5000.000	1	0	0.000	11.087	109.087	2192.751	4.690	0.307	0.025
6	4000.000	1	0	0.000	11.159	108.659	2190.050	4.638	0.302	0.025
7	3000.000	1	0	0.000	11.247	108.247	2187.640	4.578	0.297	0.025
8	2000.000	1	0	0.000	11.351	107.851	2184.914	4.508	0.292	0.025
9	1000.000	1	0	0.000	11.474	107.474	2181.803	4.427	0.285	0.025
10	0.000	3	0	0.000	11.618	107.118	2178.348	4.337	0.278	0.025

DT= 0.1000 HRS T= 3.0000 HRS ITER= 0

I	X (MI)	IC	IG	HHG (FT)	DEP(FT),	YU (FT MSL)	QU (CFS)	VU (FT/SEC)	FR NO	MANN. N
1	9000.000	2	0	0.000	10.931	110.931	2200.000	4.808	0.316	0.025

2	8000.000	1	0	0.000	10.967	110.467	2199.488	4.783	0.314	0.025
3	7000.000	1	0	0.000	11.010	110.010	2198.958	4.753	0.312	0.025
4	6000.000	1	0	0.000	11.062	109.562	2198.262	4.717	0.309	0.025
5	5000.000	1	0	0.000	11.126	109.126	2197.636	4.675	0.305	0.025
6	4000.000	1	0	0.000	11.202	108.702	2196.742	4.625	0.301	0.025
7	3000.000	1	0	0.000	11.293	108.293	2195.772	4.566	0.296	0.025
8	2000.000	1	0	0.000	11.401	107.901	2194.896	4.498	0.291	0.025
9	1000.000	1	0	0.000	11.527	107.527	2193.926	4.421	0.284	0.025
10	0.000	3	0	0.000	11.672	107.172	2192.758	4.334	0.277	0.025

DT= 0.1000 HRS T= 3.5000 HRS ITER= 2

I	X (MI)	IC	IG	HHG (FT)	DEP(FT),	YU (FT MSL)	QU (CFS)	VU (FT/SEC)	FR NO	MANN. N
1	9000.000	2	0	0.000	6.740	106.740	200.006	0.886	0.071	0.025
2	8000.000	1	0	0.000	7.289	106.789	383.927	1.523	0.119	0.025
3	7000.000	1	0	0.000	7.736	106.736	541.657	1.974	0.150	0.025
4	6000.000	1	0	0.000	8.133	106.633	699.822	2.373	0.176	0.025
5	5000.000	1	0	0.000	8.480	106.480	856.704	2.733	0.200	0.025
6	4000.000	1	0	0.000	8.775	106.275	1008.349	3.060	0.221	0.025
7	3000.000	1	0	0.000	9.016	106.016	1153.061	3.363	0.240	0.025
8	2000.000	1	0	0.000	9.204	105.704	1291.126	3.652	0.258	0.025
9	1000.000	1	0	0.000	9.340	105.340	1422.845	3.938	0.277	0.025
10	0.000	3	0	0.000	9.426	104.926	1546.089	4.222	0.295	0.025

DT= 0.1000 HRS T= 4.0000 HRS ITER= 1

I	X (MI)	IC	IG	HHG (FT)	DEP(FT),	YU (FT MSL)	QU (CFS)	VU (FT/SEC)	FR NO	MANN. N
1	9000.000	2	0	0.000	4.074	104.074	200.000	1.744	0.173	0.025
2	8000.000	1	0	0.000	4.358	103.858	227.396	1.817	0.175	0.025
3	7000.000	1	0	0.000	4.673	103.673	276.804	2.019	0.189	0.025
4	6000.000	1	0	0.000	4.927	103.427	308.593	2.098	0.192	0.025
5	5000.000	1	0	0.000	5.176	103.176	348.199	2.216	0.199	0.025
6	4000.000	1	0	0.000	5.418	102.918	398.014	2.382	0.210	0.025
7	3000.000	1	0	0.000	5.640	102.640	453.912	2.573	0.223	0.025
8	2000.000	1	0	0.000	5.837	102.337	511.663	2.767	0.236	0.025
9	1000.000	1	0	0.000	6.012	102.012	566.943	2.945	0.248	0.025
10	0.000	3	0	0.000	6.125	101.625	629.741	3.188	0.267	0.025

DT= 0.1000 HRS T= 4.5000 HRS ITER= 0

I	X (MI)	IC	IG	HHG (FT)	DEP(FT),	YU (FT MSL)	QU (CFS)	VU (FT/SEC)	FR NO	MANN. N
1	9000.000	2	0	0.000	3.310	103.310	200.000	2.270	0.246	0.025
2	8000.000	1	0	0.000	3.420	102.920	207.383	2.259	0.241	0.025
3	7000.000	1	0	0.000	3.539	102.539	216.011	2.254	0.237	0.025
4	6000.000	1	0	0.000	3.686	102.186	231.715	2.297	0.238	0.025
5	5000.000	1	0	0.000	3.822	101.822	241.717	2.288	0.233	0.025
6	4000.000	1	0	0.000	3.981	101.481	258.008	2.318	0.232	0.025
7	3000.000	1	0	0.000	4.142	101.142	278.669	2.378	0.234	0.025
8	2000.000	1	0	0.000	4.315	100.815	297.086	2.405	0.233	0.025
9	1000.000	1	0	0.000	4.495	100.495	314.582	2.414	0.230	0.025
10	0.000	3	0	0.000	4.698	100.198	330.716	2.395	0.224	0.025

DT= 0.1000 HRS T= 5.0000 HRS ITER= 0

I	X (MI)	IC	IG	HHG (FT)	DEP(FT),	YU (FT MSL)	QU (CFS)	VU (FT/SEC)	FR NO	MANN. N
1	9000.000	2	0	0.000	3.299	103.299	222.222	2.533	0.275	0.025
2	8000.000	1	0	0.000	3.307	102.807	220.564	2.506	0.271	0.025
3	7000.000	1	0	0.000	3.331	102.331	219.979	2.477	0.267	0.025
4	6000.000	1	0	0.000	3.367	101.867	220.018	2.444	0.263	0.025
5	5000.000	1	0	0.000	3.432	101.432	222.301	2.412	0.257	0.025
6	4000.000	1	0	0.000	3.513	101.013	223.598	2.355	0.248	0.025
7	3000.000	1	0	0.000	3.638	100.638	227.748	2.295	0.239	0.025
8	2000.000	1	0	0.000	3.802	100.302	232.131	2.212	0.226	0.025
9	1000.000	1	0	0.000	4.015	100.015	235.988	2.097	0.209	0.025
10	0.000	3	0	0.000	4.281	99.781	239.486	1.959	0.190	0.025

TOTAL ITERATIONS FOR EACH OF 1 RIVERS.
27

PROGRAM COMPLETED.
EXIT
EXECUTION COMPLETED O.K.
$

6.2 EXAMPLE 2

This example is an extension of Example 1 to include a tributary channel, as shown in Figure 6.6. The channel shape is shown in Figure 6.1. The channel network option was used to describe the simple network with the node types (JCOD) also listed in Figure 6.2. The downstream boundary condition is the rating curve shown in Figure 6.3. Sections 9 and 10 basically have no purpose for this example; however, the following example makes use of sections 9 and 10. For simplicity to follow to the next example, they are included. The input for this example is given in Figure 6.7.

Page _____ of _____

CLIENT _____ PROJECT _____

PROJECT NO. _____ DETAIL _____

PREPARED BY _____ DATE _____ CHECKED BY _____ DATE _____

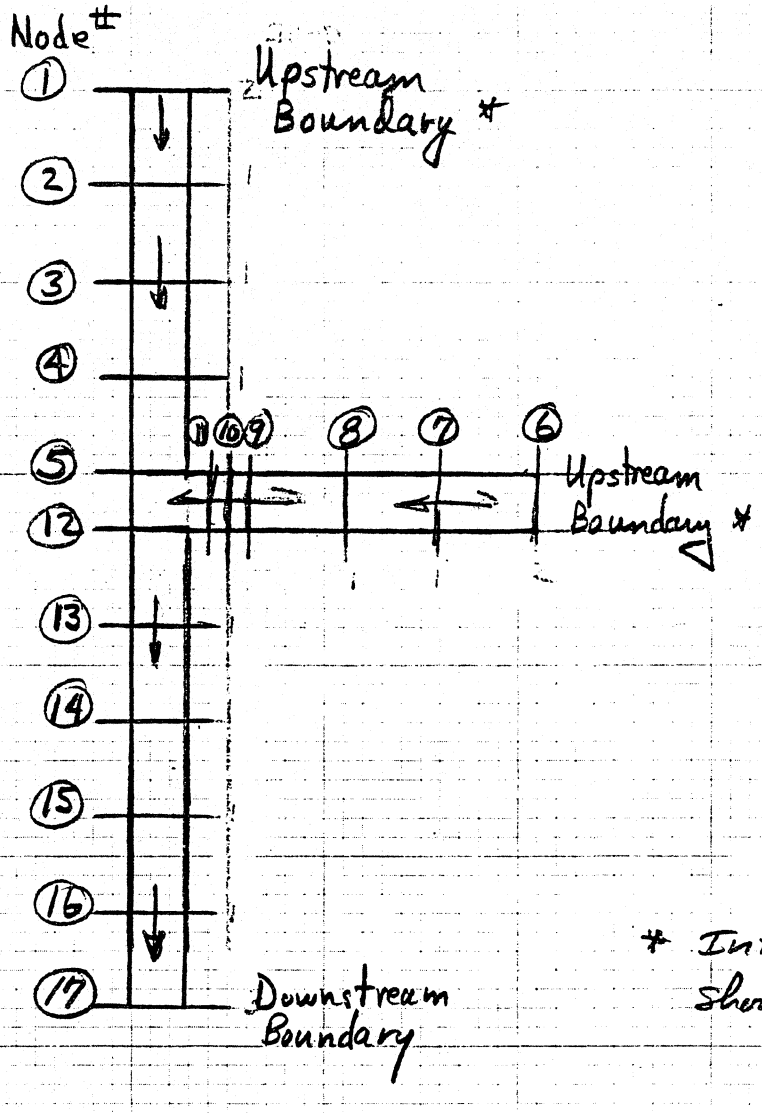

Node #	JCOD	Channel Bottom Elevation
1	2	100.
2	1	99.5
3	1	99.0
4	1	98.5
5	4	98.0
6	1	99.5
7	1	99.0
8	1	98.5
9	1	98.0
10	1	98.0
11	4	98.0
12	4	98.0
13	1	97.5
14	1	97.0
15	1	96.5
16	1	96.0
17	3	95.5

* Inflow hydrograph shown in Figure 6.2

Figure 6.6

Card

Example 6.2 Input

Card	1 (1–10)	2 (11–20)	3 (21–30)	4 (31–40)	5 (41–50)	6 (51–60)	7 (61–70)	8 (71–80)
1	1 17	100 1	1 8	1 2	2 1	1 1	1 1	2 1
1A	1 5	1 1	1 1					
2	ALONE							
3	0.1	50.	50.	0.80	0.55	1.0	0.5	
4	1	11	1	1	7	10	2	1
5	2	0	0	0	0	0	1	
6	0							
7	0							
8	0							
8A	0							
9	0							
11	17							
11A	2	1	1	1	4	2	1	1
11A	1	1	4	4	1	1	1	1
11A	3							
11B	1	2						
11C	5	11	12					
11D	2	2						
11E	1	2	3	4	5	12	13	14
11E	15	16	17	6	7	8	9	10
11E	11							
14	3							
15	1	0	1					

Card Example 6.2 Input (Cont'd)

Card	1 (10)	2 (20)	3 (30)	4 (40)	5 (50)	6 (60)	7 (70)	8 (80)
16	17							
22	200.	1200.	2200.	2200.	2200.	2200.	2200.	200.
22	200.	200.						
22	200.	1200.	2200.	2200.	2200.	2200.	2200.	200.
22	200.	200.						
25	1.00							
26	98.6	100.2	102.6	104.3	106.2	107.7	109.5	
27	200.	550.	1000.	1700.	2200.	2600.	3200.	
28	20.	100.						
28	20.	100.						
28	20.	100.						
28	20.	100.						
28	20.	100.						
28	20.	100.						
28	20.	100.						
28	20.	100.						
28	20.	100.						
28	20.	100.						
28	20.	100.						
28	20.	100.						
28	20.	100.						
28	20.	100.						
28	20.	100.						

Example 6.2 Input (Cont'd)

Card	1 (10)	2 (20)	3 (30)	4 (40)	5 (50)	6 (60)	7 (70)	8 (80)
28	20.	100.						
28	20.	100.						
29	100.	120.0						
29	99.5	119.5						
29	99.0	119.0						
29	98.5	118.5						
29	98.0	118.0						
29	99.5	119.5						
29	99.0	119.0						
29	98.5	118.5						
29	98.0	118.0						
29	98.0	118.0						
29	98.0	118.0						
29	98.0	118.0						
29	97.5	117.5						
29	97.0	117.0						
29	96.5	116.5						
29	96.0	116.0						
29	95.5	115.5						
30	0.0	0.0	0.0	0.0	0.0	0.0	0.0	0.0
30	0.0	0.0	0.0	0.0	0.0	0.0	0.0	0.0
30	0.0							
35	0.0	0.0	0.0					

Card

Example 6.2 Input (Cont'd)

Card	1 (10)	2 (20)	3 (30)	4 (40)	5 (50)	6 (60)	7 (70)	8 (80)
36	9000.	8000.	7000.	6000.	5000.	8000.	7000.	6000.
36	5000.	4995.	4990.	4990.	4000.	3000.	2000.	1000.
36	0.0							
37	0.0	0.0	0.0	0.0	0.0	0.0	0.0	0.0
37	0.0	0.0	0.0	0.0	0.0	0.0	0.0	0.0
37	0.0							
52	5.00	0.10	5					
53	0.0	0.0	0.0	0.0	0.0	0.0	0.0	0.0
53	0.0	0.0	0.0	0.0	0.0	0.0	0.0	0.0
53	100.0							
54	200.	0.	0.	0.	0.	200.	0.	0.
54	0.	0.	0.	400.	0.	0.	0.	0.
54	0.							
54A	2							
54B	6	11						
54C	6	7	8	9	10	11		
54C	1	2	3	4	5	12	13	14
54C	15	16	17					
55	0.0	10000.						
56	0.025	0.025						
57	EXAMPLE							
58	END							
59	EXIT							

```
    1   17  100    1    1    8    1    2    2    1    1    1    1    1    2    1
    1    5    1    1    1    1
ALONE
        0.1       50.       50.      0.80      0.55       1.0       0.5
          1       11         1         1         7        10         2         1
          2        0         0         0         0         0         1
          0
          0
          0
          0
          0
         17
          2         1         1         1         4         2         1         1
          1         1         4         4         1         1         1         1
          3
          1         2
          5        11        12
          2         2
          1         2         3         4         5        12        13        14
         15        16        17         6         7         8         9        10
         11
          3
          1         0         1
         17
      200.      1200.     2200.     2200.     2200.     2200.     2200.      200.
      200.       200.
      200.      1200.     2200.     2200.     2200.     2200.     2200.      200.
      200.       200.
      1.00
      98.6      100.2     102.6     104.3     106.2     107.7     109.5
      200.       550.     1000.     1700.     2200.     2600.     3200.
       20.       100.
       20.       100.
       20.       100.
       20.       100.
       20.       100.
       20.       100.
       20.       100.
       20.       100.
       20.       100.
       20.       100.
       20.       100.
       20.       100.
       20.       100.
       20.       100.
       20.       100.
       20.       100.
       20.       100.
      100.      120.0
      99.5      119.5
      99.0      119.0
      98.5      118.5
      98.0      118.0
      99.5      119.5
      99.0      119.0
      98.5      118.5
      98.0      118.0
      98.0      118.0
      98.0      118.0
      98.0      118.0
      97.5      117.5
      97.0      117.0
      96.5      116.5
      96.0      116.0
```

```
    95.5      115.5
     0.0        0.0        0.0        0.0        0.0        0.0        0.0        0.0
     0.0        0.0        0.0        0.0        0.0        0.0        0.0        0.0
     0.0
     0.0        0.0        0.0
    9000.      8000.      7000.      6000.      5000.      8000.      7000.      6000.
    5000.      4995.      4990.      4990.      4000.      3000.      2000.      1000.
     0.0
     0.0        0.0        0.0        0.0        0.0        0.0        0.0        0.0
     0.0        0.0        0.0        0.0        0.0        0.0        0.0        0.0
     0.0
    5.00       0.10          5
     0.0        0.0        0.0        0.0        0.0        0.0        0.0        0.0
     0.0        0.0        0.0        0.0        0.0        0.0        0.0        0.0
   100.0
    200.         0.         0.         0.         0.       200.         0.         0.
      0.         0.         0.       400.         0.         0.         0.         0.
      0.
       2
       6         11
       6          7          8          9         10         11
       1          2          3          4          5         12         13         14
      15         16         17
     0.0     10000.
   0.025      0.025
EX    E
END
EXIT
```

TYPE WORLD4.OUT

MODIFIED DWOPER PROGRAM (NETWORK) VERSION--7/18/84

PROGRAM DEVELOPED BY D.L.FREAD,PHD.
NWS HYDROLOGIC RESEARCH LABORATORY, 8060 13 TH ST., SILVER SPRING, MD. 20910, 301-427-7640

K1	K2	K3	K4	K5	K6	K7	K8	K9	K10	K11	K12	K13	K14	K15	K16	K17	K18	K19	K20	K21	K22	K23	K24	K25	K26
1	17	100	2	1	8	1	2	2	2	1	1	1	1	34	4	2	1	4	34	1	5	1	1	1	1

*** THE SPACE REQUIRED FOR THESE DIMENSIONS IS 6894 THE SPACE AVAILABLE IN ARRAY A IS 107600 ***

ALON

EPSY	EPSQ	EPSQJ	THETA	F1	XFACT	DHF	CFNAME
0.1000	50.0000	50.0000	0.8000	0.5500	1.0000	0.5000	

JN	NU	NCT	ICD	NYQD	ITMAX	NCML	NET
1	11	1	1	7	10	2	1

NCS	NCSS	NP	KTERM	KPL	KPL2	JNK	NPEND
2	0	0	0	0	0	1	0

NQL(J), J = 1, JN
0

NWJ(J), J = 1, JN
0

(NUMLAD(J), J = 1, JN)
0

(NG(J), J = 1, JN)
0

NCSS1(J), J = 1, JN
0

NB(1)
17

JCOD(K), K = 1, N

2	1	1	1	4	2	1	1
1	1	4	4	1	1	1	1
3							

JTN	NUPB
1	2

JU(K)	JB(K)	JL(K)	AJN(K) , K=1,JTN
5	11	12	0.00

```
KMU(K), K=1,NUPB
    2        2
  (JCPR(K),K=1,N)
[illegible]        2        3        4        5       12       13       14
[illegible]       16       17        6        7        8        9       10
   11

KD(J), J = 1, JN
    3

NRCM1(J)  NRT1(J)  NNYQ(J) , J =  1
    1        0        1

NCM(K,1), K = 1, NCRM1(1)
   17

STU(K,1), K = 1, NU
    200.00     1200.00     2200.00     2200.00     2200.00     2200.00     2200.00      200.00
    200.00      200.00        0.00

STU(K,2), K = 1, NU
    200.00     1200.00     2200.00     2200.00     2200.00     2200.00     2200.00      200.00
    200.00      200.00        0.00

GZN
  1.00

YQD(K), K = 1, NYQD
[illegible]    100.20    102.60    104.30    106.20    107.70    109.50

QYQD(K), K = 1, NYQD
200.00    550.00   1000.00   1700.00   2200.00   2600.00   3200.00

BS(K,I,1), K = 1, NCS
I =  1    20.00000 100.00000
I =  2    20.00000 100.00000
I =  3    20.00000 100.00000
I =  4    20.00000 100.00000
I =  5    20.00000 100.00000
I =  6    20.00000 100.00000
I =  7    20.00000 100.00000
I =  8    20.00000 100.00000
I =  9    20.00000 100.00000
I = 10    20.00000 100.00000
I = 11    20.00000 100.00000
I = 12    20.00000 100.00000
I = 13    20.00000 100.00000
I = 14    20.00000 100.00000
I = 15    20.00000 100.00000
I = 16    20.00000 100.00000
I = 17    20.00000 100.00000

HS(K,I,1), K = 1, NCS
I =  1     100.000   120.000
I =  [illegible]    99.500   119.500
I =  [illegible]    99.000   119.000
I =  4      98.500   118.500
I =  5      98.000   118.000
I =  6      99.500   119.500
I =  7      99.000   119.000
I =  8      98.500   118.500
```

```
I =  9      98.000   118.000
I = 10      98.000   118.000
I = 11      98.000   118.000
I = 12      98.000   118.000
I = 13      97.500   117.500
I = 14      97.000   117.000
I = 15      96.500   116.500
I = 16      96.000   116.000
I = 17      95.500   115.500

  AS(1,I,1), I = 1, NB(1)
        0.00        0.00        0.00        0.00        0.00        0.00        0.00        0.00
        0.00        0.00        0.00        0.00        0.00        0.00        0.00        0.00
        0.00

  COFW      VWIND    WINAGL
    0.00      0.00      0.00

  X(I,1), I = 1, NB(1)
9000.0000 8000.0000 7000.0000 6000.0000 5000.0000 8000.0000 7000.0000 6000.0000
5000.0000 4995.0000 4990.0000 4990.0000 4000.0000 3000.0000 2000.0000 1000.0000
  0.0000

  FKC(I,1), I = 1, NS(1)
    0.00      0.00      0.00      0.00      0.00      0.00      0.00      0.00
    0.00      0.00      0.00      0.00      0.00      0.00      0.00      0.00
    0.00

  TE(HR)    TM(HR)   KITPR
   5.000   0.10000       5      0.00

  YDI(I,1), I = 1, NB(1)
    0.00      0.00      0.00      0.00      0.00      0.00      0.00      0.00
    0.00      0.00      0.00      0.00      0.00      0.00      0.00      0.00
  100.00

  QDI(I,1), I = 1, NB(1)
        200.0       0.0       0.0       0.0       0.0     200.0       0.0       0.0
          0.0       0.0       0.0     400.0       0.0       0.0       0.0       0.0
          0.0
      2
      6      11
      6       7       8       9      10      11
      1       2       3       4       5      12      13      14
     15      16      17

  YOCM(L,K,1), K = 1, NRCM1(1)
    0.00  10000.00


  CM(L,K,1), K = 1, NRCM1(1)
  0.0250    0.0250


       EXAMPLE
```

```
(QDI(I1,1),I1=1,N)
200.00    200.00    200.00    200.00    200.00    200.00    200.00    200.00    200.00    200.00
          400.00    400.00    400.00    400.00    400.00    400.00
     100.60    134.32     38.40    411.37    400.00
         16   17    1   11   17    0    0    100.00    100.60    400.00
1    134.32    130.50   -425.30  -4857.21    100.60    100.51
2    130.97    130.50     -4.81  -4747.26    100.51    100.51
                                                                    YLLN=   100.511     I= 16

     101.10    134.32     38.40    411.37    400.00
         15   16    1   10   16    0    0    100.51    101.10    400.00
1    134.32    130.93   -391.33  -4854.38    101.10    101.02
2    131.23    130.93     -4.10  -4753.08    101.02    101.02
                                                                    YLLN=   101.018     I= 15

     101.60    134.32     38.40    411.37    400.00
         14   15    1    9   15    0    0    101.02    101.60    400.00
1    134.32    131.20   -369.98  -4852.63    101.60    101.52
2    131.40    131.20     -3.67  -4756.76    101.52    101.52
                                                                    YLLN=   101.523     I= 14

     102.10    134.32     38.40    411.37    400.00
         13   14    1    8   14    0    0    101.52    102.10    400.00
1    134.32    131.37   -356.52  -4851.53    102.10    102.03
2    131.51    131.37     -3.40  -4759.10    102.03    102.03
                                                                    YLLN=   102.026     I= 13

     102.60    134.32     38.40    413.44    400.00
         12   13    1    7   13    0    0    102.03    102.60    400.00
1    134.32    131.48   -368.88  -4845.27    102.60    102.52
2    131.41    131.48     -3.64  -4749.38    102.52    102.52
                                                                    YLLN=   102.523     I= 12

     101.20     84.48     32.80    212.04    200.00
          5   12    1    6   12    0    0    102.52    102.52    300.00
1    131.38    131.38    925.38  -4145.24    102.52    102.75
2    139.98    131.38    -31.88  -4432.35    102.75    102.74
                                                                    YLLN=   102.739     I=  5

     101.70     84.48     32.80    210.97    200.00
          4    5    1    5    5    0    0    102.74    102.74    200.00
1    120.72    139.70    495.67  -4232.37    102.74    102.86
2    125.08    139.70     -8.29  -4374.11    102.86    102.85
                                                                    YLLN=   102.854     I=  4

     102.20     84.48     32.80    210.97    200.00
          3    4    1    4    4    0    0    102.85    102.85    200.00
1    106.80    125.01    616.78  -3797.99    102.85    103.02
2    112.60    125.01    -15.27  -3986.57    103.02    103.01
                                                                    YLLN=   103.013     I=  3

     102.70     84.48     32.80    210.97    200.00
```

```
        2   3   1   3   3   0   0   103.01   103.01   200.00
1    94.94   112.46   761.38  -3441.95   103.01   103.23
2   102.57   112.46   -27.14  -3688.56   103.23   103.23
                                                          YLLN=  103.227    I=  2


    103.20    84.48    32.80   210.97   200.00
        1   2   1   2   2   0   0   103.23   103.23   200.00
1    85.36   102.31   921.45  -3171.00   103.23   103.52
2    95.09   102.31   -44.94  -3482.36   103.52   103.50
3    94.65   102.31    -0.08  -3468.25   103.50   103.50
                                                          YLLN=  103.504    I=  1


                                                          YLLN=  102.631    I= 11


    101.20    84.48    32.80   210.97   200.00
       10  11   2   6  11   5  12   102.63   102.63   200.00
1   135.51   135.51     2.51  -4280.31   102.63   102.63
                                                          YLLN=  102.632    I= 10


    101.20    84.48    32.80   210.97   200.00
        9  10   2   5  10   0   0   102.63   102.63   200.00
1   135.54   135.54     2.51  -4281.06   102.63   102.63
                                                          YLLN=  102.632    I=  9


    101.70    84.48    32.80   210.97   200.00
        8   9   2   4   9   0   0   102.63   102.63   200.00
1   116.80   135.56   525.74  -4108.65   102.63   102.76
2   121.50   135.56    -9.77  -4261.79   102.76   102.76
                                                          YLLN=  102.758    I=  8


    102.20    84.48    32.80   210.97   200.00
        7   8   2   3   8   0   0   102.76   102.76   200.00
1   103.40   121.42   653.45  -3694.37   102.76   102.93
2   109.66   121.42   -17.90  -3897.51   102.93   102.93
                                                          YLLN=  102.930    I=  7


    102.70    84.48    32.80   210.97   200.00
        6   7   2   2   7   0   0   102.93   102.93   200.00
1    92.14   109.50   803.37  -3360.76   102.93   103.17
2   100.31   109.50   -31.33  -3624.39   103.17   103.16
                                                          YLLN=  103.161    I=  6


(YDI(I1,1),I1=1,N)
 103.50   103.23   103.01   102.85   102.74   103.16   102.93   102.76   102.63   102.63
 102.63   102.52   102.03   101.52   101.02   100.51   100.00

                    INITIAL CONDITIONS AS READ IN

I   X  (MI)   IC   IG      HHG (FT)      DEP(FT),    YU (FT MSL)      QU (CFS)   VU (FT/SEC)        FR NO   MANN. N
```

DT= 0.1000 HRS T= 0.0000 HRS ITER= 0

I	X (MI)	IC	IG	HHG (FT)	DEP(FT),	YU (FT MSL)	QU (CFS)	VU (FT/SEC)	FR NO	MANN. N
1	9000.000	2	0	0.000	3.504	103.504	200.000	2.113	0.223	0.025
2	8000.000	1	0	0.000	3.727	103.227	200.000	1.955	0.201	0.025
3	7000.000	1	0	0.000	4.013	103.013	200.000	1.778	0.177	0.025
4	6000.000	1	0	0.000	4.354	102.854	200.000	1.600	0.154	0.025
5	5000.000	4	0	0.000	4.739	102.739	200.000	1.432	0.133	0.025
12	4990.000	4	0	0.000	4.523	102.523	400.000	3.045	0.289	0.025
13	4000.000	1	0	0.000	4.526	102.026	400.000	3.042	0.289	0.025
14	3000.000	1	0	0.000	4.523	101.523	400.000	3.045	0.289	0.025
15	2000.000	1	0	0.000	4.518	101.018	400.000	3.049	0.289	0.025
16	1000.000	1	0	0.000	4.511	100.511	400.000	3.055	0.290	0.025
17	0.000	3	0	0.000	4.500	100.000	400.000	3.065	0.291	0.025
6	8000.000	2	0	0.000	3.661	103.161	200.000	2.000	0.207	0.025
7	7000.000	1	0	0.000	3.930	102.930	200.000	1.827	0.184	0.025
8	6000.000	1	0	0.000	4.258	102.758	200.000	1.647	0.160	0.025
9	5000.000	1	0	0.000	4.632	102.632	200.000	1.475	0.139	0.025
10	4995.000	1	0	0.000	4.632	102.632	200.000	1.476	0.139	0.025
11	4990.000	4	0	0.000	4.631	102.631	200.000	1.476	0.139	0.025

INITIAL CONDITIONS IMPROVED BY SOLVING UNSTEADY FLOW EQUATIONS WITH BOUNDARIES HELD CONSTANT

DT= 0.1000 HRS T= 0.0000 HRS ITER= 0

I	X (MI)	IC	IG	HHG (FT)	DEP(FT),	YU (FT MSL)	QU (CFS)	VU (FT/SEC)	FR NO	MANN. N
1	9000.000	2	0	0.000	3.478	103.478	200.000	2.133	0.226	0.025
2	8000.000	1	0	0.000	3.692	103.192	199.878	1.977	0.204	0.025
3	7000.000	1	0	0.000	3.970	102.970	199.724	1.801	0.180	0.025
4	6000.000	1	0	0.000	4.305	102.805	199.544	1.620	0.157	0.025
5	5000.000	4	0	0.000	4.686	102.686	199.347	1.449	0.135	0.025
12	4990.000	4	0	0.000	4.580	102.580	398.824	2.987	0.282	0.025
13	4000.000	1	0	0.000	4.618	102.118	398.607	2.953	0.278	0.025
14	3000.000	1	0	0.000	4.669	101.669	398.364	2.908	0.272	0.025
15	2000.000	1	0	0.000	4.745	101.245	398.103	2.845	0.265	0.025
16	1000.000	1	0	0.000	4.854	100.854	397.837	2.759	0.254	0.025
17	0.000	3	0	0.000	5.003	100.503	397.580	2.648	0.241	0.025
6	8000.000	2	0	0.000	3.693	103.193	200.000	1.978	0.204	0.025
7	7000.000	1	0	0.000	3.971	102.971	199.852	1.801	0.181	0.025
8	6000.000	1	0	0.000	4.306	102.806	199.676	1.621	0.157	0.025
9	5000.000	1	0	0.000	4.687	102.687	199.479	1.449	0.135	0.025
10	4995.000	1	0	0.000	4.686	102.686	199.478	1.449	0.136	0.025
11	4990.000	4	0	0.000	4.685	102.685	199.477	1.450	0.136	0.025

DT= 0.1000 HRS T= 0.5000 HRS ITER= 1

I	X (MI)	IC	IG	HHG (FT)	DEP(FT),	YU (FT MSL)	QU (CFS)	VU (FT/SEC)	FR NO	MANN. N
1	9000.000	2	0	0.000	7.507	107.507	1200.000	4.566	0.351	0.025
2	8000.000	1	0	0.000	7.471	106.971	1079.675	4.136	0.319	0.025
3	7000.000	1	0	0.000	7.577	106.577	957.614	3.595	0.275	0.025
4	6000.000	1	0	0.000	7.813	106.313	819.407	2.944	0.223	0.025
5	5000.000	4	0	0.000	8.160	106.160	672.572	2.270	0.169	0.025
12	4990.000	4	0	0.000	7.802	105.802	1474.021	5.306	0.401	0.025

13	4000.000	1	0	0.000	7.482	104.982	1340.590	5.125	0.395	0.025
14	3000.000	1	0	0.000	7.189	104.189	1209.652	4.894	0.383	0.025
15	2000.000	1	0	0.000	6.973	103.473	1078.958	4.558	0.361	0.025
16	1000.000	1	0	0.000	6.895	102.895	942.365	4.045	0.322	0.025
17	0.000	3	0	0.000	7.005	102.505	794.656	3.336	0.264	0.025
6	8000.000	2	0	0.000	7.651	107.151	1200.000	4.443	0.339	0.025
7	7000.000	1	0	0.000	7.679	106.679	1072.212	3.949	0.301	0.025
8	6000.000	1	0	0.000	7.846	106.346	944.473	3.373	0.255	0.025
9	5000.000	1	0	0.000	8.126	106.126	802.925	2.725	0.203	0.025
10	4995.000	1	0	0.000	8.125	106.125	802.187	2.723	0.203	0.025
11	4990.000	4	0	0.000	8.124	106.124	801.449	2.721	0.202	0.025

DT= 0.1000 HRS T= 1.0000 HRS ITER= 1

I	X (MI)	IC	IG	HHG (FT)	DEP(FT),	YU (FT MSL)	QU (CFS)	VU (FT/SEC)	FR NO	MANN. N
1	9000.000	2	0	0.000	11.490	111.490	2200.000	4.455	0.287	0.025
2	8000.000	1	0	0.000	11.700	111.200	2058.746	4.054	0.259	0.025
3	7000.000	1	0	0.000	11.975	110.975	1910.640	3.630	0.230	0.025
4	6000.000	1	0	0.000	12.310	110.810	1758.016	3.201	0.200	0.025
5	5000.000	4	0	0.000	12.689	110.689	1598.230	2.776	0.171	0.025
12	4990.000	4	0	0.000	12.222	110.222	3339.986	6.149	0.386	0.025
13	4000.000	1	0	0.000	12.101	109.601	3178.377	5.942	0.374	0.025
14	3000.000	1	0	0.000	12.045	109.045	2999.106	5.647	0.357	0.025
15	2000.000	1	0	0.000	12.077	108.577	2803.939	5.258	0.332	0.025
16	1000.000	1	0	0.000	12.192	108.192	2602.555	4.809	0.302	0.025
17	0.000	3	0	0.000	12.400	107.900	2386.706	4.296	0.268	0.025
6	8000.000	2	0	0.000	11.762	111.262	2200.000	4.297	0.274	0.025
7	7000.000	1	0	0.000	12.006	111.006	2053.558	3.886	0.246	0.025
8	6000.000	1	0	0.000	12.309	110.809	1900.855	3.461	0.217	0.025
9	5000.000	1	0	0.000	12.667	110.667	1743.386	3.036	0.188	0.025
10	4995.000	1	0	0.000	12.667	110.667	1742.571	3.035	0.188	0.025
11	4990.000	4	0	0.000	12.666	110.666	1741.756	3.033	0.188	0.025

DT= 0.1000 HRS T= 1.5000 HRS ITER= 0

I	X (MI)	IC	IG	HHG (FT)	DEP(FT),	YU (FT MSL)	QU (CFS)	VU (FT/SEC)	FR NO	MANN. N
1	9000.000	2	0	0.000	13.641	113.641	2200.000	3.411	0.204	0.025
2	8000.000	1	0	0.000	14.005	113.505	2140.081	3.183	0.189	0.025
3	7000.000	1	0	0.000	14.386	113.386	2071.322	2.952	0.173	0.025
4	6000.000	1	0	0.000	14.788	113.288	2003.926	2.733	0.158	0.025
5	5000.000	4	0	0.000	15.210	113.210	1937.909	2.527	0.145	0.025
12	4990.000	4	0	0.000	14.871	112.871	3929.302	5.312	0.307	0.025
13	4000.000	1	0	0.000	15.020	112.520	3858.309	5.133	0.295	0.025
14	3000.000	1	0	0.000	15.202	112.202	3779.324	4.932	0.282	0.025
15	2000.000	1	0	0.000	15.416	111.916	3696.224	4.717	0.268	0.025
16	1000.000	1	0	0.000	15.662	111.662	3607.827	4.488	0.254	0.025
17	0.000	3	0	0.000	15.941	111.441	3513.511	4.248	0.238	0.025
6	8000.000	2	0	0.000	14.011	113.511	2200.000	3.270	0.194	0.025
7	7000.000	1	0	0.000	14.393	113.393	2135.246	3.041	0.178	0.025
8	6000.000	1	0	0.000	14.790	113.290	2062.376	2.813	0.163	0.025
9	5000.000	1	0	0.000	15.205	113.205	1992.061	2.599	0.149	0.025
10	4995.000	1	0	0.000	15.204	113.204	1991.727	2.599	0.149	0.025
11	4990.000	4	0	0.000	15.204	113.204	1991.392	2.598	0.149	0.025

DT[illegible]1000 HRS T= 2.0000 HRS ITER= 0

I	X (MI)	IC	IG	HHG (FT)	DEP(FT),	YU (FT MSL)	QU (CFS)	VU (FT/SEC)	FR NO	MANN. N
1	9000.000	2	0	0.000	14.661	114.661	2200.000	3.042	0.177	0.025
2	8000.000	1	0	0.000	15.054	114.554	2167.370	2.873	0.165	0.025
3	7000.000	1	0	0.000	15.462	114.462	2135.529	2.712	0.154	0.025
4	6000.000	1	0	0.000	15.882	114.382	2101.210	2.556	0.144	0.025
5	5000.000	4	0	0.000	16.314	114.314	2065.630	2.406	0.134	0.025
12	4990.000	4	0	0.000	16.016	114.016	4163.308	4.996	0.280	0.025
13	4000.000	1	0	0.000	16.226	113.726	4126.839	4.849	0.270	0.025
14	3000.000	1	0	0.000	16.457	113.457	4089.421	4.696	0.260	0.025
15	2000.000	1	0	0.000	16.711	113.211	4049.804	4.537	0.249	0.025
16	1000.000	1	0	0.000	16.987	112.987	4006.883	4.370	0.239	0.025
17	0.000	3	0	0.000	17.285	112.785	3961.833	4.200	0.228	0.025
6	8000.000	2	0	0.000	15.058	114.558	2200.000	2.915	0.168	0.025
7	7000.000	1	0	0.000	15.464	114.464	2165.990	2.750	0.156	0.025
8	6000.000	1	0	0.000	15.883	114.383	2132.955	2.594	0.146	0.025
9	5000.000	1	0	0.000	16.312	114.312	2098.032	2.444	0.136	0.025
10	4995.000	1	0	0.000	16.311	114.311	2097.855	2.444	0.136	0.025
11	4990.000	4	0	0.000	16.311	114.311	2097.678	2.444	0.136	0.025

DT= 0.1000 HRS T= 2.5000 HRS ITER= 0

I	X (MI)	IC	IG	HHG (FT)	DEP(FT),	YU (FT MSL)	QU (CFS)	VU (FT/SEC)	FR NO	MANN. N
[illegible]	[illegible]0.000	2	0	0.000	15.170	115.170	2200.000	2.881	0.165	0.025
2	8000.000	1	0	0.000	15.574	115.074	2183.425	2.741	0.155	0.025
3	7000.000	1	0	0.000	15.990	114.990	2166.417	2.606	0.146	0.025
4	6000.000	1	0	0.000	16.417	114.917	2149.124	2.478	0.137	0.025
5	5000.000	4	0	0.000	16.853	114.853	2130.582	2.354	0.129	0.025
12	4990.000	4	0	0.000	16.573	114.573	4277.645	4.857	0.268	0.025
13	4000.000	1	0	0.000	16.806	114.306	4258.605	4.727	0.259	0.025
14	3000.000	1	0	0.000	17.056	114.056	4238.964	4.593	0.250	0.025
15	2000.000	1	0	0.000	17.326	113.826	4218.522	4.455	0.241	0.025
16	1000.000	1	0	0.000	17.615	113.615	4196.893	4.314	0.232	0.025
17	0.000	3	0	0.000	17.922	113.422	4174.111	4.170	0.222	0.025
6	8000.000	2	0	0.000	15.577	115.077	2200.000	2.761	0.156	0.025
7	7000.000	1	0	0.000	15.992	114.992	2182.629	2.626	0.147	0.025
8	6000.000	1	0	0.000	16.417	114.917	2165.055	2.496	0.138	0.025
9	5000.000	1	0	0.000	16.852	114.852	2147.252	2.372	0.130	0.025
10	4995.000	1	0	0.000	16.852	114.852	2147.157	2.372	0.130	0.025
11	4990.000	4	0	0.000	16.852	114.852	2147.062	2.372	0.130	0.025

DT= 0.1000 HRS T= 3.0000 HRS ITER= 0

I	X (MI)	IC	IG	HHG (FT)	DEP(FT),	YU (FT MSL)	QU (CFS)	VU (FT/SEC)	FR NO	MANN. N
1	9000.000	2	0	0.000	15.432	115.432	2200.000	2.803	0.159	0.025
[illegible]	[illegible]0.000	1	0	0.000	15.841	115.341	2191.422	2.677	0.151	0.025
[illegible]	[illegible]00.000	1	0	0.000	16.261	115.261	2182.377	2.555	0.142	0.025
4	6000.000	1	0	0.000	16.691	115.191	2172.938	2.439	0.134	0.025
5	5000.000	4	0	0.000	17.129	115.129	2163.692	2.328	0.127	0.025
12	4990.000	4	0	0.000	16.857	114.857	4335.639	4.789	0.262	0.025
13	4000.000	1	0	0.000	17.100	114.600	4325.840	4.667	0.254	0.025
14	3000.000	1	0	0.000	17.360	114.360	4315.379	4.543	0.246	0.025

15	2000.000	1	0	0.000	17.637	114.137	4304.492	4.415	0.237	0.025
16	1000.000	1	0	0.000	17.933	113.933	4293.180	4.285	0.229	0.025
17	0.000	3	0	0.000	18.244	113.744	4281.449	4.154	0.220	0.025
6	8000.000	2	0	0.000	15.843	115.343	2200.000	2.687	0.151	0.025
7	7000.000	1	0	0.000	16.262	115.262	2191.128	2.565	0.143	0.025
8	6000.000	1	0	0.000	16.691	115.191	2181.784	2.449	0.135	0.025
9	5000.000	1	0	0.000	17.129	115.129	2172.041	2.337	0.127	0.025
10	4995.000	1	0	0.000	17.128	115.128	2171.994	2.337	0.127	0.025
11	4990.000	4	0	0.000	17.128	115.128	2171.947	2.337	0.127	0.025

DT= 0.1000 HRS T= 3.5000 HRS ITER= 1

I	X (MI)	IC	IG	HHG (FT)	DEP(FT),	YU (FT MSL)	QU (CFS)	VU (FT/SEC)	FR NO	MANN. N
1	9000.000	2	0	0.000	12.087	112.087	200.006	0.375	0.024	0.025
2	8000.000	1	0	0.000	12.629	112.129	448.183	0.784	0.049	0.025
3	7000.000	1	0	0.000	13.129	112.129	684.240	1.127	0.069	0.025
4	6000.000	1	0	0.000	13.608	112.108	929.801	1.447	0.087	0.025
5	5000.000	4	0	0.000	14.072	112.072	1182.582	1.745	0.103	0.025
12	4990.000	4	0	0.000	13.965	111.965	2114.886	3.160	0.187	0.025
13	4000.000	1	0	0.000	14.314	111.814	2359.457	3.390	0.199	0.025
14	3000.000	1	0	0.000	14.636	111.636	2605.656	3.613	0.210	0.025
15	2000.000	1	0	0.000	14.933	111.433	2850.005	3.827	0.221	0.025
16	1000.000	1	0	0.000	15.200	111.200	3094.699	4.040	0.231	0.025
17	0.000	3	0	0.000	15.434	110.934	3344.698	4.260	0.242	0.025
6	8000.000	2	0	0.000	12.562	112.062	200.006	0.353	0.022	0.025
7	7000.000	1	0	0.000	13.103	112.103	446.118	0.737	0.045	0.025
8	6000.000	1	0	0.000	13.606	112.106	681.681	1.061	0.064	0.025
9	5000.000	1	0	0.000	14.091	112.091	929.749	1.369	0.081	0.025
10	4995.000	1	0	0.000	14.091	112.091	931.027	1.371	0.081	0.025
11	4990.000	4	0	0.000	14.090	112.090	932.304	1.373	0.081	0.025

DT= 0.1000 HRS T= 4.0000 HRS ITER= 1

I	X (MI)	IC	IG	HHG (FT)	DEP(FT),	YU (FT MSL)	QU (CFS)	VU (FT/SEC)	FR NO	MANN. N
1	9000.000	2	0	0.000	7.708	107.708	200.000	0.733	0.056	0.025
2	8000.000	1	0	0.000	8.166	107.666	294.492	0.993	0.074	0.025
3	7000.000	1	0	0.000	8.640	107.640	411.108	1.276	0.093	0.025
4	6000.000	1	0	0.000	9.082	107.582	513.095	1.480	0.105	0.025
5	5000.000	4	0	0.000	9.511	107.511	615.045	1.657	0.115	0.025
12	4990.000	4	0	0.000	9.398	107.398	1154.941	3.168	0.222	0.025
13	4000.000	1	0	0.000	9.620	107.120	1264.546	3.350	0.232	0.025
14	3000.000	1	0	0.000	9.815	106.815	1384.463	3.560	0.245	0.025
15	2000.000	1	0	0.000	9.977	106.477	1512.730	3.795	0.259	0.025
16	1000.000	1	0	0.000	10.099	106.099	1648.071	4.060	0.276	0.025
17	0.000	3	0	0.000	10.158	105.658	1794.328	4.381	0.297	0.025
6	8000.000	2	0	0.000	8.145	107.645	200.000	0.677	0.050	0.025
7	7000.000	1	0	0.000	8.606	107.606	303.106	0.947	0.069	0.025
8	6000.000	1	0	0.000	9.079	107.579	428.522	1.237	0.088	0.025
9	5000.000	1	0	0.000	9.521	107.521	538.836	1.449	0.101	0.025
10	4995.000	1	0	0.000	9.521	107.521	539.366	1.451	0.101	0.025
11	4990.000	4	0	0.000	9.521	107.521	539.895	1.452	0.101	0.025

DT= 0.1000 HRS T= 4.5000 HRS ITER= 1

I	X (MI)	IC	IG	HHG (FT)	DEP(FT),	YU (FT MSL)	QU (CFS)	VU (FT/SEC)	FR NO	MANN. N
[illegible]	[illegible]0.000	2	0	0.000	5.272	105.272	200.000	1.242	0.111	0.025
2	[illegible]000.000	1	0	0.000	5.688	105.188	237.849	1.333	0.115	0.025
3	7000.000	1	0	0.000	6.100	105.100	275.742	1.404	0.118	0.025
4	6000.000	1	0	0.000	6.527	105.027	319.452	1.481	0.121	0.025
5	5000.000	4	0	0.000	6.945	104.945	358.390	1.523	0.121	0.025
12	4990.000	4	0	0.000	6.843	104.843	686.230	2.977	0.238	0.025
13	4000.000	1	0	0.000	7.034	104.534	727.676	3.036	0.240	0.025
14	3000.000	1	0	0.000	7.223	104.223	772.952	3.107	0.243	0.025
15	2000.000	1	0	0.000	7.413	103.913	819.975	3.176	0.245	0.025
16	1000.000	1	0	0.000	7.590	103.590	871.789	3.265	0.250	0.025
17	0.000	3	0	0.000	7.737	103.237	932.012	3.396	0.258	0.025
6	8000.000	2	0	0.000	5.651	105.151	200.000	1.131	0.098	0.025
7	7000.000	1	0	0.000	6.084	105.084	239.611	1.224	0.103	0.025
8	6000.000	1	0	0.000	6.511	105.011	280.417	1.304	0.106	0.025
9	5000.000	1	0	0.000	6.951	104.951	327.438	1.389	0.110	0.025
10	4995.000	1	0	0.000	6.951	104.951	327.639	1.390	0.110	0.025
11	4990.000	4	0	0.000	6.951	104.951	327.840	1.391	0.110	0.025

DT= 0.1000 HRS T= 5.0000 HRS ITER= 0

I	X (MI)	IC	IG	HHG (FT)	DEP(FT),	YU (FT MSL)	QU (CFS)	VU (FT/SEC)	FR NO	MANN. N
1	[illegible]000.000	2	0	0.000	3.106	103.106	0.001	0.000	0.000	0.025
[illegible]	[illegible]0.000	1	0	0.000	3.630	103.130	47.737	0.482	0.050	0.025
[illegible]	[illegible]00.000	1	0	0.000	4.115	103.115	93.629	0.806	0.080	0.025
4	6000.000	1	0	0.000	4.574	103.074	141.127	1.059	0.100	0.025
5	5000.000	4	0	0.000	5.003	103.003	194.863	1.298	0.118	0.025
12	4990.000	4	0	0.000	4.947	102.947	339.433	2.295	0.210	0.025
13	4000.000	1	0	0.000	5.183	102.683	388.763	2.470	0.221	0.025
14	3000.000	1	0	0.000	5.386	102.386	435.739	2.629	0.232	0.025
15	2000.000	1	0	0.000	5.566	102.066	481.554	2.779	0.242	0.025
16	1000.000	1	0	0.000	5.715	101.715	528.414	2.942	0.253	0.025
17	0.000	3	0	0.000	5.830	101.330	574.344	3.112	0.266	0.025
6	8000.000	2	0	0.000	3.525	103.025	0.001	0.000	0.000	0.025
7	7000.000	1	0	0.000	4.048	103.048	48.150	0.423	0.042	0.025
8	6000.000	1	0	0.000	4.540	103.040	95.598	0.724	0.069	0.025
9	5000.000	1	0	0.000	5.015	103.015	144.040	0.956	0.087	0.025
10	4995.000	1	0	0.000	5.015	103.015	144.305	0.958	0.087	0.025
11	4990.000	4	0	0.000	5.015	103.015	144.570	0.960	0.087	0.025

TOTAL ITERATIONS FOR EACH OF 1 RIVERS.
33

PROGRAM COMPLETED.
EXIT
EXECUTION COMPLETED O.K.
$

6.3 EXAMPLE 3

This example is identical to Example 2 except now a time controlled gate is placed at the station locations of 9 and 10, i.e., on the tributary just upstream of the confluence (refer to Figure 6.6). The time controlled gate operations are as follows.

Time (min)	Vertical Opening (ft)
0	2
30	4
60	4
90	4
120	4
150	4
180	4
240	4
270	4
300	4

In order to run this model with a gate, the following changes to the data input for example 3 were required.

1. K21 and K2 2 must be specified on card 1A.
2. NG must be specified on card 8A.
3. The value of JCOD = 10 must be specified on card 11A for stations 9 and 10.
4. LGX, IGT, NTG, and HGC must be specified on card 51A.
5. The gate discharge coefficients, GC, for each tail water head must be specified on card 51B.

6. The corresponding tail water head, DTW, for each gate discharge coefficint must be specified on card 51C.

7. The height of the gate opening for each time interval (NU time intervals) is specified on card 51D.

A Δt = 0.01 hr. had to be used to obtain a solution to this problem.

Card

Example 6.3 Input

Card	1 (1–10)	2 (11–20)	3 (21–30)	4 (31–40)	5 (41–50)	6 (51–60)	7 (61–70)	8 (71–80)
1	1 17	490 1	1 8	1 2	2 1	1 1	1 1	2 1
1A	1 5	1 1	1 1					
	Cards 2, 3, 4, 5, 6, 7, & 8 are the same as Example 6.2 Input							
8A	1							
	Cards 9, 11 are same as Example 6.2 Input							
11A	2	1	1	1	4	2	1	1
11A	10	10	4	4	1	1	1	1
	Cards 11B, 11C, 11D, 11E, 14, 15, 16, 22, 25, 26, 27, 28, 29, 30, 35, 36, & 37 are the							
	same as Example 6.2 Input							
51A	9	1	4	0.90				
51B	20.00	19.50	19.00	18.00				
51C	2.0	6.0	10.0	14.0				
51D	2.0	4.0	4.0	4.0	4.0	4.0	4.0	4.0
51D	4.0	4.0	4.0					
52	4.5	0.01	50					
	Cards 53, 54, 54A, 54B, 54C, 55, 56, 57, 58, & 59 are the same as Example 6.2							
	Input							

```
  1   17  490    1    1    8    1    2    2    1    1    1    1    1    2    1
  1    5    1    1    1    1
ALONE
     0.1        50.        50.       0.80       0.55       1.0       0.5
       1        11          1          1          7        10         2         1
       2         0          0          0          0         0         1
       0
       0
       0
       1
       0
      17
       2         1          1          1          4         2         1         1
      10        10          4          4          1         1         1         1
       3
       1         2
       5        11         12
       2         2
       1         2          3          4          5        12        13        14
      15        16         17          6          7         8         9        10
      11
       3
       1         0          1
      17
     200.      1200.      2200.      2200.      2200.      2200.      2200.      200.
     200.       200.
     200.      1200.      2200.      2200.      2200.      2200.      2200.      200.
     200.       200.
    1.00
    98.6       100.2      102.6      104.3      106.2      107.7      109.5
    200.        550.      1000.      1700.      2200.      2600.      3200.
     20.        100.
     20.        100.
     20.        100.
     20.        100.
     20.        100.
     20.        100.
     20.        100.
     20.        100.
     20.        100.
     20.        100.
     20.        100.
     20.        100.
     20.        100.
     20.        100.
     20.        100.
     20.        100.
     20.        100.
     20.        100.
     100.       120.0
     99.5       119.5
     99.0       119.0
     98.5       118.5
     98.0       118.0
     99.5       119.5
     99.0       119.0
     98.5       118.5
     98.0       118.0
     98.0       118.0
     98.0       118.0
     98.0       118.0
     97.5       117.5
     97.0       117.0
     96.5       116.5
```

```
  0.0      0.0      0.0      0.0      0.0      0.0      0.0      0.0
  0.0      0.0      0.0      0.0      0.0      0.0      0.0      0.0
  0.0
  0.0      0.0      0.0
 9000.    8000.    7000.    6000.    5000.    8000.    7000.    6000.
 5000.    4995.    4990.    4990.    4000.    3000.    2000.    1000.
  0.0
  0.0      0.0      0.0      0.0      0.0      0.0      0.0      0.0
  0.0      0.0      0.0      0.0      0.0      0.0      0.0      0.0
  0.0
    9        1        4     0.90
20.00    19.50    19.00    18.00
  2.0      6.0     10.0     14.0
  2.0      4.0      4.0      4.0      4.0      4.0      4.0      4.0
  4.0      4.0      4.0
  4.5     0.01       50
  0.0      0.0      0.0      0.0      0.0      0.0      0.0      0.0
  0.0      0.0      0.0      0.0      0.0      0.0      0.0      0.0
100.0
 200.       0.       0.       0.       0.     200.       0.       0.
   0.       0.       0.     400.       0.       0.       0.       0.
   0.
   2
   6       11
   6        7        8        9       10       11
   1        2        3        4        5       12       13       14
  15       16       17
 0.0    10000.
0.025    0.025
EXAMPLE
END
EXIT
```

```
TYPE WORLD5.OUT

                    MODIFIED DWOPER PROGRAM (NETWORK) VERSION--7/18/84


                    PROGRAM DEVELOPED BY D.L.FREAD,PHD.
                    NWS HYDROLOGIC RESEARCH LABORATORY, 8060 13 TH ST., SILVER SPRING, MD. 20910, 301-427-7640

  K1   K2   K3   K4   K5   K6   K7   K8   K9  K10  K11  K12  K13  K14  K15  K16  K17  K18  K19  K20  K21  K22  K23  K24  K25  K26
   1   17  490    2    1    8    1    2    2    2    1    1    1    1   34    4    2    1    4   34    1    5    1    1    1    1


*** THE SPACE REQUIRED FOR THESE DIMENSIONS IS      24054  THE SPACE AVAILABLE IN ARRAY A IS     107600 ***

       ALON

 EPSY      EPSQ      EPSQJ     THETA     F1        XFACT     DHF     CFNAME
 0.1000    50.0000   50.0000   0.8000    0.5500    1.0000    0.5000

     JN        NU        NCT       ICD       NYQD      ITMAX     NCML      NET
     1         11        1         1         7         10        2         1

     NCSS      NP        KTERM     KPL       KPL2      JNK       NPEND
     2         0         0         0         0         0         1         0

  NQL(J), J = 1, JN
     0

  NWJ(J), J = 1, JN
     0

(NUMLAD(J), J = 1, JN)
     0


(NG(J), J = 1, JN)
     1

  NCSS1(J), J = 1, JN
     0

 NB(1)
    17

  JCOD(K), K = 1, N
     2         1         1         1         4         2         1         1
    10        10         4         4         1         1         1         1


    JTN      NUPB
     1         2

   JU(K)     JB(K)     JL(K)     AJN(K) , K=1,JTN
     5        11        12       0.00
```

```
KMU(K), K=1,NUPB
    2        2
     (JCPR(K),K=1,N)
    1        2        3        4        5       12       13       14
   15       16       17        6        7        8        9       10
   11

KD(J), J = 1, JN
    3

NRCM1(J)  NRT1(J)  NNYQ(J) , J =  1
    1        0        1

NCM(K,1), K = 1, NCRM1(1)
   17

STU(K,1), K = 1, NU
    200.00      1200.00      2200.00      2200.00      2200.00      2200.00      2200.00       200.00
    200.00       200.00         0.00

STU(K,2), K = 1, NU
    200.00      1200.00      2200.00      2200.00      2200.00      2200.00      2200.00       200.00
    200.00       200.00         0.00

GZN
  1.00

YQD(K), K = 1, NYQD
 98.60   100.20   102.60   104.30   106.20   107.70   109.50

QYQD(K), K = 1, NYQD
200.00   550.00  1000.00  1700.00  2200.00  2600.00  3200.00

BS(K,I,1), K = 1, NCS
I =  1    20.00000 100.00000
I =  2    20.00000 100.00000
I =  3    20.00000 100.00000
I =  4    20.00000 100.00000
I =  5    20.00000 100.00000
I =  6    20.00000 100.00000
I =  7    20.00000 100.00000
I =  8    20.00000 100.00000
I =  9    20.00000 100.00000
I = 10    20.00000 100.00000
I = 11    20.00000 100.00000
I = 12    20.00000 100.00000
I = 13    20.00000 100.00000
I = 14    20.00000 100.00000
I = 15    20.00000 100.00000
I = 16    20.00000 100.00000
I = 17    20.00000 100.00000

HS(K,I,1), K = 1, NCS
I =  1     100.000   120.000
I =  2      99.500   119.500
I =  3      99.000   119.000
I =  4      98.500   118.500
I =  5      98.000   118.000
I =  6      99.500   119.500
I =  7      99.000   119.000
I =  8      98.500   118.500
```

```
I =  9      98.000   118.000
I = 10      98.000   118.000
I =         98.000   118.000
I =         98.000   118.000
I = 13      97.500   117.500
I = 14      97.000   117.000
I = 15      96.500   116.500
I = 16      96.000   116.000
I = 17      95.500   115.500

  AS(1,I,1), I = 1, NB(1)
        0.00        0.00        0.00        0.00        0.00        0.00        0.00        0.00
        0.00        0.00        0.00        0.00        0.00        0.00        0.00        0.00
        0.00

  COFW      VWIND    WINAGL
    0.00      0.00      0.00

  X(I,1), I = 1, NB(1)
9000.0000 8000.0000 7000.0000 6000.0000 5000.0000 8000.0000 7000.0000 6000.0000
5000.0000 4995.0000 4990.0000 4990.0000 4000.0000 3000.0000 2000.0000 1000.0000
  0.0000

  FKC(I,1), I = 1, NS(1)
    0.00      0.00      0.00      0.00      0.00      0.00      0.00      0.00
    0.00      0.00      0.00      0.00      0.00      0.00      0.00      0.00
    0.00

(          J)  IGT(K,J)  NTG(K,J)  HGC(K,J),K =   1
         9         1         4      0.90

( GC(I,K,J),I = 1,NTG(K,J))
   20.00     19.50     19.00     18.00

(DTW(I,K,J),I = 1,NTG(K,J))
    2.00      6.00     10.00     14.00

(HG(I,K,J),I =1,NU), K = 1,NG(J))
  2.0000    4.0000    4.0000    4.0000    4.0000    4.0000    4.0000    4.0000
  4.0000    4.0000    4.0000

  TE(HR)    TM(HR)   KITPR
   4.500   0.01000      50      0.00

  YDI(I,1), I = 1, NB(1)
    0.00      0.00      0.00      0.00      0.00      0.00      0.00      0.00
    0.00      0.00      0.00      0.00      0.00      0.00      0.00      0.00
  100.00

  QDI(I,1), I = 1, NB(1)
       200.0       0.0       0.0       0.0       0.0     200.0       0.0       0.0
         0.0       0.0       0.0     400.0       0.0       0.0       0.0       0.0
         0.0

          11
      6       7       8       9      10      11
      1       2       3       4       5      12      13      14
     15      16      17

  YQCM(L,K,1), K = 1, NRCM1(1)
    0.00  10000.00
```

```
CM(L,K,1), K = 1, NRCM1(1)
0.0250    0.0250


      EXAMPLE


PRECAL


(QDI(I1,1),I1=1,N)
 200.00    200.00    200.00    200.00    200.00    200.00    200.00    200.00    200.00    200.00
 200.00    400.00    400.00    400.00    400.00    400.00    400.00
     100.60    134.32     38.40    411.37    400.00
         16   17    1   11   17    0    0    100.00    100.60    400.00
 1   134.32    130.50   -425.30  -4857.21    100.60    100.51
 2   130.97    130.50     -4.81  -4747.26    100.51    100.51
                                                                    YLLN=   100.511     I= 16


     101.10    134.32     38.40    411.37    400.00
         15   16    1   10   16    0    0    100.51    101.10    400.00
 1   134.32    130.93   -391.33  -4854.38    101.10    101.02
 2   131.23    130.93     -4.10  -4753.08    101.02    101.02
                                                                    YLLN=   101.018     I= 15


     101.60    134.32     38.40    411.37    400.00
         14   15    1    9   15    0    0    101.02    101.60    400.00
 1   134.32    131.20   -369.98  -4852.63    101.60    101.52
 2   131.40    131.20     -3.67  -4756.76    101.52    101.52
                                                                    YLLN=   101.523     I= 14


     102.10    134.32     38.40    411.37    400.00
         13   14    1    8   14    0    0    101.52    102.10    400.00
 1   134.32    131.37   -356.52  -4851.53    102.10    102.03
 2   131.51    131.37     -3.40  -4759.10    102.03    102.03
                                                                    YLLN=   102.026     I= 13


     102.60    134.32     38.40    413.44    400.00
         12   13    1    7   13    0    0    102.03    102.60    400.00
 1   134.32    131.48   -368.88  -4845.27    102.60    102.52
 2   131.41    131.48     -3.64  -4749.38    102.52    102.52
                                                                    YLLN=   102.523     I= 12


     101.20     84.48     32.80    212.04    200.00
          5   12    1    6   12    0    0    102.52    102.52    300.00
 1   131.38    131.38    925.38  -4145.24    102.52    102.75
 2   139.98    131.38    -31.88  -4432.35    102.75    102.74
                                                                    YLLN=   102.739     I=  5


     101.70     84.48     32.80    210.97    200.00
          4    5    1    5    5    0    0    102.74    102.74    200.00
```

```
1    120.72    139.70    495.67  -4232.37    102.74    102.86
2    125.08    139.70     -8.29  -4374.11    102.86    102.85
                                                                YLLN=   102.854     I=  4

     102.20     84.48     32.80    210.97    200.00
          3    4    1    4    4    0    0    102.85    102.85    200.00
1    106.80    125.01    616.78  -3797.99    102.85    103.02
2    112.60    125.01    -15.27  -3986.57    103.02    103.01
                                                                YLLN=   103.013     I=  3

     102.70     84.48     32.80    210.97    200.00
          2    3    1    3    3    0    0    103.01    103.01    200.00
1     94.94    112.46    761.38  -3441.95    103.01    103.23
2    102.57    112.46    -27.14  -3688.56    103.23    103.23
                                                                YLLN=   103.227     I=  2

     103.20     84.48     32.80    210.97    200.00
          1    2    1    2    2    0    0    103.23    103.23    200.00
1     85.36    102.31    921.45  -3171.00    103.23    103.52
2     95.09    102.31    -44.94  -3482.36    103.52    103.50
3     94.65    102.31     -0.08  -3468.25    103.50    103.50
                                                                YLLN=   103.504     I=  1

                                                                YLLN=   102.631     I= 11

     101.20     84.48     32.80    210.97    200.00
         10   11    2    6   11    5   12    102.63    102.63    200.00
1    135.51    135.51      2.51  -4280.31    102.63    102.63
                                                                YLLN=   102.632     I= 10

     101.20     84.48     32.80    210.97    200.00
          9   10    2    5   10    0    0    102.63    102.63    200.00
1    135.54    135.54      2.51  -4281.06    102.63    102.63
                                                                YLLN=   102.632     I=  9

     101.70     84.48     32.80    210.97    200.00
          8    9    2    4    9    0    0    102.63    102.63    200.00
1    116.80    135.56    525.74  -4108.65    102.63    102.76
2    121.50    135.56     -9.77  -4261.79    102.76    102.76
                                                                YLLN=   102.758     I=  8

     102.20     84.48     32.80    210.97    200.00
          7    8    2    3    8    0    0    102.76    102.76    200.00
1    103.40    121.42    653.45  -3694.37    102.76    102.93
2    109.66    121.42    -17.90  -3897.51    102.93    102.93
                                                                YLLN=   102.930     I=  7

     102.70     84.48     32.80    210.97    200.00
          6    7    2    2    7    0    0    102.93    102.93    200.00
1     92.14    109.50    803.37  -3360.76    102.93    103.17
2    100.31    109.50    -31.33  -3624.39    103.17    103.16
                                                                YLLN=   103.161     I=  6
```

(YDI(I1,1),I1=1,N)

103.50	103.23	103.01	102.85	102.74	103.16	102.93	102.76	102.63	102.63
102.63	102.52	102.03	101.52	101.02	100.51	100.00			

INITIAL CONDITIONS AS READ IN

I	X (MI)	IC	IG	HHG (FT)	DEP(FT),	YU (FT MSL)	QU (CFS)	VU (FT/SEC)	FR NO	MANN. N

DT= 0.0100 HRS T= 0.0000 HRS ITER= 0

I	X (MI)	IC	IG	HHG (FT)	DEP(FT),	YU (FT MSL)	QU (CFS)	VU (FT/SEC)	FR NO	MANN. N
1	9000.000	2	0	0.000	3.504	103.504	200.000	2.113	0.223	0.025
2	8000.000	1	0	0.000	3.727	103.227	200.000	1.955	0.201	0.025
3	7000.000	1	0	0.000	4.013	103.013	200.000	1.778	0.177	0.025
4	6000.000	1	0	0.000	4.354	102.854	200.000	1.600	0.154	0.025
5	5000.000	4	0	0.000	4.739	102.739	200.000	1.432	0.133	0.025
12	4990.000	4	0	0.000	4.523	102.523	400.000	3.045	0.289	0.025
13	4000.000	1	0	0.000	4.526	102.026	400.000	3.042	0.289	0.025
14	3000.000	1	0	0.000	4.523	101.523	400.000	3.045	0.289	0.025
15	2000.000	1	0	0.000	4.518	101.018	400.000	3.049	0.289	0.025
16	1000.000	1	0	0.000	4.511	100.511	400.000	3.055	0.290	0.025
17	0.000	3	0	0.000	4.500	100.000	400.000	3.065	0.291	0.025
6	8000.000	2	0	0.000	3.661	103.161	200.000	2.000	0.207	0.025
7	7000.000	1	0	0.000	3.930	102.930	200.000	1.827	0.184	0.025
8	6000.000	1	0	0.000	4.258	102.758	200.000	1.647	0.160	0.025
9	5000.000	10	1	2.000	4.632	102.632	200.000	1.475	0.139	0.025
10	4995.000	10	0	0.000	4.632	102.632	200.000	1.476	0.139	0.025
11	4990.000	4	0	0.000	4.631	102.631	200.000	1.476	0.139	0.025

DT= 0.0100 HRS T= 0.0000 HRS ITER= 0

I	X (MI)	IC	IG	HHG (FT)	DEP(FT),	YU (FT MSL)	QU (CFS)	VU (FT/SEC)	FR NO	MANN. N
1	9000.000	2	0	0.000	3.509	103.509	200.000	2.110	0.223	0.025
2	8000.000	1	0	0.000	3.705	103.205	206.041	2.029	0.209	0.025
3	7000.000	1	0	0.000	3.950	102.950	211.339	1.918	0.193	0.025
4	6000.000	1	0	0.000	4.258	102.758	213.886	1.761	0.171	0.025
5	5000.000	4	0	0.000	4.618	102.618	215.819	1.599	0.150	0.025
12	4990.000	4	0	0.000	4.514	102.514	397.970	3.037	0.288	0.025
13	4000.000	1	0	0.000	4.512	102.012	399.841	3.053	0.290	0.025
14	3000.000	1	0	0.000	4.527	101.527	396.199	3.012	0.286	0.025
15	2000.000	1	0	0.000	4.586	101.086	386.583	2.889	0.273	0.025
16	1000.000	1	0	0.000	4.695	100.695	375.538	2.722	0.254	0.025
17	0.000	3	0	0.000	4.856	100.356	365.401	2.532	0.233	0.025
6	8000.000	2	0	0.000	3.701	103.201	200.000	1.972	0.204	0.025
7	7000.000	1	0	0.000	4.002	103.002	189.476	1.691	0.169	0.025
8	6000.000	1	0	0.000	4.359	102.859	183.262	1.464	0.141	0.025
9	5000.000	10	1	2.000	4.754	102.754	182.136	1.298	0.121	0.025
10	4995.000	10	0	0.000	4.630	102.630	182.136	1.345	0.126	0.025
11	4990.000	4	0	0.000	4.629	102.629	182.152	1.345	0.126	0.025

DT= [illegible]0100 HRS T= 0.5000 HRS ITER= 0

I	X (MI)	IC	IG	HHG (FT)	DEP(FT),	YU (FT MSL)	QU (CFS)	VU (FT/SEC)	FR NO	MANN. N
1	9000.000	2	0	0.000	7.452	107.452	1200.000	4.613	0.356	0.025
2	8000.000	1	0	0.000	7.387	106.887	1085.833	4.227	0.327	0.025
3	7000.000	1	0	0.000	7.454	106.454	963.368	3.702	0.285	0.025
4	6000.000	1	0	0.000	7.658	106.158	834.039	3.084	0.235	0.025
5	5000.000	4	0	0.000	7.975	105.975	699.794	2.441	0.183	0.025
12	4990.000	4	0	0.000	7.642	105.642	1411.015	5.233	0.399	0.025
13	4000.000	1	0	0.000	7.325	104.825	1285.471	5.065	0.393	0.025
14	3000.000	1	0	0.000	7.031	104.031	1159.438	4.841	0.382	0.025
15	2000.000	1	0	0.000	6.811	103.311	1032.250	4.508	0.361	0.025
16	1000.000	1	0	0.000	6.726	102.726	900.521	4.003	0.322	0.025
17	0.000	3	0	0.000	6.825	102.325	761.004	3.313	0.265	0.025
6	8000.000	2	0	0.000	7.905	107.405	1200.000	4.239	0.319	0.025
7	7000.000	1	0	0.000	8.043	107.043	1048.749	3.614	0.270	0.025
8	6000.000	1	0	0.000	8.323	106.823	885.048	2.902	0.214	0.025
9	5000.000	10	1	4.000	8.706	106.706	711.910	2.186	0.158	0.025
10	4995.000	10	0	0.000	7.972	105.972	711.910	2.484	0.186	0.025
11	4990.000	4	0	0.000	7.972	105.972	711.221	2.482	0.186	0.025

DT= 0.0100 HRS T= 1.0000 HRS ITER= 0

I	X (MI)	IC	IG	HHG (FT)	DEP(FT),	YU (FT MSL)	QU (CFS)	VU (FT/SEC)	FR NO	MANN. N
[illegible]	[illegible]0.000	2	0	0.000	11.132	111.132	2199.999	4.676	0.305	0.025
2	8000.000	1	0	0.000	11.278	110.778	2078.952	4.332	0.281	0.025
3	7000.000	1	0	0.000	11.491	110.491	1951.901	3.952	0.254	0.025
4	6000.000	1	0	0.000	11.768	110.268	1819.115	3.550	0.226	0.025
5	5000.000	4	0	0.000	12.100	110.100	1681.135	3.143	0.198	0.025
12	4990.000	4	0	0.000	11.699	109.699	3032.510	5.973	0.382	0.025
13	4000.000	1	0	0.000	11.579	109.079	2892.742	5.789	0.372	0.025
14	3000.000	1	0	0.000	11.507	108.507	2741.665	5.540	0.357	0.025
15	2000.000	1	0	0.000	11.507	108.007	2579.454	5.211	0.335	0.025
16	1000.000	1	0	0.000	11.595	107.595	2405.074	4.802	0.308	0.025
17	0.000	3	0	0.000	11.773	107.273	2219.451	4.329	0.276	0.025
6	8000.000	2	0	0.000	13.742	113.242	2199.999	3.371	0.201	0.025
7	7000.000	1	0	0.000	14.163	113.163	1927.443	2.816	0.166	0.025
8	6000.000	1	0	0.000	14.620	113.120	1644.387	2.284	0.133	0.025
9	5000.000	10	1	4.000	15.101	113.101	1352.085	1.784	0.102	0.025
10	4995.000	10	0	0.000	12.156	110.156	1352.085	2.510	0.158	0.025
11	4990.000	4	0	0.000	12.156	110.156	1351.375	2.509	0.158	0.025

DT= 0.0100 HRS T= 1.5000 HRS ITER= 0

I	X (MI)	IC	IG	HHG (FT)	DEP(FT),	YU (FT MSL)	QU (CFS)	VU (FT/SEC)	FR NO	MANN. N
1	9000.000	2	0	0.000	13.064	113.064	2200.000	3.651	0.223	0.025
[illegible]	[illegible]0.000	1	0	0.000	13.394	112.894	2141.275	3.417	0.206	0.025
[illegible]	[illegible]0.000	1	0	0.000	13.753	112.753	2078.859	3.182	0.190	0.025
4	6000.000	1	0	0.000	14.136	112.636	2013.188	2.950	0.174	0.025
5	5000.000	4	0	0.000	14.540	112.540	1944.684	2.725	0.159	0.025
12	4990.000	4	0	0.000	14.215	112.215	3665.872	5.325	0.314	0.025
13	4000.000	1	0	0.000	14.341	111.841	3593.330	5.147	0.302	0.025
14	3000.000	1	0	0.000	14.497	111.497	3515.276	4.949	0.289	0.025
15	2000.000	1	0	0.000	14.688	111.188	3433.021	4.734	0.275	0.025

16	1000.000	1	0	0.000	14.915	110.915	3347.191	4.504	0.260	0.025
17	0.000	3	0	0.000	15.175	110.675	3258.362	4.264	0.244	0.025
6	8000.000	2	0	0.000	18.064	117.564	2200.000	2.170	0.115	0.025
7	7000.000	1	0	0.000	18.540	117.540	2043.703	1.931	0.102	0.025
8	6000.000	1	0	0.000	19.023	117.523	1884.127	1.706	0.089	0.025
9	5000.000	10	1	4.000	19.510	117.510	1721.534	1.495	0.077	0.025
10	4995.000	10	0	0.000	14.566	112.566	1721.534	2.406	0.140	0.025
11	4990.000	4	0	0.000	14.566	112.566	1721.188	2.405	0.140	0.025

DT= 0.0100 HRS T= 2.0000 HRS ITER= 0

I	X (MI)	IC	IG	HHG (FT)	DEP(FT),	YU (FT MSL)	QU (CFS)	VU (FT/SEC)	FR NO	MANN. N
1	9000.000	2	0	0.000	14.118	114.118	2200.000	3.231	0.191	0.025
2	8000.000	1	0	0.000	14.491	113.991	2166.444	3.052	0.178	0.025
3	7000.000	1	0	0.000	14.882	113.882	2131.244	2.878	0.166	0.025
4	6000.000	1	0	0.000	15.289	113.789	2094.567	2.709	0.155	0.025
5	5000.000	4	0	0.000	15.710	113.710	2056.542	2.546	0.144	0.025
12	4990.000	4	0	0.000	15.415	113.415	3951.509	5.043	0.287	0.025
13	4000.000	1	0	0.000	15.605	113.105	3911.876	4.895	0.277	0.025
14	3000.000	1	0	0.000	15.816	112.816	3869.761	4.739	0.267	0.025
15	2000.000	1	0	0.000	16.052	112.552	3825.736	4.574	0.256	0.025
16	1000.000	1	0	0.000	16.313	112.313	3780.001	4.403	0.245	0.025
17	0.000	3	0	0.000	16.598	112.098	3732.739	4.227	0.233	0.025
6	8000.000	2	0	0.000	20.363	119.863	2200.000	1.779	0.090	0.025
7	7000.000	1	0	0.000	20.846	119.846	2100.391	1.633	0.082	0.025
8	6000.000	1	0	0.000	21.332	119.832	1998.746	1.495	0.074	0.025
9	5000.000	10	1	4.000	21.820	119.820	1895.159	1.365	0.067	0.025
10	4995.000	10	0	0.000	15.725	113.725	1895.159	2.342	0.132	0.025
11	4990.000	4	0	0.000	15.725	113.725	1894.967	2.342	0.132	0.025

DT= 0.0100 HRS T= 2.5000 HRS ITER= 0

I	X (MI)	IC	IG	HHG (FT)	DEP(FT),	YU (FT MSL)	QU (CFS)	VU (FT/SEC)	FR NO	MANN. N
1	9000.000	2	0	0.000	14.709	114.709	2200.000	3.027	0.176	0.025
2	8000.000	1	0	0.000	15.100	114.600	2179.840	2.876	0.165	0.025
3	7000.000	1	0	0.000	15.505	114.505	2158.801	2.729	0.155	0.025
4	6000.000	1	0	0.000	15.923	114.423	2136.937	2.589	0.145	0.025
5	5000.000	4	0	0.000	16.351	114.351	2114.325	2.454	0.136	0.025
12	4990.000	4	0	0.000	16.070	114.070	4113.161	4.909	0.274	0.025
13	4000.000	1	0	0.000	16.287	113.787	4089.713	4.776	0.265	0.025
14	3000.000	1	0	0.000	16.523	113.523	4064.910	4.638	0.256	0.025
15	2000.000	1	0	0.000	16.779	113.279	4039.071	4.495	0.247	0.025
16	1000.000	1	0	0.000	17.057	113.057	4012.288	4.347	0.237	0.025
17	0.000	3	0	0.000	17.354	112.854	3984.636	4.197	0.227	0.025
6	8000.000	2	0	0.000	21.753	121.253	2200.000	1.593	0.078	0.025
7	7000.000	1	0	0.000	22.238	121.238	2134.235	1.488	0.072	0.025
8	6000.000	1	0	0.000	22.726	121.226	2067.216	1.390	0.067	0.025
9	5000.000	10	1	4.000	23.215	121.215	1998.950	1.296	0.062	0.025
10	4995.000	10	0	0.000	16.361	114.361	1998.950	2.317	0.129	0.025
11	4990.000	4	0	0.000	16.361	114.361	1998.836	2.317	0.129	0.025

DT= 0.0100 HRS T= 3.0000 HRS ITER= 0

I	X (MI)	IC	IG	HHG (FT)	DEP(FT),	YU (FT MSL)	QU (CFS)	VU (FT/SEC)	FR NO	MANN. N
[illegible]	[illegible]00.000	2	0	0.000	15.064	115.064	2200.000	2.913	0.167	0.025
[illegible]	[illegible]00.000	1	0	0.000	15.464	114.964	2187.387	2.777	0.158	0.025
3	7000.000	1	0	0.000	15.876	114.876	2174.234	2.646	0.149	0.025
4	6000.000	1	0	0.000	16.299	114.799	2160.595	2.520	0.140	0.025
5	5000.000	4	0	0.000	16.732	114.732	2146.501	2.400	0.132	0.025
12	4990.000	4	0	0.000	16.458	114.458	4211.460	4.836	0.268	0.025
13	4000.000	1	0	0.000	16.689	114.189	4196.896	4.711	0.259	0.025
14	3000.000	1	0	0.000	16.938	113.938	4181.540	4.582	0.250	0.025
15	2000.000	1	0	0.000	17.205	113.705	4165.565	4.450	0.242	0.025
16	1000.000	1	0	0.000	17.492	113.492	4149.011	4.314	0.233	0.025
17	0.000	3	0	0.000	17.796	113.296	4131.942	4.177	0.223	0.025
6	8000.000	2	0	0.000	22.641	122.141	2200.000	1.488	0.072	0.025
7	7000.000	1	0	0.000	23.127	122.127	2155.820	1.407	0.067	0.025
8	6000.000	1	0	0.000	23.615	122.115	2110.824	1.330	0.063	0.025
9	5000.000	10	1	4.000	24.105	122.105	2065.030	1.256	0.059	0.025
10	4995.000	10	0	0.000	16.739	114.739	2065.030	2.307	0.127	0.025
11	4990.000	4	0	0.000	16.739	114.739	2064.960	2.307	0.127	0.025

DT= 0.0100 HRS T= 3.5000 HRS ITER= 0

I	X (MI)	IC	IG	HHG (FT)	DEP(FT),	YU (FT MSL)	QU (CFS)	VU (FT/SEC)	FR NO	MANN. N
1	9000.000	2	0	0.000	12.685	112.685	200.011	0.348	0.021	0.025
[illegible]	[illegible]000.000	1	0	0.000	13.229	112.729	374.464	0.609	0.037	0.025
[illegible]	[illegible]00.000	1	0	0.000	13.757	112.757	550.114	0.842	0.050	0.025
4	6000.000	1	0	0.000	14.271	112.771	727.542	1.050	0.062	0.025
5	5000.000	4	0	0.000	14.771	112.771	907.447	1.240	0.072	0.025
12	4990.000	4	0	0.000	14.585	112.585	2632.510	3.671	0.214	0.025
13	4000.000	1	0	0.000	14.894	112.394	2805.219	3.783	0.218	0.025
14	3000.000	1	0	0.000	15.187	112.187	2980.443	3.896	0.223	0.025
15	2000.000	1	0	0.000	15.467	111.967	3158.005	4.009	0.228	0.025
16	1000.000	1	0	0.000	15.732	111.732	3339.590	4.125	0.233	0.025
17	0.000	3	0	0.000	15.981	111.481	3527.067	4.247	0.238	0.025
6	8000.000	2	0	0.000	18.198	117.698	200.011	0.195	0.010	0.025
7	7000.000	1	0	0.000	18.713	117.713	699.831	0.651	0.034	0.025
8	6000.000	1	0	0.000	19.205	117.705	1207.142	1.076	0.056	0.025
9	5000.000	10	1	4.000	19.669	117.669	1724.150	1.477	0.076	0.025
10	4995.000	10	0	0.000	14.708	112.708	1724.150	2.372	0.138	0.025
11	4990.000	4	0	0.000	14.707	112.707	1725.063	2.374	0.138	0.025

DT= 0.0100 HRS T= 4.0000 HRS ITER= 0

I	X (MI)	IC	IG	HHG (FT)	DEP(FT),	YU (FT MSL)	QU (CFS)	VU (FT/SEC)	FR NO	MANN. N
1	9000.000	2	0	0.000	9.055	109.055	200.000	0.580	0.041	0.025
2	8000.000	1	0	0.000	9.530	109.030	315.092	0.846	0.059	0.025
3	7000.000	1	0	0.000	9.993	108.993	435.418	1.090	0.074	0.025
[illegible]	[illegible]000.000	1	0	0.000	10.444	108.944	561.134	1.314	0.088	0.025
[illegible]	[illegible]00.000	4	0	0.000	10.885	108.885	692.209	1.523	0.100	0.025
12	4990.000	4	0	0.000	10.749	108.749	1484.548	3.328	0.220	0.025
13	4000.000	1	0	0.000	10.996	108.496	1616.541	3.501	0.230	0.025
14	3000.000	1	0	0.000	11.218	108.218	1754.442	3.686	0.240	0.025
15	2000.000	1	0	0.000	11.414	107.914	1897.345	3.881	0.251	0.025
16	1000.000	1	0	0.000	11.580	107.580	2046.220	4.094	0.263	0.025
17	0.000	3	0	0.000	11.708	107.208	2202.259	4.332	0.277	0.025

6	8000.000	2	0	0.000	10.442	109.942	200.000	0.469	0.031	0.025
7	7000.000	1	0	0.000	10.920	109.920	390.897	0.856	0.056	0.025
8	6000.000	1	0	0.000	11.386	109.886	588.232	1.208	0.078	0.025
9	5000.000	10	1	4.000	11.839	109.839	791.683	1.531	0.097	0.025
10	4995.000	10	0	0.000	10.874	108.874	791.683	1.744	0.115	0.025
11	4990.000	4	0	0.000	10.873	108.873	792.339	1.746	0.115	0.025

TOTAL ITERATIONS FOR EACH OF 1 RIVERS.
2

PROGRAM COMPLETED.
EXIT
EXECUTION COMPLETED O.K.
$

CHANNEL NETWORKS

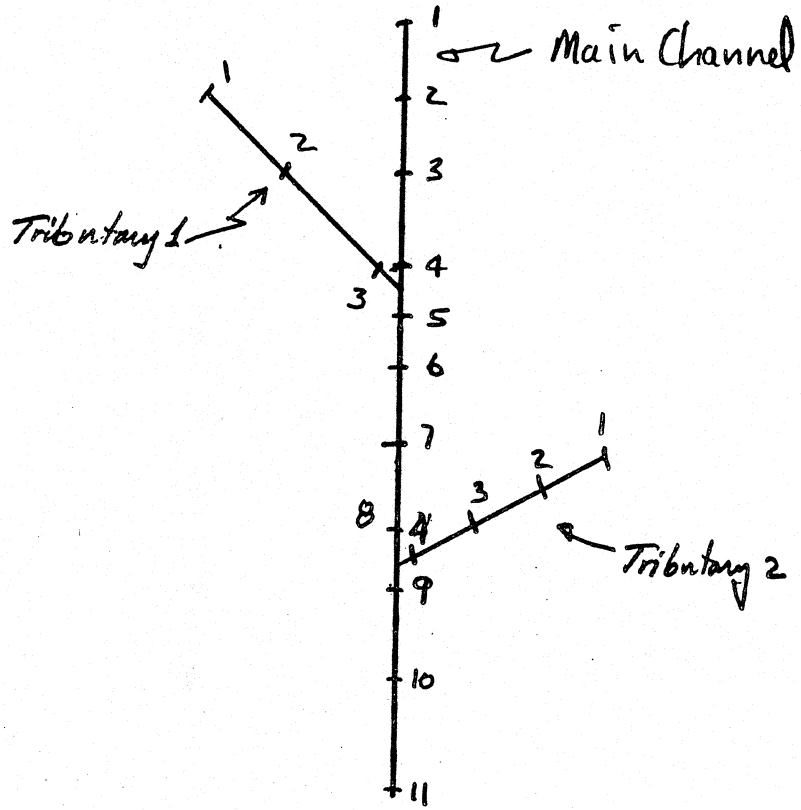

DWOPER Numbering Scheme

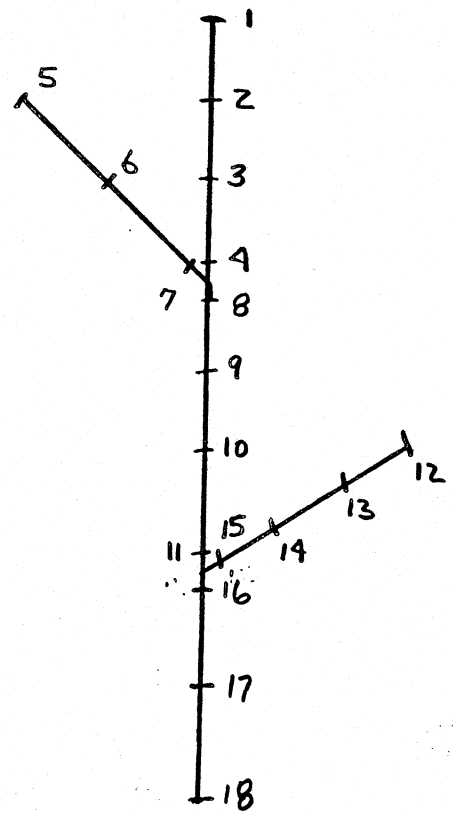

NETWORK (Channel Network Option) Number Scheme

Figure 4.2 Station Numbering Scheme for DWOPER and NETWORK

CHANNEL NETWORKS

RELAXATION METHOD

- Dendritic (tree-type)
- 1st order tributaries
- Relaxation solves S.U. eqs. for main channel, then for each trib.
- Tributary flow at each confluence with the main channel is treated as lateral inflow. (q)
- Procedure is repeated iteratively

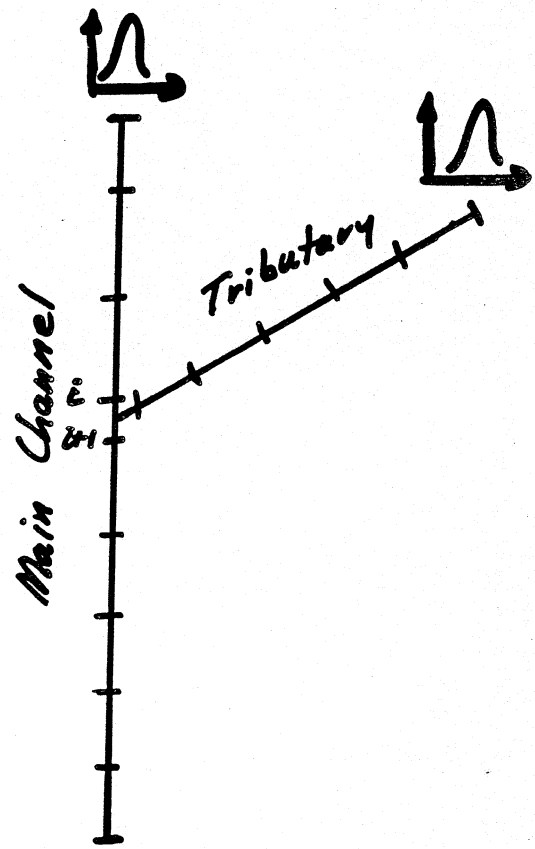

$$q^* = \alpha q + (1-\alpha) q^{**}$$

α = weighting factor ($0.6 \le \alpha \le 0.8$)

q = computed tributary flow at each confluence

q^{**} = previous estimate of q

q^* = new estimate of q.

Convergence $\quad |q - q^{**}| < \epsilon_Q$

NETWORK ALGORITHM

- Second & higher order tributaries
- Bifurcations around islands with either zero, one, or two bypasses through the island.
- Dendritic branches joining any portion of the bifurcated branches
- Dendritic network associated with river delta formations.

- Algorithm based on the treatment of the channel junctions (confluences, bifurcations) as internal boundary conditions.

Internal boundary equations.

$$Q_i^{i+1} + Q_{i'}^{i+1} - Q_{i'+1}^{i+1} - \frac{\Delta s}{\Delta t}^{i} = 0$$

$$2g\left(h_i^{i+1} - h_{i'+1}^{i+1}\right) + \left(Q^2/A\right)_i^{i+1} - \tau\left(Q^2/A^2\right)_{i'+1}^{i+1} = 0$$

$$2g\left(h_{i'}^{i+1} - h_{i'+1}^{i+1}\right) + \left(Q^2/A^2\right)_{i'}^{i+1} - \tau\left(Q^2/A^2\right)_{i'+1}^{i+1} = 0$$

$i' = i+m+1$

$\tau = 1 + C_m + C_f$

$C_m = \left(0.1 + 0.83\, Q_{i'}^{i} / Q_{i'+1}^{i}\right)\left(w_t/q_0\right)^{\mu}$

$C_f = 2g\, \Delta x_i\, \bar{n}^2 / \left[2.21\, (\bar{\delta}^{4/3})^{i}\right]$

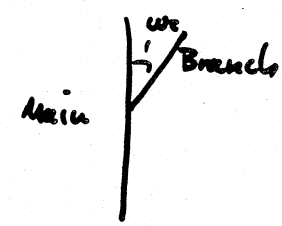

C_m & C_f related to headloss due to mixing.

NODE CODE (JCOD(K), K=1,N)

1 Internal Node

2 Upstream Boundary

3 Downstream Boundary

4 Tributary Junction

5 Tributary Junction on a Bifurcation

6 Upstream Bifurcation Junction

7 Downstream Bifurcation Junction

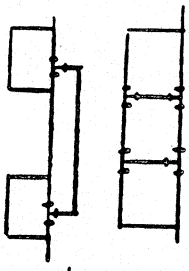

8 Double Bifurcation Junction on a Bifurcation

9 Single Bifurcation Junction on a Bifurcation

10 Gate Internal Boundary

11 Critical Flow Internal Boundary

NODE NUMBERING SCHEME

Example No. 1:

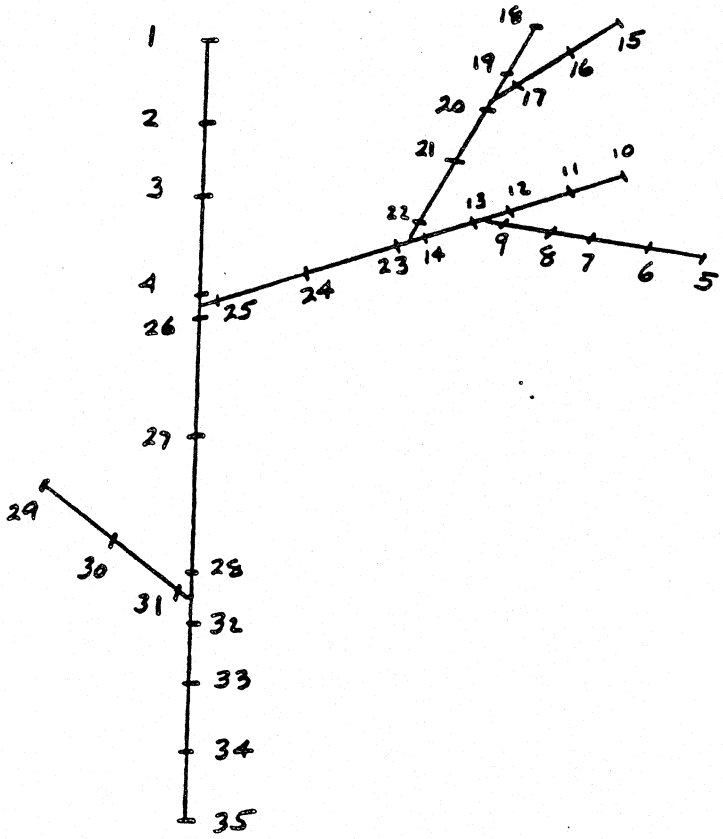

Junction No.	Upstream Node	Tributary Node	Downstream Node
1	4	25	26
2	9	12	13
3	14	22	23
4	17	19	20
5	28	31	32

NODE NUMBER SCHEME

Example No. 2:

Junct. No.	Up. Node	Trib. Node	Down. Node
1	3	5	6
2	7	8	12
3	14	11	15
4	17	18	21
5	41	20	42
6	23	38	39
7	26	28	29
8	31	34	35
9	43	44	49
10	46	52	47
11	54	48	55
12	50	51	53
13	56	57	60
14	63	59	64
15	65	66	68
16	71	67	75
17	61	72	62
18	69	74	70
19	78	82	83
20	84	89	90

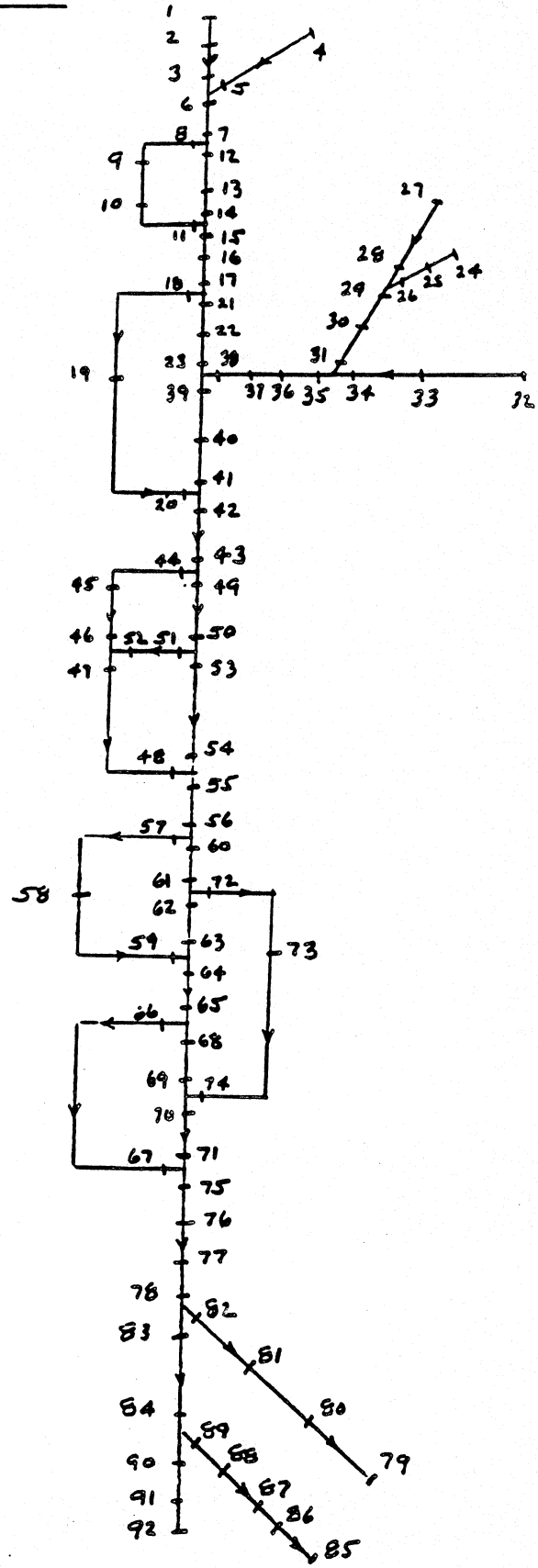

NODE NUMBERING SCHEME

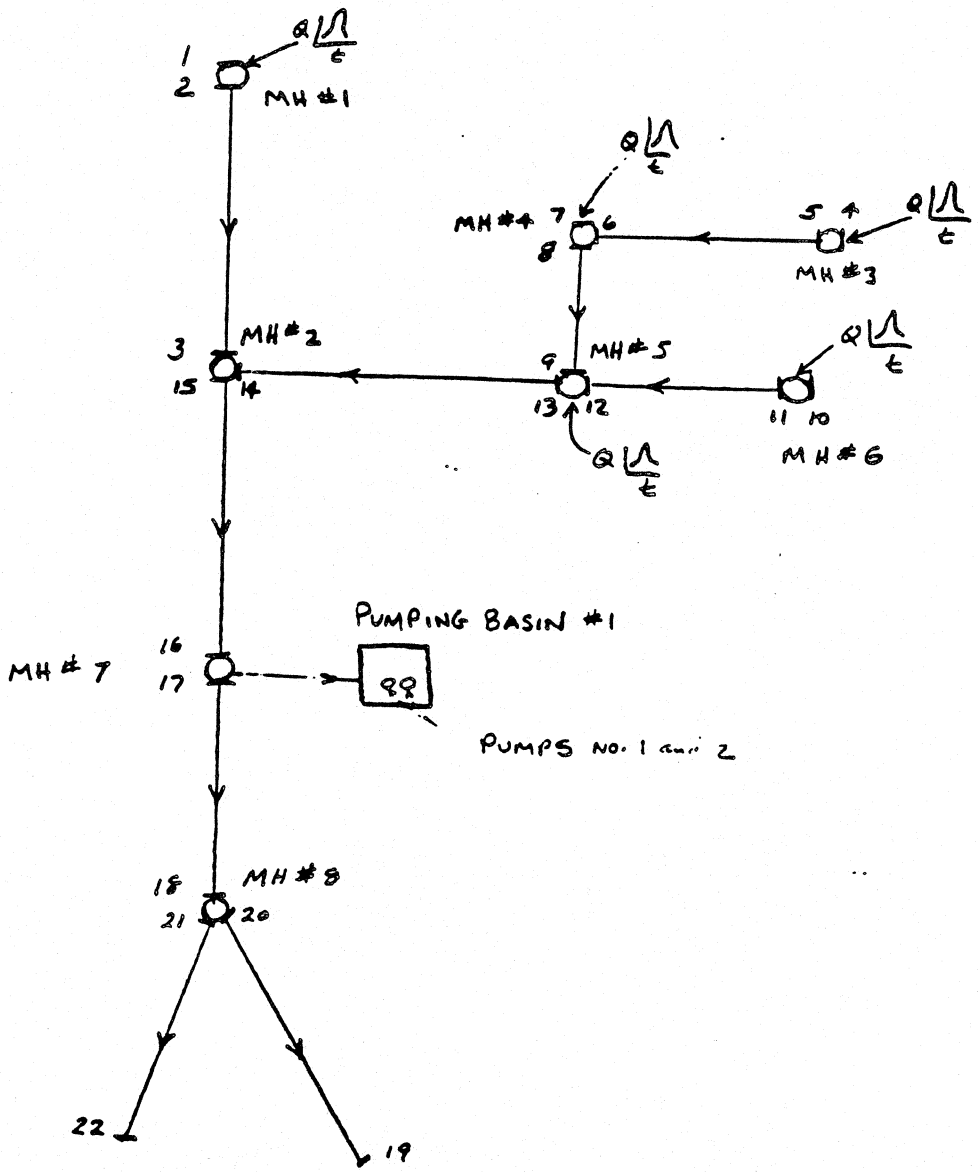

APPPENDIX B

ADDITIONAL INPUT DATA FOR "NETWORK, Critical Flow and Time-Dependent Gate" OPTIONS in DWOPER

Card input No.	Data Description - Input Format
(1)	K1,K2,K3,K4,K5,K6,K7,K8,K9,K10,K11,K12,K13,K14,K17,K18 - 16I5
	K17 — Total number of upstream boundaries in the system.
	K18 — Total number of junctions in the system.
(1A)	K21,K22 - 2I5 format
	K21 — Maximum number of gates in the system.
	K22 — Maximum number of values in the gate coefficient table.
(3)	EPSY,EPSQ,EPSQJ,THETA,F1,XFACT,DHF,CFNAME - 7F10.2,4X,A4
	CFNAME — If = IMET, the metric option is used. With this option, HGC on card no. 46C and HG on card no. 46D are input in metric; and all output data is printed in metric units.
(4)	JN,NU,NCT,ICD,NYQD,ITMAX,NCML,NET - 8I10
	NET — Parameter indicating if Channel Network option is to be used. If NET=0, this option is not used; if NET≥1, this option is to be used and JN should be set equal to 1. If NET=1, junction losses due to mixing and friction are neglected. These are included if NET=2.
(8A)	NG(J) - 8I10 Format
	NG(J) — Number of gates and/or critical flow sections in J^{th} river, J index goes from 1 to JN.

If NET≥1 (see card input no. 4), read in JCOD(K).

(11A)	JCOD(K) - 8I10 Format

(11A) JCOD(K) Code denoting the type node at each cross-section. JCOD(K) can have values of 1,2,3,...,11. K index goes from 1 to NB(J) (See Card 11).

If NET≥1 (see card input no. 4), read in JTN, NUPB

(11B) JTN,NUPB - 2I10 Format

JTN Total number of junctions in the system.
NUPB Total number of upstream boundaries in the system.

If NET≥1 (see card input no. 4), read in JU(K), JB(K), JL(K).

See not following card 11C

(11C) JU(K), JB(K), JL(K) - 3I10 Format

JU(K) Sequence number of cross-section at entry to junction.

JB(K) Sequence number of cross-section at brance of junction.

JL(K) Sequence number of cross-section at exit of junction.

Note: Repeat card 11C for each junction.

If NET ≥1 (see card input no. 4) read in KMU(K).

(11D) KMU(K) - 8 I 10 Format

KMU(K) Parameter indicating the type of upstream boundary condition: if KMU(K)=1, a stage hydrograph is the boundary condition; if KMU(K)=2, a stage hydrograph is the boundary condition; or if KMU(K)=4, a depth-discharge relation is the boundary condition. K index goes from 1 to NUPB.

(11E) JCPR(K) - 8 I 10 Format

JCPR(K) Parameter indicating sequential order that cross sections will be listed in output, K index goes from 1 to NB(J).

If NG(J)>0 (see card input no. 8A) read in LGX(K,J), IGT(K,J), NTG(I,K), HGC(K,J).

See note following card 51D

(51A) LGX(K,J), IGT(K,J), NTG(K,J), HGC(K,J) - 3I10, F10.2 Format

LGX(K,J)	Sequence number of cross section immediately upstream of gate internal boundary.
IGT(K,J)	Parameter indicating the type of gate: if IGT(K,J)=1, the gate has a continuous bottom slope; if IGT(K,J)=2, the gate has a discontinuous bottom slope; if IGT(K,J)=0, the location is a critical flow section.
NTG(K,J)	Number of values in the table of gate coefficient (GC) vs. tailwater head (DTW).
HGC(K,J)	Gate correction parameter used to correct the height of the gate opening.

If NG(J)>0 (see input no. 8A) read in GC(I,K,J).

See note following card 51D

(51B) GC(I,K,J) - 8F10.2 Format

GC(I,K,J)	Gate discharge coefficient; coefficient is determined by multiplying the width of the gate by the loss factor; I index goes from 1 to NTG(K,J).

If NG(J)>0 (see card input no. 8A) read in DTW(I,K,J).

See note following card 51D

(51C) DTW(I,K,J) - 8F10.2 Format

DTW(I,K,J)	Tailwater head (tailwater elevation - gate bottom elevation) corresponding to each gate discharge coefficient; I index goes from 1 to NTG(K,J)

If NG(J)>0 (see card input no. 8A) read in HG(I,K,J).

See note following card 51D

(51D) HG(I,K,J) - 8F10.2 Format

HG(I,K,J)	Height of gate opening; I index goes from 1 to NU.

<u>Note</u>: Omit card sequence 51B, 51C, and 51D if IGT(K,J) = 0.

<u>Note</u>: Repeat card sequence 51A, 51B, 51C, and 51D once for each K,

K=1,NG(J), and repeat this procedure for each river as J goes from 1 to JN.

(54A) NR - I10

NR - Number of separate channels or branches or storm sewers in the system.

(54B) NIRB(K) - 8I10

NIRB(K) Number of nodes in each channel or branch; K index goes from 1 to NR; most upstream branch is first with next most upstream branch following until the most downstream branch is entered, then the number of nodes along the main (principal) channel or sewer is entered.

(54C) IRB(I,K) - 8I10

IRB(I,K) Sequential number of node in each branch; node numbers commence at upstream end of each branch and proceed in the downstream direction until the last node of the branch is reached; I index goes from 1 to NIRB(K).

Note: Repeat card 54C as the K index goes from 1 to NR; branches are ordered from upstream to downstream and last entry is the main (principal) channel or storm sewer.

Note: Cards 54A,B,C are omitted if NET = 0, or QDI(2,1) not equal to zero and NET > 1.

NODE CODE (JCOD(K), K=1,N)

1 Internal Node

2 Upstream Boundary

3 Downstream Boundary

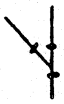

4 Tributary Junction

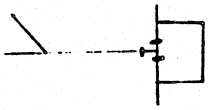

5 Tributary Junction on a Bifurcation

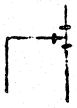

6 Upstream Bifurcation Junction

7 Downstream Bifurcation Junction

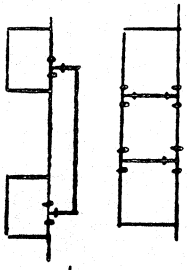

8 Double Bifurcation Junction on a Bifurcation

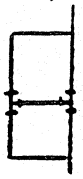

9 Single Bifurcation Junction on a Bifurcation

10 Gate Internal Boundary

11 Critical Flow Internal Boundary

NODE NUMBERING SCHEME

Example No. 1:

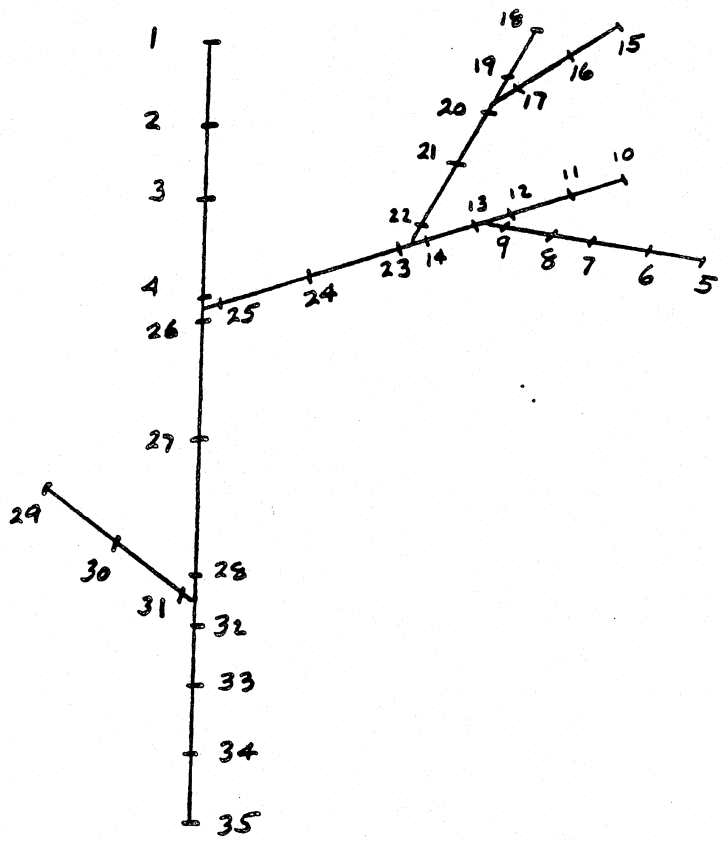

Junction No.	Upstream Node	Tributary Node	Downstream Node
1	4	25	26
2	9	12	13
3	14	22	23
4	17	19	20
5	28	31	32

NODE NUMBER SCHEME

Example No. 2:

Junct. No.	Up. Node	Trib. Node	Down. Node
1	3	5	6
2	7	8	12
3	14	11	15
4	17	18	21
5	41	20	42
6	23	38	39
7	26	28	29
8	31	34	35
9	43	44	49
10	46	52	47
11	54	48	55
12	50	51	53
13	56	57	60
14	63	59	64
15	65	66	68
16	71	67	75
17	61	72	62
18	69	74	70
19	78	82	83
20	84	89	90

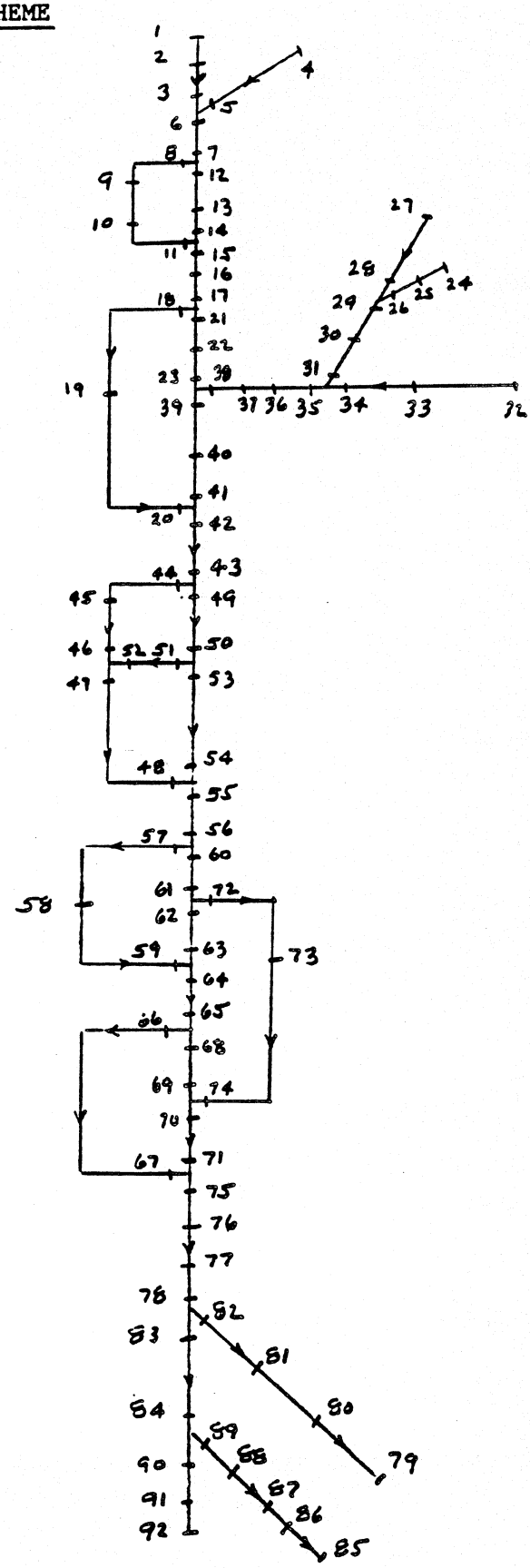

DYNAMIC WAVE MODEL FOR MIXED FLOWS IN STORM SEWER NETWORKS

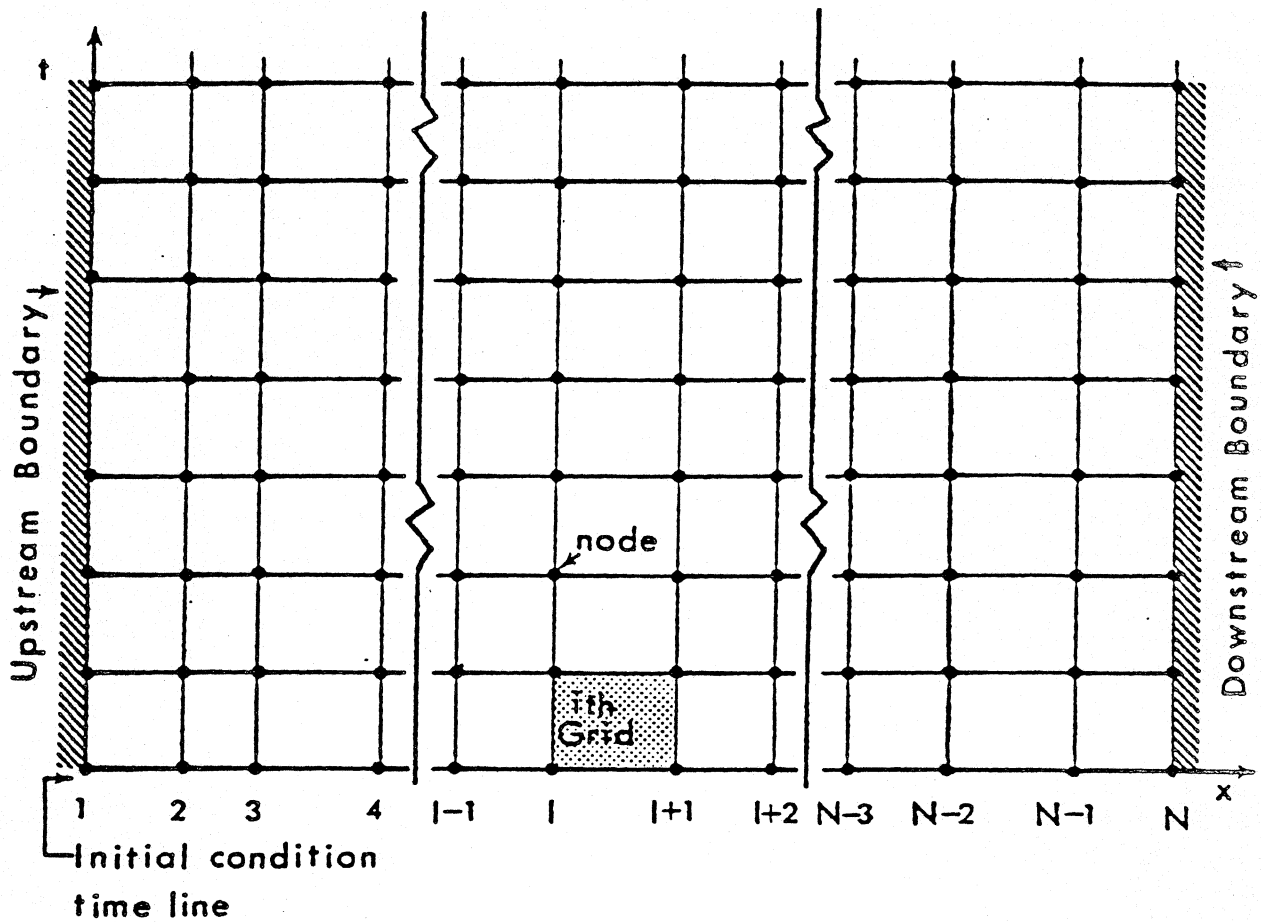

Fig. 4.4.--x-t solution plane showing time lines, nodes, grids, upstream and downstream boundaries, and initial condition time line.

$$\Theta\left(Q_{i+1}^{j+1} - Q_i^{j+1} - \bar{q}_i^{j+1}\,\Delta x_i\right) + (1-\Theta)\left(Q_{i+1}^{j} - Q_i^{j} - \bar{q}_i^{j}\,\Delta x_i\right)$$

$$+ 0.5\,\Delta x_i/\Delta t^j\left[\left(A + A_o\right)_i^{j+1} + \left(A + A_o\right)_{i+1}^{j+1} - \left(A + A_o\right)_i^{j}\right.$$

$$\left. - \left(A + A_o\right)_{i+1}^{j}\right] = 0$$

$$0.5\,\Delta x_i/\Delta t^j\left(Q_{i+1}^{j+1} + Q_i^{j+1} - Q_i^{j} - Q_{i+1}^{j}\right) + \Theta\left[\left(Q^2/A\right)_{i+1}^{j+1}\right.$$

$$- \left(Q^2/A\right)_i^{j+1} + g\,\bar{A}_i^{j+1}\left(h_{i+1}^{j+1} - h_i^{j+1} + \Delta x_i\,\bar{S}_{f_i}^{j+1} + \Delta x_i\,\bar{S}_{e_i}^{j+1}\right)$$

$$\left. + \Delta x_i\left(L + \bar{W}_f\bar{B}\right)_i^{j+1}\right] + (1-\Theta)\left[\left(Q^2/A\right)_{i+1}^{j} - \left(Q^2/A\right)_i^{j} + g\bar{A}_i^{j}\right.$$

$$\left.\left(h_{i+1}^{j} - h_i^{j} + \Delta x_i\,\bar{S}_{f_i}^{j} + \Delta x_i\,\bar{S}_{e_i}^{j}\right) + \Delta x_i\left(L + \bar{W}_f\bar{B}\right)_i^{j}\right] = 0$$

where: $\bar{A}_i = 0.5\,(A_i + A_{i+1})$

$$\bar{B}_i = 0.5\,(B_i + B_{i+1})$$

$$\bar{S}_{f_i} = \frac{\bar{n}_i^{\,2}\,|\bar{Q}_i|\,\bar{Q}_i}{2.21\,\bar{A}_i^{\,2}\,R_i^{\,4/3}} = |\bar{Q}_i|\,\bar{Q}_i/\bar{K}_{c_i}^2$$

$$\bar{Q}_i = 0.5\,(Q_i + Q_{i+1})$$

$$R_i = \bar{A}_i/\bar{B}_i$$

$$\bar{K}_{c_i} = 0.5\,(K_{c_i} + K_{c_{i+1}})$$

$$\bar{S}_{e_i} = K_{e_i}\left[\left(Q/A\right)_{i+1}^2 - \left(Q/A\right)_i^2\right]/\left(2g\Delta x_i\right)$$

$$\bar{W}_{f_i} = C_{w_i}\,|\bar{V}_{r_i}|\,\bar{V}_{r_i}$$

$$\bar{V}_{r_i} = \bar{Q}_i/\bar{A}_i - \bar{V}_{w_i}\cos\omega$$

Conduit Geometry (NETWORK)

Circular

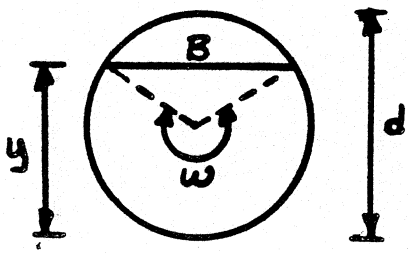

$$\omega = \pi + 2\sin^{-1}[(y-r)/r] \qquad y < d$$

ω = central angle (rad.)

Wetted perimeter

$$P = r\omega$$

Cross-sectional area of flow

$$A = 0.125\, d^2(\omega - \sin\omega) \qquad y < d$$

$$A = 0.25\,\pi d^2 \qquad y \geq d$$

$$B = d\sin(0.5\omega) \qquad y < d$$

$$B = b \quad \text{(slot width)} \qquad y \geq d$$

$$\frac{dP}{dy} = \frac{2}{\sqrt{1 - [(y-r)/r]^2}} \qquad y < d$$

$$\frac{dP}{dy} = 0 \qquad y \geq d$$

Arbitrary

Input table of conduit widths as a function of depth (B_k, Y_k), $k = 1, 2, \ldots, N_s$

$$P_k = P_{k-1} + 2\sqrt{(\Delta B_k)^2 + (\Delta Y_k)^2}$$

$$\Delta B_k = (B_k - B_{k-1})/2$$

$$\Delta Y_k = Y_k - Y_{k-1}$$

$$A_k = \sum_{l=1}^{k} 0.5\,(B_l + B_{l+1})(Y_l - Y_{l-1})$$

Arbitrary Shapes

$$B = B_k + (B_{k+1} - B_k)(y - Y_k) / (Y_{k+1} - Y_k)$$

$$P = P_k + (P_{k+1} - P_k)(y - Y_k) / (Y_{k+1} - Y_k)$$

$$A = A_k + 0.5(B + B_k)(y - Y_k)$$

$$Y_k \leq y \leq Y_{k+1}$$

Off-line Detention & Pumping Basins

Drop Inlets

Modeling Pressurized Flow

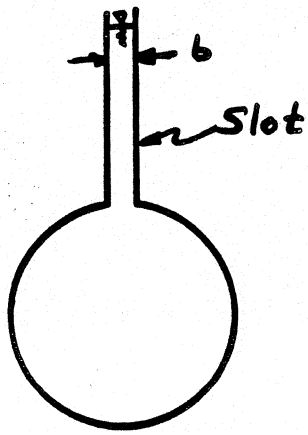

Fictitious Slot (Preissman Slot)
(chimney)

Purpose of the slot is to provide a cross-sectional area whose top width (b) is very small for all flow depths greater than the top of the conduit.

Small top width produces the proper celerity for pressurized flow as computed from the gravity wave celerity equation.

$$c = \sqrt{gA/B}$$

$$\Downarrow$$

$$b = B$$

$$c = a$$

$$\Downarrow$$

$$b = 0.25\, g\pi \left(\frac{d}{a}\right)^2 \quad \text{(required slot width)}$$

a = pressure wave celerity
(include effects of entrained air)

Slot permits a continuous transition from free surface flow to pressurized flow from one calculation section to another. For numerical reasons the transition zone between the sewer crest and the slot has been given a smooth form.

INTERNAL BOUNDARIES

MANHOLES

JUNCTIONS

DROP INLETS

CONNECTIONS TO OFFLINE DETENTION AND/OR PUMPING STATIONS.

Two equations required for each. B.C.

<u>MANHOLES</u>

$$Q_i^{i+1} + m\, Q_{i'}^{i+1} - Q_{i'+1}^{i+1} + Q_{in} - Q_w - \Delta S/\Delta t = 0$$

$\Delta S/\Delta t$ = change of storage in manhole over Δt

Q_i = inflow to manhole from upstream conduit

$Q_{i'}$ = inflow from the branch conduit, $m=1$ ($m=0$ if no branch conduit)

$Q_{i'+1}$ = outflow from the manhole through the exiting downstream conduit

Q_{in} = surface inflow to manhole ($= f(\text{time})$)

Q_w = weir flow (entering or leaving manhole via weir)

Manholes (cont'd)

$$h_i^{i+1} - h_{i'+1}^{i+1} - h_{\ell_i} = 0$$

$$h_{i'}^{i+1} - h_{i'+1}^{i+1} - h_{\ell_{i'}} = 0$$

h_i = water surface elevation of upstream conduit
$h_{i'}$ = " " " " branch "
$h_{i'+1}$ = " " " " downstream "

h_{ℓ_i} = headlosses incurred by incoming flows

$h_{\ell_{i'}}$ = " " " " exiting flows

Weir flow

$$Q_w = C \cdot C_s \, (\bar{h} - h_w)^{3/2}$$

$C \rightarrow 3.2 L_w$

$C_s \rightarrow (1 - h_r^2)^{1/2}$

Change in manhole storage

$$\Delta S = 0.25 \pi \, d_m^2 \, (\bar{h} - \bar{h}') \qquad \bar{h} < h_m \text{ (top of MH)}$$

Junction Losses

$$h_{\ell_i} = \left[(V_i^i)^2 + 0.5 (V_{i'+1}^i)^2 \right] / 2g$$

$$h_{\ell_{i'}} = \left[(V_{i'}^i)^2 + 0.5 (V_{i'+1}^i)^2 \right] / 2g$$

OFF-LINE DETENTION STORAGE & PUMPING BASINS

Water is removed from storm sewer system via the Q_w in

$$Q_i^{i+1} + m\,Q_{i'}^{i+1} - Q_{i'+1}^{i+1} + Q_{in} - Q_w - \Delta S/\Delta t = 0$$

Q_w + or − according to relative values of $\bar{h}$ & h_t (elevation of w.s. in detention basin)

h_t from storage balance of detention basin

$$S^i = S^{i-1} + (Q_w^i - Q_p^i)\,\Delta t_i$$

outflow due to pumping of one or more pumps

Head-discharge rating curve used for each pump.

$$H = h_p - h_t$$

includes friction losses

DROP INLETS

Internal boundary conditions

$$Q_i^{i+1} - Q_{i+1}^{i+1} = 0$$

$$Q_i^{i+1} - \left(\sqrt{g A^3/B}\right)_i^{i+1} = 0 \qquad \text{Critical flow}$$

When submerged, converts to solving the Saint-Venant Equations

APPENDIX C

ADDITIONAL INPUT DATA DESCRIPTION FOR "STORM SEWER" OPTION IN DWOPER

VERSION: 7/18/84

Card input no.	Data Description - Input Format
(5)	NCS, NCSS, NP, KTERM, KPL, KPL2, JNK, NPEND - 8 I·10

NPEND — Sequential number indicating the last value in the computed stage hydrograph that will be used in the statistics needed in the Automatic Calibration option to determine the Manning n. If left blank, all computed values will be used. If (-1) or (-2) is entered, the Storm Sewer option can be used. A value of (-2) indicates the storm sewers are circular pipes. A value of (-1) indicates the storm sewers are of arbitrary shape.

(51E) NMH(J),NQPU(J),NDTB(J),NPM(J) - 4I10

NMH(J) — Number of manholes in storm sewer system.

NQPU(J) — Number of inlet hydrographs in storm sewer system.

NDTB(J) — Number of detention or pumping basins in system.

NPM(J) — Number of pumps in system.

(51F) NXPI(K,J), DMH(K,J),FKV(K,J),PCWR(K,J),PWELV(K,J) - I10,4F10.2

NXPI(K,J) — Sequential number of node (cross-section) which is an entrance to a manhole; if a manhole has two channels entering, use the smallest number to denote this parameter.

DMH(K,J) — Diameter (ft) or equivalent diameter of manhole.

FKV(K,J) — Head loss coefficient for manhole; varies from about 0.10 to 0.35 (see ASCE J. Hydr., Aug 1984, p. 1150-1154, "Head Losses at Sewer Junction Manholes," by J. Marsalek).

PCWR(K,J) — Discharge coefficient for weir flow out of the top of the manhole that is permanently lost from the storm sewer system; varies from 3.1 to 3.3; if the flow out of the top of the manhole

returns thru the manhole to the sewer as the flow levels in the system recede, PCWR (K,J) represents the length (ft) of a square area equivalent to the surface area that temporarily stores the water exiting thru the top of the manhole.

PWELV(K,J) Elevation (ft) of top of manhole.

Note: Repeat card 51 F once for each K, K=1, NMH(J).
Omit card 51F if NMH(J) = 0.

(51G) NXQPU(K,J) - I10

NXQPU(K,J) Sequential number of node (cross-section) where an inlet hydrograph occurs.

(51H) QPU(I,K,J) - 8F10.2

QPU(I,K,J) Inflow (cfs) hydrograph ordinate value for K^{th} inlet hydrograph; I index goes from 1 to NU (See card 4).

Note: Repeat cards 51G and 51H once for each K, K=1, NQPU(J).
Omit cards 51G and 51H if NQPU(J) = 0.

(51I) NXDTB(K,J),PEO(K,J),DBCW(K,J),DBWELV(K,J),DBCO(K,J) - I10, 4F10.2.

NXDTB(K,J) Sequential number of node of inlet to manhole where a connection to a detention or pumping basin is located.

PEO(K,J) Elevation (ft) of water surface in detention or pumping basin at t=0.

DBCW(k,J) Weir discharge coefficient for inlet to detention or pumping basin; DBCW(K,J) = (3.1 to 3.3) x length of weir (ft).

DBWELV(K,J) Elevation (ft) of weir crest.

DBCO(K,J) Orifice discharge coefficient for inlet to detention or pumping basin; DBCO(K,J) = (0.51 to 0.98) x 8.02 x Area of orifice (ft^2).

(51J) PSA(I,K,J) - 8F10.2

PSA(I,K,J) Volume (ft^3) of Kth detention or pumping basin for a specified elevation within the basin; I index goes from 1 to a minimum value of 2 or a maximum value of 8.

(51K) PEL(I,K,J) - 8 F10.2

PEL(I,K,J) Elevation (ft) associated with each corresponding value of PSA(I,K,J); elevations start at the bottom of the basin and proceed upwards; I index goes from 1 to a minimum value of 2 or a maximum value of 8.

Note: Repeat cards 51I, 51J, 51K once for each K, K=1, NDTB(J). Omit cards 51I, 51J, 51K if NBTB(J) = 0.

(51L) NXPO(K,J),NQLP(K,J),PEMN(K,J),PEMX(K,J),PELV(K,J) - 2I10, 3F10.2.

NXPO(K,J) Sequential number of node of inlet to manhole where a connection to a basin with pumps is located.

NQLP(K,J) Parameter indicating if pump has a specified discharge hydrograph (NQLP(K,J) =1) or operates according to a specified head-discharge relation (NQLP(K,J) = 0)

PEMN(K,J) Elevation (ft) of water surface in pumping basin at which pump starts operating.

PEMX(K,J) Elevation (ft) of water surface in pumping basin at which pump stops operating.

PELV(K,J) Elevation (ft) at which pump discharges + approximate head loss thru discharge pipe.

(51M) DHP(I,K,J) - 8F10.2

DHP(I,K,J) Head differential (ft) in head-discharge relation; I index goes from 1 to minimum value of 2 or maximum value of 8; head begins at five and increases.

(51N) OP(I,K,J) - 8F10.2

OP(I,K,J) Pump discharge (cfs) associated with each corresponding (DHP(I,K,J) value.

Note: Omit cards 51M and 51N if NQLP(K,J) = 1.

(51P) QLP(I,K,J) - 8F10.2

QLP(I,K,J) Pump discharge (cfs) hydrograph; I index goes from 1 to NU.

Note: Omit card 51P if NQLP(K,J) = 0.

Note: Repeat cards 51L, 51M and 51N, or 51P once for each K, K=1, NPM(J). Omit cards 51L, 51M and 51N, or 51P if NPM(J) = 0.

Note: Repeat cards 51E thru 51P once for each J, J=1, JN where JN (card 4) is set to a value of 1 when NET(card 4) is either 1 or 2.

Note: Omit cards 51E thru 51P if NPEND > 0.

Note: When the storm sewer option is used and the sewers are circular pipes, only two values are required for the BS(K,I,J) top widths on card 28. The first value is the pipe diameter (ft) and the second value represents the diameter or width (ft) of the fictitious chimney emanating from the top of the sewer pipe. The K index goes from 1 to 2. Thus, the value of NCS (card 5) should be entered as a value of 2 when circular pipes comprise the storm sewer system.

Only one value is required for the HS(K,I,J) elevations (card 29). This value represents the invert (bottom) elevation (ft) of the pipe. The K index goes from 1 to 1.

The AS(1,I,J) values on card 30 are entered as zero's for either circular pipes or arbitrary-shaped sewers. Arbitrary-shaped sewers are described by a sufficient number of BS(K,I,J) values and corresponding HS(K,I,J) elevations.

NODE NUMBERING SCHEME

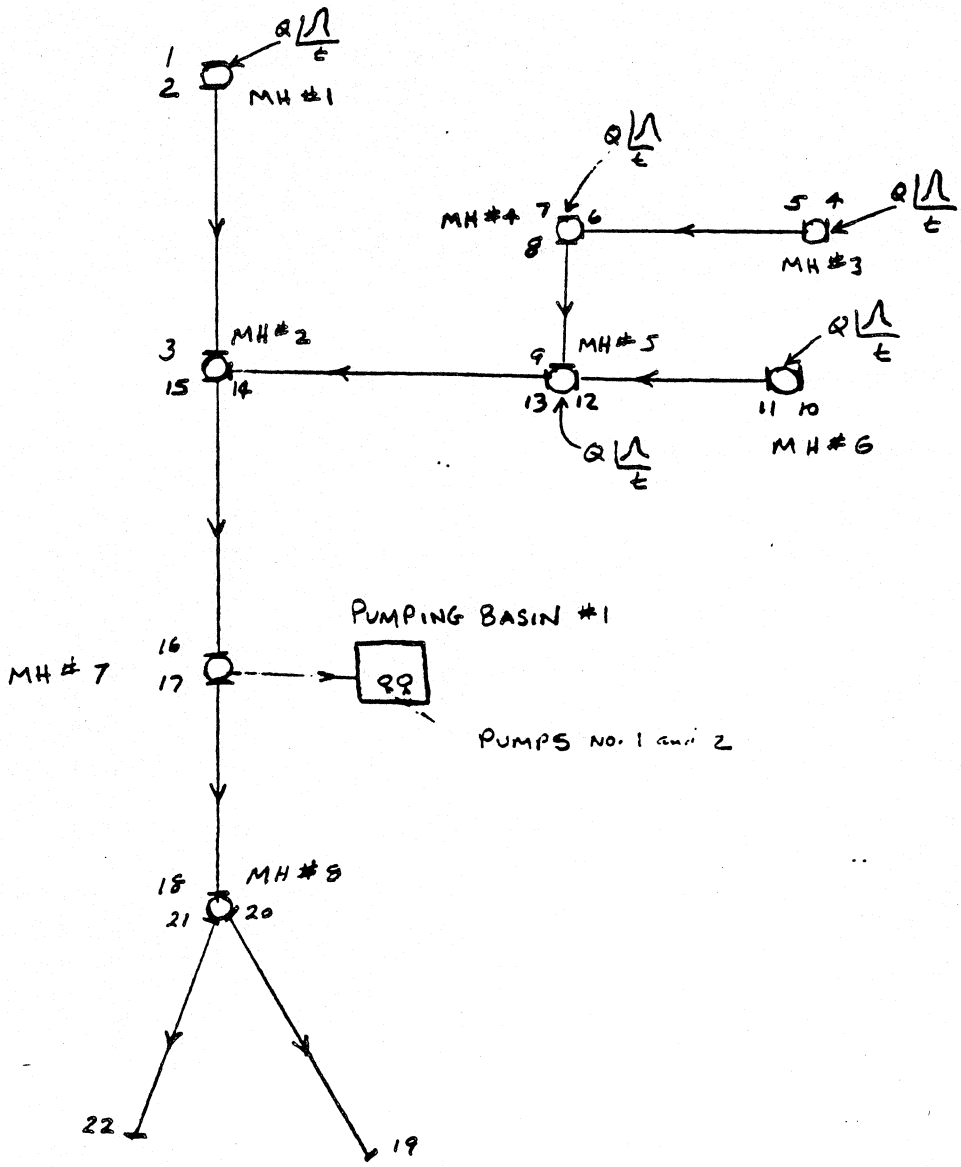

1984 International Symposium on Urban Hydrology, Hydraulics and Sediment Control
(University of Kentucky, Lexington, Kentucky – July 23-26, 1984)

AN IMPLICIT DYNAMIC WAVE MODEL FOR MIXED FLOWS IN STORM SEWER NETWORKS

by

D. L. Fread
Senior Research Hydrologist
Hydrologic Research Laboratory
National Weather Service, NOAA
Silver Spring, Maryland 20910

Abstract. Unsteady flow routing models used for real-time flow predictions or sewer network design must be capable of simulating mixed flows, i.e., flows which change with time and location along the storm sewer from free surface unsteady flow to pressurized flow and conversely. A general description of such a mathematical model is presented. The model will also properly predict backwater effects, flow reversals and surface flooding effects. The model is based on the complete one-dimensional equations of unsteady flow which are solved by a weighted four-point implicit finite difference scheme. At each time step, a system of nonlinear algebraic difference equations are solved for the unknown flow and water surface elevation at specified locations along the storm sewer network using Newton-Raphson iteration and a specially constructed Gaussian elimination matrix technique which has efficient computational properties. The model utilizes a very narrow fictitious slot emanating from the top of the sewer to effect the proper wave propagation speed when the sewer becomes pressurized. The sewer may be circular or have an arbitrary shape. The sewer network may be a single conduit or a dendritic network of conduits including multiple outlets and bypasses. Complex internal hydraulics due to the presence of manholes, overflow weirs, off-line detention storage basins and pumping stations are simulated via appropriate equations introduced within the system of flow equations as internal boundary conditions.

Introduction

When a storm sewer network receives flows from a large storm event, the flow regime may change from an initial free surface flow everywhere within the system to a mixed flow regime in which portions of the system experience pressurized flow as the sewer continues to fill. Unsteady flow routing models used for real-time flow prediction or sewer network design must be capable of simulating such mixed flows, i.e., flows which change with time and location along the storm drains from free surface unsteady flow to pressurized flow and conversely. During the time when the flow is in the free surface regime, many large trunk sewer systems are subject to backwater and reverse flow effects due to the very mild slopes dictated by outlet conditions and topography. An unsteady flow routing model must be able to properly simulate such effects which significantly deplete available storage within the system and help to actuate the pressurization of the system. For this reason, the routing model must be of either the dynamic wave or diffusion type. The degree of unsteadiness of the flow within a storm sewer network due to rapidly increasing inflows and pressurization waves favors the use of a dynamic wave type routing model.

The purpose of this paper is to present a description of an unsteady flow routing model capable of simulating mixed flows, backwater effects, reverse flows, and rapidly varying transient flows in mild sloping storm sewer networks. The model is of the dynamic wave type and is based on the complete one-dimensional equations of unsteady flow (Saint-Venant equations) which are solved by a weighted four-point implicit finite difference scheme. At each time step, a system of nonlinear algebraic difference equations are solved for the unknown flow and water surface elevation at specified locations (nodes) along the storm water conduit by using Newton-Raphson iteration coupled with a specially constructed Gaussian elimination matrix technique which provides very efficient computational properties. The storm sewer may be of circular or arbitrary shape. The network may consist of a single pipe or a dendritic system of pipes including multiple outlets, bypasses, and cross-connections. The model's mixed flow capability is made possible by introducing a very narrow fictitious chimney or slot in the top of the pipe after that introduced by Cunge and Wegner and referred to as the Preissmann slot.[1] Complex internal hydraulics due to the presence of manholes, overflow weirs, time-dependent gates, off-line detention storage basins and pumping stations, and drop inlet structures are simulated via appropriate equations introduced within the system of nonlinear flow equations as internal boundary conditions. The storage and pumping basins are connected to the storm sewer system via weir overflows where submergence effects and

possible flow reversals are considered. Each pump has its individual operating characteristics. Surface flooding, occurring at manholes when the conduit is pressurized, is either considered lost to the system or returns undiminished in volume after flooding a prescribed area. The downstream outlet(s) of the storm sewer system are governed by a specified head-discharge rating or water elevation-time history.

Relation to Previous Work

A variety of flow routing models have been developed specifically for storm sewers. Differences in the models can be attributed to their degree of simplicity, required computational effort, computational techniques utilized and their general applicability.

Some very simple models include the Chicago Hydrograph Method reported by Tholin and Keefer, the TRRL model by Watkins, and the ILLUDAS model described by Terstriep and Stall.[2,3,4] These routing models are based on steady flow hydraulics. Other simple models include the SURKNET model presented by Pansaic and Yen and the Wallingsford model described by Price.[5,6] Both of these models handle mixed flow. SURKNET uses a kinematic routing technique for free surface flow and treats the pressurized flow with a cascade solution technique from upstream to downstream. The Wallingsford model uses the Muskingum-Cunge routing method for free surface flows and solves the pressurized flow equations simultaneously for all pipe segments in which pressurization occurs.[7] Time steps are 15-30 seconds for free surface flow and 1 second for pressurized flow. Both of these models consider surface flooding due to surcharged manholes, but neither consider backwater effects or flow reversals in the free surface regime. Wood and Heitzman have developed an explicit finite element model for the complete one-dimensional equations of pressurized flow in a dendritic network of conduits.[8] They also developed two simpler models for pressurized flow only.

A few models are based on the complete one-dimensional unsteady flow (Saint-Venant) equations for the free surface regime with special treatment of the pressurized flow regime. In the popular SWMM model, the free surface flow routing uses a kinematic technique or an alternative method described by Roesner et al. based on an explicit finite difference solution of the Saint-Venant equations.[9] Pressurized flow is handled through a modified continuity relationship applied at each manhole. Any surface flooding is assumed to be lost from the system. Extremely small time steps are required for numerical stability. Song et al. have developed a model which uses an explicit finite difference solution of the characteristic form of the one-dimensional unsteady flow equations with the small disturbance celerity changed as the conduit undergoes pressurization.[10] A shock fitting technique, similar to that used by Cunge et al., is used at the interface of the two flow regimes.[11] Numerical stability restricts the allowable time step to about 0.5 - 2 seconds, depending on the propagation speed of the pressurization wave. Surface flooding is not considered. Two proprietary models developed in Europe which are not readily available have been reported in the literature. The French model, CAREDAS, developed by Sogréah, and the SYSTEM II SEWER model, developed at the Danish Hydraulics Institute, use the so-called Preissmann slot technique to enable the Saint-Venant equations to handle both free surface and pressurized flow.[12,13] Song et al. also have a model which uses the slot technique along with an explicit method of characteristics solution of the Saint-Venant equations.[10]

The model presented in this paper is similar to the European models in that a fictitious slot is used to enable the Saint-Venant equations to handle pressurized flow. It differs in the way the Saint-Venant equations are expressed in finite difference form and in the way a network of conduits are computationally treated. Other differences include the internal boundary equations used to simulate selected critical flow drop inlets, off-line detention storage and pumping basins, surface flooding and junction losses. This model is a significant extension of the work of Bhattacharyya and Fread.[14] It is an optional modification to the National Weather Service DWOPER model which has received widespread use within the engineering community for a variety of unsteady free surface flow routing applications.[15] Due to the basic DWOPER model having a modular construction with specialized subroutines and variable array sizes, the modifications required for mixed flow routing in conduit networks has little effect on its required computational resources.

Model Description

Governing Equations

The mixed flow routing model is based on the one-dimensional Saint-Venant equations of unsteady flow, i.e.,

$$\frac{\partial Q}{\partial x} + \frac{\partial A}{\partial t} - q = 0 \qquad (1)$$

$$\frac{\partial Q}{\partial t} + \frac{\partial (Q^2/A)}{\partial x} + gA\left(\frac{\partial h}{\partial x} + S_f\right) = 0 \qquad (2)$$

where:

$$S_f = \frac{n^2 |Q| Q}{2.2\, A^2\, R^{4/3}} \qquad (3)$$

and

$$n = 0.0735\, f^{1/2}\, d^{1/6} \qquad (4)$$

in which Q = flow (ft^3/sec), A = cross-sectional area (ft^2), q = lateral inflow (ft^2/sec), x = distance along the conduit (ft), t = time (sec), g = acceleration due to gravity (ft/sec^2), h = water surface elevation (ft), S_f = friction slope (ft/ft), R = hydraulic radius (ft) = A/P where P is the wetted perimeter (ft) of the cross-section, n = Manning roughness coefficient, d = the conduit diameter (ft), and f = the Darcy friction factor.

Eq (1) which conserves mass, and Eq (2) which conserves momentum, are quasi-linear hyperbolic partial differential equations. They are solved herein by using a numerical approximation procedure, the weighted four-point implicit finite difference scheme which obtains solutions of h and Q at discrete points in space (x) and time (t). In this scheme, the following approximations are used:

$$\frac{\partial K}{\partial t} \simeq \left(K_i^{j+1} + K_{i+1}^{j+1} - K_i^j - K_{i+1}^j\right)/2\Delta t_j \qquad (5)$$

$$\frac{\partial K}{\partial x} \simeq \Theta(K_{i+1}^{j+1} - K_i^{j+1})/\Delta x_i + (1-\Theta)\,(K_{i+1}^{j} - K_i^{j})/\Delta x_i \quad (6)$$

$$K \simeq \Theta(K_{i+1}^{j+1} + K_i^{j+1})/2 + (1-\Theta)\,(K_{i+1}^{j} + K_i^{j})/2 \quad (7)$$

in which K represents any variable (Q, h, q, A, S_f) in Eqs (1-2) and the (i, i+1) subscripts represent locations (nodes) along the conduit in the x-direction and the superscripts (j, j+1) represent successive points in time. The recommended value of the weighting factor (Θ) is in the range, $0.55 \leq \Theta \leq 0.65$.

Substituting Eqs (5-7) into Eq (1) and Eq (2), respectively, yields the following difference equations after some minor rearranging of terms:

$$\Theta(Q_{i+1}^{j+1} - Q_i^{j+1} - q_i^{j+1}\Delta x_i) + (1-\Theta)\,(Q_{i+1}^{j} - Q_i^{j} - q_i^{j}\Delta x_i)$$

$$+ 0.5\,\Delta x_i/\Delta t_j\,(A_i^{j+1} + A_{i+1}^{j+1} - A_i^{j} - A_{i+1}^{j}) = 0 \quad (8)$$

$$0.5\,\Delta x_i/\Delta t_j\,(Q_i^{j+1} + Q_{i+1}^{j+1} - Q_i^{j} - Q_{i+1}^{j}) + \Theta[(Q^2/A)_{i+1}^{j+1}$$

$$- (Q^2/A)_i^{j+1} + g\bar{A}_i^{\,j+1}(h_{i+1}^{j+1} - h_i^{j+1} + \bar{S}_{f_i}^{\,j+1}\,\Delta x_i)]$$

$$+ (1-\Theta)\,[(Q^2/A)_{i+1}^{j} - (Q^2/A)_i^{j} + g\bar{A}_i^{\,j}\,(h_{i+1}^{j} - h_i^{j}$$

$$+ \bar{S}_{f_i}^{\,j}\,\Delta x_i)] = 0 \quad (9)$$

where:

$$\bar{A}_i = (A_i + A_{i+1})/2 \quad (10)$$

$$\bar{S}_{f_i} = n_i^2|\bar{Q}_i|Q_i/(2.21\,\bar{A}_i^{\,2}\,R_i^{4/3}) \quad (11)$$

$$\bar{Q}_i = (Q_i + Q_{i+1})/2 \quad (12)$$

$$\bar{R}_i = \bar{A}_i/\bar{P}_i \quad (13)$$

$$\bar{P}_i = (P_i + P_{i+1})/2 \quad (14)$$

Eqs (8-9) are nonlinear with respect to the unknowns $(Q_i^{j+1}, Q_{i+1}^{j+1}, h_i^{j+1}, h_{i+1}^{j+1})$. The terms A and P are known functions of h, and S_f is a known function of Q and h. All terms with a superscript (j) are known from the initial conditions or a previous solution at the jth time.

Initial Conditions

The initial conditions are the values of h_i^j and Q_i^j for all nodes (i = 1,2, ... N) along the x-axis at time (t = 0) or j = 1. In this model, these may be obtained by either specifying them as input to the model or by letting the model compute them on the basis of the assumption of steady, spatially varied flow at t = 0.

When they are specified as input, the model uses them to obtain solutions to Eqs (8-9), and then uses the solutions to obtain another solution. This process is repeated a number of times until any small errors in the initial values have been damped out by the successive solutions. If the initial values do not contain large errors, this process converges; however, it may not if the errors are too large.

A preferable method is to let the model compute the initial conditions using the following steady gradually varied flow difference equation, i.e.,

$$(Q^2/A)_{i+1} - (Q^2/A)_i + g\bar{A}_i(h_{i+1} - h_i + \bar{S}_{f_i}\,\Delta x_i) = 0 \quad (15)$$

in which $\bar{A}_i$ and $\bar{S}_{f_i}$ are defined by Eqs (10-11). The computations proceed in the upstream direction from a specified value for h_{i+1} at the most downstream point in the system. Thus, Eq (15) is recursively solved for h_i; since A_i and $\bar{S}_{f_i}$ are nonlinear functions of h_i, Eq (15) is nonlinear and is solved by the Newton-Raphson iterative method for a single equation. The model determines all the Q values by a simple summation process using inflow values at t = 0 for all specified inflow points. The h and Q values can be determined in this way for either a single conduit or a complex dendritic network of conduits.

Boundary Conditions

Boundary conditions are specified values of either h or Q, or a known relation between them, at all the upstream-most nodes in a network of conduits and at the most downstream node. In this model, the upstream boundary conditions are known inflows as a function of time (specified discharge hydrographs). The downstream boundary can be a known water surface elevation as a function of time such as for submerged outlets in lakes or estuaries. Also, the downstream boundary can be a known relation between Q and h such as normal flow, critical flow, etc. which is input in the form of a table of Q and h values.

Solution Technique

The governing finite difference approximating equations, Eqs (8-9), can be solved once the initial conditions are obtained and all boundary conditions specified. Eqs (8-9) cannot be solved in an explicit or direct manner for the four unknowns since there are only two equations. However, if Eqs (8-9) are recursively applied to each Δx segment along a single conduit or network of conduits, a total of (2N - 4J - 2) equations with 2N unknowns can be formulated where N is the total number of nodes and J is number of junctions. Then, prescribed boundary conditions, one at the upstream end of each conduit and one at the downstream end of the main conduit, and three compatibility equations for each junction in the network, provide the necessary additional equations required for a determinate system. The resulting system of 2N nonlinear equations with 2N unknowns is solved by a functional iterative procedure, the Newton-Raphson method for a system of equations.[16]

Computations for the iterative solution of the nonlinear system are begun by assigning trial values to the 2N unknowns. Substitution of the trial values into the system of nonlinear equations yields a set of 2N residuals. The Newton-Raphson method provides a means for correcting the trial values until the residuals are reduced to a suitable tolerance level. This is usually accomplished in one or two iterations through use of linear extrapolation for the first trial values. A system of 2N x 2N linear equations relates the corrections to the residuals and to a Jacobian coefficient matrix composed of partial derivatives of each equation with respect to each unknown variable in that equation. The coefficient matrix of the linear system has a banded structure which allows the system to be solved by a compact penta-diagonal Gaussian elimination algorithm which is very efficient with respect to computing time and storage. The required storage is 2N x 4 and the required number of computational steps is approximately 38N.[17] In the case of networks, the required number of computational steps is (102 + 46J)N when using a specially constructed matrix technique which minimizes the number of off-diagonal elements due to the junctions and operates only on the non-zero elements in the Jacobian matrix.[18]

Conduit Geometry

The conduit may be circular or arbitrary shape. A very narrow fictitious slot or chimney emanates from the top of the conduit.

Circular conduit properties. Circular conduits have the following geometric properties which are used in the model:

$$\omega = \pi + 2 \sin^{-1}[(y-r)/r] \quad \ldots\ldots\ldots \quad y < d \tag{16}$$

$$P = r\,\omega \tag{17}$$

$$A = 0.125\, d^2(\omega - \sin\omega) \quad \ldots\ldots\ldots \quad y < d \tag{18}$$

$$A = 0.25\,\pi\, d^2 \quad \ldots\ldots\ldots\ldots\ldots\ldots \quad y > d \tag{19}$$

$$B = d \sin(0.5\,\omega) \quad \ldots\ldots\ldots\ldots\ldots \quad y < d \tag{20}$$

$$B > b \quad \ldots\ldots\ldots\ldots\ldots\ldots\ldots\ldots\ldots \quad y > 0 \tag{21}$$

$$dP/dy = 2/\sqrt{1 - [(y-r)/r]^2} \quad \ldots\ldots \quad y < d \tag{22}$$

$$dP/dy = 0 \quad \ldots\ldots\ldots\ldots\ldots\ldots\ldots\ldots \quad y > d \tag{23}$$

in which ω = the central angle (rad) subtended by two lines drawn from the center of the conduit to the two points where the water surface intersects the conduit perimeter, y = the depth of flow in the conduit (ft), r = the radius of the circular conduit (ft), P = the wetted perimeter (ft), A = the wetted cross-sectional area (ft^2), B = top width of the wetted area (ft), d = the diameter (ft) of the conduit, and b = the chimney width.

Arbitrary-shaped conduits. Conduits with an arbitrary shape whose geometric properties may not be readily defined analytically as with circular shapes may be modeled by inputting a table of the conduit width as a linear function of the depth, i.e., (B_k, Y_k) where $k = 1,2,\ldots N_s$; N_s is a sufficient number of widths to fully describe the geometry including the fictitious slot. The wetted perimeter and area corresponding to each are calculated initially (one time only) as follows:

$$P_k = P_{k-1} + 2\sqrt{(\Delta B_k)^2 + (\Delta Y_k)^2} \tag{24}$$

where:

$$\Delta B_k = (B_k - B_{k-1})/2 \tag{25}$$

$$\Delta Y_k = Y_k - Y_{k-1} \tag{26}$$

and,

$$A_k = \sum_{\ell=1}^{k} 0.5(B_\ell + B_{\ell-1})(Y_\ell - Y_{\ell-1}) \tag{27}$$

In Eqs (24-27), the k index goes from 2 through N_s; when k = 1, $P_1 = B_1$ and $A_1 = 0$. The values of B, P, and A, associated with any depth (y) during the unsteady flow solution, can be computed according to the following linear relations:

$$B = B_k + (B_{k+1} - B_k)(y - Y_k)/(Y_{k+1} - Y_k) \tag{28}$$

$$P = P_k + (P_{k+1} - P_k)(y - Y_k)/(Y_{k+1} - Y_k) \tag{29}$$

$$A = A_k + 0.5(B + B_k)(y - Y_k) \tag{30}$$

Eqs (28-30) are applicable when $Y_k < y < Y_{k+1}$.

Fictitious slot. From the top of the conduit, a hypothetical chimney or slot extends upward.[1,11] The purpose of the slot is to provide a cross-sectional area whose top width (b) is very small for all flow depths greater than the top of the conduit. The small top width is required to produce the proper celerity for pressurized flow as computed from the gravity wave celerity equation, i.e.,

$$c = \sqrt{gA/B} \tag{31}$$

in which c is the celerity (ft/sec) of a gravity wave. For a circular conduit, Eq (31) can be used to compute the required chimney width by replacing B with b and c with a (the celerity of a pressure wave). Solving Eq (31) for b yields the following relation:

$$b = 0.25\, g\, \pi \left(\frac{d}{a}\right)^2 \tag{32}$$

The pressure wave celerity (a) can be computed from the properties of the conduit and the storm water which may contain some entrained air.[19] Thus,

$$a = \left(\frac{K/\rho}{1 - Kdc_1/(Ee)}\right)^{1/2} \tag{33}$$

where:

$$K = \frac{K_w}{1 + V_a\left(\frac{K_w}{K_a} - 1\right)} \tag{34}$$

$$\rho = \rho_a V_a + \rho_w V_w \tag{35}$$

in which K = the bulk modulus of elasticity of the flowing water (lb/ft^2), ρ = the bulk density of the flowing water ($lb\ sec^2/ft^4$), d = the conduit diameter (ft), E = Young's modulus of elasticity for the conduit (lb/ft^2), e = the conduit wall thickness (ft), K_w = modulus of elasticity for water (lb/ft^2), K_a = modulus of elasticity for air (lb/ft^2), V_a = the ratio of air volume to the total volume, V_w = the ratio of water volume to the total volume, ρ_a = density of air ($lb\ sec^2/ft^4$), and ρ_w = density of water ($lb\ sec^2/ft^4$). In Eq (33), the term c_1 is given by the following:

$$c_1 = \alpha_o + \alpha_1 \beta \quad (36)$$

in which for thick-walled conduits ($e/d > 25$) $\alpha_o = \mu$ and $\alpha_1 = 1$, while for thin-walled conduits ($e/d < 25$):

$$\alpha_o = 2\ e/d\ (1 + \mu) \quad (37)$$

$$\alpha_1 = d/(d + e) \quad (38)$$

which μ = the Poisson ratio (- lateral stress/axial stress). The β term in Eq (36) depends on the rigidity of the conduit with respect to axial expansion, i.e., $\beta = 1.0$ if expansion joints are used throughout the length of the conduit, $\beta = 1 - \mu^2$ if it is anchored everywhere, and $\beta = 1.25 - \mu$ if it is anchored only at the upstream end.

Entrained air greatly affects the pressure wave celerity; as the air content increases from 0.0 to 1.0 percent, the celerity can decrease from about 4000 ft/sec to 700 ft/sec. Of course, field measurements of pressure celerity would be preferable for determining the chimney width (b) from Eq (32).

Internal Boundaries

Locations along the conduit network where the Saint-Venant equations are not applicable are called internal boundaries. Such locations include manholes, junctions, drop inlets where critical flow occurs, connections to off-line detention storage basins and/or pumping stations. The internal boundary consists of two equations which replace the two Saint-Venant equations. These equations relate Q and h at the entrance(s) to a short Δx reach within which the two internal boundary equations describe the hydraulics.

Manholes. Manholes are located where the conduit changes size, slope, and/or direction or where there is a junction of two or three conduits. The two internal boundary equations are:

$$Q_i^{j+1} + m\ Q_{i'}^{j+1} - Q_{i'+1}^{j+1} + Q_{in} - Q_w - \Delta s/\Delta t = 0 \quad (39)$$

$$h_i^{j+1} - h_{i'+1}^{j+1} - h_{\ell_i} = 0 \quad (40)$$

$$h_{i'}^{j+1} - h_{i'+1}^{j+1} - h_{\ell_{i'}} = 0 \quad (41)$$

in which Q_i = the inflow (ft^3/sec) to the manhole from the upstream conduit, $Q_{i'}$ = the inflow from the branch conduit ($m = 0$ if there is no branch conduit, otherwise $m = 1$), $Q_{i'+1}$ = the outflow from the manhole through the exiting downstream conduit (when there is no branch conduit, $i' = i$), h_i, $h_{i'}$, $h_{i'+1}$ are the water surface elevations (ft) of the upstream, branch, and downstream conduits, respectively, Q_{in} = the surface inflow to the manhole which is a specified function of time, Q_w = the flow entering or leaving the manhole via a weir-type control, $\Delta s/\Delta t$ = the change of storage associated with the manhole during a Δt time step, h_{ℓ_i} and $h_{\ell_{i'}}$ are the head losses incurred by the incoming and exiting flows.

The weir flow (Q_w) is further defined as follows:

$$Q_w = C\ C_s\ (\bar{h} - h_w)^{3/2} \quad (42)$$

where: $\bar{h} = \left(h_i^{j+1} + m\ h_{i'}^{j+1} + h_{i'+1}^{j+1}\right) / (m + 2)$ (43)

$$C = 3.2\ L_w \quad (44)$$

$$C_s = \left(1 - h_r^2\right)^{1/2} \quad (45)$$

$$h_r = (\bar{h} - h_w) / (h_t - h_w) \ \ldots.\ \bar{h} \text{ and } h_t > h_w \quad (46)$$

$$h_r = 0 \ \ldots.\ \bar{h} \text{ or } h_t < h_w \quad (47)$$

in which h_w is the crest elevation of the weir, $\bar{h}$ is the water elevation within the manhole as given by Eq (43) in which $m = 1$ when a branching conduit exists and $m = 0$ where there is no branch conduit, C is the weir discharge coefficient, L_w is the length (ft) of the weir crest, C_s is the submergence correction factor given by Eq (45), h_r is given by either Eq (46) or Eq (47) in which h_t is the water elevation downstream of the weir.

The change in manhole storage is given by the following:

$$\Delta s = 0.25\ \pi\ d_m^2\ (\bar{h} - \bar{h}') \ \ldots.\ \bar{h} < h_m \quad (48)$$

in which d_m = the diameter (ft) of the manhole, $\bar{h}'$ = the water elevation within the manhole at time ($t - \Delta t$), and h_m = the elevation of the top of the manhole.

The junction losses h_{ℓ_i} and $h_{\ell_{i'}}$ in Eqs (41-42) are approximated as follows:

$$h_{\ell_i} \simeq \left[\left(V_i^j\right)^2 + 0.5\left(V_{i'+1}^j\right)^2\right] / 2g \quad (49)$$

$$h_{\ell_{i'}} \simeq \left[\left(V_{i'}^j\right)^2 + 0.5\left(V_{i'+1}^j\right)^2\right] / 2g \quad (50)$$

in which V_i^j, $V_{i'}^j$, V_{i+1}^j are the velocities at time ($t - \Delta t$) of the upstream, branch, and downstream conduits, respectively. The head losses are assumed to be negligible or compensated by small drops in the inlet-outlet inverts within the manhole for all flows less than about three-fourths of the outlet conduit's full discharge capacity.

Eq (50) is not used when the branch conduit does not exist; in this case, the subscript (i') is the same as i in Eq (49).

Surface flooding. Flooding of the surrounding surface area above the top of a manhole is treated by either of two methods for each manhole. In the first, it is assumed that the flooding occurs as the water elevation of the manhole increases above the top of the manhole (h_m). When this occurs, Eq (48) becomes:

$$\Delta s = d_s^2\ (\bar{h} - \bar{h}') \ \ldots.\ \bar{h} > h_m \quad (51)$$

in which d_s is the length (ft) of the flooded surface area which is assumed to be represented by a square. It is further assumed that the surface flooding does not result in any permanent loss of

volume to the conduit system; thus, all of the flood waters return to the system as the water level in the manhole diminishes. In the second method, the surface flooding occurs when the manhole water elevation ($\bar{h}$) becomes greater than h_m and the overtopping waters are assumed to be permanently lost to the conduit system. The exiting flow is denoted by Q_w in Eq (39); it is computed from Eq (42) rewritten as follows:

$$Q_w = 3.1\ \pi\ d_m\ (\bar{h} - h_m)^{3/2} \quad \ldots\ \bar{h} > h_m \qquad (52)$$

Submergence corrections are neglected in Eq (52).

Off-line detention storage and pumping basins. Detention basins which temporarily store excess waters are connected to the conduit system via a manhole junction. The stored waters are removed from the system via the term Q_w in Eq (39) and computed using Eqs (42-47). Q_w may be plus or minus according to the relative values of $\bar{h}$ and h_t. The term h_t used in Eq (46) is the water surface elevation of the detention basin; it is computed from a storage balance of the detention basin at time $(t - \Delta t)$.

$$S^j = S^{j-1} + \left(Q_w^j - Q_p^j\right) \Delta t_j \qquad (53)$$

in which S^j and S^{j-1} are the surface storage area (ft^2) of the detention basin at times $(t - \Delta t)$ and $(t - 2\Delta t)$, respectively. Q_p represents outflow from the basin due to pumping.

If the basin has one or more pumps, Q_p represents the total discharge from the pumps as determined from a specified tabular head-discharge rating for each pump. Also, each pump has a specified elevation of the detention basin water surface at which the pump starts and one at which it stops pumping. The head (H) used to enter the head-discharge rating table to determine the pump discharge is:

$$H = h_p - h_t \qquad (54)$$

in which h_p is the average head including friction losses against which each pump discharges, and h_t is the water surface elevation of the detention (pump) basin; h_t is obtained through interpolation of the surface area (S)-elevation (H_t) table which is specified for each detention or pump basin.

Drop inlets. The invert of a conduit inlet to a manhole may be considerably higher than the other inlet and outlet. Such drop inlets must be treated as an internal boundary since the flow dropping into the manhole is governed by the critical flow equation rather than the Saint-Venant equations. Thus, a very small Δx reach is specified immediately upstream of the conduit outlet where critical flow occurs. The following two internal boundary equations are used:

$$Q_i^{j+1} - Q_{i+1}^{j+1} = 0 \qquad (55)$$

$$Q_i^{j+1} - \left(\sqrt{gA^3/B}\right)_i^{j+1} = 0 \qquad (56)$$

If the flow in the vicinity of the drop inlet starts to be pressurized such that the critical flow point becomes submerged, Eqs (55-56) are replaced by the Saint-Venant equations. The necessity of such a change is continually checked during the computations by comparing the manhole water elevation ($\bar{h}$) against the water elevation, $\left(h_i^{j+1}\right)$.

Computational Sensitivity

The model was tested for its sensitivity to the maximum distance step (Δx), the time step (Δt), and the chimney width (b). The computations were found to be insensitive to a range of Δx values representing the usual spacing of manholes. The time step recommended for free surface flow using the 4-pt. implicit solution of the Saint-Venant equations has been determined by the author.[20] For a circular conduit, the following relation is given:

$$\Delta t < 0.04\ S^{1/2}\ d^{1/6}\ Z\ T_p/n \qquad (57)$$

where:

$$Z = \left[\frac{(1 - \varepsilon^2)}{4\ \Theta^2\ \varepsilon^2 - (2\Theta - 2)^2}\right]^{1/2} \qquad (58)$$

in which ε the acceptable error expressed as a ratio of the numerical solution to an analytical solution ($0.95 < \varepsilon < 0.99$), Θ = the weighting factor in the 4-pt. implicit scheme, S = the bottom slope of the storm sewer, n = the Manning n, T_p = the duration of the rising limb of the inflow hydrograph, and d = the conduit diameter (ft). The units of Δt and T_p are the same (hr or sec).

Sensitivity of the computed results to variations in the time step (Δt) was tested on a number of sewer networks. One such system is shown in Fig. 1. It consists of six manholes, each with an inflow hydrograph having a time of rise of 0.25 hr. The system was tested with and without surcharging; the latter condition was developed by increasing the magnitude of the peak of the inflow hydrograph at manhole no. 4. Conduit diameters vary from 3 to 6 ft, and the invert slope of each is 0.00075 ft/ft. The distance (Δx) between each manhole is 580 ft. The Δt computed from Eq (57) is

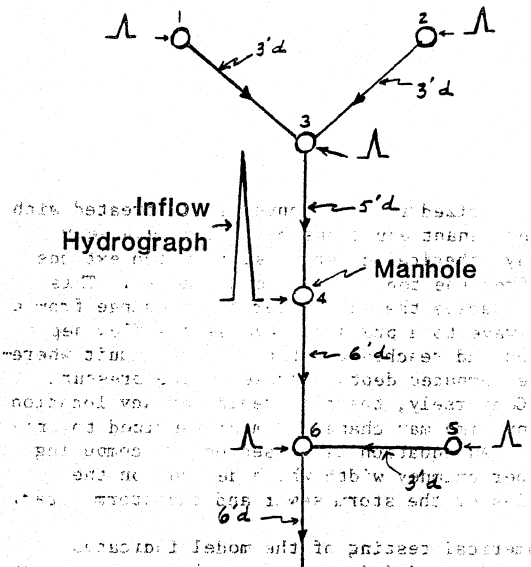

Figure 1. Test Storm Sewer System.

0.01 hr (36 sec) for $\Theta = 0.60$, $\varepsilon = 0.97$, $n = 0.010$, and $T_p = 0.25$. The computed maximum water surface elevations, discharges, and times of occurrence at manhole nos. 1, 4, 5, and 6 were compared with those computed using a very small time step of 1.8 sec. The comparative variations expressed as percent are shown in Table 1. The errors are quite small (less than 1.7 percent) for all Δt values less than or equal to 36 sec, that given by Eq (57). As Δt is considerably increased above this value, the error becomes significant. For larger T_p values, the time step which would produce insignificant errors could be increased.

Table 1. Average Errors (Percent) Associated with the Maximum Computed Values at Manhole Nos. 1, 4, 5, and 6 for Various Time Steps.

Δt (sec)	Time of Maximums	Water Surface Elevation (Head)	Discharge
1.8	0	0	0
18.	0.7	1.0	1.0
36.	0.8	1.2	1.7
180.	11.9	6.5	8.4
450.	6.7	29.8	28.1

The computational requirements on an IBM 360/195 computer are approximately 0.009 sec per manhole per time step and on a PRIME 750 computer this is increased by a factor of about seven.

Summary and Conclusions

A nonlinear weighted implicit finite difference model based on the complete Saint-Venant equations of unsteady flow has been developed. The model is capable of simulating free surface and/or pressurized flows, backwater effects and flow reversals in a single storm sewer or a complex dendritic network of sewers having cross-connections and multiple outlets. The storm conduit may have a circular or an arbitrary shape. Manhole effects (junctions of two or three conduits, head losses, storage, surface flooding with or without loss of volume), detention basin storage, pumping stations with one or more pumps with individual operating characteristics, and critical flow drop-inlets are each simulated by appropriate equations introduced as internal boundaries and solved simultaneously with the Saint-Venant finite difference equations and external boundary equations.

Pressurized flow is conveniently treated with the Saint-Venant equations by utilizing a very narrow hypothetical chimney (slot) which extends upward from the top of the storm conduit. This feature enables the wave celerity to change from a gravity wave to a pressure wave as the flow depth increases and reaches the top of the conduit whereupon the computed depth represents the pressure head. Conversely, the flow regime at any location or at any time may change from pressurized to free surface. An equation is presented for computing the proper chimney width which depends on the properties of the storm sewer and the storm water.

Numerical testing of the model indicates a desirable insensitivity to reasonable ranges of the distance step (Δx) and the time step (Δt). The former can be the normal distance between manholes where flow and conduit properties may change and the latter is selected to be less than or equal to that given by an equation which relates the storm drains' hydraulic properties, the rate of inflow to the system, and the acceptable numerical solution error.

References

1. J. A. Cunge and M. Wegner, "Numerical Integration of Barre de Saint-Venant's Flow Equations by Means of an Implicit Scheme of Finite Differences. Applications in the Case of Alternately Free and Pressurized Flow in a Tunnel," La Houille Blanche, No. 1, pp. 33-39, 1964.

2. A. L. Tholin and C. J. Keefer, "The Hydrology of Urban Runoff," Transactions, ASCE, Vol. 125, pp. 1308-1379, 1960.

3. L. H. Watkins, "A Guide for Engineers to the Design of Storm Sewer Systems," Road Research Technical paper No. 55, Dept. of Science and Industry Research, Great Britain, 1963.

4. M. L. Terstriep and J. B. Stall, "The Illinois Urban Drainage Area Simulator, ILLUDAS," Bulletin 58, Illinois State Water Survey, Urbana, Illinois, 1974.

5. N. Pansaic and B. C. Yen, "Kinematic-Wave Modelling of Storm Sewer Systems with Surcharge," Proceedings of the Second International Conference on Urban Storm Drainage, Vol. I, Hydraulics and Hydrology, ed. by B. C. Yen, University of Illinois, Urbana, Illinois, pp. 193-202, June 1981.

6. R. K. Price, "A Simulation Model for Storm Sewers," Second International Conference on Urban Storm Drainage, Urbana, Illinois, pp. 184-192, June 1981.

7. J. A. Cunge, "On the Subject of a Flood Propagation Method," Journal of Hydraulics Research, IAHR, Vol. 7, pp. 205-230, 1969.

8. D. J. Wood and G. C. Heitzman, "Hydraulic Analysis of Surcharged Storm Sewer System," Research Report No. 137, University of Kentucky Water Resources Research Institute, Lexington, Kentucky, 143 p., 1983.

9. L. A. Roesner, R. P. Shubinski, and J. A. Aldrich, "Storm Water Management Model User's Manual Version III, Addendum I Extran," U.S. Environmental Protection Agency, Cincinnati, Ohio, 1981.

10. C. C. S. Song, J. A. Cardle, and K. S. Leung, "Transient Mixed-Flow Models for Storm Sewers," Journal of Hydraulic Engineering, ASCE, Vol. 1109, No. 11, pp. 1487-1503, November 1983.

11. J. A. Cunge, F. M. Holly, Jr., and A. Verweg, Practical Aspects of Computational River Hydraulics, Pitman Advanced Publishing Program, Boston, Massachusetts, 1980.

12. Sogreah, "Mathematical Model of Flow Simulation in Urban Sewerage Systems, CAREDAS Program," Societé Grenobloise d'Etudes et d'Applications Hydrauliques, Grenoble, 1973.

13. N. E. Hoff-Clausen and A. Kej., "System II Sewer--A Storm Sewer Model," Proceedings of the Second International Conference on Urban Storm Drainage, Vol. I, Hydraulics and Hydrology, ed. by B. C. Yen, University of Illinois, Urbana, Illinois, pp. 137-145, June 1981.

14. A. K. Bhattacharyya and D. L. Fread, "Storm Surge Prediction Model and its Application to a Combined Trunk Sewer System," Proceedings of Storm Water and Water Quality Models Users Group Meeting, ed. by P. Beron and T. Barnwell, Ecole Polytechnique De Montreal, Montreal, Quebec, pp. 32-46, November 1983.

15. D. L. Fread, NWS Operational Dynamic Wave Model," Proceedings of 26th Annual ASCE Hydraulics Division Specialty Conference, University of Maryland, College Park, Maryland, pp. 455-464, August 1978.

16. M. Amein and C. S. Fang, "Implicit Flood Routing in Natural Channels," Journal of Hydraulics Division, ASCE, Vol. 96, No. HY12, pp. 2481-2500, December 1970.

17. D. L. Fread, "Discussion of Implicit Flood Routing in Natural Channels by M. Amein and C. S. Fang," Journal of Hydraulics Division, ASCE, Vol. 97, No. HY7, pp. 1156-1159, July 1971.

18. D. L. Fread, "Computational Extension to Implicit Routing Models," Proceedings of Conference on Frontiers in Hydraulic Engineering, ed. by H. T. Shen, Massachusetts Institute of Technology, Cambridge, Massachusetts, pp. 343-348, August 1983.

19. V. L. Streeter and E. B. Wylie, Hydraulic Transients, McGraw-Hill Book Co., New York, 1967.

20. D. L. Fread, "Time Step Selection for the Weighted 4-Pt. Implicit Difference Solution of the Saint-Venant Equations," Hydrologic Research Laboratory, National Weather Service, NOAA, Silver Spring, Maryland, March 1984.

DATA INPUT INSTRUCTIONS FOR DWOPER AND NETWORK

By

Larry W. Mays

DWOPER AND NETWORK INPUT
DESCRIPTION OF DATA SETS

Data Set	NETWORK & DWOPER Cards*	NETWORK Cards**	Description of Data Set	When Required?
A	1-12	1A, 8A 11A-11E	Problem size input Node and junction numbering and upstream boundary types.	Required
B	13-14		Type of boundary conditions	Required
C	15-16		Location of Manning's n reaches	Required
D	17-20		Observed stage hydrograph input and specification of hydrograph plots.	
E	21		Math function describing upstream boundary hydrograph.	
F	22-27		Upstream and downstream boundary conditions.	Required
G	28-30		Channel cross-sections.	Required
H	31-33		Off-channel storage cross-sections.	
I	34		Channel bottom slope for normal flow as the downstream boundary condition of main river.	
J	35-37		Wind coefficient, station locations, and expansion and contraction coefficients.	Required
K	38-39		Lateral inflows.	
L	40-41		Weir flow and levee overtopping.	
M	42-51	 51A-51D	Internal boundaries. Gate internal boundary condition	
N	52-54	 54A-54C	Computation time and initial conditions. Branch numbering.	Required
O	55-56		Manning's n relationship.	Required
P	57-59		Ending	Required

* These are the only required cards for DWOPER and are also required for NETWORK.

** These cards are additional cards required to run the NETWORK version.

1	2	3	4	5	6	7	8
10	20	30	40	50	60	70	80

1	2	3	4	5	6	7	8
10	20	30	40	50	60	70	80

1	2	3	4	5	6	7	8
10	20	30	40	50	60	70	80

Data Set	Card Number	Column	Format	Variable Name	Description
A	1	1-5	I5	K1	Number of rivers (main river plus number of tributaries).
		6-10	I5	K2	Maximum number of stations (cross-sections on any single tributary or the main river). K2≧ MAX[NB(J), J = 1,. . ., JN]
		11-15	I5	K3	Number of time steps. K3 ≧ MAX[NU, TE/(TM * KITPR) + 1.01]
		16-20	I5	K4	Maximum number of gaging stations. K4 ≧ MAX[NRTI(J), J = 1,. . ., JN]
		21-25	I5	K5	= 1
		26-30	I5	K6	Number of values used to describe downstream rating curve. K6 ≧ MAX[NYQD,1]
		31-35	I5	K7	Maximum number of Manning's n reaches on any river. K7 ≧ MAX[NRCM1(J), J = 1,. . ., JN]
		36-40	I5	K8	Maximum number of Manning's n values in any Manning's n reach. K8 ≧ MAX[NCML,1]
		41-45	I5	K9	Maximum number of elevation versus top width values at any cross-section. K9 ≧ MAX[NCS,1]
		46-50	I5	K10	Maximum number of lateral inflows on any river. K10 ≧ MAX[NQL(J), J = 1,. . ., JN]
		51-55	I5	K11	= 1
		56-60	I5	K12	= 1
		61-65	I5	K13	= 1
		66-70	I5	K14	Maximum number of water surface elevations versus top width values for any off-channel storage.

Data Set	Card Number	Column	Format	Variable Name	Description
A	1	71-75	I5	K17	Total number of upstream boundaries in the system.
		76-80	I5	K18	Total number of junctions in the system.
	1A	1-5	I5	K21	Maximum number of gates in the system.
		6-10	I5	K22	Maximum number of values in the gate coefficient table.
		11-15	I5	K23	= 1
		16-20	I5	K24	= 1
		21-25	I5	K25	= 1
		26-30	I5	K26	= 1
	2	1-5	A5	ALONE	Type ALONE starting in column 1.
	3	1-10	F10.0	EPSY	Depth tolerance for Newton-Rhapson method (recommend 0.05 ft.)
		11-20	F10.0	EPSQ	Discharge tolerance for Newton-Rhapson method EPSQ ≃ EPSY x (ave. velocity) x (ave. width).
		21-30	F10.0	EPSQJ	Discharge tolerance in tributary iteration scheme EPSQJ = EPSQ
		31-40	F10.0	THETA	Acceleration factor used in solving tributary junction problem (range of 0.5-1.0). Recommend 0.8.
		41-50	F10.0	F1	Weighting factor (recommend 0.55).
		51-60	F10.0	XFACT	Factor for conversion of length (location). If units are in miles, XFACT = 5280.
		61-70	F10.0	DHF	Time interval (in hours) at which discharge hydrographs are read in. If hydrographs are read in as daily values, DHF = 24.

Data Set	Card Number	Column	Format	Variable Name	Description
A	3	75-78	A4	CFNAME	= IMET if user wants the metric option to print output data in metric. All other input is the same except HGC on card 51A and HG on card 51D are input in metric. Leave blank if the metric option is not used. This metric option is only available for the NETWORK version.
	4	1-10	I10	JN	Number rivers (i.e. the main river and tributaries). JN = 1 main river only, no tributary JN = 2 main river and 1 tributary JN = 3 main river and 2 tributaries If the channel network option (NET = 1 or 2) is used, JN = 1.
		11-20	I10	NU	Number of stage or discharge hydrograph values. NU = 0 implies use of a mathematical function to describe hydrograph.
		21-30	I10	NCT	Type of extrapolation used in Newton's method. NCT = 0 no extrapolation NCT = 1 linear NCT = 2 parabolic
		31-40	I10	ICD	If any boundary hydrograph changes by more than this value from the last step, extrapolation is not used.
		41-50	I10	NYQD	Number of stage-discharge (rating curve) values for the downstream boundary.
		51-60	I10	ITMAX	Maximum number of iterations allowed in the Newton-Raphson method for solving the Saint Venant equations.
		61-70	I10	NCML	Number of values used to describe the Manning's n versus stage or discharge relationship (same number for all Manning's n reaches).

Data Set	Card Number	Column	Format	Variable Name	Description
A	4	71-80	I10	NET	= 0 Channel network option is not used. = 1 Channel network option is used. = 2 Channel network option is used and junction losses due to mixing and friction are neglected. If NET = 1 or 2 then JN <u>must</u> be read in as 1.
	5	1-10	I10	NCS	Number of values describing top width (BS) versus elevation (HS).
		11-20	I10	NCSS	Number of values describing top width (BSS) off-channel storage versus elevation (HSS).
		21-30	I10	NP	NP = 0 No automatic calibration for determining Manning's n. NP > 1 Automatic calibration is used, NP is the number of the first computed stage in the computed stage hydrograph which is used in the statistics needed in the automatic calibration to compute the Manning's n relationship. Observed stage hydrographs must be read in for the automatic calibration.
		31-40	I10	KTERM	KTERM = 1 terms in equation of motion are computed and printed. KTERM = 0 terms are not printed.
		41-50	I10	KPL	KPL = 0 no plots. KPL = 1 stage hydrographs are plotted. KPL = 2 discharge hydrographs are plotted.
		51-60	I10	KPL2	KPL2 = 0 no observed data available for plotting. KPL2 = 1 observed data available are plotted.
		61-70	I10	JNK	JNK = 0 no printout of computed water surface elevations, velocity, and discharges. JNK = 1 computed water surface elevations, velocities, and discharges are printed.
		71-80	I10	NPEND	Leave Blank.

Data Set	Card Number	Column	Format	Variable Name	Description
A	6	1-10	I10	NQL(1)	Number of Δx reaches where lateral inflows enter the main river (J = 1).
		11-20	I10	NQL(2)	Number of Δx reaches where lateral inflows enter the second river (tributary 1).
			I10	NQL(JN)	Number of Δx reaches where lateral inflows enter the JN-th river.
	7	1-10	I10	NWJ(1)	Number of Δx reaches in the main river where weir-flow occurs.
		11-20	I10	NWJ(2)	Number of Δx reaches in the second river (or tributary 1) where weir-flow occurs.
			I10	NWJ(JN)	Number of Δx reaches in the JN-th river where weir-flow occurs.
	8	1-10	I10	NUMLAD(1)	Number of internal boundaries in the first (main) river.
			I10	NUMLAD(JN)	Number of internal boundaries in the JN-th river.
	8A	1-10	I10	NG(1)	Number of gates and/or critical flow sections in the J = 1 river. For the network option JN = 1 and NET = 1 or 2 then, only NG(1) is read in.
				NG(2)	
				⋮	
				NG(JN)	

Data Set	Card Number	Column	Format	Variable Name	Description
A	9	1-10	I10	NCSS1(1)	Number of stations with off-channel storage in the main river.
				⋮	
			I10	NCSS1(JN)	Number of stations with off-channel storage in the JN-th river (tributary).
The following card 10 is used only if there are stations with off-channel storage (i.e. NCSS1 (J) > 0). If there are no stations in any of the JN rivers with off-channel storage go to card 11. Card 10 is repeated for each river starting with the main river, J = 1, then 2. . .JN.					
	10	1-10	I10	NCSSS(1,J)	First upstream station number that has off-channel storage in the J-th river.
			I10	NCSSS(2,J)	Next station (going in a downstream direction) that has off-channel storage in the J-th river.
				⋮	
			I10	NCSSS(NCSS1(J),J)	
	Card 11 must be used for all applications.				
	11	1-10	I10	NB(1)	Total number of stations on the main river. (For Network option this is the total number of stations in the system.)
If the channel network option has been selected (i.e. NET = 1 or 2 on card 4), then cards 11A through 11E must be used. If NET = 0, skip to card 12.					
	11A	1-10	I10	JCOD(1)	Denotes type of node at cross-section (node) 1 (see Figure 5.1).
		11-20	I10	JCOD(2)	Denotes type of node at cross-section (node) 2 (see Figure 5.1).
				⋮	
			I10	JCOD(NB(J))	Denotes type of node for last downstream cross-section (node).

Figure 5.1

NODE CODE (JCOD(K), K=1,N)

1 Internal Node

2 Upstream Boundary

3 Downstream Boundary

4 Tributary Junction

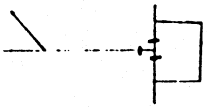

5 Tributary Junction on a Bifurcation

6 Upstream Bifurcation Junction

7 Downstream Bifurcation Junction

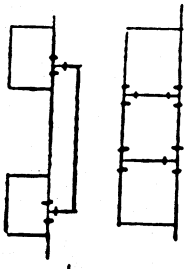

8 Double Bifurcation Junction on a Bifurcation

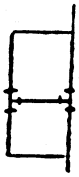

9 Single Bifurcation Junction on a Bifurcation

10 Gate Internal Boundary

11 Critical Flow Internal Boundary

Data Set	Card Number	Column	Format	Variable Name	Description
A	11B	1-10	I10	JTN	Total number of junctions in the system.
		11-20	I10	NUPB	Total number of upstream boundaries in the system.
The following card, 11C, is repeated for each junction, K = 1,. . .,JTN.					
	11C	1-10	I10	JU(K)	Cross-section number at entry to junction.
		11-20	I10	JB(K)	Cross-section number at branch of junction.
		21-30	I10	JL(K)	Cross-section number at exit of junction.
		31-40			
	11D	1-10	I10	KMU(1)	Type of upstream boundary condition for the first upstream boundary. = 1 stage hydrograph. = 2 discharge hydrograph. = 4 depth-discharge (loop rating curve developed) by the program.
				⋮	
			I10	KMU(NUPB)	
	11E	1-10	I10	JCPR(1)	Sequential order to list cross-section in output.
				⋮	
				JCPR(NB(J))	
If there are tributaries (i.e. JN > 1) the following card (12) is entered for each tributary, J = 2,. .,JN. Tributaries are numbered from upstream to downstream along the main river commencing with 2. (DWOPER OPTION ONLY)					
	12	1-10	I10	NB(J)	Number of stations for the J-th river (J-1 tributary)
		11-20	I10	NJUN(J)	Station number on the main river where tributary J enters (this station coincides with the upstream end of the small reach which is equivalent in length to the tributary width).

Data Set	Card Number	Column	Format	Variable Name	Description
A	12	21-30	F10.0	ATF(J)	Angle (in degrees) that the tributary makes with the main river at the confluence.
The following cards, 13 and 14, specify the type of boundary conditions. (DWOPER OPTION ONLY)					
B	13	1-10	I10	KU(1)	Type of upstream boundary condition for the main river. KU(J) = 1, stage hydrograph. KU(J) = 2, discharge hydrograph.
		11-20	I10	KU(2)	Type of boundary condition for the first tributary J = 2.
				⋮	
			I10	KU(JN)	Type of boundary condition for the last tributary J = JN
	14	1-10	I10	KD(1)	Type of downstream boundary condition specified for the main river. = 1, stage hydrograph (always equal to 1 for tributaries). = 2, discharge hydrograph. = 3, single value rating curve of discharge as a function of stage. (specify K6, NYQD, YQD, and QYQD) = 4, loop rating curve. = 5, normal flow computed using Manning's equation. If KD(1) = 1 and NYQD > 0, a single value rating curve is used in which Q is a function of the computed water surface elevation minus the read-in value of STN (card 24).
				KD(2)	= 1 for first tributary (J = 2) except for levee overtopping, KD(J) = 2.
				⋮	
				KD(JN)	= 1 for last tributary (J = JN), except for levee overtopping, KD(J) = 2.

Data Set	Card Number	Column	Format	Variable Name	Description
Repeat card sequence 15 and 16 once for the main river and once for each tributary (i.e. J = 1,. . .,JN)					
C	15	1-10	I10	NRCM1(J)	Number of different Manning n relationships in the main river (J = 1) or the tributaries (J = 2,. . .,JN). If KD(1) = 4 or 5, add one to NRCM1(1) for main river only.
		11-20	I10	NRT1(J)	Total number of observed stage hydrographs along the main river (J = 1) or tributary which is compared with computed water surface elevations (maximum = 9). **Also denotes total number of stations where hydrographs are plotted.**
		21-30	I10	NNYQ(J)	Indicates type of Manning's n relationship. = 0, n is a function of water surface elevation or is constant. = 1, n is a function of discharge.
	16	1-10	I10	NCM(1,J)	Most downstream station number in reach that has the same Manning's n in the J-th river.
		21-30	I10	NCM(2,J) ⋮ NCM(NRCM1(J),J)	For the main river (J = 1), if KD(1) = 4 or 5 (card 14). This last value of NCM for the main river should be one greater than the number of stations on the main river (i.e. NB(1) + 1).
Read in the following sequence of cards 17 and 18 only if observed stage hydrographs are to be compared with computed water surface elevations <u>or</u> if hydrographs are to be plotted. (i.e. (NRT1(J) > 0 on card 15.) Repeat card sequence 17 and 18 for J = 1,. . .,JN.					
D	17	1-10	I10	NT(1,J)	Station number of first observed hydrograph or hydrograph to plot on the J-river. Enter from upstream to downstream.

Data Set	Card Number	Column	Format	Variable Name	Description
D		11-20	I10	NT(2,J)	Station number of next observed hydrograph or hydrograph to plot.
				•	
				•	
				•	
			I10	NT(NRT1(J),J)	
	If stage hydrographs are to be plotted (KPL = 1 on card 5) and observed stage hydrograph is available (KPL2 = 1 on card 5) then read in card 18 (i.e. GZ(K,J); otherwise skip card 18.				
	18	1-10	I10	GZ(1,J)	Gage correction to convert observed stage hydrographs to mean sea level datum.
				•	
				•	
				•	
			I10	GZ(NRT1(J),J)	
The following sequence of cards, 19 and 20, are read in for each hydrograph to be plotted for each location, I = 1,. . .,NRT1(J), for the main river, J = 1, then for each tributary J = 2,. . ., JN. Card 19 is read in if a stage or discharge hydrograph is to be plotted or if observed hydrographs are used.					
	19	1-20	5A4	STTNAM(1,I,J)	20-character name to describe station (cross-section location.
	The following card, 20, is read in if observed stages are available. (KPL > 0 and KPL2 = 1, on card 5)				
	20	1-10	F10.0	STT(1,I,J)	Observed stage for first time interval at the I-th location on the J-th river.
		11-20	F10.0	STT(2,I,J)	Observed stage for the second time interval at the I-th location on the J-th river.
				•	
				•	
				•	
			F10.0	STT(NU,1,J)	Observed stage for the last (NU) time interval.

Data Set	Card Number	Column	Format	Variable Name	Description
Card 21 is used if a mathematical function (NU=0 on card 4) is used to describe the upstream boundary hydrograph.					
E	21	1-10	F10.0	TP	Time in hours from the initial steady flow to the peak.
		11-20	F10.0	RHO	Ratio of peak value of the specified hydrograph to the initial value of the hydrograph.
		21-30	F10.0	GAMMA	Ratio of time from the time of initial steady flow (TP) to the time of the center of gravity (TG) of the specified hydrograph (>1).
		31-40	F10.0	YI	Initial steady discharge or water surface elevation at the upstream boundary.
The following card 22 is used to describe the upstream boundary condition for (NU > 0), i.e. a stage or discharge hydrograph is read in. The following card sequence 22 and 23 are repeated for the main river, then for each tributary J = 2,. . .,JN.					
F	22	1-10	F10.0	ST1(1,J)	Stage or discharge for first time interval for upstream boundary condition for the J-th river.
		11-20	F10.0	ST1(2,J)	Stage or discharge for the second time interval for upstream boundary condition for the J-th river.
				•	
				•	
				•	
				ST1(NU,J)	Stage or discharge for the last (NU) time interval.
	Card 23 is used if the upstream boundary condition is a stage hydrograph, i.e. KU(J) = 1.				
	23	1-10	F10.0	GZ1(J)	Gage correction to convert observed stages at the upstream boundary to a mean sea level datum for the J-th river.

Data Set	Card Number	Column	Format	Variable Name	Description
If the downstream boundary condition is a stage or discharge hydrograph, then it is inputted on card 24.					
F	24	1-10	F10.0	STN(1,1)	Stage or discharge at downstream boundary of the main river for first time interval.
		11-20	F10.0	STN(2,1)	Stage or discharge for second time interval.
				⋮	
			F10.0	STN(NU,1)	Stage or discharge for the last (NU) time interval.
	The following card 25 is used when the downstream boundary condition is a stage hydrograph (KD(J) = 1) or stage-discharge values are entered to describe an empirical rating curve (NYQD > 0) at the downstream boundary.				
	25	1-10	F10.0	GZN	Gage correction to convert stages at the downstream boundary of the main river to mean sea level datum.
	The next cards, 26 and 27, are used to enter the stage-discharge rating curve.				
	26	1-10	F10.0	YQD(1)	Stages to define rating curve for downstream boundary condition. (enter with increasing stage)
		11-20	F10.0	YQD(2)	
				⋮	
			F10.0	YQD(NYQD)	
	27	1-10	F10.0	QYQD(1)	Discharge corresponding to YQD(1) used to define rating curve for downstream boundary conditions of the main river.
		11-20	F10.0	QYQD(2)	Discharge corresponding to YQD(2).
				⋮	
			F10.0	QYQD(NYQD)	Discharge corresponding to YQD(NYQD).

Data Set	Card Number	Column	Format	Variable Name	Description
Repeat the following card (28) for each cross-section I = 1,. . .,NB(J) of the J-th river, i.e. BS(1,I,J), I = 1,. . .,NB(J). Cross-sections are entered from upstream to downstream.					
G	28	1-10	F10.0	BS(1,1,J)	Top width of channel cross-section for the lowest elevation considered in the first cross-section of the J-th channel or river. NCS values are read in for each cross-section going from the bottom to the top of the channel.
		11-20	F10.0	BS(2,1,J)	Top width of the channel cross-section for the next high elevation considered in first cross-section of the J-th channel or river.
				•	
				•	
				•	
			F10.0	BS(NCS,1,J)	If NCS > 8, use an additional card.
Repeat the following card (29) for each cross-section I = 1,. . .,NB(J) of the J-th river. Cross-sections are entered from upstream to downstream.					
	29	1-10	F10.0	HS(1,1,J)	Elevation corresponding to top width BS(1,1,J) in the first cross-section of the J-th river or channel. NCS values are read in for each cross-section going from the bottom to the top.
		11-20	F10.0	HS(2,1,J)	Elevation corresponding to top width BS(2,1,J) in the first cross-section.
				•	
				•	
				•	
			F10.0	HS(NCS,1,J)	If NCS > 8, use an additional card.
	30	1-10	F10.0	AS(1,1,J)	Channel cross-sectional area below HS(1,1,J) or lowest of the HS elevations in the first cross-section of the J-th channel or river.

Data Set	Card Number	Column	Format	Variable Name	Description
G	30	11-20	F10.0	AS(1,2,J)	Channel cross-sectional area below HS(1,2,J) or lowest of the HS elevation in the second cross-section of the J-th channel or river.
		21-30	F10.0	AS(1,3,J)	Channel cross-sectional area below HS(1,3,J) or lowest of the HS elevation in the third cross-section of the J-th channel or river.
				•	
				•	
				•	
			F10.0	AS(1,NB(J),J)	

The above sequence of cards BS(K,I,J), HS(K,I,J), and AS(1,I,J) are inputted for the main river, then repeated for each tributary, J = 2,. . .,JN.

The following cards BSS, HSS, and ASS, define the top width, elevation and off-channel storage area below the lowest of the HS elevations. This sequence, BSS, HSS, and ASS, of cards 31, 32, and 33 are repeated for each cross-section or station that has off-channel storage. The cross-sections that have off-channel storage in the J-th river are defined by the array NCSSS(L,J) (card no. 10) where L = 1,. . .,NCSS1(J) which is the number of stations that have off-channel storage in the J-th river.

If none of the cross-sections have off-channel storage (i.e. NCSSS(L,J) = 0 and NCSS1(J) = 0), then skip the following sequence of cards.

H	31	1-10	F10.0	BSS(1,I,J)	Top width of off-channel storage for elevation HSS(1,I,J) for cross-section I in the J-th river.
		11-20	F10.0	BSS(2,I,J)	Top width of off-channel storage for elevation HSS(1,I,J) for cross-section I in the J-th river.
				•	
				•	
				•	
			F10.0	BSS(NCS,I,J)	Top width of off-channel storage for elevation HSS(NCSS,I,J) for cross-section I in the J-th river.
	32	1-10	F10.0	HSS(1,I,J)	Elevation corresponding to top width BSS(1,I,J).
		11-20	F10.0	HSS(2,I,J)	Elevation corresponding to top width BSS(2,I,J).

Data Set	Card Number	Column	Format	Variable Name	Description
H	32			⋮	
			F10.0	HSS(NCSS,I,J)	Elevation corresponding to top width BSS(NCSS,I,J).
	33	1-10	F10.0	ASS(1,I,J)	Cross-section area of off-channel storage that is below HSS(1,I,J) or the lowest of the HSS elevations for this cross-section.
The following card is used only if the downstream boundary condition is normal flow computed by Manning's equation (with the channel bottom slope used as the energy slope), i.e. KD(1) = 5.					
I	34	1-10	F10.6	SO	Average bottom slope of the main river or channel.
The following sequence of cards, 35, 36, and 37 are inputted for the main river J = 1, then they are repeated for each tributary, J = 2,. . .,JN. If wind is not to be considered, enter 0.0 for values on card 35.					
J	35	1-10	F10.6	COFW	Coefficient of wind stress (suggested value of 1.1×10^{-6} to 3.0×10^{-6}).
		11-20	F10.6	VWIND	Wind velocity in ft/sec. (+ if wind is directed upstream and - if wind is directed downstream).
		21-30	F10.6	WINAGL	Acute angle (degrees) of wind with the channel axis.
	36	1-10	F10.0	X(1,J)	Location of station or cross-section 1 in the J-th river (units are arbitrary since XFACT converts these to feet). The cross-sections are numbered from the upstream to the downstream.
		11-20	F10.0	X(2,J)	Location of station or cross-section 2 in the J-th river.
				⋮	
			F10.0	X(NB(J))	Eight values go on each card so several cards may be required when there are a large number of cross-sections.

Data Set	Card Number	Column	Format	Variable Name	Description
J	37	1-10	F10.0	FKC(1,J)	Expansion or contraction coefficients for cross-section 1 of the J-th river (expansion coefficients vary from -0.3 to -1.0 and contraction coefficients vary from +0.1 to +0.4; use 0.0 for no expansion or contraction effects).
		11-20	F10.0	FKC(2,J)	Expansion or contraction coefficient for cross-section 2 of the J-th river.
				•	
				•	
				•	
			F10.0	FKC(NB(J),J)	Expansion or contraction coefficient for the last downstream cross-section of the J-th river.

The above sequence of cards, 35, 36, and 37, are repeated for each river or channel J = 1,. . .,JN.

If lateral inflows are to be simulated in the J-th river (i.e. NQL(J) > 0), the following sequence of cards, 38 and 39, are repeated for each lateral inflow point and each river or channel.

K	38	1-10	I10	LQ(1,J)	Number of the cross-section at the upstream end of the first Δx reach for which lateral inflow enters.
	39	1-10	F10.0	QL(1,1,J)	Lateral inflow in cfs per Δ reach for the first inflow value at cross-section number LQ(1,J).
		11-20	F10.0	QL(2,1,J)	Lateral inflow in cfs per Δ reach for the second inflow value at cross-section number LQ(1,J).
				•	
				•	
				•	
			F10.0	QL(NU,1,J)	NU values are read in to describe the lateral inflow hydrograph at cross-section number LQ(1,J).

The above cards are repeated for each lateral inflow point for the J-th river, then the next river or channel is considered.

Data Set	Card Number	Column	Format	Variable Name	Description
The following sequence of cards, 40 and 41, are used to define weir flow or levee overtopping in each river. (NWJ(J) > 0)					
L	40	1-10	F10.0	NWJX(1,J)	Number of cross-section at upstream end of first Δx reach in which weir flow or levee overtopping occurs. Cross-section are numbered from upstream to downstream.
		11-20	F10.0	NWJX(2,J)	Number of cross-section at upstream end of second Δx reach in which weir flow or levee overtopping occurs.
				•	
				•	
				•	
			F10.0	NWJX(NWJ(J),J)	Number of cross-section at upstream end of the most downstream reach in which weir flow or levee overtopping occurs, K = 1,. . .,NWJ(J).
	41	1-10	F10.2	HWH(K)	Elevation (ft. msl) of top of levee, ridge line, etc., where weir-flow occurs; elevation is average throughout Δx reach where weir-flow occurs.
		11-20	F10.2	WC(K)	Weir-flow discharge coefficient for Δx reach where weir-flow (inflow or outflow may occur); coefficient ranges from 2.6 to 3.2.
		21-30	F10.2	TFL(K)	Time (hr.) from start of levee failure (crevasse) until the opening or breach is its maximum size.
		31-40	F10.2	BBL(K)	Final width (ft.) of levee crevasse which is assumed to have a rectangular shape.
		41-50	F10.2	HFL(K)	Elevation (ft. msl) of water surface when levee starts to fail.
		51-60	F10.2	HMINL(K)	Final elevation (ft. msl) of bottom of levee crevasse.

The above card, 41, is repeated for each section K = 1,. . .,NWJ(1) for the main river in which weir flow or levee overtopping occurs. Only card 40 is read in thereafter for J = 2,. . .,JN.

Data Set	Card Number	Column	Format	Variable Name	Description
The following sequence of cards, 42 through 51, are used to describe internal boundary conditions (NUMLAD(J) > 0). (Refer to card no. 8 if NUMLAD(J) = 0 for all J=1,. . ., JN, then go to card 51A or 52.)					
M	42	1-10	I10	LAD(1,J)	Number of cross-section at upstream end of Δx reach in which an internal boundary is located. These are entered from upstream to downstream. Negative value of LAD(I,J) is used to indicate an internal boundary condition.
	43	1-10	F10.2	POLTAR(I,J)	-1 for internal boundary condition.
	44	1-10	F10.2	CHCTW(I,J)	Specifies type of internal boundary condition. 0.00 Rating curve $Q_i = f(h_i)$ where h_i is the water surface elevation on upstream side of the internal boundary. 0.01 Rating curve $Q_i = f(h_{i+1})$, for Q_{i+1} > POLTAR(L,J); otherwise a gate rating curve GQ(K,L,J) = f(GFR(K,L,J)) is used where discharge is from the time series GFT(K,L,J) and GFR(K,L,J) is the gate opening. 0.03 Rating curve, $Q_i = f(h_i - h_{i+1})$. 0.05 Bridge internal boundary condition Contracted flow, $Q_i = C_c A_{i+1}(h_i - h_{i+1})^{1/2}$ Orifice flow, $Q_i = C_o A_{i+1}(h_i - h_{i+1})^{1/2}$ Broad-crested weir, $Q_i = S_b C_e(h_i - h_e)^{1/2}$

Data Set	Card Number	Column	Format	Variable Name	Description
M	44	1-10	F10.2	CHCTW(I,J)	(continued)
					C_e is specified as RQI(K,L,J) as a function h_i by RHI(K,L,J).
					$S_b = 1 - 27.8(r - 0.67)^3$ where
					$r = (h_{i+1} - h_e)/(h_i - h_e)$ in which h_e is the weir crest elevation specified by RHI(1,L,K).
					C_c, C_o, h_b are specified by GFT(1,L,J), GFT(2,L,J), and GFT(3,L,J).
					>0.1 Tide gate flow $Q_i = c(h_i - h_{i+1})^{1/2}$ where c is the value of CHCTW(L,J) read in.

The following cards, 45 and 46, are used to input the stage (RHI) discharge (RQI) at each station with an internal boundary condition (i.e. LAD(I,J) < 0 and CHCTW(L,J) < 0.05.

45	1-10	F10.2	RHI(1,I,J)	Stage for the internal boundary condition corresponding to RQI(1,L,J) for the L-th station in the J-th river.
	11-20	F10.2	RHI(2,I,J)	Stage for the internal boundary condition corresponding to RQI(2,1,J).
			• • •	
	71-80	F10.2	RHI(8,I,J)	Eight values of the stage can be entered.
46	1-10	F10.2	RQI(1,I,J)	Discharge corresponding to RHI(1,1,J).
	11-20	F10.2	RQI(2,I,J)	Discharge corresponding to RQI(1,1,J).
			• • •	
	71-80	F10.2	RQI(8,I,J)	Eight values of the stage can be entered.

Data Set	Card Number	Column	Format	Variable Name	Description
The following two cards, 47 and 48, are used only if there is an internal boundary condition specified as a rating curve, i.e. CHCTW(L,J) = 0.01, 0.02, or 0.03.					
M	47	1-10	F10.2	GFR(1,L,J)	Gate setting (horizontal ft. of gate opening) for station L in the J-th river. Horizontal gate opening if CHCTW(L,J) = 0.01; Differential head if CHCTW(L,J) = 0.03.
				• • •	
		71-80	F10.2	GFR(8,L,J)	Eight values can be entered for each station L.
	48	1-10	F10.2	GQ(1,L,J)	Gate discharge corresponding to the gate setting GFR(1,L,J) for station L in the J-th river.
				• • •	
		71-80	F10.2	GQ(8,L,J)	Eight values can be entered for each station L.
	49	1-10	F10.2	GTF(1,L,J)	Gate setting (horizontal ft. of gate opening) time series for first time. If CHCTW(L,J) = 0.05 enter C_c, contracted flow coefficient.
		11-20	F10.2	GFT(2,L,J)	Gate setting of time series for second time. If CHCTW(L,J) = 0.05 enter C_o, orifice coefficient.
		21-30	F10.2	GFT(3,L,J)	Gate setting of time series for third time. If CHCTW(L,J) = 0.05 enter h_b, elevation of bridge deck.
				• • •	
		71-80	F10.2	GFT(NU,L,J)	NU values are used if a time series is read in. If NU > 8, use more than one card.
M	50	1-10	F10.2	POOLT(1,L,J)	Target pool elevation for each time step. If 0.0 is entered, then POLTAR(L,J) is used for POOLT(K,L,J).
				• • •	
			F10.2	POOLT(NU,L,J)	

Data Set	Card Number	Column	Format	Variable Name	Description
M	51	1-10	I10	ITWT(1,L,J)	Indicates if gates control the flow for the first time period for the L-th station in the J-th river. If = 0, flow is controlled by gates. If = 1, flow is not controlled by gates (channel controlled).
				•	
				•	
				•	
			I10	ITWT(NU,L,J)	NU values are entered.

The above cards, 42 through 51, are repeated for each station L = 1,. . .,NUMLAD(1) for the main river, then are repeated for each tributary J = 2,. . .,JN.

The following cards are used to describe the gate internal boundary conditions (i.e. NG(J) > 0 on card number 8A. Cards 51A through 51D are inputted for each gate K = 1,. . .,NG(J) for each river J = 1,. . .,JN.

	51A	1-10	I10	LGX(K,J)	Sequence number of cross-section immediately upstream of gate internal boundary.
		11-20	I10	IGT(K,J)	Parameter indicating the type of gate: IGT(K,J) = 1, the gate has a continuous bottom slope; IGT(K,J) = 2, the gate has a discontinuous bottom slope; IGT(K,J) = 0, the location is a critical flow section.
		21-30	I10	NTG(K,J)	Number of values in the table of gate coefficient (GC) vs. tailwater head (DTW).
		31-40	F10.2	HGC(K,J)	Gate correction parameter used to correct the height of the gate opening.

The following cards, 51B, 51C, and 51D, are ommitted if the section is a critical flow section (i.e. IGT(K,J) = 0) on card 51A.

	51B	1-10	F10.2	GC(1,K,J)	Gate discharge coefficient determined by multiplying the width of the gate by the loss factor.

Data Set	Card Number	Column	Format	Variable Name	Description
M	51B	11-20	F10.2	GC(2,K,J)	
				⋮	
			F10.2	GC(NTG(K,J),K,J)	
	51C	1-10	F10.2	DTW(1,K,J)	Tailwater head corresponding to each gate discharge coefficient.
			F10.2	DTW(NTG(K,J),K,J)	
	51D	1-10	F10.2	HG(1,K,J)	Height of gate opening for time interval 1.
				⋮	
			F10.2	HG(NU,K,J)	Height of gate opening for time interval NU.

The above cards, 51A through 51D, are repeated for each gate K = 1,. . .,NG(J) for each river J = 1,. . .,JN.

N	52	1-10	F10.2	TE	Time in hours when the routing computations terminate.
			F10.2	TM	Maximum size of the computational time step Δt in hours.
			I10	KITPR	Number of computational time step intervals at which computed values are stored for plotting and/or printing.

Data Set	Card Number	Column	Format	Variable Name	Description
The following cards, 53 and 54, are used to input the initial conditions. The initial water surface elevations are entered for each station of the first river and are entered from upstream to downstream. The initial water surface elevations can be determined by a steady flow backwater analysis by entering the initial water surface at the downstream boundary and zeros for the remaining stations and entering the initial discharge for the first upstream cross-section and zeros for the remaining stations.					
N	53	1-10	F10.0	YDI(1,J)	Initial water surface elevation at station 1 in the J-th river.
		11-20	F10.0	YDI(2,J)	Initial water surface elevation at station 2 in the J-th river.
				• • •	
			F10.0	YDI(NB(J),J)	Initial water surface elevation at the downstream end of the river.
	The above card, 53, is repeated for each river J = 1,. . .,JN.				
	54	1-10	F10.0	QDI(1,J)	Initial discharge at station 1 in the J-th river. Discharge corresponding to YDI(1,J).
		11-20	F10.0	QDI(2,J)	Initial discharge corresponding to YDI(2,J).
				• • •	
			F10.0	QDI(NB(J),J)	Initial discharge corresponding. . . .
The above card, 54, is repeated for each river J = 1,. . .,JN.					
The following cards, 54A, 54B, and 54C, are only used if the channel network option is considered (i.e. NET = 1 or 2) and are ommitted if NET = 0 or if QDI(2,1) not equal to zero and NET ≥ 1.					
	54A	1-10	I10	NR	Number of separate channels or branches in the system.

Data Set	Card Number	Column	Format	Variable Name	Description
Branches are ordered from upstream to downstream to downstream with the last entry being the main or principal channel.					
N	54B	1-10	I10	NIRB(1)	Number of nodes in each channel or branch beginning with the most upstream.
				•	
				•	
				•	
			I10	NIRB(NR)	Number for most downstream node.
The following card, 54C, is repeated for each branch (k = 1,. . .,NR).					
	54C	1-10	I10	IRB(1,K)	Sequential number of node in the branch; node numbers commence at upstream end of each branch and proceed in the downstream direction until the last node of the branch is reached.
				•	
				•	
				•	
			I10	IRB(NIRB(K),K)	
The following cards, 55 and 56, are used to input the Manning's roughness factor (n) as a function of either water surface elevation or discharge. Card 55 is repeated for each of the different NRCM1(J) Manning's n relationships used in the main river, then is repeated for each tributary J = 2,. . .,JN.					
O	55	1-10	F10.0	YQCM(1,K,J)	Water surface elevation or discharge associated with the Manning's roughness factor CM(1,K,J). These values are entered with increasing water surface elevations or discharges.
		11-20	F10.0	YQCM(2,K,J)	
				•	
				•	
				•	
			F10.0	YQCM(NCML,K,J)	NCML values are used for each station.

Data Set	Card Number	Column	Format	Variable Name	Description
0	56	1-10	F10.0	CM(1,K,J)	Manning's n value associated with the water surface elevation or discharge YQCM(1,K,J).
		11-20	F10.0	CM(2,K,J)	
				⋮	
			F10.0	CM(NCML,K,J)	NCML values are used for each station.
Card 56 is repeated for each of the different NRCM1(J) Manning's n relationships used in the main river, then is repeated for each tributary, J = 2,. . .,JN.					
P	57	1-80	20A4	MESSAGE	Maximum of an 80 character message which is written at the end of the input data deck.
	58	1-4	A4	END	END indicating end of the input data deck.
	59	1-4	A4	EXIT	EXIT

SECTION 9.0

APPLICATION TO WALLER CREEK, TEXAS AND

PROPOSED FLOOD BY-PASS TUNNEL

by

Larry W. Mays

9.1 INTRODUCTION

BACKGROUND

The portion of the Waller Creek watershed from 12th Street to Town Lake is one of the most expensive commercial development areas in the City of Austin, Texas. This area is also one of the most scenic areas with the vast hike and bike trails in and along the Creek. This area is undergoing rapid development with several new high rise buildings and several either under construction or in the planning and design phase.

This portion of the Waller Creek watershed downstream of 12th Street is also one of the most flood prone areas in the City of Austin. Many structures are built below the 100 year flood elevation and are subject to extreme flooding. The purpose of this project is to study the feasibility of a major flood bypass tunnel to divert flood flows upstream of the highly developed area out of the creek and in to Town Lake.

To the investigators knowledge this type of study has never been performed on such a tunnel in Texas. Due to the possible size and expense of such a tunnel, the investigators chose to use the most highly developed state-of-the-art methods and, in most cases, more sophisticated technology than is normally used in hydrologic and hydraulic design and analysis procedures in Austin.

SCOPE OF WORK

The overall objective of this study has been to determine the engineering and economic feasibility of constructing a flood bypass tunnel for the lower portion of Waller Creek in Austin, Texas. This lower portion refers to Waller Creek downstream of 15th Street. The purpose of the proposed tunnel is to divert flood flows from Waller Creek in order to reduce flood levels along Waller Creek downstream of 15th Street.

This study has involved several major phases, many of which have been worked on simultaneously. These are briefly described as follows with more detailed descriptions provided in the appropriate section of this report:

1. Preliminary analysis to identify possible tunnel alignments, flood plain and channel characteristics, soil characteristics, possible location for inlet and outlet structures, etc.

2. Perform a hydrologic analysis of the Waller Creek watershed to determine the rainfall-runoff characteristics in the lower portion of Waller Creek. In particular, the U.S. Army Corps of Engineers HEC-1 computer program for rainfall-runoff analysis was used to determine runoff hydrographs for various return period storms. The results of this study are briefly described in Section 3.0 of this report and are given in detail in the preliminary report "Flood Plain Hydrology Study of Waller Creek Watershed" by Hydrosystems Engineering, Inc. and Camp Dresser & McKee Inc.

3. A hydraulic analysis for the portion of Waller Creek from 15th Street to Town Lake was performed to determine the steady-state water surface profiles for various return period flows. This analyis identified the extent of flood elevations for the various flow rates. The U.S. Soil Conservation Service computer program WSP2, for water surface profile determination was used. The results of this study are briefly described in Section 4.0 of this report and are described in detail in the preliminary report "Flood Plain Hydraulics Study of Waller Creek" by Hydrosystems Engineering, Inc. and Camp Dresser & McKee Inc.

4. A hydraulic transient analysis was performed to determine the amount of diversions and resulting unsteady flow effects in Waller Creek downstream of the preliminary tunnel intake structure location. The U.S. National Weather Service computer program, DWOPER, was used to perform this unsteady flow analysis. The results of this study, defining the diversion hydrographs for various intake structures sizes, are briefly described in Section 5.0 of this

report and are described in detail in the report "Hydraulic Transient Analysis and Conceptual Design of Tunnel" by Hydrosystems Engineering, Inc. and Camp Dresser & McKee Inc.

5. Preliminary designs of the tunnel were performed using a steady-state type analysis. Both a pipe flow (pressurized) tunnel design and an open channel flow tunnel design were considered. Results of these designs are presented in Section 6.0 of this report and are described in detail in the report "Hydraulic Transient Analysis and Conceptual Design of Tunnel".

6. A hydraulic transient analysis was performed for several tunnel diameters for both pressurized and open channel flow tunnel designs. The results of this study are presented in Section 7.0 of this report and are presented in more detail in the report "Hydraulic Transient Analysis and Conceptual Design of Tunnel".

7. Several types of intake and outlet structures were considered for the tunnel design. Conceptual designs of these structures are presented in Section 8.0. In addition, a dewatering system was conceptually designed for the pressurized tunnel design.

8. A comparison of the various tunnel designs and flood level reductions for these particular designs are presented in Section 9.0 of this report.

9. Other major factors that were involved in this study included a backwater analysis of Town Lake to determine the various return period water surface elevations in Town Lake in the vicinity of the proposed outlet structure. The U.S. Army Corps of Engineers HEC-2 computer program was used in this analysis. The data base was obtained from the Ft. Worth District of the U.S. Army Corps of Engineers. A preliminary survey of the utility locations was performed. Also, a preliminary evaluation of traffic was made. The results of the above analysis and surveys are presented in Section 10.0 of this report.

10. A preliminary geotechnical investigation was performed by Frank G. Bryant and Associates, Inc. Section 11.0 and parts of Section 12.0 summarize this study and more detailed results are presented in the report "Preliminary Geotechnical Investigation of Waller Creek Flood Control Tunnel" by Frank G. Bryant & Associates, Inc.

11. A preliminary assessment of the design and construction aspects has been made and are presented in Section 12.0 with more detail in the report "Feasibility Report, Waller Creek Flood Control Tunnel, City of Austin, Texas" by Jenny Engineering Corporation.

12. A preliminary cost estimate study has also been made by Jenny Engineering Corporation. The results of this study are presented in Section 13.0 with more detailed back-up data in the feasibility report by Jenny Engineering Corporation.

13. Section 15.0 presents several recommendations that should be considered for the final design phase of this project.

9.2 HYDRAULIC TRANSIENT ANALYSIS OF WALLER CREEK

TRANSIENT MODELING OF WALLER CREEK

A rather detailed transient analysis of Waller Creek is required because of the complex nature of the hydraulic transient properties of a flood wave propogating down Waller Creek with many constrictions in flow due to the bridges. The transient analysis was performed in order to develop a better understanding of:

1. the transient nature of flood waves attenuating down Waller Creek under existing conditions;

2. the transient nature of flood waves being reduced in size downstream of a proposed tunnel intake;

3. the downstream hydraulic effect in the creek of various intake structure designs including weir lengths, orifice openings, weir heights, etc.;

4. to determine the diverted volume and peak discharge diversion required by the tunnel to reduce discharges to non-damaging levels in Waller Creek downstream of the tunnel;

5. to determine the hydraulic effect of channel modification and bridge modification to reduce flood levels in Waller Creek.

The following steps were required to model Waller Creek using the transient model:

1. The input model was first developed for the Creek from 15th Street to Town Lake excluding the street bridges and the foot bridges.

2. Next the intake structure was modeled as a diversion. The model simulates the amount of flow diverted on the basis of the current simulated creek elevation.

3. In order to model the street and foot bridges, internal boundary conditions were developed which consisted of discharge versus head-loss relationships for each bridge. The development and resulting relationships for each bridge between 15th Street and Town Lake are presented in the report "Hydraulic Transient Analysis and Conceptual Design of Tunnel" by Hydrosystems Engineering Inc. and Camp Dresser & McKee Inc.

4. The internal boundary conditions (discharge versus headloss) were then incorporated in the model of Waller Creek.

5. The completed transient model was run for various intake structure sizes and elevations.

The various cross-section locations are shown in Figure 9.1. Each cross-section is described using a top width-elevation relationship. The upstream boundary is at 15th Street and the downstream boundary location is at Town Lake.

The upstream boundary condition is the discharge hydrograph (Table 9.1) at 15th Street for the 100-year runoff hydrograph determined using the U.S. Army Corps of Engineers HEC-1 computer program. The downstream boundary condition is a rating curve derived from the steady state water surface profile analysis using WSP2.

The rating curve for the downstream boundary condition is listed in Table 9.2. The lateral inflows (subarea runoff hydrographs determined from the rainfall-runoff analysis using HEC-1) were modeled at the appropriate locations along the creek. Lateral inflow points were at sections 9, 18, 27, 36 and 64.

Manning's n versus discharge relationships were used to describe the roughness characteristics of the channel and flood plain. These roughness values are described by the n vs Q relationship listed in Table 9.3.

Table 9.1

Discharge Hydrograph at 15th Street
(Upstream Boundary Condition)*

Time Hr.	Time Min.	Discharge (cfs)
	0	500.
	10	686.
	20	1227.
	30	2341.
	40	4157.
	50	5979.
1	00	7350.
	10	8264.
	20	8764.
	30	8863.
	40	8588.
	50	8020.
2	00	7259.
	10	6361.
	20	5367.
	30	4373.
	40	3464.
	50	2674.
3	00	2012.
	10	1474.
	20	1050.
	30	725.
	40	500.

*Derived from rainfall-runoff analysis with 100-year rainfall. Using the U.S. Army Corps of Engineers HEC-1 computer program.

Table 9.2

Rating Curve for Downstream Boundary Condition*

Water Surface Elevation (ft. M.S.L.)	Discharge (cfs)
428.9	0.
429.0	1000.
429.3	2000.
430.1	3000.
430.7	4000.
432.4	5444.
433.5	7035.
440.4	9424.

*Derived from steady-state analysis of water surface profiles using the U.S. Soil Conservation Service WSP2 computer program.

Table 9.3

Characteristics of Simulation Model for Waller Creek

Initial discharge = 500 cfs

Routing time interval = 0.006 hours

Total of 15 internal boundary conditions to describe bridges.

Total number of cross-sections = 67

Downstream boundary condition is rating curve from steady state analysis.

Intake structure weir elevation = 475 ft.

Intake structure weir lengths simulated = 150 ft., 200 ft., and 270 ft.

Weir location between cross-section 6 and 8 using two sections to describe the weir.

Weir coefficient = 2.6

Manning's n relationships:

Manning's n	Discharge (cfs)
0.1	0
0.09	1000.
0.075	3000.
0.09	10000.

Various initial discharges were considered to determine the smallest discharge that could be simulated and still maintain stability. The DWOPER model determines the initial conditions (water surface elevation, velocities, etc.) at each section using a backwater analysis procedure that satisfies the St. Venant equations. For small discharges (less than 500 cfs) the flows at several locations in the creek are supercritical and can cause instability problems. The creek is fairly steep with a slope of 0.006 ft/ft or 31.7 ft/mile.

One of the greatest difficulties in the modeling process was incorporation of the internal boundary condition to simulate the flow through the bridges. At first the bridges were modeled using the procedure for the bridge internal boundary using the orifice flow or contracted flow through the bridge opening and broad crested weir flow over the road embankment. This procedure resulted in stability problems due to the flow being critical or supercritical just downstream of some of the bridges for some ranges of the discharges. In order to determine the coefficients for the flow equations it would be necessary to use the rating curves for each bridge determined from the backwater analysis using the U.S. Soil Conservation Service WSP2 computer program. These ratings were essentially generated when the computer simulation were performed to determine the internal boundary conditions. However, to determine the coefficients for the flow equation using these rating curves, would require additional extrapolation of information. Instead it was felt that using the differential head over the bridge versus discharge would be more accurate. Several of these relationships showed somewhat erratic results requiring smoothing of the relationships. The input for the Waller Creek model is given in the report "Hydraulic Transient Analysis and Conceptual Design of Tunnel" by Hydrosystems Engineering, Inc. and Camp Dresser & McKee Inc.

INTERNAL BOUNDARY CONDITIONS FOR BRIDGES

The DWOPER model can incorporate bridges using four different types of internal boundary conditions: a) rating curve, $Q_i = f(h_i)$, where h_i is the water surface elevation at the upstream side of the bridge; b) rating curve, $Q_i = f(h_{i+1})$, where h_{i+1} is the water surface elevation at the

downstream end of the bridge; c) rating as a differential head, $Q_i = f(h_i - h_{i+1})$; and d) as a contracted flow or orifice flow through the bridge and broad-crested weir flow over the road embankment.

The rating curve for the bridge differential heads was used because greater accuracy could be obtained, especially because of the extensive work performed in this project using the steady-state backwater model WSP2 which simulated bridge hydraulics. The WSP2 model was used to simulate the steady-state backwater profiles for Waller Creek using several different discharges. The discharge-differential head relationships

$$Q_i = f(h_i - h_{i+1}) = f(\Delta h)$$

were determined for each of the street bridges and foot bridges from 15th Street to Town Lake. These relationships are presented in the report "Hydraulic Transient Analysis and Conceptual Design of Tunnel".

RESULTS OF MODELING EFFORT

This section describes the results of some of the simulations performed using the unsteady flow model of Waller Creek. For the purposes of this report, the simulations are used to determine the hydraulic effect in Waller Creek of using different tunnel intake designs. The DWOPER model output lists the hydraulic properties (water surface elevations, depth, velocity, Froude number, etc.) at each cross-section for each computational time interval. This essentially provides a complete picture of the flow properties throughout the creek at many times during the floodwave movement or propagation downstream. When the tunnel is modeled, then a very good description of the hydraulics in the creek downstream of the tunnel intake can be developed. This information can be used to determine the tunnel intake design and amount of flow that must be diverted to reduce flood levels in the creek below non-damaging levels.

WITH TUNNEL DIVERSIONS

The hydraulic effects in Waller Creek of using various intake structure designs (weir lengths and weir elevations) are presented. The first simulation used an intake structure design with a spillway crest (weir) length of 270 feet at an elevation of 475 feet above mean sea level. Location of the intake structure is between cross-sections 6 and 8 (in Waterloo Park above 12th Street) so that the intake for the tunnel alignment along Trinity Street is considered.

Discharge hydrographs at various locations along Waller Creek are listed in Table 9.4. The discharge hydrograph for the tunnel diversion is listed in Table 9.5.

Intake structures with weir lengths of 200 feet and 150 feet were also used to illustrate the hydraulic effects of these size structures. The resulting discharge hydrographs at various locations are presented in Tables 9.6 and 9.7. The discharge hydrographs for the diversion are listed in Table 9.5.

All the above simulations considered two sections to describe the weir length. An additional run was made considering the 200 ft. weir described by one section. A comparison of the diverted (tunnel) flows are presented in Table 9.8.

Table 9.9 lists the diverted (tunnel) flows for the following weir lengths: 50ft., 75 ft., 100 ft., 125 ft., and 200 ft.

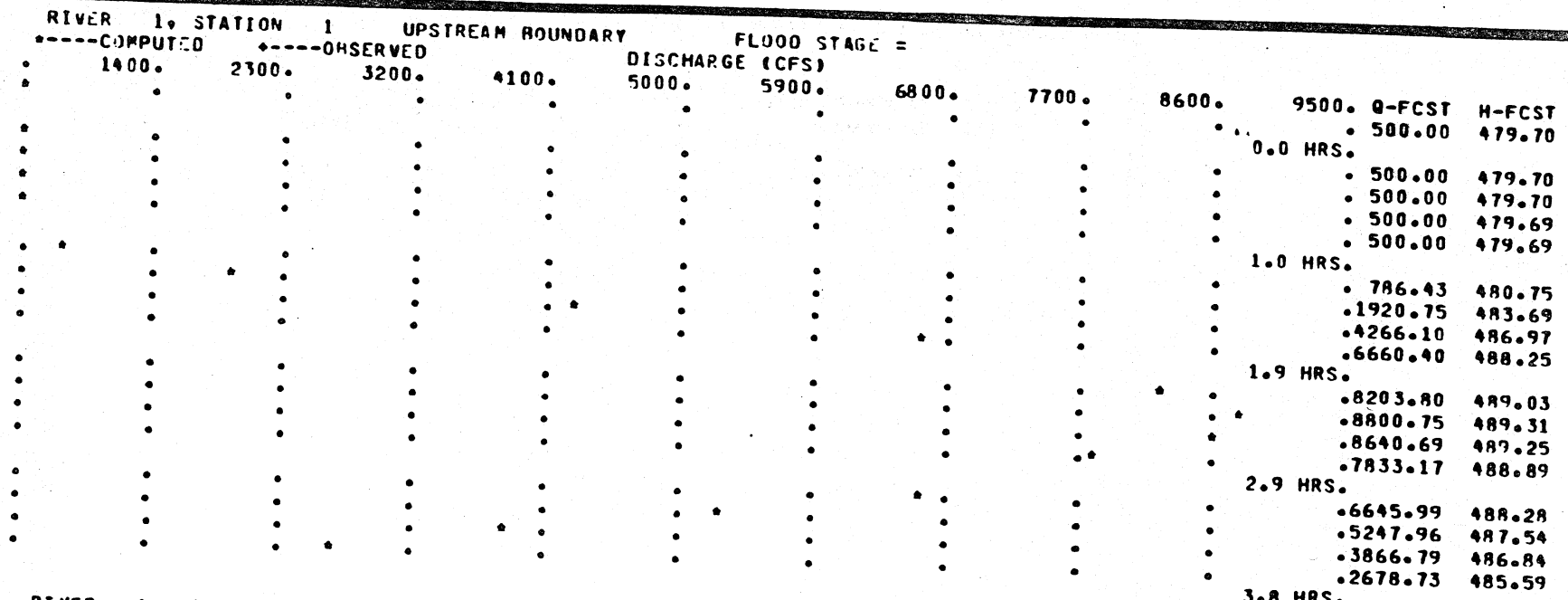

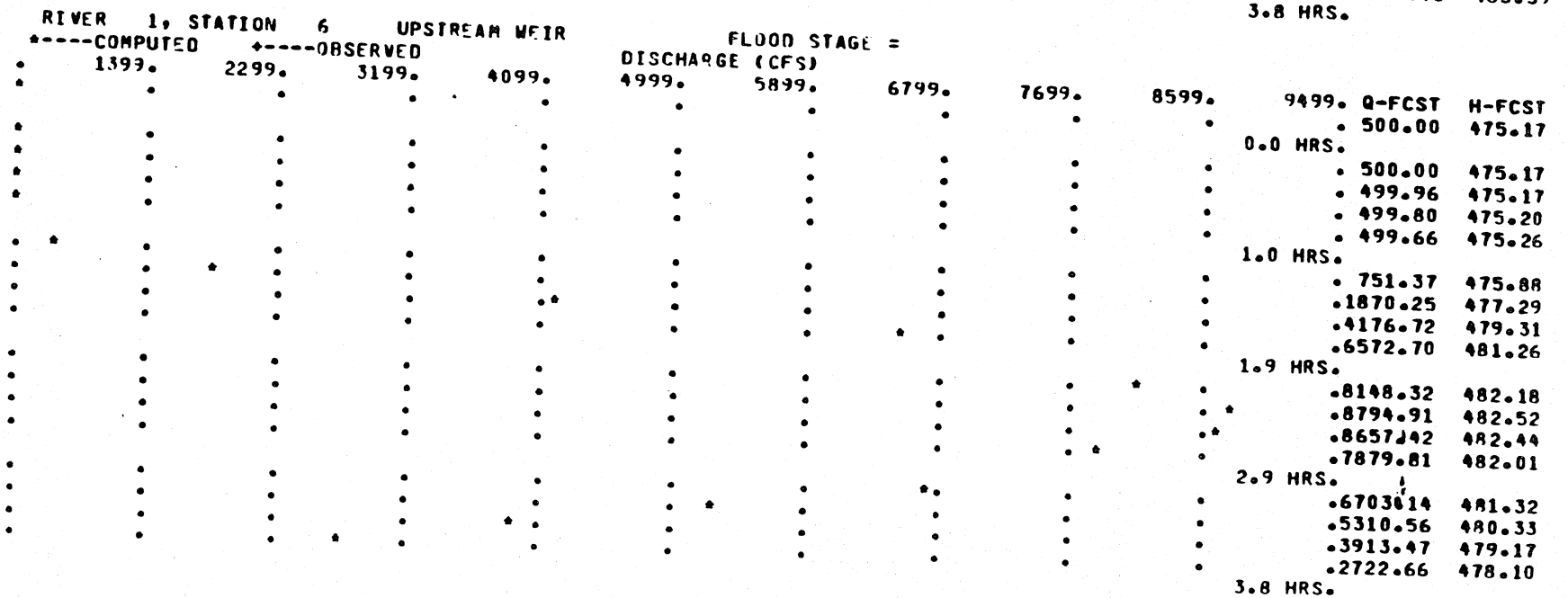

Table 9.4 Discharge Hydrographs at Various Locations (270' Weir)

RIVER 1, STATION 7 DOWNSTREAM WEIR FLOOD STAGE =

*----COMPUTED *----OBSERVED

DISCHARGE (CFS)

899.	1299.	1699.	2099.	2499.	2899.	3299.	3699.	4099.	4499.	Q-FCST	H-FCST
										499.99	474.59
									0.0 HRS.		
										500.00	474.59
										499.88	474.59
										499.43	474.64
										499.05	474.73
									1.0 HRS.		
										581.12	475.30
										1020.32	476.27
										1979.48	477.44
										2826.52	478.40
									1.9 HRS.		
										3504.07	478.99
										3793.07	479.23
										3736.76	479.19
										3404.80	478.92
									2.9 HRS.		
										2906.37	478.48
										2399.46	477.90
										1883.87	477.29
										1413.58	476.73
									3.8 HRS.		

RIVER 1, STATION 8 DOWNSTREAM WEIR FLOOD STAGE =

*----COMPUTED *----OBSERVED

DISCHARGE (CFS)

608.	718.	828.	938.	1048.	1158.	1268.	1378.	1488.	1598.	Q-FCST	H-FCST
										499.99	473.96
									0.0 HRS.		
										500.00	473.96
										499.78	473.97
										498.95	474.04
										498.35	474.17
									1.0 HRS.		
										573.76	474.72
										675.59	475.66
										852.80	476.88
										1109.68	477.34
									1.9 HRS.		
										1352.01	477.69
										1461.47	477.83
										1472.32	477.74
										1407.64	477.47
									2.9 HRS.		
										1304.[illegible]8	477.04
										1223.96	476.60
										1085.19	476.18
										934.78	475.75
									3.8 HRS.		

Table 9.4 (continued)

RIVER 1, STATION 19 9TH STREET FLOOD STAGE =

*----COMPUTED *----OBSERVED DISCHARGE (CFS)

799.	1099.	1399.	1699.	1999.	2299.	2599.	2899.	3199.	3499.	Q-FCST	H-FCST
										499.96	461.96
									0.0 HRS.		
										500.69	461.96
										514.41	462.02
										567.97	462.25
										663.94	462.63
									1.0 HRS.		
										879.20	463.47
										1450.37	464.94
										2254.49	466.62
										2133.55	466.47
									1.9 HRS.		
										1980.18	466.14
										1891.33	465.96
										1780.43	465.74
										1652.38	465.48
									2.9 HRS.		
										1487.03	465.13
										1291.10	464.66
										1117.95	464.22
										958.33	463.78
									3.8 HRS.		

RIVER 1, STATION 28 6TH STREET FLOOD STAGE =

*----COMPUTED *----OBSERVED DISCHARGE (CFS)

799.	1099.	1399.	1699.	1999.	2299.	2599.	2899.	3199.	3499.	Q-FCST	H-FCST
										499.97	451.77
									0.0 HRS.		
										501.10	451.77
										520.90	451.85
										597.42	452.16
										735.04	452.65
									1.0 HRS.		
										1004.27	453.46
										1740.74	455.11
										2848.00	456.68
										2603.53	456.41
									1.9 HRS.		
										2265.61	455.90
										2083.83	455.60
										1923.60	455.34
										1768.28	455.08
									2.9 HRS.		
										1581.96	454.74
										1333.09	454.22
										1147.54	453.79
										983.38	453.37
									3.8 HRS.		

Table 9.4 (continued)

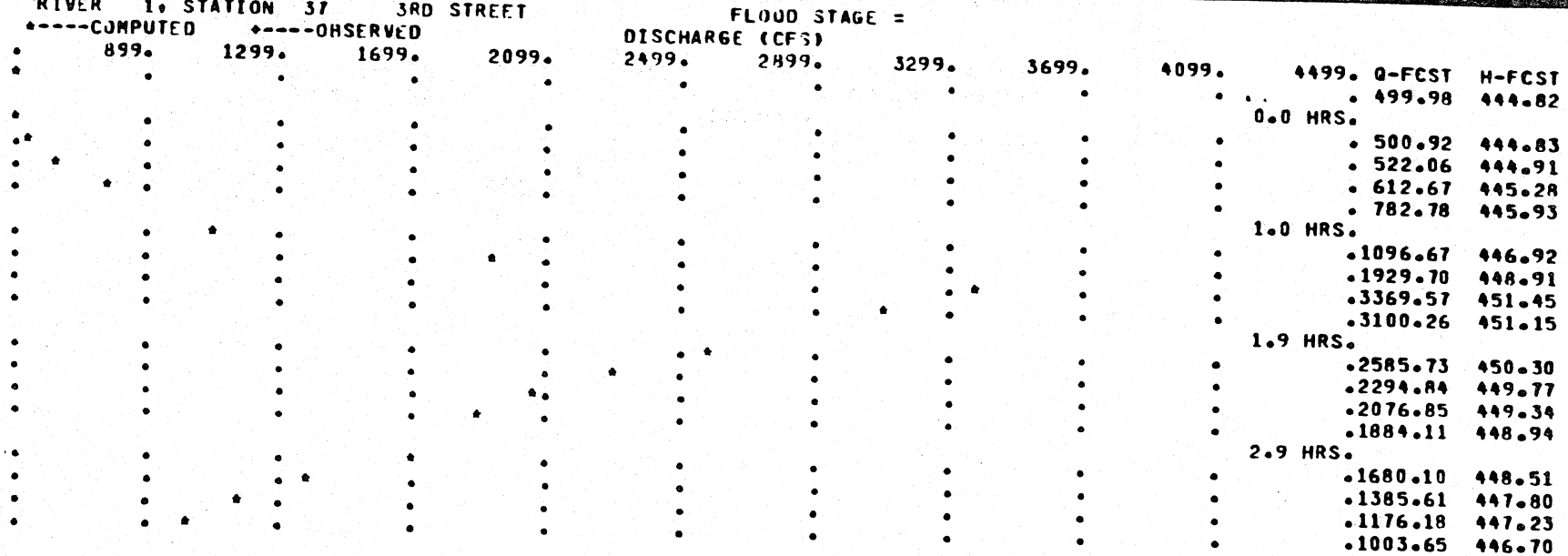

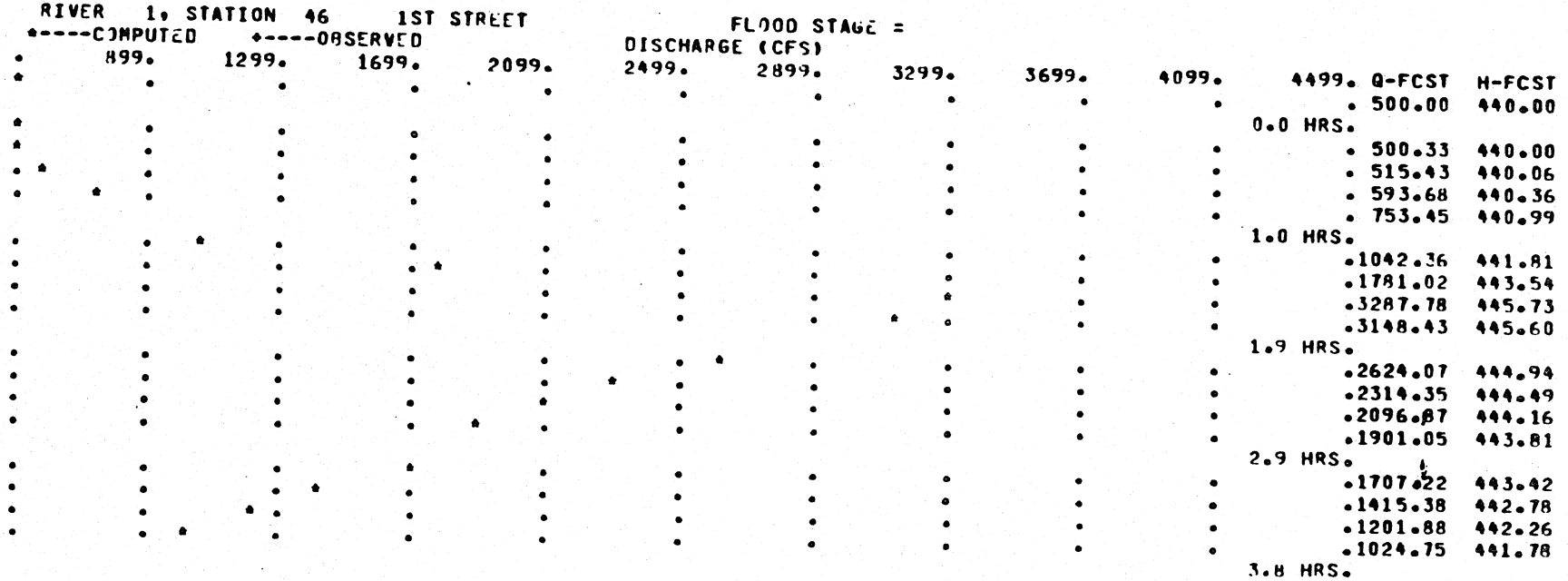

Table 9.4 (continued)

RIVER 1, STATION 67 DOWNSTREAM BOUNDARY FLOOD STAGE =

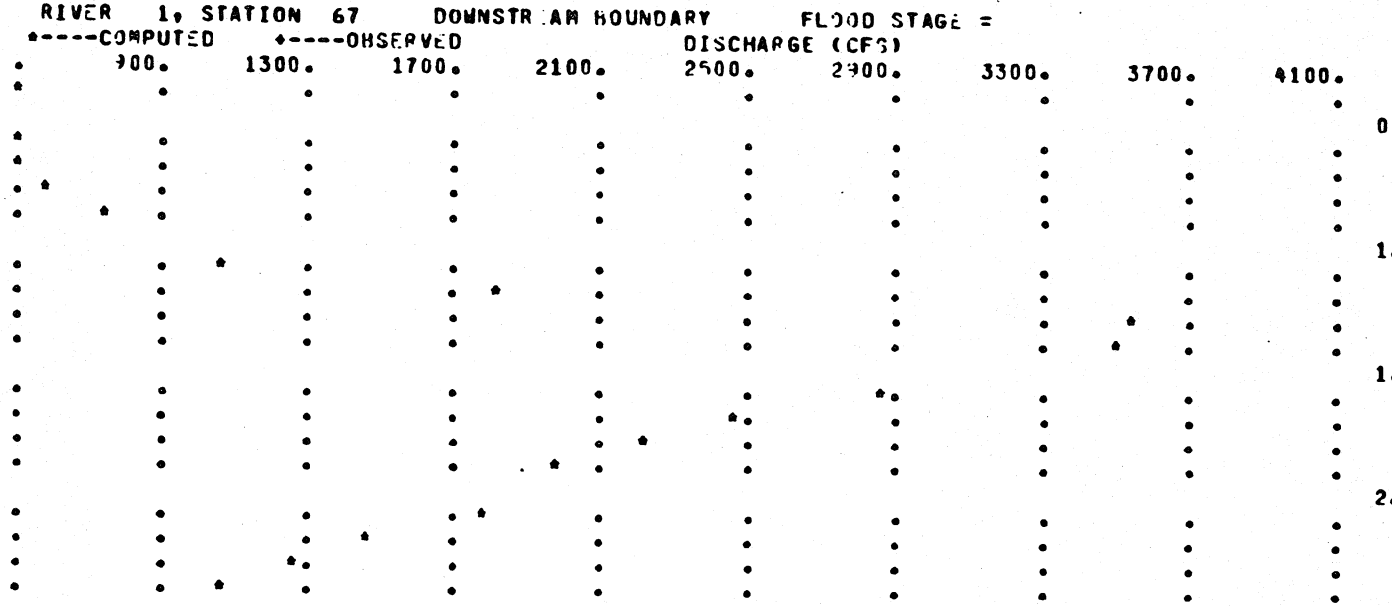

Q-FCST	H-FCST
500.06	428.95
0.0 HRS.	
500.44	428.95
512.36	428.95
589.56	428.96
752.87	428.98
1.0 HRS.	
1063.36	429.02
1817.54	429.25
3552.63	430.43
3515.41	430.41
1.9 HRS.	
2865.47	429.99
2468.60	429.67
2210.43	429.47
1990.92	429.30
2.9 HRS.	
1789.22	429.24
1476.29	429.14
1242.07	429.07
1051.97	429.02
3.8 HRS.	

Table 9.4 (continued)

Table 9.5

Tunnel Diversion Flows for Various Weir Lengths

Time (hr)	Diverted* Discharge (L = 150 ft) (cfs)	Diverted* Discharge (L = 200 ft) (cfs)	Diverted* Discharge (L = 270 ft) (cfs)
0.0	0.0	0.0	0.0
0.24	103.4	135.8	177.6
0.48	953.8	1074.2	1195.0
0.72	2721.2	3066.2	3323.9
0.96	4442.5	4967.4	5463.0
1.20	5822.5	6156.1	6796.3
1.44	6280.5	6640.3	7333.4
1.68	6151.8	6503.7	7185.1
1.92	5580.6	5879.7	6472.2
2.16	4593.4	4929.6	5398.7
2.40	3381.0	3776.2	4086.6
2.64	2381.6	2630.7	2828.3
2.88	1498.7	1639.1	1787.9

*Co = 2.6
Crest elevation = 475 ft. M.S.L.

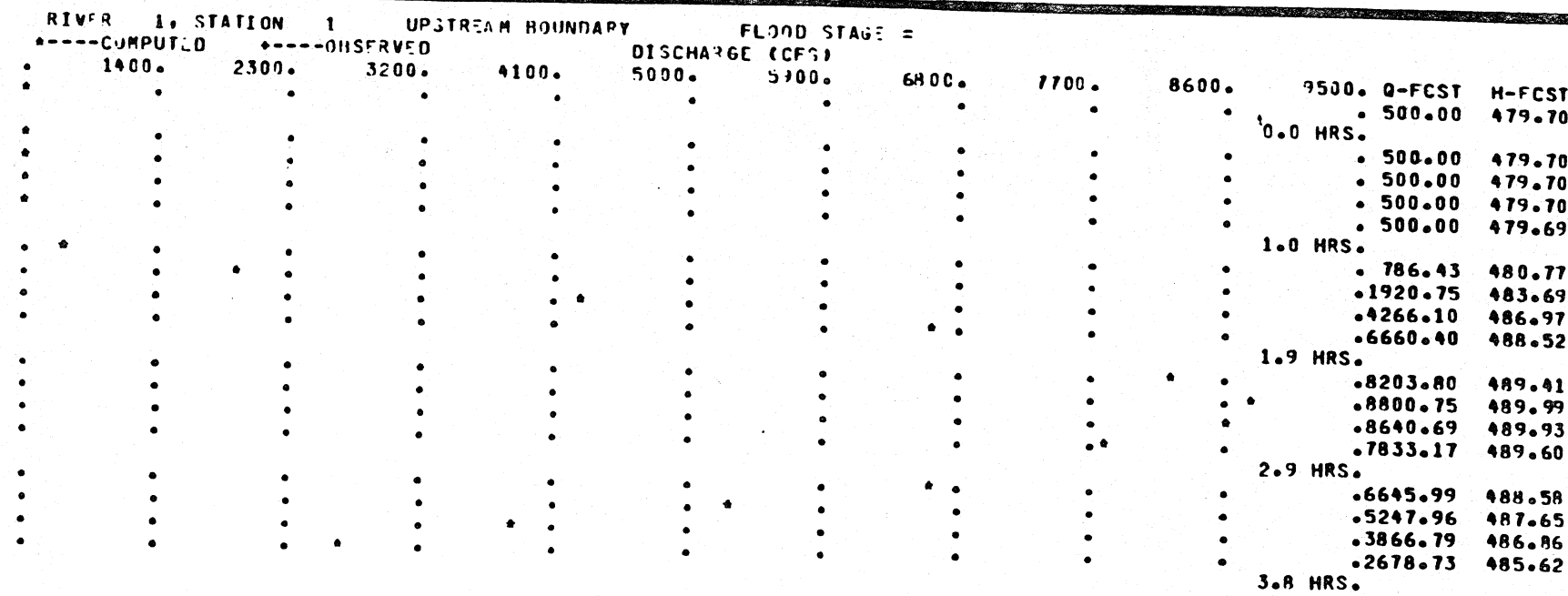

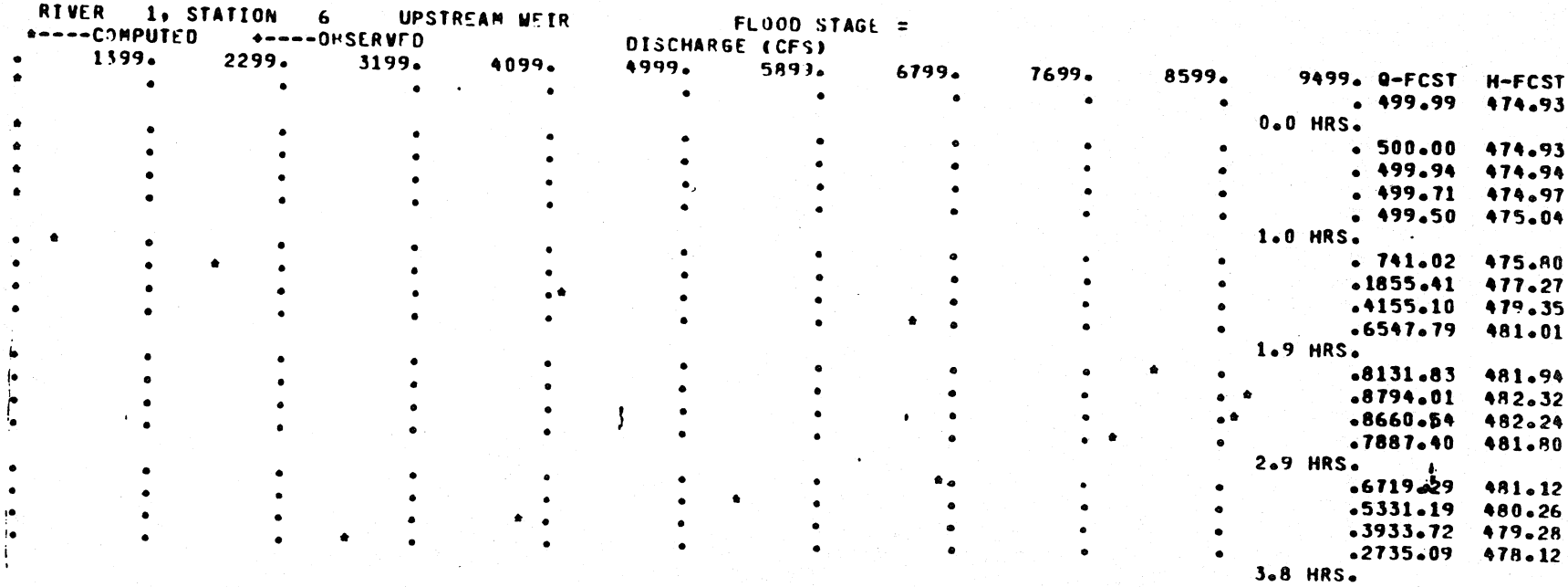

Table 9.6 Discharge Hydrographs at Various Locations (200' Weir)

RIVER 1, STATION 7 DOWNSTREAM WEIR FLOOD STAGE =

*----COMPUTED *----OBSERVED

DISCHARGE (CFS)

999.	1499.	1999.	2499.	2999.	3499.	3999.	4499.	4999.	5499.	Q-FCST	H-FCST
										499.99	474.44
									0.0 HRS.		
										500.00	474.44
										499.87	474.45
										499.39	474.50
										499.01	474.60
									1.0 HRS.		
										620.25	475.34
										1166.76	476.51
										2313.42	477.97
										3579.51	479.10
									1.9 HRS.		
										4468.11	479.71
										4852.80	479.94
										4779.94	479.89
										4350.02	479.62
									2.9 HRS.		
										3705.86	479.14
										2954.86	478.51
										2224.16	477.77
										1661.85	477.05
									3.8 HRS.		

RIVER 1, STATION 8 DOWNSTREAM WEIR FLOOD STAGE =

*----COMPUTED *----OBSERVED

DISCHARGE (CFS)

698.	898.	1098.	1298.	1498.	1698.	1898.	2098.	2298.	2498.	Q-FCST	H-FCST
										499.98	473.96
									0.0 HRS.		
										500.00	473.96
										499.79	473.97
										499.03	474.04
										498.46	474.17
									1.0 HRS.		
										605.16	474.87
										780.80	476.04
										1088.88	477.59
										1580.41	478.66
									1.9 HRS.		
										1975.72	479.30
										2153.68	479.57
										2156.84	479.46
										2007.70	479.06
									2.9 HRS.		
										1794.73	478.45
										1554.95	477.67
										1302.97	476.91
										1095.90	476.33
									3.8 HRS.		

Table 9.6 (continued)

RIVER 1, STATION 19 9TH STREET

*----COMPUTED *----OBSERVED

FLOOD STAGE =

DISCHARGE (CFS)

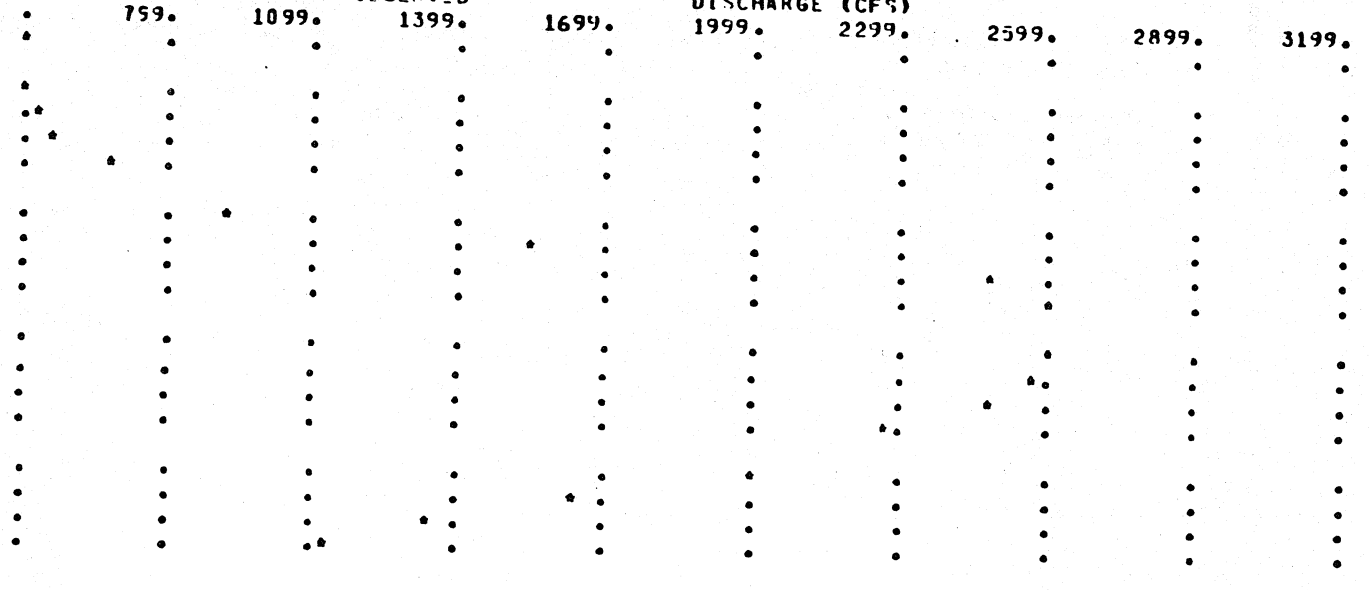

	Q-FCST	H-FCST
	499.95	461.96
0.0 HRS.		
	500.69	461.96
	514.43	462.02
	568.04	462.25
	664.05	462.63
1.0 HRS.		
	908.82	463.55
	1547.30	465.14
	2468.31	466.96
	2584.04	467.29
1.9 HRS.		
	2590.57	467.26
	2581.62	467.21
	2468.81	466.99
	2262.50	466.64
2.9 HRS.		
	1990.04	466.16
	1640.67	465.47
	1348.65	464.82
	1121.46	464.23
3.8 HRS.		

RIVER 1, STATION 28 6TH STREET

*----COMPUTED *----OBSERVED

FLOOD STAGE =

DISCHARGE (CFS)

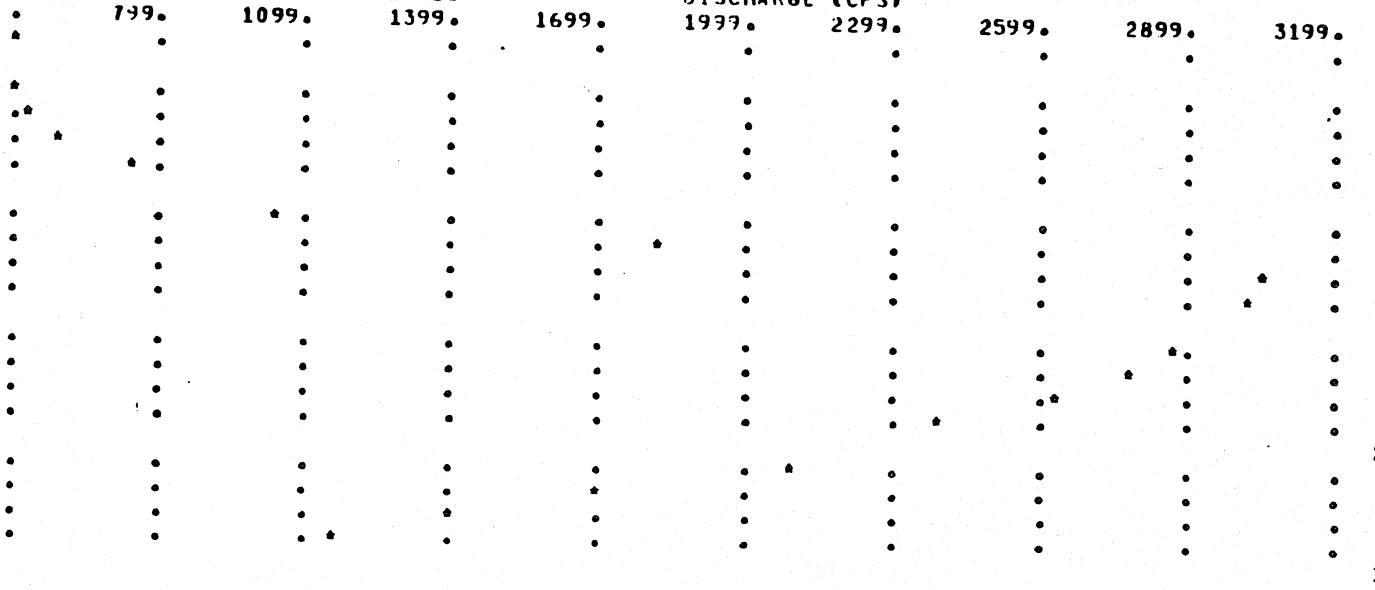

	Q-FCST	H-FCST
	499.96	451.77
0.0 HRS.		
	501.11	451.77
	520.91	451.85
	597.47	452.16
	735.14	452.65
1.0 HRS.		
	1029.63	453.52
	1823.63	455.24
	3037.16	456.79
	3028.70	456.76
1.9 HRS.		
	2859.07	456.33
	2764.58	456.16
	2616.09	456.04
	2389.15	455.84
2.9 HRS.		
	2098.50	455.53
	1700.97	454.93
	1388.65	454.33
	1149.91	453.79
3.8 HRS.		

Table 9.6 (continued)

RIVER 1, STATION 37 3RD STREET

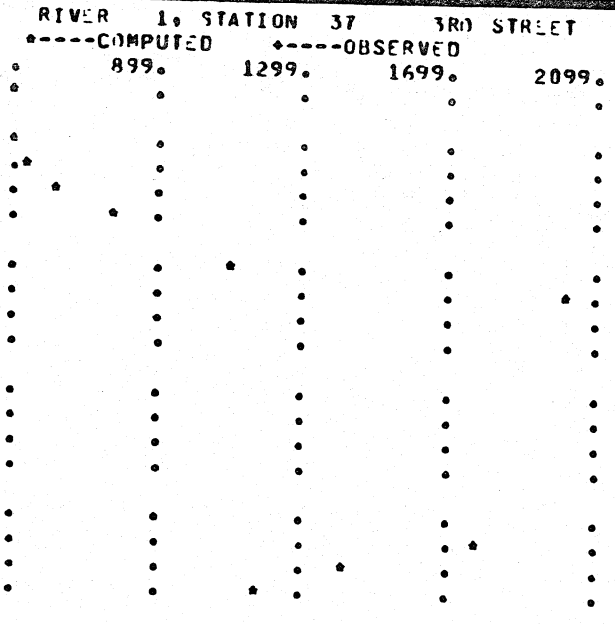

FLOOD STAGE =

DISCHARGE (CFS)

2499. 2899. 3299. 3699. 4099. 4499.

	Q-FCST	H-FCST
0.0 HRS.	499.98	444.82
	500.93	444.83
	522.06	444.91
	612.72	445.28
	782.88	445.93
1.0 HRS.	1118.26	446.97
	2006.37	449.07
	3528.79	451.71
	3515.81	451.86
1.9 HRS.	3172.87	451.22
	2968.04	450.88
	2770.85	450.56
	2508.28	450.11
2.9 HRS.	2201.38	449.58
	1765.07	448.70
	1422.73	447.89
	1172.08	447.21
3.8 HRS.		

RIVER 1, STATION 46 1ST STREET

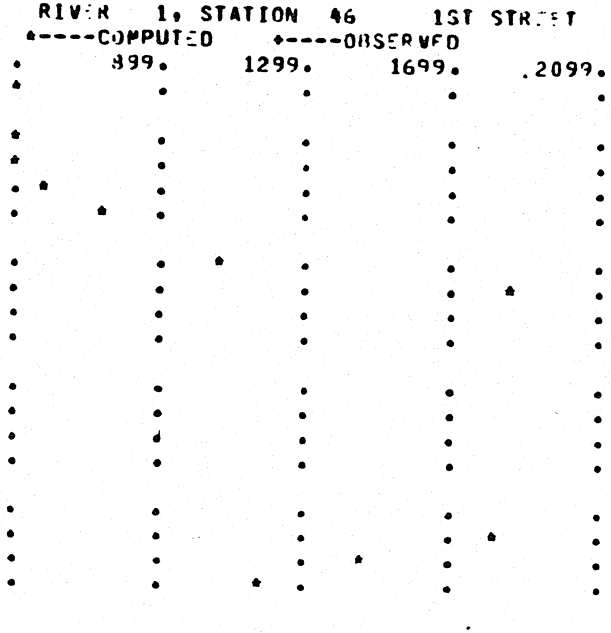

FLOOD STAGE =

DISCHARGE (CFS)

2499. 2899. 3299. 3699. 4099. 4499.

	Q-FCST	H-FCST
0.0 HRS.	500.00	440.00
	500.34	440.00
	515.43	440.06
	593.73	440.36
	753.55	440.99
1.0 HRS.	1058.48	441.85
	1850.73	443.68
	3421.13	445.94
	3547.60	446.19
1.9 HRS.	3202.41	445.64
	2976.93	445.34
	2801.58	445.13
	2529.33	444.77
2.9 HRS.	2235.27	444.36
	1808.23	443.63
	1455.63	442.87
	1197.28	442.25
3.8 HRS.		

Table 9.6 (continued)

RIVER 1, STATION 67 DOWNSTREAM BOUNDARY FLOOD STAGE =

*----COMPUTED *----OBSERVED

DISCHARGE (CFS)

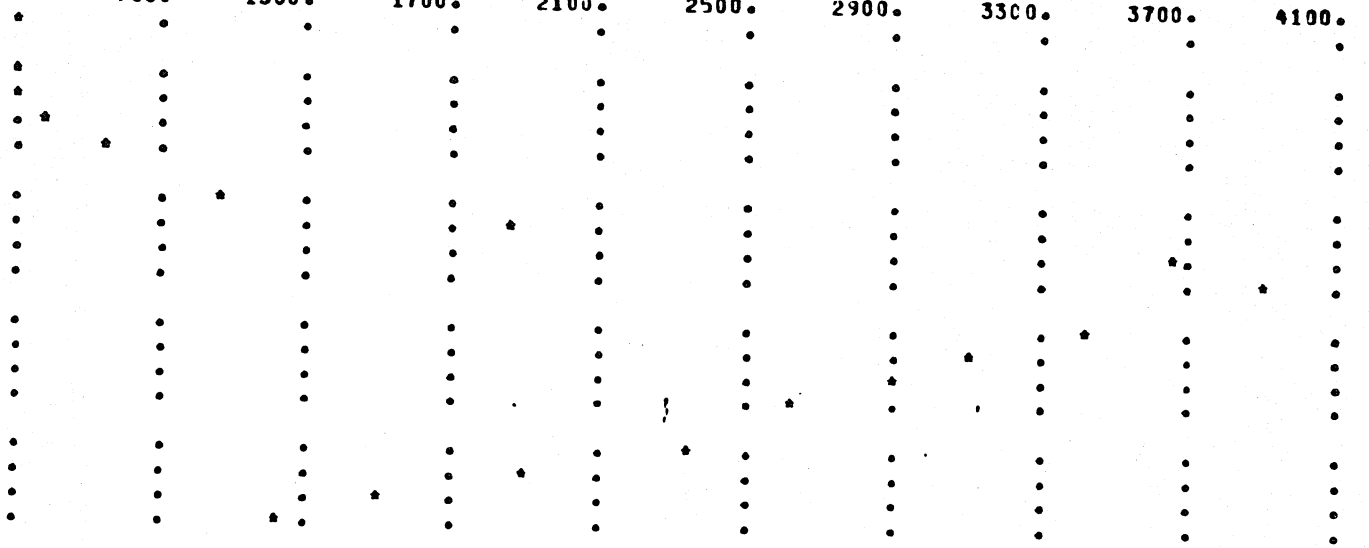

Q-FCST	H-FCST
500.06	428.95
0.0 HRS.	
500.43	428.95
512.35	428.95
589.60	428.96
752.98	428.98
1.0 HRS.	
1072.03	429.02
1879.96	429.26
3678.35	430.51
3885.53	430.63
1.9 HRS.	
3430.27	430.36
3119.84	430.17
2912.35	430.03
2623.24	429.80
2.9 HRS.	
2325.71	429.56
1882.79	429.26
1505.25	429.15
1231.59	429.07
3.8 HRS.	

Table 9.6 (continued)

RIVER 1, STATION 1 UPSTREAM BOUNDARY FLOOD STAGE =

*----COMPUTED *----OBSERVED

DISCHARGE (CFS)

1400.	2300.	3200.	4100.	5000.	5900.	6800.	7700.	8600.	9500.	Q-FCST	H-FCST
										500.00	479.71
									0.0 HRS.		
										500.00	479.71
										500.00	479.71
										500.00	479.71
										500.00	479.71
									1.0 HRS.		
										786.43	480.79
										1920.75	483.76
										4266.10	487.02
										6660.40	488.75
									1.9 HRS.		
										8203.80	489.97
										8800.75	490.27
										8640.69	490.20
										7833.17	489.84
									2.9 HRS.		
										6645.99	488.84
										5247.96	487.81
										3866.79	486.92
										2678.73	485.66
									3.8 HRS.		

RIVER 1, STATION 6 UPSTREAM WEIR FLOOD STAGE =

*----COMPUTED *----OBSERVED

DISCHARGE (CFS)

1399.	2299.	3199.	4099.	4999.	5899.	6799.	7699.	8599.	9499.	Q-FCST	H-FCST
										499.99	474.74
									0.0 HRS.		
										500.00	474.74
										499.93	474.75
										499.65	474.79
										499.40	474.87
									1.0 HRS.		
										733.20	475.73
										1839.41	477.28
										4070.46	479.27
										6529.83	480.75
									1.9 HRS.		
										8124.98	481.45
										8792.42	481.78
										8663.68	481.72
										7896.18	481.35
									2.9 HRS.		
										6729.73	480.82
										5345.41	480.10
										3937.71	479.29
										2743.60	478.24
									3.8 HRS.		

Table 9.7 Discharge Hydrographs at Various Locations (150' Weir)

RIVER 1, STATION 7 DOWNSTREAM WEIR FLOOD STAGE =

*----COMPUTED *----OBSERVED

DISCHARGE (CFS)

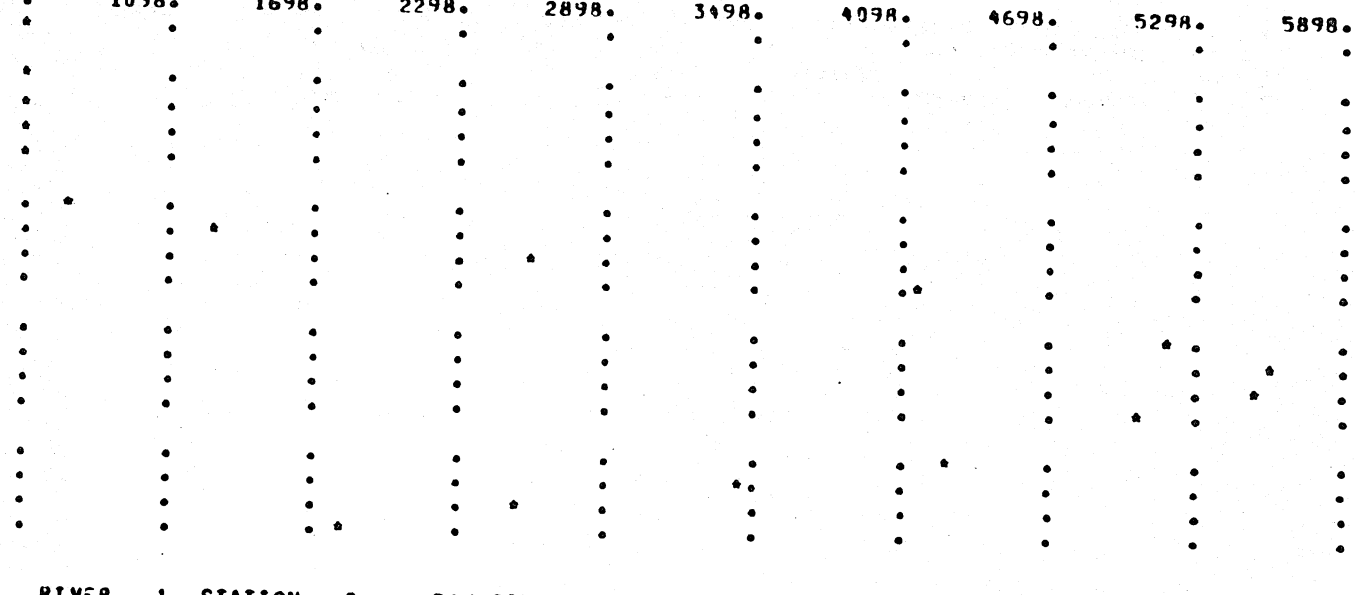

Q-FCST	H-FCST
499.99	474.33
0.0 HRS.	
500.00	474.33
499.87	474.34
499.38	474.39
498.99	474.50
1.0 HRS.	
648.74	475.36
1277.32	476.72
2576.93	478.44
4162.69	479.78
1.9 HRS.	
5160.55	480.80
5608.77	481.09
5531.84	481.02
5037.51	480.65
2.9 HRS.	
4296.89	479.98
3449.91	479.03
2528.80	478.21
1833.70	477.38
3.8 HRS.	

RIVER 1, STATION 8 DOWNSTREAM WEIR FLOOD STAGE =

*----COMPUTED *----OBSERVED

DISCHARGE (CFS)

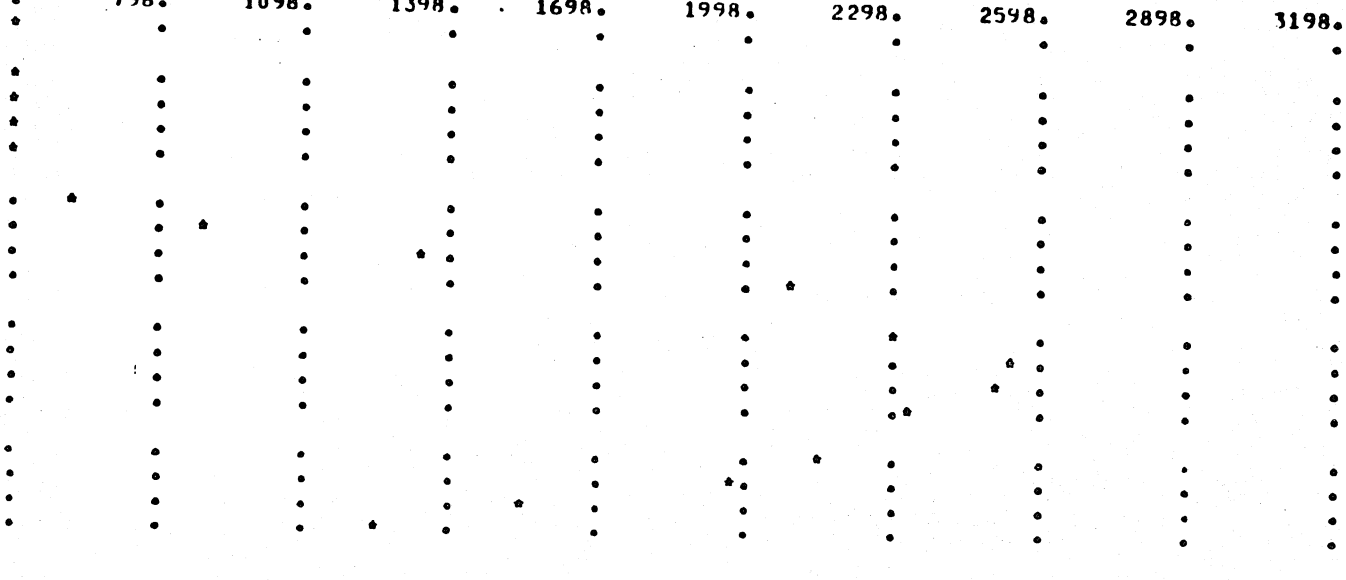

Q-FCST	H-FCST
499.99	473.96
0.0 HRS.	
500.00	473.96
499.81	473.97
499.10	474.04
498.58	474.17
1.0 HRS.	
629.82	474.98
886.33	476.40
1349.27	478.30
2087.26	479.85
1.9 HRS.	
2302.45	481.16
2527.63	481.50
2511.91	481.41
2315.58	480.97
2.9 HRS.	
2135.96	480.10
1964.41	478.75
1556.15	477.67
1244.92	476.83
3.8 HRS.	

Table 9.7 (continued)

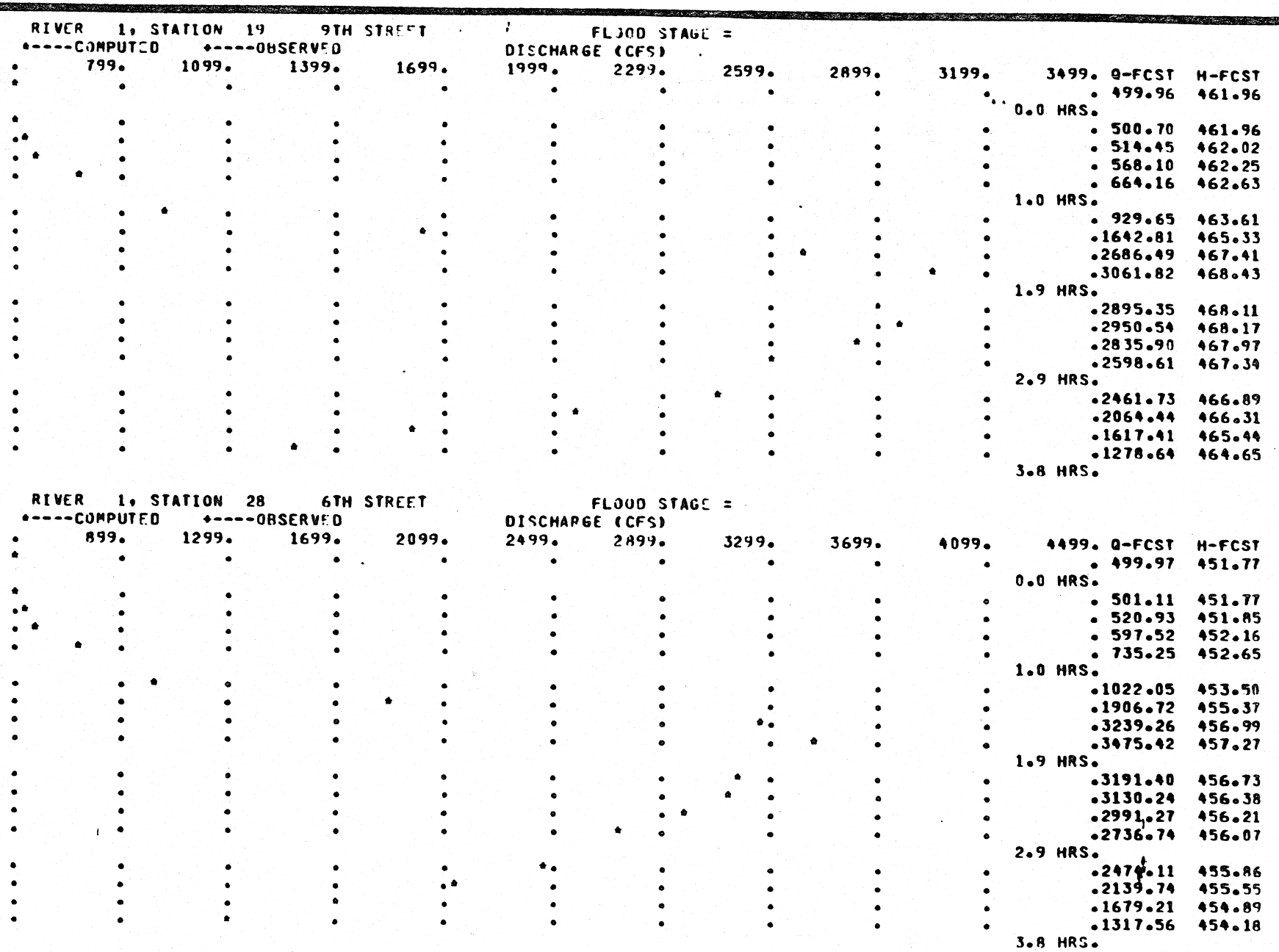

Table 9.7 (continued)

RIVER 1, STATION 37 3RD STREET FLOOD STAGE =

*----COMPUTED *----OBSERVED DISCHARGE (CFS)

899.	1299.	1699.	2099.	2499.	2899.	3299.	3699.	4099.	4499.	Q-FCST	H-FCST
										499.98	444.82
										0.0 HRS.	
										500.94	444.83
										522.08	444.91
										612.76	445.28
										782.98	445.93
										1.0 HRS.	
										1129.62	447.00
										2082.81	449.21
										3722.42	452.03
										3947.61	452.60
										1.9 HRS.	
										3537.21	451.97
										3334.27	451.51
										3149.10	451.18
										2856.83	450.71
										2.9 HRS.	
										2548.38	450.16
										2207.96	449.60
										1726.73	448.62
										1345.52	447.69
										3.8 HRS.	

RIVER 1, STATION 46 1ST STREET FLOOD STAGE =

*----COMPUTED *----OBSERVED DISCHARGE (CFS)

899.	1299.	1699.	2099.	2499.	2899.	3299.	3699.	4099.	4499.	Q-FCST	H-FCST
										500.00	440.00
										0.0 HRS.	
										500.34	440.00
										515.43	440.06
										593.77	440.36
										753.64	440.99
										1.0 HRS.	
										1066.55	441.87
										1918.85	443.81
										3588.44	446.20
										3958.84	446.82
										1.9 HRS.	
										3619.13	446.33
										3343.76	445.87
										3175.26	445.61
										2885.23	445.22
										2.9 HRS.	
										2564.20	444.81
										2256.55	444.39
										1773.31	443.56
										1378.43	442.69
										3.8 HRS.	

Table 9.7 (continued)

RIVER 1, STATION 67 DOWNSTREAM BOUNDARY FLOOD STAGE =

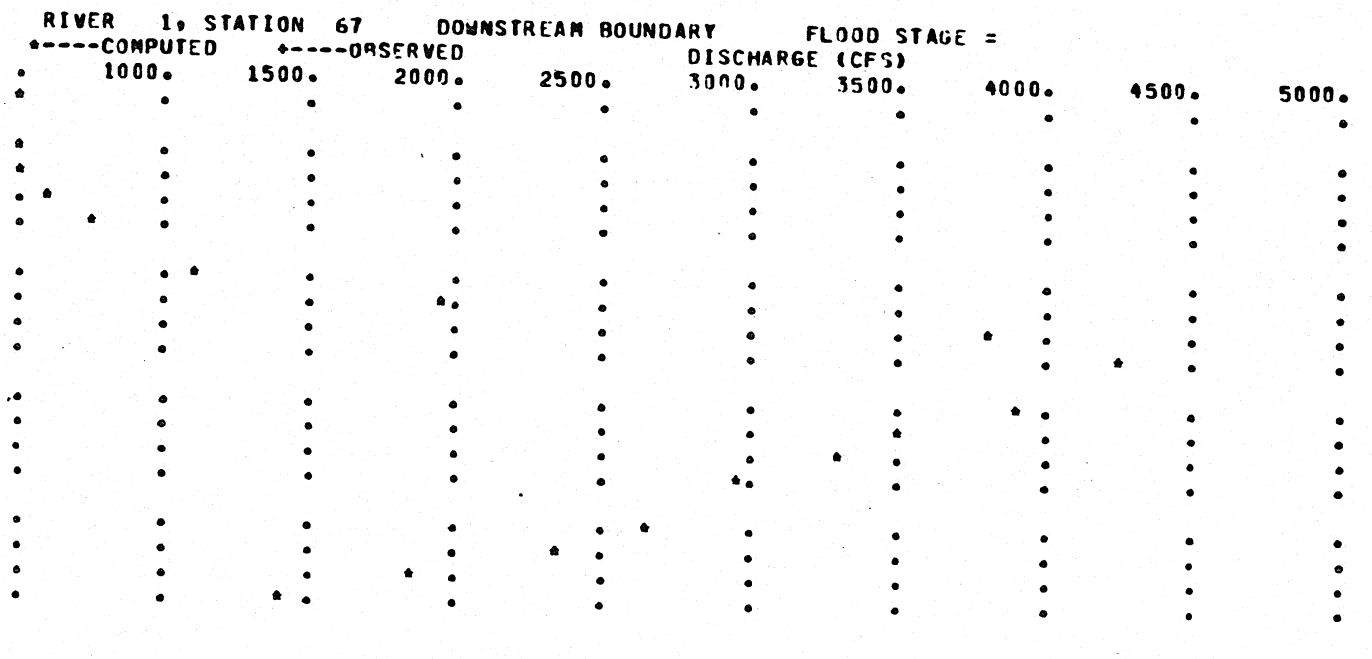

	Q-FCST	H-FCST
	500.06	428.95
0.0 HRS.		
	500.43	428.95
	512.36	428.95
	589.63	428.96
	753.07	428.98
1.0 HRS.		
	1075.10	429.02
	1939.10	429.28
	3810.91	430.59
	4269.67	431.02
1.9 HRS.		
	3912.58	430.65
	3484.73	430.39
	3294.25	430.28
	2973.31	430.08
2.9 HRS.		
	2640.65	429.81
	2336.88	429.57
	1834.27	429.25
	1423.10	429.13
3.8 HRS.		

Table 9.7 (continued)

Table 9.8

Comparison of Diverted Tunnel Inflow for Different Weir Characteristics

Time (hr)	Diverted* Discharge $C_o = 2.6$ (cfs)	Diverted* Discharge $C_o = 2.4$ (cfs)	Diverted** Discharge $C_o = 2.6$ (cfs)
0.0	0.0	0.0	0.0
0.24	135.8	133.1	140.4
0.48	1074.2	1064.0	1141.8
0.72	3066.2	4042.8	3190.2
0.96	4967.4	4918.9	5126.8
1.20	6156.1	6089.3	6347.26
1.44	6640.3	6568.6	6828.8
1.68	6503.7	6434.1	6691.4
1.92	5879.7	5815.7	6033.9
2.16	4924.6	4875.4	5039.9
2.40	3776.2	3738.7	3841.0
2.64	2630.7	2612.6	2688.5
2.88	1639.1	1628.5	1746.0

*Two sections are used in the unsteady flow model to describe the weir discharges.

**One section is used in the unsteady flow model to describe the weir discharges.

Table 9.9

Inflow Hydrographs to Tunnel for various Length Weirs

Time hr.	Time min.	Discharge[1] (cfs)	Discharge[2] (cfs)	Discharge[3] (cfs)	Discharge[4] (cfs)	Discharge[5] (cfs)
	10	171	171	171	171	171
	20	242	309	364	407	522
	30	812	1000	1141	1252	1483
	40	1838	2016	2289	2524	3066
	50	2651	3281	3732	3751	4504
1	00	3118	3864	4290	4936	5560
	10	3410	4287	4949	5477	6246
	20	3574	4494	5203	5760	6616
	30	3620	4531	5240	5802	6667
	40	3530	4405	5077	5614	6428
	50	3325	4145	4749	5245	5966
2	00	3079	3779	4315	4763	5347
	10	2719	3319	3915	4129	4601
	20	2300	2819	3135	3122	3776
	30	1880	2192	2218	2453	2943
	40	1210	1455	1689	1912	2201
	50	850	1054	1212	1328	1554
3	00	171	171	171	171	171

1 Based upon using an intake structure with a 50 ft. crest length with the crest elevation set at 475 ft. above M.S.L.

2 Based upon using an intake structure with a 75 ft. crest length with the crest elevation set at 475 ft. above M.S.L.

3 Based upon using an intake structure with a 100 ft. crest length with the crest elevation set at 475 ft. above M.S.L.

4 Based upon using an intake structure with a 125 ft. crest length with the crest elevation set at 475 ft. above M.S.L.

5 Based upon using an intake structure with a 200 ft. crest length with the crest elevation set at 475 ft. above M.S.L.

9.3 HYDRAULIC TRANSIENT ANALYSIS OF TUNNEL

MODELING OF TUNNEL

Because of the size and potential cost of a proposed tunnel to bypass flood flow from Waller Creek directly to Town Lake, a rather detailed transient analysis is required. The unsteady flow or transient analysis of the proposed tunnel must be capable of simulating flows which change with time and location along the tunnel from free surface unsteady flow to pressurized flow and conversely. Both design concepts for the open channel flow design concept and the pressurized design concept must be analyzed.

The transient analysis was performed in order to develop a better understanding of:

1. The transient nature of discharge hydrographs propagating through the tunnel for open channel flow and/or pressurized flow conditions;

2. To determine the capability of proposed tunnel alignments and designs to carry discharges diverted from Waller Creek through the intake structures;

3. To analyze the hydraulic aspects of the flow in the tunnel, in particular the range of peak velocities; and

4. To determine the hydraulic effect of various headlosses at the intake and outlet structures.

MODEL FOR OPEN CHANNEL TUNNEL DESIGN

The tunnel designed for the open channel flow concept was modeled as a 24-ft. diameter tunnel at a slope of 0.0025 ft/ft. Cross-section locations were placed every 200 ft. along the tunnel. The flows are diverted from

Waller Creek using a 270 ft. long intake structure with a crest elevation of 475 ft. Initial conditions were based upon a downstream water surface elevation of 432.9 ft. and an initial discharge of 171 cfs. The downstream boundary condition is a rating curve based upon critical flow conditions. The water surface elevations were increased by 1 ft.

The inflow hydrographs (diversions from Waller Creek) are listed in Table 9.9. The simulation for a 200 ft crest length at a crest elevation of 475 ft above M.S.L. resulted in the discharge hydrograph at Town Lake listed in Table 7.1 The maximum velocity was 20.6 ft/sec. The maximum water surface elevation at the midpoint was 459.15 ft and at the downstream was 445.57 ft.

MODEL OF PIPE FLOW (PRESSURE) TUNNEL DESIGN

The pressure tunnel design was modeled using various diameters (21 ft., 20 ft., and 18 ft.). Cross-section locations were placed every 200 ft. along the tunnel. A slope of 0. was used for the tunnel. Initial conditions assumed the tunnel was initially full (pressurized) with a discharge of 171 cfs. The downstream boundary condition was a constant elevation stage discharge hydrograph. Several values of the downstream boundary condition, ranging from water surface elevations of 429.1 ft. to 443.9 ft. were simulated.

The inflow hydrographs (diversions from Waller Creek) are listed in Table .9. Results of the simulations are summarized in Table 7.2. Discharge hydrographs for 20 ft. and 21 ft. diameter tunnels are summarized in Table 7.3.

Table 9.10

Discharge Hydrograph at Town Lake for
Open Channel Tunnel Design

Time hr.	Time min.	Downstream Discharge (cfs)	Water Surface Elevation (ft)
0	10	292.28	432.98
	20	721.40	434.96
	30	2004.43	438.36
	40	3740.09	441.65
	50	5041.55	443.61
1	00	5918.27	444.77
	10	6461.72	445.35
	20	6665.25	445.57
	30	6539.27	445.44
	40	6178.69	445.05
	50	5658.21	444.48
2	00	4984.62	443.53
	10	4221.27	442.41
	20	3411.06	441.08
	30	2639.20	439.72
	40	1964.98	438.28
	50	1155.68	436.25
3	00	392.83	433.47
	10	86.69	430.97
	20	97.47	431.15
	30	192.08	432.50
	40	232.18	432.69
	50	226.49	432.67
4	00	235.32	432.71

Table 9.11

Summary of Tunnel Simulations

Tunnel Diameter (ft)	Intake Weir Length* (ft)	Downstream Boundary Elevation (ft)	Maximum Flow Velocity (ft/sec)	Maximum Hydraulic Grade Line at Upstream (ft)	Peak Discharge Diverted** (cfs)
21.0	200.	429.1	19.2	472.1	6667.
20.0	200.	429.1	21.2	484.8	6667.
18.0	200.	429.1	26.2	523.8	6667.
21.0	200.	435.0	19.2	478.0	6667.
20.0	200.	435.0	21.2	490.3	6667.
18.0	200.	435.0	26.5	532.8	6667.
21.0	125.	435.0	16.7	467.8	5802.
20.0	125.	435.0	18.4	477.1	5802.
18.0	125.	435.0	22.7	507.0	5802.
18.0	125.	443.9	22.7	515.1	5802.
16.0	125.	435.0	27.8	562.4	5802.
20.0	75.	435.0	14.4	461.2	4531.
18.0	75.	435.0	17.3	480.0	4531.
16.0	75.	435.0	22.4	515.8	4531.
16.0	50.	435.0	17.9	487.5	3620.

* Crest elevation at 475. ft. above mean sea level. Inflow hydrographs in Table 5.9.

** Peak inflow into tunnel.

Table 9.12

Discharge Hydrographs at Town Lake for
Pressurized Tunnel Design

Time hr.	Time min.	(20.0 ft. Tunnel) Downstream Discharge* (cfs)	(21.0 ft. Tunnel) Downstream Discharge** (cfs)
0	10	521.3	521.2
	20	1481.4	1480.9
	30	3060.4	3058.8
	40	4499.5	4498.0
	50	5554.3	5552.8
1	00	6244.0	6243.2
	10	6613.5	6613.0
	20	6668.8	6669.1
	30	6429.4	6430.0
	40	5970.2	5971.1
	50	5349.9	5350.9
2	00	4605.4	4606.5
	10	3778.6	3779.5
	20	2945.9	2946.6
	30	2201.9	2202.3
	40	1555.4	1555.7
	50	257.4	173.6

* Discharge hydrograph for 21.0 ft. diameter tunnel with downstream boundary set at 429.1 ft. M.S.L. and at 435.0 ft. M.S.L.
**Discharge hydrograph for 20. ft. diameter tunnel with downstream boundary set at 429.1 ft. M.S.L. and at 435.0 ft. M.S.L.

9.4 COMPARISON OF TUNNEL DESIGNS AND FLOOD REDUCTIONS IN WALLER CREEK

WATER SURFACE PROFILES IN WALLER CREEK - EXISTING CONDITIONS

The water surface profiles from Town Lake to 14th Street for various peak flow conditions are presented in Figure 9.3 The peak flows at Town Lake for the various frequency storms are: (1) 2000 cfs, (2) 10-year frequency, 5444 cfs, (3) 25-year frequency, 7035 cfs, and (4) 100-year frequency, 9424 cfs.

At 2000 cfs, the predicted water surface elevation is below the minimum road elevation for all street crossings. At 5444 cfs (10-year frequency storm), water tops the bridge decks at 9th, 10th and 12th Streets by 3.83, 1.09, and 3.96 feet, respectively. At 7035 cfs (25-year frequency storm), the water surface elevation in Waller Creek exceeds the minimum road elevation at ten of the fifteen major road (excluding foot bridges) crossings by 0.37 to 7.08 feet. During the 100-year frequency storm, all but two major street crossings (6th and 11th Streets) will be overtopped by water ranging from 0.10 to 8.15 feet.

WATER SURFACE PROFILES IN WALLER CREEK RESULTING FROM VARIOUS DIAMETER TUNNELS

Three different size tunnels (18′ϕ, 20′ϕ, and 21′ϕ), corresponding to intake weir lengths of 75′, 125′ and 200′, have been evaluated to determine the resulting reduction in water surface elevations along Waller Creek. The maximum discharge and elevation at the cross section upstream of each street crossing for the three alternatives are listed in Tables 9.13, 9.14. and 9.15. Additionally, the water surface profiles are presented in Figure 9.4.

With the 18′ϕ tunnel, the bridges at 9th and 12th Streets will still be overtopped during the 100-year flood. With the 20′ϕ tunnel, only the bridge at 9th Street will be overtopped during the 100-year storm. With

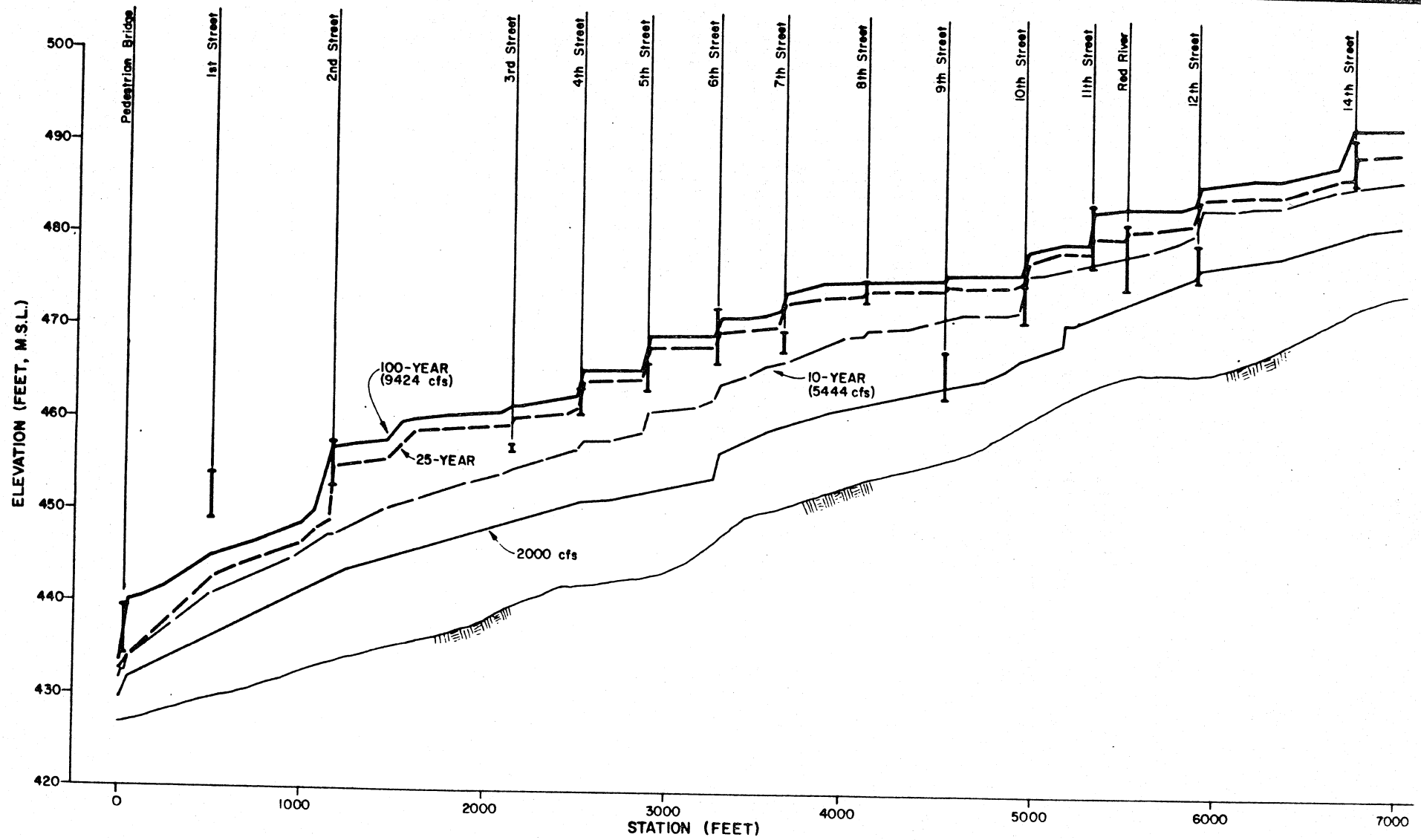

FIGURE 9.3 WALLER CREEK PROFILES FOR VARIOUS FREQUENCY STORMS

Table 9.13

Water Surface Elevations for 18 Foot Diameter Tunnel
(75′ Weir Length)

Cross Section No.	Location	Q_{max} (cfs)	Elevation* (ft M.S.L.)	Elevation** (ft M.S.L.)	Minimum Road Elevation (ft M.S.L.)
0	Town Lake	5045.8	431.9	431.3	--
1268	1st Street	4950.2	448.2	448.1	454.4
1618	2nd/Red River	4952.2	450.7	450.6	457.4
2202	3rd Street	4956.1	454.3	454.5	457.4
2590	4th Street	4795.0	457.5	456.9	463.5
2975	5th Street	4796.7	460.7	459.8	466.4
3341	6th Street	4801.0	463.6	463.9	472.5
3726	7th Street	4652.3	467.5	466.1	470.1
4161	8th Street	4659.1	470.3	468.2	475.7
4604	9th Street	4671.1	471.9	471.5	468.1
5048	10th Street	4498.0	474.8	475.3	475.6
5642	11th/Red River	4498.3	477.4	478.7	484.3/482.5
6006	12th Street	4499.1	481.8	483.2	480.1

*From DWOPER

**From WSP2

Table 9.14

Water Surface Elevations for 20 Foot Diameter Tunnel
(125′ Weir Length)

Cross Section No.	Location	Q_{max} (cfs)	Elevation* (ft M.S.L.)	Elevation** (ft M.S.L.)	Minimum Road Elevation (ft M.S.L.)
0	Town Lake	4464.3	431.3	431.0	--
1268	1st Street	4147.3	447.1	447.1	454.4
1618	2nd/Red River	4153.4	449.6	449.5	457.4
2202	3rd Street	4164.8	452.9	453.3	457.4
2590	4th Street	3648.3	455.5	455.0	463.5
2975	5th Street	3652.6	457.6	456.9	466.4
3341	6th Street	3657.7	457.7	460.8	472.5
3726	7th Street	3417.2	464.1	463.5	470.1
4161	8th Street	3414.8	466.6	465.7	475.7
4604	9th Street	3421.1	469.2	470.1	468.1
5048	10th Street	3229.2	472.0	471.8	475.6
5642	11th/Red River	3229.1	474.6	476.7	484.3/482.5
6006	12th Street	3228.6	480.5	481.1	480.1

*From DWOPER

**From WSP2

Table 9.15

Water Surface Elevations for 21 Foot Diameter Tunnel
(200′ Weir Length)

Cross Section No.	Location	Q_{max} (cfs)	Elevation* (ft M.S.L.)	Elevation** (ft M.S.L.)	Minimum Road Elevation (ft M.S.L.)
0	Town Lake	3885.5	430.6	430.6	--
1268	1st Street	3547.6	446.2	446.2	454.4
1618	2nd/Red River	3538.3	448.5	448.5	457.4
2202	3rd Street	3528.8	451.7	452.2	457.4
2590	4th Street	3041.5	454.3	453.8	463.5
2975	5th Street	3034.0	455.9	455.1	466.4
3341	6th Street	3037.2	456.8	459.6	472.5
3726	7th Street	2591.8	462.5	461.8	470.1
4161	8th Street	2591.2	465.0	464.0	475.7
4604	9th Street	2590.6	467.3	467.9	468.1
5048	10th Street	2366.4	469.7	469.2	475.6
5642	11th/Red River	2366.1	472.4	475.1	484.3/482.5
6006	12th Street	2366.3	477.9	478.8	480.1

*From DWOPER

**From WSP2

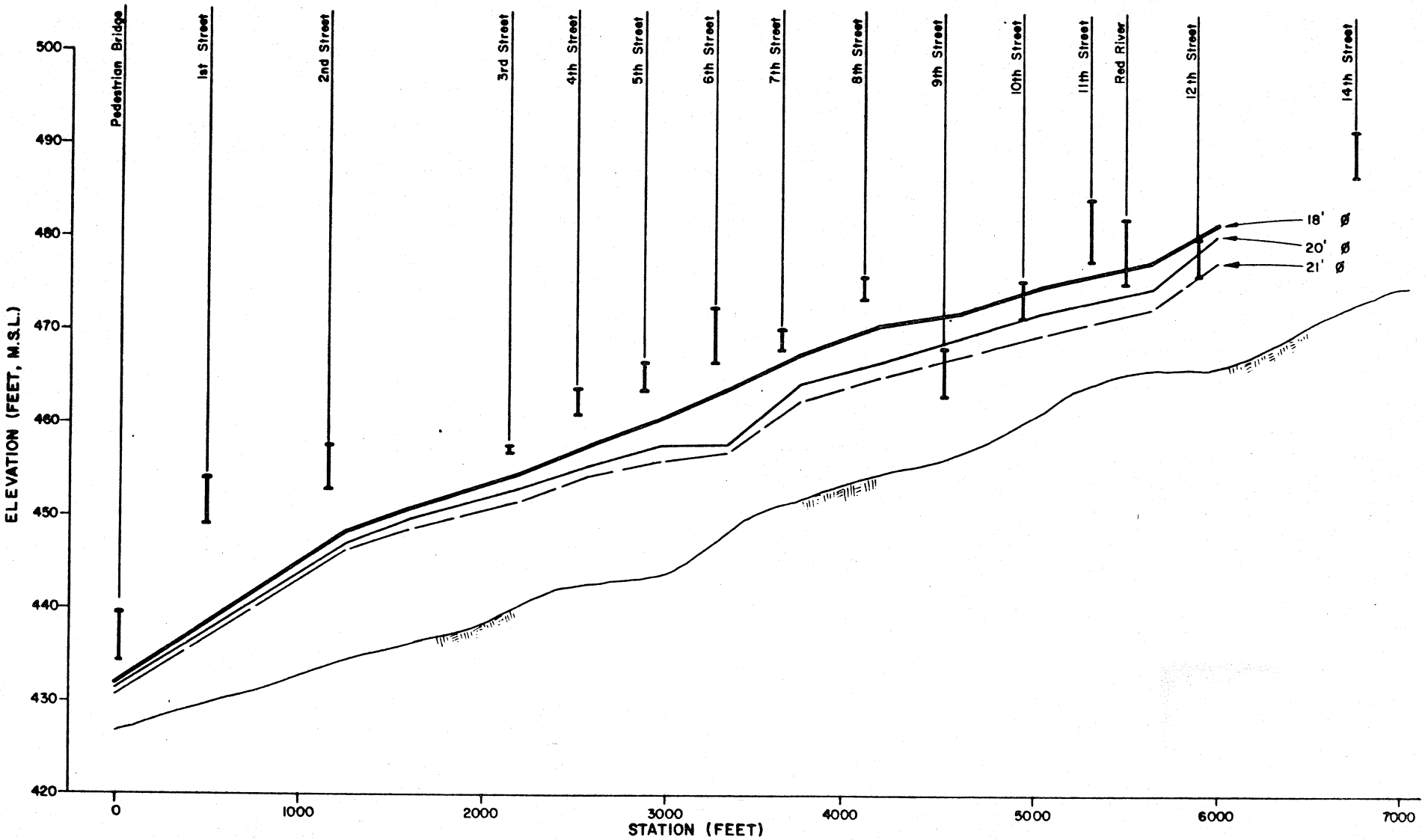

FIGURE 9. 4 WALLER CREEK PROFILES RESULTING FROM VARIOUS DIAMETER TUNNELS

the 21'ϕ tunnel, no overtopping of any major bridge will occur during the 100-year storm.

9.3 COMPARISON OF VARIOUS FREQUENCY STORMS VS. DIFFERENT TUNNEL SIZES

In a review (Figure 9.5 of the affects of the different tunnels in reducing the water surface elevations along Waller Creek during the 100-year storm, it becomes readily apparent that all three tunnel sizes reduce the water surface elevations near or below the 10-year frequency storm.

Plots of the channel cross sections at various locations (Figures 9.6 through 9.17 , however, indicates that with the 18'ϕ tunnel the floodplain is still quite wide in many locations with water in and around many buildings at elevations approaching 3 feet during the 100-year storm. The 20'ϕ tunnel reduces the elevations such that the water stays within the channel in most cases; however, there will be some flooding in and around buildings during the 100-year storm. With the 21'ϕ tunnel, water levels are reduced so that virtually all the water is maintained in the channel with little or no flooding in and around buildings.

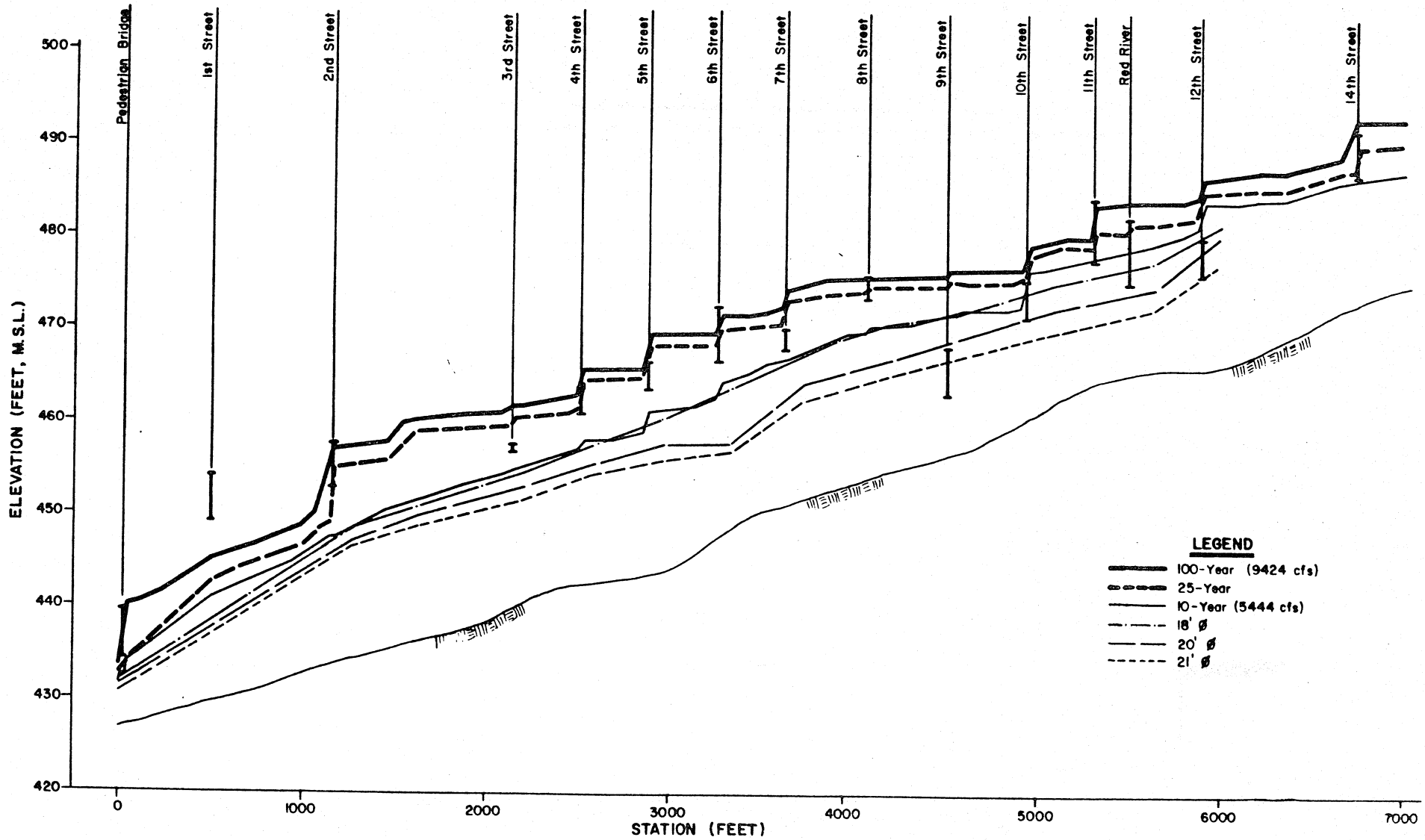

FIGURE 9.5 COMPARISON OF WALLER CREEK PROFILES FOR VARIOUS FREQUENCY STORMS AND DIAMETER TUNNELS

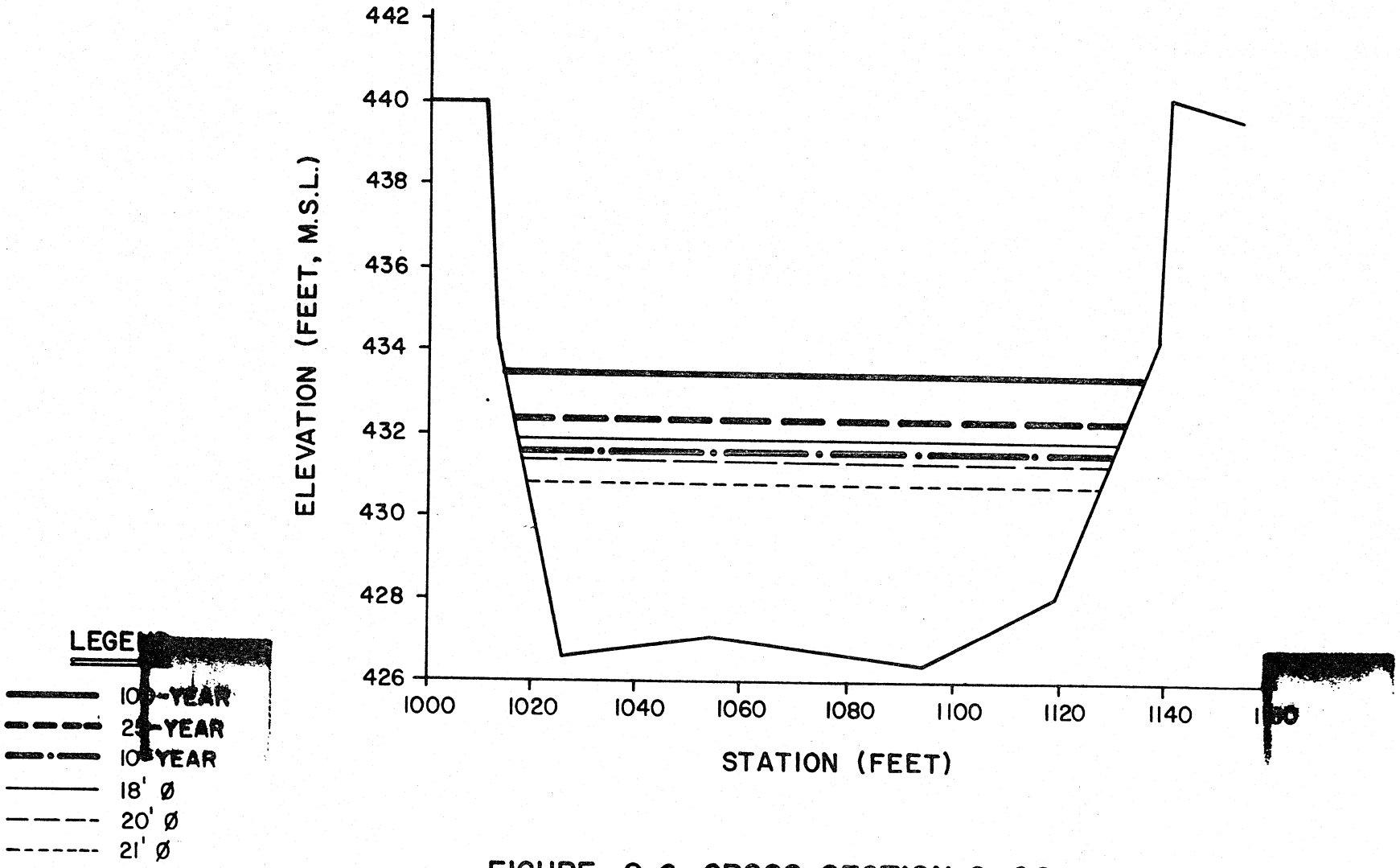

FIGURE 9.6 CROSS SECTION 0+00

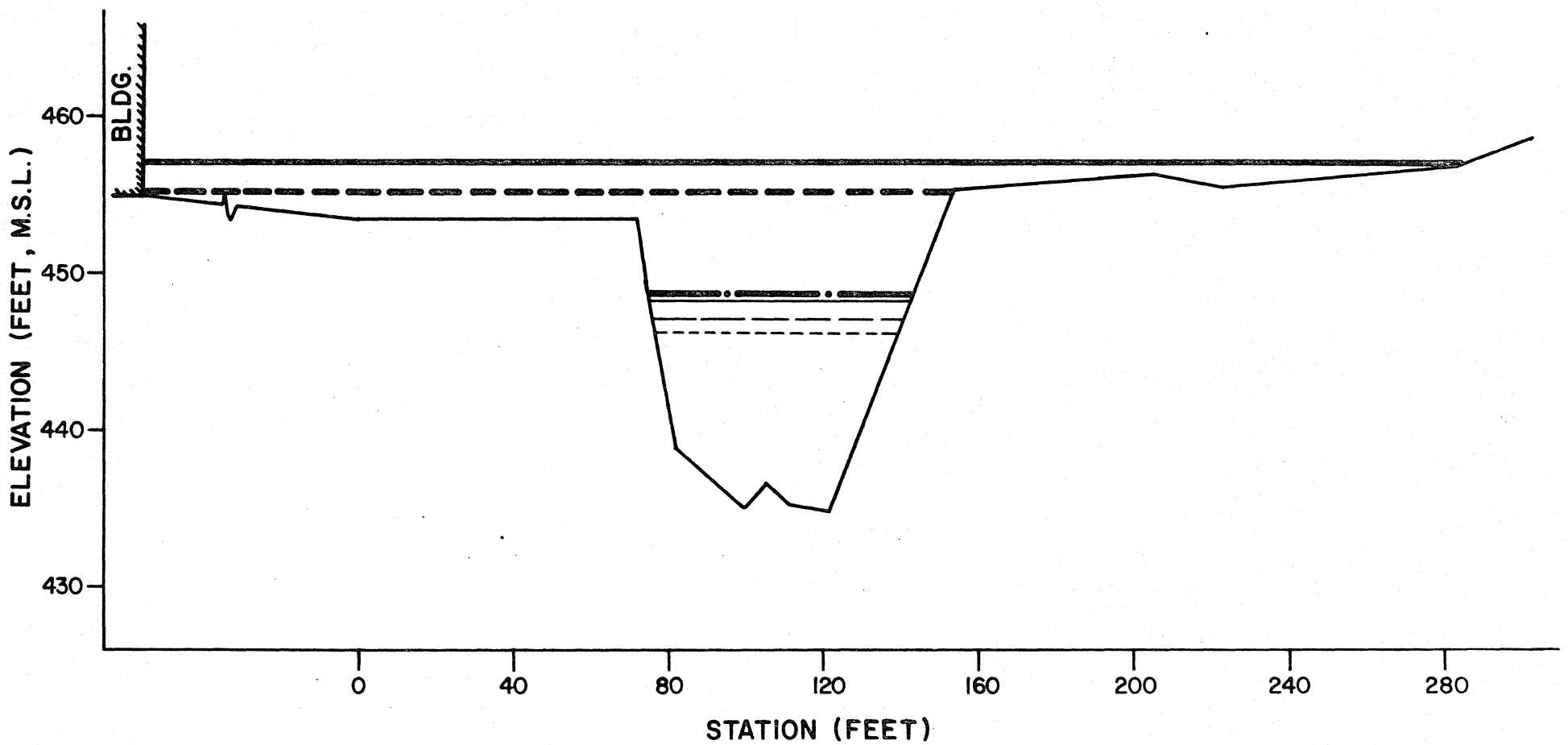

LEGEND

- 100-YEAR
- 25-YEAR
- 10-YEAR
- 18' Ø
- 20' Ø
- 21' Ø

FIGURE 9.7 1ST STREET BRIDGE + 50 FEET NORTH (STATION 12+68)

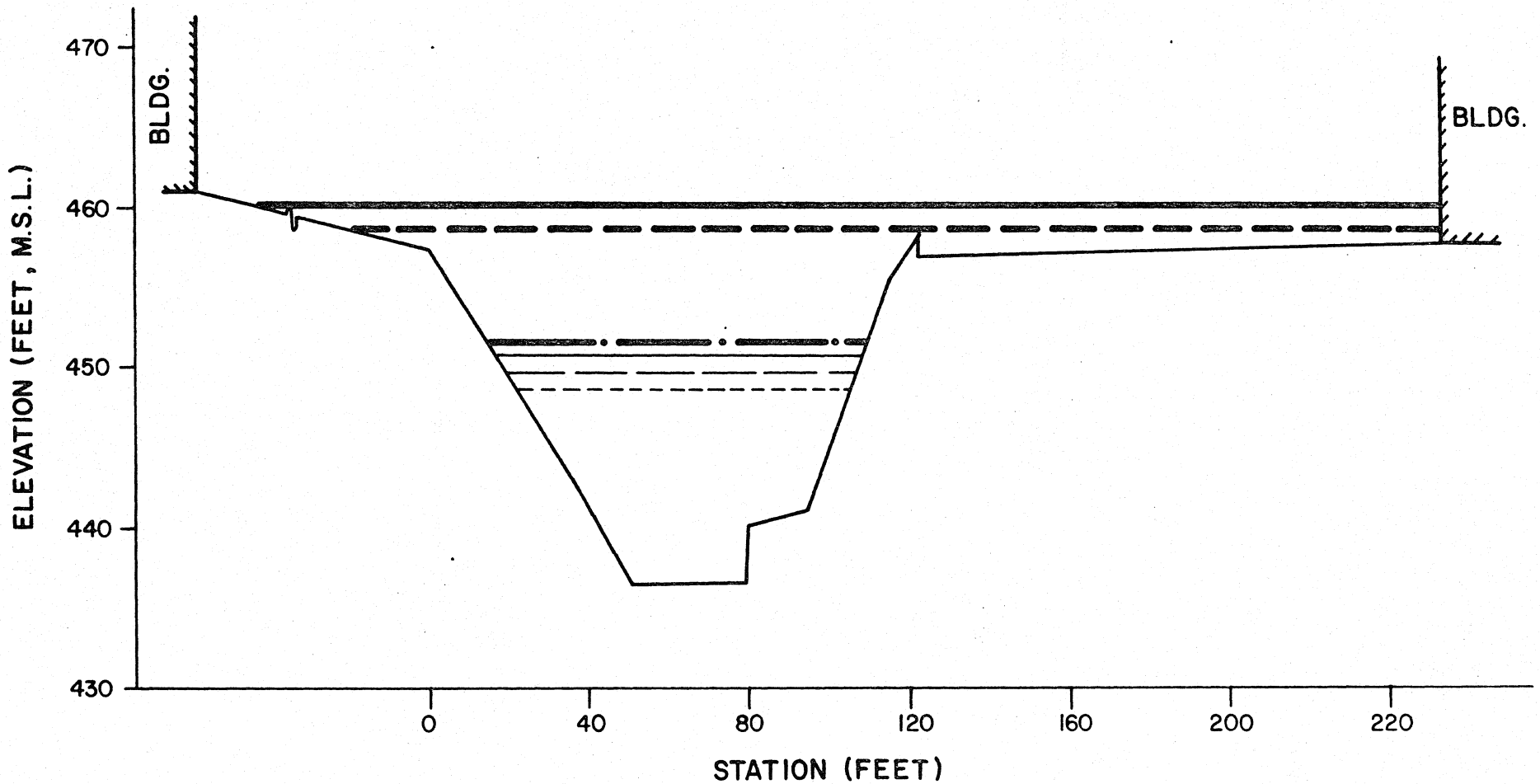

LEGEND

- 100-YEAR
- 25-YEAR
- 10-YEAR
- 18' Ø
- 20' Ø
- 21' Ø

FIGURE 9.8 2ND STREET BRIDGE + 50 FEET NORTH (STATION 16+18)

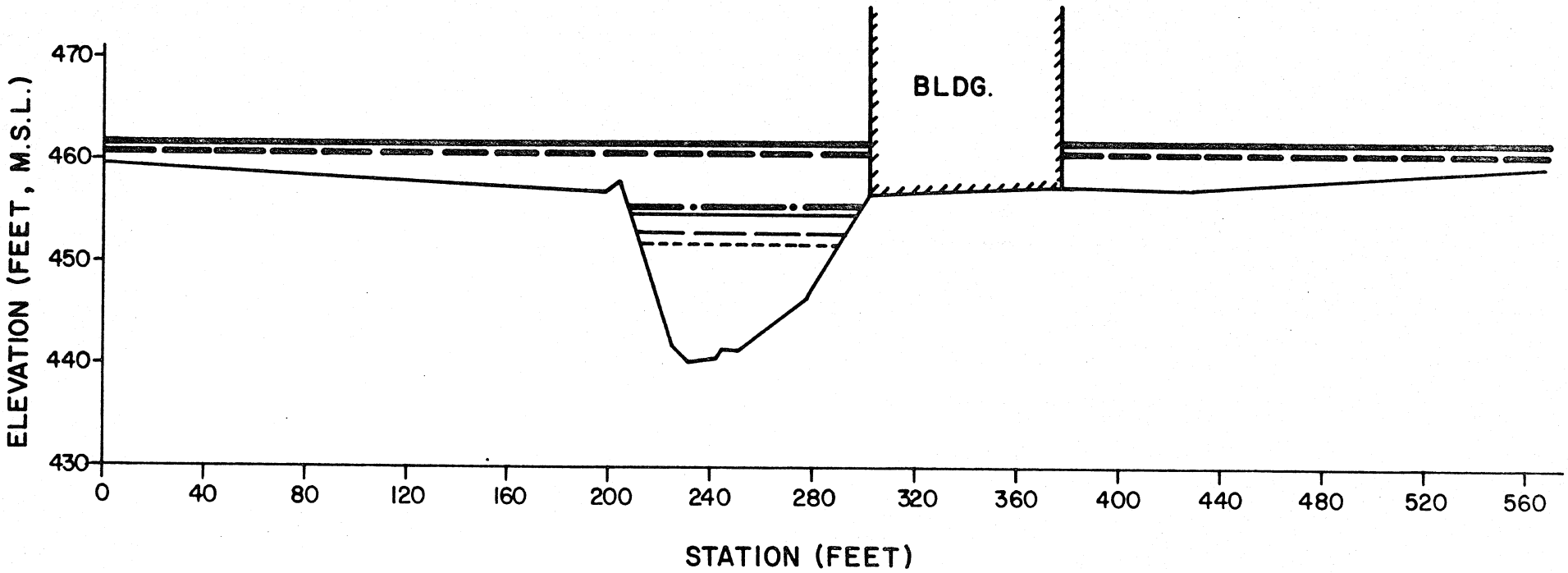

LEGEND

- 100-YEAR
- 25-YEAR
- 10-YEAR
- 18' Ø
- 20' Ø
- 21' Ø

FIGURE 9.9 3RD STREET + 50 FEET NORTH (STATION 22+02)

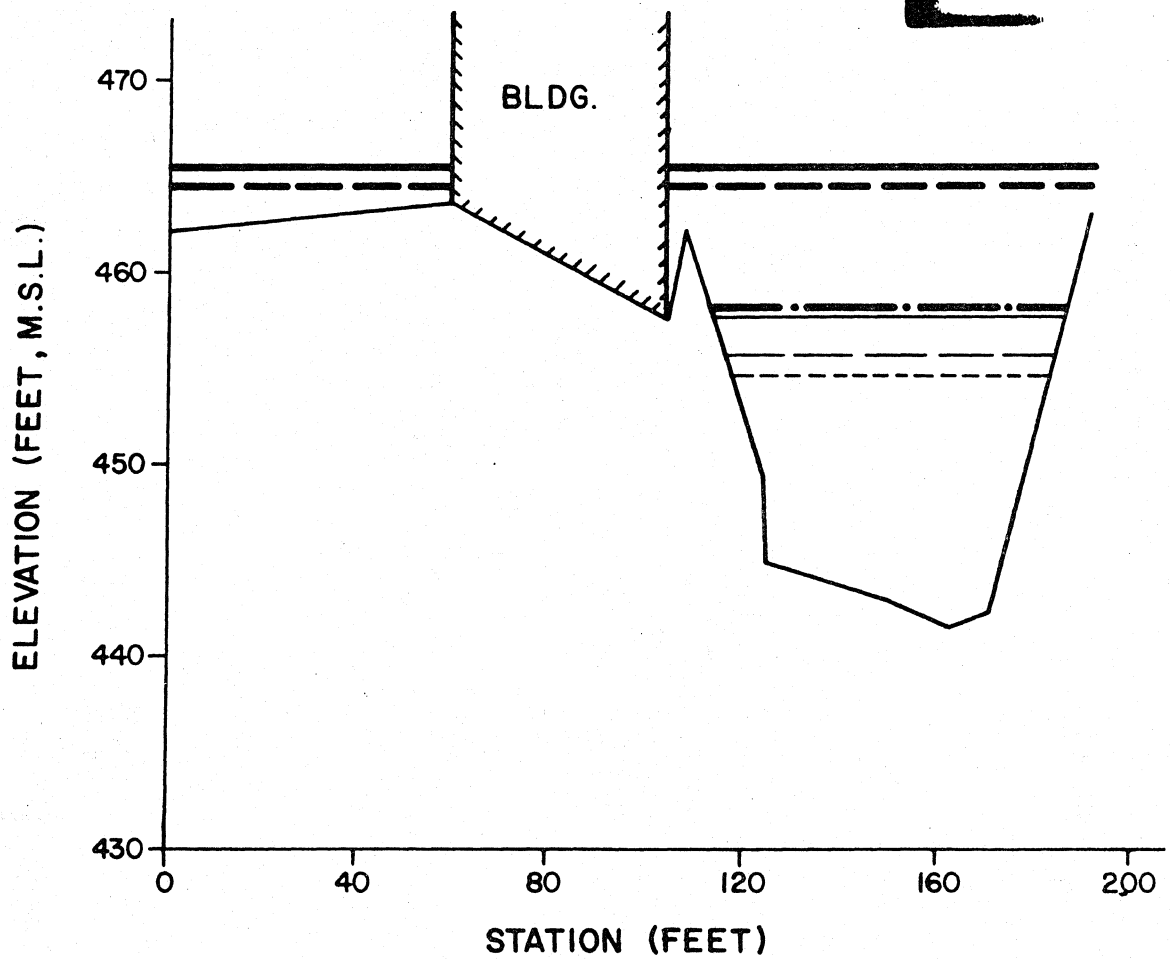

LEGEND

- 100-YEAR
- 25-YEAR
- 10-YEAR
- 18' Ø
- 20' Ø
- 21' Ø

FIGURE 9.10 4TH STREET + 50 FEET NORTH
(STATION 25 + 90)

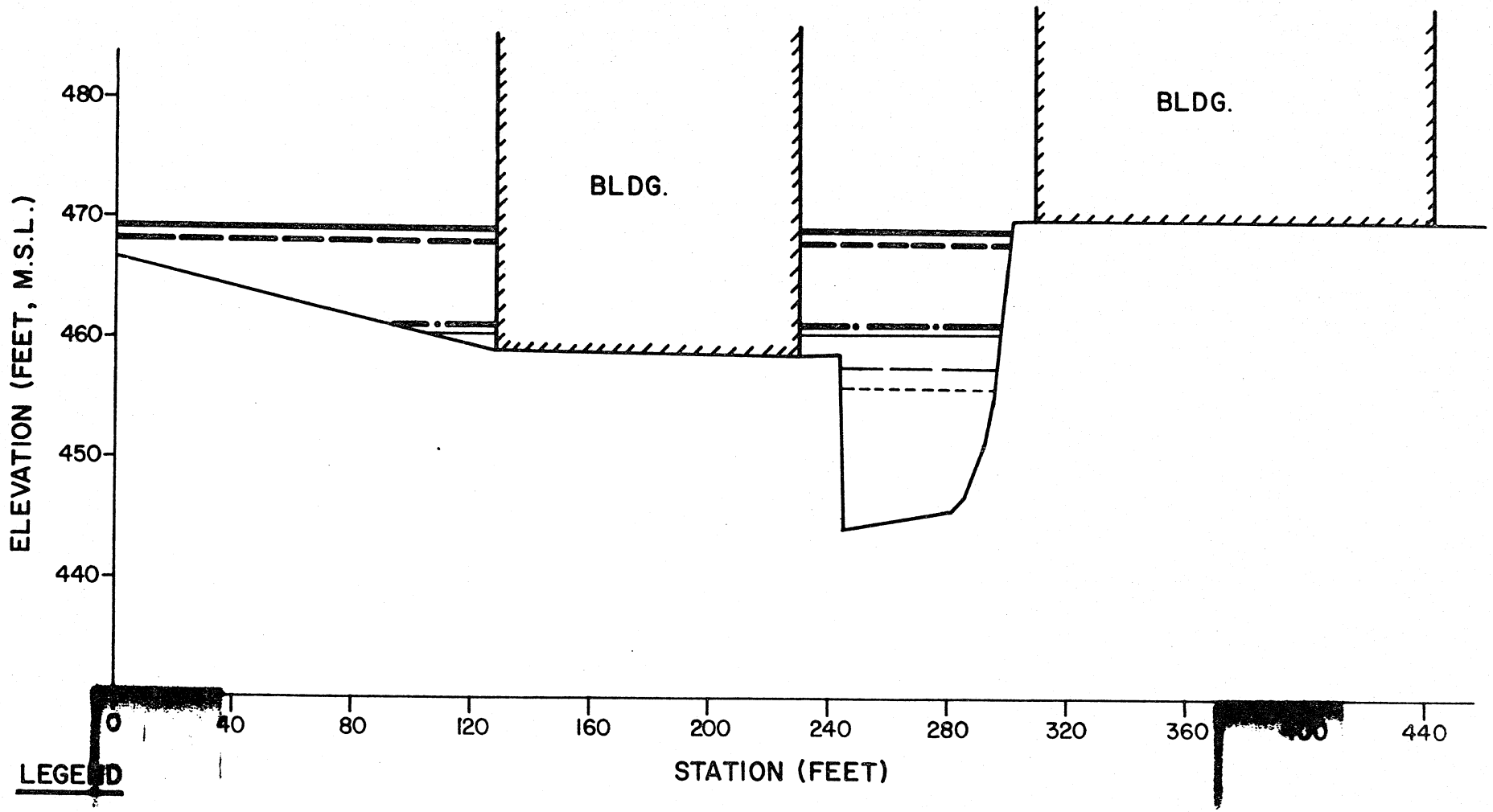

LEGEND

- 100-YEAR
- 25-YEAR
- 10-YEAR
- 18' Ø
- 20' Ø
- 21' Ø

FIGURE 9.11 5TH STREET + 50 FEET NORTH
(STATION 29 + 75)

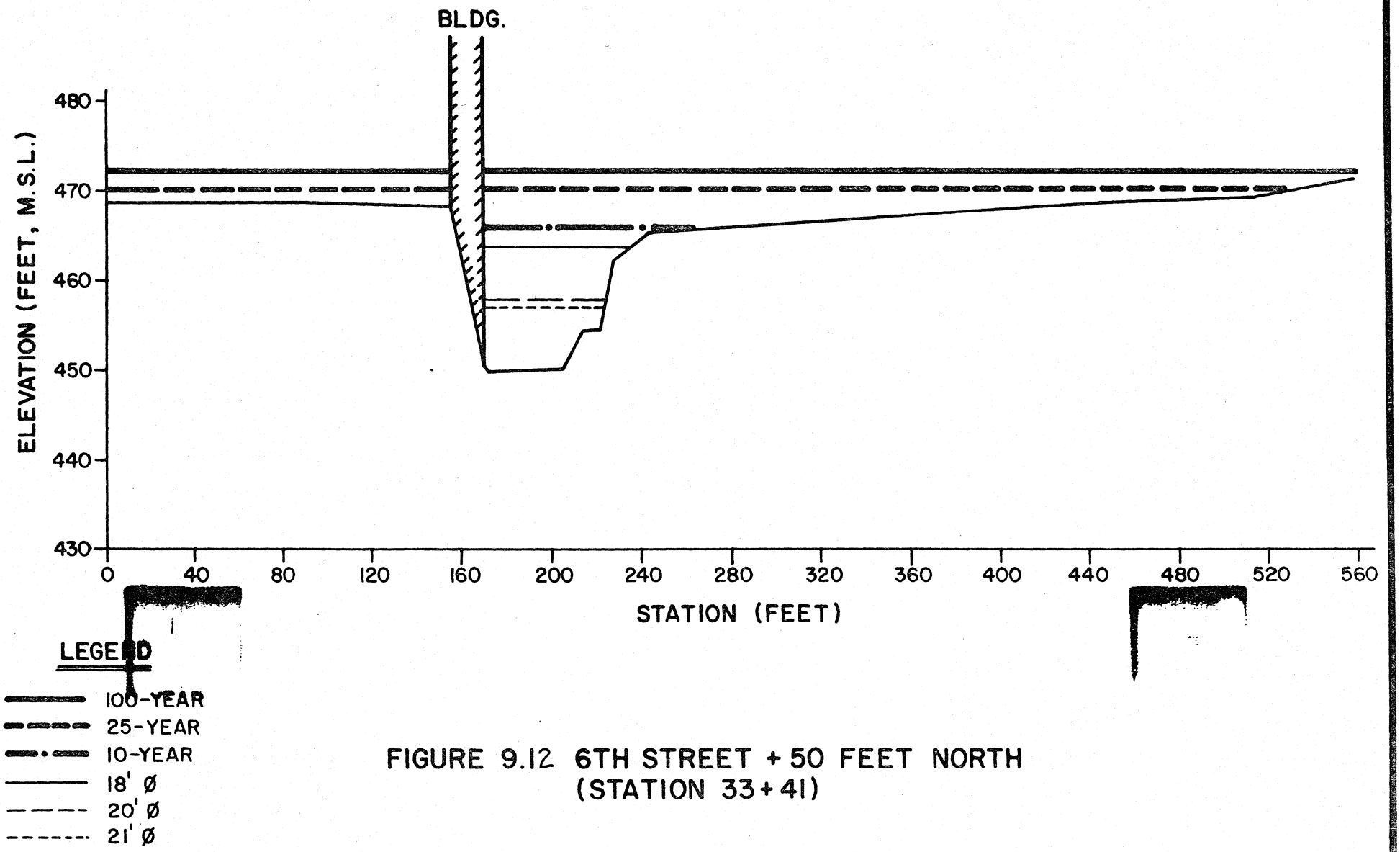

FIGURE 9.12 6TH STREET + 50 FEET NORTH
(STATION 33+41)

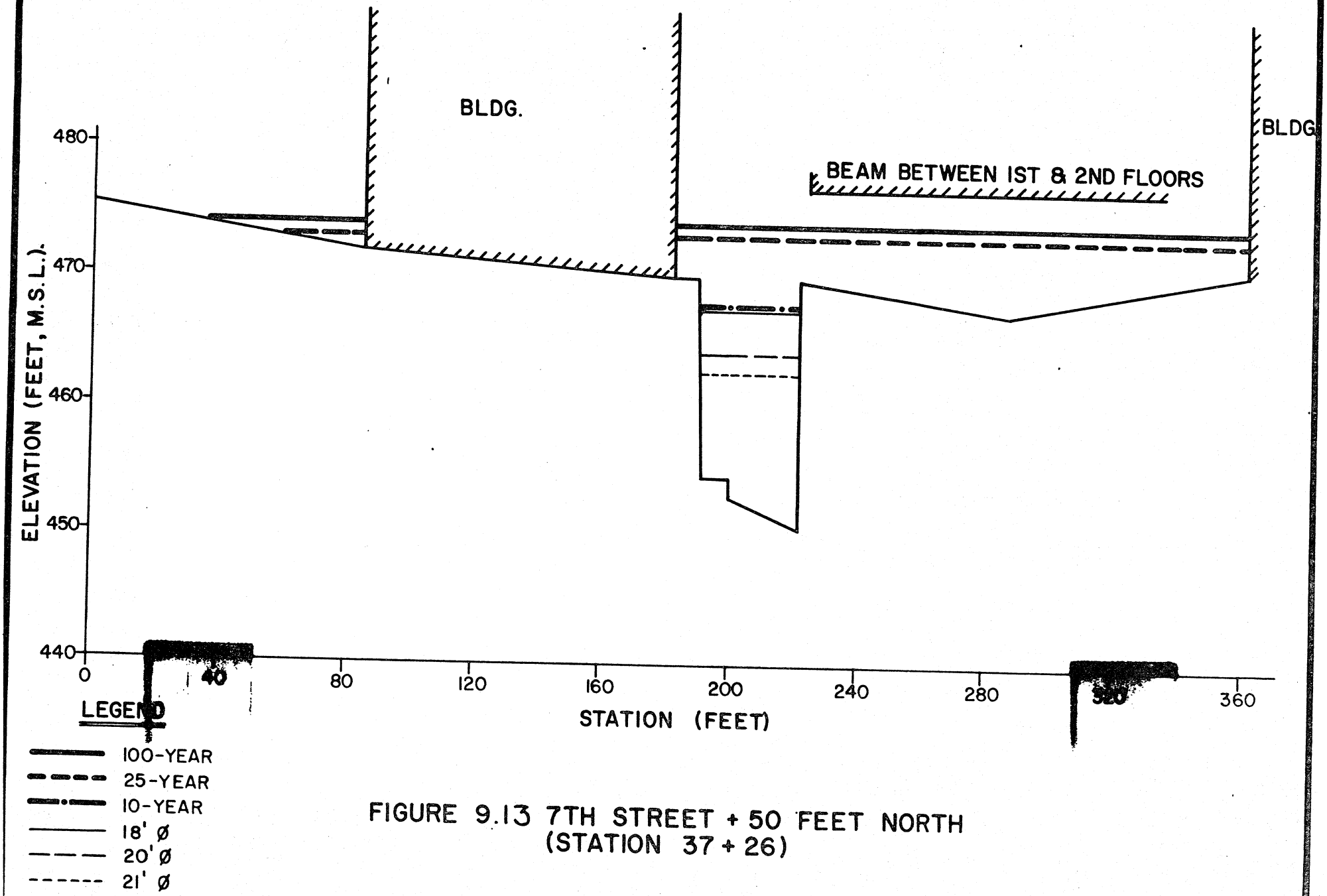

FIGURE 9.13 7TH STREET + 50 FEET NORTH
(STATION 37 + 26)

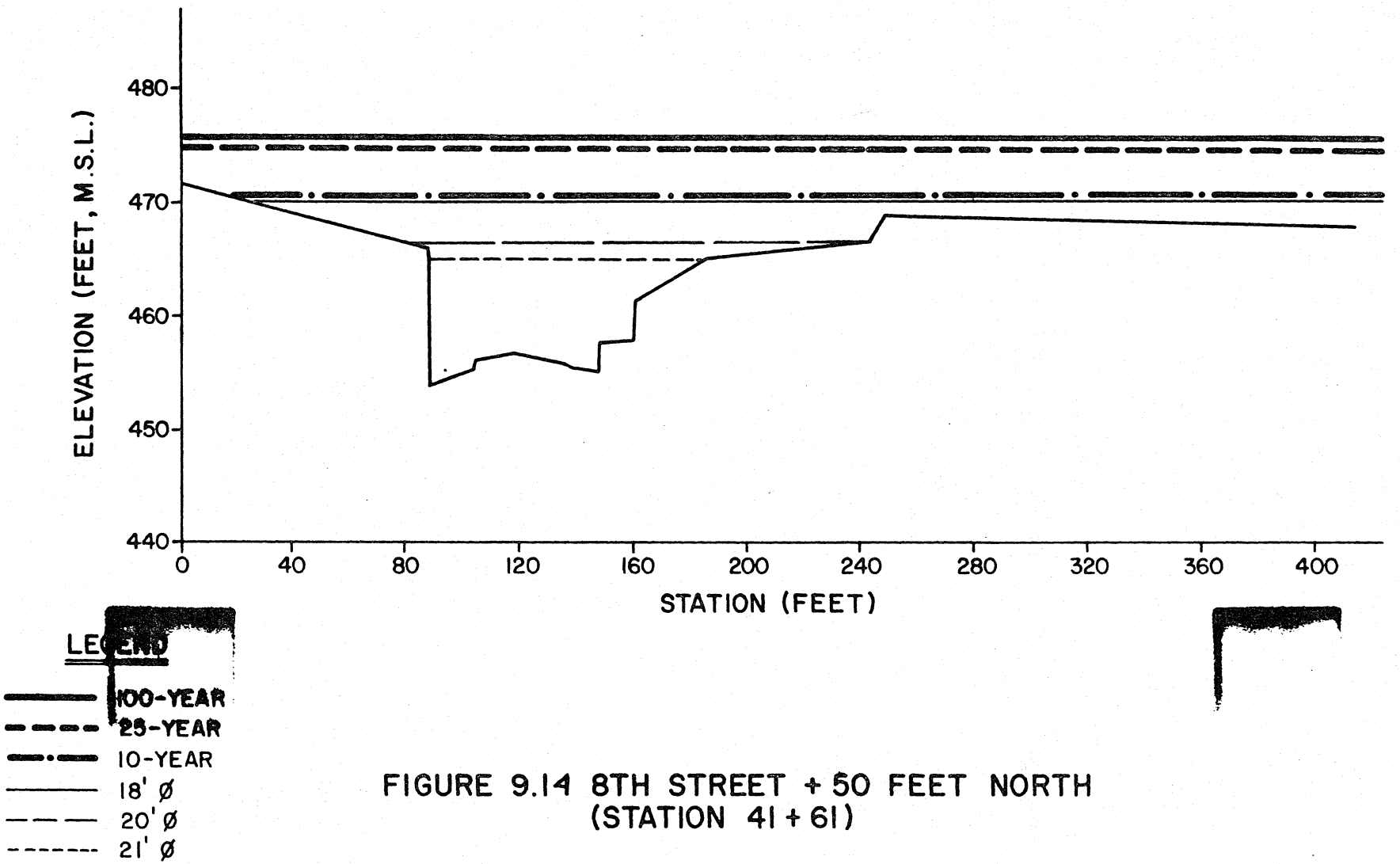

FIGURE 9.14 8TH STREET + 50 FEET NORTH
(STATION 41 + 61)

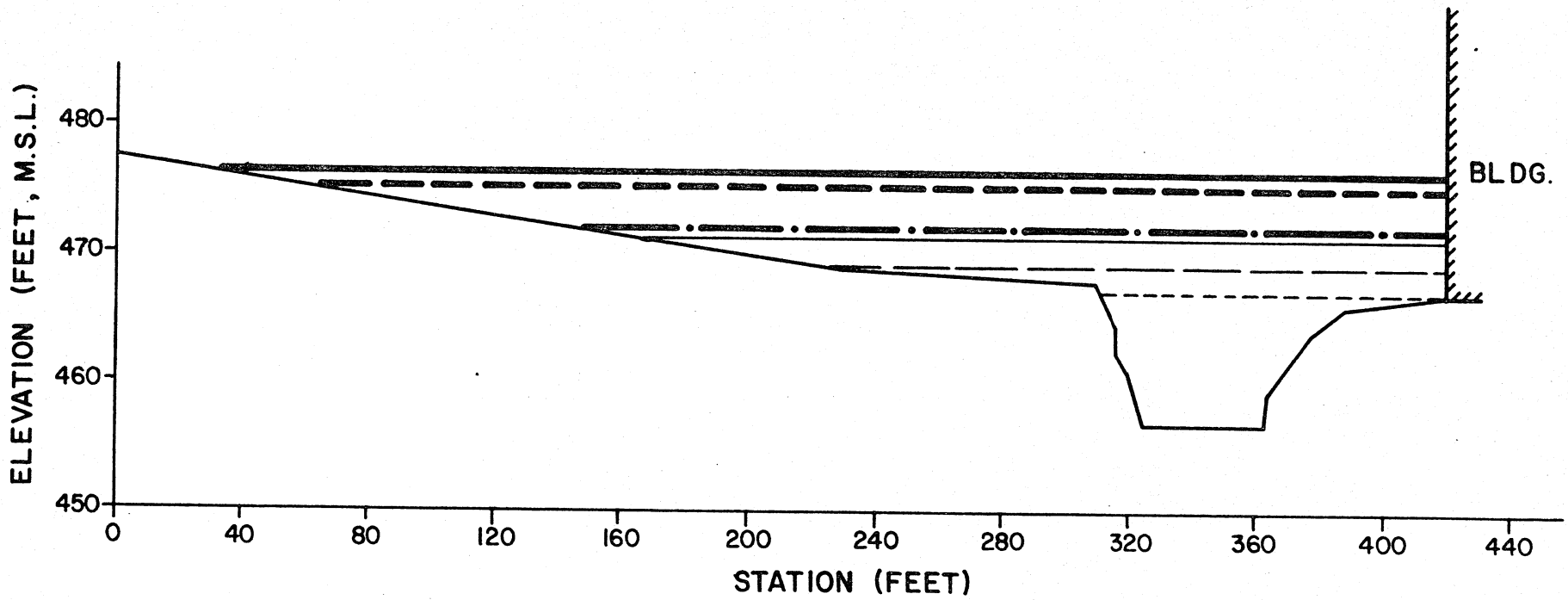

LEGEND

- 100-YEAR
- 25-YEAR
- 10-YEAR
- 18' Ø
- 20' Ø
- 21' Ø

FIGURE 9.15 9TH STREET + 50 FEET NORTH
(STATION 46+04)

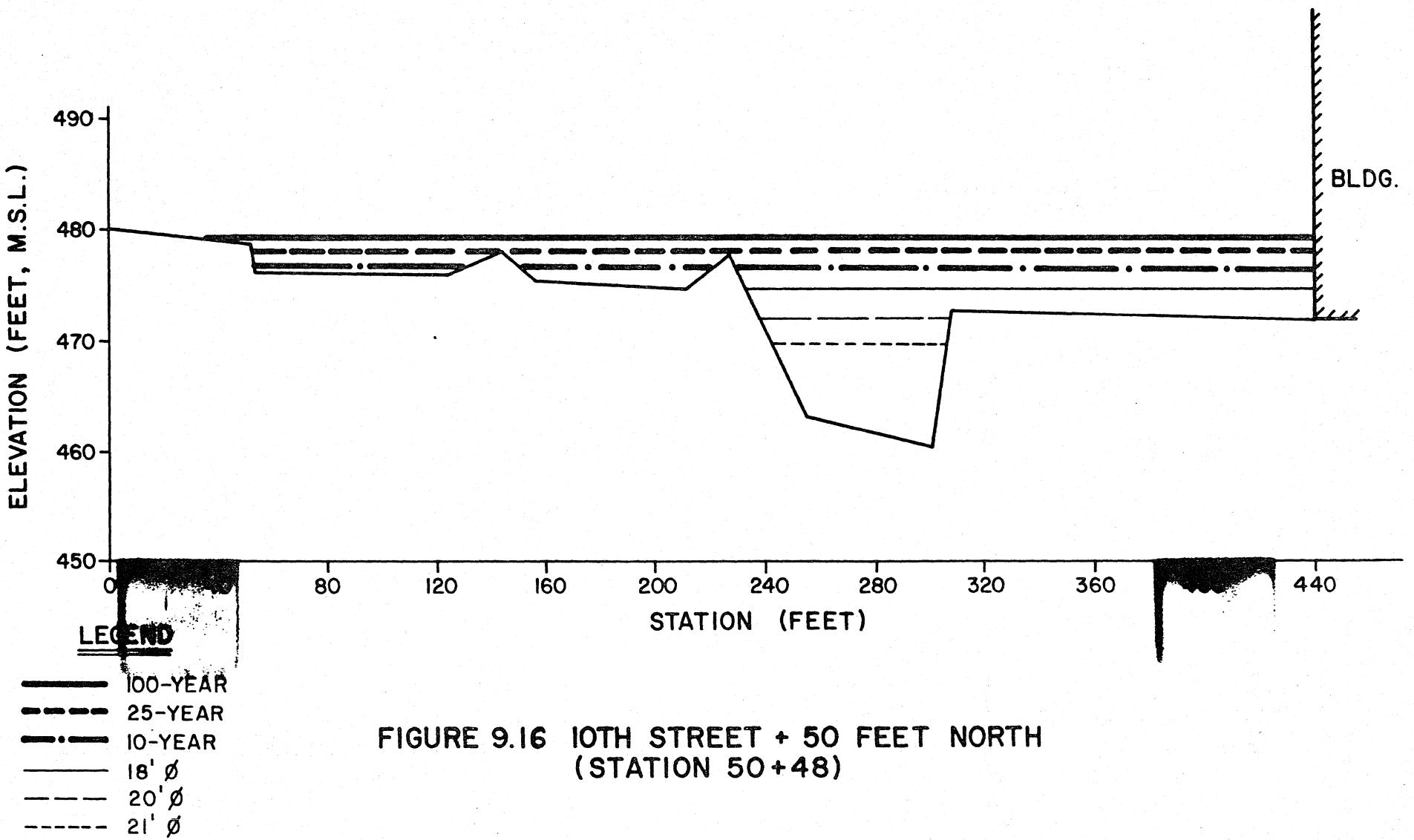

FIGURE 9.16 10TH STREET + 50 FEET NORTH
(STATION 50+48)

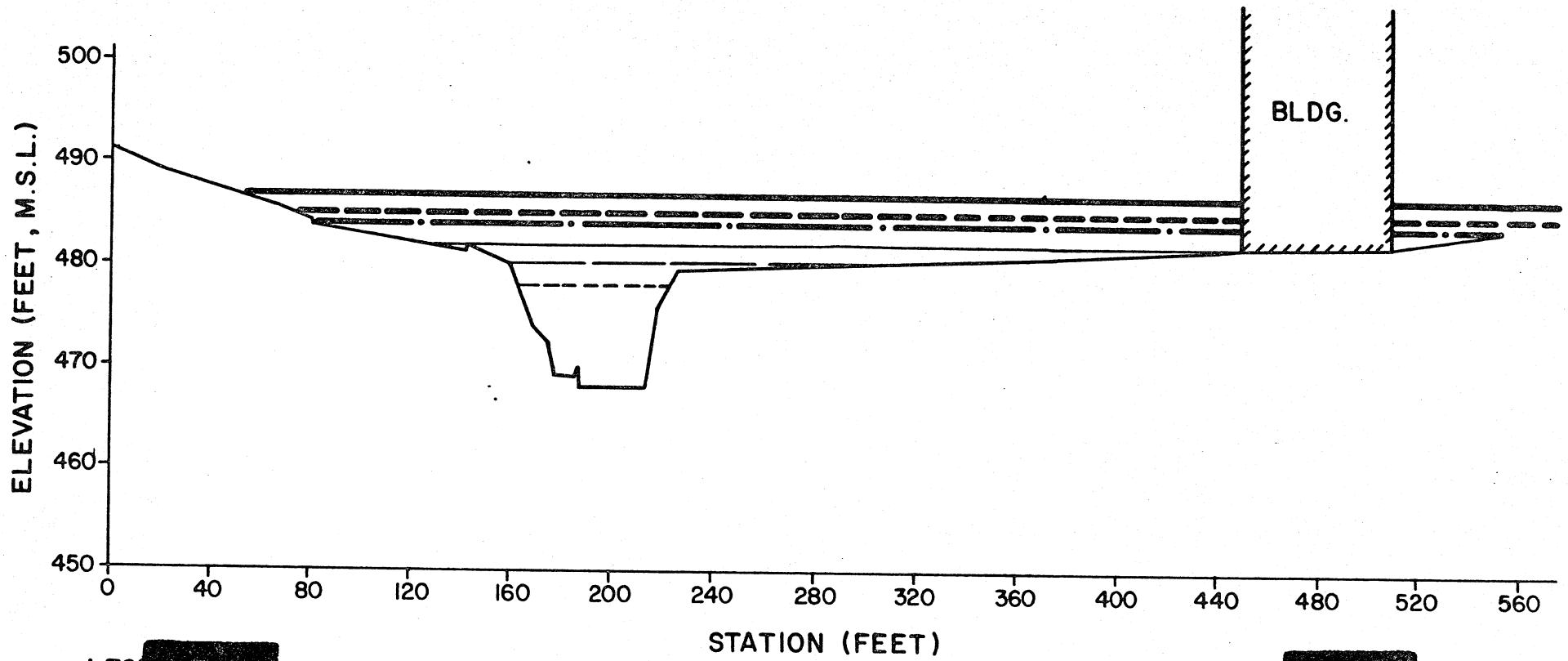

LEGEND

- 100-YEAR
- 25-YEAR
- 10-YEAR
- 18' Ø
- 20' Ø
- 21' Ø

FIGURE 9.17 12TH STREET + 50 FEET NORTH
(STATION 60+06)

```
 1 ...     2   17  100    4    1    8    1    2    2    1    1    1    1    1    2    1
 2 ... ALONE
 3 ...   0.1      50.        50.       0.80        0.55    1.0        0.5
 4 ...          2        10         1         1         7        10         2         1
 5 ...          2         0         0         0         1         0         1
 6 ...          0
 7 ...          0
 8 ...          0         1
 9 ...          0
10 ...         11
11 ...          6         5    90.
12 ...          2         2
13 ...          3         1
14 ...          1         3         1
15 ...         11
16 ...          1         3         1
17 ...          6
18 ...          1         4        11
19 ...          1         5         6
20 ... MAIN: U/S BOUNDARY
21 ... MAIN: AT 6000 FT
22 ... MAIN: D/S BOUNDARY
23 ... TRIBUT: U/S BOUNDARY
24 ... TRIBUT:10'FROM CONFL
25 ... TRIBUT:AT CONFLUENCE
26 ...     200.      1200.   2200.     2200.     2200.     2200.     2200.    1200.
27 ...     200.       200.    200.
28 ...     200.      1200.   2200.     2200.     2200.     2200.     2200.    1200.
29 ...     200.       200.    200.
30 ...  0.0
31 ...     98.6     100.2     102.6     104.3     106.2     107.7     109.5
32 ...     200.      550.     1000.     1700.     2200.     2600.     3200.
33 ...     20.       100.
34 ...     20.       100.
35 ...     20.       100.
36 ...     20.       100.
37 ...     20.       100.
38 ...     20.       100.
39 ...     20.       100.
40 ...     20.       100.
41 ...     20.       100.
42 ...     20.       100.
43 ...     20.       100.
44 ...     100.      120.
45 ...     99.5      119.5
46 ...     99.0      119.0
47 ...     98.5      118.5
48 ...     98.0      118.0
49 ...     97.5      117.5
50 ...     97.5      117.5
51 ...     97.0      117.0
52 ...     96.5      116.5
53 ...     96.0      116.0
54 ...     95.5      115.5
```

```
55 ...     0.0       0.0       0.0       0.0       0.0       0.0       0.0       0.0
56 ...    0.0       0.0       0.0
57 ...     20.       100.
58 ...     20.       100.
59 ...     20.       100.
60 ...     20.       100.
61 ...     20.       100.
62 ...     20.       100.
63 ...     99.5      119.5
64 ...     99.0      119.0
65 ...     98.5      118.5
66 ...     98.0      118.0
67 ...     98.0      118.0
68 ...     98.0      118.0
69 ...     0.0       0.0       0.0       0.0       0.0
70 ...    0.0       0.0       0.0
71 ...   9000.     8000.     7000.     6000.     5000.     4950.     4000.     3000.
72 ...   2000.     1000.       0.
73 ...     0.        0.        0.        0.        0.        0.        0.        0.
74 ...     0.        0.        0.
75 ...    0.0       0.0       0.0
76 ...   3000.     2000.     1000.       20.       10.       0.
77 ...     0.        0.        0.        0.        0.
78 ...          -5
79 ...   98.0
80 ...   0.0
81 ...   4.        6.        8.        10.       13.       16.       20.       25.
82 ...   100.      300.      700.      1000.     1300.     1500.     1750.     2000.
83 ...    5.00      0.10            5
84 ...     0.0       0.0       0.0       0.0       0.0       0.0       0.0       0.0
85 ...    0.0       0.0     99.51429
86 ...     0.0       0.0       0.0       0.0       0.0
87 ...    200.       0.0       0.0       0.0       0.0       0.0       0.0       0.0
88 ...     0.0       0.0       0.0
89 ...    200.       0.0       0.0       0.0       0.0
90 ...     0.0    10000.
91 ...     0.0    10000.
92 ...   0.025    0.025
93 ...   0.025    0.025
94 ... WORKSHOP PROBLEM 4
95 ... END
96 ... EXIT
```

Workshop 1 - DAMBRK Application for Routing

The purpose of this workshop is to illustrate the use of DAMBRK to perform reservoir routing using the storage routing procedure and dynamic routing in the downstream valley. You are to develop the DAMBRK model input and run on the computer. The PMF (probable maximum flood) inflow hydrograph to the reservoir is given in Table 1. Reservoir characteristics are presented in Table 2, listing the elevation-storage relationship and spillway characteristics. Five cross-sections (listed in Table 3) are used to describe the 12.5 mile long downstream valley. Manning's roughness factors, as a function of water surface elevation for each cross-section, are given in Table 4. Slope of the downstream valley is about 10.15 ft/mi.

The initial water surface elevation in the reservoir is 2323 ft. above M.S.L. Terminate routing computations after 57 hours of simulation. Use KDMP = 3 and JNK = 1 for the printing instructions. Use a minimum computational distance for interpolated cross-sections of 0.5 mi. for each reach.

OPTION 10

Table 1.

Time (hours)	Inflow (cfs)
0.	0.
1.	12.8
3.	239.2
5.	2000.0
7.	8028.8
9.	20339.5
11.	40906.1
13.	80570.3
15.	156116.8
17.	248330.1
19.	295681.1
21.	279367.0
23.	224737.0
25.	158232.4
27.	107019.0
29.	71600.3
31.	46295.6
33.	29862.1
35.	19363.0
37.	12561.7
39.	8143.1
41.	5275.7
43.	3460.3
45.	2205.5
47.	1218.0
49.	495.8
51.	163.4
53.	63.0
55.	15.7
57.	0.

inflow hydrograph of reservoir

Table 2. Characteristics of Reservoir

Elevation-Storage Relationship	
Elevation (ft.-M.S.L.)	Storage (acre-feet)
2342.	160710.
2330.	85120.
2320.	58460.
2305.	30075.
2290.	13400.
2275.	4125.
2260.	335.
2245.	0.

Reservoir

Top of Dam Elevation (MSL):	2347. ft.
Length of Reservoir:	5 miles
Elevation (MSL) of Bottom of Dam:	2245. ft.
Normal Pool Level (MSL):	2323. ft.

Spillway

Elevation of Uncontrolled Spillway Crest:	2333.
Discharge Coefficient for Uncontrolled Spillway:	2.5
Length of Uncontrolled Spillway:	3900. ft.

Turbine

Discharge (cfs):	800

Table 3. Cross-Sections of Downstream Valley

Cross-Section Number	Channel Location (mi)						
1	0.0	Elevation (ft)	2250.	2260.	2300.	2330.	2350.
		Top Width (ft)	0.	1024.	2737.	4508.	11812.
2	1.97	Elevation (ft)	2230.	2240.	2250.	2270.	2300.
		Top Width (ft)	0.	473.	2539.	4311.	6654.
3	5.61	Elevation (ft)	2190.	2200.	2210.	2240.	2270.
		Top Width (ft)	0.	1078.	2441.	3118.	3842.
4	8.94	Elevation (ft)	2150.	2160.	2170.	2180.	2210.
		Top Width (ft)	0.	216.	1654.	2402.	4093.
5	12.5	Elevation (ft)	2120.	2130.	2140.	2160.	2180.
		Top Width (ft)	0.	945.	1772.	3091.	3858.

Table 4. Manning's N Relationships

Reach	Manning's N Values for Respective Elevation in Table 3.				
1	0.030	0.030	0.035	0.035	0.035
2	0.030	0.030	0.035	0.035	0.035
3	0.030	0.030	0.035	0.035	0.035
4	0.030	0.030	0.035	0.035	0.035

Workshop 2 - DAMBRK Application for Dam Break Analysis for Non-Flood Event

The purpose of this workshop is to illustrate the use of DAMBRK to perform a dam break analysis for a non-flood event. The reservoir and downstream valley used in Workshop 1 is used for this application. A non-flood event is used for the inflow to the reservoir. The initial water surface elevation is at the normal pool level. Failure of the dam occurs at the initial water surface elevation in the reservoir. The breach is rectangular and the time to breach is 1.25 hours after the beginning of the breach. The breach extends down to the elevation of the bottom of the dam, 2245 ft. above M.S.L. and is 200 ft. wide at its base. The computation can be terminated after 10 hours of simulation. Perform the analysis using another time to failure to compare the results.

Workshop 3 - DAMBRK Application for Dam Break Analysis for Flood (PMF) Event

The purpose of this workshop is to illustrate the use of DAMBRK to perform a dam break analysis for a flood (PMF) event. The same reservoir and downstream valley used in Workshops 1 and 2 are used for this application. Use the same breach characteristics as used in Workshop 2. The PMF inflow into the reservoir (Workshop 1, Table 1) is to be used for this workshop. Assign an elevation of water when breaching starts (HF) equal to 2341.48 above M.S.L. and a time to maximum breach size (TFM) equal to 1.25 hr.

Perform the analysis using another time to failure to compare the results. Compare the results that you have obtained in Workshops 1, 2, and 3.

Workshop 4 - DAMBRK Application for Multiple Dams

This workshop is used to illustrate the multiple dam application. The previous workshop example is extended to include a second dam whose downstream face is at mile 12.5. Three additional cross-sections are used to define the upstream faces of both dams and the downstream channel of the second dam. Their characteristics are given in Table 5. Table 6 is a summary of the characteristics of the second dam. Notice that what used to be your cross-section at mile 0.0 is now at mile 5.0 (the length of the reservoir). The locations of the four previous cross-sections are shifted accordingly.

The initial water surface elevation for the second reservoir is at 2150 ft. The breach which starts at an elevation equal to the top of the second dam, 2180 ft. above M.S.L., extends down to elevation 2120 ft. above M.S.L. Assign a width of base of breach equal to 100 ft. Use the same value for the time to maximum breach size as in the first dam.

Table 5. Additional Cross-Sectional Information

Cross-Section Number	Channel Location (mi)						
1	4.95	Elevation (ft)	2251.	2260.	2300.	2330.	2350.
		Top Width (ft)	0.	1024.	2737.	4508.	11812.
6	17.45	Elevation (ft)	2121.	2130.	2140.	2160.	2180.
		Top Width (ft)	0.	945.	1772.	3091.	3858.
8	18.5	Elevation (ft)	2110.	2120.	2130.	2150.	2170.
		Top Width (ft)	0.	945.	1772.	3091.	3858.

Table 6. Characteristics of Second Dam

Top of Dam Elevation (MSL):	2180. ft.
Elevation (MSL) of Bottom of Dam:	2120. ft.
Elevation of Uncontrolled Spillway Crest:	2165. ft.
Discharge Coefficient for Uncontrollled Spillway:	2.5
Discharge Coefficient for Uncontrolled Weir Flow (=CDO):	4830.8
Length of Uncontrolled Spillway Length:	2000. ft.

Problem # 1

```
  1 ...     1   17   25    5    1    8    1    2    2    3    1    1    1    1    1    1
  2 ... ALONE
  3 ...   0.1      50.        50.        0.80        0.55    1.0        0.5
  4 ...          1        10         1         1         7        10         2
  5 ...          2         0         0         0         2         0         1
  6 ...          0
  7 ...          0
  8 ...          0
  9 ...          0
 10 ...         10
 11 ...          2
 12 ...          3
 13 ...          1         3         1
 14 ...         10
 15 ...          1         4        10
 16 ... MAIN: U/S BOUNDARY
 17 ... MAIN: AT 6000 FT
 18 ... MAIN: D/S BOUNDARY
 19 ...     200.      1200.   2200.     2200.     2200.     2200.     2200.     200.
 20 ...     200.       200.
 21 ...     1.0
 22 ...     98.6     100.2     102.6     104.3     106.2     107.7     109.5
 23 ...     200.      550.     1000.     1700.     2200.     2600.     3200.
 24 ...     20.       100.
 25 ...     20.       100.
 26 ...     20.       100.
 27 ...     20.       100.
 28 ...     20.       100.
 29 ...     20.       100.
 30 ...     20.       100.
 31 ...     20.       100.
 32 ...     20.       100.
 33 ...     20.       100.
 34 ...     100.      120.
 35 ...     99.5      119.5
 36 ...     99.0      119.0
 37 ...     98.5      118.5
 38 ...     98.0      118.0
 39 ...     97.5      117.5
 40 ...     97.0      117.0
 41 ...     96.5      116.5
 42 ...     96.0      116.0
 43 ...     95.5      115.5
 44 ...     0.0       0.0       0.0       0.0       0.0       0.0       0.0       0.0
 45 ...   0.0       0.0
 46 ...   0.0       0.0       0.0
 47 ...   9000.     8000.     7000.     6000.     5000.     4000.     3000.     2000.
 48 ...   1000.     0.0
 49 ...     0.0       0.0       0.0       0.0       0.0       0.0       0.0       0.0
 50 ...   0.0       0.0
 51 ...   5.00      0.10            5
 52 ...     0.0       0.0       0.0       0.0       0.0       0.0       0.0       0.0
 53 ...     0.0     98.6
 54 ...   200.       0.0       0.0       0.0       0.0       0.0       0.0       0.0
```

```
55 ...     0.0      0.0
56 ...     0.0    10000.
57 ...   0.025    0.025
58 ... EXAMPLE TO ILLUSTRATE INPUT FOR A TRAPEZOIDAL SHAPED IRRIGATION CANAL
59 ... END
60 ... EXIT
```